

**Volume 1**

# **Practical Advances in Petroleum Processing**



Edited by

**Chang Samuel Hsu** and **Paul R. Robinson**

Practical Advances in  
Petroleum Processing  
Volume 1

# Practical Advances in Petroleum Processing Volume 1

Edited by

**Chang S. Hsu**

*ExxonMobil Research and Engineering Company  
Baton Rouge, Louisiana, USA*

and

**Paul R. Robinson**

*PQ Optimization Services  
Katy, Texas, USA*

 Springer

Chang S. Hsu  
ExxonMobil Research and Engineering Co.  
10822 N. Shoreline Avenue  
Baton Rouge, Louisiana 70809  
USA  
chang.samuel.hsu@exxonmobil.com

Paul R. Robinson  
PQ Optimization Services  
3418 Clear Water Park Drive  
Katy, Texas 77450  
USA  
paul-robinson@houston.rr.com

Cover design by Suzanne Van Duyne (Trade Design Group)

Front cover photo and back cover photo insert: Two views of the OMV plant in Schwechat, Austria, one of the most environmentally friendly refineries in the world, courtesy of OMV. Front cover insert photo: The Neste Oil plant in Porvoo, Finland includes process units for fluid catalytic cracking, hydrocracking, and oxygenate production. The plant focuses on producing high-quality, low-emission transportation fuels. Courtesy of Neste Oil.

Library of Congress Control Number: 2005925505

ISBN-10: 0-387-25811-6

ISBN-13: 978-0387-25811-9

©2006 Springer Science+Business Media, Inc.

All rights reserved. This work may not be translated or copied in whole or in part without the written permission of the publisher (Springer Science+Business Media, Inc., 233 Spring Street, New York, NY 10013, USA), except for brief excerpts in connection with reviews or scholarly analysis. Use in connection with any form of information storage and retrieval, electronic adaptation, computer software, or by similar or dissimilar methodology now known or hereafter developed is forbidden.

The use in this publication of trade names, trademarks, service marks and similar terms, even if they are not identified as such, is not to be taken as an expression of opinion as to whether or not they are subject to proprietary rights.

Printed in the United States of America

9 8 7 6 5 4 3 2 1

springeronline.com

**Tribute to Dr. Esber I. Shaheen  
(1937-2003)**



Born in 1937 in a remote village in Lebanon, Dr. Esber Ibrahim Shaheen became a much-honored educator, mentor and consultant, both for technology and international affairs. He received his B.S. in chemical engineering from Oklahoma State University, his M.S. in chemical engineering from the University of Arizona in Tuscon, and his Ph.D. from the University of Tennessee in Knoxville.

He was a professor and distinguished lecturer at more than 6 universities, including the University of Wisconsin, the King Fahd University of Petroleum and Minerals in Saudi Arabia, the Illinois Institute of Technology, Chicago, and the University of Tennessee. He also served as Director of Educational Services for the Institute of Gas Technology and Director of International

Education Programs for the Gas Developments Corporation in Chicago, Illinois. He assisted and encouraged students from all over the world and was instrumental in helping many of them in developing careers throughout the world.

Dr. Shaheen authored 7 textbooks, 3 of which were on international relations and more than 50 technical articles. He was the author, co-author or editor of nearly 20 training manuals on engineering, energy, the environment and petrochemical processing.

He received many awards, including Outstanding Educator of America. Most significantly, Dr. Shaheen received medals from President Ronald Reagan and from the Governor of the Eastern Province in Saudi Arabia.

We are pleased to include, with the permission of Dr. Esber I. Shaheen's wife, Shirley K. Shaheen, selections from his writings in this volume.

Paul R. Robinson  
Chang Samuel Hsu

## Foreword

Petroleum has remained an important aspect of our lives and will do so for the next four or five decades. The fuels that are derived from petroleum supply more than half of the world's total supply of energy. Gasoline, kerosene, and diesel oil provide fuel for automobiles, tractors, trucks, aircraft, and ships. Fuel oil and natural gas are used to heat homes and commercial buildings, as well as to generate electricity. Petroleum products are the basic materials used for the manufacture of synthetic fibers for clothing and in plastics, paints, fertilizers, insecticides, soaps, and synthetic rubber. The uses of petroleum as a source of raw material in manufacturing are central to the functioning of modern industry.

Petroleum refining is now in a significant transition period as the industry has moved into the 21st century and the demand for petroleum products has shown a sharp growth in recent years, especially with the recent entry of China into the automobile market. This means that the demand for transportation fuels will, without doubt, show a steady growth in the next decade, contributing to petroleum product demand patterns that can only be fulfilled by the inclusion of heavier feedstocks into refinery operations.

In fact, the increasing supply of heavy crude oils as refinery feedstocks is a serious matter and it is essential that refineries are able to accommodate these heavy feedstocks. Indeed, in order to satisfy the changing pattern of product demand, significant investments in refining conversion processes will be necessary to profitably utilize these heavy crude oils. The most efficient and economical solution to this problem will depend to a large extent on individual country and company situations. However, the most promising technologies will likely involve the conversion of heavy crude oil, vacuum bottom residua, asphalt from deasphalting processes, and bitumen from tar sand deposits. Therefore, a thorough understanding of the benefits and limitations of petroleum processing is necessary and is introduced within the pages of this book.

The book is divided into two volumes. The first volume contains covers the origin and characterization of petroleum, major processes for fuel-

production, and environmental pollution control. The second volume focuses on lubricants, hydrogen production, process modeling, automation, and online optimization.

The 50 contributors hail from three continents – Asia, Europe, and North America. This allows the book to contain within its pages a variety of experiences that are truly worldwide in breadth and scope. Contributions come from several sources, including integrated oil companies, catalyst suppliers, licensors, consultants, and academic researchers.

I am pleased to have been asked to write the Forward to this book. In light of the world energy situation, it is a necessary and timely addition to the literature that covers the technology of petroleum.

Dr. James G. Speight



## Contributors

|                     |   |
|---------------------|---|
| Brent E. Beasley    | ExxonMobil Research & Engineering Co.<br>Process Research Lab<br>Baton Rouge, LA 70821                      |
| F. Emmett Bingham   | Haldor Topsøe, Inc.<br>770 The City Drive, Suite 8400<br>Orange, CA 92668                                   |
| Yevgenia Briker     | National Centre for Upgrading Technology<br>1 Oil Patch Drive, Suite A202<br>Devon, Alberta T9G 1A8, Canada |
| James D. Burrington | The Lubrizol Corporation<br>29400 Lakeland Blvd<br>Wickliffe, OH 44092                                      |
| Ki-Hyouk Choi       | Kyushu University<br>Kasuga, Fukuoka 816-8580, Japan  |
| Dennis Cima         | Aspen Technology, Inc.<br>2500 City West Boulevard, Suite 1500<br>Houston, Texas 77042                      |
| I. A. Cody          | ExxonMobil Research & Engineering Co.<br>Process Research Lab<br>Baton Rouge, LA 70821                      |
| Barry H. Cooper     | Haldor Topsøe A/S<br>Nymøllevej 55, DK2800<br>Lyngby, Denmark   |
| M. Andrew Crews     | CB&I Process and Technology<br>3102 E. Fifth St<br>Tyler, TX 75701-5013                                     |
| Geoffrey E. Dolbear | G.E. Dolbear & Associates<br>23050 Aspen Knoll Drive<br>Diamond Bar, California 91765, USA                  |
| T. Rig Forbus       | The Valvoline Co. of Ashland, Inc.<br>Lexington, KY 40512 USA   |
| Thomas Gentzis      | CDX Canada Co<br>1210, 606-4th Street SW,<br>Calgary, Alberta, Canada T2P 1T1                               |

|                      |  |
|----------------------|--|
| Adrian Gruia         | UOP LLC<br>Des Plaines, Illinois, USA  |
| Nick Hallale         | AspenTech UK Limited<br>Warrington, UK   |
| Suzzy C. Ho          | ExxonMobil Chemical Co.<br>Edison, NJ. 08818-3140  |
| Teh C. Ho            | ExxonMobil Research & Engineering Co.<br>Annandale, NJ 08801, USA  |
| Gang Hou             | Department of Chemical Engineering<br>University of Delaware, Newark, DE 19716   |
| Maurice D. Jett      | Aspen Technology, Inc.<br>2500 City West Boulevard, Suite 1500<br>Houston, Texas 77042                                 |
| Michael T. Klein     | Dept. of Chemical and Biochemical Engineering<br>School of Engineering<br>Rutgers University, Piscataway, NJ 08854     |
| Ian Moore            | AspenTech UK Limited<br>Warrington, UK   |
| Sriganesh Karur      | Aspen Technology, Inc.<br>2500 City West Boulevard, Suite 1500<br>Houston, Texas 77042                                 |
| Kim G. Knudsen       | Haldor Topsøe A/S<br>Nymøllevej 55, DK2800<br>Lyngby, Denmark  |
| Zaiting Li           | Research Institute of Petroleum Processing<br>SINOPEC<br>Beijing, China  |
| Xiaoliang Ma         | Dept. of Energy & Geo-Environmental Engineering<br>The Pennsylvania State University<br>University Park, PA 16802, USA |
| Blaine McIntyre      | Aspen Technology, Inc.<br>125 9th Avenue SE, Suite 900<br>Calgary, Alberta T2G OP6 Canada                              |
| Milo D. Meixell, Jr. | Aspen Technology, Inc.<br>2500 City West Boulevard, Suite 1500<br>Houston, Texas 77042                                 |
| Isao Mochida         | Kyushu University<br>Kasuga, Fukuoka 816-8580, Japan   |
| Dale R. Mudt         | Suncor Inc<br>1900 River Road<br>Sarnia, Ontario N7T 7J3 Canada  |

- Douglas E. Nelson Haldor Topsøe, Inc.  
770 The City Drive, Suite 8400  
Orange, CA 92668
- Paul O'Connor Albemarle Nobel Catalysts  
Stationsplein 4, P.O.Box 247, 3800AE  
Amersfoort, The Netherlands
- Clifford C. Pedersen Suncor Inc.  
1900 River Road  
Sarnia, Ontario N7T 7J3 Canada
- J. L. Peña-Díez Technology Centre, Repsol-YPF  
P.O. Box 300  
28930 Móstoles – Madrid, Spain
- John K. Pudelski The Lubrizol Corporation  
29400 Lakeland Blvd  
Wickliffe, OH 44092
- Parviz M. Rahimi National Centre for Upgrading Technology  
1 Oil Patch Drive, Suite A202  
Devon, Alberta, Canada T9G 1A8
- Zbigniew Ring National Centre for Upgrading Technology  
1 Oil Patch Drive, Suite A202  
Devon, Alberta T9G 1A8, Canada
- Paul R. Robinson PQ Optimization Services  
3418 Clearwater park Drive  
Katy, Texas 77450, USA
- James P. Roski The Lubrizol Corporation  
29400 Lakeland Blvd  
Wickliffe, OH 44092 USA
- Stilianos G. Roussis Sarnia Research Centre, Imperial Oil  
Sarnia, Ontario, N7T 8C8 Canada
- B. Gregory Shumake CB&I Process and Technology  
3102 E. Fifth St  
Tyler, TX 75701-5013 USA
- Eli I. Shaheen International Institute of Technology, Inc.  
830 Wall Street  
Joplin, MO 64801 USA
- Ebbe R. Skov Hetagon Energy Systems Inc.  
Mission Viejo, California, USA
- Chunshan Song Dept. of Energy & Geo-Environmental Engineering  
The Pennsylvania State University  
University Park, Pennsylvania 16802, USA
- Dennis Vauk Air Liquide America L.P.  
Houston, Texas

|                     |   |
|---------------------|---|
| Clifford C. Walters | ExxonMobil Research & Engineering Co.<br>Annandale, NJ 08801, USA   |
| Murray R. Watt      | Sarnia Research Centre, Imperial Oil<br>Sarnia, Ontario, N7T 8C8 Canada                                     |
| Xieqing Wang        | Research Institute of Petroleum Processing<br>SINOPEC<br>Beijing, China                                     |
| Margaret M. Wu      | ExxonMobil Research & Engineering Co.<br>Annandale, NJ 08801, USA   |
| Chaogang Xie        | Research Institute of Petroleum Processing<br>SINOPEC<br>Beijing, China                                     |
| Hong Yang           | National Centre for Upgrading Technology<br>1 Oil Patch Drive, Suite A202<br>Devon, Alberta T9G 1A8, Canada |
| Genquan Zhu         | Research Institute of Petroleum Processing<br>SINOPEC<br>Beijing, China                                     |

## Preface

In 1964, Bob Dylan released an album and song named, *The Times They Are A-Changin'*. He was right. Times were changing, but nobody, not even Dylan, could have foreseen just how dramatically the great, wide world – and the smaller world of petroleum processing – would change during the next forty years.

In 1964, a wall divided Berlin. The moon was free of foot-prints. And in America we said, “Fill ‘er up with ethyl” as a team of fueling-station attendants hurried to wash the windows of our thirsty Fords and Chevies.

In 1970, the Nixon administration created the U.S. Environmental Protection Agency (EPA), which, in 1973, initiated a lead phase-down program for gasoline. By the end of the decade, thanks to an oil embargo in 1973-74 and a revolution in Iran in 1978-79, fuel-efficient Japanese cars were displacing home-made brands in the United States and Europe.

In the 1980s, refiners built new process units to close the “octane gap” created by ever-tighter limits on lead in gasoline. Due to record-high prices, the worldwide demand for petroleum actually was decreasing. The drive to conserve energy created a market for rigorous models and advanced process control in refineries and petrochemical plants.

The Clean Air Act Amendments (CAAA) of 1990 again changed the industry. For gasoline, the CAAA required the addition of oxygenates such as MTBE. Billions of dollars, francs, marks, and yen were spent building methanol and MTBE plants. For on-road diesel, the CAAA emulated California by limiting sulfur content to 500 wppm. Across the Atlantic, the European Commission imposed a different set of limits. By the end of 2003, refiners were making low-sulfur gasoline and preparing to make ultra-low-sulfur diesel. Ironically, in 1999, Governor Gray Davis issued an executive order banning the use of MTBE in California gasoline. Soon thereafter, Davis was replaced by Arnold Schwarzenegger.

***Purpose of this Book.*** This historical digression illustrates, we hope, that petroleum processing is a dynamic industry driven by global political, economic, and environmental forces. That’s one of the reasons we’re writing this book: to explain how the industry has changed during the past 40 years,

particularly since 1994. We also wanted to cover cutting-edge topics usually missing from other general books on refining – FCC gasoline post-treatment, catalytic production of lubes, optimization of hydrogen and utility networks, process modeling, model-predictive control, and online optimization. And in addition: pollution control, staffing, reliability and safety.

**Target Audience.** Our target audience includes engineers, scientists and students who want an update on petroleum processing. Non-technical readers, with help from our extensive glossary, will benefit from reading Chapter 1 and the overview chapters that precede each major section.

**Contributors.** We are pleased to have contributions from several sources, including integrated oil companies, catalyst suppliers, licensors, consultants, and academic researchers. Our 50 contributors hail from three continents – Asia, Europe, and North America.

Many of the chapters are based on presentations given at a symposium at the 222<sup>nd</sup> National Meeting of the American Chemical Society (ACS), which was held in Chicago, Illinois in 2001. The symposium was entitled, “Kinetics and Mechanisms of Petroleum Processes.” We thank ACS and the Division of Petroleum Chemistry, Inc. for allowing us to co-chair that session.

**Organization and Overview.** The book is divided into two volumes. The first contains 14 chapters, which cover the origin and characterization of petroleum, major processes for fuel-production, and environmental pollution control. The second volume contains 13 chapters, which focus on lubricants, hydrogen production, process modeling, automation, and refining management.

Chapter 1 introduces the book by giving an overview of petroleum and petroleum processing. Chapters 2-4 focus on the origin and characterization of oil and gas. Chapter 5 reports recent advances in the production of light olefin feedstocks for petrochemicals by catalytic processes, especially the balance between propylene and ethylene. Chapter 6 gives an overview of the kinetics and mechanism of fluidized catalytic cracking, an important process for producing gasoline.

The next five chapters discuss hydroprocessing and alternative ways to remove sulfur from fuels. Chapter 7 gives an overview of hydrotreating and hydrocracking and Chapter 8 gives more detail on hydrocracking. Chapters 9-11 discuss aspects of hydrotreating catalysts and processes, especially those related to meeting clean fuel specifications. Chapter 12 describes an extractive desulfurization process, and Chapter 13 discusses improvements in reactor design for hydroprocessing units.

One of the most important elements in modern petroleum refining is to keep the environment clean. Chapter 14 covers a wide range of pollution

control issues: regulations, types of pollutants, informative examples of major environmental incidents, and pollution control technology.

The first four chapters in Volume 2 describe processes for making lubricating oils, including synthetic lubes. Chapter 15 gives an overview of conventional manufacturing processes for lube base-stocks, Chapter 16 discusses selective hydroprocessing for making high quality lubricants to meet new standards, Chapter 17 discusses synthetic lube base stocks, and Chapter 18 describes additives and formulation technology for engine oils.

As the world's supplies of light crude oils dwindle, processes for refining heavy oils and bitumen are becoming increasingly important. Chapter 19 deals with heavy oil processing. It reviews the chemical composition, physical and chemical properties, and upgrading chemistry of bitumen and heavy oils.

During the past twenty years, competitive pressures, including industry consolidation, forced the closure of some refineries even as others expanded. More and more, surviving refiners are using automation – model-predictive control, composition-based modeling, and computerized analysis of analytical data – to gain or maintain a competitive edge. Chapter 20 describes the application of kinetic modeling tools based on molecular composition to the development of a mechanistic kinetic model for the catalytic hydrocracking of heavy paraffins. Chapter 21 provides a general survey of process models based on two types of kinetic lumping: partition-based lumping and total lumping. Chapter 22 describes how model-predictive control can increase throughput, product quality, and stability in refining operations. Chapter 23 describes the real-time, online refinery-wide optimization application at Suncor-Sarnia.

As refiners reconfigure their plants to produce clean fuels, they are looking at ways to optimize the value of the hydrogen they now produce. They are also looking at different ways to supply the extra hydrogen required to make clean fuels. Chapter 24 discusses the online application of models of hydrogen production from the steam reforming of naphtha and other hydrocarbons. Chapter 25 addresses the issues of hydrogen demand, production and supply in refineries, and Chapter 26 tells refiners why they should think of their hydrogen as an asset, not a liability.

Chapter 27 reviews a new methodology to generate complete and reliable crude oil assays from limited laboratory data. Better crude quality control can improve refinery planning to ensure the profitability to survive in highly competitive global markets. It has also potential to be used in upstream operations for preliminary assessment of the oil quality of new reservoirs and new wells.

Putting this book together has been a rewarding challenge. We hope that you, our readers, will find it useful.

***Acknowledgements.*** We wish to thank Dr. Kenneth Howell, Senior Editor for Chemistry at Springer, for his guidance and limitless patience. We also want to thank our many contributors for their time and effort. Obviously, without them, this book would not exist.

Most of all, we wish to thank our devoted, magnificent wives, Grace Miao-Miao Chen and Carrie, for putting up with our absences – mental if not physical – during so many nights and lost weekends throughout the past two years.



## CONTENTS

### 1. Petroleum Processing Overview

*Paul R. Robinson*

|  |    |
|--|----|
| 1. Introduction .....                                  | 1  |
| 1.1 History of Petroleum Production .....              | 1  |
| 1.2 What is Petroleum? .....                           | 4  |
| 1.2.1 The Chemicals in Petroleum .....                 | 7  |
| 1.2.1.1 Paraffins .....                                | 7  |
| 1.2.1.2 Aromatics and Naphthenes .....                 | 8  |
| 1.2.1.3 Hetero-atom Compounds .....                    | 9  |
| 1.2.1.4 Olefins .....                                  | 9  |
| 1.3 History of Petroleum Processing .....              | 11 |
| 1.3.1 Demand for Conversion .....                      | 11 |
| 1.3.2 Demand for a Clean Environment .....             | 13 |
| 1.4 Modern Petroleum Processing .....                  | 14 |
| 2. Separation .....                                    | 15 |
| 2.1 Distillation .....                                 | 15 |
| 2.1.1 Atmospheric Distillation .....                   | 15 |
| 2.1.2 Vacuum Distillation .....                        | 19 |
| 2.2 Solvent Refining .....                             | 19 |
| 2.2.1 Solvent Deasphalting .....                       | 19 |
| 2.2.2 Solvent Extraction .....                         | 20 |
| 2.2.3 Solvent Dewaxing, Wax Deoiling .....             | 21 |
| 3. Conversion .....                                    | 21 |
| 3.1 Visbreaking .....                                  | 22 |
| 3.2 Coking .....                                       | 22 |
| 3.2.1 Delayed Coking .....                             | 22 |
| 3.2.2 Fluid Coking .....                               | 24 |
| 3.3 Fluid Catalytic Cracking .....                     | 25 |
| 3.3.1 FCC Process Flow .....                           | 25 |
| 3.3.2 Heat Balance .....                               | 26 |
| 3.3.3 Houdry Catalytic Cracking (HCC) .....            | 27 |
| 3.3.4 Residue FCC .....                                | 28 |
| 3.4 Hydrotreating and Hydrocracking .....              | 28 |
| 3.4.1 Chemistry of Hydrotreating and Hydrocracking ... | 29 |
| 3.4.2 Hydrotreating Process Flow .....                 | 29 |
| 3.4.3 Hydrotreating Objectives .....                   | 31 |

|       |   |    |
|-------|---|----|
| 3.4.4 | Hydrocracking .....   | 33 |
| 3.4.5 | Hydrocracking Objectives .....                                  | 33 |
| 3.4.6 | Hydrocracker Feeds .....  | 33 |
| 3.4.7 | Hydrocracking Process Flow .....                                | 33 |
| 3.4.8 | Hydrocracker Products .....                                     | 34 |
| 3.5   | Ebullated Bed Units .....                                       | 34 |
| 4.    | Upgrading Naphtha .....   | 35 |
| 4.1   | Catalytic Reforming .....                                       | 35 |
| 4.1.1 | Catalytic Reforming Objective .....                             | 35 |
| 4.1.2 | Chemistry of Catalytic Reforming .....                          | 35 |
| 4.1.3 | Catalytic Reforming Catalysts .....                             | 37 |
| 4.1.4 | Process Flows .....   | 37 |
| 4.2   | Isomerization .....   | 40 |
| 4.2.1 | Isomerization Objectives .....                                  | 40 |
| 4.2.2 | Isomerization Catalysts .....                                   | 41 |
| 4.2.3 | Process Flow: C <sub>4</sub> Isomerization .....                | 41 |
| 4.2.4 | Process Flow: C <sub>5</sub> C <sub>6</sub> Isomerization ..... | 41 |
| 4.3   | Catalytic Oligomerization .....                                 | 43 |
| 4.3.1 | Catalytic Oligomerization Objectives .....                      | 43 |
| 4.3.2 | Catalysis .....   | 43 |
| 4.3.3 | Process Flow .....  | 43 |
| 4.4   | Alkylation .....  | 44 |
| 4.4.1 | Alkylation Objectives .....                                     | 44 |
| 4.4.2 | Process Flow: Sulfuric Acid Alkylation .....                    | 44 |
| 4.4.3 | Process Flow: HF Alkylation .....                               | 45 |
| 5.    | Lubes, Waxes and Greases .....                                  | 46 |
| 5.1   | Lube Base Stocks .....  | 46 |
| 5.1.1 | Catalytic Dewaxing .....  | 46 |
| 5.2   | Waxes .....   | 46 |
| 5.3   | Greases .....   | 47 |
| 6.    | Asphalt Production .....  | 47 |
| 7.    | Drying, Sweetening, and Treating .....                          | 48 |
| 7.1   | Drying and Sweetening .....                                     | 48 |
| 7.2   | Treating .....  | 48 |
| 8.    | Product Blending .....  | 49 |
| 8.1   | Product Specifications .....                                    | 49 |
| 8.2   | Gasoline Blending .....   | 50 |
| 8.2.1 | Octane Numbers for Hydrocarbons .....                           | 50 |
| 8.2.2 | Reformulated Gasoline (RFG) .....                               | 51 |
| 8.2.3 | Gasoline Additives .....  | 53 |
| 8.2.4 | Low-Sulfur Gasoline and Ultra-Low-Sulfur Diesel .....           | 54 |
| 8.2.5 | FCC Gasoline Post-Treating .....                                | 55 |
| 8.3   | Kerosene and Jet Fuel .....                                     | 55 |

|   |    |
|---|----|
| 8.4 Diesel Blending .....                                   | 56 |
| 8.4.1 Diesel Additives .....                                | 58 |
| 9. Protecting the Environment .....                         | 59 |
| 9.1 Air Quality .....                                       | 59 |
| 9.1.1 Sulfur Recovery .....                                 | 59 |
| 9.2 Waste Water Treatment .....                             | 62 |
| 9.2.1 Primary Treatment .....                               | 62 |
| 9.2.2 Secondary Treatment .....                             | 63 |
| 9.2.3 Tertiary Treatment .....                              | 63 |
| 9.3 Solid Waste .....                                       | 63 |
| 10. Power, Steam, Hydrogen, and CO <sub>2</sub> .....       | 63 |
| 10.1 Power .....  | 64 |
| 10.2 Steam .....  | 64 |
| 10.3 Hydrogen and CO <sub>2</sub> .....                     | 64 |
| 11. Refining Economics .....                                | 65 |
| 11.1 Costs .....  | 65 |
| 11.2 Revenues .....   | 67 |
| 11.3 Margins .....  | 68 |
| 11.3.1 Location, Location, Location .....                   | 68 |
| 11.3.2 Size .....   | 69 |
| 11.3.3 Conversion Capability and Complexity .....           | 69 |
| 11.3.4 Automation .....                                     | 70 |
| 12. Safety, Reliability, and Maintenance .....              | 70 |
| 12.1 Refinery Staffing .....                                | 70 |
| 12.2 Safety .....   | 71 |
| 12.3 Reliability and Maintenance .....                      | 72 |
| 13. Petroleum Processing Trends .....                       | 73 |
| 13.1 Industry Consolidation .....                           | 73 |
| 13.2 Environmental Regulations .....                        | 74 |
| 13.3 Residue Upgrading .....                                | 75 |
| 13.4 Increased Oil Consumption in Developing Countries .... | 75 |
| 13.5 Automation .....                                       | 76 |
| 14. Summary .....   | 76 |
| 15. References .....  | 76 |

## 2. The Origin of Petroleum

*Clifford C. Walters*

|   |    |
|---|----|
| 1. Historical Overview .....  | 79 |
| 2. The Petroleum System .....   | 81 |
| 3. Deposition of Organic-Rich Sedimentary Rocks .....                     | 82 |
| 4. Kerogen Formation and the Generative Potential of Source<br>Rocks..... | 86 |

|  |    |
|--|----|
| 5. Generation and Expulsion of Oil and Gas ..... | 91 |
| 6. Composition of Produced Petroleum .....       | 95 |
| 7. Summary .....                                 | 97 |
| 8. References .....                              | 97 |

### 3. Crude Assay

*Murray R. Watt and Stilianos G. Roussis*

|   |     |
|---|-----|
| 1. Introduction .....   | 103 |
| 2. Property Measurements/Crude Inspections .....                            | 104 |
| 2.1 API Gravity .....   | 104 |
| 2.2 Sulfur Content .....  | 104 |
| 2.3 Pour Point .....  | 104 |
| 2.4 Whole Crude Simulated Distillation .....                                | 104 |
| 2.5 Full Assay .....  | 105 |
| 2.6 Physical Distillation – ASTM D 2892 Method .....                        | 105 |
| 2.7 ASTM D5236 Method .....   | 106 |
| 2.8 TBP Curves .....  | 106 |
| 2.9 Property Measurement/Assay Grid .....                                   | 106 |
| 2.10 Physical Property Test .....   | 107 |
| 2.10.1 API Gravity .....  | 107 |
| 2.10.2 Aniline Point .....  | 107 |
| 2.10.3 Cloud Point .....  | 107 |
| 2.10.4 Freeze Point .....   | 108 |
| 2.10.5 Metals .....   | 108 |
| 2.10.6 Mercaptan Sulfur .....   | 108 |
| 2.10.7 Micro Carbon Residue .....   | 108 |
| 2.10.8 Nitrogen .....   | 108 |
| 2.10.9 Pour Point .....   | 109 |
| 2.10.10 Refractive Index .....  | 109 |
| 2.10.11 Reid Vapor Pressure RVP .....                                       | 109 |
| 2.10.12 Salt Content .....  | 109 |
| 2.10.13 Smoke Point .....   | 109 |
| 2.10.14 Sulfur Content .....  | 110 |
| 2.10.15 Total Acid Number .....   | 110 |
| 2.10.16 Viscosity .....   | 110 |
| 2.10.17 Water & Sediment .....  | 110 |
| 2.11 Asphalt Properties .....   | 111 |
| 2.11.1 Penetration .....  | 111 |
| 2.11.2 Softening Point .....  | 111 |
| 3. The Prediction of Crude Assay Properties .....                           | 111 |
| 3.1 Needs for Rapid and Accurate Prediction of Crude Assay Properties ..... | 111 |

|     |   |     |
|-----|---|-----|
| 3.2 | Predictions from Measurement of Selected Whole Crude Oil Properties ..... | 112 |
| 3.3 | Predictions from NMR Measurements .....                                   | 112 |
| 3.4 | Predictions from Chromatographic Data .....                               | 113 |
| 3.5 | Predictions from GC/MS Measurements .....                                 | 113 |
| 3.6 | Predictions from NIR Data .....   | 114 |
| 3.7 | Property Determination from First Principles .....                        | 115 |
| 4.  | References .....  | 115 |

#### **4. Integrated Methodology for Characterization of Petroleum Samples and Its Application for Refinery Product Quality Modeling**

*Yevgenia Briker, Zbigniew Ring, and Hong Yang*

|       |  |     |
|-------|--|-----|
| 1.    | Introduction .....                                 | 117 |
| 2.    | Class-Type Separation .....                        | 118 |
| 2.1   | Modification of ASTM D2007 LC Separation .....     | 119 |
| 2.2   | SPE Method .....                                   | 121 |
| 2.2.1 | SAP (Saturates, Aromatics and Polars) .....        | 121 |
| 2.2.2 | SOAP (Saturates, Olefins, Aromatics, Polars) ..... | 123 |
| 3.    | Detailed Hydrocarbon Type Analysis .....           | 131 |
| 3.1   | Mass Spectrometry .....                            | 131 |
| 3.2   | Distributions by Boiling Point .....               | 137 |
| 4.    | Neural Network Correlations .....                  | 142 |
| 5.    | Acknowledgments .....                              | 147 |
| 6.    | References .....                                   | 147 |

#### **5. Catalytic Processes for Light Olefin Production**

*Wang Xieqing, Xie Chaogang, Li Zaiting, and Zhu Genquan*

|     |  |     |
|-----|--|-----|
| 1.  | Introduction .....   | 149 |
| 2.  | Fundamentals of the Cracking Mechanism for Light Olefin Production ..... | 151 |
| 3.  | Catalysts .....  | 153 |
| 4.  | New Technology .....   | 155 |
| 4.1 | Deep Catalytic Cracking (DCC) .....                                      | 156 |
| 4.2 | Catalytic Pyrolysis Process (CPP) .....                                  | 157 |
| 4.3 | PetroFCC .....   | 160 |
| 4.4 | Propylur .....   | 161 |
| 4.5 | Superflex .....  | 162 |
| 4.6 | Mobil Olefin Interconversion (MOI) .....                                 | 163 |
| 4.7 | Propylene Catalytic Cracking (PCC) .....                                 | 164 |
| 4.8 | Olefins Conversion Technology (OCT) .....                                | 164 |
| 4.9 | Methanol to Olefin (MTO) Process .....                                   | 166 |
| 5.  | Prospects .....  | 167 |
| 6.  | References .....   | 168 |

## 6. Kinetics and Mechanisms of Fluid Catalytic Cracking

*P. O'Connor*

|   |     |
|---|-----|
| 1. Introduction .....                             | 169 |
| 2. Process Development .....                      | 169 |
| 3. Chemistry and Kinetics .....                   | 171 |
| 4. Catalysts .....                                | 171 |
| 5. Catalyst Aging and Deactivation .....          | 173 |
| 6. Feedstocks, Products and the Environment ..... | 174 |
| 7. Future Challenges .....                        | 175 |
| 8. References .....                               | 175 |

## 7. Hydrotreating and Hydrocracking: Fundamentals

*Paul R. Robinson and Geoffrey E. Dolbear*

|   |     |
|---|-----|
| 1. Introduction .....   | 177 |
| 1.1 Hydroprocessing Units: Similarities and Differences ..... | 178 |
| 2. Process Objectives .....                                   | 180 |
| 2.1 Clean Fuels .....   | 181 |
| 2.2 The Process In-Between .....                              | 181 |
| 3. Chemistry of Hydroprocessing .....                         | 182 |
| 3.1 Saturation Reactions .....                                | 182 |
| 3.2 HDS Reactions .....                                       | 185 |
| 3.3 HDN Reactions .....                                       | 186 |
| 3.4 Cracking Reactions .....                                  | 187 |
| 3.5 Coke Formation .....                                      | 189 |
| 3.6 Mercaptan Formation .....                                 | 190 |
| 3.7 Reaction Kinetics .....                                   | 192 |
| 4. Hydroprocessing Catalysts .....                            | 195 |
| 4.1 Catalyst Preparation .....                                | 196 |
| 4.1.1 Precipitation .....                                     | 196 |
| 4.1.2 Filtration, Washing and Drying .....                    | 198 |
| 4.1.3 Forming .....   | 198 |
| 4.1.4 Impregnation .....                                      | 198 |
| 4.1.5 Activation .....  | 199 |
| 4.1.6 Noble-Metal Catalysts .....                             | 199 |
| 4.2 Hydrotreating Catalysts .....                             | 199 |
| 4.3 Hydrocracking Catalysts .....                             | 200 |
| 4.4 Catalyst Cycle Life .....                                 | 200 |
| 4.4.1 Catalyst Regeneration and Rejuvenation .....            | 202 |
| 4.4.2 Catalyst Reclamation .....                              | 203 |
| 5. Process Flow .....   | 204 |
| 5.1 Trickle-Bed Units .....                                   | 204 |
| 5.2 Slurry-Phase Hydrocracking .....                          | 210 |
| 5.3 Ebullating Bed Units .....                                | 210 |

|     |                                     |     |
|-----|-------------------------------------|-----|
| 6.  | Process Conditions .....            | 211 |
| 7.  | Yields and Product Properties ..... | 212 |
| 8.  | Overview of Economics .....         | 212 |
| 8.1 | Costs .....                         | 212 |
| 8.2 | Benefits .....                      | 214 |
| 8.3 | Catalyst Cycle Life .....           | 214 |
| 9.  | Hydrocracker-FCC Comparison .....   | 215 |
| 10. | Operational Issues .....            | 215 |
| 11. | Licensors .....                     | 216 |
| 12. | Conclusion .....                    | 217 |
| 13. | References .....                    | 217 |

## 8. Recent Advances in Hydrocracking

*Adrian Gruia*

|     |  |     |
|-----|--|-----|
| 1.  | Introduction .....                                 | 219 |
| 2.  | History .....                                      | 219 |
| 3.  | Flow Schemes .....                                 | 221 |
| 3.1 | Single Stage Once-Through Hydrocracking .....      | 221 |
| 3.2 | Single Stage with Recycle Hydrocracking .....      | 222 |
| 3.3 | Two Stage Recycle Hydrocracking .....              | 224 |
| 3.4 | Separate Hydrotreat Two Stage Hydrocracking .....  | 224 |
| 4.  | Chemistry .....                                    | 225 |
| 4.1 | Treating Reactions .....                           | 225 |
| 4.2 | Cracking Reactions .....                           | 227 |
| 5.  | Catalysts .....                                    | 231 |
| 5.1 | Acid Function of the Catalyst .....                | 232 |
| 5.2 | Metal Function of the Catalyst .....               | 234 |
| 6.  | Catalyst Manufacturing .....                       | 234 |
| 6.1 | Precipitation .....                                | 235 |
| 6.2 | Forming .....                                      | 235 |
| 6.3 | Drying and Calcining .....                         | 238 |
| 6.4 | Impregnation .....                                 | 238 |
| 7.  | Catalyst Loading and Activation .....              | 239 |
| 7.1 | Catalyst Loading .....                             | 239 |
| 7.2 | Catalyst Activation .....                          | 240 |
| 8.  | Catalyst Deactivation and Regeneration .....       | 241 |
| 8.1 | Coke Deposition .....                              | 241 |
| 8.2 | Reversible Poisoning .....                         | 242 |
| 8.3 | Agglomeration of the Hydrogenation Component ..... | 242 |
| 8.4 | Metals Deposition .....                            | 242 |
| 8.5 | Catalyst Support Sintering .....                   | 242 |
| 8.6 | Catalyst Regeneration .....                        | 243 |

|        |   |     |
|--------|---|-----|
| 9.     | Design and Operation of Hydrocracking Reactors .....    | 243 |
| 9.1    | Design and Construction of Hydrocracking Reactors ...   | 243 |
| 9.2    | Hydrocracking Reactor Operation .....                   | 245 |
| 10.    | Hydrocracking Process Variables .....                   | 246 |
| 10.1   | Catalyst Temperature .....                              | 247 |
| 10.2   | Conversion .....  | 248 |
| 10.3   | Fresh Feed Quality .....                                | 249 |
| 10.3.1 | Sulfur and Nitrogen Compounds .....                     | 249 |
| 10.3.2 | Hydrogen Content .....                                  | 249 |
| 10.3.3 | Boiling Range .....                                     | 250 |
| 10.3.4 | Cracked Feed Components .....                           | 250 |
| 10.3.5 | Permanent Catalyst Poisons .....                        | 250 |
| 10.4   | Fresh Feed Rate (LHSV) .....                            | 250 |
| 10.5   | Liquid Recycle .....                                    | 251 |
| 10.6   | Hydrogen Partial Pressure .....                         | 252 |
| 10.7   | Recycle Gas Rate .....                                  | 253 |
| 10.8   | Makeup Hydrogen .....                                   | 253 |
| 10.8.1 | Hydrogen Purity .....                                   | 254 |
| 10.8.2 | Nitrogen and Methane Content .....                      | 254 |
| 10.8.3 | CO + CO <sub>2</sub> Content .....                      | 254 |
| 11.    | Hydrocracker Licensors and Catalyst Manufacturers ..... | 255 |
| 11.1   | Licensors .....   | 255 |
| 11.2   | Catalyst Suppliers .....                                | 255 |
| 12.    | References .....  | 255 |

## **9. Current Progress in Catalysts and Catalysis for Hydrotreating**

*Isao Mochida and Ki-Hyouk Choi*

|     |   |     |
|-----|---|-----|
| 1.  | Introduction .....  | 257 |
| 2.  | Hydrotreating Process .....   | 261 |
| 3.  | Bases for Hydrotreating .....   | 262 |
| 3.1 | Hydrotreating Catalysts .....   | 262 |
| 3.2 | Chemistry of Hydrodesulfurization .....   | 264 |
| 4.  | Deep Hydrodesulfurization of Gasoline .....   | 269 |
| 5.  | Deep Hydrodesulfurization of Diesel .....   | 271 |
| 6.  | HDN, HDO and HDM Reactions .....  | 273 |
| 7.  | Inhibition of HDS .....   | 275 |
| 8.  | Deactivation and Regeneration of Hydrotreating Catalysts .....                          | 275 |
| 9.  | Process Flow of Hydrotreating .....   | 276 |
| 10. | Two Successive Layers in Catalyst Beds .....  | 279 |
| 11. | Process and Catalyst Development for Deep and Selective<br>HDS of FCC Gasoline .....    | 280 |
| 12. | Progress in Support Materials for More Active HDS<br>Catalysts .....                    | 283 |
| 13. | Recognition and Control of the Shape and Size of Active Sites<br>of HDS Catalysts ..... | 286 |



|   |     |
|---|-----|
| 14. Catalytic Active Sites for HDS and Hydrogenation .....                        | 288 |
| 15. Roles of Steric Hindrance in Adsorption and Kinetic Processes<br>of HDS ..... | 291 |
| 16. Further Scope and Acknowledgements .....                                      | 293 |
| 17. References .....  | 294 |

## 10. Ultra Deep Desulfurization of Diesel: How an Understanding of the Underlying Kinetics Can Reduce Investment Costs

*Barry H. Cooper and Kim G. Knudsen*

|  |     |
|--|-----|
| 1. Changes in Diesel Specifications and Demand .....                               | 297 |
| 2. Challenges Facing the Refiner .....   | 298 |
| 3. The Selection of Catalyst for Ultra Deep Desulfurization .....                  | 299 |
| 3.1 Desulfurization .....  | 299 |
| 3.2 Choice of Catalysts for Ultra Deep Desulfurization .....                       | 301 |
| 3.3 Inhibitors for the Hydrogenation Route .....                                   | 303 |
| 3.4 Consequences for the Choice of Catalyst in Ultra Deep<br>Desulfurization ..... | 309 |
| 4. Case Studies for the Production of Ultra Low Sulfur Diesel ...                  | 309 |
| 4.1 Case 1: Straight-run, Low Sulfur Feed at 32 Bar .....                          | 310 |
| 4.2 Case 2: Straight-run, High Sulfur Feed at 32 Bar .....                         | 311 |
| 4.3 Case 3: Blended, High Sulfur Feed at 32 Bar .....                              | 312 |
| 4.4 Case 4: Blended, High Sulfur Feed at 54 Bar .....                              | 314 |
| 4.5 Revamp vs. Grassroots Unit .....   | 315 |
| 5. Conclusion .....  | 316 |
| 6. References .....  | 316 |

## 11. Ultra-Clean Diesel Fuels by Deep Desulfurization and Deep Dearomatization of Middle Distillates

*Chunshan Song and Xiaoliang Ma*

|   |     |
|---|-----|
| 1. Introduction .....   | 317 |
| 2. Sulfur Compounds in Transportation Fuels .....                                   | 321 |
| 3. Challenges of Ultra Deep Desulfurization of Diesel Fuels .....                   | 324 |
| 3.1 Reactivities of Sulfur Compounds in HDS .....                                   | 324 |
| 3.2 Mechanistic Pathways of HDS .....   | 328 |
| 4. Design Approaches to Ultra Deep Desulfurization .....                            | 330 |
| 4.1 Improving Catalytic Activity by New Catalyst<br>Formulation .....               | 332 |
| 4.2 Tailoring Reaction and Processing Conditions .....                              | 336 |
| 4.3 Designing New Reactor Configurations .....                                      | 338 |
| 4.4 Developing New Processes .....  | 340 |
| 4.4.1 S Zorb Process for Sulfur Absorption and Capture                              | 340 |
| 4.4.2 Selective Adsorption for Deep Desulfurization at<br>Ambient Temperature ..... | 341 |

|       |  |     |
|-------|--|-----|
| 4.4.3 | New Integrated Process Concept Based on Selective Adsorption ..... | 344 |
| 4.4.4 | Adsorption Desulfurization Using Alumina Based Adsorbents .....    | 345 |
| 4.4.5 | Charge Complex Formation .....                                     | 345 |
| 4.4.6 | Oxidative Desulfurization .....                                    | 346 |
| 4.4.7 | Biodesulfurization .....   | 348 |
| 5.    | FCC Feed Hydrotreating and LCO Undercutting .....                  | 352 |
| 5.1   | FCC Feed Hydrotreating and Sulfur Reduction in LCO .....           | 352 |
| 5.2   | Undercutting LCO .....   | 353 |
| 6.    | Deep Hydrogenation of Diesel Fuels .....                           | 355 |
| 6.1   | Benefits of Aromatics Reduction .....                              | 355 |
| 6.2   | Challenges of Deep Aromatization .....                             | 356 |
| 6.3   | Application of Noble Metal Catalysts .....                         | 356 |
| 7.    | Design Approaches to Deep Hydrogenation .....                      | 358 |
| 7.1   | Deep Hydrogenation at Low Temperatures .....                       | 358 |
| 7.2   | Saturation of Aromatics in Commercial Process .....                | 360 |
| 8.    | Summary and Conclusions .....                                      | 361 |
| 9.    | Acknowledgment .....   | 362 |
| 10.   | Glossary of Terms .....  | 362 |
| 11.   | References .....   | 363 |

## 12. Synergistic Extractive Desulfurization Processes

*Ebbe R. Skov and Geoffrey E. Dolbear*

|    |  |     |
|----|--|-----|
| 1. | Introduction .....                         | 373 |
| 2. | Extractive Desulfurization Processes ..... | 375 |
| 3. | Synergism Between HDS and EDS .....        | 376 |
| 4. | Summary .....                              | 378 |
| 5. | References .....                           | 379 |

## 13. Advanced Reactor Internals for Hydroprocessing Units

*F. Emmett Bingham and Douglas E. Nelson*

|     |  |     |
|-----|--|-----|
| 1.  | Introduction .....   | 381 |
| 2.  | Elements of Hydroprocessing Reactor Design .....           | 382 |
| 3.  | Liquid Distribution Tray Design .....                      | 383 |
| 4.  | Quench Mixing Chamber Design .....                         | 388 |
| 5.  | Example of Reactor Internals Revamp .....                  | 389 |
| 5.1 | Reactor Internals Performance (Pre-revamp) .....           | 390 |
| 5.2 | New Reactor Internals Modifications and Improvements ..... | 391 |
| 5.3 | Performance Improvement Results .....                      | 392 |
| 5.4 | Radial Temperature Differences .....                       | 392 |
| 5.5 | Weighted Average Bed Temperature .....                     | 393 |
| 6.  | Conclusions .....  | 393 |

## 14. Environmental Pollution Control

*Paul R. Robinson, Eli I. Shaheen, and Esber I. Shaheen*

|  |     |
|--|-----|
| 1. Why Control Pollution? .....                            | 395 |
| 2. Pollution from Petroleum Processing .....               | 395 |
| 2.1 Particulate Matter .....                               | 395 |
| 2.2 Carbon Monoxide .....                                  | 396 |
| 2.3 Sulfur Oxides .....                                    | 396 |
| 2.4 Nitrogen Oxides, VOC, and Ozone .....                  | 397 |
| 2.5 Chemicals that React with Stratospheric Ozone .....    | 397 |
| 2.6 Greenhouse Gases .....                                 | 399 |
| 2.6.1 Global CO <sub>2</sub> and Temperature Balances..... | 399 |
| 2.6.2 Global Warming .....                                 | 400 |
| 2.7 Waste Water .....                                      | 400 |
| 2.8 Solid Waste .....                                      | 401 |
| 2.9 Oil Spills .....                                       | 401 |
| 3. Environmental Incidents .....                           | 401 |
| 3.1 London Fog (1952) .....                                | 402 |
| 3.2 Amoco Cadiz (1978) .....                               | 402 |
| 3.3 Bhopal, India (1984) .....                             | 403 |
| 3.4 Chernobyl (1986) .....                                 | 404 |
| 3.5 The Rhine (1986) .....                                 | 406 |
| 3.6 Prince William Sound, Alaska (1989) .....              | 407 |
| 3.7 Kuwait (1991) .....                                    | 408 |
| 3.8 Lessons Learned .....                                  | 409 |
| 4. Environmental Agencies .....                            | 411 |
| 4.1 Environmental Protection Agency .....                  | 411 |
| 4.2 Other Environmental Agencies .....                     | 412 |
| 4.3 Occupational Safety and Health Administration .....    | 412 |
| 4.3.1 Material Safety Data Sheets (MSDS) .....             | 413 |
| 5. Key Regulations .....                                   | 414 |
| 5.1 Clean Air Acts .....                                   | 415 |
| 5.1.1 Title I – Non-Attainment.....                        | 416 |
| 5.1.2 Title II – Mobile Sources .....                      | 417 |
| 5.1.3 Title III – Air Toxics .....                         | 419 |
| 5.1.4 Title IV – Acid Rain.....                            | 420 |
| 5.1.5 Title VIII – Enforcement.....                        | 420 |
| 5.2 River and Harbors Act, Refuse Act .....                | 421 |
| 5.3 Federal Water Pollution Control Act .....              | 421 |
| 5.4 Clean Water Acts, Water Quality Act .....              | 422 |
| 5.5 Marine Protection, Research, and Sanctuaries Act ..... | 423 |

|        |  |            |
|--------|--|------------|
| 5.6    | Safe Drinking Water Act .....                                    | 423        |
| 5.7    | Resource Conservation and Recovery Act (RCRA) ....               | 423        |
| 5.8    | Superfund, CERCLA .....  | 425        |
| 5.9    | Toxic Substance Control Act (TSCA) .....                         | 426        |
| 5.10   | Asbestos School Hazard Abatement Act .....                       | 427        |
| 5.11   | Stockholm Conference .....                                       | 427        |
| 5.12   | Control of Dumping at Sea .....                                  | 427        |
| 5.13   | Climate Control: Rio and Kyoto .....                             | 427        |
| 5.13.1 | Rio Earth Summit .....   | 427        |
| 5.13.2 | Kyoto Protocol .....   | 428        |
| 5.13.3 | Plan B for Climate Control: Contraction and<br>Convergence ..... | 429        |
| 6.     | Pollution Control Technology .....                               | 430        |
| 6.1    | Particulate Matter .....   | 430        |
| 6.2    | Carbon Monoxide and VOC .....                                    | 431        |
| 6.3    | Sulfur Oxides .....  | 431        |
| 6.4    | Nitrogen Oxides .....  | 433        |
| 6.5    | Greenhouse Gases, Stratospheric Ozone .....                      | 434        |
| 6.6    | Waste Water .....  | 434        |
| 6.6.1  | Primary Treatment .....  | 434        |
| 6.6.2  | Secondary Treatment .....  | 436        |
| 6.6.3  | Tertiary Treatment .....   | 436        |
| 6.7    | Cleaning Up Oil Spills .....                                     | 436        |
| 6.7.1  | Natural Forces .....   | 436        |
| 6.7.2  | Containment and Physical Removal .....                           | 437        |
| 6.7.3  | Adsorbents .....   | 438        |
| 6.7.4  | Dispersion Agents .....  | 439        |
| 6.7.5  | Non-dispersive Methods .....                                     | 439        |
| 6.7.6  | Cleanup of Oil Contaminated Beaches .....                        | 440        |
| 6.7.7  | Amoco Cadiz Oil Spill Cleanup: A Case Study                      | 441        |
| 6.8    | Solid Waste Recovery and Disposal .....                          | 442        |
| 6.8.1  | Super-critical Fluid Extraction .....                            | 443        |
| 6.8.2  | Sludge .....   | 444        |
| 6.8.3  | Spent Catalysts .....  | 445        |
| 7.     | Fiction vs. Fact .....   | 445        |
| 8.     | References .....   | 446        |
|        | <b>Index</b> .....   | <b>449</b> |

## Chapter 1

# PETROLEUM PROCESSING OVERVIEW

Paul R. Robinson

*PQ Optimization Services, Inc.*

*3418 Clearwater park Drive, Katy, Texas, 77450*

## 1. INTRODUCTION

The ground begins to rumble, then shake. The hero of the film – a lean ex-cowboy with a square jaw under his hat and a gorgeous brunette on his arm – reaches out to brace himself against his horse. A smile creases his face as the rumbling grows louder. Suddenly, a gush of black goo spurts into the air and splashes down on him, his side-kick and his best gal. They dance with ecstasy until the music swells and the credits start to roll.

Why is our hero so happy? Because he's rich! After years of drilling dry holes in every county between the Red River and the Rio Grande, he finally struck oil.

### 1.1 History of Petroleum Production

So why is he rich? What makes oil so valuable?

Actually, crude oil straight from the ground has some value, but not a lot. *Table 1* shows the history of petroleum before 1861. Before 1859, oil that was mined or that simply seeped up out of the ground was used to water-proof ships, as an adhesive in construction, for flaming projectiles, and in a wide variety of ointments.<sup>1-4</sup>

After 1859, petroleum became more and more important to the world's economy, so important that today, without a steady flow of oil, most human activities on this planet would grind to a halt. Petroleum accounts for 60% of the world's shipping on a tonnage basis.<sup>3</sup> It provides fuels and lubricants for our trucks, trains, airplanes, and automobiles. Ships are powered by fuel oil derived from petroleum. Bottom-of-the-barrel petroleum derivatives pave our roads and provide coke for the steel industry. Together with natural gas,

petroleum provides precursors for the world's petrochemical industries. At the end of 2003, the world was consuming 78 million barrels of oil per day.<sup>5</sup> In August 2005, that volume of petroleum was worth \$4.6 billion per day, or \$1.7 trillion per year.

*Table 1. History of Petroleum Before 1861*

| <b>Date</b>  | <b>Description</b>   |
|--------------|--|
| 3000 BC      | Sumerians use asphalt as an adhesive for making mosaics. Mesopotamians use bitumen to line water canals, seal boats, and build roads. Egyptians use pitch to grease chariot wheels, and asphalt to embalm mummies.               |
| 1500 BC      | The Chinese use petroleum for lamps and for heating homes.   |
| 600 BC       | Confucius writes about the drilling of 100-foot (30-meter) natural gas wells in China. The Chinese build pipelines for oil using bamboo poles.   |
| 600-500 BC   | Arab and Persian chemists mix petroleum with quicklime to make Greek fire, the napalm of its day.  |
| 1200-1300 AD | The Persians mine seep oil near Baku (now in Azerbaijan).  |
| 1500-1600 AD | Seep oil from the Carpathian Mountains is used in Polish street lamps. The Chinese dig oil wells more than 2000 feet (600 meters) deep.  |
| 1735 AD      | Oil is extracted from oil sands in Alsace, France.   |
| Early 1800s  | Oil is produced in United States from brine wells in Pennsylvania.   |
| 1847         | James Oakes builds a "rock oil" refinery in Jacksdale, England. <sup>6</sup> The unit processes 300 gallons per day to make "paraffin oil" for lamps. James Young builds a coal-oil refinery in Whitburn, Scotland. <sup>7</sup> |
| 1848         | F.N. Semyenov drills the first "modern" oil well near Baku.  |
| 1849         | Canadian geologist Abraham Gesner distills kerosene from crude oil.  |
| 1854         | Ignacy Lukasiewicz drills oil wells up to 150 feet (50 meters) deep at Bóbrka, Poland.   |
| 1857         | Michael Dietz invents a flat-wick kerosene lamp (Patent issued in 1859).   |
| 1858         | Ignacy Lukasiewicz builds a crude oil distillery in Ulaszowice, Poland. <sup>8</sup> The first oil well in North America is drilled near Petrolia, Ontario, Canada.  |
| 1859         | Colonel Edwin L. Drake triggers the Pennsylvania oil boom by drilling a well near Titusville, Pennsylvania that was 69-feet deep and produced 35 barrels-per-day.  |
| 1859         | An oil refinery is built in Baku (now in Azerbaijan).  |
| 1860-61      | Oil refineries are built near Oil Creek, Pennsylvania; Petrolia, Ontario, Canada; and Union County, Arkansas.  |

So what happened in 1859? What began the transformation of petroleum from a convenience into the world's primary source of energy? As often is the case with major socioeconomic shifts, the move toward oil was instigated not by just a single event, but by the juxtaposition of several:

- In the 1850s, most home-based lamps burned whale oil or other animal fats. Historically, whale-oil prices had always fluctuated wildly, but they peaked in the mid-1850s due to the over-hunting of whales; by some estimates, in 1860 several species were almost extinct. Whale oil sold for an average price of US\$1.77 per gallon between 1845 and 1855. In contrast, lard oil sold for about US\$0.90 per gallon.<sup>9,10</sup> Lard oil was more abundant, but it burned with a smoky, smelly flame.

- Michael Dietz invented a flat-wick kerosene lamp in 1857. The Dietz lamp was arguably the most successful of several devices designed to burn something other than animal fats.
- The availability of kerosene got a sudden boost on August 27, 1859, when Edwin L. Drake struck oil with the well he was drilling near Titusville, Pennsylvania. By today's standards, the well was shallow – about 69 feet (21 meters) deep and it produced only 35 barrels per day. Drake was able to sell the oil for US\$20 per barrel, a little less than the price of lard oil and 70% less than the price of whale oil. In 1861, US\$700 per day was a tidy sum, equivalent to US\$5 million per year in 2002 dollars.<sup>11</sup> Drake's oil well was not the first – according to one source, the Chinese beat Drake by about 2200 years – but it may have been the first drilled through rock, and it certainly triggered the Pennsylvania oil rush. Figure 1 shows some of the closely spaced wells that sprang up in 1859 in the Pioneer Run oil field a few miles from Titusville.

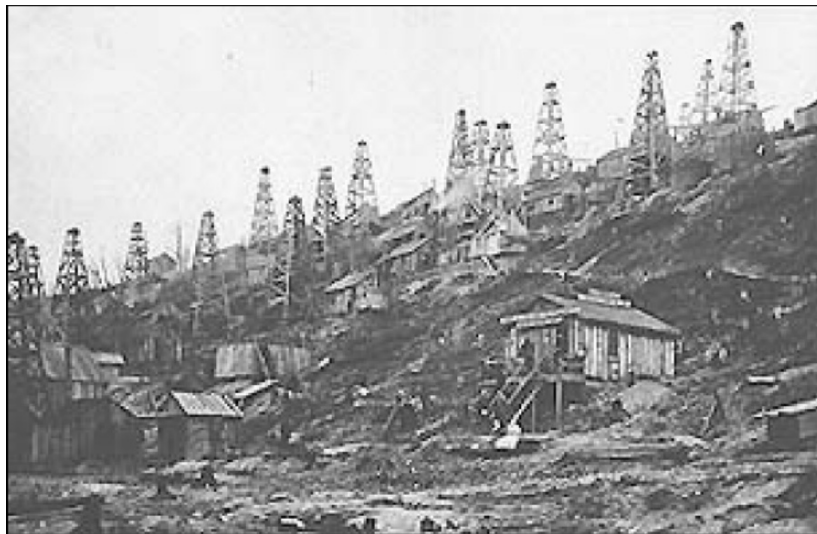


Figure 1. Pioneer Run oil field in 1859. Photo used with permission from the Pennsylvania Historical Collection and Museum Commission, Drake Well Museum Collection, Titusville, PA.

According to a report issued in 1860 by David Dale Owens,<sup>12</sup> the state geologist of Arkansas:

“On Oil Creek in the vicinity of Titusville, Pennsylvania, oil flows out from some wells at the rate of 75 to 100 gallons in 24 hours already fit for the market. At least 2000 wells are now in progress and 200 of these are already pumping oil or have found it.”

According to *The Prize*,<sup>13</sup> a prize-winning book by Daniel Yergin:

“When oil first started flowing out of the wells in western Pennsylvania in the 1860’s, desperate oil men ransacked farmhouses, barns, cellars, stores, and trash yards for any kind of barrel – molasses, beer, whiskey, cider, turpentine, sale, fish, and whatever else was handy. But as coopers began to make barrels especially for the oil trade, one standard size emerged, and that size continues to be the norm to the present. It is 42 gallons.

“The number was borrowed from England, where a statute in 1482 under King Edward IV established 42 gallons as the standard size barrel for herring in order to end skullduggery and “divers deceits” in the packing of fish. At the time, herring fishing was the biggest business in the North Sea. By 1866, seven years after Colonel Drake drilled his well, Pennsylvania producers confirmed the 42-gallon barrel as their standard, as opposed to, say, the 31½ gallon wine barrel or the 32 gallon London ale barrel or the 36 gallon London beer barrel.”

In sharp contrast to the situation today, in 1870 America was the world’s leading oil producer, and oil was America’s 2<sup>nd</sup> biggest export.<sup>4</sup> Agricultural products were first, accounting for 79% of exports that were worth, on average, US\$573 million per year from 1870 to 1879.<sup>14</sup> Despite the ravages of the U.S. Civil War, the main agricultural export was still “King Cotton.”

## 1.2 What Is Petroleum?

Before we go on to talk about petroleum processing, it is important to know something about petroleum itself. Petroleum is called a fossil fuel because it is formed from the bodies of ancient organisms – primarily one-celled plants and animals (see Chapter 2). Contrary to modern myth, only a tiny fraction (if any) of the molecules in crude oil are from dinosaurs. When these creatures died, their remains accumulated at bottoms of ancient lakes or seas, along with sand and other sediments. Over time, a combination of pressure, heat, and bacterial action transformed the deposits into sedimentary rock. The incorporated organic matter was transformed into simpler chemicals, such as hydrocarbons, water, carbon dioxide, hydrogen sulfide, and others.

The chemicals didn’t always stay put. If the surrounding rock was porous, liquids and gases could migrate, either up to the surface or into a reservoir (*Figure 2*) that was capped by impermeable rock or a dome of salt. Today, when petroleum geologists look for oil, they actually are looking for structures that might be traps for liquid hydrocarbons.



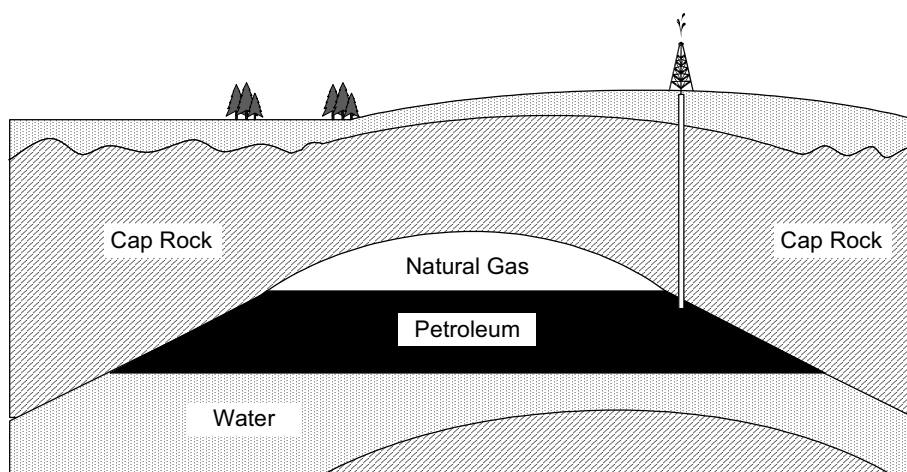


Figure 2. Petroleum Reservoir

In solid sources of fossil fuel – coal, oil shale, oil sands and tar sands – the mineral content is higher and the hydrocarbon molecules usually are heavier. In China and South Africa, a significant amount of coal is converted into synthesis gas, which is used to make chemicals and/or synthetic petroleum. In Canada, oil sands are converted into more than 700,000 barrels-per-day of synthetic petroleum, which is sent to conventional oil refineries in Canada and the United States. A well-written book by Berger and Anderson<sup>15</sup> provides additional general information about the formation, production, and refining of petroleum.

Due to its origin, crude oil is a complex mixture containing thousands of different hydrocarbons.<sup>16,17</sup> As the name implies, hydrocarbons are chemicals containing hydrogen and carbon. In addition to hydrogen and carbon, most crude oils also contain 1 to 3 wt% sulfur along with smaller amounts of nitrogen, oxygen, metals, and salts. The salts can be removed with a hot-water wash (see Section 2), but the other major contaminants – sulfur, nitrogen, oxygen and metals – are harder to remove because they are linked to hydrocarbons by chemical bonds.

Crude oils from some wells are as clear as vegetable oil. Other wells produce green, brown or black crudes. Some taste sour or smell like rotten eggs. Some flow as easily as water, others don't flow unless they are heated, and some are so solid they have to be mined.

Table 2 compares properties for 21 selected crudes. Traders characterize a crude by citing its source, API gravity (a measure of density), and sulfur content. The source is the oil field from which the crude was produced. The API gravity is a rough indication of distillation properties, which determine how much gasoline, kerosene, etc., can be distilled from the crude. Along with other factors, the sulfur content affects processing costs. Figure 3 shows

that light crudes (those with high API gravities) often contain less sulfur and nitrogen than heavy crudes, but not always.

Table 2. Properties of 21 Selected Crude Oils

| Crude Oil                | API Gravity <sup>†</sup> | Specific Gravity | Sulfur (wt%) | Nitrogen (wt%) |
|--------------------------|--------------------------|------------------|--------------|----------------|
| Alaska North Slope       | 26.2                     | 0.8973           | 1.1          | 0.2            |
| Arabian Light            | 33.8                     | 0.8560           | 1.8          | 0.07           |
| Arabian Medium           | 30.4                     | 0.8740           | 2.6          | 0.09           |
| Arabian Heavy            | 28.0                     | 0.8871           | 2.8          | 0.15           |
| Athabasca (Canada)       | 8                        | 1.0143           | 4.8          | 0.4            |
| Beta (California)        | 16.2                     | 0.9580           | 3.6          | 0.81           |
| Brent (North Sea)        | 38.3                     | 0.8333           | 0.37         | 0.10           |
| Bonny Light (Nigeria)    | 35.4                     | 0.8478           | 0.14         | 0.10           |
| Boscan (Venezuela)       | 10.2                     | 0.9986           | 5.3          | 0.65           |
| Ekofisk (Norway)         | 37.7                     | 0.8363           | 0.25         | 0.10           |
| Henan (China)            | 16.4                     | 0.9567           | 0.32         | 0.74           |
| Hondo Blend (California) | 20.8                     | 0.9291           | 4.3          | 0.62           |
| Kern (California)        | 13.6                     | 0.9752           | 1.1          | 0.7            |
| Kuwait Export            | 31.4                     | 0.8686           | 2.5          | 0.21           |
| Liaohi (China)           | 17.9                     | 0.9471           | 0.26         | 0.41           |
| Maya (Mexico)            | 22.2                     | 0.9206           | 3.4          | 0.32           |
| Shengli (China)          | 13.8                     | 0.9738           | 0.82         | 0.72           |
| Tapis Blend (Malaysia)   | 45.9                     | 0.7976           | 0.03         | nil            |
| West Hackberry Sweet*    | 37.3                     | 0.8383           | 0.32         | 0.10           |
| West Texas Intermediate  | 39.6                     | 0.8270           | 0.34         | 0.08           |
| Xinjiang (China)         | 20.5                     | 0.9309           | 0.15         | 0.35           |

\* Produced from a storage cavern in the U.S. Strategic Petroleum Reserve

<sup>†</sup> **API Gravity** is related to specific gravity by the formula:

$$^{\circ}\text{API} = 141.5 \div (\text{specific gravity @ } 60^{\circ}\text{F}) - 131.5$$

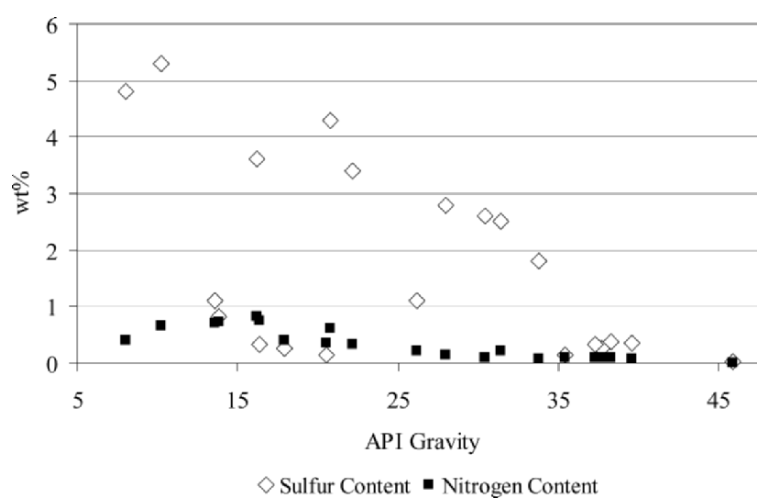


Figure 3. Sulfur and nitrogen versus API gravity for selected crude oils

## 1.2.1 The Chemicals in Petroleum

Carbon is present in almost all of the chemical compounds in petroleum. If you've ever taken a chemistry class, you know that carbon, more than any other element, binds to itself to form straight chains, branched chains, rings, and complex three-dimensional structures. The most complex molecules are biological – proteins, carbohydrates, fats and nucleic acids, which are present in every living thing, from the smallest bacterium to the largest tree. This is significant here because (as stated above) petroleum was formed from ancient organisms, and its molecules retain certain structural characteristics of the organic compounds from which it formed.

### 1.2.1.1 Paraffins

The lightest paraffin is methane (CH<sub>4</sub>) which is the major constituent of natural gas. Paraffins have the general formula C<sub>n</sub>H<sub>2n+2</sub>. The carbon chains in paraffins can be straight or branched. Compounds with the same formula but different structures are called isomers. Straight-chain paraffins are “normal,” while branched paraffins with the same chemical formula are called “iso.”

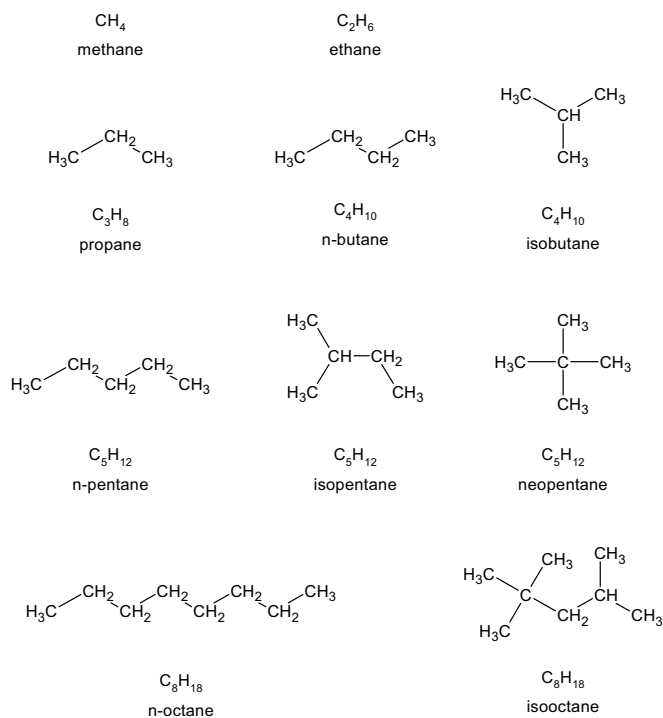


Figure 4. Isomers of selected light paraffins

Tables 3 and 4 show that isomers have different physical properties.<sup>18</sup> They also can have significantly different chemical properties. For gasoline, one of the most important chemical properties is octane number. The research octane number (RON) for n-octane is -27 compared to a RON of 100 (by definition) for isooctane (2,2,3-trimethylpentane). For heptane isomers, RON values range from 45 for 2-methyl-hexane to >100 for 2,2,3-trimethylbutane, compared to zero (by definition) for n-heptane. Octane numbers are discussed in more detail in Section 8.2.

Table 3. Boiling Points of Selected Light Paraffins

| Name       | Formula                        | Boiling Point (°F) | Boiling Point (°C) |
|------------|--------------------------------|--------------------|--------------------|
| Methane    | CH <sub>4</sub>                | -259.9             | -162.2             |
| Ethane     | C <sub>2</sub> H <sub>6</sub>  | -127.4             | -88.6              |
| Propane    | C <sub>3</sub> H <sub>8</sub>  | -43.7              | -42.1              |
| n-Butane   | C <sub>4</sub> H <sub>10</sub> | 31.7               | -0.1               |
| Isobutane  | C <sub>4</sub> H <sub>10</sub> | 11.9               | -11.2              |
| n-Pentane  | C <sub>5</sub> H <sub>12</sub> | 96.9               | 36.1               |
| Isopentane | C <sub>5</sub> H <sub>12</sub> | 82.3               | 28.0               |
| Neopentane | C <sub>5</sub> H <sub>12</sub> | 49.0               | 9.5                |
| n-Octane   | C <sub>8</sub> H <sub>18</sub> | 258.0              | 125.6              |
| Isooctane  | C <sub>8</sub> H <sub>18</sub> | 210.7              | 99.3               |

The melting points of paraffin isomers also can differ significantly. As shown in Table 5, long-chain n-paraffins melt at relatively high temperatures, while their branched-chain isomers melt at lower temperatures. This explains their different behaviours as lubricants. Long-chain normal paraffins are waxy, so as lubricants they are terrible. Conversely, iso-paraffins with the same number of carbons are excellent lube base stocks.

Table 4. Fusion Points for Selected C<sub>16</sub> Paraffins.

| Name                    | Formula                         | Melting Point (°F) | Melting Point (°C) |
|-------------------------|---------------------------------|--------------------|--------------------|
| Hexadecane              | C <sub>16</sub> H <sub>34</sub> | 64.1               | 17.9               |
| 5-Methylpentadecane     | C <sub>16</sub> H <sub>34</sub> | -29.5              | -34.2              |
| 7,8-Dimethyltetradecane | C <sub>16</sub> H <sub>34</sub> | -123.1             | -86.2              |

### 1.2.1.2 Aromatics and Naphthenes

Aromatics and naphthenes are also found in petroleum. Aromatics contain one or more unsaturated 5 to 6-carbon rings. In naphthenes, carbon rings are saturated with hydrogen.

Figure 5 shows structures for a few of the aromatics and naphthenes that have been found in crude oils. For aromatics with one six-carbon ring, the general formula is C<sub>n</sub>H<sub>2n-6</sub>, and for naphthenes with one ring, the general formula is C<sub>n</sub>H<sub>2n</sub>.

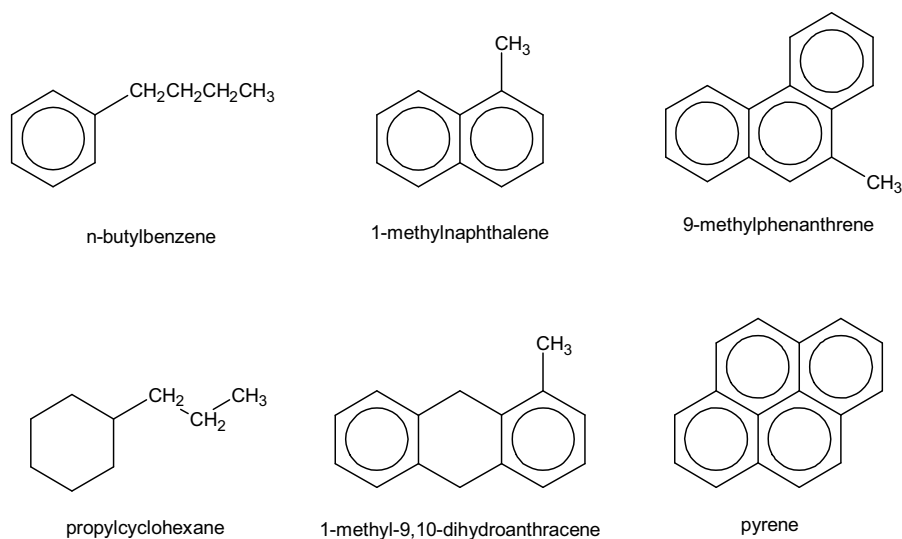


Figure 5. Aromatics and naphthenes found in crude oil

Aromatics and naphthenes display significantly different chemical and physical properties. Compared to paraffins and naphthenes with the same carbon number, aromatics are denser and have higher octane numbers.

### 1.2.1.3 Hetero-atom Compounds

When present in organic compounds, atoms other than carbon and hydrogen are called hetero-atoms. As mentioned above, sulfur, nitrogen, oxygen and metals are minor constituents of crude oil, but as we shall see, their impact on processing costs can be major. *Figure 6* shows some of the sulfur and nitrogen compounds that present problems to oil refiners. When burned in vehicles or power plants, high-sulfur fuels cause acid rain. For many refining processes, sulfur is a catalyst poison. Nitrogen and metals also are catalyst poisons. Therefore, refiners devote a considerable amount of time and money to remove hetero-atoms from intermediate streams and finished products.

### 1.2.1.4 Olefins

We need to discuss one more class of molecules before moving on. Due to their high reactivity, olefins are not common in natural crude oil. However, in refineries they are generated by several “cracking” processes. *Figure 7* shows structures for some common light olefins.

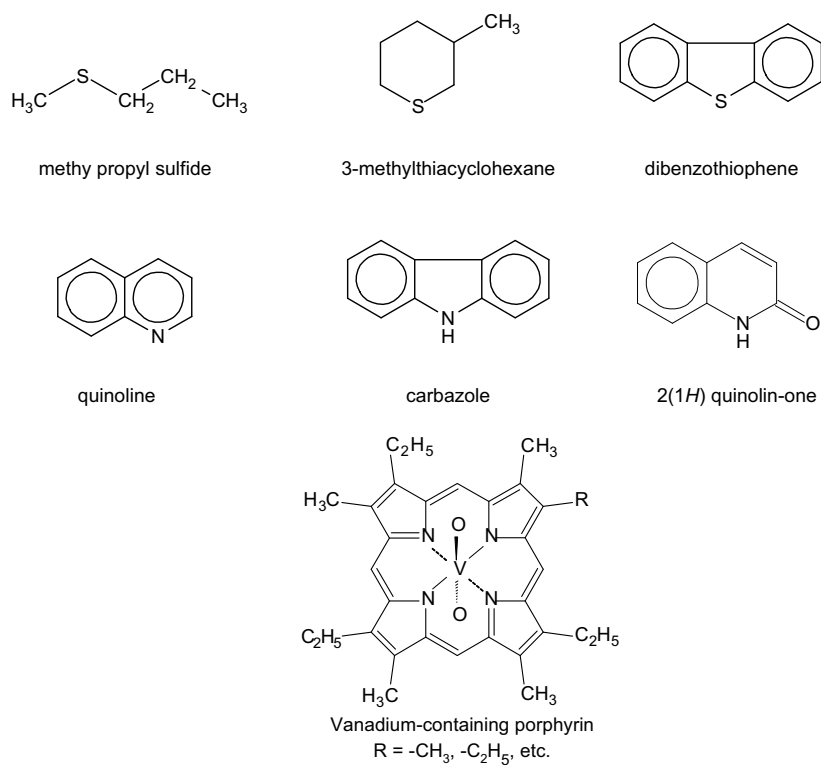


Figure 6. Hetero-atom compounds found in crude oil

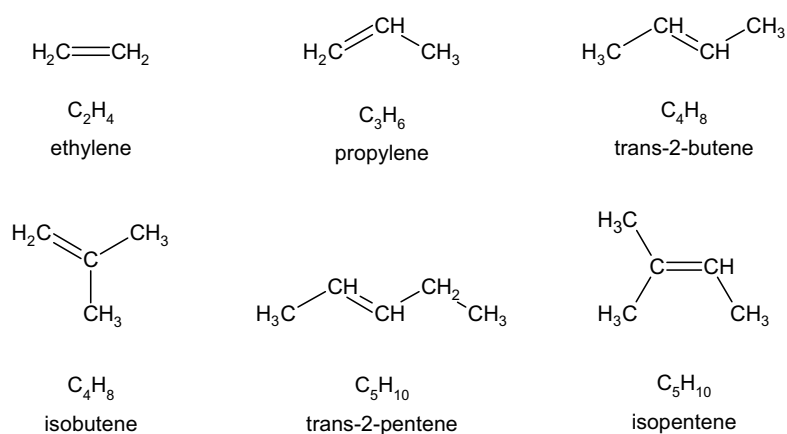


Figure 7. Selected light olefins

## 1.3 History of Petroleum Processing

These days, it's extremely rare for oil to flow out of a well already fit for the market as it did in the 1860s near Oil Creek, Pennsylvania.<sup>12</sup> Crudes from the Tapis field in Malaysia are almost good enough for direct use in diesel engines, but even these high-quality "boutique crudes" are sent to refineries for separation into higher-value components.

As mentioned in Section 1.1, in the 1860s the most valuable crude-oil fraction was kerosene. From the first crude distillation units – which truly were crude, comprising cast-iron kettles, water-cooled coils and wooden product-collection vats – part of the lightest fraction (naphtha) was sold as a solvent, but most of it was burned off. Distillates heavier than kerosene (gas oils) found some use as lubricants, but the undistilled residues were discarded.

### 1.3.1 Demand for Conversion

The demand for petroleum remained relatively flat throughout the last half of the 19<sup>th</sup> Century. In 1878, thanks to the inventions of Thomas Edison, electric lighting slowly but surely began to displace kerosene as a preferred illuminant. (*Table 5*)

But the biggest blow to kerosene came from the gasoline-powered automobile. Developed in 1889 by Gottlieb Daimler, Wilhelm Maybach, and (separately) by Karl Benz, the motor car was a curiosity until 1901, when Ransom Eli Olds started assembly-line production of the Curved Dash Oldsmobile Runabout.<sup>19</sup>

Henry Ford built his first gasoline-powered car in 1896 and founded the Ford Motor Company in 1903. In 1908 he began selling Model T's for the low, low price of US\$950. The resulting boom in automobile sales triggered tremendous growth in petroleum demand, which continued unabated until the Arab Oil Embargo of 1973. Over 15 million Model T Fords were sold in the United States alone between 1908 and 1917, with prices as low as US\$280 per unit.<sup>19</sup>

In addition to increasing the overall demand for petroleum, the advent of the automobile increased the relative demand for naphtha (from which gasoline is derived) versus kerosene. In response, refiners developed conversion processes. The first of these was the thermal cracking process patented by William Burton and Robert Humphreys, who were working for Standard Oil of Indiana. The Burton-Humphreys process doubled the yield of gasoline from crude oil, and it is credited for averting a gasoline shortage during World War I. Moreover, gasoline from thermal crackers performed better in automobiles than straight-run products distilled from crude petroleum.

Table 5. Significant Events in Petroleum Processing, 1861 – 2000

| <b>Date</b> | <b>Description</b>   |
|-------------|--|
| 1878        | Thomas Edison invents the light bulb. The use of kerosene lamps starts to decline.   |
| 1889        | Gottlieb Daimler, Wilhelm Mayback and (separately) Karl Benz build gasoline-powered automobiles.   |
| 1901        | Ransom E. Olds begins assembly-line production of the Curved Dash Oldsmobile.  |
| 1908        | Ford Motor Company offers Model T's for US\$950 each.  |
| 1912        | William Burton and Robert Humphreys develop thermal cracking.  |
| 1913        | Gulf Oil builds the world's first drive-in filling station in Pittsburgh, Pennsylvania.  |
| 1919        | UOP commercializes the Dubbs thermal cracking process.   |
| 1929        | Standard Oil of Indiana (now BP) commercializes the Burton process for delayed coking at Whiting, Indiana.   |
| 1933        | UOP introduces the catalytic polymerization of olefins to form gasoline.   |
| 1934        | Eugene Houdry, working for Sun Oil, patents Houdry Catalytic Cracking (HCC).   |
| 1938        | A consortium of refiners develops sulfuric acid alkylation, which is first commercialized at the Humble (now ExxonMobil) refinery in Baytown, Texas.   |
| 1940        | Phillips develops HF alkylation.   |
| 1942        | Standard Oil of New Jersey (now ExxonMobil) commercializes the FCC process at Baton Rouge, Louisiana.  |
| 1949        | Old Dutch Refining in Muskegon, Michigan starts the world's first catalytic reformer based on the UOP Platforming processes.   |
| 1950        | Catalytic hydrotreating is patented by Raymond Fleck and Paul Nahin of Union Oil.  |
| 1960s       | UOP introduces C <sub>4</sub> and C <sub>5</sub> /C <sub>6</sub> isomerization processes.  |
| 1961        | Standard Oil of California (now Chevron) introduces catalytic hydrocracking.   |
| 1970        | The world celebrates Earth Day. The newly created U.S. Environmental Protection Agency passes the Clean Air Act, which requires a 90% reduction in auto emissions by 1975. The European Union issues similar requirements. |
| 1972        | Mobil invents ZSM-5. During the next three decades, this shape-selective catalyst finds uses in numerous processes, including FCC, catalytic dewaxing, and the conversion of methanol to gasoline.                         |
| 1975        | The catalytic converter goes commercial. The phase-out of tetraethyl lead begins.  |
| 1990        | The U.S. Congress issues the Clean Air Act Amendments of 1990, which lay the framework for reformulated gasoline and low-sulfur diesel.  |
| 1990s       | Several processes are developed to remove sulfur from gasoline. These include SCANfining (Exxon), OCTGAIN (Mobil), Prime G (Axens), and S Zorb (Phillips).   |
| 1993        | Chevron commercializes Isodewaxing for converting waxy paraffins into high-quality lube base stock.  |
| 2000        | The European Commission issues the Auto Oil II report, which includes a timetable for low-sulfur gasoline and ultra-low-sulfur diesel.   |

In 1914, Jesse A. Dubbs and J. Ogden Armour founded the National Hydrocarbon Company, which later became Universal Oil Products (UOP).<sup>20</sup> UOP grew to become the world's largest licensor of process technology for the oil refining industry. In 1919, UOP commercialized the Dubbs process, which solved some of the problems associated with the Burton-Humphreys process. The Dubbs process produced fewer coke deposits, it could process heavier petroleum fractions, and it ran longer between shutdowns.

Standard Oil of Indiana commercialized the delayed coking process at Whiting, Indiana in 1929. In 1933, UOP commercialized the conversion of olefins to gasoline via catalytic polymerization. Later in the 1930s, refiners began using tetraethyl lead to boost the octane of gasoline. A consortium of



refining companies – Anglo-Iranian, Humble, Shell Oil, Standard Oil, and Texaco – developed sulfuric acid alkylation, which was commercialized in 1938 at the Humble (now ExxonMobil) refinery in Baytown, Texas. In 1940, Phillips Petroleum (now ConocoPhillips) developed HF alkylation.

Eugene Houdry patented the Houdry Catalytic Cracking (HCC) process in 1934. HCC was commercialized in 1937. With amazing foresight, Houdry also invented the catalytic converter, which started appearing on automobiles in the 1970s.

In 1942, Standard Oil of New Jersey (now ExxonMobil) commercialized the fluidized catalytic cracking (FCC) process, which dramatically increased a refiner's ability to convert heavy gas oils into gasoline. The four inventors of this process, which still produces more than half of the world's gasoline, were Donald L. Campbell, Homer Z. Martin, Eger V. Murphree, and Charles W. Tyson. During 1942-45, several FCC-based refineries were built in the United States to produce automotive and aviation gasoline during World War II.

After 1945, the development of new refining processes was stimulated by a continuing increase in demand for petroleum products, coupled with the increased availability of oil from the Middle East and elsewhere. The quality of gasoline got a large boost from catalytic reforming, which first appeared in 1949 at the Old Dutch refinery in Muskegon, Michigan. The unit was based on technology developed by UOP, which employed a platinum-based catalyst invented by Vladimir N. Ipatieff.

In 1961, hydrocracking was introduced to convert gas oil into naphthene-rich heavy naphtha, which is a superb feed for a catalytic reformer. The first unit used the Isocracking process developed by Standard Oil of California (now Chevron Texaco).

### **1.3.2 Demand for a Clean Environment**

In 1970, President Richard M. Nixon established the U.S. Environmental Protection Agency (EPA) and the U.S. Congress passed the Clean Air Act (CAA). The CAA required a 90% reduction in auto emissions by 1975. The scope and timing of this requirement presented a challenge to the automobile industry.<sup>21</sup> After reviewing several alternatives, auto makers focused on developing catalytic converters to remove carbon monoxide and hydrocarbons from automobile exhaust. Also in 1970, the European Union issued directive 70/220/EEC, which specified similar emission limits for passenger cars.

Lead poisons the active metal (platinum) in catalytic converters, so in 1975 EPA promulgated a phase-out plan to remove lead from gasoline.

In the 1990s and 2000s, the California Air Resources Board (CARB), the U.S. EPA and the European Commission promulgated requirements for reformulated gasoline, low-sulfur diesel, low-sulfur gasoline and ultra-low-sulfur diesel (ULSD). ULSD will enable the use of advanced emission

controls (including catalytic converters) on diesel-powered cars and trucks. Refiners are responding by installing additional hydrotreating capacity.

## 1.4 Modern Petroleum Processing

All refineries are different. They have different histories, locations, and market drivers. Therefore, no single illustration can capture all of the possible combinations and permutations of the processes that fit together to comprise an oil refinery. But despite their differences, most refineries perform the seven basic operations named in *Table 6*.

*Table 6.* Seven Basic Operations in Petroleum Processing

|  |  |
|--|--|
| <b>Separation</b>  | <b>Combination</b>   |
| <ul style="list-style-type: none"> <li>• Distillation</li> <li>• Solvent refining</li> </ul>                   | <ul style="list-style-type: none"> <li>• Catalytic polymerization</li> <li>• Alkylation</li> </ul>                                 |
| <b>Conversion</b>  | <b>Treating, finishing, blending</b>   |
| <ul style="list-style-type: none"> <li>• Carbon removal</li> <li>• Hydrogen addition</li> </ul>                | <ul style="list-style-type: none"> <li>• Gasoline, kerosene and diesel</li> <li>• Lubes and waxes</li> <li>• Asphalt</li> </ul>    |
| <b>Reforming</b>   | <b>Protecting the Environment</b>  |
| <ul style="list-style-type: none"> <li>• Catalytic reforming</li> <li>• Steam/hydrocarbon reforming</li> </ul> | <ul style="list-style-type: none"> <li>• Waste water treatment</li> <li>• Disposal of solids</li> <li>• Sulfur recovery</li> </ul> |
| <b>Rearrangement</b>   |  |
| <ul style="list-style-type: none"> <li>• Isomerization</li> </ul>  |  |

*Figure 8* shows a simplified layout for a high-conversion refinery in the United States. The diagram doesn't show product blending and sulfur recovery units, but these are almost always present. Lube-oil processing and hydrogen production units also may be present.

The depicted plant is configured for maximum fuels production. In a typical European refinery, the coker would be replaced with a visbreaker. In many Asian refineries, where diesel demand is higher than gasoline demand, the coker would be replaced by a visbreaker and the FCC by a hydrocacker.

The rest of this chapter provides a brief overview of the processes shown or mentioned above. The chapters that follow provide detailed process descriptions, with emphasis on recent developments. General information on refining technology can be found in the excellent books by E.I. Shaheen,<sup>22</sup> and W.L. Leffler,<sup>23</sup> and in a manual published by the U.S. Occupational Safety and Health Administration.<sup>24</sup> Each year, *Hydrocarbon Processing* compiles a widely read refining process handbook, which gives descriptions of about 120 licensed processes offered by engineering contractors, oil companies, and of course process licensors.<sup>25</sup>

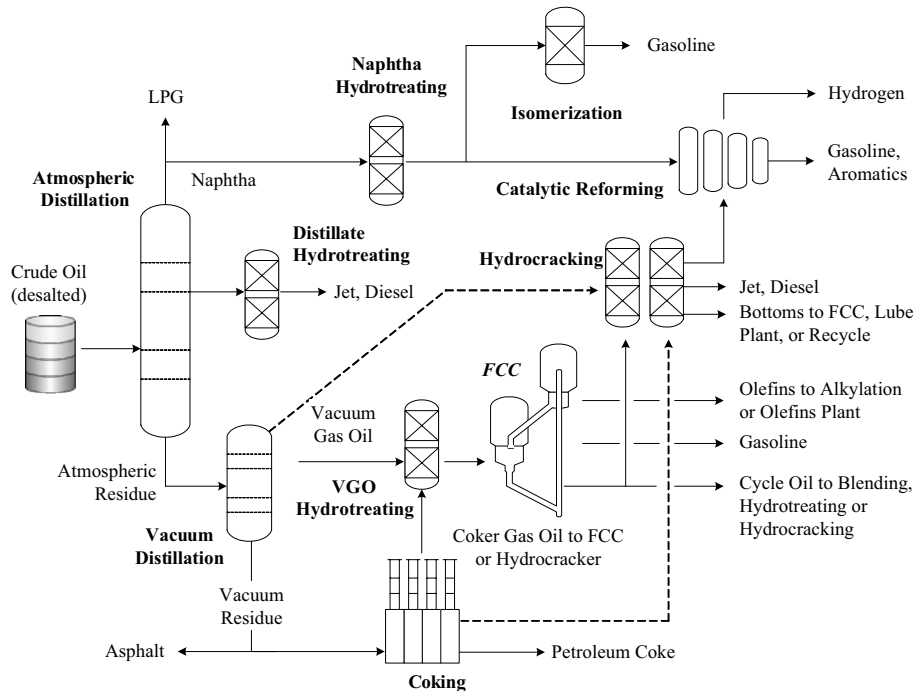


Figure 8. Typical layout for an oil refinery

## 2. SEPARATION

### 2.1 Distillation

In terms of throughput, the biggest unit in most plants is the crude distillation unit (*Figure 9*). Many downstream conversion units also use distillation for production separation. For example, in a coker, hydrocracker, or FCC unit, an atmospheric tower, a vacuum tower, and a multi-column gas plant may be required.

#### 2.1.1 Atmospheric Distillation

Crude oil distillation is more complicated than product distillation, in part because crude oils contain water, salts, and suspended solids. To reduce corrosion, plugging, and fouling in crude heaters and towers, and to prevent the poisoning of catalysts in downstream units, these contaminants are removed by a process called desalting.

The two most typical methods of crude-oil desalting – chemical and electrostatic separation – use hot water to dissolve the salts and collect

suspended solids. In chemical desalting, water and surfactants are added to the crude, heated to dissolve salts and other impurities, and then sent to a settling tank where the water and oil separate. In electrostatic desalting, chemicals are replaced with a strong electrostatic charge, which drives the separation of water from oil.

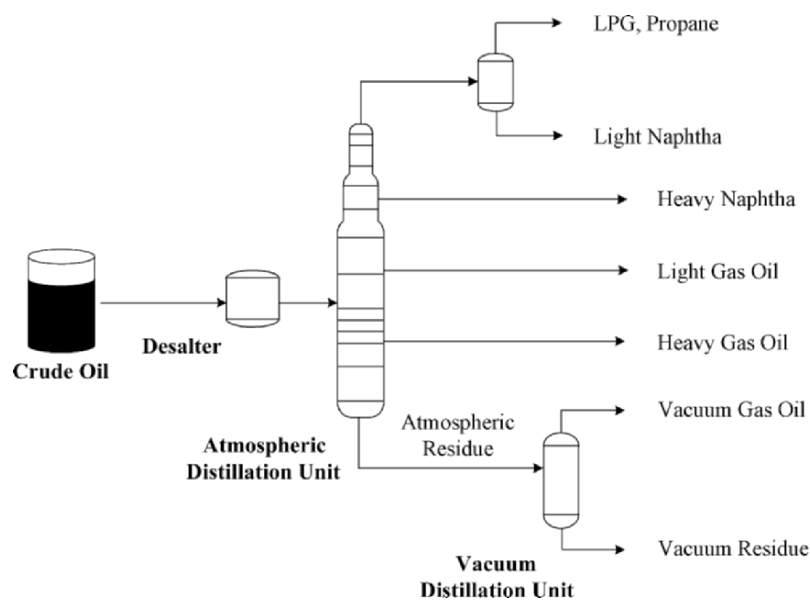


Figure 9. Crude distillation

Modern crude distillation towers can process 200,000 barrels of oil per day. They can be up to 150 feet (50 meters) tall and contain 20 to 40 fractionation trays spaced at regular intervals. In some towers, the trays in the top section are replaced with structured packing.

Before reaching the tower, desalted oil goes through a network of pre-heat exchangers to a fired heater, which brings the temperature up to about 650°F (343°C). If the oil gets much hotter than this, it starts to crack and deposit carbon inside the pipes and equipment through which it flows. The hot crude enters the distillation tower just above the bottom. Steam is added to enhance separation; it does so largely by decreasing vapor pressure in the column.

When hot oil enters the tower, most of it vaporizes. Unvaporized heavy fuel oil and/or asphalt residue drops to the bottom of the tower, where it is drawn off. The vapors rise through the distillation trays, which contain perforations and bubble caps (Figure 10). Each tray permits vapors from below to bubble through the cooler, condensed liquid on top of the tray. This

provides excellent vapor/liquid contacting. Condensed liquid flows down through a pipe to the hotter tray below, where the higher temperature causes re-evaporation. A given molecule evaporates and condenses many times before finally leaving the tower.

Products are collected from the top, bottom and side of the column. Side-draw products are taken from trays at which the temperature corresponds to the cutpoint for a desired product. In modern towers, a portion of each side-draw stream is returned to the tower to control tray temperatures and further enhance separation. Part of the top product is also returned; this “reflux” flow plays a major role in controlling temperature at the top of the tower.

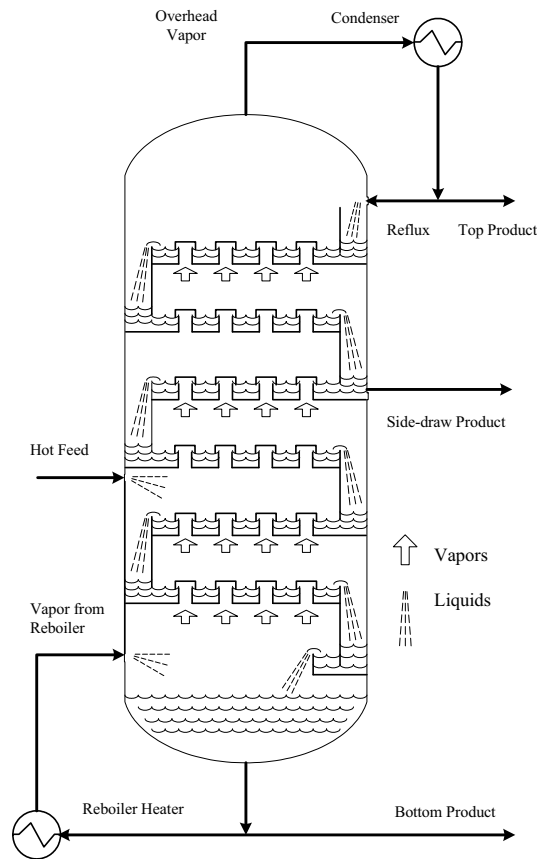


Figure 10. Distillation column with bubble-cap trays

After leaving the tower, product streams go to holding tanks or directly to downstream process units. As shown in Figure 9 and Table 7, products can include heavy fuel oil, heating oil, kerosene, gasoline, and uncondensed gases.

Table 7. Destinations for Straight-Run Distillates

| Fraction       | Approx. Boiling Range |            | Next Destination | Ultimate Product(s)                             |
|----------------|-----------------------|------------|------------------|---|
|                | °C                    | °F         |                  |   |
| LPG            | -40 to 0              | -40 to 31  | Sweetener        | Propane fuel                                    |
| Light Naphtha  | 39 - 85               | 80 - 185   | Hydrotreater     | Gasoline  |
| Heavy Naphtha  | 85 - 200              | 185 - 390  | Cat. Reformer    | Gasoline, aromatics                             |
| Kerosene       | 170 - 270             | 340 - 515  | Hydrotreater     | Jet fuel, No. 1 diesel                          |
| Gas Oil        | 180 - 340             | 350 - 650  | Hydrotreater     | Heating Oil, No. 2 diesel                       |
| Vacuum Gas Oil | 340 - 566             | 650 - 1050 | FCC              | Gasoline, LCO, gases                            |
|                |                       |            | Hydrotreater     | Fuel oil, FCC feed                              |
|                |                       |            | Lube Plant       | Lube basestock                                  |
|                |                       |            | Hydrocracker     | Gasoline, jet, diesel, FCC feed, lube basestock |
| Vacuum Residue | >540                  | >1000      | Coker            | Coke, coker gas oil                             |
|                |                       |            | Visbreaker       | Visbreaker gas oil, resid                       |
|                |                       |            | Asphalt Unit     | Deasphalted oil, asphalt                        |
|                |                       |            | Hydrotreater     | FCC feed  |

Table 8 shows that straight-run yields from various crude oils can differ substantially. The naphtha content of Brent is twice as high as Ratawi, and its vacuum residue content is 60% lower. Bonny Light yields the most middle distillate and the least vacuum residue.

Table 8. Typical Straight-run Yields from Various Crudes<sup>26,27</sup>

| Source field            | Brent  | Bonny Lt. | Green Canyon | Ratawi   |
|-------------------------|--------|-----------|--------------|----------|
| Country                 | Norway | Nigeria   | USA          | Mid East |
| API gravity             | 38.3   | 35.4      | 30.1         | 24.6     |
| Specific gravity        | 0.8333 | 0.8478    | 0.8752       | 0.9065   |
| Sulfur, wt%             | 0.37   | 0.14      | 2.00         | 3.90     |
| <b>Yields, wt% feed</b> |        |           |              |          |
| Light ends              | 2.3    | 1.5       | 1.5          | 1.1      |
| Light naphtha           | 6.3    | 3.9       | 2.8          | 2.8      |
| Medium naphtha          | 14.4   | 14.4      | 8.5          | 8.0      |
| Heavy naphtha           | 9.4    | 9.4       | 5.6          | 5.0      |
| Kerosene                | 9.9    | 12.5      | 8.5          | 7.4      |
| Atmospheric gas oil     | 15.1   | 21.6      | 14.1         | 10.6     |
| Light VGO               | 17.6   | 20.7      | 18.3         | 17.2     |
| Heavy VGO               | 12.7   | 10.5      | 14.6         | 15.0     |
| Vacuum residue          | 12.3   | 5.5       | 26.1         | 32.9     |
| Total naphtha           | 30.1   | 27.7      | 16.9         | 15.8     |
| Total middle distillate | 25.0   | 34.1      | 22.6         | 18.0     |

Atmospheric distillation of the best crudes yields about 60% naphtha plus middle distillates (kerosene and gas oil), but the average is closer to 40%. In contrast, Table 9 shows that during 1991-2003, the United States consumed, on average, 70% of its petroleum as gasoline and middle distillates. This

leaves a gap of about 30%, which is satisfied by converting residual oils into lighter products (Section 3).

Table 9. Average U.S. Consumption of Petroleum Products, 1991-2003<sup>28</sup>

| <b>Product</b>                    | <b>Consumption<br/>(barrels/day)</b> | <b>Percent of Total</b> |
|-----------------------------------|--------------------------------------|-------------------------|
| Gasoline                          | 8,032                                | 43.6%                   |
| Jet Fuel                          | 1,576                                | 8.6%                    |
| Total Distillates                 | 3,440                                | 18.7%                   |
| Residual Fuel Oil                 | 867                                  | 4.8%                    |
| Other Oils                        | 4,501                                | 24.4%                   |
| Total Consumption                 | 18,416                               | 100%                    |
| Sum of Gasoline, Jet, Distillates | 13,048                               | 70.8%                   |

### 2.1.2 Vacuum Distillation

The residue from an atmospheric distillation tower can be sent to a vacuum distillation tower, which recovers additional liquid at 0.7 to 1.5 psia (4.8 to 10.3 kPa). The vacuum, which is created by a vacuum pump or steam ejector, is pulled from the top of the tower. Relative to atmospheric columns, vacuum columns have larger diameters and their internals are simpler. Often, instead of trays, random packing and demister pads are used.

The overhead stream – light vacuum gas oil – can be used as a lube base stock, heavy fuel oil, or as feed to a conversion unit. Heavy vacuum gas oil is pulled from a side draw. The vacuum residue can be used to make asphalt, or it can be sent to a coker or visbreaker unit for further processing.

## 2.2 Solvent Refining

Distillation splits a mixture into fractions according to the boiling points of the mixture constituents. In contrast, solvent refining segregates compounds with similar compound types, such as paraffins and aromatics. The three main types of solvent refining are solvent deasphalting, solvent extraction, and solvent dewaxing.

### 2.2.1 Solvent Deasphalting

Solvent deasphalting takes advantage of the fact that aromatic compounds are insoluble in paraffins. Propane deasphalting is commonly used to precipitate asphaltenes from residual oils. Deasphalted oil (DAO) is sent to hydrotreaters, FCC units, hydrocrackers, or fuel-oil blending. In hydrocrackers and FCC units, DAO is easier to process than straight-run residual oils. This is because asphaltenes easily form coke and often contain catalyst poisons such as nickel and vanadium, and the asphaltene content of DAO is (by definition) almost zero.

In traditional solvent deasphalting, residual oil and propane are pumped to an extraction tower at 150 to 250°F (65 to 120°C) and 350 to 600 psig (2514 to 4240 kPa). Separation occurs in a tower, which may have a rotating disc contactor (*Figure 11*). Liquid products are evaporated and steam stripped to recover the propane solvent, which is recycled.

An advanced version of solvent deasphalting is “residuum oil supercritical extraction,” or ROSE. The ROSE™ Process was developed by the Kerr-McGee Corporation and now is offered for license by KBR Engineering and Construction, a subsidiary of Halliburton. In this process, the oil and solvent are mixed and heated to above the critical temperature of the solvent, where the oil is almost totally insoluble. Advantages include higher recovery of deasphalted liquids, lower operating costs due to improved solvent recovery, and improved energy efficiency. The ROSE process can employ three different solvents, the choice of which depends upon process objectives:

- Propane: Preparation of lube base stocks
- Butane: Asphalt production
- Pentane: Maximum recovery of liquid

### 2.2.2 Solvent Extraction

Solvent extraction is used to remove aromatics and other impurities from lube and grease stocks. The feedstock is dried, then contacted with the solvent in a counter-current or rotating disk extraction unit (*Figure 11*). The solvent is separated from the product stream by heating, evaporation, or fractionation. Remaining traces of solvent are removed from the raffinate by steam stripping or flashing. Electrostatic precipitators may be used to enhance separation of inorganic compounds. The solvent is then regenerated and recycled.

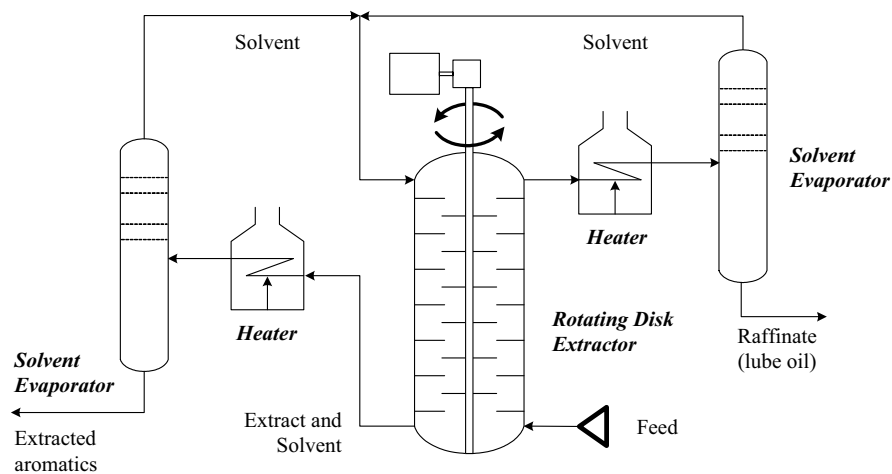


Figure 11. Rotating-disk solvent extraction



Today, phenol, furfural, and cresylic acid are widely used as solvents. In the past, some refiners installed the Edeleanu process, in which the solvent is liquid sulfur dioxide, but the hazards of potential leaks made it undesirable. Chlorinated ethers and nitrobenzene also have been used.

### 2.2.3 Solvent Dewaxing, Wax Deoiling

Solvent dewaxing removes wax (normal paraffins) from deasphalted lube base stocks. The main process steps include mixing the feedstock with the solvent, chilling the mixture to crystallize wax, and recovering the solvent. Commonly used solvents include toluene and methyl ethyl ketone (MEK). Methyl isobutyl ketone (MIBK) is used in a wax deoiling process to prepare food-grade wax.

## 3. CONVERSION

As mentioned in Section 1.1, the decreased use of kerosene lamps (thanks to Thomas Edison) coupled with rising demand for automotive gasoline provided incentives to convert kerosene and other heavier fractions into gasoline.

*Table 10* illustrates the fundamental principle behind conversion. For a given class of hydrocarbons, “lighter” means lower molecular weight, lower boiling point, lower density, and higher hydrogen-to-carbon ratios (H/C). Methane, the lightest hydrocarbon, has an H/C of 4.0. Benzopyrene has an H/C of 0.6. The H/C of commonly used crude oils ranges from 1.5 to 2.0, and the H/C for asphaltenes is 1.15.

*Table 10.* Molecular Weight, H/C and Boiling Point for Selected Hydrocarbons

| Compound        | Molecular Weight | Formula                         | H/C  | Boiling Point |        |
|-----------------|------------------|---------------------------------|------|---------------|--------|
|                 |                  |                                 |      | °C            | °F     |
| Paraffins       |                  |                                 |      |               |        |
| Methane         | 16.04            | CH <sub>4</sub>                 | 4.0  | -164          | -263.2 |
| Ethane          | 30.07            | C <sub>2</sub> H <sub>6</sub>   | 3.0  | -88.6         | -127.5 |
| Propane         | 44.10            | C <sub>3</sub> H <sub>8</sub>   | 2.67 | -42.1         | -43.7  |
| Butane (iso)    | 58.12            | C <sub>4</sub> H <sub>10</sub>  | 2.50 | -6.9          | 19.6   |
| Octane (iso)    | 114.23           | C <sub>8</sub> H <sub>18</sub>  | 2.25 | 99.2          | 210.6  |
| Cetane (normal) | 226.44           | C <sub>16</sub> H <sub>34</sub> | 2.13 | 287           | 548.6  |
| Aromatics       |                  |                                 |      |               |        |
| Benzene         | 78.11            | C <sub>6</sub> H <sub>6</sub>   | 1.0  | 80.1          | 176.2  |
| Naphthalene     | 128.17           | C <sub>10</sub> H <sub>8</sub>  | 0.8  | 218           | 424.4  |
| Benzopyrene     | 252.32           | C <sub>20</sub> H <sub>12</sub> | 0.6  | –             | –      |

Most conversion processes – FCC, thermal cracking, and deasphalting – increase the H/C by rejecting carbon. A few processes – hydrotreating to a small extent and hydrocracking to a great extent – increase the H/C by adding hydrogen. In this context, “rejecting carbon” does not mean that a little bit of

carbon is removed from every molecule. Rather, it means that heavy molecules are split (“cracked”) into a smaller molecule with a higher H/C and another smaller molecule with a lower H/C. Molecules with low H/C – polyaromatic hydrocarbons (PAH) – can condense to form coke (*Figure 12*). Condensation reactions release hydrogen, lowering H/C even more.

### 3.1 Visbreaking

Visbreaking is a mild form of thermal cracking that achieves about 15% conversion of atmospheric residue to gas oils and naphtha. At the same time, a low-viscosity residual fuel is produced.

Visbreaking comes in two basic flavors – “short-contact” and “soaker.” In short-contact visbreaking, the feed is heated to about 900°F (480°C) and sent to a “soaking zone” (reactor) at 140 to 300 psig (1067 to 2170 kPa). The elevated pressure allows cracking to occur while restricting coke formation. To avoid over-cracking, the residence time in the soaking zone is short – several minutes compared to several hours in a delayed coker – and the hot oil is quenched with cold gas oil to inhibit further cracking and sent to a vacuum tower for product separation. “Soaker” visbreaking keeps the hot oil at elevated temperature for a longer time to increase the yield of middle distillates. The low-viscosity visbreaker gas oil can be sent to an FCC unit or hydrocracker for further processing, or used as heavy fuel oil.

### 3.2 Coking

Coking processes come in two basic forms – delayed coking, which is a semi-batch process, and fluid-bed coking, which is continuous.

#### 3.2.1 Delayed Coking

In a delayed coker, vacuum residue feed is heated to about 900 to 970°F (487 to 520°C) and sent to a large coke drum. Cracking begins immediately, generating coke and cracked, vaporized products. Coke stays behind in the drum while the vapors rise to the top and flow to the product fractionator.

Liquid products include coker naphtha, light coker gas oil (LCGO), and heavy coker gas oil (HCGO). All of these require further processing due to their high olefins content, which makes them unstable and poorly suited for direct blending into finished products. The coker naphtha and LCGO are hydrotreated. The HCGO can go either to an FCC unit or a hydrocracker.

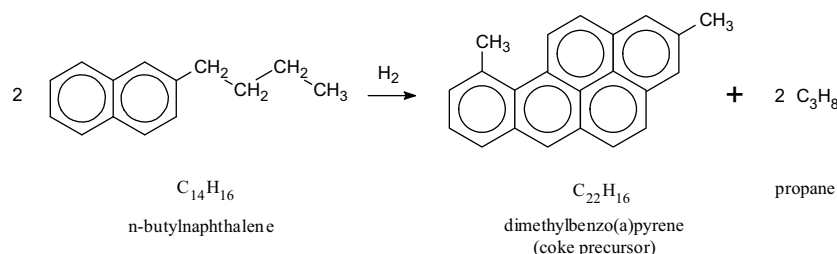


Figure 12. Representative thermal-cracking reaction. The reaction shown here is the sum of a condensation reaction, which generates hydrogen, and dealkylation, which consumes hydrogen.

Meanwhile, hot residue keeps flowing into the drum until it is filled with solid coke. To remove the coke, the top and bottom heads of the drum are removed. A rotating cutting tool uses high-pressure jets of water to drill a hole through the center of the coke from top to bottom. In addition to cutting the hole, the water also cools the coke, forming steam as it does so. The cutter is then raised, step by step, cutting the coke into lumps, which fall out the bottom of the drum. Typically, coke drums operate on 18- to 24-hour cycles, which include preheating the drum, filling it with hot oil, allowing coke and liquid products to form, cooling the drum, and decoking.

Coke can account for up to 30 wt% of the product. It can be shipped by rail, truck, or conveyor belt to a calciner, which converts *green coke* fresh from the drum into various grades of petroleum coke. Green coke can also be used for fuel.

**Sponge Coke.** Sponge coke is named for its sponge-like appearance. It is produced from feeds that have low-to-moderate asphaltene concentrations. If sponge coke meets certain specifications, it can be used to make carbon anodes for the aluminum industry. Otherwise, it is used for fuel. “Green” sponge coke must be calcined before it can be used for anodes. Fuel coke may not require calcination.

**Needle Coke.** Needle coke, named for its needle-like structure, is made from feeds that contain nil asphaltenes, such as hydrotreated FCC decant oils. Needle coke is a high-value product used to make graphite electrodes for electric-arc furnaces in the steel industry. At present (April 2004), needle coke fetches more than US\$500 per ton, which is significantly greater than the US\$40 to US\$45 per ton price for metallurgical coke exported from the United States.

**Shot Coke.** Shot coke is an undesirable product because it is inconsistent and in some cases dangerous. It is produced when the concentration of feedstock asphaltenes and/or coke-drum temperatures are too high. Excessive feedstock oxygen content can also induce its formation.

Shot coke begins to form as the oil flows into the coke drum. As light ends flash away, small globules of heavy tar are left behind. These globs of tar

coke rapidly grow due to the heat produced by asphaltene polymerization, producing discrete mini-balls 0.1 to 0.2 inches (2 to 5 mm) in diameter. In the center of the drum, the mini-balls can stick together to form clusters as large as 10 inches (25 cm). On occasion, a cluster breaks apart when the coke drum is opened, spraying a volley of hot mini-balls in every direction. Adding aromatic feeds, such as FCC decant oil, can eliminate shot coke formation. Other methods of eliminating shot coke – decreasing temperature, increasing drum pressure, increasing the amount of product recycle – decrease liquid yields, which is not desired.

A quantitative measure of the quality of coke is the coefficient of thermal expansion (CTE). A low CTE means that the product has a low tendency to expand when heated. Ranges of CTE for the three major types of petroleum coke are shown in *Table 11*.

*Table 11. Coefficients of Thermal Expansion for Petroleum Coke Products*

| Product     | CTE (cm/cm/°C x 10 <sup>-7</sup> ) |
|-------------|------------------------------------|
| Needle coke | 0 to 4                             |
| Sponge coke | 8 to 18                            |
| Shot coke   | >20                                |

Shot coke cannot be used in making anodes for aluminum production, because the outer layer of a shot sphere has a very low CTE while the inside has a very high CTE. When rapidly heated, the interior expands, cracking the outer layer like an egg shell. Consequently, in aluminum smelters, shot-coke anodes quickly turn to dust.

Other specialty carbon products made from petroleum include recarburizer coke, which is used to make specialty steel, and titanium dioxide coke, which is used as a reducing agent in the titanium dioxide pigment industry.<sup>29</sup>

### 3.2.2 Fluid Coking

Fluid coking, also called continuous coking, is a moving-bed process for which the operating temperature is higher than the temperatures used for delayed coking. In continuous coking, hot recycled coke particles are combined with liquid feed in a radial mixer (reactor) at about 50 psig (446 kPa). Vapors are taken from the reactor, quenched to stop any further reaction, and fractionated. The coke goes to a surge drum, then to a classifier, where the larger particles are removed as product. The smaller coke particles are recycled to a preheater, where they mix with fresh feed. Coking occurs both in the reactor and in the surge drum.

Installation costs for fluid coking are somewhat higher than for delayed coking, but feeds can be heavier and heat losses are lower.

### 3.3 Fluid Catalytic Cracking

Fluid catalytic cracking (FCC) produces more than half the world's gasoline. A typical FCC unit comprises three major sections – riser/reactor, regenerator, and fractionation. *Table 12* provides important details on FCC.

*Table 12.* FCC in a Nutshell

|                                   |   |                              |
|-----------------------------------|---|------------------------------|
| <b>Purpose</b>                    | Convert heavy oils into gasoline and/or light olefins               |                              |
| <b>Licensors</b>                  | Axens (IFP)   | ExxonMobil                   |
|                                   | KBR   | Stone & Webster              |
|                                   | UOP   |                              |
| <b>Catalysts and Additives</b>    | Zeolite (highly acidic, catalyzes cracking)                         |                              |
|                                   | Rare-earth oxide (increases catalyst stability)                     |                              |
|                                   | ZSM-5 (increases octane and production of light olefins)            |                              |
|                                   | Pt (promotes combustion of CO to CO <sub>2</sub> in regenerator)    |                              |
|                                   | Desox (transfers SO <sub>x</sub> from regenerator to riser/reactor) |                              |
| <b>Feeds</b>                      | Atmospheric gas oil   | Vacuum gas oil               |
|                                   | Coker gas oil   | Deasphalted oil              |
|                                   | Lube extracts   | Vacuum resid (up to 20 vol%) |
| <b>Typical Feed Properties</b>    | Nitrogen <3000 wppm   |                              |
|                                   | Carbon residue <5.0 wt%   |                              |
|                                   | Nickel + Vanadium <50 wppm  |                              |
|                                   | 90% boiling point <1300°F (704°C)                                   |                              |
| <b>Typical Process Conditions</b> | Feed temperature 300 – 700°F (150 – 370°C)                          |                              |
|                                   | Reactor temperature 920 – 1020°F (493 – 550°C)                      |                              |
|                                   | Regenerator temperature 1200 – 1350°F (650 – 732°C)                 |                              |
|                                   | Catalyst/Oil ratio 4.0 – 10.0                                       |                              |
|                                   | Reactor pressure 10 – 35 psig (170 – 343 kPa)                       |                              |
| <b>Typical Product Yields</b>     | Conversion 70 – 84 vol%   |                              |
|                                   | H <sub>2</sub> , H <sub>2</sub> S, methane, ethane 3.0 – 3.5 wt%    |                              |
|                                   | Propane and propylene 4.5 – 6.5 wt%                                 |                              |
|                                   | Butanes and butenes 9.0 – 12.0 wt%                                  |                              |
|                                   | Gasoline 44 – 56 wt%  |                              |
|                                   | LCO 13 – 20 wt%   |                              |
|                                   | Slurry oil 4 – 12 wt%   |                              |
|                                   | Coke 5 – 6 wt%  |                              |
|                                   | Total C <sub>3</sub> -plus 106 – 112 vol%                           |                              |

#### 3.3.1 FCC Process Flow

Figure 13 shows a sketch for the riser/reactor section of an FCC unit. In the reaction section, preheated oil is mixed with hot, regenerated catalyst. The mixture acts as a fluid because the catalyst particles are small – about the size of sifted flour. The hot catalyst vaporizes the oil, and the vaporized oil carries the catalyst up the riser/reactor. A book by Magee and Dolbear<sup>30</sup> provides

specific information on the manufacture and use of catalysts used for FCC and other refining processes.

The cracking reaction is very fast. It produces light gases, high-octane gasoline, and heavier products called light cycle oil (LCO), heavy cycle oil (HCO), slurry oil, and decant oil. It also leaves a layer of coke on the catalyst particles, making them inactive.

At the top of the riser, the temperature can reach 900 to 1020°F (482 to 549°C). The temperature at the riser outlet is a key factor in determining conversion and product selectivity, so FCC operators control it as tightly as possible. Higher temperatures favor production of olefin-rich light gas at the expense of gasoline, moderate temperatures favor gasoline production, and at lower temperatures gasoline yields decrease in favor of middle distillates.

In the disengaging section, steam is used to help separate the now-deactivated catalyst from the reaction products. The catalyst goes to the regenerator, where the coke is burned away by fluidized combustion in the presence of air. The hot catalyst at temperatures up to 1350°F (732°C) returns to the riser/reactor, where the cycle begins again.

In a 60,000 barrels-per-day unit processing a typical mixture of vacuum gas oils, the total catalyst in the unit (the “inventory”) is 400 to 500 tons. To maintain activity, about 0.5 to 1 wt% of the inventory is replaced each day. If the feed to the unit contains significant amounts of residue, the replacement rate is higher. The discharged catalyst is cooled and shipped either to a land fill for disposal or to another refiner, which may have a particular use for “conditioned” FCC catalyst.

### 3.3.2 Heat Balance

FCC units must be heat-balanced, or they won’t run. Understanding heat balance is the key to understanding how FCC variables interact. The burning of coke in the regenerator provides all of the heat required by the process. *Table 13* gives a representative breakdown of FCC heat requirements.

*Table 13.* Breakdown of FCC Heat Requirements

| <b>Heat-Consuming Event</b>                           | <b>Percent of Total</b>            |
|---|------------------------------------|
| Heat up and vaporize fresh feed                       | 40-50%                             |
| Heat recycled oil                                     | 0-10%                              |
| Heat of reaction (endothermic)                        | 15-30%                             |
| Heat steam  | 2-8%                               |
| Heat losses   | 2-5%                               |
| Heat air to regenerator temperature                   | 15-25%                             |
| Heat coke from the reactor to regenerator temperature | 1-2%                               |
| Total Heat Duty                                       | 500-1000 Btu/lb<br>1160-2325 kJ/kg |

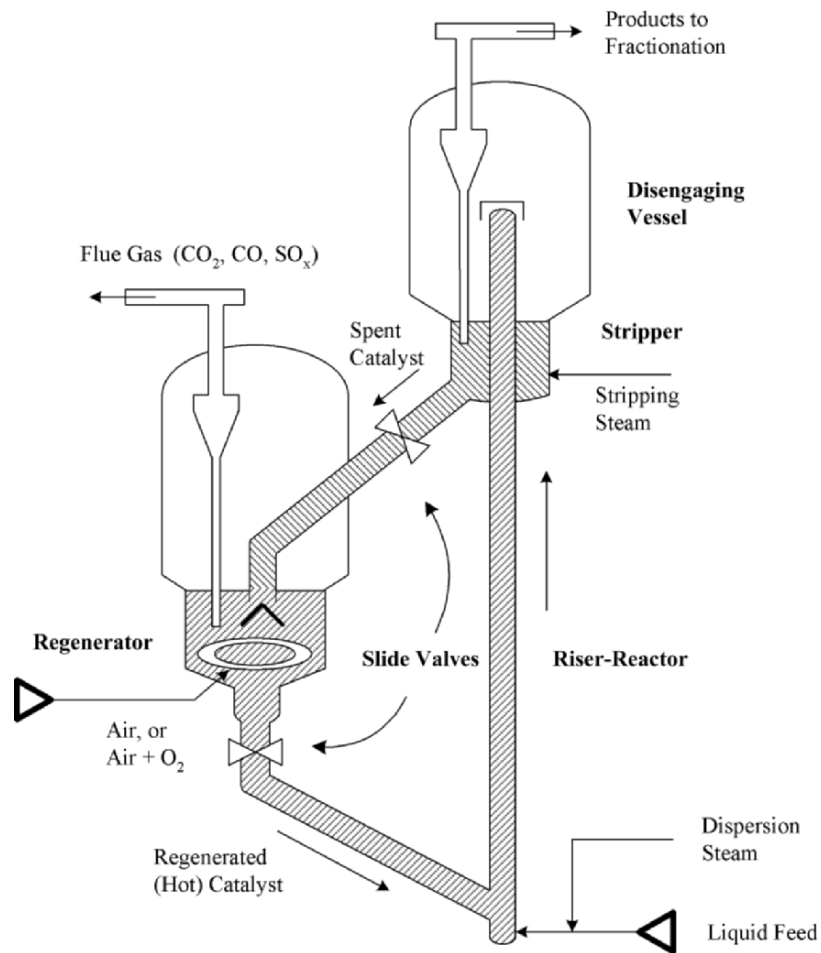


Figure 13. FCC riser-reactor and regenerator sections

### 3.3.3 Houdry Catalytic Cracking (HCC)

The Houdry Catalytic Cracking (HCC) process was a precursor to FCC. Houdry catalyst particles are pellets, which are carried to a storage hopper by a conveyor belt or pneumatic lift tubes. The pellets flow down from the hopper through the reactor, and from the reactor to a regenerator. The HCC product slate is similar to that for FCC, but FCC conversions and gasoline yields are significantly higher.

### 3.3.4 Residue FCC

Many modern FCC units are designed to process significant amounts of vacuum residue. These units use catalyst coolers (e.g., steam coils) in the regenerator or a second regeneration zone to remove excess heat from the unit. This is because vacuum residue generates substantially more coke than conventional FCC feeds, and excess heat is generated when the extra coke is burned away from catalyst.

In vacuum residue, the metals content can be very high – sometimes more than 200 wppm nickel-plus-vanadium. In an FCC unit, these metals are bad news. Nickel increases coke formation and decreases liquid yields. Vanadium reduces conversion, decreases liquid yields, and destroys the catalyst. For these reasons, refiners pretreat the residue in a hydrotreater before sending it on to the FCC.

In addition to removing most of the Ni and V, the pretreater decreases the concentration of sulfur, nitrogen, and aromatics. In the FCC, part of the feed sulfur ends up in liquid products and part ends up as sulfur oxides (SO<sub>x</sub>) in the flue gas, so removing sulfur from the feed is beneficial. Removing nitrogen is beneficial because feed nitrogen suppresses FCC catalyst activity. Saturating feed aromatics increases FCC conversion by as much as 10 vol%. This alone can justify the cost of building the pretreater.

## 3.4 Hydrotreating and Hydrocracking

A modern petroleum refinery may have four or more hydrotreating units. Strictly speaking, hydrotreaters are not conversion units because the breaking of carbon-to-carbon bonds is minimal. However, it is convenient to discuss hydrotreating together with hydrocracking and mild hydrocracking because they employ similar catalysts and process flow schemes.

The key differences are presented in Table 14. Hydrocrackers tend to operate at higher pressure, using different catalysts, and with lower linear hourly space velocity (LHSV). LHSV is equal to the volume of feed per hour divided by the catalyst volume. A lower required LHSV means that a given volume of feed requires more catalyst. In terms of process conditions and conversion, mild hydrocracking lies somewhere between hydrotreating and full-conversion hydrocracking.



Table 14. Comparison of Hydrotreating, Hydrocracking and Mild Hydrocracking

| Process, Feedstock Types  | H <sub>2</sub> Partial Pressure |                 | Conversion |
|---------------------------|---------------------------------|-----------------|------------|
|                           | psig                            | kPa             |            |
| <i>Hydrotreating</i>      |                                 |                 |            |
| Naphtha                   | 250 – 300                       | 1825 – 2170     | 0 – 5%     |
| LGO (Kerosene)            | 250 – 600                       | 1825 – 4238     | 0 – 5%     |
| HGO (Diesel), LCO         | 600 – 800                       | 4238 – 5617     | 5 -15%     |
| VGO, VBGO, CGO, HCO       | 800 – 2000                      | 5617 – 13,890   | 5 -15%     |
| Residual Oil              | 2000 – 3000                     | 13,890 – 20,786 | 5 -15%     |
| <i>Mild Hydrocracking</i> |                                 |                 |            |
| VGO, VBGO, CGO, LCO, HCO  | 800 – 1500                      | 5617 – 10,443   | 20 – 40%   |
| <i>Hydrocracking</i>      |                                 |                 |            |
| VGO, VBGO, CGO, LCO, HCO  | 1500 – 2000                     | 10,443 – 13,890 | 60 – 99%   |
| Residual Oil              | 2000 – 3000                     | 13,890 – 20,786 | 15 – 25%   |
| LGO = Light Gas Oil       |                                 |                 |            |
| HGO = heavy Gas Oil       |                                 |                 |            |
| LCO = FCC Light Cycle Oil |                                 |                 |            |
| HCO = FCC Heavy Cycle Oil |                                 |                 |            |
| VGO = Vacuum Gas Oil      |                                 |                 |            |
| VBGO = Visbreaker Gas Oil |                                 |                 |            |
| CGO = Coker Gas Oil       |                                 |                 |            |

### 3.4.1 Chemistry of Hydrotreating and Hydrocracking

To one extent or another, all of the chemical reactions listed in Table 15 occur in hydrotreaters and hydrocrackers. The reactions are discussed in greater detail in Chapters 7-9.

Table 15. List of Hydrotreating and Hydrocracking Reactions

| <b>Hydrotreating<br/>(C-C bond breaking is minimal)</b> | <b>Hydrocracking<br/>(C-C bond breaking is significant)</b> |
|---|---|
| Hydrodesulfurization (HDS)                              | Dealkylation of aromatic rings                              |
| Hydrodenitrogenation (HDN)                              | Opening of naphthene rings                                  |
| Hydrodemetallation (HDM)                                | Hydrocracking of paraffins                                  |
| Saturation of aromatics                                 |   |
| Saturation of olefins                                   |   |
| Isomerization   |   |

### 3.4.2 Hydrotreating Process Flow

Figure 14 illustrates the process flow for a fixed-bed hydrotreater. At moderate-to-high pressure – 300 to 1800 psig (2170 to 12,512 kPa) – mixtures of preheated oil and hydrogen pass down over fixed beds of catalyst, in which the desired reactions occur.

Hydrotreating is exothermic (heat-releasing), so many commercial units comprise several catalyst beds separated by quench zones. In a quench zone, hot process fluids from the preceding bed are mixed with relatively cold, hydrogen-rich quench gas before passing to the next bed.

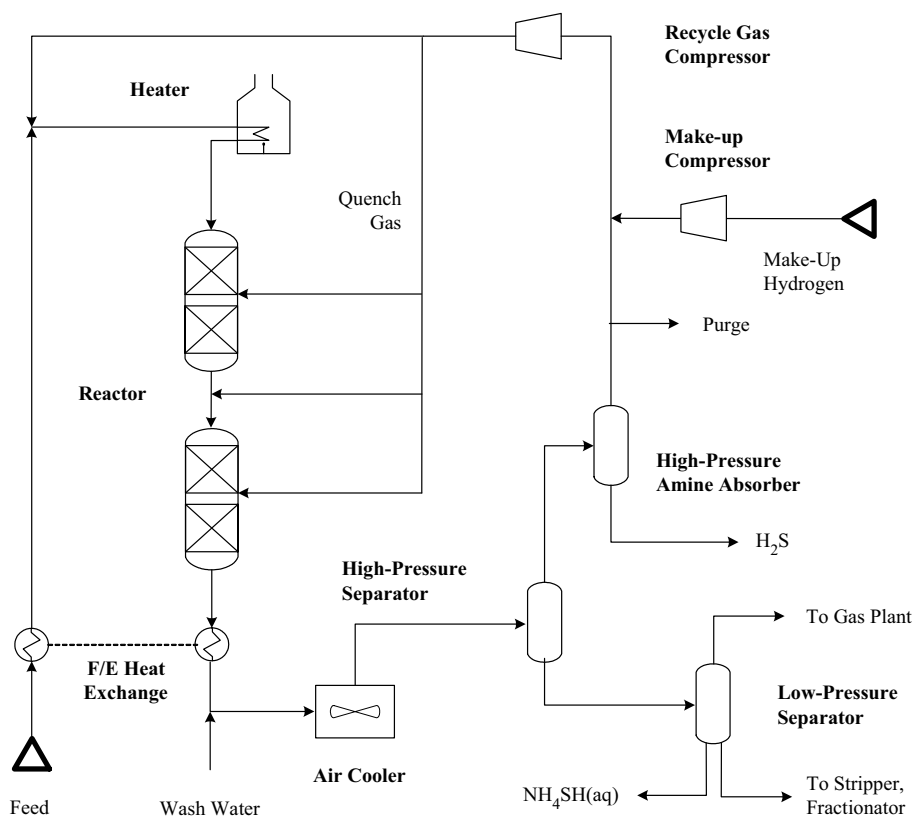


Figure 14. Gas-oil hydrotreating and once-through hydrocracking

HDS and HDN reactions produce  $\text{H}_2\text{S}$  and  $\text{NH}_3$ , respectively. Wash water is injected into the effluent from the last reactor to remove ammonia, which goes into the aqueous phase as ammonium bisulfide,  $\text{NH}_4\text{HS}(\text{aq})$ . The  $\text{NH}_4\text{HS}(\text{aq})$  is rejected from the unit as sour water in downstream flash drums.

In the high-pressure flash drum, liquid products are separated from the hydrogen-rich gas, which is recycled to the reactors. In most hydrotreaters designed for deep desulfurization,  $\text{H}_2\text{S}$  is removed from the recycle gas with a high-pressure amine absorber. The liquids go to a stripping column, which removes entrained  $\text{H}_2\text{S}$  and other light gases. These go to a low-pressure amine absorber and then to either a gas plant or the refinery fuel-gas system.

The destination of the liquid is unit-specific. In some hydrotreaters, the stripped liquid goes directly to product blending. In others, it goes to one or more fractionation towers.

**Naphtha Hydrotreating.** Heavy naphthas generally have low octane numbers, often less than 60 RON. To raise the octane, refiners use catalytic reforming units. Alternatively, heavy naphtha can go to an isomerization unit, which also makes high-octane products. In both reforming and isomerization, the catalysts are sulfur-sensitive, so a naphtha hydrotreater is used to lower the feed sulfur content, usually to <1 wppm. Some nitrogen is removed, too, which also is beneficial.

Table 16 provides additional details on hydrotreating.

Table 16. Hydrotreating in a Nutshell

|                                   |   |   |
|-----------------------------------|---|---|
| <b>Purpose</b>                    | Sulfur removal (HDS)<br>Olefin saturation<br>Metals removal   | Nitrogen removal (HDN)<br>Aromatic saturation (HDA) |
| <b>Licensors</b>                  | Axens (IFP)<br>Chevron Lummus (CLG)<br>Haldor-Topsoe<br>Shell Global Solutions                          | CDTECH<br>ExxonMobil<br>KBR<br>UOP                  |
| <b>Catalysts</b>                  | CoMo on $\gamma$ -alumina for HDS<br>NiMo or NiW on $\gamma$ -alumina for HDS, HDN, aromatic saturation |   |
| <b>Feeds</b>                      | Naphtha<br>Heavy gas oil<br>Coker gas oil   | Kesosene<br>Vacuum gas oil<br>Residual oils         |
| <b>Typical Process Conditions</b> |   |   |
|                                   | <i>Reactor temperature</i>  | 600 – 800°F (315 – 425°C)                           |
|                                   | <i>Reactor pressure</i>   | 250 – 2000 psig (1825 – 13,890 kPa)                 |

### 3.4.3 Hydrotreating Objectives

Catalytic hydrotreating removes contaminants from liquid petroleum fractions. It also saturates most olefins and many aromatic compounds. Sulfur, nitrogen, oxygen, and metals are the most troublesome impurities. If not removed, they can deactivate catalysts, contaminate finished products, and accelerate corrosion in downstream equipment.

**Gasoline Hydrotreating.** In the context of post-treating gasoline to meet recent sulfur specifications, Section 8.2.5 discusses gasoline hydrotreating. Temperatures and pressures are relatively mild, but the leading processes use multiple catalysts, multiple catalyst beds, and/or pre-fractionation to minimize loss of gasoline octane.

**Kerosene Hydrotreating.** Straight-run kerosene streams may not meet specifications for jet-fuel. By using mild hydrodearomatization (HDA) to convert some aromatic compounds into cleaner-burning naphthenes, low-severity hydrotreating can convert kerosene into jet fuel. In many parts of the world, low-sulfur kerosene is used for home heating. In those regions, straight-run kerosene and other light gas oils usually must be hydrotreated.

**Diesel Hydrotreating.** From 1991 in Sweden, 1995 in California, and 1998 in the rest of the U.S., hydrotreating was used to make diesel containing <500 wppm sulfur. Generally, diesel hydrotreaters operate at higher pressures than naphtha and kerosene units, and they often use different catalysts. These days, under pressure to make ULSD by the end of 2006, most U.S. refiners either have or will be (a) building new diesel hydrotreaters, (b) revamping existing units by changing catalysts, modifying reactor internals, adding a high-pressure H<sub>2</sub>S absorber, and/or adding a new reactor, or (c) converting other units to diesel service.

**FCC Feed Pretreating: VGO, CGO, and VBGO.** For hydrotreaters that prepare feed for conventional FCC units, removing nitrogen (HDN) from the feed is beneficial, because organic nitrogen (especially basic nitrogen) inhibits cracking by binding to the highly acidic active sites in FCC catalysts. The removal of sulfur (HDS) can reduce the size of, or eliminate the need for, FCC gasoline post-treating units. By converting aromatics to naphthenes (HDA), FCC feed pretreaters increase feed “crackability.” In FCC and other thermal cracking units, naphthenes convert to lighter products. But except for losing side chains, aromatics are rather inert. If anything, they tend to form polyaromatic hydrocarbons (PAH) and coke. Pretreaters also benefit FCC units by removing metals (primarily nickel and vanadium) and Conradson carbon (CCR). CCR correlates strongly with the tendency of a feed to form coke in a delayed coking unit. It also correlates with coke-formation in an FCC unit. By reducing feed CCR, a pretreater allows an FCC to operate at higher feed rates and/or higher conversion. If the feed rate stays constant, the conversion can increase by 10 to 20 vol%. The extent of the increase depends upon the properties of the raw feed and the conditions under which the feed is hydrotreated.

**FCC Feed Pretreating: Residue.** Originally, residue hydrotreaters were built to reduce the sulfur content of heavy fuel oil. These days, a large percentage of residue hydrotreaters are used to pretreat FCC feeds. Residue hydrotreating requires higher pressure, lower LHSV, and at least one hot flash drum after the reactors. Another main difference is the need to use one or more HDM catalysts to protect the HDS catalyst from metals such as nickel and vanadium. If not removed, Ni and V accelerate deactivation and the buildup of pressure-drop. In the Resid Unionfining process offered by UOP, HDM catalyst is loaded into a guard reactor upstream from the main reactors. In the RDS process offered by Chevron Lummus Global, an OCR (“onstream catalyst replacement”) or UFR (“up-flow reactor”) unit removes metals from the RDS feed. With OCR, a refiner can process residues containing 400 wppm metals (Ni + V).

**Lube Hydrotreating.** The mild hydrotreating (“hydrofinishing”) of lube oils improves color, odor, and stability by removing olefins, sulfides and mercaptans. Severe hydrotreating also removes aromatics, nitrogen, and refractory sulfur compounds.

**Pyrolysis Gasoline Hydrotreating.** Hydrotreating improves the quality of pyrolysis gasoline (pygas), a by-product from olefins plants. In the past, due to its high octane, some pygas was blended into gasoline. Pygas contains diolefins, which react with air to form gums. Mild hydrotreating converts diolefins into mono-olefins. This improves the stability of pygas.

#### 3.4.4 Hydrocracking

As shown in Table 14, the major difference between hydrotreating, hydrocracking, and mild hydrocracking is the extent to which conversion occurs. In a hydrocracking unit designed for high conversion of vacuum gas oil, the process flow is more complex. The unit probably operates at a much higher pressure. It may include an additional reactor, a hot high-pressure separator, and a multiple-column fractionation section. To achieve near-total conversion of fresh feed, unconverted oil may be recycled. Some details about hydrocracking are given in Table 17.

#### 3.4.5 Hydrocracking Objectives

For a given hydrocracker, process objectives can include:

- Maximum production of naphtha
- Maximum production of middle distillate fuels
- Flexibility to swing between production of naphtha and middle distillates
- Production of ultra-clean lube base stocks
- Production of olefin plant feeds.

#### 3.4.6 Hydrocracker Feeds

Liquid feeds can be atmospheric or vacuum gas oils from crude distillation units; gas oils (light and heavy) from delayed cokers, fluid cokers, or visbreakers; and cycle oils (light and heavy) from FCC units.

#### 3.4.7 Hydrocracking Process Flow

The process flow scheme in Figure 14 can describe a gas-oil hydrotreater, a mild hydrocracking, or a once-through high-conversion hydrocracker. In a hydrocracker, the first few beds are likely to contain hydrotreating catalyst while subsequent beds contain hydrocracking catalyst. In some hydrocrackers designed for maximum production of diesel fuel, all catalyst beds contain hydrocracking catalyst. Other hydrocracking process flow schemes are described in Chapters 7 and 8.

### 3.4.8 Hydrocracker Products

Middle distillates (jet and diesel) from high-conversion hydrocrackers meet or exceed finished product specifications. The heavy naphtha, however, usually goes to a catalytic reformer for octane improvement. The fractionator bottoms from partial conversion units can be sent to an FCC unit, an olefins plant, or a lube plant.

Due to the fact that products from a hydrocracker are less dense than the feeds, the total volume of liquid products is greater than the feed volume by 10 to 30 vol%. This phenomenon is called volume swell.

Table 17. Hydrocracking in a Nutshell

|                                   |   |  |
|-----------------------------------|---|--|
| <b>Purpose</b>                    | Convert heavy hydrocarbons into lighter hydrocarbons      |  |
| <b>Uses for Unconverted Oil</b>   | FCC feed  | Lube base stock                            |
|                                   | Olefin plant feed   | Recycle to extinction                      |
| <b>Other Reactions</b>            | Sulfur removal (HDS)                                      | Nitrogen removal (HDN)                     |
|                                   | Olefin saturation   | Aromatic saturation                        |
| <b>Licensors</b>                  | Axens (IFP) (IFP)   | Chevron Lummus                             |
|                                   | ExxonMobil  | KBR  |
|                                   | Shell Global Solutions                                    | UOP  |
| <b>Catalysts</b>                  | NiMo on $\gamma$ -alumina (HDS, HDN, aromatic saturation) |  |
|                                   | NiMo or NiW on zeolite (hydrocracking)                    |  |
|                                   | NiMo or NiW on amorphous silica-alumina (hydrocracking)   |  |
|                                   | Pd on zeolite (hydrocracking)                             |  |
| <b>Feeds</b>                      | Heavy gas oil   | Vacuum gas oil                             |
|                                   | Coker gas oil   | Residual oils                              |
| <b>Typical Process Conditions</b> | Reactor temperature                                       | 600 – 800°F (315 – 425°C)                  |
|                                   | Reactor pressure  | 1200 – 2500 psig (8375 – 17,338 kPa)       |
| <b>Range of Product Yields</b>    | Conversion (once-through)                                 | 20 – 90 vol%                               |
|                                   | Conversion (with recycle)                                 | 90 – 99 vol% fresh feed                    |
|                                   | C <sub>4</sub> -plus naphtha                              | Up to 120 vol% fresh feed                  |
|                                   | Middle distillates  | Up to 90 vol% fresh feed                   |
|                                   | Hydrogen consumption                                      | 1000 to 3000 scf/bbl                       |
|                                   |   | 175 to 525 Nm <sup>3</sup> /m <sup>3</sup> |

### 3.5 Ebullated Bed Units

In fixed-bed hydrocrackers designed to process VGO, residual oils in the feed can reduce catalyst cycle life if they contain even trace amounts of salts, asphaltenes, refractory carbon, trace metals (Fe, Ni, V), or particulate matter. As mentioned in Section 3.4.2, fixed-bed units designed to process residue remove metals and other contaminants with upstream guard beds or onstream catalyst replacement technology. In contrast, ebullated bed hydrocrackers can and do process significant amounts of residual oils. This is because fresh

catalyst is added and spent catalyst is removed continuously. Consequently, catalyst life does not impose limitations on feed selection or conversion.

Ebullated bed processes are offered for license by Axens (IFP) ABB Lummus. In ebullated bed reactors, hydrogen-rich recycle gas bubbles up through a mixture of oil and catalyst particles to provide three-phase turbulent mixing. The reaction environment can be nearly isothermal, which improves product selectivity. At the top of the reactor, catalyst particles are disengaged from the process fluids, which are separated in downstream flash drums. Most of the catalyst goes back to the reactor. Some is withdrawn and replaced with fresh catalyst.

## 4. UPGRADING NAPHTHA

Gasoline is produced by blending several different refinery streams – butanes, straight-run gasoline, reformat, alkylate, isomate, FCC gasoline, oxygenates, and others. This section gives an overview of the processes that either upgrade or generate gasoline blend stocks.

### 4.1 Catalytic Reforming

#### 4.1.1 Catalytic Reforming Objectives

Catalytic reforming converts low-octane heavy naphtha into a high-octane product (reformat) that is an excellent gasoline blend stock. Reformat has a high content of BTX (benzene-toluene-xylene), so it also serves as a great source of aromatics for petrochemical plants.

In addition to making aromatic compounds, catalytic reformers produce hydrogen, which is used in hydrotreaters, hydrocrackers, and other hydrogen-addition processes.

#### 4.1.2 Chemistry of Catalytic Reforming

The chemistry of catalytic reforming includes the reactions listed in *Table 18*. All are desirable except hydrocracking, which converts valuable C<sub>5</sub>-plus molecules into light gases. The conversion of naphthenes to aromatics and the isomerization of normal paraffins provide a huge boost in octane. H<sub>2</sub> is produced by dehydrocyclization of paraffins and naphthene dehydrogenation, which are shown in *Figure 15*.

*Table 18.* List of Catalytic Reforming Reactions

| <b>Naphthene Reactions</b>                 | <b>Paraffin Reactions</b>                   |
|--|---|
| Dehydrogenation to form aromatics          | Dehydrocyclization to form aromatics        |
| Isomerization to form different naphthenes | Isomerization to form other paraffins       |
|  | Hydrocracking to form C <sub>4</sub> -minus |

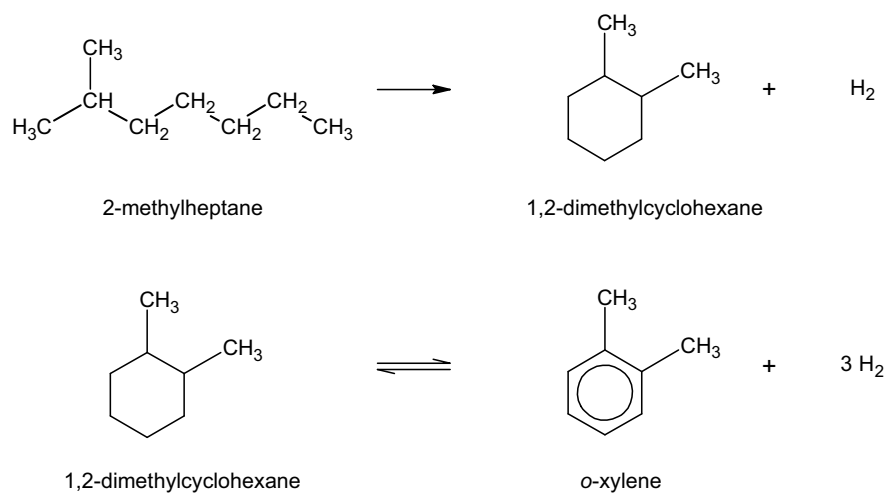


Figure 15. Dehydrocyclization and dehydrogenation

Hydrocracking and isomerization reactions are shown in *Figure 16* and *Figure 17*, respectively. Hydrocracking, which is undesirable in this process, occurs to a greater extent at high temperatures.

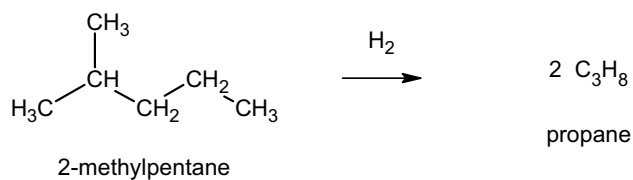


Figure 16. Hydrocracking in catalytic reformers.

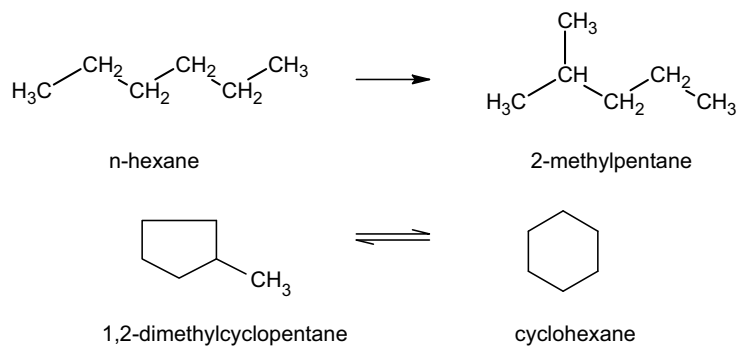


Figure 17. Isomerization of paraffins and naphthenes in catalytic reformers.



Additional details about catalytic reforming are given in *Table 19*.

*Table 19. Catalytic Reforming in a Nutshell*

|  |  |   |
|--|--|---|
| <b>Purpose</b>                               | Increase heavy-naphtha octane  |   |
| <b>Other</b>                                 | Produce aromatics (BTX) for petrochemical plants<br>Produce hydrogen |   |
| <b>Licensors</b>                             | Axens (IFP)<br>ExxonMobil  | BP<br>UOP   |
| <b>Catalysts</b>                             | Pt on $\gamma$ -alumina<br>Pt-Re-Sn on $\gamma$ -alumina             | Pt-Re on $\gamma$ -alumina                                      |
| <b>Promoters</b>                             | HCl  |   |
| <b>Feeds</b>                                 | Hydrotreated heavy naphtha, 40 to 62 RON                             |   |
| <b>Typical Process Conditions</b>            |  |   |
|  | H <sub>2</sub> /HC ratio   | Up to 6.0   |
|  | Reactor inlet temperature  | 900 – 970°F (482 – 521°C)                                       |
|  | Pressure (Semi-regen., Cyclic)                                       | 200 – 500 psig (1480 – 3549 kPa)                                |
|  | Pressure (CCR)   | 100 – 150 psig (791 – 1136 kPa)                                 |
| <b>Typical Product Yields and Properties</b> |  |   |
|  | Total C <sub>5</sub> -plus   | 84 to 85 vol%   |
|  | H <sub>2</sub> production  | 650 – 1100 scf/bbl (115 – 195 Nm <sup>3</sup> /m <sup>3</sup> ) |
|  | RONC (Semi-regen., Cyclic)   | 85 to 95  |
|  | RONC (CCR)   | Up to 105   |

### 4.1.3 Catalytic Reforming Catalysts

Catalytic reforming catalysts contain highly dispersed platinum (Pt), the activity of which is inhibited by sulfur. Therefore, an upstream hydrotreater lowers the sulfur content of reformer feeds to <1 wppm. In addition to Pt, modern multi-metallic catalysts contain highly dispersed rhenium (Re) and in some cases tin (Sn).

### 4.1.4 Process Flows

There are three major process flows for catalytic reforming:

- Semi-regenerative
- Cyclic
- Continuous catalyst regeneration (CCR)

*Figure 18* shows a semi-regenerative reformer, a fixed-bed unit in which catalyst cycles last from 6 to 12 months. A catalyst cycle ends when the unit is unable to meet its process objectives – typically octane and overall C<sub>5</sub>-plus yields. At the end of a cycle, the entire unit is brought down and catalyst is regenerated. In a cyclic reformer, catalyst cycles are shorter – 20 to 40 hours – but they are staggered so that only one reactor goes down at a time. In a CCR unit, the catalyst is slowly but constantly moving from the reactor to the regenerator and back again.

In a semi-regenerative unit, desulfurized naphtha is mixed with hydrogen, heated to  $>900^{\circ}\text{F}$  ( $>480^{\circ}\text{C}$ ) and passed through a series of fixed-bed reactors. The major chemical reactions – dehydrogenation and dehydrocyclization – are endothermic (heat absorbing), and the reactors themselves are essentially adiabatic. This means that heat can't enter or leave except by the cooling or heating of reaction fluids. Consequently, the temperature drops as reactants flow through a reactor. Between reactors, fired heaters bring the process fluids back to desired reactor inlet temperatures.

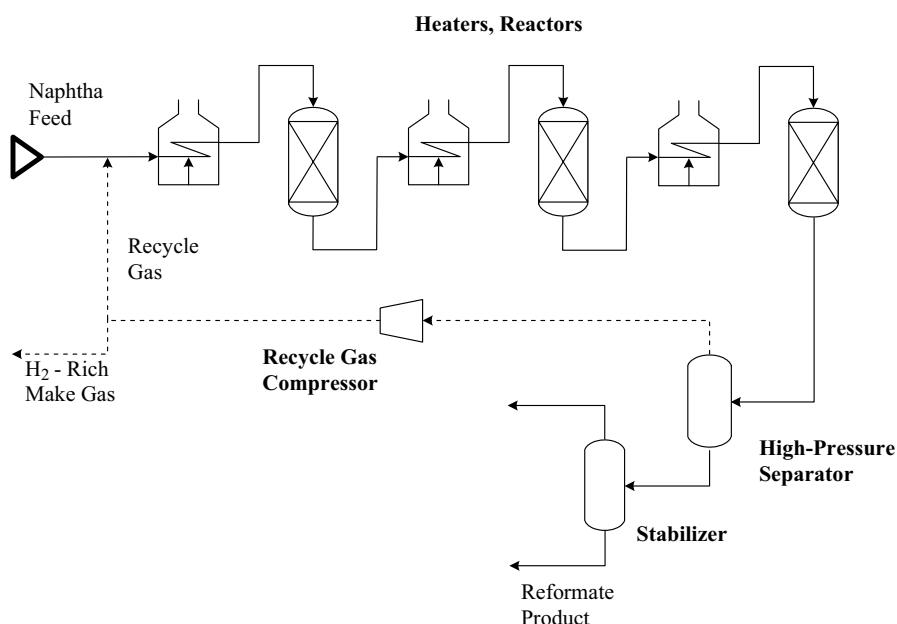
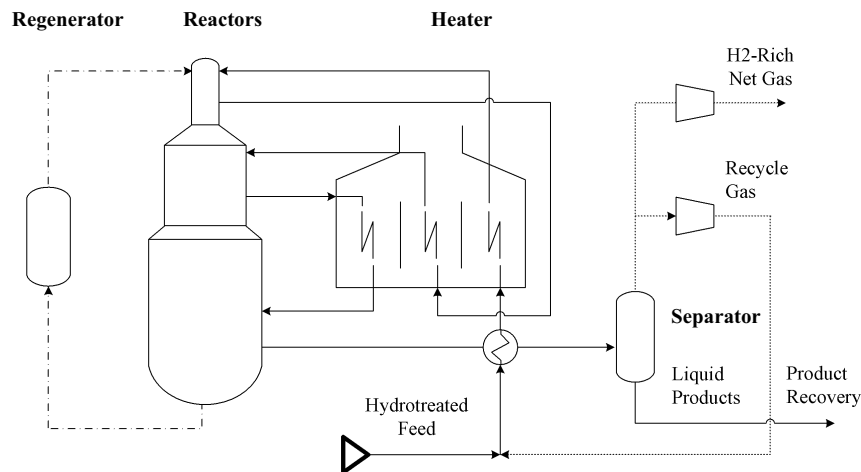


Figure 18. Semi-regenerative catalytic reforming

Some catalytic reformers operate at low pressure (100 psig, 791 kPa), while others operate at  $>500$  psig (3549 kPa). Low operating pressure improves yields of aromatics and hydrogen, but it accelerates catalyst deactivation by increasing the rate at which coke forms on the catalyst. In a CCR reformer, the catalyst always is being regenerated, so increased coking is less problematic. Therefore, CCR units can operate at very low pressures. In most reformers, the feed is spiked with an organic chloride, which converts to hydrogen chloride (HCl) in the reactors. The HCl increases catalyst acidity and helps to minimize catalyst coking.

The effluent from the last reactor is cooled and sent to a separator, from which hydrogen-rich gas is removed and recycled to the reactors. The liquid product flows to a stabilizer column, where entrained gases are removed, before going to the gasoline blender or aromatics plant.

In a CCR unit (*Figure 19*), the hydrotreated feed mixes with recycle hydrogen and goes to series of adiabatic, radial-flow reactors arranged in a vertical stack. Catalyst flows down the stack, while the reaction fluids flow radially across the annular catalyst beds. The predominant reforming reactions are endothermic, so heaters are used between reactors to reheat the charge to reaction temperature. Flue gas from the fired heaters is typically used to generate steam.



*Figure 19.* CCR catalytic reforming

The effluent from the last reactor is cooled and sent to a separator. Part of the vapor is compressed and recycled to the reactors. The rest is compressed, combined with separator liquids, and sent to the product recovery section. Liquids from the recovery section go to a stabilizer, where light saturates are removed from the  $C_6$ -plus aromatic products.

Partly deactivated catalyst is continually withdrawn from the bottom of the reactor stack and sent to the regenerator. As the catalyst flows down through the regenerator, the coke is burned away. Regenerated catalyst is lifted by hydrogen to the top of the reactor stack. Because the reactor and regenerator sections are separate, each operates at its own optimum conditions. The regeneration section can be temporarily shut down for maintenance without affecting the operation of the reactor and product recovery sections.

## 4.2 Isomerization

### 4.2.1 Isomerization Objectives

As we have seen, isomerization occurs as a side-reaction in all conversion processes. But in refining, when we say “isomerization process,” we are referring specifically to the on-purpose isomerization of n-butane, n-pentane, and n-hexane. The main purpose of n-paraffin isomerization is to produce iso-paraffins with substantially higher octane numbers. An isomerization reaction for normal hexane was shown in *Figure 17*.

Some details about paraffin isomerization processes are given in *Table 20*.

*Table 20.* Isomerization in a Nutshell

|   |   |                                  |
|---|---|----------------------------------|
| <b>Purpose</b>  | Convert n-butane to isobutane<br>Convert n-pentane and n-hexane to branched isomers |                                  |
| <b>Licensors (C<sub>4</sub>)</b>                                      | ABB Lummus Global<br>UOP  | BP                               |
| <b>Licensors(C<sub>5</sub>C<sub>6</sub>)</b>                          | Axens (IFP)<br>UOP  | BP                               |
| <b>Catalysts(C<sub>4</sub>)</b>                                       | Pt on $\gamma$ -alumina, HCl promoter   | Pt on zeolite                    |
| <b>Catalysts(C<sub>5</sub>C<sub>6</sub>)</b>                          | Pt on $\gamma$ -alumina, HCl promoter   | Pt on zeolite                    |
| <b>Feeds(C<sub>4</sub>)</b>   | dry n-butane  |                                  |
| <b>Feeds(C<sub>5</sub>)</b>   | Light straight-run, end point <160°F (71°C)   |                                  |
|   | Light reformat  | Light hydrocrackate              |
|   | Natural gasoline  | Light aromatics raffinate        |
| <b>Process Conditions (Pt on alumina, chlorided)</b>                  |   |                                  |
|   | Reactor temperature   | 250 – 300°F (121 – 149°C)        |
|   | Reactor pressure  | 400 – 450 psig (2859 – 3204 kPa) |
| <b>Process Conditions (Pt on zeolite)</b>                             |   |                                  |
|   | Reactor temperature   | 445 – 545°F (230 – 285°C)        |
|   | Reactor pressure  | 190 – 440 psig (1411 – 3135 kPa) |
| <b>Conversion and Product Properties (C<sub>5</sub>C<sub>6</sub>)</b> |   |                                  |
|   | Conversion (with recycle)   | up to 97%                        |
|   | RON   | 85 to 90                         |

Section 8.2.1 lists octane numbers for heavy naphtha and some normal and iso-paraffins. N-butane has a high octane number (92), so refiners blend as much of it as possible into gasoline. But n-butane also evaporates easily, which means that tighter restrictions on the RVP (volatility) of gasoline limit its C<sub>4</sub> content (see Section 8.2.2). In many locales, this creates an excess of n-butane. By converting it into isobutane, which is consumed in alkylation units, refiners can reduce or eliminate this excess of n-butane.

#### 4.2.2 Isomerization Catalysts

The most common catalyst for isomerising n-butane is platinum (Pt) on alumina promoted by chloride. The high activity of this catalyst allows operation at relatively low temperature. This is beneficial because the reaction is controlled by equilibrium; at low temperature, equilibrium favors isobutane. Pt/alumina catalysts can't be regenerated, and they are highly sensitive to water and other contaminants.

In units that isomerize n-pentane and n-hexane, the reactions are catalyzed either by Pt/alumina or Pt on zeolite. The zeolite catalysts require higher temperatures, but they are less sensitive to water. As with butane isomerization, the reactions are controlled by equilibrium, so lower reaction temperatures favor branched isomers. The high temperatures required by zeolite catalysts reduce the octane of the product relative to products made at lower temperatures with chlorided alumina catalysts.

#### 4.2.3 Process Flow: C<sub>4</sub> Isomerization

The feed to a butane (C<sub>4</sub>) isomerization unit should contain maximum amounts of n-butane and only small amounts of isobutane, pentanes, and heavier material. The feed is dried, combined with dry makeup hydrogen, and charged to the reactor section at 230 to 340° F (110 to 170°C) and 200 to 300 psig (1480 to 2170 kPa). H<sub>2</sub> is not consumed by isomerization reactions, but it suppresses polymerization of the olefin intermediates that are formed during the reaction. A small amount of organic chloride promoter, which is added to maintain catalyst activity, converts completely to HCl in the reactors.

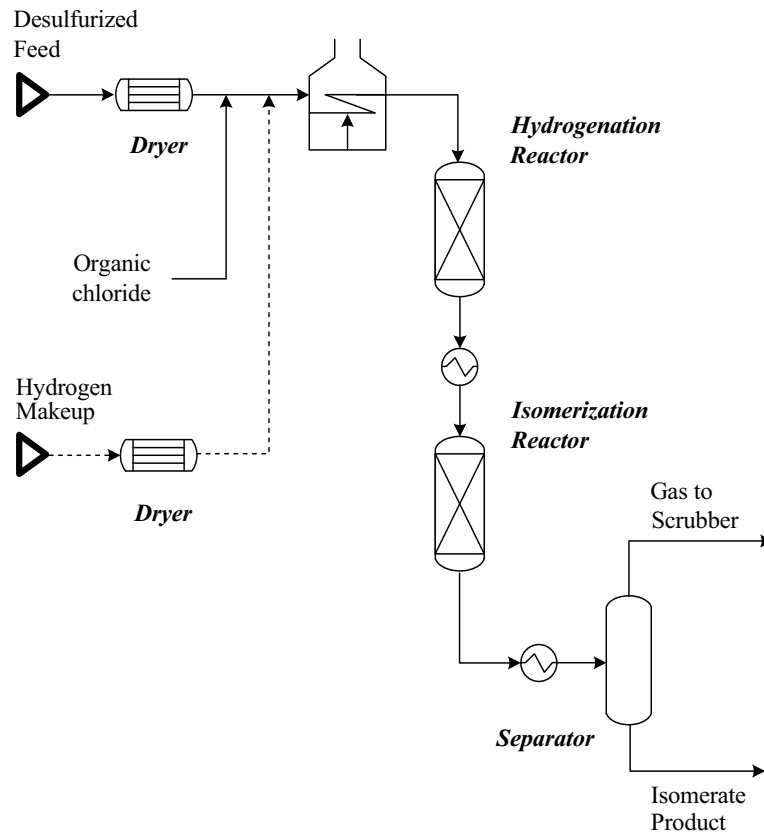
Often, two reactors in series are used to increase on-stream efficiency. The catalyst in one reactor can be replaced while the other continues to operate. The reactor effluent (isomerate) flows to a stabilizer. A caustic scrubber removes HCl from the separated light gases. The stabilized liquid product comprises a near-equilibrium mixture of n-butane and isobutanes, plus a small amount of heavier hydrocarbons. Losses due to cracking are less than 1 wt%.

The isomerate can be blended directly into gasoline or sent to an alkylation unit. N-butane from an alkylation unit can be recycled to a butane isomerization unit to achieve nearly total conversion of n-butane into isobutane or alkylate.

#### 4.2.4 Process Flow: C<sub>5</sub>C<sub>6</sub> Isomerization

Pentane/hexane (C<sub>5</sub>C<sub>6</sub>) isomerization processes increase the octane of light gasoline. In a typical unit, dried, hydrotreated feed is mixed with a small amount of organic chloride and recycled hydrogen, then heated to reaction temperature.

Process objectives determine whether one or two reactors are used. In two-reactor units (*Figure 20*), the feed flows first to a saturation reactor, which removes olefins and (to a large extent) benzene. After saturation, the feed goes to an isomerization reactor, where normal paraffins are converted to isoparaffins.



*Figure 20.*  $C_5C_6$  isomerization: two reactors, once-through hydrogen

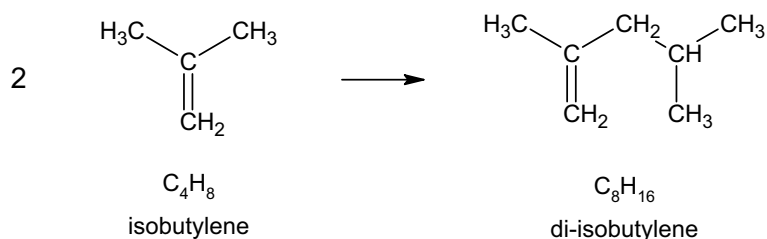
The reactor effluent flows to a product separator, where hydrogen is separated from the other reaction products. Recovered hydrogen can go to a recycle compressor, which returns it to the reactors, or it can be treated and sent to the fuel gas system. Separator liquids go to a stabilizer column, which removes light gases and remaining dissolved hydrogen. The stabilized liquid goes to storage or gasoline blending. If sent to a fractionator, n-pentane and n-hexane can be recycled to the isomerization unit for increased conversion.

## 4.3 Catalytic Oligomerization

### 4.3.1 Catalytic Oligomerization Objectives

Catalytic oligomerization also is called catalytic polymerization, catpoly, and catalytic condensation. The process converts  $C_3$  and  $C_4$  olefins into  $C_6$  to  $C_9$  olefins, which are excellent gasoline blend stocks. Per *Table 22*, the research octane numbers for  $C_6$  and  $C_8$  olefins such as methyl-2-pentenes and 2,2,4-trimethylpentenes are greater than 97.

Variations on the process make higher olefins and aromatics such as cumene for petrochemical applications. *Figure 21* shows the main chemical reaction for the dimerization of isobutylene.



*Figure 21.* Dimerization of isobutylene

### 4.3.2 Catalysts

Sulfuric acid, phosphoric acid, and solid phosphoric acid on kieselguhr pellets (SPA) are used as catalysts. The SPA catalyst is non-corrosive, so it can be used in less-expensive carbon-steel reactors.

### 4.3.3 Process Flow

*Figure 22* presents a sketch for a unit designed to use SPA catalysts. After pre-treatment to remove sulfur and other undesirable compounds, the olefin-rich feed is sent to the reactor. The reaction is exothermic, so temperatures are controlled by diluting the feed with product and by injecting relatively cold feedstock (quench) between beds in the reactor. Temperatures range from 300 to 450°F (150 to 230°F) and pressures range from 200 to 1,200 psig (1480 to 8375 kPa).

Reaction products go to stabilization and/or fractionator systems to separate gases – saturated and unsaturated  $C_3$ - $C_4$  compounds – from the liquid product. The gases are recycled to the reactor, and the liquid product goes to gasoline blending.

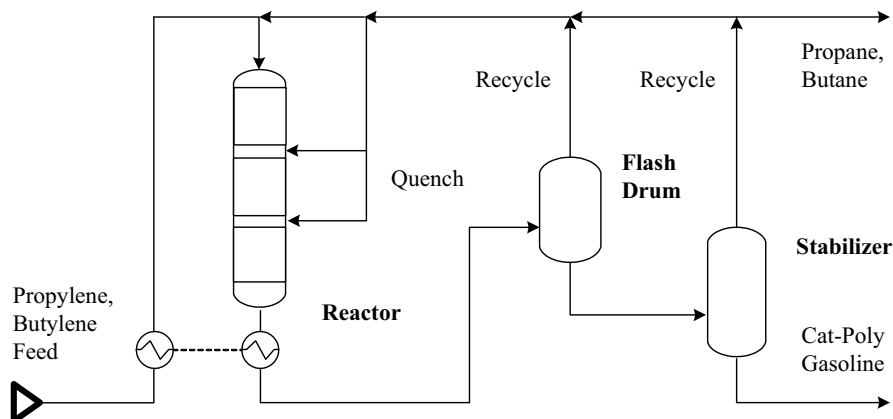


Figure 22. Catalytic oligomerization of olefins

## 4.4 Alkylation

### 4.4.1 Alkylation Objectives

Alkylation processes combine light olefins (primarily propylene and butylene) with isobutane in the presence of a highly acidic catalyst, either sulfuric acid or hydrofluoric acid. The product (alkylate) contains a mixture of high-octane, branched-chain paraffinic hydrocarbons. *Figure 23* illustrates the reaction between isobutane and trans-2-butene. Alkylate is a highly desirable gasoline blend stock because, in addition to its high octane, it has a low vapor pressure. The octane of the product depends on the operating condition and the kinds of olefins used.

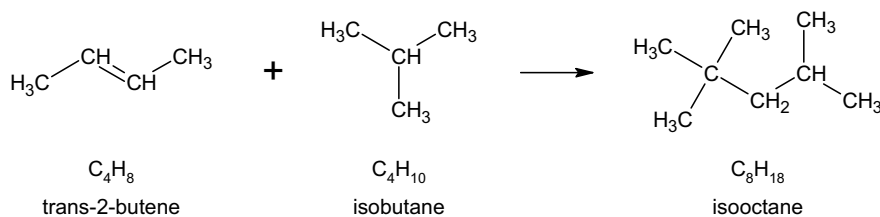


Figure 23. Alkylation of trans-2-butene

### 4.4.2 Process Flow: Sulfuric Acid Alkylation

In sulfuric acid ( $\text{H}_2\text{SO}_4$ ) alkylation units, the feeds – propylene, butylene, amylene, and fresh isobutane – enter the reactor and contact sulfuric acid



with a concentration of 85 to 95%. The reactor is divided into zones. Olefins are fed through distributors to each zone, and sulfuric acid and isobutanes flow over baffles from one zone to the next.

The reactor effluent goes to a settler, in which hydrocarbons separate from the acid. The acid is returned to the reactor. The hydrocarbons are washed with caustic and sent to fractionation. The fractionation section comprises a depropanizer, a deisobutanizer, and a debutanizer. Alkylate from the deisobutanizer can go directly to motor-fuel blending, or it can be reprocessed to produce aviation-grade gasoline. Isobutane is recycled.

### 4.4.3 Process Flow: HF Alkylation

Figure 24 shows a process schematic for hydrofluoric acid (HF) alkylation. Olefins and isobutane are dried and fed to a reactor, where the alkylation reaction takes place over the HF catalyst. The reactor effluent flows to a settler, where the acid phase separates from the hydrocarbon phase. The acid is drawn off and recycled. The hydrocarbon phase goes to a deisobutanizer (DIB). The overhead stream, containing propane, isobutane, and residual HF, goes to a depropanizer (DeC3). The DeC3 overhead goes to an HF stripper. It is then treated with caustic and sent to storage. Isobutane from the DIB main fractionator is recycled. The bottom stream from the debutanizer goes to product blending.

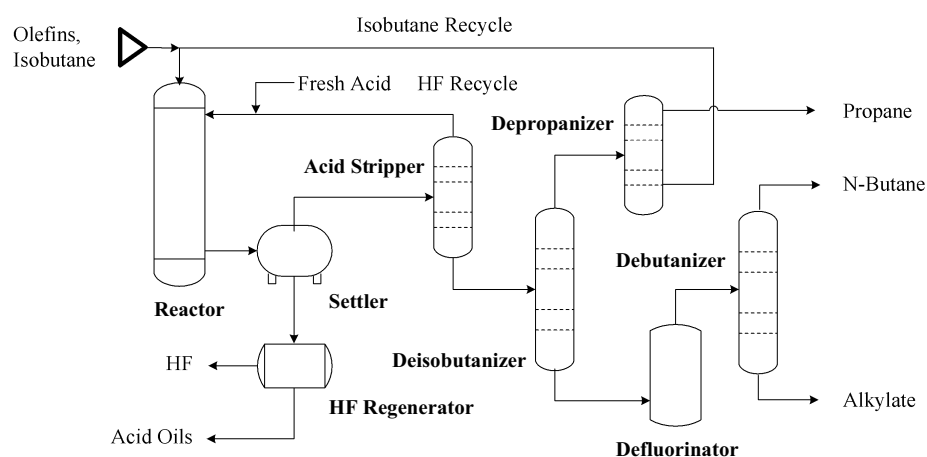


Figure 24. HF alkylation

## 5. LUBES, WAXES AND GREASES

“Bottom of the barrel” fractions – atmospheric and vacuum residues – can be converted by the processes described in Sections 2 and 3, or they can be used to make lubes, waxes and greases.

### 5.1 Lube Base Stocks

Refiners prepare lube base stocks from residual oils by removing asphaltenes, aromatics, and waxes. Lube base stocks are hydrofinished, blended with other distillate streams for viscosity adjustment, and compounded with additives to produce finished lubricants.

Solvent-based processes for removing asphaltenes, aromatics and waxes were discussed in Section 2.2. The next few paragraphs give a quick overview of catalytic dewaxing.

#### 5.1.1 Catalytic dewaxing

Catalytic dewaxing (CDW) was developed by Exxon Mobil in the 1980s. The process employs a shape-selective zeolite called ZSM-5, which selectively converts waxy n-paraffins into lighter hydrocarbons.

The Isodewaxing Process, commercialized in 1993 by ChevronTexaco, catalytically isomerizes n-paraffins into iso-paraffins. This decreases the wax content and increases the concentration low-viscosity hydrocarbons, both of which are desirable. Isodewaxing also removes sulfur and nitrogen, and it saturates aromatics. Products have a high viscosity index (VI), low pour point, and excellent response to additives.

Catalytic dewaxing and Isodewaxing are discussed in more detail in the second volume of this book.

### 5.2 Waxes

The raffinate from the solvent extraction unit in a traditional lube plant contains a considerable amount of wax. To recover the wax, the raffinate is mixed with a solvent, usually propane, and cooled in a series of heat exchangers. Further cooling is provided by the evaporation of propane in the chiller and filter feed tanks. The wax forms crystals, which are continuously removed, filtered, and washed with cold solvent. The solvent is recovered by flashing and steam stripping. The wax is purified by heating with hot solvent, after which it is re-chilled, re-filtered and given a final wash.

Paraffin waxes are used to make candles and coated papers for use as bread wrappers, cold-drink cups, and beverage cartons. They are also used in

building materials. The market for packaging is declining, but other uses are on the rise, especially in construction.<sup>31</sup>

### 5.3 Greases

Greases are made by blending salts of long-chained fatty acids into lubricating oils at temperatures of 400 to 600°F (204 to 315°C). Antioxidants are added to provide stability. Some greases are batch-produced, while others are made continuously. The characteristics of a grease depend to a great extent on the counter-ion (calcium, sodium, aluminum, lithium, etc.) in the fatty-acid salt.

## 6. ASPHALT PRODUCTION

Asphalt can be produced directly from vacuum residue or by solvent deasphalting (see Section 2.2).

**Road-Tar Asphalt.** Vacuum residue is used to make road-tar asphalt. To drive off remaining light ends, it is heated to about 750°F (400°C) and charged to a column where a vacuum is applied.

In road-paving, the petroleum residue serves as a binder for aggregate, which can include stone, sand, or gravel. The aggregate comprises about 95% of the final mixture. Polymers are added to the binder to improve strength and durability.

The recommended material for paving highways in the United States is Superpave<sup>32</sup> hot-mix asphalt. Superpave was developed in 1987-93 during a US\$50 million research project sponsored by the Federal Highway Administration.

**Roofing Asphalt.** Roofing asphalt is produced by blowing, which involves the oxidation of asphalt flux by bubbling air through liquid asphalt at 260°C (500°F) for 1 to 10 hours. During this process, organic sulfur is converted to H<sub>2</sub>S and SO<sub>2</sub>. Catalytic salts such as ferric chloride (FeCl<sub>3</sub>) may be used to adjust product properties and increase the rates of the blowing reactions, which are exothermic. To provide cooling, water is sprayed into the top of the blowing vessel, creating a blanket of steam that captures sulfur-containing gases, light hydrocarbons, and other gaseous contaminants. These are recovered downstream. Cooling water may also be sprayed on the outside of the vessel.

The length of the blow depends on desired product properties, such as softening temperature and penetration rate. A typical plant blows four to six batches of asphalt per 24-hour day. There are two primary substrates for roofing asphalt – organic (paper felt) and fiberglass. The production of felt-based roofing shingles consists of:

- Saturating the paper felt with asphalt
  - Coating the saturated felt with filled asphalt
  - Pressing granules of sand, talc or mica into the coating
  - Cooling with water, drying, cutting and trimming, and packaging
- If fiberglass is used as the base instead of paper felt, the saturation step is eliminated.

## **7. DRYING, SWEETENING, AND TREATING**

Drying, sweetening and treating are not as glamorous as extraction and conversion, or even distillation, but they are essential to the performance and safety of finished products. In lubricating oils, traces of olefins and sulfur compounds can form gums and accelerate degradation. At high altitude, excess water in jet fuel can freeze and plug fuel lines. Traces of mercaptans and disulfides in “sour” gasoline can react with water in storage tanks to produce toxic levels of hydrogen sulfide.

### **7.1 Drying and Sweetening**

Light gas streams produced by various refinery units are collected and piped to treating plants, where:

- Propane is recovered for LPG
- Propylene is removed for use in petrochemical plants
- Butanes and butenes are removed for use as alkylation feeds
- Heavier components are recovered and sent to gasoline blending

Knock-out drums collect easy-to-condense liquids, but if necessary drying agents – alumina, silica, or molecular sieves – are used to remove the final traces of water. Some processes use beds of molecular sieves to dry and sweeten at the same time.

Gases containing hydrogen sulfide are scrubbed in trayed contactors with aqueous amines such as diethanolamine (DEA). Hydrogen sulfide is stripped from the “rich” amine with steam and recycled to the contactor. In a properly operating unit, the sweetened gas contains <10 wppm H<sub>2</sub>S.

### **7.2 Treating**

Treating improves the odor, color, and stability of straight-run liquids and conversion-unit products. Sulfuric acid treating removes olefins, sulfur, nitrogen, oxygen compounds, and other contaminants. Clay/lime treating of acid-treated oil removes any residual traces of asphaltenes. Caustic treating

with sodium (or potassium) hydroxide removes naphthenic acids, phenols, mercaptans, and H<sub>2</sub>S.

If the concentration of organic sulfur exceeds the capacity of a caustic or acid treater, the stream must be sent to a hydrotreater.

## 8. PRODUCT BLENDING

### 8.1 Product Specifications

Liquid products from modern refineries comprise several individual streams, which are blended to meet desired specifications. Product specifications developed by ASTM – the American Society for Testing and Materials – are widely used throughout the world. *Table 21* lists some common refinery products along with their ASTM designations.

*Table 21.* ASTM Specification Numbers for Hydrocarbon Fuels

| <b>Product</b> | <b>ASTM Specification</b> | <b>Last Updated</b> | <b>Description</b>   |
|----------------|---------------------------|---------------------|--|
| Gasoline       | D4814                     | 2003                | Standard Specification for Automotive Spark-Ignition Engine Fuel |
| Jet            | D1655                     | 2003                | Standard Specification for Aviation Turbine Fuels                |
| Kerosene       | D3699                     | 2003                | Standard Specification for Kerosene                              |
| Diesel         | D975                      | 2004                | Standard Specification for Diesel Fuel Oils                      |
| Fuel Oil       | D396                      | 1998                | Standard Specification for Fuel Oils                             |

Analogous institutions in other countries – for example, the Japanese Industrial Standards Committee (JISC) and the British Standards Institution (BSI) – serve similar functions. BSI developed the ISO9000 series of standards for managing manufacturing processes.

In addition to setting specifications, these institutions develop and publish test methods used to analyze a wide variety of materials. ASTM and its international cousins cooperate with each other, and they work closely with government regulators. For example, recent low-sulfur gasoline and diesel directives from the U.S. Environmental Protection Agency are incorporated into D975-04 and D4814-03a, respectively.

Other widely used tests and specifications are defined by licensors. For example, UOP's *Laboratory Test Methods*, distributed by ASTM, defines several hundred procedures for analyzing catalysts, chemicals and fuels. Axens (IFP), ChevronTexaco, ExxonMobil and other licensors also distribute test methods to process licensees.

Additives are an essential component of finished fuels. They increase stability, improve flow properties and enhance performance. For example, cetane-improvers are routinely added to diesel fuel, and additives that prevent intake-valve deposits are now required in all grades of gasoline in the United States.

## 8.2 Gasoline Blending

Forty years ago, making gasoline was a relatively simple task. If a mixture of components met specifications for volatility and octane, it could be shipped to retail outlets and sold as-was. If the octane was low, the problem could be fixed by adding a little tetraethyl lead. Butanes could be added as needed to adjust volatility.

In fact, volatility and octane are still the two most important properties of gasoline. The volatility must be high enough to vaporize during cold weather; otherwise, engines won't start. And octane is still one of the best predictors of performance in a spark-ignition gasoline engine.

### 8.2.1 Octane Numbers for Hydrocarbons

In a spark-ignition engine, some compounds start to burn before they reach the spark plug. This premature ignition causes knocking, which reduces the power of the engine, increases engine wear, and in some cases causes serious damage.

Octane number is a measure of the propensity of fuels to knock in gasoline engines. It is based on an arbitrary scale in which the octane number of n-heptane is zero and the octane number of isooctane (2,2,4-trimethylpentane) is 100. When a fuel is tested in a standard single-cylinder engine, mixtures of isooctane and n-heptane are used as standards. ASTM D2699 and ASTM D2700 describe methods for measuring research octane number (RON) and motor octane number (MON), respectively. The engine speed for the RON test is 600 rpm, while 900 rpm is used for the MON test. RONC and MONC are sometimes used instead to RON and MON. The "C" stands for clear, which means that the fuel does not contain lead or manganese additives.

*Table 22* presents RON and MON values for several pure compounds. Aromatics, olefins, and branched isomers have higher octane numbers than straight-chain isomers with similar carbon numbers. Octane numbers for naphthenes are substantially lower than those for aromatics.

Octane numbers do not blend linearly. For example, while the RON for pure 4-methyl-2-pentene is 99, its blended RON is 130.

In North America, the pump octane of gasoline is the average of RON and MON:  $(R+M)/2$ . This is the number displayed on pumps at filling stations.

Typical grades are "regular" with a pump octane of 87, "mid-grade" with a pump octane of 89, and "premium" with a pump octane of 91 to 93. In some locales, customers can dial in any octane they want between 87 and 93.

Table 22. Octane Numbers for Selected Pure Compounds

| Compound                  | Type       | Formula                        | RON  | MON |
|---------------------------|------------|--------------------------------|------|-----|
| n-Butane                  | n-Paraffin | C <sub>4</sub> H <sub>10</sub> | 92   | 93  |
| n-Pentane                 | n-Paraffin | C <sub>5</sub> H <sub>12</sub> | 62   | 62  |
| Cyclopentane              | Naphthene  | C <sub>5</sub> H <sub>10</sub> | 101  | 85  |
| 2-Methylbutane            | i-Paraffin | C <sub>5</sub> H <sub>12</sub> | 92   | 90  |
| 2-Methyl-2-butene         | Olefin     | C <sub>5</sub> H <sub>10</sub> | 97   | 85  |
| n-Hexane                  | n-Paraffin | C <sub>6</sub> H <sub>14</sub> | 25   | 26  |
| Methylcyclopentane        | Naphthene  | C <sub>6</sub> H <sub>12</sub> | 91   | 80  |
| 2,2-Dimethylbutane        | i-Paraffin | C <sub>6</sub> H <sub>14</sub> | 92   | 93  |
| 3-Methyl-2-pentene        | Olefin     | C <sub>6</sub> H <sub>12</sub> | 97   | 81  |
| 4-Methyl-2-pentene        | Olefin     | C <sub>6</sub> H <sub>12</sub> | 99   | 84  |
| Benzene                   | Aromatic   | C <sub>6</sub> H <sub>6</sub>  | >100 | 106 |
| n-Heptane                 | n-Paraffin | C <sub>7</sub> H <sub>16</sub> | -27  | 0   |
| Methylcyclohexane         | Naphthene  | C <sub>7</sub> H <sub>14</sub> | 75   | 71  |
| 2-Methylhexane            | i-Paraffin | C <sub>7</sub> H <sub>16</sub> | 42   | 46  |
| 2,2-Dimethylpentane       | i-Paraffin | C <sub>7</sub> H <sub>16</sub> | 93   | 96  |
| 2,2,3-Trimethylbutane     | i-Paraffin | C <sub>7</sub> H <sub>16</sub> | 116  | 101 |
| Toluene                   | Aromatic   | C <sub>7</sub> H <sub>8</sub>  | >100 | 109 |
| n-Octane                  | n-Paraffin | C <sub>8</sub> H <sub>18</sub> | <0   | <0  |
| Isooctane                 | n-Paraffin | C <sub>8</sub> H <sub>18</sub> | 100  | 100 |
| 2,2,4-Trimethyl-1-pentene | Olefin     | C <sub>8</sub> H <sub>16</sub> | >100 | 86  |
| 2,2,4-Trimethyl-2-pentene | Olefin     | C <sub>8</sub> H <sub>16</sub> | >100 | 86  |
| o-, m-, and p-Xylene      | Aromatic   | C <sub>8</sub> H <sub>10</sub> | >100 | 100 |
| Ethylbenzene              | Aromatic   | C <sub>8</sub> H <sub>10</sub> | >100 | 98  |

Many refinery streams have the right vapor pressure, boiling range, and octane to end up in the gasoline pool. Table 23 shows properties for stocks recently used to make gasoline in a European refinery. The raffinate came from an aromatics extraction unit, and the pyrolysis gasoline came from a nearby ethylene plant.

Table 23. Gasoline Blend Stock Properties: Example

| Component             | Density<br>(kg/m <sup>3</sup> ) | RVP<br>(bar) | Boiling Range |           | RON   | MON  |
|-----------------------|---------------------------------|--------------|---------------|-----------|-------|------|
|                       |                                 |              | °C            | °F        |       |      |
| Butanes               | 0.575                           | 3.6          | -12 to -0.5   | 10.4 – 31 | 97    | 95   |
| Straight-run Gasoline | 0.64                            | 1.15         | 27 – 80       | 81 – 176  | 80.2  | 76.6 |
| Reformate             | 0.815                           | 0.08         | 78 – 197      | 172 – 387 | 100.5 | 89.5 |
| Raffinate             | 0.685                           | 0.3          | 65 – 112      | 149 – 234 | 60.3  | 54.5 |
| Hvy FCC Gasoline      | 0.76                            | 0.2          | 43 – 185      | 109 – 365 | 90.5  | 79.5 |
| Light FCC Gasoline    | 0.66                            | 1.3          | 25 – 89       | 77 – 192  | 94.5  | 81.5 |
| Pyrolysis Gasoline    | 0.845                           | 0.3          | 47 – 180      | 117 – 356 | 101.5 | 86.5 |
| Alkylate              | 0.705                           | 0.3          | 39 – 195      | 102 – 383 | 98    | 93.5 |
| MTBE                  | 0.746                           | 0.5          | 48 – 62       | 118 – 144 | 115   | 97   |

## 8.2.2 Reformulated Gasoline (RFG)

In 1970, gasoline blending became more complex. The U.S. Clean Air Act required the phase-out of tetraethyl lead, so refiners had to find other ways to provide octane. In 1990, the Clean Air Act was amended. It empowered EPA

to impose emissions limits on automobiles and to require reformulated gasoline (RFG).

Phase I RFG regulations (*Table 24*) required a minimum amount of chemically bound oxygen, imposed upper limits on benzene and Reid Vapor Pressure (RVP), and ordered a 15% reduction in volatile organic compounds (VOC) and air toxics. VOC react with atmospheric NO<sub>x</sub> to produce ground-level ozone. Air toxics include 1,3-butadiene, acetaldehyde, benzene, and formaldehyde.

Oxygen can be supplied as ethanol or C<sub>5</sub> to C<sub>7</sub> ethers. The ethers (*Table 25*) have excellent blending octanes and low vapor pressures. This makes them highly desirable gasoline blend stocks. Due to the detection of MTBE in ground water, the future for MTBE is questionable, especially since 1999, when the Governor of California issued an executive order requiring the phase-out of MTBE as a component of gasoline. But in Finland and many other European countries, MTBE is still considered a premium, relatively safe blend stock.<sup>33</sup>

*Table 24.* Simple Model RFG Specifications

| Property                 | Specification |
|--------------------------|---------------|
| Oxygen, wt%              | 2.0 max       |
| Benzene, vol%            | 1.0 max       |
| RVP, Summer              |               |
| Class B (psi)            | 7.2 max       |
| Class B (kPa)            | 50 max        |
| Class C (psi)            | 8.1 max       |
| Class C (kPa)            | 56 max        |
| VOC (summer)             | 15% reduction |
| Air toxics               | 15% reduction |
| Sulfur                   | Same as 1990  |
| T90*, olefins, aromatics | Same as 1990  |

\*T90 is the temperature at which 90% of a gasoline blend evaporates.

RFG was implemented in two phases. The Phase I program started in 1995 and mandated RFG for 10 large metropolitan areas. Several other cities and four entire states joined the program voluntarily. In the year 2000, about 35% of the gasoline in the United States was reformulated.

The regulations for Phase II, which took force in January 2000, are based on the EPA Complex Model, which estimates exhaust emissions for a region

*Table 25.* Blending octane and RVP of ethers and alcohols

| Ether or Alcohol            | Blending Octane (RON) | Blending RVP (psi) | Blending RVP (kPa) |
|-----------------------------|-----------------------|--------------------|--------------------|
| Methanol                    | 133                   | 58-62              | 400-427            |
| Ethanol                     | 130                   | 18-22              | 124-152            |
| Methyl-t-butyl ether (MTBE) | 118                   | 8-10               | 55-69              |
| Ethyl-t-butyl ether (ETBE)  | 118                   | 3-5                | 21-34              |
| t-Amyl methyl ether (TAME)  | 111                   | 1-2                | 7-14               |



based on geography, time of year, mix of vehicle types, and – most important to refiners – fuel properties (*Table 26*).

By intent, Phase II is a regulation based on emissions instead of a formula. But refiners don't have to measure the tail-pipe emissions of every gasoline blend. Instead, they can use EPA's computer model – called MOBILE6 – to calculate emissions. By law, complex-model calculations are just as valid as dynamometer tests with vehicles.

*Table 26.* Example of Product Property Ranges Calculated by the Phase II Complex Model

| Property  | Reformulated gasoline |          | Conventional gasoline |          |
|-----------|-----------------------|----------|-----------------------|----------|
|           | Low end               | High end | Low end               | High end |
| Oxygen    | 0                     | 3.7      | 0                     | 3.7      |
| Sulfur    | 0                     | 500      | 0                     | 1000     |
| RVP       | 6.4                   | 10       | 6.4                   | 11       |
| E200      | 30                    | 70       | 30                    | 70       |
| E300      | 70                    | 95       | 70                    | 100      |
| Aromatics | 10                    | 50       | 0                     | 55       |
| Olefins   | 0                     | 25       | 0                     | 30       |
| Benzene   | 0                     | 2        | 0                     | 4.9      |
| MTBE      | 0                     | 3.7      | 0                     | 3.7      |
| ETBE      | 0                     | 3.7      | 0                     | 3.7      |
| Ethanol   | 0                     | 3.7      | 0                     | 3.7      |
| TAME      | 0                     | 3.7      | 0                     | 3.7      |

In practice, blending under the complex model can be less restrictive than blending to a recipe, because changing the amount of one blend-stock (for examples, due to a sudden increase or decrease in availability) can be offset by changes in others.

### 8.2.3 Gasoline Additives

*Table 27* lists the kinds of additives used to prepare finished gasoline. Additive packages vary from season-to-season, region-to-region, and retailer to retailer. “After-market” additives contain similar types of ingredients and usually are more concentrated. They are packaged so that they can be added by consumers to the fuel tanks of individual automobiles.

*Table 27.* Additives Used in Gasoline

| Additive Type           | Function  |
|-------------------------|---|
| Anti-oxidation          | Minimize oxidation and gum formation during storage   |
| Metal passivation       | Deactivate trace metals that can accelerate oxidation |
| Corrosion inhibition    | Minimize rust throughout the gasoline supply chain    |
| Anti-icing              | Minimize ice in carburetors during cold weather       |
| IVD control (detergent) | Control deposition of carbon on intake valves         |
| CCD control             | Control deposition of carbon in combustion chambers   |
| Anti-knock              | Methylcyclopentadienyl manganese tricarbonyl (MMT)    |

### 8.2.4 Low-Sulfur Gasoline and Ultra-Low-Sulfur Diesel

In recent years, the U.S. Environmental Protection Agency (EPA) and the European Parliament promulgated clean-fuel regulations that are lowering the sulfur content of gasoline and diesel fuel. New sulfur-content standards for several developed countries are shown in *Table 28*, which also shows the target dates for implementation.

*Table 28. Clean Fuels: Limits on Sulfur*

| Country                     | Fuel Sulfur Content, wppm |              |              |
|-----------------------------|---------------------------|--------------|--------------|
|                             | 2004 Level                | Target Level | Target Date  |
| US <sup>34-36</sup>         |                           |              |              |
| Gasoline                    | >300                      | 30           | 2004 – 2008  |
| Diesel, on-road             | 500                       | 15           | July 1, 2006 |
|                             | -                         | -            | July 1, 2010 |
| Diesel, off-road            | 2000 – 3500               | 500          | 2007         |
|                             | -                         | 15           | 2010         |
| Canada <sup>37</sup>        |                           |              |              |
| Gasoline                    | 150                       | 30           | 2005         |
| Diesel                      | 500                       | 15           | 2006         |
| Germany <sup>38</sup>       |                           |              |              |
| Gasoline                    | 10                        | 10           | 2003         |
| Diesel                      | 10                        | 10           | 2003         |
| Sweden <sup>39</sup>        |                           |              |              |
| Diesel                      | 10                        | 10           | 1995         |
| Other EU <sup>38</sup>      |                           |              |              |
| Gasoline                    | 150                       | 50           | 2005         |
|                             | -                         | 10           | 2008         |
| Diesel                      | 350                       | 50           | 2005         |
|                             | -                         | 10           | 2008         |
| Australia <sup>40</sup>     |                           |              |              |
| Gasoline                    | 500                       | 150          | 2005         |
| Diesel                      | 500                       | 30           | 2008         |
| Korea (South) <sup>41</sup> |                           |              |              |
| Gasoline                    | 100                       | 30           | 2006         |
| Diesel                      | 300                       | 50           | 2006         |
| Japan <sup>42</sup>         |                           |              |              |
| Gasoline                    | 100                       | 10           | 2008         |
| Diesel                      | 500                       | 50           | 2004         |
|                             | -                         | 10           | 2008         |

Table 29 shows that, prior to 2004, FCC gasoline was by far the major source of sulfur in gasoline,<sup>43</sup> typically accounting for 85 – 95% of the total sulfur in the blending pool.<sup>44</sup> Obviously, to reduce the sulfur content of gasoline, sulfur either must be kept out of FCC feed or removed from FCC product(s). Both approaches are being used. FCC feed desulfurization is discussed in Section 3.4.2. FCC gasoline post-treating is discussed below.

Table 29. Sources of Sulfur in Gasoline (before 2004)

| Component                  | Contribution to the Gasoline Pool (vol%) | Contribution to Sulfur in the Pool (%) |
|----------------------------|--|--|
| Alkylate                   | 12                                       | 0                                      |
| Coker naphtha              | 1  | 1                                      |
| Hydrocracker naphtha       | 2  | 0                                      |
| FCC gasoline               | 36                                       | 98                                     |
| Isomerate                  | 5  | 0                                      |
| Light straight-run naphtha | 3  | 1                                      |
| Butanes                    | 5  | 0                                      |
| MTBE                       | 2  | 0                                      |
| Reformate                  | 34                                       | 0                                      |
| Total                      | 100                                      | 100                                    |

### 8.2.5 FCC Gasoline Post-Treating

**Hydrotreating FCC Gasoline.** Conventional hydrotreating does a good job of removing sulfur from FCC gasoline. Unfortunately, it also does a good job of reducing octane by saturating C<sub>6</sub>-C<sub>10</sub> olefins. In recent years, the industry has developed several processes to remove sulfur at minimum octane loss. Licensors include Axens (IFP), CDTECH, ExxonMobil, and UOP.

**Sulfur Removal by Selective Adsorption.** The ConocoPhillips S Zorb process uses selective adsorption to remove sulfur from FCC gasoline.<sup>44</sup> The feed is combined with a small amount of hydrogen, heated, and injected into an expanded fluid-bed reactor, where a proprietary sorbent removes sulfur from the feed. A disengaging zone in the reactor removes suspended sorbent from the vapor, which exits the reactor as a low-sulfur stock suitable for gasoline blending.

The sorbent is withdrawn continuously from the reactor and sent to the regenerator section, where the sulfur is removed as SO<sub>2</sub> and sent to a sulfur recovery unit. The clean sorbent is reconditioned and returned to the reactor. The rate of sorbent circulation is controlled to help maintain the desired sulfur concentration in the product.

## 8.3 Kerosene and Jet Fuel

Kerosene, jet fuel, and turbine fuel have similar boiling ranges. The key product properties are:

- Flash point
- Freezing point
- Sulfur content
- Smoke point

The flash point is the lowest temperature at which a liquid gives off enough vapor to ignite when an ignition source is present. The freezing point is especially important for jet aircraft, which fly at high altitudes where the outside temperature is very low. Sulfur content is a measure of corrosiveness.

The measurement of smoke point goes back to the days when the primary use for kerosene was to fuel lamps. To get more light from a kerosene lamp, you could turn a little knob to adjust the wick. But if the flame got too high, it gave off smoke. Even today, per ASTM D1322, smoke point is the maximum height of flame that can be achieved with calibrated wick-fed lamp, using a wick “of woven solid circular cotton of ordinary quality.”

The smoke point of a test fuel is compared to reference blends. A standard 40%/60% (volume/volume) mixture of toluene with 2,2,4-trimethylpentane has a smoke point of 14.7, while pure 2,2,4-trimethylpentane has a smoke point of 42.8. Clearly, isoparaffins have better smoke points than aromatics.

*Table 30* shows specifications for five grades of jet fuel, otherwise known as aviation turbine fuel. The JP fuels are for military aircraft.

*Table 30. Specifications for Aviation Turbine Fuels*

| Specification          | Jet A                        | Jet B   | JP-4    | JP-5    | JP-8    |
|------------------------|------------------------------|---------|---------|---------|---------|
| Flash point, °C (min)  | 38                           | -       | -       | 60      | 38      |
| Freeze point, °C (max) | -40 (Jet A)<br>-47 (Jet A-1) | -50     | -58     | -46     | -47     |
| API Gravity            | 37 – 51                      | 45 – 57 | 45 – 57 | 36 – 48 | 37 – 51 |
| Distillation, °C       |                              |         |         |         |         |
| 10% max                | 205                          | -       |         | 205     | 205     |
| 20% max                | -                            | 145     | 145     | -       | -       |
| 50% max                | -                            | 190     | 190     | -       | -       |
| 90% max                | -                            | 245     | 245     | -       | -       |
| EP                     | 300                          | -       | 270     | 290     | 300     |
| Sulfur, wt% max        | 0.3                          | 0.3     | 0.4     | 0.4     | 0.3     |
| Aromatics, vol% max    | 22                           | 22      | 25      | 25      | 25      |
| Olefins, vol% max      | -                            | -       | 5       | 5       | 5       |

## 8.4 Diesel Blending

Diesel blending is simpler than gasoline blending because the limitations are fewer. Only sulfur, cetane number, and (in some countries) aromatics and density are regulated for environmental reasons. Sulfur contributes heavily to particulate emissions from diesel engines, and cetane number is a measure of burning quality in a diesel engine. As with octane number, cetane number measures the tendency of fuels to auto-ignite in a standard test engine. It is easier to start a diesel engine when the cetane number of the fuel is high.

The reference fuels for ASTM D613, which describes the test method for cetane number, are n-cetane,  $\alpha$ -methyl-naphthalene, and heptamethylnonane, for which cetane numbers are defined to be 100, 0, and 15, respectively. *Table 31* shows cetane numbers for selected pure compounds.<sup>45</sup>

Table 31. Cetane Numbers for Selected Pure Compounds

| Compound                    | Type           | Carbons | Formula                         | Cetane No. |
|-----------------------------|----------------|---------|---------------------------------|------------|
| n-Decane                    | Paraffin       | 10      | C <sub>10</sub> H <sub>22</sub> | 76         |
| Decalin                     | Naphthene      | 10      | C <sub>10</sub> H <sub>18</sub> | 48         |
| α-Methylnaphthalene         | Aromatic       | 11      | C <sub>11</sub> H <sub>10</sub> | 0*         |
| n-Pentylbenzene             | Aromatic       | 11      | C <sub>11</sub> H <sub>16</sub> | 8          |
| 3-Ethyldecane               | Paraffin (iso) | 12      | C <sub>12</sub> H <sub>26</sub> | 48         |
| 4,5-Diethyloctane           | Paraffin (iso) | 12      | C <sub>12</sub> H <sub>26</sub> | 20         |
| 3-Cyclohexylhexane          | Naphthene      | 12      | C <sub>12</sub> H <sub>24</sub> | 36         |
| Biphenyl                    | Aromatic       | 12      | C <sub>12</sub> H <sub>10</sub> | 21         |
| α-Butylnaphthalene          | Aromatic       | 14      | C <sub>14</sub> H <sub>16</sub> | 6          |
| n-Pentadecane               | Paraffin       | 15      | C <sub>15</sub> H <sub>32</sub> | 95         |
| n-Nonylbenzene              | Aromatic       | 15      | C <sub>15</sub> H <sub>24</sub> | 50         |
| n-Hexadecane (cetane)       | Paraffin       | 16      | C <sub>16</sub> H <sub>34</sub> | 100*       |
| 2-Methyl-3-cyclohexylnonane | Naphthene      | 16      | C <sub>16</sub> H <sub>34</sub> | 70         |
| Heptamethylnonane           | Paraffin (iso) | 16      | C <sub>16</sub> H <sub>34</sub> | 15*        |
| 8-Propylpentadecane         | Paraffin (iso) | 18      | C <sub>18</sub> H <sub>38</sub> | 48         |
| 7,8-Diethyltetradecane      | Paraffin (iso) | 18      | C <sub>18</sub> H <sub>38</sub> | 67         |
| 2-Octylnaphthalene          | Aromatic       | 18      | C <sub>18</sub> H <sub>24</sub> | 18         |
| n-Eicosane                  | Paraffin       | 20      | C <sub>20</sub> H <sub>42</sub> | 110        |
| 9,10-Dimethyloctane         | Paraffin (iso) | 20      | C <sub>20</sub> H <sub>42</sub> | 59         |
| 2-Cyclohexyltetradecane     | Naphthene      | 20      | C <sub>20</sub> H <sub>40</sub> | 57         |

\* Used as a standard for ASTM D976

Cetane index, as defined by ASTM D976, is not a measurement, but the result of a calculation based on density and mid-boiling point. It is nearly the same as the cetane number for diesel fuels comprised mostly of straight-run gas oils blended with lesser amounts of cracked stocks. Diesel index is a simpler calculation based on density and aniline point. The streams listed in Table 32 are typical candidates for making diesel fuel.

Table 32. Properties of U.S. Diesel Blend Stocks, Year 2000 (California Excluded)<sup>46</sup>

| Blend Stock                  | Percent of Total U.S. Pool | Sulfur (wt%) | API Gravity | Cetane (no additives) |
|------------------------------|----------------------------|--------------|-------------|-----------------------|
| Straight-run gas oil         | 12.4                       | 0.222        | 30.3 – 42.2 | 40.3 – 45.0           |
| Hydrotreated straight-run    | 51.9                       | 0.036        | 29.9 – 42.9 | 44.5 – 50.4           |
| FCC light cycle oil          | 3.1                        | 0.532        | 22.3 – 33.1 | <<30                  |
| Hydrotreated light cycle oil | 19.4                       | 0.087        | 30.7 – 45.0 | 42.7 – 44.1           |
| Coker gas oil                | 1.0                        | 0.342        | 32.3 – 42.4 | <<30                  |
| Hydrotreated coker gas oil   | 8.2                        | 0.026        | 29.9 – 34.8 | 36.1 – 45.3           |
| Hydrocrackate                | 4.0                        | 0.008        | 32.9 – 41.8 | 50.2                  |

Table 33 presents clean-diesel specifications for the European community, which were based on two extensive research programs – Auto Oil I and Auto Oil II. Automobile manufacturers, oil refining companies, and government agencies participated in both programs. Auto Oil I lasted four years, from 1992 to 96. Auto Oil II was launched in 1997, and the final report was issued in October 2000. The purpose of the programs was to find ways to reduce emissions from gasoline and diesel-powered vehicles, considering public health, technology and economics.

Table 33. EU Specifications for Automotive Diesel

| Specification                   | Units             | Year 2000 Limits | Possible Future Limits |
|---------------------------------|-------------------|------------------|------------------------|
| Cetane number                   |                   | 51 (min)         | 55 (min)               |
| Cetane index                    |                   | No spec          | 52 (min)               |
| Density @ 15°C                  | g/cm <sup>3</sup> | 0.845 (max)      | 0.84                   |
| Distillation                    |                   |                  |                        |
| 90% boiling point               | °F                | no spec          | 608 (max)              |
| 95% boiling point               | °F                | 680 (max)        | 644 (max)              |
| Final boiling point             | °F                | no spec          | 662 (max)              |
| 90% boiling point               | °C                | no spec          | 320 (max)              |
| 95% boiling point               | °C                | 360 (max)        | 340 (max)              |
| Final boiling point             | °C                | no spec          | 350 (max)              |
| Polyaromatic hydrocarbons (PAH) | wt%               | 11 (max)         | 2 (max)                |
| Total aromatics                 | wt%               | no spec          | 15 (max)               |
| Sulfur                          | wppm              | 350 (max)*       | 10 (max)               |

- As discussed elsewhere, diesel sulfur will be limited to 50 wppm in 2005.

Catalytic converters led to the elimination of lead from gasoline, because lead poisons the converter catalyst. Similarly, sulfur poisons catalysts that may be used on future vehicles. Hence, the reduction of sulfur in gasoline and diesel fuel to ultra-low levels is a key requirement of Auto Oil II.

Around the world, the transportation and fungibility of ultra-clean fuels is a major concern. For common-carrier pipelines, which transport various products made by different refiners, cross-contamination is a major concern. The interface layer between shipments is called “trans mix.” If a shipment of gasoline containing 30 wppm of sulfur follows a batch of diesel containing 500 wppm of sulfur, the sulfur-contaminated trans mix could comprise more than 20% of the gasoline. Consequently, several pipeline companies have announced that in the future they will not transport any high-sulfur material.

Other important diesel-fuel properties include flash point, cloud point, pour point, kinematic viscosity, and lubricity. Cloud point and pour point indicate the temperature at which the fuel tends to thicken and then gel in cold weather. In addition to providing energy, diesel fuel also serves as a lubricant for fuel pumps and injectors, which prolongs the life of the engine. Viscosity measures the tendency of a fluid to flow. In a diesel engine, viscosity indicates how well a fuel atomizes in spray injectors. It also measures its quality as a lubricant for the fuel system. Lubricity measures the fuel’s ability to reduce friction between solid surfaces in relative motion. It indicates how the engine will perform when loaded.

#### 8.4.1 Diesel Additives

Chemical additives improve the performance and extend the tank-life of diesel fuels. Typical types of additives are shown in *Table 34*.

Table 34. Additives Used in Diesel Fuel

| Additive Type         | Function  |
|-----------------------|---|
| Anti-oxidation        | Minimize oxidation and gum formation during storage   |
| Cetane improvement    | Increase cetane number                                |
| Dispersion            | Improve behavior in fuel injectors                    |
| Anti-icing            | Minimize ice formation during cold weather            |
| Detergent             | Control deposition of carbon in the engine            |
| Metal passivation     | Deactivate trace metals that can accelerate oxidation |
| Corrosion inhibition  | Minimize rust throughout the diesel fuel supply chain |
| Cold-flow improvement | Improve flow characteristics in cold weather          |

## 9. PROTECTING THE ENVIRONMENT

The ways in which the refining industry protects the environment are discussed in more detail in Chapter 14, Environmental Pollution Control. In this section, we provide a brief overview of the methods used to improve air quality, prevent water pollution, and dispose of solid wastes.

### 9.1 Air Quality

In the 1970s and 1980s, environmental laws compelled refineries to reduce emissions of SO<sub>x</sub>, NO<sub>x</sub>, CO<sub>2</sub>, and hydrocarbons. In the atmosphere, SO<sub>x</sub> reacts with water vapor to make sulfurous and sulfuric acids, which return to earth as acid rain. Volatile hydrocarbons react with NO<sub>x</sub> to make ozone. CO<sub>2</sub> is a major “green-house” gas. To reduce these pollutants, the industry tightened its operation by:

- Reducing fugitive hydrocarbon emissions from valves and fittings
- Removing sulfur from refinery streams and finished products
- Adding tail-gas units to sulfur recovery plants
- Reducing the production of NO<sub>x</sub> in fired heaters
- Scrubbing SO<sub>x</sub> and NO<sub>x</sub> from flue gases
- Reducing the production of CO<sub>2</sub> by increasing energy efficiency

#### 9.1.1 Sulfur Recovery

Conversion processes, hydrotreaters, and sweetening units remove chemically bound sulfur from petroleum fractions. That’s a good thing, but where does the sulfur go? The answer depends upon the form in which it is produced.

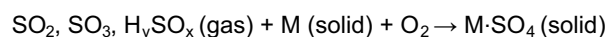
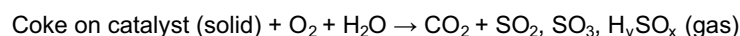
**SO<sub>x</sub> Abatement.** Fuel-oil fired heaters and the regenerators of FCC units are major sources of refinery SO<sub>x</sub> and NO<sub>x</sub> emissions. The most obvious way to reduce SO<sub>x</sub> emissions from a heater is to use low-sulfur fuels. Unfortunately, although that solution requires no investment, it is probably

the most expensive due to the relatively high cost of buying low-sulfur fuel oil or hydrotreating high-sulfur fuel oil.

A large fraction of the sulfur in the feed to an FCC unit ends up in coke on the catalyst. SO<sub>x</sub> is formed in the regenerator when the coke is burned away. Therefore, removing sulfur from the feed decreases SO<sub>x</sub> emissions.

As stated in Section 3.4.2, using a hydrotreater or hydrocracker for feed HDS eliminates or minimizes the cost of post-FCC desulfurization equipment. Removing basic nitrogen decreases deactivation of acid sites on the FCC catalyst, which allows the FCC to reach a given conversion at lower temperatures. The saturation of aromatics in the feed pretreater provides the biggest benefit, because it converts hard-to-crack aromatics into easier-to-crack naphthenes. This alone can justify the installation of an FCC feed pretreater. Therefore, in addition to abating SO<sub>x</sub>, hydrotreating the feed to an FCC can generate a substantial return.<sup>43</sup>

#### FCC Regenerator (Oxidizing Environment)



#### FCC Riser/Reactor (Reducing Environment)

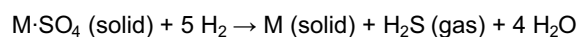


Figure 25. Mechanism of SO<sub>x</sub> transfer in FCC units.

**SO<sub>x</sub> Transfer Additives.** Arguably, SO<sub>x</sub> transfer additives are the most cost-effective way to lower SO<sub>x</sub> emissions in an FCC unit. These materials, first developed by Davison Chemical, react with SO<sub>x</sub> in the FCC regenerator to form sulfates (Figure 25). When the sulfated additive circulates to the riser/reactor section, the sulfate is reduced to H<sub>2</sub>S, which is recovered by amine absorption and sent to the sulfur plant. In some units, these additives reduce FCC SO<sub>x</sub> emissions by more than 70%. Consequently, if a pre-treater or post-treater still must be installed, its size can be reduced.

**Flue-Gas (Stack-Gas) Scrubbing.** Flue-gas scrubbing is a refiner's last chance to keep NO<sub>x</sub> and SO<sub>x</sub> out of the air. In wet flue-gas desulfurization, gas streams containing SO<sub>x</sub> react with an aqueous slurry containing calcium hydroxide Ca(OH)<sub>2</sub> and calcium carbonate CaCO<sub>3</sub>. Reaction products include calcium sulfite (CaSO<sub>3</sub>) and calcium sulfate (CaSO<sub>4</sub>), which precipitate from the solution.

NO<sub>x</sub> removal is more difficult. Wet flue-gas scrubbing removes about 20% of the NO<sub>x</sub> from a typical FCC flue gas. To remove the rest, chemical reducing agents are used. In the Selective Catalytic Reduction (SCR) process, anhydrous ammonia is injected into the flue gas as it passes through a bed of



catalyst at 500 to 950°F (260 to 510°C). The chemical reaction between NO<sub>x</sub> and ammonia produces N<sub>2</sub> and H<sub>2</sub>O.

**Hydrogen Sulfide Removal.** When sulfur-containing feeds pass through hydrotreaters or conversion units, some or most of the sulfur is converted into H<sub>2</sub>S, which eventually ends up in off-gas streams. Amine absorbers remove the H<sub>2</sub>S, leaving only 10 to 20 wppm in the treated gas streams. H<sub>2</sub>S is steam-stripped from the amines, which are returned to the absorbers. The H<sub>2</sub>S goes to the refinery sulfur plant.

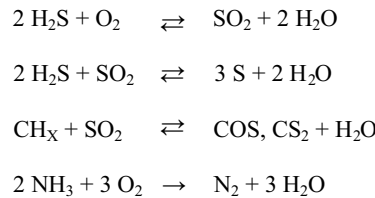


Figure 26. Claus reactions.

**Claus Sulfur Recovery Process.** At the sulfur plant, H<sub>2</sub>S is combined with sour-water stripper off-gas and sent to a Claus unit. Invented in 1881 by Carl Freidrich Claus,<sup>47</sup> almost every refinery in the world uses some version of this process to convert H<sub>2</sub>S into elemental sulfur. A simplified version of Claus-reaction chemistry is shown in Figure 26.

Figure 27 shows a process schematic for a Claus unit. H<sub>2</sub>S and a carefully controlled amount of air are mixed and sent to a burner, where about 33% of the H<sub>2</sub>S is converted to SO<sub>2</sub> and water. From the burner, the hot gases go to a reaction chamber, where the reactions shown in Figure 26 reach equilibrium. In several units, the air is enriched with oxygen to increase plant capacity.

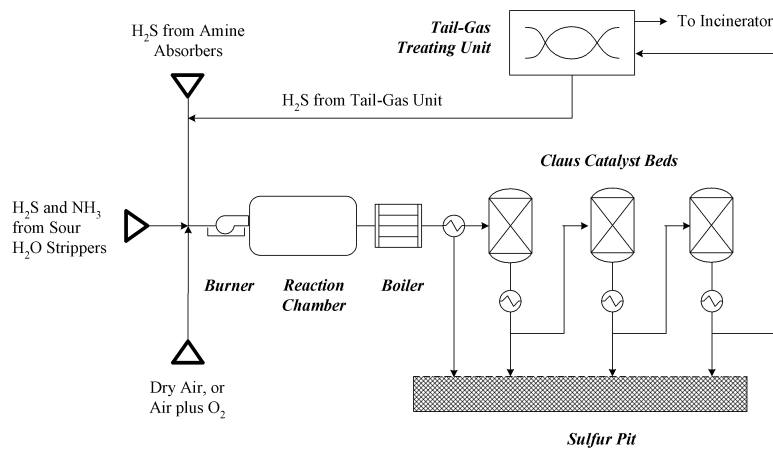


Figure 27. Claus process.

As shown, elemental sulfur is produced by the reversible reaction between  $\text{SO}_2$  and  $\text{H}_2\text{S}$ .  $\text{COS}$  and  $\text{CS}_2$  appear in small amounts, but even traces of these compounds are hard to remove in tail-gas treating units. Ammonia comes in with the sour-water stripper off-gas. In the Claus process, it is thermally decomposed into nitrogen and water.

In the Claus burner, combustion temperatures reach  $2200^\circ\text{F}$  ( $1200^\circ\text{C}$ ). Needless to say, this generates a tremendous amount of heat. Much of the heat is recovered in a waste-heat boiler, which generates steam as it drops the temperature to  $700^\circ\text{F}$  ( $370^\circ\text{C}$ ).

Next, the process gas goes to a condenser, where it is cooled to about  $450^\circ\text{F}$  ( $232^\circ\text{C}$ ). At this temperature, sulfur vapors condense, and the resulting molten sulfur flows through a drain to a heated sulfur-collection pit. At the bottom of the drain, a seal leg maintains system pressure and keeps unconverted gases out of the pit.

Uncondensed sulfur and other gases flow to a series of catalyst beds, which recover additional sulfur by promoting the reaction between left-over  $\text{H}_2\text{S}$  and  $\text{SO}_2$ . With fresh catalyst and a stoichiometric gas composition, the cumulative recovery of sulfur after the four condensers is about 50%, 80%, 95%, and 96-98%, respectively.

Tail-gas treating units (TGTU) bring the total sulfur recovery up to  $>99.9\%$ . Most tail-gas treating processes send the tail gas to a hydrotreater, which converts all sulfur-containing compounds ( $\text{SO}_2$ ,  $\text{SO}_3$ ,  $\text{COS}$ ,  $\text{CS}_2$  and  $\text{S}_x$ ) into  $\text{H}_2\text{S}$ . In the SCOT process, offered by Shell Global Solutions, the  $\text{H}_2\text{S}$  is absorbed by an amine and returned to the front of the Claus furnace. In the LO-CAT<sup>®</sup> process, offered by Merichem,  $\text{H}_2\text{S}$  is air-oxidized to sulfur in an aqueous solution containing a chelated iron catalyst.

For all tail-gas treatment processes, the last traces of unrecovered sulfur go to an incinerator, where they are converted into  $\text{SO}_2$  and dispersed into the atmosphere.

## 9.2 Waste Water Treatment

Waste water treatment is used to purify process water, runoff, and sewage. As much as possible, purified waste-water streams are re-used in the refinery. Wastewater streams may contain suspended solids, dissolved salts, phenols, ammonia, sulfides, and other compounds. The streams come from just about every process unit, especially those that use wash water, condensate, stripping water, caustic, or neutralization acids.

### 9.2.1 Primary Treatment

Primary treatment uses a settling pond to allow most hydrocarbons and suspended solids to separate from the wastewater. The solids drift to the

bottom of the pond, hydrocarbons are skimmed off the top, and oily sludge is removed. Difficult oil-in-water emulsions are heated to expedite separation.

Acidic wastewater is neutralized with ammonia, lime, or sodium carbonate. Alkaline wastewater is treated with sulfuric acid, hydrochloric acid, carbon dioxide-rich flue gas, or sulfur.

### 9.2.2 Secondary Treatment

Some suspended solids remain in the water after primary treatment. These are removed by filtration, sedimentation or air flotation. Flocculation agents may be added to consolidate the solids, making them easier to remove by sedimentation or filtration. Activated sludge is used to digest water-soluble organic compounds, either in aerated or anaerobic lagoons. Steam-stripping is used to remove sulfides and/or ammonia, and solvent extraction is used to remove phenols.

### 9.2.3 Tertiary Treatment

Tertiary treatment processes remove specific pollutants, including traces of benzene and other partially soluble hydrocarbons. Tertiary water treatment can include ion exchange, chlorination, ozonation, reverse osmosis, or adsorption onto activated carbon. Compressed oxygen may be used to enhance oxidation. Spraying the water into the air or bubbling air through the water removes remaining traces of volatile chemicals such as phenol and ammonia.

## 9.3 Solid Waste

Refinery solid wastes may include the following materials:

- Spent catalyst and catalyst fines
- Acid sludge from alkylation units
- Miscellaneous oil-contaminated solids

All oil-contaminated solids are treated as hazardous and sent to sanitary landfills. Recently, super-critical extraction with carbon dioxide has been used with great success to remove oil from contaminated dirt.

## 10. POWER, STEAM, HYDROGEN, AND CO<sub>2</sub>

Utilities are a critical ingredient in petroleum processing. After excluding the cost of crude oil and other raw materials, power and steam account for almost half of a refinery's operating costs.

Due to clean-fuel regulations, many refineries are implementing hydrogen recovery/purification projects and/or installing steam/hydrocarbon reformers to generate on-purpose hydrogen.

## 10.1 Power

Refineries purchase electricity from outside sources, but they also produce much of their own power with steam turbines or gas engines. Electrical substations distribute power throughout the facility. For safety reasons, substations are located far away from sources of combustible vapors.

## 10.2 Steam

Steam production and distribution systems are quite complex, involving 3 to 4 different steam qualities and hundreds of pipes and valves. Cooling towers and evaporators are used to dispose of unused steam.

Steam is generated by boilers and heat-producing process units. FCC units, Claus units, and steam/hydrocarbon reformers (hydrogen plants) are major sources of refinery steam.

Steam boilers are fired with refinery fuel gas, natural gas, and/or fuel oil. Fuel oil is a blend of residual oils with flow-improving cutter stocks. Usually, it is pumped through a series of strainers before being burned.

Refinery fuel gas is collected from process units, sweetened in amine absorbers, and sent to a balance drum. Natural gas and LPG may be used to augment the fuel gas supply, and to replace it when needed. The balance drum stabilizes system pressure and calorific content. It also provides a place for suspended liquids to separate from the gas.

Boiler feedwater (BFW) is used for steam generation. BFW must be free of contaminants, because salts and dissolved gases, particularly CO<sub>2</sub> and O<sub>2</sub>, can cause extensive corrosion.

## 10.3 Hydrogen and CO<sub>2</sub>

Due to the extra hydrotreating required by clean-fuel regulations, refiners are looking for additional sources of hydrogen, which can be recovered from off-gas streams or generated by new hydrogen plants. Chapter 26 by Nick Hallale, Ian Moore and Dennis Vauk describes a methodology for optimizing hydrogen recovery from existing refinery hydrogen networks. For new hydrogen plants, steam-hydrocarbon reforming is used. This process is described in detail in Chapter 25 by Andrew Crews and Gregory Shumake and in the Chapter 24 by Milo Meixell. A brief overview is given in this section.

The feed gas for a steam-hydrocarbon reformer can be natural gas, refinery off-gas, or a mixture of the two. The feed gas is desulfurized, mixed with

superheated steam and sent through tubes packed with a nickel-based catalyst. Reaction temperatures are very high – 1100 to 1600°F (593 to 871°C).

The reformed gas, which contains water vapor, H<sub>2</sub>, CO, and CO<sub>2</sub>, is sent through a high-temperature shift (HTS) converter. In the HTS converter, carbon monoxide reacts with steam over an iron-based catalyst to form additional CO<sub>2</sub> and hydrogen.

In modern units, the CO<sub>2</sub> and residual CO and CH<sub>4</sub> are removed by pressure-swing adsorption (PSA). As an option, residual CO is converted to methane in a hydrotreater.

In older units, CO<sub>2</sub> is removed with an absorber containing an amine, Sulfinol<sup>®</sup>, Rectisol<sup>®</sup> or by the Benfield<sup>™</sup> process, which uses hot potassium carbonate. Recovered CO<sub>2</sub> can be sold as a product.

## 11. REFINING ECONOMICS

### 11.1 Costs

The purchase of crude oil and external blend stocks accounts for about 85% of a refinery's operating costs. About half of the remaining 15% is due to energy in the form of fuel and electrical power. Table 35 shows a typical breakdown of plant-wide operating costs. For the refining industry, labor costs are about 2.3% of sales compared to 7.6% for making automobile bodies, 8.3% for plastics, and 12.7% for computers.<sup>48</sup>

About half of the energy used by a refinery is generated from crude oil. In Table 35, crude oil used for energy production is included with "Crude oil and blend stocks." Corporate overhead, interest payments, taxes, and capital depreciation are not included in this analysis.

*Table 35.* Typical breakdown of refinery operating costs.

| <b>Item</b>                | <b>Percent of "Other"</b> | <b>Percent of Total</b> |
|----------------------------|---------------------------|-------------------------|
| Crude oil and blend stocks | –                         | 85                      |
| Other operating costs      |                           |                         |
| Fuel oil, fuel gas         | 40.7                      | 6.1                     |
| Electrical power           | 5.3                       | 0.8                     |
| Maintenance                | 23.3                      | 3.5                     |
| Operations                 | 18                        | 2.7                     |
| Catalysts and chemicals    | 12.7                      | 1.9                     |
| <b>Totals</b>              | <b>100</b>                | <b>100</b>              |

Ultimately, prices for crude oil are set by members of the Organization of Petroleum Exporting Countries (OPEC), which are listed in *Table 36*. The members of OPEC supply about 40% of the world's oil production and own

about 75% of the world's proven oil reserves; consumption within OPEC is very low, so almost all of the produced oil is exported.

Table 36. OPEC Oil Reserves and Production<sup>49</sup>

| Country              | Daily Production, 2002<br>(million barrels) | Proven Reserves, 2003<br>(billion barrels) |
|----------------------|---|--|
| Algeria              | 1.58  | 9.2  |
| Indonesia            | 1.35  | 5.0  |
| Iran                 | 3.53  | 89.7                                       |
| Iraq                 | 2.04  | 112.5                                      |
| Kuwait               | 2.02  | 96.5                                       |
| Libya                | 1.38  | 29.5                                       |
| Nigeria              | 2.12  | 24.0                                       |
| Qatar                | 0.84  | 15.2                                       |
| Saudi Arabia         | 8.71  | 261.8                                      |
| United Arab Emirates | 2.38  | 97.8                                       |
| Venezuela            | 2.91  | 77.8                                       |

Figure 28 illustrates how oil prices have changed since 1861.<sup>50</sup> The bottom trend shows the actual historical prices. The top trend converts the historical prices into 2002 dollars. The big spikes in 1973 and 1978-81 correspond to actions taken by the OPEC cartel. In 1973, the first Arab Oil Embargo caused the average price of oil to rise from about US\$4 per barrel to more than US\$10 per barrel. In 1978, the revolution in Iran triggered another steep increase in prices, which peaked in 1981 at about US\$38 per barrel.

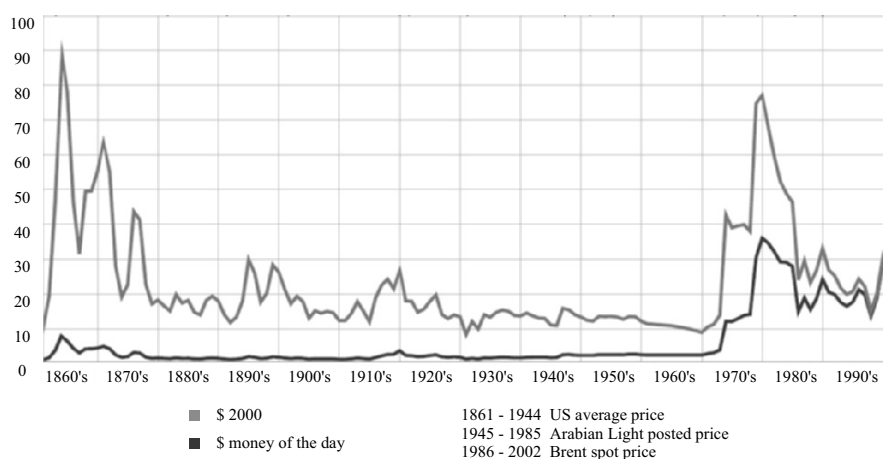


Figure 28. Oil Prices Since 1861 (\$US)

In response to these severe price increases, major oil-consuming countries developed alternatives and implemented energy conservation measures. The member countries of OEDC (Organization for Economic Co-operation and Development) decreased oil demand from 44 million b/d in 1979 to 37

million b/d in 1985. Significantly, France now gets more than 75% of its electricity from nuclear power plants, and most of the rest is hydroelectric.

Slowly but steadily, oil consumption rose from 58 million b/d in 1983 to 75 million b/d in 2002. Most of the rise came from developing countries (*Figure 29*). The price run-up in 2003-05 was caused by increased rates of rising demand in China and India, whose economies were booming. At the same time, there was an (apparent) inability of exporters to keep pace with demand and a lack of spare refining capacity, especially in North America.

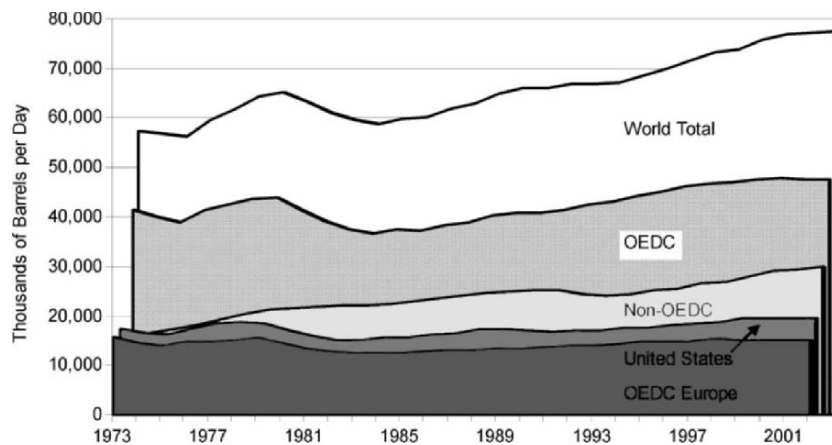


Figure 29. Worldwide Petroleum Processing Capacity Since 1973

Sudden changes in consumption, either up or down, are unlikely due to the long lead-time needed to increase population, build new refining capacity, build plants that produce energy from alternative sources, or implement energy conservation measures. It takes 18 to 24 months to design and install a new crude distillation unit. Alternative energy production plants take a lot longer, especially in the United States, where it takes years to obtain permits for a new plant of significant size.

“Everybody wants power, but nobody wants a power plant in his yard.”

In contrast, supply can change overnight – at least in the minds of oil traders.

## 11.2 Revenues

The economics of some important conversion units are summarized in Table 37. In each case, one major contributor accounts for most of the operating costs. Hydrotreating is an “enabling” process with low margins, but it is essential to the proper functioning of many other units in a refinery.

Table 37. Economics for Selected Conversion Units.

| Process        | Operating Costs<br>(US\$ per bbl) | Major Cost<br>Factor | Percent of<br>Total Cost | Net margin<br>(\$US per bbl) |
|----------------|-----------------------------------|----------------------|--------------------------|------------------------------|
| FCC            | 2.0 – 2.2                         | Fuel                 | 70                       | 4.0 to 5.0                   |
| Cat. Reforming | 3.0                               | Utilities            | 90                       | 2.0 to 2.5                   |
| Alkylation     | 4.8 – 5.5                         | Utilities            | 65 to 75                 | 3.5 to 4.5                   |
| Hydrotreating  | 1.7                               | Hydrogen             | 60 to 70                 | 0.5                          |
| Hydrocracking  | 4.0 to 4.5                        | Hydrogen             | 75 to 80                 | 1.5 to 3.0                   |

## 11.3 Margins

Refinery margins depend on location, size, automation, complexity, and crude and product prices. A good indicator of margins is the “crack spread” – the difference in price between crude oil and refined products.

### 11.3.1 Location, Location, Location

A well-located refinery has lower operating costs and increased operating flexibility. When located near other refineries and petrochemical plants in a coastal industrial basin such as Rotterdam, the Houston Ship Channel, etc., it has access to a wide variety of crudes, blend stocks, transportation options, additives, supplies, and services. This enhances its ability to cope with upsets and to react aggressively to sudden changes in price differentials.

In a basin, the infrastructure – seaports, pipelines, laboratories, waste-handling facilities – is extensive. Often, a single large supplier provides utilities and commodities such as hydrogen to several different customers, reducing costs for all concerned. This is because, due to economies of scale, production and distribution costs for a large plant are lower than those for multiple smaller plants with equivalent total capacity.

As long as space is available, industrial basins tend to grow. They also attract and support large pools of operators and engineers. Contractors, who perform as-needed engineering, maintenance, and other important service work, also are attracted by “basin gravitation.”

Lest we leave you with the idea that non-basin facilities are inherently handicapped, we should emphasize that other locations also can have advantages. For example, the ConocoPhillips refinery in Borger, Texas was built in 1932 in an area that still produces large quantities of natural-gas liquids. Except for a few nearby chemical plants, the Borger refinery seems isolated. However, it is connected by pipelines to the U.S. Gulf Coast and to the mammoth hub of pipelines in Cushing, Oklahoma. Through these various pipelines, the Borger complex receives crude oil from the Texas Gulf Coast and supplies products to Houston, Denver, Kansas City, and beyond. Also, in



addition to gasoline and other fuels, it produces a large number of ultra-pure chemicals, some of which are not manufactured in quantity anywhere else in the United States.

### 11.3.2 Size

Size isn't everything, but it certainly helps. On a per-ton basis, it costs less to design and build large process units. Engineering costs are essentially capacity-independent. This economy of scale translates into higher returns on investments, faster paybacks, and/or reduced interest payments as percentages of total project costs.

Similarly, bigger plants have lower per-barrel operating costs because many fixed costs, especially labor, are nearly size-independent.

Size and weight determine the maximum size of for the vessels in large process units. High-pressure reactors can only be built in a few special factories in Italy and Japan. They can weigh more than 2200 tons and their diameters may exceed 15 feet (5 meters), but it must be possible to move them over existing road and to lift them with available cranes.

### 11.3.3 Conversion Capability and Complexity

The most profitable refineries tend to be more complex. In the 1960s, W.L. Nelson developed an index for calculating the relative costs of refineries based on complexity.<sup>51</sup> *Table 38* presents complexity indices for individual processes, and *Table 39* compares complexity in different parts of the world.

*Table 38.* Nelson Complexity Indices for Individual Process Units

| Process Unit               | Complexity Index |
|----------------------------|------------------|
| Crude distillation         | 1                |
| Vacuum distillation        | 2                |
| Visbreaking                | 2.75             |
| Delayed and fluid coking   | 6                |
| FCC                        | 6                |
| Catalytic reforming        | 5                |
| Hydrotreating              | 2-3              |
| Hydrocracking              | 6                |
| Alkylation, polymerization | 10               |
| Aromatics, isomerization   | 15               |
| Lubes                      | 10               |
| Asphalt                    | 1.5              |
| Hydrogen production        | 1                |

To compute the Nelson Index for a given refinery or regions, the complexity factors for each individual unit is multiplied by the percentage of the incoming crude that it processes. The individual unit results are summed to give a total plant complexity rating.

Table 39. Nelson Complexity Indices for Selected Regions

| Region        | Refineries | Throughput<br>(million bpcd) | Complexity Index |
|---------------|------------|------------------------------|------------------|
| C.I.S.        | 58         | 10.0                         | 3.8              |
| Latin America | 80         | 6.3                          | 4.7              |
| Asia          | 135        | 14.7                         | 4.9              |
| Europe        | 116        | 14.5                         | 6.5              |
| Canada        | 23         | 1.8                          | 7.1              |
| United States | 153        | 15.3                         | 9.5              |

In short: The petroleum refining business is highly capital-intensive and competition is fierce. The predominant cost – purchase of crude oil – is beyond a refiner’s control, due to the fact that crude-oil costs are, for the most part, determined by OPEC. Even so, large, well-located, high-conversion refineries can be very profitable, especially during spikes in product prices. In 2005, crack spreads reached all-time highs, exceeding \$15 per barrel in most of the United States and >\$20 per barrel in California.

#### 11.3.4 Automation

As discussed in Chapter 22, model-predictive control (MPC) and real-time optimization (RTO) can improve the profitability of a major conversion unit by 5 to 10%. Refinery-wide, benefits from MPC and RTO can exceed US\$0.40 per barrel, or \$US30 million per year for a high-conversion 200,000 b/d refinery.

## 12. SAFETY, RELIABILITY, AND MAINTENANCE

This section could have been a part of Section 11: Refining Economics, because the most profitable refineries are also the safest and most reliable. Just consider this: For a 200,000 barrels-per-day refinery, a minor accident that shuts down the plant for just one week can cost US\$3 to 6 million in lost revenue. An accident that damages a major conversion unit can cost between US\$80 and US\$120 million in lost revenue during the 12-18 months required for reconstruction, plus US\$20 to 50 million (or more) in reconstruction expenses. These estimates don’t include the cost of repairing damage to the surrounding community. To settle lawsuits and pay penalties for a “minor” incident that occurred in 1994, a California refiner paid more than US\$83 million.<sup>52</sup>

### 12.1 Refinery Staffing

Figure 30 shows a typical refinery organization chart.

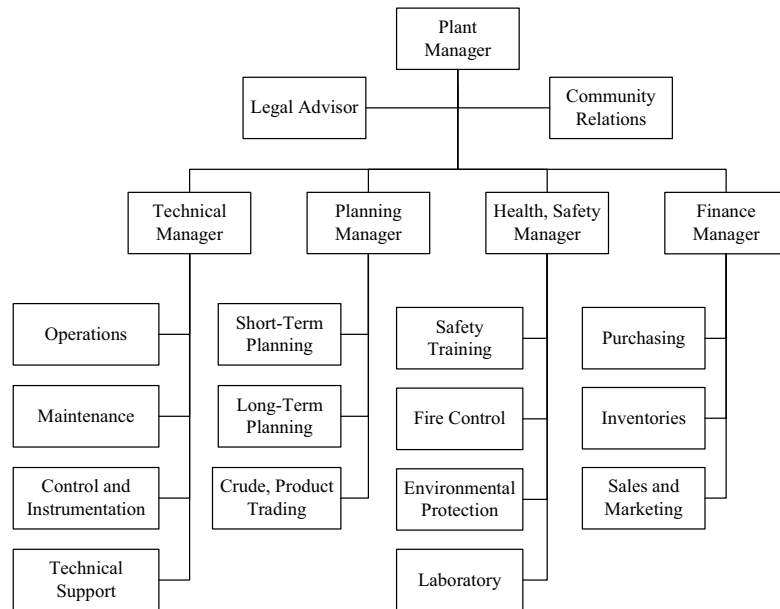


Figure 30. Refinery Organization Chart

More than anything else, safety and reliability depend on people who work in a plant. A typical U.S. or Canadian refinery employs 500 to 750 people. About half of these are operators and 20 to 25% are engineers.

## 12.2 Safety

“Safety first!”

“Safety is a state of mind.”

“All accidents are preventable.”

In safely operated plants, these maxims are emphasized over and over again to each and every employee. Industry studies show that safe plants share the following characteristics:

- Top managers demonstrate personal commitment to safety.
- Safety goals are aggressive. A perfect example of an aggressive goal is “Zero Lost-Time Accidents.”
- Safe performance is rewarded. For achieving aggressive safety goals, individual workers can receive thousands of dollars per year.
- Safety takes priority over (false) economics. In safety-first plants, operators are encouraged to shut a unit down at the first sign of serious trouble. Historically, far too many incidents are caused (or aggravated) by someone who decides to keep running a unit despite indications that something is wrong.<sup>52</sup>

- Protective clothing is required. Anyone in an operations area must wear fire-proof coveralls, a helmet, and safety goggles. Hearing protection and steel-toed shoes may also be required.
- Safety equipment is well-maintained and readily available. Safety equipment includes alarms, intercoms, sprinkler systems, self-contained breathing units, and first-aid kits.
- Safety training is rigorous and continuous. Training topics include:
  - **Safety regulations.** In the United States, safety regulations are issued and enforced by the Occupational Safety and Health Administration (OSHA). Per OSHA requirements, for every chemical in the plant, a Material Safety Data Sheet (MSDS) must be available. An MSDS describes the substance, classifies its danger, if any, and describes proper storage and handling.
  - **Emergency procedures,** including where to go and what to do when they hear different alarms. Usually, there are at least two kinds of alarm sounds – a fire alarm and a toxic-release alarm. Possible toxic releases include H<sub>2</sub>S, which is actually more poisonous than hydrogen cyanide, and carbon monoxide.
  - **Maintenance safety.** Historically, most refinery accidents occurred during maintenance. Now, all proposed maintenance work is reviewed and pre-approved by operations, engineering, craftspeople and management. Lock-out, tag-out procedures prevent unsuspecting employees from trying to start equipment that shouldn't be started.
- Contractors must be trained, too. Before they can enter the plant, all contractors are required to complete safety training.

Safety programs work! For example, a report by ChevronTexaco claims that, between 1990-91 and 2000-01, safety programs reduced injuries by 90% at its large refinery in Pascagoula, Mississippi.<sup>53</sup> In 2003, Valero's Paulsboro refinery had no lost-time injuries and a total recorded injury rate of 0.7, which is three times better than the industry average. For this and other achievements, the refinery was one of only 13 in the United States to be honored as "Star Site" within OSHA's Voluntary Protection Program (VPP). In addition, the plant earned four national safety awards from the National Petroleum Refiners Association (NPRA). "Our successful VPP efforts have taken the commitment of every person in this refinery, and I'm proud of how everybody has worked together as a team to make it a safety leader," said Mike Pesch, vice president and manager of the refinery.<sup>54</sup>

### 12.3 Reliability and Maintenance

Most refinery maintenance takes place during scheduled shut-downs, when refinery personnel, often with help from contractors, clean, inspect, maintain and (if necessary) repair equipment.

During a major turnaround, process vessels are drained and filled or blanketed with nitrogen gas. In conversion units, catalysts are unloaded and the reactors are metallurgically “pacified” with chemicals such as aqueous sodium carbonate. The process units are inspected, and pre-planned revamps are implemented. Reactors are re-loaded, either with fresh or regenerated catalysts, and the unit is re-started.

Maintenance planning is complex. Complete planning and competent management are prerequisites to success.<sup>55</sup>

### 13. PETROLEUM PROCESSING TRENDS

#### 13.1 Industry Consolidation

The oil industry has been consolidating since oil prices exploded during 1978-81, after the revolution in Iran. According to the United States Energy Information Administration,<sup>56</sup> in 1981 there were 324 refineries in the United States (*Figure 31*). Ten years later, there were 202, and by the end 2002 there were 153. Interestingly, during that same time-frame, the total capacity dropped from 18.6 million b/d to a low of 15.0 million b/d in 1994. It then climbed back to 16.8 million b/d by the end of 2002. The average capacity nearly doubled, from 57,400 b/d in 1981 to 109,700 b/d in 2002.

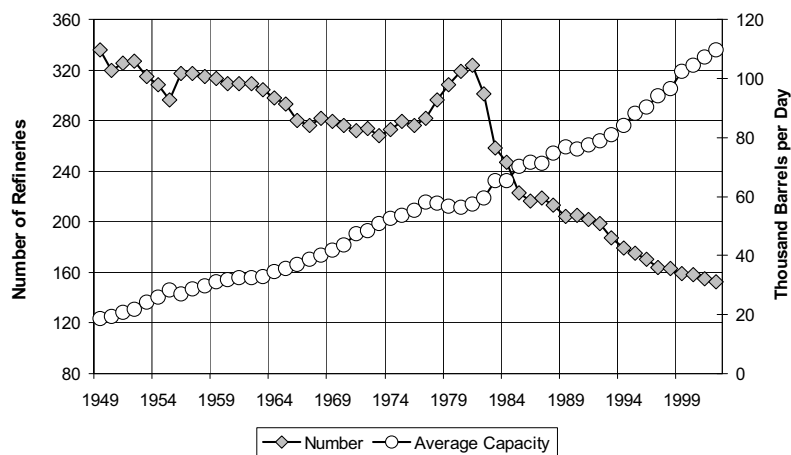


Figure 31. Average Capacity of U.S. Refineries 1949-2002

It’s tempting to conclude that 171 refineries were shut down during the past 20-plus years and the remaining plants got a whole lot bigger. Indeed, there were a lot of shut-downs and expansions, but that’s not the whole story. In many cases, mergers between neighbors decreased the apparent number of

plants without affecting capacity, because equipment from both predecessors continues to run at full rate. For example, the 300,000 b/d Flint Hills refinery in Corpus Christi, Texas used to be three separate plants owned by Koch Refining, Gulf States and Kerr-McGee.

Trends are similar in Western Europe. Total capacity has levelled off, but the number of refineries has decreased, in part due to mergers. Plants owned by BP and Texaco were merged to form the 380,000 b/d Netherlands Refining Company (NeRefCo). MiRO, a 283,000 b/d refinery in Karlsruhe, Germany, was created by a merger between refineries owned by Esso and by the by the four OMW partners – DEA, Conoco, Veba, and Petroleos de Venezuela.

In recent years, consolidation has evolved from relatively small mergers between neighboring refineries into mega-mergers between fully integrated oil corporations. Many of these are listed in *Table 40*.

*Table 40. Large Mergers and Acquisitions in the Oil Industry*

| Present Name   | Component Parts                                      |
|----------------|--|
| BP             | BP, Amoco, Arco, Castrol, Veba                       |
| ChevronTexaco  | Chevron, Texaco, Gulf                                |
| ConocoPhillips | Conoco, Phillips, Tosco, Unocal                      |
| ExxonMobil     | Exxon, Mobil   |
| Total          | Total, Fina, Elf                                     |
| Valero         | Valero, Phibro, Diamond Shamrock, Premcor, Ultramar* |

\*Valero acquired its Paulsboro refinery from Mobil and its Benicia refinery from Exxon

## 13.2 Environmental Regulations

A second main trend in petroleum processing – tightening environmental regulations – started in 1970 and accelerated in recent years. Major areas of improvement include:

- Reduced fugitive emissions. This requires modification or replacement of valves and compressor seals, along with more-vigilant maintenance.
- Reduced particulate emissions. To reduce emission of particulates, better cyclones and high-efficiency electrostatic precipitators are being added to FCC units. At delayed coking units, enclosed coke conveyors and storage systems have been installed.
- Reduced CO, SO<sub>x</sub>, and NO<sub>x</sub> emissions. Reduction of carbon monoxide emissions requires improved efficiency in the CO boilers of FCC units. SO<sub>x</sub> emissions from FCC units are being reduced by the hydrotreating of feedstocks, the use of SO<sub>x</sub>-transfer additives, and the addition of flue-gas scrubbing. At some plants, limitations on NO<sub>x</sub> may require the addition of post-combustion NO<sub>x</sub>-removal on boilers and heaters.
- Heat-efficiency, CO<sub>2</sub>. Energy is the largest controllable cost for a refinery. Therefore, the drive to increase heat efficiency is ever-present, especially in crude distillation units and other major energy consumers. In countries honoring the Kyoto protocol, decreased energy consumption also

decreases CO<sub>2</sub> emissions. Therefore, refineries in some of these countries are receiving tax credits for energy conservation projects.

- Clean water. Regulations in OECD countries require that the quality of water leaving a refinery must be at least as good as the water that enters. Tertiary treatment technology is being installed to remove lingering traces of benzene, phenols, nitrates, ammonia, and other undesirable chemicals.
- Reformulated gasoline. The need for higher octane and lower RVP in reformulated gasoline is increasing the need for alkylate and isomerate. In some catalytic reformers, severity is being reduced. Others are being converted to BTX service. More recently, MTBE units are being used for alternative purposes, such as alkylate production.
- Low-sulfur fuels. Recent rules limiting the sulfur content of gasoline and diesel fuel are stimulating hydrotreater revamps and the installation of a large number of new hydrotreaters. This in turn is requiring an increase in sulfur recovery and hydrogen-production capacity. From a process-development standpoint, the need to produce low-sulfur fuels has driven the development of new processes – SCANfining, OCTGAIN, S Zorb Prime-G, and others – for post-treating gasoline. To prevent the contamination of ultra-clean products, storage tanks and pipelines are being re-rated.

### 13.3 Residue Upgrading

The need for more and more heavy oil processing has been a trend since the start of the industry. Year by year the density and sulfur content of available crudes has slowly but surely been rising. Perhaps the discovery of some new oil field will change this trend, but for now, if refiners wish to continue meeting the demand for light products, they'll have to be able to process heavier feeds.

Several residue upgrading processes were mentioned in previous sections, and are described in the following chapters. The main processes are:

- Delayed coking
- Fluid-bed coking (FLEXIcoking)
- Residue hydrotreating (RDS, OCR/UFR, Resid Unionfining)
- Residue FCC (RFCC)
- Solvent deasphalting (ROSE® process)

### 13.4 Increased Oil Consumption in Developing Countries

The trends in *Figure 29* show that consumption of oil in OECD countries has stabilized, but consumption in the non-OECD world continues to increase. According to an article by Jeffrey Brown of FACTS Inc.,<sup>57</sup> China led the way

with 451,000 b/d of growth in 2003. Overall, Asia accounted for 664,000 b/d of the 1.6 million b/d of global incremental demand growth in 2003.

China will continue to drive consumption growth and affect regional product trade, prices, and refining margins. India is also likely to return to higher growth, and the region's midsized markets, such as Thailand and Indonesia, will post strong growth. In 2004, FACTS Inc. expects demand growth of 386,000 b/d in China, 22,000 b/d in South Korea, and 31,000 b/d in India. After 2004, average worldwide petroleum demand will increase by 2.5 to 3.0% per year, with Asia accounting for about half of the growth.

### 13.5 Automation

Advanced process control (APC) and model-predictive control (MPC) are widely used in the industry. Real-time optimization (RTO) is rather new, but its acceptance is growing Chapter 22.

APC, MPC and RTO require modern instrumentation, which includes actuator valves, distributed control systems (DCS), high-flux data highways, analyzers, and dedicated computers. They also require trained support staff, which at this writing is in short supply.

## 14. SUMMARY

Modern petroleum processing started in 1860. During the past 14 decades, it has grown in response to market drivers, particularly the demand for transportation fuels. In recent years, in response to economic drivers and pressure from environmental regulations, the industry has been changing.

We sincerely hope this book is a help to people who wish to gain a better understanding of the industry today.

## 15. REFERENCES

1. Energy in the United States, 1635-2000, Energy Information Administration, U.S. Department of Energy: Washington, D.C., 2003
2. Moldauer, B. (ed.) *All About Petroleum*, American Petroleum Institute: Washington, D.C., 1998
3. Weinkauf, K. "The Many Uses of Petroleum from Discovery to Present," Desk and Derrick Club of Tulsa: Tulsa, Oklahoma, 2003
4. *Significant Events in the History of Energy*, Energy Information Administration, U.S. Department of Energy: Washington, D.C., 2003
5. "World Oil Balance Data" *International Petroleum Monthly*, 2004 (2) Table 2.1
6. Scotese, D. "Jacksdale and the Surrounding Neighborhood" *A Village Remembered*, from the Ironville Post Office, Number 1 Market Street: Ironville, Nottingham, UK
7. "Oil Shale" *Wikipedia, The Free Encyclopedia*, 2004 (<http://en.wikipedia.org>)
8. "Major Developments in the History of the Polish Oil Industry" Polish Oil and Gas Company: Warsaw, 2003 (<http://www.pgnig.pl/en/pgnig/firma/histria/przemysl>)



9. Robbins, J.S. *How Capitalism Saved the Whales*, Foundation for Economic Education, Irvington-on-Hudson, New York, 1997
10. Pees, S.T. "Whale Oil Versus the Others" *Oil History*, Samuel T. Pees, Meadville, Pennsylvania, 2004
11. McCusker, J.J. *How Much Is That in Real Money? A Historical Commodity Price Index for Use as a Deflator of Money Values in the Economy of the United States* (2nd Ed.), American Antiquarian Society: Worcester, MA, 2001
12. Spencer, A.L. "Arkansas' First Oil Refinery" *Arkansas Historical Quarterly* 1957 (16), 335
13. Yergin, D. *The Prize: The Epic Quest for Oil, Money and Power*, The Free Press: New York, 1993
14. Economic Research Service "A History of American Agriculture, 1776-1990," United States Department of Agriculture, Washington, D.C., 2004
15. Berger, B.D.; Anderson, K.E. *Modern Petroleum: A Basic Primer of the Industry* (2nd ed.) PennWell: Tulsa, 1981
16. Robbins, W.K.; Hsu, C.S. "Composition," in the *Kirk-Othmer Encyclopedia of Chemical Technology* (4th ed.) John Wiley & Sons: New York, 1996
17. Altgelt, K.H.; Boduszynski, M.M. *Composition and Analysis of Heavy Petroleum Fractions*, Marcel Dekker: New York, 1994.
18. *NIST Standard Reference Database, No. 69*, National Institute of Standards and Technology: Boulder, Colorado, 2003
19. Coffey, F., Layden, J., Allerton, C. (ed.) *America on Wheels: The First 100 Years*, General Publishing Group: Santa Monica, California, 1996
20. "UOP's History" *About UOP*, UOP LLC: Des Plaines, Illinois, 2003
21. Palucka, T. "Doing the Impossible" *Invention & Technology* **2004** (3), 22
22. E.I. Shaheen *Catalytic Processing in Petroleum Refining*, PennWell: Tulsa, Oklahoma, 1983
23. Leffler, W.L. *Petroleum Refining for the Non-Technical Person* (2nd ed.), PennWell: Tulsa, Oklahoma, 1979, 1985
24. "Petroleum Refining Processes" OSHA Technical Manual (Section IV: Ch. 2), Occupational Health and Safety Administration: Washington, D.C., 2001
25. "Refining Processes" *Hydrocarbon Processing* **2002** (1), 85-148
26. CVX crude marketing web page, <http://www.chevrontexaco.com/crudemarketing>, 2004
27. Yields for Green Canyon crude were taken from the following reference and adjusted to match the boiling ranges used for the other 3 assays: "BP Assays Field in Gulf of Mexico" *Oil & Gas Journal*, February 17, 2003
28. "Weekly Production by Product," Energy Information Administration, U.S. Department of Energy: Washington, D.C., 2004
29. "Types of Petroleum Coke" *Products and Services: Global Carbon*, ConocoPhillips: Houston, Texas, 2004 ([http://www.conoco.com/products/global\\_carbon/types.asp](http://www.conoco.com/products/global_carbon/types.asp))
30. Magee, J.S.; Dolbear, G.E. *Petroleum Catalysis in Nontechnical Language*, PennWell: Tulsa, Oklahoma, 1998
31. "Wax Facts" National Petroleum Refiners Association: Washington, D.C., 2003
32. For more information, refer to: <http://www.utexas.edu/research/superpave/index.html>
33. "MTBE Questions and Answers" Fortum Corporation, [www.fortum.com](http://www.fortum.com), 2004
34. *EPA's Program for Cleaner Vehicles and Cleaner Gasoline, Document No. EPA420-F-99-051*, U.S. Environmental Protection Agency: Washington, D.C., 1999
35. *Heavy-Duty Engine and Vehicle Standards and Highway Diesel Fuel Sulfur Control Requirements, Document No. EPA 420-F-00-057*, U.S. Environmental Protection Agency: Washington, D.C., 2000
36. *Reducing Nonroad Diesel Emissions: Low Emission Program Summary, Document No. EPA420-F-03-008*, U.S. Environmental Protection Agency: Washington, D.C., 2003
37. *Final Report of the Government Working Group in Sulfur in Gasoline and Diesel Fuel, Summary and Recommendations*, Environment Canada: Ottawa, 1999

38. Hanson, R.; Lee, C.K.; Rost, K-D.; Herold, R.; Chou, T-S. "German Refiner Produces Ultra-Low Sulfur Diesel" *Oil & Gas Journal*, 6/2/03
39. "Sweden Natur Vards Verket: Input from Swedish Experts to the European Auto-Oil Programme" *Directive on Fuel Quality*, European Commission: Brussels, 1995
40. *Setting National Fuel Standards. Paper 3. Proposed Model for Standards Implementation*, Environment Australia: Canberra, 2000
41. Walsh, M.P. *Car Lines*, 2000 (4)
42. *Motor Vehicle Environmental Pollution Control in Japan*, Environment Agency of Japan, Automotive Pollution Control Division: Tokyo, 1999
43. Shorey, S.W.; Lomas, D.A.; Keesom, W.H. "Improve Refinery Margins and Produce Low-Sulfur Fuels," *World Refining Special Edition*, 1999 (Summer), p. 41
44. Stynes, P.C.; Shepherd, T.; Thompson, M.; Kidd, D. "Innovation Key to New Technology Project Success: Phillips S Zorb Becomes Low Sulfur Gasoline Solution," AM-01-43 National Petroleum Refiners Association, Washington, D.C., 2001
45. Bacha, J., et al. *Diesel Fuels Technical Review (FTR-2)*, Chevron Products Company: Richmond, California, 1998
46. *Heavy-Duty Standards / Diesel Fuel RIA, Document No. EPA 420-R-00-026*, Table IV.A-1, U.S. Environmental Protection Agency, Washington, D.C., 2000
47. Claus, C.F. **German Patent DE 17399**, August 26, 1881
48. Markum, J. "Refiners Urged to Capture, Defend Prosperity," *Oil & Gas Journal*, November 10, 1977
49. *International Energy Annual 2002*, U.S. Energy Information Administration: Washington, D.C., 2004
50. *Statistical Review of World Energy (52<sup>nd</sup> Ed.)*, BP plc: London, 2003.
51. Johnston, D. "Refining Report: Complexity Index Indicates Refinery Capability, Value," *Oil & Gas Journal*, May 18, 1996
52. Flournoy, C. "Refinery Accidents, Anxiety Increase," *Dallas Morning News*, October 1, 2000
53. <http://www.chevron.com/about/pascagoula/safeoperations/>
54. "Valero's Paulsboro Refinery Honored with OSHA's Highest Safety Recognition," Valero Energy Corporation, San Antonio, Texas, July 28, 2004
55. Oliver, R. "Complete Planning for Maintenance Turnarounds Will Ensure Success" *Oil & Gas Journal*, April 29, 2002
56. *Annual Energy Review 2002*, U.S. Energy Information Administration: Washington, D.C., 2004.
57. Brown, J. "China will continue leading product demand growth in Asia-Pacific," *Oil & Gas Journal*, May 17, 2004.

## Chapter 2

# THE ORIGIN OF PETROLEUM

Clifford C. Walters  
*ExxonMobil Research & Engineering Co.*  
*Annandale, NJ 08801*

### 1. HISTORIC OVERVIEW

Man has used petroleum since Biblical times, yet the origin of this natural resource remained a mystery for much of man's history. Classical literature is noticeably devoid of insight and even Roger Bacon laments in his 1268 treatise *Opus Tertium* on the lack of discussion on the origins of oils and bitumen by Aristotle and other natural philosophers.<sup>1</sup> Two theories on petroleum emerged during the Renaissance. In his 1546 text *De Natura eorum quae Effluunt ex Terra*, Georgius Agricola, a German physician, expanded on the Aristotilian concept of exhalations from deep within the Earth<sup>2</sup> and proposed that bitumen, like other minerals, condensed from sulfur. Andreas Libavius, another German physician, theorized in his 1597 text *Alchemia* that bitumen formed from the resins of ancient trees. These early discussions mark the beginnings of one of the longest running scientific debates: whether petroleum is formed by abiogenic processes that occur deep within the Earth, or from sedimentary organic matter that was once living organisms.

As fossil evidence emerged during the 18<sup>th</sup> century that coals were derived from plant remains, many scientists proposed similar origins to explain petroleum. The historic record is somewhat questionable, but Mikhailo Lomonosov is credited by some to have proposed the theory that liquid oil and solid bitumen originate from coal through underground heat and pressure as early as 1757<sup>3</sup> and certainly by 1763<sup>4</sup>. Various biogenic theories emerged during the early 19<sup>th</sup> century suggesting that petroleum was derived directly from biological remains or through a distillation process<sup>5</sup>.

Modern theories that petroleum originated from ancient sedimentary, organic-rich rocks emerged during the 19<sup>th</sup> century. T.S. Hunt of the Canadian Geological Survey concluded in 1863 that the organic matter in

some North American Paleozoic rocks must be derived from marine vegetation or marine animals, and that the transformation of this organic matter to bitumen must be similar to the processes involved in coal formation<sup>6</sup>. Leo Lesquereux, the American father of paleobotany, reached similar conclusions after studying Devonian shales in Pennsylvania<sup>7</sup>, as did Newberry in his study of Devonian shales in Ohio.<sup>8</sup> Early 20th century field<sup>9</sup> and chemical<sup>10</sup> studies of the Monterey Formation by the U.S. Geologic Survey provided convincing evidence that the oil was derived from diatoms in the organic-rich shales. Similar studies of organic-rich shales conducted in Europe during this time arrived at the same conclusion.<sup>11,12</sup>

Full ascendancy of the biogenic hypothesis began in the mid-20<sup>th</sup> century with a convergence of scientific advances in paleontology, geology, and chemistry. In 1936, Alfred Treibs established a link between chlorophyll in living organisms and porphyrins in petroleum.<sup>13</sup> Additional geochemical evidence followed with the discoveries that low to moderate maturity oils still retained hydrocarbon fractions with optical activity<sup>14</sup>, that the stable isotopes of carbon of petroleum bear a biological fractionation<sup>15</sup>, and that oils contain in addition to porphyrins, a host of hydrocarbons that can be traced back to specific biological precursors<sup>16</sup>. Concurrent with these findings were field studies recognizing that organic-rich strata occur in all petroliferous sedimentary basins, that this sedimentary organic matter (kerogen) is derived from biota, that it has been chemically altered from its initial state<sup>17,18</sup> and, that oil and gas is produced from this kerogen as the sediments are buried and heated.<sup>19</sup>

Although there is overwhelming evidence for a biogenic origin, some still advocate abiotic theories. The development of the modern abiogenic concept is rooted in the mid-19<sup>th</sup> century. The prolific French chemist Marcelin-Pierre Berthelot described in 1860 experiments where *n*-alkanes formed during the acid dissolution of steels.<sup>20</sup> Dmitri Mendeleev reasoned in 1877 that surface waters could percolate deep within the Earth, react with metallic carbides forming acetylene, which could then condense further into larger hydrocarbons.<sup>21</sup> Mendeleev's abiotic theory, further refined in 1902<sup>22</sup>, was viewed initially as particularly attractive as it offered an explanation for the growing awareness of the widespread occurrence of petroleum deposits that suggested some sort of deep, global process.

Advocates of abiotic origin theories dwindled under the mounting evidence for a biogenic origin of petroleum. By the 1960's, there was little support for an abiotic origin, except among a small group within in the Former Soviet Union. First proposed in 1951 by Nikolai Kudryavtsev<sup>23</sup> and advanced over the years in numerous Soviet publications,<sup>3</sup> a modernized version of Mendeleev's hypothesis emerged. This theory relies on a thermodynamic argument, which states that hydrocarbons greater than methane cannot form spontaneously except at the high temperatures and

pressures of the lowest most crustal depths. The theory ignores the fact all of life relies on being in thermodynamic disequilibrium with its environment.

In the West, astronomers have been the most vocal advocates for abiotic petroleum. Carbonaceous chondrites and other planetary bodies, such as asteroids, comets, and the moons and atmospheres of the Jovian planets, certainly contain hydrocarbons and other organic compounds that were generated by abiotic processes.<sup>24</sup> Sir Fredrick Hoyle reasoned in 1955 that as the Earth was formed from similar materials, there should be vast amounts of abiogenic oil.<sup>25</sup> In more recent years, Thomas Gold is the strongest promoter for abiotic petroleum.<sup>26,27</sup> Against the advice of nearly all geochemists and petroleum geologists, Gold convinced the Swedish government to drill two deep wells (Gravberg 1 in 1986-1990 and Stenberg 1 in 1991-1992) into fractured granite under the Siljan ring, the site of an ancient meteorite crater. The wells failed to find economic reserves and evidence for even trace amounts of abiotic hydrocarbons is controversial.<sup>28</sup>

Geochemists do not deny the existence of abiogenic hydrocarbons on Earth. Small amounts of abiotic hydrocarbon gases are known to be generated by rock-water interactions involving serpentinization of ultramafic rocks,<sup>29,30</sup> the thermal decomposition of siderite in the presence of water,<sup>31</sup> and during magma cooling as a result of Fischer–Tropsch type reactions.<sup>32</sup> However, commercial quantities of abiotic petroleum have never been found and the contribution of abiogenic hydrocarbons to the global crustal carbon budget is inconsequential.<sup>33</sup>

## 2. THE PETROLEUM SYSTEM

The accumulation of economic volumes of petroleum (oil and/or gas) in the subsurface requires that several essential geological elements and processes be present at specific time and space.<sup>34,35</sup> *Source rocks* generate and expel petroleum when sufficient thermal energy is imparted to the sedimentary organic matter (kerogen) to break chemical bonds. This heating is induced usually by burial by *overburden rock*. Once expelled, petroleum migrates either along faults and/or highly permeable strata. Accumulations form only when high porosity strata (*reservoir rocks*) are charged with migrating petroleum and the petroleum is prevented from further migration. These petroleum *traps* are formed only when geologic movements result in subsurface topographies (structural and stratigraphic) that block migration and when the reservoir rocks are covered by low permeability strata (*seal rocks*). The mere presence of these geologic elements is insufficient to form petroleum reserves. Traps must be available at the time of oil expulsion and, once charged, their integrity must be preserved until exploited. These elements and processes constitute the *Petroleum System* (Figure 1).

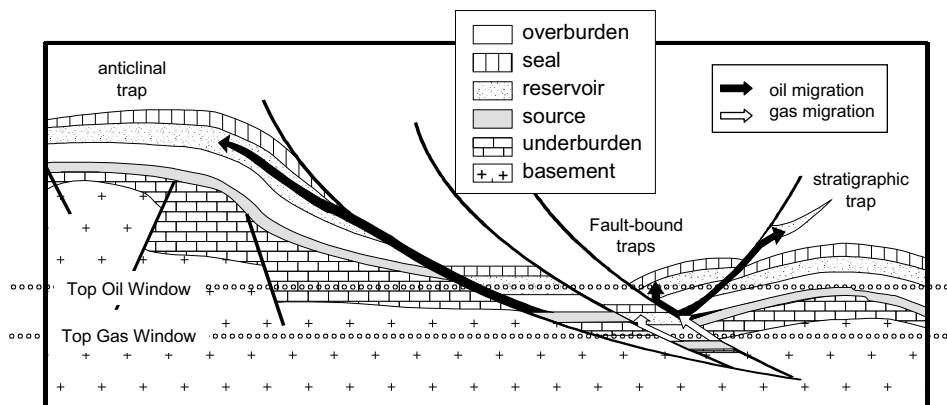


Figure 1. Elements of a Petroleum System. All petroleum systems contain: 1. at least one formation of organic-rich sediments that has been buried to a sufficient depth by overburden rock such that petroleum is generated and expelled, 2. Pathways (permeable strata and faults) that allow the petroleum to migrate, 3. Reservoir rocks with sufficient porosity and permeability to accumulate economically significant quantities of petroleum, and 4. Sealing rock (low permeability) and structures that retain migrated petroleum within the reservoir rock. The top and bottom of the oil window is approximated as a function of burial depth. In actual basins, these depths are not uniform and vary as a function of organic matter type, regional heat flow from basement, in thermal conductivity of the different lithologies, and burial history (e.g., deposition rates, uplift, erosion, and hiatus events).

A rigorous discussion of the origin of petroleum should encompass all of the interrelated elements of the petroleum system. Such a discourse is beyond the scope of this review, which will focus only on the deposition of organic-rich strata and the generation of petroleum from these sources. The reader is referred to *Exploring for Oil and Gas Traps*, a publication of the American Association of Petroleum Geologists, for a complete discussion of all aspects involved with defining the petroleum system for effective exploration.<sup>36</sup> Books by Tissot and Welte<sup>37</sup> and Hunt<sup>38</sup> provide detailed discussions of the principles of petroleum geochemistry, and a recent paper by Peters and Fowler<sup>39</sup> is an excellent review of the application of modern geochemical techniques to exploration and production practices.

### 3. DEPOSITION OF ORGANIC-RICH SEDIMENTARY ROCKS

Petroleum *source rocks* are water-deposited sedimentary rocks that contain sufficient amounts of organic matter to generate and expel commercial quantities of oil and/or gas when heated. Such organic-rich strata were deposited throughout Earth's history, in nearly all geologic environments, and in most sedimentary basins. Source rocks, however,

typically represent only a minor amount of basinal strata and are formed only when specific conditions exist.

Three general factors control the deposition of organic-rich sediments: productivity, dilution, and preservation (Figure 2).<sup>40,41,42</sup> Biological productivity determines the amount of organic matter that is contributed to sediments. Dilution refers to the amount of inorganic minerals that mixes with the organic matter. Once deposited, the organic matter must be preserved in a form that may later generate petroleum. There was once an active debate as to which factor was the most important in forming organic-rich sediments.<sup>43</sup> It is now recognized that these three factors are inherently interrelated in a highly complex, and variable manner.

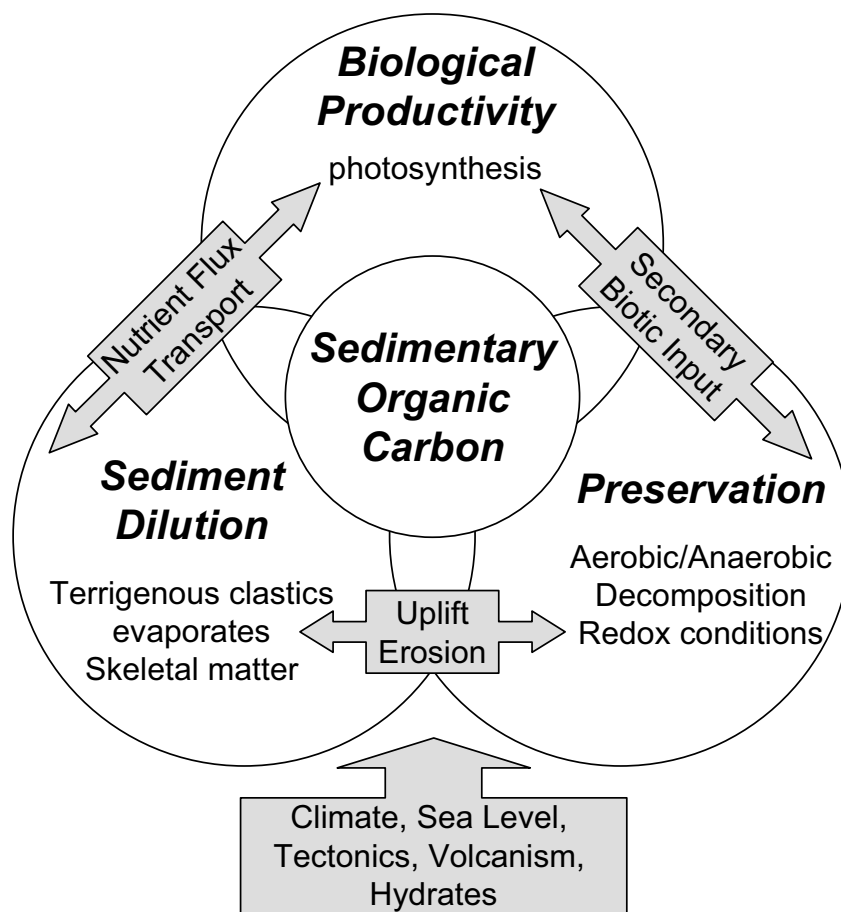
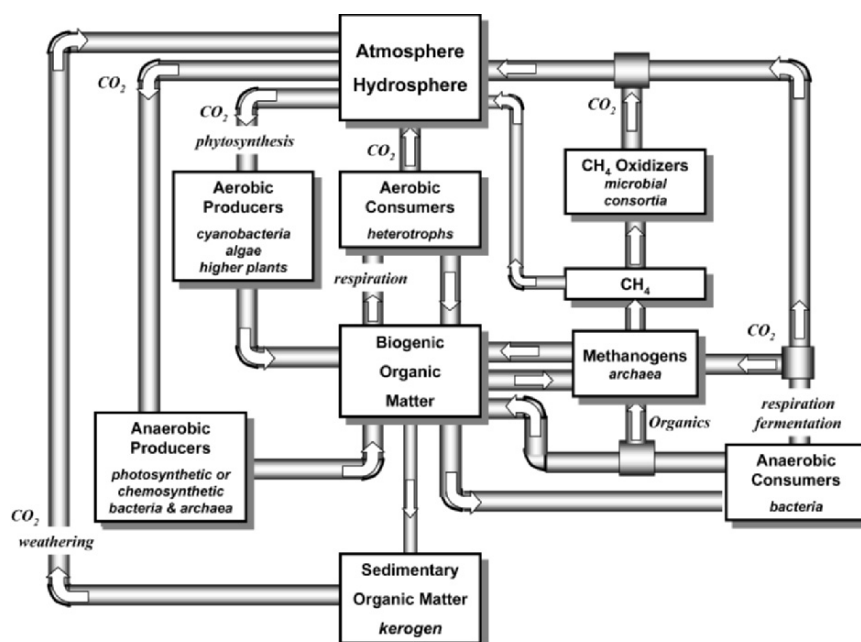


Figure 2. Three major factors, primary productivity, preservation, and dilution, determine whether organic-rich source rocks are deposited. These factors are interrelated and influenced by a number of geologic conditions.

Photosynthetic organisms, which include aerobic cyanobacteria, algae, phytoplankton, land-plants, and some anaerobic bacteria, provide most of the initial organic matter by fixing  $\text{CO}_2$  into biomass. The contribution of organic matter by non-photosynthetic chemotrophs is minor, except in some unusual environments, such as the deep-sea hydrothermal vents. Most of the non-photosynthetic biosystems, such as methanotropic communities<sup>44</sup>, rely on recycled carbon that was fixed originally by photosynthetic organisms. Many factors moderate the biota and the primary productivity (e.g., such as nutrient input from rivers and coastal upwellings,  $\text{pCO}_2$ , temperature, and turbidity) that are influenced by global climatic and tectonic conditions.



*Figure 3.* Generalized redox cycle for organic carbon. Production of new organic matter by the photosynthetic fixation of  $\text{CO}_2$  (primary productivity) can occur with (aerobic) or without oxygen (anaerobic) as a byproduct. Respiration and other processes result in the nearly complete oxidation of this organic matter back to  $\text{CO}_2$ . A small amount of the organic matter in sediments escapes biological recycling and is preserved in rocks. Eventually, this carbon is recycled to the surface as  $\text{CO}_2$  by geologic processes, such as subduction and venting, erosion and weathering – or more recently, by the combustion of fossil fuels.

Much of the primary organic matter created by photosynthetic or chemosynthetic autotrophs undergoes degradation by other organisms during the secondary production of organic matter. Heterotrophic organisms in the water column, sediments, and rock continually degrade and rework primary aquatic and terrigenous organic matter (Figure 3). Aerobic respiration is very rapid and efficient and primary organic matter may pass through a chain of



water and mud dwelling animals, protozoa, and bacteria, until fully consumed and returned to the atmosphere/hydrosphere as  $\text{CO}_2$ . Anaerobic bacteria also degrade organic matter either by fermentation or by respiration using terminal electron acceptors other than  $\text{O}_2$  (e.g., nitrate, sulfate, iron). These microbial metabolisms are generally slower and may be curtailed by limited nutrient and electron acceptors within the sediment porewaters. Consequently, some of sedimentary organic matter, both from primary and secondary biogenic sources, may escape recycling and become preserved in lithified rock. Hence, anoxic conditions enhance the preservation of oil-prone organic matter and promote the deposition of potential source rocks (Figure 4).

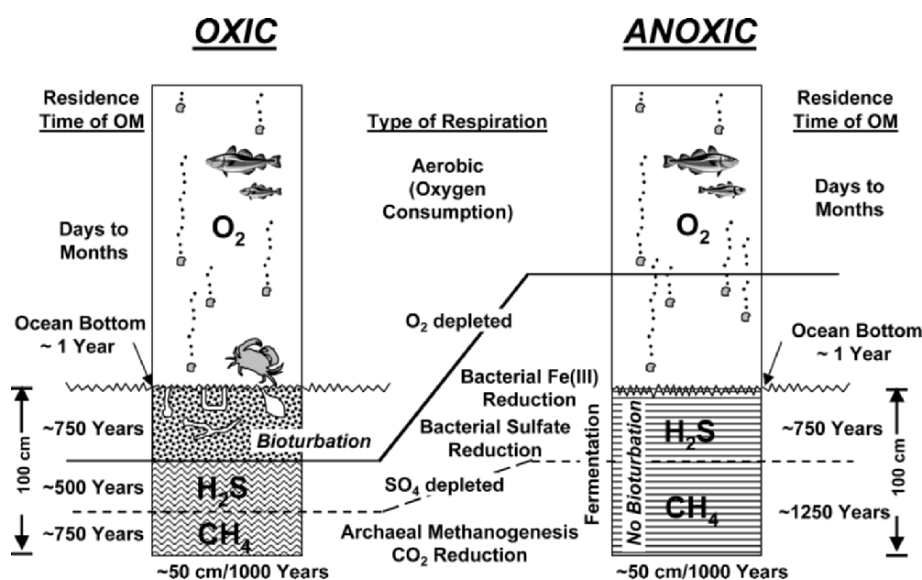


Figure 4. Oxic (left) and anoxic (right) depositional environments generally result in poor and good preservation of deposited organic matter, respectively (after Demaison and Moore, 1980<sup>45</sup>). The solid horizontal line separates oxic (above) from anoxic (below). In oxic settings, bottom dwelling metazoa bioturbate the sediments and oxidize most organic matter. In anoxic settings, especially where the oxic-anoxic boundary occurs in the water column, bottom-dwelling metazoa are absent and sediments are not bioturbated.

The amount of oxygen in bottom waters or sediments is determined by its rate of influx from the photic zone (via circulation and/or diffusion) and its rate of consumption (biological oxygen demand). Topographical barriers, currents, or water stratification due to temperature and salinity gradients may limit water circulation and diffusion. A high supply of primary organic matter raises the biological oxygen demand, rendering pore waters, and even the lower water column, anoxic. This mechanism is seen in terrigenous environments with high input of land-plant material (e.g. swamps, and coastal

plains), and in lake and marine environments with high nutrient influx (e.g., seasonal rains and overturn of water columns, and upwelling zones).

In anoxic marine environments, the most prevalent organisms are bacteria that utilize sulfate and produce  $H_2S$ . If not precipitated as pyrite by iron from clays and other clastic minerals,  $H_2S$  may react with organic matter, incorporating sulfur. If the production of  $H_2S$  is greater than its rate of sequestering, *euxinic* conditions (waters with free  $H_2S$ ) occur. The transition between oxic and euxinic waters may occur within the sediments or water column. Some strata with excellent source potential were deposited where euxinic conditions extended into the photic zone.<sup>46</sup> Biological activity may also be restricted by hypersaline conditions that occur in playa lakes, lagoons, and restricted marine settings.

Sedimentation rate influences both the preservation and concentration of organic matter. The inorganic materials may be clastic (eroded clays and sands), chemical precipitates (carbonates, salts), or biogenic (siliceous and carbonate shells). Organic matter may be removed from biological recycling by rapid burial, such as in deltaic settings. However, preservation is offset by dilution and the resulting rocks may be relatively low in organic carbon. Similarly, sediments resulting from high primary productivity, such as diatomaceous cherts, may have an upper limit in organic carbon because of high autodilution. In general, sedimentary rocks with the highest concentrations of organic matter are deposited under conditions of moderate to high influx of primary organic matter, anoxic (possibly euxinic) bottom waters, and low sedimentation rates.

#### **4. KEROGEN FORMATION AND THE GENERATIVE POTENTIAL OF SOURCE ROCKS**

Although derived from biochemicals, the sedimentary organic matter in source rocks, is markedly different in structure and chemical composition. Living organisms are composed mostly of proteins, nucleic acids, and lipids. Structural materials, such as lignin and cellulose, and various resins are fairly well-defined biopolymers composed of a limited number of monomers. With the exception of some halophilic green algae and a few bacteria<sup>47</sup>, only trace amounts of hydrocarbons are produced directly as biomass by most living organisms. In contrast, immature sedimentary rocks contain only low concentrations of the functionalized biochemicals. Most of the organic carbon is bound in a condensed, insoluble macromolecular material, termed kerogen, which has comparatively few functional groups. Kerogen has been called a "geopolymer" but this is a misnomer, as the term implies that there is a repetition of distinct monomers and some structural order. Kerogen has no unique molecular structure and can only be defined in terms of bulk elemental composition and average molecular distributions.

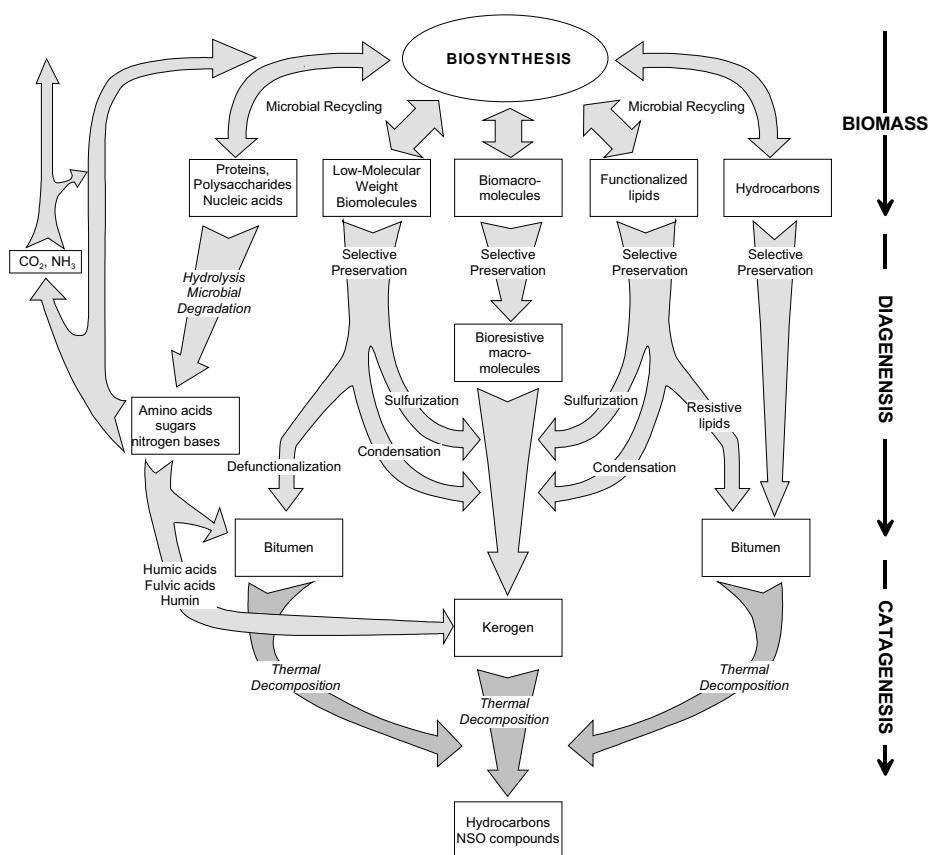
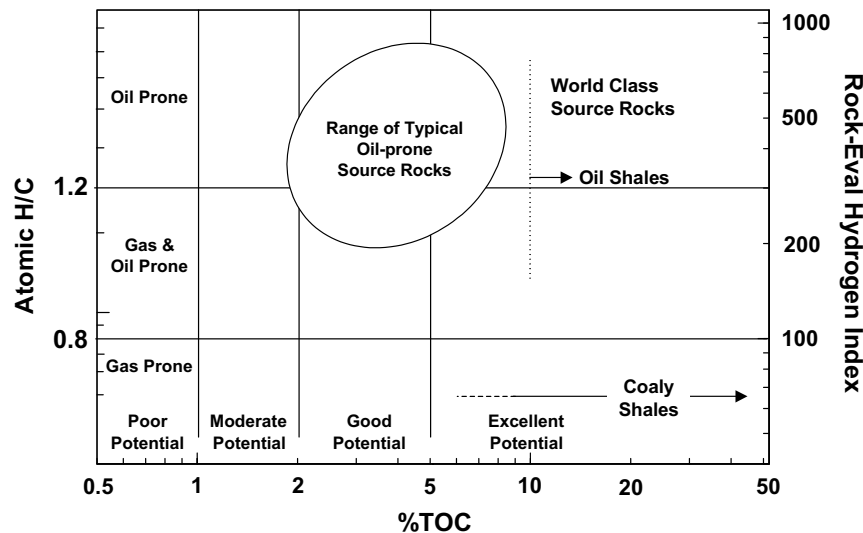


Figure 5. Kerogen is formed during diagenesis by the selective preservation of bio-resistant macromolecules and from the incorporation of lower-molecular weight species. Modified from Tegelaar et al. (1989)<sup>49</sup>.

Optically, kerogen is often described as mixtures of amorphous organic matter and *macerals*, morphologically distinct particles that are mostly derived from land-plants. The amorphous matter was once thought to be derived from the complete breakdown of biological macromolecules that then re-assembled in a random fashion with low molecular-weight biochemicals (e.g., lipids).<sup>48</sup> We now realize that there are biological macromolecules that are alkyl-rich and resist microbial recycling.<sup>49</sup> These bio-macromolecules (e.g., cutan, sporopollenin, tannins, and algaenan) may constitute only a small fraction of the initial biomass, but are selectively preserved and enriched during early diagenesis (Figure 5). They provide a core for the incorporation of functionalized low molecular-weight biochemicals, such as membrane lipids and the breakdown products of less resistant bio-macromolecules. A small fraction of this material may remain soluble, which along with biogenic

hydrocarbons and lipids that resist incorporation, becomes the bitumen that can be extracted from immature source rocks using organic solvents.

Kerogen formation begins at the point when living cells die and their biochemicals are exposed to the geologic environment. Microbial processes are mostly responsible for the breakdown of biological macromolecules and the recycling of lower molecular-weight biochemicals, resulting in the selective preservation of the more bio-resistant compounds. Low temperature chemical reactions further alter kerogen through the loss of functional groups (e.g.,  $-\text{NH}_3$ ,  $-\text{COOH}$ ), sulfur incorporation, condensation, cross-linking, and aromatization. The processes and thermal regime under which kerogen forms, termed *diagenesis*, occurs under mild thermal conditions ( $<80^\circ\text{C}$ ).



*Figure 6.* The quantity and quality of kerogen determines the generative potential of a source rock. Boundaries for the classifications of generative potential are approximate. Typical marine source rocks from productive basins contain ~2 to 6% TOC. Basins with world class reservoirs may contain source units with appreciably higher amounts of carbon. Expulsion of oil may be difficult from rocks with  $<1\text{-}2\%$  TOC. The hydrogen content of the organic carbon determines the quality of the expelled hydrocarbons (during metagenesis). Kerogens with high H/C ratios tends to generate oil, while those with low H/C ratios tend to generate gas. The Hydrogen Index is based on the Rock-Eval instrumentation. This pyrolysis method, commonly used by petroleum geochemists to rapidly screen rocks for their generative potential, heats a ground sample and measures the pyrolyzate response on a flame ionization detector and a  $\text{CO}_2$  response by an infrared detector. These responses can be calibrated to a rough approximation of the kerogen H/C and O/C atomic ratios.

The quantity and quality of organic matter preserved during diagenesis of sediment determines the generative potential of the source rock and whether it will be prone to expel oil or gas. Quantity is determined by amount of organic input, the degree to which it is preserved (either as primary or

secondary biogenic matter), and by its dilution with inorganic mineral matter. Typical oil-prone, marine source rocks contain 2-5 wt.% total organic carbon (TOC), but strata in the range of 10-20% are known to occur in high yield petroleum systems (Figure 6). Oil shales, many of which are lake deposits, contain over 10% TOC. Coals are >80% TOC, and may be dilute with varying amounts of clastic minerals to yield coaly shales with a wide range of carbon content.

Kerogen quality is mainly a function of hydrogen content – kerogens with high H/C ratios (> 1.2) are oil-prone, while those with lower H/C ratios (0.5 to 0.8) tend to generate mostly gas. Biogenic input of organic matter and the manner of its preservation determine the hydrogen content of kerogen. Some algae and bacteria are extremely rich in membrane lipids and aliphatic biopolymers, such as algaenan. Sediments that receive this input have the potential to be hydrogen-rich (kerogen H/C >1.5). Conversely, land-plant lignins have low H/C ratios and sediments that received only this input are hydrogen-poor (kerogen H/C ratios < 1.0). The hydrogen, sulfur, and oxygen content of kerogen can be modified greatly during deposition and diagenesis. Oxic conditions favor rapid and fairly complete heterotrophic consumption of primary organic matter. The organic matter remaining in the sediments tends to be oxidized or inert. Anoxic conditions conserve, or even enhance, the initial H/C ratio of the primary organic matter via selective preservation and/or contributions from secondary biota. Euxinic conditions promote the incorporation of sulfur, resulting in high S/C ratios.

There are many schemes that attempt to classify kerogen types by their morphology, maceral and palynological assemblages, and/or bulk chemical composition. The most widely used is a modification of a method developed for coals<sup>50</sup>, whereby the H/C and O/C ratios are plotted (Figure 7). Kerogens are assigned designations as being Type I, II, III, or IV depending where they fall on the plot. Type I and II are oil-prone, Type III is gas-prone, and Type IV is inert carbon.

This classification scheme can be sub-divided further by considering the variation in sulfur content (Table 1). Since the incorporation of sulfur into sedimentary organic matter involves the generated of H<sub>2</sub>S by sulfate reducing bacteria, kerogens with high S/C ratios (0.04 to > 0.10) are found mostly in marine (non-clastic) rocks where euxinic conditions may prevail. Type I kerogens are deposited typically in continental lakes, which have no contact with marine waters and lack a ready supply of sulfate. Consequently, sulfur-rich Type IS kerogens arise only in unusual geologic settings where older evaporite beds (e.g., gypsum or anhydrite) are exposed and dissolved into normally fresh lake water.<sup>51</sup>

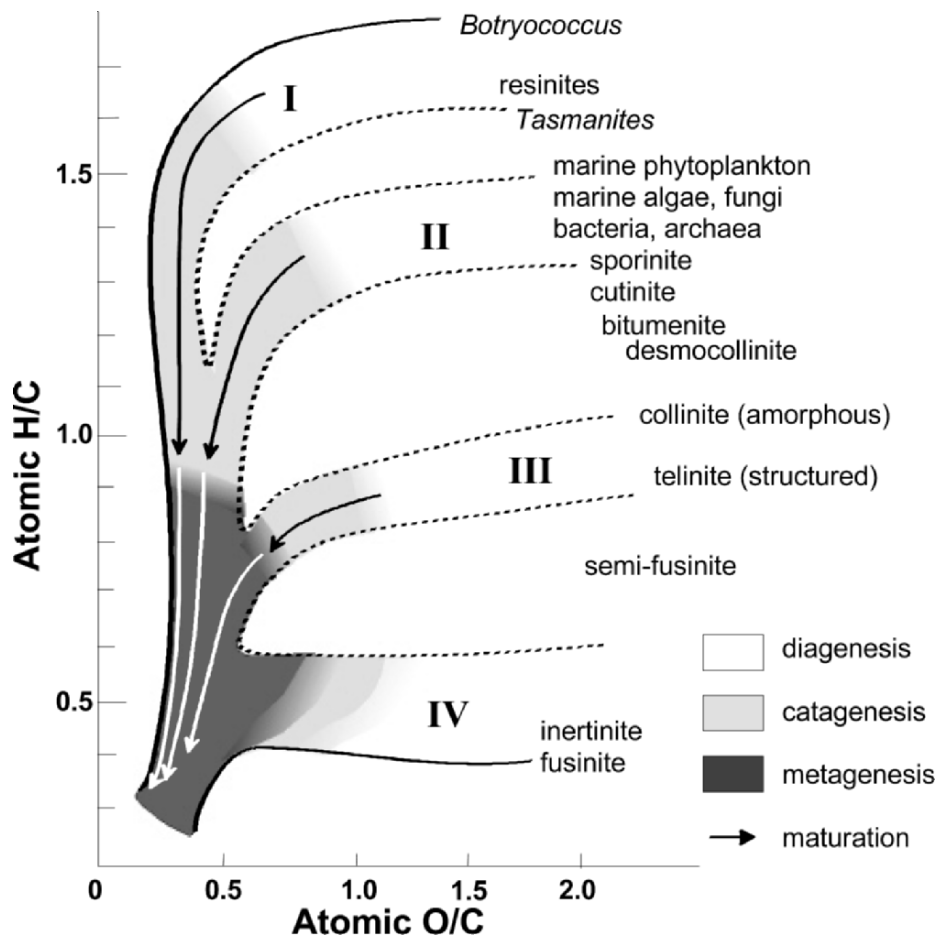


Figure 7. van Krevelen type diagram showing the distribution of kerogen types and some of their precursor macerals in relationship to their H/C and O/C atomic ratios. A substantial portion of their oxygen content is lost during diagenesis. Oil generation occurs during catagenesis, whereby the H/C ratio of the residual kerogens decrease. When the H/C ratio is < 0.5, the residual kerogens are capable of generating only methane.

Type II kerogens are deposited primarily in marine settings dominated by photosynthetic organisms. During early diagenesis, this organic matter may react with  $H_2S$  produced by sulfate-reducing bacteria that thrive in marine, anoxic waters and sediments.  $H_2S$  also reacts with iron and other metals, forming inorganic sulfides. Consequently, marine Type II kerogens may have varying sulfur content. Marine shales and mudstones, which contain iron oxides and iron-rich clays, yield low-sulfur Type II kerogens and pyrite. Carbonate, evaporite, and chert deposits, which are iron-poor, yield high-sulfur Type IIS kerogens.

Type III kerogens form in swamps and coastal plains. As these depositional environments may or may not have marine influence, the sulfur content of coals can vary, but is generally low. Type III kerogens are frequently allochthonous; that is, they are transported by fluvial systems into delta and nearshore marine sediments where they may mix with locally produced (autochthonous) Type II kerogens. Most Type III kerogens are dominated by vitrinite, a land-plant maceral that has a low H/C ratio and is gas-prone. Some coals, however, contain oil-prone material (Type IIIC) that are derived from associated algae or from the selective preservation of cutinous macromolecules. Many oils from Southeast Asia are generated from Tertiary coaly shales that contain this type of kerogen.

Table 1. Kerogen types, their occurrence and bulk chemistry (at end of diagenesis)

| Type | Depositional Setting                               | Primary Biotic Input                            | H/C        | O/C    | S/C                 |
|------|--|---|------------|--------|---------------------|
| I    | Lakes, restricted lagoons                          | green algae<br>cyanobacteria<br>dinoflagellates | > 1.4      | < 0.1  | < 0.02              |
| IS   | Lakes with a source of sulfate (rare)              | green algae<br>cyanobacteria                    | >1.4       | < 0.1  | > 0.04              |
| II   | Marine shales                                      | marine algae,<br>phytoplankton                  | 1.2 - 1.4  | ~ 0.1  | 0.02 - 0.04         |
| IIS  | Marine carbonates, evaporites, silicates           | marine algae,<br>phytoplankton                  | 1.2 - 1.4  | ~ 0.1  | > 0.04              |
| III  | Coals, coaly shales, deltas                        | vascular land-plants                            | 0.7 - 1.0  | > 0.1  | < 0.02 <sup>1</sup> |
| IIIC | Coastal plains (oil-prone coals)                   | vascular land-plants, algae                     | 1.0 to 1.2 | > 0.1  | < 0.02 <sup>1</sup> |
| IV   | Inert carbon due to oxidation or advanced maturity | All possible                                    | < 0.5      | < 0.15 | < 0.02 <sup>2</sup> |

<sup>1</sup> Coals generally are low in sulfur. Depositional settings with marine influence may result in coals with S/C > 0.02.

<sup>2</sup> Some inert pyrobitumens may have higher S/C ratios as a result of secondary sulfur incorporation.

## 5. GENERATION AND EXPULSION OF OIL AND GAS

During *catagenesis*, kerogen thermally cracks and produces bitumen. Weak C—S and C—O bonds break preferentially during the early stages of catagenesis producing bitumen that is highly enriched in polar (NSO) compounds. With additional heating (~90-140°C), C—C bonds break within the evolved polar compounds and from residual kerogen, yielding a hydrocarbon-rich fluid that is then expelled from the source rock's mineral matrix. With additional thermal stress, kerogen yields primarily condensate and then wet gas (C<sub>1</sub>-C<sub>6</sub>). Catagenesis is complete when the kerogen has expended its capacity to generate C<sub>2+</sub> hydrocarbons (~150-175°C). *Metagenesis* may then take place under still more severe thermal alteration,

where only methane is produced as methyl-groups are cleavage from highly condensed, aromatic structures.

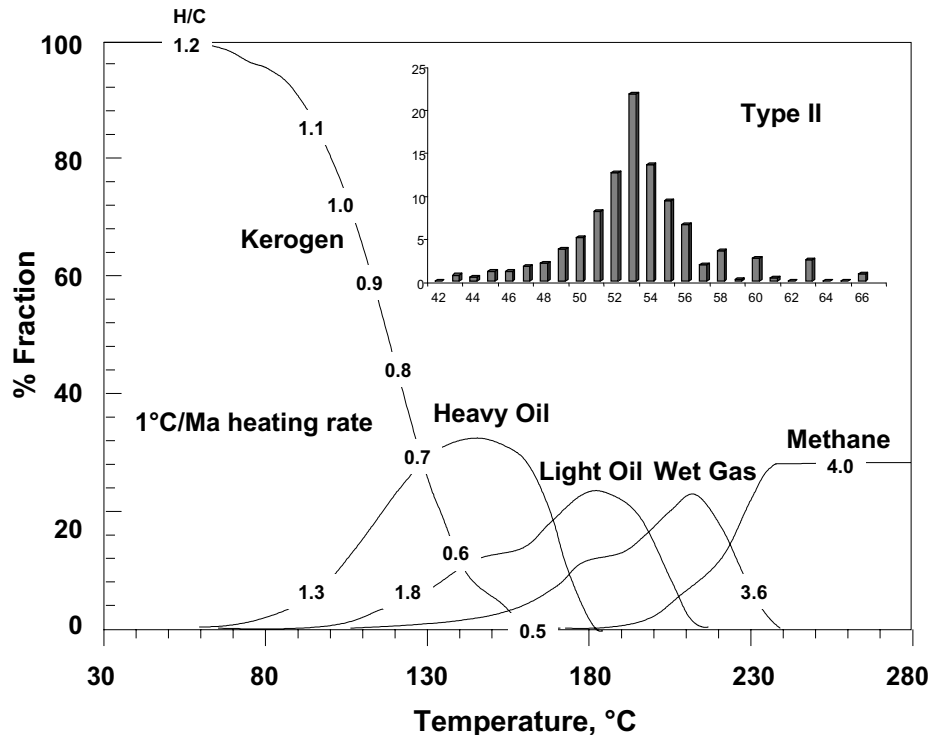


Figure 8. Example of a kerogen decomposition kinetic model with predictions of expelled fluid composition. The rate of kerogen conversion is assumed to follow a series of parallel first order kinetic reactions defined by the Arrhenius equation,  $k = Ae^{-(E/RT)}$ , where  $k$  is the rate coefficient,  $A$  is a constant termed the frequency factor,  $E$  is the activation energy,  $R$  is the universal gas constant, and  $T$  is the temperature. The kerogen model was derived by fitting the yield curves of pyrolyzates that evolved from a marine shale source rock containing Type II kerogen heated at several different heating rates under anhydrous conditions. In this case, the model was fitted using a fixed frequency factor,  $A = 1 \times 10^{14} \text{ sec}^{-1}$ . The evolved products are predicted from a more advanced model that accounts for expulsion and secondary cracking of retained bitumen and residual kerogen.

Oil generation is a kinetic process – both time and temperature are critical<sup>52</sup>. The kinetic parameters of kerogen decomposition can be determined by artificially heating immature source rocks using relatively fast heating rates ( $\sim 300$  to  $550^\circ\text{C}$  at  $\sim 1$  to  $50^\circ\text{C}/\text{min}$ ) or lower isothermal temperatures ( $275$ - $350^\circ\text{C}$  for several days) and measuring either product yield or the residual generative potential. Data are fitted to kinetic models defined by a series of first order parallel reactions, usually at a single frequency factor. When geologic heating rates are applied ( $\sim 1$  to  $10^\circ\text{C}/\text{Ma}$ ), the derived kinetic models yield kerogen maturation results comparable to what is observed in



petroliferous basins.<sup>53,54</sup> More advanced models describe the fluid composition of the expelled products and include secondary cracking reactions (Figure 8).

Although simple thermogenesis adequately describes petroleum generation, geocatalysis involving reactive mineral surfaces, clays, trace metals, or organic species have been proposed.<sup>55,56</sup> Such processes are highly speculative, and it is difficult to image how inorganic agents would remain activated under subsurface conditions or how mass transport limitations inherent in solid-solid interactions could be circumvented<sup>57</sup>.

Once generated from the kerogen, petroleum is expelled into mineral pore spaces (primary migration) and then through permeable rock and faults to the trap (secondary migration). Oil expelled from a source rock is enriched in saturated and aromatic hydrocarbons relative to the bitumen that remains (Figure 9). The factors that control primary expulsion and bitumen fractionation are largely unknown; and, although there is generally a lack of experimental or observational evidence for the underlying mechanisms, there is no shortage of hypotheses. Expulsion models that attempt to account for these chemical differences generally assume rate-limiting processes occur in the release of generated hydrocarbons from the kerogen or in the movement of hydrocarbons within the mineral matrix.

Hypotheses based on kerogen-oil interaction postulate that the expulsion of oil is controlled by absorption or adsorption of the products onto the surface of the kerogen,<sup>58,59,60</sup> diffusion of the hydrocarbons through the kerogen<sup>61,62,63,64</sup> and/or relative solubility.<sup>65</sup> These hypotheses attribute little importance to movement of petroleum within the source rock mineral matrix and the efficiency of the release of oil is controlled primarily by the amount of organic carbon and its composition (see, Pepper & Corvi, 1995; and references therein<sup>53</sup>). Expulsion models based on the interactions of generated products with the source kerogen have gained favor in recent years as they have the potential to account for compositional differences between bitumens and expelled oil and for expulsion efficiencies that depend on kerogen type and richness. This thinking can be traced to observations made on source rocks<sup>66</sup> and to recognition of the absorptive capacity of solid organic matter as revealed by solvent swelling experiments.<sup>67,68,69,70</sup> It is now clear that Type I and II kerogens and Type III and IIIC coals have sufficient sorptive properties to explain residual oil concentrations in mature source rocks.

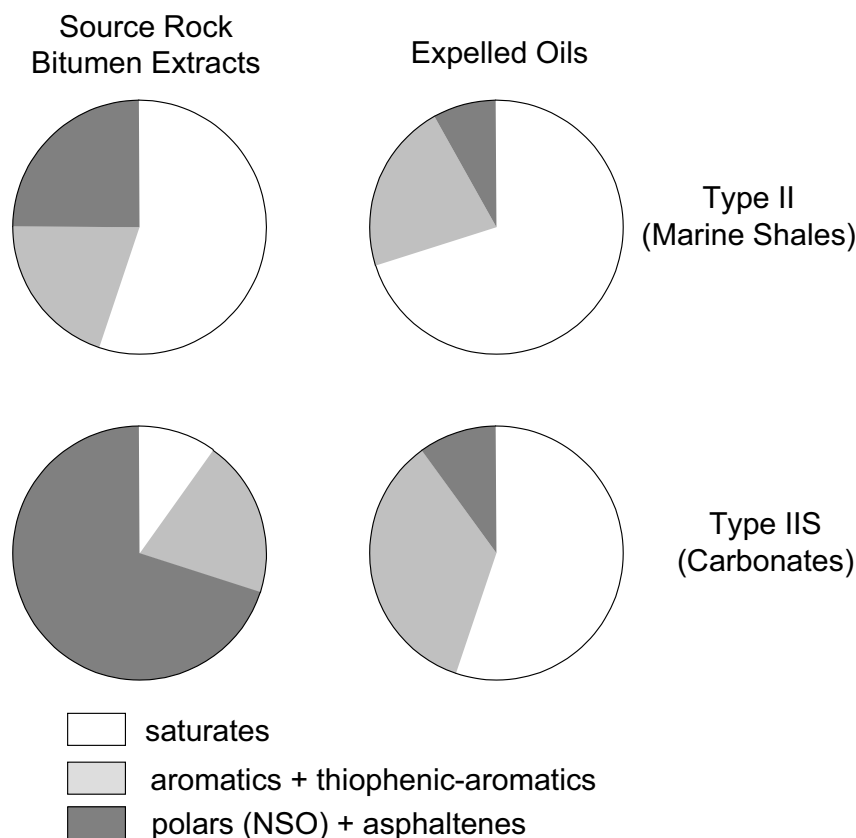


Figure 9. Comparison of  $C_{15+}$  chemical group type distributions of expelled oil and retained bitumens for typical Type II (marine shale) and Type IIS (carbonate) source rocks (middle of the oil window).

There are many expulsion models that target chemical or physical processes of oil moving within the source rock mineral matrix as the rate determining step. Different aspects have been considered to be important in this movement. Some consider the amount and type of organic matter as being critical to generating sufficient bitumen to exceed a pore saturation threshold.<sup>71,72,73</sup> Others postulate that the establishment of effective and continuous migration pathways within the source rocks is critical.<sup>74,75,76</sup>

Other factors suggested to be key elements in expulsion are: pressure build-up from generation and compaction and the failure of the rock fabric resulting in micro-fracturing,<sup>77</sup> gas availability and movement of oil in a gas or supercritical phase,<sup>78,79</sup> or movement of oil in an aqueous phase.<sup>80,81</sup> For the most part, the conditions that determine these elements are controlled by the primary sedimentological conditions in the depositional environment of the source rock and secondary diagenetic processes. Consequently, the

mechanisms that define oil movement differ according to the lithofacies of the source rock.

## 6. COMPOSITION OF PRODUCED PETROLEUM

The molecular and isotopic composition of produced petroleum is determined by complex chemical, physical, and biological processes. Generation and expulsion from the source rocks, phase behavior as the petroleum moves from source to reservoir, reservoir fill history, and secondary alteration processes all influence oil and gas compositions.

Each source facies generates oil with distinct chemical composition that reflects biotic input, depositional setting, and thermal history (Figure 10). For example, lacustrine and coaly source rocks generate waxy, low-sulfur crudes, while carbonate and evaporite source rocks generate asphaltic, high-sulfur crudes. These compositional differences are most apparent during the initial stages of oil expulsion and become less distinct as the source proceeds through catagenesis where secondary cracking reactions become prevalent. Although petroleum is derived from biological organic matter, most of the individual compounds cannot be assigned to a specific biochemical precursor. Some petroleum hydrocarbons, termed *biomarkers*, retain enough of their original carbon structure that a likely biochemical precursor can be assigned.<sup>82</sup> The abundance and distribution of biomarkers allow geochemists to infer the origin and thermal history of oils.

Once generated and expelled from the source rock, petroleum composition can be further modified during migration and entrapment within the reservoir. In most petroleum systems, the source formation is at greater temperature and pressure than the reservoir and migrating petroleum fluid may separate into gas and liquid phases that can then migrate independently.<sup>83,84,85</sup> Petroleum also interacts with water and the more soluble hydrocarbons may selectively partition into the aqueous phase.<sup>86</sup>

Once in the reservoir, secondary processes can alter oil composition. Biodegradation, the consumption of hydrocarbons by microorganisms, is likely to occur in shallow, cool reservoirs (<80°C).<sup>87,88</sup> This process selectively removes saturated hydrocarbons, enriching the residual crude oil in polar and asphaltic material. Biodegradation forms acids and biogenic CH<sub>4</sub>, CO<sub>2</sub>, and H<sub>2</sub>S. Microbial alteration of crude oils is a relatively fast process and may occur naturally or result from poor production practices. Thermochemical sulfate reduction (TSR) is another reservoir alteration process that can affect oil quality and quantity. It is a chemical redox process that occurs at relatively high temperatures (>120°C), where hydrocarbons are oxidized to CO<sub>2</sub> and sulfate is reduced to H<sub>2</sub>S.<sup>89,90</sup> The residual oil is depleted in saturated hydrocarbons and enriched in sulfur-aromatic species. Reservoir charging and fill history also can alter oil composition. For example, mixing

of gaseous hydrocarbons with a heavy oil can cause asphaltenes to precipitate, forming a tar mat.<sup>91</sup>

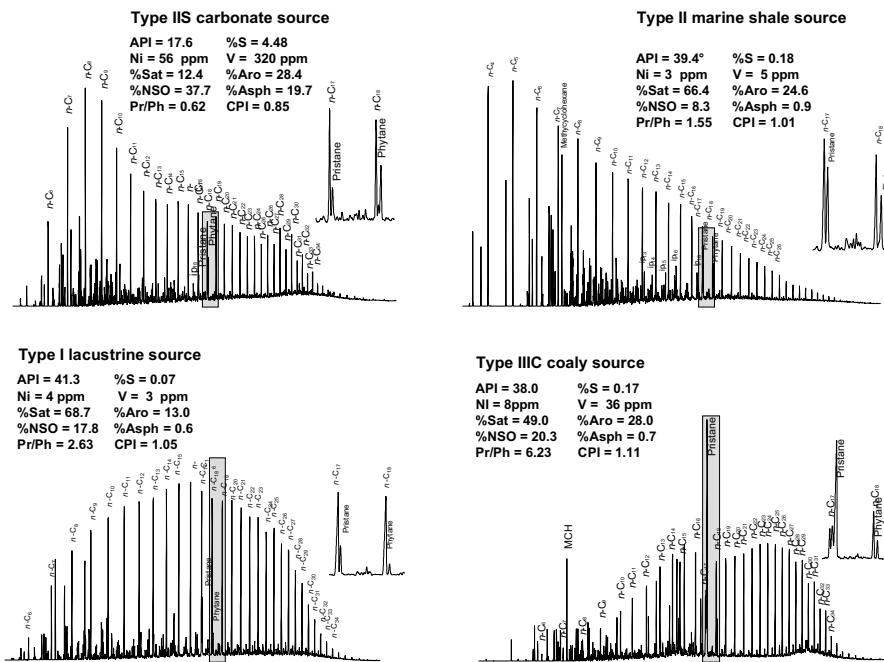


Figure 10. Whole-oil gas chromatograms showing examples of oils from different source kerogens. The grayed area, showing the elution of  $n\text{-C}_{17}$ , pristane (Pr),  $n\text{-C}_{18}$ , and phytane (Ph), is enlarged. Pr/Ph is the pristane/phytane ratio, which is used to infer the depositional environment (anoxic, hypersaline Pr/Ph<1, oxic water column/anoxic sediments Pr/Ph 1~2, oxic deposition Pr/Ph>2). CPI is the carbon preference, which is used to infer carbonate/evaporite source facies <1, and higher land-plant input CPI > 1. API gravity, the concentrations of sulfur (S), nitrogen (N), nickel (Ni) and vanadium (V) and the  $\text{C}_{15+}$  chemical group-type compositions are influenced by of the organic matter, depositional environment, and thermal history of their source rocks and by reservoir alteration processes.

The composition of crude oil that arrives at a refinery is not identical to reservoir fluids. Gas and water is separated at the well head and emulsions are broken. Consequently, oils lose some light hydrocarbons (< $\text{C}_6$ ) by evaporation during production and transport. Pipeline and tanker oils are frequently blends of oils from multiple fields and reservoirs, which individually may be of varying composition and quality. For these reasons, testing of subsurface fluids from individual reservoirs is necessary to determine field economics and design reservoir management practices.

## 7. SUMMARY

The theory that petroleum originates from sedimentary organic matter that was once living organisms is consistent with all natural observations, laboratory analyses and experiments, theoretical considerations, and basin simulations. The accumulation of economic quantities of petroleum (oil and gas) requires that a series of processes occur within sedimentary basins. Organic-rich sediments are deposited only under specific conditions that promote the production of biota and/or transport of biogenic organic compounds and the selective preservation of this material. The sedimentary organic matter converts to kerogen, an insoluble macromolecule with a composition that reflects the biotic input and chemical alterations (sulfurization, condensation, defunctionalization, and aromatization) that occur during diagenesis. Once lithified, these organic-rich strata have the potential to generate oil and gas when buried and heated to promote thermal cracking. Expelled petroleum migrates from the source through fractures and permeable strata. Economic reserves occur when geological conditions allow for the accumulation, retention, and preservation of significant volumes of migrated petroleum. Collectively, these processes describe a petroleum system.

## 8. REFERENCES

- <sup>1</sup> Bacon, Roger. *Fr. Rogeri Bacon Opera quaedam hactenus inedita. I. I. Opus tertium. II. Opus minus. III. compendium philosophiae.* J. S. Brewer (Ed.). London, 1859.
- <sup>2</sup> Aristotle, *Meteorology* in *The Complete Works of Aristotle*, Jonathan Barnes (Eds) Princeton Univ. Press, 1995; pp. 555-625.
- <sup>3</sup> Kenney, J.F. Considerations about recent predictions of impending shortages of petroleum evaluated from the perspective of modern petroleum science, *Energy World* **1996**, *240*, 16-18.
- <sup>4</sup> Wellings, F.E. Geological aspects the origin of oil. *Inst. Petrol. J.* **1966**, *52*, 124-130.
- <sup>5</sup> Dott, R.H. Hypotheses for an organic origin. In *Sourcebook for Petroleum Geology, Part I. Genesis of Petroleum.* R.H. Dott and M.J. Reynolds (Eds). AAPG Memoir 5, Tulsa, 1969; pp. 1-244.
- <sup>6</sup> Hunt, T.S. Report on the geology of Canada. Canadian Geological Survey Report: Progress to 1863. Canadian Geological Survey, 1863.
- <sup>7</sup> Lesquereux, L. Report on the fossil plants of Illinois: III. Geol. Survey, **1866**, *2*, 425-470.
- <sup>8</sup> Newberry, J.S. The general geological relations and structure of Ohio: *Ohio Geological Survey Report 1*, **1873**, pt. 1, 222 p.
- <sup>9</sup> Arnold, R. & Anderson, R. Geology and oil resources of the Santa Maria Oil District, Santa Barbara County, California. *USGS Bulletin* **1907**, No. 322.
- <sup>10</sup> Clarke, F.W. Data of geochemistry. *USGS Bulletin* **1916**, No. 616.
- <sup>11</sup> Pompeckj, J.F. Die Juraablagerungen zwischen Regensburg und Regensburg. *Geologisches Jahrbuch*, **1901**, *14*, 139-220.
- <sup>12</sup> Schuchert, C. The conditions of black shale deposition as illustrated by Kupferschiefer and Lias of Germany. *Proc. Am. Philos. Soc.* **1915**, *54*, 259-269.

- <sup>13</sup> Treibs, A. Chlorophyll and hemin derivatives in organic mineral substances. *Angewandte Chemie* **1936**, 49, 682-686.
- <sup>14</sup> Oakwood, T.S.; Shriver, D.S.; Fall, H.H.; Mcaleer, W.J.; Wunz, P.R. Optical activity of petroleum. *Ind. Eng. Chem.* **1952**, 44, 2568-2570.
- <sup>15</sup> Craig, H. The geochemistry of the stable carbon isotopes. *Geochim. Cosmochim. Acta* **1953**, 3, 53-92.
- <sup>16</sup> Eglinton, G.; Calvin, M. Chemical fossils. *Sci. Amer.* **1967**, 216, 32-43.
- <sup>17</sup> Forsman, J.P.; Hunt, J.M. Insoluble organic matter (kerogen) in sedimentary rocks of marine origin. In: Weeks, L.G. (Ed.), *Habitat of Oil: A Symposium*. American Association of Petroleum Geologists, Tulsa, Oklahoma, 1958; pp. 747-778.
- <sup>18</sup> Abelson, P.H. Organic geochemistry and the formation of petroleum. *6th World Petroleum Congress Proc.*, **1963**, Sec 1, 397-407.
- <sup>19</sup> Tissot, B. Premières données sur les mécanismes et la cinétique de la formation du pétrole dans les sédiments. Simulation d'un schéma réactionnel sur ordinateur. *Rev. Inst. Fran. Pét.* **1969**, 24, 470-501.
- <sup>20</sup> Berthelot, M.-P. *Chimie organique fondée sur la synthèse*, 1860
- <sup>21</sup> Mendeleev, D. L'origine du pétrole. *Revue Scientifique*, **1877**, 2e Ser., VIII, 409-416.
- <sup>22</sup> Mendeleev, D. *The Principles of Chemistry*, vol. 1. Second English edition translated from the sixth Russian edition. Collier: New York, 1902; 552 pp.
- <sup>23</sup> Kudryavtsev, N.A. Against the organic hypothesis of the origin of petroleum *Petroleum Economy [Neftianoye Khozyaistvo]*, **1951**, 9, 17-29.
- <sup>24</sup> Cronin J.; Pizzarello S.; Cruikshank D.P. Organic matter in carbonaceous chondrites, planetary satellites, asteroids, and comets. In *Meteorites and the Early Solar System*, Kerridge, J.F.; Mathews, M.S. (Eds), University of Arizona Press, 1988; pp. 819-857
- <sup>25</sup> Hoyle, F. *Frontiers of Astronomy*, Heineman: London, 1955; 360 pp.
- <sup>26</sup> Gold T. The origin of natural gas and petroleum and the prognosis for future supplies. *Annual Review of Energy*, **1985**, 10, 53-77.
- <sup>27</sup> Gold T. *The Deep Hot Biosphere*, Copernicus: New York, 1999; 235 p.
- <sup>28</sup> Kerr, R.A. When a radical experiment goes bust, *Science* **1990**, 247, 1177.
- <sup>29</sup> Sherwood Lollar B.S.; Frape, S.K.; Weise, S.M.; Fritz, P.; Macko, S.A.; Whelan, J.A. Abiogenic methanogenesis in crystalline rocks. *Geochim. Cosmochim. Acta* **1993**, 57, 5087-5097.
- <sup>30</sup> McCollom, T.M.; Seewald, J.S. A reassessment of the potential for reduction of dissolved CO<sub>2</sub> to hydrocarbons during serpentinization of olivine. *Geochim. Cosmochim. Acta* **2001**, 65(21), 3769-3778.
- <sup>31</sup> McCollom, T.M. Formation of meteorite hydrocarbons from thermal decomposition of siderite (FeCO<sub>3</sub>). *Geochim. Cosmochim. Acta* **2003**, 67(2), 311-317.
- <sup>32</sup> Potter J.; Rankin, A.H.; Treloar, P.J. The nature and origin of abiogenic hydrocarbons in the alkaline igneous intrusions, Khibina and Lovozero in the Kola Peninsula, N.W. Geological Society London Hydrocarbons in Crystalline Rocks Joint Meeting, London, England, 13-14 February, 2001.
- <sup>33</sup> Sherwood, Lollar B.; Westgate, T.D.; Ward, J.A.; Slater, G.F.; Lacrampe-Couloume, G. Abiogenic formation of alkanes in the Earth's crust as a minor source for global hydrocarbon reservoirs, *Nature* **2002**, 416, 522-524.
- <sup>34</sup> *The Petroleum System—From Source to Trap*, Vol. AAPG Memoir No. 60, Magoon, L.B.; Dow, W.G. (Eds.) American Association of Petroleum Geologists, Tulsa, 1994; pp. 655..
- <sup>35</sup> Magoon, L.B.; Beaumont, E.A. Petroleum Systems. In: *Handbook of Petroleum Geology: Exploring for Oil and Gas Traps*, Beaumont, E.A.; Foster, H.N. (Eds), American Association of Petroleum Geologists, Tulsa, 1999; pp. 3-1 to 3-34..
- <sup>36</sup> Beaumont, A.; Foster N.H. *Treatise of Petroleum Geology/Handbook of Petroleum Geology: Exploring for Oil and Gas Traps*, The American Association of Petroleum Geologists, Tulsa, 1999.

- <sup>37</sup> Tissot, B.P.; Welte, D.H. *Petroleum Formation and Occurrence*, Springer-Verlag: New York, 1984; 699 p.
- <sup>38</sup> Hunt, J.M. *Petroleum Geochemistry and Geology*. W. H. Freeman: New York, 1996; 743 p.
- <sup>39</sup> Peters K.E.; Fowler, M.G. Applications of petroleum geochemistry to exploration and reservoir management, *Org. Geochem.* **2002**, *33*, 5-36.
- <sup>40</sup> Arthur, M.A.; Sageman, B.B. Marine black shales: a review of depositional mechanisms and significance of ancient deposits. *Annual Review of Earth & Planetary Science* **22**, 499-551.
- <sup>41</sup> Canfield, D.E. (1994) Factors influencing organic carbon preservation in marine sediments. *Chemical Geology*, **1994**, *114*, 315-329.
- <sup>42</sup> Tyson, R.V. *Sedimentary Organic Matter: Organic Facies and Palynofacies*. Chapman and Hall: London, 1995; 615 pp.
- <sup>43</sup> Pedersen, T.F.; Calvert, S.E. Anoxia vs. productivity: what controls the formation of organic-carbon-rich sediments and sedimentary rocks? *AAPG Bulletin* **1990**, *74*, 454-466.
- <sup>44</sup> Michaelis, W.; Seifert, R.; Nauhaus, K.; Treude, T.; Thiel, V.; Blumenberg, M.; Knittel, K.; Gieseke, A.; Peterknecht, K.; Pape, T.; Boetius, A.; Amann, R.; Jørgensen, B.B.; Widdel, F.; Peckmann, J.; Pimenov, N.V.; Gulin, M.B. Microbial reefs in the Black Sea fueled by anaerobic oxidation of methane. *Science* **2002**, *297*, 1013-1015.
- <sup>45</sup> Demaison, G.L.; Moore, G.T. Anoxic environments and oil source bed genesis. *AAPG Bulletin* **1980**, *64*, 1179-1209.
- <sup>46</sup> Koopmans, M.P.; Schouten, S.; Kohnen, M.E.L.; Sinninghe Damsté, J.S. Restricted utility of aryl isoprenoids as indicators for photic zone anoxia. *Geochim. Cosmochim. Acta* **1996**, *60*, 4467-4496.
- <sup>47</sup> Metzger, P.; Largeau, C.; Casadevall, E. Lipids and Macromolecular Lipids of the hydrocarbon-rich Microalga *Botryococcus Braunii*. *Progress in the Chemistry of Organic Natural Products*, **1991**, *57*, 1-70.
- <sup>48</sup> *Kerogen. Insoluble Organic Matter From Sedimentary Rocks*, Durand, B. (Ed.) Éditions Technip: Paris, 1980; 519 p.
- <sup>49</sup> Tegelaar E.W.; De Leeuw, J.W.; Derenne, S.; Largeau, C. A reappraisal of kerogen formation. *Geochim. Cosmochim. Acta* **1989**, *53*, 3103-3106.
- <sup>50</sup> van Krevelen D.W. *Coal*, Elsevier: New York, 1961; 514 pp.
- <sup>51</sup> Sinninghe Damsté, J.S.; de las Heras, F.X.C.; van Bergen, P.F.; de Leeuw, J.W. Characterization of Tertiary Catalan lacustrine oil shales; discovery of extremely organic sulphur-rich Type I kerogens. *Geochim. Cosmochim. Acta* **1993**, *57*, 389-415.
- <sup>52</sup> Connan, J. Time-temperature relation in oil genesis. *AAPG Bulletin* **1974**, *58*, 2516-2521.
- <sup>53</sup> Tissot, B.P.; Pelet, R.; Ungerer, P. Thermal history of sedimentary basins and kinetics of oil and gas generation. *AAPG Bulletin* **1986**, *70*, 656.
- <sup>54</sup> Ungerer, P.; Bessis, F.; Chenet, P.Y.; Durand, B.; Nogaret, E.; Chiarelli, A.; Oudin, J.L.; Perrin, J.F. Geological and geochemical models in oil exploration; principles and practical examples. In: *Petroleum geochemistry and basin evaluation* Demaison, G.; Murriss, R. J. (Ed.), American Association of Petroleum Geologists, Tulsa, OK, 1984; pp. 53-77.
- <sup>55</sup> Mango, F.D. Transition metal catalysis in the generation of petroleum and natural gas. *Geochim. Cosmochim. Acta* **1992**, *56*, 553-555.
- <sup>56</sup> Sabate, R.W.; Baker, C.C. Synergetic catalysis in hydrocarbon generation. In *Gulf Coast Association of Geological Societies Transactions*, 1994; pp. 657-661.
- <sup>57</sup> Schoonen, M.A.A.; Xu, Y.; Strongin, D.R. An introduction to geocatalysis. *J. Geochem. Expl.* **1998**, *62*, 201-215.
- <sup>58</sup> McAuliffe, C.D. Oil and gas migration: chemical and physical constraints. In *Problems of Petroleum Migration*, Roberts, W. H.; Cordell, R. J. (Eds.) AAPG Geological Studies 10, 1980; p. 89-107.
- <sup>59</sup> Sandvik, E.I.; Young, W.A.; Curry, D.J. Expulsion from hydrocarbon sources; the role of organic absorption. *Org. Geochem.* **1992**, *19*, 77-87
- <sup>60</sup> Pepper, A.S.; Corvi, P.J. Simple kinetic models of petroleum formation; Part III, Modelling an open system. *Marine Petrol. Geol.* **1995**, *12*, 417-452.

- <sup>61</sup> Thomas, M.M.; Clouse, J.A. Primary migration by diffusion through kerogen; I, Model experiments with organic-coated rocks, *Geochim. Cosmochim. Acta* **1990**, *54*, 2775-2779.
- <sup>62</sup> Thomas, M.M.; Clouse, J. A. Primary migration by diffusion through kerogen; II, Hydrocarbon diffusivities in kerogen. *Geochim. Cosmochim. Acta* **1990**, *54*, 2781-2792.
- <sup>63</sup> Thomas, M. M.; Clouse, J. A. Primary migration by diffusion through kerogen; III, Calculation of geologic fluxes. *Geochim. Cosmochim. Acta* **1990**, *54*, 2793-2797.
- <sup>64</sup> Stainforth, J.G.; Reinders, J.E.A. Primary migration of hydrocarbons by diffusion through organic matter networks, and its effect on oil and gas generation. *Org. Geochem.* **1990**, *16*, 61-74.
- <sup>65</sup> Ritter, U. Solubility of petroleum compounds in kerogen: implications for petroleum expulsion *Org. Geochem.* **2003**, *34*, 319-326
- <sup>66</sup> Pepper, A. S. Estimating the petroleum expulsion behaviour of source rocks; a novel quantitative approach. In *Petroleum Migration*, England, W. A.; Fleet, A. J. (Eds.) Geological Society of London Special Publication 59, 1991; pp. 9-31.
- <sup>67</sup> Shadle, L.J.; Khan, M.R.; Zhang, G.Q.; Bajura, R.A. Investigation of oil shale and coal structures by swelling in various solvents, *Prep. Div. Petr. Chem.* **1989**, *34(1)*, 55-61.
- <sup>68</sup> Larsen, J.W.; Li, Shang. Changes in the macromolecular structure of a Type I kerogen during maturation," *Energy Fuels* **1987**, *11*, 897-901.
- <sup>69</sup> Larsen, J.W.; Li, Shang. An initial comparison of the interactions of type I and III kerogens with organic liquids, *Org. Geochem.* **1987**, *26*, 305-309.
- <sup>70</sup> Larsen, J.W.; Li, Shang. Solvent swelling studies of Green River Kerogen, *Energy Fuels* **1994**, *8*, 932-936.
- <sup>71</sup> Tissot, B. Migration of hydrocarbons in sedimentary basins; a geological, geochemical and historical perspective. *Migration of hydrocarbons in sedimentary basins*, 1987; 1-19.
- <sup>72</sup> Ungerer, P. State of the art of research in kinetic modelling of oil formation and expulsion. *Org. Geochem.* **1990**, *16*, 1-25.
- <sup>73</sup> Burnham, A.K.; Braun, R.L. Development of a detailed model of petroleum formation, destruction, and expulsion from lacustrine and marine source rocks. *Org. Geochem.* **1990**, *16*, 27-39.
- <sup>74</sup> Dickey, P.A. Possible migration of oil from source rock in oil phase. *AAPG Bulletin* **1975**, *72*, 337-345.
- <sup>75</sup> Palciauskas, V.V.; Domenico, P.A. Microfracture development in compacting sediments: relation to hydrocarbon-maturation kinetics. *AAPG Bulletin* **1980**, *64*, 927-937.
- <sup>76</sup> Mann, U. Sedimentological and petrophysical aspects of primary migration pathways. In *Sediments and Environmental Geochemistry*, Heling, D.; Rothe, P.; Förstner, U.; Stoffers, P. (Eds.), Springer: New York, 1990; pp. 152-178.
- <sup>77</sup> Düppenbecker, S. J.; Welte, D. H. Petroleum expulsion from source rocks; insights from geology, geochemistry and computerized numerical modelling. *Thirteenth World Petroleum Congress*, **1992**; 165-177.
- <sup>78</sup> Price, L.C. Primary petroleum migration from shales with oxygen-rich organic matter. *J. Petrol. Geol.*, **1989**, *12*, 289-324.
- <sup>79</sup> Leythaeuser, D.; Poelchau, H.S. Expulsion of petroleum from type III kerogen source rocks in gaseous solution; modeling of solubility fractionation. In *Petroleum migration*, Vol. 59, England, W. A.; Fleet, A. J. (Eds.), Geological Society of London: London, 1991; pp. 33-46.
- <sup>80</sup> Barker, C. Aquathermal pressuring: role of temperature in development of abnormal pressure zones. *AAPG Bulletin* **1972**, *56*, 2068-2071.
- <sup>81</sup> Magara, K. Agents for primary hydrocarbon migration; a review. In *Problems of petroleum migration*, Roberts, III W. H.; Cordell, R. J. (Eds.), American Association of Petroleum Geologists, Tulsa, OK, 1980; pp. 33-45..
- <sup>82</sup> Peters, K.E.; Moldowan, J.M. *The Biomarker Guide; Interpreting Molecular Fossils in Petroleum and Ancient Sediments*. Prentice Hall: Englewood Cliffs, NJ, 1993; 363 pp.



- <sup>83</sup> Werner, A.; Behar, F.; de Hemptinne, J.C.; Behar, E. Thermodynamic properties of petroleum fluids during expulsion and migration from source rocks. *Org. Geochem.* **1996**, *24*, 1079-1095.
- <sup>84</sup> Kuo, L.C. Gas exsolution during fluid migration and its relation to overpressure and petroleum accumulation. *Marine Petrol. Geol.* **1997**, *14*, 221-229.
- <sup>85</sup> Di Primio, R.; Dieckmann, V.; Mills, N. PVT and phase behaviour analysis in petroleum exploration. *Org. Geochem.* **1998**, *29*, 207-222.
- <sup>86</sup> Palmer, S.E. Effect of water washing on C<sub>15+</sub> hydrocarbon fraction of crude oils from northwest Palawan, Phillipines. *AAPG Bulletin*, **1984**, *68*, 137-149.
- <sup>87</sup> Connan, J. Biodegradation of crude oils in reservoirs. In *Advances in Petroleum Geochemistry, 1*, Brooks, J.; Welte, D.H. (Eds.), . Academic Press: London, 1984; pp. 299-335.
- <sup>88</sup> Seifert, W.K.; Moldowan, J.M.; Demaison G. J. Source correlation of biodegraded oils: *Org. Geochem.* **1984**, *6*, 633-643.
- <sup>89</sup> Orr, W.L. Changes in sulfur content and isotopic ratios of sulfur during petroleum maturation-Study of Big Horn Paleozoic oils. *AAPG Bulletin*, **1974**, *58*, 2295-2318.
- <sup>90</sup> Machel, H.G. Bacterial and thermochemical sulfate reduction in diagenetic settings - old and new insights. *Sedimentary Geology* **2001**, *140*, 143-175.
- <sup>91</sup> Wilhelms, A.; Larter, S.R. Origin of tar mats in petroleum reservoirs: part II: formation mechanisms for tar mats. *Marine Petrol. Geol.* **1994**, *11*, 442-456.

## Chapter 3

### **CRUDE ASSAY**

Murray R. Watt and Stilianos G. Roussis

*Imperial Oil*

*Sarnia Research Centre*

*Sarnia, Ontario, N7T 8C8*

#### **1. INTRODUCTION**

The well-developed crude assay program is crucial to the success of an organization that deals with diverse crude slates. Purchasing decisions and ultimately processing capability all begin with having high quality assay data that reflect the needs of the organization. Most crude oils have a lot of variability in their compositions from one source to another. Also as a crude oil field ages property data will change. These needs are especially important if the organization wants to deal with spot market crude purchasing from various parts of the world.

Crude assay programs can be subdivided into various formats, one format being Whole Crude property measurements/inspections and the other being a full assay including distillations and inspection data. The quality of either program is dependent on the care and attention paid to crude sampling and storage. Care is needed in some geographic locations, in the sampling from the crude container, especially in hot climates. In this case, the container may need to be cooled prior to the measurement in order to insure that light ends are not lost. Conversely, in colder climates containers need to be brought up gradually to room temperatures. ASTM D 4057 and D 5854 methods provide information on the sampling/mixing of petroleum products.<sup>1</sup>

## **2. PROPERTY MEASUREMENTS/CRUDE INSPECTIONS**

### **2.1 API Gravity**

This industry standard that is based on ASTM D287/1298, is the single most utilized crude property measurement for making crude purchases. It is quite common for measurements to range from values in the low teens (asphaltic crude) to those having values in the 50's (condensates). While this test normally is done by the hydrometer method and is simple to perform, it does have some crucial steps that need to be performed. The first step is to insure that the crude aliquot taken is representative. API is measured along with the temperature of the crude that is then converted to an API at 60 °F (the industry standard).

### **2.2 Sulfur Content**

The sulfur content of crude oils is normally in the range of 0.1-5.0-wt %. Sulfur is normally measured utilizing an x-Ray technique such as the following two methods ASTM D4294 or D5291 using a technique known as X-Ray Fluorescence. The methods have large dynamic ranges and allow analysis to be completed in about 3-5 minutes. Samples having sulfur contents greater than 5.0 % are measured by methods such as D1552, a combustion technique. For extremely low levels an Ultraviolet fluorescence technique is employed (ASTM D5453). Again most of these methods are very robust, but can be influenced by not having a representative sample.

### **2.3 Pour Point**

The pour point of a sample is defined as the temperature normally 3 degrees above the point a sample no longer moves when inverted. This value is of particular importance for crudes that are transported through pipelines from source to load ports.

Currently the method of choice for whole crudes is ASTM D5853 which handles crudes that have pour points greater than -36 °C. For crudes that have pour points lower than -36 °C ASTM D97 tends to be the method of choice.

### **2.4 Whole Crude Simulated Distillation**

This method normally is performed by ASTM D5307.<sup>1</sup> This gas chromatography method is a quick and robust method for determining a true boiling point curve and predicting crude yields. This external standard method is done on 5 metre fused silica columns having thin film thickness allowing

the analysis to be completed within an hour. A true boiling point curve can be determined by plotting % off (cumulative yield) versus temperature. Comparing a full assay TBP curve to this data and then monitoring the crude over time is a valuable tool to determine whether or not a full assay may need to be done/updated.

## 2.5 Full Assay

Assay analyses of whole crudes are done by combining an atmospheric and vacuum distillation run. These two runs when combined will provide a TBP (True Boiling Point Curve). While these batch distillation methods are labor intensive, taking between three to five days, they allow the collection of distillation fractions that can be utilized for testing. While each of the distillations techniques have been standardized by ASTM, cut schemes tend to mimic Refinery product classifications and there is no standardization of the individual inspection formats. Each corporation tends to perform both physical and chemical testing that best meet the needs of their refining operations and product suites.

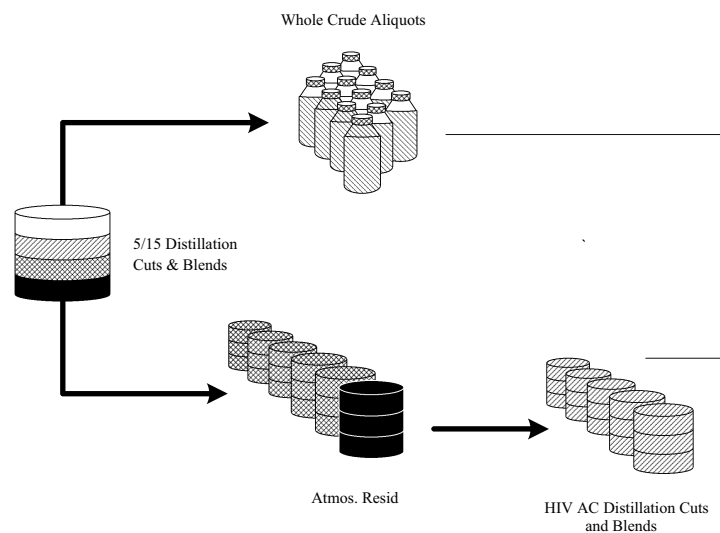


Figure 1. Crude Distillation

## 2.6 Physical Distillation - ASTM D 2892 Method

This technique is performed on a 15 theoretical plate fractionation column to obtain a true boiling point curve while maintaining an approximate 5:1 reflux ratio. The still pressure is reduced in order to prevent decomposition

due to high pot temperatures. This fractionation determines accurate boiling points (TBP) and agrees with the fractionation produced in the refinery.

These narrow fractions are sent for physical property measurements as well as chemical typing analysis. A typical cutting scheme is listed below.

*Table 1. Temperature Ranges for Typical Distillation Cuts*

| Distillation Cut       | Temperature Range in °C |
|------------------------|-------------------------|
| Light Ends/Natural Gas | Trap                    |
| Light Gasoline         | Trap-70                 |
| Light Naphtha          | 70-100                  |
| Medium Naphtha         | 100-150                 |
| Heavy Naphtha          | 150-190                 |
| Light Kerosene         | 190-235                 |
| Heavy Kerosene         | 235-265                 |
| Atmospheric Gas Oil    | 265-343                 |
| Atmospheric Resid      | 343+                    |

## 2.7 ASTM D 5236 Method

The atmospheric resid taken from the D 2892 distillation run is charged into the vacuum potstill. The method produces distillation fractions in the gas oil and traditional lube oil range as well as producing a vacuum resid. While there is no industry standard cutting scheme for Hivac distillation runs, narrow cuts in the 25-50 degree intervals are common. The final cut temperature is normally done to 565°C, a temperature that most crudes can attain.

Care needs to be taken to identify the early stages of cracking. It is recommended that the last distillation cut be taken within one hour of the pot temperature reaching 310°C.

## 2.8 TBP Curves

The physical distillation data from the D 2892 and D 5236 distillation runs are used to create a True Boiling Point Curve (TBP). These two curves will have a disparity in the area corresponding to the overlap between the 15/5 and Hivac distillation runs. This artifact is due to the Hivac still not being at optimum conditions at the early stages of the run. Once a TBP curve has been created property measurements can then be curve fit.

## 2.9 Property Measurement/Assay Grid

At present there is not a standardize grid for physical property and chemical typing information. The grid inspection format is based on customer need as well affordability. Please refer to Figure 2 as an example of a typical grid.

| CRUDE  | Whole Crude |        | Whole Crude |       | DISTILLATION and AIR |   |        |      |      |     |     |      |      |    |    |   |    |      |     |     |      |      |      |         |         |         |         |         |          |          |      |             |     |      |         |                    |     |   |  |
|--------|-------------|--------|-------------|-------|----------------------|---|--------|------|------|-----|-----|------|------|----|----|---|----|------|-----|-----|------|------|------|---------|---------|---------|---------|---------|----------|----------|------|-------------|-----|------|---------|--------------------|-----|---|--|
|        |             |        |             |       | X                    | X | SULFUR | MERC | H2SD | H2S | IN2 | BENZ | CCAR | FE | NI | V | NA | FOUR | CLD | FRZ | RIB7 | ANPT | SMOK | VIS 20C | VIS 40C | VIS 50C | VIS 60C | VIS 80C | VIS 100C | VIS 135C | IPAN | ASPHALTINES | RVP | SALT | GC COMP | PNAs (MS or GC/MS) | FIA |   |  |
| D2892  | Trap        | 158.0  | Trap        | 70.0  | X                    | X |        |      |      |     |     |      |      |    |    |   |    |      |     |     |      |      |      |         |         |         |         |         |          |          |      |             |     |      |         |                    |     |   |  |
| D2892  | Trap        | 158.0  | Trap        | 70.0  | X                    | X |        |      |      |     |     |      |      |    |    |   |    |      |     |     |      |      |      |         |         |         |         |         |          |          |      |             |     |      |         |                    |     | X |  |
| D2892  | 158.0       | 212.0  | 70.0        | 100.0 | X                    | X |        |      |      |     |     |      |      |    |    |   |    |      |     |     |      |      |      |         |         |         |         |         |          |          |      |             |     |      |         |                    |     | X |  |
| D2892  | 212.0       | 257.0  | 100.0       | 125.0 | X                    | X |        |      |      |     |     |      |      |    |    |   |    |      |     |     |      |      |      |         |         |         |         |         |          |          |      |             |     |      |         |                    |     |   |  |
| D2892  | 257.0       | 302.0  | 125.0       | 150.0 | X                    | X |        |      |      |     |     |      |      |    |    |   |    |      |     |     |      |      |      |         |         |         |         |         |          |          |      |             |     |      |         |                    |     |   |  |
| D2892  | 302.0       | 347.0  | 150.0       | 175.0 | X                    | X |        |      |      |     |     |      |      |    |    |   |    |      |     |     |      |      |      |         |         |         |         |         |          |          |      |             |     |      |         |                    |     |   |  |
| D2892  | 347.0       | 392.0  | 175.0       | 200.0 | X                    | X |        |      |      |     |     |      |      |    |    |   |    |      |     |     |      |      |      |         |         |         |         |         |          |          |      |             |     |      |         |                    |     |   |  |
| D2892  | 392.0       | 437.0  | 200.0       | 225.0 | X                    | X |        |      |      |     |     |      |      |    |    |   |    | X    | X   |     |      | X    | X    |         |         |         |         |         |          |          |      |             |     |      |         |                    |     |   |  |
| D2892  | 437.0       | 482.0  | 225.0       | 250.0 | X                    | X |        |      |      |     |     |      |      |    |    |   |    | X    | X   | X   |      | X    | X    |         |         |         |         |         |          |          |      |             |     |      |         |                    |     |   |  |
| D2892  | 482.0       | 527.0  | 250.0       | 275.0 | X                    | X |        |      |      |     |     |      |      |    |    |   |    |      |     |     |      | X    | X    |         |         |         |         |         |          |          |      |             |     |      |         |                    |     | X |  |
| D2892  | 527.0       | 572.0  | 275.0       | 300.0 | X                    | X |        |      |      |     |     |      |      |    |    |   |    |      | X   | X   | X    |      | X    |         |         |         |         |         |          |          |      |             |     |      |         |                    |     |   |  |
| D2892  | 572.0       | 617.0  | 300.0       | 325.0 | X                    | X |        |      |      |     |     |      |      |    |    |   |    |      |     |     |      | X    | X    |         |         |         |         |         |          |          |      |             |     |      |         |                    |     | X |  |
| D2892  | 617.0       | 650.0  | 325.0       | 343.3 | X                    | X |        |      |      |     |     |      |      |    |    |   |    |      |     |     |      | X    | X    |         |         |         |         |         |          |          |      |             |     |      |         |                    |     |   |  |
| D2892  | 650.0       | FBP    | 343.3       | FBP   | X                    | X |        |      |      |     |     |      |      |    |    |   |    |      |     |     |      |      |      |         |         |         |         |         |          |          |      |             |     |      |         |                    |     |   |  |
| D5236  | 650.0       | 734.0  | 343.3       | 390.0 | X                    | X |        |      |      |     |     |      |      |    |    |   |    |      |     |     |      |      |      |         |         |         |         |         |          |          |      |             |     |      |         |                    |     |   |  |
| D5236  | 734.0       | 779.0  | 390.0       | 415.0 | X                    | X |        |      |      |     |     |      |      |    |    |   |    |      | X   |     |      | X    | X    |         |         |         |         |         |          |          |      |             |     |      |         |                    |     |   |  |
| D5236  | 779.0       | 824.0  | 415.0       | 440.0 | X                    | X |        |      |      |     |     |      |      |    |    |   |    |      |     |     |      |      |      |         |         |         |         |         |          |          |      |             |     |      |         |                    |     |   |  |
| D5236  | 824.0       | 869.0  | 440.0       | 465.0 | X                    | X |        |      |      |     |     |      |      |    |    |   |    |      |     |     |      |      |      |         |         |         |         |         |          |          |      |             |     |      |         |                    |     |   |  |
| D5236  | 869.0       | 914.0  | 465.0       | 490.0 | X                    | X |        |      |      |     |     |      |      |    |    |   |    |      |     |     |      |      |      |         |         |         |         |         |          |          |      |             |     |      |         |                    |     |   |  |
| D5236  | 914.0       | 959.0  | 490.0       | 515.0 | X                    | X |        |      |      |     |     |      |      |    |    |   |    |      |     |     |      |      |      |         |         |         |         |         |          |          |      |             |     |      |         |                    |     |   |  |
| D5236  | 959.0       | 1004.0 | 515.0       | 540.0 | X                    | X |        |      |      |     |     |      |      |    |    |   |    |      |     |     |      |      |      |         |         |         |         |         |          |          |      |             |     |      |         |                    |     |   |  |
| D5236  | 1004.0      | 1049.0 | 540.0       | 565.0 | X                    | X |        |      |      |     |     |      |      |    |    |   |    |      |     |     |      |      |      |         |         |         |         |         |          |          |      |             |     |      |         |                    |     |   |  |
| D5236  | 1049.0      | FBP    | 565.0       | FBP   | X                    | X |        |      |      |     |     |      |      |    |    |   |    |      |     |     |      |      |      |         |         |         |         |         |          |          |      |             |     |      |         |                    |     |   |  |
| BLEND5 | 650.0       | FBP    | 565.0       | FBP   | X                    | X |        |      |      |     |     |      |      |    |    |   |    |      |     |     |      |      |      |         |         |         |         |         |          |          |      |             |     |      |         |                    |     |   |  |

Figure 2. Typical Crude Testing Grid

## 2.10 Physical Property Test

### 2.10.1 API Gravity

This is the most common measurement performed on petroleum products; density is expressed in terms of API gravity. This measurement determines the weight of a crude oil per unit volume at 60°F, normally measured by the Hydrometer method ASTM D 287.

### 2.10.2 Aniline Point

This point is defined as the lowest temperature at which aniline is soluble in a specified amount of sample. This measure is used to determine the solvency of the hydrocarbons Typically paraffinic hydrocarbons have higher aniline points than aromatic hydrocarbons. This method is usually performed under the guidelines of ASTM D 611. Aniline point can be used to determine the quality of ignition in diesel cuts.

### 2.10.3 Cloud Point

This is defined as the temperature at which a haze appears in a sample which is attributed to the formation of wax crystals. Cloud point data is used to determine the tendency of small orifices to plug in cold operating temperatures, normally measured on middle distillate cuts. This property can

be measured manually by utilizing ASTM D 2500, since many laboratories utilize similar equipment to perform pour points. With the development of new analytical equipment many laboratories are now utilizing phase technology and are performing ASTM D 5773 which is less labor intensive and more robust.

#### **2.10.4 Freeze Point**

The temperature at which crystal start to form in hydrocarbon liquids and then disappear when the liquid is heated is the freeze point. Normally performed by ASTM D2386, this method like cloud point is done by ASTM D 5972 by phase technology.

#### **2.10.5 Metals**

The metals concentration in crude can range from a few to several thousand ppm. Low values of certain elements such as nickel vanadium can severely affect catalyst activity. In the past metals were determined by Atomic Absorption, but now most metals are determined by Inductively Coupled Plasma Emission Spectroscopy ICPAES. X-ray fluorescence can be a viable technique depending on the concentration.

#### **2.10.6 Mercaptan Sulfur**

Mercaptan Sulfur species are undesirable in crude oils, and in some cases are toxic. These species are normally attributed to sour crudes. Analysis is normally based on UOP 163, a potentiometric titration method. A hydrocarbon sample is added to a solution of isopropyl alcohol containing a small amount of ammonium hydroxide. The solution is then titrated with a solution of silver nitrate.

#### **2.10.7 Micro Carbon Residue**

The carbon residue of a petroleum crude oil is proportional to the asphalt content, normally measured by Conradson Carbon ASTM D 189. In most cases the lower the carbon residue, the higher the value that can be placed on the crude oil.

#### **2.10.8 Nitrogen**

Nitrogen species in crude oils can cause catalyst poisoning. ASTM D 3228 or ASTM D 4629 normally determines nitrogen content. Either a syringe inlet or boat inlet analyzes distillate cuts by Oxidative Combustion and Chemiluminescence detection. Whole crude, atmospheric and vacuum

resids are analyzed by Kjeldahl methodology, a labor intensive method involving digestion/distillation and finishing up with a titration.

### **2.10.9 Pour Point**

The lowest temperature at which a hydrocarbon fraction is observed to pour when cooled under prescribed conditions. The pour point of a sample is determined to be 3 degrees Celsius above the point at which a sample can be horizontally held and no movement occurs for five seconds. The most frequently utilized method for this test is ASTM D 97, which can be used for all assay fractions/ blends. For whole crudes that have pour points greater than -36°C, a new method has been developed (ASTM D 5853). Also for fractions that contain wax, a new method utilizing phase technology ASTM D 5949. Normally low pour points are due to low paraffin content and high aromatics.

### **2.10.10 Refractive Index**

Refractive index is a ratio technique that takes the velocity of light in air at a specific wavelength and compares that to the velocity in the sample tested. Normally this is performed under the guidelines of ASTM D 1218. This test method can be performed at various temperatures. The refractive index can be used to estimate the distribution of PNA molecules in oil fractions.

### **2.10.11 Reid Vapor Pressure (RVP)**

RVP is measurement of the volatility of a liquid hydrocarbon. Normally this is performed by ASTM D 323. This measurement is normally used to predict gasoline performance, normally expressed in pounds per square inch (psi). This is normally an inspection that is performed on Whole Crudes having relatively high API's.

### **2.10.12 Salt Content**

The salt content is measured by ASTM D 3230 to determine the corrosiveness of a Crude oil. It is this conductivity method that measures a sample of crude oil dissolved in water and compares that to reference solutions of salt.

### **2.10.13 Smoke Point**

Performed by ASTM D 1322, this test determines the maximum flame height in a lamp without smoke forming. Normally high values represent



clean burning fuels. In normally practice this test is performed on jet fuels and kerosene cuts.

#### **2.10.14 Sulfur Content**

The sulfur content of crude oils is normally in the range of 0.1-5.0-wt %. Sulfur is normally measured by an x-ray technique such as ASTM D 4294 or D 5291. These methods have large dynamic ranges and allow analysis to be completed in about 3-5 minutes. Samples having sulfur contents greater than 5.0 % are measured by methods such as ASTM D 1552, a combustion technique. For extremely low levels an ultraviolet fluorescence technique is employed (ASTM D 5453) Again most of these methods are very robust, but can be influenced by not having a representative sample. Crudes are determined to be sweet or sour based on the amount of dissolved hydrogen sulfide.

#### **2.10.15 Total Acid Number**

The industry standard for this test is based on ASTM D 664. Normally expressed as Neutralization Number, this test predicts the acidity of an oil/distillate fraction. The sample normally dissolved in Toluene/IPA/Water is titrated with potassium hydroxide and the results are expressed as mg KOH per gram of sample. Crude Oils having high acid numbers are purchased cautiously due to possible corrosion problems in the refineries. Crudes typically have TAN values form 0.05-6.0 mg KOH/gm of sample. While whole crudes are outside the scope of this titration method, it is the only recognized method in the industry.

#### **2.10.16 Viscosity**

Viscosity is a measurement of a fluid resistance to flow. Most measurements use the force of gravity to produce the flow through a small capillary tube called a viscometer; thus the measurement is known as kinematic viscosity having a unit of centistoke (cSt). The viscosity of a fluid is always reported with a temperature, since viscosity will vary inversely with temperature. Most viscosity measurements follow the guidelines of ASTM D445. Normally in an inspection grid the viscosity will be measured at three different temperatures and then plotted on semi-log graph paper. If all measurements are performed properly a straight line will result.

#### **2.10.17 Water & Sediment**

Sediment and water values in crude oils are critical parameters as to whether problems will occur in the processing in the refinery. In many cases, desalting equipment may be required in order to handle a given crude slate.

## **2.11 Asphalt Properties**

### **2.11.1 Penetration**

Penetration is a method for determining the consistency of semi-solid material normally performed by ASTM D 5. A sample of resid is weighed, cooled, and a needle is positioned above the surface and allowed to penetrate the sample. The penetration measure in millimeters is also based on the temperature of the sample.

### **2.11.2 Softening Point**

Usually determined by ASTM D 36, softening point determines the temperature at which hard asphalts reach an arbitrary degree of softening.

## **3. THE PREDICTION OF CRUDE ASSAY PROPERTIES**

### **3.1 Needs for Rapid and Accurate Prediction of Crude Assay Properties**

Conventional crude assays provide accurate and detailed information about the physicochemical properties of crude oils across the boiling range. This information is used for critical purchasing and processing decisions. However, the determination of the crude oil properties is a lengthy, tedious, and costly process. Crude oils must be transported in large volumes (e.g., barrels) over significant geographic distances to analytical facilities capable of performing the required tests. Physical distillation must be conducted for the determination of the distillation yield profiles (weight and volume %) and is a prerequisite to the collection of narrow distillation cuts for further testing. The time period for crude oil transportation from the well to the analytical lab can range from several weeks to several months. Once in the lab, distillation can take 2-4 days for completion and complete testing of the various properties for each distillation cut may require 2 to 6 weeks. It is obvious, that despite the great accuracy and detailed information provided by conventional crude assay methodologies, newer analytical methodologies are required to provide timely information for rapid decision making.

The ideal crude oil assay should be able to provide on-line, instantaneous and detailed determination of all crude oil properties across the boiling range. Unfortunately, such a method is not yet available. However, several efforts have been made to that end. The most successful approach has been the prediction of the physicochemical properties of crude oils by correlating the data obtained by a rapid, surrogate method (usually spectroscopic) to the data

obtained by the conventional, lengthy crude assays. The testing time, degree of accuracy and extent of information greatly depend on the characteristics of the surrogate method. The following sections present some of the efforts associated with the development of analytical approaches for the prediction of the properties of crude oils.

### **3.2 Predictions from Measurement of Selected Whole Crude Oil Properties**

Gaylor and Jones developed an early method for the rapid and comprehensive determination of crude oil properties without the need for distillation.<sup>2</sup> Information for all fractions through asphalt was obtained in two to three hours. The method relied on six measurements made on the whole crude oil: gravity, sulfur, nitrogen, pentane insolubles, condensed aromatics, and gas chromatography. Using multiple regression equations, it was possible to correlate the six properties of the whole crude oils to the properties of selected crude oil fractions. The method allowed for the rapid evaluation of important properties, such as: gravity of all fractions, smoke point and freezing point of kerosine, wax content and viscosity index of lubricating oils. Correlations were obtained for yields, paraffins, aromatics, gas oil, cracking stock, and asphalt quality properties. The 3-hour test allowed for the determination of a total of 59 parameters from the six measurements on the whole crude oil. The Gaylor and Jones approach is a relatively simple approach that can be readily implemented in most labs capable of performing the six tests on whole crude oils. The suitability of the approach to specific applications will depend on the accuracy required for reliable decision making.

### **3.3 Predictions from NMR Measurements**

NMR is not an obvious analytical method suitable for the prediction of crude oil properties. However, it has been used for the estimation of the physical properties of petroleum reservoir fluids leading to the performance of phase equilibrium calculations (PVT properties). Using NMR data, it has been possible to solve the equation of state and to predict the changes in the relative volume versus pressure.<sup>3</sup> Crude oil cuts were collected and separated into aromatic and (paraffin and naphthene) fractions. Group contribution methods were developed using several structural hypotheses to improve the efficiency of NMR data in the characterization of the petroleum fluids. The NMR data used in this study led to the successful prediction of PVT properties, in good agreement with the experimental data. The authors, however, concluded that despite the good predictions, NMR is a lengthy and expensive method with no particular advantage over other methods. Although

these conclusions are still valid, the methods and structural hypotheses developed by these authors may be useful in the future, when smaller and less costly NMR instruments become available.

### 3.4 Predictions from Chromatographic Data

Burg and co-workers developed a chromatographic approach for the prediction of the kinematic viscosity of crude oil.<sup>4</sup> The ability to predict viscosity is very important as it has direct impact on the production and transportation of crude oils and their products. Prediction using compositional information can be problematic since the property can be modified by small amounts of molecules. In this study, the fractions boiling higher than 200 °C were used as stationary phases, and retention time measurements were made with 13 solutes at 50°C. Five parameters were determined relating the intermolecular interactions to kinematic viscosity. The interaction parameters are: a dispersive/cavity term (London forces), a dipolarity/polarizability term (Keesom and Debye forces), an acidic term, a basicity term, and a term for the tendency of crude oil to interact with polarizable solutes. The obvious advantage of this approach, in comparison to other approaches, is that the parameters have physical meaning and are directly linked to the molecular interactions. Crude oil viscosity was found to depend primarily on dipole-dipole and dipole-induced dipole interactions. Hydrogen bonds were not found to play a predominant role in the viscosity of the crude oils examined. Understanding of the different effects the five intermolecular parameters have on viscosity can lead to the development of novel approaches for the modification of the viscosity of crude oils and their products.

### 3.5 Predictions from GC/MS Measurements

A simple and rapid method was developed using gas chromatography-mass spectrometry (GC/MS) for the prediction of the properties of crude oils and their boiling fractions.<sup>5</sup> The method creates a statistical correlation between the known properties of a training set of crude oils and their GC/MS data. The properties of unknown crude oils are thus predicted from the training set and the measured GC/MS data of the unknown crude oils. A major advantage of this method is that the simulated distillation information provided naturally by gas chromatography is coupled to detailed compositional information possible by the mass spectrometer. The method not only provides detailed information rapidly which can be used for the chemometric predictions of the crude oils properties across the boiling range, it can also provide molecular information for the determination of the properties of crude oils and their fractions from first principles. Most importantly, the molecules affecting specific crude oil properties can be determined by the method and the information can be used for the design of

products with desirable properties. The approach, although based on relatively simple low-resolution GC/MS instrumentation, it currently requires skilled operators and a laboratory environment for the performance of tests. Future developments in miniaturized, rugged and portable GC/MS systems are expected to significantly improve the practicality of the approach and provide routine molecular characterization in the field.

### 3.6 Predictions from NIR Data

Near infrared (NIR) spectroscopic methods have been developed to rapidly determine the properties of crude oils.<sup>6</sup> The method is used to control the separation of components in crude oil downstream of a well head. Measurements are made at or before the pipeline between the analyzer and the separator. Optimization of the separation process is based on the NIR results. The method is also used to determine crude oil properties (e.g., content of naphtha, gas oil and/or fuel oil). Chemical, physical, physicochemical, optical and mechanical properties can be determined by the method at the same time, from the same oil sampling. The spectroscopic analysis is done in a standard cell maintained at a constant temperature. The analysis is performed in real time or near real time. The absorption of the oil is measured in the region 600-2700 nm. The properties of the oils are then determined by direct, indirect, or statistical correlations with a set of standard oils of known properties. The capability of the method for on line or at line measurements makes it highly suitable for automated control applications. The wavelengths used in the calculations are generally chosen by statistical means. Multiple linear regression, principle component regression, canonic regression and partial least squares statistical methods can be used for the correlations. Most interestingly, a preferred method is the direct comparison of the absorptions of the unknown crude oils with those of a set of standard crude oils of known properties. Unknown crude oils with the nearest absorption values at the same wavelengths to the standards have similar properties to the properties of the nearest standards. The advantage of the direct comparison of absorptions is that there is no need for development of rigorous statistical correlations between the measured NIR data and the known properties of crude oils. Accurate property determination is possible by the direct comparison method, provided that very similar crude oils are present in the database. The simplicity and practicality of the NIR method makes it the most suitable current approach for rapid, on-line prediction of the properties of crude oils. Real time decisions can be made using the method. The main disadvantage over the GC/MS method is the lack of specific information about the molecular makeup of the crude oils. This can be problematic for properties that can be affected by small amounts of molecules (e.g., additives).

NIR has been used for the determination of the total boiling point profiles and densities of crude oils.<sup>7</sup> 110 crude oils were used for the development of

the correlations. The reproducibility limits of the approach are equivalent to those of the ASTM reference procedures. The correlation coefficients were better than 0.98. The success of the method clearly demonstrates the capabilities of NIR to provide rapid information on critical properties of crude oils.

### 3.7 Property Determination from First Principles

The optimization of the refinery performance for individual crude oil feedstocks requires the development of simulation and prediction models of the individual refinery processes. Such a model is Quann and Jaffe's Structure-Oriented Lumping.<sup>8</sup> Individual hydrocarbon molecules are represented by this model, as vectors of incremental structural features that can describe the composition, reactions and properties of petroleum mixtures. The approach allows for the molecular modeling of all refinery processes.

The accuracy and utility of such molecular-based models greatly depend on the availability of detailed molecular information. Most importantly, for timely decision making, real time molecular characterization of petroleum feeds and products would be ideally required for continuous input to the models. Stand-alone NMR and NIR spectroscopic methods are limited due to their inability to identify individual molecules in complex mixtures. Mass spectrometry is more suitable for the characterization of complex petroleum mixtures and it has been extensively applied to that end.<sup>9</sup> Increased molecular speciation can be obtained by coupling chromatographic means of separation to the spectroscopic detection methods. A multitude of hyphenated analytical methods has been developed for the acquisition of detailed molecular information of petroleum samples.<sup>10</sup> At present, not a single analytical methodology can provide complete characterization of crude oils at the molecular level. Limitations range from the inability of the methods to separate overlapping components to the inability to introduce the heavy petroleum fractions into the analytical instruments. The most successful current approach involves tedious sample preparation procedures, followed by lengthy component separation steps, using advanced analytical instrumentation. Significant future advances in analytical instrumentation will be required for the ideal rapid and complete characterization of crude oils at the molecular level by a single comprehensive hyphenated technique.

## 4. REFERENCES

1. ASTM Book.
2. Gaylor, V. F.; Jones, C. N. "Rapid and Comprehensive Crude Oil Evaluation Without Distillation", *Ind. & Eng. Chem. Prod. Res. and Develop.*, **1968**, 7(3), 191-8.
3. Jaubert, J.-N.; Neau, E.; Peneloux, A.; Fressigne, C.; Fuchs, A. "Pressure, Volume, and Temperature Calculations on an Indonesian Crude Oil Using Detailed NMR Analysis or a

- Predictive Method To Assess the Properties of the Heavy Fractions”, *Ind. & Eng. Chem. Res.*, **1995**, *34*(2), 640-55.
4. Burg, P.; Selves, J.-L.; Colin, J.-P. “Prediction of Kinematic Viscosity of Crude Oil From Chromatographic Data”, *Fuel*, **1997**, *76*(11), 1005-1011.
  5. Ashe, T. R.; Roussis, S. G.; Fedora, J. W.; Felsky, G.; Fitzgerald, W. P. “Method for Predicting Chemical or Physical Properties of Crude Oils”, U. S. Patent 5,699,269. 1997.
  6. Kelly, J.; Lambert, D.; Martens, A. “Determination of crude oil properties”, *PCT Int. Appl.*, **1998**, 27 pp. WO 9836274.
  7. Hidajat, K.; Chong, S. M. “Quality Characterization of Crude Oils by Partial least Squares Calibration of NIR Spectral Profiles”, *J. Near Infrared Spectrosc.*, **2000**, *8*, 53-59.
  8. Quann, R. J.; Jaffe, S. B. “Structure-Oriented Lumping: Describing the Chemistry of Complex Hydrocarbon Mixtures”, *Ind. Eng. Chem. Res.*, **1992**, *31*, 2483-2497.
  9. Altgelt, K. H.; Boduszynski, M. M. *Composition and Analysis of Heavy Petroleum Fractions*, Marcel Dekker, Inc.: New York, 1994.
  10. Hsu, C. S. *Analytical Advances for Hydrocarbon Research*, Kluwer Academic/Plenum Publishers: New York, 2003.

## Chapter 4

# **INTEGRATED METHODOLOGY FOR CHARACTERIZATION OF PETROLEUM SAMPLES AND ITS APPLICATION FOR REFINERY PRODUCT QUALITY MODELING**

Yevgenia Briker, Zbigniew Ring, and Hong Yang  
*National Centre for Upgrading Technology*  
*1 Oil Patch Drive, Suite A202*  
*DEVON, Alberta T9G 1A8, Canada*

### **1. INTRODUCTION**

Accurate compound type analysis of complex hydrocarbon mixtures is of utmost importance for the refining industry both in terms of analyzing day-to-day operation of the conversion processes and in terms of model-aided optimization of the processes and their predictive simulation at the design stage. The optimization and simulation of refining processes relies on complex models that require detailed composition data to deliver reliable results. In principle, a modern mathematical model of a refining process such as hydrocracking or catalytic cracking consists of the reactor model and the product quality model. The reactor model may use a molecular representation of the feedstock to produce molecular representation of the effluent.<sup>1</sup> The product quality model may use the molecular representation of the effluent to estimate the refinery-type characterization of the individual fractions of this effluent. Of course, even a relatively narrow vacuum gas oil fraction, common feed for conversion units, consists of such a large number of various molecules that it is not possible to know its exact molecular composition. However, high resolution mass spectrometry or, alternatively, low resolution mass spectroscopy coupled with gas chromatography allow quantification of isomeric lumps that can be further broken down into representative molecules – a molecular representation.



This chapter describes a suite of relatively fast and inexpensive analytical techniques to be used as the basis for the development of modern process models at the National Centre for Upgrading Technology (NCUT). Derived from various standard methods, the methodology presented below delivers a unique result – a matrix of hydrocarbon types distributed by carbon number or boiling point, depending on the need, that describes bulk composition of a refinery stream. We show that this detailed characterization can be reliably generated for a wide variety of materials by a combination of liquid chromatography (LC) and high voltage low-resolution electron impact mass spectrometry (EIMS). This methodology, developed mostly for diesel range materials, has been successfully used at NCUT to characterize full-range distillates. The adaptation and further development of LC separation, the development of MS techniques by boiling point distribution, and the development of the FIMS (field ionization mass spectrometry) method provide results that allow development of product quality correlations between the chemical composition and physical properties, along with refinery-type characterization.

## **2. CLASS-TYPE SEPARATION**

The chemical complexity of refinery feedstocks and finished products containing thousands of various compounds poses major problems in analysis. In order to identify minor components with greater accuracy, the fuel has to be separated into sub-fractions before analysis. Separation techniques include distillation (by boiling point), solvent extraction (by solubility), and open column liquid chromatographic techniques that allow separation by molecular size (gel permeation chromatography - GPC) or by polarity. The Open column chromatographic techniques, ASTM D2007 and ASTM D2549, have corresponding HPLC (high-pressure or high performance liquid chromatography) versions such as the IP391/95 method for determination of aromatic compounds in middle distillates. In addition, supercritical fluid chromatography (SFC, CAN/CGSB-3.0 No. 15.0-94) and hot fluorescent indicator absorption (Hot FIA, UOP 501-83) methods also provide hydrocarbon class separation for fuels.

The separation method described later in this chapter was gradually developed into its final stage currently used at NCUT by first modifying the ASTM D2007 method, and then developing a miniature version utilizing the SPE (solid phase extraction) methodology that also rendered separation of the olefins.

## 2.1 Modification of ASTM D2007 LC Separation

The original class separation procedure, ASTM D2007, covers the boiling range 177-525°C and uses n-pentane to elute the saturate and the aromatic fractions by volume.<sup>2</sup> It yields mainly mono- and di-aromatics in the total aromatic fraction. The aromatics consist of a larger number of rings that are eluted together with the polars. This fraction is defined as “polyaromatics”. The MS methods – ASTM D2786 for saturates and ASTM D3239 for aromatics – provide a detailed hydrocarbon-type analysis of separated fractions.<sup>3</sup> The characterization of aromatics by ASTM D3239 goes far beyond the di-aromatic range, and stretches to pentaaromatics and further to multi-ring aromatics, namely unidentified classes. Therefore it is necessary to modify the ASTM D2007 method and extend the extraction of aromatics to full scale, leaving behind only the “true polars”, i.e. the compounds having some strong polar functionality. The modification of ASTM D2007 includes replacing n-pentane solvent, used in the original ASTM method for the elution of the aromatic fraction, with the binary solvent mixture (n-pentane/toluene in a ratio of 1:1) in order to elute polyaromatic hydrocarbons. To summarize our modifications to the ASTM D2007 method, it should be noted that we did not change the apparatus and the columns dimensions. For collection of saturates we slightly increase the volume of n-pentane from 280 mL to 300±10 mL to cover the samples with high paraffin content. In any case, the elution of saturates is always monitored by HPLC equipped with photo diode array detector (PDA) at 254nm. For the elution of aromatics we use 1560 mL of solvent mixture of n-pentane and toluene in a ratio of 1:1. The rest of the method follows the ASTM procedure. Since we sometimes work with heavy samples having high polar content, and these samples have limited solubility in n-pentane or cyclohexane, the solvents recommended in the original ASTM, we sonicate the sample with the solvent. If complete solubility cannot be achieved, the sample is dissolved in a minimum amount of dichloromethane and added to a beaker containing a pre-weighed amount of Attapulugus clay. This amount is later deducted from the amount in the upper column section. The mixture is placed in a warm water bath (40°C) and the solvent evaporates slowly while stirring the mixture. After most of the solvent evaporates, the mixture is placed in a vacuum oven for 1 h at 45°C to get rid of traces of solvent. The sample is now evenly distributed on the surface of the clay and the clay mixture is added on top of the upper column to start the elution. Sample size requirements for this method are 5 to 10 g depending on polar content. To reduce the solvent consumption and sample size, we scale down the column assembly 5 times and reduce the sample size to 1 - 2 g. The solvent elution volumes are changed to: 80 mL for n-pentane, 312 mL for n-pentane-toluene mixture, and 50 mL for acetone-toluene mixture.

There is another widely used LC separation method, ASTM D2549. It is good for analyzing fuels in the diesel range that have low or no polar content

(below 2wt%).<sup>2</sup> In this method n-pentane is used to elute the saturates and dichloromethane is used to elute the aromatics. It should be noted that dichloromethane may move some polars into the aromatic fraction. When polar content exceeds the 2wt% limit (sometimes we have to analyze samples having polar content 20wt% and higher), the ASTM2549 method may produce erroneous results.

The modified ASTM2007M method was verified against ASTM2549 and other separation techniques such as SFC, HPLC and FIA. The comparison of results obtained by different laboratories and different methods for various diesel fuels is shown in Table 1. The results are shown for five commercial diesel fuels, two synthetic crude blends and two conventional diesel blends prepared by Shell Canada Ltd. with approximately 20wt% and 30wt% aromatics. Results are also shown for a certified low aromatic fuel supplied by Chevron Research and Technology Company (Chevron low aromatic), and a commercial low sulfur diesel (Ref1).

Table 1. LC Separation of Fuels by Different Methods

| wt%     | NCUT <sup>a</sup> |       |        |        | Syncrude <sup>b</sup> |       |        | Core <sup>c</sup> |       |        | Shell <sup>d</sup> |        | Shell <sup>d</sup> |        |
|---------|-------------------|-------|--------|--------|-----------------------|-------|--------|-------------------|-------|--------|--------------------|--------|--------------------|--------|
|         | Sats.             | Arom. | Polars | Method | Sats.                 | Arom. | Method | Sats.             | Arom. | Method | Arom.              | Method | Arom.              | Method |
| Diesel1 | 70.0              | 29.7  | 0.3    | D2007M | 70.4                  | 29.7  | SFC    | 71.9              | 28.1  | D2549  | -                  | -      | -                  | -      |
| Diesel2 | 70.0              | 29.6  | 0.4    | D2007M | 70.0                  | 30.0  | SFC    | 70.5              | 29.5  | D2549  | -                  | -      | -                  | -      |
| Diesel3 | 14.3              | 84.5  | 1.2    | D2007M | 14.9                  | 85.1  | SFC    | 14.6              | 85.4  | D2549  | -                  | -      | -                  | -      |
| Diesel4 | 94.5              | 5.5   | 0.0    | D2007M | 95.1                  | 4.9   | SFC    | 95.5              | 4.5   | D2549  | -                  | -      | -                  | -      |
| Diesel5 | 87.5              | 12.5  | 0.0    | D2007M | 87.2                  | 12.9  | SFC    | -                 | -     | -      | -                  | -      | -                  | -      |
| S20B    | 77.7              | 22.3  | -      | D2549  | 76.5                  | 23.5  | SFC    | -                 | -     | -      | 22.8               | HPLC   | 20.8               | FIA    |
| S30B    | 69.8              | 30.2  | -      | D2549  | 68.6                  | 31.4  | SFC    | -                 | -     | -      | 31.3               | HPLC   | 27.6               | FIA    |
| C20B    | 80.6              | 19.4  | -      | D2549  | 79.8                  | 20.2  | SFC    | -                 | -     | -      | 19.8               | HPLC   | 17.7               | FIA    |
| C30B    | 71.2              | 28.8  | -      | D2549  | 70.2                  | 29.8  | SFC    | -                 | -     | -      | 30.2               | HPLC   | 25.4               | FIA    |
| Chevron | 95.6              | 4.4   | -      | D2549  | 95.2                  | 4.8   | SFC    | -                 | -     | -      | 4.2                | HPLC   | 4.7                | FIA    |
| Ref1    | 74.6              | 25.4  | -      | D2549  | 72.7                  | 27.3  | SFC    | -                 | -     | -      | 25.9               | HPLC   | 24.2               | FIA    |

a. National Centre for Upgrading Technology, Devon

b. Syncrude Canada, Edmonton

c. Core Laboratories, Inc., Houston

d. Shell, Canada, Calgary

The results suggest a very good correlation between the methods and the laboratories. So the modified ASTM D2007M method together with the ASTM2549 method allow us to have two comparable techniques for separating samples with various polar content.

Class-type separations by open column chromatography are highly time and solvent consuming. They can also have problems achieving good mass balances for samples containing a lot of very light material. For example, the boiling point of toluene, the solvent used to elute the aromatic fraction in the modified ASTM D2007M, may overlap with the boiling points of lighter sample components, making it virtually impossible to remove solvent and maintain a good mass balance. The method requires solvent removal by rotary evaporation to obtain solvent-free fractions for calculation of the material balances. In this case usually a small amount of toluene is left in the fraction and it must be taken into consideration when calculating the mass balance. To accomplish this, the removal of toluene by rotary evaporation is not carried out to the end. Some solvent is left in the fraction and it is analyzed by gas

chromatography. The toluene peak is quantified; its amount is subtracted from the amount of aromatics, and the material balance is then recalculated.

The amount of sample required for analysis can also pose a problem in some cases when only small quantities are available (e.g. fluid catalytic cracking-micro-activity test - FCC-MAT).

Given some constraints of the above methods, we turned our attention to solid phase extraction (SPE) methodology. It is an alternative technique for class-type separation and is well described in the literature.<sup>4</sup> The procedure has been tested on standard hydrocarbon mixtures. It is simple, fast, and inexpensive, and it yields hydrocarbon fractions in solutions that are ready to be analyzed by GC-MS. It removes the need for a number of laboratory procedures such as removal of solvents, handling the large quantities of solvents and adsorbents, and sieving and washing the Attapulugus clay adsorbent required for ASTM2007M.

## 2.2 SPE method

The original SPE method used an activated silica gel-filled micro glass 6 mL column (13 mm diameter) to separate fuel into groups of aliphatic, and mono-, di-, and polyaromatic hydrocarbons using a stepwise gradient of dichloromethane in n-pentane.<sup>4</sup> Originally, it was developed to analyze fuels mainly in the diesel boiling range. The separated fractions were analyzed by GC-MS to identify various hydrocarbon types. We adapted this method with some modifications to replace the ASTM D2007M method. Furthermore, the SPE method was expanded to provide the separation of olefins.

### 2.2.1 SAP (Saturates, Aromatics and Polars)

Silica gel used in the original method had a mean particle size of 40  $\mu\text{m}$ , particle distribution of 30-60  $\mu\text{m}$ , pore diameter of 6 nm, active surface of 480  $\text{m}^2/\text{g}$ , and was obtained from Baker (Grob-Garau, Germany). In our study, silica gel used for analysis had a BET surface area of 500  $\text{m}^2/\text{g}$ , pore volume of 0.75  $\text{cm}^3/\text{g}$ , particle distribution of 70-230 mesh (210-63 $\mu\text{m}$ ), 60 $\text{\AA}$  pore diameter, and was obtained from Aldrich Chemical Company, Inc. The sample load was about 20mg. It was applied on top of the cartridge as 200  $\mu\text{l}$  of 10% solution in n-pentane. We used the same type of cartridge as in the original method, and the same volume of n-pentane used for elution of the saturate fraction (6 mL). HPLC PDA was used to monitor the cut point for elution of the saturate fraction during the development stage. As the fractions were subsequently analyzed by GC-MS, there was no need to separate mono-, di- and poly-aromatics. Instead, all these aromatic groups were collected as a single fraction eluted with 18.5 mL of dichloromethane (DCM). Another modification involved the solvent composition used to elute the polar fraction. A mixture of methanol and DCM in ratio 40:60 (18.5 mL) was used instead of

25% acetic acid in methanol. This method is applied to samples having little (less than 2wt%) or no polars. For heavy samples with high polar content, the ASTM 2007M method is used to separate and gravimetrically quantify the polars, and the SPE method is used for all the other fractions. However, we also introduced an SPE method that resembled a miniaturized ASTM D2007M separation. It utilized two cartridges where the top cartridge was filled with 2g of activated Attapulgus clay and the bottom cartridge was filled with activated silica. Sample load was 20mg. Elution volumes were changed to 12 mL of n-pentane for saturates, 55 mL of n-pentane/toluene mixture for aromatics, and 18.5 mL of methanol/DCM mixture for polars. For heavy samples with high polar content and poor solubility in n-pentane the preparation and application of the sample was similar to the ASTM2007M method.

In our modified method, it is not necessary to remove all solvents as in ASTM D2007M. Quantification is done by GC-FID (gas chromatography - flame ionization detection) with an external standard prepared from a selected standard fuel at a concentration of about 1mg/mL and analyzed at identical conditions. For quantification purposes each fraction collected from SPE cartridges is reduced to a certain volume (1 mL, for example) using the nitrogen gas sweep, and the calculation is done by using the response factor calculated from an external standard, and the total integration areas of the GC-FID chromatograms of the fractions. The same solutions (with exception of the polar fraction) are simultaneously analyzed by the GC-MS. However, for samples having a large amount of light ends, even an insignificant volume reduction with mild nitrogen blow can lead to some undesirable losses of light ends. The quantification for these types of samples is done only from 200°C to FBP. The retention time is calibrated by analyzing the paraffin standards (C<sub>5</sub>-C<sub>44</sub>) by GC-FID at the identical conditions, and the exact retention time corresponding to 200°C is calculated from the calibration curve. The chromatogram is integrated from this point (200°C) to the end for each fraction. Calculated sum of the fractions (saturates, aromatics, and polars) is compared to the 200°C-FBP fraction of the total sample, as determined from the simulated distillation data. Usually the comparison is very good. Then the total balance is calculated as sum of the fractions from the SPE analysis plus the IBP-200°C fraction determined from the simulated distillation of the sample. The number for the total balance is usually close to 100wt%. For further calculations, the yields of the SPE fractions are normalized so that the total balance equals 100wt%. The calculation of the hydrocarbon types in saturate and aromatic fractions analyzed by the GC-MS is also done from 200°C to FBP. This is achieved by calibrating the retention time of the GC-MS chromatogram with the paraffin standards (C<sub>5</sub>-C<sub>44</sub>) analyzed at the identical conditions, and by averaging the spectra from the retention time corresponding to 200°C point on the chromatogram. The class-type composition of IBP-200°C fraction is determined by PIONA (paraffins,

isoparaffins, olefins, naphthenes and aromatics) analysis that gives the distribution of n-paraffins, iso-paraffins, naphthenes, aromatics, and olefins if they are present in the sample.

Some examples of SPE results are shown in Table 2. The DECSE3 diesel is a sample from another study that was used to investigate the effects of sulfur levels on the operation of diesel exhaust emission control devices,<sup>5</sup> and the remaining samples were obtained from various refineries across Canada. These fuels were prepared for a collaborative research program “Canadian Diesel Fuel Composition and Emissions”.<sup>6</sup>

Table 2. SPE in Comparison with Other Methods

| <i>HC Type</i>                   | <i>LC</i> | <i>SFC</i> | <i>SPE</i>        |
|----------------------------------|-----------|------------|-------------------|
| <i>Ref2</i>                      |           |            |                   |
| Saturates                        | 70.5      | 70.2       | 69.5              |
| Aromatics                        | 29.5      | 29.8       | 30.6              |
| Polars                           | 0.0       | 0.0        | 0.0               |
| Total                            | 100.0     | 100.0      | 100.1             |
| <i>Ref5</i>                      |           |            |                   |
| Saturates                        | 73.6      | 73.8       | 72.1              |
| Aromatics                        | 26.4      | 26.2       | 25.0              |
| Polars                           | 0.0       | 0.0        | 2.9               |
| Total                            | 100.0     | 100.0      | 100.0             |
| <i>SWRI</i>                      |           |            |                   |
| Saturates                        | 66.1      | 67.4       | 66.2              |
| Aromatics                        | 33.9      | 32.6       | 33.3              |
| Polars                           | 0.0       | 0.0        | 0.5               |
| Total                            | 100.0     | 100.0      | 100.0             |
| <i>HGO</i>                       |           |            |                   |
| Saturates                        | 58.9      | N/A        | 58.8              |
| Aromatics                        | 36.4      | N/A        | 36.3              |
| Polars                           | 4.7       | N/A        | 4.9               |
| Total                            | 100.0     | N/A        | 100.0             |
| <i>DECSE3</i>                    |           |            |                   |
| Saturates                        | -         | -          | 68.8 <sup>b</sup> |
| Aromatics                        | -         | -          | 15.4 <sup>b</sup> |
| Polars                           | -         | -          | 0.0               |
| Total (IBP-200°C)                | -         | -          | 84.2 <sup>b</sup> |
| SimDist <sup>a</sup> (200°C-FBP) | -         | -          | 15.8 <sup>b</sup> |
| Total (IBP-FBP)                  | -         | -          | 100.0             |

a-quantified from 200°C to FBP

b-calculated from simulated distillation

The results point to a very good agreement between LC (ASTM D2549 and ASTM D2007M – NCUT), SFC (Syncrude Research, Edmonton), and modified SPE results for all the tested fuels.

### 2.2.2 SOAP (Saturates, Olefins, Aromatics, Polars)

During analysis of some specific samples, such as shale-oil-derived distillates and products from FCC-MAT, we encountered high contents of olefinic compounds. The SAP method cannot provide separation of olefins.

They elute with n-pentane as part of the saturate fraction. We further developed the SPE method to facilitate olefins separation (SOAP).

Olefins are found predominantly in cracked materials as a result of thermal processing (thermal and catalytic cracking, coking, pyrolysis, etc.), which converts these materials into lower boiling point products such as diesel and gasoline. The presence of olefins and diolefins in feedstocks may lead to instability during processing, transportation and storage. Knowledge of the olefin content and their boiling point distribution may help to develop better processing and useful product models. Therefore, it is important to develop a reliable method for rapid identification and quantification of this hydrocarbon type.

There are several methods that offer olefins determination. Olefins can be determined by electrometric titration and reported as 'Bromine Number', which is defined as the number of grams of bromine that will react with 100g of the sample - ASTM D1159-89. This method is applicable to gasolines, kerosenes and distillates in the light gas oil range (90% distillate point under 327°C). There is a correlation between the Bromine number and the olefin content. Depending on the value of the Bromine number, the mole concentration of double bonds can be calculated by using ASTM formulas. The other way of calculating the olefins content is by introducing a factor of 2.2 by which the Bromine Number should be divided.<sup>7</sup> The method is simple but it covers only the naphtha range. Its accuracy depends on the boiling range and the olefins-to-aromatics ratio. For fractions with boiling points ranging from 120°C to 190°C, the values for olefins calculated by this method are higher than those determined by PONA (paraffins, olefins, naphthenes, aromatics). These values are also higher if the olefins-to-aromatics ratio (O/A) in the sample is less than one. Another method to quantify olefins is the ASTM D1319 method. It is based on open column liquid chromatography coupled with fluorescent indicator adsorption (FIA). This method has a high level of uncertainty attributable to a significant saturate zone broadening in the open column system. It covers only a certain boiling range (below 315°C) and cannot be applied to dark-colored samples. There are also methods involving olefins determination by multidimensional gas chromatography (MD-GC)<sup>8</sup> and multicolumn systems<sup>9</sup>. The hydroboration-oxidation method is based on selective and quantitative conversion of olefins to alcohols, which are then recovered from the hydrocarbon fraction by elution on an alumina column, followed by GC-MS quantification.<sup>10</sup> In another method, selective olefin stripping (SOS) is used to differentiate between alkanes and alkenes to enhance the GC-FID detection of alkenes. To achieve this, selective bromination of alkenes by saturated aqueous bromine is performed followed by adsorption chromatography and GC-FID.<sup>11</sup> The latest development includes selective and quantitative olefin bromination in the presence of saturates and aromatics, followed by GC-AED (atomic emission detection) that can detect any element and monitor molecular functionality by means of

specific reactions with derivatives containing elemental ‘tags’, in this particular case, Br (bromine).<sup>12</sup> All these methods are time consuming and sometimes not very selective.

In our modified SOAP method the olefins separation is carried out by using a double cartridge procedure where the top cartridge is filled with an activated silica, and the bottom cartridge is filled with 2g of silver nitrate (10%) impregnated silica gel (200 mesh - obtained from Aldrich Chemicals). The cartridges are connected together with the help of a PTFE adaptor –PN IS1201104 from Chromatographic Specialties INC. The saturate fraction is eluted with n-pentane. In this case the volume of n-pentane is increased from 6 mL to 10.5 mL to elute the olefins. Elution of the olefin fraction is monitored by HPLC PDA at 220nm for the olefins, and at 254nm for the aromatics. When the collection of saturate fraction is completed, the cartridges are separated, and the bottom cartridge is washed with an additional 2 mL of n-pentane to remove the left over saturates. This wash is combined with the 10.5 mL of n-pentane and the whole fraction is treated as saturates. In the next step the dichloromethane (18.5 mL) is used to elute both the aromatic and the olefin fractions from the top and the bottom cartridges, respectively. Finally, the polars are eluted from the top cartridge with 18.5 mL of methanol/dichloromethane (40:60) mixture. The fractions are quantified as described before.

There are not many ways to verify the quality of olefin separation. To compare the SPE results for olefins with the results by other methods such as FIA (ASTM D1319), a number of diesel samples were analyzed by both methods. Since there is a correlation between the Bromine number and the olefin content of the sample, the criteria for sample selection was a relatively high value of the Bromine Number. The selected samples were:

- a standard D-916 that was analyzed by ASTM D1319 in a number of laboratories included in the ASTM National Exchange Group;
- a set of four diesel cuts from various thermal cracking processes donated by RIPP (Research Institute of Petroleum Processing) in China, with Bromine numbers (determined by ASTM D1159) varying between 5.22 and 21.52;
- a set of four samples from Canadian sources - coker LGO, coker gas oil, the feed, and the product from partial hydrotreating - with Bromine numbers varying between 29.8 and 79.3.

Results of SPE separation of diesel fuel standard D-916 are presented in Table 3.



Table 3. Comparison of FIA (ASTM) and SPE Results for standard D-916

| Laboratory          | Method       | Hydrocarbon Types (vol%) |         |           |
|---------------------|--------------|--------------------------|---------|-----------|
|                     |              | Saturates                | Olefins | Aromatics |
| ARC                 | ASTM D1319   | 60.0                     | 2.7     | 37.3      |
| Chevron, El Segundo | ASTM D1319   | 58.3                     | 6.2     | 35.5      |
| Core, Carson        | ASTM D1319   | 63.4                     | 2.3     | 34.4      |
| Core, Houston       | ASTM D1319   | 57.4                     | 1.8     | 40.8      |
| Dixie Services      | ASTM D1319   | 54.3                     | 1.3     | 44.4      |
| Lyonell-Citgo       | ASTM D1319   | 56.8                     | 3.6     | 39.6      |
| Motiva              | ASTM D1319   | 56.9                     | 5.8     | 37.3      |
| Octel Starreon      | ASTM D1319   | 61.0                     | 1.9     | 37.1      |
| Phillips            | ASTM D1319   | 63.5                     | 1.1     | 35.5      |
| Average             | ASTM D1319   | 59.0                     | 3.0     | 38.0      |
| NCUT (wt%)          | SPE Modified | 60.8                     | 4.3     | 34.9      |

Usually, there is a large variation in results for olefins determined by the FIA method in different laboratories, as shown in Table 3. The olefins content varies from 1.1 to 6.2vol%, the aromatic content ranges from 34.4 to 44.4vol% and the saturate content from 54.3 to 63.5vol%. The SPE results, 60.8wt% for saturates, 4.3wt% for olefins and 34.9wt% for aromatics, fall well within the range of these round robin FIA test results.

Table 4 shows the SPE separation results for a set of four samples from China and for a set of four samples from Canadian sources. These samples were also analyzed by the ASTM D1319 method (FIA) and ASTM D1159 (Bromine number).

The last two columns of Table 4 also show the amount of olefins estimated from the Bromine number by using two different factors, instead of dividing the Bromine number by a factor of 2.2 to estimate the amount of olefins, as mentioned before. These factors were experimentally determined by Lubeck and Cook.<sup>13</sup> Lubeck and Cook's argument was that the presence of di- and higher olefins would increase Bromine numbers significantly, and the correlation between the olefin content and Bromine number would vary. The upper and lower limits for these ratios were found to be 1.8 and 2.9. There was also an indication from some earlier works that the correlation between the PONA olefins and the olefins calculated from the Bromine number could depend on the olefin-to-aromatic ratio in the sample.<sup>7</sup> All the above conclusions are mainly related to the gasoline-range samples. The presence of di- and higher olefins in cracked gasolines was reported earlier.<sup>14</sup> Diesel or full boiling-range samples cannot be analyzed by MD-GC (multi-dimensional gas chromatography) or FIA because of poor accuracy. Using the SPE separation technique, the olefin fraction can be quantitatively separated from these sample types, giving an advantage over the FIA method.

The first three samples in Table 4 are LCO cuts from the FCC (fluid catalytic cracking) process. They all have relatively low levels of olefins (between 2.0 and 4.5wt% determined by SPE). Conversion of the Bromine numbers to olefin content by using high (2.9) and low (1.8) ratio values produced results that were close to those experimentally found by the SPE

Table 4. Estimation of Olefin Content by SPE, FIA and Bromine Number

|  | SPE<br>Modified<br>wt% | FIA<br>ASTMD1319<br>vol% | Br.No.<br>ASTMD1159<br>gBr/100g | Calculated<br>from Br.No. <sup>a</sup><br>wt% | Calculated<br>From Br.No. <sup>b</sup><br>wt% |
|--|------------------------|--------------------------|---------------------------------|---|---|
| <b><u>Hydrocarbon Type Samples from RIPP</u></b> |                        |                          |                                 |   |   |
| <i>FCC Diesel Pipeline</i>                       |                        |                          |                                 |   |   |
| Saturates  | 32.5                   | 34.1                     |                                 |   |   |
| Aromatics  | 62.7                   | 51.0                     |                                 |   |   |
| Olefins  | 4.5                    | 14.9                     | 11.68                           | 4.0   | 6.4   |
| Polars   | 1.5                    | 0.0                      |                                 |   |   |
| <i>FCC Diesel Mideast</i>                        |                        |                          |                                 |   |   |
| Saturates  | 20.3                   | 21.6                     |                                 |   |   |
| Aromatics  | 76.5                   | 67.4                     |                                 |   |   |
| Olefins  | 2.0                    | 11.0                     | 5.22                            | 1.8   | 2.9   |
| Polars   | 1.2                    | 0.0                      |                                 |   |   |
| <i>FCC Diesel Liaohe</i>                         |                        |                          |                                 |   |   |
| Saturates  | 31.1                   | 29.1                     |                                 |   |   |
| Aromatics  | 64.6                   | 64.6                     |                                 |   |   |
| Olefins  | 2.6                    | 6.3                      | 6.44                            | 2.2   | 3.5   |
| Polars   | 1.7                    | 0.0                      |                                 |   |   |
| <i>Coker Diesel</i>                              |                        |                          |                                 |   |   |
| Saturates  | 46.5                   | -                        |                                 |   |   |
| Aromatics  | 31.9                   | -                        |                                 |   |   |
| Olefins  | 18.1                   | -                        | 21.52                           | 7.4   | 12.0  |
| Polars   | 1.9                    | -                        |                                 |   |   |
| <b><u>Samples from Canadian sources</u></b>      |                        |                          |                                 |   |   |
| <i>Coker LGO</i>                                 |                        |                          |                                 |   |   |
| Saturates  | 22.7                   | -                        |                                 |   |   |
| Aromatics  | 54.1                   | -                        |                                 |   |   |
| Olefins  | 17.9                   | -                        | 30.8                            | 10.6  | 17.1  |
| Polars   | 5.2                    | -                        |                                 |   |   |
| <i>Coker Gas Oil</i>                             |                        |                          |                                 |   |   |
| Saturates  | 24.7                   | -                        |                                 |   |   |
| Aromatics  | 52.0                   | -                        |                                 |   |   |
| Olefins  | 18.0                   | -                        | 29.8                            | 10.3  | 16.6  |
| Polars   | 4.8                    | -                        |                                 |   |   |
| <i>Feed</i>                                      |                        |                          |                                 |   |   |
| Saturates  | 5.5                    | -                        |                                 |   |   |
| Aromatics  | 68.8                   | -                        |                                 |   |   |
| Olefins  | 11.9                   | -                        | 79.3                            | 27.3  | 44.0  |
| Polars   | 8.7                    | -                        |                                 |   |   |
| <i>Product</i>                                   |                        |                          |                                 |   |   |
| Saturates  | 14.4                   | -                        |                                 |   |   |
| Aromatics  | 54.9                   | -                        |                                 |   |   |
| Olefins  | 18.9                   | -                        | 54.6                            | 18.8  | 30.3  |
| Polars   | 4.3                    | -                        |                                 |   |   |

a-bromine number divided by factor 2.9

b- bromine number divided by factor 1.8

method. The scatter between values obtained by using either ratio was not very large, however the results obtained with factor 2.9 were closer to the SPE values, suggesting that there was a small amount of di- or higher olefins present in these samples. In Figure 1, most of the values for FCC products were close to the dotted line in the parity plot, representing good agreement between the two methods.

The FIA results for these samples, on the other hand, were high compared to the results from the other two methods. The coloration of the samples probably interfered with the precision of the FIA method.

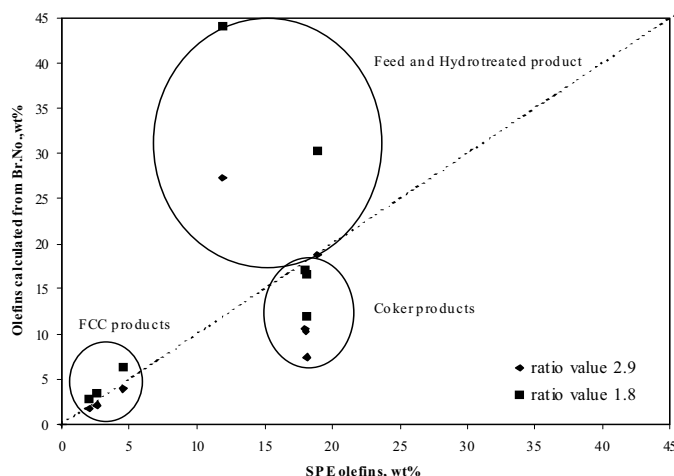


Figure 1. Correlation of olefin content determined by SPE and Bromine Number

The next two samples, representing coker products, coker diesel, coker LCO and coker gas oil, had similar olefin contents as determined by the SPE method (18.1wt%, 17.9wt% and 18.0wt%, respectively). The olefin contents calculated from the Bromine numbers by using a low ratio value of 1.8 were 12.0wt%, 17.1wt% and 16.6wt%, respectively for the three products. For coker diesel, the olefins by SPE were slightly higher than those calculated from the Bromine numbers (by about 5%). One reason could be that this sample was lighter than the other two products, and a small amount of monoaromatic fraction could co-elute with the n-pentane during SPE separation increasing the amount of olefin fraction. Generally, there is a good agreement between the SPE and the calculated values. The fact that the lower ratio value of 1.8 produced a better correlation suggests that mostly mono-olefinic types were present in these samples.

For the last two samples, the feed and partially-hydrotreated product, the Bromine numbers were significantly higher than for coker products, although their SPE olefins were in a similar range (11.9wt% for the feed and 18.9wt% for product with the corresponding Bromine numbers 79.3 and 54.6, respectively). In this case, when the high ratio value of 2.9 was used for the calculation, the results were 27.3wt% for the feed and 18.8wt% for the product. When the low ratio of 1.8 was used, these results were 44.0wt% and 30.3wt%, respectively. The calculated value for the feed using high ratio value 2.9 was still higher (27.3wt%) than the SPE result (11.9wt%), however both calculated results obtained with the high ratio 2.9 appeared to be much closer to the SPE results than those calculated using the low ratio 1.8. This implies the presence of di- and higher olefins in these samples, especially in the feed.

Lastly, we compared the olefin content in the commercial diesel DECSE from DOE (Department of Energy). It was determined by ASTM D1319 method in the US laboratory to be 2.3 vol%. The saturate and the aromatic contents measured by ASTM D5186 were 71.2 and 28.5 respectively. In comparison, SOAP results for this diesel were 72.1 wt% for saturates, 28.1wt% for aromatics and 1.8wt% for olefins. Analysis by SFC at Syncrude Research Ltd. rendered total saturates 71.2 wt% and total aromatics 28.8 wt%.

All of the above results suggest that the SOAP method shows good results for a variety of samples and it works when other methods fail or are not applicable.

Figure 2 displays an overlaid GC-FID chromatogram of SOAP separated fractions from shale oil.

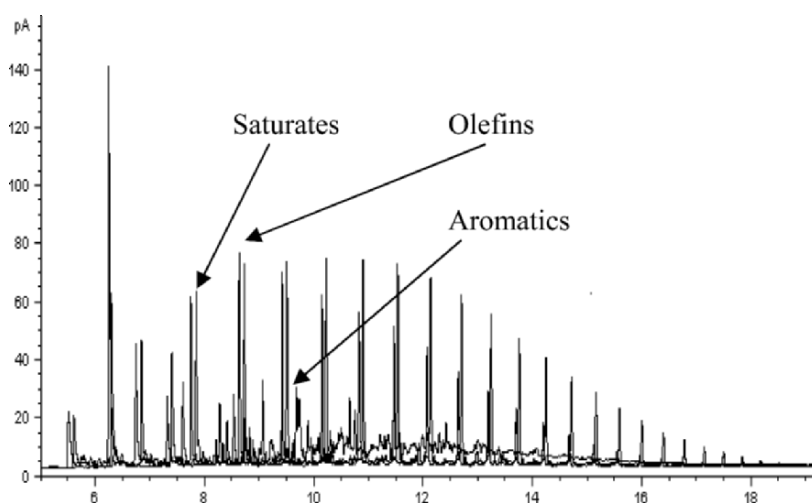


Figure 2. GC-FID chromatograms of SOAP separated fractions

This particular shale oil sample was very rich in olefins. The chromatogram of saturate compounds displays typical features characteristic for the homologous series of normal paraffins with increasing carbon number, shown as separate peaks, as well as a variety of other saturate compounds shown as smaller peaks. The other chromatogram follows the homologous series of olefinic compounds, where each preceding peak represents an olefin with a carbon number identical to the carbon number of a corresponding paraffinic compound, displayed by the following neighboring peak. The third chromatogram belongs to the aromatic compounds. This example points to a very good separation between these compound types.

All our separation methods are summarized in Figure 3.

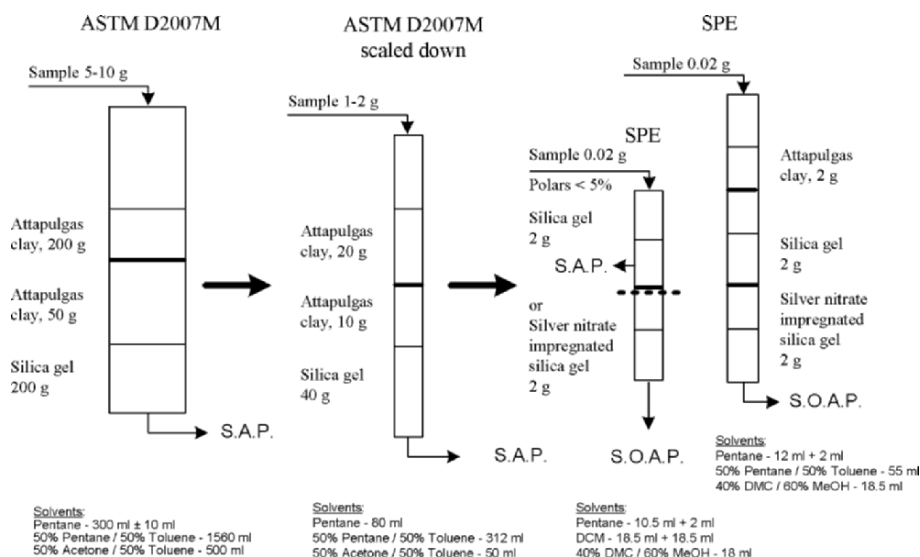


Figure 3. Summarized diagram of NCUT's class separation methods

As noted earlier, in our practice we have to deal with samples that have a wide boiling range. In some cases the light ends (200°C -) can be as high as 50wt% of the total sample. Integrating GC-FID chromatograms from 200°C to FBP allows for a good material balance for 200°C+ material. However, volume reduction of fractions with nitrogen gas sweep involves some tedious handling that can be avoided. Recently, we made few modifications to the SPE method that improved the balance even more and helped to simplify the procedure. We increased the sample size from 20 mg to 35 mg. It means that now a sample is prepared by dissolving about 0.35g of sample in 2 mL solution and 200 $\mu$ l of this solution is applied on the top cartridge. The cartridge size, therefore, is increased to 14 mL so that it can be filled with 5g of silica. The cartridge has the same diameter (13 mm) but is increased lengthwise and has a wide top end to hold more solvent. In the SOAP method the bottom cartridge now is filled with 3g of silver nitrate impregnated silica. The saturate fraction is eluted with 14 mL of n-pentane and the olefin and the aromatic fractions are eluted with 20 mL of DCM each. Each fraction is collected into a 25 mL volumetric flask and then topped up with the corresponding solvent to the 25 mL mark. There is no volume reduction with nitrogen gas after that. These solutions are more diluted than before and are injected into GC-FID using a splitless injection mode to avoid any possible discrimination and also to obtain a stronger signal. The same solutions are used for GC-MS analysis. The RF calibrant is prepared by dissolving about 0.2g of diesel blend in 2 mL of DCM and then transferring 200 $\mu$ l of this

solution into a 25 mL volumetric flask, and bringing to a volume with DCM. The resulting concentration will be about 0.8 mg/mL.

This modification simplified the procedure and seems to improve the material balance.

### 3. DETAILED HYDROCARBON TYPE ANALYSIS

However the fractions are separated, the next step is their analysis by various mass-spectrometry techniques, directly or in combination with gas chromatography. What follows are the methods used for detailed hydrocarbon type analysis.

#### 3.1 Mass Spectrometry

The SPE separated fractions (saturates and aromatics) are analyzed by electron impact mass spectrometer (EIMS) with gas chromatograph (GC) used for sample introduction (GC-EIMS). The saturate fraction is calculated by ASTM D2786 method, and the aromatic fraction is calculated by ASTM D3239 method.<sup>3</sup> The computer programs for calculation of hydrocarbon types were written by R. Teeter<sup>15</sup> based on modification of the original method by Robinson/Cook<sup>16</sup>, and supplied by PSMASPEC. These methods combined together provide full characterization of samples in the 200-525°C boiling range (resolving up to 7 saturate, 18 aromatic and 3 thiophenic types). The values for total saturates and aromatics in these calculations are taken from the SPE or LC material balance. The olefins and the polars are also included into the total hydrocarbon balance.

NCUT places an emphasis on process modeling and developing correlations between the chemical composition and physical properties of fuels. Therefore, we face the task of building a large database containing the information about chemical composition and physical properties of a number of fuels, particularly diesel fuels, that later will be used to derive various correlations. Having a method that does not require pre-separation of samples into fractions would be very beneficial. In cooperation with SRI International we developed a new GC-FIMS (Gas Chromatograph-Field Ionization Mass Spectrometry) method for fuels boiling in the diesel range (200-343°C). The method, well described in open literature, provides detailed characterization for up to 5 saturates (including isoparaffins), 6 aromatics and 2 aromatic thiophenotypes.<sup>17,18</sup> It does not require pre-separation of the sample and the results are also reported by carbon number.

Since physical properties of diesel fuels are directly related to their chemical composition, it is of great importance to be able to rely on the results provided by any of the methods used for hydrocarbon type analysis. As with separation methods, we have done some work on comparing our MS results

(EIMS and FIMS) with the results from other laboratories and other methods. Some of them are summarized here and can also be found in the literature.<sup>17</sup>

Table 5. Aromatic types by different methods

| HC Type                 | LC/GC-MS | SFC  | SPE/GC-MS | GC-FIMS | HPLC |
|-------------------------|----------|------|-----------|---------|------|
| <i>Ref2</i>             |          |      |           |         |      |
| Aromatics               | 29.5     | 29.8 | 30.6      | 29.7    | -    |
| Monoaromatics           | 23.8     | 23.4 | 24.1      | 23.8    | -    |
| Diaromatics             | 5.4      | 5.7  | 5.1       | 5.5     | -    |
| Polyaromatics           | 0.3      | 0.7  | 1.4       | 0.4     | -    |
| <i>Ref5</i>             |          |      |           |         |      |
| Aromatics               | 26.4     | 26.2 | 25.0      | 29.0    | -    |
| Monoaromatics           | 20.6     | 19.9 | 19.7      | 21.9    | -    |
| Diaromatics             | 5.7      | 5.9  | 4.1       | 6.9     | -    |
| Polyaromatics           | 0.2      | 0.4  | 1.2       | 0.2     | -    |
| <i>SWRII</i>            |          |      |           |         |      |
| Aromatics               | 33.9     | 32.6 | 33.3      | 33.3    | -    |
| Monoaromatics           | 23.5     | 21.3 | 22.0      | 23.4    | -    |
| Diaromatics             | 9.8      | 10.4 | 8.7       | 11.9    | -    |
| Polyaromatics           | 0.6      | 1.0  | 2.6       | 0.7     | -    |
| <i>Shell Low Sulfur</i> |          |      |           |         |      |
| Aromatics               | -        | 14.2 | 14.2      | 14.2    | -    |
| Monoaromatics           | -        | 11.7 | 11.7      | 12.1    | -    |
| Diaromatics             | -        | 2.3  | 2.4       | 2.0     | -    |
| Polyaromatics           | -        | 0.2  | 0.1       | 0.1     | -    |
| <i>S20B</i>             |          |      |           |         |      |
| Aromatics               | 22.3     | 23.5 | -         | 26.4    | 22.8 |
| Monoaromatics           | 19.2     | 20.3 | -         | 23.5    | 20.9 |
| Diaromatics             | 2.8      | 2.7  | -         | 2.7     | 1.3  |
| Polyaromatics           | 0.3      | 0.5  | -         | 0.1     | 0.6  |
| <i>S30B</i>             |          |      |           |         |      |
| Aromatics               | 30.2     | 31.4 | -         | 32.1    | 31.3 |
| Monoaromatics           | 26.2     | 27.4 | -         | 29.0    | 28.8 |
| Diaromatics             | 3.9      | 3.6  | -         | 2.9     | 2.2  |
| Polyaromatics           | 0.1      | 0.3  | -         | 0.2     | 0.3  |
| <i>C20B</i>             |          |      |           |         |      |
| Aromatics               | 19.4     | 20.2 | -         | 20.1    | 19.8 |
| Monoaromatics           | 15.7     | 16.8 | -         | 16.3    | 17.4 |
| Diaromatics             | 3.6      | 3.2  | -         | 3.6     | 2.2  |
| Polyaromatics           | 0.1      | 0.3  | -         | 0.1     | 0.2  |
| <i>C30B</i>             |          |      |           |         |      |
| Aromatics               | 28.8     | 29.8 | -         | 27.3    | 30.2 |
| Monoaromatics           | 24.5     | 25.1 | -         | 24.6    | 26.9 |
| Diaromatics             | 4.2      | 4.4  | -         | 3.5     | 3.0  |
| Polyaromatics           | 0.1      | 0.3  | -         | 0.1     | 0.3  |

The results for total saturates and aromatics from different class-type separations for these fuels were shown previously in Tables 1 and 2. The results in Table 5 provide a more detailed composition. Methods like supercritical fluid chromatography (SFC) and high performance liquid chromatography (HPLC) can only determine the aromatic subgroups (mono-, di-, and polyaromatics). We used these data to evaluate the reliability of hydrocarbon types determined by both EIMS and FIMS methods. In all cases there is a very good agreement between the methods. There are no independent techniques that would allow estimation of the MS performance

by verifying the hydrocarbon types in the aromatic subgroups (alkylbenzenes, benzocycloalkanes, benzodicycloalkanes, naphthalenes etc.). However, based on the good agreement between the methods for major subgroups, there is reason to believe that the results for more detailed distribution in the aromatic subgroups are also correct. While in LC/GC-MS and SPE/GC-MS methods the values for total saturates and aromatics were obtained from separation of the sample prior to MS analysis, in the GC-FIMS method these values were calculated from a single analysis. The following two graphs display excellent correlations obtained for a large number of diesel fuels, where GC-FIMS calculated data for total saturates and aromatics are compared with the SPE separation results.

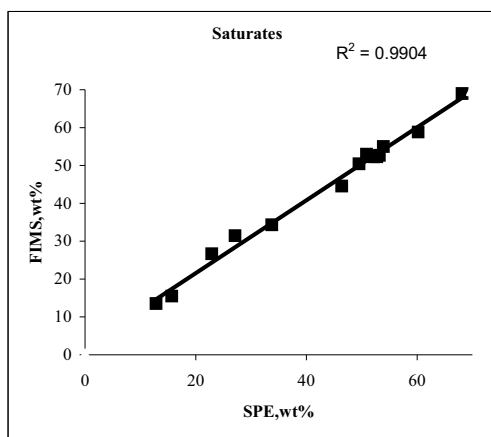


Figure 4. Correlation between GC-FIMS and SPE results for total saturates

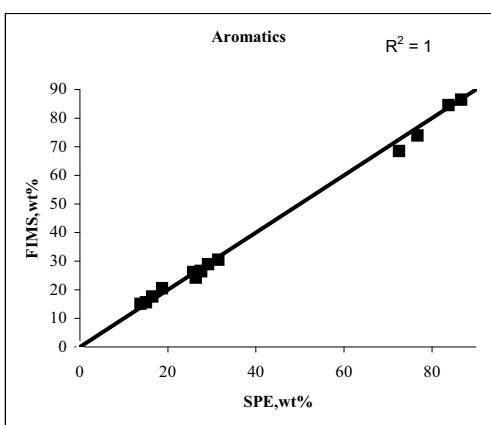


Figure 5. Correlation between GC-FIMS and SPE results for total aromatics



To confirm the reliability of FIMS results in a different way, we analyzed a large number of diesel blends by the GC-FIMS method. The blends were manually prepared from individual diesel components. Before using GC-FIMS results for the model development, the GC-FIMS method was first verified by comparing the chemical composition of blends analyzed by GC-FIMS with the calculated weight averaged chemical composition derived from original components by the following equation:

$$W = \sum_1^n W_i X_i \quad (1)$$

where  $n$  equals to the number of original diesel components that contributed to the blend,  $W_i$  is the weight fraction of a hydrocarbon type in  $i^{\text{th}}$  original component,  $X_i$  is the specific hydrocarbon type (for example, saturate or aromatics) in the chemical composition matrix of the original components, and  $W$  represents the fraction of this specific hydrocarbon type in the final blend.

Figure 6 shows a comparison between calculated and measured results for various hydrocarbon groups for a hundred diesel blends. “Analyzed” results were obtained from the GC-FIMS and PIONA analysis of the blends, and “calculated” results were calculated from the GC-FIMS and PIONA analysis of the individual components using their blending ratios. Good agreement between the two sets of data was observed.

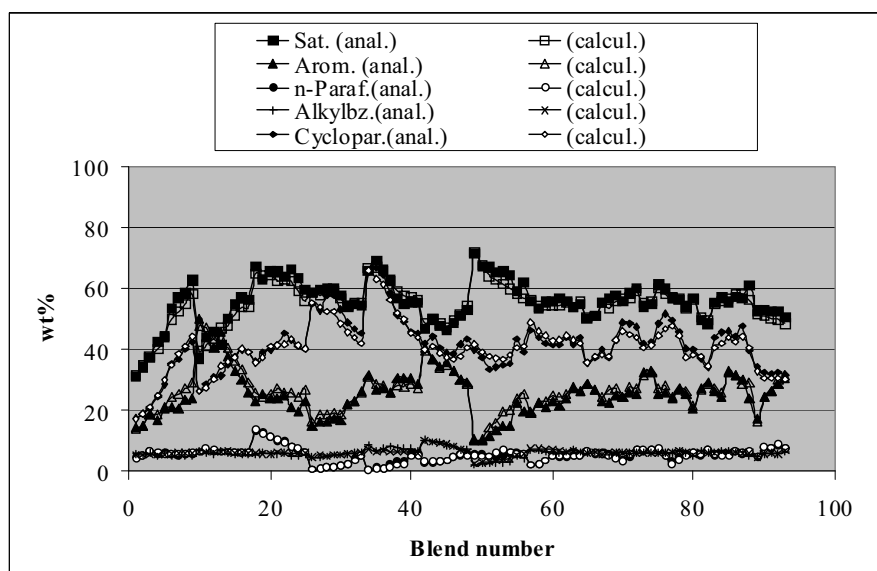


Figure 6. Composition of diesel blends-Analyzed vs Calculated

Analysis of diesel blends on one hand helped to establish the GC-FIMS method as being a reliable tool for quick diesel analysis, and on the other hand provided valuable data for the general product quality model database

In terms of saturate types, it is very difficult to evaluate the MS data. GC-EIMS ASTM D2786 method reports total paraffin content, while SRI/NCUT GC-FIMS method calculates iso- and n-paraffins separately. All the other methods independent of MS report only total saturate content. In our previous communications we showed the results for normal paraffins calculated by high resolution GC. We compared these values with those calculated by the GC-FIMS, and those obtained by Core Laboratories in Houston, Texas<sup>17</sup>. There was good agreement between the data suggesting that n-paraffins by GC-FIMS or total paraffins by GC-EIMS reflect their real concentration. To verify the distribution of cycloparaffins by MS, we attempted a physical separation of the saturate fraction into subgroups.<sup>18</sup> The *n*-paraffins were separated by 5Å molecular sieve, and iso-paraffins and mono-, di- and tri-cycloparaffins were separated by open column LC using Sephadex LH-20 gel. Again, the correlations between the physically separated fractions, GC-EIMS and GC-FIMS results were quite good.

One more way of checking the viability of the MS results was to determine the aromatic sulfur by some independent method. We chose the GC-FID/SCD (sulfur chemiluminescence detector) to determine the total aromatic sulfur and the aromatic sulfur types in the aromatic fraction of one of the cracked distillates (LCO). The GC-SCD chromatogram of this fraction contained a number of peaks corresponding to various sulfur compounds grouped into two distinguished groups. The total sulfur was calculated by integrating the total chromatogram area and using a response factor (RF) from an external calibration. The two distinguished groups of peaks belonged to benzothiophenes starting with benzothiophene-BT, and dibenzothiophenes starting with dibenzothiophene-DBT (Figure 7).

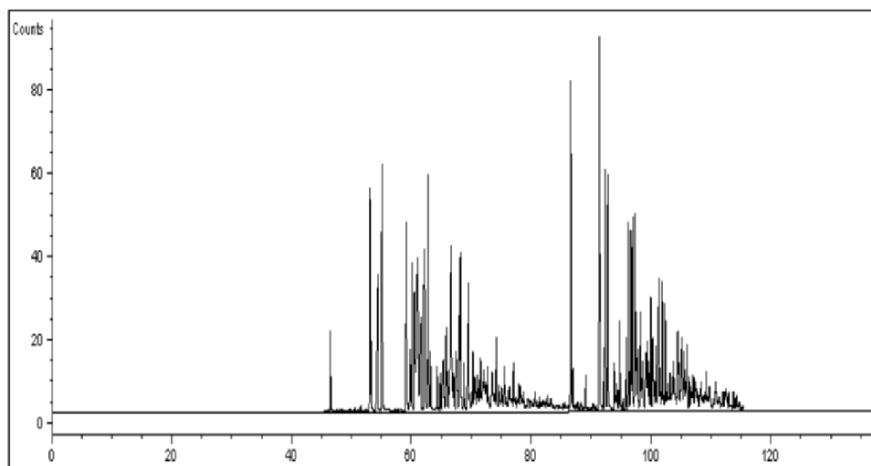


Figure 7. Sulfur trace of diesel sample

After the retention times for benzo- and dibenzothiophene standards analyzed separately were determined, the total sulfur chromatogram of the sample was split into two parts. The first group of peaks starting from and ending at the retention times corresponding to benzothiophene and dibenzothiophene, respectively, was integrated separately and sulfur was calculated using the RF. This sulfur corresponded to benzothiophene types. The second group of peaks was integrated starting from and ending at the retention times corresponding to dibenzothiophene and the end of chromatogram, respectively. This sulfur corresponded to dibenzothiophene types. To calculate the wt% of benzothiophenes (BT) from the sulfur wt% (S), we assumed that the average molecular weight of benzothiophenes was 190 Da and calculated their wt% as follows:  $BT = S * 32.0643 / 190$ , where 32.0643 is the atomic weight of sulfur. Similarly, the wt% of dibenzothiophenes was calculated by assuming the average molecular weight for dibenzothiophenes 220 Da. The third group of aromatic sulfur usually reported in the MS report belongs to benzonaphthothiophenes. In our LCO sample this group was not present but the calculation would be done the same way as for the other two groups. Lastly, the aromatic fraction was analyzed by ASTM D4294 method (Dispersive x-Ray Fluorescence Spectroscopy) for total sulfur. Table 6 summarizes these results.

Table 6. Aromatic Sulfur Types by different methods

| Aromatic sulfur types<br>wt% of total | X-Ray<br>ASTM D4294 | GC-SCD | GC-FIMS | GC-EIMS<br>ASTM D3239 | GC-EIMS<br>Robinson |
|---------------------------------------|---------------------|--------|---------|-----------------------|---------------------|
| Benzothiophenes                       | -                   | 2.70   | 3.30    | 3.60                  | 3.40                |
| Dibenzothiophenes                     | -                   | 6.00   | 6.50    | 4.00                  | 3.90                |
| Benzonaphthothiophenes                | -                   | N/D    | N/D     | 0.20                  | 0.20                |
| Total aromatic sulfur                 | -                   | 8.70   | 9.80    | 7.80                  | 7.50                |
| Total sulfur                          | 1.45                | 1.38   | 1.50    | 1.19                  | 1.14                |

For comparison, the last column also shows the results calculated by the Robinson method<sup>16</sup>. For the GC-SCD, the total sulfur was calculated from the sulfur chromatogram as mentioned before, but for all the MS methods it was calculated back from the sulfur types using the average molecular weights. Considering the fact that the values for an average molecular weight were assumed, these results compare reasonably well. For sulfur types, the GC-FIMS results are closer to the GC-SCD results than the results from the other two MS methods, and both methods render total sulfur that is in better agreement with the x-ray result.

### 3.2 Distributions by Boiling Point

The MS analysis, whether it is done by EI or FI, determines the hydrocarbon type composition of the whole analyzed sample. In real practice very often it is necessary to estimate the composition of a certain distillation fraction without having to distill the sample (e.g. when the sample is available in a very small amount), or to prepare a blend that meets requirements in a specified boiling range. It may also be necessary to know sulfur distribution in order to choose the right cut point for a refinery stream to make a fuel-blending component that will help maintain fuel spec in the particular situation at a specific refinery. All of these needs could be addressed by presenting the MS data distributed by boiling point.

Initially, we developed a manual method for the GC-EIMS. The saturates and the aromatics were analyzed separately as required by ASTM. The method was based on retention time slicing of the total ion chromatogram (TIC) of the fraction into desirable temperature intervals. The retention times for desired temperatures were calculated from the calibration curve obtained by analyzing the normal paraffins standard at the identical conditions. The mass in each temperature interval was calculated from the simulated distillation data of the fraction. After analysis of the fractions and processing the data, the saturate and aromatic reports were combined together into a total report, the sum of the slices was calculated weighted by corresponding yields of the fractions from LC separation, and this report was compared to a report for the whole sample. An example of these calculations is given in Table 7. The numbers in the last two columns agree very well suggesting that the slicing can be safely applied without undermining the integrity of the total report.

Another way of verifying the validity of the method was to produce physical slices by distilling the sample into several distillation cuts (A, B, C, and D), analyzing them by LC/GC-MS and comparing results for the sum of the cuts with the analysis of the total sample and with the sum of manual slices, making allowance for the overlap between the distillation fractions. These results are shown in Table 8.



Table 8. Sum of Manual Slices vs Sum of Distillation Cuts vs Total

| Hydrocarbon C <sub>n</sub> H <sub>2n+z</sub>                           | Z No. | CutA         | CutA        | CutB         | CutB        | CutC         | CutC        | CutD         | CutD         | Sum of cuts  | Total        | Sum of       |
|--|-------|--------------|-------------|--------------|-------------|--------------|-------------|--------------|--------------|--------------|--------------|--------------|
| Start of slice   |       |              |             |              |             |              |             |              |              |              |              |              |
| End of slice   |       | % of A       | % total     | % of B       | % total     | % of C       | % total     | % of D       | % total      | % total      | Sample       | slices       |
| <b>Saturates</b>   |       | <b>75.1</b>  | <b>16.8</b> | <b>82.8</b>  | <b>22.0</b> | <b>85.6</b>  | <b>23.7</b> | <b>87.8</b>  | <b>20.38</b> | <b>82.8</b>  | <b>82.9</b>  | <b>82.9</b>  |
| Paraffins  | 2     | 26.0         | 5.8         | 29.2         | 7.8         | 32.23        | 8.9         | 35.1         | 5.2          | 30.6         | 30.9         | 30.2         |
| Monocycloparaffins   | 0     | 24.2         | 5.4         | 22.8         | 6.1         | 15.9         | 6.3         | 22.5         | 3.5          | 23.0         | 23.3         | 23.4         |
| Dicycloparaffins   | -2    | 15.9         | 3.6         | 16.4         | 4.3         | 15.0         | 4.4         | 14.9         | 3.5          | 15.8         | 15.7         | 16.2         |
| Polycycloparaffins   | -4    | 9.1          | 2.0         | 14.5         | 3.8         | 14.1         | 4.1         | 15.3         | 2.8          | 13.4         | 13.2         | 13.1         |
| <b>Aromatics</b>   |       | <b>24.7</b>  | <b>5.5</b>  | <b>16.9</b>  | <b>4.6</b>  | <b>7.8</b>   | <b>3.9</b>  | <b>11.7</b>  | <b>1.2</b>   | <b>16.8</b>  | <b>16.9</b>  | <b>16.8</b>  |
| <b>MonoAromatics</b>   |       | <b>21.5</b>  | <b>4.8</b>  | <b>11.5</b>  | <b>3.1</b>  | <b>4.0</b>   | <b>2.2</b>  | <b>5.3</b>   | <b>0.7</b>   | <b>11.3</b>  | <b>11.6</b>  | <b>11.5</b>  |
| Alkylbenzenes  | -6    | 11.3         | 2.5         | 5.4          | 1.4         | 2.3          | 1.1         | 2.9          | 0.3          | 5.7          | 6.0          | 6.1          |
| Benzocycloalkanes  | -8    | 9.1          | 2.1         | 4.2          | 1.1         | 1.6          | 0.6         | 1.5          | 0.2          | 4.1          | 4.2          | 4.1          |
| Benzodicycloalkanes  | -10   | 1.0          | 0.2         | 1.9          | 0.6         | 5.2          | 0.5         | 0.9          | 1.1          | 1.5          | 1.4          | 1.3          |
| <b>Diaromatics</b>   |       | <b>3.2</b>   | <b>0.7</b>  | <b>4.8</b>   | <b>1.3</b>  | <b>1.3</b>   | <b>1.5</b>  | <b>4.7</b>   | <b>0.2</b>   | <b>4.6</b>   | <b>4.7</b>   | <b>4.2</b>   |
| Naphthalenes   | -12   | 1.9          | 0.4         | 1.6          | 0.4         | 3.0          | 0.4         | 0.8          | 0.6          | 1.4          | 1.5          | 1.4          |
| Naphthocycloalkanes  | -14   | 1.0          | 0.2         | 2.5          | 0.7         | 1.0          | 0.8         | 2.5          | 0.3          | 2.3          | 2.3          | 2.1          |
| Fluorenes  | -16   | 0.3          | 0.1         | 0.7          | 0.2         | 0.3          | 0.3         | 1.4          | 0.2          | 0.9          | 0.8          | 0.7          |
| <b>Triaromatics</b>  |       | <b>0.1</b>   | <b>0.1</b>  | <b>0.2</b>   | <b>0.1</b>  | <b>0.3</b>   | <b>0.1</b>  | <b>0.7</b>   | <b>0.1</b>   | <b>0.4</b>   | <b>0.3</b>   | <b>0.3</b>   |
| Phenanthrenes  | -18   | 0.1          | 0.1         | 0.2          | 0.1         | 0.0          | 0.1         | 0.5          | 0.1          | 0.3          | 0.3          | 0.3          |
| Phenanthrocycloalkanes   | -20   | 0.0          | 0.0         | 0.0          | 0.0         | 0.1          | 0.0         | 0.2          | 0.1          | 0.1          | 0.0          | 0.0          |
| <b>Tetraaromatics</b>  |       | <b>0.0</b>   | <b>0.0</b>  | <b>0.0</b>   | <b>0.0</b>  | <b>0.1</b>   | <b>0.0</b>  | <b>0.3</b>   | <b>0.1</b>   | <b>0.1</b>   | <b>0.1</b>   | <b>0.1</b>   |
| Pyrenes/Benzofluorenes   | -22   | 0.0          | 0.0         | 0.0          | 0.0         | 0.0          | 0.0         | 0.3          | 0.0          | 0.1          | 0.1          | 0.1          |
| Chrysenes  | -24   | 0.0          | 0.0         | 0.0          | 0.0         | 0.0          | 0.0         | 0.0          | 0.0          | 0.0          | 0.0          | 0.0          |
| <b>Pentaaromatics</b>  |       | <b>0.0</b>   | <b>0.0</b>  | <b>0.0</b>   | <b>0.0</b>  | <b>0.0</b>   | <b>0.0</b>  | <b>0.0</b>   | <b>0.0</b>   | <b>0.0</b>   | <b>0.0</b>   | <b>0.0</b>   |
| Benzopyrenes/Perylenes   | -28   | 0.0          | 0.0         | 0.0          | 0.0         | 0.0          | 0.0         | 0.0          | 0.0          | 0.0          | 0.0          | 0.0          |
| Dibenzanthracenes  | -30   | 0.0          | 0.0         | 0.0          | 0.0         | 0.0          | 0.0         | 0.0          | 0.0          | 0.0          | 0.0          | 0.0          |
| <b>Unidentified</b>  |       | <b>0.0</b>   | <b>0.0</b>  | <b>0.0</b>   | <b>0.0</b>  | <b>0.0</b>   | <b>0.0</b>  | <b>0.0</b>   | <b>0.0</b>   | <b>0.0</b>   | <b>0.0</b>   | <b>0.0</b>   |
| C <sub>n</sub> H <sub>2n-32</sub> /C <sub>n</sub> H <sub>2n-46</sub>   | -32   | 0.0          | 0.0         | 0.0          | 0.0         | 0.0          | 0.0         | 0.0          | 0.0          | 0.0          | 0.0          | 0.0          |
| C <sub>n</sub> H <sub>2n-36</sub> /C <sub>n</sub> H <sub>2n-26</sub> S | -36   | 0.0          | 0.0         | 0.0          | 0.0         | 0.0          | 0.0         | 0.0          | 0.0          | 0.0          | 0.0          | 0.0          |
| C <sub>n</sub> H <sub>2n-38</sub> /C <sub>n</sub> H <sub>2n-28</sub> S | -38   | 0.0          | 0.0         | 0.0          | 0.0         | 0.0          | 0.0         | 0.0          | 0.0          | 0.0          | 0.0          | 0.0          |
| C <sub>n</sub> H <sub>2n-40</sub> /C <sub>n</sub> H <sub>2n-30</sub> S | -40   | 0.0          | 0.0         | 0.0          | 0.0         | 0.0          | 0.0         | 0.0          | 0.0          | 0.0          | 0.0          | 0.0          |
| C <sub>n</sub> H <sub>2n-42</sub> /C <sub>n</sub> H <sub>2n-32</sub> S | -42   | 0.0          | 0.0         | 0.0          | 0.0         | 0.0          | 0.0         | 0.0          | 0.0          | 0.0          | 0.0          | 0.0          |
| C <sub>n</sub> H <sub>2n-44</sub> /C <sub>n</sub> H <sub>2n-34</sub> S | -44   | 0.0          | 0.0         | 0.0          | 0.0         | 0.0          | 0.0         | 0.0          | 0.0          | 0.0          | 0.0          | 0.0          |
| <b>Aromatic Sulfur</b>   |       | <b>0.0</b>   | <b>0.0</b>  | <b>0.4</b>   | <b>0.1</b>  | <b>0.5</b>   | <b>0.1</b>  | <b>0.7</b>   | <b>0.2</b>   | <b>0.3</b>   | <b>0.3</b>   | <b>0.7</b>   |
| Benzothiophenes  | -10S  | 0.0          | 0.0         | 0.4          | 0.1         | 0.5          | 0.1         | 0.4          | 0.1          | 0.3          | 0.3          | 0.5          |
| Dibenzothiophenes  | -16S  | 0.0          | 0.0         | 0.0          | 0.0         | 0.0          | 0.0         | 0.3          | 0.1          | 0.0          | 0.0          | 0.2          |
| Benzenaphthothiophenes   | -22S  | 0.0          | 0.0         | 0.0          | 0.0         | 0.0          | 0.0         | 0.0          | 0.0          | 0.0          | 0.0          | 0.0          |
| <b>Polar Compounds</b>   |       | <b>0.2</b>   | <b>0.1</b>  | <b>0.3</b>   | <b>0.1</b>  | <b>0.3</b>   | <b>0.1</b>  | <b>0.5</b>   | <b>0.1</b>   | <b>0.4</b>   | <b>0.2</b>   | <b>0.2</b>   |
| <b>Total</b>   |       | <b>100.0</b> | <b>22.4</b> | <b>100.0</b> | <b>26.7</b> | <b>100.0</b> | <b>27.7</b> | <b>100.0</b> | <b>23.2</b>  | <b>100.0</b> | <b>100.0</b> | <b>100.0</b> |

The results in the column titled “Sum of cuts” are calculated by summation of the results for each individual cut taken as a percent of the total sample. The results for each distillation cut were calculated from the GC-MS analysis of saturate and aromatic fractions of the cut weighed by the mass fraction of this cut. This procedure was reversed and the TIC of the total sample was manually “cut” into four slices having boiling ranges similar to the actual cuts. However, based on simulated distillation data there was a significant overlapping between the real cuts. This fact had to be taken into account to calculate the weight percentages for the slices. The slicing was done as described before, and the sum of the results for the slices is shown in the last column of Table 8. There is very good agreement between the results in the last three columns.

Lastly, we verified the by-boiling-point distribution method by looking specifically into the calculation of individual compounds present in the MS

report and whether we could identify and quantify them by other methods. We analyzed one of the aromatic fractions by GC-MS, calculated the hydrocarbon types by ASTM 3239, and did the manual slicing by 30°C intervals (the yield of this fraction from LC separation was 39.60wt%). Afterwards, this aromatic fraction was separated into mono-, di-, polyaromatic and polar fractions using normal phase semi-preparative HPLC separation with the following yields: 46.50wt%, 28.15wt%, 23.81wt%, and 1.54wt%, respectively. The polyaromatic fraction was separated into individual aromatic compounds using a reversed phase HPLC. Our specific interest was to identify and quantify pyrene (B.P.=393°C), phenanthrene (B.P.=340°C), and fluorine (B.P.=298°C) in this fraction and compare these results with those calculated by GC-MS for the same compounds in the corresponding temperature intervals. For HPLC quantitation, pure standards were analyzed to obtain the calibration curve for each compound. Peak assignments on the HPLC chromatogram were given based on the retention times of the standards. The results of these calculations are presented in Table 9.

Table 9. Comparison of GC-MS and HPLC Results for Individual Compounds

| <i>HC Type</i>         | <i>HPLC<br/>wt% of<br/>LC fraction</i> | <i>HPLC<sup>a</sup><br/>wt% of<br/>total sample</i> | <i>GC-MS<br/>wt% of<br/>LC aromatics</i> | <i>GC-MS<sup>b</sup><br/>wt% of<br/>total sample</i> |
|------------------------|--|---|--|--|
| Pyrene (390-420)       | 0.92                                   | 0.22  | 0.50                                     | 0.20   |
| Phenanthrene (330-360) | 0.40                                   | 0.10  | 0.30                                     | 0.12   |
| Fluorene (270-300)     | 0.22                                   | 0.05  | 0.10                                     | 0.04   |

a. results in column 1\* 0.2381

b. results in column 3\* 0.3960

The results based on the total sample shown in the second and the fourth columns are almost identical. The compounds of interest were found in the right temperature interval of the GC-MS calculations, in an amount that was confirmed by HPLC calculations.

Once we had confidence in manual slicing, the computer software was developed to perform the automatic calculations. The yields of fractions from LC or SPE separation, their simulated distillation results, and the retention time calibration from GC-MS (together with the MS data) were fed into the software that utilized the original Teeter's programs<sup>15</sup>. In LC separation, the fractions have to be submitted for simulated distillation analysis separately. In the case of SPE separation, the GC-FID signal of separated fractions is used simultaneously for quantification and also for producing the simulated distillation results that are calculated by the software (Separation Systems Inc.). In the SOAP method, the GC-FID signal of the olefin fraction that is used for quantification is also used for calculating the cut-point table with the same software, where the temperature intervals are chosen as they are used in the GC-MS distribution of hydrocarbon types.

As indicated earlier, all calculations are done for the 200-525°C boiling range. To analyze the naphtha fraction, the sample is injected into a PIONA

analyzer with a prefractionator. The PIONA report reflects the composition of the IBP-200°C fraction of the sample. The PIONA report is combined with the GC-MS report and a final report that reflects detailed composition in full boiling range is produced. An example of this report is shown in Table 10.

Table 10. Hydrocarbon Types Characterization – Full Boiling Range

| Start BP Deg. C  | Method      | IBP        | Method     | 200        | 210        | 220        | 230        | 240        | 250        | -          | 510        | 520        | 530        | 200         | IBP          |
|--|-------------|------------|------------|------------|------------|------------|------------|------------|------------|------------|------------|------------|------------|-------------|--------------|
| End BP Deg. C  |             | 200        |            | 210        | 220        | 230        | 240        | 250        | 260        | -          | 520        | 530        | 540        | 540         | FBP          |
| Weight Percent   | SimDist     |            | SimDist    | 0.6        | 0.7        | 0.8        | 1.0        | 1.1        | 2.0        |            | 1.1        | 0.9        | 0.6        |             |              |
| <b>Hydrocarbon Types</b>   | <b>Z</b>    |            |            |            |            |            |            |            |            |            |            |            |            |             |              |
|  | PIONA       |            | GC-MS      |            |            |            |            |            |            |            |            |            |            |             |              |
| <b>Saturates</b>   |             | <b>2.0</b> | SPE/FID    | <b>0.4</b> | <b>0.5</b> | <b>0.5</b> | <b>0.7</b> | <b>0.7</b> | <b>0.9</b> |            | <b>0.3</b> | <b>0.2</b> | <b>0.1</b> | <b>31.1</b> | <b>33.2</b>  |
| <b>Total Paraffins</b>   |             | <b>1.4</b> | ASTM2786   | <b>0.1</b> | <b>0.2</b> | <b>0.1</b> | <b>0.1</b> | <b>0.1</b> | <b>0.1</b> |            | <b>0.0</b> | <b>0.0</b> | <b>0.0</b> | <b>4.5</b>  |              |
| iso-Paraffins  | <b>2</b>    | PIONA      | 0.7        | -          |            |            |            |            |            |            |            |            |            |             |              |
| n-Paraffins  | <b>2</b>    | PIONA      | 0.7        | -          |            |            |            |            |            |            |            |            |            |             |              |
| <b>Cycloparaffins</b>  |             | <b>0.6</b> | ASTM2786   | <b>0.3</b> | <b>0.3</b> | <b>0.4</b> | <b>0.5</b> | <b>0.6</b> | <b>1.0</b> |            | <b>0.2</b> | <b>0.2</b> | <b>0.1</b> | <b>26.6</b> |              |
| <b>Olefins</b>   | <b>0</b>    | PIONA      | <b>1.1</b> | SPE/FID    | <b>0.1</b> | <b>0.2</b> | <b>0.2</b> | <b>0.3</b> | <b>0.2</b> | <b>0.3</b> | <b>0.1</b> | <b>0.1</b> | <b>0.1</b> | <b>10.7</b> | <b>11.7</b>  |
| Monocycloparaffins   | <b>0</b>    |            | ASTM2786   | 0.1        | 0.1        | 0.1        | 0.1        | 0.1        | 0.2        |            | 0.0        | 0.0        | 0.0        | 5.8         |              |
| Dicycloparaffins   | <b>-2</b>   |            | ASTM2786   | 0.2        | 0.2        | 0.3        | 0.3        | 0.4        | 0.4        |            | 0.1        | 0.0        | 0.0        | 9.0         |              |
| Tricycloparaffins +  | <b>-4</b>   |            | ASTM2786   | 0.0        | 0.0        | 0.1        | 0.1        | 0.2        | 0.4        |            | 0.1        | 0.1        | 0.0        | 11.9        |              |
| <b>Aromatics</b>   |             | <b>1.5</b> | SPE/FID    | <b>0.2</b> | <b>0.2</b> | <b>0.3</b> | <b>0.3</b> | <b>0.4</b> | <b>0.6</b> |            | <b>0.8</b> | <b>0.7</b> | <b>0.5</b> | <b>46.0</b> | <b>47.5</b>  |
| <b>Monoaromatics</b>   |             |            | ASTM3239   | <b>0.2</b> | <b>0.2</b> | <b>0.3</b> | <b>0.2</b> | <b>0.3</b> | <b>0.4</b> |            | <b>0.2</b> | <b>0.2</b> | <b>0.1</b> | <b>15.8</b> |              |
| Alkylbenzenes  | <b>-6</b>   |            | ASTM3239   | 0.1        | 0.1        | 0.1        | 0.1        | 0.1        | 0.1        |            | 0.1        | 0.1        | 0.1        | 4.4         |              |
| Benzocycloalkanes  | <b>-8</b>   |            | ASTM3239   | 0.0        | 0.1        | 0.1        | 0.1        | 0.1        | 0.2        |            | 0.0        | 0.0        | 0.0        | 5.1         |              |
| Benzodicycloalkanes  | <b>-10</b>  |            | ASTM3239   | 0.0        | 0.0        | 0.0        | 0.1        | 0.1        | 0.1        |            | 0.1        | 0.0        | 0.0        | 6.3         |              |
| <b>Diaromatics</b>   |             |            | ASTM3239   | <b>0.0</b> | <b>0.0</b> | <b>0.0</b> | <b>0.0</b> | <b>0.0</b> | <b>0.1</b> |            | <b>0.3</b> | <b>0.5</b> | <b>0.3</b> | <b>12.1</b> |              |
| Naphthalenes   | <b>-12</b>  |            | ASTM3239   | 0.0        | 0.0        | 0.0        | 0.0        | 0.0        | 0.1        |            | 0.1        | 0.1        | 0.0        | 3.4         |              |
| Naphthocycloalkanes  | <b>-14</b>  |            | ASTM3239   | 0.0        | 0.0        | 0.0        | 0.0        | 0.0        | 0.0        |            | 0.0        | 0.0        | 0.0        | 3.4         |              |
| Fluorenes  | <b>-16</b>  |            | ASTM3239   | 0.0        | 0.0        | 0.0        | 0.0        | 0.0        | 0.0        |            | 0.3        | 0.3        | 0.3        | 5.2         |              |
| <b>Triaromatics</b>  |             |            | ASTM3239   | <b>0.0</b> | <b>0.0</b> | <b>0.0</b> | <b>0.0</b> | <b>0.0</b> | <b>0.0</b> |            | <b>0.0</b> | <b>0.0</b> | <b>0.0</b> | <b>4.0</b>  |              |
| Phenanthrenes  | <b>-18</b>  |            | ASTM3239   | 0.0        | 0.0        | 0.0        | 0.0        | 0.0        | 0.0        |            | 0.0        | 0.0        | 0.0        | 2.3         |              |
| Phenanthrocycloalkanes   | <b>-20</b>  |            | ASTM3239   | 0.0        | 0.0        | 0.0        | 0.0        | 0.0        | 0.0        |            | 0.0        | 0.0        | 0.0        | 1.7         |              |
| <b>Tetraaromatics</b>  |             |            | ASTM3239   | <b>0.0</b> | <b>0.0</b> | <b>0.0</b> | <b>0.0</b> | <b>0.0</b> | <b>0.0</b> |            | <b>0.0</b> | <b>0.0</b> | <b>0.0</b> | <b>2.9</b>  |              |
| Pyrenes/Benzofluorenes   | <b>-22</b>  |            | ASTM3239   | 0.0        | 0.0        | 0.0        | 0.0        | 0.0        | 0.0        |            | 0.0        | 0.0        | 0.0        | 2.0         |              |
| Chrysenes  | <b>-24</b>  |            | ASTM3239   | 0.0        | 0.0        | 0.0        | 0.0        | 0.0        | 0.0        |            | 0.0        | 0.0        | 0.0        | 0.8         |              |
| <b>Pentaaromatics</b>  |             |            | ASTM3239   | <b>0.0</b> | <b>0.0</b> | <b>0.0</b> | <b>0.0</b> | <b>0.0</b> | <b>0.0</b> |            | <b>0.0</b> | <b>0.0</b> | <b>0.0</b> | <b>1.2</b>  |              |
| Benzopyrenes/Perylenes   | <b>-28</b>  |            | ASTM3239   | 0.0        | 0.0        | 0.0        | 0.0        | 0.0        | 0.0        |            | 0.0        | 0.0        | 0.0        | 1.1         |              |
| Dibenzanthracenes  | <b>-30</b>  |            | ASTM3239   | 0.0        | 0.0        | 0.0        | 0.0        | 0.0        | 0.0        |            | 0.0        | 0.0        | 0.0        | 0.1         |              |
| <b>Unidentified</b>  |             |            | ASTM3239   | <b>0.0</b> | <b>0.0</b> | <b>0.0</b> | <b>0.0</b> | <b>0.0</b> | <b>0.0</b> |            | <b>0.1</b> | <b>0.0</b> | <b>0.1</b> | <b>1.7</b>  |              |
| C <sub>n</sub> H <sub>2n-32</sub> /C <sub>n</sub> H <sub>2n-46</sub>   | <b>-32</b>  |            | ASTM3239   | 0.0        | 0.0        | 0.0        | 0.0        | 0.0        | 0.0        |            | 0.0        | 0.0        | 0.0        | 0.2         |              |
| C <sub>n</sub> H <sub>2n-36</sub> /C <sub>n</sub> H <sub>2n-36</sub> S | <b>-36</b>  |            | ASTM3239   | 0.0        | 0.0        | 0.0        | 0.0        | 0.0        | 0.0        |            | 0.0        | 0.0        | 0.0        | 0.0         |              |
| C <sub>n</sub> H <sub>2n-38</sub> /C <sub>n</sub> H <sub>2n-28</sub> S | <b>-38</b>  |            | ASTM3239   | 0.0        | 0.0        | 0.0        | 0.0        | 0.0        | 0.0        |            | 0.1        | 0.0        | 0.1        | 1.4         |              |
| C <sub>n</sub> H <sub>2n-40</sub> /C <sub>n</sub> H <sub>2n-30</sub> S | <b>-40</b>  |            | ASTM3239   | 0.0        | 0.0        | 0.0        | 0.0        | 0.0        | 0.0        |            | 0.0        | 0.0        | 0.0        | 0.0         |              |
| C <sub>n</sub> H <sub>2n-42</sub> /C <sub>n</sub> H <sub>2n-32</sub> S | <b>-42</b>  |            | ASTM3239   | 0.0        | 0.0        | 0.0        | 0.0        | 0.0        | 0.0        |            | 0.0        | 0.0        | 0.0        | 0.0         |              |
| C <sub>n</sub> H <sub>2n-44</sub> /C <sub>n</sub> H <sub>2n-34</sub> S | <b>-44</b>  |            | ASTM3239   | 0.0        | 0.0        | 0.0        | 0.0        | 0.0        | 0.0        |            | 0.0        | 0.0        | 0.0        | 0.0         |              |
| <b>Aromatic Sulfur</b>   |             |            | ASTM3239   | <b>0.0</b> | <b>0.0</b> | <b>0.0</b> | <b>0.0</b> | <b>0.0</b> | <b>0.1</b> |            | <b>0.1</b> | <b>0.1</b> | <b>0.0</b> | <b>8.3</b>  |              |
| Benzothiophenes  | <b>-10S</b> |            | ASTM3239   | 0.0        | 0.0        | 0.0        | 0.0        | 0.0        | 0.1        |            | 0.1        | 0.1        | 0.0        | 4.8         |              |
| Dibenzothiophenes  | <b>-16S</b> |            | ASTM3239   | 0.0        | 0.0        | 0.0        | 0.0        | 0.0        | 0.0        |            | 0.0        | 0.0        | 0.0        | 2.8         |              |
| Benzenaphthiophenes  | <b>-22S</b> |            | ASTM3239   | 0.0        | 0.0        | 0.0        | 0.0        | 0.0        | 0.0        |            | 0.0        | 0.0        | 0.0        | 0.7         |              |
| <b>Polars</b>  |             |            | SPE/FID    |            |            |            |            |            |            |            |            |            |            |             | <b>7.4</b>   |
| <b>Asphaltenes</b>   |             |            | SE         |            |            |            |            |            |            |            |            |            |            |             | <b>0.2</b>   |
| <b>Total</b>   |             |            |            |            |            |            |            |            |            |            |            |            |            |             | <b>100.0</b> |

This same idea was used in the development of the software for by-boiling-point distribution of the GC-FIMS results, with the exception that there was no need to input the SPE or LC separation results. FIMS reports the hydrocarbon types by carbon number (up to C<sub>21</sub> for diesel range). The by-boiling point distribution added another dimension, and a full FIMS report now consisted of a series of reports by carbon number in each temperature interval. For lighter diesels the GC-FIMS results were calculated also from



the 200°C+ boiling interval, and in combination with PIONA analysis the final report that captured the full sample range was produced.

Having such a convenient and comprehensive method for diesel analysis made it possible to create a database containing the results for a large number of samples. These data were used to draw various correlations between the chemical composition and the physical properties of the fuels, and also predict the blending ratios for diesel blends having specific cetane number requirements.

#### 4. NEURAL NETWORK CORRELATIONS

According to NCUT's definition, the product quality model links the molecular representation of the process effluent to its physical properties (e.g. density and viscosities at two different temperatures) and refinery-type characterization (e.g. smoke point and cetane number). In this section we will illustrate the development of product quality correlations for diesel-range materials using density of liquid and cetane number as examples.

Density and cetane number are two important specifications of diesel fuel that have been targeted for regulation along with sulfur content, aromatic content, boiling range, etc. For example, studies show that increasing cetane number and reducing density improve fuel combustion properties and benefit engine particulate matters emissions.<sup>19-22</sup> It is worth noting that although density is easily measured in the refinery using a small amount of sample, this option is not available until the stream in question is actually produced. Any predictive simulation model has to be able to estimate density based on other information generated by the model. In our case, this information is hydrocarbon-type characterization as described above. While density can be measured relatively easily, the measurement of cetane number by ASTM D613 engine test requires much more time and a relatively large sample. It cannot be used as a rapid measurement to control diesel quality in the refinery. Therefore, accurate prediction of the cetane number can be of use for both model predictions as well as day-to-day refinery operation. One important application would be optimization of diesel fuel blending.

We have not been able to find open literature publications on predicting the density of hydrocarbon liquids based on chemical composition. In contrast, there have been many attempts to develop empirical correlations to predict the cetane number.<sup>23-26</sup> Unfortunately, most of those attempts have had rather limited success, which, in the end, led to the introduction of the term "cetane index" to describe cetane number estimates generated with the various correlations.

Most of these correlations used 2 to 3 bulk properties and they were developed using multiple linear or nonlinear regression techniques. This kind of approach requires the developer to specify *a priori* a mathematical form of the empirical correlation. Therefore, the development of a satisfactory

empirical correlation and the associated parameter estimation may be quite tedious despite relatively few variables involved.

The neural network approach is an alternative way of solving the problem. Unlike multiple linear or nonlinear regression techniques, which require a predefined empirical form, the neural network can identify and learn the correlative patterns between the input and the corresponding output values once a training set is provided. This approach avoids some of the shortcomings encountered in more traditional correlative methods, and with modern software it can provide useful models in a relatively short time for both linear and non-linear systems.<sup>27-29</sup>

NCUT has been working on the development of neural network correlations to predict, among other things, cetane number (CN) and density of diesel fuel from its chemical compositions using a three-layer Ward back propagation network (NeuroShell® software, Ward System Group Inc. MD, USA)<sup>30</sup>. Two steps are required to create such a model: a training step and a validation step. In the training step, the neural network is supplied with a training data set, including the correlation input and corresponding output values. The network learns the trends contained in the data set and correlates the inputs and outputs by finding the optimum set of weights that minimize the differences between the predicted and actual output values. The training terminates when the predefined “stop training criterion” is reached. In our work, the training stopped after 20,000 epochs had passed since the reaching of the minimum average error for the test data set. The best model saved was the one that had the smallest prediction error on the test data. Sixty-nine diesel fuels were analyzed using the LC/GC-EIMS methods described above and were used for correlation development with 48 samples in the training set and 21 samples in the test set. Twelve hydrocarbon groups, including paraffins (normal paraffins and isoparaffins), monocycloparaffins, dicycloparaffins, tricycloparaffins and heavier, alkylbenzenes, benzocycloalkanes, benzo-dicycloalkanes, naphthalenes, naphthocycloalkanes, fluorenes, triaromatics and heavier, and aromatic sulfur, were used as neural network inputs. Cetane number (ASTM D613) or density (ASTM D4502) was the output. Using the entire data set, mean absolute errors of 1.32 and 0.004 g/mL were obtained for cetane number and density, respectively. The mean absolute error for cetane number prediction was below the reproducibility limits of the ASTM D613 engine test method, which is between 2.8 to 4.8 depending on the cetane number of diesel fuel. However, the mean error for the density prediction was far worse than the reproducibility of the ASTM D4052 test (0.0005).

Two actions were taken in an effort to improve the neural network model. First, more diesel blends were analyzed to increase the number of data points. For this purpose 114 diesel blends were prepared using 15 diesel blending components obtained from a number of Canadian refineries and derived from conventional crude oils and synthetic materials. The blending components and

the diesel blends (129 samples altogether) were characterized by ASTM standard methods for their physical properties including aniline point, cetane number, density, viscosity, refractive index and molecular weight. Second, the GC-MS method was replaced by PIONA and GC-FIMS methods for the determination of the chemical composition. GC-FIMS method was used for the boiling range 200–343°C, and PIONA was used for the boiling range IBP–200°C. The mass-balanced combinations of the GC-FIMS and PIONA results for all the blends were used to develop the neural network correlations. The GC-FIMS method has several advantages over GC-EIMS. In the diesel range, this method makes it possible to analyze a whole sample without pre-separation into saturate and aromatic fractions. This reduces errors caused by loss of lighter materials due to handling during the separation procedure. NCUT's GC-FIMS procedure can also distinguish between n-paraffins and iso-paraffins. Since n-paraffins and iso-paraffins differently affect cetane number, this approach was expected to improve the cetane number correlation. In this part of the study, new neural network correlations (to predict cetane number and density) were developed using a larger diesel database (in total 129 samples were analyzed). The same three-layer Ward back propagation network configuration was used for the new model development. Twelve hydrocarbons, iso-paraffins, n-paraffins, monocycloparaffins, dicycloparaffins, polycycloparaffins, alkylbenzenes, benzocycloalkanes, benzodicycloalkanes, diaromatics, tricaromatics, tetraomatics, and aromatic sulfur were used as neural network inputs. Cetane number or density was the network output. Most of the hydrocarbon types used in the new models are the same as in our previous work. However, two major modifications were made: 1) n-paraffins and iso-paraffin were used separately and 2) two-ring aromatics (naphthalenes, naphthocycloalkanes, fluorenes) were lumped together. Figures 8 and 9 present the plots of predicted cetane numbers and densities plotted against the measured ones.

Figures 10 and 11 compare the differences between the measured and predicted values (residuals) of cetane numbers and densities.

The new neural network correlations give mean absolute errors of 1.06 for cetane number and 0.003 for density, which represent significant improvements over the correlations developed in the first attempt. Work on improving these correlations and developing correlations for the other properties available in our database continues.

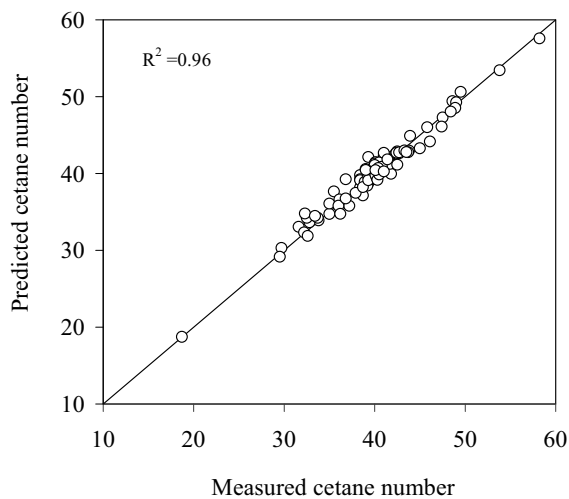


Figure 8. Comparison between predicted and measured cetane numbers

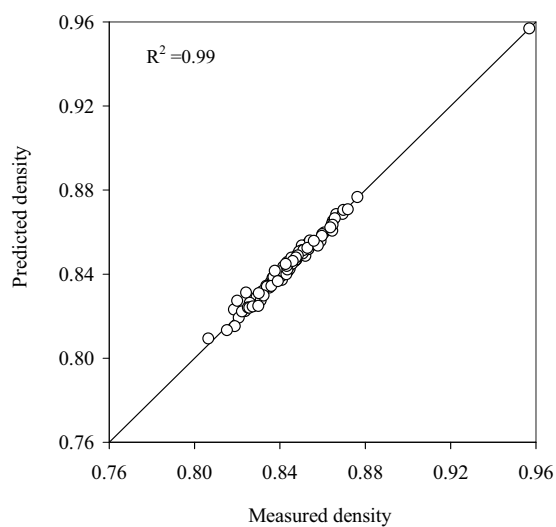


Figure 9. Comparison between predicted and measured densities

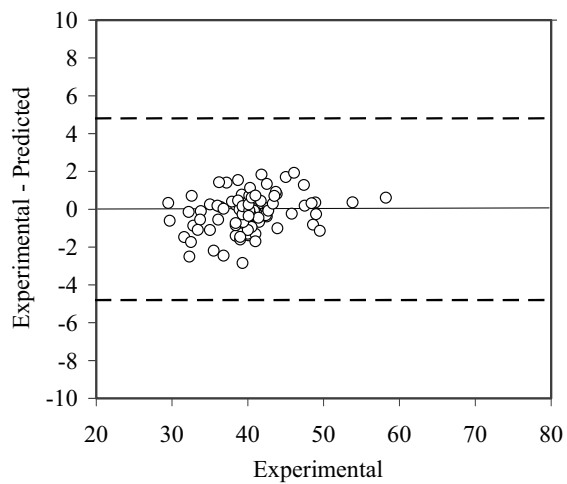


Figure 10. Comparison of the residuals from the neural network model (circles) with the ASTM D613 for cetane number obtained reproducibility (dotted line).

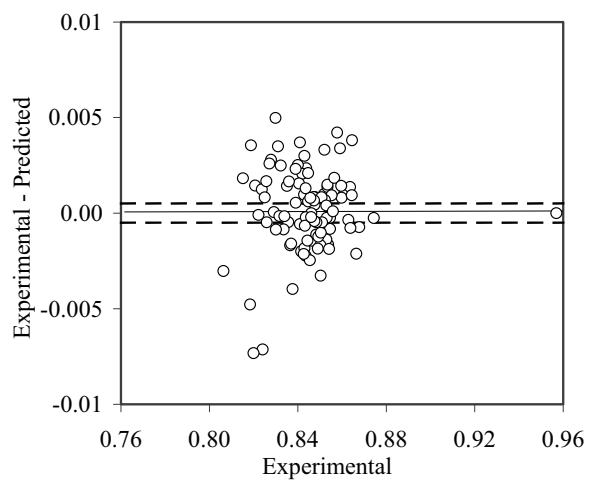


Figure 11. Comparison of the residuals for density obtained from the neural network model (circles) with the ASTM D4502 reproducibility (dotted line).

The results presented in this section demonstrate that, in the diesel range, the type of characterization of hydrocarbon samples developed at NCUT provides sufficient input for product quality estimation in any process model.

## 5. ACKNOWLEDGMENTS

The authors would like to acknowledge Syncrude Canada Ltd. for performing the SFC tests and Alberta Research Council for performing the FIA tests. Partial funding for NCUT has been provided by the Canadian Program for Energy Research and Development (PERD), the Alberta Research Council and the Alberta Energy Research Institute.

## 6. REFERENCES

1. Hu, Shanying; Towler, G.; Zhu, X.X., *Ind.Eng.Chem.Res.*, **2002**, *41*, 825-841.
2. Annual Book of ASTM Standards, Section 5 Petroleum Products, Lubricants, and Fossil Fuels; American Society for Testing and Materials: (Test method for characteristic groups in rubber extender and processing oils by the clay-gel adsorption chromatographic method; **Designation: D2007**. Method for Separation of Representative Aromatics and Nonaromatic Fractions of High Boiling Oils by Elution Chromatography; **Designation D2549**).
3. Annual Book of ASTM Standards, Section 5 Petroleum Products, Lubricants, and Fossil Fuels; American Society for Testing and Materials: Easton, MD (Standard test method for hydrocarbon type analysis of gas-oil saturate fractions by high ionizing voltage mass spectrometry; **Designation: D2786**. Method for aromatic types analysis of gas-oil aromatic fractions by high ionizing voltage mass spectrometry; **Designation: D3239**).
4. Bundt, J.; Herbel, W.; Steinhart, H.; Franke, S.; Francke, W., Structure-type Separation of Diesel Fuels by Solid Phase Extraction and Identification of the Two- and Three-ring Aromatics by Capillary GC-Mass Spectrometry, *J. High Res. Chromatogr.*, **1991**, *14*, 91-98.
5. Diesel Emission Control – Sulfur Effects (DECSE) Program. Phase I. August 1999. Interim Data Report No.1. World Wide Web Document. Available from <http://www.ctt.doe.gov/decse>.
6. Neill, W.S.; Li, X.; Chippior, W.L.; Gülder, Ö.L., **1999**. Canadian diesel fuel composition and emissions-II. Ottawa: Combustion Research Group, Institute for Chemical Process and Environmental Technology, National Research Council Canada.
7. Ceballo, C.D.; Dambrosio, F.; Torres, N., Estimation of Olefins to Aromatics Ratio (O/A) in Cracked Naphthas by Bromine Number Assay, *Pet. Sci. Technol.*, **1998**, *16(1&2)*, 179-189.
8. Kosal, N.; Bhairi, A.; Ali, M.A., Determination of Hydrocarbon Types in Naphthas, Gasolines and Kerosenes: a Review and Comparative Study of Different Analytical Procedures, *Fuel*, **1990**, *69*, 1012-1019.
9. Selucky, M.L.; Chu, Y.; Ruo, T.; Strausz, O.P., Chemical composition of Athabasca bitumen, *Fuel*, **1977**, *56*, 369-381.
10. Poirier, M.A.; George, A.E., Selective Separation and Identification of Olefins in Petroleum and Synthetic Fuel Naphtha, *Fuel*, **1982**, *61*, 182-184.
11. DeLaet, M.; Tilquin, B. *Talanta*, **1992**, *39*, 769.
12. Hardas, N.R.; Adam, R.; Uden, P.C., Alkene Determination by Bromination and Gas Chromatography with Element-selective Atomic Plasma Spectroscopic Detection, *J. Chromatogr. A*, **1999**, *844*, 249-258.

13. Lubeck, A.J.; Cook, R.D., Bromine number should replace FIA in gasoline olefins testing, *Oil Gas J.*, **1992**, 90(52), 86.
14. Sriča, V.; Mühl, J.; Jednačak, M.; Durić, A., Determination of Hydrocarbon Type Distribution of Coking Gasolines by N.M.R. Spectrometry, *Fuel*, **1992**, 72, 775-778.
15. Teeter, R.M. 1992. Software for calculation of hydrocarbon types. Walnut Creek, CA: PCMASPEC.
16. Robinson, C.J.; Cook, G.L., Low-resolution Mass Spectrometric Determination of Aromatic Fractions from Petroleum, *Anal. Chem.*, **1969**, 41(12), 1548-1554.
17. Briker, Y.; Ring, Z.; Iacchelli, A.; Rahimi, P.; Fairbridge, C.; Malhotra, R.; Coggiola, M.; Young, S., Diesel Fuel Analysis by GC-FIMS – Aromatics, n-Paraffins and Isoparaffins, *Energy Fuels*, **2001**, 15(1), 23-37.
18. Malhotra, R.; Coggiola, M.; Yound, S.; Spindt, C.; Hsu, C.S.; Dechert, G.; Rahimi, P.; Briker, Y., Rapid Detailed Analysis of Transportation Fuels by GC-FIMS, *Chemistry of Diesel Fuels*, Song, C.; Hsu, C.S.; Mochida, I. (Eds.), Taylor & Francis: New York, 2000; Chapter 3, pp. 77-92.
19. Briker, Y.; Ring, Z.; Iacchelli, A.; McLean, N.; Fairbridge, C.; Malhotra, R.; Coggiola, M.; Young, S., Diesel Fuel Analysis by GC-FIMS – n-Paraffins, Isoparaffins, and Cycloparaffins, *Energy Fuels*, **2001**, 15(4), 996-1002.
20. Mitchell, K., SAE Paper 2890. Jan. **2000**.
21. Naber, D.; Lange, W.W.; Reglitzky, A.A.; Schater, A.; Gairing, M.; Le'Jeune, A., SAE Paper 932685, **1993**.
22. McCarty, C.I.; Slodowske, W.J.; Sienicki, E.J.; Jass, R.E., *Fuel Reformulation*, **1994**, 3-4, 34.
23. *Diesel Fuel Technical Review*, Chevron Products Company: San Francisco, 1998.
24. *Literature review of Cetane number and its Correlations*. GEO-Centers, Inc.: Newton Upper Falls, MA. 1987.
25. Yui, S.M.; Sanford, E.C., *AOSTRA J. Res.*, **1991**, 7, 47.
26. Cookson, D.J.; Lloyd, C.P.; Smith, B.E., *Energy Fuels*, **1988**, 2, 854.
27. Ladommatos, N.; Goacher, J., *Fuel*, **1995**, 74(7), 1083.
28. Bhaga, P., *Chem. Eng. Progress*, **1990**, 8, 55.
29. Zupan, J.; Gasteiger, J., *Anal. Chim. Acta*, **1991**, 248, 1.
30. Eberhart, R.C.; Dobbins, R.W. (Eds), *Neural Network PC Tools: A Practical Guide*, Academic Press: New York, 1990.
31. Yang, H.; Ring, Z.; Briker, Y.; Mclean, N.; Friesen, W.; Fairbridge, C., *Fuel*, **2002**, 81, 65-74.

## Chapter 5

# CATALYTIC PROCESSES FOR LIGHT OLEFIN PRODUCTION

Wang Xieqing, Xie Chaogang, Li Zaiting, and Zhu Genquan  
*Research Institute of Petroleum Processing, SINOPEC*  
*Beijing, China*

### 1. INTRODUCTION

Consumption of petroleum in the transportation fuel sector is expected to show only a modest rate of growth in the near future. Fuel specifications are becoming increasingly stringent due to new environmental regulations, and energy sources such as biofuel and especially fuel cells for vehicles are becoming increasingly attractive as environmentally friendly alternatives. In the petrochemical sector however, consumption of hydrocarbon raw materials is expected to grow more rapidly. The building blocks for the petrochemical industry are mainly light olefins, principally ethylene and propylene, and aromatics including benzene, toluene and xylenes (BTX). Steam cracking has been the major source of light olefins and aromatics for more than half a century. The proportions of different steam cracking feedstocks used worldwide are shown in Figure 1. Naphtha is currently the dominant feedstock, accounting for 50~55% of the total. It is expected that ethane, associate gas and condensates will gradually replace naphtha as the major feedstock because the former are easier to obtain, at a lower price, in the most productive oilfields. In North America and the Middle East, ethane and associate gas already make up 25~40% of the feedstock for steam cracking. This threatens to induce an imbalance in the ethylene to propylene ratio in the overall output from steam cracking because typical ethane pyrolysis gives 79% selectivity to ethylene and less than 1% selectivity to propylene at 70% conversion, whereas steam cracking of naphtha gives approximately 30% ethylene and 15% propylene. It is predicted that by 2010, the annual demand for ethylene and propylene will be 120 Mt and 82 Mt respectively (a propylene to ethylene ratio of 0.68). The propylene stream from refineries



currently accounts for one third of the total supply, and it is clearly necessary to develop new ways of increasing propylene production. A variety of new processes for modifying the propylene to ethylene ratio are emerging, such as transformation or product shift by isomerization, hydroisomerization, metathesis, interconversion, skeletal isomerization and catalytic cracking.

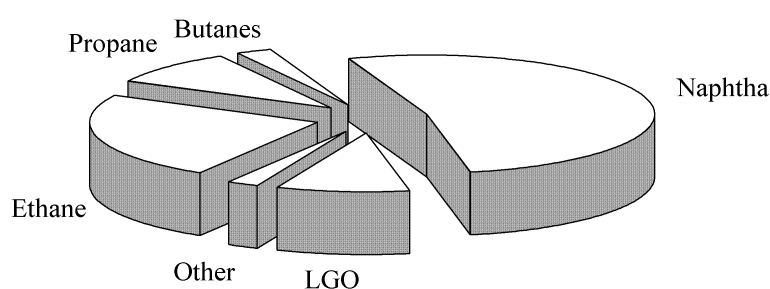


Figure 1. Proportions of different feedstocks used in steam cracking

Increasing integration of petroleum refining with petrochemicals is an inevitable tendency not only for economic and environmental reasons but also because of an increasing reliance on deep upgrading of crude oil. Statistics show that reserves of heavy crude are much larger than those of conventional crude and deep upgrading of heavy crude, for both refining and petrochemicals, is attracting more and more attention from scientists and engineers. Integration will also lead to a rational development of both refinery product slates and petrochemical building blocks.

In the manufacture of the key building blocks for petrochemicals, i.e. ethylene, propylene and other olefins as monomers for polymerization, and BTX as the basic raw material for various synthetic pathways, thermal steam crackers currently still predominate. Catalytic processes such as FCC, alkylation, isomerization, catalytic reforming and hydroprocessing play a decisive role in the production of clean fuels and lubricants in refineries. The integration of refining with petrochemicals leads to optimization of all the processes involved, and development of processes with an adjustable ratio of ethylene to propylene production is now becoming possible. It can be expected that catalytic processes will play an increasingly significant role in the production of light olefins, especially when heavy or low-grade oil is used as the feedstock. This Chapter introduces the latest progress towards the aim of increasing propylene production in FCC and related processes for light olefins.

## 2. FUNDAMENTALS OF THE CRACKING MECHANISM FOR LIGHT OLEFIN PRODUCTION

There are two routes for production of light olefins by catalytic cracking, which differ according to whether heavy or light hydrocarbons are employed as feedstock. When heavy hydrocarbons are used, they undergo primary cracking to form light naphtha olefins followed by secondary cracking to produce light olefins. Light hydrocarbon feedstocks are by-products from refining and petrochemical plants, i.e. C<sub>4</sub> and C<sub>5</sub> fractions of relatively low added value, which are suitable for further cracking to ethylene and propylene. The reaction pathways involved for the two types of feedstock differ to some extent.

The complex composition of heavy feedstocks means that a large number of reactions can take place, both in parallel and consecutively, on the catalyst. The relative rates of the various reactions, taken together with the relative ease of formation of various carbocations from the parent molecules, lead to a bewildering array of possible reaction pathways. The matter is complicated by the presence of a variety of active sites on the heterogeneous catalysts. These sites not only differ in their acid strength but also in their nature. A variety of reactions of carbocations can take place on these acid sites, including cracking, isomerization, hydrogen transfer, alkyl transfer and C-C bond formation as well as coke formation. Cracking reactions of large molecules tend to predominate however.

In the FCC process using heavy feedstocks, light olefins are probably produced by secondary cracking of primary olefins in the FCC naphtha fraction. The reaction proceeds readily over ZSM-5 zeolite-containing catalysts. It is widely accepted that olefin cracking over catalysts with Brønsted acidity involves initial protonation of the double bond to form a tricoordinate carbenium ion, with subsequently scission of a carbon-carbon bond in the beta position, to form a free olefin and a smaller carbenium ion.

Anderson et al.<sup>1</sup> recently attempted to predict the optimum zeolite-based catalyst for selective cracking of naphtha range hydrocarbons by the pathway proposed by Haag and Dessau in 1984. According to this mechanism, light olefins are produced from alkanes via “protolytic cracking”, in which alkanes are protonated to form carbonium ion transition states that can undergo either C-C bond cleavage yielding alkanes (including methane and ethane) or C-H bond cleavage yielding dihydrogen and carbenium ions. These carbenium ions subsequently form alkenes via back-donation of a proton to the zeolite. Formation of ethylene is probably via this pathway.

Weitkamp et al.<sup>2</sup> introduced a classification of carbenium ion beta scission processes. The process where the carbenium ions before and after scission are both tertiary, is denoted as Type A. Type B1 scission refers to reaction of a secondary ion to give a tertiary ion, while type B2 involves a change from a tertiary to a secondary ion. Type C involves conversion of a secondary ion to

another secondary ion, and type D involves transformation of a secondary ion to a primary ion. Buchanan<sup>3</sup> added an additional category of primary to tertiary ion transformation, designated as type E. Although the beta scission of primary carbenium ions can produce ethylene, formation of other types of carbenium ion, which mostly produce propylene by terminating the reaction pathway, is more likely.

Cracking of the second category of feedstock - light hydrocarbons such as C<sub>4</sub> olefins - is likely to involve a bimolecular process and probably proceeds via initial oligomerization to form C<sub>8</sub> species, which then undergo further cracking to form light olefins. Our study of C<sub>4</sub> saturates and that of Wakui et al.<sup>4</sup> both showed that butanes are difficult to crack directly. They must first be dehydrogenated to form butenes, which are then consecutively cracked following the usual olefin reaction pathways.

It should be noted that in addition to Brønsted acid sites, Lewis acid sites also play a very important role in olefin production, although in fact these two types of acid sites can be interconverted at high temperatures. In general, heating the zeolite catalyst to a high temperature results in a loss of Brønsted acidity with a corresponding increase in Lewis acidity. This alters the activity and selectivity of the zeolite in favor of a high light olefin yield. We have found it is of great importance to maintain an optimum L/B ratio in order to maximize ethylene yield under severe operating conditions.

Table 1 shows that when ZSM-5 zeolite is modified by treatment with silver (samples AGZ-1 and AGZ-2) the number of Brønsted and Lewis acid sites both increase, but the increase in the number of Lewis sites is much more marked. By using these zeolites as catalysts for cracking of heavy oil at 650 °C, substantially higher yields of ethylene and propylene can be obtained compared with the reaction over quartz as a representative inert solid. Furthermore, increasing the number of acid sites, especially Lewis sites, leads to an enhanced ethylene yield. Our experimental data are summarized in Table 2.

Table 1. Acid sites in modified ZSM-5 zeolites (Aging conditions: 800 °C for 4 hrs under 100% steam)

| Sample | Acid amount, mmol.g <sup>-1</sup> |        | L/B  | L+B    |
|--------|-----------------------------------|--------|------|--------|
|        | B-acid                            | L-acid |      |        |
| ZSM-5  | 20.34                             | 5.95   | 0.29 | 26.29  |
| AGZ-1  | 32.20                             | 48.81  | 1.51 | 81.01  |
| AGZ-2  | 44.07                             | 64.09  | 1.45 | 108.16 |

Corma et al.<sup>5</sup> postulated that in highly dealuminated zeolites the cracking reactions take place on extra-framework aluminum sites following a radical-type pathway, which will give more C<sub>1</sub> and C<sub>2</sub> hydrocarbons, mostly ethylene. The mechanism for the cracking reactions we observe at 650 °C (results shown in Table 2) may involve either carbenium ion or radical ion intermediates but this still has to be determined.

Table 2. Ethylene and propylene yields (in wt%) from heavy oil cracked over different catalytic materials

| Zeolite        | H <sub>2</sub> | Methane | Ethylene | Propylene | C <sub>2</sub> <sup>=</sup> /C <sub>3</sub> <sup>=</sup> | C <sub>2</sub> <sup>=</sup> +C <sub>3</sub> <sup>=</sup> |
|----------------|----------------|---------|----------|-----------|--|--|
| Quartz (inert) | 0.08           | 2.12    | 4.74     | 4.01      | 1.18   | 8.75   |
| ZSM-5          | 0.09           | 2.17    | 5.08     | 8.70      | 0.58   | 13.78  |
| AGZ-1          | 0.27           | 2.61    | 8.23     | 11.78     | 0.70   | 20.01  |
| AGZ-2          | 0.27           | 2.80    | 8.99     | 12.77     | 0.70   | 21.76  |

### 3. CATALYSTS

In the FCC process, it is generally accepted that after vaporization the large molecules of heavy hydrocarbons undergo cracking on both the surface of the Y-zeolite and on the surrounding silica-alumina matrix as a primary reaction. The smaller molecules thus formed permeate into the pores of the Y-zeolite and reach the active sites of the catalyst where the desired catalytic cracking reactions take place. Great efforts have been made to redesign the catalyst formulation as well as improve the process of catalyst manufacture in order to optimize the yield of light olefins.

As far as improvement of catalyst formulation is concerned, there are two approaches to the goal of enhanced light olefin yields in the FCC process: incorporation of ZSM-5 containing additives into conventional FCC host catalysts or reformulation of the catalysts especially for olefin production.

Both of these methods have their advantages and disadvantages. Mixing the conventional FCC catalyst with ZSM-5 containing additives gives the advantage of flexibility in FCCU operation according to changes in the market demand for gasoline or olefins. The disadvantage is the difficulty in providing the pore size distribution gradient in the mixed zeolite catalyst which gives the desired ratio of light olefins as products of primary and secondary cracking. Furthermore, according to the accepted reaction mechanism, the intermediates from primary cracking should first be desorbed from the acid sites of the main catalyst and then enter the pores of the ZSM-5 containing additive. In the course of this migration, the intermediate species can undergo some undesired reactions. As a result, the yield of light olefins may be adversely affected. From the viewpoint of the physical properties of a mixed catalyst in an FCCU, the two kinds of solids should be closely matched in density and attrition index in order to keep their relative proportions constant over time. This necessitates a careful choice by the user of both host catalysts and additives.

A specially formulated catalyst for maximizing the yield of light olefins can be tailored in the light of the feed properties and target products by optimizing the composition of a mixture of different natural zeolites. The pore size distribution of the matrix should be such as to allow access to the large molecules of the feedstock, whilst incorporation of large pore Y zeolite favors intermediate molecule formation and mesoporous ZSM-5 favors production

of light olefins. The gradient in pore size distribution allows ready access to a series of reactants of different molecular sizes. Furthermore, the acidity of natural catalytic materials, as well as their strength and density can be adjusted to give predominantly light olefins.

Modification of ZSM-5 is crucial if olefins are to be produced under much more severe operating conditions than those employed for conventional FCC. In the Research Institute of Petroleum Processing (RIPP) of SINOPEC, there has been a long-term program aimed at enhancing the hydrothermal stability and selectivity of ZSM-5.

It is well known that incorporation of rare earth cations can greatly improve the hydrothermal stability of Y zeolite. Shu et al.<sup>6</sup> have reported the incorporation of rare earth ions into the ZSM-5 structure by a seeding method in which an REY zeolite is dispersed in a gel containing Si-, Al-, Na- sources and water and the mixture converted into an MFI type zeolite. The resulting ZSM-5 zeolite containing rare earth ions was further modified under hydrothermal conditions and the final catalyst, denoted ZRP-1, has outstanding hydrothermal stability as shown in Table 3.

Table 3. Activity retention of ZRP-1 based catalyst in n-C<sub>14</sub> cracking<sup>7</sup>

| Conditions                         | Conversion, wt% |
|------------------------------------|-----------------|
| 780 °C, 100% H <sub>2</sub> O, 4 h | 77.1            |
| 800 °C, 100% H <sub>2</sub> O, 4 h | 74.2            |
| 820 °C, 100% H <sub>2</sub> O, 4 h | 74.0            |

It was found that introduction of phosphorus into the ZRP series of zeolites further stabilized the crystal structure and was successful in reducing dealumination at high reaction temperatures allowing a large fraction of the acidity, and hence activity, to be maintained. Based on this experience, a modified MFI type catalyst CEP-1<sup>6</sup> was developed by RIPP especially for the Catalytic Pyrolysis Process (CPP) with the aim of giving high activity and selectivity for light olefins under severe operating conditions. The hydrothermal stability of the catalyst is shown in Table 4.

Table 4. Hydrothermal stability of the CEP-1 catalyst\*

| Aging time, h  | 4  | 8  | 12 | 16 | 20 | 24 | 28 |
|----------------|----|----|----|----|----|----|----|
| Activity Index | 65 | 62 | 55 | 55 | 54 | 54 | 52 |

\*At 820 °C, 100% steam

The stability of carbenium ions decreases in the order tertiary>secondary>primary, meaning that the yield of ethylene is generally much less than that of propylene. Zhang et al.<sup>8</sup> found that by adjusting the acid type, acid strength and acid distribution, the ratio of ethylene to propylene can be altered in favor of ethylene. A modified MFI type zeolite PMZ was formed by treatment of ZRP-1 with alkaline earth metal ions. When PMZ is used as the catalyst for middle distillate cracking at 520 °C, the ratio

of ethylene to propylene is increased compared with that obtained over the ZRP-1 precursor, as indicated in Table 5.

Table 5. Comparison of ethylene yields obtained with modified MFI type zeolites

| MFI Zeolite | Conversion, % | Ethylene, wt% | Ethylene/Propylene |
|-------------|---------------|---------------|--------------------|
| ZSM-5       | 44.06         | 0.82          | 0.13               |
| ZRP-1       | 63.06         | 2.63          | 0.31               |
| PMZ         | 63.01         | 3.30          | 0.49               |

It should be noted that in addition to the catalytic carbenium ion pathways for light olefin production, thermal reactions involving free radicals are also a significant source of ethylene and indeed predominate at higher temperatures. Table 6 gives a comparison of the impact of such thermal reactions on the yields of ethylene and propylene at different temperatures.

Table 6. MAT results with PMZ as catalytically active material and quartz as inert carrier

| Reaction temp., °C  | 650    |       | 680    |       |
|---|--------|-------|--------|-------|
|   | Quartz | PMZ   | Quartz | PMZ   |
| Product yields, wt%   |        |       |        |       |
| Cracked gas   | 17.05  | 37.94 | 30.68  | 45.08 |
| in which, Ethylene  | 5.19   | 8.48  | 9.31   | 11.20 |
| Propylene   | 4.39   | 15.95 | 8.07   | 17.95 |
| Butylenes   | 2.35   | 6.80  | 4.59   | 7.56  |
| C <sub>5</sub> +Naphtha   | 23.21  | 18.22 | 25.10  | 18.33 |
| LCO   | 49.02  | 37.40 | 34.92  | 26.31 |
| HCO   | 7.66   | 5.20  | 5.33   | 3.41  |
| Coke  | 0.12   | 0.98  | 0.49   | 1.80  |
| Loss  | 2.94   | 0.26  | 3.48   | 4.35  |
| Conversion, wt%   | 43.32  | 57.40 | 59.75  | 70.28 |
| C <sub>2</sub> <sup>=</sup> +C <sub>3</sub> <sup>=</sup> +C <sub>4</sub> <sup>=</sup> , wt% | 11.93  | 31.23 | 21.79  | 36.71 |
| Olefin selectivity, wt/wt   |        |       |        |       |
| C <sub>2</sub> <sup>=</sup>   | 0.12   | 0.15  | 0.16   | 0.16  |
| C <sub>3</sub> <sup>=</sup>   | 0.10   | 0.28  | 0.14   | 0.25  |
| C <sub>4</sub> <sup>=</sup>   | 0.05   | 0.12  | 0.08   | 0.11  |

#### 4. NEW TECHNOLOGY

In the last few decades, great efforts have been made to produce light olefins by catalytic processes in order to achieve a rational utilization of heavy feedstocks or petrochemical by-products. Some papers in this area presented at the 17<sup>th</sup> WPC attracted considerable attention from both academic and industrial researchers. A variety of very promising processes have been developed, and some have already been commercialized. All of the new catalytic processes aim to tackle the problem of low propylene to ethylene ratio caused by the recent feedstock change for steam crackers.

#### 4.1 Deep Catalytic Cracking (DCC) <sup>7</sup>

Deep Catalytic Cracking (DCC) is a new fluidized catalytic cracking process using a proprietary catalyst for selective cracking of a wide variety of heavy feedstocks to give light olefins. The process, developed by RIPP of SINOPEC, has been commercially proven with seven units built since 1990, six in China and one in Thailand. The DCC-I process is similar to that of conventional FCC with a modified reactor consisting of a riser plus fluidized dense bed. The dense bed at the end of the riser results in a longer residence time at a high catalyst/oil ratios favoring secondary cracking of primary intermediates, which is thought to enhance propylene production at the cost of gasoline yield. In the DCC-II system, the dense bed is removed in order to allow flexibility in propylene and gasoline yield according to market demand. Table 7 shows a comparison of the key features of DCC with those of conventional FCC.

Table 7. Comparison between DCC and FCC processes

| Process              | FCC                        | DCC   |
|----------------------|----------------------------|---|
| Feedstock            | A wide range of heavy oils | A wide range of heavy oils preferably paraffinics |
| Catalyst             | Various types of Y zeolite | A modified pentasil structure zeolite             |
| Hardware             |                            |   |
| Reactor              | Riser                      | Riser and bed                                     |
| Regenerator          | Base                       | Similar   |
| Main fractionator    | Base                       | Higher vapor/liquid ratio                         |
| Stabilizer/absorber  | Base                       | Bigger  |
| Compressor           | Base                       | Larger capacity                                   |
| Operating conditions |                            |   |
| Reaction temp.       | Base                       | +30~50°C  |
| Regeneration temp.   | Base                       | Similar   |
| Catalyst/oil ratio   | Base                       | 1.5~2 times                                       |
| Residence time       | Base                       | More  |
| Oil partial pressure | Base                       | Lower   |
| Dilution steam       | Base                       | More  |

The experience accumulated over eight years in four refineries and one petrochemical complex has shown that light olefin yields are greatly dependent on the feedstock properties as detailed in Table 8. Daqing paraffinic feedstock gives the highest propylene and isobutylene yields, with 23.0 wt% and 6.9 wt% respectively. For intermediate base feeds, propylene yield is more than 18 wt% for DCC-I and 14.4 wt% for DCC-II operation with an FCC naphtha yield near 40 wt%.

Table 8. DCC light olefin yields

| Refinery           | Daqing                | Anqing                   | TPI                      | Jinan                        | Jinan  |
|--------------------|-----------------------|--------------------------|--------------------------|------------------------------|--------|
| Operation mode     | DCC-I                 | DCC-I                    | DCC-I                    | DCC-I                        | DCC-II |
| Feedstock          | Paraffinic<br>VGO+ATB | Intermediate<br>base VGO | Arabian HVGO+<br>DAO+WAX | Intermediate base<br>VGO+DAO |        |
| Reaction temp., °C | 545                   | 550                      | 565                      | 564                          | 530    |
| Olefin yields, wt% |                       |                          |                          |                              |        |
| Ethylene           | 3.7                   | 3.5                      | 5.3                      | 5.3                          | 1.8    |
| Propylene          | 23.0                  | 18.6                     | 18.5                     | 19.2                         | 14.4   |
| Butylenes          | 17.3                  | 13.8                     | 13.3                     | 13.2                         | 11.4   |
| In which           |                       |                          |                          |                              |        |
| Isobutylene        | 6.9                   | 5.7                      | 5.9                      | 5.2                          | 4.8    |

The DCC gasoline fraction is rich in BTX especially xylenes. Table 9 lists the BTX content in the DCC gasoline fraction and DCC 75°C~150 °C light gasoline range. Recovery of BTX from the narrow cut for petrochemical applications is economically viable.

Table 9. BTX content in DCC gasoline fraction

|                   | DCC naphtha | 75~150°C cut |
|-------------------|-------------|--------------|
| BTX content, vol% | 25.90       | 57.56        |
| In which          |             |              |
| Benzene           | 2.41        | 5.36         |
| Toluene           | 9.84        | 21.87        |
| Xylenes           | 13.65       | 30.33        |

It has been clearly demonstrated that increasing propylene production, even at the expense of gasoline yield, is a commercial proposition in an integrated refining-petrochemical complex.

## 4.2 Catalytic Pyrolysis Process (CPP) <sup>9</sup>

The Catalytic Pyrolysis Process (CPP), also developed by RIPP of SINOPEC, is an extension of DCC which gives an increased ethylene yield while keeping propylene production at a reasonable rate. The key features of this process are as follows:

- A new catalytic material has been developed which reduces the activation energy required, thus allowing the reaction to be carried out at a significantly lower temperature compared with that required for steam cracking, and also favors the production of light olefins.
- The catalyst possesses excellent hydrothermal stability and attrition resistance.
- The operating conditions for CPP are more severe than for Resid FCC (RFCC) to an extent that it is allowed to be operated in existing idle RFCC units without the risk of damage to the fabric of the plant.
- The heat required for the cracking reaction can be provided by burning



coke and HCO in the regenerator, making the reaction fully self-supporting.

- A specially designed stripper located between the regenerator and reactor removes the flue gas carried over from the regenerator.
- Since the reaction temperature is higher than for conventional RFCC, a post-riser quench has been introduced for heat recovery as well as termination of secondary reactions in order to prevent further thermal degradation of the target products.

Commercial trial runs were successfully completed in early 2001 at the PetroChina Daqing Refining & Chemical Co. using a revamped DCC unit with a capacity of 80,000 t/a. Three sets of conditions were employed: Mode 1 – for maximum propylene yield; Mode 3 – for maximum ethylene yield; Mode 2 - intermediate between the two. Feedstock properties, major operating parameters and product distribution can be seen in Tables 10, 11 and 12. Across the three modes, the combined yield of ethylene and propylene ranges between 34 and 38 wt% and the total yield of C<sub>2</sub> ~ C<sub>4</sub> olefins is around 45 wt% in each case. The ethylene to propylene ratio can be adjusted by variation of the operating conditions.

*Table 10. Feedstock properties*

| Operating mode                     | Mode 1 | Mode 2 | Mode 3 |
|------------------------------------|--------|--------|--------|
| Density (20 °C), g/cm <sup>3</sup> | 0.9002 | 0.9015 | 0.9012 |
| CCR, wt%                           | 4.7    | 4.9    | 4.7    |
| Hydrogen, wt%                      | 12.82  | 12.86  | 12.84  |
| Sulfur, wt%                        | 0.16   | 0.16   | 0.16   |
| Nitrogen, wt%                      | 0.29   | 0.26   | 0.25   |
| Nickel, ppm                        | 5.8    | 6.2    | 6.3    |
| Composition, wt%                   |        |        |        |
| Saturates                          | 56.3   | 54.8   | 55.5   |
| Aromatics                          | 27.2   | 28.4   | 28.0   |
| Resin                              | 15.7   | 16.0   | 15.7   |
| Asphaltene                         | 0.8    | 0.8    | 0.8    |

*Table 11. Main operating parameters*

| Operating mode          | Mode 1 | Mode 2 | Mode 3     |
|-------------------------|--------|--------|------------|
| Feed rate, t/h          | 9.73   | 8.00   | 5.90       |
| Reaction temp., °C      | 576    | 610    | 640        |
| Reaction press., MPa(g) | 0.08   | 0.08   | 0.08       |
| Regeneration temp., °C  | 720    | 725    | 760        |
| WHSV, h <sup>-1</sup>   | 2.5    | 4.0    | Zero level |
| Catalyst/oil ratio      | 14.5   | 16.9   | 21.1       |
| Steam/oil ratio         | 0.30   | 0.37   | 0.51       |

Table 12. Product distribution and olefin yields

| Operating mode                     | Mode 1 | Mode 2 | Mode 3 |
|------------------------------------|--------|--------|--------|
| Product yield, wt%                 |        |        |        |
| C <sub>2</sub> mines               | 17.64  | 26.29  | 37.13  |
| C <sub>3</sub> plus C <sub>4</sub> | 43.72  | 36.55  | 28.46  |
| C <sub>5</sub> +naphtha            | 17.84  | 17.61  | 14.82  |
| LCO                                | 11.75  | 8.98   | 7.93   |
| Coke                               | 8.41   | 9.67   | 10.66  |
| Loss                               | 0.64   | 0.90   | 1.00   |
| Olefin yield, wt%                  |        |        |        |
| Ethylene                           | 9.77   | 13.71  | 20.37  |
| Propylene                          | 24.60  | 21.45  | 18.23  |
| Butylenes                          | 13.19  | 11.34  | 7.52   |

We suggest that in order to optimize use of crude oil as a petrochemical feedstock, a combination of steam cracking and CPP may be the best choice, as depicted in the flow scheme in Figure 2.

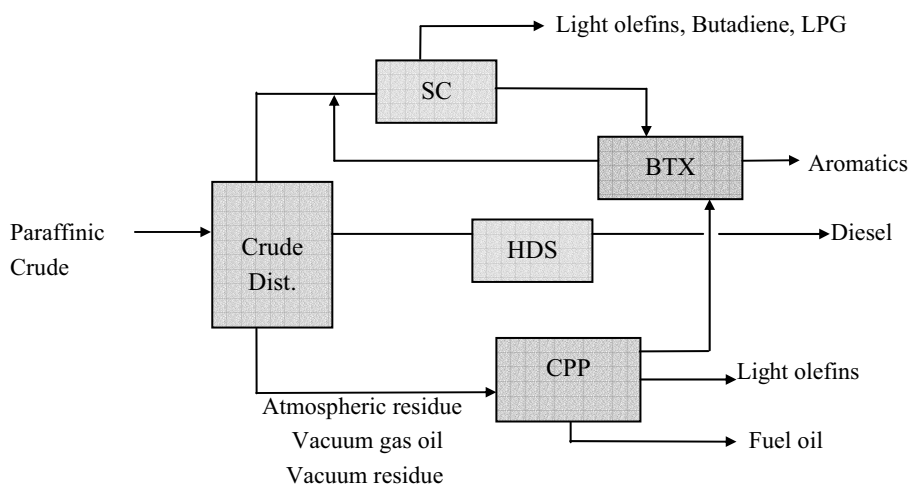


Figure 2. The scheme of crude to petrochemicals

Key economic data for a CPP plant with integrated steam cracker are shown in Table 13. Based on 500 KTA of ethylene produced by CPP and 1000 KTA of ethylene produced by steam cracking, the estimated net product revenue is 450 \$MM/A.

Table 13. Key economic data for a CPP integrated olefins plant \*

|   | CPP/SC<br>\$MM | SC  | $\Delta$ |
|---|----------------|-----|----------|
| TIC   |                |     |          |
| CPP (50MBPD, 500 KTA C <sub>2</sub> H <sub>4</sub> )                    | 150            |     |          |
| SC, Recovery (1000 KTA C <sub>2</sub> H <sub>4</sub> )<br>(SC P/E 0.45) | 600            | 650 |          |
|   | 750            | 650 | 100      |
| Operating Cost (including Catalyst)                                     | \$MM/A         |     |          |
|   | 30             | 20  | 10       |
| Net Product Revenue   | \$MM/A         |     |          |
|   | 450            | 320 | 130      |

$\Delta$ TIC/Revenue < 1 Year Pay Out

\*By courtesy of Mr. Colin P. Bowen of Stone & Webster, A Shaw Group Company

### 4.3 PetroFCC<sup>10,11</sup>

The PetroFCC process is licensed by UOP LLC and features RxCAT technology. The process gives high yields of propylene, light olefins and aromatics for petrochemical applications, from feedstocks which can include conventional FCC feeds and higher boiling or residual feeds. The feed comes into contact with the blended catalyst in the riser under very severe processing conditions. The blended catalyst consists of the regenerated catalyst and coked catalyst.

The PetroFCC process employs several measures to improve the yield and selectivity of propylene and lower the yield of dry gas:

- The PetroFCC catalyst has two components. The first component comprises a large pore zeolite, such as a Y-type zeolite. The second component involves medium or small pore zeolites such as ZSM-5 or ST-5, which have high coking resistance.
- The riser inlet temperature is reduced to about 620 °C by cooling the regenerated catalyst with the recycled coked catalyst. The ratio of catalyst to feed can be increased to an extent without any adverse influence on the heat balance in the unit.
- The residence time for the feed in contact with the catalyst in the riser is less than or equal to 2 seconds. The short residence time ensures that the target products are not further converted to undesired products. The diameter and height of the riser should be varied to give the desired residence time.

The expected yield patterns for a typical VGO feedstock in a traditional FCC unit and a PetroFCC unit are compared in Table 14.

Table 14. Yield patterns of traditional FCC and PetroFCC units

| Component, wt%   | Traditional FCC | PetroFCC |
|--|-----------------|----------|
| H <sub>2</sub> S, H <sub>2</sub> , C <sub>1</sub> & C <sub>2</sub> | 2.0             | 3.0      |
| Ethylene   | 1.0             | 6.0      |
| Propane  | 1.8             | 2.0      |
| Propylene  | 4.7             | 22.0     |
| Butanes  | 4.5             | 5.0      |
| Butenes  | 6.5             | 14.0     |
| Naphtha  | 53.5            | 28.0     |
| Distillate   | 14.0            | 9.5      |
| Fuel oil   | 7.0             | 5.0      |
| Coke   | 5.0             | 5.5      |

#### 4.4 Propylur<sup>12,13</sup>

The Propylur process converts low value light hydrocarbons enriched in olefins into petrochemicals such as propylene and is based on a shape-selective heterogeneous zeolitic catalyst of the ZSM-5 type.

The feedstock for the Propylur process can be C<sub>4</sub> cuts, Raffinate I, Raffinate II or gasoline fraction. Naturally, a feedstock with high olefin content is more favorable. Compounds such as paraffins, cycloalkanes, and aromatics are rarely converted when they pass through the reactor. The diolefin content should be limited to approximately 1.5 % in order to reduce the formation of gum and coke during the reaction.

The Propylur reactor is an adiabatic fixed bed type, similar to that employed in a Claus unit. The operating temperature is approximately 500 °C and pressure is slightly above atmospheric. The hydrocarbon partial pressure is reduced by diluting the feedstock with steam, in order to shift the equilibrium towards the desired product (propylene). This also minimizes coking and gum formation. The reaction is endothermic and requires additional heat.

By cooling the reactor effluent, the steam is condensed and then separated together with some gasoline by-products. The remaining vapor is compressed in order to allow C<sub>3</sub>/C<sub>4</sub> separation at reasonable temperatures. Most of C<sub>4</sub>+ fraction is recycled to the reactor to increase the ultimate propylene yield. Further separation of the C<sub>3</sub> fraction can be done in the ethylene plant. The single-pass propylene yield is 40% to 45%, and the ethylene yield is 10%. The ultimate yield of propylene is 60% and that of ethylene is 15%, with the butenes recycled.

The catalyst lifetime is predicted to exceed 15 months based on the laboratory pilot-plant experience. The catalyst can be regenerated off-stream in situ by burning the coke deposited on it by controlled combustion with a nitrogen cycle and small air makeup.

When integrated with an ethylene plant, the Propylur plant can give increased propylene to ethylene ratios in a steam cracker. The typical yields of

different products from the Propylur process are shown in Table 15.

Table 15. Typical yields from the Propylur process

|           | Typical yields, wt% |                         |
|-----------|---------------------|-------------------------|
|           | Single pass         | C <sub>4</sub> -recycle |
| Propylene | 40-45               | 60                      |
| Ethylene  | 10                  | 15                      |
| Butylenes | 30                  |                         |

#### 4.5 SUPERFLEX<sup>14,15</sup>

The SUPERFLEX process is a proprietary technology patented by ARCO Chemical Technology, Inc. (now Lyondell Chemical Co.), and is exclusively offered for license by Kellogg Brown & Root. It uses an FCC system with a proprietary catalyst to convert low-value feedstock with high olefin content to petrochemical products such as propylene and ethylene.

The feedstock can be olefin-rich light hydrocarbons in the carbon range C<sub>4</sub> to C<sub>8</sub>, and the ideal feedstocks are C<sub>4</sub> and C<sub>5</sub> streams generated in the steam cracker. Diolefins and acetylenes in the feedstock can be partially hydrogenated to olefins, or the diolefins extracted for other petrochemical applications. Other possible feedstocks are MTBE Raffinate-2, aromatics plant raffinate and refinery streams that are rich in olefins, such as light naphthas from an FCCU, coker or visbreaker. Refinery streams do not require pretreatment or hydrogenation of dienes - there is no limit on feed aromatic or diene content.

The SUPERFLEX FCC system is similar to that of a conventional FCC unit and consists of riser reactor, regenerator vessel and units for air compression, catalyst handling, flue gas handling and feed and effluent heat recovery. The SUPERFLEX system should be integrated into an ethylene plant in order to minimize capital investment, with the feedstock obtained directly from the steam cracker and shared common product recovery. The cooled reactor effluent can be processed in a nearby existing ethylene plant recovery unit. Alternatively, the effluent can be processed in a partial recovery unit to recover recycle streams and olefin-rich streams concentrated for further processing in a nearby ethylene plant.

The conditions involve low hydrocarbon partial pressures, high temperatures and low per pass conversions in order to favor propylene production. The catalyst is very robust, and there is no need to pretreat for typical feed contaminants such as sulfur, water, oxygenate or nitrogen in feeds. The typical ultimate light olefin yields after the recycle operation are listed in Table 16.

Table 16. Ultimate yields from the SUPERFLEX process

| Yields, wt% | C <sub>4</sub> Raffinate | Partially Hydrog. C <sub>5</sub> S | FCC Lt. Naphtha |
|-------------|--------------------------|------------------------------------|-----------------|
| Fuel gas    | 7.2                      | 12.0                               | 13.6            |
| Ethylene    | 22.5                     | 22.1                               | 20.0            |
| Propylene   | 48.2                     | 43.8                               | 40.1            |
| Propane     | 5.3                      | 6.5                                | 6.6             |
| Gasoline    | 16.8                     | 15.6                               | 19.7            |

#### 4.6 Mobil Olefin Interconversion (MOI) <sup>16</sup>

MOI was developed by the Mobil Oil Corporation and converts light hydrocarbons containing C<sub>4</sub>-C<sub>7</sub> olefins to more valuable light olefins by contacting the feed with a catalyst containing ZSM-5 and/or ZSM-11.

The feedstocks will typically be low value refinery or petrochemical streams, such as steam cracker by-products rich in C<sub>4</sub>'s, which have poor propylene selectivity when recycled to the steam cracker. The feedstock can include raffinates, catalytic cracked naphtha, coker naphtha, steam cracker pyrolysis gasoline, as well as synthetic chemical streams containing sufficient amounts of C<sub>4</sub>-C<sub>7</sub> olefins. Dienes, sulfur, nitrogen and oxygenates in the feeds are preferably selectively hydrotreated prior to the conversion process. However, feeds with low levels of dienes, sulfur, nitrogen, metal compounds and oxygenates can be processed directly from FCC units, cokers or steam crackers without any pretreatment.

The process uses a dense fluidized bed and the hydrocarbon feed containing the C<sub>4</sub>-C<sub>7</sub> olefins is continuously passed through the bed under conversion conditions in the presence of the catalyst. The catalyst is continuously circulated between the fluidized bed and a regenerator. The fluidizable catalyst can transfer heat from the latter to the former thereby helping to supply some of the thermal needs of the conversion reaction, which is endothermic. The operation of the process is similar to that of conventional FCC.

The dense fluidized bed conversion conditions include temperature in the range 540 °C to 650 °C and pressure from 0.10 to 0.45 MPa, catalyst/oil weight ratio of 0.1 to 10, and a weight hourly space velocity (WHSV) of 1 to 10 h<sup>-1</sup>. Because the catalyst used in the process has lower cracking activity relative to conventional FCC catalysts, a higher temperature compared with that for conventional FCC may be used in order to achieve a higher conversion to the desired light olefins.

The catalyst in MOI contains only ZSM-5 and/or ZSM-11 without any large pore zeolites. The ZSM-5 and/or ZSM-11 preferably have a high initial silica/alumina molar ratio and are modified by phosphorus and metals such as gallium.

The products from MOI include light olefins such as propylene and ethylene. A higher yield of propylene is produced than is usually obtained in conventional catalytic cracking processes utilizing a ZSM-5 additive. The

propylene/ethylene weight ratio is related to the conversion and feed but almost always exceeds 3.0. The combined yield of ethylene plus propylene is about 20 to 30 wt%. Propylene purities of 85 wt% or greater can be achieved. In addition, only relatively small amounts of aromatics such as benzene, toluene and xylenes (BTX) are produced.

#### 4.7 Propylene Catalytic Cracking (PCC)<sup>17</sup>

The ExxonMobil PCC<sup>SM</sup> Process is a new fluid solids naphtha cracking process to convert naphtha olefins to light olefins such as propylene, which employs an optimum catalyst, reactor design, and patented combination of optimum operating conditions to achieve a high degree of reaction selectivity.

The feed can be obtained from cat naphtha, coker naphtha, and steam cracker's C4's and pyrolysis gasoline. The largest source of olefinic feedstock molecules is cat naphtha, which contain 20-60% olefins. Most of linear cat naphtha olefins are converted to light olefins, and at the same time, an increased octane and reduced olefin content naphtha is produced by the concentration of higher octane aromatics, plus isomerization and some additional aromatics formation.

A fluid solids reactor/regenerator configuration is designed for large capacity units. Feed naphtha is preheated and is injected into the reactor of a fluid solids reactor/regenerator system. The hot, regenerated catalyst contacting the preheated feed supplies the necessary sensible heat to complete preheating the feed to reaction temperature, and supplies the heat of reaction. These fluid solids systems can use ZSM-5 containing fluid solids catalysts. In this way, coke make on the catalyst when cracking naphtha is low. Therefore, it requires a means to provide supplemental fuel to burn in the regenerator to supply the necessary sensible heat and heat of reaction. The regeneration of catalyst provides the flexibility to process a variety of feeds, which can contain diolefins, aromatics, or heavy ends to a certain degree.

Reactor effluent is cooled and vapors are compressed for product recovery. Once-through yields of ethylene and propylene typically are in the range of 10-20 wt.% and 30-40 wt.% on feed olefin content, respectively. The propylene's concentration is ranging from 85% to 90% and can be further purified to supply as polypropylene feed. Ethylene can also be recovered in order to achieve maximum economic benefit. Butylenes can be recovered as product, or can be recycled (optionally with unconverted C<sub>5</sub>+) for additional propylene production.

#### 4.8 Olefins Conversion Technology (OCT)<sup>18,19,20</sup>

OCT was originally developed by Phillips Petroleum and was first commercialized in 1965 when it was used to produce ethylene and butenes from propylene, due to the over-supply of the latter at that time. With the

increasing demand for propylene, the OCT process is currently being licensed by ABB Lummus for production of propylene from ethylene and butene-2 by metathesis.

OCT converts normal butene-2 and ethylene to polymer grade propylene via metathesis (Figure 3). The metathesis is essentially equilibrated, with the equilibrium position depending on the temperature and the ratio of reactants. In addition to the main reaction, numerous side reactions between olefins also occur which lower the yield of propylene and cause deactivation of the catalyst.



Figure 3. Metathesis of ethylene and butene-2

The ethylene feed can be polymer grade or lower purity as long as the impurities are below a certain limit. Any saturated hydrocarbons, such as ethane and methane, do not react. A variety of C<sub>4</sub> streams, including mixed C<sub>4</sub>'s produced by FCC or steam cracking, or C<sub>4</sub> Raffinate from butadiene extraction or MTBE production, can be used in the process. In order to achieve the full potential propylene production. However, the raw C<sub>4</sub> cut requires pretreatment to maximize its butene-2 content.

The catalysts used in the metathesis process are highly selective and flexible and can operate over a broad range of temperatures and pressures. There are two classes: tungsten-based operating at high (300-400 °C) temperatures, and rhenium-based working at low (20-50 °C) temperatures. Both catalyst types can be deactivated and fouled by heavier organic compounds formed by side reactions. The deactivated catalyst can be regenerated by calcination at 500-600 °C.

A simplified flow process for Lummus OCT can be described as follows. Fresh and recycled C<sub>4</sub>'s are mixed with ethylene and recycled ethylene feeds and sent through a guard bed which removes trace impurities from the mixed feed. The feed is heated prior to entering the vapor phase fixed-bed metathesis reactor where the equilibrium reaction takes place. The catalyst is regenerated in situ on a regular basis. The per-pass conversion of butene is greater than 60 wt% with overall selectivity to propylene exceeding 90 wt%. The product from the metathesis reactor contains mainly propylene and unreacted feed.

A standalone OCT unit requires a polymer grade ethylene feed and specific invest. When integrated with an ethylene plant, however, OCT provides the flexibility to economize on feedstock while varying the ratios of light olefins produced. The typical propylene to ethylene ratio of 0.4 to 0.6 in an ethylene plant can be extended to greater than 1. OCT can also be combined with FCC in order to reduce the investment cost per ton of propylene produced.



#### 4.9 Methanol to Olefin (MTO) Process<sup>21,22</sup>

The UOP/HYDRO MTO process converts methanol to light olefins. The process provides greater selectivity to ethylene and propylene versus C<sub>4</sub>+ by-products.

The MTO reaction scheme is shown in Figure 4.

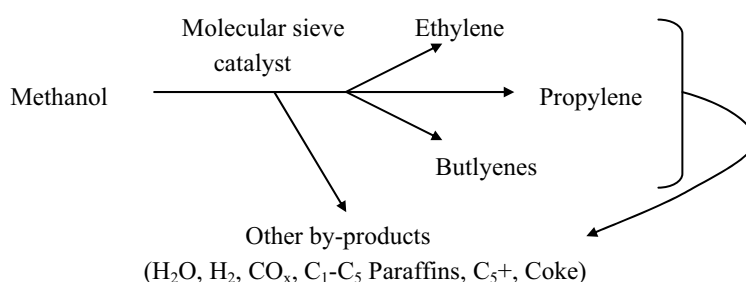


Figure 4. MTO reaction scheme

The ethylene and propylene are produced from a dimethylether (DME) intermediate in the MTO process. Some by-products such as butenes and other higher olefins are also produced. The MTO reaction is exothermic. The coke deposited on the catalyst can be removed by combustion with air in a catalyst regenerator system in order to prolong the active life of the catalyst.

The UOP/Hydro MTO process utilizes the highly selective metalloaluminophosphate molecular sieve catalyst MTO-100, which is based on SAPO-34. The main olefin products are ethylene and propylene, but the catalyst is rapidly deactivated by aromatic coking. An alternative MTO catalyst is the medium-pore zeolite ZSM-5. In this case the main olefin product is propylene, and the deactivation of catalyst caused by aromatic coke is slow, but significant quantities of C<sub>5</sub>+aromatic by-products are formed.

In the UOP/Hydro MTO process unit, the methanol and recycled DME come into contact with the catalyst in the reactor and are converted into light olefins. Residence times are very short and the reactor operates in a stable steady-state in the vapor phase at temperatures between 350 and 600 °C, and pressures between 0.1 and 0.3 MPa. In the process, the catalyst is deactivated by coke accumulation, and a part of catalyst is transferred to the fluidized bed regenerator in order to restore its activity.

Oxygenates in the reactor effluent are recovered and recycled. Polymer grade ethylene and propylene can be produced from the reactor effluent by a series of purification steps. The results from an MTO demonstration plant show that the conversion of methanol is 100 %, selectivity to ethylene is above 40 %, and selectivity to propylene is close to 40 %.

## 5. PROSPECTS

The production of ethylene and propylene is one of the cornerstones of the petrochemical industry and developments in this area are a key to progress in the industry as a whole.

According to reliable forecasts, the world's recoverable conventional oil resources amount to 310 billion tons,<sup>23</sup> while non-conventional oil resources (including extra-heavy oil, oil sands, asphalt and oil shale) total 400-700 billion tons. It is predicted that the output of conventional crude oil will peak in 2030, and by 2060 the production of conventional and non-conventional crude oil will reach 6.54 billion tons. Refineries will face the tough task of upgrading more heavy oils, not only for clean fuels, but also for provision of petrochemical raw materials.

Olefin production technology can be separated into non-catalytic and catalytic processes. Conventional pyrolysis of light hydrocarbons, a non-catalytic process, plays the dominant role in ethylene production and there have been significant advances in reaction selectivity through innovative designs as well as in energy saving. Catalytic processes have been developed in recent decades in an effort to extend the range of possible feedstocks to include heavy hydrocarbons and by-products from refineries and petrochemical streams. Principal issues to consider in the selection of olefin technology for a grass roots plant or a revamped refining-petrochemical complex with expanded capacity are feedstock optimization, by-product slate and markets, capital return, and environmental constraints. Many of these issues are site-specific, especially feedstock supply which varies considerably from region to region. Feedstock preparation for olefin plants mainly involves limited modification of the hydrogen to carbon ratio, either by hydrogen addition or carbon rejection. By virtue of the shortfall in light fraction supply as feedstock, integration of a steam cracker with FCC modified processes such as DCC, CPP or PetroFCC is generally the best choice. Such a combination means making full use of crude by coupling a non-catalytic with a catalytic process.

To comply with current or probable future clean gasoline specifications, the aromatic content as well as the olefin and sulfur content should be strictly limited. In order to increase the isoparaffin content of the gasoline pool, Chen<sup>24</sup> has proposed a new clean refinery system with the production and upgrading of light olefins at its heart. He proposed that production of light olefins by catalytic hydrotreating be coupled with high temperature catalytic cracking and upgrading of light olefins based on isomerization, oligomerization and hydration or etherification. All of these processes lead to the manufacture of clean fuels and high quality synthetic lubricants. Catalytic processing for production of light olefins is the key step in the future integration of refining and petrochemicals plants.

## 6. REFERENCES

1. Anderson, B.G.; Schumacher, R. R.; Duren, R.; Singh, A. P.; Santen, R. A. *J. Mol. Catal. A*, **2002**, 181, 291-301.
2. Weitkamp, J.; Jacobs, P. A.; Martens, J. A. *Appl. Catal.* **1983**, 8, 123.
3. Buchanan, J. S.; Santiesteban, J. G.; Haag, W. O. *J. Catal.* **1996**, 158, 279-287.
4. Wakui, K.; Satoh, K.; Sawada, G.; Shiozawa, K.; Matano, K.; Suzuki, K.; Hayakawa, T.; Yoshimura, Y.; Murata, K.; Mizukami, F. *Appl. Catal.* **2002**, 230, 195-202.
5. Corma, A.; Orchilles, A. V. *J. Catal.* **1989**, 115, 115.
6. Shu X.T.; Fu W.; He M.Y., et al. U.S. Patent 5,232,675, **1993**.
7. Hou X.L. Advances in Refining Technology in China, *China Petrochemical Press*, **1997**, 12-25, 68-78.
8. Zhang F.M. et al. U.S. Patent 6,080,698, **1998**.
9. Wang X.Q.; Shi W.Y.; Xie C.G.; Li Z.T. *5<sup>th</sup> International Conference on Refinery Processing*, AIChE **2002**, 241-249.
10. Greer, D.; Houdek, M.; Pittman, R.; Woodcock J. Creating Value from Light Olefins – Production and Conversion, *Proc. the DGMK Conference*, Hamburg, Germany, **2001**, 31-43.
11. Pittman, R. M.; Upson, L.L. U.S. Patent 6,538,169, 2003.
12. Bolt, H. V.; Glanz S. *Hydrocarbon Process.*, **2002**, 77.
13. Bolt, H. V.; Zimmermann H. *Proc. 13<sup>th</sup> Ethylene Producers' Conference*, American Institute of Chemical Engineers: New York, 2001; pp. 518-547.
14. Niccum, P. K.; Gilbert, M. F.; Tallman, M. J.; Santner, C. R. *Hydrocarbon Process.*, November 2001, 47-53.
15. Leyshon, D. W.; Cozzone, G. E. U.S. Patent, 5,043,522, 1991.
16. Johnson, D. L.; Nariman, K. E.; Ware, R. A. U.S. Patent 6,222,087, 2001.
17. Ruziska P. A.; Steffens T. R. 2001 Technology Session of the 12th Ethylene Producers' Conference, 2001 AIChE Spring National Meeting, Houston, TX.
18. de Barros, J., *Proc. 17<sup>th</sup> World Petroleum Congress*, Rio de Janeiro, Brazil, September 2002.
19. Cosyns, J.; Chodorge, J.; Commereuc, D.; Tork, B. *Hydrocarbon Process.*, **1998**, 61-65.
20. Laugier, J. P. *Proc. 12<sup>th</sup> Ethylene Producers' Conference*, New York: American Institute of Chemical Engineers, **2000**, 123-138.
21. Kvisle, S.; Nilsen H. R.; Fuglerud, T.; Gronvold, A.; Vora, B. V.; Pujado, P. R.; Barger, P. T.; Andersen, J. M. *DGMK Conference "Creating Value from Light Olefins – Production and Conversion"*, Hamburg, Germany, **2001**, 73-84.
22. Barger, P. T.; Vora, B. V. U.S. Patent 6,534,692, 2003.
23. Haddock, P.W. *NPRA*, 1999.
24. Chen, N.Y. *Chemical Innovation*, April 2001, 11-20.

## Chapter 6

# KINETICS AND MECHANISMS OF FLUID CATALYTIC CRACKING

P. O'Connor

*Albemarle Catalysts*

*Stationsplein 4, P.O.Box 247, 3800AE Amersfoort, The Netherlands*

## 1. INTRODUCTION

Catalytic cracking is a very flexible process to reduce the molecular weight of hydrocarbons. Today fluid catalytic cracking (FCC) remains the dominant conversion process in petroleum refineries. Prior to 1925, the higher boiling heavy crude oil molecules were chemically changed to smaller naphtha (gasoline) molecules by thermal decomposition using a process called thermal cracking. In the late twenties Eugene Jules Houdry demonstrated that a catalytic cracking process yields more gasoline of a higher octane. The first full-scale commercial fixed bed catalytic cracking unit began production in 1937.

## 2. PROCESS DEVELOPMENT

During the catalytic cracking process the catalysts are after a short time covered by a deactivating layer of coke. This coke can be removed and regenerated by burning, but the regeneration time is relatively slow compared to the reaction time. An efficient way to solve this problem is to move the catalyst from one reactor (for hydrocarbon cracking) to another reactor (for catalyst regeneration). The first continuous circulating catalyst process using a bucket elevator thermofor catalytic cracking (TCC) was started up in Paulsboro, NJ in 1941.

The moving-bed solved the problem of moving the catalyst between efficient contact zones. However the catalyst beads used still were too large, limiting the regenerator temperatures to avoid intra particle temperature excursions and therefore requiring a large regenerator and catalyst hold up.<sup>1</sup>

Moving the solid catalyst in this way remains a challenge, which was solved by making use of the invention that it is possible to make a powder to flow in a manner similar to a liquid if enough gas flows through it. This phenomenon is called fluidization and the FCC process was introduced which uses fine powdered catalysts which can be fluidized. The first commercial circulating fluid bed process went on stream in 1942 in Baton Rouge, Louisiana.<sup>2</sup> By the 1970's FCC units replaced most of the fixed and moving-bed crackers.

Generally FCC units operate in a heat balanced mode whereby the heat generated by the burning of coke is equal to heat needed for the vaporization of the feed plus the heat of cracking. Also the pressure balance of an FCC unit is very important in order to ensure proper catalyst circulation and to prevent the contact between hydrocarbons (reactor) and air (regenerator). Overall this makes the optimal operation of a unit a very interesting challenge.

The FCC process hardware and operation have continued to co-evolve with the catalyst and the changing economical and environmental requirements.

Key development in FCC process and hardware are:<sup>1,3</sup>

- Short contact time riser reactor.
- Feed distribution, atomization.
- Feed pre vaporization or "supercritical" injection.
- Multiple feed injection.
- Quick product disengaging and separation from catalyst.
- Quick product quench.
- More efficient stripping.
- Downer (downflow) reactor.
- Improved regenerator efficiency, lower inventory.
- Improved control of combustion (CO, CO<sub>2</sub>, SO<sub>x</sub>, NO<sub>x</sub>).
- Improved airgrid designs.
- Catalyst coolers (internal and external heat-removal).
- Power recovery from fluegas.
- Improved high flux standpipes.
- High efficiency cyclone separators.
- Cyclones without diplegs.
- Third-, Fourth- and Fifth- stage particulate capture systems.
- Erosion and high temperature resistant metallurgy.

These developments have led to dramatic reductions in the size (elevation, volume, catalyst inventory) and hence costs of a FCC unit required per barrel of feed charged and converted.

### 3. CHEMISTRY AND KINETICS

The catalytic cracking of hydrocarbons is a chain reaction that is believed to follow the carbonium ion theory involving three steps: Initiation, propagation and termination. The initiation step is represented by the attack of an active site on a reactant molecule to produce the active complex that corresponds to the formation of a carbocation. The chain propagation is represented by the transfer of a hydride ion from a reactant molecule to an adsorbed carbenium ion. Finally the termination step corresponds to the desorption of the adsorbed carbenium ion to give an olefin whilst restoring the initial active site.<sup>4</sup>

Carbenium-ion cracking mechanism produces a higher yield of a much more desirable gasoline than thermal cracking. While thermally cracked gasoline is quite olefinic, cat cracked gasoline contains a large amount of aromatics and branched compounds which is beneficial for the gasoline octane numbers (RON and MON). The following table illustrates the differences in the kinetics of thermal and catalytic cracking at about equal conversion.

Table 1. Catalytic vs. thermal cracking

| Conversion       | iC <sub>5</sub> /nC <sub>5</sub> ratio | (C <sub>1</sub> +C <sub>2</sub> )/iC <sub>4</sub> ratio | Fuel gas, mol/mol cracked |
|------------------|--|---|---------------------------|
| Thermal          | 0                                      | 66  | 2                         |
| Activated Carbon | 0.06                                   | 27  | 0.54                      |
| Alumina          | 0.2                                    | 14  | 2.72                      |
| Silica-Alumina   | 3.8                                    | 0.6   | 0.41                      |

The above data indicate that also for catalytic cracking strong differences in are possible. Only carbenium-ion cracking involving a tertiary carbenium-ion will produce branched compounds. A second type of cracking, protolytic cracking,<sup>5</sup> can be assumed to yield more “radical-cracking” like products such as methane and ethane (fuel gas).

### 4. CATALYSTS

Table 2 gives the types and forms of cracking catalysts developed and used over the years. The way in which catalysts are built up from the separate components (catalyst assembly) and catalyst form, have an important impact.<sup>6</sup>

The first FCC catalyst, the Super Fitol, were produced by activating clays with acid these materials were originally used for bleaching edible oils and decolorizing hydrocarbons. Synthetic mixed oxide catalysts followed, some of which were 2 to 3 times more active than the activated clay based types. The Al<sub>2</sub>O<sub>3</sub> of the SiO<sub>2</sub>•Al<sub>2</sub>O<sub>3</sub> was optimized impregnating dry SiO<sub>2</sub> gels in the 10 to 25% Al<sub>2</sub>O<sub>3</sub> range. The high Al<sub>2</sub>O<sub>3</sub> catalysts (HA, 25% Al<sub>2</sub>O<sub>3</sub>) exceeded the low Al<sub>2</sub>O<sub>3</sub> catalysts (LA) and Super Fitol steamed activity level. Later on

clay was added in the preparation of synthetic  $\text{SiO}_2 \bullet \text{Al}_2\text{O}_3$  catalysts to provide additional macro porosity.

Table 2. Early days of cracking catalysts

| Year | Process            | Reactor System | Catalyst type   | Catalyst form                             |
|------|--------------------|----------------|---|---|
| 1920 | McAfee             | Batch          | $\text{AlCl}_3$   | Granulated                                |
| 1939 | Houdry             | Fixed bed      | Clay  | Acid treated<br>Granulated                |
| 1940 | Suspensoid         | Liquid phase   | Clay  | Ex-luboil<br>decolorizing.<br>Powdered    |
| 1942 | FCC                | Fluid bed      | Clay  | Super Filtrol<br>Acid treated<br>Powdered |
| 1945 | TCC Houdry<br>Flow | Moving bed     | Clay  | Acid treated<br>Pellets                   |
| 1942 | FCC                | Fluid bed      | Synthetic<br>$\text{SiO}_2 \bullet \text{Al}_2\text{O}_3$ | Ground                                    |
| 1946 | FCC                | Fluid bed      | Synthetic<br>$\text{SiO}_2 \bullet \text{Al}_2\text{O}_3$ | Microspheres                              |
| 1965 | FCC                | Fluid bed      | X, Y Zeolites   | Microspheres                              |

Co-currently micro spheroidal (MS) catalysts were developed, recognizing the advantages for a higher alumina content catalyst and improvements in impregnation efficiency with small particles compared to the traditional lumps of silica hydro-gel. The original process was quite burdensome and involved an emulsion process which was replaced soon by spray drying of the impregnated gel. Spray drying still is today the way all FCC manufacturers compound and form their MS catalysts.

In the 1950's zeolites were invented along with their potential application in catalysis.<sup>7</sup> In the 1960's Mobil introduced zeolites into FCC catalysts leading to very substantial increases in conversion and gasoline production,<sup>8</sup> as shown in the following example:

Table 3. Improvements in zeolite cracking catalysts

| Catalyst           | Conversion (vol.%) | Gasoline (vol.%) |
|--------------------|--------------------|------------------|
| Silica-Alumina gel | 56                 | 40               |
| REHX               | 68                 | 52               |
| REHY               | 75                 | 58               |

The first generation zeolite catalysts were based predominately on  $\text{SiO}_2 \bullet \text{Al}_2\text{O}_3$  gels ("matrix") in which the zeolite is added at some point prior to spray drying. In the "In-situ" crystallization method as applied by Engelhard, kaolin based microspheres are prepared and calcined, where after zeolites are crystallized in the microsphere, leaving zeolite in an " $\text{Al}_2\text{O}_3$ -enriched matrix".

In the early 1970s Grace Davison introduced the use of a silica hydro-sol based binder for the incorporation of zeolites. Silica hydro sol is a polymerized silica dispersed in water to form a clear continuous phase, which

is a binder giving dramatic improvements in attrition resistance and density. The result is the creation of particles which are encased in a hard resilient shell of a vitreous material. The low activity of the silica hydro-sol relative to the  $\text{SiO}_2 \bullet \text{Al}_2\text{O}_3$  based systems enabled the selectivities of nearly pure zeolite cracking, resulting in further improvements in gasoline and coke yields. Nevertheless, alternate routes of using  $\text{Al}_2\text{O}_3$  gel and/or  $\text{SiO}_2 \bullet \text{Al}_2\text{O}_3$  gels as binders and as catalytic functional materials are also still pursued, because of the significance of porosity and permeability of the microsphere.

The importance of diffusion restrictions in FCC catalysis is often questioned. Short contact time pilot riser experiments confirm that combining zeolites with a “diffusion enhancing” matrices can result in significant product selectivity and product property improvements. The industrial benefits of non-zeolite “matrix” on bottoms cracking in Heavy VGO and resid FCC have also been confirmed in practice. Recently new methods are used to measure the accessibility of FCC catalysts.<sup>6,11</sup>

Besides faujasite (Y) zeolites, today’s catalysts contain several additional functional materials such as metal traps, nickel resistant matrices, bottoms cracking matrices and small pore zeolites as for instance ZSM-5.<sup>9</sup> These zeolites are often added in separate (additive) particles with the intention of boosting the gasoline octane numbers and/or the production of light olefins (propylene)

Also various FCC additives are produced usually consisting of metals (Pt, Pd, Ce, V, Cu, Co, Zn) on alumina and or alumina-magnesia supports for  $\text{CO}_2$ , CO,  $\text{SO}_x$  and  $\text{NO}_x$  control of the regenerator off-gas<sup>10</sup> and for Sulfur reduction of gasoline.

## 5. CATALYST AGING AND DEACTIVATION

FCC catalysts are deactivated via several mechanisms,<sup>11</sup> which all result in a loss in activity and a change in yield selectivity: Catalyst will age, meaning change chemical and physical structure due to the (hydro) thermal conditions during the 10,000 to 50,000 reaction and regeneration cycles it will endure. The catalysts can also be poisoned, whereby the active sites are covered by coke and/or polars (nitrogen) that neutralize the catalytic activity or by metals (vanadium, nickel, sodium) which can destroy or alter the activity.

Catalysts can also be deactivated by fouling whereby coke and/or metals deposits and block the catalyst pores and thereby limit the mass transfer.

Reversible deposits (nitrogen, coke) are removed during regeneration. If we assume that the poisoning effect will increase with the concentration, then the poisoning effect will be inversely proportional to the catalyst-to-oil ratio (CTO), and therefore will be dependent on the coke selectivity of the catalyst. Irreversible catalyst poisons (metals), on the other hand, will build up and continue to interact with the catalyst.



The very detrimental effects of contaminants like Iron and calcium on the accessibility and performance of catalysts has been reported.<sup>6,12,13</sup> Apparently these contaminants can result in (liquid) eutectic melts on the surface of the catalyst particles, which can block the important entrance pores and even glaze catalyst surface completely.

## 6. FEEDSTOCKS, PRODUCTS AND THE ENVIRONMENT

To strike a balance between product demand and refinery feed composition, more residue (high metals, concarbon) is being included in FCC feedstocks. Improvements in process and catalyst technology has resulted in a further opening of the feedstock processability window (Fig. 1).

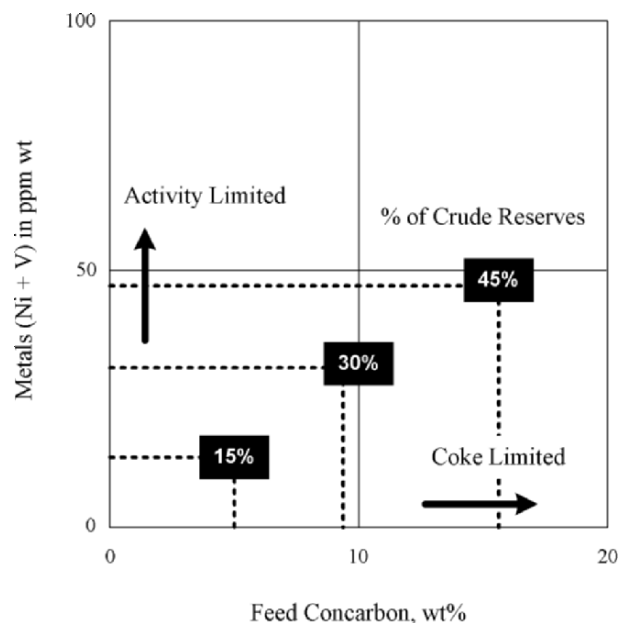


Figure 1. Resid properties and processability (from Ref. 9)

Environmental regulations are becoming more a key driving force for reducing FCC process air-pollutant emissions<sup>10</sup> and for changing the composition of fuel products<sup>9</sup>. This is affecting the design and operation of the FCC and is providing new opportunities for the development of catalyst and additive technology.

## 7. FUTURE CHALLENGES

Although FCC is sometimes considered to be a fully matured process, new challenges and opportunities in its application and a continuing stream of innovations in the process and catalyst field ensure that it will remain an important and dynamic process in the future of refining.

## 8. REFERENCES

1. Avidan, A.A. Origin, development and scope of FCC. in Fluid Catalytic Cracking Science & Technology, Magee, J.S.; Mitchell, M.M (Eds.), *Stud. Surf. Sci. Catal.*, **1993**, Vol. 76.
2. *The Fluid Bed Reactor, A National Historic Chemical Landmark*, published by American Chemical Society to commemorate the designation of the Fluid Reactor as a National Historic Chemical Landmark, 1998.
3. Schlosser, C.R.; Pinho, A.; O'Connor, P.; Baptista, R.D.; Sandes, E.F.; Torem, M.A. Residue Catalytic Cracking Technology: State of the Art and future developments, Akzo Nobel Catalysts Symposium, June 2001.
4. Corma, A.; Orchilles, A.V. Current views on the mechanism of catalytic cracking. In *Microporous and Mesoporous Materials*, **2000**, 35-36, 21-30.
5. Wojciechowski, B.V.; Corma, A. *Catalytic Cracking: Catalysis, Chemistry, Kinetics*, Marcel Dekker Inc: New York, 1986.
6. O'Connor, P.; Imhof, P.; Yanik, S.J. Catalyst Assembly Technology in FCC in Fluid Catalytic Cracking V. Materials and Technology Innovations, *Studies in Surface Science and Catalysis*, Occelli, M.L.; O'Connor, P. (Eds.), **2001**, Vol. 134.
7. Boyle, J.; Pickert, J.; Rabo, J.; Stamiros, D. in 2<sup>nd</sup> International Congress in Catalysis, July 1960, Paris.
8. Plank, C.J. The invention of zeolite cracking catalysts, *Chem. Tech.*, **1984**, 243.
9. Biswas, J.; Maxwell, I.E. Recent process and catalyst related developments in FCC, *Appl. Catal.*, **1990**, 63, 197-258.
10. Cheng, W.C.; Kim, G.; Peters, A.W.; Zhao, X.; Rajagopalan, K. Environmental FCC technology, *Catal. Rev – Sci. Eng.*, **1998**, 40 (1&2), 39-79.
11. O'Connor, P.; Pouwels, A.C. FCC Catalyst deactivation" in Catalyst Deactivation, *Stud. Surf. Sci. Catal.*, 1994, Vol. 88..
12. Hodgson, M.C.J.; Looi, C.K.; Yanik, S.J. Avoid excessive catalyst deactivation, Akzo Nobel Catalysts Symposium, June 1998.
13. Yaluris, G.; Cheng, W.; Hunt, J.L.; Boock, L.T. The effects of Fe poisoning on FCC catalysts, NPRA Annual meeting 2001, AM-01-59.

## Chapter 7

# HYDROTREATING AND HYDROCRACKING: FUNDAMENTALS

Paul R. Robinson<sup>1</sup> and Geoffrey E. Dolbear<sup>2</sup>

1. *PQ Optimization Services, 3418 Clear Water Park Drive, Katy, TX 77450*

2. *G.E. Dolbear & Associates, 23050 Aspen Knoll Drive, Diamond Bar, CA 91765*

### 1. INTRODUCTION

Hydrotreaters are the most common process units in modern petroleum refineries. As shown in Table 1, the world's hydrotreating capacity is nearly half as large as the world's crude distillation capacity.<sup>1</sup> In more than 700 refineries around the globe, there are more than 1300 hydrotreating units. A typical Western petroleum refinery (*Figure 1*) uses at least three hydrotreaters – one for naphtha, one or two for light gas oil, and one or two for heavy gas oil and/or vacuum gas oil.

*Table 1. Worldwide Refining Process Units (as of January 1, 2004)<sup>1</sup>*

|                          | Crude<br>Distillation | Coking +<br>Visbreaking | FCC    | Catalytic<br>Reforming | Hydro-<br>treating | Hydro-<br>cracking |
|--------------------------|-----------------------|-------------------------|--------|------------------------|--------------------|--------------------|
| Number of<br>Units       | >710                  | >330                    | 360    | 550                    | 1316               | 168                |
| Total World<br>Capacity* | 82.0                  | 8.0                     | 14.3   | 11.3                   | 40.3               | 4.6                |
| Average<br>Capacity†     | 114,000               | 45,700                  | 39,700 | 20,500                 | 30,600             | 27,400             |

\* million barrels per calendar day

† barrels per calendar day

Hydrocracking is far less common than hydrotreating, but the number of partial-conversion “mild” hydrocrackers is increasing as refiners build new units to meet clean fuel regulations.

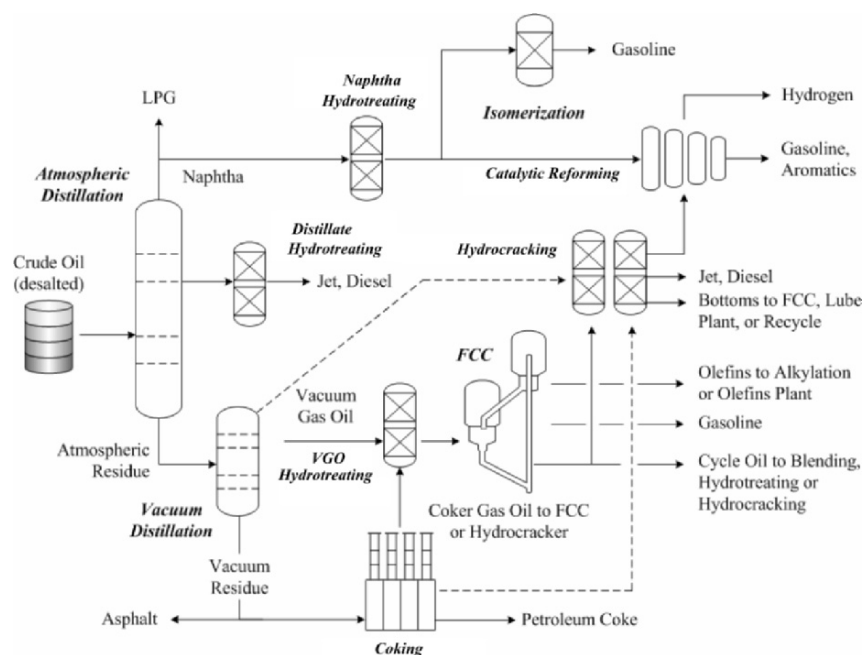


Figure 1. Layout of a Typical High-Conversion Oil Refinery

## 1.1 Hydroprocessing Units: Similarities and Differences

Process flow schemes for hydrotreating and hydrocracking are similar. Both use high-pressure hydrogen to catalytically remove contaminants from petroleum fractions. Both achieve at least some conversion, and they use the same kinds of hardware. Therefore, to avoid redundancy, we decided to discuss them together. As is common in the refining industry, we use the term “hydroprocessing” when a statement applies to both hydrotreating and hydrocracking.

As shown in *Table 2*, the extent of conversion is the most significant difference between hydrotreating and hydrocracking. In this context, the term “conversion” is defined as the difference in amount of unconverted oil between feed and product divided by the amount of unconverted oil in the feed. Unconverted oil is defined as material that boils above a specified temperature. For vacuum gas oil (VGO), a typical specified temperature is 650°F (343°C). Conversion in hydrotreaters is less than 15 wt%, while conversion in hydrocrackers and mild hydrocrackers exceeds 20 wt%.

In hydrotreating units, reactions that convert organic sulfur and nitrogen into  $\text{H}_2\text{S}$  and  $\text{NH}_3$  also produce light hydrocarbons. For example, as shown in *Figure 5*, the removal of sulfur from dibenzothiophene (boiling point =

630°F, 332°C) generates biphenyl (492.6°F, 255.9°C). This reaction does not break any carbon-to-carbon bonds, but it does convert a molecule that boils above 600°F (315.5°C) into one that boils below 600°F (315.5°C).

In hydrotreaters, conversion due to the removal of sulfur, nitrogen and oxygen usually is less than 15 wt%.

Table 2. Hydrotreating and Hydrocracking: Ranges of H<sub>2</sub> Partial Pressure and Conversion

| Process, Feedstock Types           | H <sub>2</sub> Partial Pressure |                  | Conversion<br>wt% |
|------------------------------------|---------------------------------|------------------|-------------------|
|                                    | psig                            | kPa              |                   |
| <i>Hydrotreating</i>               |                                 |                  |                   |
| Naphtha                            | 250 to 450                      | 1825 to 3204     | 0.5 to 5%         |
| LGO (Kerosene)                     | 250 to 600                      | 1825 to 4238     | 0.5 to 5%         |
| HGO (Diesel), LCO                  | 600 to 800                      | 4238 to 5617     | 5 to 15%          |
| VGO, VBGO, DAO, CGO, HCO           | 800 to 2000                     | 5617 to 13,891   | 5 to 15%          |
| Residual Oil                       | 2000 to 3000                    | 13,891 to 20,786 | 5 to 15%          |
| <i>Mild Hydrocracking</i>          |                                 |                  |                   |
| VGO, VBGO, DAO, CGO, LCO, HCO      | 800 to 1200                     | 5617 to 8375     | 20 to 40%         |
| <i>Once-Through Hydrocracking</i>  |                                 |                  |                   |
| VGO, VBGO, DAO, CGO, LCO, HCO      | 1500 to 2000                    | 10,443 to 13,891 | 60 to 90%         |
| Residual Oil                       | 2000 to 3000                    | 13,891 to 20,786 | 15 to 25%         |
| <i>Recycle Hydrocracking</i>       |                                 |                  |                   |
| VGO, VBGO, DAO, CGO, LCO, HCO      | 1500 to 2000                    | 10,443 to 13,891 | 80 to 99%         |
| <i>Ebullated-Bed Hydrocracking</i> |                                 |                  |                   |
| VGO, VBGO, DAO, HCO                | 2000                            | 13,891           | 80 to 99%         |
| Residual Oil                       | 2000 to 3000                    | 13,891 to 20,786 | >50%              |
| LGO = light gas oil                | HGO = heavy gas oil             |                  |                   |
| LCO = FCC light cycle oil          | HCO = FCC heavy cycle oil       |                  |                   |
| VGO = vacuum gas oil               | VBGO = visbreaker gas oil       |                  |                   |
| DAO = deasphalted oil              | CGO = coker gas oil             |                  |                   |

Hydrotreating and hydrocracking differ in other ways. For a given amount of feed, hydrocrackers use more catalyst and operate at higher pressures. They also use different catalysts. Because they make large amounts of light products, hydrocracker fractionation sections must be more complex. In some hydrocrackers, unconverted oil from the fractionation section is recycled, either back to the front of the unit or to a separate cracking reactor.

Many mild hydrocrackers contain at least one bed of cracking catalyst, which allows them to achieve higher conversion – between 20 and 40 wt%. The unconverted bottoms can go to an FCC unit, a lube plant, or fuel-oil blender. Due to its high value in other applications, the bottoms are blended into fuel oil only when there is no other feasible option.

In hydrocrackers that process vacuum gas oils or other feeds with similar boiling ranges, the typical once-through conversion exceeds 60 wt%. If the unconverted oil is recycled, the overall conversion can exceed 95 wt%. As

with mild hydrocracking, the unconverted bottoms are high-value oils, which usually are sent to FCC units, lube plants, or olefin plants. For heavier feeds – atmospheric and vacuum residues – conversions are much lower, especially in fixed-bed units. In ebullated-bed units, the conversion of 1050°F-plus (566°C-plus) residue can exceed 60 wt%.

Catalytic isomerization and dewaxing is a special kind of hydrocracking used to make high-quality lube base stocks. This topic is well-covered elsewhere, so we won't elaborate here.

## 2. PROCESS OBJECTIVES

Table 3 presents a list of feeds and product objectives for different kinds of hydrotreaters and hydrocrackers. In the 1950s, the first hydrotreaters were used to remove sulfur from feeds to catalytic reformers. In the 1960s, the first hydrocrackers were built to convert gas oil into naphtha.

Table 3. Feeds and Products for Hydroprocessing Units

| Feeds                      | Products from Hydrotreating                      | Products from Hydrocracking   |
|----------------------------|--|---|
| Naphtha                    | Catalytic reformer feed                          | LPG   |
| Straight-run light gas oil | Kerosene, jet fuel                               | Naphtha   |
| Straight-run heavy gas oil | Diesel fuel                                      | Naphtha   |
| Atmospheric residue        | Lube base stock, low-sulfur fuel oil, RFCC* feed | Naphtha, middle distillates, FCC feed                                     |
| Vacuum gas oil             | FCC feed, lube base stock                        | Naphtha, middle distillates, FCC feed, lube base stock, olefin plant feed |
| Vacuum residue             | RFCC* feed                                       | Naphtha, middle distillates, RFCC* feed                                   |
| FCC light cycle oil        | Blend stocks for diesel, fuel oil                | Naphtha   |
| FCC heavy cycle oil        | Blend stock for fuel oil                         | Naphtha, middle distillates   |
| Visbreaker gas oil         | Blend stocks for diesel, fuel oil                | Naphtha, middle distillates   |
| Coker gas oil              | FCC feed   | Naphtha, middle distillates, FCC feed, lube base stock, olefin plant feed |
| Deasphalted oil            | Lube base stock, FCC feed                        | Naphtha, middle distillates, FCC feed, lube base stock                    |

\*RFCC = “residue FCC unit” or “reduced crude FCC unit,” which are specially designed to process feeds that contain high concentrations carbon-forming compounds.

Today, in addition to naphtha, hydrotreaters process kerosene, gas oil, vacuum gas oil, and residue. Hydrocrackers process vacuum gas oil, coker gas oil, visbreaker gas oil, FCC heavy cycle oil, and/or other feeds that boil between 650°F and 1050°F (343°C and 566°C). Most residue hydrocrackers use fluidized bed or ebullated bed technology.

For hydroprocessing units, product specifications are set to meet plant-wide objectives. For example, the naphtha that goes to catalytic reforming and isomerization units must be (essentially) sulfur free. Before it can be sold as

jet fuel, the aromatics content of kerosene must be low enough to meet smoke-point specifications (ASTM D1655). Heavier distillates cannot be sold as diesel fuel unless they meet stringent sulfur specifications.

## 2.1 Clean Fuels

As mentioned in Chapter 1 (Section 8.2.4), on-road diesel in the United States must contain <15 wppm sulfur by 2006. The sulfur limit for non-road diesel will be 500 wppm in 2007. The present U.S. specification for gasoline is <30 wppm sulfur. In the European Union, the sulfur content of both gasoline and diesel must be <50 wppm by 2005 and <10 wppm by 2008.

To meet clean fuel specifications, refiners in North America and Europe are increasing their hydroprocessing capabilities and adjusting operations. Two real-world examples are described below.

**Example 1.** A U.S. refinery is planning to produce diesel fuel that contains <15 wppm sulfur by June 2006. At present, the hydrocracker makes 39,000 barrels/day of middle distillate that is nearly sulfur-free. The existing 60,000 barrels/day distillate hydrotreater (DHT) gives a product with 600 to 700 wppm sulfur. Mixing the two streams yields a blend containing 425 to 485 wppm sulfur, which meets existing specifications for low-sulfur diesel fuel (per ASTM D975). To make ultra-low-sulfur diesel (ULSD), the refiner is adding a reactor and a high-pressure amine absorber to the existing DHT, enabling the unit to make a stream with 12 to 18 wppm sulfur. Blending this with distillate from the hydrocracker will give a final product containing 7 to 12 wppm sulfur.

**Example 2.** A European refiner now runs a mild hydrocracker (MHC) to maximize conversion of VGO and to pretreat the feed to its FCC unit. The plant cannot post-treat its FCC gasoline, so the sulfur content of the MHC bottoms must be less than 500 wppm to guarantee that the sulfur content of the FCC gasoline is less than 150 wppm. Other low-sulfur streams (reformate, alkylate and hydrotreated gas oil) go into the final gasoline blend, so sulfur in the FCC gasoline can exceed the final-product limit of 50 wppm.

## 2.2 The Process In-Between

As shown in *Figure 1*, hydrocracking often is an “in-between” process. The required hydrogen comes from catalytic reformers, steam/methane reformers or both. Liquid feeds can come from atmospheric and/or vacuum distillation units; delayed cokers; fluid cokers; visbreakers; or FCC units. Middle distillates from a hydrocracker usually meet or exceed finished product specifications, but the heavy naphtha from a hydrocracker usually is sent to a catalytic reformer for octane improvement. The fractionator bottoms can be recycled or sent to an FCC unit, an olefins plant, or a lube plant.

### 3. CHEMISTRY OF HYDROPROCESSING

Chemically, the boundaries between hydrotreating, mild hydrocracking, and hydrocracking are blurry. Hydrocracking occurs in many hydrotreaters, especially at high temperatures near the end of a catalyst cycle. *Table 4* lists the chemical reactions that occur in hydroprocessing units.<sup>2</sup> Most of the reactions are exothermic, so controlling heat release is a primary consideration in the design and operation of hydrotreaters and hydrocrackers.

*Table 4.* List of Hydroprocessing Reactions

| Reaction Type                        | Illustration                                     | $\Delta H_R^*$ |
|--------------------------------------|--|----------------|
| <b>Minimal C-C Bond Breaking</b>     |  |                |
| Hydrodesulfurization (HDS) †         | $R-S-R' + 2 H_2 \rightarrow RH + R'H + H_2S$     | -2.5 to -3.0   |
| Hydrodenitrogenation (HDN)           | $R=N-R' + 3 H_2 \rightarrow RH + R'H + NH_3$     | -2.5 to -3.0   |
| Hydrodeoxygenation (HDO)             | $R-O-R' + 2 H_2 \rightarrow RH + R'H + H_2O$     | -2.5 to -3.0   |
| Hydrodemetallation (HDM)             | $R-M + \frac{1}{2} H_2 + A \rightarrow RH + M-A$ | -3             |
| Saturation of aromatics              | $C_{10}H_8 + 2 H_2 \rightarrow C_{10}H_{12}$     | -3             |
| Saturation of olefins                | $R=R' + H_2 \rightarrow HR-R'H$                  | -5.5           |
| Isomerization                        | $n-RH \rightarrow i-RH$                          | n/a            |
| <b>Significant C-C Bond Breaking</b> |  |                |
| Dealkylation of aromatic rings       | $\Phi-CH_2-R + H_2 \rightarrow \Phi-CH_3 + RH$   | -1.3 to -1.7   |
| Opening of naphthene rings           | $Cyclo-C_6H_{12} \rightarrow C_6H_{14}$          | -1.3 to -1.7   |
| Hydrocracking of paraffins           | $R-R' + H_2 \rightarrow RH + R'H$                | -1.3 to -1.7   |
| <b>Other Reactions</b>               |  |                |
| Coke formation                       | $2 \Phi H \rightarrow \Phi\Phi + 2 H_2$          | +3             |
| Mercaptan formation                  | $R=R' + H_2S \rightarrow HS-R-R'H$               | -3             |

\* Kilojoules per standard m<sup>3</sup> of H<sub>2</sub> consumed. For exothermic reactions,  $\Delta H_R$  is negative.

† R = alkyl;  $\Phi$  = aromatic; M = Fe, Ni or V; A = metals-adsorbing material

Enthalpies for the reactions ( $\Delta H_R$ ) can be grouped into three categories. For HDS, HDN, HDO, HDM, and aromatics saturation,  $\Delta H_R$  are about -2.5 to -3.0 kJ per standard cubic meter of consumed H<sub>2</sub>. For reactions that break carbon-to-carbon bonds,  $\Delta H_R$  are about -1.3 to -1.7 kJ per m<sup>3</sup> of consumed H<sub>2</sub>. And for saturation of olefins,  $\Delta H_R$  are about -5.5 kJ per m<sup>3</sup> of consumed H<sub>2</sub>. Isomerization reactions produce a small amount of heat, but this can be neglected.

The following sections describe most of these reactions in more detail. In-depth information is provided in Chapter 20 by Michael Klein and Gang Hou, in Chapter 9 by I. Mochida and Ki-Hyouk, in Chapter 10 by Barry Cooper and Kim Knudsen, and in Chapter 11 by Chunshan Song and Xiaoliang Ma.

#### 3.1 Saturation Reactions

*Figure 2* shows examples of saturation reactions for olefins and aromatics.



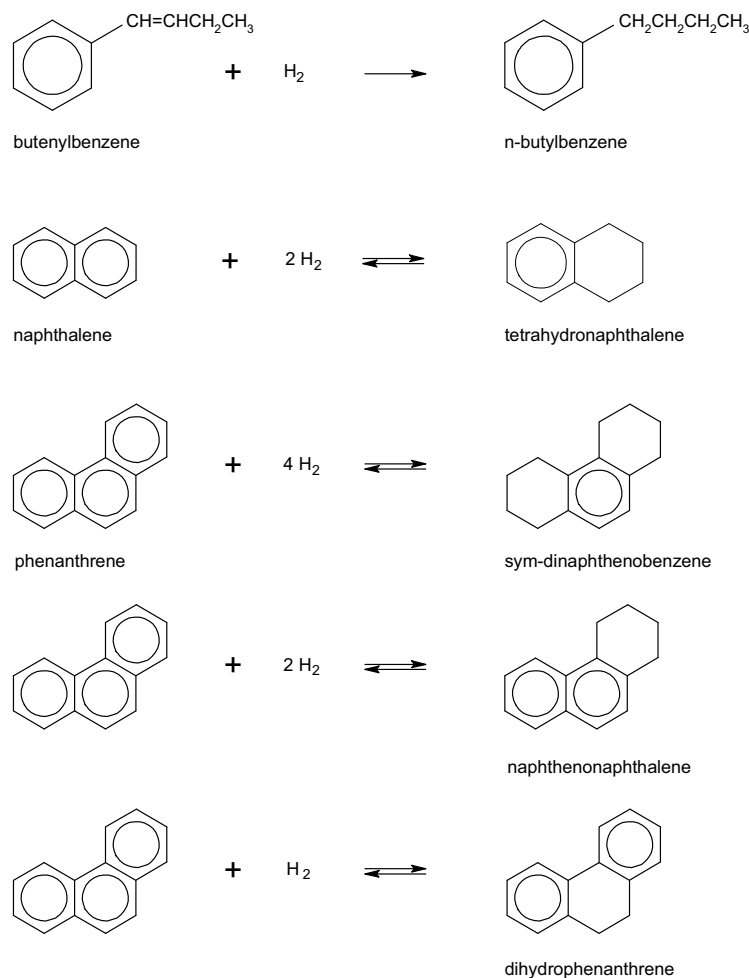


Figure 2. Saturation of butenylbenzene, naphthalene, and phenanthrene.

Practically speaking, the saturation of olefins is irreversible. The saturation of aromatics is reversible. In hydroprocessing units, at temperatures below about 700°F (370°C), forward (hydrogenation) reactions dominate and the extent of saturation goes up at higher temperatures. In the full-range product, the naphthene-to-aromatic (N/A) ratio is greater than the N/A ratio predicted by thermodynamic calculations. This indicates that the reactions are not at equilibrium and are governed by kinetics. Above about 740°F (393°C), equilibrium starts to compete with kinetics and the reverse (dehydrogenation) reactions become more important. *Figure 3* shows how LHSV affects product N/A ratio of the four saturation reactions in *Figure 2*. The product N/A ratio closest to equilibrium is for the phenanthrene/naphthenonaphthalene pair at

low space velocity (0.51). At a more typical space velocity (1.04), the N/A ratio for this pair is 1.5 times higher than the equilibrium value.

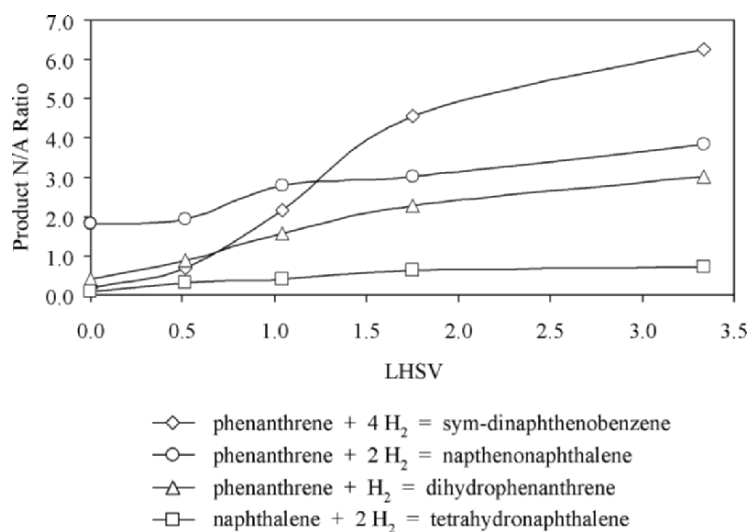


Figure 3. Product naphthene/aromatic (N/A) ratios for saturating naphthene and phenanthrene at 800°F, 2000 psig (426°C, 13,891 kPa) over a non-acidic catalyst. N/A ratios at zero LHSV (infinite reaction time) come from equilibrium calculations, not measurements.<sup>3</sup>

The saturation cross-over temperature – above which the N/A ratio of the full-range product starts to decrease – depends on feed composition, catalyst type, and reaction conditions; H<sub>2</sub> partial pressure is especially important. This phenomenon, illustrated by Figure 4, affects important product properties, such as kerosene smoke point and diesel cetane.

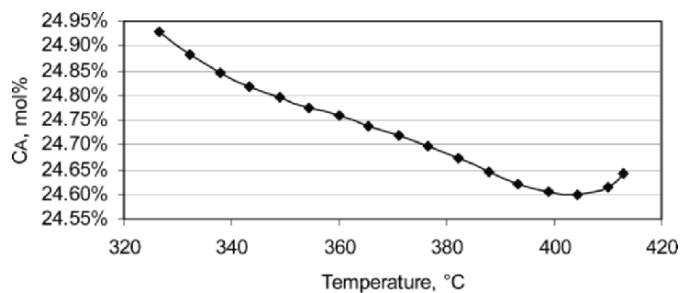


Figure 4. Aromatics cross-over in a 1500 psig (10,443 kPa) VGO hydrotreater.

### 3.2 HDS Reactions

Hydrodesulfurization (HDS) reactions proceed via two major pathways.<sup>4</sup> “Direct” HDS (*Figure 5*) is relatively simple. However, “indirect” HDS (*Figure 6*) requires preliminary reactions, such as saturation of aromatics or ring dealkylation.

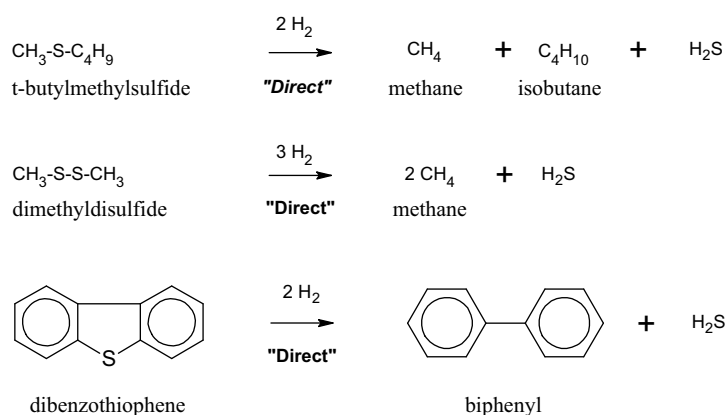


Figure 5. Hydrodesulfurization (HDS) of a sulfide, a disulfide, and dibenzothiophene

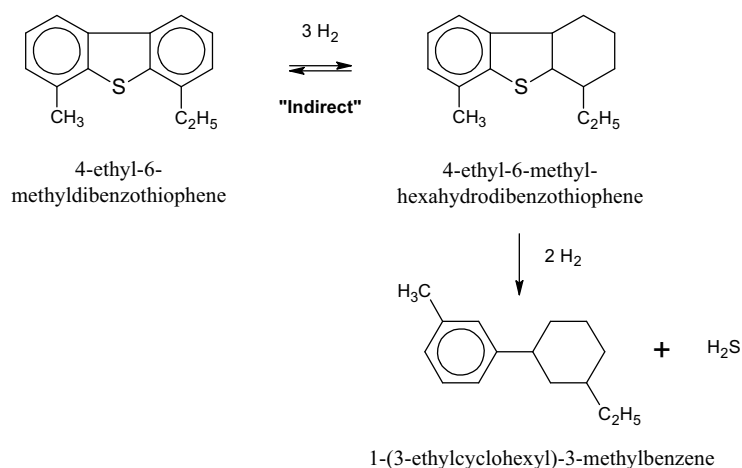

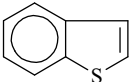
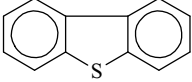
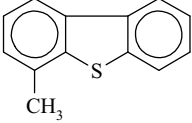
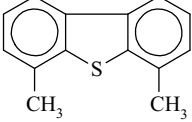
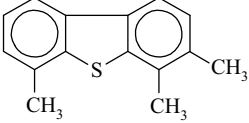


Figure 6. Mechanism for hydrodesulfurization of a hindered dibenzothiophene.

Note that the “direct” removal of a sulfur atom from dibenzothiophene requires 2 molecules of hydrogen, while the “indirect” removal of sulfur from a hindered dibenzothiophene requires 5 molecules of hydrogen per sulfur atom. This is important when estimating hydrogen requirements for deep-

desulfurization. In sterically hindered compounds, such as dibenzothiophenes with alkyl groups in the 4- and/or 6-position, HDS rates are low because the alkyl groups keep the sulfur atom away from the catalyst surface. The benzothiophene core is planar because it is aromatic. But after saturation removes aromaticity from one or both of the 6-carbon rings, the molecule can twist, allowing the sulfur atom to reach the catalyst. *Figure 7* compares HDS rates for hindered and unhindered compounds.<sup>5</sup>

|   | Compound                  | Relative Rate |
|---|---------------------------|---------------|
|    | Thiophene                 | 100           |
|   | Benzothiophene            | 50            |
|  | Dibenzothiophene          | 30            |
|  | Methyldibenzothiophene    | 5             |
|  | Dimethyldibenzothiophene  | 1             |
|  | Trimethyldibenzothiophene | 1             |

*Figure 7.* Relative rates of HDS for hindered and unhindered compounds

### 3.3 HDN Reactions

Almost all of the nitrogen in petroleum is found in ring compounds. These must be saturated and opened before the nitrogen can be removed. *Figure 8* shows a widely accepted mechanism for the HDN of quinoline.<sup>6</sup> The fast pathway requires 7 molecules of hydrogen per nitrogen atom. The slow one

uses 4 molecules of hydrogen per nitrogen atom; however, the slow pathway is so slow that, for most practical purposes, it can be neglected.

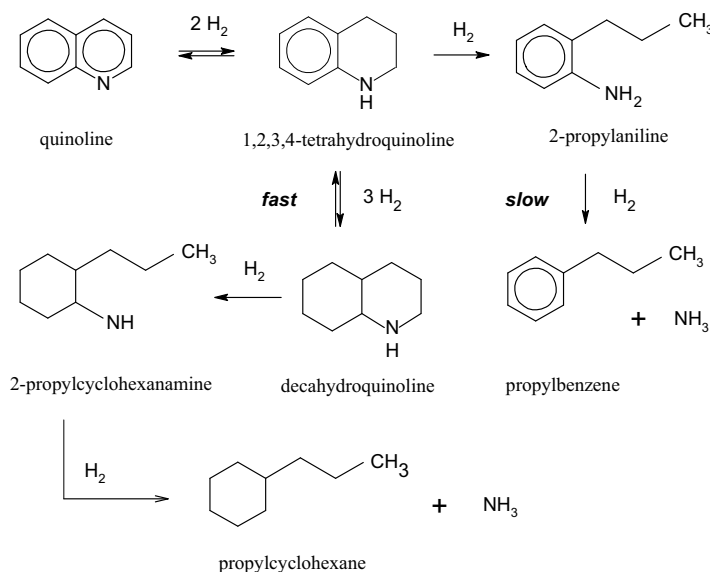


Figure 8. Hydrodenitrogenation (HDN) of quinoline.

### 3.4 Cracking Reactions

In hydroprocessing units, cracking reactions – those that break carbon-to-carbon bonds – can be grouped into three main categories:

- Paraffin hydrocracking
- Naphthene ring opening
- Dealkylation of aromatic and naphthenic rings

The dual mechanism for paraffin hydrocracking<sup>7,8</sup> includes the steps shown in *Figure 9*. “Dual” means that catalyst has two kinds of active sites – acid-based and metal-based. Section 3.7 lists the acids and metals that are used to make these catalysts.

Step 1 of the dual mechanism involves adsorption of a paraffin molecule to a metal site, followed by reversible dehydrogenation to form an olefin. In Step 2, the olefin migrates to an acid site, where it reacts with a proton to form a carbenium ion. The carbenium ion can rearrange into a more-stable carbenium ion (Step 3), which explains why products from hydrocrackers are relatively rich in iso-paraffins. In Step 4,  $\beta$ -scission of the carbenium ion produces an olefin and a smaller carbenium ion. The olefin can undergo further cracking on an acid site, or it can react with hydrogen at a metal site

(Step 5) to form a saturated iso-paraffin. The carbenium ion from Step 4 can also convert to a paraffin via deprotonation (Step 6).

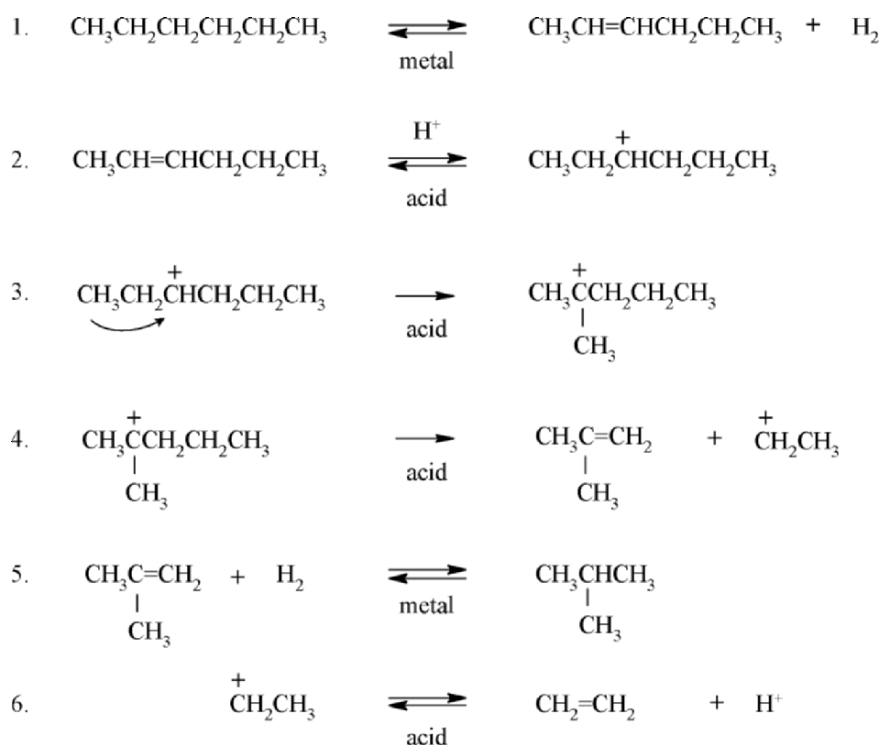


Figure 9. Metal/acid ("dual") mechanism for paraffin hydrocracking.

Organic nitrogen compounds inhibit hydrocracking by adsorbing strongly to acid sites. Therefore, the organic nitrogen content of a feed must be greatly reduced before it can be hydrocracked. In all but a few commercial units, nitrogen is removed in one or more beds of HDN catalyst. Per Section 3.3, HDN converts organic nitrogen into ammonia, which also adsorbs to acid sites but not nearly so tightly.

Figure 10 shows the opening of a naphthene ring, and Figure 11 shows a ring dealkylation reaction. Note that both reactions leave a methyl group attached to the remaining ring. This is characteristic of  $\beta$ -scission cracking reactions (see Step 4 above).

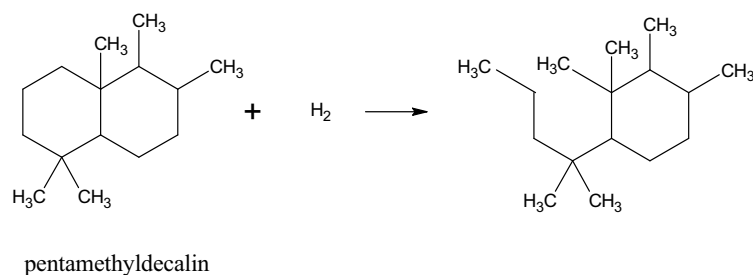


Figure 10. Naphthene ring opening.

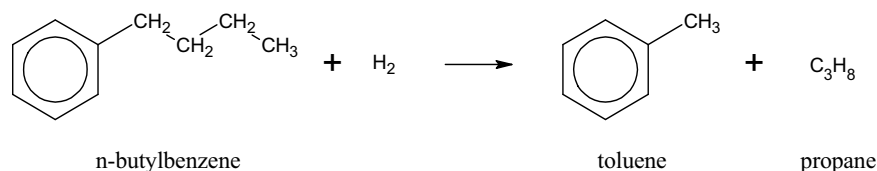


Figure 11. Ring dealkylation.

In vacuum gas oils and other 650°F-plus (343°C-plus) material, more than half of the carbon atoms may be found in ring compounds – polyaromatic hydrocarbons (PAH), partially saturated PAH (naphthene-aromatics) and fully saturated naphthenes. According to Qader and McOmber<sup>9</sup> and Lapinas, et al.,<sup>10</sup> hydrocracking converts complex ring compounds into light products by the following sequence of reactions:

- Saturation of an aromatic ring
- Opening of the resulting naphthenic ring
- Removal of paraffinic side chains (ring dealkylation)
- Isomerization of paraffins and naphthene-aromatics

Hydrocracking of paraffins, including long alkyl side chains *Figure 12* shows how these reactions might convert 2-butyl naphthalene into propane, butane and toluene.

### 3.5 Coke Formation

Due to the presence of a large excess of hydrogen, coke formation in hydroprocessing units is slow – so slow that it can be neglected in material balances for commercial units. However, coke formation is one of four major causes of catalyst deactivation. The other three are poisoning, fouling, and sintering (see Section 4.1).

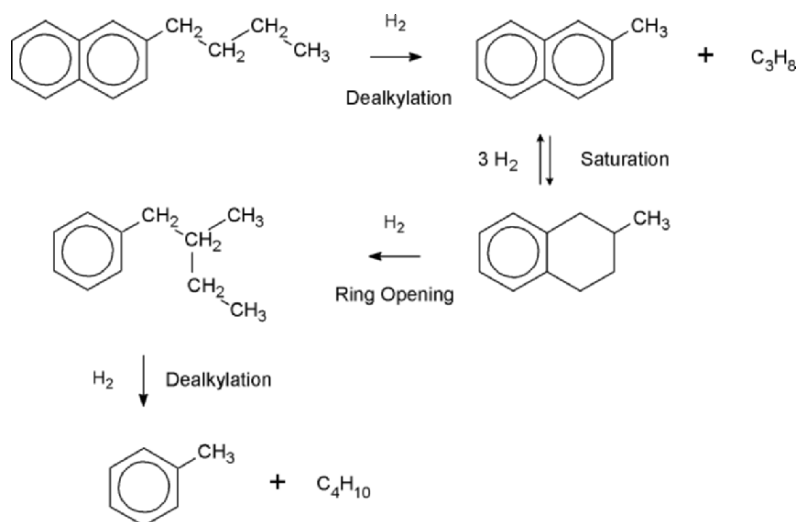


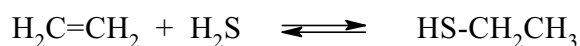
Figure 12. Reaction chain for the hydrocracking of 2-butylnaphthalene.

At the start of a catalyst cycle, a layer of coke quickly forms on the clean catalyst surface. When most of the catalyst is coated with coke, additional formation of coke is comparatively slow. A recent paper by van Speybroeck, et al.,<sup>11</sup> refers to widely cited mechanisms for coke growth. Small olefins add rings to coke nuclei with alkylation/cyclization reactions, which involve free-radical intermediates. By the same mechanism, small olefins can add rings to polyaromatic hydrocarbons (PAH). Figure 13 illustrates the addition of a ring to phenanthrene. In hydroprocessing units, coke formation and PAH growth must compete with saturation, ring-opening and hydrocracking.

The inspection of catalyst deactivation data from several commercial hydrocracking units reveals another possibility.<sup>12</sup> Kinetic expressions derived from these data indicate with a mechanism in which two PAH condense to form a large PAH (Figure 14). In the reactants have side chains, condensation may be accompanied by side-chain cracking.

### 3.6 Mercaptan Formation

In high-conversion hydrocrackers, olefins react with  $\text{H}_2\text{S}$  to form small amounts of mercaptans:



If not removed, mercaptans in hydrocracker naphtha may cause problems for downstream catalytic reforming units. Often, they are removed with a "post-treat" bed – a small layer of hydrotreating catalyst underneath the last



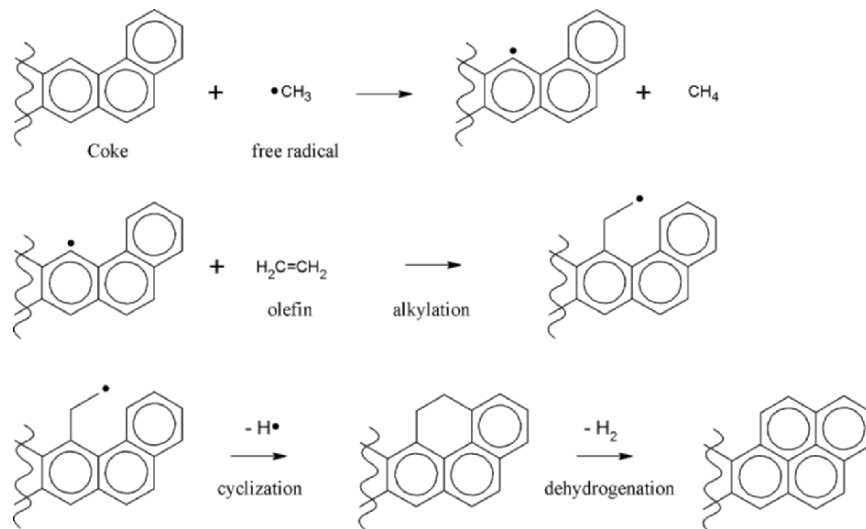


Figure 13. Free-radical mechanism for coke growth in hydroprocessing units.

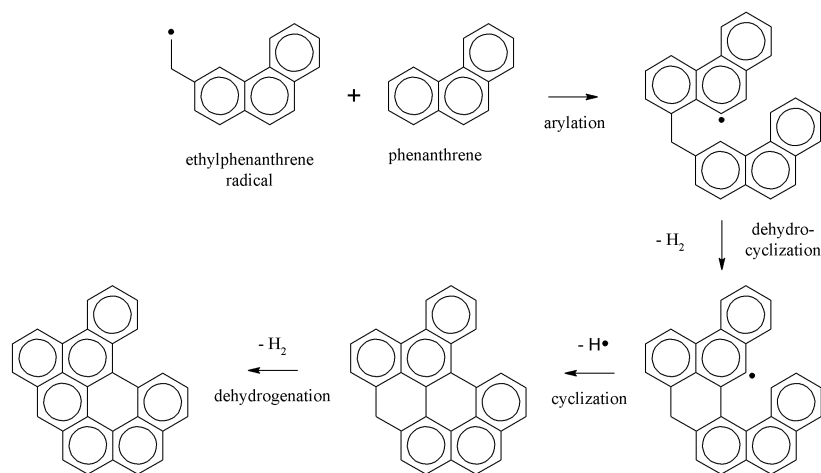


Figure 14. Proposed PAH condensation reaction.

bed of cracking catalyst. Others are removed with a hydrotreater or a guard bed loaded with a sulfur-selective sorbent.

### 3.7 Reaction Kinetics

Due to the tremendous complexity of heavy petroleum fractions, lumping is used to formulate reaction kinetics for conversion units. The simplest schemes treat the feed as a single entity, assume first-order kinetics and use empirical correlations to adjust for product objectives and feed properties, such as density, distillation, sulfur, nitrogen, olefins, and CCR. These models may seem austere, but they have been used for the design of commercial units since the early 1960s.

Recently, Hu, et al.<sup>13</sup> used a steady-state hydrotreater model (HTR-SIM) in combination with typical single-lump kinetics to monitor the performance of a commercial HDS unit in Japan. The equations used to model the conversion of feed sulfur into product sulfur are:

1.  $k_{\text{HDS}} = (\text{LHSV}) \ln (S_{\text{F}}/S_{\text{P}})$
2.  $k_{\text{HDS}} = [(\text{LHSV})/(n-1)](S_{\text{P}}^{(1-n)} - S_{\text{F}}^{(1-n)})$
3.  $k_{\text{T}} = (k_0) \exp[-E_a/RT]$

where  $k_{\text{HDS}}$ ,  $K_{\text{T}}$ , and  $K_0$  are rate constants, LHSV is the liquid hourly space velocity,  $n$  is the reaction order,  $S_{\text{P}}$  is the product sulfur concentration,  $S_{\text{F}}$  is the feed sulfur concentration,  $E_a$  is the activation energy,  $R$  is the gas-law constant, and  $T$  is temperature. Equation 1 is used for any 1<sup>st</sup> order process in which one material is transformed into another. Equation 2 applies to any  $n^{\text{th}}$  order process in which  $n \neq 1$ . Equation 3 is the well-known Arrhenius expression for calculating the effect of temperature on reaction rate. For single-lump HDS kinetics,  $E_a$  ranges between 100 and 140 kJ/mol.  $E_a$  varies with feed composition, catalyst type, and reaction conditions.

Sue and Sugiyama,<sup>14</sup> Steinberg et al.,<sup>15</sup> and Mohanty et al.<sup>16</sup> have written reviews of kinetic studies on hydrocracking reactions. In most of the cited literature, pure compounds or simple mixtures were processed in small isothermal reactors. For example, a publication by Rappaport<sup>17</sup> reported that the rate of hydrocracking for pure normal paraffins increases as shown in Table 5.

Table 5. Relative Rates of Hydrocracking for Pure n-Paraffins

| Carbon Number   | Relative Rate |
|-----------------|---------------|
| C <sub>5</sub>  | 1             |
| C <sub>10</sub> | 32            |
| C <sub>15</sub> | 72            |
| C <sub>20</sub> | 120           |

Figure 15 and Table 6 show data from an especially informative study by Filimonov, et al.,<sup>18</sup> which determined relative reaction rates for different

classes of compounds at temperatures between 716°F and 482°F (380°C and 450°C). In the table, negative relative rates indicate that a reverse reaction is faster than its corresponding forward reaction. In agreement with Section 3.1, the rates of aromatics saturation reactions decrease at higher temperature.

*Table 6. Relative Rates for Groups of Hydrocracking Reactions (as Shown in Figure 15)*

| Rxn No. | Reactants / Products  | Reaction Type | Relative Reaction Rate at: |       |       |       |
|---------|---|---------------|----------------------------|-------|-------|-------|
|         |   |               | 380°C                      | 400°C | 425°C | 450°C |
| 1       | Pyrenes, chrysenes / Polybenzonaphthenes                            | Saturation    | –                          | –     | –     | –     |
| 2       | Phenanthrenes / Dinaphthenobenzenes, acenaphthenes, fluorenes       | Saturation    | –                          | –     | –     | –     |
| 3       | Naphthalenes / Indanes  | Saturation    | 0.6                        | 0.5   | 0.5   | 0.5   |
| 4       | Polybenzonaphthenes / Dinaphthenobenzenes, acenaphthenes, fluorenes | Saturation    | –                          | –     | –     | –     |
| 5       | Benzonaphthenes / Dinaphthenobenzenes, acenaphthenes, fluorenes     | Saturation    | 3.7                        | 3.0   | 2.6   | 2.4   |
| 6       | Indanes / Alkylbenzenes   | Ring opening  | 4.2                        | 3.5   | 3.4   | 3.2   |
| 7       | Alkylbenzenes / Single-ring naphthenes                              | Saturation    | 4.5                        | 2.4   | 0.3   | -0.8  |
| 8       | Polycyclic naphthenes / Three-ring naphthenes                       | Ring opening  | 1.0                        | 1.0   | 1.0   | 1.0   |
| 9       | Three-ring naphthenes / Two-ring naphthenes                         | Ring opening  | 1.1                        | 1.6   | 1.9   | 2.1   |
| 10      | Two-ring naphthenes / Single-ring naphthenes                        | Ring opening  | 1.3                        | 1.7   | 2.7   | 3.1   |
| 11      | Single-ring naphthenes / Paraffins                                  | Ring opening  | 0.9                        | -1.8  | -2.8  | -3.2  |
| 12      | Long paraffins / Short paraffins                                    | Cracking      | 0.3                        | 2.1   | 3.3   | 3.8   |
| 13      | Alkylbenzenes / Methyl benzenes, paraffins                          | Cracking      | 2.2                        | 2.9   | 3.4   | 4.1   |

In 1974, Stangeland<sup>19</sup> developed a pseudo-component approach to the modelling of conversion kinetics in hydrocrackers. Conceptually, he divided the feed and products into a set of 50°F-wide slices – 100°F to 150°F, 150°F to 200°F, etc. He then built a set of rate expressions for converting higher-boiling slices into lower-boiling slices and linked them with an expression that reflects the fact that heavy hydrocarbons react faster than light ones:

$$k_{(T)} = k_0[T + A(T^3 - T)]$$

In this equation,  $T = \text{TBP}/1000$  (TBP = true boiling point) and  $A$  is a tuning parameter that usually falls between 0 and 1.

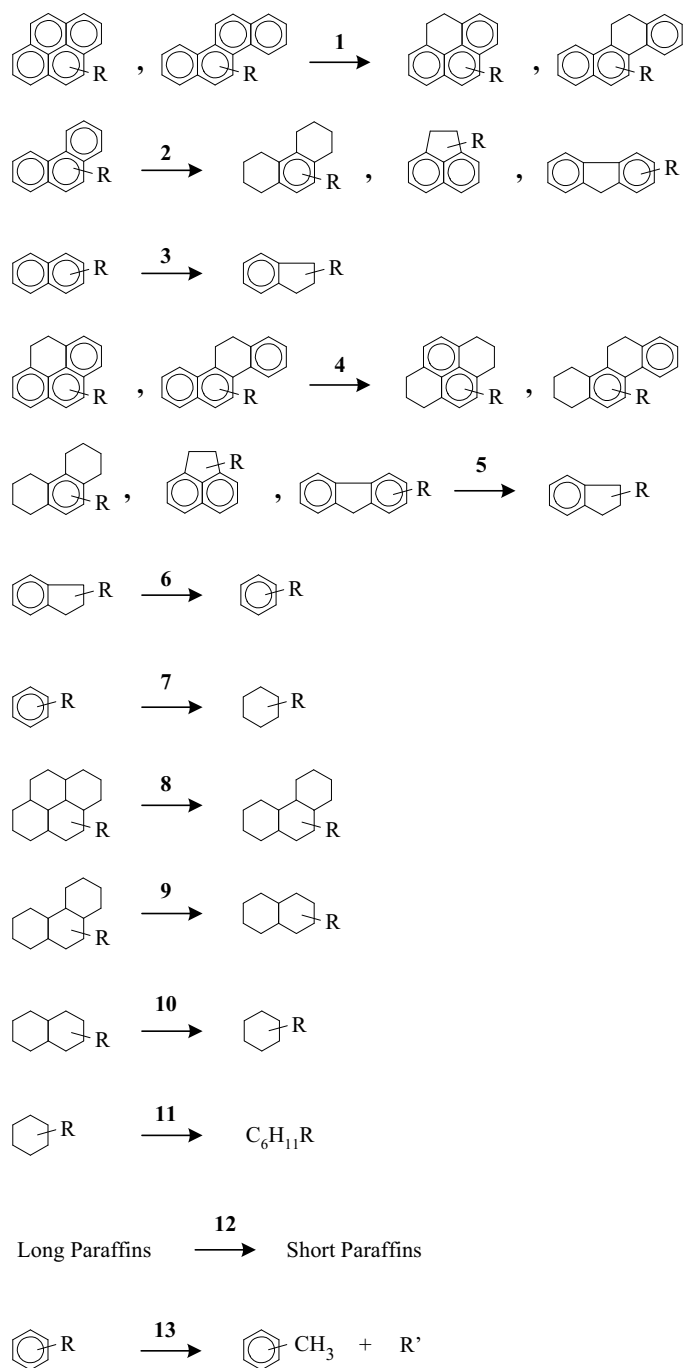


Figure 15. Hydrocracking reaction chain for polyaromatic and naphtheno-aromatic compounds, per Filimonov, et al.<sup>18</sup> The relative rates of Reactions 1 to 12 are shown in Table 6.

During the past 20 years, academic and industrial researchers developed composition-based kinetic models with hundreds or even thousands of lumps and pure compounds. The QSRC (quantitative structure-reactivity correlation) and LFER (linear free energy relationship) lumping techniques are discussed in Chapter 20 by Professor Klein and Chapter 9 by Professor Mochida. The structure-oriented lumping (SOL) approach of Quann and Jaffe<sup>20,21</sup> yields models rigorous enough for use in closed-loop real-time optimizers (CLRTO), which automatically adjust setpoints for commercial process units several times each day.<sup>22</sup>

In the composition-based model developed by Lapinas, et al.,<sup>10</sup> and applied to a commercial hydrocracker by Pedersen, et al.,<sup>22</sup> rate equations are based on the Langmuir-Hinshelwood-Hougen-Watson (LHHW) mechanism for heterogeneous reactions. In brief, the LHHW mechanism describes (a) the adsorption of reactants to acid and metal sites on a catalyst surface, (b) reactions between the reactants, including saturation, cracking, ring opening, dealkylation, HDS, HDN, etc., and (c) desorption of products. Inhibition effects are modelled, too. These include the adsorption of organic nitrogen to acid sites and the inhibition of HDS reactions by H<sub>2</sub>S.

Rigorous, flow-sheet-based models for hydrocrackers include sub-models for furnaces, pumps, compressors, reactors, quench zones, flash drums, recycle gas scrubbers, fractionation towers, and – importantly – economic data. As discussed in Chapter 23 by Mudt, et al., such models can comprise hundreds of reactions and hundreds of thousands of equations. The model grows when inequalities are included to ensure a feasible solution that honors process constraints. To solve such models in real time (i.e., in less than an hour), open-equation mathematics and high-powered solvers are used.

#### 4. HYDROPROCESSING CATALYSTS

Recent books by Magee and Dolbear<sup>23</sup> and by Scherzer and Gruia<sup>2</sup> are superb sources of technical information on hydroprocessing catalysts, which are also discussed in Chapters 9-12. The hydroprocessing catalyst business is big, with annual sales approaching US\$800 million per year. The materials most commonly used to make these catalysts are shown in *Table 7* and *Table 8*.

*Table 7.* Supports Used in Hydroprocessing Catalysts

| Support                      | Major Use                                    | Acidity   |
|------------------------------|--|-----------|
| $\gamma$ -Alumina            | Hydrotreating catalysts                      | Low       |
| Amorphous aluminosilicates   | Distillate-selective hydrocracking catalysts | High      |
| Zeolites (X, Y or mordenite) | High-stability hydrocracking catalysts       | Very high |

Table 8. Active Metals Used in Hydroprocessing Catalysts

| Metals  | Major Use          | Activation Method           | Hydrogenation Acitivity |
|---------|--------------------|-----------------------------|-------------------------|
| CoMo    | HDS                | Sulfiding                   | Moderate                |
| NiMo    | HDN, hydrocracking | Sulfiding                   | High                    |
| NiW     | HDN, hydrocracking | Sulfiding                   | Very high               |
| Pd, Pt* | Hydrocracking      | Reduction by H <sub>2</sub> | Highest                 |

\*Pd and Pt are poisoned by sulfur and can only be used in low-H<sub>2</sub>S environments

In fixed-bed hydroprocessing units, the catalysts must be able to drive the desired reactions, but they also must possess a high surface area and great physical strength, enough to resist crushing under the forces imposed by rapidly flowing high-pressure fluids and the weight of the catalyst itself. A single bed can contain several hundred of tons of catalyst.

Chemical reactions take place inside small pores, which account for most of the catalyst surface area. The diameters of these pores range from 75Å to 85Å for catalysts that process light and heavy gas oils. For catalysts that process residue, the average pore size ranges from 150Å to 250Å.

## 4.1 Catalyst Preparation

The following steps may be used to prepare the supported metal catalysts used in hydrotreaters and hydrocrackers.<sup>2,23</sup>

- Precipitation
- Filtration (or centrifugation), washing and drying
- Forming
- Calcining
- Impregnation
- Activation

Other steps, such as kneading, mulling, grinding, and/or sieving also may be used. For some catalysts, some of the above-listed steps are eliminated or additional steps are added. For example, if mulling is used to mix active metals with a support, precipitation and impregnation may not be needed.

### 4.1.1 Precipitation

In the catalyst world, precipitation involves combining two solutions to form a desired solid. For example, mixing an aqueous solution of aluminum nitrate [Al(NO<sub>3</sub>)<sub>3</sub>] with sodium aluminate [Na<sub>2</sub>Al<sub>2</sub>O<sub>4</sub>] yields aluminum hydroxide [Al(OH)<sub>3</sub>], which forms a gelatinous solid. As the gel ages, tiny crystals grow larger and a pore structure starts to develop.

The zeolites used in hydrocracking catalysts also are prepared by precipitation. Zeolites occur naturally, but the ones used for catalysis are synthetic. *Figure 16* outlines a common procedure for synthesizing Na-Y and H-Y zeolites.

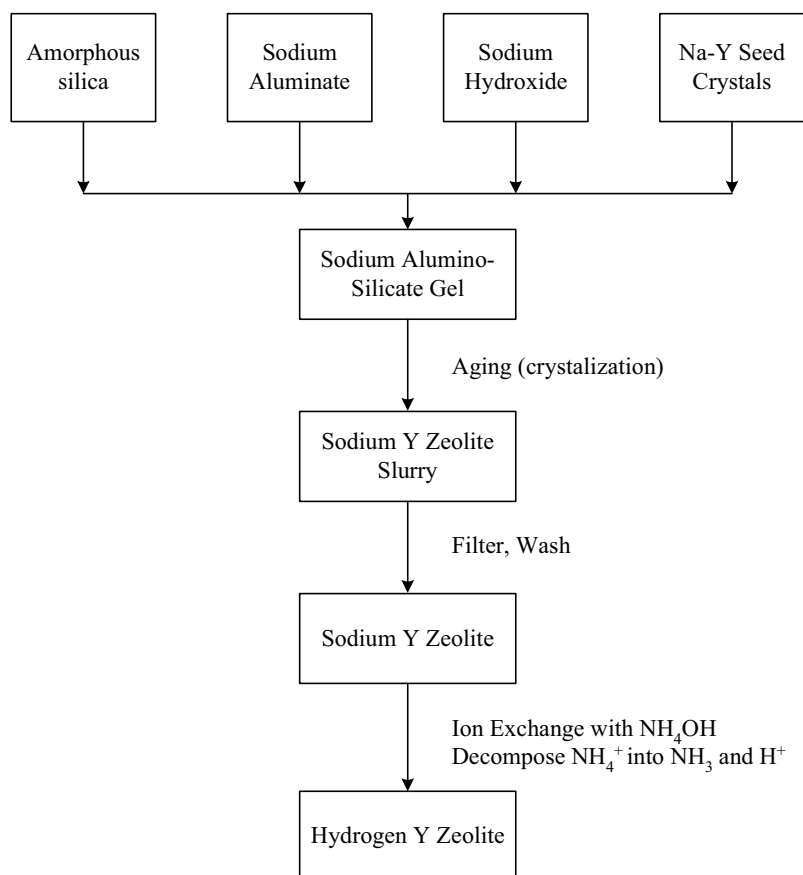


Figure 16. Synthesis procedure for H-Y zeolite.

These remarkable aluminosilicates can be used as drying agents, ion-exchangers, and molecular sieves for gas separation. Their microporosity provides them with high surface area, and they can be converted into solid acids with superb catalytic activity.

The Al(III) atoms in zeolites replace Si(IV) atoms in a  $\text{SiO}_2$  superstructure. To maintain a neutral charge, every aluminum atom must be accompanied by a counter-ion such as  $\text{Na}^+$ ,  $\text{K}^+$ ,  $\text{H}^+$ ,  $\text{NH}_4^+$ , etc. Counter ions can be swapped via ion exchange. When Na-Y zeolite is exchanged with an ammonium salt, the  $\text{Na}^+$  ion is replaced by  $\text{NH}_4^+$ . When  $\text{NH}_4$ -Y is heated to the right temperature, the ammonium ion decomposes, releasing  $\text{NH}_3$ (gas) and leaving behind highly acidic H-Y zeolite.

The synthetic zeolites used in catalysts for hydrocracking include X, Y, mordenite and ZSM-5. The latter is made by including a soluble organic

template, such as a quarternary ammonium salt, in the mix of raw materials. ZSM-5 is used for catalytic dewaxing. Due to its unique pore structure, it selectively cracks waxy n-paraffins into lighter molecules. It is also used in FCC catalysts to increase propylene yields.

#### 4.1.2 Filtration, Washing and Drying

Filtration, washing and drying remove undesired impurities. In our  $\text{Al}(\text{OH})_3$  example, sodium nitrate is washed away with water. Sometimes, ammonium hydroxide is added to expedite sodium removal. Subsequent air- and oven-drying removes most of the excess water and initiates the transformation of  $\text{Al}(\text{OH})_3$  into alumina [ $\text{Al}_2\text{O}_3$ ].

#### 4.1.3 Forming

Catalyst and support precursors can be formed into extrudates, spheres or pellets. Extrudates are generated by forcing a paste (e.g., a mixture of powdered  $\gamma$ -alumina with water) through a die. Adding peptizing agents such as nitric acid increases the average pore size of the product. Raising the extrusion pressure tends to decrease the average pore size.

The resulting spaghetti-like strands are dried and broken into short pieces with a length/diameter ratio of 3 to 4. The particles are dried then calcined. In our alumina example, calcination decomposes residual ammonium nitrate. It also hardens the particles and completes the conversion of  $\text{Al}(\text{OH})_3$  into  $\text{Al}_2\text{O}_3$ . The preferred alumina for catalyst supports is  $\gamma$ -alumina, also known as bohemite. This material has a high surface area, great physical strength, and a well-defined network of pores. If the calcination temperature gets too high,  $\gamma$ -alumina transforms into  $\alpha$ -alumina or  $\beta$ -alumina, whose physical properties are far less desirable.

An extrudate cross-section can be circular or shaped like 3-leaf or 4-leaf clover without the stem (see Chapter 8 by Adrian Gruia). Compared to cylindrical extrudates, clover-leaf ("multi-lobe") catalysts have a higher surface-to-volume ratio. In trickle-bed hydroprocessing reactors, they have less resistance to diffusion and lower pressure drop. Spherical catalysts are made (a) by spray-drying slurries of catalyst precursors, (b) by spraying liquid onto powders in a tilted rotating pan, or (c) by dripping a silica-alumina slurry into hot oil.<sup>2</sup> Pellets are made by compressing powders in a die.

#### 4.1.4 Impregnation

Impregnation is a common technique for distributing active metals within the pores of a catalyst support. Calcined supports are especially porous. Like sponges, they use capillary action to suck up aqueous solutions containing



active metals. For some catalysts, the support is soaked in excess metal-containing solution, which saturates the pores fully.

In the “incipient wetness” method, precise amounts of solution are added – just enough to leave the support dry to the touch. After a drying step, addition solution may be added to increase loading of the same or different active metal.

#### 4.1.5 Activation

Prior to use, most non-noble-metal catalysts are activated (“sulfided”) by circulating hydrogen and a light, sulfur-containing start-up oil through the catalyst. Often, the start-up oil is spiked with dimethyl sulfide ( $\text{CH}_3\text{-S-CH}_3$ ) or dimethyl disulfide ( $\text{CH}_3\text{-S-S-CH}_3$ ). The temperature is raised slowly to the decomposition temperature of the sulfiding agent. The process continues until breakthrough, i.e., the point at which significant amounts of  $\text{H}_2\text{S}$  appear in the recycle gas. After breakthrough, sulfiding continues until the catalyst is completely saturated with sulfur.

During “dry sulfiding,” a mixture containing 2 to 5 vol%  $\text{H}_2\text{S}$  in hydrogen is circulated through the catalyst. The temperature is increased slowly to the temperature at which the unit is expected to operate. The process continues until the exit gas contains the same amount of  $\text{H}_2\text{S}$  as the inlet gas.

Most manufacturers offer pre-sulfided catalysts, which allow a refiner to shorten the start-up of a unit by two or three days. That may not seem like much, but for a 40,000 barrel/day FCC feed pretreater, it can generate up to US\$500,000 in extra income.

#### 4.1.6 Noble-Metal Catalysts

Some hydrocracking catalysts contain highly dispersed platinum or palladium. These noble metals are expensive, but their loading is low – 0.6 to 1.0 wt% – and their high activity justifies the cost. They are added by impregnation with tetraamine complexes –  $\text{Pt}(\text{NH}_3)_4^{2+}$  or  $\text{Pd}(\text{NH}_3)_4^{2+}$ . When the catalysts are heated in air to about 840°F (450°C), the complexes decompose, giving off ammonia and leaving behind divalent metal oxides. In commercial hydrocrackers, catalysts containing noble-metal oxides are activated by direct reduction with high-pressure hydrogen at 700°F (350°C).

## 4.2 Hydrotreating Catalysts

Hydrotreating catalysts comprise oxides of either Mo or W and either Co or Ni on a support comprised of  $\gamma$ -alumina. Usually, CoMo catalysts are used for HDS. NiMo catalysts are used for HDS and HDN. NiW catalysts are especially active for the saturation of aromatics. Typical physical properties are shown in Table 9.

Hydrotreating catalyst particles are surprisingly small, with diameters of 1.5 to 3.0 mm and length/diameter ratios of 3 to 4. In many units, ceramic balls and/or successively larger catalyst particles are loaded on top of the first catalyst bed. This “graded bed” protects the bulk of the catalyst by filtering particulate matter out of the feed.

Table 9. Physical Properties for Hydrotreating Catalysts

| Property   | Low | High |
|--|-----|------|
| Surface area, m <sup>2</sup> /gram                     | 150 | 250  |
| Pore volume, ml/gram                                   | 0.5 | 1.0  |
| Pore diameter (average), Ångströms                     | 75  | 250  |
| Bulk density, lbs/ft <sup>3</sup>                      | 30  | 60   |
| Bulk density, kg/m <sup>3</sup>                        | 490 | 980  |
| Co or Ni (as CoO or NiO), wt%                          | 3   | 8    |
| Mo or W (as MoO <sub>3</sub> or WO <sub>3</sub> ), wt% | 10  | 30   |

### 4.3 Hydrocracking Catalysts

Commercial hydrocracking catalysts comprise active metals on solid, highly acidic supports. The active metals are Pd, NiMo or NiW, all of which catalyze both hydrogenation and dehydrogenation reactions. The most common supports are synthetic crystalline zeolites and amorphous silica-aluminas.

Hydrocracking catalyst shapes can be spherical or cylindrical, with gross dimensions similar to those for hydrotreating catalysts.

As already mentioned, in most hydrocrackers, the first few catalyst beds contain a high-activity HDN catalyst, which also is active for HDS, saturation of olefins, and saturation of aromatics. Other hydrocrackers use a bifunction catalyst – one that is active for both hydrotreating and hydrocracking – in all catalyst beds.

### 4.4 Catalyst Cycle Life

Catalyst cycle life has a major impact on the economics of fixed-bed refinery units, including hydrotreaters and hydrocrackers. Cycles can be as short as 12 months and as long as 60 months. Two-year cycles are typical. At the start of a cycle, average reactor temperatures are low – 580°F to 660°F (304°C to 349°C). As the cycle proceeds, the catalyst deactivates and refiners must raise temperatures to maintain conversion. A catalyst cycle is terminated for one of the following reasons, whichever occurs first. Note that only one of the listed events relates directly to catalyst activity.

1. **The temperature required to achieve the unit’s main process objective hits a metallurgical limit.** Or alternatively, the main process objective can be met only at reduced feed rate. To ensure safe operation, the maximum

average reactor temperature is about 760°F (404°C) and the maximum peak temperature is about 800°F (427°C).

2. **Side reactions are starting to cause process or economic problems.** If the production of light gases exceeds the capacity of one or more towers in the downstream gas plant, operators must decrease feed rate or reduce conversion. Both options are expensive. Excess gas production consumes expensive hydrogen and converts it into low-value LPG. This also is expensive. Running at high temperature decreases selectivity to middle distillates and increases aromatics in middle distillates. At some point, due to one or more of these factors, refinery-wide economics show that it's better to shut down for a catalyst change versus trying to keep limping along – even though metallurgical limits have not yet been reached.
3. **The recycle compressor cannot overcome pressure drop across the unit.** The overall pressure drop is the difference in pressure between the recycle compressor suction and the recycle compressor discharge. At start-of-run, the pressure drop across the catalyst is low – 3 to 10 psi (0.2 to 0.7 bar) for each bed – but it increases as the run proceeds. Usually, the increase is largest in the first catalyst bed, which is most susceptible to fouling. Attempts to continue running a unit despite very high pressure drop can deform the quench-deck support beams inside a reactor.
4. **A related unit has to shut down for more than a few weeks.** Related units might include an upstream vacuum distillation unit, an upstream hydrogen source, or a downstream FCC unit. In refineries with enough intermediate tankage, hydroprocessing units can continue to run for a few days despite an interruption in the supply of liquid feed, but a loss of hydrogen supply can cause an immediate shut-down. At best, if the unit gets hydrogen from multiple sources, the feed rate must be reduced.
5. **Major process upsets.** Most process upsets are caused by sudden changes in feed quality. For a fixed-bed VGO hydrotreater, a slug of residue can poison part of the catalyst with trace metals such as Fe, Ni, V, and/or Si; or foul it with particulates, asphaltenes and/or refractory carbon. In fixed-bed units, poisoning and fouling usually are confined to the top few feet of the first catalyst bed. If so, the ruined catalyst can be skimmed off the top and replaced during a brief, scheduled shutdown. A brief, scheduled shut-down does not require a cycle-ending catalyst change-out.
6. **Equipment failure.** Hardware problems occur most frequently in rotating equipment – pumps and compressors. Fortunately, many problems can be detected in advance, allowing operators to schedule a brief shut-down for preventive maintenance.

Process variables that increase or decrease the rate of catalyst deactivation are shown in Table 10.

Table 10. Factors Affecting Catalyst Cycle Life

|   | Effect on Cycle Life | Comment  |
|---|----------------------|--|
| Higher H <sub>2</sub> partial pressure    | +                    |  |
| Higher recycle gas rate                   | +                    | Increases H <sub>2</sub> partial pressure  |
| Higher makeup gas purity                  | +                    | Increases H <sub>2</sub> partial pressure  |
| Increased purge of recycle gas            | +                    | Increases H <sub>2</sub> partial pressure  |
| Higher fresh feed rate                    | -                    |  |
| Higher conversion                         | -                    |  |
| Higher fresh feed endpoint                | -                    | Increases rate of catalyst coking. Also can increase pressure-drop buildup rate. |
| Higher fresh feed impurities <sup>1</sup> | -                    | Related to feed type and feed endpoint   |
| Process upsets <sup>2</sup>               | -                    |  |

1. Deleterious feed impurities include sulfur, nitrogen, refractory carbon, asphaltenes, metals (nickel, vanadium, iron, silicon) and particulate matter (coke fines, FCC catalyst fines).
2. Process upsets include "burps" in upstream units that feed the hydrocracker, equipment failures (typically, loss of a feed pump or compressor) or temperature excursions requiring de-pressuring.

Hydrogen keeps the catalyst clean by inhibiting coke formation. This explains why increasing the hydrogen partial pressure decreases the rate of catalyst deactivation.

Raising the temperature increases the rates of most hydrocracking reactions, including coke formation. Raising the hydrogen/oil ratio increases heat removal, which limits temperature rise.

If the feed rate goes up and targets for HDS, HDN or conversion remain the same, the temperature must go up. If the feed rate goes up and the temperature does not, then HDS, HDN or conversion will decrease.

Increasing the feed endpoint and/or density tends to increase the amount of coke precursors in the feed. The precursors include asphaltenes, refractory carbon, and PAH.

#### 4.4.1 Catalyst Regeneration and Rejuvenation

After working 24/7 for a year or two (or in some cases five) in a fixed-bed hydroprocessing unit, the catalyst is spent. The entire unit is shut down and catalyst is removed. During the shut-down, which typically lasts 3 to 4 weeks, refiners inspect and repair equipment. Meanwhile, the catalyst is shipped to an off-site facility, where it is regenerated by controlled combustion in air, air plus oxygen, or air plus steam. During combustion, accumulated coke is converted to CO<sub>2</sub> and CO plus small amounts of SO<sub>2</sub> and NO<sub>x</sub>, which are formed from the sulfur and nitrogen in the coke. Typically, the temperature used for regeneration in air is (750°F to 930°F) 400°C to 500°C.

The regenerated catalyst may also undergo rejuvenation, a wet process in which the active metals are chemically re-dispersed. A combination of regeneration and rejuvenation can restore a catalyst to more than 95% of its original activity.

Inevitably, some particles break apart during the unloading, transportation, regeneration, and rejuvenation of spent catalysts. If part of the catalyst is

contaminated with excessive amounts of Fe, Ni, V, or Si, that part cannot be regenerated. Typically, losses due to fragmentation and fouling amount to 10 to 15%.

In the bad old days, regeneration meant burning coke off the catalyst while it was still inside the reactor. Today, “in situ” regeneration is rare because it is hard to control and often gives poor results. A poor regeneration is costly, because afterwards the unit’s performance will be poor. With a crippled catalyst, the unit may have to limp along for several months at lower feed rates and/or lower severity. Worst of all, the catalyst won’t last long, which means that it will have to be regenerated or replaced sooner rather than later.

#### 4.4.2 Catalyst Reclamation

Even though noble-metal hydrocracking catalysts contain only small amounts of Pd or Pt, these metals are so expensive that recovering the metals is more cost-effective than throwing them away. Other hydroprocessing catalysts contain Mo or W, Ni, and/or Co. Spent hydrotreating catalysts – especially those used to hydrotreat residue – can be very rich in vanadium, richer than many ores.

Reclamation companies convert these materials into salable products using different combinations of oxidation, pyrolysis, dissolution in acid or alkali, precipitation, extraction or ion exchange. Depending on the process used, the salable products may include several of the materials shown in Table 11.

The book by Scherzer and Gruia<sup>2</sup> provides a well-written description of catalyst reclamation processes used by four major companies – CRI-MET, Eurecat, Gulf Chemical, and TNO/Metrex.

Table 11. Some of the Materials Sold by Catalyst Reclamation Companies

| Material                         | Formula  |
|----------------------------------|--|
| Palladium metal or chloride salt | Pd or Na <sub>2</sub> PdCl <sub>4</sub>  |
| Platinum metal or chloride salt  | Pt or Na <sub>2</sub> PtCl <sub>4</sub>  |
| Molybdenum trisulfide            | MoS <sub>3</sub>   |
| Molybdenum oxide                 | MoO <sub>3</sub>   |
| Ammonium molybdate               | (NH <sub>4</sub> ) <sub>2</sub> Mo <sub>4</sub> O <sub>13</sub> •2H <sub>2</sub> O   |
| Sodium molybdate                 | Na <sub>2</sub> MoO <sub>4</sub> •2H <sub>2</sub> O                                  |
| Tungsten trioxide                | WO <sub>3</sub>  |
| Ammonium para-tungstate          | (NH <sub>4</sub> ) <sub>10</sub> W <sub>12</sub> O <sub>41</sub> •5 H <sub>2</sub> O |
| Sodium tungstate                 | Na <sub>2</sub> WO <sub>4</sub> •2H <sub>2</sub> O                                   |
| Vanadium pentoxide               | V <sub>2</sub> O <sub>5</sub>  |
| Sodium (meta) vanadate           | NaVO <sub>3</sub>  |
| Nickel metal or chloride         | Ni or NiCl <sub>2</sub>  |
| Cobalt metal or chloride         | Co or CoCl <sub>2</sub>  |
| Nickel-cobalt concentrate        | Ni <sub>x</sub> Co <sub>y</sub>  |
| Iron-molybdenum concentrate      | Fe <sub>x</sub> Mo <sub>y</sub>  |
| Alumina hydrate                  | Al <sub>2</sub> O <sub>3</sub> •3H <sub>2</sub> O                                    |

## 5. PROCESS FLOW

### 5.1 Trickle-Bed Units

Most hydrotreaters and hydrocrackers are trickle-bed units. A classic article by Satterfield<sup>24</sup> describes the fundamental behaviour of such units, in which mixtures of liquid and gaseous reactants pass down over fixed beds of catalyst. In hydroprocessing units, the liquid reactants are petroleum fractions, and the gaseous reactant is hydrogen.

Figure 17 shows a flow scheme for a once-through unit designed to process heavy gas oil feeds. Designs offered by major process licensors can differ in several areas.

(1) **Heaters.** Units with gas-only heaters mix hot gas with pre-heated liquid feed just before the reactants enter the first reactor. Other designs use a gas-plus-oil heater to bring the mixed fluids up to reaction temperature.

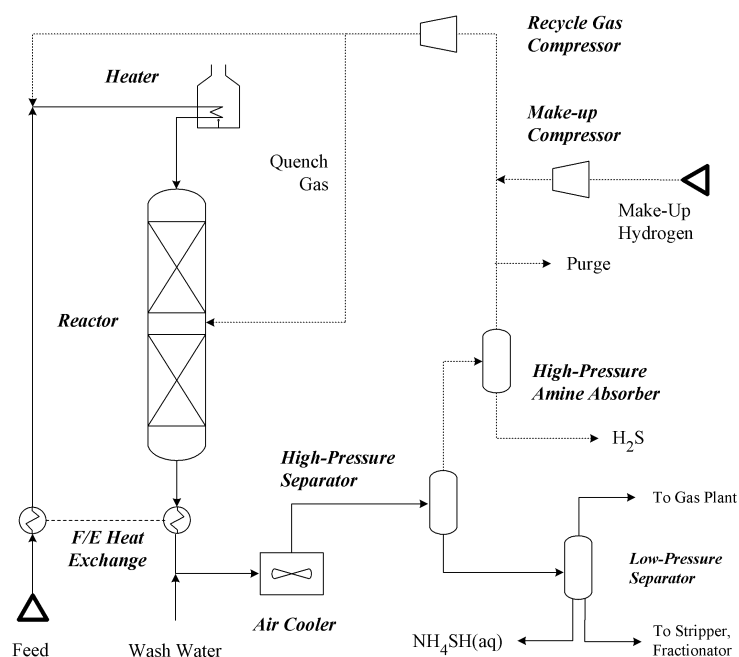


Figure 17. Once-through hydroprocessing unit: two separators, recycle gas scrubber.

(2) **Reactors, Catalyst Beds and Quench Zones.** As shown in Table 4, most hydroprocessing reactions are exothermic. The heat released in naphtha and kerosene hydrotreaters is relatively low, so units designed for these feeds may use just one reactor that contains a single catalyst bed. However, for heavier feeds and/or feeds that contain large amounts of sulfur, aromatics or

olefins, the total increase in temperature can exceed 180°F (100°C). It is unsafe to allow that much temperature rise in a single bed of catalyst. To divide the heat release into smaller, safer portions, commercial units use multiple catalyst beds with cooling in between. A unit can have one bed per reactor, or multiple beds in each reactor with quench zones in between. For simplicity, Figure 18 shows only 2 catalyst beds, but most hydrocrackers have more; some have as many as 30!

In a quench section (*Figure 18*), hot process fluids from the preceding bed are combined with relatively cold hydrogen-rich quench gas before the mixture passes into the next bed. We can think of a catalyst bed as a stack of thin, horizontal discs. Ideally, the top disc is the coolest, the bottom disc is the hottest, and at every point in each given disc, temperatures are identical. But in real units, the downward flow of reactants is never perfectly uniform, so the temperatures within the discs are different, especially near the bottom.

The difference between the highest and lowest temperature at the bottom of a catalyst bed is called the “radial temperature difference” (RTD). The truth is, we never know the actual highest and lowest temperature, because we can’t place thermocouples everywhere. But if the measured RTD is small – less than 5°F (3°C) – we can assume that the actual RTD also is small, and that flow through the bed is nearly uniform. If the measured RTD is large, the actual RTD is almost certainly larger, and we have to be concerned about hot spots, flow blockages, and other potentially dangerous symptoms of mal-distribution.

Modern quench sections are designed to do three things: (a) to lower the overall temperature of the reacting fluids, (b) to reduce radial mal-distribution with radial mixing, and (c) to redistribute the reactants and deliver them to the next bed. The major parts of a quench deck are the quench tube, the liquid collector and re-distributor, the gas/liquid mixing zone, and the final distributor.

Quench tubes bring quench gas into the reactor. Some are very simple – just a tube with a series of holes in it. Others, such as the ExxonMobil “spider vortex” design, are more complex, distributing gas horizontally through several “spokes” to different parts of the quench deck.

In the liquid collector and re-distributor, liquids are forced to flow down two angled slides into a raceway. The slides give the liquids some angular momentum, and the raceway gives them time to mix. More than anything else, this part of the quench deck reduces RTD.

In the gas/liquid mixing zone, a bubble-cap tray or similar device provides intimate contact between gases and liquids from the redistribution zone. The final distributor sends a fine spray of fluids down to the catalyst bed below.

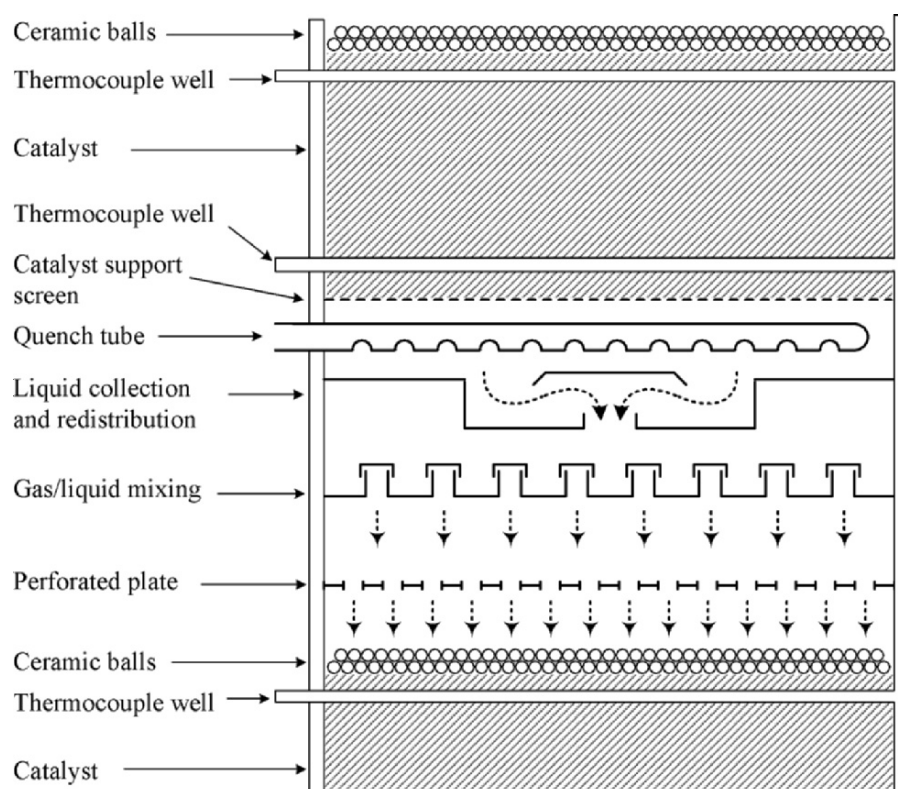


Figure 18. Hydroprocessing reactor: quench zone

In residue hydroprocessing units, heat release is high, but some licensors avoid using intra-reactor quench because residue feeds often form lumps of coked-bonded catalyst in fixed-bed units. In reactors with complex internals, such lumps are very hard to remove during a catalyst change-out. Therefore, fixed-bed residue units often comprise three or more 1-bed reactors in series with quench in between. In many cases, the first reactor is “guard bed” filled with one or catalysts designed to remove metals.

**(3) Catalysts.** Hydrotreaters are loaded either with a CoMo HDS catalyst, a NiMo HDN catalyst, or both. NiMo catalysts are better for the saturation of aromatics, which is required for the removal of hindered sulfur compounds during deep desulfurization. Therefore, some refiners load a layer of NiMo catalyst on top of a CoMo catalysts in diesel desulfurization units. Recently, catalyst manufacturers have been offering trimetallic (CoNiMo) hydrotreating catalysts.

Most of the cracking in hydrocracking units is driven by catalysts with high acidity. The acidic sites are inhibited by organic nitrogen, so the first several catalyst beds in a hydrocracking unit typically contain a high activity HDN catalyst. In a few units, all beds in a hydrocracker are filled with an



amorphous “dual function” catalyst, which catalyzes both HDN and cracking. This type of catalyst has a high selectivity for producing middle distillates from VGO.

As mentioned in Section 3.6, the last bed in a hydrocracker often contains a final layer of “post-treat” catalyst to remove mercaptans.

**(4) Makeup and Recycle Hydrogen.** Compressors for makeup hydrogen are reciprocating machines, most of which are driven by electric motors. Recycle gas compressors can be reciprocating or centrifugal; the latter are often driven by steam. In naphtha hydrotreaters, the high-pressure off-gas can be purer than the makeup gas, because (a) conversion is nil, and (b) liquids in the makeup gas are absorbed by the naphtha. In most other units, the makeup gas is purer than the recycle gas.

Makeup hydrogen can enter the unit at the cold high-pressure separator (CHPS), at the suction of the recycle gas compressor, or at the discharge of the recycle gas compressor. If the makeup comes in at the CHPS, the makeup compressor discharge pressure is lower, which can reduce electricity costs. However, if part of the recycle gas is purged after leaving the CHPS, part of the incoming makeup gas goes right back out again. If the makeup comes in at the discharge of the recycle gas compressor, the discharge pressure of the makeup compressor is higher, but none of the high-purity makeup is lost with purge gas.

**(5) High-Pressure Amine Absorption.** Prior to the advent of ultra-low-sulfur fuels, it was rare to find hydroprocessing units with a high-pressure amine absorber to remove  $H_2S$  from the recycle gas.  $H_2S$  inhibits HDS reactions and lowers the purity of the recycle gas. For both of these reasons, high-pressure amine absorbers are now included in most new and revamped diesel hydrotreaters and mild hydrocrackers.

**(6) Product Cooling and Separation.** Commercial units comprise a number of different product cooling and flash drum configurations. The simplest comprises a feed/effluent heat exchanger train, a large air- or water-cooled heat exchanger, and one or two flash drums.

Heavy-feed units have at least a cold high-pressure separator (CHPS) and a low-pressure separator (LPS). The CHPS overhead stream can go directly to the recycle gas system or through a high-pressure amine absorber for removal of  $H_2S$ . The CHPS bottoms go to the CLPS. Sometimes the pressure differential between the CHPS and the CLPS is used to drive a power recovery turbine. As shown in *Figure 19*, some units include a hot high-pressure separator (HHPS) upstream from the CHPS. The HHPS overhead goes through a cooler to the CHPS, and HHPS bottoms go through a cooler to the LPS. This arrangement provides better heat recovery. In single-stage hydrocrackers with recycle of unconverted oil, hot separation minimizes fouling caused by the accumulation of PAH in the recycle oil.

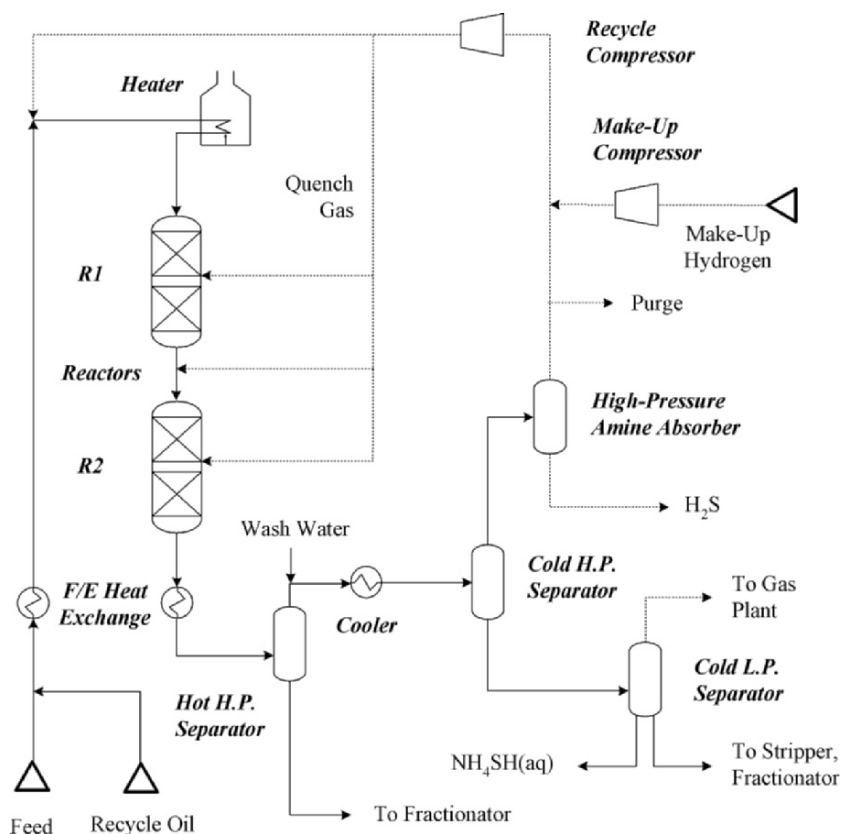


Figure 19. Single-stage hydrocracker: hot H.P. separator, recycle to R1

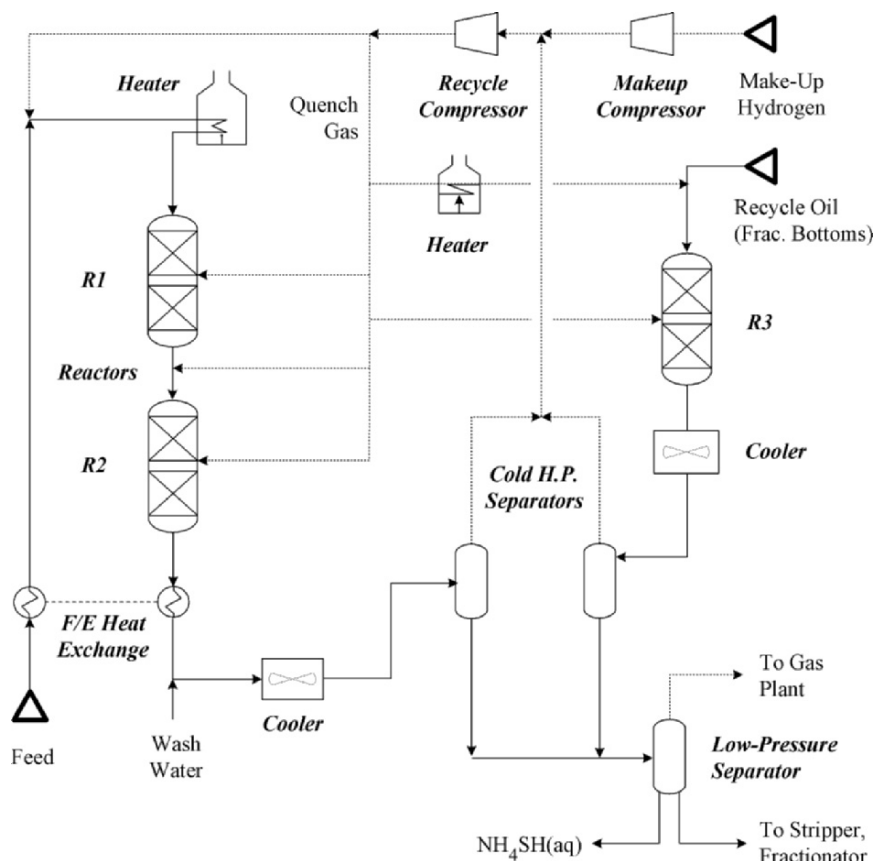
(7) **Wash Water Addition.** As mentioned above, HDS and HDN reactions produce  $\text{H}_2\text{S}$  and  $\text{NH}_3$ , respectively. Wash water is injected into the effluent from the last reactor to convert almost all of the  $\text{NH}_3$  and some of the  $\text{H}_2\text{S}$  into aqueous ammonium bisulfide,  $\text{NH}_4\text{HS}(\text{aq})$ . The  $\text{NH}_4\text{HS}(\text{aq})$  is rejected from the unit as sour water in the low-pressure flash drum.

(8) **Fractionation.** For product fractionation, HDS units that treat naphtha or light gas oil may use a simple steam stripper to remove  $\text{H}_2\text{S}$  and traces of light hydrocarbons from the liquid product (CLPS bottoms). An absorber may be used to recover  $\text{C}_3$ -plus compounds from the CLPS overhead.

Conversion units may employ a full-fledged fractionation train, with a pre-flash tower to remove light ends; an atmospheric fractionator to separate light naphtha, heavy naphtha, middle distillates, and unconverted oil; and a vacuum tower to maximize the recovery of diesel. Some hydrocrackers use the atmospheric tower to produce full-range naphtha, which is then separated into light and heavy fractions in a naphtha splitter.

**(9) Recycle of Fractionator Bottoms.** In full-conversion hydrocrackers, unconverted oil from the fractionator is recycled. Single-stage units with multiple reactors (*Figure 19*) send the recycled oil either to the hydrotreating reactor (R1) via the feed surge drum or to the hydrocracking reactor (R2). Recycle to R1 means that R1 must be larger, but recycle to R2 eliminates an expensive and troublesome high-pressure pump.

*Figure 20* shows a two-stage hydrocracker. In these units, unconverted oil goes to a separate cracking reactor (R3) with its own high-pressure separator.



*Figure 20.* Two-stage hydrocracker: common recycle gas system.

The unit shown in *Figure 20* uses a single makeup and recycle gas system to supply all reactors. In other units, the 2<sup>nd</sup> stage has a separate gas system. Units with a common recycle gas system need only one recycle compressor, but in units with two gas systems, the 2<sup>nd</sup> stage can operate at lower pressure, which can reduce both investment and operating costs. Also, the 2<sup>nd</sup> stage can use sweet gas (no H<sub>2</sub>S) rather than sour, allowing the refiner to employ a wider range of catalysts.

Early fixed-bed hydrocrackers used a “separate hydrotreat” flow scheme, which resembles a 2-stage design with nothing but hydrotreating catalyst in the 1<sup>st</sup> stage. This flow scheme is discussed in further detail in Chapter 8 by Adrian Gruia.

## 5.2 Slurry-Phase Hydrocracking

Slurry-phase hydrocracking converts residue in the presence of hydrogen under severe process conditions – more than 840°F (450°C) and 2000 to 3000 psig (13,891 to 20,786 kPa). To prevent excessive coking, finely powdered additives made from carbon or iron salts are added to the liquid feed. Inside the reactor, the liquid/powder mixture behaves as a single phase due to the small size of the additive particles. Residue conversion can exceed 90%, and the quality of converted products is fairly good.

Unfortunately, the quality of the unconverted pitch is poor, so poor that it can't be used as a fuel unless it is blended with something else – coal or heavy fuel oil. Even then, its high metals and sulfur content can create problems.

At the 5,000 b/d CANMET demonstration plant in Canada, the pitch is sent to a cement kiln for use as clinker. Other slurry-phase processes include COMBIcracking (developed by Veba Oel), Aurabon (UOP), and HDH Cracking (Intevap). Although several slurry-phase demonstration plants have been built, the pitch-disposal problem has kept it from gaining industry-wide acceptance.

## 5.3 Ebullating Bed Units

In contrast to fixed-bed VGO hydrocrackers, ebullating bed units can (and do) process residual oils. In ebullating bed units (*Figure 21*), hydrogen-rich recycle gas is bubbled up through a mixture of oil and catalyst particles. This provides three-phase turbulent mixing, which is needed to ensure a uniform temperature distribution. At the top of the reactor, catalyst is disengaged from the process fluids, which are separated in downstream flash drums. Most of the catalyst is returned to the reactor. Some is withdrawn and replaced with fresh catalyst. The two major ebullating-bed processes are H-Oil, which is offered for license by Axens (IFP), and LC-Fining, which is offered by Chevron Lummus Global. Their main advantages are:

- High conversion of atmospheric residue, up to 90 vol%.
- Better product quality than many other residue conversion processes, especially delayed coking.
- Long run length. Catalyst life does not limit these units. Fresh catalyst is added and spent catalyst is removed continuously. Therefore, barring any mechanical problems, the units can run for a much longer time than fixed-bed residue units.

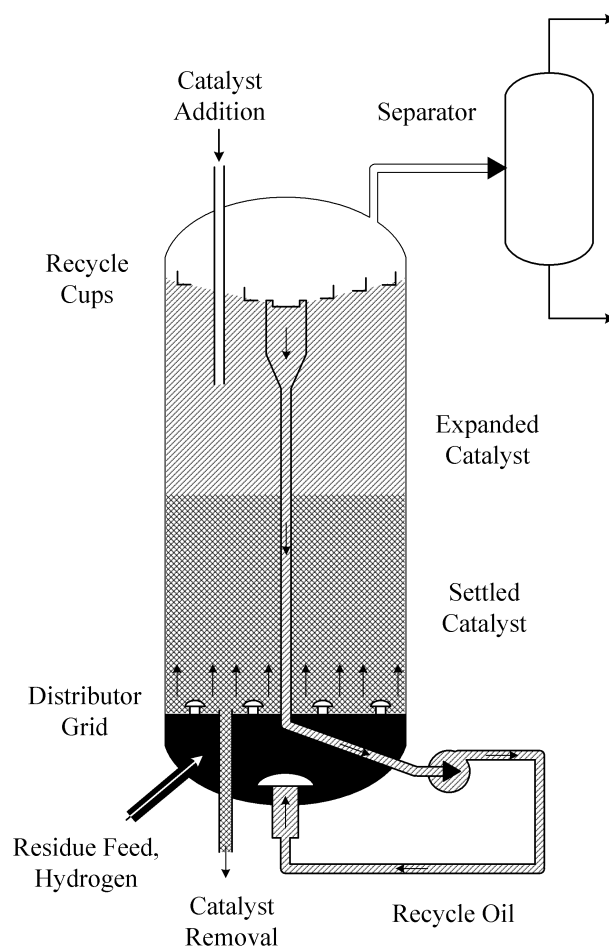


Figure 21. Ebullating bed hydrocracking reactor.

## 6. PROCESS CONDITIONS

For fixed-bed hydroprocessing units, the process conditions – pressure, temperature, space velocity, and catalyst – are determined by feed quality and process objectives. Table 12 shows typical process conditions for the hydrotreating of different feeds in fixed-bed hydrotreating units. The values shown are approximate.

The  $H_2/Oil$  ratios are for units in which off-gas from the high-pressure separator is recycled. For once-through naphtha hydrotreaters associated with catalytic reformers, the  $H_2/Oil$  ratio can be much higher than 350 scf/bbl ( $60 \text{ m}^3/\text{m}^3$ ). For units that treat olefinic cracked stocks from FCC or coking units,  $H_2/Oil$  ratios are higher to control the extra heat released by olefin saturation.

Table 12. Typical Process Conditions for Hydrotreating Different Petroleum Fractions

|                                | Naphtha      | Kerosene     | Diesel       | VGO            | Residue    |
|--------------------------------|--------------|--------------|--------------|----------------|------------|
| WART*                          |              |              |              |                |            |
| °F                             | 530          | 550          | 575 to 600   | 680 to 700     | 700 to 725 |
| °C                             | 277          | 288          | 300 to 315   | 360 to 370     | 370 to 385 |
| H <sub>2</sub> Pressure†       |              |              |              |                |            |
| psig                           | 250 to 450   | 250 to 600   | 600 to 800   | 800 to 2000    | >2000      |
| kPa                            | 1825 to 3204 | 1825 to 4238 | 4238 to 5617 | 5617 to 13,891 | >13,891    |
| LHSV                           | 5            | 4            | 2 to 3       | 0.8 to 1.5     | 0.5        |
| H <sub>2</sub> /Oil Ratio‡     |              |              |              |                |            |
| scf/bbl                        | 350          | 450          | 800          | 1200           | >3000      |
| M <sup>3</sup> /m <sup>3</sup> | 60           | 80           | 140          | 210            | >525       |

\*Approximate weighted average reactor temperature at start of run

†Approximate hydrogen partial pressure at the high-pressure separator

‡Approximate hydrogen-to-oil ratio at the first reactor inlet

## 7. YIELDS AND PRODUCT PROPERTIES

Table 13 illustrates the yield flexibility of recycle hydrocracking. The ability to swing in just a day or two from 90 vol% full-range naphtha to >75 vol% full-range diesel provides unparalleled capability to respond to short-term changes in market conditions – if the refinery has sufficient blending, storage and distribution capacity. To shift the product slate, operators adjust reactor temperatures and change cut points in the fractionation section.

For all process units, product specifications are set to meet refinery-wide objectives. For example, if a refinery wants to produce diesel fuel containing <15 wppm sulfur, and if its hydrocracker makes 40,000 barrels/day of sulfur-free middle distillate, the product sulfur specification for its 20,000 barrels/day distillate hydrotreater (DHT) could be as high as 45 wppm – if a blend of the two streams satisfies the requirements of ASTM D975, which is the standard specification for heavy-duty diesel fuel in the United States. In practice, the DHT sulfur target would be lower than 45 wppm to cushion the refinery against upsets and measurement error. For a diesel fuel containing 10 wppm sulfur, the analytical reproducibility for ASTM Method D5453 is  $\pm 1.8$  wppm. For a diesel containing 50 wppm sulfur, the reproducibility is  $\pm 8.1$  wppm. ASTM D5453 is an x-ray fluorescence method for measuring sulfur in distillate fuels, including ultra-low-sulfur diesel.

## 8. OVERVIEW OF ECONOMICS

### 8.1 Costs

Throughput, operating pressure and process configuration – once-through or recycle of unconverted oil – are the major factors affecting construction costs for hydroprocessing units, which range from \$1000 to \$4000 per daily

barrel. On this basis, a fully-installed 25,000 barrels-per-day hydrocracker can cost between US\$40 million and US\$100 million. These estimates do not include costs for a hydrogen plant and off-site utilities.

Table 13. Feed and Product Properties for a flexible Single-Stage Hydrocracker

| <u>Feedstock Type</u>                        | <u>Straight-run Vacuum Gas Oil</u> |            |               |
|--|------------------------------------|------------|---------------|
| Boiling Range, °C                            | 340 to 550                         |            |               |
| Boiling Range, °F                            | 644 to 1022                        |            |               |
| API Gravity                                  | 22.0                               |            |               |
| Specific Gravity                             | 0.9218                             |            |               |
| Nitrogen, wppm                               | 950                                |            |               |
| Sulfur, wt%                                  | 2.5                                |            |               |
| <u>Product Objective</u>                     | <u>Naphtha</u>                     | <u>Jet</u> | <u>Diesel</u> |
| Weighted Average Reactor Temp, °C            | "base"                             | -6         | -12           |
| Weighted Average Reactor Temp, °F            | "base"                             | -11        | -22           |
| <u>Yields, vol% Fresh Feed</u>               |                                    |            |               |
| C <sub>4</sub>                               | 11                                 | 8          | 7             |
| C <sub>5</sub> -82°C (C <sub>5</sub> -180°F) | 25                                 | 18         | 16            |
| 82°C-plus (180°F-plus) Naphtha               | 90                                 | 29         | 21            |
| Jet A-1 or Diesel                            | ---                                | 69         | 77            |
| Total C <sub>4</sub> -plus                   | 126                                | 124        | 121           |
| Chemical H <sub>2</sub> Consumption          |                                    |            |               |
| Nm <sup>3</sup> /m <sup>3</sup>              | 345                                | 315        | 292           |
| Scf/bbl                                      | 2050                               | 1870       | 1730          |
| <u>Product Qualities</u>                     |                                    |            |               |
| <i>C<sub>5</sub>-82°C</i>                    |                                    |            |               |
| RONC   | 79                                 | 79         | 80            |
| <i>Heavy Naphtha</i>                         |                                    |            |               |
| P/N/A  | 45/50/5                            | 44/52/4    | ---           |
| RONC   | 41                                 | 63         | 67            |
| End Point, °C (°F)                           | 216 (421)                          | 121 (250)  | 118 (244)     |
| <i>Jet A-1</i>                               |                                    |            |               |
| Flash Point, °C (°F)                         | ---                                | 38 (100)   | ---           |
| Freeze Point, °C (°F)                        | ---                                | -48 (-54)  | ---           |
| Smoke Point, mm                              | ---                                | 34         | ---           |
| FIA Aromatics, vol%                          | ---                                | 7          | ---           |
| End Point, °C (°F)                           | ---                                | 282 (540)  | ---           |
| <i>Diesel</i>                                |                                    |            |               |
| Cloud Point, °C (°F)                         | ---                                | ---        | -15 (5)       |
| API Gravity                                  | ---                                | ---        | 44            |
| Cetane Number                                | ---                                | ---        | 55            |
| Flash Point, °C (°F)                         | ---                                | ---        | 52 (126)      |
| End Point, °C (°F)                           | ---                                | ---        | 349 (660)     |

For hydrotreaters, operating costs are roughly US\$1.7 per barrel. The cost of producing and compressing hydrogen accounts for 60% to 70% of this. For high-conversion hydrocrackers, operating costs are roughly US\$4.0 to US\$4.5 per barrel, of which 75% to 80% is due to hydrogen.

## 8.2 Benefits

Many hydrotreaters are stay-in-business investments, so it's difficult to quantify their upgrade value, which is the value of products minus costs – labor, materials (liquid feed, hydrogen, catalysts and chemicals), utilities, maintenance, and investment amortization. In some plants, the refinery planning LP assigns equal value to treated and untreated naphtha, and even to treated and untreated distillates. This reflects the underlying assumption that the increase in value across a hydrotreater is equal to the cost of running the unit, i.e., the upgrade value is zero. In other LPs, the NHT that pretreats catalytic reformer feed is lumped in with the reformer. Certainly, if a key naphtha or distillate hydrotreater shuts down, the refinery may have to run at reduced rate, but that can be said of most units.

For an FCC feed pretreater, the upgrade value can be more than US\$3 per barrel if the calculation includes its positive impact on FCC yields. Usually, benefits to the FCC are greater than the value of conversion and volume swell in the hydrotreater itself. Typically, the upgrade value for a high-conversion VGO hydrocracker is US\$3 to US\$4 per barrel.

With hydroprocessing units, most refiners try to maximize feed rate while (a) meeting other process objectives and (b) maintaining a high on-stream factor. Some try to maximize conversion, while others just want to hit a key process target at minimum cost.

## 8.3 Catalyst Cycle Life

For fixed-bed units, catalyst cycle life dominates economics. Catalysts can't be changed if the units are operating, so shorter catalyst cycles mean decreased production. For a typical 25,000 b/d unit, one day of lost production can cost US\$100,000.

Here are some of the many economic tradeoffs that must be considered when setting hydrocracker process targets:

- Higher feed rates and higher conversion are desirable economically, but they increase consumption of hydrogen and decrease catalyst cycle life.
- In units that can recycle fractionator bottoms, higher recycle oil rates can increase selectivity, but they may impose limits on fresh feed rate.

For many recycle units, switching to once-through (zero recycle) operation is attractive economically if the unconverted oil (i.e., the fractionator bottoms) goes to an FCC, olefins plant or lube plant for further upgrading. Conversion goes down in the hydrocracker, but it may be possible to increase fresh feed rates without decreasing catalyst cycle life, and operating costs may go down due to decreased hydrogen consumption.



## 9. HYDROCRACKER-FCC COMPARISON

In a petroleum refinery, heavy molecules with low hydrogen-to-carbon ratios (H/C) are converted into light molecules with higher H/C. The FCC process increases H/C by rejecting carbon, while hydrocracking increases H/C by adding hydrogen. Consequently, FCC and hydrocracking have marked differences in operating conditions, volume swell, product yields and product properties. *Table 14* summarizes some of these differences.

*Table 14.* Comparison of Hydrocracking with FCC

|  | <i>FCC</i>   | <i>Hydrocracking</i>               |
|--|--|------------------------------------|
| Operating pressure                       | Low  | High 1500 – 2800 psi               |
| Operating temperature                    | High 900 – 1000°F                                  | Moderate 600 – 780°F               |
| Construction costs                       | Moderate   | High                               |
| Volume swell                             | 112 – 118 vol%<br>Incl. fuel gas FOEB <sup>1</sup> | 115 – 140 vol%<br>Fresh feed basis |
| Product olefins                          | High   | Nil                                |
| Light naphtha octane (RONC) <sup>2</sup> | >100   | 78-81                              |
| Heavy naphtha octane (RONC) <sup>2</sup> | 95 – 100   | 40-64                              |
| Distillate cetane index                  | Low  | 56 – 60                            |
| Distillate sulfur content                | Moderate to High                                   | Very low                           |
| Bottoms sulfur content                   | Moderate to High                                   | Very low                           |

1. FOEB = fuel oil equivalent barrels

2. RONC = research octane number clear (without tetraethyl lead)

## 10. OPERATIONAL ISSUES

Hydroprocessing – especially hydrocracking – is exothermic. Effective control of produced heat is the primary concern of designers, owners and operators of hydrocracking units. In modern units, a high flux of recycle gas provides a sink for process heat. It also promotes plug flow and the transport of heat through the reactors. Most licensors recommend that the ratio of recycle gas to makeup gas should exceed 4:1.

During design, limits on temperature rise ( $T_{\text{rise}} = T_{\text{out}} - T_{\text{in}}$ ) set the size of catalyst beds and determine the number and location of quench zones. During operation, when feeds (and maybe catalysts) are different, the  $T_{\text{rise}}$  is also different – sometimes dangerously different. A sudden spike in  $T_{\text{rise}}$  can lead to a “temperature runaway” or “temperature excursion.” These are dangerous. The rates of cracking reactions increase exponentially with temperature – the hotter they get, the faster they get hot. In a few cases, temperature runaways have melted holes in the stainless steel walls of hydrocracking reactors. This is remarkable, because the walls were more than 8 inches (20 cm) thick.

The best way to stop a temperature excursion is to de-pressure the unit by venting recycle gas through a special valve at the CHPS. This decelerates all hydrocracking reactions by rapidly reducing  $H_2$  partial pressure in the reactors. De-pressuring can also lead to catalyst mal-distribution, decreased

catalyst activity, and/or increased pressure drop. For these reasons, operators are extremely careful when re-starting a unit after a temperature excursion.

Due to the presence of hydrogen, leaks in hydroprocessing units often cause fires. Such fires can be devastating, if not deadly. The replacement of a reactor and the reconstruction of other equipment damaged by the accident can take 12 months. The cost of lost production can exceed US\$50 million.

Safety concerns are responsible for several operating constraints, such as:

- An upper limit on temperature in the reactors. This and other temperature constraints prevent damage to the reactor.
- Upper limits on the  $T_{\text{rise}}$  in each bed and each reactor, and upper limits on the rate at which  $T_{\text{rise}}$  changes. These are designed to decrease the likelihood of temperature excursions.
- An upper limit on the velocity of fluid flow through elbows in high-pressure piping. This constraint emerged after erosion-corrosion cut a hole in a high-pressure pipe in a hydrocracker, causing a major accident.
- A lower limit on reserve quench gas – usually 15% of the total flow of recycle gas. Reserve quench provides a way to react quickly to non-emergency changes in  $T_{\text{rise}}$ .
- A lower limit on wash water injection. This ensures the near-total removal of ammonia from the system.

## 11. LICENSORS

Leading licensors of hydroprocessing technology are listed in Table 15.

*Table 15. Leading Licensors of Hydroprocessing Technology*

| Company         | Process Name      | Description                                    |
|-----------------|-------------------|--|
| Axens (IFP)     | Prime-G           | Gasoline desulfurization                       |
|                 | IFP Hydrotreating | Naphtha, Distillate, VGO hydrotreating         |
|                 | IFP Hydrocracking | High-conversion fixed-bed hydrocracking        |
|                 | T-Star            | Ebullating bed hydrotreating                   |
|                 | H-Oil             | Ebullating bed hydrocracking                   |
| CDTECH          | CDHydro, CDHDS    | Hydrotreating with catalytic distillation      |
| Chevron Lummus  | ISOCRACKING       | High-conversion hydrocracking                  |
|                 | RDS               | Atmospheric residue hydrotreating              |
|                 | VRDS              | Vacuum residue hydrotreating                   |
|                 | OCR               | Onstream catalyst replacement                  |
|                 | ISODEWAXING       | Catalytic dewaxing                             |
|                 | LC-Fining         | Ebullating bed hydrocracking                   |
| Criterion/ABB / | SynSat            | Distillate hydrotreating, aromatics saturation |
| Shell Global    | Deep Gasoil HDS   | Hydrotreating to make ultra-low-sulfur diesel  |
| ExxonMobil      | SCANfining        | Hydrotreating to make low-sulfur gasoline      |
|                 | OCTGAIN           | Hydrotreating to make low-sulfur gasoline      |
|                 | ULSD-fining       | Hydrotreating to make ultra-low-sulfur diesel  |
|                 | MAXSAT            | Saturation of aromatics in distillate streams  |

Table 15. (Continued)

| Company       | Process Name      | Description                                |
|---------------|-------------------|--|
|               | LCO-finishing     | LCO hydrotreating                          |
|               | GO-finishing      | FCC feed pretreating                       |
|               | RESIDfinishing    | Residue hydrotreating                      |
|               | MIDW              | Lube isomerization/dewaxing                |
| Haldor Topsøe |                   | Naphtha, distillate, VGO hydrotreating     |
| KBR           | MAK Hydrotreating | Distillate and VGO hydrotreating           |
|               | MAK Hydrocracking | Mild hydrocracking, FCC feed pre-treatment |
| UOP           | ISAL              | Gasoline desulfurization                   |
|               | Unifining         | Naphtha hydrotreating                      |
|               | Unionfinishing    | Distillate, VGO, residue hydrotreating     |
|               | Unicracking       | High-conversion VGO hydrocracking          |

Many engineering contractors gladly will build un-licensed hydrotreaters. However, for hydrocrackers and special-application hydrotreaters, especially those designed to meet clean-fuel specifications, refiners almost always select licensed technology from an experienced vendor willing to offer guarantees.

## 12. CONCLUSION

Advances in hydroprocessing are driven by competitive forces and clean-fuel regulations. These advances include improved catalysts (Chapters 9-11), better reactor design (Chapters 7-8), advanced process control (Chapter 22), and online optimization (Chapter 23). As clean-fuel regulations migrate from North America and the EU into the rest of the world, and as globalization of the oil industry continues apace, the need will continue for new (and better) hydroprocessing units. Hopefully, within a few years, this chapter will be obsolete and we'll have to write an update.

## 13. REFERENCES

1. "Worldwide Refineries, Capacities as of January 1, 2004," *Oil & Gas J.*, Dec. 22, 2003
2. Scherzer, J.; Gruia, A.J., *Hydrocracking Science and Technology*, Marcell Dekker, Inc.: New York, 1996
3. Wu, W.L.; Haynes, H.W. "Hydrocracking Condensed Ring Aromatics over Nonacidic Catalysts," in *Hydrocracking and Hydrotreating* (Ward, J.W.; Qader, S.A., eds), ACS Symposium Series 20, 1975, pp. 65-81
4. Knudsen, K.G.; Cooper, B.H.; Topsøe, H. "Catalyst and Process Technologies for Ultra Low Sulfur Diesel," *Appl. Catal.*, A 189, 1999, 205
5. Sapre, A. "Advanced Distillate Hydroprocessing Technology," 4th Conference on Oil Refining and Petrochemicals in the Middle East, Abu Dhabi, January 28, 2003
6. Dolbear, G.E., "Hydrocracking: Reactions, Catalysts, and Processes," in *Petroleum Chemistry and Refining* (Speight, J.G. ed.), Taylor & Francis: Washington, D.C., 1998
7. Mills, G.A.; Heinemann, H.; Milliken, T.H.; Oblad, A.G. *Ind. Eng. Chem.* 1953, 45, 134.

8. Weisz, D.B. *Adv. Catal.* 1962, 13, 137.
9. Qader, S.A.; McOmber, D.B. "Conversion of Complex Aromatic Structures to Alkyl Benzenes," *Hydrocracking and Hydrotreating*, Oxford University Press, 1975, pp. 82-98
10. Lapinas, A.T.; Klein, M.T.; Gates, B.D.; Macris, A.; Lyons, J.E. "Catalytic Hydrogenation and Hydrocracking of Fluorene: Reaction Pathways, Kinetics and Mechanisms," *Ind. Eng. Chem. Res.*, 1991, 30 (1), 42
11. Van Speybroeck, V.; Reyniers, M-F.; Marin, G.B.; Waroquier, M. "The Kinetics of Cyclization Reactions on Polyaromatics from First Principles," *CHEMPHYSICHEM* 2002, 3, 863-870
12. Robinson, P.R. "Catalyst Life Management with a Predictive Deactivation Model," 2004 NPRA PADS Conference, PD-04-171, September 19-21, 2004
13. Hu, M.C.; Powell, R.T.; Yomojio, N.; Ohshima, D. "Steady-state Simulator to Monitor Treater Performance," *Petroleum Technology Quarterly*, Spring 2001, 47
14. Sue, H.; Sugiyama, H. *Petrotech* (Tokyo), 1982, 5, 942
15. Steinberg, K.H.; Becker, K.; Nestles, K.H. *Acta Phys. Chem.*, 1985, 31, 441
16. Mohanty, S.; Kunzru, D.; Saraf, D.N. *Fuel*, 1990, 69, 1467
17. Rappaport, I.B. *Chemistry and Technology of Synthetic Liquid Fuels*, 2nd ed., Israel Program for Scientific Translation, Jerusalem, 1962
18. Filimonov, V.A.; Popov, A.A.; Khavkin, V.A.; Perezehigina, I.Ya.; Osipov, L.N.; Rogov, S.P.; Agafonov, A.V. "The Rates of Reaction of Individual Groups of Hydrocarbons in Hydrocracking," *International Chem. Eng.*, 1972, 12 (1), 21
19. Stangeland, B. "A Kinetic Model for the Prediction of Hydrocracker Yields," *Ind. Eng. Chem., Process Des. Develop.*, 1974 (13), 1, 71
20. Quann, R.J.; Jaffe, S.B. "Structure Oriented Lumping: Describing the Chemistry of Complex Hydrocarbon Mixtures," *I&EC Research* 31, 1992, 2483
21. Quann, R.J.; Jaffe, S.B. "Building Useful Models of Complex Reaction Systems in Petroleum Refining," *Chem. Eng. Science* 51, 1996, 1615
22. Pedersen, C.C.; Mudt, D.R.; Bailey, J.K.; Ayala, J.S. "Closed Loop Real Time Optimization of a Hydrocracker Complex," 1995 NPRA Computer Conference, CC-95-121, November 6-8, 1995
23. Magee, J.S.; Dolbear, G.E. *Petroleum Catalysis in Nontechnical Language*, PennWell: Tulsa, Oklahoma, 1998
24. Satterfield, C.N., "Trickle-Bed Reactors," *AIChE Journal*, 1975, 21 (2), 209

## Chapter 8

# RECENT ADVANCES IN HYDROCRACKING

Adrian Gruia  
*UOP LLC*

### 1. INTRODUCTION

Hydrocracking is a versatile catalytic refining process that upgrades petroleum feedstocks by adding hydrogen, removing impurities and cracking to a desired boiling range. Hydrocracking requires the conversion of a variety of types of molecules and is characterized by the fact that the products are of significantly lower molecular weight than the feed. Hydrocracking feeds can range from heavy vacuum gas oils and coker gas oils to atmospheric gas oils. Products usually range from heavy diesel to light naphtha. Hydrocrackers are designed for and run at a variety of conditions depending on many factors such as type of feed, desired cycle length, expected product slate but in general they will operate at the following range of conditions: LHSV - 0.5-2.0 hr<sup>-1</sup>, H<sub>2</sub> circulation - 5,000-10,000 SCFB (850-1,700 NM<sup>3</sup>/M<sup>3</sup>), H<sub>2</sub>PP 1,500-2,000 psia (103-138 bars) and SOR temperatures ranging between 675 and 725 °F (357-385 °C). Hydrocracking is particularly well suited to generating products that meet or exceed all of the present tough environmental regulations.

### 2. HISTORY

While the first commercial installation of a unit employing the type of technology in use today was started up in Chevron's Richmond, California refinery in 1960, hydrocracking is one of the oldest hydrocarbon conversion processes. Its origin is the work done by Sabatier and Senderens, who in 1897 published the discovery that unsaturated hydrocarbons could be hydrogenated in the vapor phase over a nickel catalyst.<sup>1</sup> In 1904, Ipatieff extended the range of feasible hydrogenation reactions by the introduction of

elevated hydrogen pressures.<sup>2</sup> At the time, the progress of the automobile industry was expected to entail a considerable increase in the consumption of gasoline. This led to the experimental work by Bergius,<sup>3</sup> started in 1910 in Hanover, Germany. He sought to produce gasoline by cracking heavy oils and oil residues as well as converting coal to liquid fuels. He realized that to remedy the inferior quality of the unsaturated gasoline so produced, the hydrogen removed mostly in the form of methane during the cracking operation has to be replaced by addition of new hydrogen. Thus, formation of coke was avoided and the gasoline produced was of a rather saturated character. Bergius also noted that the sulfur contained in the oils was eliminated for the most part as H<sub>2</sub>S. Ferric oxide was used in the Bergius process to remove the sulfur. Actually, the ferric oxide and sulfides formed in the process acted as catalysts, though the activity was poor. Actual hydrocracking technology for coal conversion was developed in Germany as early as 1915 designed to secure a supply of liquid fuels derived from domestic deposits of coal. The first plant for hydrogenation of brown coal was put on stream in Leuna Germany in 1927,<sup>4</sup> applying what may be considered the first commercial hydrocracking process. Conversion of coal to liquid fuels was a catalytic process operating at high pressures, 3000 - 10,000 psig (207-690 bar) and high temperatures, 700 - 1000 °F (371-538 °C).

The large scale industrial development of hydrogenation in Europe, particularly in Germany, was due entirely to military considerations. Germany used hydrogenation extensively during World War II to produce gasoline: 3.5 million tons were produced in 1944.<sup>5</sup> The emergent availability of Middle Eastern crude after World War II removed the incentive to convert coal to liquid fuels, so continuing the development of hydrocracking technology became less important.

Even though hydrogenation has been of interest to the petroleum industry for many years, little commercial use of hydrogen-consuming processes has been made because of the lack of low-cost hydrogen. That changed in the early 1950s with the advent of catalytic reforming, which made available by-product hydrogen. That brought up an extensive and increased interest in processes that will utilize this hydrogen to upgrade petroleum stocks.

Another factor was that in the mid-1950's the automobile industry started manufacturing high-performance cars with high-compression ratio engines, which required high-octane gasoline. Thus catalytic cracking expanded rapidly and generated, in addition to gasoline, large quantities of refractory cycle stock that was difficult to convert to gasoline and lighter products. This need to convert refractory stock to gasoline was filled by hydrocracking. Furthermore, the switch of railroads from steam to diesel engines after World War II and the introduction of commercial jet aircraft in the late 1950s increased the demand for diesel fuel and jet fuel. The flexibility of the newly developed hydrocracking processes made possible the production of such fuels from heavier feedstocks.<sup>6</sup>

The early hydrocrackers used amorphous silica alumina catalysts. The rapid growth of hydrocracking in the 1960s was accompanied by the development of new, zeolite based hydrocracking catalysts. They showed a significant improvement in certain performance characteristics as compared with amorphous catalysts: higher activity, better ammonia tolerance and higher gasoline selectivity. While hydrocracking was used in the United States primarily in the production of high-octane gasoline, it grew in other parts of the world, starting in the 1970s primarily for the production of middle distillates. The amorphous catalysts remained the catalysts of choice for this application, though some 'flexible' catalysts were developed that made it possible to maximize the yield of different products by using the same catalyst but changing the operating conditions. As of the beginning of 2002, there were more than 150 hydrocrackers operating in the world with a total capacity in excess of 3,800,000 B/D (500,000 MT/D).<sup>7</sup>

### 3. FLOW SCHEMES

Various licensors have slightly different names for their hydrocracking units flow schemes, but in general, they can be grouped into major two categories: single stage and two stage. Table 1 shows the general evolution of flows schemes, generally driven by improvements in catalysts.<sup>8</sup>

Table 1. Evolution of Hydrocracking Units Flow Schemes

| Date                       | Process Scheme                                   | Reason  |
|----------------------------|--|---|
| Early 60's                 | Separate Hydrotreating                           | Low activity amorphous catalyst   |
| Mid 60's                   | Two Stage Hydrocracking                          | Advent of zeolitic catalysts<br>More economical scheme  |
| Late 60's<br>70's and 80's | Single Stage<br>Once through, partial conversion | More efficient design & cost<br>Upgraded unconverted oil for FCC or ethylene plant feed,<br>lube oil base stock |

#### 3.1 Single Stage Once-Through Hydrocracking

Figure 1 shows a schematic of a single stage, once through hydrocracking unit, which is the simplest configuration for a hydrocracker. It is a variation of the single stage hydrocracking with recycle configuration (described in 3.2). The feed mixes with hydrogen and goes to the reactor. The effluent goes to fractionation, with the unconverted material being taken out of the unit as unconverted material. This type of unit is the lowest cost hydrocracking unit, can process heavy, high boiling feed stocks and produces high value unconverted material which becomes feed stock for FCC units, ethylene plants or lube oil units. In general, the conversion of the feed stock to products is 60-70 vol%, but can range as high as 90 vol%.

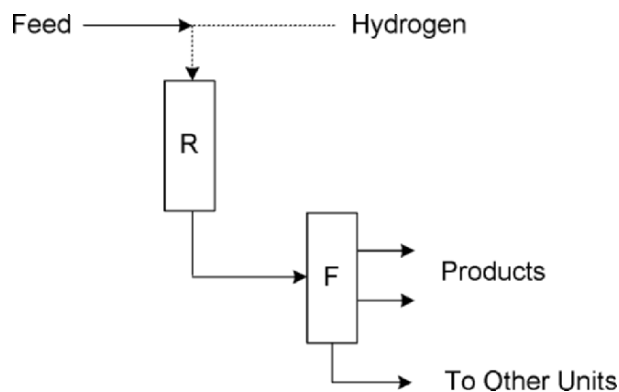


Figure 1. Single Stage Once Through Hydrocracking Unit. R = Reactor(s), F = Fractionation

### 3.2 Single Stage with Recycle Hydrocracking

The most widely found hydrocracking unit is the single stage with recycle in which the unconverted feed is sent back to the reactor section for further conversion. Figure 2 depicts this type unit. It is the most cost-effective design for 100% (or near 100%) conversion and is especially used to maximize diesel product.

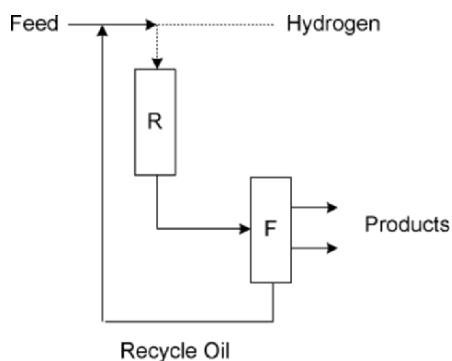


Figure 2. Single Stage Hydrocracking unit with Recycle. R = Reactor(s), F = Fractionation

A more detailed flow diagram (than those shown in either Figures 1 & 2) of the reactor section in a single stage hydrocracker is shown in Figure 3. The fresh feed is passed downward through the catalyst in presence of hydrogen, after being preheated to reaction temperature by passing it through heat exchangers and a heater. The effluent from the reactors goes through a series of separators where hydrogen is recovered and, together with make up hydrogen, is recycled to the reactors.



The liquid product is sent to fractionation where the final products are separated from unconverted oil. In once-through units, the unconverted oil leaves the unit, as previously described. In units designed to operate with recycle, the unconverted oil combines with the fresh feed (Figure 3). As described in the next section, the reaction section fulfills two functions: pre-treating and cracking. In most units, these functions occur in separate reactors, though both can occur in one reactor when using amorphous catalysts

When using a pre-treat & cracking catalyst configuration, the first catalyst (a hydrotreating catalyst) converts organic sulfur and nitrogen from hetero compounds in the feedstock to hydrogen sulfide and ammonia, respectively. The deleterious effect of  $H_2S$  and  $NH_3$  on hydrocracking catalysts is considerably less than that of the corresponding organic hetero compounds. The hydrotreating catalyst also facilitates the hydrogenation of aromatics. In the single stage, two reactor configuration, the products from the first reactor are passed over a hydrocracking catalyst in the second reactor where most of the hydrocracking takes place. The conversion occurs in the presence of  $NH_3$ ,  $H_2S$ , and small amounts of unconverted amounts of hetero compounds. The hydrotreating catalyst in the first reactor is designed to convert the hetero compounds in the feed stock. Typically, such catalysts comprise sulfided molybdenum and nickel on an alumina support. The reactor operates at temperatures varying from 570 to 800 °F (300-425 °C) and hydrogen partial pressures between 1,250 and 2,500 psig (85-170 bar). Under these conditions, in addition to heteroatom elimination, significant hydrogenation occurs and some cracking also takes place. The cracking reactor operates at the same hydrogen pressures but at temperatures varying from 570 to as high as 840 °F (300 - 450 °C) for amorphous hydrocracking catalysts and up to 440 °C (825 °F) for zeolite containing catalysts.

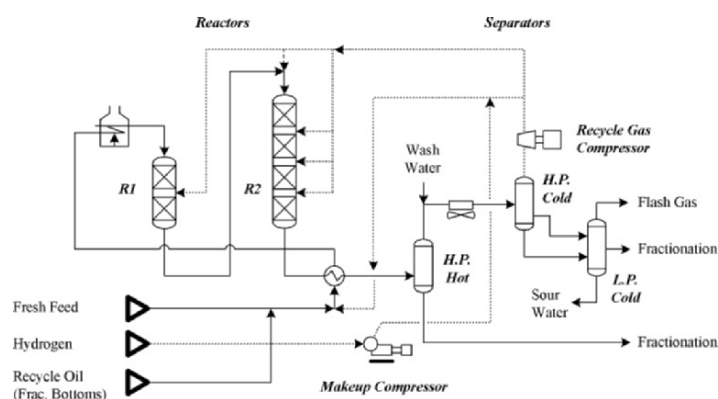


Figure 3. Typical Flow Diagram of Reactor Section of Single Stage Hydrocracker (or first stage of a two stage hydrocracker)

### 3.3 Two Stage Recycle Hydrocracking

The two stage hydrocracking process configuration is also widely used, especially for large throughput units. In two stage units, the hydrotreating and some cracking takes place in the first stage. The effluent from the first stage is separated and fractionated, with the unconverted oil going to the second stage. The unconverted oil from the second stage reaction section goes back to the common fractionator. A simplified schematic of a two stage hydrocracker is shown in Figure 4. The catalysts in the first stage are the same types as those used in the single stage configuration. The catalyst in the second stage is operating in near absence of ammonia, and depending on the particular design, in the absence or presence of hydrogen sulfide. The near absence of  $\text{NH}_3$  and  $\text{H}_2\text{S}$  allows the use of either noble metal or base metal sulfide hydrocracking catalysts.

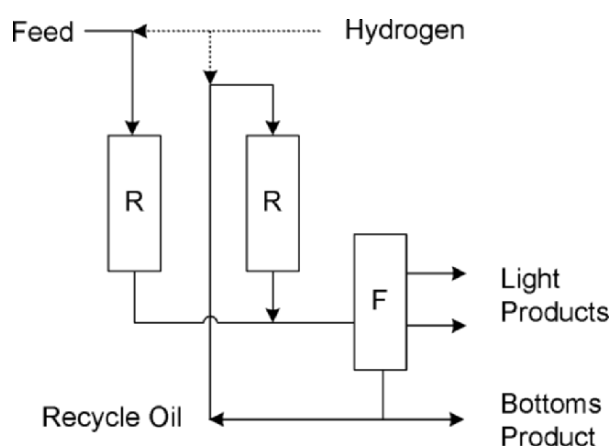


Figure 4. Two Stage Hydrocracking. R = Reactor(s), F = Fractionation

### 3.4 Separate Hydrotreat Two Stage Hydrocracking

A variation of the typical two stage hydrocracking with common hydrogen circulation loop is the separate hydrotreat hydrocracking shown in Figure 5 in which each stage has a separate hydrogen circulation loop, allowing for operation of the second stage in the near absence of hydrogen sulfide (and ammonia).

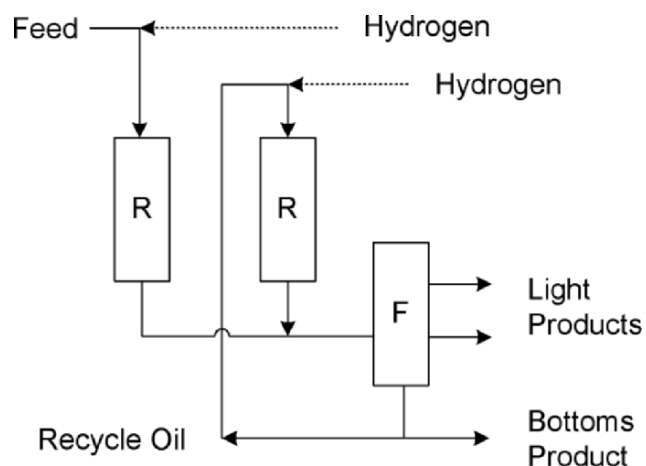


Figure 5. Separate Hydrotreat Two Stage Hydrocracking. R = Reactor(s), F = Fractionation

## 4. CHEMISTRY

Hydrocracking converts the heavy feed stock to lower molecular weights products, removes sulfur and nitrogen and saturates olefins and aromatics. The organic sulfur is transformed into  $H_2S$ , the nitrogen is transformed into  $NH_3$  and the oxygen compounds (not always present) are transformed into  $H_2O$ . The reactions in hydrocracking can be classified in two categories: desirable and undesirable. Desirable are the treating, saturation and cracking reactions. Undesirable reactions are contaminant poisoning as well as coking of the catalyst. There are two types of reactions taking place in hydrocracking units: treating (also called pre-treating) and cracking (also called hydrocracking). The cracking reactions require bi-functional catalyst, which possess a dual function of cracking and hydrogenation.

### 4.1 Treating Reactions

The treating reactions that will take place (if the respective contaminants are present) are the following: sulfur removal, nitrogen removal, organo-metallic compound removal, olefin saturation, oxygen removal and halides removal. The first three types of compounds are always present though in varying amounts depending on the source of feed stock. The others are not always present. In general, the treating reactions proceed in the following descending order of ease: (organo) metals removal, olefin saturation, sulfur removal, nitrogen removal, oxygen removal and halide removal. Some aromatic saturation also occurs in the pre-treating section. Hydrogen is

consumed in all treating reactions. In general, the desulfurization reaction consumes 100-150 SCFB/wt% change (17-25 NM<sup>3</sup>/M<sup>3</sup>/wt% change) and the denitrogenation reaction consumes 200-350 SCFB/wt% change (34-59 NM<sup>3</sup>/M<sup>3</sup>/wt% change). Typically, the heat released in pretreating is about 0.02 °F/SCFB H<sub>2</sub> consumed (0.002 °C/NM<sup>3</sup>/M<sup>3</sup> H<sub>2</sub>).

The postulated mechanism for the desulfurization reaction is shown in Figure 6: first, the sulfur is removed followed by the saturation of the intermediate olefin compound. In the example below the thiophene is converted to butene as an intermediate which is then saturated into butane.

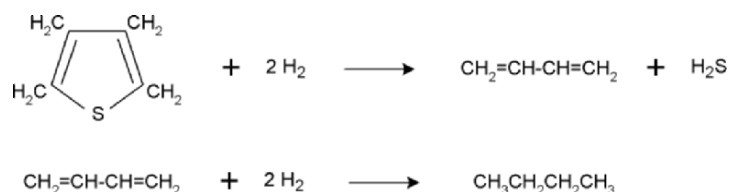


Figure 6. Postulated Mechanism for Hydrodesulfurization

Listed below in Figure 7 are several desulfurization reactions arranged in increasing order of difficulty.

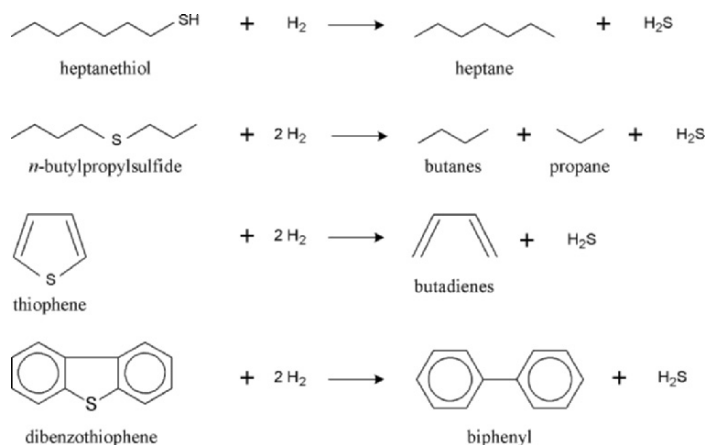


Figure 7. Typical Desulfurization Reactions

The denitrogenation reaction proceeds through a different path. In the postulated mechanism for hydrodenitrogenation the aromatic hydrogenation occurs first, followed by hydrogenolysis and, finally denitrogenation. This is shown in Figure 8. Figure 9 shows a few typical examples of denitrogenation reactions.

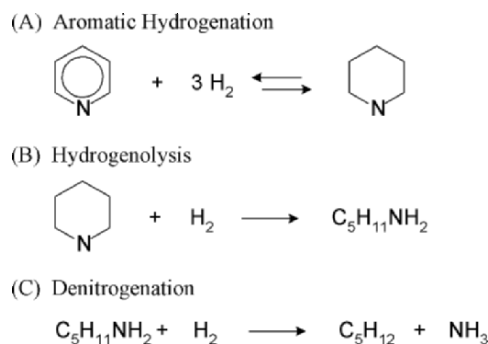


Figure 8. Postulated mechanism for Hydrodenitrogenation

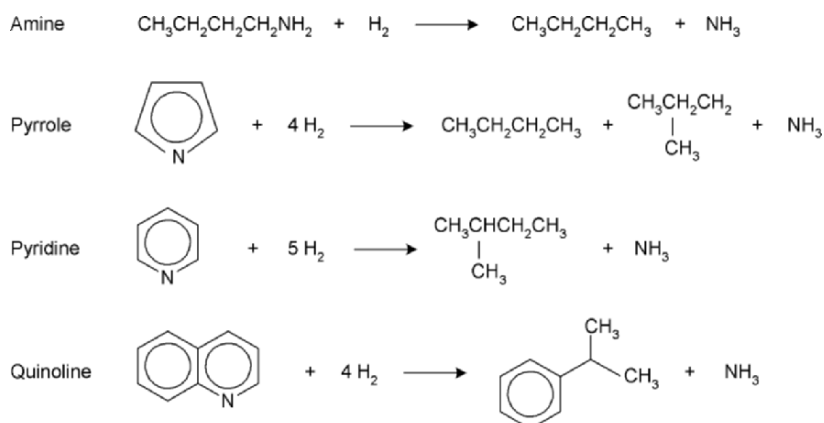


Figure 9. Typical Denitrogenation Reactions

## 4.2 Cracking Reactions

Hydrocracking reactions proceed through a bifunctional mechanism. A bifunctional mechanism is one that requires two distinct types of catalytic sites to catalyze separate steps in the reaction sequence. These two functions are the acid function, which provide for the cracking and isomerization and the metal function, which provide for the olefin formation and hydrogenation. The cracking reaction requires heat while the hydrogenation reaction generates heat. Overall, there is heat release in hydrocracking, and just like in treating, it is a function of the hydrogen consumption (the higher the consumption, the more important the exotherm). Generally, the hydrogen consumption in hydrocracking (including the pretreating section) is 1200-2400 SCFB/wt% change (200-420  $\text{NM}^3/\text{M}^3/\text{wt}\%$  change) resulting in a typical heat release of 50-100 BTU/SCF  $\text{H}_2$  (2.1-4.2  $\text{Kcal}/\text{M}^3 \text{H}_2$ ) which translates into a temperature increase of about 0.065 °F/SCF  $\text{H}_2$  consumed

(0.006 °C/NM<sup>3</sup>/M<sup>3</sup> H<sub>2</sub>). This includes the heat release generated in the treating section.

In general, the hydrocracking reaction starts with the generation of an olefin or cycleolefin on a metal site on the catalyst. Next, an acid site adds a proton to the olefin or cycloolefin to produce a carbenium ion. The carbenium ion cracks to a smaller carbenium ion and a smaller olefin. These products are the primary hydrocracking products. These primary products can react further to produce still smaller secondary hydrocracking products. The reaction sequence can be terminated at primary products by abstracting a proton from the carbenium ion to form an olefin at an acid site and by saturating the olefin at a metal site. Figure 10 illustrates the specific steps involved in the hydrocracking of paraffins. The reaction begins with the generation of an olefin and the conversion of the olefin to a carbenium ion. The carbenium ion typically isomerizes to form a more stable tertiary carbenium ion. Next, the cracking reaction occurs at a bond that is  $\beta$  to the carbenium ion charge. The  $\beta$  position is the second bond from the ionic charge. Carbenium ions can react with olefins to transfer charge from one fragment to the other. In this way, charge can be transferred from a smaller hydrocarbon fragment to a larger fragment that can better accommodate the charge. Finally, olefin hydrogenation completes the mechanism. The hydrocracking mechanism is selective for cracking of higher carbon number paraffins. This selectivity is due in part to a more favorable equilibrium for the formation of higher carbon number olefins. In addition, large paraffins adsorb more strongly. The carbenium ion intermediate causes extensive isomerization of the products, especially to  $\alpha$  methyl isomers, because tertiary carbenium ions are more stable. Finally, the production of C<sub>1</sub> to C<sub>3</sub> is low because the production of these light gases involves the unfavorable formation of primary and secondary carbenium ions. Other molecular species such as alkyl naphthenes, alkyl aromatics and so on react via similar mechanisms eg via the carbenium ion mechanism.

In summary, hydrocracking occurs as the result of a bifunctional mechanism that involves olefin dehydrogenation-hydrogenation reactions on a metal site, carbenium ion formation on an acid site, and isomerization and cracking of the carbenium ion. The hydrocracking reactions tend to favor conversion of large molecules because the equilibrium for olefin formation is more favorable for large molecules and because the relative strength of adsorption is greater for large molecules. In hydrocracking, the products are highly isomerized, C<sub>1</sub> and C<sub>3</sub> formation is low, and single rings are relatively stable.

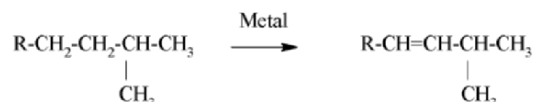
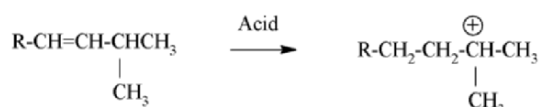
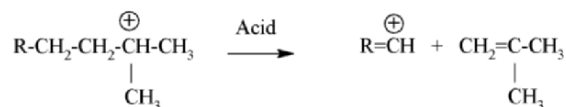
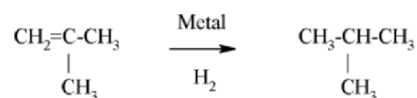
**(A) Formation of Olefin****(B) Formation of Tertiary Carbenium Ion****(C) Isomerization and Cracking****(D) Olefin Hydrogenation**

Figure 10. Postulated Hydrocracking Mechanism of n-Paraffins

In addition to treating and hydrocracking several other important reactions take place in hydrocrackers. These are aromatic saturation, polynuclear aromatics (PNA) formation and coke formation. Some aromatic saturation occurs in the treating section and some in the cracking section. Aromatic saturation is the only reaction in hydrocracking which is equilibrium limited at the higher temperatures reached by hydrocrackers toward the end of the catalyst cycle life. Because of this equilibrium limitation, complete aromatic saturation is not possible toward the end of the catalyst cycle when reactor temperature has to be increased to make up for the loss in catalyst activity resulting from coke formation and deposition. Figure 11 shows the thermodynamics of the major reactions taking place in a hydrocracker. Of course, the principles of thermodynamics provide the means to determine which reactions are possible. In general, the thermodynamic equilibrium for hydrocracking is favorable. Cracking reactions, desulfurization and denitrogenation are favored at the typical hydrocracker operating conditions. The initial step in the hydrocracking of paraffins or naphthenes is the generation of an olefin or cycloolefin. This step is unfavorable under the high hydrogen partial pressure used in hydrocracking. The dehydrogenation of the smaller alkanes is most unfavorable. Nevertheless, the concentration of olefins and cycloolefins is sufficiently high, and the conversion of these intermediates to carbenium ions is sufficiently fast so that the overall hydrocracking rate is not limited by the equilibrium olefin levels.

| <u>Reaction</u>            | <u>Equilibrium</u>                     | <u>Heat of Reaction</u> |
|----------------------------|--|-------------------------|
| <b>Olefin Formation</b>    | <b>Unfavorable But Not Limiting</b>    | <b>Endothermic</b>      |
| <b>Aromatic Saturation</b> | <b>Unfavorable At High Temperature</b> | <b>Exothermic</b>       |
| <b>Cracking</b>            | <b>Favorable</b>                       | <b>Endothermic</b>      |
| <b>HDS</b>                 | <b>Favorable</b>                       | <b>Exothermic</b>       |
| <b>HDN</b>                 | <b>Favorable</b>                       | <b>Exothermic</b>       |

Figure 11. Thermodynamics of Major Reactions in Hydrocracking

Polynuclear aromatics (PNA), sometimes called polycyclic aromatics (PCA) or polyaromatic hydrocarbons (PAH) are compounds containing at least two benzene rings in the molecule. Normally, the feed to a hydrocracker can contain PNA with up to seven benzene rings in the molecule. PNA formation is an important, though undesirable, reaction that occurs in hydrocrackers. Figure 12 shows the competing pathways for conversion of multiring aromatics. One pathway starts with metal-catalyzed ring saturation and continues with acid-catalyzed cracking reactions. The other pathway begins with an acid-catalyzed condensation reaction to form a large aromatic-ring compound. This molecule may undergo subsequent condensation reactions to form a large PNA.

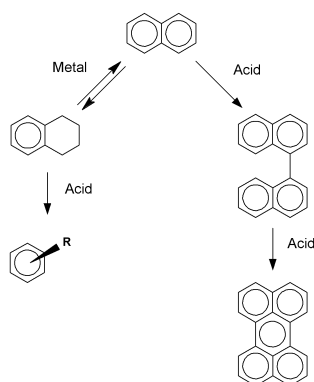


Figure 12. Possible Pathways for Multiring Aromatics

When a hydrocracker is operated with recycle of the unconverted feed, PNA with more than seven benzene rings are created. These are called HPNA (heavy polynuclear aromatics). The consequences of PNA formation are shown in Figure 13. The HPNA produced on the catalyst may exit the reactor and cause downstream fouling; or they may deposit on the catalyst and form coke, which deactivates the catalyst. Their presence results in plugging



of equipment. For mitigation a stream of 5 to as much as 10% of unconverted material might have to be taken out of the hydrocracker, resulting in much lower than expected conversion of the feed.

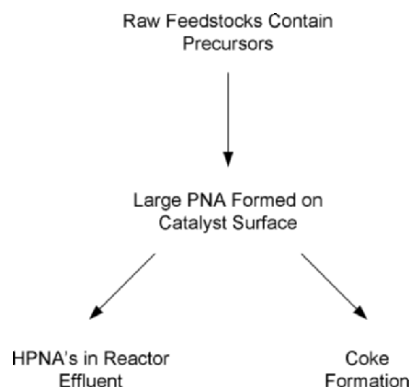


Figure 13. HPNA Formation

## 5. CATALYSTS

Hydrocracking catalysts are dual function catalysts. For the cracking reaction to occur (as well as some of the other reactions taking place in hydrocracking, such as hydroisomerization and dehydrocyclization), both metallic sites and acidic sites must be present on the catalyst surface. Hydrocracking catalysts have a cracking function and hydrogenation function. The cracking function is provided by an acidic support, whereas the hydrogenation function is provided by metals.

The acidic support consists of amorphous oxides (e.g., silica-alumina, a crystalline zeolite (mostly modified Y zeolite) plus binder (e.g., alumina), or a mixture of crystalline zeolite and amorphous oxides. Cracking and isomerization reactions take place on the acidic support. The metals providing the hydrogenation function can be noble metals (palladium, platinum), or nonnoble (or base) metal sulfides from group VIA (molybdenum, tungsten) and group VIIIA (cobalt, nickel). These metals catalyze the hydrogenation of the feedstock, making it more reactive for cracking and heteroatom removal, as well as reducing the coking rate. They also initiate the cracking by forming a reactive olefin intermediate via dehydrogenation.

The ratio between the catalyst's cracking function and hydrogenation function can be adjusted in order to optimize activity and selectivity. Activity and selectivity are but two of the four key performance criteria by which hydrocracking catalysts are measured:

- Initial activity, which is measured by the temperature required to obtain desired product at the start of the run
- Stability, which is measured by the rate of increase of temperature required to maintain conversion
- Product selectivity, which is a measure of the ability of a catalyst to produce the desired product slate
- Product quality, which is a measure of the ability of the process to produce products with the desired use specifications, such as pour point, smoke point, or cetane number.

For a hydrocracking catalyst to be effective, it is important that there be a rapid molecular transfer between the acid sites and hydrogenation sites in order to avoid undesirable secondary reactions. Rapid molecular transfer can be achieved by having the hydrogenation sites located in the proximity of the cracking (acid) sites.

## 5.1 Acid Function of the Catalyst

A solid oxide support material supplies the acid function of the hydrocracking catalyst. Amorphous silica-alumina provides the cracking function of amorphous catalysts and serves as support for the hydrogenation metals. Amorphous silica-alumina catalysts are commonly used in distillate producing hydrocracking catalysts. Amorphous silica-alumina also plays a catalytic role in low-zeolite hydrocracking catalysts. In high-zeolite hydrocracking catalysts it acts primarily a support for metals and as binder. Zeolites, particularly Y zeolite, are commonly used in high activity distillate catalysts and in naphtha catalysts. Other acidic support components such as acid-treated clays, pillared clays, layered silicates, acid metal phosphates and other solid acids have been tried in the past, however, present day hydrocracking catalysts do not contain any of these materials.

Amorphous mixed metal oxide supports are acidic because of the difference in charge between adjacent cations in the oxide structure. The advantages of amorphous silica-alumina for hydrocracking are that it has large pores, which permit access of bulky feed stock molecules to the acidic sites, and moderate activity, which makes the metal-acid balance needed for distillate selectivity easier to obtain. Figure 14 is an illustration of silica-alumina acid sites. The substitution of an  $\text{Al}_3^+$  cation for a  $\text{Si}_4^+$  cation leaves a net negative charge on the framework that can be balanced by an acidic proton. The removal of water from this Bronsted acid site creates a Lewis acid site. A Bronsted acid site on a catalyst is an acid site where the acidic entity is an ionizable hydrogen. A Lewis acid site on a catalyst is an acid site where the acidic entity is a positive ion such as  $\text{Al}_3^+$  rather than an ionizable hydrogen. Although plausible hydrocracking mechanisms can be written for

both Bronsted or Lewis sites, Bronsted acidity is believed to be more desirable because Lewis acid sites may catalyze coke formation.

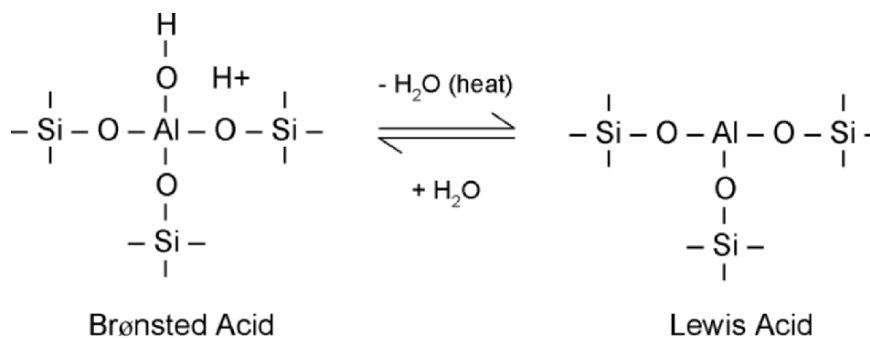


Figure 14. Silica-Alumina Acid Sites

Zeolites are crystalline aluminosilicates composed of  $\text{Al}_2\text{O}_3$  and  $\text{SiO}_2$  tetrahedral units that form a negatively charged microporous framework structure enclosing cavities occupied by large ions and water molecules, both of which have considerable freedom of movement, permitting ion-exchange and reversible dehydration. Mobile cations, which are not part of the framework but are part of the zeolites, are readily exchanged. If the mobile cations are exchanged with  $\text{NH}_4^+$ , followed by calcination to remove  $\text{NH}_3$ , a Bronsted acid site is formed. The zeolite used in hydrocracking, Y zeolite, is synthetic. It has a structure nearly identical to the naturally found zeolite faujasite. The Y zeolite has both a relatively large free aperture, which controls access of reactants to acid sites, and a three-dimensional pore structure, which allows diffusion of the reactants in and products out with minimal interference. Both Bronsted and Lewis acids are possible in zeolites. The number of acid sites and the strength of the acid sites may be varied. These sites are highly uniform, but each zeolite may have more than one type of site. The following factors influence the number and strength of acid sites in zeolites: the types of cations occupying the ion exchange sites, thermal treatments that the sample has received, and the ratio of silica to alumina of the framework. For example, Y zeolite can be dealuminated by a variety of methods, including thermal and hydrothermal treatments. Dealumination decreases the total number of acid sites because each proton is associated with a framework aluminum. However, dealumination also increases the strength of the acid sites to a certain point. As a result, the total acidity of the zeolite, which is a product of the number of sites and strength per site, peaks at an intermediate extent of dealumination. Clearly, the acid site concentration and strength of zeolites affect the final hydrocracking catalyst properties. The principal advantage of zeolites for hydrocracking is their high acidity.

## 5.2 Metal Function of the Catalyst

A metal, a metal oxide, a metal sulfide, or a combination of these compounds may supply the metal function of the catalyst. The key requirement for the metal function is that it must activate hydrogen and catalyze dehydrogenation and hydrogenation reactions. In addition, metal-catalyzed hydrogenolysis (carbon-carbon breaking) is undesirable because the distribution of the hydrogenolysis products is less desirable relative to hydrocracking.

The most commonly used metal function for hydrocracking catalysts is a combination of Group VIA (Mo,W) and Group VIIIA (Co,Ni) metal sulfides. The major advantage of this combination of metal sulfides is that it is sulfur tolerant; however, it has only moderate activity compared to Pd or Pt. The combination of Group VIA and Group VIIIA metal sulfides has been extensively characterized because of its importance to hydrocracking. Although Group VIIIA metal sulfides have some hydrogenation activity, these sulfides alone are much less active than the Group VIA metal sulfides and are considered to be promoters. The Group VIIIA metal promoter interacts synergistically with the Group VIA metal sulfide to produce a substantial increase in activity.

Because the Group VIA and Group VIIIA metals are most conveniently prepared as oxides, a sulfiding step is necessary. That will be discussed in Section 7 (Catalyst Loading and Activation).

## 6. CATALYST MANUFACTURING

Hydrocracking catalysts can be manufactured by a variety of methods. The method chosen usually represents a balance between manufacturing cost and the degree to which the desired chemical and physical properties are achieved. Although there is a relationship between catalyst formulation, preparation procedure, and catalyst properties, the details of that relationship are not always well understood due to the complex nature of the catalyst systems. The chemical composition of the catalyst plays a decisive role in its performance; the physical and mechanical properties also play a major role.

The preparation of hydrocracking catalysts involves several steps:

- Precipitation
- Filtration (decantation, centrifugation)
- Washing
- Drying
- Forming
- Calcination
- Impregnation

Other steps, such as kneading or mulling, grinding, and sieving, may also be required. Depending on the preparation method used, some of these steps may be eliminated, whereas other steps may be added. For example, kneading or comulling of the wet solid precursors is used in some processes instead of precipitation. When the metal precursors are precipitated or comulled together with the support precursors, the impregnation step can be eliminated. Described below are the steps that are an integral part of any hydrocracking catalyst manufacturing process

## 6.1 Precipitation

Precipitation involves the mixing of solutions or suspension of materials, resulting in the formation of a precipitate, which may be crystalline or amorphous. Mulling or kneading of wet solid materials usually leads to the formation of a paste that is subsequently formed and dried. The mulled or kneaded product is submitted to thermal treatment in order to obtain a more intimate contact between components and better homogeneity by thermal diffusion and solid state reactions. Precipitation or mulling is often used to prepare the support for the catalyst and the metal component is subsequently added by impregnation.

The support determines the mechanical properties of the catalyst, such as attrition resistance, hardness, and crushing strength. High surface area and proper pore size distribution is generally required. The pore size distribution and other physical properties of a catalyst support prepared by precipitation are also affected by the precipitation and the aging conditions of the precipitate as well as by subsequent drying, forming and calcining.

## 6.2 Forming

The final shape and size of catalyst particles is determined in the forming step. Catalysts and catalyst supports are formed into several possible shapes such as spheres, cylindrical extrudates or shaped forms such as trilobes or quadrilobes. Spherical catalyst support catalyst is obtained by 'oil dropping' whereby precipitation occurs upon the pouring of a liquid into a second immiscible liquid. Spherical bead catalyst are obtained by this process which is shown in Figure 15.

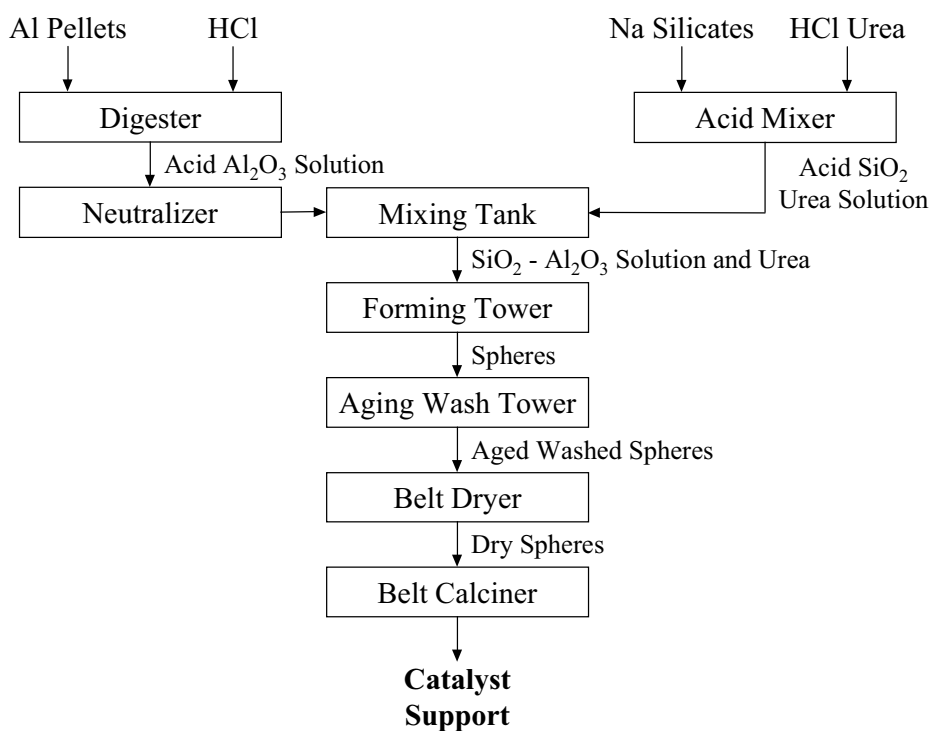


Figure 15. Spherical Catalyst Support Manufacturing

Generally, because of cost considerations, the majority of catalysts are formed in shapes other than spheres. Only amorphous silica-alumina catalysts are formed as spheres.

Extrudates are obtained by extruding a thick paste through a die with perforations. Peptizing agents are usually included in the paste. The spaghetti-like extrudate is usually dried and then broken into short pieces. The typical length to diameter ratio of the extrudates varies between 2 and 4. The extrudate is then dried and/or calcined. The water content of the paste submitted to extrusion is critical because it determines the density, pore size distribution, and mechanical strength of the product. The water content of the paste is usually kept close to the minimum at which extrusion is still possible. Figure 16 shows a typical extrudate support manufacturing.

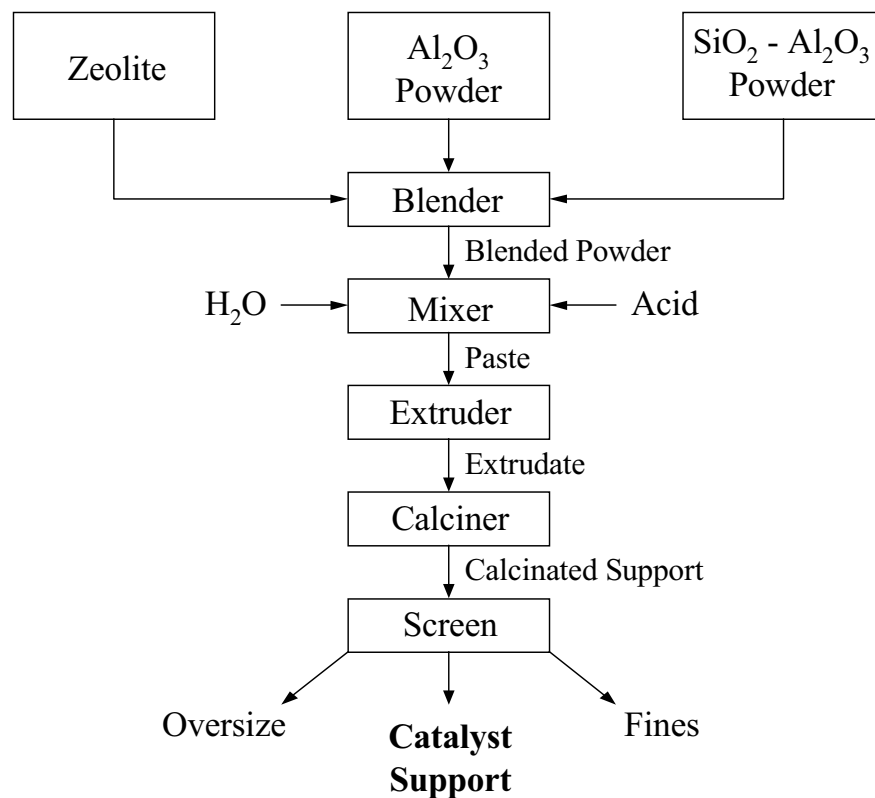


Figure 16. Extrudate Catalyst Support Manufacturing

The form of extrudates may vary. The simplest form is cylindrical, but other forms such as trilobes, twisted trilobes, or quadrilobes, are also found commercially. Catalysts with multilobal cross-sections have a higher surface-to-volume ratio than simple cylindrical extrudates. When used in a fixed bed, these shaped catalyst particles help reduce diffusional resistance, create a more open bed, and reduce pressure drop. Figure 17 depicts several shapes of commercial catalysts used in hydrocracking.

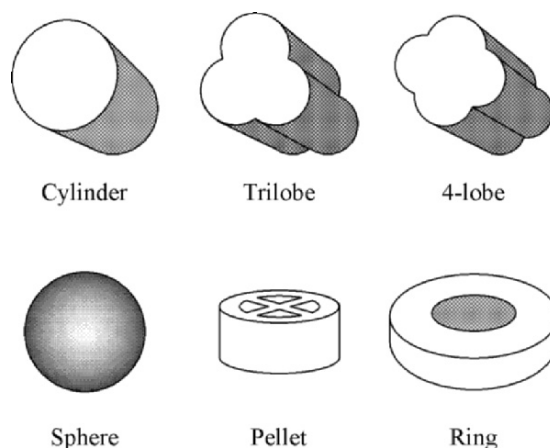


Figure 17. Commercial Catalyst Shapes

### 6.3 Drying and Calcining

Thermal treatment is generally applied before or after impregnation of the formed catalyst. For catalysts prepared by precipitation or comulling of all the components (including the metal components), only drying may be required prior to forming, with subsequent calcination of the formed product. Thermal treatment of the catalyst or support eliminates water and other volatile matter. The drying and calcination conditions are of critical importance in determining the physical as well as catalytic properties of the product. Surface area, pore size distribution, stability, attrition resistance, crushing strength, as well as the catalytic activity are affected by the drying and calcination conditions.

### 6.4 Impregnation

Impregnation is used to incorporate a metal component into a preformed catalyst support. Several impregnation methods may be used for catalyst preparation: a) impregnation by immersion (dipping), b) impregnation by incipient wetness, and c) diffusional impregnation. In the first method, which is the most commonly used, the calcined support is immersed in an excess of solution containing the metal compound. The solution fills the pores and is also adsorbed on the support surface. The excess volume is drained off. Impregnation to incipient wetness is carried out by tumbling or spraying the activated support with a volume of solution having the proper concentration of metal compound, and equal to or slightly less than the pore volume of the support. The impregnated support is dried and calcined. Because metal oxides are formed in the process,



The calcination step is also called oxidation. In diffusional impregnation the support is saturated with water or with acid solution, and immersed into the aqueous solution containing the metal compound. That compound subsequently diffuses into the pores of the support through the aqueous phase. Figure 18 shows an example of catalyst finishing (impregnation).

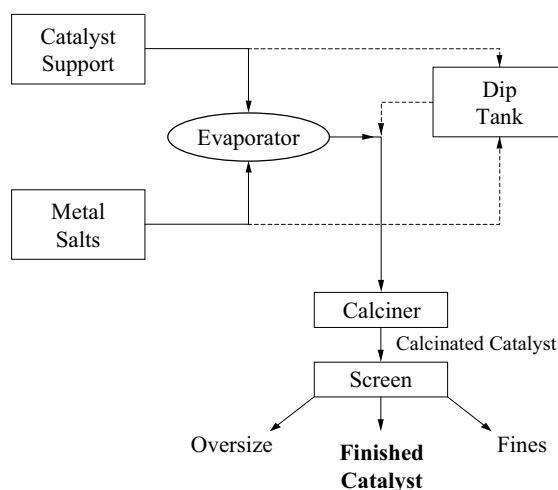


Figure 18. Example of Catalyst Finishing

## 7. CATALYST LOADING AND ACTIVATION

### 7.1 Catalyst Loading

There are two methods of catalyst loading sock loading and dense loading. Sock loading is done by pouring catalyst into a hopper mounted on top of the reactor and then allowing it to flow through a sock into the reactor. Dense loading or dense bed packing is done with the help of a mechanical device. The dense loading method was introduced in mid 1970's. Catalyst loaded by sock loading will have a higher void fraction than catalyst that was dense loaded. Dense bed packing and the resulting higher pressure drop provides a more even distribution of liquid in a trickle flow which is the flow regime for most hydrocracker applications. If diffusion limitations are negligible, dense loading is desirable in order to maximize the reaction rate per unit reactor volume. This is often the case in hydrocracking reactors. The other advantage of dense loading is that it orients the catalyst particles in a horizontal and uniform manner. This improves the vapor/liquid distribution through the catalyst beds. Catalyst particle orientation is important especially for cylindrically shaped extruded catalyst in vapor/liquid reactant systems. When the catalyst particles are oriented in a horizontal position in the catalyst bed, liquid maldistribution or channeling is eliminated. This maldistribution

tends to occur when the catalyst loading is done by the sock loading method, which generally causes the extrudates to be oriented in a downward slant toward the reactor walls increasing bed voids and creating liquid maldistribution. Of all the factors influencing catalyst utilization, catalyst loading has generally proven to be the most important factor. Except for the hydrocrackers that have reactor pressure drop limitations mainly due to operation at higher than design throughputs, the great majority of units worldwide are dense loaded.

## 7.2 Catalyst Activation

Hydrocracking catalysts have to be activated in order to be catalytically active. Several names are used for that purpose, such as sulfiding, presulfiding, presulfurizing in addition to activation. The metals on the greatest majority of catalysts are in an oxide form at the completion of the manufacturing process. The noble metal catalysts are activated by hydrogen reduction of the finished catalyst, in which the metal is also in an oxide form. Calcination in air prior to reduction is necessary to avoid metal sintering. The presence of water vapors is generally avoided, also to prevent metal sintering. By using an excess of hydrogen, the water formed during reduction can be swept away. The activation of noble metal catalysts by hydrogen reduction occurs at 570-750 °F (300-400 °C).

The nonnoble (base metal) catalysts are activated by transforming the catalytically inactive metal oxides into active metal sulfides (thus the name sulfiding, etc). This is accomplished mainly in situ though some refiners have started to do the activation outside the unit (ex situ). It is likely more and more refiners will opt to receive the catalyst at the refinery site in presulfided state to accelerate the start up of the unit. In situ sulfiding can be accomplished either in vapor or liquid phase. In vapor phase sulfiding, the activation of the catalyst is accomplished by injecting a chemical which decomposes easily to H<sub>2</sub>S, such as di-methyl-di-sulphide (DMDS) or di-methyl-sulfide (DMS); use of H<sub>2</sub>S was fairly common until a few years ago, but now it is only rarely used because of environmental and safety concerns. Liquid phase sulfiding can be accomplished with or without spiked feedstocks. In the latter case, the feedstock is generally a gas oil type material that contains sulfur compounds in ranges from a few thousand to twenty thousand ppm. The H<sub>2</sub>S necessary for the activation of the catalyst is generated by the decomposition of the sulfur compounds. This method is in very little use today, but it was 'state of the art' in the 1960's and early 1970's. The preferred sulfiding procedure in the industry is liquid phase with a spiking agent (generally DMDS or DMS). It results in important savings of time when compared to either vapor phase or liquid phase without spiking agents. Another advantage of liquid phase over gas phase sulfiding is that by having all the catalyst particles wet from the very beginning there is very little

chance of catalyst bed channelling which can occur if the catalyst particles are allowed to dry out. The in-situ sulfiding occurs at temperatures between 450 and 600 °F (230-315 °C) regardless of the method used. Some catalyst manufacturers recommend the sulfiding be conducted at full operating pressure while others prefer it be done at pressures lower than the normal operating pressure. Ammonia injection is practiced during the sulfiding of high activity (high zeolite content) catalysts to prevent premature catalyst deactivation.

In the case of ex-situ presulfurization of catalyst, sulfur compounds are loaded onto the catalyst. The activation occurs when the catalyst, which has been loaded in the reactor, is heated up in the presence of hydrogen. The activation can be conducted either in vapor or liquid phase. Generally, activation of ex-situ presulfurized catalyst is accomplished faster than if the sulfiding is done in situ, however there is the additional expense due to the need for the ex-situ presulfurization step.

The economics vary from refiner to refiner, however ex-situ presulfurization is rarely used for hydrocracking catalysts.

## **8. CATALYST DEACTIVATION AND REGENERATION**

Catalyst deactivation is the gradual loss of the catalyst's ability to convert the feed into useful products. Catalyst activity is a measure of the relative rate of feedstock conversion. In practical terms it is the temperature required obtaining a fixed conversion. As the run progresses, the catalyst loses activity. Catalyst will lose activity in several ways described below.

### **8.1 Coke Deposition**

Coke deposition is a byproduct of the cracking reactions. The laydown of coke on a catalyst is a time-temperature phenomenon in that the longer the exposure and/or the higher the temperature the catalyst is subjected to, the more severe the deactivating effect. It begins with adsorption of high-molecular weight, low hydrogen/carbon ratio ring compounds; it proceeds with further loss of hydrogen content, and ends with varying degrees of hardness of coke. This coke can cover active sites and/or prevent access to these sites by physical blockage of the entrance to the pores leading to the sites. Coke is not a permanent poison. Catalyst, which has been deactivated by coke deposition, can be, relatively easily, restored to near original condition by regeneration.

## 8.2 Reversible Poisoning

Catalyst poisoning is primarily the result of strong chemisorption of impurities on active sites. This type of poisoning is reversible - that is, when the deactivating agent is removed, the deactivating effect is gradually reversed. In some cases, raising the catalyst temperature can compensate for the deactivating effect. But, raising temperatures will, however, increase the rate of coke deposition. One example of a reversible poison is carbon monoxide, which can impair the hydrogenation reactions by preferential adsorption on active sites. Another example is  $H_2S$ , which in moderate to high concentrations can reduce the desulfurization, rate constant. In this case, the removal of  $H_2S$  from the recycle gas system solves the problem.

## 8.3 Agglomeration of the Hydrogenation Component

Another reversible form of catalyst deactivation is the agglomeration of the hydrogenation component of the catalyst. It can be caused by poor catalyst activation conditions in which a combination of high water partial pressure and high temperature may exist for a prolonged period.

Regeneration can restore the catalyst to near original condition.

## 8.4 Metals Deposition

Deposition of metals is not reversible, even with catalyst regeneration. The metals may come into the system via additives, such as silicon compounds used in coke drums to reduce foaming, or feedstock contaminants such as Pb, Fe, As, P, Na, Ca, Mg, or as organometallic compounds in the feed primarily containing Ni and V. The deposition of Ni and V takes place at the pore entrances or near the outer surface of the catalyst, creating a 'rind' layer - effectively choking off access to the interior part of the catalyst, where most of the surface area resides. Metals deposition can damage the acid sites, the metal sites, or both.

## 8.5 Catalyst Support Sintering

This is another reason for loss of catalyst activity and it also is irreversible. This is also a result of high temperatures and particularly in connection with high water partial pressures. In this case the catalyst support material can lose surface area from a collapse of pores, or from an increase in the diameter of pores, with the pore volume remaining approximately constant.

## 8.6 Catalyst Regeneration

A coked catalyst is usually regenerated by combustion in a stream of diluted oxygen or air, although steam or steam-air mixtures have also been used in the past. Upon combustion, coke is converted to  $\text{CO}_2$  and  $\text{H}_2\text{O}$ . In the absence of excess oxygen,  $\text{CO}$  may also form. Except for the noble metal catalysts, hydrocracking catalysts contain sulfur, as the metals are in a sulfide form. In the regeneration process, the sulfur will be emitted as  $\text{SO}_2$ . In general, sulfur oxide emission starts at lower temperature than  $\text{CO}_2$  emission. Regeneration of commercial catalysts can be done in-situ or ex-situ. The majority of commercial catalysts regeneration is performed ex-situ because of environmental considerations as well as because it results in a better performing catalyst. There are several companies that perform ex-situ regeneration by using different equipment for burning off the coke. One company uses a continuous rotolouver, which is a cylindrical drum rotating slowly on a horizontal axis and enclosing a series of overlapping louvers. The spent catalyst passes slowly through the rotolouver, where it encounters a countercurrent of hot air. Another company uses a porous moving belt as a regenerator. The catalyst is moved with the stainless steel belt through a stationary tunnel furnace vessel where the regeneration takes place. A third company regenerator uses ebullated bed technology to perform the catalyst regeneration. Regardless of the process, the spent catalyst is submitted to de-oiling prior to regeneration. This is to eliminate as much hydrocarbon as possible as well as to remove as much sulfur as possible to prevent formation of sulfates which could deposit on the catalyst and not be removed during regeneration. Sulfates are deleterious to catalyst performance.

## 9. DESIGN AND OPERATION OF HYDROCRACKING REACTORS

### 9.1 Design and Construction of Hydrocracking Reactors

Hydrocracking reactors are downflow, fixed-bed catalytic reactors, generally operating in trickle flow regime. Because hydrocracking occurs at high pressure and relatively high temperature and in the presence of hydrogen and hydrogen sulfide the reactors are vessels with thick wall constructed from special materials. The reactors are usually cylindrical vessels fabricated from  $2\frac{1}{4}$  Cr - 1 Mo or 3 Cr - 1 Mo material with stabilized austenitic stainless steel weld overlay or liner, for added corrosion protection. More specialized materials, in which a small amount of Vanadium is added to the  $2\frac{1}{4}$  Cr - 1 Mo or 3 Cr - 1 Mo reactor base metal to increase its strength characteristics, started being used by some fabricators in the last 3 - 5 years. A typical drawing of a hydrocracking reactor is shown in Figure 19.

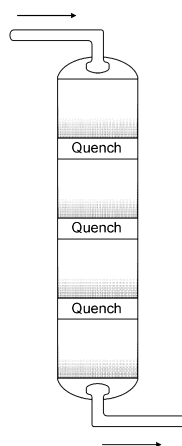


Figure 19. Typical Hydrocracking Reactor

The size of the hydrocracking reactors varies widely depending on the design conditions and is dependent on the desired mass velocity and acceptable pressure drops. Commercially, reactors with inside diameters of up to 16 ft (4.9 m) have been fabricated. Depending on the design pressure and inside diameter, the thickness of the reactor walls can be as much as 1 ft (30 cm). Since heat release is a common feature for all hydrocrackers, reactor temperature control has to be exercised. As shown schematically in Figure 8.1, a hydrocracking reactor will contain several separate catalyst beds. The number of catalytic beds in a reactor and their respective lengths are determined from the temperature rise profile. The maximum acceptable temperature rise per bed defines the length of the catalyst bed. The acceptable temperature maximum, in turn, depends on the operating mode of the hydrocracker. For example, operations designed to maximize naphtha have a different maximum from those designed the production of middle distillate. A typical reactor operated to maximize naphtha yields will have five or six beds. A typical reactor operated to produce middle distillate will have three or four beds. Commercial catalyst beds can reach lengths up to 20 ft (6 m). A typical pretreating reactor will have two or three beds if the feed is straight run material, and up to five beds if the feed contains appreciable amounts of cracked material. Cold hydrogen gas, introduced in the quench zones, is used for reactor temperature control. The quench zones separating successive catalyst beds have the following functions: (a) to cool the partially reacted fluids with hydrogen quench gas; (b) to assure a uniform temperature distribution the fluids entering the next catalyst bed; and (c) to mix efficiently and disperse evenly the fluids over the top of the next catalyst bed. Since hydrocracking is an exothermic process, the fluids exiting one catalyst bed have to be cooled prior to entering the next catalyst bed, in order to avoid overheating and to provide a safe and stable operation. This is accomplished

by thorough mixing with cool hydrogen. Furthermore, the temperature distribution in the cooled fluids entering the next catalyst bed has to be uniform in order to minimize the radial temperature gradients in successive catalyst beds. Unbalanced temperatures in a catalyst bed may result in different reaction rates in the same bed. This can lead to different deactivation rates of the catalyst, and, in worse cases, to temperature excursions. In addition to a uniform temperature distribution, it is also important to achieve a good mass flow distribution. The effective vapor/liquid mixing and uniform distribution of fluids over the top of the catalyst bed, accomplished in the quench zone, reestablishes an even mass flow distribution through the bed. There is a multitude of companies providing vapor/liquid distribution devices, from process licensors, to catalyst manufacturers and, engineering contractors. Most distribution devices perform well, provided they are properly installed. Another important parameter is liquid flux (lbs/hr/sq ft of cross-sectional area). While gas mass flux has practically no influence on liquid distribution, liquid mass flux is determinant in avoiding maldistribution in the catalyst bed. Operation at a liquid mass flux of more than 2,000 lbs/hr/sq ft is recommended; operation at liquid fluxes lower than 1,500 lbs/hr/sq ft is strongly discouraged. Furthermore, it should be noticed that if the liquid mass flux is below the recommended limit, increasing the gas mass flux will have very little effect, if any, on the liquid distribution (eg it will not improve it).

## 9.2 Hydrocracking Reactor Operation

During operation, the hydrocracking catalyst gradually loses some of its activity. In order to maintain the conversion of feedstock to products constant, the average bed temperature is gradually increased. The temperature increase in many cases is very small, less than 2 °F/month (1 °C/month). When the average bed temperature reaches a value close to the designed maximum, the catalyst has to be replaced or reactivated. Because the required temperature increase per unit time is relatively small, the reactor can be operated with the same catalyst for several years before replacement of the deactivated catalyst becomes necessary. Similar changes take place in the pretreating reactor.

Kinetics is the study of the rates of reaction. The rates of reaction determine the key properties of a hydrocracking catalyst: initial activity, selectivity, stability and product quality. The temperature required to obtain the desired product at the start of the run measures the initial activity. In general, the catalyst activity is a measure of the relative rate of feedstock conversion. In hydrocracking, activity is defined as the temperature required obtaining fixed conversion under certain process conditions. Hydrocracking conversion is usually defined in terms of change of endpoint:

$$\% \text{ Conversion} = ((EP^+_{\text{feed}} - EP^+_{\text{product}})/EP^+_{\text{feed}}) \times 100$$

where  $EP^+$  indicates the fraction of material in the feed or product boiling above the desired endpoint.

Catalyst selectivity is a measure of the rate of formation of a desired product relative to the rate of conversion of the feed (or formation of other products). Hydrocracking selectivity is expressed as the yield of desired product at a specific conversion. Yield is determined by the rate of formation of the desired product relative to the feed rate. At 100% conversion, catalyst yield equals catalyst selectivity. Hydrocracking selectivity is affected by operating conditions. In general, more severe operating conditions cause higher selectivity for secondary products.

Catalyst stability is a measure of change of reaction rate over time. Hydrocrackers are typically operated in the constant conversion mode, with temperature adjustments made to maintain the desired conversion. Hydrocracking activity stability is defined as the temperature change required maintaining constant conversion. Changes in product yield over time on-stream occur when using zeolitic catalysts. Hydrocracking yield stability is defined as the yield change with time at constant conversion and is usually expressed as a function of temperature change.

The product quality is a measure of the ability of the process to yield products with the desired use specification such as pour point, smoke point or octane. Table 8.2 shows some of the important product quality measurements and the chemical basis for these measurements.

*Table 2. Chemical Basis for Product Quality*

| Quality Measurement | Chemical Basis                   |
|---------------------|----------------------------------|
| High Smoke Point    | Low Concentration of Aromatics   |
| Low Pour Point      | Low Concentration of n-Paraffins |
| Low Freeze Point    | Low Concentration of n-Paraffins |
| Low Cloud Point     | Low Concentration of n-Paraffins |
| Low CFPP            | Low Concentration of n-Paraffins |
| High Octane         | High Ratio of i/n Paraffins      |
|                     | High Concentration of Aromatics  |
|                     | High Concentration of Naphthenes |

## 10. HYDROCRACKING PROCESS VARIABLES

The proper operation of the unit will depend on the careful selection and control of the processing conditions. By careful monitoring of these process variables the unit can operate to its full potential.



## 10.1 Catalyst Temperature

The amount of conversion which takes place in the reactors is going to be determined by several variables; the type of feedstock, the amount of time the feed is in the presence of catalyst, the partial pressure of hydrogen in the catalyst bed, and, most important, the temperature of the catalyst and reactants. The obvious generalization about temperature is that the higher the temperature, the faster the rate of reaction and therefore, the higher the conversion. Since hydrocracking is exothermic, overall, the temperature increases as the feed and recycle gas proceed through the catalyst beds. It is very important that the temperature increase ( $\Delta T$ ) be controlled carefully at all times. It is possible to generate more heat from the reactions than the flowing streams can remove from the reactors. If this happens, the temperature may increase very rapidly. This condition is called a temperature excursion or a temperature runaway. A temperature runaway is a very serious situation since extremely high temperatures can be generated within a short period of time. These high temperatures can cause damage to the catalyst and/or to the reactors. To avoid these situations temperature guidelines have to be observed. These guidelines are dependent on the type of feedstock, and the type of catalyst, and vary from catalyst supplier to catalyst supplier, but by and large, limit the temperature rise of catalyst beds loaded with noble metal catalyst to about 30 °F (17 °C). The temperature rise of catalyst beds loaded with high activity base metal catalysts (for naphtha production) is limited to about 40 °F (22 °C) and those loaded with low zeolite content catalyst (for middle distillate production) the temperature rise is limited to 50 °F (28 °C). Finally, maximum bed temperature rises of about 75 °F (42 °C) are recommended for amorphous catalysts. The same maximum bed temperature rise is also recommended for most pretreating reactors. To properly monitor the reactions as the reactants pass through the catalyst bed, it is not sufficient to just measure the temperature of the flowing stream at the inlet and outlet of each bed and/or the reactor. It is necessary to observe the temperature at the inlet, outlet, and radially throughout the catalyst bed. A temperature profile plot is a useful tool for evaluating performance of catalyst, effectiveness of quench, and reactor flow patterns. A temperature profile can be constructed by plotting the catalyst temperature versus distance into the catalyst bed (or more accurately versus weight percent of catalyst). The hydrocracking reactor should be operated with equal catalyst peak temperatures. In this manner the total catalyst volume is utilized during the entire cycle. The weight average bed temperature (WABT) is typically used to compare the catalyst activity. Figure 20 gives a general description of how the WABT is calculated for a reactor.

The rate of increase of the reactor WABT to maintain both hydrotreating and hydrocracking functions, in order to obtain the desire conversion level and product quality, is referred to as the deactivation rate. It is one of the key

variables used to monitor the performance of the catalyst systems. The deactivation rate can be expressed in °F per barrel of feed processed per pound of catalyst (°C per m<sup>3</sup> of feed per kilogram of catalyst) or more simply stated as °F per day (°C per day). The decrease in catalyst activity for hydrotreating catalyst will show up in a decrease in its ability to maintain a constant nitrogen level in the hydrotreating catalyst effluent. For hydrocracking catalyst, a decrease in catalyst activity will generally show up in its ability to maintain a constant conversion to the desired product slate. To hold the same conversion level to the desired product slate the reactor WABT is gradually increased.

Attribute a weight-fraction of the catalyst to each temperature indicator (TI).  
For example:

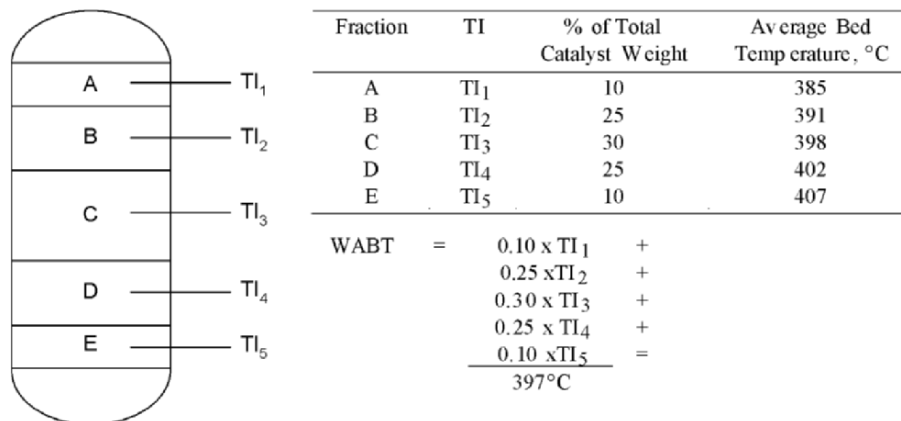


Figure 20. Example Calculation of Weight Average Reactor Temperature (WABT)

## 10.2 Conversion

The term “conversion” is usually defined as:

$$\text{Conversion, vol\%} = (\text{Fresh Feed} - ((\text{Fractionator Bottoms})/\text{Fresh Feed})) * 100$$

where:

FF = Fresh feed rate, BPD or m<sup>3</sup>/hr

Frac Bottoms = Net fractionator bottoms product to storage, BPD or m<sup>3</sup>/hr

Conversion is useful as a measure of the severity of the operation. It requires higher severity (meaning higher catalyst temperature) to go to higher conversion levels and higher severity to reduce the endpoint of the product at a constant conversion. Conversion is normally controlled by catalyst temperature.

### 10.3 Fresh Feed Quality

The quality of the raw oil charged to a Hydrocracker will affect the temperature required in the catalyst bed to reach the desired conversion, the amount of hydrogen consumed in the process, the length of time before the catalyst is deactivated, and the quality of products. The effect of the feedstock quality on the performance of the unit is important and should be well understood, especially with regard to contaminants that can greatly reduce the life of the catalyst.

#### 10.3.1 Sulfur and Nitrogen Compounds

In general, increasing the amount of organic nitrogen and sulfur compounds contained in the feed results in an increase in severity of the operation. The sulfur content of the feed for a normal vacuum gas oil charge stock can vary up to as high as 2.5 to 3.0 wt. percent. The higher sulfur levels will cause a corresponding increase in the H<sub>2</sub>S content of the recycle gas that will normally have little or no effect on catalyst activity.

The organic nitrogen compounds are converted to ammonia which, if allowed to build up in the recycle gas, competes with the hydrocarbon for the active catalyst sites. This results in a lower apparent activity of the catalyst as the ammonia concentration increases. Because of this, feedstocks with high organic nitrogen contents are more difficult to process and require higher catalyst temperatures.

#### 10.3.2 Hydrogen Content

The amount of unsaturated compounds (such as olefins and aromatics) contained in the feed will have an effect on the heat released during the reaction and on the total hydrogen consumption on the unit. In general, for a given boiling range feedstock, a reduction in API gravity (increase in specific gravity) indicates an increase in the amount of unsaturated compounds and, therefore, higher heats of reaction and higher hydrogen consumption. Large amounts of unsaturated hydrocarbons can also cause a heat balance problem if the unit has not been designed to process this type of feed.

### 10.3.3 Boiling Range

The typical charge stock to a Hydrocracker is a 700°F+ (370°C+) boiling range HVGO. Increasing the boiling range usually makes the feed more difficult to process which means higher catalyst temperatures and shorter catalyst life. This is especially true if the feed quality is allowed to decrease significantly due to entrainment of catalyst poisons in the feed. Higher endpoint feeds also usually have higher sulfur and nitrogen contents, which again make it more difficult to process.

### 10.3.4 Cracked Feed Components

Cracked feedstocks derived from catalytic cracking or thermal cracking can also be processed in a Hydrocracker. These cracked components tend to have higher contaminants such as sulfur, nitrogen, and particulates. They are also more refractory, with high aromatics content and polynuclear aromatic precursors. These compounds make cracked stocks harder to process to produce quality products.

### 10.3.5 Permanent Catalyst Poisons

Organo-metallic compounds contained in the feed will be decomposed and the metals will be retained on the catalyst, thus decreasing its activity. Since metals are normally not removable by oxidative regeneration, once metals have poisoned a catalyst, its activity cannot be restored. Therefore, metals content of the feedstock is a critical variable that must be carefully controlled. The particular metals which usually exist in vacuum gas oil type feeds are naturally occurring nickel, vanadium and arsenic as well as some metals which are introduced by upstream processing or contamination such as lead, sodium, silicon and phosphorous. Iron naphthenates are soluble in oil and will be a poison to the catalyst. Iron sulfide as corrosion product is normally not considered a poison to the catalyst and is usually omitted when referring to total metals.

The tolerance of the catalyst to metals is difficult to quantify and is somewhat dependent upon the type of catalyst being employed and the severity of the operation, i.e., the higher the severity, the lower will be the metals' tolerance since any impairment of activity will affect the ability to make the desired conversion. It is recommended to keep the total metals in the feedstock as low as possible and certainly not higher than 2 wt-ppm.

## 10.4 Fresh Feed Rate (LHSV)

The amount of catalyst loaded into the reactors is based upon the quantity and quality of design feedstock and the desired conversion level. The variable

that is normally used to relate the amount of catalyst to the amount of feed is termed liquid hourly space velocity (LHSV). LHSV is the ratio of volumetric feed rate per hour to the catalyst volume. Hydrocrackers are normally designed for a LHSV that depends on the severity of the operation. Increasing the fresh feed rate with a constant catalyst volume increases the LHSV and a corresponding increase in catalyst temperature will be required to maintain a constant conversion. The increased catalyst temperature will lead to a faster rate of coke formation and, therefore, reduce the catalyst life. If the LHSV is run significantly higher than the design of the unit, the rate of catalyst deactivation may become unacceptable. Liquid Hourly Space Velocity (LHSV) can be defined as:

$$\text{LHSV (hr}^{-1}\text{)} = \frac{\text{Total Feed to Reactor Inlet}}{\text{Total Catalyst Volume}}$$

## 10.5 Liquid Recycle

Most Hydrocrackers are designed to recycle unconverted feed from the product fractionator bottoms back to the reactors. This stream is normally material distilled above the heaviest fractionator side cut product. For a distillate producing Hydrocracker, the recycle stream is normally a 600-700°F (315-370°C) heavy diesel plus material.

The liquid recycle rate is normally adjusted as a ratio with fresh feed. This variable is called combined feed ratio (CFR), and is defined as follows:

$$\text{CFR} = \frac{\text{Fresh Feed Rate} + \text{Liquid Recycle Rate}}{\text{Fresh Feed Rate}}$$

It can be seen that if the unit has no liquid recycle from the fractionator back to the reactors, the CFR is 1.0 and the unit is said to operate once-through, i.e., the fresh feed goes through the catalyst bed only once. If the amount of liquid recycle is equal to fresh feed, the CFR will be 2.0.

An important function of liquid recycle is to reduce the severity of the operation. Considering conversion per pass that is defined as follows can show this:

$$\text{Conversion per Pass} = \left( \frac{\text{Feed Rate} - \text{Frac Bottoms Rate to Storage}}{\text{Feed Rate} + \text{Liquid Recycle Rate}} \right) \times 100$$

If a unit were operating once-through (CFR = 1.0), and 100 percent of the feed were converted into products boiling below, i.e. 700°F (370°C), the conversion per pass is 100 percent since the feed only makes one pass through the catalyst. At the other extreme, if a unit is designed at a CFR of 2.0 and

100 percent of the feed converted into products, the conversion per pass is only 50 percent. In this way, it can be seen that as the CFR increases, the conversion per pass decreases. It is also seen that the catalyst temperature requirement is reduced as the CFR is increased (at a constant fresh feed conversion level). Therefore, reducing the CFR below the design value can lead to higher catalyst temperatures and shorter catalyst cycle life. Increasing the CFR above design can be helpful when operating at low fresh feed rates since it does not allow the total mass flow through the catalyst bed to reach such a low value that poor distribution patterns are established.

## 10.6 Hydrogen Partial Pressure

The reactor section operating pressure is controlled by the pressure that is maintained at the high pressure separator. This pressure, multiplied by the hydrogen purity of the recycle gas, determines the partial pressure of hydrogen at the separator. The hydrogen partial pressure required for the operation of the unit is chosen based on the type of feedstock to be processed and the amount of conversion desired.

The function of hydrogen is to promote the saturation of olefins and aromatics and saturate the cracked hydrocarbons. It is also necessary to prevent excessive condensation reactions from forming coke. For this reason, running the unit for extended periods of time at lower than design partial pressure of hydrogen will result in increased catalyst deactivation rate and shorter time between regeneration.

Hydrogen partial pressure has an impact on the saturation of aromatics. A decrease in system pressure or recycle gas purity has a sharp effect on the product aromatic content. This will be especially true for kerosene aromatic content, which will in turn affect the kerosene product smoke points.

A reduction in operating pressure below its design will have a negative effect on the activity of the catalyst and will accelerate catalyst deactivation due to increased coke formation.

Operating at higher than design pressure may not be possible. There will be a practical equipment limitation on most units that will not allow significantly higher pressure than design, such as the pressure rating of the heaters, exchangers, and vessels. The major control variable for hydrogen partial pressure is the recycle gas purity that should be monitored closely to assure it is always maintained above the minimum value. The hydrogen purity can be improved by increasing the hydrogen purity of the makeup hydrogen, venting gas off the high-pressure separator, or reducing the temperature at the high-pressure separator.

## 10.7 Recycle Gas Rate

In addition to maintaining a prescribed partial pressure of hydrogen in the reactor section, it is equally important to maintain the physical contact of the hydrogen with the catalyst and hydrocarbon so that the hydrogen is available at the sites where the reaction is taking place. This is accomplished by circulating the recycle gas throughout the reactor circuit continuously with the recycle gas compressor. The amount of gas that must be recycled is a design variable again set by the design severity of the operation. The standard measure of the amount of gas required is the ratio of the gas being recycled to the rate fresh feed is being charged to the catalyst.

As with hydrogen partial pressure, the recycle gas/feed ratio should be maintained at the design ratio. The actual calculation for the gas-to-oil ratio, can be defined as:

$$\text{Gas - To - Oil Ratio} = \frac{\text{Total Circulating Gas to Reactor, Nm}^3/\text{hr}}{\text{Total Feed to Reactor Inlet, m}^3/\text{hr}} = \text{Nm}^3/\text{m}^3 \text{ Feed}$$

As with hydrogen partial pressure, any reduction of the gas-to-oil ratio below the design minimum will have adverse effects on the catalyst life. During normal operations and through out the cycle length, there will be a gradual increase in the reactor section pressure drop. As the pressure drop increases, there will be a tendency for the gas-to-oil ratio to decrease. When the pressure drop through the system increases to the point where the minimum gas-to-oil ratio can not be kept, either the unit throughput will have to be decreased to bring the gas-to-oil ratio back above the minimum, or the unit shutdown for catalyst replacement.

Gas-to-oil ratio recommendations vary between licensors and/or catalyst vendors but in general the minimums recommended are as follows: (a) 4,000 SCFB (675  $\text{nm}^3/\text{m}^3$ ) for amorphous catalyst systems and 5,500 SCFB (925  $\text{nm}^3/\text{m}^3$ ) for zeolitic catalyst systems.

## 10.8 Makeup Hydrogen

The quality of the hydrogen-rich gas from the hydrogen plant is an important variable to the performance of Hydrocrackers since it can affect the hydrogen partial pressure and recycle gas/feed ratio and thereby influence the catalyst stability (deactivation rate). The following guidelines should be used in operating the hydrogen plant to produce acceptable feed gas to a Hydrocracker.

### 10.8.1 Hydrogen Purity

The purity of hydrogen in the makeup gas to a Hydrocracker will have a major influence on the hydrogen partial pressure and recycle gas/feed ratio. Therefore, the minimum purity on the makeup gas should be set to provide the minimum recycle gas purity allowed. If the hydrogen plant is unable for some reason to produce minimum hydrogen purity product, it may be possible to purge sufficient recycle gas off the high-pressure separator to maintain the recycle gas purity requirements.

### 10.8.2 Nitrogen and Methane Content

The total of the nitrogen and methane contained in the makeup gas is only harmful as a diluent, i.e., it will reduce the hydrogen partial pressure and as long as the minimum hydrogen purity is maintained, it will not affect the unit. However, it should be noted that excessive quantities of molecular nitrogen entering a hydrocracker in the makeup gas stream can cause a buildup of nitrogen in the recycle gas since the nitrogen is non-condensable. If this is the case, the nitrogen will have to be removed from the reactor circuit by a small, continuous purge of recycle gas off the high-pressure separator.

### 10.8.3 CO + CO<sub>2</sub> Content

The normal specification for CO plus CO<sub>2</sub> in the makeup gas stream to a Hydrocracker is in low two-digit mol-ppm maximum. Larger quantities can have a harmful effect on catalyst activity. CO is considered the worst impurity due to the fact that it has a limited solubility in both hydrocarbon and water and will, therefore, build up in the recycle gas. CO<sub>2</sub>, on the other hand, is much more soluble and is readily removed from the system in the high-pressure separator liquids.

Both CO and CO<sub>2</sub> have similar effects on the Hydrocracking catalyst; they are converted on the active sites of the catalyst in the presence of hydrogen to methane and water. This methanation of CO and CO<sub>2</sub> competes with the normal hydrocarbon reactants for the catalyst. Therefore, if CO + CO<sub>2</sub> is allowed to build up, higher catalyst temperatures will be required. In an extreme case where a large quantity of CO or CO<sub>2</sub> would be introduced to the Hydrocracker in a short period of time, it is theoretically possible that a temperature excursion would result since the methanation reaction is highly exothermic.

It is recommended practice that if the CO + CO<sub>2</sub> content exceeds the maximum design limit, the catalyst temperature should not be increased to compensate for a resulting decrease in conversion. Catalyst temperature should be maintained at the same level or reduced until the problem causing the high CO + CO<sub>2</sub> is eliminated. In this way the catalyst will not be harmed



by increased deactivation at a higher temperature and it will also eliminate the possibility of a temperature runaway due to methanation.

## 11. HYDROCRACKER LICENSORS AND CATALYST MANUFACTURERS

### 11.1 Licensors

Hydrocracking licensing started in 1960. Chevron, UOP, Unocal, Shell and Exxon were active from the beginning. Since that time, some 250 hydrocrackers have been licensed worldwide. As of the beginning of 2001, 154 hydrocrackers were in operation. Through the years, the licensing 'landscape' has changed. Currently, the active licensors are Chevron, EMAK (ExxonMobil-Akzo Nobel-Kellogg), IFP and UOP.

### 11.2 Catalyst Suppliers

Catalysts used in hydrocrackers are pretreating catalysts and cracking catalysts. Following is a list of the current major suppliers of pretreating catalysts: Advanced Refining Technology (in conjunction with Chevron), Albemarle, Criterion, Haldor Topsoe, Procatalyse (in connection with IFP) and UOP. The major cracking catalyst suppliers are: Albemarle, Chevron, Criterion & Zeolyst, Procatalyse (in connection with IFP and UOP).

## 12. REFERENCES

1. Sabatier, P., Senderens, J.B. Acad. Sci. Paris, **1897**, (124), 1358-1360.
2. Ipatieff, V.N. *Catalytic Reactions at High Pressures and Temperatures*, Macmillan (New York) 1936.
3. Bergius, F. Nobel Prize Lecture, Stockholm, Sweden, 1931
4. Borkin, J. *The Crime and Punishment of I.G. Farben*, Free Press (New York), 1978.
5. Radovic, L.R. in "Synthetic Fuels, Oil Shale, and Tar Sands," <http://www.ems.psu.edu/~Radovic/Chapter10.pdf>
6. Sullivan, R.F., Egan, C.J., Langolis, G.E., Seig, R.P. *J. Amer. Chem. Soc.*, **1961** (83) 1156.
7. "Worldwide Refineries, Capacities as of January 1, 2004," *Oil & Gas J.*, Dec. 22, 2003
8. Scherzer, J.; Gruia, A.J., *Hydrocracking Science and Technology*, Marcell Dekker, Inc.: New York, 1996

## Chapter 9

# CURRENT PROGRESS IN CATALYSTS AND CATALYSIS FOR HYDROTREATING

Isao Mochida and Ki-Hyouk Choi  
*Kyushu University*  
*Kasuga, Fukuoka 816-8580*  
*Japan*

### 1. INTRODUCTION

There are a number of processes used in petroleum refining as shown in Fig. 1. These include thermal, catalytic and hydroprocessing upgrading processes. The hydroprocessing processes include three major classes, namely, hydrotreating, hydrocracking, and hydrofinishing. Hydrotreating includes hydrogenative heteroatom removal and hydrogenation. Hydrocracking performs hydrogenation and cracking successively and simultaneously. There are differences between combined hydrotreating/catalytic cracking and hydrotreating/hydrocracking in terms of conditions and reactions interactions, with associated advantages and disadvantages being included in these processes. Hydrofinishing is really another form of hydrotreating that is used to achieve the final specifications of fuels. Each process is individually optimized according to the boiling range and molecular composition of the specific petroleum fraction being treated.<sup>1</sup> Hence, it is very important to understand correctly the process objectives, conditions and configurations, the chemistry of feeds and products, catalytic materials and their functions and working mechanisms for all of the important hydroprocesses currently operated.<sup>2</sup>

The products in the refining processes are also hydrotreated, and are basically classified according to their boiling ranges. This overview describes the detailed chemistry of feeds, products, and their conversion mechanisms on the catalysts in hydrotreating on a molecular level, including the detailed structures of the reactants, their chemical and physical properties and the mechanisms of their conversion. The influences of the detailed molecular

interactions on reactivity and inhibition are also reviewed. The preparation, activation, composition and structure of the catalysts in each process are discussed along with the associated causes of catalyst deactivation and ultimate catalyst lifetime for each process. Approaches to new and improved catalytic processes and more active catalysts are also discussed, even if the structure of the catalyst is still not fully described on atomic levels.

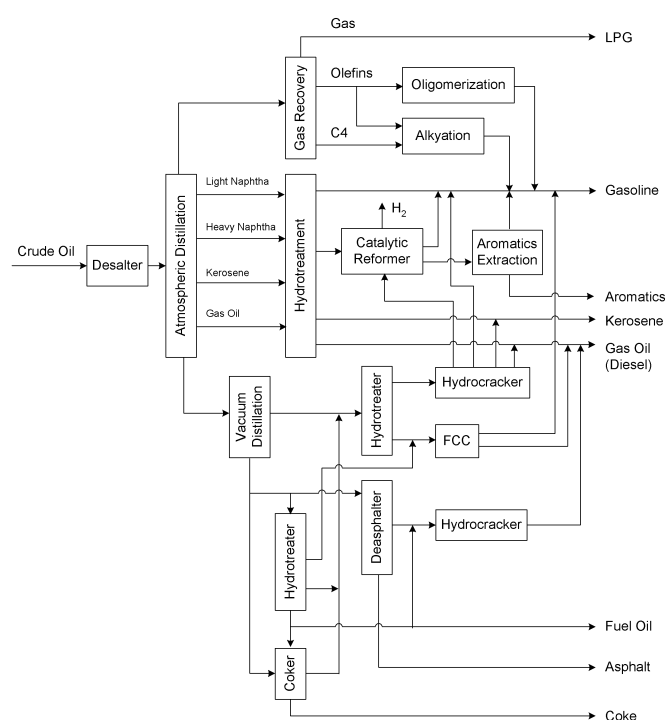


Figure 1. Stream of Petroleum Processes

Recently, some reviews on the hydrodesulfurization of middle distillates have been published. Song summarized the new aspects of deep HDS of diesel and gasoline fractions including a brief review of some commercial processes.<sup>3</sup> Moulijn also reported the recent advances in deep HDS.<sup>4</sup> His review described the conventional and non-conventional technology including adsorption and oxidation. In contrast, French groups summarized the chemical nature of HDS systems, including new acid catalysts and adsorption technology.<sup>5</sup>

Fig. 2 illustrates the diversity of composition by showing the elemental distribution of some typical petroleum fractions, such as LCO (light cycle oil), MCO (medium cycle oil), SRGO (straight run gas oil), H-SRGO (hydrotreated straight run gas oil), and gasoline, as determined by GC-AED

(Gas Chromatography with Atomic Emission Detection).<sup>6,7</sup> GC-AED chromatograms of hexane soluble fraction of VGO were also included. Also shown in this figure are the distributions of specific molecular species that must be converted into hydrocarbons by hydrotreating in the presence of partner species.

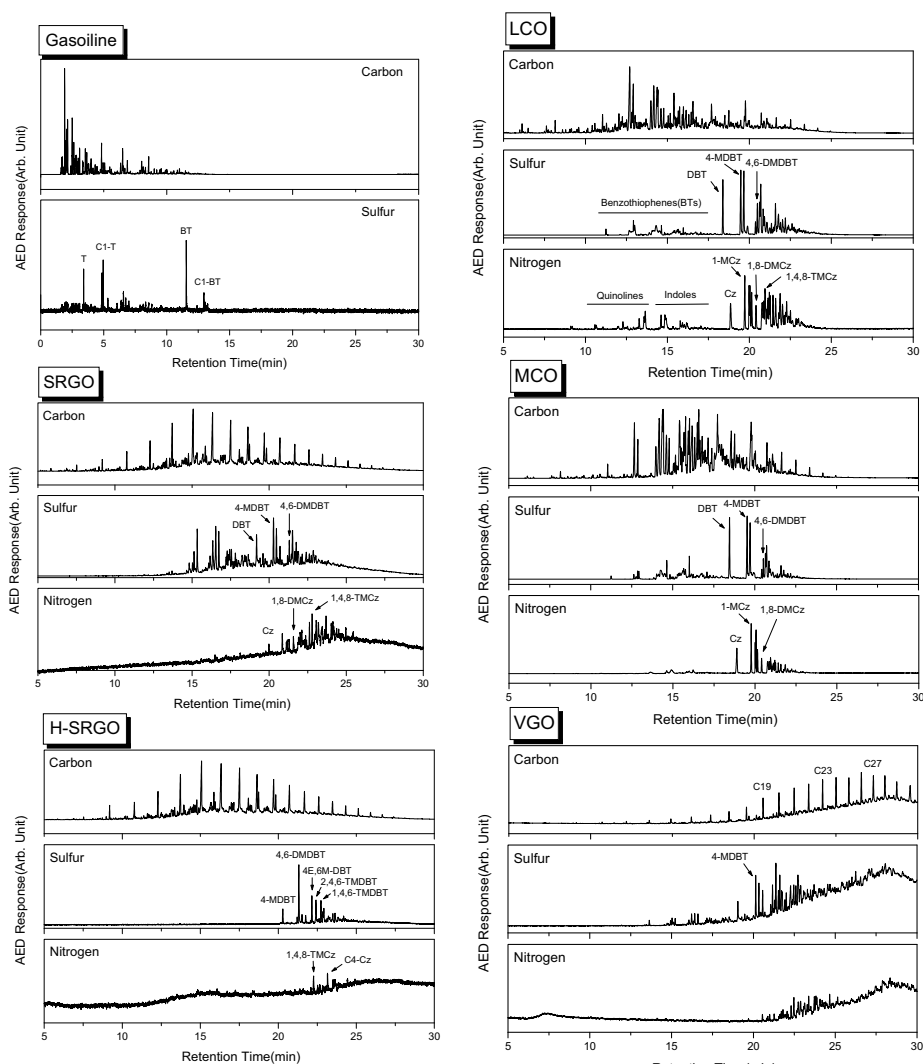


Figure 2. AED Chromatograms of Various Fuel Oils. LCO: light cycle oil, MCO: medium cycle oil, VGO(hexane soluble fraction):Vacuum Gas Oil, SRGO: straight run gas oil, H-SRGO: hydrotreated straight run gas oil. (Cn: Paraffin with n carbons, T: Thiophene, BT: Benzothiophenes, DBT:Dibenzothiophene, Cz: Carbazole, DM: Dimethyl, EM: Ethylmethyl, TM: Trimethyl.)

The molecular composition of heavier fractions such as atmospheric and vacuum residues are not fully solved at present, although high pressure liquid chromatography (HPLC), time-of-flight mass spectroscopy (TOF-MS) and their combinations have provided some clues to their molecular composition.<sup>8,9</sup> These heavier fractions are believed to be polymeric substances of aromatic unit structures that are basically similar to those found in the lighter fractions. It has been postulated that strong molecular associations of polymeric chains are present in the residual fractions.<sup>10,11</sup> Such intermolecular association is schematically illustrated in Fig. 3.<sup>10</sup> Thus, the major target of residue hydrotreating is to convert asphaltenes by liberating molecular association first and then breaking down to lower molecular weight molecular species. This kind of hydroprocess is very important and becomes even more important in the near future. However, the present review excludes this topic.

Light and medium cycle oils (MCO) in FCC products of the gas oil range are further hydroprocessed to yield high quality fuels. The problems originating from aromatic components in LCO and MCO have been clearly indicated in their deep HDS. Thermally cracked product can be characterized to have olefinic composition.

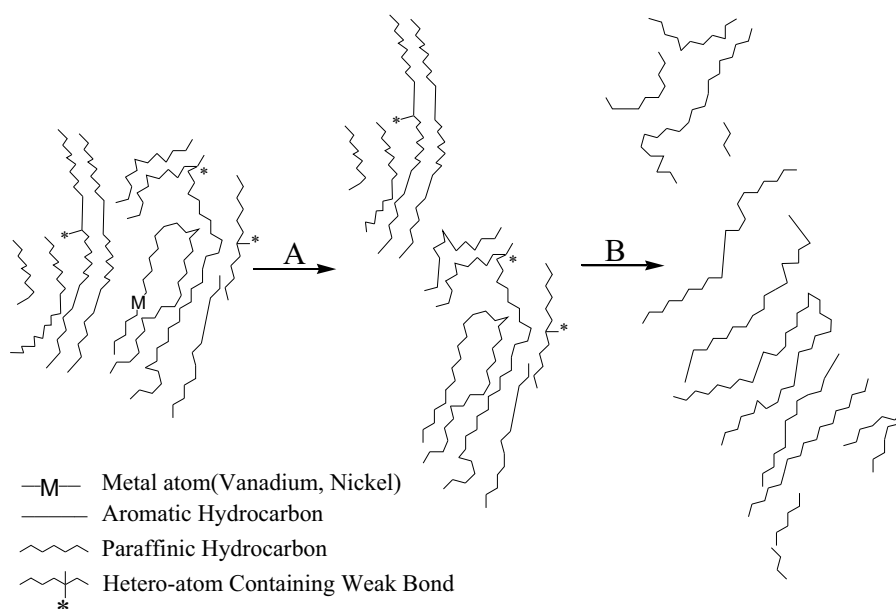


Figure 3. Model of Hydrocracking of Asphaltene. A: De-agglomeration of Asphaltene due to demetallation, B: Depolymerization due to desulfurization. \* means heteroatom<sup>10</sup>

## 2. HYDROTREATING PROCESS

The primary objectives of hydrotreating are (a) to remove impurities, such as heteroatom and metal-containing compounds, from a feedstock, (b) to increase the hydrogen content of the feedstock, and (c) to lower molecular weight without a substantial loss in liquid product yield. The impurities of concern depend on the molecular weight of the feedstock being processed. Lower molecular weight feedstocks such as naphtha, gasoline, intermediate distillates (atmospheric and light vacuum), diesel fuels and home heating oils (kerosene etc.) have undesired impurities such as sulfur-containing compounds (S-compounds), nitrogen-containing compounds (N-compounds), oxygen-containing compounds (O-compounds), and polynuclear aromatic (PNA) compounds. Higher molecular weight feedstocks, such as high vacuum distillates, atmospheric and vacuum residues, have the same impurities as the above and in addition have significant concentrations of metal-containing compounds (M-compounds). V and Ni are the major metals in petroleum which are present in the form of porphyrin complexes of  $V^{4+}=O$  and  $Ni^{2+}$ .<sup>10</sup> The crude oils often contain NaCl,  $MgCl_2$ ,  $CaCl_2$ ,  $CaSO_4$  and naphthenates of some metals such as Ca, Mg and Fe. The former metal compounds can be removed rather easily by washing before the distillation. However, small amounts of remaining metal compounds, particularly Fe or its derived FeS, often result in operational problems. Naphthenates may dissolve iron from valves or the reactor and transfer lines, which can be included in the feeds to downstream processes as described below.<sup>12</sup> In general, the concentration of these impurities increases with increasing boiling point. Thus, the hydrotreating process of choice depends primarily on the boiling range of the feedstock of concern. The boiling range is dictated by the molecular weight distribution of the feedstock. The next most important consideration in choosing a hydrotreating process is the product quality specification, which is predominantly related to the total hydrogen content of the product, which in turn is related to the content of PNA compounds.

O-compounds are generally not considered as major environmental hazards in petroleum products. Nevertheless, some O-impurity compounds such as phenols and naphthenic acids lead to corrosion problems in the reactors and storage vessels.<sup>13</sup> Some crudes which contain a large amount of naphthenic acids are classified as naphthenic crudes. Such naphthenic acids are extracted to be sold as lubricants. Iron dissolved by naphthenic acid in crude causes plugging by forming FeS in the catalyst bed or on the filter. Finely dispersed FeS may enhance coking reactions.<sup>10</sup> The O-compounds in the petroleum are much more reactive than other impurities and generally, hydrotreating is not developed specifically to remove O-compounds in the usual crudes. However, less reactive O-compounds such as phenols and

benzofurans are found in significant amounts in coal derived oils. Hence their removal is one of the major concerns in the hydrotreating of coal derived oils.<sup>15</sup>

S-compounds, N-compounds and M (Metal) compounds have different reactivities and chemistry depending on the boiling ranges of fractions in which they are found. Thus, specific processes have been developed for the removal of each of these impurities. These are classified as hydrodesulfurization (HDS), hydrodenitrogenation (HDN) and hydrodemetallation (HDM) processes, respectively. These are in turn subdivided into processes, which are optimized for the boiling range of the particular feedstock being treated.

In general, the sulfur impurity is the major concern because S-compounds are often serious poisons and inhibitors for other secondary upgrading process catalysts. Their combustion products create serious environmental hazards such as acid rain. Thus, the main processes that have been developed for distillable feedstocks are HDS processes. N-compound impurities are also removed during HDS processes. When the successive acid-catalysis is important in conversion mechanisms, extensive N-removal is required since the basic N-compounds are both serious poisons and coke precursors on acid catalysts.<sup>16</sup> Lowering aromatic content through hydrotreating is classified as hydrodearomatization (HDA). HDA reactions occur during HDS and HDN processes, but product quality requirements often demand that an HDA process is conducted subsequent to an initial HDS and/or HDN process. Future environmental regulations may emphasize HDA further.<sup>17</sup>

M-compound impurities are found particularly in high boiling feedstocks, such as atmospheric and vacuum residues. Thus, HDM processes are tailored for high boiling and very viscous feedstocks.<sup>18</sup> Nevertheless, trace amounts of M compounds in the gas oil must not be overlooked since they cause the catalyst deactivation in long run.

### **3. BASES FOR HYDROTREATING**

#### **3.1 Hydrotreating Catalysts**

Currently, catalysts for hydrotreating are alumina supported Mo and W based sulfides with promoters of Ni or Co sulfides. Alumina is believed to be the best and most balanced support in terms of surface area (200 - 300 m<sup>2</sup>/g), pore size control, affinity to sulfide for high dispersion, mechanical strength and cost. Molybdenum precursor (15 - 20wt%) is first impregnated to be highly dispersed onto alumina and then the Co or Ni precursor (1 - 5wt%) is impregnated hopefully onto the Mo phase. The impregnated catalyst is

carefully calcined and sulfided in the commercial application for the stable catalytic activity. The active species is believed to be the Co(Ni) MoS phase. Commercial catalysts also contain isolated Co(Ni)<sub>9</sub>S<sub>8</sub>, and Co(Ni)/Al<sub>2</sub>O<sub>3</sub> which are not active. The Co(Ni)MoS phase consists of small layered crystals of S and Co/Mo as illustrated in Fig. 4.<sup>19</sup> The bottom of the CoMo layers, which contact the Al<sub>2</sub>O<sub>3</sub> surface, is believed difficult to sulfide into the active form,<sup>2</sup> hence multi-layered stacks of these are believed to be more active on alumina supports. In order to disperse Mo and Co(Ni) to form more active crystallites, impregnation procedures have been developed which use P<sub>2</sub>O<sub>5</sub> and chelating agents in commercial catalyst preparation as described below. The sulfiding medium and conditions have been extensively studied in order to achieve higher activity. The edge and rim of the Co(Ni)MoS phases are believed particularly active for hydrotreating reactions. However, active sites for hydrogenation and C-X fission are not fully solved.

Microscopic analyses have been used to understand the morphology of Co(Ni)MoS phase crystals on alumina. TEM and STM have shown that the crystal size of this phase in commercial catalysts is very small.<sup>20</sup>

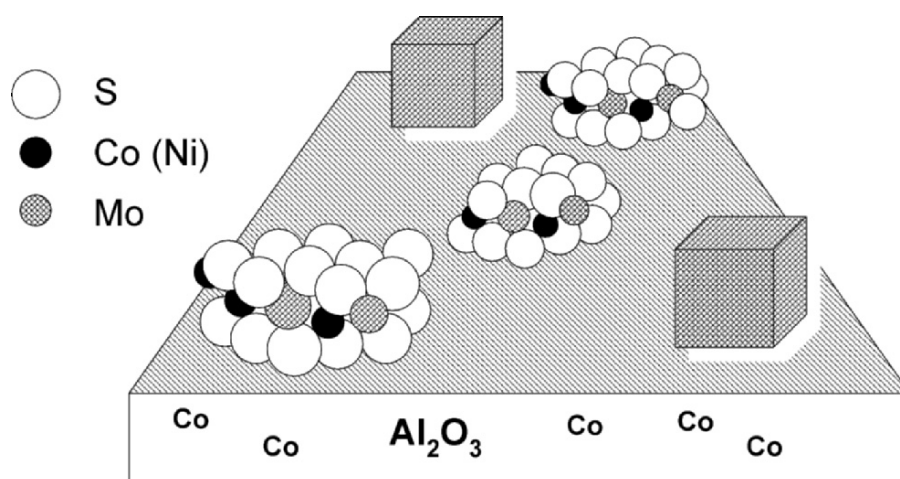


Figure 4. The Structure of CoMo Catalyst<sup>2</sup>



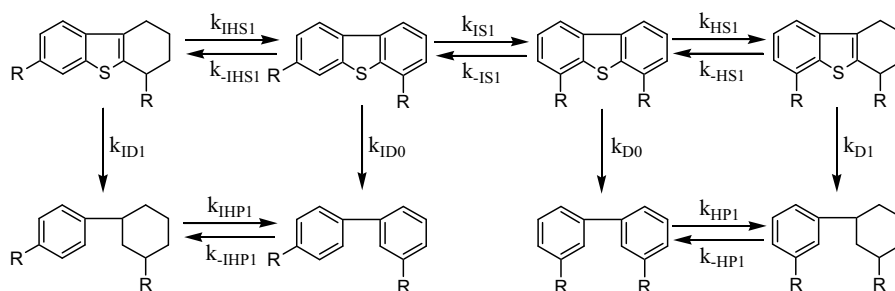
### 3.2 Chemistry of Hydrodesulfurization

The ease of removal of sulfur from a petroleum stream depends greatly on the structure of the sulfur compound being treated. The rates of sulfur removal can vary by several orders of magnitude. Generally, acyclic sulfur compounds such as thiols and disulfides are highly reactive and can be removed under very mild conditions. Saturated cyclic sulfur compounds and aromatic systems in which sulfur is present in six-membered rings are also highly reactive. However, compounds in which the sulfur atom is incorporated into a five-membered aromatic ring structure (such as thiophene), are much less reactive and the reactivity decreases as the ring structure becomes increasingly condensed (e.g. one ring > two rings > three rings).<sup>2</sup> For highly condensed ring structures (four or more rings), the reactivity trend reverses and reactivity tends to increase as the ring structure increases in size.<sup>2</sup> The reason for such behavior is that there are several different chemical pathways through which sulfur can be removed from a molecule and the preferred pathway changes for different sulfur compound structures.

An illustration of the various pathways is shown in Fig. 5 for dibenzothiophenes. In this scheme, there are two major pathways to desulfurized products. The first is called direct hydrodesulfurization, in which the sulfur atom is removed from the structure and replaced by hydrogen, without hydrogenation of any of the other carbon-carbon double bonds. The rate constant associated with this direct route is shown as  $k_{D0}$  in Fig. 5. The second route is called the hydrogenative route and assumes that at least one aromatic ring adjacent to the sulfur containing ring is hydrogenated before the sulfur atom is removed and replaced by hydrogen. The associated rate constants for hydrogenation and hydrodesulfurization routes are shown as  $k_{HS1}$  and  $k_{D1}$  in Fig. 5. In addition to hydrogenation of an aromatic ring before sulfur is removed, an aromatic ring may be hydrogenated after sulfur removal, and the associated rate constant for this reaction is shown as  $k_{HP1}$  in Fig. 5. This often leads to confusion in interpreting the results of experimental data as both routes can produce the cyclohexylbenzene final product.

It should also be noted that the hydrogenation pathways are subject to thermodynamic equilibrium constraints. Thus, the partially hydrogenated intermediates (such as tetrahydrodibenzothiophenes) have lower equilibrium concentrations at higher temperatures. This results in a maximum in the observed rates of HDS via the hydrogenative route, as a function of temperature. Thus, hydrodesulfurization via the hydrogenative route becomes limited at low pressures and high temperatures. Another route includes the isomerization and transmethylation of methyl groups at 4- or 6-position, which reduces the steric hindrance as in Fig. 5. The direct pathway is believed to involve the insertion of a metal atom on the surface of the catalyst into a sulfur-carbon bond in the sulfur-containing compound

as shown in Fig. 6.<sup>2</sup> This insertion can occur even for fully aromatic sulfur compounds, such as thiophene, benzothiophene and dibenzothiophene. Such a pathway is possible because the resultant metal-sulfur bond is energetically favorable. After the insertion, several other steps occur in which the sulfur is expelled as hydrogen sulfide and the catalyst is restored to its original state.



Where R=H, CH<sub>3</sub> or Other

Figure 5. Reaction Pathways for Desulfurization of Dibenzothiophenes.

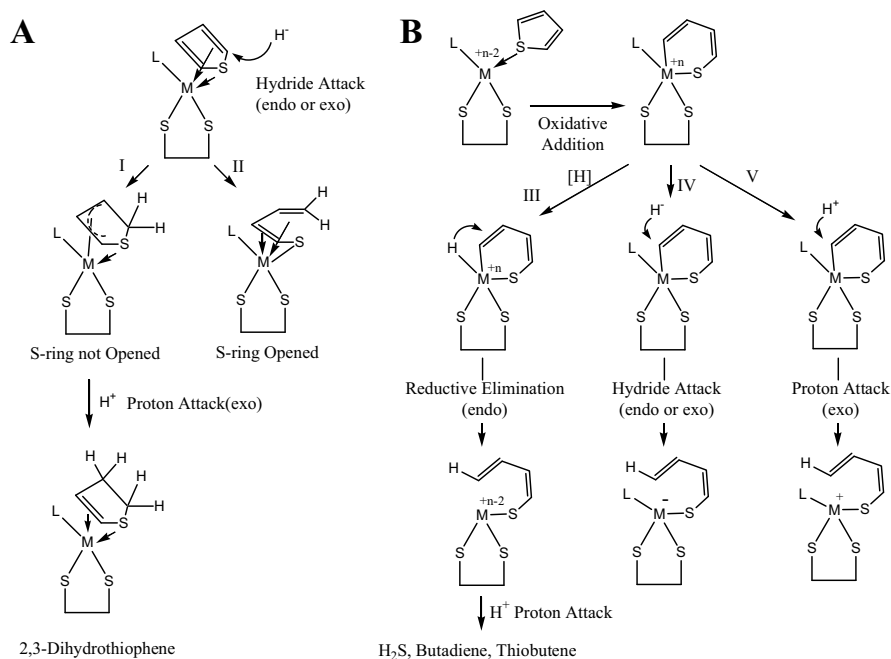


Figure 6. Possible Routes to Hydrogenation and Ring-opening Reactions<sup>2</sup>

The hydrogenative pathway involves the initial hydrogenation of one or more of the carbon-carbon double bonds adjacent to the sulfur atom in the aromatic system. Hydrogenation destabilizes the aromatic ring system, weakens the sulfur-carbon bond and provides a less sterically hindered environment for the sulfur atom. Metal insertion is thus more facile.

There are two active sites (functions) postulated on HDS catalysts based on the above discussion, S-extrusion and hydrogenation. Fig. 7 illustrates the schemes of both reactions including details of the active sites. The active center is a coordinatively unsaturated metal site where the S ligand is facile. Sulfur in aromatic rings can coordinate to the active center of both functions. It is believed that the initial adsorption of the S-compound is through  $\sigma$ -bonding, in the case of direct S-extrusion. However, in the hydrogenative function, S-compound coordination is through  $\pi$ -bonding. Neighboring S-H groups are believed to be involved in hydrogen transfer for both S extraction and hydrogenation. Differences in the active sites for S extraction and ring hydrogenation are not yet clear although they appear to be interconvertible.  $H_2S$ ,  $NH_3$  and nitrogen containing compounds can also coordinate to the active center, inhibiting the S-extraction and hydrogenation as discussed later.

The direct pathway becomes more difficult as the ring structure becomes larger because the aromatic structures become increasingly more stable and because the insertion becomes more hindered for the more condensed rings. To illustrate these factors, Fig. 8 provides examples of hydrodesulfurization reactivities of sulfur compounds having different ring structures.<sup>21,22</sup> For ease of discussion, all of the rate constants in this and following illustrations have been normalized relative to dibenzothiophene having a value of 100.

In Fig. 8 it can be seen that the overall hydrodesulfurization reactivity of the sulfur compounds decreases with increasing ring condensation from one ring to two rings to three rings, but then reverses for the four ring system. This is due to a switch in the preferred pathway from the direct route to the hydrogenative route. As mentioned above, increasing ring condensation is detrimental to the insertion step in the direct route, while with increasing ring condensation, hydrogenation becomes more facile.

Another complicating factor in reactivity is the proximity of alkyl groups to the sulfur atom in aromatic ring structures. Generally, as the sulfur atom becomes more crowded by adjacent alkyl groups the reactivity decreases. This has been attributed to steric crowding of the sulfur during adsorption on the catalyst surface or during some transition state. This steric crowding affects the direct hydrodesulfurization route most severely. Fig. 9 illustrates this factor for several alkyl-substituted benzothiophenes and dibenzothiophenes. In Fig. 9 it can be seen that the reactivity for hydrodesulfurization decreases as the number of substituents around the sulfur

atom increases.<sup>23</sup> Alkyl groups that are not close to the sulfur atom have little effect. Recently, migration of alkyl groups before the hydrodesulfurization was proved to enhance the direct hydrodesulfurization on the catalyst of strong acidity as illustrated in Fig. 5.

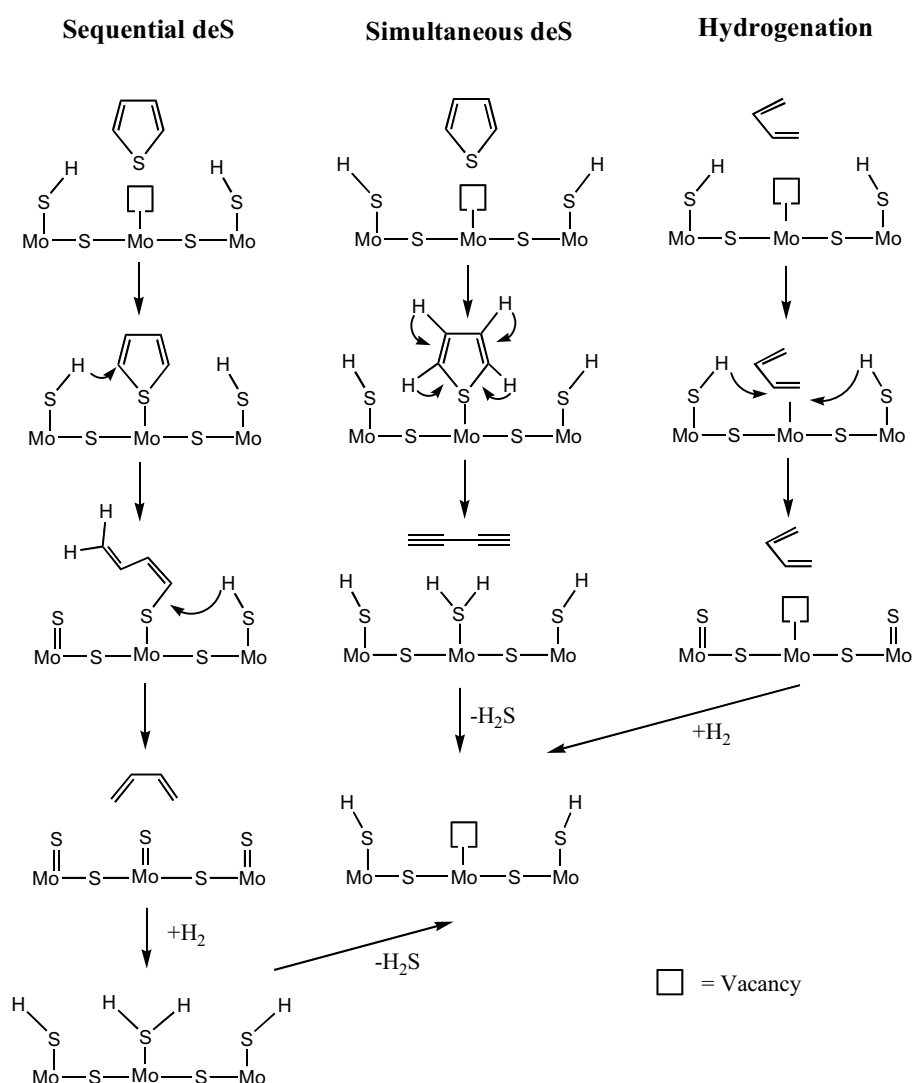


Figure 7. Vacancy Model of the HDS Mechanism<sup>2</sup>

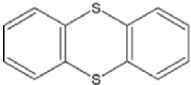

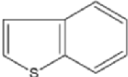
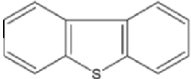
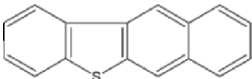
| <u>Sulfur Compound Structure</u>  | <u>Relative Reactivity</u> |
|---|----------------------------|
|    | Very Fast                  |
|    | 2250                       |
|    | 1300                       |
|    | 100                        |
|  | 260                        |

Figure 8. Desulfurization Reactivities of Compounds Having Different Ring Structures<sup>21,22</sup>


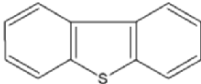
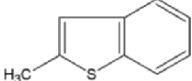
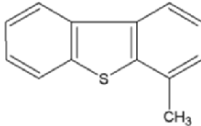
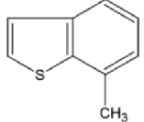
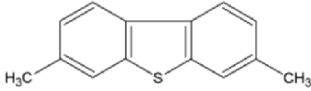
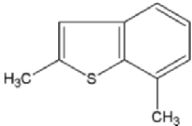
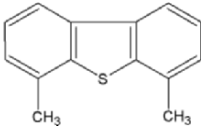
| <u>Alkyl Benzothiophenes</u>  | <u>Relative Reactivity</u> | <u>Alkyl Dibenzothiophenes</u>   | <u>Relative Reactivity</u> |
|---|----------------------------|--|----------------------------|
|  | 1330                       |  | 100                        |
|  | 596                        |  | 38                         |
|  | 466                        |  | 90                         |
|  | 310                        |  | 11                         |

Figure 9. Desulfurization Reactivities of Alkyl-substituted Aromatic Sulfur Compounds<sup>23</sup>

It has been shown that the hydrogenative routes are not significantly affected by alkyl-substitution on the aromatic rings, while the direct route becomes lower when alkyl groups are adjacent to the sulfur atom. Thus, the relative rate changes shown in Fig. 9 are primarily due to loss in the ability for hydrodesulfurization to proceed via the direct route. For this reason, the catalyst, which is preferred for hydrodesulfurization, is often different for light and heavy feedstocks, as the numbers of alkyl groups and of condensed aromatic rings in the sulfur containing compounds increases with their boiling points.

#### 4. DEEP HYDRODESULFURIZATION OF GASOLINE

Current regulations on the accepted sulfur levels in gasoline and diesel are becoming increasingly stringent in order to protect the environment from the exhaust gases of motor vehicles. Several different streams are blended to produce commercial gasoline in a refinery.<sup>24</sup> These include straight run gasoline, reformat, alkylate, crude FCC gasoline, RFCC gasoline, gasoline from HDS and hydrocracking of vacuum gas oil and residue. Reformat and alkylate are sulfur free. However, the other streams contain various amounts of S-compounds. Currently sulfur levels of such gasolines are separately controlled before blending.

Recent regulation forces deeper hydrodesulfurization. While HDS of FCC gasoline is rather difficult without hydrogenation of olefin and aromatic components, which are major sources for high octane number, sulfur species in gasoline are reactive forms of thiols, thiophenes and benzothiophenes, which are readily desulfurized. Selective HDS without olefin hydrogenation is being extensively explored at present.<sup>25</sup>

Such a selective hydrodesulfurization must clarify the active sites of CoMo and NiMo sulfides supported on alumina for hydrodesulfurization and hydrogenation. CoMo is certainly more selective for hydrodesulfurization with limited hydrogenation activity than NiMo. Hence, cobalt is applied for the present purpose. Coordinatively unsaturated Co sulfide on MoS<sub>2</sub> is often postulated as the active site for both reactions (see Fig.7). The metal with unsaturated valence is proposed as the hydrogenative site in cooperation with a Mo-S-H group while the metal with the unsaturated valences must be the hydrodesulfurization site. H<sub>2</sub>S concentration in HDS can be reduced to enhance the hydrodesulfurization selectivity.

Several patents are issued for selective HDS of FCC gasoline by poisoning the hydrogenation site more than the hydrodesulfurization one over CoMoS/alumina.<sup>25</sup> Amines, alkali metal ions, and carbon deposition have been proposed in the patents to increase the selectivity for hydrogenation,

although the hydrodesulfurization itself is also poisoned by reacting with CoMoS. The mechanism for selective poisoning is not clarified, but alumina support appears to principally be poisoned. Acidic natures of the support may be responsible for the hydrogenation activity as described with hydrogenative HDS of refractory sulfur species in diesel fuel.<sup>26</sup> Separated HDS of fractions in FCC gasoline was also proposed to fractionate olefins and aromatic sulfur species in the respective fractions.<sup>3</sup> More kinds of catalyst supports are worthwhile for detail examination.

Although FCC feed can be extensively desulfurized to produce FCC gasoline with lower sulfur content, the deep desulfurization of FCC gasoline is required. Vacuum gas oil feeds provide gases, gasoline, light cycle oil (LCO), heavy cycle oil (HCO), decant oil, and coke on the catalyst.<sup>27</sup> RFCC (Resid FCC) gives the same products, except it yields cracked residue instead of decant oil. Sulfur is produced from paraffins and aromatics. Other types of compounds may not yield gasoline, but they still can produce hydrogen sulfide, which influences product sulfur content. The opening of aromatic rings hardly occurs in the FCC process even though hydrogen-transfer reactions take place.

The strong acidity of zeolites is sometimes postulated to desulfurize through hydrogen transfer, however, its contribution must not be exaggerated. Thus, sulfur balances in FCC process are being carefully described to discover the origins of S-compounds in FCC products.<sup>28</sup>

Recombination of H<sub>2</sub>S with olefins can not be neglected, even at sulfur levels below 30 ppm in FCC process.<sup>29</sup> Thiols may cyclize and dehydrogenate into thiophenes, which are the major sulfur species in very low sulfur level gasolines. A substantial amount of sulfur ends up in coke on FCC catalysts. Such sulfur is combusted into SO<sub>2</sub> in the regeneration stage. RFCC catalysts have been sophisticatedly designed as shown in Fig. 10.<sup>79</sup> A special additive can be added to prevent the crystal structure of zeolite from being destroyed by impurity metals. In Fig. 10, CMT-40 functions as metal trap. The next generation FCC promises to be a very sophisticated composite catalyst that carries out specified functions particular locations in the catalyst particles. Increasing SO<sub>2</sub> at the stack can be handled by dry desulfurization over active carbon fibers.<sup>30</sup>

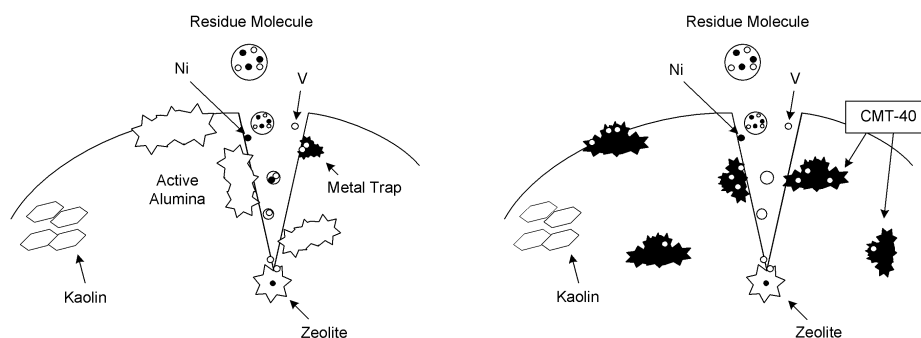


Figure 10. New Design Concept of RFCC Catalyst <sup>79</sup>

## 5. DEEP HYDRODESULFURIZATION OF DIESEL

Deep HDS of diesel fuel is currently a very important topic in refining. Basically, deep hydrodesulfurization of diesel involves the extensive elimination of refractory sulfur species such as 4-MDBT, 4,6-DMDBT, and 4,6,X-TMDBTs. Such deep hydrodesulfurization is difficult because of the lower reactivities of these compounds and strong inhibition by coexisting species such as  $H_2S$ ,  $NH_3$ , nitrogen species and even aromatic species, especially when the sulfur level must be lowered to <300 ppm.  $H_2S$  and  $NH_3$  are produced from the reactive sulfur and nitrogen species contained in the same feed.

There are four approaches for improving reactivity.

1. Introduction of more active sites by impregnating more active metals on the catalyst.
2. Removal or reduction of inhibitors in the process during or before HDS.
3. Novel catalyst designs to introduce new mechanistic pathways that are less subjective to inhibition.
4. A series of catalysts in two successive layers to remove reactive sulfur species and in the first layer, and to remove remaining refractory sulfur species to less than 10 ppm under the presence of  $H_2S$ ,  $NH_3$  and other remaining inhibitors, such as nitrogen species and aromatic compounds, in the other layer.

Currently the first method is the major commercial approach. The second approach has been proposed as a two-stage HDS process. Fig. 11 shows the efficiency of two-stage HDS, in which the produced  $H_2S$  and  $NH_3$  in the first stage are eliminated before the second stage.<sup>7</sup>



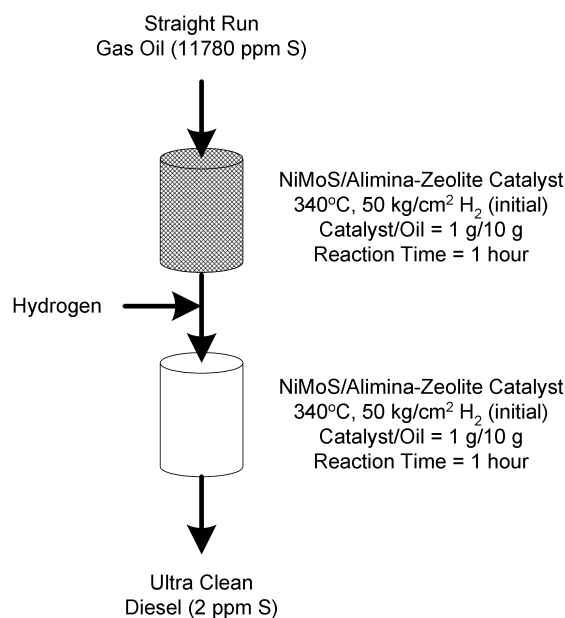


Figure 11. Schematic Diagram and Performance of Two-Stage Reaction Concept <sup>7</sup>

Another type of two stage HDS is to remove nitrogen species prior to HDS with silica-gel, silica-alumina or active carbon. The present authors suggest the high efficiency of active carbon for nitrogen species removal.<sup>31</sup> Some refractory sulfur species are also removed by the active carbon, which significantly helps deep hydrodesulfurization. Post removal of sulfur species after hydrodesulfurization can also be used to lower the total sulfur content below 10 ppm. However, the capacity for sulfur removal is rather limited, compared to the removal of nitrogen species. Hence the application of this approach is restricted to preparation of the ultra clean hydrodesulfurization for fuel cells.

The third approach has high potential and is being investigated extensively. The use of acidic supports appears to enhance catalyst activity by enhancing hydrogenation, methyl group migration, and by lowering H<sub>2</sub>S inhibition. However, coking and NH<sub>3</sub> inhibition also must be overcome. TiO<sub>2</sub> and carbon are interesting supports for producing higher activity catalysts. High surface area TiO<sub>2</sub> is now available, due to a novel development. Deeper sulfiding is one of the proposed reasons for its higher activity. Strong interaction between active oxides and the support is designed for better dispersion of active species, but may hinder sulfiding. Reactive sulfide is recommended for sulfidation. Strong interaction between active sulfide and support must be explored. Carbon inclusion at the active species during the

the sulfiding stage is claimed to give higher HDS activity. Some metals are reported to give high HDS activity. Precise evaluation is still necessary by comparing the activity of catalysts currently lined up.

Highly aromatic feeds such as LCO and MCO appear now to require more severe conditions for their deep HDS because aromatic species exert strong inhibition on refractory sulfur species, especially at their very low concentrations. Catalytic species having higher affinity for sulfur than for olefins and aromatic hydrocarbons are currently targets of extensive research for achieving deep HDS of aromatic diesel. A sulfur atom can be an anchor to be ported to the soft acid site of the catalyst for the preferential hydrogenation of neighboring aromatic rings. Process design has been proved very effective for such feeds to separate the major aromatics from the refractory sulfur species fraction.

## 6. HDN, HDO AND HDM REACTIONS

Removal of nitrogen, oxygen and metal is also important to purify petroleum products. Such reactions progress concurrently together with HDS. Activated hydrogen can break C-X bonds over the same catalyst, although the affinity to the active site, the necessity of hydrogenation in the ring structure, and C-X bond reactivity are very different according to their own mechanisms.

HDM, HDS, HDN and HDO (hydrodeoxygenation) are generally recognized in the order of easiness, although the HDS and HDN of refractory sulfur and nitrogen species are comparable at deep levels of removal. HDN of the last non-basic carbazoles is completed before HDS reaches to the 10 ppm level. Basic nitrogen species occupy the active sites before sulfur compounds. HDN of aromatic nitrogen species is generally believed to proceed through the complete hydrogenation of aromatic rings because the aromatic C – N< bond is too strong to be fissioned by hydrogenolysis. In contrast, the aliphatic C – N< bond is easily broken. Thus, NiMoS and NiWS catalysts are often applied for HDN. Large hydrogen consumption is inevitable. An acidic support helps HDN on NiMoS by accelerating hydrogenation, although it also enhances the chance of deactivation due to coking. There is a competition between hydrogenation and acidic reactions on the same catalysts.

Recently, the C – N< bond was proposed to be associated with H<sub>2</sub>S in the formation of C – SH and NH<sub>3</sub>. The C – SH bond is easily eliminated under hydrotreating conditions. Prins et al.<sup>32,33</sup> reported that 2-methylcyclohexylamine (MCHA) is hydrodenitrogenated through three ways: (a) direct elimination of ammonia, (b) nucleophilic removal of the NH<sub>2</sub> group by H<sub>2</sub>S followed by removal of the -SH group, and (c) direct

hydrogenolysis of the C-N bond. They estimated the contribution of each pathway as shown in Fig. 12.<sup>33</sup> Such contribution of nucleophilic substitution was dependent on H<sub>2</sub>S partial pressure. However, it is not clear that such a mechanism is relevant to the HDN of refractory nitrogen species, such as carbazole, because H<sub>2</sub>S is a strong inhibitor for the HDN of such inert nitrogen species. The natures of the catalysts are also important since a variety of catalysts are now available.

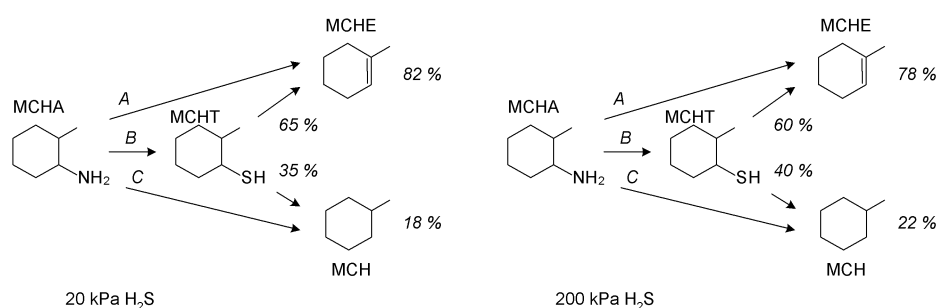


Figure 12. Selectivities for elimination (A), nucleophilic substitution (B), and hydrogenolysis (C) in the HDN of 2-methylcyclohexylamine (MCHA), and the observed selectivities of methylcyclohexene (MCHE) and methylcyclohexane (MCH) in the HDN of 2-ethylcyclohexylamine and in the HDS of 2-methylcyclohexanethiol (MCHT) in the presence of 20 kPa (left-hand side) and 200 kPa (righthand side) H<sub>2</sub>S<sup>33</sup>

The involvement of aromatic C – N<, especially derivatives from carbazoles, is not definite yet. Such a mechanism would be desired to reduce hydrogen consumption. HDO is not an important reaction for petroleum products, but it is very important in stabilizing coal-derived liquids. HDO of dibenzofuran is very slow. An acidic support is helpful for the HDO of dibenzofuran species.

HDM is a key for the hydrotreatment of heavy oil because it removes asphaltenes and affects the capacity of downstream catalysts to hold eliminated metal sulfides.<sup>18</sup> Liberation of asphaltene aggregation as well as the pore-mouth size and pore volume are important criteria for the design of catalysts to enhance HDM of heavy feeds.

## 7. INHIBITION OF HDS

The active sites postulated for HDS catalysts promote sulfur extraction, hydrogenation and acid catalyzed reactions. Such active sites are all commonly or selectively subject to occupancy by the inhibitors. As mentioned above, several species in the feed and product are inhibitors for HDS. Reactive sulfur species appear to be less inhibited than the refractory species. This is because the S atom in the reactive species can easily undergo metal insertion to break the C-S bond via the direct HDS route. They are also the major S-compounds present and can compete effectively with inhibitors for the active sites on catalysts. By contrast, when proceeding by way of the direct HDS route, the sulfur atom in refractory sulfur species may be sterically hindered. Hence, their desulfurization must be performed after hydrogenation. Inhibition for their hydrogenation must be concerned. Also, their concentrations become very low while H<sub>2</sub>S and NH<sub>3</sub> inhibitors increase their concentration during the initial stage of the HDS process. These inhibitors are in high concentration where the refractory species of very low content must be desulfurized. It must be recognized that the initial and last stages of the HDS of refractory species are very different in their rate. Some processes have been developed which remove H<sub>2</sub>S and NH<sub>3</sub> between stages to minimize this problem as described above.

Other feed impurities, such as N-compounds, are severe inhibitors for the hydrogenative HDS route. They are strong  $\pi$ -bonding species and they hinder the interaction of the refractory S-compounds with the active hydrogenation site. The overall HDS process has been shown to be much more facile when the N-compound inhibitors are removed prior to hydrotreating. In addition, nitrogen species are removed during HDS, reducing their concentration through concurrent HDN.

Aromatic species are also inhibitors for HDS of refractory sulfur species as described above, because refractory sulfur species are desulfurized through the hydrogenation route. Aromatic species can be highly concentrated and can inhibit the last stages of HDS. Overcoming this difficulty is not easy.

## 8. DEACTIVATION AND REGENERATION OF HYDROTREATING CATALYSTS

Hydrotreating catalysts lose their activity in several ways:<sup>34</sup>

- (1) Sintering of the active phase into large crystal units;
- (2) Degradation of the active phase, including degradation of sulfided forms;
- (3) Covering of the active sites by reactants and/or products including coke;

- (4) Deposition of inactive metal sulfides (such as V and Ni sulfides);
- (5) Deposition of other impurities such as salt and silica.

The deactivation usually occurs in three steps: initial rapid deactivation, intermediate slow but steady deactivation and rapid deactivation at the end of the cycle. Commercial processes are operated at constant conversion. This constant conversion is achieved by gradually heating the reactor to higher temperatures to compensate for the slow but steady catalyst deactivation.

The initial rapid deactivation phase is believed to be due to rapid coking on active sites having very high acidity.<sup>34</sup> Deposited carbon can be characterized by temperature programmed combustion and Raman spectroscopy.<sup>35</sup> The slow but steady deactivation is associated with metal deposition, sintering and/or coking during the course of the process cycle. Higher reaction temperatures utilized at the end of the process cycle may cause rapid deactivation at the final stage.

Currently, acidic supports are utilized to achieve high activity, hence coking deactivation appears important in current processes. Such deactivation schemes suggest that catalysts may be regenerable if suitable methods can be developed. Removal of strongly adsorbed heavier organic materials or coke precursor and coke could possibly be achieved by thermal extraction and/or combustion. However, during regeneration of the catalyst, the active sulfide form must be maintained or it must subsequently be regenerated.

More important to the design of the catalyst is to improve the hydrogenation activity in the vicinity of acidic sites. This could hydrogenate hydrogenate the coke precursors by cracking them or making them soluble in the matrix.

## 9. PROCESS FLOW OF HYDROTREATING

A typical hydrotreating flow diagram is shown in Fig. 13, where single stage hydrotreating is illustrated. The feed oil is pumped up to the required pressure and mixed with make-up and recycle hydrogen-rich gas. The temperature is initially raised by heat exchange with the reactor effluent then further increased by a furnace to achieve the required temperature. The feed oil is hydroprocessed over the catalyst in the reactor under a flow of pressurized hydrogen-rich gas. The figure shows one reactor, but the numbers of reactors may be increased even in single stage processes, depending upon the conditions or throughput rate.

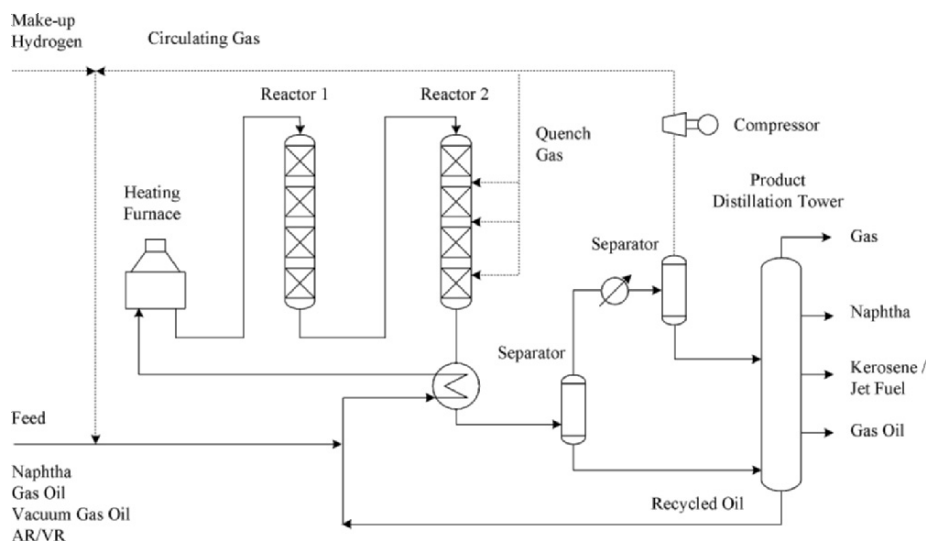


Figure 13. Single-Stage Process Flow Diagram

In general, a fixed bed reactor is employed for hydrotreating process. However, a series of catalysts having different functions are generally packed sequentially in the reactor(s). Thus, optimum catalysts are packed in each bed according to the requirements of the bed. The feed oil and hydrogen rich gas are normally supplied from the top of the reactor. Quenching hydrogen gas is commonly injected at several points along the reactor to control the reaction temperature, because hydrotreating reactions are always exothermic. The reactor effluent is then cooled down by feed to the reactor in the heat exchanger. This recovers some of the exothermic heat of the reaction and improves the thermal efficiency of the overall process. Following heat exchange, the gas and liquid products are separated by a high temperature, high-pressure vessel followed by a low temperature, high-pressure vessel. Liquid products are further fractionated into the required products in the fractionating column according to their boiling points. The gaseous products from the high-pressure vessel are fed to an absorbing column to remove hydrogen sulfide, and the cleaned hydrogen-rich gas is recycled to the reactor after repressurizing with a recycle compressor.

There are two types of processes. One is called a single stage process, while another is termed a two or multiple stage process. The single stage

process has the same process flow as mentioned above. The feed is hydroprocessed consecutively without obvious separation in between the reactors. However, a single stage process does not mean that only one reactor is employed, only that no separations are done until the final conversion is achieved.

In a two-stage process, the unwanted products of the first stage are separated and eliminated before the second stage. Thus, the unwanted secondary reactions of the product, poisons and inhibitors produced in the first stage are eliminated before beginning the second stage of the conversion.<sup>7,36,37</sup> This reduces the load on the second stage and enhances its reactivity. With staged processes, very high conversions, so called deep refining, are easily achieved.

The present authors proposed a new type of reactor as shown in Fig. 14, where fractions of a gas oil were reacted separately in upper and lower parts of the catalyst bed.<sup>37</sup> Hydrogen was charged from the bottom of the reactor. H<sub>2</sub>S inhibition on the heavier fraction can be avoided. The optimum catalysts can be applied for the respective parts of the bed. Pressure drop is a possible worry at the lower part of the reactor, where the hydrogen is up flow while liquid feed is down flow. A honeycomb type catalyst bed is now available for this problem.

By lowering the end point of the starting diesel fuel, hydrotreating the lower end point diesel fuel feed to ultra low sulfur levels is much easier. For example, when the 90% distillation point (T90) of diesel fuel is lowered by 20 °C, the required reactor size is only about half that needed for the full range feed.<sup>38</sup> This diesel with lower T90 has another merit. It will produce less particulate matter in diesel exhaust gas. The downside of this approach would be the requirement for increasing the cracking capacity of the refinery to produce the required volume of diesel fuel with this T90. One solution is to revamp a VGO hydrotreater to mild hydrocracking service.

The color of finished diesel oil is a stringent requirement in some countries. Presently, hydrodesulfurization of faintly yellow diesel oil feedstocks produces colorless and transparent products at 500 ppm S. However, when severe conditions are used for deep HDS, the diesel oil becomes, a fluorescent yellowish green product. High hydrogen pressures suppress color formation, while a high reaction temperature conversely retards hydrogenation and enhances color formation.<sup>39</sup>

Finally, we must emphasize the advantage of fractionated HDS for LCO.<sup>40</sup> We may be able to avoid the real difficulty for HDS of refractory sulfur species in the presence of aromatic inhibitions.

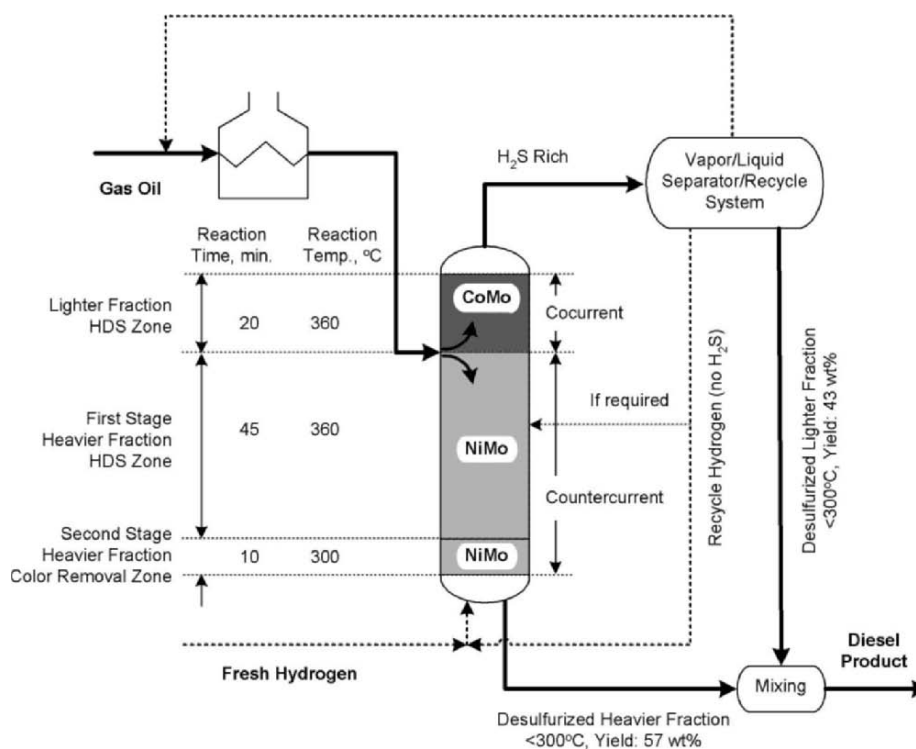


Figure 14. Reactor Design for Deep HDS <sup>37</sup>

## 10. TWO SUCCESSIVE LAYERS IN CATALYST BEDS<sup>7</sup>

Fig. 2 illustrates the sulfur distribution of a current 300 ppm diesel fuel (HSRGO). Comparison of its sulfur distribution to that of the straight run gas oil (SRGO) revealed that 100% of reactive sulfur species and 80% of refractory sulfur species are removed to obtain 300 ppm by current HDS units. The nitrogen species in the 300 ppm diesel are also illustrated in the same figure, showing carbazole of 50 ppm.

We can achieve sulfur levels less than 15 ppm when we can desulfurize remaining refractory sulfur species in the presence of inhibiting products such



as H<sub>2</sub>S and NH<sub>3</sub>.<sup>7</sup> Table 1 summarizes the activity of some catalysts under such conditions. NiMo on acidic supports achieved a sulfur level less than 15 ppm. Acidic supports of proper strength overcome the inhibitions by H<sub>2</sub>S and NH<sub>3</sub>. The sulfur level of 300 ppm can be achieved with a space velocity larger than 3 over CoMo catalysts on acidic supports. Hence, in combination the two catalysts in the layers can achieve deep hydrodesulfurization with a overall space velocity larger than 1. It must be noted that the catalysts of the two layers are not always same. Optimum catalysts must be selected. The catalysts in the first layer and second layer are designed by selecting active species and supports. The activity of the catalyst for reactive and refractory sulfur species, and its resistance to inhibitors at the respective concentration levels of sulfur species must be taken into account. The activity for the reactive species reflects direct desulfurization access to rather small molecules. Larger surface area for a CoMoS catalyst, even if the pore size is rather small, is advised. Furthermore, denitrogenation in the first layer must be also considered since remaining nitrogen strongly influences the hydrodesulfurization of remaining refractory sulfur species. Examination of this reactor scheme is now under evaluation.

Table 1. Remaining Sulfur and Nitrogen Content (ppmS, ppmN) over Catalysts after 1 hour reaction at 340°C. (Catalyst/Oil=1g/10g, H<sub>2</sub>=50 kg/cm<sup>2</sup> (initial charging pressure), H<sub>2</sub>S=1.66 vol% in H<sub>2</sub>, NH<sub>3</sub>=200 ppmN).

| Name    | SRGO<br>(ppmS) | SRGO<br>(ppmN) | HSRGO in the Absence<br>of H <sub>2</sub> S and NH <sub>3</sub> (ppmS) | HSRGO in the Presence<br>of H <sub>2</sub> S and NH <sub>3</sub> (ppmS) |
|---------|----------------|----------------|--|---|
| CoMo-A  | 1,118          | 81.0           | 22.5   | 36.7  |
| NiMo-A  | 2,229          | 12.2           | 2.1  | 5.9   |
| CoMo-SA | 576            | 41.6           | 7.1  | 36.4  |
| NiMo-SA | 477            | 19.6           | 4.4  | 32.7  |
| CoMo-AZ | 323            | 17.1           | 5.3  | 17.8  |
| NiMo-AZ | 242            | 5.4            | 3.6  | 15.5  |

\* A:Alumina support, SA: silica-alumina support, AZ:alumina-zeolite support

## 11. PROCESS AND CATALYST DEVELOPMENT FOR DEEP AND SELECTIVE HDS OF FCC GASOLINE

As described above, catalytic deep hydrodesulfurization of FCC gasoline must make ultra low sulfur gasoline while maintaining octane number. Hence, novel catalytic and non-catalytic processes have been proposed and evaluated.

First of all, selective HDS of cracked gasoline by novel catalysts has been developed by ExxonMobil and IFP, named as SCANfining<sup>41,42</sup> and Prime G<sup>3</sup>, respectively. In the SCANfining process, RT-225 catalyst, jointly developed by Albemarle and ExxonMobil Research and Engineering Co., is

used. The catalyst is known to be based on CoMo catalyst of low metals content and high dispersion to avoid hydrogenation of olefins while maintaining HDS activity. In order to block the hydrogenation active site, which is believed to lie on rim sites of sulfide crystals, a selective poison is added<sup>41-43</sup> as shown in Fig. 15. Over 20 refineries have selected SCANfining as their major clean gasoline production process.

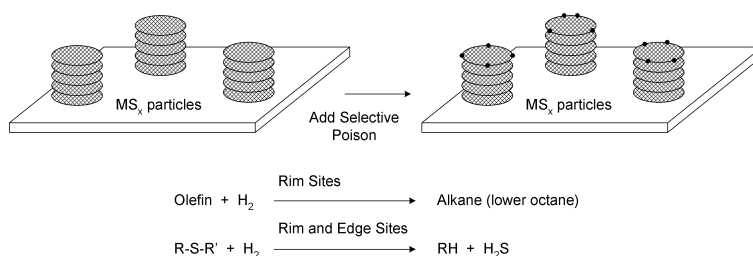


Figure 15. Schematic Diagram for Selective HDS catalyst for Gasoline<sup>41</sup>

Prime G+ process uses two reactors. In the first reactor, selective hydrogenation of diolefins and conversion of mercaptans occurs, as shown in Fig.16.<sup>44</sup> FRCN means full range catalytic naphtha. The bottom stream from the splitter, which separates Light Catalytic Naphtha (LCN) and Heavy Catalytic Naphtha (HCN) after the first reactor, is desulfurized by a novel catalyst. The Prime G+ process is reported to be operating at more than 50 refineries. Fractionation is a practical approach to separate competing components to be treated separately over the best catalysts.

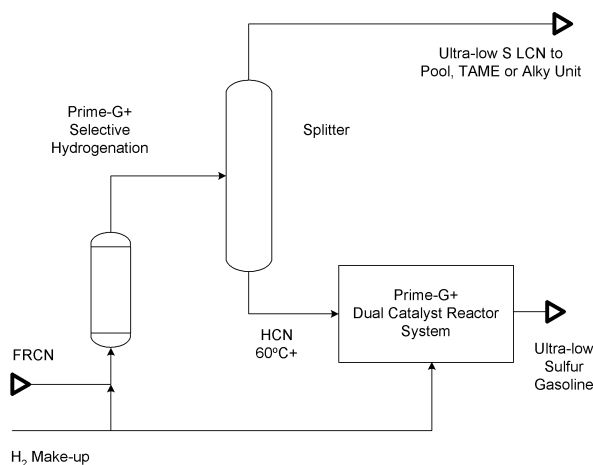


Figure 16. Process Diagram of Prime G+<sup>44</sup>

Like the Prime G+ process concept, CDTech proposed the catalytic distillation process, in which olefin and sulfur-rich streams are separated. Those are called CDHydro and CDHDS. The C<sub>5</sub>+ gasoline fraction from the FCC is fed into the CDHydro reactor, in which fractionation into light cut naphtha (LCN) and middle/heavy cut naphtha (MCN/HCN) occurs simultaneously with the combination reaction between mercaptans and diolefins. MCN/HCN from the bottom of CDHydro is fed into the CDHDS unit. The CDHDS unit is packed with two catalyst layers. The upper and lower catalyst layers desulfurize MCN and HCN, respectively. Because olefins are concentrated in the upper part of the CDHDS unit, selective HDS of rather heavy sulfur species can be performed in its lower part without saturation of olefins.

Table 2 shows the comparison of various technologies for low sulfur gasoline.<sup>45</sup>

Table 2. Comparison of FCC Gasoline Desulfurization Technology<sup>44</sup>

|                                  | OCTGain<br>125 | OCTGain<br>220 | SCAN<br>Fining | Prime G+ | CDTech | S Zorb |
|----------------------------------|----------------|----------------|----------------|----------|--------|--------|
| Processing capacity<br>(BBL/day) | 1500           | 31,000         | 25,000         | 24,000   | 30,000 | 25,000 |
| Investment<br>(million \$)       | 14.9           | 23.8           | 16.8           | 21.7     | 18.5   | 13.8   |
| Hydrogen<br>consumption (M3/kL)  | 66             | 23             | 14             | 22       | 18     | 12     |
| Power Consumption<br>(KWH/kL)    | 12.6           | 9.4            | 3.8            | 8.2      | 2.8    | 4.4    |
| Steam Use (kG/kL)                | 214            | 128            | 180            | 70       | 13     |        |
| Home-use Fuel (L/kL)             | 13.6           | 5.8            | 2.4            | 1.5      | 5.3    | 6.3    |
| Catalyst Cost (\$/BBL)           | 0.43           | 0.22           | 0.22           | 0.01     | 0.25   | 0.27   |
| Cooling Water<br>(Ton/kL)        | 6              | 5.4            | 3.2            | 3.1      | 1.3    | 3.1    |
| Yield Loss (%)                   | 5              | 0.7            | 0              | 0.8      | 0      | 0      |
| Octane Loss                      | 0              | 0.1            | 1              | 1.3      | 1      | 0.75   |

Zeolite-based adsorbents for gasoline desulfurization were proposed by R. T. Yang.<sup>46</sup> He used Cu or Ag-exchanged Y-type zeolite in purifying gasoline and diesel. The capacity of such an adsorbent was reported to be 14.7 cc/1g. Regeneration was not intensively discussed, although such  $\pi$ -complexation may require rather severe regeneration conditions.

There is still a sacrifice of octane number due to olefin saturation, which can be made-up by isomerization and alkylation of saturated olefins. The OCTGain process developed by ExxonMobil lies in this category. In such a process, olefins are saturated to a large extent, but octane number loss is compensated by subsequent isomerization and alkylation steps. A more

selective catalyst is needed. Selective poisons are targeted. The alumina support is also neutralized by alkali hydroxide or carbon deposition.<sup>47,48</sup>

In spite of these efforts to produce ultra low sulfur gasoline, catalytic processes will require large investment and a meaningful increase of operating costs. Hence, non-catalytic processes with lower investment and operating cost have been proposed, especially by applying adsorption technology.

S-Zorb, developed by Phillips Petroleum, may be the first adsorption process to remove sulfur molecules contained in cracked gasoline. In the process, the adsorbent encounters sulfur molecules and selectively traps them on its surface. Sulfur-bearing adsorbent is regenerated by combusting sulfur in to  $\text{SO}_2$ . The S-Zorb Process looks very attractive to reduce the sulfur content of gasoline below a few ppm to a few tens of ppb. S Zorb consumes the least amount of hydrogen among the gasoline desulfurization technologies. Olefin loss is also very small, as low as 1 vol%.

Activated carbon materials have been proven to have enough sulfur retaining capacity in gas oil adsorption by the present authors.<sup>31</sup> However, its application to gasoline seems to have some problems due to strong adsorption of co-present olefins and aromatic compounds.

Besides the technologies on the way to commercialization, new catalysts have been proposed to achieve the effective desulfurization of gasoline without loss of octane number. Yin et al.<sup>49</sup> reported that FCC naphtha could be desulfurized over Ni/HZSM-5 catalyst without octane loss due to aromatization activity of the catalyst. In their concept, an olefin is aromatized before the hydrogenation. Excess cracking as well as rapid saturation are a concern. The present authors are examining CoMoS catalysts supported on carbon materials in HDS of cracked gasoline.

## 12. PROGRESS IN SUPPORT MATERIALS FOR MORE ACTIVE HDS CATALYSTS

There have been several significant advances in HDS catalysts. Although some suggest active species other than CoMo and NiMo, enhancement of catalytic activity has been intended particularly for the HDS of refractory sulfur species to find more active support materials. Some oxides and carbon materials have been evaluated to show their superiority to alumina in HDS reactions, although it could not be generalized due to the wide variation of reaction conditions and feed characteristics in HDS. Support influences the catalytic activity in HDS through two ways, modifying the active species on itself and participating in the HDS reaction as a co-catalyst.

Acidic supports, such as zeolites, have been tested by many researchers, and show superiority in the HDS reaction. Acidic zeolite was reported to facilitate isomerization and trans-alkylation of alkylated DBT, resulting in the enhanced HDS activity of such refractory sulfur species.<sup>50</sup>

Acidity has been recognized as important in deep HDS to improve resistivity against inhibition by H<sub>2</sub>S. Strong acidity must be inhibited by basic polar nitrogen species, such as NH<sub>3</sub> and pyridines, and carbazoles. Nevertheless HDN is also accelerated due to reduced N inhibition. A series of CoMo and NiMo catalysts supported on alumina, silica-alumina, and alumina-zeolite were examined in the deep HDS of SRGO to evaluate enhanced activity by such supports in the presence of H<sub>2</sub>S and NH<sub>3</sub>, by the present authors.<sup>7</sup> Although H<sub>2</sub>S and NH<sub>3</sub> inhibit the HDS of refractory sulfur species over all catalysts examined, a catalyst of high acidity achieved deep HDS even under such conditions. Adsorption of gas-phase inhibitors on the acidic sites and weakening of the metal-sulfur bond in the active sulfide caused by acidity of the support are believed to improve the resistivity against H<sub>2</sub>S. Reduction of inhibition by NH<sub>3</sub> is moderate.

Functions of zeolite, as a representative acidic support, have been discussed just from the viewpoint of enhanced hydrogenation and isomerization. In addition, zeolite itself has been found to desulfurize some sulfur species, such as thiophene. Acidic C-S bond breakage and hydrogen transfer can be postulated over the acidic zeolite. More research is needed.

In spite of the above advantages in using zeolite as a support material, an inevitable problem is present in such an acidic catalyst system, that is fast coking. Strong acidic sites cause extensive coking, which shortens the lifetime of the catalyst, covering particularly the strong acid sites. Although such behavior can not be discussed in detail now due to the lack of information, a disadvantage such as fast coking may be moderated by blocking particular acidic sites by a third ingredient. We examined CoMoS and NiMoS catalysts supported on USY, modified by an alumina additive. Acidity, measured by NH<sub>3</sub> desorption, was lower on the modified USY. However, its activity toward refractory sulfur species contained in the conventionally hydrotreated gas oil was only slightly improved over that of the zeolite support. Furthermore, cracking occurring on acid site was much less over the alumina-coated zeolite catalyst. It is also important to locate the hydrogenation active site in the vicinity of the acidic site to hydrogenate strongly adsorbed species on the acidic site for desorption before coking.

Incorporation of MCM-41 into alumina provided higher activity for the CoMo catalyst in DBT HDS.<sup>51</sup> MCM-41 was reported to reduce the interaction of Co and Mo with the support. As a result, it enhances the formation of polymeric Mo octahedral species, which are regarded as an active form on alumina. Furthermore, it modifies the dispersion of Co to suppress the

formation of an inactive  $\text{CoAl}_2\text{O}_4$  phase. Such results indicate the importance of the acidic nature of the support in modifying active sites. Such a function can be ascribed to finer particles of alumina among the matrix with poor affinity for the active oxides, such as  $\text{SiO}_2$ ,  $\text{TiO}_2$ ,  $\text{B}_2\text{O}_3$  and  $\text{P}_2\text{O}_5$ . It is intended to incorporate active species in the pore of zeolite. Difficulty for diffusion of large refractory species must be considered.

$\text{SiO}_2\text{-Al}_2\text{O}_3$  is also an acidic support like zeolites. HDS activity toward 4,6-DMDBT was reported to increase from the mixing of the conventional  $\text{NiMo/Al}_2\text{O}_3$  catalyst with  $\text{SiO}_2\text{-Al}_2\text{O}_3$ .<sup>52</sup> Such observation is believed to be caused by enhanced hydrogenation and isomerization by the acidic component in the catalyst. However, there are many questions on the fundamental aspects of HDS catalysts supported on  $\text{SiO}_2\text{-Al}_2\text{O}_3$ . First of all, the difference in  $\text{MoS}_2$  morphology on  $\text{Al}_2\text{O}_3$  and  $\text{SiO}_2\text{-Al}_2\text{O}_3$  must be clarified. It is generally accepted that  $\text{SiO}_2$  can't disperse  $\text{MoO}_3$  well in a monolayer due to very weak interaction with  $\text{MoO}_3$ .<sup>53</sup> However,  $\text{Al}_2\text{O}_3$  incorporation alters the nature of surface to increase the monolayer capacity. Hence, the form of active species may be different from that observed on  $\text{Al}_2\text{O}_3$  supports. Higher activity of  $\text{SiO}_2\text{-Al}_2\text{O}_3$  supported catalysts may come from a more favorable form of active species in addition to the stronger acidity of the support, but definite evidence has not been found yet.

Addition of  $\text{P}_2\text{O}_5$ ,  $\text{ZrO}_2$ , and  $\text{B}_2\text{O}_3$  to  $\text{Al}_2\text{O}_3$  were reported to increase the acidity of catalysts and as a result enhance the HDS of refractory sulfur species.<sup>54</sup> Phosphorus was also known to form  $\text{NiP}$ , which is active for hydrodesulfurization.<sup>55</sup> However, their effects on the morphology of active species are not confirmed yet. Roles of acidic supports in HDS by sulfide catalysts are summarized in Table 3.

Table 3. Role of Acidic Supports in HDS by Sulfide Catalyst.

|  |
|--|
| 1. Influences on the Active Species(Catalyst-Support Interaction)  |
| (1) Acidic modification on the natures of active sulfides<br>-Long and short-range interaction                                     |
| (2) Restriction of the area(site) for dispersion of active oxide precursors  |
| (3) Reverse spillover of proton from support to active sulfides  |
| 2. Catalytic Functions of Support(Bifunctional Catalysts)  |
| (1) Acidic activation of substrate<br>- Cracking, isomerization, trans-alkylation  |
| (2) Acidic adsorption of substrate in $\sigma$ - and $\pi$ -coordination<br>- Spillover of coordinated substrate to active sulfide |
| 3. Influence of Active Species on the Substrate Adsorbed on the Support)   |
| (1) Hydrogen spillover for sulfide to oxide support  |

TiO<sub>2</sub> was evaluated as an active support material for HDS. Its main drawback, low surface area, was reported to be overcome by a kind of sol-gel process, giving as high as 120 m<sup>2</sup>/g.<sup>256</sup> It could carry a higher loading of Mo as (19 wt% as MoO<sub>3</sub>) than conventional TiO<sub>2</sub> supports, allowing well dispersed Mo species. This catalyst showed higher HDS activity for 4,6-DMDBT than the alumina supported one. An Al<sub>2</sub>O<sub>3</sub>-TiO<sub>2</sub> composite support was also tested to provide higher surface area. It showed higher activity than Al<sub>2</sub>O<sub>3</sub> and TiO<sub>2</sub> alone in HDS of 4,6-DMDBT while its activity for the HDS of DBT was inferior to the alumina support.<sup>57,58,59</sup> Such binary oxides carry more Brønsted acidic sites and as a result have rather high activity in hydrogenation. This gives an increase in the activity for 4,6-DMDBT HDS. It should be also noted that TiO<sub>2</sub> is believed to have much less interaction with active species than Al<sub>2</sub>O<sub>3</sub>, inducing a more easily reducible oxide phase of Mo and Co(Ni) due to the partial sulfidation of TiO<sub>2</sub>.<sup>60</sup>

Carbon has been regarded as a promising catalyst support due to its very high surface area, peculiar pore structure, and surface-functional groups.<sup>24</sup> HDS catalysts supported on carbon can provide higher activity than alumina supported ones.<sup>36,61,62</sup> Presumably, weak interaction of carbon with sulfide precursors provides the more sulfidable species on carbon than on alumina, resulting in the more active sites for HDS. The very large surface area of carbon supports must be also helpful although the acidic contribution is not expected.

Life of catalysts due to the sintering of active species must be carefully tested since such supports interact weakly with active species.

### 13. RECOGNITION AND CONTROL OF THE SHAPE AND SIZE OF ACTIVE SITES ON HDS CATALYSTS

There have been several proposals to describe the active sites for HDS, such as intercalation, surface complex, and rim-edge models of cobalt and nickel in their location.<sup>63</sup> Such models include the stacked layer structure of MoS<sub>2</sub>, which is believed to constitute the major part of the active sites. Daage and Chianelli suggested that there are two types of active sites on a MoS<sub>2</sub> slab, rim and edge.<sup>63</sup> Rim sites are assumed to be responsible for the hydrogenation while edge sites are for both hydrogenation and direct hydrodesulfurization, respectively. Such images have provided design concepts of active sites for higher activity toward HDS by larger numbers of slabs or stacking providing higher activity.<sup>64</sup> Furthermore, Mo species directly contacting the support surface could not easily be sulfided, showing lower activity. Such concepts distinguish Type I and Type II phases. The former is a highly dispersed monolayer of MoS<sub>2</sub> and latter has lower dispersion and a higher extent of stacking.<sup>65,66</sup>

Although extensive examination to clarify the morphology of active species has been conducted by several research groups, it is not definitely concluded whether MoS<sub>2</sub> slabs sit with perpendicular or parallel orientation on supports.<sup>67</sup> Two types of MoS<sub>2</sub> slabs are depicted in Fig. 17.

Hence, methods to make the MoS<sub>2</sub> phase taller have been attempted. Among several types of anchoring sites on  $\gamma$ -Al<sub>2</sub>O<sub>3</sub>, an OH group bound to a tetrahedrally coordinated aluminum cation has been proposed to give strong interaction with Mo, resulting in less sulfidable Mo species.<sup>68</sup> In order to suppress the anchoring of Mo precursor on such inactive sites, Ti could be deposited on alumina prior to the impregnation of Mo.<sup>68</sup> This observation may be related to the dependence of the morphology of MoS<sub>2</sub> on the support type and preparation conditions. Additive agents are used to improve the dispersion of active species. There are two approaches. One is to disperse MoO<sub>2</sub> on the support to be highly stacked. The additive on the support restricts the site, leading to MoO<sub>2</sub> accumulation to make tall crystals. B<sub>2</sub>O<sub>3</sub> and P<sub>2</sub>O<sub>5</sub> can be such additives. Their acidic natures must not be excluded by mixing B<sub>2</sub>O<sub>3</sub>, P<sub>2</sub>O<sub>5</sub> and TiO<sub>2</sub> with alumina.

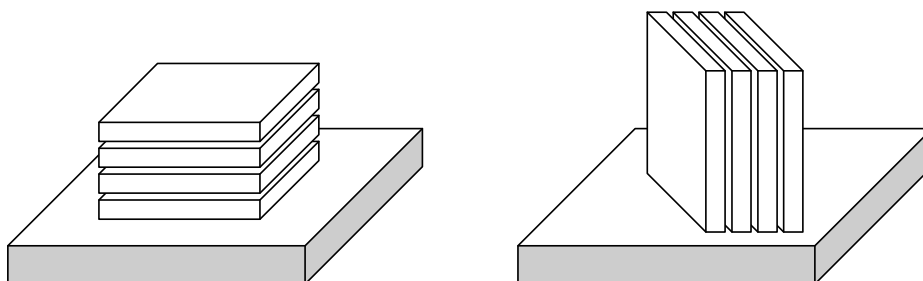


Figure 17. Schematic models for MoS<sub>2</sub> slabs sitting on support with parallel (left) and perpendicular (right) orientation

The second approach is to disperse Co and Ni on the particular sites of MoO<sub>2</sub>. In practical catalysts, EDTA (ethylenediaminetetraacetic acid), NTA (nitriloacetic acid) complexing agents can be applied to prevent interaction of Co(Ni) ions with the Al<sub>2</sub>O<sub>3</sub> surface.<sup>64,68,69,70</sup>

A more sophisticated approach is to make microcrystal shapes of nano size by micelle technology, which is a common methodology in nanotechnology. Atomic scale observation of HDS catalyst could provide deep insight for morphological understanding. Examination of model Mo-S structures on well defined substrates by scanning tunneling microscopy (STM) revealed that Co changes the morphology of MoS<sub>2</sub> from triangular to



truncated hexagonal by preferred siting of Co at the sulfur edge site of MoS<sub>2</sub>.<sup>20,71</sup> STM observation on the thiophene adsorbed model of MoS<sub>2</sub> provided information on the adsorption site, which was suggested to be the metallic edge site of MoS<sub>2</sub>. Such an approach is strongly expected to accelerate in-situ structural analysis of the practical catalyst. It must be noted that dynamic natures of catalyst structure and substrate conversion are important targets.

TEM observation of HDS catalysts was widely applied to evaluate the stacking degree and width of each stack of MoS<sub>2</sub>. It must be recognized that TEM can not detect the stacking of MoS<sub>2</sub> when its C axis is perpendicular to the surface of alumina. A number of stacks observed under TEM are placed to direct their C axis parallel to the surface. Detailed design of Co(Ni)MoS<sub>2</sub> can be achieved by molecular design of Co(Ni)M clusters with definite structure. Interaction of clusters with the surface of the support must be further clarified for complete sophistication.<sup>68</sup> The present authors believe now that most MoS<sub>2</sub> sits on its edge on the active support while weak interaction may allow the flat sitting of MoS<sub>2</sub> on an inactive support.

#### 14. CATALYTIC ACTIVE SITES FOR HDS AND HYDROGENATION

Co(Ni)MoS supported on alumina shows catalytic activity for hydrogenation as well as HDS. These catalysts include activation of hydrogen to substitute the counterpart of C-S bond or saturate the C-C double bond, which occur simultaneously. However, some features of these catalysts suggest that there are different active sites on Co(Ni)MoS/Al<sub>2</sub>O<sub>3</sub>. It is good to design catalysts of HDS with less hydrogenation. NiMoS is believed more active for hydrogenation than CoMoS.<sup>1,2</sup> Very low concentrations of H<sub>2</sub>S appear to retard hydrodesulfurization while it accelerates hydrogenation, although high concentration prohibits both reactions.<sup>72,73</sup> Acidic supports accelerate hydrogenation and hydrodesulfurization through the hydrogenation of refractory sulfur species. Acidity strengthens resistance to H<sub>2</sub>S inhibition of hydrodesulfurization. Such results suggest that the active sites for these catalysts are more coordinatively unsaturated for HDS than for hydrogenation. HDS requires two open valences to insert hydrogen into a C-S bond as illustrated in Fig. 6. In contrast,  $\pi$ -coordination of an aromatic ring or unsaturated bond in the aromatic ring to one of the active sites is followed by the addition of hydrogen from S-H on the sulfide for the first stage of hydrogenation. Strong adsorption of a partially hydrogenated aromatic ring continues the successive hydrogenation of other unsaturated bonds to

complete the aromatic hydrogenation. An acidic support moderates the electron density of active metals to be more acidic, activating S-H or Ni-H bonds to transfer the proton for hydrogenation. Nickel is certainly more active for hydrogenation than cobalt.

Other metals, including iron or noble metals, are worthwhile for examination to compare the selectivity between hydrodesulfurization and hydrogenation, although a series of metals are compared in the relationship between strength of metal-S and -H bonds and catalytic activity to confirm the Sabatier principle.<sup>74</sup>

Another important point not much discussed yet is the chemistry of  $\pi$ -coordination in heterogeneous catalysis.<sup>75,76,77</sup> The authors are particularly interested in the contribution of heteroatoms, especially sulfur, in the same or adjacent rings of the  $\pi$ -coordination. Fig. 18 shows the possible coordination geometry of thiophene. The catalytic sites must be clarified in such  $\pi$ -coordination. It may be important to distinguish carbon and S atoms in the aromatic ring for the selective hydrogenation of DBT against pure aromatic hydrocarbons as found in LCO and HCO from FCC the process. Roles of alkyl groups on the DBT ring are also considered. It is necessary to define the desulfurization mechanism of the target species such as thiols, thiophene and benzothiophene in the hydrodesulfurization of cracked gasoline.

Selective poisoning of hydrogenation has been patented to demonstrate selectivity for hydrodesulfurization. Sulfur compounds are postulated to adsorb on the support to reduce hydrogenation activity more than hydrodesulfurization as describe above. It is in line with a conclusion that the acidic support accelerates the hydrogenation. Unfortunately, such selective poisoning is still not very selective, as it also reduces hydrodesulfurization activity. More details and deeper understanding of the active sites and influential factors in the mechanism of hydrodesulfurization and hydrogenation are still being explored. The authors believe that the detailed description of the molecular structures of the catalyst, support, substrate, intermediate and then dynamic intermediates are logically established to build up catalysts frameworks.

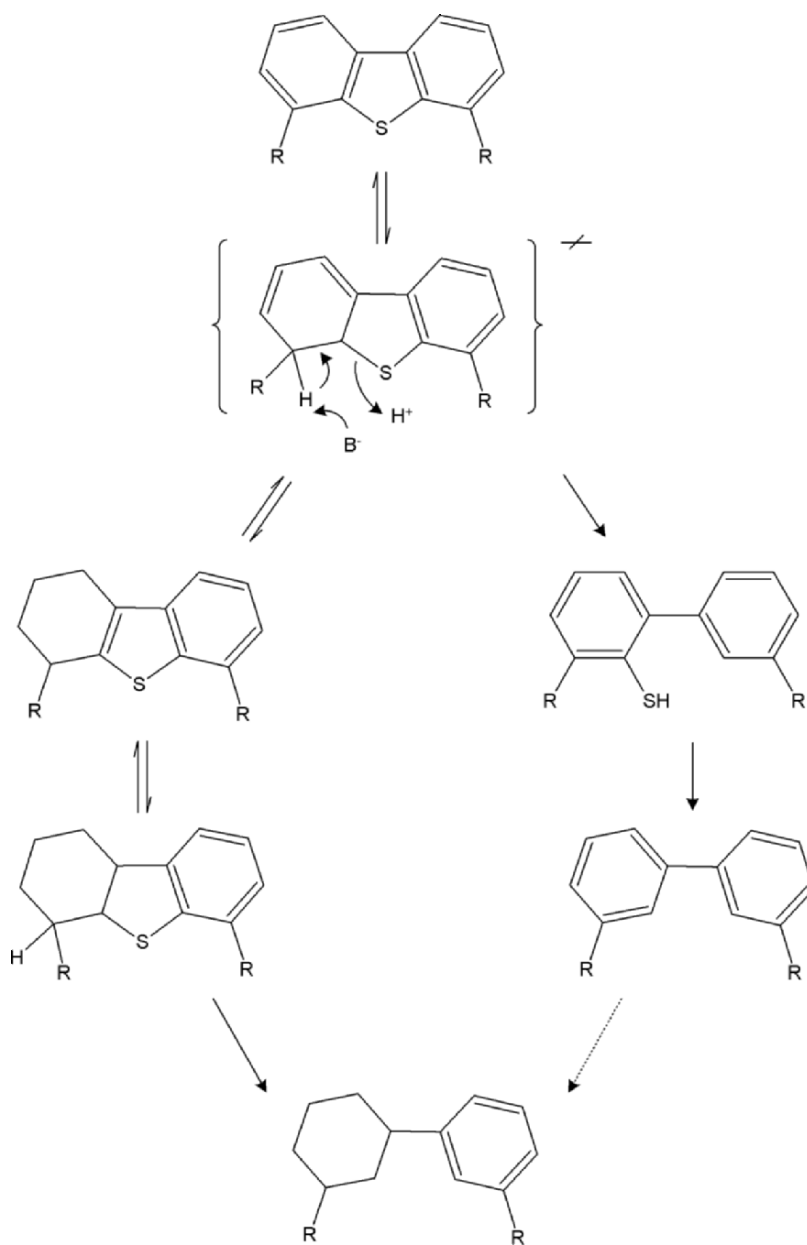


Figure 18. Reaction mechanism of HDS of 4,6-dialkylIDBT, assuming the formation of dihydro intermediate<sup>5</sup>

## 15. ROLES OF STERIC HINDRANCE IN ADSORPTION AND KINETIC PROCESSES OF HDS

It is definitely recognized that the deep hydrodesulfurization of gas oil relies upon the deep hydrodesulfurization of refractory sulfur species, which tend to stay almost exclusively at a significant level in conventional hydrodesulfurization processes. The refractory sulfur species are of low reactivity and suffer high inhibition by  $H_2S$ , nitrogen compounds including  $NH_3$ , and even aromatic compounds. The refractory sulfur species carry alkyl groups at the 4 and 6 positions on the DBT ring. The influence of 1 and 9 positions have not been examined yet. Other positions – 2, 3, 7, and 8 – do not deactivate but accelerate the hydrodesulfurization. Refractory sulfur species have been recognized to be desulfurized mainly through the hydrogenation of at least one phenyl ring prior to sulfur elimination. Hydrodesulfurization of hydrogenated intermediates is very rapid under typical hydrodesulfurization conditions.<sup>78</sup> In contrast, the reactive sulfur species are mainly desulfurized through direct elimination of sulfur atoms without hydrogenation of any phenyl ring, even if the hydrogenated intermediate could be desulfurized more rapidly. Thus, hydrogenation of one phenyl ring in refractory sulfur species is the rate-determining step. At higher temperature than  $360^\circ C$ , direct hydrodesulfurization becomes dominant even with the refractory sulfur species because higher temperature under the constant hydrogen pressure very sharply reduces obstacles against the direct elimination.<sup>78</sup> Such results indicate steric hindrance of alkyl groups at 4 and 6 positions on the DBT ring. The question is, which step is sterically hindered? Sulfur species can be adsorbed onto a sulfide catalyst first through  $\pi$ -coordination of the DBT ring. It is not clear how much and which place on the catalyst  $\pi$ -electrons of S atoms are coordinated at this stage. The  $\pi$ -coordinated species is transformed into  $\sigma$ -coordination of the sulfur atom on an active site of probably Co or Ni of coordinative unsaturation. This leads to the insertion of the active metal between aromatic C and S atoms as described above. The C-active site and C-S bonds are hydrogenatively fissioned, probably in a successive manner with two hydrogen atoms coming from the catalyst surface for S extraction. The SH group on the active site is further hydrogenated and desorbed eventually as  $H_2S$ . The steric hindrance can work during  $\sigma$ -coordination, at insertion, and during the hydrogenative fission steps.

The  $\sigma$ -coordinating step is often considered to be the most sensitive to steric effects. Strong inhibition against refractory sulfur species, especially at concentrations less than 300 ppm, favors steric hindrance at this stage. Inhibition is basically competition for active sites among the substrates, including inhibitors.  $\sigma$ -coordination of aromatic rings may not be probable.  $\pi$ -coordination to an active site, a  $\sigma$ -coordination site or a hydrogenation site may hinder hydrodesulfurization. In the latter case, only the hydrogenation route is inhibited and no inhibition can be observed with direct elimination of sulfur atoms. Detailed kinetic analyses are still needed to clarify the true features. High measured heat of adsorption suggests strong adsorption of refractory sulfur species. The measured heat is consistent with  $\pi$ -coordination adsorption. Hence, steric hindrance at  $\sigma$ -coordination sites is not excluded by this result. Kinetic analyses are necessary to estimate the heat of adsorption of real intermediates.

It is necessary to clarify more details of  $\pi$ -coordination on the catalyst in terms of its relation with the hydrogenation of aromatic species and which sites of sulfided catalysts are involved. Selectivity among aromatic species of pure hydrocarbons and of nitrogen, sulfur or oxygen containing rings can be discussed by clarifying such questions. Steric hindrance of alkyl groups on hydrogenation has been discussed for lower temperature.<sup>16</sup> However, no evidence has been observed in HDS above 300°C.

The hydrogenative bond fission step can be also postulated to suffer steric hindrance.<sup>2</sup> Alkyl groups at other locations may be involved in this stage. In this sense, reactivities of 1,9-dialkyl DBTs are interesting to discuss at these stages. The same questions have been posed in the HDN of aromatic nitrogen species. So far, in depth discussion has not been attempted.

Perot et al.<sup>5</sup> proposed the formation of dihydro intermediates during the HDS of DBT and dialkyl-DBT, regardless of whether the route involves hydrogenolysis or direct desulfurization as seen in Fig. 19. They ascribed the inertness of 4,6-DMDBT to hindered  $\beta$ -elimination by substituted methyl groups.

In conclusion, we believe that steric hindrance plays its role dominantly at the  $\sigma$ -coordination stage. Details of  $\pi$ -coordination must be involved in competition for the catalyst surface even if the step may not be rate-determining. Even so, participation of  $\pi$ -coordination may be influential in some petroleum refining reactions.

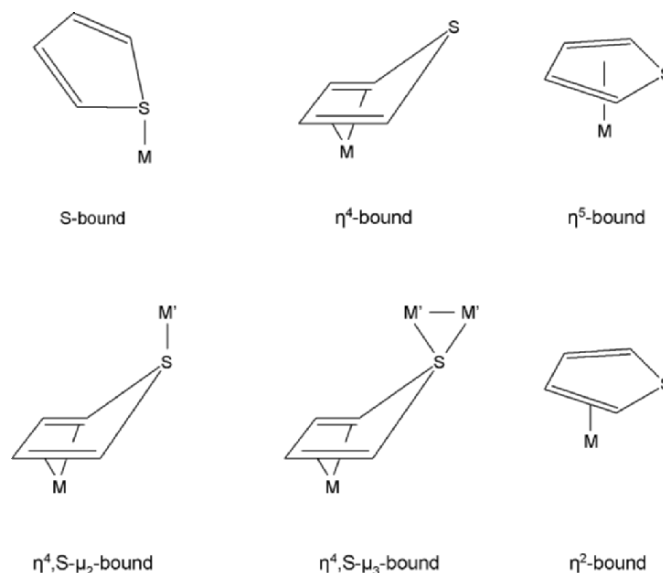


Figure 19. Coordination of thiophen in organometallic complexes <sup>77</sup>

## 16. FURTHER SCOPE AND ACKNOWLEDGMENTS

The present authors intended to cover the overall chemistry of hydrotreating processes in terms of feed and intermediates. The authors are grateful to the editors for giving us a chance to summarize our current research in hydrotreating catalysis and catalysts. One of the present authors (IM) has been involved in hydrotreating research for two decades. It is now time to establish the feeds and products, as well as the nature of catalysts, at the molecular level, including both structures and dynamics. Contributions of steric hindrance must be considered when discussing  $\pi$ -coordination. The authors believe that the present days are the turning point in catalytic research. Past assumptions must be deeply reviewed, based on modern techniques of analysis and the testing of more catalytic species, with due respect for the past 50 years of research, to establish current refining technologies.

The present review did not include the hydrotreatment of very heavy oils such as bitumen which must become very competitive resources in the near future.

The authors are grateful to New Energy & Industrial Technology Development Organization (NEDO), Petroleum Energy Center (PEC) and Ministry of Economy, Trade and Industry (METI) of Japan for financial

support for many years to their research. The authors are particularly grateful to a number of students and colleagues in Kyushu University. A number of friends in universities, research institutes, petroleum engineering and catalyst vendors from all over the world helped them to continue their research in the field of petroleum refining. Special thanks to Dr. D. D. Whitehurst for his long term and vivid friendship.

## 17. REFERENCES

1. Topsoe, H.; Clausen, B. S.; Massoth, F. E. *Hydrotreating Catalysis*, Springer: Berlin, 1996.
2. Whitehurst, D. D.; Isoda, T.; Mochida, I. *Adv. Catal.*, **1998**, *42*, 345.
3. Song, C. *Catal. Today*, **2003**, *86*, 211.
4. Babich, I. V.; Moulijn, J. A. *Fuel*, **2003**, *82*, 607.
5. Breysse, M.; Djega-Mariadassou, G.; Pessayre, S.; Geantet, C.; Vrinat, M.; Pérot, G.; Lemaire, M. *Catal. Today*, **2003**, *84*, 129.
6. Shin, S.; Yang, H.; Sakanishi, K.; Mochida, I.; Grudoski, D. A.; Shinn, J. H. *Appl. Catal. A*, **2001**, *205*, 101.
7. Choi, K.-H.; Kunisada, N.; Korai, Y.; Mochida, I.; Nakano, K. *Catal. Today*, **2003**, *86*, 277.
8. Qian, K.; Dechert, G. J. *Anal. Chem.*, **2002**, *74*, 3977.
9. Yongzhi, L.; Xianliang, D.; Weile, Y. *Fuel*, **1998**, *77*, 277.
10. Takatsuka, T. *Hydrotreatment - Science & Technology*, Kabe, T. (Ed.), IPC: Tokyo, 2000.
11. Ma, X.; Sakanishi, K.; Isoda, T.; Mochida, I. *Fuel*, **1997**, *76*, 329.
12. Sakanishi, K.; Yamashita, N.; Whitehurst, D. D.; Mochida, I. *Catal. Today*, **1998**, *43*, 241.
13. Furimsky, E. *Appl. Catal. A*, **2000**, *199*, 147.
14. Gentzis, T.; Parker, R. J.; McFarlane, R. A. *Fuel*, **2000**, *79*, 1173.
15. Sumbogo Murti, S. D.; Sakanishi, K.; Okuma, O.; Korai, Y.; Mochida, I. *Fuel*, **2002**, *81*, 2241.
16. Massoth, F. E. *Catal. Lett.*, **1999**, *57*, 129.
17. Kaufmann, T. G.; Kaldor, A.; Stuntz, G. F.; Kerby, M. C.; Ansell, L. L. *Catal. Today*, **2000**, *62*, 77.
18. Wei, J. *Catalyst Design - Progress and Perspective*, Hegedus, L. L. (Ed.), John Wiley & Sons: New York, 1987.
19. Topsøe, H.; Clausen, B. S. *Catal. Rev. -Sci. Eng.*, **1984**, *26*, 395.
20. Lauritsen, J. V.; Nyberg, M.; Vang, R. T.; Bollinger, M. V.; Clausen, B. S.; Topsøe, H.; Jacobson, K. W.; Lagsgaard, E.; Norskov, J. K.; Besenbacher, F. *Nanotechnol.*, **2003**, *14*, 385.
21. Girgis, M. J.; Gates, B. C. *Ind. Eng. Chem. Res.*, **1991**, *30*, 2021.
22. Nag, N. K.; Sapre, A. V.; Broderiok, D. H.; Gates, B. C. *J. Catal.*, **1979**, *57*, 509.
23. Ma, X.; Sakanishi, K.; Mochida, I. *Ind. Eng. Chem. Res.*, **1994**, *33*, 218.
24. Mata, J. M.; Smith, R. L.; Young, D. M.; Cost, C. A. V. *Environ. Sci. Technol.*, **2003**, *37*, 3724.
25. Yoskihiko, F. *Idemitsu Tech. Report*, **2000**, *45*, 140.
26. Perot, G. *Catal. Today*, **2003**, *86*, 111.
27. Romanow-Garcia, S. *Hydrocarbon Process*, **2000**, *79*, 17.
28. Dupain, X.; Rogier, L. J.; Games, E. D.; Makkee, M.; Moulijn, J. A. *Appl. Catal. A*, **2003**, *238*, 223.
29. Leflaive, P.; Lemberon, J. L.; Perot, G.; Mirgain, C.; Carriat, J. Y.; Colin, J. M. *Appl. Catal. A*, **2002**, *227*, 201.

30. Mochida, I.; Korai, Y.; Shirahama, M.; Kawano, S.; Hada, T.; Seo, Y.; Yoshikawa, M.; Yasutake, A. *Carbon*, **2000**, 38, 227.
31. Sano, Y.; Choi, K. -H.; Korai, Y.; Mochida, I. *Appl. Catal. B*, **2003**, submitted.
32. Egorova, M.; Zhao, Y.; Kukula, P.; Prins, R. *J. Catal.*, **2002**, 206, 263.
33. Rota, F.; Prins, R. *J. Catal.*, **2002**, 202, 195.
34. Furimsky, E.; Massoth, F. E. *Catal. Today*, **1999**, 52, 381.
35. Amemiya, M.; Korai, Y.; Mochida, I. *J. Japan Petroleum Institute*, **2003**, 46, 99.
36. Farag, H.; Whitehurst, D. D.; Sakanishi, K.; Mochida, I. *Catal. Today*, **1999**, 50, 9.
37. Mochida, I.; Sakanishi, K.; Ma, X.; Nagao, S.; Isoda, T. *Catal. Today*, **1996**, 29, 185.
38. Inoue, S.; Takatsuka, T.; Wada, Y.; Hirohama, S.; Ushida, T. *Fuel*, **2000**, 79, 843.
39. Ma, X.; Sakanishi, K.; Mochida, I. *Fuel*, **1994**, 73, 1667.
40. Choi, K.-H.; Korai, Y.; Mochida, I. *Prep. Am. Chem. Soc. Fuel Div.*, **2003**; p. 653.
41. Kaufmann, T.G.; Kaldor, A.; Stuntz, G. F.; Kerby, M. C.; Ansell, L. L. *Catal. Today*, **2000**, 62, 77.
42. Plantenga, F. L.; Leliveld, R. G. *Appl. Catal. A*, **2003**, 248, 1.
43. Sweed, N. H. *SCANFinishing for Low Sulfur Gasoline*, [http://www.prod.exxonmobil.com/refiningtechnologies/pdf/JPI\\_Paper\\_on\\_SCANfining\\_for\\_Low\\_Sulfur\\_Mogas.pdf](http://www.prod.exxonmobil.com/refiningtechnologies/pdf/JPI_Paper_on_SCANfining_for_Low_Sulfur_Mogas.pdf)
44. Marion, P., 4th International Conference on Petroleum Refining Technology and Economics in Russia, the CIS and Baltics, 2002. [www.axens.net/upload/presentations/fichier/presaxenscleanfuelstechnologies.pdf](http://www.axens.net/upload/presentations/fichier/presaxenscleanfuelstechnologies.pdf)
45. T. Hagiwara *Gasoline Production Technology and Methods and an Evaluation of Their Economic Viability*, Petroleum Energy Center (PEC) of Japan, 2001.
46. Yang, R. T.; Hernández-Maldonado, A. Z.; Yang, F. H. *Science*, **2003**, 301, 79.
47. Mey, D.; Brunet, S.; Perot, G.; Diehl, F. *Prep. Am. Chem. Soc. Fuel Div.*, **2003**; p. 44.
48. Hatanaka, S.; Sadakane, O. U.S. Patent, 6,120,679, **2000**.
49. Yin, C.; Zhao, R.; Liu, C. *Energy Fuels*, **2003**, 17, 1356.
50. Isoda, I.; Nagao, S.; Ma, X.; Korai, Y.; Mochida, I. *Energy Fuels*, **1996**, 10, 1078.
51. Ramirez, J.; Contreras, R.; Castillo, P.; Klimova, T.; Zárate, R.; Luna, R. *Appl. Catal. A*, **2000**, 197, 69.
52. Michaud, P.; Lemberton, J. L.; Pérot, G. *Appl. Catal. A*, **1998**, 169, 343.
53. Rana, M. S.; Maity, S. K.; Ancheyta, J.; Murali Dhar, J.; Prasada Rao, T. S. R. *Appl. Catal. A*, **1998**, 253, 165.
54. Lecrenay, E.; Sakanishi, K.; Mochida, I.; Suzuka, T., *Appl. Catal. A*, **1998**, 175, 237.
55. Koranyi, T. I., *Appl. Catal. A*, **2003**, 239, 253.
56. Dzwigaj, S.; Louis, C.; Breysse, M.; Cattenot, M.; Bellière, V.; Geantet, C.; Vrinat, M.; Blanchard, P.; Payen, E.; Inoue, S.; Kudo, H.; Yoshimura, Y. *Appl. Catal. B*, **2003**, 41, 181.
57. Lecrenay, E.; Sakanishi, K.; Nagamatsu, T.; Mochida, I.; Suzuka, T. *Appl. Catal. B*, **1998**, 18, 325.
58. Kaneko, E. Y.; Pulcinelli, S. H.; da Silva, V. T.; Santilli, C. V. *Appl. Catal. A*, **2002**, 235, 71.
59. Pahal, C.; Kameda, F.; Hoshino, K.; Yoshinaka, S.; Segawa, K. *Catal. Today*, **1997**, 39, 21.
60. Ramirez, J.; Cedeno, L.; Busca, G. *J. Catal.*, **1999**, 184, 59.
61. Auer, E.; Freund, A.; Pietsch, J.; Tacke, T. *Appl. Catal. A*, **1998**, 173, 259.
62. Whitehurst, D. D.; Farag, H.; Nagamatsu, T.; Sakanihi, K.; Mochida, I. *Catal. Today*, **1998**, 45, 299.
63. Daage, M.; Chianelli, R. R. *J. Catal.*, **1994**, 149, 414.
64. Hensen, E. J. M.; Kooyman, P. J.; van der Meer, Y.; van der Kraan, A. M.; de Beer, V. H. J.; van Veen, J. A. R.; van Santen, R. A., *J. Catal.*, **2001**, 199, 224.
65. Candia, R.; Sorensen, O.; Villadsen, J.; Topsoe, N. -Y.; Clausen, B. S.; Topsoe, H., *Bull. Soc. Chim. Belg.*, **1987**, 93, 763.



66. Hensen, E. J. M.; de Beer, V. H. J.; van Veen, J. A. R.; van Santen, R. A. *Catal. Lett.*, **2002**, *84*, 59.
67. Reardon, J.; Datye, A. K.; Sault, A. G. *J. Catal.*, **1998**, *173*, 14.
68. Inamura, K.; Uchikawa, K.; Matsuda, S.; Akai, Y. *App. Surf. Sci.*, **1997**, *121-122*, 468.
69. Cattaneo, R.; Rota, F.; Prins, R. *J. Catal.*, **2001**, *199*, 318.
70. Hiroshima, T.; Mochizuki K.; Honma, T.; Shimizu, T.; Yamada, M. *Appl. Surf. Sci.*, **1997**, *121*, 433.
71. Lauritsen, J. V.; Helveg, S.; Lagsgaard, E.; Stensgaard, I.; Clausen, B. S.; Topsøe, H.; Besenbacher, F. *J. Catal.*, **2001**, *197*, 1.
72. Hensen, E. J. M.; de Beer, V. H. J.; van Veen, J. A. R.; van Santen, R. A. *J. Catal.*, **2003**, *215*, 353.
73. Kunisada, N.; Choi, K.-H.; Korai, Y.; Mochida, I. *Appl. Catal. A.*, **2003**, In press.
74. Chianelli, R. R.; Berhaut, G.; Kasztelan, S.; Hafner, J.; Touhoat, H. *Appl. Catal. A.*, **2002**, *227*, 83.
75. Angelici, R. J. *Polyhedron*, **1997**, *16*, 3073.
76. Sánchez-Delgado, R. A. *J. Mol. Catal.*, **1994**, *86*, 287.
77. Wiegand, B. C.; Friend, C. M. *Chem. Rev.*, **1992**, *92*, 491.
78. Farag, H.; Mochida, I.; Sakanishi, K. *Appl. Catal. A.*, **2000**, *194-195*, 147.
79. Seijiro Nonaka, *The 11<sup>th</sup> CCIC Technical Seminar (Catalysts & Chemical Ind. Co. Ltd.)*, 2002; pp.2-1.

## Chapter 10

### **ULTRA DEEP DESULFURIZATION OF DIESEL: HOW AN UNDERSTANDING OF THE UNDERLYING KINETICS CAN REDUCE INVESTMENT COSTS**

Barry H. Cooper and Kim G. Knudsen  
*Haldor Topsøe A/S*  
*Nymøllevvej 55, DK2800 Lyngby, Denmark*

#### **1. CHANGES IN DIESEL SPECIFICATIONS AND DEMAND**

In recent years, the development and use of “environmentally friendly” fuels has had high priority throughout the world. The driving force is the improvement in air quality, especially in metropolitan areas. Reductions in vehicle emissions require improvements in both engine and exhaust technologies, and in fuel quality. The vehicle manufacturers have issued a “World-Wide Fuel Charter”, which stipulates their minimum requirements for fuel quality to meet future emission standards.

In the European Union (EU), new specifications were introduced in 2000 covering sulfur content, specific gravity (SG or density), poly-aromatic hydrocarbon (PAH) content, cetane number and the maximum 95% ASTM distillation point. Legislation has been passed that will further limit the sulfur content to 50 wppm by the year 2005, and to 10 wppm by 2009 at the latest. Ultra low sulfur diesel (ULSD) with a cap of 10 wppm sulfur was introduced in Germany and the UK in 2003.

In the United States, new legislation limits the sulfur content of diesel fuel to 15 wppm by mid 2006. In California, transit bus fleets were required to use max. 15 wppm sulfur diesel by October 2002.

Current diesel sulfur specifications in Asia vary over a wide range from 0.5 wt% to less than 0.05 wt%. The average sulfur level, estimated to be 0.19 wt% for year 2000, will continue to drop due to the definite movement away from 0.5% grades toward 0.05% grades. In Japan, diesel with max. 50 wppm

will be mandatory by 2005, and max. 10 wppm has been proposed for 2007. Future diesel specifications for selected countries are shown in Table 1.

*Table 1. Future Diesel Specifications for Selected Countries*

|        | Current Spec. wppm | Future Specs. wppm (year) |
|--------|--------------------|---------------------------|
| EU     | 350                | 50/10 (2005/9)            |
| USA    | 500                | 15 (2006)                 |
| Canada | 500                | 15 (2006)                 |
| Japan  | 500                | 50/10 (2005/7)            |
| Korea  | 500                | 50 (2005)                 |

At the same time as diesel fuel specifications are tightening, the demand for diesel is growing in Asia as well as in Europe. Although the growth rate for middle distillate in Asia Pacific was relatively stagnant from 1996-1998, it rose to 4.6% in 1999,<sup>1</sup> and future demand in developing Asia is forecast to be 5.1% per year.<sup>2</sup> In the EU, the increase in demand for mid-distillates has been at about 1.2%/annum over the past 5 years. It is predicted that the diesel demand in the EU will increase by 30% over the next 15 years.<sup>3</sup> There is a reduced demand for home heating oil and fuel oil cutter stocks, which can help meet the increased need for diesel, but these lower quality stocks will require severe hydrotreatment to meet the future specifications for diesel fuel.

## 2. CHALLENGES FACING THE REFINER

The refining industry is facing a double-edged challenge: to meet new, more stringent specifications for diesel product, while simultaneously producing more diesel product from lower quality feedstocks. The combination of these factors places a heavy burden on the refiner's hydroprocessing capabilities. As a result, increased new hydrotreating capacity and revamp of existing facilities will be needed to meet the future diesel specifications. Since each refinery is unique with respect to crude supplies, upgrading facilities, product slate, hydroprocessing units and the availability of hydrogen, there is no single answer on how to best meet this challenge. Added to this is the uncertainty of what further restrictions on diesel quality will be imposed in the future.

Each refiner has to make decisions with respect to:

- Whether equipment in existing units can be revamped to obtain future diesel specifications, or whether it is necessary to build a grassroots unit.
- Whether changes made now will be sufficient to meet likely future changes in specifications.
- What extent investments can be staged.
- What extent achieving low sulfur specifications can improve other key diesel properties.

In the following, we will address the issues raised by these considerations.

### 3. THE SELECTION OF CATALYST FOR ULTRA DEEP DESULFURIZATION

When hydrotreating to lower and lower sulfur levels, it becomes necessary to remove sulfur from those compounds which are the most difficult to desulfurize.<sup>4,6</sup> The most refractive sulfur compounds are higher molecular weight dibenzothiophenes that contain side chains in positions close to the sulfur atom (Figure 1). Two such compounds that are known to be difficult to desulfurize are 4-methyl dibenzothiophene (4-MDBT) and 4,6-dimethyl dibenzothiophene (4,6-DMDBT). These compounds are normally found in a higher concentration in aromatic feeds such as cycle oils and coker gas oils.

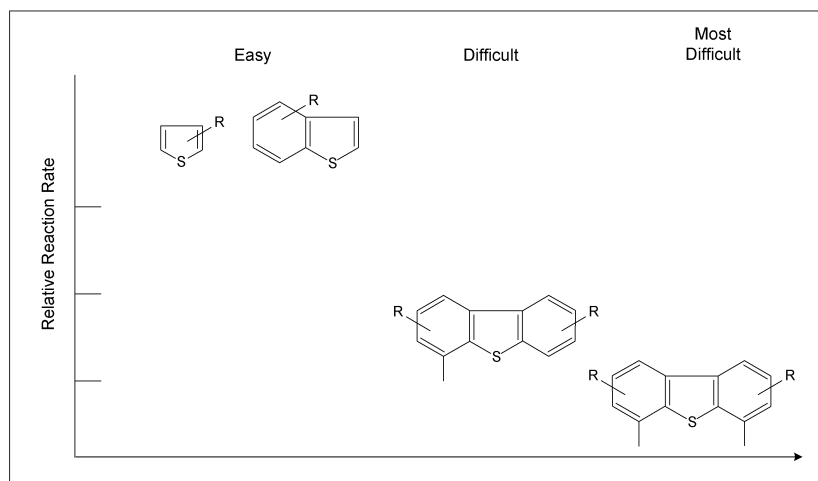


Figure 1. Impact of Sulfur Species

These compounds react quite differently over CoMo and NiMo catalysts, and the response of the two catalysts to the hydrogen sulfide produced during reaction and to inhibitors in the feed is dissimilar. To appreciate the criteria governing the choice of catalyst for ultra deep desulfurization and the consequences for product properties and hydrogen consumption, it is important to understand how the most refractive sulfur compounds react as well as the role played by inhibitors.

#### 3.1 Desulfurization

In general, there are two possible reaction pathways for removal of sulfur from dibenzothiophene (DBT) and alkylated dibenzothiophenes as shown in Figure 2.<sup>7</sup> The first pathway is by direct extraction of the sulfur atom from the molecule. The second pathway is by prehydrogenation of one aromatic ring followed by extraction of the sulfur atom.

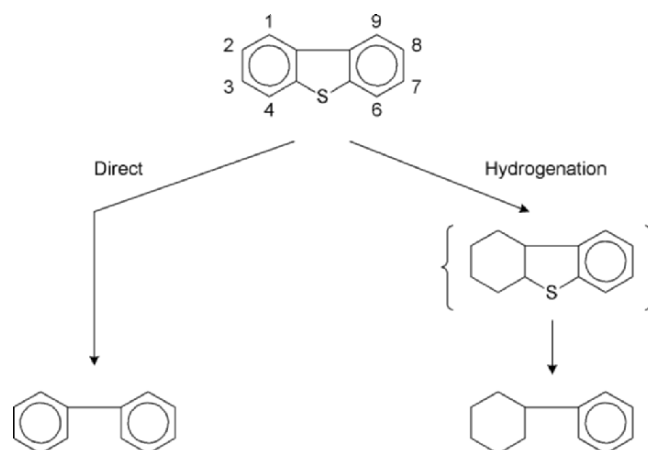


Figure 2. Reaction Pathways for HDS of DBT

Desulfurization of DBT progresses preferentially via the direct extraction route. When alkyl substituents are attached to the carbon atoms adjacent to the sulfur atom, the rate of direct sulfur extraction is diminished, whereas the rate of sulfur removal via the prehydrogenation route is relatively unaffected.

For DBT-molecules with alkyl substituents in the 4- and/or the 6-position, both routes are important, but for all other sulfur-containing molecules in the diesel boiling range, only the direct route is important for HDS.

CoMo catalysts desulfurize primarily via the direct desulfurization route. NiMo catalysts, which exhibit a higher hydrogenation activity, have a relatively higher selectivity for desulfurization via the hydrogenation route. The extent to which a given catalyst desulfurizes via one route or the other determines the effect of  $H_2$  partial pressure,  $H_2S$  partial pressure and feed properties on the catalyst activity.

The effect on catalyst activity of process variables such as LHSV, temperature, hydrogen partial pressure, hydrogen sulfide partial pressure and gas/oil ratio can be predicted by a suitable kinetic expression. It was found that the expression shown in equation 1 could be used to describe the kinetics of CoMo and NiMo catalysts for very deep desulfurization of diesel.<sup>7</sup>

Equation 1:

$$\frac{-dC_s}{dt} = \frac{k_D \cdot C_s^n \cdot P_{H_2}^\alpha}{(1 + K_{H_2S} \cdot P_{H_2S})} + \frac{k_H \cdot C_s^m \cdot P_{H_2}^\beta}{1 + K_F \cdot C_F}$$

In the expression for the rate of desulfurization ( $-dC_s/dt$ ), the first term represents the direct desulfurization route, which is enhanced by an increase of the hydrogen partial pressure and inhibited by the presence of  $H_2S$ . The second term represents the hydrogenation route, which is also enhanced by an increase of the hydrogen partial pressure and inhibited by certain nitrogen-

containing compounds present in the oil (denoted F in the equation). The effect of inhibitors on the hydrogenation route is described in detail below.

For CoMo catalysts, the second term can to a good approximation be neglected, and the rate constant,  $k_D$ , can be determined by integration of the expression. For NiMo catalysts, both terms are important.

### 3.2 Choice of Catalysts for Ultra Deep Desulfurization

The choice of the best catalyst for a given feedstock and for given operating conditions is influenced by the different ways that CoMo and NiMo catalysts desulfurize the most refractive sulfur compounds. In contrast to conventional wisdom, it is found for deep desulfurization that CoMo catalysts generally perform better than NiMo catalysts on feeds containing cracked stocks. A series of tests were performed to illustrate the changes in catalyst ranking as a function of feed and operating conditions. Three catalysts from Haldor Topsøe A/S were used:

- TK-554, a CoMo catalyst for low sulfur diesel service
  - TK-574, a CoMo catalyst for ultra low sulfur diesel service
  - TK-573, a NiMo catalyst for ultra low sulfur diesel service
- Characteristics of the feeds used in the tests are shown in Table 2.

Table 2. Properties of Test Feedstocks

|                         | Kuwait Straight Run<br>Gas Oil (SRGO) | Blend of 25% light coker oil<br>(LCO) and 75% SRGO |
|-------------------------|---------------------------------------|--|
| Sulfur (wt %)           | 1.30                                  | 1.52   |
| SG (60/60°F)            | 0.846                                 | 0.857  |
| Aromatic content, wt%   |                                       |  |
| Total / mono / di / tri | 24.0 / 14.9 / 7.4 / 1.7               | 29.9 / 15.2 / 11.5 / 3.2                           |
| Distillation D86 in °C  |                                       |  |
| IBP / 10 / 30 / 50 /    | 203 / 242 / 270 / 293 /               | 211 / 246 / 294 / 303 /                            |
| 70 / 90 / 95 / FBP      | 323 / 365 / 385 / 403                 | 332 / 372 / 378 / 379                              |
| 4-Me-DBT (wppm)         | 140                                   | 300  |
| 4,6-DiMe-DBT (wppm)     | 90                                    | 150  |

Figure 3 shows results obtained for the three catalysts on the Kuwait straight-run gas oil. The figure shows product sulfur as a function of LHSV for each catalyst. The tests were operated at a hydrogen pressure of 30 bar,  $H_2$ /oil ratio of 250 NI/l and at constant temperature. Of the two CoMo catalysts, TK-574 is between 30 and 40% better on a relative volume activity basis than TK-554 for all space velocities. The NiMo catalyst, TK-573, exhibits a lower activity than TK-574 at high LHSV, where the benzothiophenes, DBT's and to some extent 4-MDBT are removed. These molecules are predominantly removed via the direct extraction route, for which the CoMo catalyst has the highest activity. At low LHSV (i.e. high degree of HDS), where the 4,6-DiMe-DBT's have to be removed, the TK-573 is more active than the CoMo catalysts. The reason for this is the fact that at these conditions, the NiMo catalyst is a better hydrogenation catalyst and

thereby better for removal of the inhibitors of the hydrogenation route, which is the preferred route for removal of the 4,6-DMDBT's.

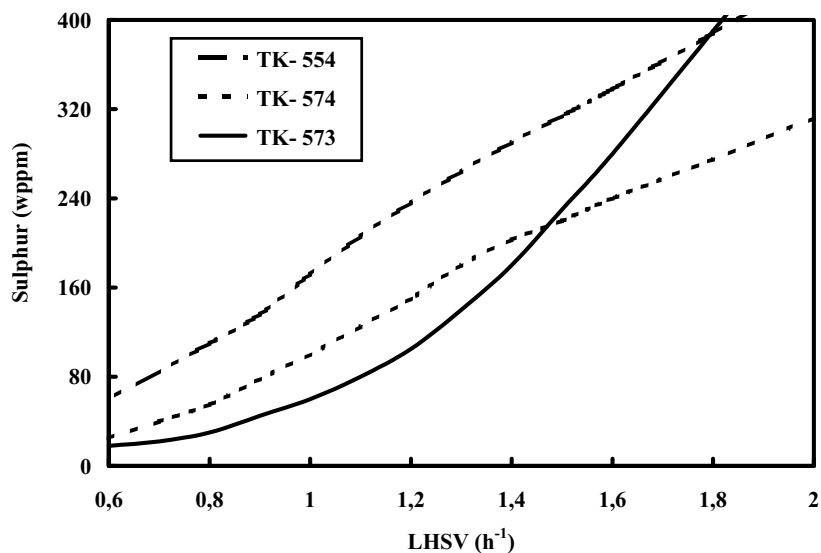


Figure 3. Product Sulfur vs. LHSV (SRGO)

Figure 4 shows product sulfur as a function of temperature for the three catalysts on the blend of 75% straight run gas oil and 25% light coker oil (LCO). In these tests, the hydrogen to oil ratio was 500 NI/l, and the hydrogen pressure was 30 bar. LHSV was held constant.

Of the two CoMo catalysts, TK-574 is always between 6 and 8°C better than TK-554. At low temperatures, TK-573 exhibits a lower activity than the CoMo catalysts, but ranks second in activity at higher temperatures. The reason for the good performance of the CoMo catalysts at low temperatures (i.e. at a low degree of HDS) is the same as that given above: CoMo catalysts are better at removing sulfur via the direct extraction route. What perhaps is surprising, is that the NiMo catalyst is not the best catalyst at the highest conversion level as was found in the tests on straight run gas oil. There are two reasons for this. Firstly, the feed containing cracked material has a higher concentration of inhibitors for the hydrogenation route. Secondly, removal of sulfur and inhibitors via the hydrogenation route suffers from a thermodynamic equilibrium constraint in the hydrogenation step, and the apparent activation energy for HDS via the hydrogenation route is therefore relatively low. This favors the use of a CoMo catalyst for deep HDS of this feedstock.

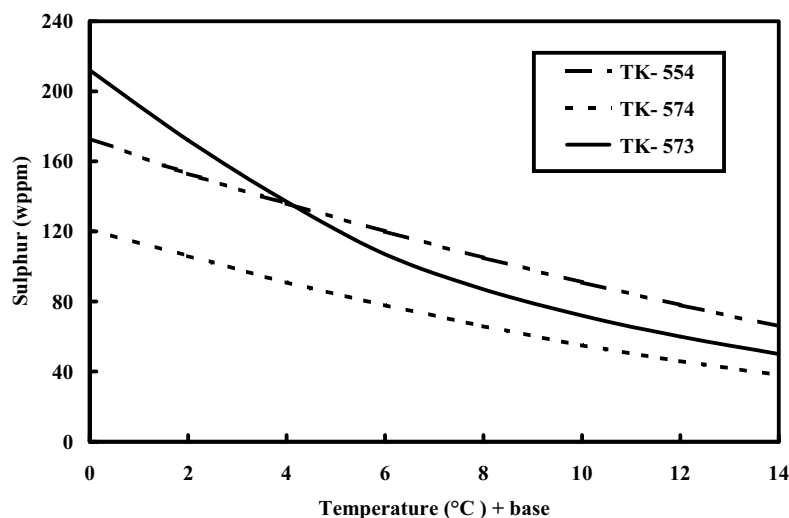


Figure 4. Product Sulfur vs. Temperature (LCO/SRGO)

Increasing the hydrogen pressure leads to a relatively better performance of the NiMo catalyst. This is illustrated in Figure 5 in which product sulfur is plotted versus pressure for TK-573 and TK-574 at two different temperatures on the blend of 75% straight run gas oil and 25% LCO. At the low temperature, the CoMo catalyst is better than the NiMo catalyst at all but the highest pressures, but at the higher temperature, the two catalysts change ranking at a much lower pressure. It is clear that the hydrogen partial pressure dependency is different for the two different reaction routes. The direct extraction route (for which the CoMo catalyst has the highest activity) has a relatively low hydrogen pressure dependency, whereas the hydrogenation route (for which the NiMo catalyst has the highest activity) exhibits a high hydrogen partial pressure dependency. If the hydrogen partial pressure is high, the thermodynamic equilibrium constraint for removal of sulfur via the hydrogenation route is moved to a higher temperature, and the apparent activation energy of HDS via the hydrogenation route is therefore pressure dependent.

### 3.3 Inhibitors for the Hydrogenation Route

It has already been mentioned that the hydrogenation route is severely inhibited by nitrogen-containing compounds. It is important to understand what types of N-compounds inhibit, and how they interfere with the HDS reactions. Model compound studies have shown that some basic nitrogen-containing molecules (such as acridine) are orders of magnitude more inhibiting than other N-containing molecules (such as aniline and indole) and



also more inhibiting than DBT itself.<sup>8</sup> The interesting results from these model compound tests called for additional real feed studies, where the inhibition of HDS in typical diesel fuels was investigated. In the following, the results from such real feed studies will be described.

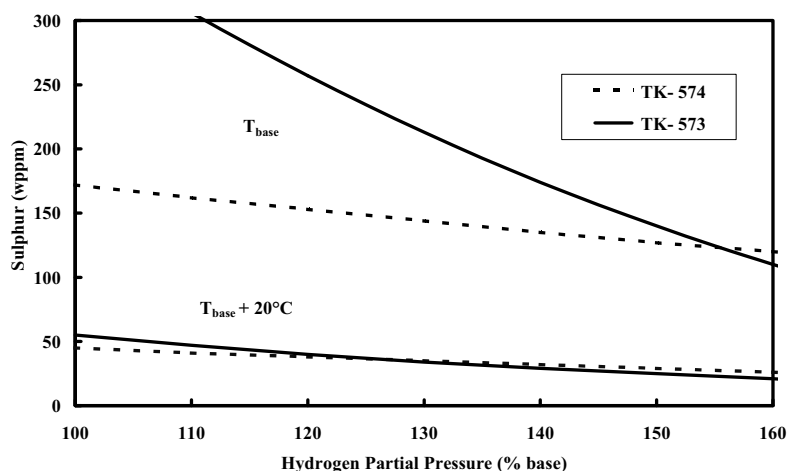


Figure 5. Product Sulfur vs. Pressure at Two Temperatures (LCO/SRGO)

In a series of experiments, hydrotreated diesel fuels were extensively characterized using a state-of-the-art technique for N-compound analysis. This procedure has been reported elsewhere.<sup>9</sup> Briefly, it consists of a novel pre-concentration step for the N-compounds on a silica SPE column followed by recovery of the N-compounds. The GC analysis was performed on a Hewlett-Packard 6890 equipped with an atomic emission detector (AED) model G2350A. In most cases, more than 60% of the N-containing molecules in the feed and products can be accounted for, and all the major peaks have been identified. The results of these studies showed that alkylcarbazoles were the least reactive N-compound class. Furthermore, it was established that the reactivity was the lowest for carbazoles with a high degree of substitution. These results led to the question of whether alkylcarbazoles were the major inhibitors in the HDS of the refractory S-compounds.

Previous studies of the N-compounds in diesel fuels showed that alkylcarbazoles are the major N-compound class in the diesel fuel.<sup>9</sup> Alkyl indoles and quinolines are also present but are not as prevalent. Basic N-compounds such as anilines are only present as trace components in diesel hydrotreating feeds, but are found in hydrotreated fuels. It was decided to simplify the inhibition studies by removing essentially all N-compounds from the diesel fuel and adding known model compounds from different classes of N-compounds. In this way a clear assessment of the relative effects of different classes of N-compounds in diesel fuels could be made. The selective

removal of N-compounds, leaving all the sulfur compounds unaltered, was accomplished by preparative chromatography over silica gel. Details of the separation are given in Ref. 10. The original diesel feedstock used for these studies contained 300 wppm of nitrogen. Three different feeds were prepared by blending 300 wppm of different N-compound classes into the N-free diesel fuel. The compounds chosen were 3-methylindole, 1,4-dimethylcarbazole and acridine. In addition, a blend containing 100 wppm N of each compound was made using the N-free fuel. The modified diesel fuels were then hydrotreated over a NiMo catalyst, and the results were compared with those obtained from hydrotreatment of the untreated fuel.

The results are shown in Figure 6. It can clearly be seen that 3-methylindole and 1,4-dimethylcarbazole are not major inhibitors, whereas acridine is. The three component blend behaves essentially as an additive combination of the three different N-compounds. There are also indications to the effect that acridine strongly inhibits the conversion of 1,4-dimethylcarbazole. In the absence of acridine, a high degree of conversion was obtained even for this low reactivity alkylcarbazole. The results indicate that alkylcarbazoles are not the major species of concern in HDS inhibition, even though they are the major species detected in hydrotreated diesel fuels.<sup>9</sup> This suggests that there may be some components of diesel fuels that inhibit both HDN of alkylcarbazoles and HDS of alkyldibenzothiophenes. To see whether or not this is the case, additional studies were conducted on the N-free diesel fuel.

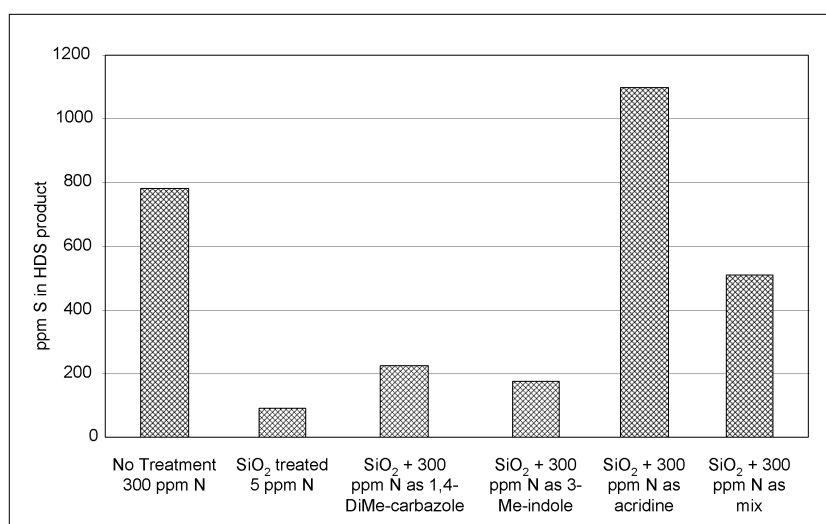


Figure 6. The Effect of Various Nitrogen Compounds on HDS Activity

Specific N-compound classes were recovered from the silica gel used in the preparative chromatography to produce the N-free oil by sequential elution using different solvents.<sup>11</sup> Several different classes of N-compounds were isolated, but in this chapter we will focus on three of them: basic + polar compounds, hindered carbazoles (having alkyl substituents adjacent to the N atom) and unhindered carbazoles. Figures 7-11 show the distribution of the various N-compounds within the diesel fuel and isolated fractions as determined by SPE-GC/AED analysis.<sup>8,9,11</sup> All chromatograms are presented on the same scale, with the exception of the “N-free” sample, which is shown on a 10 times larger scale. It is seen that there are traces of N-compounds in that sample. An analysis of the sample showed that it contained about 5 wppm of total N. The differences in composition of the two carbazole fractions are shown in Figures 9 and 10, respectively. The basic fraction (Figure 11) does not resemble the carbazole fractions since there are no high concentrations of individual components, but a multitude of overlapping species. The three fractions were analyzed for N-content and blended back into the “N-free” diesel fuel to produce modified diesel feeds with about 200 wppm of total N in the form of different chemical classes. The three feedstocks were used together with the N-free diesel fuel and the raw feed (from which the N-free diesel is produced and from which the different classes of N-compounds are separated) in a comparative hydrotreating study over a NiMo catalyst.

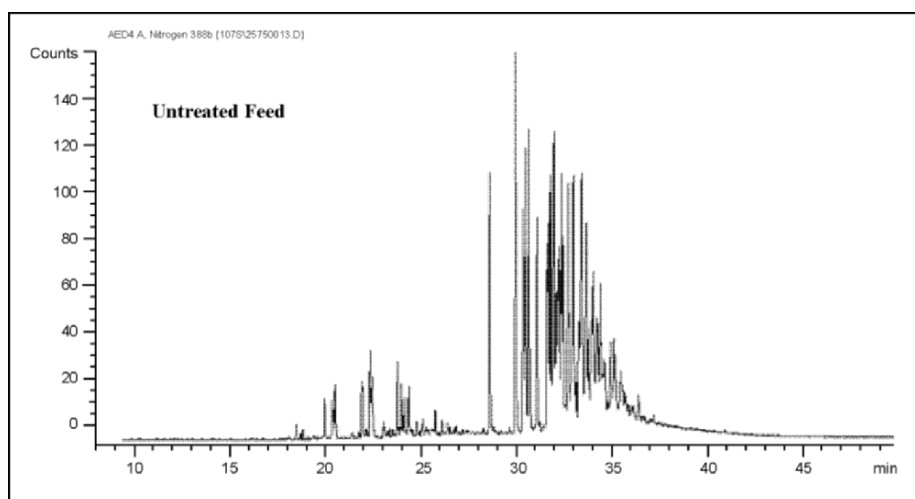


Figure 7. GC/AED Analysis of Untreated Feed

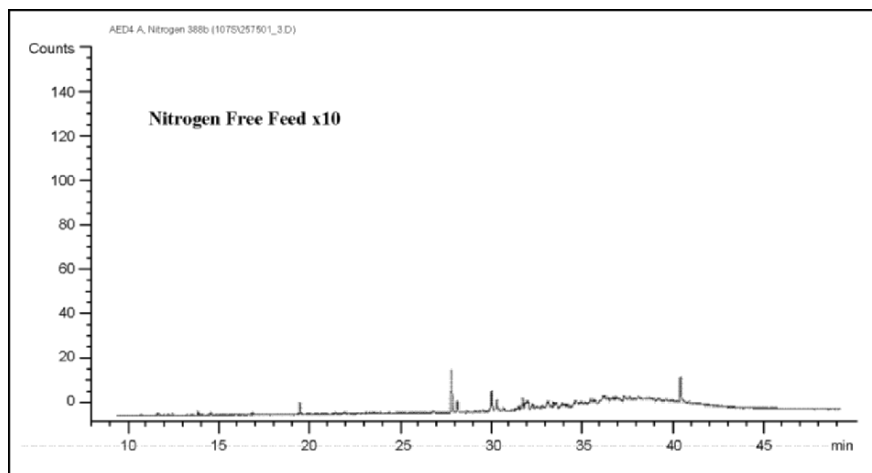


Figure 8. GC/AED Analysis of Nitrogen Free Feed (X 10)

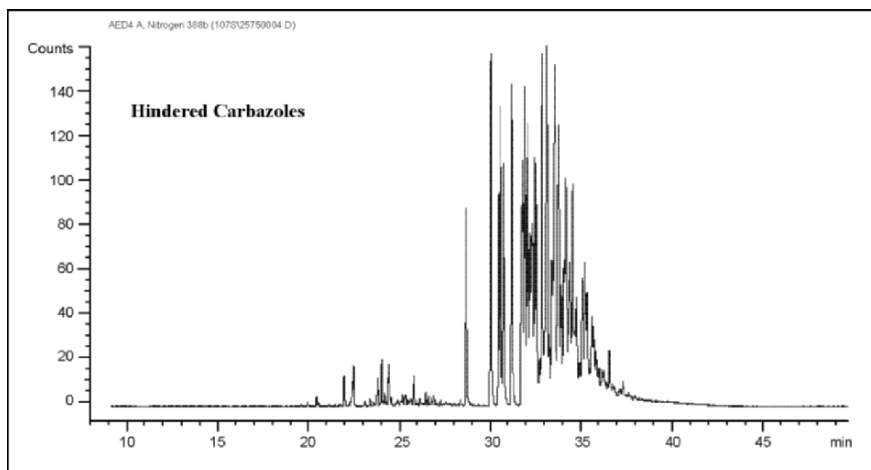


Figure 9. GC/AED Analysis of Hindered Carbazoles

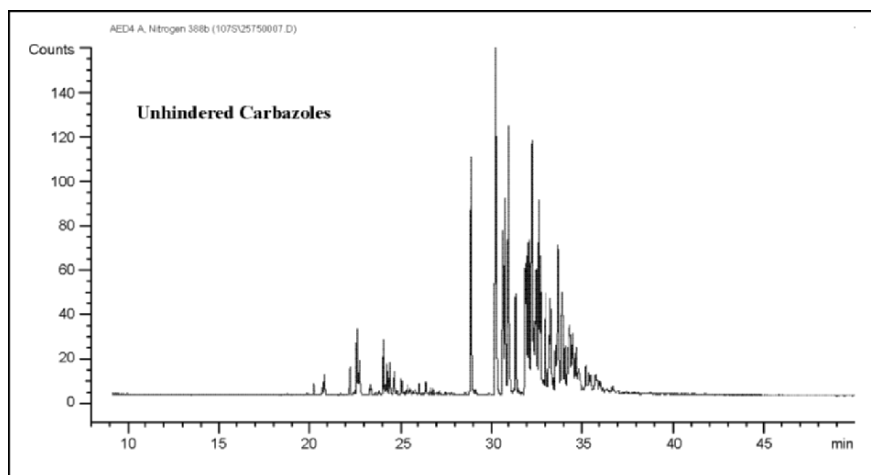


Figure 10. GC/AED Analysis of Unhindered Carbazoles

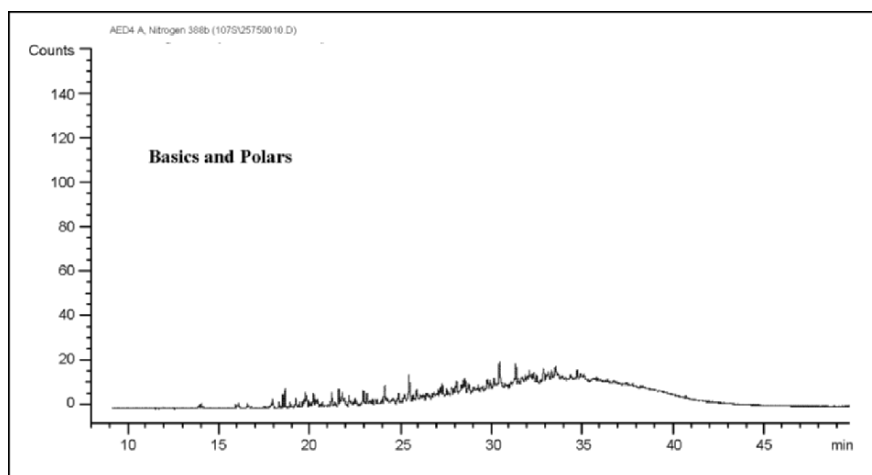


Figure 11. GC/AED Analysis of Basics and Polars

Table 3 summarizes the results. The data again confirm the observations made with model N-compound inhibitors<sup>9</sup> to the effect that basic compounds are by far the worst inhibitors and that in the absence of basic N-compounds, carbazoles are not serious inhibitors. Even though the hindered carbazoles were converted a little more slowly than the unhindered carbazoles, they both appeared to inhibit the refractory sulfur compounds to the same low degree.

Table 3. Effect of Added N-Compound Fractions on Hydrotreating Rates

|                          | Feed                |                 | Product                                   |   |   |
|--------------------------|---------------------|-----------------|---|---|---|
|                          | Composition of feed |                 | (340°C, 30 bar, TK-573)                   |   |   |
|                          | Total S<br>wt%      | Total N<br>wppm | LHSV=3 h <sup>-1</sup><br>Total S<br>wppm | LHSV=2 h <sup>-1</sup><br>Total S<br>wppm | LHSV=1 h <sup>-1</sup><br>Total S<br>wppm |
| No treatment             | 1.680               | 270             | 590                                       | 295                                       | 40  |
| SiO <sub>2</sub> treated | 1.668               | 5               | 160                                       | 60  | 7   |
| Hindered carbazoles      | 1.668               | 185             | 305                                       | 135                                       | 14  |
| Unhindered carbazoles    | 1.668               | 186             | 310                                       | 135                                       | 13  |
| Bases and polars         | 1.668               | 211             | 1380                                      | 880                                       | 400                                       |

### 3.4 Consequences for the Choice of Catalyst in Ultra Deep Desulfurization

Due to different reactivities towards removal of the inhibitors and the refractive sulfur molecules, a NiMo catalyst behaves differently than a CoMo catalyst. The NiMo catalyst does not become very active until almost all of the inhibitors have been removed, at this point it will become more active than a CoMo catalyst. NiMo catalysts are preferable to CoMo catalysts at high pressure and when the content of inhibitors (specific basic nitrogen compounds) is low. Furthermore, some of the first reaction steps via the hydrogenation route are equilibrium limited, which results in a lower reactivity (and low apparent activation energy), and at low pressures and high temperatures, a CoMo catalyst can therefore be a better choice than a NiMo catalyst.

Hydrogenation reactions such as aromatic saturation also proceed via the hydrogenation route and are inhibited by the same nitrogen compounds. If NiMo catalysts can be applied, more aromatic saturation occurs (compared with using CoMo catalysts) resulting in a greater improvement in cetane number and density, and a lower product PAH content. There will also be higher hydrogen consumption, which may have consequences for the hydrogen availability, hydrogen recycle rate and compression costs.

## 4. CASE STUDIES FOR THE PRODUCTION OF ULTRA LOW SULFUR DIESEL

As mentioned earlier, the refiner needs to decide whether the desired reduction in diesel sulfur content can be achieved by revamping an existing unit (e.g. adding more hydrotreating reactor capacity, revamping reactor internals, revamping the treat gas system, etc.) or whether it is necessary to build a grassroots unit. The decision will depend on many factors including the quality of feedstocks, the design criteria for the existing unit, and whether or not improvements of other diesel properties are required. The optimum solution with respect to overall investment and operating costs will depend on the correct choice of catalyst based on the considerations outlined above. To

illustrate how the required additional reactor volume depends on operating conditions and feedstock properties, we present four case studies below. The case studies also serve to illustrate the effects on other key parameters for diesel fuel quality that might be a result of tightening diesel fuel sulfur specifications, and the extent to which there is a need for more hydrogen.

The four cases are:

- **Case 1:** Hydrotreater producing 500 wppm sulfur operating at 32 bar hydrogen pressure on a low sulfur, straight-run feedstock.
- **Case 2:** Hydrotreater producing 500 wppm sulfur operating at 32 bar hydrogen pressure on a high sulfur, straight-run feedstock.
- **Case 3:** Hydrotreater producing 500 wppm sulfur operating at 32 bar hydrogen pressure on a high sulfur, blended feedstock containing 25% LCO and 75% straight-run feedstock.
- **Case 4:** Hydrotreater producing 500 wppm sulfur operating at 54 bar hydrogen pressure on a high sulfur, blended feedstock containing 25% LCO and 75% straight-run feedstock.

For each case, calculations have been made to estimate the incremental reactor volume needed to reach a 50 wppm, a 30 wppm and a 10 wppm sulfur specification, and key product properties have been estimated. The basis for the calculations and estimates is extensive testing performed in our laboratories at ultra deep desulfurization conditions.

#### 4.1 Case 1: Straight-run, Low Sulfur Feed at 32 bar

This case is based on straight-run low sulfur gas oil containing 0.2 wt% sulfur operating at a hydrogen partial pressure at the inlet of 32 bar. Feedstock properties are given in Table 4. The catalyst is TK-574, a high activity CoMo catalyst. Catalyst cycle length is fixed at 2½ years.

Table 4. Feed Properties for Straight-Run Low Sulfur Gas Oil

|   |           |
|---|-----------|
| Density, kg/m <sup>3</sup>                | 850       |
| Sulfur, wt%                               | 0.2       |
| ASTM D86, °C                              |           |
| 10 vol% / 50 vol%                         | 243 / 287 |
| 90 vol% / 95 vol%                         | 342 / 360 |
| Total aromatics content, wt%              | 25.5      |
| PAH content, wt%                          | 9.0       |
| Calculated cetane index (CCI), ASTM D4737 | 52.8      |

Table 5 shows the reactor volumes required to reach 50 wppm, 30 wppm and 10 wppm sulfur relative to the reactor volume required to reach 500 wppm, and the relative chemical hydrogen consumption. The table also shows changes in other key product properties.

Table 5. Relative Reactor Volume and Hydrogen Consumption and Product Properties (Case 1)

|   | Product S =<br>500 wppm | Product S =<br>50 wppm | Product S =<br>30 wppm | Product S =<br>10 wppm |
|---|-------------------------|------------------------|------------------------|------------------------|
| Relative reactor volume                   | 1.0                     | 2.0                    | 2.5                    | 3.3                    |
| Relative hydrogen consumption (SOR)       | 1.00                    | 1.02                   | 0.99                   | 0.98                   |
| <u>Product Properties at Start-of-Run</u> |                         |                        |                        |                        |
| PAH content, wt%                          | 2.7                     | 2.7                    | 3.0                    | 3.2                    |
| Density, kg/m <sup>3</sup>                | 844                     | 844                    | 844                    | 844                    |
| CCI, ASTM D4737                           | 54.7                    | 54.7                   | 54.7                   | 54.7                   |

a. SOR: start-of-run.

For Case 1, reducing the product sulfur content from 500 wppm to 50 wppm whilst maintaining cycle length requires a doubling of reactor volume, and further reduction from 50 wppm to 10 wppm requires the addition of approximately 65% more reactor volume. There is little or no change in other key product properties. The hydrogen consumption is very similar for all four cases.

Whether or not it is necessary to implement other changes (e.g. revamp of the recycle gas compressor to cope with the increased pressure drop over the reactor system) will depend on the equipment already in place.

In Case 1, a CoMo catalyst is the best choice at all product sulfur levels. For a feed having a higher sulfur content, and a similar level of nitrogen-containing inhibitors, there will be more sterically hindered sulfur compounds, and a higher degree of HDS is necessary to obtain 10-50 wppm product sulfur. In this situation, a NiMo catalyst might be preferred to a CoMo catalyst as illustrated in the following example.

## 4.2 Case 2: Straight-run, High Sulfur Feed at 32 bar

This case is based on straight-run high sulfur gas oil containing 1.2 wt% sulfur operating at a hydrogen partial pressure at the inlet of 32 bar. Feedstock properties are given in Table 6. For ease of comparison, only the sulfur content has been changed in relation to the feed used in Case 1. A comparison is made between TK-574, a CoMo catalyst, and TK-573, a NiMo catalyst. Catalyst cycle length is fixed at 2½ years.

Table 6. Feed Properties for Straight-Run High Sulfur Gas Oil

|   |         |
|---|---------|
| Density, kg/m <sup>3</sup>                | 850     |
| Sulfur, wt%                               | 1.2     |
| ASTM D86, °C                              |         |
| 10 vol% / 50 vol%                         | 243/287 |
| 90 vol% / 95 vol%                         | 342/360 |
| Total Aromatics Content, wt%              | 25.5    |
| PAH content, wt%                          | 9.0     |
| Calculated cetane index (CCI), ASTM D4737 | 52.8    |



Table 7 shows the reactor volumes required to reach 50 wppm and 10 wppm sulfur relative to the reactor volume required to reach 50 wppm on the CoMo catalyst, and the relative chemical hydrogen consumption. The table also shows changes in other key product properties.

*Table 7. Relative Reactor Volume and Hydrogen Consumption and Product Properties (Case 2)*

|  | Product S =<br>50 wppm<br>TK-574 | Product S =<br>10 wppm<br>TK-574 | Product S =<br>50 wppm<br>TK-573 | Product S =<br>10 wppm<br>TK-573 |
|--|----------------------------------|----------------------------------|----------------------------------|----------------------------------|
| Relative reactor volume                          | 1.0                              | 1.9                              | 0.85                             | 1.5                              |
| Relative hydrogen consumption (SOR) <sup>a</sup> | 1.00                             | 0.96                             | 1.27                             | 1.33                             |
| <u>Product Properties at Start-of-Run</u>        |                                  |                                  |                                  |                                  |
| PAH content, wt%                                 | 3.2                              | 3.8                              | 2.4                              | 2.9                              |
| Density, kg/m <sup>3</sup>                       | 841                              | 842                              | 839                              | 838                              |
| CCI, ASTM D4737                                  | 55.9                             | 55.7                             | 56.9                             | 57.2                             |

a. SOR: start-of-run.

For Case 2, reducing the product sulfur content from 50 wppm to 10 wppm whilst maintaining cycle length requires almost a doubling of reactor volume for the CoMo catalyst, and a 75% increase in reactor volume for the NiMo catalyst. The NiMo catalyst can remove the inhibitors to the hydrogenation route at the conditions needed to reach the two product sulfur levels, and as a result performs better than the CoMo catalyst. Similarly, the NiMo catalyst exhibits more hydrogenation, and this results in improved product properties with respect to PAH content, density and cetane index, and correspondingly higher hydrogen consumption.

### 4.3 Case 3: Blended, High Sulfur Feed at 32 bar

This case is based on a blend of 25% light cycle oil and 75% straight-run gas oil containing 1.5 wt% sulfur operating at a hydrogen partial pressure at the inlet of 32 bar. Feedstock properties are given in Table 8. The catalyst is TK-574, a high activity CoMo type catalyst. Catalyst cycle length is fixed at 2½ years.

*Table 8. Feed Properties for High Sulfur Blended Gas Oil*

|   |           |
|---|-----------|
| Density, kg/m <sup>3</sup>                | 870       |
| Sulfur, wt%                               | 1.5       |
| ASTM D86, °C                              |           |
| 10 vol% / 50 vol%                         | 243 / 287 |
| 90 vol% / 95 vol%                         | 342 / 360 |
| Total aromatics content, wt%              | 30.0      |
| PAH content, wt%                          | 14.0      |
| Calculated cetane index (CCI), ASTM D4737 | 45.1      |

Table 9 shows the reactor volumes required to reach 50 wppm, 30 wppm and 10 wppm sulfur relative to the reactor volume required to reach 500

wppm, and the relative chemical hydrogen consumption. The table also shows changes in other key product properties.

*Table 9. Relative Reactor Volume and Hydrogen Consumption and Product Properties (Case 3)*

|   | Product S =<br>500 wppm            | Product S =<br>50 wppm | Product S =<br>30 wppm | Product S =<br>10 wppm |
|---|------------------------------------|------------------------|------------------------|------------------------|
| Relative reactor volume                             | 1.0                                | 1.9                    | 2.3                    | 3.4                    |
| Relative hydrogen<br>Consumption (SOR) <sup>a</sup> | 1.0                                | 0.94                   | 0.93                   | 0.91                   |
| <u>Product Properties</u>                           |                                    |                        |                        |                        |
| PAH content, wt%                                    | 4.2 (SOR)<br>9.1(EOR) <sup>b</sup> | 5.6 (SOR)<br>8.5 (EOR) | 5.9 (SOR)<br>8.4 (EOR) | 6.3 (SOR)<br>8.3(EOR)  |
| Density, kg/m <sup>3</sup>                          | 855 (SOR)                          | 856 (SOR)              | 856 (SOR)              | 856 (SOR)              |
| CCI, ASTM D4737                                     | 49.2 (SOR)                         | 48.9 (SOR)             | 48.8(SOR)              | 48.7 (SOR)             |

a. SOR: start-of-run. b. EOR: end-of-run.

For Case 3, reducing the product sulfur content from 500 wppm to 50 wppm whilst maintaining cycle length requires almost a doubling of reactor volume, and further reduction from 50 wppm to 10 wppm requires the addition of approximately 80% more reactor volume.

The percentage increase is similar to Case 1, but the absolute reactor volumes are much higher (approximately 3 times) owing to the higher feed sulfur content and a higher proportion of sterically hindered sulfur compounds in the cracked material. The large additional volume required to meet the low product sulfur levels will result in an increase in pressure drop and may necessitate a revamp of the recycle gas system.

The low LHSV required at the lowest product sulfur levels may result in significant hydrocracking (to naphtha and gas), thereby reducing diesel yield. The additional cracking will probably also require additional investment in product fractionator overhead equipment.

The chemical hydrogen consumption is almost 2.5 times that of Case 1 due to the higher feed sulfur content. The hydrogen consumption is similar for all four product sulfur levels.

There is a deterioration in the other key product properties when the product sulfur level is lowered. Furthermore, the quality of the product with respect to the three properties shown in Table 6.2 deteriorates throughout the run as the temperature is increased to counteract catalyst deactivation. This is illustrated in Table 9 by comparing the PAH content at start-of-run (SOR) and end-of-run (EOR). The PAH content in all cases is very high at EOR, because the equilibrium between mono-ring aromatics and poly-ring aromatics becomes less favorable at the temperatures used at EOR. The PAH concentration affects product density and cetane index (and cetane number), and at EOR, the density will be higher in all three cases and the cetane index (and cetane number) will be lower.

#### 4.4 Case 4: Blended, High Sulfur Feed at 54 bar

This case is based on the same blend of 25% light cycle oil and 75% straight-run gas oil used in Case 3, but the unit operates at a hydrogen partial pressure at the inlet of 54 bar. The feedstock properties are the same as those given in Table 8. The CoMo catalyst, TK-574, is chosen for the 500 wppm product sulfur case, and the NiMo catalyst, TK-573, for all the low sulfur cases. Catalyst cycle length is fixed at 2½ years.

Table 10 shows the reactor volumes and chemical hydrogen consumption for the four product sulfur levels. *The reactor volumes are relative to the reactor volume required for Case 3, 500 wppm sulfur.* The table also shows changes in other key product properties.

Table 10. Relative Reactor Volume and Product Properties (Case 4)

|   | Product S =<br>500 wppm<br>TK-574 | Product S =<br>50 wppm<br>TK-573 | Product S =<br>30 wppm<br>TK-573 | Product S =<br>10 wppm<br>TK-573 |
|---|-----------------------------------|----------------------------------|----------------------------------|----------------------------------|
| Relative reactor volume                             | 0.65                              | 1.1                              | 1.25                             | 1.6                              |
| Relative hydrogen<br>Consumption (SOR) <sup>a</sup> | 1.15                              | 1.5                              | 1.65                             | 1.8                              |
| <b>Product properties</b>                           |                                   |                                  |                                  |                                  |
| PAH content, wt%                                    | 1.4 (SOR)                         | 1.8 (SOR)                        | 1.8 (SOR)                        | 2.1 (SOR)                        |
|   | 6.3 (EOR) <sup>b</sup>            | 5.9 (EOR)                        | 5.6 (EOR)                        | 5.3 (EOR)                        |
| Density, kg/m <sup>3</sup>                          | 853 (SOR)                         | 848 (SOR)                        | 845 (SOR)                        | 843 (SOR)                        |
| CCI, ASTM D4737                                     | 49.7 (SOR)                        | 51.6 (SOR)                       | 52.1 (SOR)                       | 52.5 (SOR)                       |

a. SOR: start-of-run. b. EOR: end-of-run.

For Case 4, reducing the product sulfur content from 500 wppm to 50 wppm whilst maintaining cycle length requires a 70% increase in reactor volume, and a further reduction from 50 wppm to 10 wppm requires the addition of approximately 45% more reactor volume. The percentage increase is less than that for Case 3, and the absolute increase in reactor volume is only 40% of that for Case 3.

The effect of pressure on the performance of TK-574 is seen by comparing the results for 500 wppm product sulfur in Tables 9 and 10. Increasing the pressure by almost 70% results in a reduction in required reactor volume by 35%. At the higher pressure, even the CoMo catalyst exhibits a higher hydrogenation activity as reflected in higher hydrogen consumption and improved product properties.

For the remaining product sulfur levels, the difference in required reactor volumes for Case 3 and Case 4 may be explained by the higher reactivity of the NiMo catalyst in Case 4. At the higher pressure in Case 4, the NiMo catalyst can remove the inhibiting species, enabling desulfurization of the sterically hindered DBTs via the (quicker) hydrogenation route.

The higher hydrogenation activity of the NiMo catalyst as compared with the CoMo catalyst is reflected in the key product properties of the three product sulfur levels. Although the diesel quality with respect to these

properties will deteriorate at EOR (for the same reason as given above), the extent of deterioration will be less because the aromatics equilibria are more favorable at the higher pressure in Case 4. This has been illustrated in Table 10 for the PAH content at both SOR and EOR.

The higher level of aromatics saturation obtained in Case 4 may be desirable, depending on future diesel specification requirements. It does, however, give higher operating costs due to higher chemical hydrogen consumption, especially for the low sulfur product levels. Higher hydrogen consumption results in a lower partial pressure of hydrogen at the reactor outlet, adversely affecting the rate of catalyst deactivation and the key product properties. It is therefore necessary to increase the recycle gas to oil ratio in order to maintain outlet hydrogen partial pressure, and this will very often require revamp of the recycle gas system.

Yield loss due to cracking is less at the higher space velocities used in Case 4 than in Case 3, and is furthermore countered by volume swell due to a higher hydrogen addition.

#### 4.5 Revamp vs. Grassroots Unit

Case 3 and 4 can be used to illustrate the considerations involved when deciding between revamping a unit or building a grassroots unit. Take the case of an European refiner who has a unit producing a diesel with 500 wppm sulfur at 32 bar hydrogen partial pressure using the feed shown in Table 8. The refiner is faced with having to meet 50 wppm sulfur in 2005, and 10 wppm sulfur by 2009 at the latest. Should the refiner choose to revamp the existing unit by adding additional reactor volume, i.e. Case 3, or build a new grassroots unit operating at higher pressure, i.e. Case 4?

If the only consideration is to reduce sulfur, the preferred solution would probably be to add reactor volume as in Case 3, but this assumes that the existing gas recycle system can manage the increased pressure drop and that the diesel yield loss due to cracking is acceptable. It may be necessary to revamp the recycle gas system and the overhead fractionator. In many cases, the performance of the existing reactor can also be improved by installing state-of-the-art liquid distribution trays and quench mixers.<sup>12-14</sup>

If PAH content, density or cetane number are also important, the refiner may choose to build a new high pressure unit to meet the 50 wppm product sulfur level, i.e. the Case 4 solution. This involves more costly investments and the intelligent use of existing equipment may help reduce overall costs.<sup>15</sup> In this case, incremental investment to meet the 10 wppm sulfur specification in 2009 will be lower.

## 5. CONCLUSION

Refiners will need to invest heavily in hydrotreating units as legislation for ultra low sulfur diesel fuel is adopted. For optimum design in which the cost of new units is kept to a minimum and the best use is made of existing equipment, it is necessary to have a deep understanding of the factors governing the removal of the most refractive compounds in diesel fuels. This chapter outlines how the identification of the compounds present in diesel feedstocks that inhibit the removal of the most refractive sulfur compounds can be used to define the correct choice of catalyst for a given service. The choice of catalyst also affects other key diesel properties such as density, PAH content and cetane index, as well as hydrogen consumption and the required treat gas/oil ratio.

## 6. REFERENCES

1. <http://www.bp.com/worldenergy/oil/index.htm>
2. International Energy Outlook, March 2002, [www.eia.doe.gov/oiaf/ieo/index.html](http://www.eia.doe.gov/oiaf/ieo/index.html)
3. Purvin; Gertz, Hart's 4<sup>th</sup> Annual World Fuel Conference, Brussels, May 19-21, 1999
4. Mochida, I.; Sakanishi, K.; Ma, X.; Nagao, S.; Isoda, T., *Catal. Today*, **1996**, *29*, 185.
5. Whitehurst, D.D.; Isoda, I.; Mochida, I., *Adv. Catal.*, **1998**, *42*, 343.
6. Knudsen, K.G.; Ovesen, C.V.; Nielsen, I.V.; Andersen, K., *JECAT '97*, Nov. 25-28, 1997, Tsukuba, Japan.
7. Knudsen, K.G.; Topsøe, H.; Cooper, B. H., *Appl. Catal. A*, **1999**, *189*, 205-215.
8. Whitehurst, D.D.; Knudsen, K.G.; Nielsen, I.V.; Wiwel, P.; Zeuthen, P., *Prepr. Am. Chem. Soc. Div. Petr. Chem.*, **2000**, *45(4)*, 692.
9. Wiwel, P.; Knudsen, K.G.; Zeuthen, P.; Whitehurst, D.D., *I&E Proc. Res.*, in press.
10. Knudsen, K.G.; Whitehurst, D.D.; Zeuthen, P., A detailed understanding of the inhibition effect of organic nitrogen compounds for ultra deep HDS and the consequences for the choice of catalyst, Presented at the AIChE Spring National Meeting, Atlanta, GA, March 5-9, 2000
11. Whitehurst, D.D.; Knudsen, K.G.; Wiwel, P.; Zeuthen, P., *Prepr. Am. Chem. Soc. Div. Petr. Chem.*, **2000**, *45(2)*, 367.
12. Bingham, F.E.; Müller, M.; Christensen, P.; Moyse, B.M., Performance Focused Reactor Design to Maximise Benefits of High Activity Hydrotreating Catalysts, ERTC Conference, London, Nov. 17-19, 1997.
13. Yearly, D.; Wrisberg, J.; Moyse, B.M., Revamp of Low Sulfur Diesel: A Case Study, NPRA Annual Meeting, March 16-18, 1997, Paper AM-97-14.
14. Bingham, F.E.; Chan, E.; Mankowski, T.; Hubbard, P., Improved Reactor Internals for Syncrude's HGO Hydrotreaters, NPRA Annual Meeting, March 26-28, 2000, Paper AM-00-19.
15. Bingham, F.E.; Christensen, P., Revamping HDS Units to Meet High Quality Diesel Specifications, Asian Refinery Technology Conference, March 8-10, 2000, Kuala Lumpur, Malaysia.

## Chapter 11

# **ULTRA-CLEAN DIESEL FUELS BY DEEP DESULFURIZATION AND DEEP DEAROMATIZATION OF MIDDLE DISTILLATES**

Chunshan Song\* and Xiaoliang Ma  
*Department of Energy & Geo-Environmental Engineering  
The Pennsylvania State University  
University Park, PA 16802, USA*

### **1. INTRODUCTION**

Increasing attention worldwide is being paid to chemistry of diesel fuel processing. This heightened interest is related to both the thermal efficiency and the environmental aspects, which include both the pollutants and greenhouse gas emissions. Clean fuels research including desulfurization and dearomatization has become an important subject of environmental catalysis studies worldwide. The U.S. Clean Air Act Amendments of 1990 and new regulations by the U.S. EPA and government regulations in many countries call for the production and use of more environmentally friendly transportation fuels with lower contents of sulfur and aromatics.<sup>1-4</sup> In the mean time, the demand for transportation fuels has been increasing in most countries for the past two decades. According to a recent analysis, diesel fuel demand is expected to increase significantly in the early part of the 21st century and both the U.S. and Europe will be increasingly short of this product.<sup>5</sup> Sulfur content in diesel fuel is an environmental concern because, upon combustion, sulfur is converted to SO<sub>x</sub> during combustion which not only contributes to acid rain, but also poisons the catalytic converter for exhaust emission treatment.

Sulfur content is usually expressed as the weight percent (wt %) of sulfur in the fuel, since there are many different sulfur-containing compounds in petroleum-derived fuels. Dramatic changes occurred in many countries concerning diesel sulfur regulations in the past decade.<sup>6</sup> The maximum sulfur

content of highway diesel fuel in the U.S. was reduced by regulations, from about 0.20-0.50 wt% in late 1980s<sup>7-8</sup>, to 0.05 wt% on October 1, 1993 for all highway (on-road) diesel fuels<sup>3</sup>. The sulfur content of diesel fuel in Western Europe was limited to 0.3 wt% in 1989, to 0.2 wt% in 1994, and further reduced to 0.05 wt% from October 1, 1996. The diesel sulfur content in Japan was reduced by regulation from 0.4 wt% to  $\leq 0.2$  wt% in 1993, and further to  $\leq 0.05$  wt% in 1997. Canadian government regulations required all diesel fuels sold must contain no more than 0.05 wt% sulfur since January 1998.

Tables 1 and 2 show the current US EPA regulations for gasoline<sup>9-11</sup> and diesel fuels<sup>11-13</sup>, including non-road diesel fuels<sup>14</sup>, respectively, along with earlier fuel specification data in the US for comparison<sup>15-17</sup>. Currently the fuel specifications for all highway diesel fuels in the U.S., Japan, and Western Europe limit the sulfur content of the diesel fuels to less than 0.05 wt% or 500 parts per million by weight of sulfur (ppmw). The new government regulations in many countries will further lower the contents of sulfur and aromatics in the year 2004-2007.<sup>12</sup> In January 2001, the U.S. EPA announced new rules that will require a 97% reduction in sulfur content of highway diesel fuel to 15 ppmw from current 500 ppmw, starting from June 2006<sup>18</sup>. New gasoline sulfur regulations will require most refiners to meet a 30 ppmw sulfur average with an 80 ppmw cap for both conventional and reformulated gasoline by January 1, 2006.<sup>9-10</sup>

Table 1. US EPA Tier II Gasoline Sulfur Regulations as of 2002

| Category                | Year                           |  |                   |                   |                   |
|-------------------------|--------------------------------|--|-------------------|-------------------|-------------------|
|                         | 1988 <sup>a</sup>              | 1995 <sup>b</sup>  | 2004 <sup>c</sup> | 2005 <sup>c</sup> | 2006 <sup>c</sup> |
| Compliance as of year   |                                |  |                   |                   |                   |
| Refinery average, ppmw  | 1000 <sup>a</sup><br>(maximum) | 330 <sup>b</sup><br>( $<330$ ppm S and $<29.2\%$ aromatics required for national certification; $< 850$ ppm S and $<41.2\%$ aromatics as national maximum) | --                | 30                | 30                |
| Corporate average, ppmw |                                |  | 120               | 90                | --                |
| Per gallon cap, ppmw    |                                |  | 300               | 300               | 80                |

Source: (a) SAE, Automotive Gasoline - SAE J312 Oct88, Society of Automotive Engineers, Warrendale, PA, February, 1992; (b) K. Owen, and T. Coley, Automotive Fuels Reference Book, 2<sup>nd</sup> Ed., Society of Automotive Engineers, Warrendale, PA, 1995; (C) US EPA, 2001.

Table 2. US EPA Sulfur Regulations for Diesel and Jet Fuels as of April 2003

| Category              | Year  |   |  |   |
|-----------------------|---|---|--|---|
|                       | 1989 <sup>a</sup>   | 1993 <sup>b</sup>                       | 2006 <sup>b</sup>  | 2010 <sup>b</sup>                                     |
| Compliance as of year |   |   |  |   |
| Highway diesel, ppmw  | 5000 <sup>a</sup><br>(Maximum for No. 1-D & 2-D, with minimum cetane No. of 40) | 500<br>(Current upper limit since 1993) | 15<br>(Regulated in 2001; exclude some small refineries) | 15<br>(Regulated in 2001; apply to all US refineries) |
| Nonroad diesel, ppmw  | 20000 <sup>a</sup>  | 5000<br>(Current upper limit)           | 500<br>(Proposed in 2003 for 2007)                       | 15<br>(Proposed in 2003 for 2010)                     |
| Jet fuel, ppmw        | 3000  | 3000                                    | ?  | ?   |

Source: (a) SAE, Diesel Fuels - SAE J313 Jun89, Society of Automotive Engineers, Warrendale, PA, February, 1992; (b) US EPA, 2003.

More recently, the EPA has announced plan to reduce non-road diesel fuel sulfur from the current average of 3400 ppm to 500 ppm by 2007 and further to 15 ppm by 2010<sup>14</sup>. The U.S. Clean Air Act Amendments of 1990 and related new fuel regulations by the U.S. EPA and government regulations in many countries call for the production and use of more environmentally friendly transportation fuels with lower contents of sulfur and aromatics.

Table 3 shows the average properties of crude oils refined in the US during 1981-2001, along with the US and worldwide petroleum consumption during 1981-2001, based on published statistic data.<sup>19-23</sup> The demand for transportation fuels has been increasing in most countries for the past three decades. The total world petroleum consumption increased from 49.42 million barrels per day (MBPD) in 1971 to 77.12 MBPD in 2001, representing a 56% increase [EIA/IEA, 2002]. The total US consumption of petroleum products reached 19.59 MBPD in 2001, about a 39 % increase from 1971 (14.11 MBPD).<sup>19</sup> Of the petroleum products consumed in the US in 2001, 8.59 MBPD was supplied as motor gasoline, 3.82 MBPD as distillate fuels, including 2.56 MBPD as highway diesel fuels and 1.26 MBPD as off-road fuels and industrial fuels, 1.65 MBPD as jet fuel, 0.93 MBPD as residual fuel oil, and 1.13 MBPD as liquefied petroleum gas (LPG), and 3.47 MBPD for other uses in the US.<sup>19</sup>

The problem of deep removal of sulfur has become more serious due to the lower and lower limit of sulfur content in finished gasoline and diesel fuel products by regulatory specifications, and the higher and higher sulfur contents in the crude oils. A survey of the data on crude oil sulfur content and API gravity for the past two decades reveals a trend that U.S. refining crude slates continue towards higher sulfur contents and heavier feeds. The average sulfur contents of all the crude oils refined in the five regions of the U.S. known as the five Petroleum Administration for Defense Districts (PADDs) increased from 0.89 wt% in 1981 to 1.42 wt% in 2001, while the corresponding API gravity decreased from 33.74 °API in 1981 to 30.49 °API



in 2001.<sup>21-23</sup> In the past 2 decades, average sulfur contents in crude oils refined in the US increased by 265 ppm/year and API gravity decreased by 0.16 °API/year, while the total crude oil refined in US refineries increased from 12.47 MBPD in 1981 (11.20 MBPD in 1971) to 15.13 MBPD in 2001.<sup>19</sup>

*Table 3. Average Properties of Crude Oils Refined in the US During 1981-2001 and US and World Petroleum Consumption During 1981-2001*

| Property  | Year  |       |       |
|---|-------|-------|-------|
|   | 1981  | 1991  | 2001  |
| Total amounts of crude oils refined in US, million barrel per day   | 12.47 | 13.30 | 15.13 |
| Average sulfur content of crude oils refined in US, wt% based on sulfur                                   | 0.89  | 1.13  | 1.42  |
| API gravity of crude oils refined in US, °API   | 33.74 | 31.64 | 30.49 |
| Total petroleum products supplied in the US including imported crude and products, million barrel per day | 16.06 | 16.71 | 19.59 |
| Total worldwide petroleum consumption, million barrel per day   | 60.90 | 66.72 | 77.12 |

The crude oils refined in the US tend to have higher sulfur contents than those in the Western Europe. For example, the average crude oil feeds to US refineries in 2000 have 1.35 wt% sulfur and 31.0° API gravity, whereas European refinery feed by comparison was sweeter at 1 wt% sulfur and 35 ° API gravity.<sup>24</sup> The total world consumption of refined petroleum product in 2000 was 76.896 MBPD, in which the consumptions in the US and Western Europe were 19.701 and 14.702 MBPD, respectively. The problem for diesel desulfurization is also somewhat more serious in the US because a higher proportion of light cycle oil from FCC is used in the diesel pool in the US, which has higher contents of more refractory sulfur compounds (see below). H<sub>2</sub> demand increase is another challenge to the refinery operations. Hydrogen deficits are processing restraints and will impact future hydrotreating capabilities and decisions.<sup>25</sup>

The heightened interests in ultra-clean fuels are also due to the need for using new emission control technologies for IC engines (especially those for diesel fuels), and for using on-board or on-site reforming of hydrocarbon fuels for fuel cells. Our studies on clean fuels have focused on deep desulfurization and dearomatization of diesel and jet fuels as well as gasoline<sup>26-36</sup>. One new application area which presents a great challenge to ultra-deeper desulfurization of liquid hydrocarbon fuels is the hydrocarbon fuel processor for proton-exchange membrane fuel cells, which require essentially zero-sulfur fuels such as gasoline and diesel fuels<sup>26,27,30,37</sup>. The general chemistry of diesel fuels is covered in a recent book<sup>33</sup>. This Chapter is a selective overview on new design approaches and associated catalysis and chemistry as well as processes for deep desulfurization and deep hydrogenation of hydrocarbon fuels, particularly diesel fuels.

## 2. SULFUR COMPOUNDS IN TRANSPORTATION FUELS

There are three major types of transportation fuels: gasoline, diesel and jet fuels that differ in composition and properties. The common types of sulfur compounds in liquid fuels are listed below.

- Gasoline Range: Naphtha, FCC-naphtha (Selective HDS)
  - Mercaptanes RSH; Sulfides R<sub>2</sub>S; Disulfides RSSR
  - Thiophene and its alkylated derivatives
  - Benzothiophene
- Jet Fuel Range: Heavy naphtha, Middle distillate
  - Benzothiophene (BT) and its alkylated derivatives
- Diesel Fuel Range: Middle distillate, Light cycle oil
  - alkylated benzothiophenes
  - Dibenzothiophene (DBT) and its alkylated derivatives
- Boiler Fuels Feeds: Heavy oils and distillation residues
  - ≥3-ring Polycyclic sulfur compounds, including DBT, benzonaphthothiophene (BNT), phenanthro[4,5-b,c,d]thiophene (PT) and their alkylated derivatives

Table 4. Volume Fraction of U.S. Highway Diesel Pool from Each Feedstock Component

| Diesel Blendstock          | % of U.S. Highway Diesel Fuel Pool per Blendstock Boiling Fraction |                  |                  |               |                                |
|----------------------------|--|------------------|------------------|---------------|--------------------------------|
|                            | Naphtha  | Light Distillate | Heavy Distillate | Light Gas Oil | All Boiling Fractions Combined |
| Straight Run               | 0.1  | 6.4              | 4.9              | 1.0           | 12.4                           |
| Hydrotreated Straight Run  | 0.3  | 8.1              | 41.2             | 2.3           | 51.9                           |
| Cracked Stock              | -  | 0.1              | 0.8              | 2.2           | 3.1                            |
| Hydrotreated Cracked Stock | -  | 2.1              | 15.6             | 1.7           | 19.4                           |
| Coker Gas Oil              | -  | -                | 1.0              | -             | 1.0                            |
| Hydrotreated Coker Gas Oil | 0.1  | 2.1              | 3.7              | 2.3           | 8.2                            |
| Hydrocrackate              | -  | 1.3              | 2.7              | -             | 4.0                            |

Source: EPA, EPA420-R-00-026, 2000.

Table 4 shows the volume fraction of U.S. highway diesel pool, and Table 5 shows the corresponding sulfur levels of U.S. highway diesel blendstocks<sup>12</sup>. Among the diesel blendstocks, the light cycle oil (LCO) from fluid catalytic cracking (FCC) contains highest amount of sulfur and aromatics, and the LCO also tends to have the highest contents of refractory sulfur compounds, especially 4-methyldibenzothiophene (4-MDBT) and 4,6-dimetyldibenzothiophene (4,6-DMDBT)<sup>12</sup>.

Table 5. Sulfur Levels of U.S. Highway Diesel Blendstocks (CA Excluded)

| Diesel Blendstock          | Sulfur Content (ppmw) by Boiling Fraction |                  |                  |                   |                                |
|----------------------------|---|------------------|------------------|-------------------|--------------------------------|
|                            | Naphtha                                   | Light Distillate | Heavy Distillate | Light Gas Oil     | All Boiling Fractions Combined |
| Straight Run               | 827                                       | 1770             | 2269             | 4980              | 2218                           |
| Hydrotreated straight Run  | 362                                       | 119              | 394              | 548               | 358                            |
| Cracked Stock              | -   | 2219             | 2892             | 6347 <sup>c</sup> | 5322                           |
| Hydrotreated Cracked Stock | 18  | 37               | 939              | 1306 <sup>c</sup> | 874                            |
| Coker Gas Oil              | 540                                       | 1800             | 3419             | -                 | 3419 (?)                       |
| Hydrotreated Coker Gas Oil | 8   | 25               | 310              | 400               | 258                            |
| Hydrocrackate              | -   | 12               | 120              | -                 | 85                             |

C: Indicating properties that were not reported in the refiner survey. These values were calculated by EPA using the reported sulfur contents of like boiling fractions in other diesel blendstocks by assuming the same relative sulfur levels between boiling fractions. Source: EPA, EPA420-R-00-026, 2000.

There are various 2-ring and 3-ring sulfur compounds in middle distillates from various refinery streams that can be used to make middle distillate fuels—diesel fuels and jet fuels. Kabe and coworkers have analyzed the sulfur compounds in a light gas oil and hydrotreated gas oils using gas-chromatography with atomic emission detector (GC-AED) and GC-mass spectrometer (GC-MS)<sup>38-39</sup>. They identified 42 alkylated benzothiophene compounds and 29 alkylated dibenzothiophene compounds in the oil. Among them the 4,6-DMDBT was found to remain even after deep hydrodesulfurization<sup>38,40</sup>. Ma et al. have analyzed the sulfur compounds in a gas oil and a non-polar fraction of vacuum gas oil<sup>41-43</sup>. They found that the major sulfur compounds are alkyl benzothiophenes in the gas oil, and alkyl thiophenes, alkyl benzothiophenes, alkyl DBT, alkyl BNT and alkyl PT in the vacuum gas oil. The dibenzothiophenes with two alkyl substituents at 4- and 6-positions, respectively, were found to be the most difficult to remove from the oils. Hsu and coworkers have performed mass spectrometric analysis of many diesel fuels and petroleum fractions<sup>44,45</sup>. They have identified not only the major compounds in all classes, but also trace amounts of heteroatom-containing compounds. Trace amounts of nitrogen compounds in diesel fuels include indoles, carbazoles, quinolines, acridines, and phenanthridines. The oxygen compounds include alkylated phenols and dibenzofurans. Formulated diesel fuels also contain trace amounts of additives.

Figure 1 shows the GC-FPD chromatograms of the three transportation fuel samples analyzed in our laboratory.<sup>26,27</sup> For obtaining the results in Figure 1, we have conducted a detailed analysis to identify the type of sulfur compounds and their alkylated isomers in a commercial gasoline sample and a commercial diesel fuel sample, which were purchased in 2001 from a local fuel station in State College, Pennsylvania, and a JP-8 type jet fuel sample from

Wright Laboratory of US Air Force. The identification of different alkylated polycyclic sulfur compounds and their isomers is complicated, since there are few commercially available standards and their mass spectra (e.g., fragmentation patterns) are often similar for most isomers of alkyl thiophenic compounds. In our group, we did the identification of the sulfur components in the gasoline, jet fuel and diesel fuel based on a combination of various techniques, standard sample, HPLC separation<sup>43</sup>, sulfur-selective ligand exchange chromatography<sup>43</sup>, GC-MS<sup>41,43</sup>, retention time comparison with the literature data<sup>46,47</sup>, reactivities of various sulfur compounds in HDS<sup>41,42</sup> and understanding of the elution order of the isomers<sup>48</sup>.

As shown in Figure 1, the major sulfur compounds existing in the commercial gasoline are thiophene, 2-methylthiophene, 3-methylthiophene, 2,4-dimethylthiophene and benzothiophenes, indicating that most sulfur compounds with higher HDS reactivity, including thiols (mercaptanes), disulfides and sulfides, have been removed in current processes for making the commercial gasoline. The major sulfur compounds in the commercial and military jet fuel JP-8 are dimethylthiophenes and trimethylthiophenes with two methyl groups at the 2- and 3-positions, respectively, implying that these alkyl benzothiophenes are more difficult to be removed than their isomers. No alkyldibenzothiophenes were detected in the JP-8. The sulfur compounds in the commercial diesel fuel include alkyl benzothiophenes and alkyl dibenzothiophenes, but the major sulfur compounds are the alkyl dibenzothiophenes with alkyl groups at the 4- or/and 6-positions, indicating that the major sulfur compounds remaining in the commercial diesel fuel are the refractory sulfur compounds, which are difficult to be removed by the conventional HDS process.

Figure 1 also clearly demonstrates that sulfur compounds tend to become larger in ring size and higher in number of substitutes as the fuel becomes higher in boiling point ranges from gasoline to jet fuels to diesel fuels. The current sulfur contents in highway (on-road automotive) diesel fuel and gasoline are limited to 500 ppm and 350 ppmw, respectively, by regulations in the U.S. The jet fuel sulfur is limited to 3000 ppmw. The sulfur content of off-road diesel fuels is limited to 2000 to 3000 ppmw. The real sulfur contents in commercially available gasoline and diesel fuel samples are typically lower than the regulatory upper limits. This statement applies to commercial and military jet fuels as well. The average content of sulfur in typical jet fuels was reported to be 490 ppmw.<sup>49</sup>

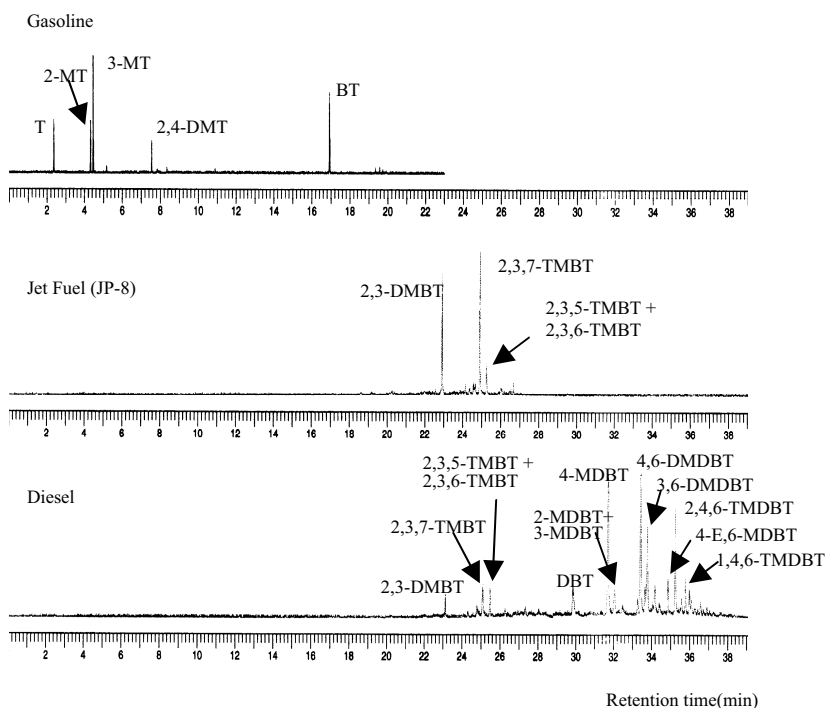


Figure 1. GC-FPD Chromatograms of Commercial Gasoline, Jet Fuel and Diesel

### 3. CHALLENGES OF ULTRA DEEP DESULFURIZATION OF DIESEL FUELS

#### 3.1 Reactivities of Sulfur Compounds in HDS

Figure 2 shows the qualitative relationship between reactivities of sulfur compounds and their ring size and substitution patterns. It covers the gasoline, jet fuel and diesel fuel ranges. Figure 2 illustrates that there are major differences in reactivity of sulfur compounds depending on both their ring size and substitution pattern. In particular, differences in the position of alkyl groups on benzothiophene and on dibenzothiophene can have major impacts on their reactivity due to steric hindrance. The organic sulfur compounds present in petroleum vary widely in their reactivities in catalytic hydrodesulfurization. Deeper hydrodesulfurization (HDS) is not a simple increase in conversion of total sulfur compounds by a pseudo first order. There are many different sulfur compounds in diesel fuels. Earlier research has shown that certain sulfur compounds are easier to convert. The reactivities

of the 1- to 3-ring sulfur compounds decrease in the order of thiophenes > benzothiophenes > dibenzothiophenes<sup>50-54</sup>. In naphtha, thiophene is so much less reactive than the thiols, sulfides, and disulfides that the latter can be considered to be virtually infinitely reactive in practical high-conversion processes<sup>55,56</sup>.

Figure 3 shows the GC-FPD chromatograms that illustrate reactivities of various sulfur compounds in gas oil HDS for diesel fuel production. In deep HDS, the conversion of these key substituted dibenzothiophenes largely determines the required conditions. In gas oils, the reactivities of (alkyl-substituted) 4-methyldibenzothiophene and 4,6-dimethyldibenzothiophene are much lower than those of other sulfur-containing compounds<sup>38,41,56,57</sup>. Gates and Topsoe<sup>56</sup> pointed out in 1997 that 4-methyldibenzothiophene and 4,6-dimethyldibenzothiophene are the most appropriate compounds for investigations of candidate catalysts and reaction mechanisms.

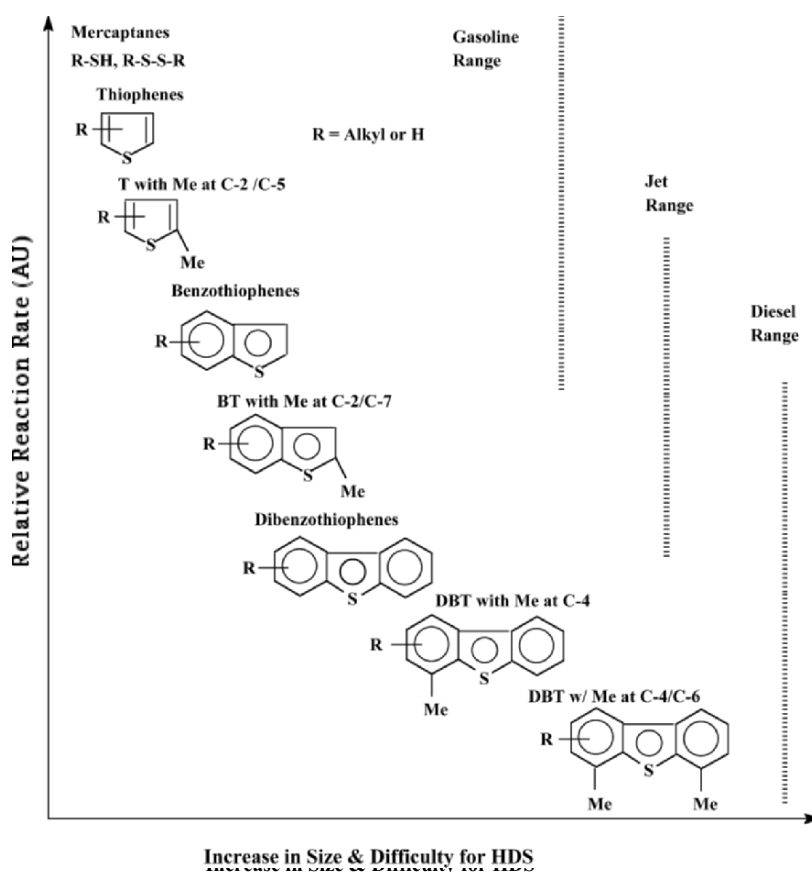


Figure 2. Dependence of reactivity of sulfur compounds vs their ring size and substitution patterns (for sulfur compounds in gasoline, jet fuel and diesel fuel feedstock)<sup>37</sup>.

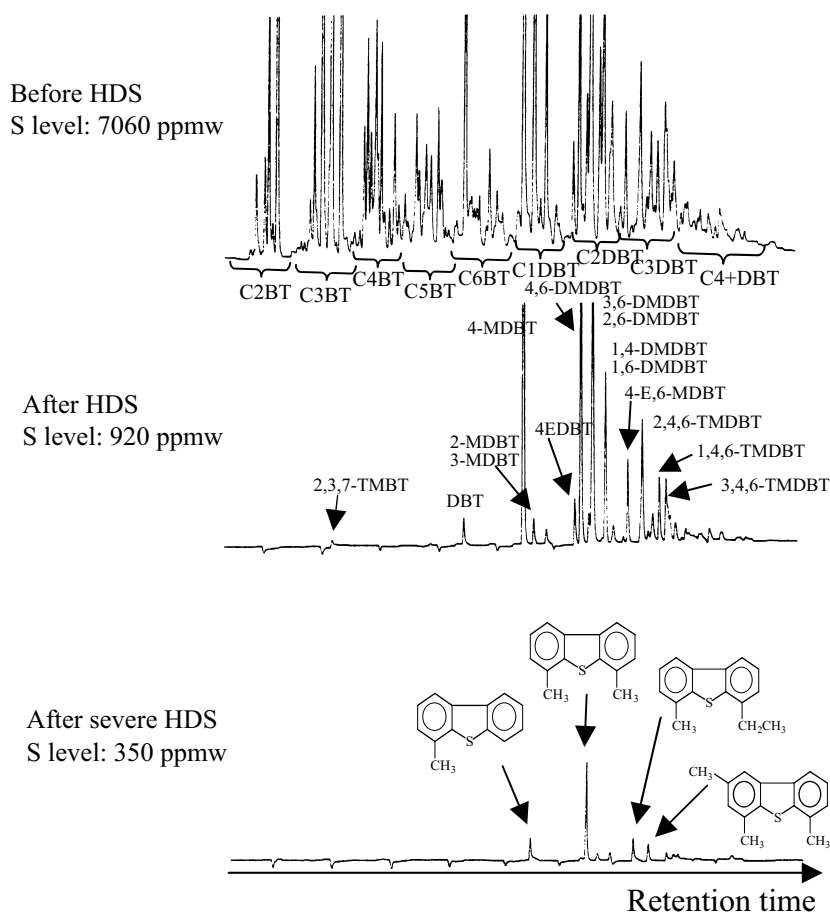


Figure 3. GC-FPD Chromatograms showing Reactivities of Various Sulfur Compounds in Gas Oil in HDS<sup>181</sup>

While the new regulation will further reduce the environmental impact of diesel emissions, it creates a major technical challenge for fuel processing<sup>58,59</sup>. It is the most refractory sulfur species that remains in the diesel fuel after the sulfur reduction to 500 ppmw level by conventional hydrodesulfurization<sup>38,41,42,56,57,60,61</sup>. For desulfurization of sulfur species in it gasoline, is not difficult to remove the sulfur compounds in the naphtha range by current catalytic HDS processes. For the U.S. refineries, most sulfur in the gasoline pool is found in FCC naphtha. The challenge in deep desulfurization of FCC naphtha is selective conversion of sulfur compounds without saturation of olefinic compounds, which contribute to octane number enhancement. For straight run kerosene that is used for making jet fuels, the sulfur removal by HDS is

more difficult than that from naphtha, but less difficult compared to that from gas oil.

Recently, investigations have demonstrated that sulfur compounds remaining in diesel fuels at sulfur levels lower than 500 ppm are the dibenzothiophenes (DBTs) with alkyl substituents at the 4- and/or 6-position, and are lower in HDS reactivity<sup>38,41,42,56,62</sup>. These species are termed refractory sulfur compounds. Both steric hindrance and electronic factors are responsible for the observed low reactivity of 4- and 6-substituted DBTs<sup>63,64</sup>.

Based on recent studies on gas oil HDS<sup>41,57</sup>, the sulfur compounds can be classified into four groups according to their HDS reactivities that were described by the pseudo-first-order rate constants. The first group is dominantly alkyl BTs; the second, DBT and alkyl DBTs without alkyl substituents at the 4- and 6-positions; the third, alkyl DBTs with only one alkyl substituent at either the 4- or 6-position; the fourth, alkyl substituents at the 4- and 6- positions (as shown in Scheme 1). The sulfur distribution of the four groups in the gas oil is 39, 20, 26 and 15 wt %, respectively, and the relative rate constant of HDS for each of the four groups is 36, 8, 3, and 1, respectively<sup>41,57</sup>.

Figure 4 shows the relative reactor volume requirements for various degrees of sulfur removal by conventional single-stage HDS of diesel fuels. The estimation of volume requirements is based on the results from HDS kinetics studies using a commercial Co-Mo/Al<sub>2</sub>O<sub>3</sub> catalyst 41, assuming 1.0 wt% S in feed. When the total sulfur content is reduced to 500 ppmw, the sulfur compounds remaining in the hydrotreated oil are the third and fourth group sulfur compounds. When the total sulfur content is reduced to 30 ppmw, the sulfur compounds remaining in the hydrotreated oil are only the fourth group sulfur compounds, indicating that the less the sulfur content is the lower the HDS reactivity, which has been discussed by Whitehurst et al. in their review<sup>60</sup>. More recent studies using various straight-run gas oils from different crude oils confirmed the differences in reactivity between different sulfur compounds<sup>65,66</sup>.

To put these problems into perspective based on conventional approaches for HDS of diesel fuels, for reducing the sulfur level from current 500 ppmw to 15 ppmw (the regulation in 2006) by conventional HDS processing, the volume of catalyst bed will need to be increased by 3.2 times as that of the current HDS catalyst bed. This is consistent in general with the analysis on a typical Co-Mo catalyst by Haldor Topsøe regarding the required increase in catalyst activity and bed temperature for further reduction of sulfur from 500 to 50 ppmw<sup>61,67</sup>. Furthermore, as shown in Figure 3, for reducing the sulfur level to 0.1 ppmw by conventional HDS process for fuel cell applications, the volume of catalyst bed will need to be increased by about 7 times. Increasing the volume of the high-temperature and high-pressure reactor is very expensive. In another scenario, with current commercial HDS processes



without changing the reactor volume the catalyst activity will have to be increased by a factor of 3.2 and 7 to meet the new regulation and fuel cell applications, respectively. It is difficult to meet such a demand by making small incremental improvements in the existing hydrotreating catalysts that have been developed during the last 50 years.

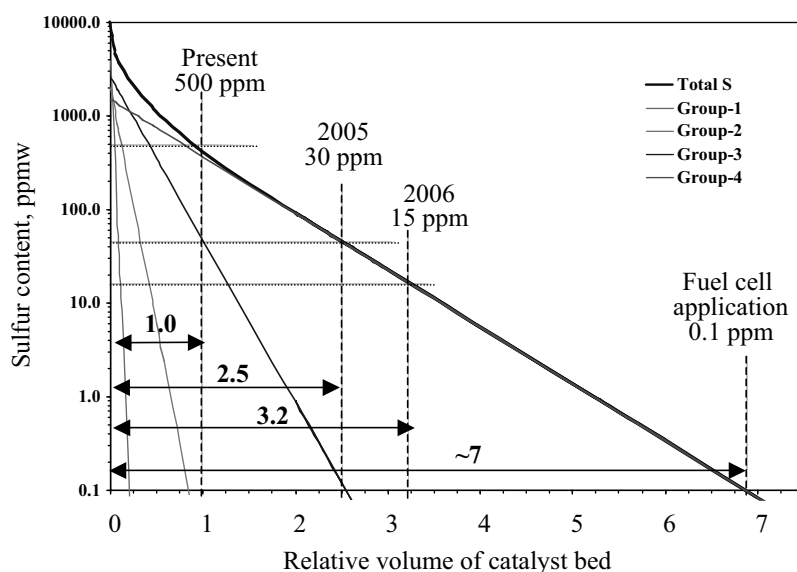


Figure 4. Simulated HDS of diesel to meet 15 and 0.1 ppm level on the basis of a conventional single-stage reactor, assuming 1.0 wt% S in feed; HDS kinetic model:  $C_{S, total} = C_{S10} e^{-k1t} + C_{S20} e^{-k2t} + C_{S30} e^{-k3t} + C_{S40} e^{-k4t}$

The NPRA (National Petroleum Refiners Association) estimates that imposing a 15-ppmw sulfur maximum on diesel could result in a 10% to 20% shortfall in supply<sup>68</sup>. The above trends and discussion indicate that the petroleum refining industry is facing a major challenge to meet the new stricter sulfur specifications for producing ultra clean transportation fuels in the early 21<sup>st</sup> century<sup>69</sup> when the quality of the crude oils continue to decline in terms of increased sulfur content and decreased API gravity.

### 3.2 Mechanistic Pathways of HDS

Substantial progress has been made in fundamental understanding and practical applications of hydrotreating catalysis and metal sulfide-based catalysts for HDS, as discussed in several excellent reviews<sup>40,60,61,64,67,70,71</sup>. The following discussion focuses on deep desulfurization of polycyclic sulfur compounds as shown in Scheme 1.

HDS of thiophenic compounds proceeds through two pathways: hydrogenation pathway (hydrogenation followed by hydrogenolysis) and the

direct hydrogenolysis pathway (direct elimination of S atom via C-S bond cleavage)<sup>31,32,62,72-77</sup>. A third pathway is isomerization of alkyl groups on the rings which affect the HDS conversion and selectivity<sup>31</sup>. Hydrogenation and hydrogenolysis may occur at different active sites. Polyaromatic compounds have been found to be the main inhibitors towards the hydrogenation pathway<sup>78-81</sup>. Girgis and Gates published an excellent review on reactivities of various compounds and their reaction networks as well as kinetics of high-pressure catalytic hydroprocessing<sup>53</sup>. Kabe et al.<sup>82</sup> compared the reactivities of DBT, 4-MDBT and 4,6-DMDBT under deep hydrodesulfurization conditions (sulfur concentration < 0.05 wt.%) using Co-Mo/Al<sub>2</sub>O<sub>3</sub>. The conversion of DBTs into cyclohexylbenzenes (CHBs) was nearly the same while that of DBTs into biphenyls (BPs) decreased in order DBT > 4-MDBT > 4,6-DMDBT. Data for DBTs could be arranged by the Langmuir-Hinshelwood rate equation. Activation energies of DBT, 4-MDBT and 4,6-DMDBT were 24, 31 and 40 kcal/mol, respectively<sup>82</sup>. Heats of adsorption for DBT, 4-MDBT and 4,6-DMDBT were 12, 20 and 21 kcal/mol, respectively<sup>82</sup>. Kabe et al. proposed that 4-MDBT or 4,6-DMDBT can be adsorbed on the catalyst through a pi-electron in the aromatic rings more strongly than that of DBT, and that the C-S bond cleavage of adsorbed DBTs is disturbed by steric hindrance of the methyl group<sup>82</sup>. Previous studies by Mochida and coworkers<sup>62,83-85</sup> have demonstrated that over the industrial HDS catalysts, the refractory sulfur compounds, particularly 4,6-DMDBT, are desulfurized dominantly by the hydrogenation pathway as the alkyl groups at the 4 and/or 6-position of DBT strongly blocks the hydrogenolysis pathway. The rate constant of DBT and 4,6-DMDBT for hydrogenation pathway is similar, being 0.015 and 0.010 min<sup>-1</sup> over a commercial Co-Mo catalyst, while the rate constant of 4,6-DMDBT for hydrogenolysis pathway is 0.004 min<sup>-1</sup>, less than that of DBT (0.048) by 12 times. Quantum chemical calculation on the conformation and electronic property of the various sulfur compounds and their HDS intermediates by Ma et al. shows that the hydrogenation pathway favors desulfurization of the refractory sulfur compounds by both decreasing the steric hindrance of the methyl groups and increasing the electron density on the sulfur atom in the sulfur compounds<sup>63</sup>. As desulfurization of the refractory sulfur compounds occurs dominantly through the hydrogenation pathway, the inhibition of the coexistent aromatics towards HDS of the refractory sulfur compounds by competitive adsorption on the hydrogenation active sites becomes stronger in deep HDS<sup>80,81</sup>. H<sub>2</sub>S produced from reactive sulfur compounds in the early stage of the reaction is one of the main inhibitors for HDS of the unreactive species.<sup>41,86</sup>

Computer modeling and simulation in the active sites on the catalyst surface and their interaction with sulfur compounds have also been applied in our laboratory to understand the reaction pathways and mechanism<sup>87-90</sup>. Figure 5 shows 2 types of chemisorption patterns of 4,6-DMDBT on MoS<sub>2</sub>, the flat adsorption and S-μ<sub>3</sub> type adsorption. Semi-empirical calculations have

been carried out to illustrate the difference in chemisorption patterns between DBT and 4,6-DMDBT. Both DBT and 4,6-DMDBT can interact well with 3030 edge of MoS<sub>2</sub> catalyst by flat chemisorption. The chemisorption of 4,6-dialkyldibenzothiophenes, different from that of the DBTs without any alkyl group at both 4- and 6-positions, is difficult by the S-μ<sub>3</sub> type coordination due to the steric hindrance of the alkyl groups. This steric hindrance is expected to increase with increasing size of the alkyl groups (from methyl to ethyl to propyl). Milenkovic et al.<sup>91</sup> synthesized various alkyldibenzothiophenes bearing bulky groups in positions 4 and 6 and compared their sensitivity to HDS over a NiMo/Al<sub>2</sub>O<sub>3</sub> industrial catalyst in a batch reactor at 573 K and under 5 MPa H<sub>2</sub> pressure. It was further demonstrated that their reactivity is correlated to the steric hindrance near the sulfur atom. Some recent studies were directed at understanding the surface reaction pathways for deep HDS of alkyldibenzothiophenes<sup>92</sup>.

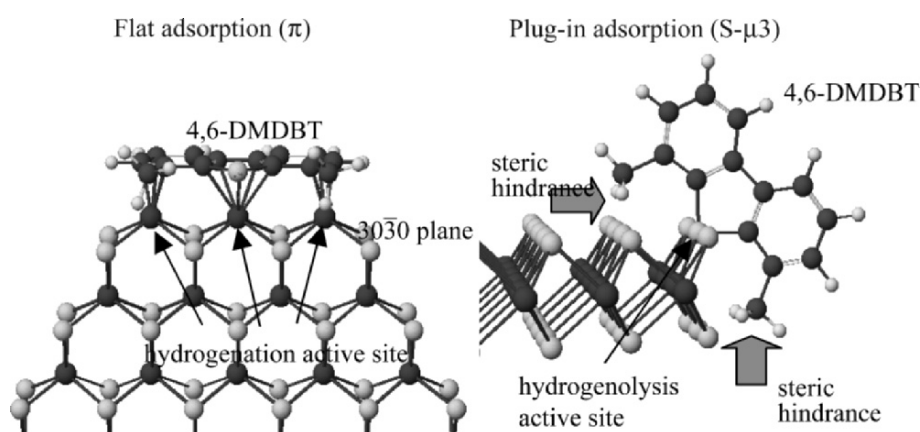


Figure 5. Adsorption conformations of 4,6-DMDBT at the hydrogenation active site and the hydrogenolysis active site. There is a strong steric hindrance in the plug-in adsorption<sup>181</sup>.

#### 4. DESIGN APPROACHES TO ULTRA DEEP DESULFURIZATION

Approaches to ultra-deep desulfurization include (1) improving catalytic activity by new catalyst formulation for HDS of 4,6-DMDBT; (2) tailoring reaction and process conditions; (3) designing new reactor configurations; and (4) developing new processes. One or more approaches may be employed by a refinery to meet the challenges of producing ultra-clean fuels at affordable cost.

Design approaches for developing more active catalysts are based on the ideas to tailor the active sites for desired reactions. The exact nature of active

sites in Co-Mo or Ni-Mo catalysts is still a subject of debate, but the Co-Mo-S model (or Ni-Mo-S model for Ni-Mo catalysts) is currently the one most widely accepted<sup>70,71</sup>. According to the model, the Co-Mo-S structure or Ni-Mo-S structure is responsible for the catalytic activity of the Co-promoted or Ni-promoted MoS<sub>2</sub> catalyst, although the model does not specify whether the catalytic activity arises from Mo promoted by Co or from cobalt promoted by molybdenum. Density-functional theory (DFT) calculations show that addition of Co to MoS<sub>2</sub> structure lowers the sulfur binding energy at the edges and thereby provides more active sites<sup>93</sup>. Recently, the formation of sulfur vacancy in MoS<sub>2</sub> under H<sub>2</sub> atmosphere has been observed directly for the first time by scanning tunneling electron microscope (STM)<sup>94</sup>. Comparison of STM images for Mo sulfide based particles with and without cobalt promoter atoms shows that without cobalt, the MoS<sub>2</sub> particles assume a neat triangular shape. Once cobalt enters the crystals, the particles become truncated hexagons--triangles with clipped-off vertices.<sup>94</sup> These new findings from experimental STM observations are consistent also with the FT-IR studies for NO chemisorption on Co-Mo catalysts. Co-Mo catalysts with more Co sites exposed (Co edge sites) tend to have higher activity for HDS<sup>70</sup>, and this trend has been observed also for Co-Mo/MCM-41 and Co-Mo/Al<sub>2</sub>O<sub>3</sub> catalysts based on DBT HDS and FT-IR of chemisorbed NO<sup>33</sup>.

Among the Co-Mo-S structures for alumina-supported catalysts, the intrinsically more active phase was referred to as type II (Co-Mo-S II), and the less active phase as type I (Co-Mo-S I); the type I structure is assumed to be bonded to support through Mo-O-Al linkages and has less stacking, whereas the type II structure has higher stacking and few linkages with support<sup>71</sup>. For steric reasons, catalyst-support linkages in Co-Mo-S I probably hinder reactant molecules from approaching the catalytically active sites, and thus Co-Mo-S II is more active than Co-Mo-S I, although Mossbauer and EXAFS signals of type I and type II structures are the same. Daage and Chianelli reported that the top and bottom layers (rim) of unsupported MoS<sub>2</sub> stacks (slabs) have a much higher activity than the surface of intermediate layers (edge) for hydrogenation of DBT, while the hydrogenolysis of the C-S bond in DBT occurs equally well on all MoS<sub>2</sub> layers<sup>64</sup>. They proposed a rim-edge model, and explained that the flat pi-adsorption on MoS<sub>2</sub> surface results in hydrogenation of DBT, which can take place on rim sites but this adsorption is more difficult on edge sites, whereas vertical adsorption of sulfur is assumed to be necessary for C-S bond hydrogenolysis, which can take place on surface Mo sites of all layers (both rim and edge). The Co-Mo-S model makes no distinction between rim and edge, but Co-Mo-S II would seem to have relatively more rim sites that are not likely to be influenced by steric hindrance of reactant adsorption. Consequently, more Co-Mo-S II structures can lead to more active catalysts for desulfurization of polycyclic sulfur compounds.

## 4.1 Improving Catalytic Activity by New Catalyst Formulation

Design approaches for improving catalytic activity for ultra deep hydrodesulfurization focus on how to remove 4,6-DMDBT more effectively, by modifying catalyst formulations to (1) enhance hydrogenation of aromatic ring in 4,6-DMDBT by increasing hydrogenating ability of the catalyst; (2) incorporate acidic feature in catalyst to induce isomerization of methyl groups away from the 4- and 6-positions; and (3) remove inhibiting substances (such as nitrogen species in the feed, H<sub>2</sub>S in gas) and tailoring the reaction conditions for specific catalytic functions. The catalytic materials formulations may be improved for better activity and/or selectivity by using different supports (MCM-41, carbon, HY, TiO<sub>2</sub>, TiO<sub>2</sub>-Al<sub>2</sub>O<sub>3</sub>, etc.) for preparing supported CoMo, NiMo and NiW catalysts; by increasing loading level of active metal (Mo, W, etc.); by modifying preparation procedure (using different precursor, using additives, or different steps or sequence of metal loading); by using additives or additional promoters (P, B, F, etc.); by adding one more base metal (e.g., Ni to CoMo or Co to NiMo, Nb etc.); and by incorporating a noble metal (Pt, Pd, Ru, etc.).

New and improved catalysts and different processing schemes are among the subjects of active research on deep HDS<sup>33,60,61,67</sup>. For example, some recent studies examined carbon-supported CoMo catalysts for deep HDS<sup>81,95,96</sup>. Binary oxide supports such as TiO<sub>2</sub>-Al<sub>2</sub>O<sub>3</sub> have been examined for making improved HDS catalysts<sup>97-99</sup>.

In 1992, novel mesoporous molecular sieve MCM-41 was invented by Mobil researchers<sup>100,101</sup>. The novel mesoporous molecular sieve of MCM-41 type has also been examined as support for Co-Mo/MCM-41 catalyst for HDS. Al-MCM-41 has been synthesized with improved aluminum incorporation into framework<sup>102-104</sup> and applied to prepare Co-Mo/MCM-41 for deep HDS of diesel fuels<sup>31,32,105,106</sup> and for HDS of petroleum resid<sup>104</sup>.

The design approach makes use of high surface area of MCM-41 for higher activity per unit weight, uniform meso pore to facilitate diffusion of polycyclic sulfur compounds, and mild acidity of Al-containing MCM-41 to facilitate metal dispersion and possible isomerization<sup>31</sup>. We synthesized MCM-41 type aluminosilicate molecular sieves using different Al sources, and established a proper procedure for making acidic MCM-41<sup>31,103</sup>. Several recent studies have explored the design of new catalysts for HDS of refractory DBT-type sulfur compounds, based on synthesis and application of mesoporous aluminosilicate molecular sieves of MCM-41 type<sup>32,34,35</sup>. Compared to Co-Mo/Al<sub>2</sub>O<sub>3</sub>, higher activity for HDS has been observed for Co-Mo/MCM-41 with a higher metal loading. When MCM-41 with proper SiO<sub>2</sub>/Al<sub>2</sub>O<sub>3</sub> ratio was used to prepare Co-Mo/MCM-41 at suitable metal loading, the catalyst is much more active for HDS of dibenzothiophene, 4-

methyl- and 4,6-dimethyl dibenzothiophene than a commercial Co-Mo/Al<sub>2</sub>O<sub>3</sub> catalyst.<sup>32,34,35</sup>

Figure 6 shows the results for HDS of various polycyclic sulfur compounds in a light cycle oil (LCO) over Co-Mo/MCM-41 (SiO<sub>2</sub>/Al<sub>2</sub>O<sub>3</sub> ratio = 50) and Co-Mo/Al<sub>2</sub>O<sub>3</sub> (C-344)<sup>107</sup>. The conversions of refractory sulfur compounds in LCO such as 4-MDBT and 4,6-DMDBT are much higher with the Co-Mo/MCM-41 catalyst than with the Co-Mo/Al<sub>2</sub>O<sub>3</sub>. FT-IR spectra of chemisorbed NO on sulfided Co-Mo/MCM-41 and in comparison the sulfided Co-Mo/Al<sub>2</sub>O<sub>3</sub> catalyst<sup>108,109</sup> revealed that there is a higher degree of Co edge site exposure on sulfided Co-Mo/MCM-41 as compared to that on sulfided Co-Mo/Al<sub>2</sub>O<sub>3</sub> catalyst,<sup>108</sup> since Co site has a distinct NO chemisorption peak<sup>109</sup>. The reason for the higher degree of Co site exposure in Co-Mo on MCM-41 relative to Co-Mo on Al<sub>2</sub>O<sub>3</sub> (based on FT-IR spectra for NO on Co-Mo/MCM-41) remains to be clarified. It is possible that relatively more hydrophobic support could lead to a higher layer of stacking and more Co site on the edge when compared to a more hydrophilic surface such as Al<sub>2</sub>O<sub>3</sub>, but it is difficult to quantify such an effect due to support surface hydrophobicity. In this context, the surface hydrophobicity consideration may partially rationalize why carbon-supported MoS<sub>2</sub> catalyst can be more active than alumina-supported MoS<sub>2</sub> catalyst for desulfurization of dibenzothiophene-type sulfur compounds. Recently, the use of silicalite MCM-41 without aluminum has also been reported for DBT HDS.<sup>110</sup>

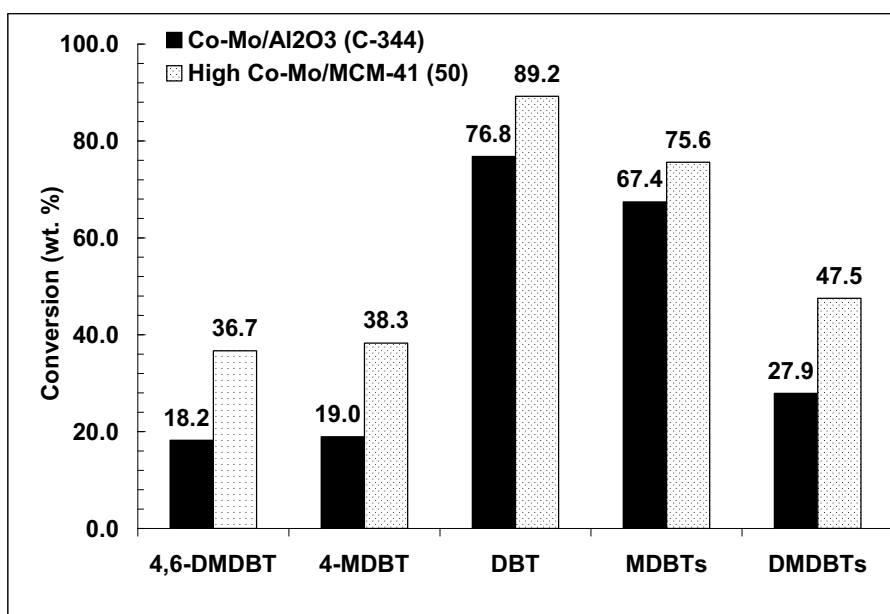


Figure 6. HDS of various PASCs in LCO over Co-Mo/MCM-41 (50) and Co-Mo/Al<sub>2</sub>O<sub>3</sub> (C-344) (Temperature, 300 °C; hydrogen pressure, 45 atm; WHSV, 4 h<sup>-1</sup>; hydrogen/hydrocarbon, 300 ml/ml; conversion data obtained after 4 h of time on stream)<sup>107</sup>.

The catalyst development has been one of the focuses of industrial research and development for deep hydrodesulfurization.<sup>69</sup> For example, new and improved catalysts have been developed and marketed by Albemarle, Haldor Topsøe, Criterion, IFP, United Catalyst/Sud-Chemie, Advanced Refining, and ExxonMobil.

Akzo Nobel has developed and commercialized various catalysts that can be used for HDS of diesel feed: KF 752, KF 756 and KF 757, and KF 848<sup>111</sup>. KF 752 can be considered to be typical of an Akzo Nobel catalyst of the 1992-93 timeframe. KF 756 is a Co-Mo catalyst with high HDS activity; it was jointly developed by Albemarle and Exxon Mobil Research and Engineering by applying a new alumina-based carrier technology and a special promoter impregnation technique to allow high and uniform dispersion of metals such as Co and Mo on support with moderate density<sup>112</sup>. KF 757 is Albemarle's latest Co-Mo with higher HDS activity and optimized pore structure; it was announced in 1998<sup>111</sup>. Albemarle estimates that under typical conditions (e.g., 500 ppmw sulfur), KF 756 is 25 % more active than KF 752, while KF 757 is 50 % more active than KF 752 and 30 % more active than KF 756<sup>113</sup>. KF 756 is widely used in Europe (20 % of all distillate hydrotreaters operating on January 1, 1998), while KF 757 has been used in a large number of hydrotreaters commercially<sup>12</sup>. Under more severe conditions (e.g., <50 ppmw sulfur), KF 757 is 35-75 % more active than KF 756.

KF 757 and KF 848 were developed by using what Albemarle calls STARS (Super Type II Active Reaction Sites) technology. Type II refers to a specific kind of catalyst site, which is more effective for removing sulfur from sterically hindered compounds. KF 848 was announced in 2000<sup>113</sup>. KF 848 is 15-50% more active than KF757 under medium to high pressure. Commercial experience exists for both advanced catalysts at BP refineries. In terms of sulfur removal, Akzo Nobel projects that a desulfurization unit which produces 500 ppmw sulfur with KF 752, would produce 405, 270 and 160 ppm sulfur with KF 756, KF757, and KF 842, respectively<sup>12</sup>. As evidenced by the STARS technology, the advances in basic understanding of fundamental pathways of HDS reactions over transition metal sulfides has also resulted in major advances in commercial catalyst developments.

Researchers at Haldor Topsøe and their collaborators in academic institutions have contributed significantly to both the advances in research on fundamental aspects of catalytically active sites of transition metal sulfides<sup>61,70</sup> and the development of new and more active commercial hydrotreating catalysts and processes<sup>67</sup>. Haldor Topsøe has commercialized more active catalysts for HDS. Its TK-554 catalyst is analogous to Akzo Nobel's KF 756 catalyst, while its newer, more active catalyst is termed TK-574. For example, in pilot plant studies, under conditions where TK-554 produces 400 ppmw sulfur in SRGO, TK 574 will produce 280 ppmw. Under more severe conditions, TK-554 will produce 60 ppmw, while TK 574 will produce 30 ppmw, and similar benefits are found with a mixture of straight run and

cracked stocks<sup>12</sup>. In addition to catalyst development, Haldor Topsøe has also developed new processes for HDS.

Criterion Catalyst Company announced two new lines of catalysts. One is called Century, and the other is called Centinel. These two lines of catalysts are reported to be 45-70% and 80% more active, respectively, at desulfurizing petroleum fuel than conventional catalysts used in the mid-90s<sup>12</sup>. These improvements have come about through better dispersion of the active metal on the catalyst substrate.

Albemarle recently reported on their commercial experience of their STARS catalyst for diesel fuel feedstock HDS at two BP refineries (Grangemouth, and Coryton) in UK. The original unit at Grangemouth refinery was designed to produce 35,000 barrels per day of diesel fuel at 500 ppmw treating mostly straight run material, but some LCO was treated as well. Albemarle's newest and best catalyst (KF 757 at that time) was dense-loaded into the reactor to produce 45,000 barrels per day diesel fuel at 10 - 20 ppmw (to meet the 50 ppmw cap standard). As the space velocity changed, the sulfur level changed inversely proportional to the change in space velocity. Usually when the space velocity decreased to below 1.0, the sulfur level dropped below 10 ppmw. At that refinery, however, it was not necessary to maintain the sulfur level below 10 ppmw<sup>12</sup>.

More recently, NEBULA catalyst has been developed jointly by Exxon Mobil, Albemarle, and Nippon Ketjen and announced in 2001<sup>114</sup>. The NEBULA catalyst is even more active than KF 848 STARS catalyst with respect to HDN and diesel hydrotreating; it has been successfully applied in several diesel hydrotreaters for months as of early 2002<sup>114</sup>. Hydrocracking pretreatment was the first application where very high activity was found for NEBULA-1. For good hydrocracking pretreatment one traditionally needs the best possible HDN catalyst and, since HDN usually correlates with good hydrogenation, the typical hydrocracking pretreat catalysts have excellent HDN and HDA combined. HDS activity used to be of secondary importance for hydrocracking pretreatment but with the new low sulfur specifications it can also limit the performance of the pretreater<sup>115</sup>. A similar improvement in activity is found for HDS and hydrogenation over NEBULA, this will lead to highly improved product qualities like lower sulfur, higher cetane, lower density, etc.

The choice of commercial hydrotreating catalysts, represented by alumina-supported Co-Mo, Ni-Mo and Ni-Co-Mo, depends on the capability of reactor equipments, operating conditions (pressure, temperature), feedstock type and sulfur contents, and desired levels of sulfur reduction. In general, for low-pressure and high-temperature desulfurization of distillate fuels, Co-Mo catalysts may be better than Ni-Mo catalysts. For high-pressure and low-temperature conditions, Ni-Mo catalysts perform better than Co-Mo catalysts. Ni-Mo catalysts generally have higher hydrogenating ability than Co-Mo counterparts, and higher H<sub>2</sub> pressure and lower temperature favor the



hydrogenation reactions and thus facilitate HDS by hydrogenation pathway. The trimetallic Ni-Co-Mo catalysts can combine the features of Co-Mo and Ni-Mo, and this new formulation feature is being used in some recent commercial catalysts.

## 4.2 Tailoring Reaction and Processing Conditions

Tailoring process conditions aims at achieving deeper hydrodesulfurization with a given catalyst in an existing reactor without changing the processing scheme, with no or minimum capital investment. The parameters include those that can be tuned without any new capital investment (space velocity, temperature, pressure), and those that may involve some relatively minor change in the processing scheme or some capital investment (expansion in catalyst volume or density, H<sub>2</sub>S scrubber from recycle gas, improved vapor-liquid distributor)<sup>116,117</sup>. First, space velocity can be decreased to increase the reactant-catalyst contact time. More refractory sulfur compounds would require lower space velocity for achieving deeper HDS. Second, temperatures can be increased, which increases the rate of HDS. Higher temperatures facilitate more of the high activation-energy reactions. Third, H<sub>2</sub> pressure can be increased. Fourth, improvements can be made in vapor-liquid contact to achieve uniform reactant distribution, which effectively increases the use of the surface area of the catalyst. Fifth, the concentration of hydrogen sulfide in the recycle stream can be removed by scrubbing. Since H<sub>2</sub>S is an inhibitor to HDS, its build-up in high-pressure reactions through continuous recycling can become significant. Finally, more volume of catalyst can be used, either through catalyst bed volume expansion or more dense packing.

Some of these factors are elaborated further below. It should be noted that conventional approaches for fuel desulfurization in response to the 1993 diesel fuel sulfur regulation (500 ppmw sulfur) in the U.S. were to increase process severity of HDS, increase catalysts to fuel ratio, increase residence time, and enhance hydrogenation, or to use additional low-sulfur blending stocks either from separate process streams or purchased. It is becoming more difficult to meet the ultra-low-sulfur fuel specifications by fuel hydrodesulfurization using the conventional approaches.

Liquid-hourly space velocity (LHSV) and catalytic bed volume are inter-related parameters that control both the level of sulfur reduction and the process throughput. Increase in catalyst bed volume can enhance desulfurization. UOP projects that doubling reactor volume would reduce sulfur from 120 to 30 ppmw<sup>12</sup>. Haldor-Topsøe reports that doubling the catalyst volume results in a 20 °C decrease in average temperature if all other operating conditions are unchanged, and there is a double effect of the increased catalyst volume<sup>67</sup>. The deactivation rate decreases because the

start-of-run temperature decreases, and the lower LHSV by itself reduces the deactivation rate even at the same temperature.

Increasing the temperature of reaction can enhance the desulfurization of more refractory sulfur compounds. Haldor Topsøe has shown that an increase of 14 °C while processing a mix of SRLGO and LCO with its advanced TK-574 Co-Mo catalyst will reduce sulfur from 120 ppmw to 40 ppmw<sup>12</sup>. UOP projects that a 20 °F increase in reactor temperature would decrease sulfur from 140 to 120 ppmw<sup>12</sup>. The downside of increased temperature is reduced catalyst life (i.e., the need to change catalyst more frequently). This increases the cost of catalyst, as well as affects highway diesel fuel production while the unit is down for the catalyst change. Still, current catalyst life ranges from 6 to 60 months, so some refiners could increase temperature and still remain well within the range of current industry performance. The relationship between temperature and life of a catalyst is a primary criterion affecting its marketability; thus, catalyst suppliers generally do not publish these figures<sup>12</sup>.

The decrease in the concentration of hydrogen sulfide in the gas phase could reduce the inhibition of the desulfurization<sup>41,85,86,118</sup> and hydrogenation reactions. The role of H<sub>2</sub>S in deep HDS of gas oils has been discussed in detail by Sie<sup>119</sup>. H<sub>2</sub>S can be removed by chemical scrubbing. Haldor-Topsøe indicates that decreasing the concentration of hydrogen sulfide at the inlet to a co-current reactor by three to six volume% can decrease the average temperature needed to achieve a specific sulfur reduction by 15-20°C, or reduce final sulfur levels by more than two-thirds<sup>12</sup>. UOP projects that scrubbing hydrogen sulfide from recycled hydrogen can reduce sulfur levels from roughly 285 to 180 ppmw in an existing hydrotreater<sup>12</sup>.

The increase in hydrogen partial pressure and/or purity can improve hydrodesulfurization and hydrogenation. Haldor-Topsøe indicates that increasing hydrogen purity is preferable to a simple increase in the pressure of the hydrogen feed gas, since the latter will also increase the partial pressure of hydrogen sulfide later in the process, which inhibits both beneficial reactions<sup>12</sup>. Haldor-Topsøe projects that an increase in hydrogen purity of 30% would lower the temperature needed to achieve the same sulfur removal rate by eight to nine °C. Or temperature could be maintained while increasing the amount of sulfur removed by roughly 40%. Hydrogen purity can be increased through the use of a membrane separation system or a PSA unit. UOP project that purifying hydrogen can reduce distillate sulfur from 180 to 140 ppmw from an existing hydrotreater<sup>12</sup>.

Increasing the recycle gas/oil ratio (increase in the amount of recycle gas sent to the inlet of the reactor) could increase the degree of desulfurization, but the effect is relatively small, so a relatively large increase is needed to achieve the same effect as scrubbing the recycle gas<sup>67</sup>. Haldor-Topsøe indicates that a 50% increase in the ratio of total gas/liquid ratio only decreases the necessary reactor temperature by 6 to 8°C; or the temperature can be maintained and the final sulfur level reduced by 35-45%<sup>12</sup>.

The improvement in vapor-liquid contact can enhance the performance of distillate hydrotreaters. As an example, in testing of an improved vapor-liquid distributor in commercial use, Haldor-Topsoe and Phillips Petroleum found that the new Topsøe Dense Pattern Flexible Distribution Tray (installed in 1996 to replace a chimney type distributor installed in 1995 in a refinery) allowed a 30% higher sulfur feed to be processed at 25°C lower temperatures, while reducing the sulfur content of the product from 500 to 350 ppmw<sup>67</sup>. Albemarle estimates that an improved vapor-liquid distributor can reduce the temperature necessary to meet a 50 ppmw sulfur level by 10 °C, which in turn would increase catalyst life and allow an increase in cycle length from 10 to 18 months<sup>12</sup>. Based on the above data from Haldor-Topsoe, if temperature were maintained, the final sulfur level could be reduced by 50%<sup>12</sup>. Maintaining temperature should have allowed an additional reduction in sulfur of more than two-thirds. Thus, ensuring adequate vapor-liquid contact can have a major impact on final sulfur levels.

The above-mentioned individual improvements described cannot be simply combined, either additively or multiplicatively. As mentioned earlier, each existing distillate hydrotreater is unique in its combination of design, catalyst, feedstock, and operating conditions. While the improvements described above are probably indicative of improvements which can be made in many cases, it is not likely that all of the improvements mentioned are applicable to any one unit; the degree of improvement at one refinery could either be greater than, or less than the benefits that are indicated for another refinery.

### 4.3 Designing New Reactor Configurations

Industrial reactor configuration for deep hydrodesulfurization of gas oils in terms of reaction order and effect of H<sub>2</sub>S has been discussed by Sie<sup>119</sup>. The reactor design and configuration involve 1-stage and 2-stage desulfurization. Desulfurization processes in use today in the U.S. generally use only one reactor, due to the need to only desulfurize diesel fuel to 500 ppmw or lower. Hydrogen sulfide strongly suppresses the activity of the catalyst for converting the refractory sulfur compounds, which should occur in the major downstream part of a cocurrent trickle-bed reactor during deep desulfurization. The normally applied cocurrent trickle-bed single reactor is therefore not the optimal technology for deep desulfurization<sup>119</sup>. However, a second reactor can be used, particularly to meet lower sulfur levels. Adding a second reactor to increase the degree of desulfurization is an option, and both desulfurization and hydrogenation in the second reactor can be improved by removing H<sub>2</sub>S and NH<sub>3</sub> from the exit gas of first reactor before entering the second reactor. This last technical change is to install a complete second stage to the existing, one-stage hydrotreater. This second stage would consist of a second reactor, and a high pressure, hydrogen sulfide scrubber between

the first and second reactor. The compressor would also be upgraded to allow a higher pressure to be used in the new second reactor. Assuming use of the most active catalysts available in both reactors, UOP projects that converting from a one-stage to a two-stage hydrotreater could produce 5 ppm sulfur relative to a current level of 500 ppm today<sup>12</sup>.

A new way of reactor design is to have two or three catalyst beds, that are normally placed in separate reactors, within a single reactor shell and have both co-current and counter-current flows<sup>119</sup>. This new design was developed by ABB Lummus and Criterion, as represented by their SynSat process<sup>120,121</sup>. The SynAlliance (consisting of ABB Lummus, Criterion Catalyst Corp., and Shell Oil Co.) has patented a counter-current reactor design called SynTechnology. With this technology, in a single reactor design, the initial portion of the reactor will follow a co-current design, while the last portion of the reactor will be counter-current<sup>12</sup>. Traditional reactors are cocurrent in nature. The hydrogen is mixed together with the distillate at the entrance to the reactor and the mixture flows through the reactor. Because the reaction is exothermic, heat must be removed periodically. This is sometimes done through the introduction of fresh hydrogen and distillate at one or two points further down the reactor. The advantage of cocurrent design is practical; it eases the control of gas-liquid mixing and contact with the catalyst. The disadvantage is that the concentration of H<sub>2</sub> is the highest at the front of the reactor and lowest at the outlet. The opposite is true for the concentration of H<sub>2</sub>S. This increases the difficulty of achieving extremely low sulfur levels due to the low H<sub>2</sub> concentration and high H<sub>2</sub>S concentration at the end of the reactor. A new solution to this problem is to design a counter-current reactor, where the fresh H<sub>2</sub> is introduced at one end of the reactor and the liquid distillate at the other end. Here, the hydrogen concentration is highest (and the hydrogen sulfide concentration is lowest) where the reactor is trying to desulfurize the most difficult (sterically hindered) compounds. The difficulty of counter-current designs in the case of distillate hydrotreating is vapor-liquid contact and the prevention of hot spots within the reactor.

In a two reactor design, the first reactor will be co-current, while the second reactor will be counter-current. ABB Lummus estimates that the counter-current design can reduce the catalyst volume needed to achieve 97% desulfurization by 16 % relative to a co-current design<sup>12</sup>. The impact of the counter-current design is even more significant when aromatics control (or cetane improvement) is desired in addition to sulfur control. However, operation of countercurrent flow reactor might not be possible in packed beds of the usual catalyst particles because of the occurrence of flooding at industrially relevant fluid velocities. Some novel reactor concepts based on special structured packings or monoliths that allow such countercurrent operation have been presented<sup>119</sup>.

## 4.4 Developing New Processes

Among the new process concepts, design approaches for ultra deep desulfurization focus on (1) adsorption and sulfur atom extraction - remove sulfur by using reduced metals or metal oxides to react with sulfur to form metal sulfides at elevated temperatures under  $H_2$  atmosphere without hydrogenation of aromatics; (2) selective adsorption for removing sulfur compounds (SARS) – remove sulfur by selective interaction with sulfur compounds in the presence of aromatic hydrocarbons under ambient or mild conditions without using hydrogen; (3) oxidation and extraction – oxidize sulfur compounds by liquid-phase oxidation reactions with or without ultrasonic radiation, followed by separation of the oxidized sulfur compounds and (4) biodesulfurization – attack sulfur atoms by using bacteria via microbial desulfurization.

### 4.4.1 S Zorb Process for Sulfur Absorption and Capture.

Phillips Petroleum (now Conoco Phillips) conducted an internal study of its refineries and concluded that the use of hydrotreating technologies to reach ultra-low sulfur levels in gasoline to be a cost-prohibitive option<sup>122</sup>. A new diesel desulfurization process called S Zorb Diesel, was recently announced by Phillips Petroleum. This is an extension of their S Zorb Gasoline process for gasoline (at 377-502°C, 7.0-21.1 kg/cm<sup>2</sup>)<sup>122</sup>. S-Zorb for diesel contacts highway diesel fuel (typically with about 350 ppm sulfur) with a solid sorbent in a fluid bed reactor at relatively low pressures and temperature in the presence of hydrogen. The sulfur atom of the sulfur-containing compounds adsorbs onto the sorbent and reacts with the sorbent. Phillips Petroleum uses a proprietary sorbent that attracts sulfur-containing molecules and removes the sulfur atom from the molecule. The sulfur atom is retained on the sorbent while the hydrocarbon portion of the molecule is released back into the process stream. Hydrogen sulfide is not released into the product stream and therefore prevents recombination reactions of hydrogen sulfide and olefins to make mercaptans, which would otherwise increase the effluent sulfur concentration.

Scheme 2 illustrates the principle of S Zorb process<sup>122</sup>. Based on the principle, it appears that the sorbent is based on reduced metal that reacts with sulfur to become metal sulfide. The spent sorbent is continuously withdrawn from the reactor and transferred to the regenerator section. In a separate regeneration vessel, the sulfur is burned off of the sorbent and  $SO_2$  is sent to the sulfur plant. The cleansed sorbent is further reduced by hydrogen and the regenerated sorbent is then recycled back to the reactor for removing more sulfur. The rate of sorbent circulation is controlled to help maintain the desired sulfur concentration in the product. Because the sorbent is continuously regenerated, Phillips estimates that the unit will be able to

operate 4-5 years between shutdowns<sup>12</sup>.

Phillips Petroleum's first commercial S Zorb – Gasoline unit began operations successfully in its Borger refinery in Texas, USA, in early 2001, for processing 6000 barrels of gasoline feed per day to produce gasoline with 10 ppmw sulfur<sup>123</sup>. The S Zorb diesel desulfurization process has been demonstrated in the laboratory using two different diesel feedstocks, which has shown that diesel feeds containing 17-20% hydrotreated LCO can be desulfurized down below 10 ppmw sulfur<sup>123</sup>.

Table 6 shows the performance of S Zorb process for diesel streams under the following general operating conditions: reactor temperature, 650-775 °F (343-413 °C); reactor pressure, 100-300 psig (7-21 atm); space velocity, 4-10 WHSV; H<sub>2</sub> gas purity, > 50%<sup>123</sup>. The S Zorb diesel desulfurization process has been demonstrated in the laboratory using two different diesel feedstocks (Table 6), which has shown that diesel feeds containing 17-20% hydrotreated LCO can be desulfurized down below 10ppmw sulfur<sup>123</sup>. Conoco Phillips is currently operating a S Zorb diesel pilot plant unit where they are processing feeds with a wide range of sulfur content. Plans are underway for a commercial S Zorb diesel unit<sup>124</sup>. A recent article from Conoco Phillips presents a summary of S-Zorb process performance, historical development and future perspective of S-Zorb for gasoline and diesel desulfurization<sup>125</sup>. RTI group also tested their TreND process, initially developed for gasoline, for diesel desulfurization<sup>126</sup>.

Table 6. Impact of Hydrodesulfurization on FCC Feed Properties

|                                | Raw Feed  |         | HDS     |         |
|--------------------------------|-----------|---------|---------|---------|
|                                | Untreated | 90% HDS | 98% HDS | 99% HDS |
| Operating pressure, psig       | —         | 900     | 1,000   | 1,000   |
| Feed properties                |           |         |         |         |
| Gravity, °API                  | 20.5      | 23.5    | 24.8    | 26.0    |
| Sulfur, wt%                    | 2.6       | 0.25    | 0.06    | 0.02    |
| Nitrogen, wppm                 | 880       | 500     | 450     | 400     |
| Carbon residue, wt%            | 0.4       | 0.25    | 0.1     | 0.1     |
| Metals (Ni + V), wppm          | 1         | <1      | <1      | <1      |
| Hydrogen addition to feed, wt% | 0         | 0.51    | 0.74    | 0.94    |

Source:<sup>160</sup>.

#### 4.4.2 Selective Adsorption for Deep Desulfurization at Ambient Temperature

An alternate process is being explored at Pennsylvania State University for deep desulfurization of distillate fuels (diesel, gasoline and jet fuels) based on selective adsorption for removal of sulfur compounds (PSU-SARS) at ambient conditions without using H<sub>2</sub><sup>26,36,127</sup>. Figure 7 illustrates the known coordination geometries of thiophene in organometallic complexes, which indicate likely adsorption configurations of thiophenic compounds on the surface of adsorbents. Both thiophenic compounds and non-sulfur aromatic

compounds can interact with metal by pi-electrons. However, in Figure 5 only two types of interaction of thiophene with metal involve the sulfur atom in thiophene, the  $\eta^1\text{S}$  bonding interaction between the sulfur atom and one metal atom, and the  $\text{S}-\mu_3$  bonding interaction between the sulfur atom and two metal atoms.

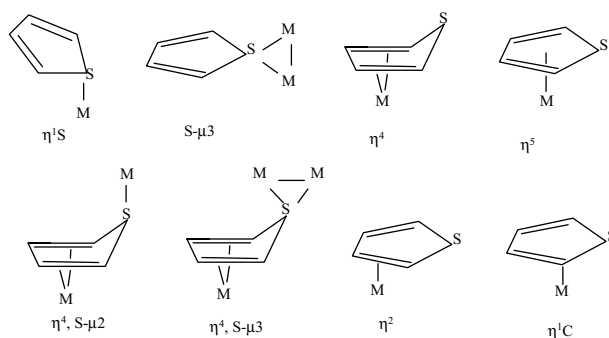


Figure 7. Known coordination geometries of thiophene in organometallic complexes, indicating likely adsorption configurations of thiophenic compounds on the surface of adsorbents<sup>127</sup>

Figure 8 shows the preliminary results from our laboratory for selective adsorption of sulfur compounds from a commercial diesel fuel using a transition metal complex based adsorbent A-1<sup>127</sup>. Figure 9 shows the corresponding results for a model diesel fuel that contains naphthalene, 2-methylnaphthalene, DBT and 4,6-DMDBT<sup>127</sup>. Based on the computational and experimental results, it is theoretically possible and experimentally doable to distinguish between sulfur compounds and aromatic compounds in diesel fuels using a solid adsorbent.

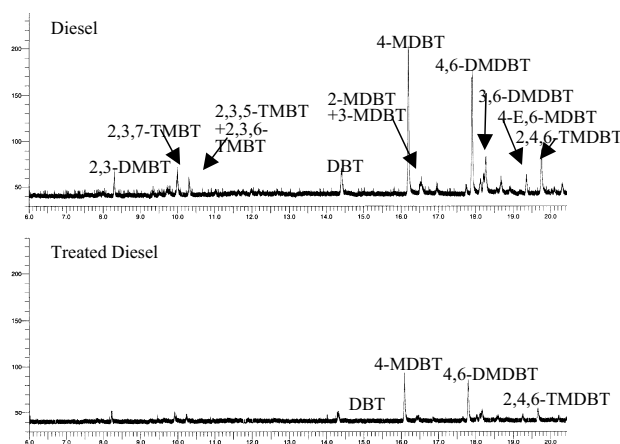


Figure 8. GC-FPD chromatogram of diesel and treated diesel. Adsorbent: A-1, Feed: a commercial diesel

Selective separation of sulfur compounds has also been conducted in analytical characterization using ligand-exchange chromatography. For example, Pyell et al.<sup>128</sup> has examined 2-amino-1-cyclopentene-1-dithiocarboxylic acid silica gel (ACDA-SG) loaded with Ag(I) or Pd(II) ions for the group fractionation of polycyclic aromatic sulfur heterocycles (PASH) from polycyclic aromatic hydrocarbons (PAH) via ligand-exchange chromatography in the normal phase mode. It is shown that metal loading has a great impact on the selectivity of ACDA-SG for PASH and PAH. Pd(II) loaded ACDA-SG proved to be suitable for the group isolation of PASH from the aromatic fractions of petroleum mixtures (number of condensed rings less than or equal to 3)<sup>128</sup>. Rudzinski et al.<sup>129</sup> analyzed the Maya crude oil by the saturates-aromatics-resins-asphaltenes (SARA) method. They separated sulfur-containing compounds in the saturate and aromatic fractions using a ligand-exchange chromatography method based on organosulfur affinity for  $\text{Cu}^{2+}$  and  $\text{Pd}^{2+}$ , respectively.

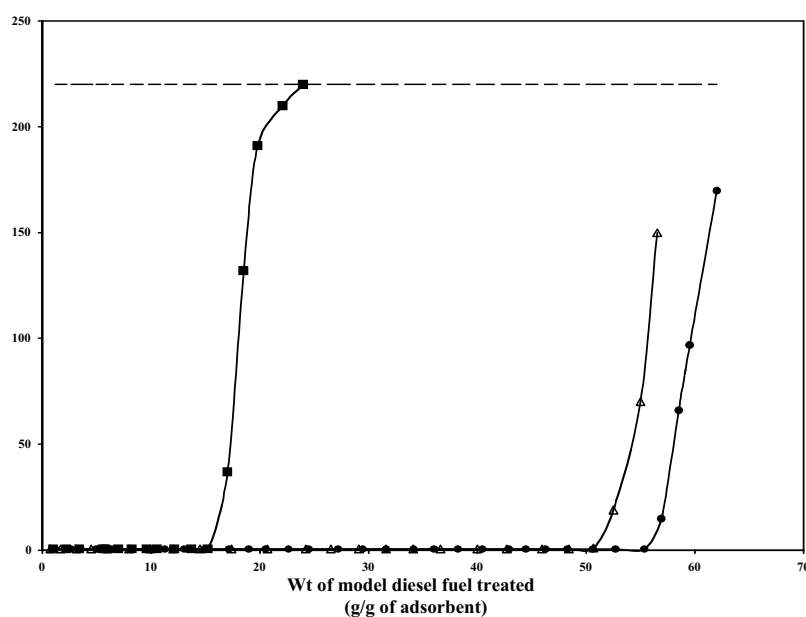


Figure 9. Breakthrough curves for the adsorptive desulfurization of a model diesel fuel containing 4,6-DMDBT at 60°C over Transition metal oxides supported on MCM-41 and activated carbon

More recently, Yang and coworkers<sup>130-134</sup> have reported on adsorption separation of thiophenic sulfur compounds from aromatic compounds based on  $\pi$ -complexation using Cu- and Ag-exchanged Y zeolites. The Cu(I)-Y zeolite was prepared by reducing the Cu(II)-Y zeolite at 450°C in He atmosphere. Better adsorption performance was noticed over Cu(I)-Y zeolites.



However, it is not clear how the  $\pi$ -complexation can differentiate between sulfur-containing aromatic compounds and non-sulfur containing aromatic compounds in real liquid fuels, although they have shown by theoretical calculations that the  $\pi$ -complexation strength is higher for thiophene compared to benzene<sup>131</sup>. The authors have noted that the adsorption performance of the Cu(I)-Y zeolite is decreased when aromatics are present in the fuel<sup>132-134</sup> probably due to the competitive adsorption of sulfur compounds and aromatics by  $\pi$ -complexation.

#### 4.4.3 New Integrated Process Concept Based on Selective Adsorption

By using existing HDS processes, we will need to process 100% of the fuel to deal with sulfur compounds that account for less than 0.3 wt% of the feed with 500 ppmw sulfur level. We are proposing a new approach for an integrated process. Figure 10 shows the flow diagram of the proposed concept of the new integrated desulfurization process, which consists of selective adsorption for removal of sulfur compounds (PSU-SARS)<sup>26,36,127</sup> followed by HDS of concentrated sulfur compounds (HDSCS) using high-activity catalysts such as Co-Mo/MCM-41<sup>34,35</sup>. The subsequent hydrodesulfurization of sulfur compounds removed by selective adsorption is expected to be much easier than conventional HDS of diesel streams for two reasons. First, it is more concentrated and thus reactor utilization is more efficient. Second, the rate of HDS reaction is faster because of the removal of aromatics which inhibit the HDS by competitive adsorption on the hydrogenation sites. Third, and most importantly for practical application, the required reactor volume can be substantially smaller because the amount of fuel to be processed is smaller by 95% or more.

The PSU-SARS-HDSCS concept represents an attempt to make deep desulfurization in a future refinery fundamentally more efficient and consumes less hydrogen, which is a significant cost factor for both capital investment ( $H_2S$  scrubber for recycle  $H_2$  gas, compressor) and process operation (consumption of  $H_2$ ). It is known that for current commercial hydrotreater operations, each 1 wt% sulfur removal results in about 18-20  $Nm^3/m^3$  feed (110-120 SCFB) of  $H_2$  consumption; each 1000 ppm nitrogen removal results in about 5.9-6.1  $Nm^3/m^3$  (35-36 SCFB) of  $H_2$  consumption; each 1 wt% aromatics removal yields about 5.0-8.4 (use half of these numbers if aromatics are reported as volume %); each one unit increase in °API gravity requires about 17  $Nm^3/m^3$  feed (100 SCFB) of  $H_2$  consumption, as does each one unit increase in cetane number for diesel stocks<sup>69</sup>.

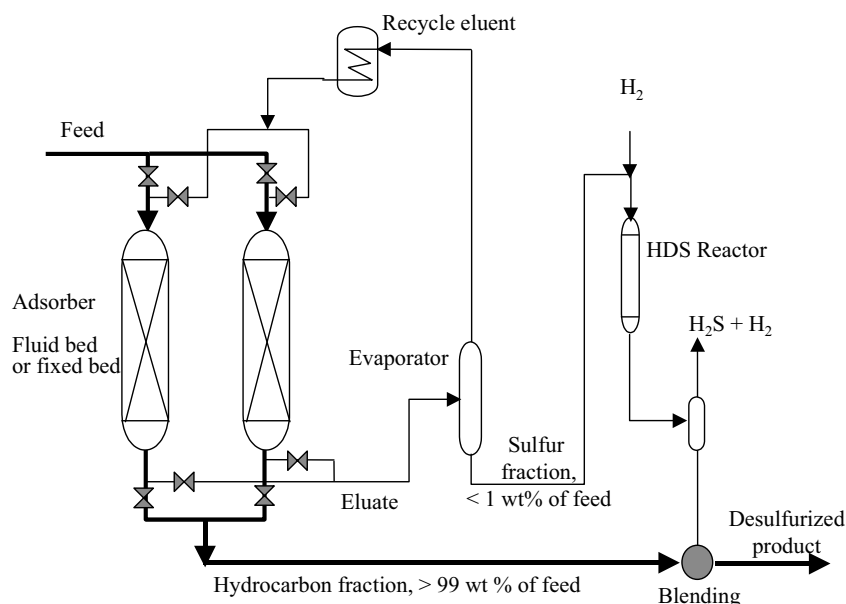


Figure 10. The proposed integrated PSU-SARS-HDSCS process based on adsorption for deep desulfurization<sup>127</sup>

#### 4.4.4 Adsorption Desulfurization Using Alumina Based Adsorbents

The IRVAD process by Black & Veatch Pritchard Inc. and Alcoa Industrial Chemicals is claimed to be a low-cost process for low-sulfur gasoline<sup>135,136</sup>. The process uses an alumina-based selective adsorbent to counter-currently contact liquid hydrocarbon in a multistage adsorber. The adsorbent is regenerated in a continuous cross-flow reactivator using heated reactivation gas. The process operates at lower pressure, and does not consume hydrogen or saturate olefins. The adsorption mechanism is based on the polarity of sulfur compounds. It is not very selective for gasoline sulfur, and no information is available on diesel sulfur.

#### 4.4.5 Charge Complex Formation

It is well established that among all sulfur-containing compounds present in gas oil, alkyldibenzothiophenes are the most refractory to the achievement of deep classical hydrodesulfurization. Focusing on these refractory sulfur compounds in gas oil, Milenkovic et al.<sup>91,137</sup> explored an approach to selective elimination of alkyldibenzothiophenes from gas oil by formation of insoluble charge-transfer complexes. They have noted the electron-rich structure of alkyl DBTs and studied their ability to form charge-transfer complexes (CTC) with pi-acceptors in order to develop a new highly

selective method for their specific removal from gas oil. A new method based on the selective formation of insoluble charge transfer complexes for removing the refractory compounds is described. They reported the selective formation of insoluble CTC between dibenzothiophene derivatives and tetranitrofluorenone in synthetic solutions, which model the gas oil matrix. By the same procedure the global sulfur level was lowered in gas oils. Furthermore, they have shown that the charge transfer complexation method is specific for dibenzothiophenes with regard to benzothiophenes. The complexation activity and selectivity have been correlated to the frontier molecular orbital energies and their shapes<sup>137</sup>.

#### 4.4.6 Oxidative Desulfurization

Oxidation of sulfur atoms in liquid phase into corresponding sulfones, with or without radiation by ultrasound or UV light, followed by extraction of oxidized species can lead to desulfurization of diesel fuels. As the regulations for sulfur in fuels become more and more stringent, it becomes increasingly more difficult for existing hydrodesulfurization processes to achieve affordable “ultra-deep desulfurization” to produce ultra-low-sulfur diesel fuels. Oxidative desulfurization is an alternative process, which may have niche applications<sup>138</sup>. Otsuki et al.<sup>139</sup> studied the oxidation of dibenzothiophene (DBT) using t-butyl hypochlorite (t-BuOCl) in the presence of several catalysts. In a flow reactor under ambient pressure at 30-70 °C, more than 90% of DBT could be oxidized in the decahydronaphthalene (decalin) solution. The catalyst was necessary to oxidize dibenzothiophene with t-BuOCl, and gamma-Al<sub>2</sub>O<sub>3</sub> supported catalysts have relatively high activities. At the same time, the activities of the metal-loaded Al<sub>2</sub>O<sub>3</sub> catalysts showed the same activities as those of the Al<sub>2</sub>O<sub>3</sub> support, indicating that the Al<sub>2</sub>O<sub>3</sub> support itself possessed such activity<sup>139</sup>. Aida et al.<sup>140</sup> discussed the oxidation processes for reducing the sulfur content in diesel fuel. The oxidation method has capabilities, not only to decrease the sulfur content in light oil below 0.1 ppm, but also to recover the sulfur component as an organic sulfur compound such as sulfone or dibenzothiophene derivatives that has a potential industrial use<sup>140</sup>. Hangun et al.<sup>141</sup> studied oxidative desulfurization using a series of iron (III) complexes (tetra amido macrocyclic ligand) as activators that enhance the oxidizing ability of hydrogen peroxide for dibenzothiophene derivatives at low catalyst concentrations and mild conditions such as 40 °C. Otsuki et al.<sup>139</sup> also examined the effect of a variety of model compounds found in light gas oil (LGO) such as n-pentadecane, 2,4,4-trimethylpentene, xylene, and indole on the oxidation of DBTs.

Shiraishi et al.<sup>142</sup> explored a new two-stage oxidative desulfurization process of light oil, effected by a combination of photochemical reaction and organic two-phase liquid-liquid extraction. The first consists of the transfer of the sulfur-containing compounds from the light oil to an aqueous-soluble

polar solvent. This is then followed by the photooxidation and photodecomposition of the sulfur-containing compounds in the solvent by UV irradiation, using a high-pressure mercury lamp. The operations are carried out under conditions of room temperature and atmospheric pressure. Acetonitrile was found to be the most suitable polar solvent for the process. The same group<sup>143</sup> reported photochemical desulfurization using hydrogen peroxide ( $\text{H}_2\text{O}_2$ ) aqueous solution extraction system for high-sulfur-content straight-run light gas oil and aromatic-rich light cycle oil. Photochemical desulfurization of light oils of different sulfur contents and aromatic components, such as straight-run light gas oil (LGO) and light cycle oil (LCO), in an oil/hydrogen peroxide aqueous solution two-phase liquid-liquid extraction system was investigated<sup>143</sup>. The entire wavelength region of light from a high-pressure mercury lamp was utilized to realize the direct excitation of sulfur-containing compounds. In the case of LGO of high sulfur content, 77% of the sulfur is removed by 36 h of photo-irradiation, and the quantity of sulfur removed from LGO is six-fold greater than in the case of commercial light oil. Although the desulfurization of LCO is suppressed by the presence of a large quantity of 2-ring aromatics, the sulfur content is reduced to less than 0.05 wt% to meet with regulations in Japan<sup>143</sup>. GC-AED analysis shows that benzothiophenes in all the feedstocks are more easily desulfurized than dibenzothiophenes. Highly substituted dibenzothiophenes in LCO, especially those having substituted carbon number of 4-6, are hardly desulfurized by the proposed method<sup>143</sup>.

With respect to commercial oxidation process development, Petro Star Inc. recently announced a desulfurization technology which removes sulfur from diesel fuels using chemical oxidation<sup>144,145</sup>. Desulfurization of diesel fuel is accomplished by first forming a water emulsion with the diesel fuel. In the emulsion, the sulfur atom is oxidized to a sulfone using peroxyacetic acid<sup>138,145</sup>. This is followed by liquid/liquid extraction to remove the oxidized sulfur compounds using a solvent such as DMSO<sup>145</sup>. With oxygen atoms attached to the sulfur atom, the sulfur-containing molecules (sulfones) becomes polar and hydrophilic and then move into the aqueous phase. The overall oxidative desulfurization process may include liquid-phase oxidation, solvent extraction, solvent recovery, raffinate polishing by adsorption onto silica or alumina, and extract treatment such as chemical reaction or biochemical digestion<sup>138,145</sup>. Like biodesulfurization, some of the sulfones could be converted to a surfactant which could be sold to the soap industry at an economically desirable price; the earnings made from the sales of the surfactant could offset some of the cost of oxidative desulfurization<sup>144</sup>. Oxidative desulfurization has also been studied by other companies such as Unipure and Texaco<sup>146</sup>.

#### 4.4.7 Biodesulfurization

Biodesulfurization is a process that removes sulfur from fossil fuels using a series of enzyme-catalyzed reactions.<sup>147</sup> Biodesulfurization is another alternative processing method that has some similarity to the above-mentioned oxidative desulfurization, in that both methods oxidize sulfur atoms in the sulfur-containing compounds. Certain microbial biocatalysts have been identified that can biotransform sulfur compounds found in fuels, including ones that selectively remove sulfur from dibenzothiophene-type heterocyclic compounds.<sup>147</sup> Biocatalytic sulfur removal from fuels may have applicability for producing low sulfur gasoline and diesel fuels.

Figure 11 shows the general steps in the biodesulfurization system based on studies of various bacterial species.<sup>148</sup> Attention has been given to the microbial chemical pathway which can remove sulfur from substituted dibenzothiophenes with alkyl groups that hinder chemical catalysis and that resist removal by hydrodesulfurization. Monticello recently outlined sulfur-specific C<sub>x</sub>-DBT metabolism via the hydrocarbon-conserving (4S) pathway first proposed by Campbell and Kee Rhee<sup>148</sup>. The activity has been observed in many species of bacteria since the first confirmed isolation by Kilbane in 1988<sup>148</sup>. In most cases, the bacteria have been closely related and catalyze the same reaction.

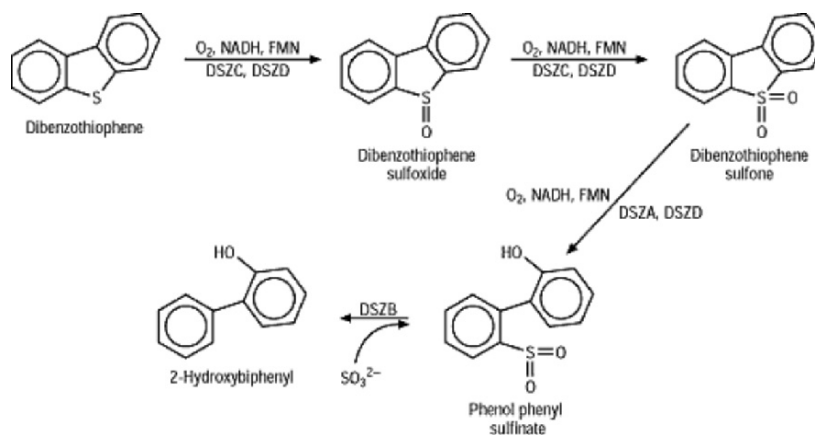


Figure 11. The pathway of biological desulfurization of model compound dibenzothiophene relies on biocatalysts for specificity. NADH is reduced nicotinamide adenosine dinucleotide; FMN is flavin mononucleotide; DSZA, DSZB, DSZC, and DSZD are the catalytic gene products of *dszA*, *dszB*, *dszC*, and *dszD*, respectively<sup>148</sup>.

A biodesulfurization process has been reported by Energy Biosystems<sup>148</sup>. It involves the removal of sulfur-containing hydrocarbon compounds from distillate (diesel) fuel or naphtha (gasoline) streams using bacteria. The distillate stream is first mixed with an aqueous media containing the bacteria,

caustic soda and nutrients for the bacteria. Enzymes in the bacteria first oxidize the sulfur atoms and then cleaves some of the sulfur-carbon bonds. Designs based on pilot plant studies combine biodesulfurization with conventional hydrotreating to produce diesel fuel containing 50 ppmw sulfur<sup>12</sup>. The sulfur leaves the process in the form of hydroxyphenyl benzene sulfonate, which can be used commercially as a feedstock to produce surfactants. Recently, utilization of by-products from biodesulfurization has also been reported and the process system is being explored<sup>149</sup>.

Better understanding of the mechanism of biodesulfurization, as shown in Figure 8, may be gained from some recent studies<sup>150-153</sup>. Gallagher et al.<sup>150</sup> reported a sulfur-specific pathway in microbial desulfurization of DBT. *Rhodococcus rhodochrous* strain IGTS8 metabolizes DBT in a sulfur-specific manner. Two routes of desulfurization have been identified. Under growth conditions, the intermediates are dibenzothiophene sulfoxide, dibenzothiophene sulfone, 2'-hydroxybiphenyl-2-sulfonate, and 2,2'-dihydroxybiphenyl<sup>150</sup>. Stationary phase cells produce 2-hydroxybiphenyl as the desulfurized product and use the 2'-hydroxybiphenyl-2-sulfinate, rather than the sulfonate, as the key intermediate<sup>150</sup>.

Piddington et al.<sup>152</sup> studied the sequence and molecular characterization of a DNA region encoding the DBT desulfurization operon of *Rhodococcus* sp. strain IGTS8. DBT can be desulfurized to 2-hydroxybiphenyl (2-HBP) by *Rhodococcus* sp. strain IGTS8<sup>152</sup>. Izumi et al.<sup>154</sup> isolated a DBT-degrading bacterium, *Rhodococcus erythropolis* D-1, which utilized DBT as a sole source of sulfur from soil. DBT was metabolized to 2-hydroxybiphenyl (2-HBP) by the strain, and 2-HBP was almost stoichiometrically accumulated as the dead-end metabolite of DBT degradation. DBT degradation by this strain was shown to proceed as DBT --> DBT sulfone --> 2-HBP. DBT at an initial concentration of 0.125 mM was completely degraded within 2 days of cultivation. DBT at up to 2.2 mM was rapidly degraded by resting cells within only 150 min. It was thought this strain had a higher DBT-desulfurizing ability than other microorganisms reported previously<sup>154</sup>.

Gray et al.<sup>153</sup> reported on the molecular mechanisms of biocatalytic desulfurization of DBT. *Rhodococcus* sp. strain IGTS8 has the ability to convert DBT to 2-hydroxybiphenyl (HBP) with the release of inorganic sulfur. The conversion of DBT to HBP is catalyzed by a multienzyme pathway consisting of two monooxygenases and a desulfinate. The final reaction catalyzed by the desulfinate appears to be the rate limiting step in the pathway<sup>153</sup>. Each of the enzymes has been purified to homogeneity and their kinetic and physical properties studied. Neither monooxygenase has a tightly bound cofactor and each requires an NADH-FMN oxidoreductase for activity (NADH is reduced nicotinamide adenosine dinucleotide; FMN is flavin mononucleotide). An NADH-FMN oxidoreductase has been purified from *Rhodococcus* and is a protein of approximately 25,000 molecular weight with no apparent sequence homology to any other protein in the databases. Gray et

al.<sup>153</sup> described a unique sulfur acquisition system that *Rhodococcus* uses to obtain sulfur from very stable heterocyclic molecules. According to Denome et al.<sup>151</sup>, *rhodococcus* sp. strain IGTS8 possesses an enzymatic pathway that can remove covalently-bound sulfur from DBT without breaking carbon-carbon bonds. The DNA sequence of a 4.0-kb BstBI-BsiWI fragment that carries the genes for this pathway was determined. Frameshift and deletion mutations established that three open reading frames were required for DBT desulfurization, and the genes were designated soxABC (for sulfur oxidation). Each sox gene was subcloned independently and expressed in *Escherichia coli* MZ1 under control of the inducible lambda p(L) promoter with a lambda cII ribosomal binding site. SoxC is similar to the 45-kDa protein that oxidizes DBT to DBT-5,5'-dioxide. SoxA is similar to the 50-kDa protein responsible for metabolizing DBT-5,5'-dioxide to an unidentified intermediate. SoxB is similar to the 40-kDa protein that, together with the SoxA protein, completes the desulfurization of DBT-5,5'-dioxide to 2-hydroxybiphenyl. Protein sequence comparisons revealed that the predicted SoxC protein is similar to members of the acyl coenzyme A dehydrogenase family but that the SoxA and SoxB proteins have no significant identities to other known proteins. The sox genes are plasmidborne and appear to be expressed as an operon in *Rhodococcus* sp. strain IGTS8 and in *E. coli*<sup>151</sup>.

Kobayashi et al.<sup>155</sup> studied the reaction mechanism of biodesulfurization using whole cells of *Rhodococcus erythropolis* KA2-5-1, which have the ability to convert DBT into 2-hydroxybiphenyl. The desulfurization patterns of alkyl DBTs were represented by the Michaelis-Menten equation. The values of rate constants, the limiting maximal velocity (V-max) and Michaelis constant (K-m), for desulfurization of alkyl DBTs were calculated. The relative desulfurization activities of various alkyl DBTs were reduced in proportion to the total carbon numbers of alkyl substituent groups. Alkyl DBTs that had a total of six carbons of alkyl substituent groups were not desulfurized. The type or position of alkyl substituent groups had little effect on desulfurization activity<sup>155</sup>. The desulfurization activity of each alkyl DBT, when mixed together, was reduced. This phenomenon was caused by apparent competitive inhibition of substrates. Using the apparent competitive inhibition model, the desulfurization pattern of a multiple components system containing alkyl DBTs was elucidated. This model was also applicable for biodesulfurization of light gas oil<sup>155</sup>.

Lee et al.<sup>156</sup> studied microbial desulfurization of DBTs bearing alkyl substitutions adjacent to the sulfur atom, such as 4,6-diethyldibenzothiophene (4,6-DEDBT), which are referred to as sterically hindered with regard to access to the sulfur moiety. By using enrichment cultures with 4,6-DEDBT as the sole sulfur source, bacterial isolates which selectively remove sulfur from sterically hindered DBTs were obtained. The isolates were tentatively identified as *Arthrobacter* species, 1,6-DEDBT sulfone was shown to be an

intermediate in the 4,6-DEDBT desulfurization pathway, and 2-hydroxy-3,3'-diethylbiphenyl (HDEBP) was identified as the sulfur-free end product<sup>156</sup>.

Omori et al.<sup>157</sup> isolated Strain SY1, identified as a *Corynebacterium* sp., on the basis of the ability to utilize DBT as a sole source of sulfur. Strain SY1 could utilize a wide range of organic and inorganic sulfur compounds, such as DBT sulfone, dimethyl sulfide, dimethyl sulfoxide, dimethyl sulfone, CS<sub>2</sub>, FeS<sub>2</sub>, and even elemental sulfur. Strain SY1 metabolized DBT to dibenzothiophene-5-oxide, DBT sulfone, and 2-hydroxybiphenyl, which was subsequently nitrated to produce at least two different hydroxynitrobiphenyls during cultivation<sup>157</sup>. These metabolites were separated by silica gel column chromatography and identified by nuclear magnetic resonance, UV, and mass spectral techniques. Resting cells of SY1 desulfurized toluenesulfonic acid and released sulfite anion. On the basis of these results, a new DBT degradation pathway is proposed.<sup>157</sup>

Several recent reviews outline the progress in the studies of the microbial desulfurization from the basic and practical point of view<sup>117,148,158</sup>. Biocatalytic sulfur removal from fuels has potential applicability for producing low sulfur gasoline and diesel. Microbial biocatalysts (microorganisms) have been identified that can biotransform sulfur compounds found in fuels, including ones that selectively remove sulfur from dibenzothiophene heterocyclic compounds to form 2-hydroxyl biphenyl and similar compounds. They are promising as biocatalysts in the microbial desulfurization of petroleum because, without assimilation of the carbon content, they remove only sulfur from the heterocyclic compounds, which are refractory to conventional chemical desulfurization<sup>158</sup>. Various bioreactor and bioprocess designs are being tested for use with biocatalysts, including recombinant biocatalysts, for use in removing sulfur from fuels and feedstocks within the petroleum refinery stream<sup>147</sup>. Both enzymological and molecular genetic studies are now in progress for the purpose of obtaining improved desulfurization activity of organisms. The genes involved in the sulfur-specific DBT desulfurization were identified and the corresponding enzymes have been investigated. Most attention is given to the 4S pathway of *Rhodococcus*, which can remove sulfur from substituted and unsubstituted dibenzothiophenes, including sulfur compounds that hinder chemical catalysis and that resist removal by mild hydrotreatment<sup>147</sup>. From the practical point of view, it has been proved that the microbial desulfurization proceeds in the presence of high concentrations of hydrocarbons, and more complicated DBT analogs are also desulfurized by the microorganisms<sup>148</sup>.

As summarized by McFarland et al.<sup>147</sup>, microbial sulfur-specific transformations have been identified that selectively desulfurize organic sulfur compounds in fossil fuels. Recent discoveries related to biodesulfurization mechanisms may lead to commercial applications of biodesulfurization through engineering recombinant strains for over-expression of biodesulfurization genes, removal of end product repression,



and/or by combining relevant industrial and environmental traits with improvements in bioprocess design<sup>147,159</sup>. With bioprocess improvements that enhance biocatalyst stability, achieve faster kinetics, improve mass transfer limitations, temperature and solvent tolerance, as well as broaden substrate specificity to attack a greater range of heterocyclic compounds, biocatalysis may be a cost-effective approach to achieve the production of low sulfur gasoline<sup>147</sup>. The challenge will be to accomplish these improvements by the time the regulations for ultra low sulfur gasoline and other vehicle fuels go into effect in order to be competitive with emerging non-biological desulfurization technologies<sup>147</sup>.

## **5. FCC FEED HYDROTREATING AND LCO UNDERCUTTING**

### **5.1 FCC Feed Hydrotreating for Sulfur Reduction in LCO**

Tables 6 and 7 show the properties of raw FCC feed and hydrotreated FCC feedstock<sup>160</sup>. The diesel fuel is produced from several blending stocks, of which light cycle oil (LCO) from FCC is a major blending stock that contributes to the sulfur in diesel pool. The FCC unit primarily produces gasoline, but it also produces a significant quantity of LCO. LCO is high in aromatics and sulfur and contains a relatively high fraction of the sterically hindered DBT-type compounds such as 4-MDBT and 4,6-DMDBT<sup>35,107</sup>. In general, sulfur could be removed before, after, or during FCC. Early in the processing train prior to the FCC unit, the most practical place to remove sulfur is feed hydrotreater. Many refineries already have an FCC feed hydrotreating unit; the LCO from these refineries should contain a much lower concentration of sterically hindered DBT compounds than refineries without hydrotreating their FCC feed<sup>12</sup>. However, adding an FCC feed hydrotreating unit is much more costly than distillate hydrotreating. Just on the basis of sulfur removal, FCC feed hydrotreating is more costly than distillate hydrotreating, even considering the need to reduce gasoline sulfur concentrations<sup>111</sup>. On the other hand, FCC feed hydrotreating provides environmental and economic benefits.

In conjunction with Tables 5 and 6, the data in Table 7 shows the impact of feed hydrotreating on FCC product yield and quality<sup>160</sup>. FCC feed hydrotreating decreases the sulfur contents of gasoline and diesel fuel significantly. It also increases the yield of relatively high value gasoline and LPG from the FCC unit and reduces the formation of coke on the FCC catalyst. For individual refiners, these additional benefits may offset the cost of FCC feed hydrotreating to make it more economical than post-FCC distillate hydrotreating. There are newly developed catalysts that have

optimized activity and pore structure for FCC feed hydrotreating, such as Akzo Nobel's KF 841 (NiMo) and KF 902 (NiCoMo).<sup>111</sup>

Table 7. Impact of Feed Hydrotreating on FCC Unit Performance

|                                | Raw Feed     |              | HDS          |              |
|--------------------------------|--------------|--------------|--------------|--------------|
|                                | Untreated    | 90% HDS      | 98% HDS      | 99% HDS      |
| <b>Yields, wt%</b>             |              |              |              |              |
| H <sub>2</sub> S               | 1.1          | 0.1          | 0.0          | 0.0          |
| C <sub>2</sub> -               | 3.3          | 3.5          | 3.2          | 2.8          |
| C <sub>3</sub> +C <sub>4</sub> | 16.3         | 17.6         | 18.7         | 19.9         |
| Full-range naphtha             | 48.3         | 51.5         | 52.5         | 53.6         |
| LCO                            | 16.7         | 15.7         | 15.0         | 14.0         |
| CSO                            | 9.0          | 6.6          | 5.9          | 5.2          |
| Coke                           | 5.4          | 5.0          | 4.7          | 4.4          |
| <b>Total</b>                   | <b>100.0</b> | <b>100.0</b> | <b>100.0</b> | <b>100.0</b> |
| <b>Conversion, vol%</b>        | 74.3         | 77.7         | 79.1         | 80.8         |
| <b>Key product properties</b>  |              |              |              |              |
| Naphtha RON                    | 93.2         | 93.0         | 92.9         | 92.7         |
| Naphtha MON                    | 80.5         | 80.8         | 81.1         | 81.0         |
| LCO cetane index               | 25.7         | 25.7         | 26.4         | 26.5         |
| <b>Product sulfur, wppm</b>    |              |              |              |              |
| H <sub>2</sub> S               | 10,066       | 753          | 188          | 94           |
| Naphtha                        | 3,600        | 225          | 55           | 18           |
| LCO                            | 29,700       | 3,400        | 900          | 300          |
| CSO                            | 57,800       | 11,000       | 3,000        | 1,100        |
| Coke                           | 30,300       | 5,700        | 1,554        | 516          |
| SOx, vppm                      | 2,030        | 410          | 120          | 42           |

Source:<sup>160</sup>

## 5.2 Undercutting LCO

It is conceivable that the sulfur-rich fractions, if they have a narrow boiling range, could be separated out (undercut) by a distillation operation. Undercutting has been considered for both gasoline feed<sup>162</sup>, which may require better naphtha fractionation<sup>163</sup>, and for diesel feeds, in which sulfur compounds and nitrogen compounds tend to concentrate more in high boiling point range of 300-400 °C<sup>164</sup>. A major stumbling block to ultra deep hydrodesulfurization to sulfur levels meeting the 15 ppm cap is the presence of sterically hindered DBT-type compounds, particularly those with two methyl or ethyl groups at 4- and 6-positions blocking the sulfur atom. These compounds are found in greatest concentration in LCO, which itself is highly aromatic. These compounds can be desulfurized readily if saturated. However, due to the much higher hydrogen cost of doing so, it is better economically if this can be avoided. One option is to drop the sulfur-rich fraction out of diesel feed. Because these compounds are inherently large in molecular weight due to their chemical structure, they distill near the high end of the diesel range of distillation temperatures. This makes it possible to segregate these compounds from the rest of the cracked stocks via distillation

and avoid the need to desulfurize them. Once separated, this LCO material could be mixed into the refinery streams currently being used to produce off-highway diesel fuel (maximum sulfur: 2000 ppmw to 3000 ppmw) and heating oil (maximum sulfur: 2000 ppmw to 5000 ppmw depending on the state). These fuels would still have to meet applicable quality specifications, such as cetane, density, sulfur and distillation. For example, the industry specification for non-road diesel fuel is a minimum of 40 cetane number, and a maximum sulfur concentration of 5,000 ppm. An analysis of off-highway diesel fuel shows that off-highway diesel fuel averages 44.4 cetane number, 3,300 ppm sulfur, 34.5 API gravity, T10 of 438 °F, T50 of 517 °F, and T90 of 600 °F<sup>165</sup>. Refiners may need to use cetane additives to compensate for the addition of LCO to maintain off-highway fuel cetane levels similar to those of current in-use fuels. Additional cold-flow additives<sup>166</sup> might also be necessary for off-highway diesel fuel in the winter to maintain cold-flow performance at current levels. Refiners would allow other off-highway and heating oil properties to change as a result of the addition of LCO, while continuing to ensure that all specifications on these fuels are met<sup>12</sup>.

Since LCO contains more refractory sulfur compounds, shifting LCO to off-highway diesel fuel and heating oil could prevent the need to desulfurize a sizeable fraction of the sterically hindered DBT compounds currently present in highway diesel fuel. For example, Albemarle studies indicate that a drop of 10 °C in the T95 (temperature for 95 % distillation) of diesel fuel decreases sulfur from 50 - 60 ppmw<sup>12,167</sup>. Of course, such a shift to non-highway diesel fuel markets would decrease the amount of highway diesel fuel produced, about 3 % for the typical refinery, if more easy-to-hydrotreat material was not switched from non-highway diesel fuels to the highway diesel fuel pool. A decrease of T95 of this magnitude effected by undercutting only LCO would decrease sulfur even more because the sulfur levels in the heaviest portions of LCO are much greater than those in SRLGO and are the most difficult to be desulfurized. Shifting only heavy LCO would increase the sulfur reduction per volume of highway diesel fuel lost, but would still result in a net loss of highway diesel fuel production if no other feedstocks replaced it.

While this heavy LCO material could be shifted to other markets, this does not necessarily have to be the case. Under certain conditions, this material can be recycled to the FCC unit<sup>168</sup>. For this to be feasible, the refiner must hydrotreat the FCC feed at a pressure sufficient to desulfurize the sterically hindered sulfur containing compounds and the feed hydrotreater must have sufficient excess capacity to handle the additional material. This material could also be sent to an existing hydrocracker, if sufficient capacity existed, and converted into gasoline blendstock. Alternatively, it could be hydrotreated separately under more severe conditions to remove the sulfur, such as with SynAlliance's SynShift process<sup>169</sup>. This would entail higher hydrogen consumption per barrel of treated material because of some aromatic saturation. However, the amount of material being processed would

be small, so overall hydrogen consumption would still be low. There are various projections on the distillate hydrodesulfurization technology needed to meet a range of highway diesel fuel sulfur levels<sup>12</sup>. These projections were developed to support refining cost studies conducted by the Engine Manufacturers Association and the American Petroleum Institute, and the National Petroleum Council<sup>12</sup>. These projections addressed compliance with three different average sulfur levels: 10, 30 and 100 ppmw. Generally, these projections indicate that it will be possible for refiners to meet the 10 ppmw average sulfur level without resorting to catalysts and operating conditions which reduce aromatic levels dramatically.

## 6. DEEP HYDROGENATION OF DIESEL FUELS

### 6.1 Benefits of Aromatics Reduction

High aromatic content in distillate fuels lowers the fuel quality and contributes significantly to the formation of environmentally harmful emissions<sup>170,171</sup>. Reducing aromatic content along with sulfur content is generally desirable with respect to diesel fuel quality, as aromatic reductions increase cetane levels and generally improve combustion characteristics. California Air Resources Board (CARB) passed legislative measures to limit the sulfur and aromatic contents of diesel fuel to 0.05 wt% and 10 vol%, respectively, effective October 1993<sup>1,3</sup>. More recently, the Texas Natural Resources Conservation Commission<sup>172</sup> has announced new Low Emission Diesel Fuel Program. This program, which begins April 1, 2005, limits all diesel fuel sold or supplied for use in on-road vehicles and in nonroad equipment in the affected 110 county region in Texas, to a maximum sulfur content of 500 ppmw, a maximum aromatic hydrocarbons content of 10%, and a minimum cetane number of 48. Beginning June 1, 2006, the maximum sulfur content of LED (low emission diesel) used in both on-road vehicles and non-road equipment in the affected 110 county regions in Texas will be reduced to 15 ppm<sup>172</sup>.

Aromatics saturation by catalytic hydrotreating can increase cetane number significantly<sup>1</sup>. One of the significant findings by the US Auto/Oil Air Quality Improvement Research Program (which involved Ford, General Motors, Chrysler, and the 14 largest US petroleum companies) is that lowering aromatic content lowers toxic emissions<sup>2,173</sup>. The significant findings of the European Program on Emissions, Fuels, and Engine Technologies (EPEFE) also include the following related to aromatics: 1) decreasing aromatics reduces catalytic converter light-off time, improves the converter efficiency and decreases exhaust hydrocarbons; and 2) decreasing fuel polyaromatics reduces light-duty diesel exhaust nitrogen oxides, particulate material and

heavy-duty exhaust hydrocarbons, nitrogen oxides, and particulate material<sup>173</sup>.

## 6.2 Challenges of Deep Dearomatization

Currently, conventional hydrotreating technology is adapted for dearomatization by aromatics saturation<sup>170</sup>. Typical conventional catalysts for fuel hydroprocessing are sulfided Co-Mo and Ni-Mo supported on alumina. Some studies have shown that complete hydrogenation of aromatics is not possible owing to equilibrium limitations under typical hydrotreating conditions. Conventional middle distillate hydrotreaters designed to reduce sulfur and nitrogen levels would lower the diesel aromatics only marginally.<sup>170,174</sup> For example, Ali and Siddiqui<sup>175</sup> compared 3 types of hydrotreating catalysts, CoMo/Al<sub>2</sub>O<sub>3</sub>, NiMo/Al<sub>2</sub>O<sub>3</sub> and NiW/Al<sub>2</sub>O<sub>3</sub>, for dearomatization of light cycle oil. They observed that the type of catalyst has a critical influence on the composition and properties of the product<sup>175</sup>. Divergent effects of aromatics content and molecular weight on the cetane index by these catalysts occurred. Their data show that it was not possible to obtain a diesel product that meets stringent specifications using one type of catalyst in a single-stage reactor, even under severe operating conditions<sup>175</sup>.

Deep hydrogenation may become necessary in the near future for reducing aromatic contents of distillate fuels to meet increasingly stringent regulations. As hydrogenation is exothermic, deep hydrogenation is favored at a lower temperature. However, conventional hydrotreating catalysts are active only at relatively high temperatures (e.g., >300°C). It is therefore natural to consider deep hydrogenation at low temperatures (e.g., <300°C). The potential candidate catalysts for low-temperature hydrotreating include noble metals. Since it is known that noble metal catalysts are easily deactivated by sulfur compounds, a two-stage processing strategy is being adopted. The first stage involves deep desulfurization of the fuels using metal sulfide catalysts, and the second stage deals with hydrogenation over a noble metal catalysts. Such a two-stage processing scheme is being practiced by the industry in both the U.S. and Europe, as discussed below. Aromatic structures in diesel fuels are shown in Scheme 3.

## 6.3 Application of Noble Metal Catalysts

While noble metals are active for hydrogenation at low temperatures, their use is limited because of their sensitivity to sulfur poison. In current processing schemes involving noble metal catalysts, two or more stages with multiple catalyst beds are used to achieve deep desulfurization and deep hydrogenation. Hydrodesulfurization occurs in the first stage over a Ni-Mo or Co-Mo catalyst, followed by intermediate byproduct gas removal. Finally, hydrogenation over the noble metal catalyst operates in the last stage or

bottom bed where the concentrations of catalyst poisons (organosulfur and  $\text{H}_2\text{S}$ ) are extremely low<sup>120,176</sup>. Commercial examples of two-stage or multi-stage hydroprocessing technology include the Shell Middle Distillate Hydrogenation process by Shell<sup>176,177</sup>, the Dual-Stage Process by Haldor-Topsøe<sup>171</sup>, and hydrotreating process by IFP<sup>178</sup>, and the SynSat process developed by Criterion/Lummus<sup>120,179</sup>. There are no reports of noble metal catalysts that can operate without such intermediate  $\text{H}_2\text{S}$  removal<sup>176</sup>.

Figure 12 shows the SynSat process based on published information.<sup>120,179,180</sup> The SynSat process is considered to be an innovation across the boundary between catalysis and reactor engineering<sup>120</sup>. SynSat employs several different catalyst beds within a single reactor shell with intermediate by-product gas ( $\text{H}_2\text{S}$  etc.) removal, and optional counter-current gas-flow. Catalysts **A** and **B** in Figure 9 are metal sulfide catalysts such as sulfided Ni-Mo. Catalyst **C** is a noble metal loaded on an acidic support such as zeolite. There is an intermediate gas removal between the beds of Catalysts **B** and **C**. Nearly all the sulfur compounds must be converted and removed as  $\text{H}_2\text{S}$  on beds **A** and **B** before the fuel feed reaches the noble metal catalyst bed **C**.

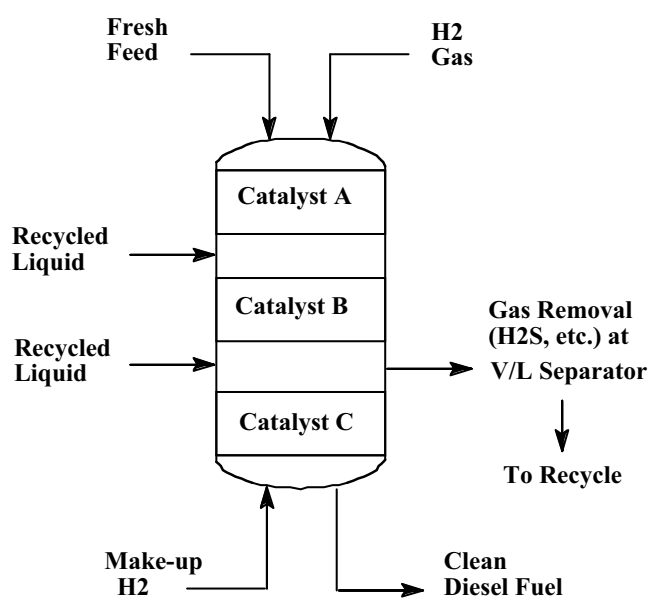


Figure 12. SynSat/SynShift process with Criterion/Lummus catalytic hydrotreating reactor technology, with intermediate by-product gas removal and counter-current gas-flow<sup>181</sup>.

In addition to the SynSat process, which was developed to provide an economic solution to aromatic reduction of diesel fuels, the SynShift process was recently developed for making high-quality diesel fuels with higher cetane number<sup>169,179</sup>. SynShift is a selective ring-opening process; it aims at not only heteroatom removal, but also ring-opening, thus shifting the product

boiling range for the production of lighter diesel fuel with higher quality. The typical reactor pressures and temperatures in SynSat and SynShift process range from 30 to 61 atm (450-900 psig) and from 315 to 400 °C (600 to 750 °F), depending on the feedstocks and required product properties<sup>180</sup>. SynShift upgrading of a feed that was made of 28% SRGO, 33% LCO, and 39% LCGO gave the following improvements<sup>180</sup>:

| Property                   | Feed   | Product |
|----------------------------|--------|---------|
| Gravity, °API              | 25.0   | 33.1    |
| Sulfur, ppmw               | 15,150 | 2       |
| Nitrogen, ppmw             | 631    | <1      |
| Aromatics, wt%             | 64.7   | 34.3    |
| Cetane Index, D-976        | 34.2   | 43.7    |
| Liquid Yield on feed, vol% | 103.5  |         |

A recent report by Shell Research and Technology Center<sup>176</sup> showed that commercial noble metal-based catalysts for deep hydrogenation of fuels operate in a regime where the large majority of the metal sites are poisoned by sulfur, even when sulfur tolerance has been improved by choosing modern support functions and metals. Thus, these catalysts are currently used only after a deep desulfurization over Ni-Mo catalysts and subsequent removal of H<sub>2</sub>S, as is also the case in the Shell Middle Distillate Hydrogenation process and the Lummus/Criterion SynSat process<sup>120,176</sup>. Noble metal catalysts that can operate in a stacked-bed reactor with a Ni-Mo catalyst without intermediate H<sub>2</sub>S removal have not been reported<sup>176</sup>.

## 7. DESIGN APPROACHES TO DEEP HYDROGENATION

### 7.1 Deep Hydrogenation at Low Temperatures

We have been exploring sulfur-resistant noble metal catalysts for more efficient hydrotreating of sulfur-containing distillates at low temperatures to produce cleaner transportation fuels. More recently, a new approach has been proposed for the design of sulfur-resistant noble metal catalysts for low-temperature hydrotreating and dearomatization (LTHDA) of sulfur-containing distillates to produce clean distillate fuels<sup>28,29</sup> such as diesel fuels and jet fuels. The proposed concept invokes the use of acidic zeolite support, shape-selective exclusion, differentiation of sulfur resistance, and hydrogen spillover for the design of highly sulfur-tolerant noble-metal catalysts<sup>29</sup>. Because of its importance, sulfur resistance of noble metal catalysts has been the subject of a number of studies<sup>32,106,174,182-185</sup>.

Figure 13 shows a simplified representation of the LTHDA catalyst design concept recently proposed<sup>28</sup>. It invokes some unique acidic zeolites with bimodal pore structure as supports for noble metals and utilizes (1) shape-selective exclusion, (2) hydrogen spillover, and (3) two types of sulfur resistance. Unique zeolite supports can be used to prepare bimodal distributions of noble metal particles. Some metals are located in small pores (**Sm**: pore opening less than about 5 Å); whereas, others will be contained in large pores (**La**: pore opening larger than 6 Å). Preferably, the two pore systems inter-connect, or are at least uniformly distributed so that they are in close proximity. Diffusion of organosulfur compounds such as thiophenic molecules into the small-pores would be inhibited by size (shape-selective exclusion). The large pores (large micropore or mesopore range) would preferably allow fast diffusion and reaction of bulky polycyclic aromatic and sulfur compounds. The thiophenic molecules could enter the large pores, but not the small pores. However, H<sub>2</sub> molecules can readily enter both types of pores, dissociatively adsorb on metal contained within, and be transported between pore systems by spillover. When the metal in the large pores becomes inactivated by adsorbed sulfur, spillover hydrogen could recover the poisoned metal sites by elimination of R-S-R and R-S-H. It is also of interest to classify sulfur resistance as either type I, resistance to organic sulfur compounds, or type II, resistance to inorganic H<sub>2</sub>S. The metal species, particularly those in small pores, should have higher type II sulfur resistance.

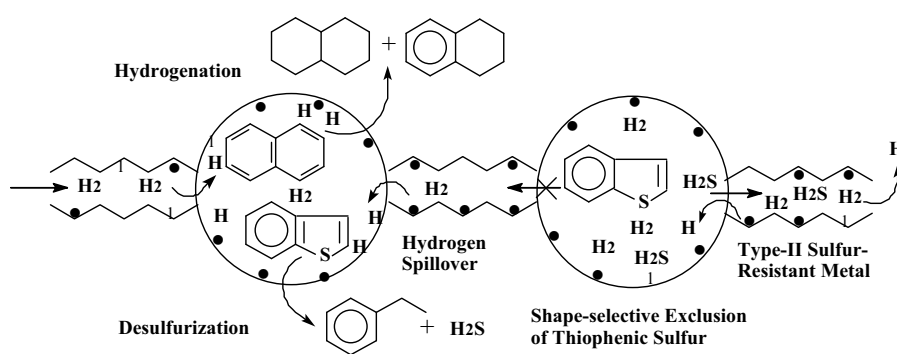


Figure 13. The proposed new concept for LTHDA catalyst design based on shape-selective exclusion, hydrogen spillover, and two types of sulfur resistance. The black dots indicate metal particles on internal surface<sup>28</sup>.

Mesoporous molecular sieve MCM-41 has been used as support for new hydrogenation catalysts<sup>186-188</sup>. In the study by Corma et al., the hydrogenation activity of Pt supported on two mesoporous MCM-41 samples differing in their chemical composition has been examined by following the kinetics of the hydrogenation of naphthalene at 225-275 °C and 5.0 MPa total pressure and by comparing the kinetic parameters obtained with Pt supported



on a mesoporous amorphous silica-alumina (MSA) and other conventional supports, such as commercial amorphous silica-alumina (ASA), zeolite USY, gamma-alumina, and silica. The two mesoporous MCM-41 and MSA materials having very high surface areas allowed for a better dispersion of the Pt particles, and they showed a superior overall hydrogenation activity as compared to the other supports. However; Pt/USY displayed the highest turnover (activity per exposed surface Pt), owing to the interaction of small Pt aggregates in the supercage of the zeolite with the strong Bronsted acid sites associated to framework aluminum forming electron-deficient Pt species of known enhanced activity<sup>188</sup>. Moreover, both the Al-MCM-41 and USY-based catalysts presented the highest sulfur tolerance during the hydrogenation of a naphthalene feed containing 200 ppmw sulfur added as DBT<sup>188</sup>. The high metal dispersion and the interaction of the small Pt clusters with the mildly acidic sites present in Al-MCM-41 may account for its high sulfur tolerance. The superior hydrogenation activity and sulfur tolerance of Pt-MCM-41 catalyst observed in the naphthalene experiments were further confirmed during the hydrogenation of a hydrotreated LCO feed containing about 70 wt% aromatics and 400 ppmw sulfur<sup>188</sup>.

Fujikawa et al.<sup>189</sup> examined the potential of B<sub>2</sub>O<sub>3</sub>-Al<sub>2</sub>O<sub>3</sub>-supported bimetallic Pt-Pd catalysts for aromatic hydrogenation of middle distillate fuels. The activity measurements were carried out with hydrotreated LCO/straight-run light gas oil (SRLGO) feed containing 33 vol% aromatics and 320 ppm sulfur under practical conditions. They observed that Pt-Pd/B<sub>2</sub>O<sub>3</sub>-Al<sub>2</sub>O<sub>3</sub> catalysts have much higher activity for aromatic hydrogenation as compared to Pt-Pd/Al<sub>2</sub>O<sub>3</sub> catalysts

## 7.2 Saturation of Aromatics in Commercial Process

Haldor Topsøe has developed a two-stage HDS/HDA process for deep hydrogenation of aromatics in distillate fuels, in which the first stage uses their base-metal catalyst such as TK-573 for hydrodesulfurization, while the second stage uses their noble metal catalysts, either TK-907/TK908 or TK-915, which is a newly developed high-activity dearomatization catalyst<sup>190</sup>. United Catalysts and Sud-Chemie AG have published data on the performance of their ASAT catalyst, which uses platinum and palladium<sup>12</sup>. The focus of their study was to reduce aromatics to less than 10 volume % starting with a feed distillate containing up to 500 ppmw sulfur and at least 100 ppmw nitrogen. Starting with a feed distillate containing 400 ppmw sulfur and 127 ppmw nitrogen and 42.5 volume % aromatics, the ASAT catalyst was able to reduce sulfur to eight to nine ppmw, essentially eliminate nitrogen and reduce aromatics to two to five vol%. Hydrogen consumption was 800-971 standard cubic feet per barrel (SCFB).<sup>12</sup>

IFP, in conjunction with various catalyst manufacturers, offers its Prime D technology for deep desulfurization, aromatics saturation and cetane

improvement. Using a NiMo catalyst, IFP's Prime D process can produce distillate sulfur levels of 10 ppmw from SRLGO and of less than 20 ppmw from distillate containing 20-100% cracked material using a single stage reactor. With a two-stage process, less than one ppmw sulfur can be achieved.<sup>12</sup>

Criterion and ABB Lummus have been licensing their SynTechnology, and as of August 2, 1999, there were 24 units either in operation or in the process of being constructed. Their purposes range from desulfurization to desulfurization plus dearomatization to mild hydrocracking. Of particular interest here is a revamp of an existing two reactor distillate hydrotreater at the Lyondell / Citgo refinery in Texas. The revamped unit was designed to process a low-cost feed very heavily weighted towards cracked material (65-70 % LCO and LCGO).<sup>12</sup> One existing reactor was converted to SynSat Technology, while the other was used simply as a flash drum. A new first-stage reactor was added. Both reactors were designed to operate in a co-current fashion. Pilot plant studies predicted average sulfur and aromatics levels of seven ppmw and 31 volume %, respectively, based on feed sulfur and aromatics levels of 11,900 ppmw and 53 volume %, respectively. The unit exceeded expectations in the case of sulfur, producing an average sulfur level of less than five ppmw from a feed sulfur level of 13,800 ppmw. The actual aromatic level achieved was above the target by four volume %, but the feed aromatic level was five volume % higher than expected. Thus, the net reduction in aromatic content in terms of volume % was still higher than found in the pilot plant. ABB Lummus and Criterion indicate that their catalyst technology is sufficiently flexible to focus on the deep desulfurization with or without the significant aromatics reduction seen.<sup>12</sup>

## 8. SUMMARY AND CONCLUSIONS

There exist various sulfur compounds in transportation fuels that differ in ring size, substitution pattern, and reactivities. Heightened concerns for cleaner air and increasingly more stringent regulations on sulfur contents in transportation fuels will make desulfurization more and more important. The sulfur problem is becoming more serious in general, particularly for diesel fuels, as the regulated sulfur content is getting an order of magnitude lower, while the sulfur contents of crude oils refined in the U.S. are becoming higher and higher.

The chemistry of diesel fuel processing has evolved significantly around the central issue of how to produce ultra-low sulfur diesel fuels and low-aromatic diesel fuels in a more efficient and environmentally friendly fashion. New design approaches are necessary for making affordable ultra-clean diesel and gasoline.

Design approaches include (1) shift in thinking paradigms; (2) new catalyst design concepts; (3) new processing schemes; (4) novel integrated and compact sulfur removal systems. It has become more and more difficult for making ultra-low-sulfur fuels by using conventional processes, and new approaches are needed to remove sulfur more effectively and to even far below sulfur levels required by US EPA Tier II regulations in 2006.

Catalysis, adsorption, material formulation, reactor configuration, processing and engineering studies all have important roles to play for developing affordable ultra-clean fuels.

We need to begin with end in mind: road to zero-sulfur. One case which presents a great challenge to ultra-deeper desulfurization of liquid hydrocarbon fuels is the fuel processor for proton-exchange membrane fuel cells and also solid oxide fuel cells, which require essentially near zero-sulfur fuels.

## 9. ACKNOWLEDGMENTS

We are grateful to Prof. Harold H. Schobert of PSU for his encouragement and general discussions on fuel chemistry, to our coworkers including Dr. Uday Turaga, Mr. Gang Wang, Dr. Jian Zheng, and Mr. Michael Sprague of PSU for helpful discussions on diesel fuel desulfurization and hydrogenation. We also wish to thank Prof. Isao Mochida of Kyushu University, Japan, Dr. Henrik Topsøe of Haldor Topsøe, and Dr. Slavik Kasztelan of IFP, France, for helpful discussions on diesel hydrodesulfurization. We are pleased to acknowledge the US Department of Energy, National Energy Technology Laboratory, US Department of Defense, US Air Force Office of Scientific Research, US Defense Advanced Research Project Agency, and New Energy and Industrial Development Organization (NEDO) of Japan for partial financial support of various portions of our research.

## 10. GLOSSARY OF TERMS

DBT: dibenzothiophene  
4,6-DMDBT: 4,6-dimethyldibenzothiophene  
4,6-DEDBT: 4,6-diethyldibenzothiophene  
EIA: Energy Information Administration  
EPA: Environmental Protection Agency  
FCC: Fluid catalytic cracking  
GO: gas oil, a middle distillate fraction from  
HBP: hydroxybiphenyl  
HDS: hydrodesulfurization  
HDSGS: HDS of concentrated sulfur fraction  
LCO: light cycle oil, derived from FCC

LED: low emission diesel  
LGO: light gas oil  
LHSV: liquid hourly space velocity  
LTHDA: low-temperature hydrotreating and dearomatization  
MBPD: million barrels per day  
4,6-MDBT: 4-methyldibenzothiophene  
ppm: parts per million  
ppmw: parts per million by weight  
RIA: regulatory impact analysis  
PASH: polycyclic aromatic sulfur heterocycles  
SARS: selective adsorption for removing sulfur  
SRGO: straight-run gas oil  
ULSD: ultra low sulfur diesel fuel

## 11. REFERENCES

1. Lee, S. L., De Wind, M., Desai, P. H., Johnson, C. C., and Asim Mehmet, Y. Aromatics Reduction and Cetane Improvement of Diesel Fuels. *Fuel Reformulation*, 1993, 5, 26-31.
2. Unzelman, G. H. Fuel Projections and Technology Closer to Reality. *Fuel Reformulation*, 1993, 5, 38-44.
3. Khan, M. R., and Reynolds, J. G. Formulating a Response to the Clean Air Act. *Chemtech*, 1996, 26, 56-61.
4. US EPA. Diesel Fuel Quality: Advance Notice of Proposed Rulemaking. EPA420-F-99-011, Office of Mobile Sources, May 1999.
5. Brady, A. Global Refining Margins Look Poor in Short Term, Buoyant Later Next Decade. *Oil Gas J.*, 1999, 97 (46), 75-80.
6. Song, C., Hsu, S. and Mochida, I. Eds. *Chemistry of Diesel Fuels*, New York: Taylor & Francis 2000.
7. Dyroff, G. V. Manual on Significance of Tests for Petroleum Products. 5<sup>th</sup> Ed. Philadelphia: ASTM, 1989, 169 pp.
8. Corbett, R. A. Tougher Diesel Specs Could Force Major Refining Industry Expenditures. *Oil Gas J.*, 1987, May 30 issue, 56-59.
9. EPA-Gasoline RIA. Regulatory Impact Analysis – Control of Air Pollution from New Motor Vehicles: Tier 2 Motor Vehicle Emissions Standards and Gasoline Sulfur Control Requirements. U.S. Environmental Protection Agency, Air and Radiation EPA420-R-99-023, December 1999.
10. EPA-RFG-II. Phase II RFG Report on Performance Testing. U.S. Environmental Protection Agency, Air and Radiation EPA420-R-99-025, April 1999.
11. EPA, Control of Air Pollution from New Motor Vehicles Amendment to the Tier-2/ Gasoline Sulfur Regulations, US Environmental Protection Agency, April 13, 2001, <http://www.epa.gov/fedrgstr/EPA-AIR/2001/April/Day-13/a8927.htm>.
12. EPA-Diesel RIA. Regulatory Impact Analysis: Heavy-Duty Engine and Vehicle Standards and Highway Diesel Fuel Sulfur Control Requirements. United States Environmental Protection Agency, Air and Radiation EPA420-R-00-026, December 2000.
13. EPA, EPA Gives the Green Light on Diesel Sulfur Rule, Press Release, United States Environmental Protection Agency, February 28, 2001.
14. EPA. Reducing Nonroad Diesel Emissions. US Environmental Protection Agency, April 2003. <http://www.epa.gov/nonroad/f03008.htm#q3>,
15. SAE, Automotive Gasoline, SAE J312 October 1988, Society of Automotive Engineers, Warrendale, PA, February 1992.

16. SAE, Diesel Fuels, SAE J313 June 1989, Society of Automotive Engineers, Warrendale, PA, February 1992.
17. Owen, K., Coley, T., Automotive Fuels Reference Book, 2<sup>nd</sup> ed. Society of Automotive Engineers, Warrendale, PA, February 1995, 963 pp.
18. News-EPA. Government Developments-EPA. *Oil Gas J.*, Jan 1, 2001, p.7.
19. EIA/AER, Annual Energy Review 2001, Energy information administration, U.S. Department of Energy, Washington D.C., 2002.
20. IA/IEA. International Energy Annual 2001, Energy information administration, U.S. Department of Energy, Washington D.C., 2002.
21. Swain E.J. US Crude Slate Gets Heavier, Higher in Sulfur. *Oil Gas J.*, 1991, 89 (36), 59-61.
22. Swain E.J. US Refining Crude Slates Continue Towards Heavier Feeds, Higher Sulfur Contents. *Oil Gas J.*, 1998, 96 (40), 43-48.
23. Swain, E.J. Crudes Processed in the US Refineries Continue to Decline in Quality. *Oil Gas J.*, 2002, 100, 40-45.
24. Lawson, W.F. Clean Transportation Fuels in the United States. Paper presented at Third US-China Oil and Gas Industry Forum. Beijing, China, September 10-12, 2001.
25. Romanow-Garcia, S. Cleaner fuel-it's just not that simple, *Hydrocarbon Process.* 2000, 79, 17.
26. Ma, X., Lu, S., Yin, Z. and Song, C. *Am. Chem. Soc. Div. Fuel. Chem. Prepr.* 2001, 46(2), 648-649.
27. Ma, X., Sprague, M., Lu, S., and Song, C. *Am. Chem. Soc. Div. Fuel. Chem. Prepr.* 2002, 47(2), 452.
28. Song, C. Designing Sulfur-Resistant, Noble-Metal Hydrotreating Catalysts. *Chemtech*, 1999, 29 (3), 26-30.
29. Song, C. Sulfur-Resistant Noble Metal Catalysts Based on Shape-Selective Exclusion and Hydrogen Spillover. Chapter 27 in *Shape-Selective Catalysis. Chemicals Synthesis and Hydrocarbon Processing* (ACS Symposium Series 738), C. Song, J. M. Garces and Y. Sugi, eds. Washington D.C.: American Chemical Society, 1999, pp. 381-390.
30. Song, C. Catalytic Fuel Processing for Fuel Cell Applications. Challenges and Opportunities. *Am. Chem. Soc. Div. Fuel Chem. Prepr.*, 2001, 46 (1), 8-13. 33.
31. Song, C., and Reddy, K. M. Mesoporous Zeolite-Supported Co-Mo Catalyst for Hydrodesulfurization of Dibenzothiophene in Distillate Fuels. *ACS Div. Petrol. Chem. Preprints*, 1996, 41, 567-573.
32. Song, C., Reddy, K. M. Mesoporous Molecular Sieve MCM-41 Supported Co-Mo Catalyst for Hydrodesulfurization of Dibenzothiophene in Distillate Fuels. *Appl. Catal. A: Gen.*, 1999, 176, 1-10.
33. Song, C. Introduction to Chemistry of Diesel Fuel. Chapter 1 in *Chemistry of Diesel Fuels*. C. Song, S. Hsu and I. Mochida, eds., New York: Taylor & Francis, 2000.
34. Turaga, U.T.; Song, C. Deep Hydrodesulfurization of Diesel and Jet Fuels Using mesoporous Molecular Sieve-Supported Co-Mo/MCM-41 Catalysts. *Am. Chem. Soc. Div. Petrol Chem. Preprints*, 2001, 46 (3), 275-279.
35. Turaga, U.T.; Song, C. *Am. Chem. Soc. Div. Fuel Chem. Preprints*, 2002, 47 (2), 457.
36. Velu, S., Ma, X. Song, C. Selective Adsorption for Removing Sulfur from Jet Fuel over Zeolite-Based Adsorbents. *Ind. Eng. Chem. Res.* 2003, 42, 5293-5304.
37. Song, C. Fuel Processing for Low-Temperature and High-Temperature Fuel Cells. Challenges, and Opportunities for Sustainable Development in the 21<sup>st</sup> Century. *Catalysis Today*, 2002, 77 (1), 17-50.
38. Kabe, T., Ishiharam A. and Tajima, H. Hydrodesulfurization of Sulfur-Containing Polyaromatic Compounds in Light Oil. *Ind. Eng. Chem. Res.*, 1992, 31, 1577-1580.
39. Tajima, H., Kabe, T., and Ishiharam A. Separation and Analysis of Sulfur-Containing Polyaromatic Hydrocarbons in Light Oil. *Bunseki Kagaku*, 1993, 42, 6775.
40. Kabe, T., Ishiharam A. and Qian, W. Hydrodesulfurization and Hydrodenitrogenation. *Chemistry and Engineering*. Kodansha, Tokyo, Japan, 1999, 374 pp.

41. Ma, X., Sakanishi, K., and Mochida, I. Hydrodesulfurization Reactivities of Various Sulfur Compounds in Diesel Fuel, *Ind. Eng. Chem.*, 1994, 33, 218-222.
42. Ma, X., Sakanishi, K., and Mochida, I. Hydrodesulfurization Reactivities of Various Sulfur Compounds in Vacuum Gas Oil. *Ind. Eng. Chem. Res.* 1996b, 35, 2487-2494.
43. Ma, X., Sakanishi, K., Isoda, T., and Mochida, I. Determination of Sulfur Compounds in Non-polar Fraction of Vacuum Gas Oil. *Fuel* 1997, 76, 329-339.
44. Hsu, C. S., Genowitz, M. W., Dechert, G. J., Abbott, D. J. and Barbour, R. Molecular Characterization of Diesel Fuels by Modern Analytical Techniques. Chapter 2 in *Chemistry of Diesel Fuels*. C. Song, S. Hsu and I. Mochida, eds., New York: Taylor & Francis, 2000.
45. Drinkwater, D., Hsu, C. S. GC/MS in the Petroleum Industry. in *Current Practice in GC/MS*. New York: Marcel Dekker, 2001.
46. Depauw, G.A.; Froment, G.F. Molecular analysis of the sulphur components in a light cycle oil of a catalytic cracking unit by gas chromatography with mass spectrometric and atomic emission detection. *Journal Of Chromatography A*, 1997, 761 (1-2), 231-247.
47. Chawla, B. and Sanzo, F. D. Determination of sulfur components in light petroleum streams by high-resolution gas chromatography with chemiluminescence detection. *J. Chromatogr.* 1992, 589, 271-279
48. Lai, W.-C. and Song, C. Temperature-Programmed Retention Indices for GC and GC-MS Analysis of Coal- and Petroleum-derived Liquid Fuels. *Fuel*, 1995, 74 (10), 1436-1451.
49. Edwards, T., System Drivers for High Heat Sink Fuels. *Am. Chem. Soc. Div. Petrol. Chem. Prepr.*, 2000, 45 (3), 436-439.
50. Frye, C.G; Mosby, J. F. Kinetics of Hydrodesulfurization. *Chem. Eng. Prog.* 1967, 63, 66.
51. Kilanowski, D. R.; Teeuwen, H.; De Beer, V. H. J.; Gates, B. C.; Schuit, B. C. A.; Kwart, H. Hydrodesulfurization of Thiophene, Benzothiophene, Dibenzothiophene, and Related Compounds Catalyzed by Sulfided CoO-MoO<sub>3</sub>/γ-Al<sub>2</sub>O<sub>3</sub>: Low-Pressure Reactivity Studies. *J. Catal.*, 1978, 55, 129.
52. Houalla, M.; Broderick, D. H.; Sapre, A.V.; Nag, N. K.; De Beer, V. H. J.; Gates, B. C.; Kwart, H. Hydrodesulfurization of Methyl-substituted Dibenzothiophene Catalyzed by Sulfided CoO-MoO<sub>3</sub>/γ-Al<sub>2</sub>O<sub>3</sub>. *J. Catal.*, 1980, 61, 523.
53. Girgis, M. J. and Gates, B. C. 1991. Reactivities, Reaction Networks, and Kinetics in High-Pressure Catalytic Hydroprocessing. *Ind. Eng. Chem.* 1991, 30, 2021.
54. Vasudevan P. T., Fierro, J. L. G. A Review of Deep Hydrodesulfurization Catalysis. *Catal. Rev.-Sci. Eng.*, 1996, 38 (2), 161-188.
55. Phillipson, J. J. Kinetics of Hydrodesulfurization of Light and Middle Distillates, paper presented at Am. Inst. Chem. Engrs. Meeting, Houston, 1971.
56. Gates, B. C.; H. Topsøe. Reactivities in Deep Catalytic Hydrodesulfurization: Challenges, Opportunities, and the Importance of 4-Methyldibenzothiophene and 4,6-Dimethyl-dibenzothiophene. *Polyhedron*. 1997, 16, 3213.
57. a) Ma, X., Sakanishi, K., Isoda, T., and Mochida, I. Hydrodesulfurization Reactivities of Narrow-Cut Fractions in a Gas Oil. *Ind. Eng. Chem. Res.* 1995, 34, 748-754. b) Ma, X. Ph.D. Thesis, Deep Hydrodesulfurization of Diesel Fuel: Chemistry and Reaction Processing Design. 1995, Kyushu University, Japan.
58. UOP. Diesel Fuel. Specifications and Demand for the 21<sup>st</sup> Century. UOP, 1998.
59. Grisham, J. L. EPA's Sulfur Rule Sparks Debate. *Chem. Eng. News*, June 7, 1999, p.21.
60. Whitehurst, D. D., Isoda, T., and Mochida, I. Present State of the Art and Future Challenges in the Hydrodesulfurization of Polyaromatic Sulfur Compounds. *Advan. Catal.* 1998, 42, 345.
61. a) Topsøe, H. Environmental Catalysis for the 21<sup>st</sup> Century: Introduction of New Low Sulfur Transport Fuels. Presented at the 16<sup>th</sup> North American Catalysis Society Meeting, Boston, May 30-June 6, 1999, Paper A-5. b) Topsøe, H., Knudsen, K. G., Byskov, L. S., Norskov, J. K. and Clausen, B. S. Advances in Deep Desulfurization. *Stud. Surf. Sci. Catal.*, 1999, 121, 13-22.

62. Ma, X., Sakanishi, K., Isoda, T., and Mochida, I. Comparison of Sulfided CoMo/Al<sub>2</sub>O<sub>3</sub> and NiMo/Al<sub>2</sub>O<sub>3</sub> Catalysts. in *Hydrodesulfurization of Gas Oil Fractions and Model Compounds, in Hydrotreating Technology for Pollution Control*. M. L. Occelli and R. Chianelli, eds., New York: Marcel Dekker, 1996, p 183.
63. Ma, X., Sakanishi, K., Isoda, T., and Mochida, I. Quantum Chemical Calculation on the Desulfurization Reactivities of Heterocyclic Sulfur Compounds. *Energy & Fuels*, 1995, 9, 33-37.
64. Daage, M. and Chianelli, R. R. Structure-Function Relations in Molybdenum Sulfide Catalysts: The Rim-Edge Model. *J. Catal.*, 1994, 194, 414-427.
65. van Veen, J. A. R., Sie, S. T. Editorial: Deep Hydrodesulfurization of Diesel Fuel. *Fuel Processing Technol.*, 1999, 61, 1-4.65.
66. Schulz, H. Bohringer, W., Ousmanov, F., and Waller, F. Refractory Sulfur Compounds in Gas Oils. *Fuel Processing Technol.*, 1999, 61, 5-42.
67. Knudsen, K. G., Cooper, B. H. and Topsøe, H. Catalyst and Process Technologies for Ultra Low Sulfur Diesel. *Appl. Catal. A: Gen.*, 1999, 189 (2), 205-215.
68. Swaty, T.E.; Nocca, J.L.; Ross, J. What Are the Options to Meet Tier II Sulfur Requirements? *Hydrocarbon Processing*, 2001, 80 (2), 62-70.
69. Shiflett, W.K.; Krenzke, L. D. Consider Improved Catalyst Technologies to Remove Sulfur. *Hydrocarbon Processing*, 2001, 81 (2), 41-43.
70. Topsøe, H., Clausen, B. S., Massoth, F. E. *Hydrotreating Catalysis. Science and Technology*. Springer-Verlag, Berlin, 1996, 310 pp.
71. Prins, R. Catalytic Hydrodenitrogenation. *Advances in Catalysis*, 2001, 46, 399-464.
72. Houalla, M.; Nag, N. K.; Sapre, A. V.; Broderick, D. H.; Gates, B. C. Hydrodesulfurization of Dibenzothiophene Catalyzed by Sulfided CoO-MoO<sub>3</sub>/γ-Al<sub>2</sub>O<sub>3</sub>: The Reaction Network. *AIChE J.* 1978, 24, 1015.
73. Sapre, A. V., Broderick, D. H., Fraenkel, D., Gates, B. C., and Nag, N. K. Hydrodesulfurization of Benzo[b]naphtho[2,3-d]thiophene Catalyzed by Sulfided CoO-MoO<sub>3</sub>/γ-Al<sub>2</sub>O<sub>3</sub>: The Reaction Network. *AIChE J.*, 1980, 26, 690.
74. Devanneaux, J.; Maurin, J. Hydrogenolysis and Hydrogenation of Thiophene Compounds on a Co-Mo/Al<sub>2</sub>O<sub>3</sub> Catalyst. *J. Catal.* 1981, 69, 202.
75. Virnat, M. L. The Kinetics of the Hydrodesulfurization Process: A Review. *Appl. Catal.* 1983, 6, 137.
76. Aubert, C.; Durand, R.; Geneste, P.; Moreau, C. Hydroprocessing of dibenzothiophene, phenothiazine, phenoxathiin, Thianthrene, and thioxanthene on a sulfided NiO-MoO<sub>3</sub>/γ-Al<sub>2</sub>O<sub>3</sub> catalyst. *J. Catal.* 1986, 97, 169-176.
77. Vanrysselberghe, V., Froment, G. Hydrodesulfurization of Ddibenzothiophene on a CoMo/AL<sub>2</sub>O<sub>3</sub> Catalyst: Reaction Network and Kinetics. *Ind. Eng. Chem. Res.* 1996, 35, 3311.
78. Nagai, M. and Kabe, T. Selectivity of Molybdenum Catalyst in Hydrodesulfurization, Hydro-denitrogenation, and Hydrodeoxygenation: Effect of Additives on Dibenzothiophene Hydrodesulfurization. *J. Catal.* 1983, 81, 440.
79. Lavopa, V.; Satterfield, C. N. Poisoning of Thiophene Hydrodesulfurization by Nitrogen Compounds. *J. Catal.* 1988, 110, 375.
80. Isoda, T.; Ma, X. and Mochida, I. Reactivity of Refractory Sulfur Compounds in Diesel Fuel (Part 2) Inhibition of Hydrodesulfurization Reaction of 4,6-Dimethyldibenzothiophene by Aromatic Compound. *J. Japan Petrol. Inst.* 1994, 37, 506.
81. Farag, H.; Sakanishi, K.; Mochida, I.; Whitehurst, D. D. Kinetic Analyses and Inhibition by Naphthalene and H<sub>2</sub>S in Hydrodesulfurization of 4,6-Dimethyldibenzothiophene (4,6-DMDBT) over CoMo-Based Carbon Catalyst. *Energy Fuels* 1999, 13, 449.
82. Kabe, T., Ishihara, A. and Zhang, Q. Deep Desulfurization of Light Oil. 2. Hydrodesulfurization of Dibenzothiophene, 4-Methyldibenzothiophene and 4,6-Dimethyldibenzothiophene. *Appl. Catal. A-Gen.* 1993, 97, L1-L9.

83. Ma, X., Sakanishi, K., Isoda, T., and Mochida, I. Comparison of Sulfided CoMo/Al<sub>2</sub>O<sub>3</sub> Catalysts in Hydrodesulfurization of Gas Oil Fractions. *Prepr., Div. Pet. Chem., Am. Chem. Soc.* 1994, 39, 622-626.
84. Isoda, T.; Ma, X.; Mochida, I. Reactivity of Refractory Sulfur Compounds in Diesel Fuel (Part 1) Desulfurization Reactivity of Alkyldibenzothiophenes in Decalin. *J. Japan Petrol. Inst.* 1994, 37, 368.
85. Mochida, I., Sakanishi, K., Ma, X., Nagao, S., and Isoda, T. Deep Hydrodesulfurization of Diesel Fuel: Design of Reaction Process and Catalysis. *Catalysis Today*, 1996, 29, 185.
86. Isoda, T.; Ma, X.; Nagao, S.; Mochida, I. Reactivity of Refractory Sulfur Compounds in Diesel Fuel (Part 3) Coexisting Sulfur Compounds and By-produced H<sub>2</sub>S Gas as Inhibitors in HDS of 4,6-Dimethyldibenzothiophene. *J. Japan Petrol. Inst.* 1995, 38, 25.
87. Ma, X., Schobert, H. H. Hydrodesulfurization of thiophenic Compounds on MoS<sub>2</sub>, A Computational Study using ZINDO. *Prepr. Div. Fuel Chem. ACS*, 1997, 42, 48.
88. Ma, X. and Schobert, H. H. Hydrogenolysis of Thiophenic Compounds on MoS<sub>2</sub>- A Computational Modeling of Heterogeneous Catalysis. *ACS Prepr. Div. Petrol. Chem.*, 1997, 42, 657.
89. Ma, X. and Schobert, H. H. Computational Modeling on Hydrodesulfurization of Thiophenic Compounds on MoS<sub>2</sub> and Ni-Promoted MoS<sub>2</sub>. *Prepr. Div. Petrol. Chem., ACS*, 1998, 43, 24.
90. Ma, X. and Schobert, H. H. Molecular Simulation on Hydrodesulfurization of Thiophenic Compounds over MoS<sub>2</sub> Using ZINDO. *J. Mol. Catal.* 2000, 160, 409-427.
91. Milenkovic A, Macaud M, Schulz E, Koltai T, Loffreda D, Vrinat M, Lemaire M. How could organic synthesis help the understanding of the problems of deep hydrodesulfurization of gasoils? *Comptes Rendus De L Academie Des Sciences Serie Ii Fascicule C-Chimie*, 2000, 3 (6), 459-463.
92. Bataille, F.; Lemberton, J.L.; Michaud, P.; Perot, G.; Vrinat, M.; Lemaire, M.; Schulz, E.; Breyse, M.; Kasztelan, S. Alkydibenzothiophenes Hydrodesulfurization-Promoter Effect, Reactivity, and Reaction Mechanism. *J. Catal.*, 2000, 191, 409-422.
93. Byskov, L.S., Hammer, B., Norskov, J.K., Clausen, B.S., Topsøe, H. Sulfur bonding in Mo-Mo-S catalyst particles, *Catal. Lett.* 2000, 64, 95.
94. Helveg, S.; J. V. Lauritsen, E. Lægsgaard, I. Stensgaard, J. K. Nørskov, B. S. Clausen H. Topsøe and F. Besenbacher. *Phys. Rev. Lett.*, 2000, 84, 951.
95. Pawelec, B.; Mariscal, R.; Fierro J.L.G.; Greenwood, A.; Vasudevan, P.T. Carbon-supported tungsten and nickel catalysts for hydrodesulfurization and hydrogenation reactions. *APPLIED CATALYSIS A-GENERAL* 2001, 206 (2): 295-307.
96. Kaluza L, Zdrzil M. Carbon-supported Mo catalysts prepared by a new impregnation method using a MoO<sub>3</sub>/water slurry: saturated loading, hydrodesulfurization activity and promotion by Co. *Carbon* 2001, 39 (13): 2023-2034
97. Olguin-Orozco, E., Vrinat, M., Cedeno, L., Ramirez, J., Boroque, M., and Lopez, A. A. The Use of TiO<sub>2</sub>-Al<sub>2</sub>O<sub>3</sub> Binary Oxides as Supports for Mo-Based Catalysts in Hydrodesulfurization of Thiophene and Dibenzothiophene. *Appl. Catal. A:Gen*, 1997, 165, 1-13.
98. Murali Dhar, G., Rana M. S., Maity, S. K., Srinivas, B. N. and Prasada Rao, T. S. R. Performance of Mo Catalysts Supported on TiO<sub>2</sub>-Based Binary Supports for Distillate Fuel Hydroprocessing. Chapter 8 in *Chemistry of Diesel Fuels*. C. Song, S. Hsu and I. Mochida, eds., New York: Taylor & Francis, 2000.
99. Segawa, K., Takahashi, K. and Satoh, S. Development of new catalysts for deep hydrodesulfurization of gas oil. *Cata. Today* 2000, 63, 123-131.
100. Kresge, C. T., Leonowicz, M. E., Roth, W. J., Vartuli, J. C., and Beck, J. S. Ordered Mesoporous Molecular-Sieves Synthesized by a Liquid-Crystal Template Mechanism. *Nature*, 1992, 359, 710-712.
101. Vartuli, J. C., Shi, S. S., Kresge, C. T., and Beck, J. S. Potential Applications for M41S Type Mesoporous Molecular Sieves. *Stud. Surf. Sci. Catal.*, 1998, 117, 13.



102. Reddy, K. M. and Song, C. Synthesis of Mesoporous Molecular Sieves: Influence of Aluminum Source on Al Incorporation in MCM-41. *Catalysis Letters*, 1996, 36(1), 103-109/122.
103. Reddy, K. M. and Song, C. Effect of Al Sources on the Synthesis and Acidic Characteristics of Mesoporous Aluminosilicates of MCM-41 Type. *Stud. Surf. Sci. Catal.*, 1998, 117, 291-99.
104. Reddy, K. M., Wei, B., and Song, C. Mesoporous Molecular Sieve MCM-41 Supported Co-Mo Catalyst for Hydrodesulfurization of Petroleum Resids. *Catalysis Today*, 1998, 43 (3), 261-272.
105. Song, C., Reddy, K. M., and Leta, H. Mesoporous Aluminosilicate Molecular Sieve MCM-41 as Support of Co-Mo Catalysts for Hydrodesulfurization of Diesel Fuels. *Am. Chem. Soc. Div. Petrol. Chem. Prepr.*, 1998, 43 (4), 534-538.
106. Song, C., Reddy, K. M. Chap. 1 in *Recent Trends in Catalysis*. Edited by V. Murugesan, B. Arabindoo, and M. Palanichamy, New Delhi, India: Narosa Publishing House, 1999, pp. 1-13.
107. Turaga, U. T., Song, C. MCM-41-supported Co-MO catalysts for deep hydrodesulfurization of light cycle oil. *Catal. Today*, 2003, 86, 129-140.
108. Song, C., Reddy, K.M., Leta, H., Yamada, M., Koizumi, N. Mesoporous aluminosilicate molecular sieve MCM-41 as support of Co-MO catalysts for deep hydrodesulfurization of diesel fuels, in Song, C., Hsu, S. and Mochida, I. Eds. *Chemistry of Diesel Fuels*, New York, 2000. Chapter 7, p. 139.
109. Yamada, M., Koizumi, N., Yamazaki, M. High pressure ( $\leq 5.1$  Mpa) DRIFT study on surface structure of Co-Mo/ $\text{Al}_2\text{O}_3$  and Ni-Mo/ $\text{Al}_2\text{O}_3$  using NO as probe molecule, *Catal. Today* 1999, 50, 3.
110. Wang, A.J., Wang, Y., Kabe, T. Chen, Y.Y., Ishihara, A. Qian, W.H. Hydrodesulfurization of dibenzothiophene over siliceous MCM-41-supported catalysts. I. Sulfided Co-Mo catalysts, *J. Catal.* 2001, 199, 19.
111. AkzoNobel. <http://www.akzonobel-catalysts.com/html/hydroprocessing/catalysts/hccatze.htm>. 2002.
112. Kaufmann, T.G.; Kaldor, A.; Stuntz, G.F., Kerby, M.C.; Ansell, L.L. Catalysis Science and Technology for Cleaner Transportation Fuels. *Catalysis Today*, 2000, 62, 77-90.
113. Gerritsen, L.A. Production of Green Diesel in the BP Amoco Refineries, Presentation by Akzo Nobel at the WEFA conference in Berlin, Germany, June 2000.
114. Meijburg, G. Production of Ultra Low-Sulfur Diesel in Hydrocracking with the Latest and Future Generation Catalysts. *Catalyst Courier* 46, Akzo Nobel, 2001.
115. Plantenga, F.L. "Nebula" A Hydroprocessing Catalyst With Breakthrough Activity. *Catalysts Courier - Courier* 47, [http://www.akzonobel-catalysts.com/html/catalystcourier/courier47/c47\\_a3.htm](http://www.akzonobel-catalysts.com/html/catalystcourier/courier47/c47_a3.htm), Akzo Nobel, 2002. 128.
116. Bharvani, R.R.; Henderson, R.S. Revamp Your Hydrotreater for Deep Desulfurization. *Hydrocarbon Processing*, 2002, 81 (2), 61-64.
117. Lawler, D.; Robinson, S. Update Hydrotreaters to Process "Green" Diesel. *Hydrocarbon Processing*, 2002, 80 (11), 61-68.
118. Ma, X., Sakanishi, K., and Mochida, I. Three-stage Deep Hydrodesulfurization and Decolorization of Diesel Fuel with CoMo and NiMo catalysts at Relatively Low Pressure. *Fuel*, 1994, 73, 1667-1671.
119. Sie, S. T. Reaction Order and Role of Hydrogen Sulfide in Deep Hydrodesulfurization of Gas Oil : Consequences for Industrial Reactor Configuration. *Fuel Proc. Tech.* 1999, 61, 149-171.
120. Maxwell, I. E. Innovation in Applied Catalysis. *Cattech*, 1997, 1, 5-3.
121. Dautzenberg, F. A Call for Accelerating Innovation. *Cattech*, 1999, 3 (1), 54-63.
122. Phillips Petroleum. <http://www.fuelstechnology.com/szorbiesel.htm>, Viewed December 2001.
123. Gislason, J. Phillips Sulfur-Removal Process Nears Commercialization. *Oil Gas J.*, 2002, 99 (47), 74-76.132.

124. Sughrue, E. Conoco Phillips, Personal communication on desulfurization. April 19, 2003.
125. Tucker, C.; Sughrue, E.; Vanderlaan, J. Production of Ultra-Low Sulfur Fuels: Today and Tomorrow. AM-03-48, NPRA 2003 Annual Meeting, March 23-25, 2003, San Antonio, TX.
126. Turk, B. S.; Gupta, R. P.; Arena, B. A New Continuous Process for Desulfurization of Syngas and Hydrocarbons. 2002 NPRA Annual Meeting, San Antonio, TX, paper No. AM-02-10, 2002a.
127. Ma, X., Sun, L., Song, C. A new approach to deep desulfurization of gasoline, diesel fuel and jet fuel by selective adsorption for ultra-clean fuels and for fuel cell applications. *Catal. Today*, 2002, 77, 107-116.
128. Pyell, U.; Schober S, Stork G. Ligand-exchange chromatographic separation of polycyclic aromatic hydrocarbons and polycyclic aromatic sulfur heterocycles on a chelating silica gel loaded with palladium (II) or silver (I) cations. *Fresenius Journal Of Analytical Chemistry*, 1997, 359 (7-8), 538-541.
129. Rudzinski WE, Aminabhavi TM, Sassman S, Watkins LM. Isolation and characterization of the saturate and aromatic fractions of a Maya crude oil. *Energy & Fuels*, 2000, 14 (4), 839-844.
130. Yang, R.T.; Takahashi, A.; Yang, F.H. New Sorbents for Desulfurization of Liquid fuels by  $\pi$ -Complexation. *Ind.Eng.Chem.Res.* 2001, 40, 6236.
131. Takahashi, A.; Yang, F.H.; Yang, R.T. New Sorbents for Desulfurization by  $\pi$ -Complexation: Thiophene/Benzene Adsorption. *Ind.Eng.Chem.Res.* 2002, 41, 2487.
132. Hernandez-Maldonado, A. J., Yang, R. T. Desulfurization of commercial liquid fuels by selective adsorption via pi-complexation with Cu(I)-Y Zeolite. *Industrial Engineering Chemistry Research*, 2003, 42, 123-129.
133. Hernandez-Maldonado, A. J., Yang, R. T. Desulfurization of liquid fuels by adsorption via pi complexation with Cu(I)-Y and Ag-Y zeolites. *Industrial Engineering Chemistry Research*, 2003, 42, 3103-3110.
134. Yang, R. T., Hernandez-Maldonado, A. J., Yang, F. H. Desulfurization of Transportation Fuels with Zeolites Under Ambient Conditions. *Science* 2003, 301, 79-81.
135. *Hydrocarbon Processing*, May 1999, p. 39.
136. Irvine, R. L. 1998. U.S. Pat. No. 5,730,860. 116. Bharvani, R.R.; Henderson, R.S. Revamp Your Hydrotreater for Deep Desulfurization. *Hydrocarbon Processing*, 2002, 81 (2), 61-64.
137. Milenkovic A, Schulz E, Meille V, Loffreda D, Forissier M, Vrinat M, Sautet P, Lemaire M. Selective elimination of alkyldibenzothiophenes from gas oil by formation of insoluble charge-transfer complexes. *Energy & Fuels*, 1999, 13 (4), 881-887.
138. Dolbear, G. E.; Skov, E. R. Selective Oxidation as a Route to Petroleum Desulfurization. *Am. Chem. Soc. Div. Petrol. Chem. Prep.*, 2000, 45, 375-378.
139. Otsuki S, Nonaka T, Qian WH, Ishihara A, Kabe T. Oxidative desulfurization of middle distillate – oxidation of dibenzothiophene using t-butyl hypochlorite. *SEKIYU GAKKAISHI*, 2001, 44 (1), 18-24.
140. Aida T, Yamamoto D, Iwata M, Sakata K. Development of oxidative desulfurization process for diesel fuel. *Reviews on Heteroatom Chemistry*, 2000, 22, 241-256.
141. Hangun, Y.; Alexandrova, L.; Khetan, S.; Horwitz, C.; Cugini, A.; Link, D. D.; Howard, B.; Collins, T. J. Oxidative Desulfurization of Fuels Through TAML Activators and Hydrogen Peroxide. *Am. Chem. Soc. Div. Petrol. Chem. Prep.*, 2002, 47, 42-44.
142. Shiraishi Y, Hirai T, Komasaawa I. A deep desulfurization process for light oil by photochemical reaction in an organic two-phase liquid-liquid extraction system. *Industrial & Engineering Chemistry Research*, 1998, 37 (1), 203-211.
143. Shiraishi Y, Hirai T, Komasaawa I. Photochemical desulfurization of light oils using oil hydrogen peroxide aqueous solution extraction system: Application for high sulfur content straight-run light gas oil and aromatic rich light cycle oil. *J. Chem. Eng. Jap.* 1999, 32 (1), 158-161.

144. Chapados, D. Desulfurization by Selective Oxidation and Extraction of Sulfur-Containing Compounds to Economically Achieve Ultra-Low Proposed Diesel Fuel Sulfur Requirements, Paper presented at the 2000 NPRA Annual Meeting.
145. Bonde, S. E.; Gore, W.; Dolbear, G. E.; Skov, E. R. Selective Oxidation and Extraction of Sulfur-Containing Compounds to Economically Achieve Ultra-Low Diesel Fuel Sulfur Requirements. *Am. Chem. Soc. Div. Petrol. Chem. Prep.*, 2000, 45, 364-366.
146. Nero, V. P.; DeCanio, S.J.; Rappas, A. S.; Levy, R. E.; Lee, F.-M. Oxidative Process for Ultra-Low Sulfur Diesel. *Am. Chem. Soc. Div. Petrol. Chem. Prep.*, 2002, 47, 41-41.
147. McFarland, B. L., Boron, D. J., Deever, W., Meyer, J. A., Johnson, A. R. and Atlas, R. M. Biocatalytic Sulfur Removal from Fuels: Applicability for Producing Low Sulfur Gasoline. *Crit. Rev. Microbiol.*, 1998, 24 (2), 99-147.
148. Monticello, D. J. Biodesulfurization of Diesel Fuels. *CHEMTECH* 1998, 28(7), 38-45.
149. Lange, E. A. and Lin, Q. Preparation of Surfactants from a Byproduct of Fossil Fuel Biodesulfurization. Chapter 9 in *Chemistry of Diesel Fuels*. C. Song, S. Hsu and I. Mochida, eds., Philadelphia: Taylor & Francis, 2000.
150. Gallagher, J.R., Olson E.S., Stanley, D.C. Microbial Desulfurization of Dibenzothiophene - A Sulfur-Specific Pathway. *Fems Microbiology Letters*, 1993, 107 (1), 31-36.
151. Denome, S.A.; Oldfield, C.; Nash, L.J, Young, K.D. Characterization of the Desulfurization Genes from *Rhodococcus* Sp Strain Igts8. *J. Bacteriology*, 1994, 176 (21), 6707-6716.
152. Piddington, C.S.; Kovacevich, B.R.; Rambosek, J. Sequence and Molecular Characterization of a DNA Region Encoding the Dibenzothiophene Desulfurization Operon of *Rhodococcus* sp. Strain IGTS8. *Applied and Environmental Microbiology*, 1995, 61 (2), 468-475.
153. Gary, J. H. and Handwerk, G. E. *Petroleum Refining Technology and Economics*. New York: Marcel Dekker, 1994, 465 pp..
154. Izumi, Y; Ohshiro, T.; Ogino, H.; Hine, Y, Shimao, M. Selective Desulfurization Of Dibenzothiophene By *Rhodococcus-Erythropolis* D-1. *Applied and Environmental Microbiology*, 1994, 60 (1), 223-226.
155. Kobayashi M, Horiuchi K, Yoshikawa O, Hirasawa K, Ishii Y, Fujino K, Sugiyama H, Maruhashi K. Kinetic analysis of microbial desulfurization of model and light gas oils containing multiple alkyl dibenzothiophenes. *Bioscience Biotechnology and Biochemistry*, 2001, 65 (2): 298-304.
156. Lee, M.K.; Senius, J.D.; Grossman, M. J. Sulfur-Specific Microbial Desulfurization of Sterically Hindered Analogs of Dibenzothiophene. *Applied And Environmental Microbiology*, 1995, 61 (12), 4362-4366.
157. Omori, T, Monna, L, Saiki, Y.; Kodama, T. Desulfurization of Dibenzothiophene by *Corynebacterium* Sp Strain-Sy1. *Applied and Environmental Microbiology*, 1992, 58 (3), 911-915.
158. Ohshiro T, Izumi Y. Microbial desulfurization of organic sulfur compounds in petroleum. *Bioscience Biotechnology and Biochemistry*, 1999, 63 (1), 1-9.
159. McFarland, B.L. Biodesulfurization. *Current Opinion in Microbiology*, 1999, 2 (3), 257-264.
160. Shorey, S.W., Lomas, D. A., Keesom, W. H. Use FCC feed pretreating methods to remove sulfur. *Hydroc. Proce.* 1999, 78 (11), 43-51.
161. Fredrick, C. Sulfur Reduction: What Are the Options. *Hydrocarbon Processing*, 2002, 81 (2), 45-50.
162. Sloley, A. W. Cat Naphtha Sulfur Management: Undercut or Not? *Hydrocarbon Processing*, 2001, 80 (2), 75-78.
163. Golden, S.W.; Hanson, D.W.; Fulton, S.A. Use Better Fractionation to Manage Gasoline Sulfur Concentration. *Hydrocarbon Processing*, 2002, 81 (2), 67-72.
164. De la Fuente, E.; Low, G. Cost-Effectively Improve Hydrotreater Designs. *Hydrocarbon Processing*, 2002, 81 (2), 43-46.
165. Diesel Fuel Oils, October, 1996, Cheryl Dickson, and Gene Sturm, Jr., National Institute

- for Petroleum and Energy Research, Bartlesville, Oklahoma, NIPER-197 PPS, 96/5.
166. Pipenger, G.G. How to 'Spec' Diesel Fuel Additives for Winterization. *Hydrocarbon Processing*, 2001, 80 (11), 79-84.
  167. Gerritsen, L.A., Sonnemans, J.W M, Lee, S.L., and Kimbara, M. Options to Meet Future European Diesel Demand and Specifications. ERTC Conference, Berlin, November 1998.
  168. Mayo, S.W., Mid-Distillate Hydrotreating: The Perils and Pitfalls of Processing LCO, Akzo Nobel Catalysts.
  169. Van der Linde, B.; Menson, R.; Dave, D.; Gustas, S. SYN Technology. An Attractive Solution for Meeting Future Diesel Specifications. ARTC-99, ARTC Annual Meeting, 1999.
  170. Stanislaus, A, and Cooper, B. H. Aromatic Hydrogenation Catalysis: A Review. *Catal. Rev. - Sci. Eng.*, 1994, 36, 75-123.
  171. Cooper, B. H.; Sogaard-Anderson, P.; Nielsen-Hannerup, P. Production of Swedish Class I Diesel Using Dual-Stage Process, in *Catalytic Hydroprocessing of Petroleum and Distillates*. M. C. Oballa and S. S. Shih, eds., New York: Marcel Dekker, 1994, pp. 279-290.
  172. TNRCC. Texas Motor Vehicle Fuel Programs. Texas Natural Resources Conservation Commission, <http://www.tnrcc.state.tx.us/air/ms/fuelprograms.html>, May 2002.
  173. Kreucher, W. M. In *The Alternative: New Reasons For Old Fuels*. *Chem. Ind.*, 1995, 15, 601-604.
  174. Cooper, B. H. and Donnis, B. B. L. Aromatic Saturation of Distillates: An Overview. *Appl. Catal. A.*, 1996, 37, 203-223.
  175. Ali S. A, Siddiqui M. A. B. Dearomatization, cetane improvement and deep desulfurization of diesel feedstock in a single-stage reactor. *Reac. Kine. Catal. Let.* 1997, 61 (2), 363-368.
  176. Stork, W. H. J. Performance Testing Of Hydroconversion Catalysts. *Am. Chem. Soc. Sym. Ser.*, 1996, 634, 379-00.
  177. Lucien, J. P., van den Berg, J. P., Germaine, G., van Hooijdonk, H. M. J. H., Gjers, M. and Thielemans, G. L. B. Shell Middle Distillate Hydrogenation Process, in *Catalytic Hydroprocessing of Petroleum and Distillates*. M. C. Oballa and S. S. Shih, eds., New York: Marcel Dekker, 1994, pp. 291-313.149.
  178. Marchal, N., Kasztelan, S., and Mignard, S. A Comparative Study of Catalysts for the Deep Aromatic Reduction in Hydrotreated Gas Oil. in *Catalytic Hydroprocessing of Petroleum and Distillates*. M. C. Oballa and S. S. Shih, eds., New York: Marcel Dekker, 1994, pp. 315-327.
  179. Suchanek, A. How To Make Low-Sulfur, Low Aromatics, High Cetane Diesel Fuel. *ACS Div. Petrol. Chem. Preprints*, 1996, 41, 583-84.
  180. ABB Lummus Global, Inc. Hydrotreating. *Hydrocarbon Processing*, 1998, 77 (11), 90.
  181. Song, C., Ma, X. *Appl. Catal. B: Envi.* 2003, 41, 207-238.
  182. Absi-Halabi, M., Stanislaus, A. and Qabazard, H. Trends in Catalysis Research to Meet Future Refining Needs. *Hydrocarbon Process.*, 1997, 76 (2), 45-55.
  183. Lin, S.D., and Song, C. Noble Metal Catalysts for Low-Temperature Naphthalene Hydrogenation in the Presence of Benzothiophene. *Catalysis Today*, 1996, 31(1), 93-04.
  184. Song, C., and Schmitz, A. D. Zeolite-Supported Noble-Metal Catalysts for Low-Temperature Hydrogenation of Aromatics in the Absence and Presence of Benzothiophene. *Am. Chem. Soc. Div. Petrol Chem. Preprints*, 1996, 41, 609-14.
  185. Song, C., and Schmitz, A. D. Zeolite-Supported Pd and Pt Catalysts for Low-Temperature Hydrogenation of Naphthalene in the Absence and Presence of Benzothiophene. *Energy & Fuels*, 1997, 11(3), 656-61.
  186. Reddy, K. M., and Song, C. Synthesis of Mesoporous Zeolites and Their Application for Catalytic Conversion of Polycyclic Aromatic Hydrocarbons. *Catalysis Today*, 1996, 31(1), 137-44.
  187. Reddy, K. M. and Song, C. Mesoporous Molecular Sieve MCM-41 Supported Pt and Pd Catalysts for Low-Temperature Hydrogenation of Aromatics in Distillate Fuels. Chapter

- 15 in *Designing Transportation Fuels for a Cleaner Environment*. J. G. Reynolds and M. R. Khan eds. Philadelphia: Taylor & Francis, 1999, pp. 173-185.
188. Corma A, Martinez A, MartinezSoria V. Hydrogenation of aromatics in diesel fuels on Pt/MCM-41 catalysts. *J. Catal*, 1997, 169 (2), 480-489.
189. Fujikawa T, Idei K, Usui K. Aromatic hydrogenation of distillate over B<sub>2</sub>O<sub>3</sub>-Al<sub>2</sub>O<sub>3</sub> supported Pt-Pd catalysts. *SEKIYU GAKKAISHI*, 1999, 42 (4), 271-274.
190. News-HDS/HDA. Hydrodearomatization. *Hydrocarbon Processing*, 2000, 79 (11), 118.

## Chapter 12

# SYNERGISTIC EXTRACTIVE DESULFURIZATION PROCESSES

Ebbe R. Skov<sup>1</sup> and Geoffrey E. Dolbear<sup>2</sup>

1. *Hetagon Energy Systems Inc.*

*Mission Viejo, CA*

2. *G.E.Dolbear & Associates*

*Diamond Bar, CA 91765*

### 1. INTRODUCTION

The refinery industry in the United States and Europe confronts major challenges at the start of the new millennium. Within this decade it must meet new very stringent rules for ultra-low-sulfur diesel (ULSD) fuels while producing larger volumes of motor fuels from increasingly lower-quality feedstocks. In the U.S., the most recent EPA rules call for ULSD fuel with a maximum of 15 wppm sulfur in 2006; these levels may be extended to non-road diesel by the end of the decade. Similar specifications calling for 50 wppm sulfur in diesel are going into effect in the EU in 2005 (see Table 1).

*Table 1. Diesel Fuel Specifications*

| <b>Governing Body</b>         | <b>United States</b> | <b>California</b> | <b>United States</b> | <b>EU</b>   |
|-------------------------------|----------------------|-------------------|----------------------|-------------|
| <b>Year</b>                   | <b>1993</b>          | <b>1993</b>       | <b>2006</b>          | <b>2005</b> |
| Boiling Range, ASTM D86, °F * | 356 - 662            | 338 - 662         | 356 - 662            | 329 - 680   |
| 90%, °F (max)                 | 640                  | 608               | 640                  | 680         |
| Boiling Range, ASTM D86, °C * | 180 - 350            | 170 - 350         | 180 - 350            | 165-360     |
| 90%, °C (max)                 | 338                  | 320               | 338                  | 360         |
| Flash Point, °F (min)         | 100                  | 129               | 104 - 219*           | 131         |
| Flash Point, °C (min)         | 38                   | 54                | 40 - 54*             | 55          |
| Total Aromatics, vol% (max)   | 35                   | 10                | 35                   | —           |
| Sulfur, wppm (max)            | 500                  | 500               | 15                   | 50          |
| Cetane Index (min)            | 40                   | —                 | 40                   | —           |
| Cetane Number (min)           | —                    | 48                | —                    | 51          |

\* Expected range

Several new processes have been announced that, when used in connection with the more conventional hydrodesulfurization (HDS) processes, promise to facilitate the achievement of that goal at lower capital and operating costs than required for high-severity HDS. Economic synergism is expected in the application of these new processes in tandem with the existing processes for HDS.

The physical basis for this synergism in process application is based in the chemistry of the alkylated aromatic thiophenic compounds in diesel fuel feedstock; those most resistant to conversion to hydrocarbons by HDS are those most readily amenable to oxidation and extractive desulfurization. Refiners expanding their processing capacity or adjusting to the new ULSD rule may want to consider the new extractive desulfurization (EDS) alternatives to high severity HDS, including debottlenecking HDS units by feedstock pretreatment or post-treatment, or parallel operation to reduce the load on their units.

To meet the ULSD fuel specifications, the refining industry initially turned to hydrodesulfurization (HDS) processes for better, more effective catalysts, improved hydrotreating selectivity and higher severity.<sup>1,2</sup> However, the 350–650 wppm sulfur remaining in the diesel fuel after conventional HDS is mostly present as alkylated aryl-thiophenic (AAT) compounds. These include benzo- and dibenzothiophenes (BT, DBT), benzo-naphtho-thiophenes (BNT), hydro-dibenzo- and hydro-di-naphtho-thiophenes (HDBT, HDBT), and their C<sub>1</sub> to C<sub>6</sub> alkylated homologues, representing dozens or perhaps hundreds of discrete compounds (see Table 2).

Table 2. Alkylated Aryl-Thiophenic (AAT) Compounds

| Abbrev.   | Compound Type                       | Example Alkyl Groups  |                 |                 |                 |                       |       |
|---|-------------------------------------|---|-----------------|-----------------|-----------------|-----------------------|-------|
| BT  | Benzothiophenes                     | Mono substituted: methyl-, ethyl-, propyl-, etc.<br>Di-substituted: dimethyl-, ethylmethyl-, diethyl-, etc. |                 |                 |                 |                       |       |
| DBT   | Dibenzothiophenes                   | Mono-substituted: methyl-, ethyl-, propyl-, etc.<br>Di-substituted: dimethyl-, ethylmethyl-, diethyl-, etc. |                 |                 |                 |                       |       |
| BNT   | Benzonaphthothiophenes              | Mono-substituted: methyl-, ethyl-, propyl-, etc.<br>Di-substituted: dimethyl-, ethylmethyl-, diethyl-, etc. |                 |                 |                 |                       |       |
| HDBT  | Di- and tetrahydrodibenzothiophenes |   |                 |                 |                 |                       |       |
| THBNT   | Tetrahydrobenzonaphthothiophenes    |   |                 |                 |                 |                       |       |
| OHDNT   | Octahydrodinaphthothiophenes        |   |                 |                 |                 |                       |       |
| THDNT   | Tetrahydrodinaphthothiophenes       |   |                 |                 |                 |                       |       |
| <b>Properties</b>   |                                     |   |                 |                 |                 |                       |       |
| Boiling range   | 428 – 665°F<br>220 – 350°C          | Molecular Weight 134 – 345<br>No. of Carbon Atoms 8 – 24  |                 |                 |                 |                       |       |
| Sulfur, wt%   | 11 – 24                             |   |                 |                 |                 |                       |       |
| <b>Example: AAT in Alaska North Slope Light Atmospheric Gas Oil</b> |                                     |   |                 |                 |                 |                       |       |
| No. of Carbons  | C <sub>8</sub>                      | C <sub>9</sub>  | C <sub>10</sub> | C <sub>11</sub> | C <sub>12</sub> | C <sub>13</sub> -plus | Total |
| MW  | 134                                 | 148   | 162             | 176             | 184-190         | 204-218               | avg   |
| Fraction, wt%   | 2                                   | 3   | 34              | 27              | 26              | 8                     | 100%  |
| Sulfur, wt%   | 24                                  | 21  | 20              | 18              | 17              | <15                   | 5000  |

These AAT compounds are to various degrees refractory to hydrogenation under conventional operating conditions.<sup>1,3,4</sup> Studies have shown that the more refractory sulfur compounds in diesel streams are the alkyl-substituted DBTs and BNTs, in which the alkyl groups are located in the 4 and 6 positions adjacent to the thiophenic sulfur atom.<sup>2,4,5</sup> In order to reduce the sulfur to meet ULS diesel fuel specifications, very high severity HDS processing is required. This will require expensive equipment and significantly increased hydrogen consumption, resulting in elevated conversion costs.<sup>6</sup>

Successful refinery technology developers generally focus on their specialty, adapting and optimizing their processes and catalysts to solve new arising challenges. When confronted with the new ULSD specifications, HDS catalyst and process developers, therefore, began by improving the catalysts and designing for more severe operating conditions. It sometimes happens that a new combination of different processes, where a new process may be used for feed pretreatment or post-treatment for another, will result in a less expensive solution. The application of extractive desulfurization (EDS) processes in combination with conventional HDS may be such a case.

## 2. EXTRACTIVE DESULFURIZATION PROCESSES

The removal of AAT sulfur compounds from the diesel fuel feedstock by extractive desulfurization (EDS), either adsorption or solvent extraction, is a viable alternative to HDS.<sup>4,7,8,9</sup> This approach is based on the polarity difference between the AAT family of compounds and the hydrocarbons found in the diesel fraction. Because AATs comprise several dozen different compounds, they represent a range of solvent polarities, in some cases quite similar to the aromatic compounds found in diesel fuel. The critical “polarity difference” between individual hydrocarbon and thiophenic compounds is therefore variable, and in some cases may be insufficient to allow a functional separation by extraction. Polarity difference can, however, be increased by oxidizing the thiophenic sulfur to the corresponding more polar mono- and dioxides, the alkylated-aryl-thiophene-sulfoxide or sulfone (AATS). This in turn facilitates the separation, and several EDS processes therefore are designed to oxidize the AAT before extraction of the sulfur.<sup>4,7,8,9,10</sup>

An examination of the chemical reactivity of AAT shows that it correlates with the electron density on the sulfur atom. Interestingly, the affinity for oxidation is directly proportional to the electron density on the sulfur atom,<sup>4,5,11</sup> while the affinity for hydrogenation is inversely proportional.<sup>4,12</sup> Alkyl-groups positioned near the sulfur atom are incremental electron donors and they also are responsible for steric hindrance that has been shown to block access of the thiophene sulfur to the active site on the surface<sup>5</sup>. This obviously is an important consideration, because AAT compounds that are refractory to



HDS are more readily oxidized and more amenable to EDS, which can provide the basis for synergistic application of these two processes for ULSD.

During the past several years, several new desulfurization processes have been announced that utilize the solvent polarity differences between AAT, AATS and hydrocarbons. While several of these EDS processes are designed around a combination of oxidation and solvent extraction,<sup>4,7,8</sup> at least two are based on solid-phase adsorption of the AAT.<sup>13,14</sup> One of these, the ConocoPhillips S Zorb process for gasoline, has commercial experience with a 6,000 b/d facility that started up in mid 2001.<sup>15</sup>

Table 3. Extractive Desulfurization Processes

| Process / Developer            | Features  | Status                          |
|--------------------------------|---|---------------------------------|
| S Zorb / ConocoPhillips        | Solid adsorbent                                     | 6,000 b/d plant started in 2001 |
| IRVAD /Black & Veach Pritchard | Solid adsorbent                                     | Pilot plant                     |
| Unipure                        | Oxidation, solvent extraction                       | Pilot test in 2003              |
| UOP LLC                        | Oxidation, solvent extraction                       | U.S. patent issued              |
| CED / Petro-Star, Inc.         | Oxidation, solvent extraction                       | DOE R&D grant                   |
| Osaka University               | Oxidation, solvent extraction<br>UV photoactivation | R&D stage                       |

The S Zorb and IRVAD processes are based on adsorbing the more polar AAT compounds on solid material such as treated alumina or silica. Continuous removal of the saturated adsorbent permits recovery of the AAT compound and recycle of the activated adsorbent. Processing cost results primarily from the consumption of fuel, makeup adsorbent and capital charges. The cost of adsorbent regeneration may represent a limitation for the applicability of this type EDS process, and other constraints may be limitations to the feedstock boiling range and sulfur content.

In the oxidative solvent extraction processes, the AAT compounds are first oxidized to AATS using various oxidants (notably hydrogen peroxide) before they are removed by solvent extraction. Solvent is recovered by distillation for recycle from the ultra-low-sulfur raffinate and high-sulfur extract. The conversion cost consists primarily of the cost of oxidant, solvent losses, fuel cost and capital charges. Where the reduction of poly-aromatics from the ULS diesel is desired, the solvent-based EDS processes may present advantages, because the extract fraction can be adjusted to meet this need. However, high levels of olefins may limit the oxidation approach because they can consume additional oxidant and produce undesired byproducts.

### 3. SYNERGISM BETWEEN HDS AND EDS

Extractive desulfurization (EDS) probably will be economically attractive as a stand-alone process in some refinery applications. However, it seems likely that many refineries also will look to employ a synergistic combination

of HDS and EDS processing to expand and debottleneck their HDS capacity and achieve ULSD specifications at the lowest cost.

*Table 4. Preliminary Process Economic Assessment – Diesel Fuel*

| Process Type               | Capital Cost *           | Conversion Cost *      |
|----------------------------|--------------------------|------------------------|
|                            | TIC, US\$/barrel/day     | US\$/barrel            |
| HDS, conventional          | 2500 – 3500 <sup>a</sup> | 1.8 – 2.5 <sup>b</sup> |
| HDS, high-severity         | 3500 – 4500 <sup>b</sup> | 2.3 – 3.8 <sup>b</sup> |
| Extractive desulfurization | 1000 - 2000 <sup>c</sup> | 1.0 – 2.0 <sup>c</sup> |

\* The estimates assume 3000 wppm sulfur feed and 15 wppm sulfur diesel (350 wppm sulfur diesel for conventional HDS).

a. Total installed cost within battery limits, US Gulf Coast; variability due to feedstock, product spec, plant size and location. [See published studies, e.g., API, NCP, DOE as reported by MathPro 9/21/00 H-WFC.]

b. Conversion cost includes hydrogen, catalyst, labor, general, and capital charges; variability due to feedstock type and sulfur content, final spec, plant size, fuel cost.

c. Conversion cost based on generic assessment of similar processes [author's assessment].

Based on the “complementary reactivity” of AAT compounds towards oxidation and hydrogenation mentioned above, it seems probable that the EDS processes, when used as post- or pre-treatment in connection with existing conventional HDS processes, will achieve the objectives of lowest combined capital and conversion costs for ULSD production. Preliminary estimates indicate that conversion cost will be below what is expected for high-severity hydrodesulfurization.

*Table 5. Process Configurations and Comparative Costs*

| Example | Process Configuration                | Sulfur, wppm         | Conversion Cost |
|---------|--------------------------------------|----------------------|-----------------|
|         |                                      | Feed/Process/Product | US\$/barrel *   |
| I       | C-HDS <sup>b</sup>                   | 3000 / — / 350       | 1.80 – 2.50     |
| II      | HS-HDS <sup>c</sup>                  | 3000 / — / 15        | 2.50 – 3.80     |
| III     | C-HDS / EDS <sup>d</sup>             | 3000 / 350 / 15      | 2.80 – 3.10     |
| IV      | EDS / C-HDS <sup>d</sup>             | 3000 / 1000 / 15     | 2.80 – 3.50     |
| V       | EDS (several processes) <sup>d</sup> | 3000 / — / 15        | 1.00 – 2.00     |

a. Conversion cost assessments reference Tables 3 and 4.

b. C-HDS = Conventional HDS

c. HS-HDS = High-Severity HDS

d. EDS process assumes recycle of the EDS-extract stream to HDS unit for full credit.

Another symbiotic relationship may exist between EDS and HDS due to the production of high-sulfur extract from the EDS processes. The byproduct EDS extract will have a content of 65–85% poly-aromatics and 3–15 w% sulfur, and it will typically represent 15–30% of the feedstock. When the feedstock is first processed by EDS, the feed designated for HDS therefore may only need to be a fraction of the original volume. The resulting EDS extract will require processing by medium- or high-severity HDS, but pretreatment will unload the HDS unit by a substantial fraction, and the extract may indeed be a preferred, higher value feed than the feedstock it substitutes.

In addition to its potential as stand-alone processes for ULSD production, the EDS processes, therefore, may find application as ancillary process units for the debottlenecking of HDS units by:

- Placing EDS in front of the HDS for feedstock pretreatment will function to eliminate the most refractory AAT compounds and decrease the sulfur content overall.
- Placing EDS after the HDS unit provides a polishing step by removing the residual 300–500 PPM sulfur fraction that was too refractory for conventional HDS.
- Placing the EDS unit in parallel with the HDS will serve to unload the HDS unit by a factor of four with respect to the EDS feed stream.

The EDS processes may have limitations that must be considered for each individual refinery application. These limitations may include the boiling range of the feedstock, its density and its composition, especially olefins and sulfur levels. This suggests that refineries with both HDS and EDS units, located close together, may look for additional operating synergism in the area of fuel desulfurization.

#### 4. SUMMARY

There are several reasons why refinery engineers will want to consider using the new extractive desulfurization (EDS) processes. First, EDS can be considered for stand-alone desulfurization to produce ultra-low-sulfur diesel fuel (ULSD), similarly to HDS processing. Second, EDS may be considered for tandem operation with HDS, either as HDS feed pretreatment or effluent post-treatment to achieve the new ULSD specifications.<sup>10</sup> In these cases EDS promises to be an alternative for very-high severity HDS processing.

There are valid chemical reasons for the synergism between HDS and EDS. These surround the difficulties of treating alkyl-aryl-thiophene sulfur containing compounds in naphtha and gas-oil by high-severity hydrogenation, while the same compounds are readily oxidized under mild process conditions. It therefore makes sense to remove some of the sulfur via the conventional HDS processing, perhaps to reach 350–750 wppm S, and then to remove the rest via EDS.

Alternatively, one can consider unloading the HDS unit by processing the feedstock with EDS, and then processing only the smaller EDS-extract fraction by HDS.

Several EDS processes with differing design and operating characteristics are currently under development. As they mature within the next few years, we can expect that achieving the ULSD goal will become a more accessible challenge for the refinery industry.

## 5. REFERENCES

1. Sieli, G. M. "Optimizing Sulfur Reduction in Gasoline," *Today's Refiner*, **2000** (10), 11
2. Cooper, B. H.; Knudsen, K. G. "What Does It Take to Produce Ultra-Low-Sulfur Diesel?" *World Refining*, **2000** (11), 14-18
3. Shiraishi, Y, Hirai, T.; Komasaawa, I. "Petrochemical Desulfurization and Denitrogenation Process for Vacuum Gas Oil Using an Organic Two-Phase Extraction System," *Ind. Eng. Chem. Res.* **2001** (40), 293-303
4. Otsuki, S. (et al.) "Oxidative Desulfurization of Light Gas Oil and Vacuum Gas Oil by Oxidation and Solvent Extraction," *Energy & Fuels* **2000** (14), 1232-1239
5. Whitehurst D. D.; Isoda, T.; and Mochida, I.; "Present State of the Art and Future Challenges in the Hydrodesulfurization of Polyaromatic Sulfur Compounds," in Eley, D. D.; et al, *Advances in Catalysis*, **1998**, 345-472.
6. Richardson, N.; du Preez, P. "Study Says 2005 EU Product Specs May Cost Refiners up to \$9 Billion," *Oil & Gas Journal*, 11/27/00
7. Cabrera, C.A.; Imai, T. **U.S. Patent 6,171,478**, January 9, 2001
8. Bonde, S.E. (et al.) "Desulfurization by Selective Oxidation and Extraction of Sulfur-Containing Compounds in Diesel Fuel," NPRA Annual Meeting, March 27, 2000
9. Dolbear, G.E.; Skov, E.R. "Selective Oxidation as a Route to Petroleum Desulfurization," American Chemical Society National Meeting, San Francisco, March 2000
10. Ho, T.C.; Hsu, C.S.; Dupre, G.D.; Liotta, R.; Buckholz, V.B. "A Process for Deep Desulfurization Using Combined Hydrotreating-Oxidation," **US Patent 5,958,224**, August 14, 1998
11. Paybarah, A.; Bone, R.L.; Corcoran, W.H. "Selective Oxidation of Dibenzothiophene by Benzoic Acid Formed in Situ" *Ind. Chem. Process Des. Dev.* **1982** (21), 431-440
12. Collins, F.M.; Lucy, A.R.; Sharp, C. "Oxidative Desulphurization of Oils via Hydrogen Peroxide and Heteropolyanion Catalysis," *J. Molecular Catalysis A: Chem.* **117** **1997**, 397-403
13. Bui, K.. "Phillips Launches New Sulfur Removal Process," *Today's Refinery* **2000** (4) 17
14. Black & Veach, "IRVAD Process," NPRA, AM-99-42, March 1999
15. Stynes, P.C.; Shepherd, T.; Thompson, M.; Kidd, D. "Innovation Key to New Technology Project Success: Phillips S Zorb Becomes Low Sulfur Gasoline Solution," AM-01-43 National Petroleum Refiners Association, Washington. D.C., 2001

## Chapter 13

# ADVANCED REACTOR INTERNALS FOR HYDROPROCESSING UNITS

F. Emmett Bingham and Douglas E. Nelson  
*Haldor Topsoe, Inc.*  
*Orange, CA*

### 1. INTRODUCTION

Since the introduction of fixed bed hydroprocessing technology in the early 1950's, catalyst suppliers have made significant advances in improving the relative activities of hydroprocessing catalysts. As illustrated in Figure 1, the activities of current commercial hydrotreating catalysts are an order of magnitude higher than those initially introduced.

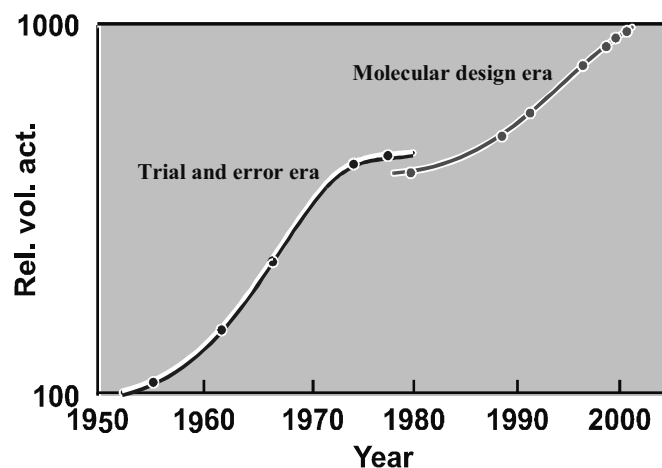


Figure 1. Development of Hydrodesulfurization Catalysts

In the mid 1990's it became apparent that the design of hydroprocessing reactors had not advanced at the same pace as the development of hydroprocessing catalysts, and that the existing reactors were not capable of utilizing the benefits of the high activity catalysts. As a result, licensors began to develop high performance reactor internals to address the demands of ultra-low sulfur diesel production.

## **2. ELEMENTS OF HYDROPROCESSING REACTOR DESIGN**

The following describes the reactor internals elements that should be considered in the design of hydroprocessing reactors:

- **Inlet Impingement Device:** The purpose of the inlet impingement device is to diffuse the velocity profile of the fluids entering the reactor inlet nozzle and create an even pattern of liquid dispersion across the top liquid distribution tray.
- **Top liquid distribution tray:** The top liquid distribution tray evenly distributes the liquid charge across the surface of the top catalyst bed.
- **Catalyst support:** Multiple beds are often utilized in reactors that have high temperature rises or would benefit from re-distribution of the reactants. These reactors would have catalyst support grids and beams to carry the weight of each catalyst bed.
- **Quench distributor:** In multibed reactors, quench fluids are introduced into a quench zone through a quench distributor for cooling purposes or replenishment of depleted reactants.
- **Quench Mixing Chamber:** In multibed reactors, the mixing chamber insures that liquid and vapor phases entering the quench zone make sufficient contact to reach an equilibrium temperature and composition.
- **Liquid re-distribution tray:** The re-distribution tray evenly distributes the quenched liquid and vapor exiting the mixing chamber across the surface of the subsequent catalyst bed.
- **Thermocouples:** Thermocouples monitor the temperature of the fluids reacting throughout the catalyst bed. They should be located to provide sufficient data to indicate that the reaction in each section of the catalyst bed is even.
- **Outlet collector:** The outlet collector supports the bottom catalyst bed and is designed to promote even flow in the bottom of the reactor.

Although the entire reactor internals elements listed above are important to the performance of the hydroprocessing reactor, the distribution trays and mixing chambers are critical to insuring the efficient utilization of the hydroprocessing catalyst.

### 3. LIQUID DISTRIBUTION TRAY DESIGN

Liquid distribution trays are typically used to establish good flow distribution in hydroprocessing reactors. By obtaining even distribution of the liquid reactants over the entire reactor cross sectional area, all the catalyst at a given level is evenly wetted. Thus all the catalyst at a given level operates at the same efficiency, which increases the overall efficiency of the reactor. Additionally, even liquid distribution minimizes the radial temperature profile across the reactor. This minimizes the occurrence of hot spots which, over time, causes coking and high catalyst deactivation. Consequently, the reactor operates more efficiently, which enables a longer cycle length. Value is achieved by reduced catalyst requirements, higher processing capability and/or longer cycle lengths.

Most liquid distribution devices are proprietary designs developed by process licensors and internals fabricators. Most of the known designs fall into one of four categories.

The first is a series of troughs and overflow weirs that systematically subdivide the liquid into multiple streams before it contacts the bed. This type is often used in liquid contactors or counter-current absorbers. The trough type distribution device is mechanically complex and very sensitive to levelness. Depending on the design of the troughs, the quality of the distribution may be susceptible to fouling. An example of this type is U.S. Patent 5,192,465 by Petrich, et al, assigned to Glitsch, Inc.

A second type of liquid distribution device is a perforated tray. This may or may not have notched weirs around the perforations. The tray may also have chimneys for vapor flow. This type of distribution device is often used for rough liquid distribution in conjunction with a more sophisticated final liquid distribution tray. A perforated tray is possibly the least expensive design with regard to materials and fabrication cost, and it can offer a large number of distribution points. However, it is not an efficient primary distribution device because it must be absolutely level to provide even distribution of liquids, and it is very prone to plugging by debris collecting on the tray. Examples of this type are U.S. Patent 4,836,989 by Ali, et al, assigned to Mobil Oil Co. and U.S. Patent 3,824,080 by Smith, et al, assigned to Texaco.

A third common type of liquid distribution device is a chimney tray. This device uses a number of standpipes laid out typically on a regular square or triangular pitch pattern on a horizontal tray. The standpipes typically have holes or notches cut through the sides for the passage of liquid. The tops of the standpipes are open to allow vapor flow down through the center of the chimneys. Some designs use special vapor chimneys to handle the bulk of the vapor flow. Functionally, the chimney tray design is very similar to the perforated tray design, except the holes or perforations are elevated above the surface of the tray to allow some capacity to maintain a liquid level and hold debris that may collect on the tray. The chimney design is an improvement over a perforated tray, since it can be designed for a wider range of liquid/vapor loadings and is less susceptible to fouling. However, the spacing of the chimney risers typically reduces the number of distribution points compared to a perforated tray. A properly designed chimney must either become taller or have smaller holes drilled in the side to maintain a liquid level on the tray as the liquid rate changes. At turndown, it is possible that some holes will be covered with liquid and others will not. This results in uneven liquid distribution over the surface below the tray. Examples of this type are U.S. Patent 4,126,540 by Grossboll, et al., assigned to ARCO, and U.S. Patent 3,353,924 by Riopelle assigned to Shell Oil Co.

The fourth type of liquid distribution device is a bubble cap tray, originally designed for application in fractionation towers. This device employs a number of bubble caps laid out on a regular pitched pattern on a horizontal tray. The bubble cap distributor works on a vapor-assist principle that offers a relatively stable operation compared to a chimney device. The bubble cap is a cap centered concentrically over a standpipe. The sides of the cap are slotted for vapor flow. Liquid flows under the cap and is aspirated by the vapor, flowing upward in the annular area between the cap and the standpipe, and then down through the standpipe.



The advantage of a bubble cap device over a chimney type design is the wider turndown range possible with the bubble cap. As the liquid charge rate drops the level drops on a bubble cap tray and the slot area increases, resulting in a reduced vapor velocity through the slots. The reduced vapor velocity pulls less liquid through the distributor, and the liquid level is re-established. Another advantage of the bubble cap over the chimney type design is that the bubble cap is less sensitive to an out-of-level tray. Due to fabricating tolerances, installation difficulties and deflection due to operating load, not all of the distribution devices will be at the same level in the vessel. With proper design, the bubble cap device will minimize the liquid flow differences between bubble caps at different elevations better than can be achieved with a chimney type design. A final advantage of the bubble cap over the chimney type design is the increased contacting of the liquid and vapor phases. The intimate contacting that occurs in the up flow portion of the device provides closer approaches to thermal and compositional equilibrium than would be achieved in the chimney tray.

The primary disadvantage of a bubble cap tray is the comparatively large size of the bubble caps relative to a chimney device. The large size and necessarily wider spacing of the bubble caps reduces the number of distribution points over the cross section of the tray and catalyst bed below. The wide spacing and pitched array of the bubble cap tray also results in poorer distribution coverage adjacent to the reactor wall, further reducing catalyst utilization. An example of this type is U.S. Patent 5,158,714 by Shih, et al., assigned to Union Oil Co.

A comparison of the performance characteristics of a typical multi-port chimney type distributor and a standard bubble cap distributor is illustrated in Figure 2.

The performance parameter, Sensitivity %, is a measurement of the difference in the liquid delivered by adjacent distributors at different elevations. This parameter is described by the following formula:

$$S = [(F_l - F_h) / F_{ave}] * 100$$

Where: S = Performance Sensitivity

$F_l$  = Liquid flow through low distributor

$F_h$  = Liquid flow through high distributor

$F_{ave}$  = Average flow through all distributors

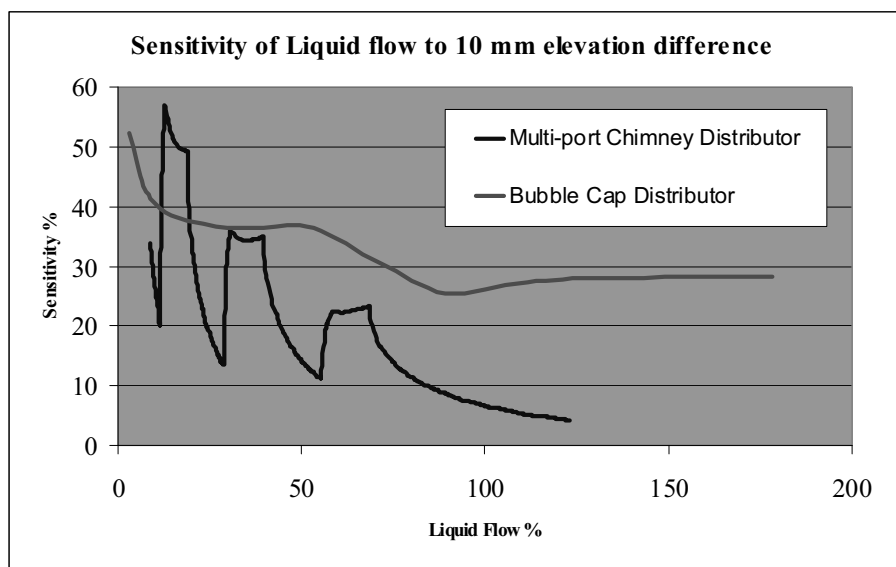


Figure 2. Liquid Distributor Performance Sensitivity

Figure 2 illustrates the deterioration in performance of a nonlevel chimney type tray as the liquid rate is reduced and the liquid level drops. Each time the liquid level reaches the nominal elevation of one of the chimney's holes, holes of the low chimneys may be covered with liquid while holes of the high chimneys are dry. Thus some distributors deliver more liquid. This causes flow mal-distribution across the catalyst bed.

When Haldor Topsøe began to investigate the design of a high performance distribution tray, several parameters were recognized as critical to achieve the desired performance efficiency. These are as follows:

1. **Spacing Density:** Because of the difficulty to visualize the performance of the distribution devices under actual operating conditions of a hydroprocessing reactor, assumptions as to the effectiveness of overlapping spray patterns, or deflection splash patterns, should be discounted. The only positive approach to insure adequate liquid distribution is to achieve a high number of liquid drip points across the surface of catalyst by reducing the spacing of the distribution devices as much as is practically possible. Increasing the spacing density also enables a greater number of distribution points in the area adjacent to the reactor wall. This is very important to improved catalyst utilization, because over 35% of the catalyst in the reactor is contained within an annular ring between the reactor wall and 80% of the reactor diameter.

2. **Sensitivity to Levelness:** An out-of-level condition should have a very low impact on the operation of a high performance distribution tray. As described earlier, a distributor device operating on a vapor-assist principle will have a greater tolerance to levelness compared to a chimney type distributor device. In addition, the geometry of the distributor device can further improve the sensitivity to levelness. Leveling devices can also be incorporated into the tray design to compensate for out-of-levelness due to ring warpage, beam deflection, or plumbness of the reactor.
3. **Operating Stability:** A distribution tray may have very good performance at the design conditions. However, as the operation diverges from the design point due to changes in the charge rate or changes in vaporization due to temperature or feed quality, the performance of the distribution tray can deteriorate rapidly. A high performance tray should be capable of maintaining a relatively level height of liquid and an even flow rate through the distributor devices as the operation of the reactor changes.

The distribution device developed through the research and development efforts undertaken by Haldor Topsøe is a combination of bubble cap and chimney devices referred to as a Vapor-Lift Tray, or VLT. The VLT device has an operating concept similar to a bubble cap device but has several advantages. The VLT device has a smaller footprint and closer spacing which enables an increase in the number of liquid distribution points across the tray area. Furthermore, since the spacing pattern has a square rather than triangular pitch, gaps in liquid distribution coverage along beams and near the vessel wall are minimized. Overall wetting efficiency of the catalyst below the tray is improved when the liquid distributors have a smaller pitch compared to a larger pitch.

A standard bubble cap tray design is limited by the relatively large spacing and modifications have been attempted to improve the dispersion pattern of the liquid exiting from the cap, e.g. the shear plate described in the Shih patent or the turbine baffles described in the Jacobs patent. Increasing the number of bubble caps by reducing the spacing would increase the number of distribution points. However, doing so would negatively impact the liquid/vapor flow relationships through each cap. Smaller bubble caps with fewer slots will not be as efficient as a VLT due to the geometry of the concentric caps. The geometry of the VLT enhances the stability over a wide operating range compared to a bubble cap. A further advantage for the VLT device is that its simplicity makes it easier and less costly to fabricate in the optimal size prescribed by the process conditions. The performance characteristics of a VLT compared to bubble caps and chimney tray designs are illustrated in Figure 3.

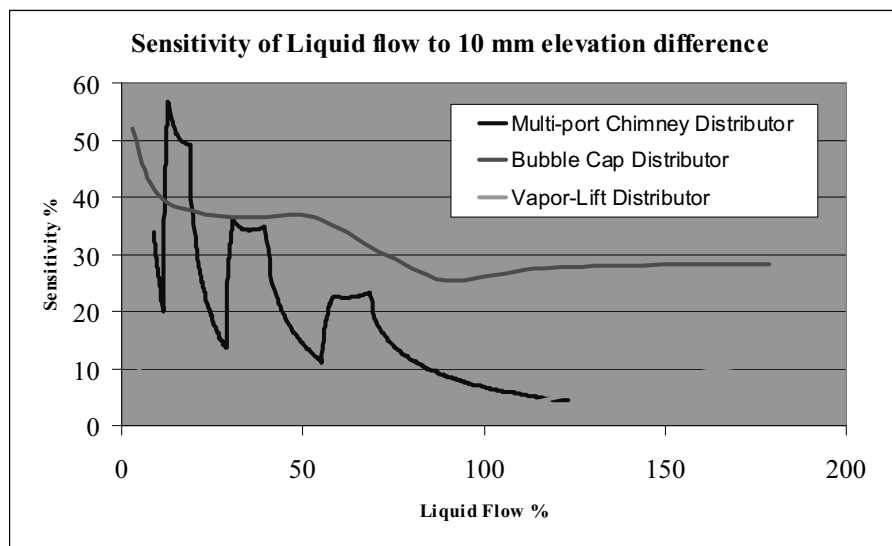


Figure 3. VLT Distributor Performance

Sensitivity is, as described previously, a gauge of the difference in the liquid flow measured from adjacent liquid distributors positioned at different elevations. These plots show that the percentage difference in the liquid flow from VLT distributors is much smaller compared to other distributor types. This ensures an even distribution of liquid over a broad range of operations, even though the tray may not be perfectly level. Poorly designed distributor devices can become very unstable and sensitive to differences in elevation as the liquid level on the tray drops. At very low liquid levels, a poorly designed distributor can actually cause mal-distribution of liquid across the catalyst bed beneath the tray.

#### 4. QUENCH MIXING CHAMBER DESIGN

The catalyst in hydroprocessing reactors with high temperature rises or large catalyst volumes is separated into multiple catalyst beds. A quench section separating each of the catalyst beds is designed to mix the reactants and introduce a quenching medium to typically reduce the equilibrium temperature before the reactants are distributed over the following catalyst bed. Since distributor trays are basically plug-flow devices, an apparatus is needed to mix the liquid into a homogeneous blend before it is delivered onto the distribution tray. Several different mixing chamber designs have evolved during the development of hydroprocessing reactor internals.

Baffle mixer designs such as ribbon blenders and disc-and-donut type mixers promote mixing by changing the direction of the fluid streams. These designs can be effective mixing devices, but they usually have comparatively high differential pressures to achieve mixing and they can be comparatively large, requiring more reactor shell length to accommodate the quench section.

Impingement type quench boxes promote mixing by injecting or directing separate portions of the reactant fluids and impinging them against one another in a small area. This type of mixer can be designed with a reduced depth. However, test work has shown that it is difficult to achieve an equilibrium temperature with an impingement type mixer. In a low pressure drop design, the vapor and liquid phases typically follow separate paths through the mixing chamber and can segregate and inhibit the mixing of liquid collected from different quadrants of the reactor.

A preferred type of mixing chamber is a centrifugal or vortex type design, typical of the design introduced by U.S. Patent 4,836,989 by Ali, et al., assigned to Mobil Oil Co. This mixer collects liquid and vapor from all quadrants of the reactor and introduces them close to the perimeter of a circular chamber where they make several rotations before being ejected out through a central exit port. This design can have a comparatively shallow depth, a very low pressure drop, and can achieve an equilibrium temperature of the liquid passing through the mixer. Several licensors skilled in the design of hydroprocessing reactors employ a vortex type mixing chamber.

## 5. EXAMPLE OF REACTOR INTERNALS REVAMP

The following is an example of improved performance that has been realized by replacing a classic reactor internals design with a recently developed high performance design.

The original reactor internals included bubble-cap liquid distribution trays and impingement-type, quench mixing chambers similar to those described in U.S. Patent No. 3,218,249 and U.S. Patent No. 3,502,445 –Ballard, et al., Union Oil of Cal. (Figure 4). The original thermometry comprised three vertical thermowells running the length of the reactors and horizontal thermowells traversing the top and bottom of each of three catalyst beds.

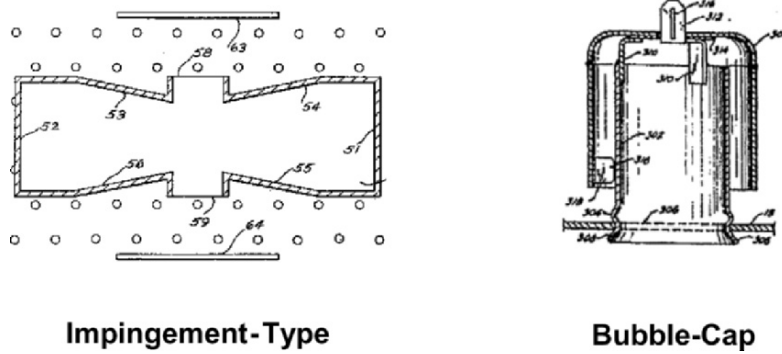


Figure 4. Pre-Revamp Reactor Internals

### 5.1 Reactor Internals Performance (Pre-revamp)

Due to changes in the plant operation subsequent to the initial installation, the performance of the impingement-type quench mixing chambers deteriorated and the distribution trays could no longer maintain an even flow distribution across the catalyst beds. The degradation in performance of the reactor internals resulted in wide radial temperature variations ranging from 7– 10°C at the catalyst bed inlets to 15 – 40°C at the catalyst bed outlets. The flow/temperature mal-distribution is documented by temperature profiles plotted from thermocouple measurements (Figure 5).

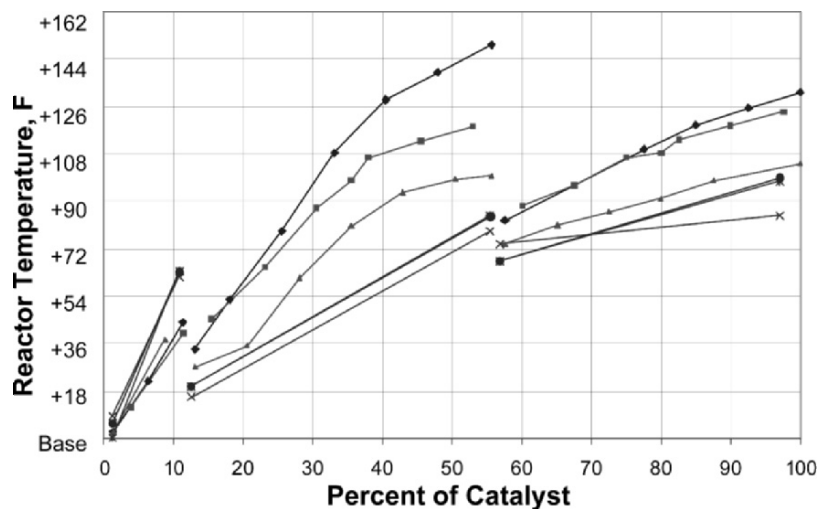


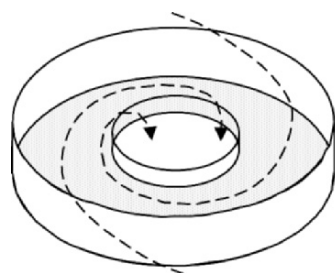
Figure 5. Pre-Revamp Performance

As seen, significant radial temperature differences were measured by the thermocouples in the vertical thermowells, especially at the bottom of the second catalyst bed in the reactor. The temperature difference measured at the top of the middle and lower catalyst beds is an indication that the quench boxes were not adequately mixing the liquid to an equilibrium temperature before passing it on to the re-distribution trays. Further, the vapor-liquid mixing through the distributors was not sufficient to evenly quench the liquid before it was distributed onto the next bed. In addition to the temperature mal-distribution, the original re-distribution trays were not providing an even liquid flow onto the following catalyst beds. This flow mal-distribution is indicated by the widening of the radial temperature differences measured by thermocouples descending through the beds.

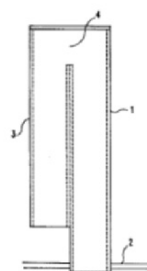
Large radial temperature differences are problematic because they reduce the length of the operating cycle between turnarounds. High peak temperature areas adjacent to the reactor wall lead to premature unit shutdown as the temperature approaches the reactor design limit. Furthermore, because of limited thermocouple coverage, there is real concern that the existing temperature indicators might not record the actual hot spot in the catalyst bed, and that damage to the reactor wall could occur unknowingly.

## 5.2 New Reactor Internals Modifications and Improvements

To improve unit performance, the existing reactor internals were replaced by high performance vortex type mixing chambers to optimize liquid-liquid mixing and VLT distribution trays to increase the number of drip points and minimize the dead flow zones adjacent to the reactor wall (Figure 6). The VLT distribution trays also offered low sensitivity to tray levelness and improved stability over a wide operating range.



**Vortex-Mixer**



**Vapor-Lift Distributor**

Figure 6. High Performance Reactor Internals

To improve monitoring of the temperature profiles, the existing thermocouple arrangement was replaced by 84 flexible-type thermocouples in the catalyst beds.

### 5.3 Performance Improvement Results

Following the restart of operations, the temperature profile across the reactor with the new internals is plotted in Figure 7. The improved performance of the new internals is readily seen when comparing this plot with that previously shown in Figure 5.

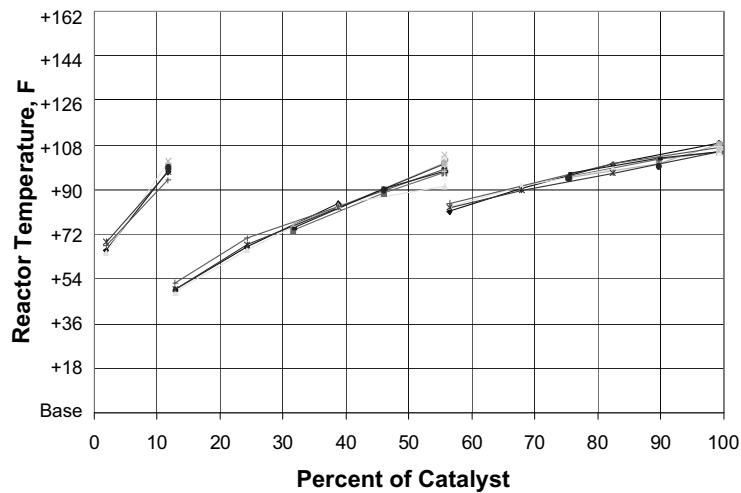


Figure 7. Revamped Reactor Performance

Several observations from such a comparison are immediately apparent:

### 5.4 Radial Temperature Differences

The radial temperature spreads for the revamped operation are significantly improved compared to the original equipment. At the start of the operating cycle conditions, the actual deviation in bed inlet temperature is approximately 1°C. With the old internals, the temperature deviation at the bed inlets ranged from 7-10°C. With the new internals, the radial temperature spread at the bed outlets ranges from 2-4°C. This is significantly lower than the 15-40°C bed outlet temperature deviation experienced with the old internals.



## **5.5 Weighted Average Bed Temperature**

A reduction in average bed temperature is typically observed when less efficient distribution trays are replaced. This is due to more efficient utilization of the catalyst resulting from improved liquid flow distribution. It appears that a directional 2-4°C reduction in weighted average bed temperature (WABT) may have been achieved. However, it is difficult to estimate the degree of improvement with any precision because the widely divergent temperatures measured by the three vertical thermowells during the pre-revamp operation makes estimating the actual WABT very speculative.

## **6. CONCLUSIONS**

Hydroprocessing reactors originally designed for low severity service typically are not adequate to handle increased severity with high activity catalysts or to achieve the operating efficiency demanded by the current and future fuels specifications.

High performance reactor mixing chamber and distribution tray designs have been developed by some licensors which can often be incorporated into existing reactors to improve their performance.

## Chapter 14

# ENVIRONMENTAL POLLUTION CONTROL

Paul R. Robinson,<sup>1</sup> Eli E. Shaheen,<sup>2</sup> and Esber I. Shaheen<sup>3</sup>

1. *PQ Optimization Services, 3418 Clear Water Park Drive, Katy, TX 77450*

2. *International Institute of Technology Inc., 830 Wall Street, Joplin, MO 64801*

3. *In memorium*

### 1. WHY CONTROL POLLUTION?

The best-selling book, *Technology of Environmental Pollution Control* by Esber I. Shaheen,<sup>1</sup> serves as the primary technical reference for this chapter.

While addressing the question *What Is Life?* Margulis and Sagan<sup>2</sup> remind us that “every species of organism produces wastes that are incompatible with its own existence.” As humans living on an ever-more-crowded planet, our main reason for abating pollution is self-preservation. Observing nature tells that that some day, if we don’t control it, our own waste will kill us.

### 2. POLLUTION FROM PETROLEUM PROCESSING

This section describes the predominant gaseous, liquid and solid pollutants generated by the petroleum industry. It also explains why these pollutants can be harmful. Section 5 of this chapter describes selected pollution-control regulations, and Section 6 discusses technology for abating these pollutants.

#### 2.1 Particulate Matter

The main sources of air pollution from petroleum refineries are listed in *Table 1*. Refineries can be significant sources of particulate matter (PM), which can irritate the respiratory tract. PM is especially harmful when it is associated with sulfur and nitrogen oxides (SO<sub>x</sub> and NO<sub>x</sub>).

Table 1. Main Sources of Refinery Air Pollution

| Source                                  | PM | SO <sub>2</sub> | CO | VOC | NO <sub>x</sub> |
|---|----|-----------------|----|-----|-----------------|
| Fluid catalytic cracking (FCC) units    | x  | x               | x  | x   | x               |
| Coking units                            | x  | x               | x  | x   | x               |
| Compressor engines                      |    | x               | x  | x   | x               |
| Vapor recovery and flare systems        |    | x               | x  | x   | x               |
| Vacuum distillation unit and condensers |    |                 |    | x   |                 |
| Sulfur recovery units                   |    | x               | x  |     | x               |
| Waste water treatment plants            |    |                 |    | x   |                 |
| Boilers and process heaters             |    | x               | x  |     | x               |
| Storage tanks                           |    |                 |    | x   |                 |

PM = particulate matter

SO<sub>2</sub> = sulfur dioxide

CO = carbon monoxide

VOC = volatile organic compounds

NO<sub>x</sub> = nitric oxide (NO) and nitrogen dioxide (NO<sub>2</sub>)

Most refinery PM comes from two sources – delayed coking units and the regenerators of fluid catalytic cracking (FCC) units. FCC regenerators also emit ammonia, which combines with SO<sub>x</sub> and NO<sub>x</sub> in the air to form ammonium sulfates and nitrates. According to the South Coast Air Quality Management District (AQMD)<sup>3</sup> in Southern California, 1 ton of ammonia can generate 6 tons of PM<sub>10</sub> – airborne particulates with particle diameters less than 10 microns. PM<sub>2.5</sub> stands for airborne particulates with diameters less than 2.5 microns.

## 2.2 Carbon Monoxide

In refineries, carbon monoxide (CO) is formed by incomplete combustion in boilers, process heaters, power plants, and FCC regenerators. CO is toxic because it binds strongly to the hemoglobin in blood, displacing oxygen. It is colorless and odorless, so without a special analyzer, it is hard to detect. This adds to its danger.

## 2.3 Sulfur Oxides

At oil and gas production sites, sulfur dioxide (SO<sub>2</sub>) and sulfur trioxide (SO<sub>3</sub>) are produced by the burning of sulfur-containing fuels. In oil refineries, SO<sub>x</sub> are produced by the combustion of sulfur-containing fuels, including the coke that is burned off of catalysts in FCC regenerators. SO<sub>x</sub> irritate the respiratory tracts of people and other animals. When adsorbed to particulate matter, SO<sub>x</sub> are especially bad. While gaseous SO<sub>x</sub> molecules are trapped by mucous in the upper respiratory tract, inhaled particulates can penetrate deep into lungs.

In the atmosphere, SO<sub>x</sub> react with water vapor to make sulfurous and sulfuric acids. The acids return to earth as “acid rain,” which poisons trees and

contaminates lakes and rivers. Experts estimate that SO<sub>2</sub> can remain in the air for 2 to 4 days. During that time, it can travel 600 miles (1,000 km) before returning to the ground. Consequently, SO<sub>2</sub> emissions have caused a number of international disputes. Acid rain from neighboring countries in Eastern Europe may have caused the death of about 1/3 of Germany's forests. In the past, the United States and Canada argued bitterly about the cross-border impact of SO<sub>x</sub> emissions from U.S. power plants. Fortunately, since 1983, the passage and enforcement of clean-air legislation has reduced the problem dramatically.

## 2.4 Nitrogen Oxides, VOC, and Ozone

Like CO and SO<sub>x</sub>, nitric oxide (NO) and nitrogen dioxide (NO<sub>2</sub>) are emitted by fired heaters, power plants and FCC regenerators. NO<sub>x</sub> also damage respiratory tissues and contribute to acid rain.

Ozone, a nasty component of smog, is generated by reactions between oxygen and NO<sub>x</sub>. The reactions are triggered by sunlight. In the troposphere, ozone reacts with volatile organic hydrocarbons (VOC) to form aldehydes, peroxyacetyl nitrate (PAN), peroxybenzoyl nitrate (PBN) and a number of other substances. PAN irritates nasal passages, mucous membranes, and lung tissue. Collectively, these compounds are called "photochemical smog." They are toxic to humans, animals and plants, and they accelerate the degradation of rubber and other materials. In some areas, smog looks like a brownish cloud just above the horizon. It makes for spectacular sunsets, but nothing else about it is good.

In the United States, areas with the worst air are Los Angeles, Houston, Eastern Connecticut, and New York. In recent years, due to better air in Los Angeles and worse air in Houston (caused in part by accidental releases from chemical plants along the Ship Channel), Houston led the United States in 1<sup>st</sup>-stage smog alerts.

Standards for selected pollutants in the air over Los Angeles are given in *Table 2*.

*Table 2.* Standards for Selected Pollutants in the Air over Los Angeles

| Pollutant       | Maximum Allowable Concentration, ppm |       |        |
|-----------------|--------------------------------------|-------|--------|
|                 | Warning                              | Alert | Danger |
| Carbon monoxide | 100                                  | 200   | 300    |
| Nitrogen oxides | 3                                    | 5     | 10     |
| Sulfur dioxide  | 3                                    | 5     | 10     |
| Ozone           | 0.5                                  | 1.0   | 1.5    |

## 2.5 Chemicals that React with Stratospheric Ozone<sup>4</sup>

The previous section mentions the harmful effects of ground-level ozone. The stratosphere, located about 6 to 30 miles (10 to 50 km) above the ground,

contains a layer of ozone that is beneficial, because it protects organisms from harmful ultraviolet-B (UV-B) solar radiation.

Over the past 3 decades, scientists have concluded that this protective shield has been damaged. Each year, an “ozone hole” forms over Antarctica. Ozone levels there can fall to 60% below normal. Even over the United States, stratospheric ozone levels are about 3% below normal in summer and 5% below normal in winter.

In the 1970s, scientists linked several man-made substances to ozone depletion, including carbon tetrachloride (CCl<sub>4</sub>), chlorofluorocarbons (CFCs), halons, methyl bromide, and methyl chloroform. These chemicals leak from air conditioners, refrigerators, insulating foam, and some industrial processes. Winds carry them through the lower atmosphere into the stratosphere, where they react with strong solar radiation to release chlorine and bromine atoms. These atoms initiate chain reactions that consume ozone. Scientists estimate that a single chlorine atom can destroy 100,000 ozone molecules.

The 1998 and 2002 Scientific Assessments of Stratospheric Ozone firmly established the link between decreased ozone and increased UV-B radiation. In humans, UV-B is linked to skin cancer. It also contributes to cataracts and suppression of the immune system. The effects of UV-B on plant and aquatic ecosystems are not well understood. However, the growth of certain plants can be slowed by excessive UV-B. Some scientists suggest that marine phytoplankton, which are the foundation of the ocean food chain, are already under stress from UV-B. If true, this could adversely affect supplies of food from the oceans.

In 1987, 27 countries signed the Montreal Protocol, which recognized the international consequences of ozone depletion and committed the signatories to limit production of ozone-depleting substances. Today, more than 180 nations have signed the Protocol, which now calls for the elimination of ozone-depleting chemicals.

In the United States, production of halons ended in January 1994. In January 1996, production virtually ceased for several other ozone-depleting chemicals, including CFCs, CCl<sub>4</sub>, and methyl chloroform. New products less damaging to the ozone layer have gained popularity. For example, computer makers now use ozone-safe solvents to clean circuit boards, and automobile manufacturers use HFC-134a, an ozone-safe refrigerant, for air conditioners in new vehicles.

Studies indicate that the Montreal Protocol has been effective to date. The 2002 Scientific Assessment of Ozone Depletion shows that the rate of ozone depletion is slowing. Stratospheric concentrations of methyl chloroform are falling, indicating that emissions have been reduced. Concentrations of other ozone-depleting substances, such as CFCs, are also decreasing. It takes years for these substances to reach the stratosphere and release chlorine and bromine atoms. For this reason, stratospheric chlorine levels are still near their peak, but they are expected to decline slowly in years to come. If all parties to

the Montreal Protocol abide by their commitments, the ozone layer may fully recover during the second half of this century.

## 2.6 Greenhouse Gases<sup>5,6</sup>

In a greenhouse or in an automobile with the windows rolled up, sunlight comes in through the glass and gets absorbed by various objects inside. These objects reradiate the adsorbed energy as heat, which can't go back out through the glass, at least not very quickly. Consequently, on a sunny day the inside of a greenhouse and inside of a sealed car is hotter than the outside air.

In the earth's atmosphere, gases such as CO<sub>2</sub>, CH<sub>4</sub>, and N<sub>2</sub>O are called "greenhouse gases," because they are nearly transparent to visible sunlight, but they absorb infrared (IR) radiation. In essence, they warm the atmosphere by slowing the release of heat into space. (The analogy with a real greenhouse isn't perfect, but it comes close.)

On average, every person in the world is responsible for just over a ton of CO<sub>2</sub> emissions each year. Most of this is due to the burning of fossil fuels in power plants and vehicles. According to some estimates, to prevent dangerous climate change while allowing for some increase in population, that number must be reduced to about 0.3 tons per person per year.

### 2.6.1 Global CO<sub>2</sub> and Temperature Balances

We are lucky to live on a planet that has a stable balance between *heat sources* (sunlight, volcanoes, forest fires, power plants, animal metabolism, natural radioactive decay, etc.) and *heat sinks* (consumption of sunlight by plants, radiation of heat into space, etc.). We also are lucky that our oceans and ice caps do such an excellent job of regulating temperature. In the past, when the amount of heat from sources exceeded the heat consumed by sinks, the ice caps shrank and sea level rose, but the average global temperature changed just a little – less than a few degrees. When heat sinks exceeded heat sources (for example, after a meteor strike or a major volcanic explosion hurled dust into the atmosphere, reducing incident sunlight for several months or even years), the ice caps grew and sea level fell, but again the average global temperature stayed nearly the same.

The oceans also serve as a buffer for carbon dioxide. On average, the oceans hold 60 times more CO<sub>2</sub> than the atmosphere. When dissolved in water, CO<sub>2</sub> forms carbonic acid (H<sub>2</sub>CO<sub>3</sub>), bicarbonate (HCO<sub>3</sub><sup>-</sup>) and carbonate (CO<sub>3</sub><sup>2-</sup>). Sea water is slightly alkaline, with a surface pH of 8.2, so it readily reacts with H<sub>2</sub>CO<sub>3</sub>. However, rapid exchange with the atmosphere only occurs in the upper wind-mixed layer, which is about 300 feet (100 meters) thick. This layer contains roughly one atmosphere equivalent of CO<sub>2</sub>.

CO<sub>2</sub> in its various forms is removed from the sea by foraminifera, coral reefs, and other marine organisms, which produce solid calcium carbonate,

the main component of sea shells. About 30 to 50% of the CO<sub>2</sub> released into the air stays there. The rest goes into the hydrosphere and biosphere.

*Table 3* provides estimates of the global carbon distribution.<sup>7</sup>

*Table 3.* Global Distribution of Carbon

| Source   | Moles of Carbon x 10 <sup>18</sup> | Relative to the Atmosphere |
|--|------------------------------------|----------------------------|
| Sediments  |                                    |                            |
| Carbonates   | 1530                               | 28,500                     |
| Organic carbon                                     | 572                                | 10,600                     |
| Land   |                                    |                            |
| Organic carbon                                     | 0.065                              | 1.22                       |
| Oceans   |                                    |                            |
| CO <sub>2</sub> and H <sub>2</sub> CO <sub>3</sub> | 0.018                              | 0.3                        |
| HCO <sub>3</sub> <sup>-</sup>                      | 2.6                                | 48.7                       |
| CO <sub>3</sub> <sup>2-</sup>                      | 0.33                               | 6.0                        |
| Dead organic                                       | 0.23                               | 4.4                        |
| Living organic                                     | 0.0007                             | 0.01                       |
| Atmosphere   |                                    |                            |
| CO <sub>2</sub>                                    | 0.0535                             | 1.0                        |

## 2.6.2 Global Warming

The global greenhouse effect – also called global warming – concerns us now because atmospheric CO<sub>2</sub> concentrations are increasing faster than ever, and because most of the increase is due to industrial growth. Many scientists predict that unless we do something to impede global warming, it may:

- Increase the number and intensity of dangerous heat waves
- Increase severe storm activity
- Damage certain crops
- Raise the average sea level

These in turn will increase weather-related deaths, damage coastal cities and towns, and ruin coastal ecosystems.

It is still hard to find a consensus on global warming. Different experts use different models and even different data sets.<sup>6</sup> Some believe global warming is imminent and predict that it will cause catastrophic damage. Others are far less concerned. Until the science is more definitive, the global-warming debate will continue to be governed by Robinson's Rule of Expert Testimony:

“For any given PhD, there is an equal and opposite PhD.”

## 2.7 Waste Water

Refineries generate contaminated process water, oily runoff, and sewage. Water is used by just about every process unit, especially those that require wash water, condensate, stripping water, caustic, or neutralization acids. Contaminated process water may contain suspended solids, dissolved salts, phenols, ammonia, sulfides, and other compounds. As much as possible, waste-water streams are purified and re-used. Present requirements ensure that

the water going out of a refinery is at least as clean as the water coming in. Additional details are provided in Section 6.

## 2.8 Solid Waste

Solid wastes from petroleum processing may include the following:

- Cuttings from the drilling of oil wells
- Used drilling mud
- Spent catalyst and catalyst fines
- Acid sludge from alkylation units
- Sludge from the bottom of storage tanks
- Miscellaneous oil-contaminated solids

Wastes that cannot be recycled are cleaned on site, sent to land fills, or transported to reclamation facilities. Some of the technology used for cleanup and reclamation is discussed in Section 6.

## 2.9 Oil Spills

Large spills of oil from tankers are not very uncommon, but they can cause tremendous damage to the environment. Small spills come from leaks in tanks or mishaps during the loading or unloading of trucks, ships, or rail cars. Spills are discussed in more detail in Sections 3, 4, and 6.

## 3. ENVIRONMENTAL INCIDENTS

Pollution-causing incidents can be divided into four major categories:

**1. Usual-practice pollution.** In this case, we know that we are discharging waste into the environment. We know the associated risk, but we conclude that the cost of decreasing the discharge is too high. To different groups, “risk” and “cost” can mean entirely different things. Usually, nothing changes until some government body decides to force a change.

**2. Accidental pollution.** This category includes industrial accidents, some of which are described below. Post-disaster investigations often show that the accidents were preventable. In many cases, an entire industry learns from the accident and implements safeguards to prevent a recurrence.

**3. Inappropriate response to pollution.** As shown in the examples below, many industrial accidents would have been far less harmful if the people involved had responded in a more appropriate way. Inappropriate responses reflect lack of preparation, both mental and physical. Studies conclude that careful emergency planning coupled with thorough employee training (and re-training) prevents accidents and leads to faster, better responses to accidents.

**4. Malicious acts.** These include illegal “midnight dumping,” cover-ups, sabotage, and acts of war.



The examples described below cover all four categories. In every case, the damage was mitigated by the heroic efforts of doctors, nurses, firemen, and/or cleanup crews. These people put themselves at risk to save the lives of others. When we give statistics for lost lives, we don't enumerate all the lives saved by these heroes, not because we don't want to, but because we can't find the numbers.

### **3.1 London Fog (1952)**

In December 1952, thick fog rolled across many parts of the British Isles. In the Thames Valley, the fog mixed with smoke, soot and sulfur dioxide from coal-burning homes and factories, turning the air over London into a dense yellow mass. Due to a temperature inversion, the fog stayed put for several days, during which the city's hospitals filled to over-flowing. According to the Parliamentary Office of Science and Technology,<sup>8</sup> more than 4,000 people died that month because of the polluted air. Similar, less-severe episodes occurred in 1956, 1957, and 1962. The 1956 event killed more than 1,000 people.

London's deadly smog was caused by "usual-practice" pollution. Due to the widespread use of cheap, high-sulfur coal, the air in London had been bad for decades, but post-war growth made it worse than ever. In response to the incidents, Parliament passed Clean Air Acts in 1956 and 1962, prohibiting the use of high-sulfur fuels in critical areas.

### **3.2 Amoco Cadiz (1978)<sup>9</sup>**

On March 16, 1978, the supertanker *Amoco Cadiz* was three miles off the coast of Brittany when its steering mechanism failed. The ship ran aground on the Portsall Rocks.

For two weeks, severe weather restricted cleanup efforts. The wreck broke up completely before any of the remaining oil could be pumped out, so the entire cargo – more than 1.6 million barrels of Arabian and Iranian crude oil – spilled into the sea.

The resulting slick was 18 miles wide and 80 miles long. It polluted 200 miles of coastline, including the beaches of 76 Breton communities. On several beaches, oil penetrated the sand to a depth of 20 inches. Piers and slips in small harbors were covered with oil. Other polluted areas included the pink granite rock beaches of Tregastel and Perros-Guirrec, and the popular bathing beaches at Plougasnou. The oil persisted for only a few weeks along exposed rocky shores, but in the areas protected from wave action, the oil remained as an asphalt crust for several years.

At the time, the *Amoco Cadiz* incident caused more loss of marine life than any other oil spill. Cleanup activities on rocky shores, such as pressure-washing, also caused harm. Two weeks after the accident, millions of dead

mollusks, sea urchins, and other bottom-dwelling organisms washed ashore. Nearly 20,000 dead birds were recovered. About 9,000 tons of oysters died. Fish developed skin ulcerations and tumors.

Years later, echinoderms and small crustaceans had disappeared from many areas, but other species had recovered. Even today, evidence of oiled beach sediments can be seen in sheltered areas, and layers of sub-surface oil remain under many impacted beaches.

### **3.3 Bhopal, India (1984)**

On December 2, 1984, a worker observed a build-up of pressure in a storage tank at the Union Carbide chemical plant near Bhopal, India. The tank contained about 15 tons of methylisocyanate (MIC), a chemical used to make pesticides. It is flammable, and at high concentrations it is deadly. At low concentrations, it causes lung damage and blindness.

The pressure increase probably was caused by water inside the tank. Water reacts with MIC to form methylamine and gaseous carbon monoxide. The reaction releases heat, which would have contributed to the pressure rise by vaporizing some MIC. Normally, a refrigeration unit would have controlled the temperature, but that unit had been out of service for several months. Eventually, the pressure rise opened a safety valve. When this happened, the vented gas should have been routed to a caustic scrubber, which would have absorbed and hydrolyzed the MIC, rendering it harmless. Instead, the vented gas went to the flare. The flare should have converted the MIC into relatively harmless CO<sub>2</sub>, H<sub>2</sub>O and N<sub>2</sub>. But the flare system failed, perhaps because it wasn't designed to handle such a large surge of gas. Consequently, tons of MIC poured into the air and spread across the countryside, covering 25 square miles (65 square kilometers). If operators had noticed the leak immediately, they might have been able to stop it before it did much damage. But leak did not show up on their monitors because a critical panel had been removed from the control room.

How did water get into the tank? The MIC was stored under a blanket of dry nitrogen. Some experts suggest that the nitrogen was wet. Others guess that a water hose was inadvertently connected to the nitrogen line. A Union Carbide official suggested possible sabotage.

Even if the incident on December 2, 1984 was an accident, the MIC unit at Bhopal was a disaster waiting to happen. During a press conference, a Union Carbide executive acknowledged that the unit was in a state of sorry disrepair, and that its condition was so poor that it shouldn't have been running.

Up to 200,000 people were exposed to MIC in Bhopal and surrounding towns. More than 2,500 died. Thousands more suffered permanent lung and/or eye damage. All told, there were 524,000 personal injury claims, 2,800 lost-cattle claims, 4,600 business claims, and 3,400 wrongful death claims.

Eventually, Union Carbide reached a US\$470 million settlement with the Parliament of India.

### 3.4 Chernobyl (1986)

SCRAM stands for “safety critical reactor ax man.” It is a term from the early days of nuclear power development, when control rods were raised and lowered into the reactor core with a rope on a pulley. The ax man stood ready to cut the rope in an emergency, dropping all control rods all way down, shutting down the reactor.

After a SCRAM at the Chernobyl nuclear power plant near Pripyat, Ukraine, the cooling water pumps would stop due to lost electrical power. Emergency power was supplied by diesel generators, but starting the diesels took almost a minute. During the delay, residual heat remained in the reactor until the cooling pumps were running again.

To Deputy Chief Engineer Anatolij Diatlov, this delay was unacceptable. He thought of a solution. Right after a SCRAM, he knew, the plant’s power turbines kept spinning for several minutes due to their massive inertia. Diatlov calculated that, as the turbines slowed down, they could produce enough power to run the water pumps until the diesels were up and running. He designed a complex network of switches to keep the current steady as the turbines lost momentum.

Diatlov talked to the chief engineer of the plant, who gave him permission to run his “electrical engineering” experiment. The test began on April 25, 1986, as Unit 4 was shutting down for long-delayed maintenance. With Diatlov’s approval, the operators decided to run the test manually instead of using the unit’s “unimaginative automatics.”

At 2:00 PM, in violation of safety regulations, the operators switched off the emergency cooling system. Just after midnight on April 26th, they violated another rule by switching off the reactor’s power-density controls.

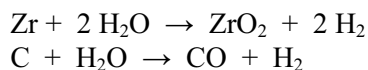
Under manual operation, the reactor became unstable. At 1:07 AM, the power output suddenly dropped to 0.03 gigawatts (GW), far less than the specified minimum of 0.70 GW. To generate more power, the operators raised the control rods to the maximum height allowed by regulations. Diatlov ordered them to raise the rods further. When the operators balked, Diatlov insisted, and the operators complied.

At 1:23 AM, the power output seemed to be stable at 0.2 GW. The operators violated yet another regulation by disabling the emergency SCRAM, an automatic interlock designed to stop the reactor whenever the neutron flux exceeds a safe limit. (In modern nuclear power plants, it is physically impossible to disable this control.)

Now the experiment could begin. To see how long the turbine would spin without a supply of steam, they closed the valve that channelled steam from

the reactor to the turbine. Steam that should have been taking heat out of the reactor was now trapped inside.

In less than 45 seconds, the reactor started to melt. Super-hot pellets of uranium-oxide fuel ruptured their zirconium-alloy containers, coming into direct contact with cooling water. The water flashed into steam, causing the first of two explosions that blew the top off the reactor. The second blast was caused by a H<sub>2</sub>-CO-air explosion. The H<sub>2</sub> and CO were generated by reactions of zirconium and carbon with super-heated steam:



About 15 tons of radioactive material from the reactor core was blown into the atmosphere, where it spread across Europe. More than 36 hours after the accident, plant personnel told local officials about the accident. About 14 hours after that – 50 hours after the accident – radiation from the explosion was detected by technicians at the Forsmark nuclear power plant in Sweden. That radiation was the first notification to the world outside the Soviet Union that something had happened in Pripyat.

At the site, more than 30 fires broke out, including an intensely hot graphite fire that burned until May 9. About 250 people fought the various fires. During 1800 helicopter sorties, pilots dropped 5000 tons of lead, clay, dolomite and boron onto the reactor. Near term, the explosion and high-level radiation killed 31 people, including operators, fire-fighters, and helicopter pilots. Thousands more died later.

In June 1987, 14 months after the disaster, some 27 villages within the restricted zone were still heavily contaminated, because the cleanup operation had stopped. Nearby cities and towns were reporting dramatic rises in thyroid diseases, anemia, and cancer. Hardest hit were children. Frequently, calves were born without heads, eyes, or limbs. The three remaining nuclear reactors were still running, and two new reactors were under construction. Despite ambient radiation levels 9 times higher than widely accepted limits, workers at the power-plant were living in newly built colonies inside the “dead zone.”

During a trial that ended in August 1987, the Chernobyl plant director (Brukhanov) was convicted and sentenced to 10 years in a labor camp. The chief engineer (Fomin), and Diatlov received shorter sentences. The two operators were acquitted, but both of them died soon afterwards from radiation poisoning. More than 60 other workers were fired or demoted.

In 1991, Unit 2 was damaged beyond repair by a fire in the turbine room. That left Units 1 and 3, which kept running for the next nine years.

According to government figures, more than 4,000 Ukrainians who took part in the clean-up had died, and 70,000 were disabled by radiation. About 3.4 million of Ukraine's 50 million people, including some 1.26 million children, were affected by Chernobyl.<sup>10</sup> According to Gernadij Grushevoi, co-

founder of the Foundation for the Children of Chernobyl, the long-term danger is even worse in Belorussia. In 1992, in testimony at the World Uranium Hearing,<sup>11</sup> he said, "... 70 percent of the radioactive stuff thrown up by the explosion at Chernobyl landed on White Russian territory. There is not a centimeter of White Russia where radioactive cesium cannot be found."

On December 14, 2000, the plant was shut down. The shut-down was expedited by the European Commission, which approved a US\$585 million loan to help Ukraine build two new reactors, and by the European Bank for Reconstruction and Development, which provided US\$215 million.

### 3.5 The Rhine (1986)<sup>12</sup>

On November 1, 1986, a fire broke out in a riverside warehouse at the Sandoz chemical plant in Schweizerhalle, Switzerland. While extinguishing the flames, firemen sprayed water over exploding drums of chemicals, washing as much as 30 tonnes of pesticides, chemical dyes and fungicides into the Rhine River. Up to 100 miles (160 km) downstream, the river was sterilized. All told, more than 500,000 eels and fish were killed. More than 50 million people in France, Germany, and The Netherlands suffered through drinking water alerts.

Afterwards, while checking the Rhine for chemicals as it rolled through Germany, officials discovered high levels of a herbicide (Atrazine) that wasn't on the list provided by Sandoz. Eventually, Ciba-Geigy admitted that it had spilled Atrazine into the river just a day before the Sandoz fire. As monitoring continued, more chemicals were discovered alerting German authorities to the fact that many different companies were discharging dangerous chemicals. BASF admitted to spilling more than a tonne of herbicide, Hoechst discovered a chlorobenzene leak, and Lonza confessed to "losing" 2,000 gallons (4,500 liters) of chemicals.

In response to the Sandoz disaster, companies all along the Rhine joined the Rhine Action Program for Ecological Rehabilitation, agreeing to cut the discharge of hazardous pollutants in half by 1995. Although many experts thought the target could never be reached, samples showed that from 1985 to 1992, mercury in the river at the German town of Bimmen-Lobith, near the Dutch border, fell from 6.0 to 3.2 tonnes, cadmium from 9.0 to 5.9 tonnes, zinc from 3,600 to 1,900 tonnes, and polychlorinated biphenyls (PCBs) from 390 to 90 kilograms.

The payoff for this program came in December 1990, when for the first time in 30 years a large Atlantic salmon was fished from the Sieg, a tributary of the Rhine in West-Central Germany. The catch proved what officials had hoped: If you clean the water and clear the way, someday the fish will come back. The event gave new life to the Salmon 2000 project, and further success followed. In 1994, researchers found recently hatched salmon in the Sieg, and in 1996 a salmon was hooked near Baden-Baden. In 1998, encouraged by the

success of the Rhine Action Program, targets were set to designate a large protected ecosystem from the mouth of the Rhine in The Netherlands to streams in the Jura Mountains, the Alps, the Rhine mountains, the Rhineland-Palatinate, the Black Forest, and the Vosges.

Meanwhile, not all of the Rhine's pollution problems have been solved. One of the most serious is a huge basin in the Netherlands, into which toxin-laden mud dredged from the Port of Rotterdam has been dumped since the 1970s. Contamination levels are falling, but several toxins are very stubborn.

All along the Rhine, the main source of remaining pollution comes from farm fertilizers, which seep into the river every time it rains.

### **3.6 Prince William Sound, Alaska (1989)**

On March 23, 1989, the 987-foot supertanker Exxon *Valdez* left port carrying more than 1.2 million barrels of North Slope crude. The ship was headed south toward refineries in Benicia and Long Beach, California. At 10:53 PM, it cleared the Valdez Narrows and headed for Prince William Sound in the Gulf of Alaska. To avoid some small icebergs, Captain Joseph Hazelwood asked for and received permission to move to the northbound shipping lane. At 11:50 PM, just before retiring to his cabin, the captain gave control of the ship to the third mate, Gregory Cousins, instructing him to steer the vessel back into the southbound lane after it passed Busby Island.

Cousins did tell the helmsman to steer to the right, but the vessel didn't turn sharply enough. At 12:04 AM, it ran aground on Bligh Reef. It still isn't known whether Cousins gave the order too late, whether the helmsman didn't follow instructions properly, or if something went wrong with the steering system.

Captain Hazelwood returned to the bridge, where he struggled to hold the tanker against the rocks. This slowed the rate of oil leakage. He contacted the Coast Guard and the Alyeska Pipeline Service Company. The latter dispatched containment and skimming equipment. According to the official emergency plan, this equipment was supposed to arrive at a spill within 5 hours. In fact, it arrived in 13 hours – eight hours late.

The Exxon *Baton Rouge* was sent to off-load the un-spilled cargo and to stabilize the *Valdez* by pumping sea water into its ballast tanks. The oil transfer took several days. By the time it was finished, more than 250,000 barrels of oil had spilled into the Sound. Eventually, 33,000 birds and 1,000 otters died because of the spill.

Captain Hazelwood was tried and convicted of illegally discharging oil, fined US\$50,000, and sentenced to 1000 hours of community service. Exxon spent US\$2.2 billion to clean up the spill, continuing the effort until 1992 when both the State of Alaska and the U.S. Coast Guard declared the cleanup complete. The company also paid about US\$1 billion for settlements and compensation.

Eleven thousand workers treated 1,200 miles (1,900 kilometers) of shoreline around Prince William Sound and the Gulf of Alaska, using 82 aircraft, 1,400 vessels, and 80 miles (128 kilometers) of oil-containing booms.

In response to the disaster, the U.S. Congress passed the Oil Pollution Act of 1990. The Act streamlined and strengthened the ability of the U.S. Environmental Protection Agency (EPA) to prevent and react to catastrophic oil spills. A trust fund, financed by a tax on oil, was established to pay for cleaning up spills when the responsible party cannot afford to do so. The Act requires oil storage facilities and vessels to submit plans to the Federal government, telling how they intend to respond to large oil discharges. EPA published regulations for above-ground storage facilities, and the U.S. Coast Guard published regulations for oil tankers. The Act also requires the development of area contingency plans to prepare for oil spills on a regional scale.

The efforts seem to be working. On July 10, 2004, *USA Today* reported:<sup>13</sup> “Not one drop of crude oil spilled into Prince William Sound from oil tankers in 2003 – the first spill-free year since the ships started carrying crude from the trans-Alaska pipeline terminal in 1977.”

### **3.7 Kuwait (1991)**

On January 25-27, 1991, during Iraqi’s occupation of Kuwait, pumping stations at Mina Al-Ahmadi sent 4 to 6 million barrels of oil – 16 to 25 times more than the amount spilled by the Exxon *Valdez* – into the Arabian Gulf. On January 27, allied bombers stopped the spill by destroying the pumping stations.

Ad Daffi Bay and Abu Ali Island experienced the greatest pollution. The spill damaged sensitive mangrove swamps and shrimp grounds. Marine birds, such as cormorants, grebes, and auks, were killed when their plumage was coated with oil. The beaches around the shoreline were covered with oil and tar balls.

Despite the ongoing war, the clean-up of the oil spill proceeded rapidly. Kuwaiti crude is rich in light ends, and water in the Arabian Gulf water is relatively warm. For these reasons, about half of the spilled oil evaporated, Kuwaiti crude simply evaporated, leaving behind a thick emulsion which eventually solidified and sank to the bottom of the sea. Another 1.5 million barrels were recovered by skimming. Operators of sea-water cooled factories and desalination plants were concerned that the oil might foul their intake systems. To prevent this, protective booms that extended three feet (1 meter) below the surface were installed around intakes in Bahrain, Iran, Qatar, Saudi Arabia, and the United Arab Emirates.

On February 23-27, 1991, retreating Iraqi soldiers damaged three large refineries and blew up 732 Kuwaiti oil wells, starting fires on 650 of them. Up to 6 million barrels per day were lost between February 23 and November 8,

1991. Crews from 34 countries assembled to fight the oil-well fires. Initially, experts said the fires would rage for several years. But due to the development of innovative fire-fighting technology, the job took less than 8 months.

The oil-well fires burned more than 600 million barrels, enough to supply the United States for more than a month. The fire-fighting effort cost US\$1.5 billion. Rebuilding Kuwait's refineries cost another US\$5 billion. In all, Kuwait spent between US\$30 and US\$50 billion to recover from the Iraqi invasion.

### 3.8 Lessons Learned

Hopefully, we have learned from these terrible examples. Here are some suggested tenets:

***Needs determine priorities.*** According Maslow's "Hierarchy of Needs," people must satisfy basic physiological needs before they can afford to focus on safety, love, self-esteem and self-actualization.<sup>14</sup>

Those of us lucky enough to live in wealthy countries are justly proud of our recent environmental progress, which qualifies as self-actualization. But in poorer countries, people are less inclined to care about long-term dangers of pollution. After the nuclear accident at Chernobyl, the power plant ran for 14 more years because the Soviet Union (and then Ukraine) needed electric power and decided that it was too expensive to build a new plant. After 1986, the old plant was staffed by workers who lived in towns where the ambient radiation exceeded the safety threshold by a factor of nine. Despite a second accident in 1991, and despite daily reminders of the dangers radiation, the workers stayed on because they needed jobs and couldn't find other work. Without incentives from the European Community, the Chernobyl nuclear power plant might still be running today.

***Follow the rules.*** On their own or under duress, people ignore safety rules all the time, all over the world, not just in factories, but in homes and offices, on farms and highways. If we include exceeding the speed limit on public highways, it's safe to say that only a fraction of rule violations cause accidents. While the accidents can be tragic for the people who are involved, they seldom cause catastrophic damage to the environment.

When the consequences of an accident might be severe, adhering to safety rules is crucial. On the Exxon *Valdez*, Captain Hazelwood violated a U.S. Coast Guard guideline when he left the third mate in charge before the ship reached open water. At Chernobyl, Diatlov and his operators violated three major safety rules when they (a) shut off the emergency cooling water system, (b) raised the control rods too high, and (c) disabled the emergency SCRAM. Any one of the idled systems might have prevented the accident.

***Encourage whistle-blowing.*** When told to raise the control rods too high, the Chernobyl operators hesitated, citing safety regulations. But when Diatlov insisted, the operators complied. Undoubtedly, the fear of losing their jobs



outweighed their fear of breaking a rule. After all, they already had broken several rules, and nothing awful had happened.

Over the years, the U.S. Congress has passed at least seven laws to protect environmental whistle-blowers from retribution from their employers. Even so, according to Edmund Seebauer,<sup>15</sup> “Studies confirm the intuitive perception that whistleblowers tend to face hostility within their organizations and commonly leave their jobs, either voluntarily or otherwise. Lengthy and costly litigation often follows.” Seebauer goes on to say: “Some employers are happy to hire workers who demonstrate such a strong commitment to high ethical standards. Nevertheless, there is no guarantee of employment, especially in a slow market. The whistleblower may lose seniority and retirement benefits, and must often move to another city. The needs of family members must be considered.” When faced with these realities, insiders are reluctant to report environmental wrong-doing.

Smart companies encourage whistle-blowing. They send employees to courses that teach them about safety and environmental protection. They establish internal whistleblower hot lines and encourage employees to use them when they think their concerns haven’t properly been addressed by the normal chain of command. These companies are smart. They recognize that, in today’s litigious society, whistleblowers can save a company billions of dollars in fines and cleanup costs.

***If your automation works, use it.*** Control systems aren’t perfect. In fact, we have seen more than one process unit in which an advanced control application is so bad that the operators won’t use it.

On the other hand, safety-related interlocks are equivalent to safety rules. They are there for a reason. They must not be broken. Operators, engineers, and managers should be trained to understand exactly how the controls work and why certain controls are critical. If the guidelines are wrong, unsafe or inadequate, they must be discussed thoroughly before changes are made.

***Prepare, then test your preparation.*** In 1978, the world simply was not prepared for oil spills as large as the *Amoco Cadiz*. The main lesson learned there was that quick response is critical. By the time help finally arrived, the *Cadiz* was destroyed and its entire cargo was in the sea.

In 1987, the Alyeska Pipeline Service Company seemed better prepared for a large spill. As mentioned, in its emergency plan submitted to the federal government, Alyeska promised a 5-hour response to a 200,000-barrel oil spill in the Prince William Sound area. But after the Exxon *Valdez* ran aground, Alyeska took 13 hours to reach the ship. During those extra eight hours, the size of the oil spill more than doubled. Was it even possible for Alyeska to respond in five hours? We don’t know. Was the plan ever tested? We don’t know that either. We do know that, when filing its plan, Alyeska said: “It is highly unlikely that a spill of this magnitude would occur. Catastrophic events of this nature are further reduced because the majority of the tankers calling

on Port Valdez are of American registry and all of these are piloted by licensed masters or pilots.”

Despite the 8-hour delay, action by Alyeska and Exxon was relatively fast. Most of the oil stayed inside the ship until it was off-loaded. Consequently, instead of losing the entire cargo of 1.2 million barrels, “only” 250,000 barrels spilled into the sea.

***If it's broken, don't run it.*** At Bhopal, the refrigeration system had been down for months. A faulty valve that should have sent the leaking gas to a scrubber sent it instead to the flare system, which failed. Operators didn't detect the leak immediately, because a key panel was missing from the control room. As stated by a Union Carbide executive, the plant should not have been running.

***War is the biggest polluter of all.***

## **4. ENVIRONMENTAL AGENCIES**

Under pressure from the American public, in 1970 the U.S. Congress established the Environmental Protection Agency (EPA) and the Occupational Safety and Health Administration (OSHA). Together, these agencies are responsible for dramatic improvements in air and water quality and increases safety in workplaces throughout the United States.

### **4.1 Environmental Protection Agency**

EPA's mission is “to enforce federal laws to control and abate pollution of air and water, solid waste, noise, radiation, and toxic substances. It is also to administer the Superfund for cleaning up abandoned waste sites, and award grants for local sewage treatment plants.”

After its creation, EPA quickly took the following actions:

1. Established 10 regional offices throughout the nation.
2. In 1971, established National Ambient Air Quality Standards, which specified maximum permissible levels for major pollutants.
3. Required each state to develop plans to meet air quality standards.
4. Established and enforced emission standards for hazardous pollutants such as asbestos, beryllium, cadmium, and mercury.
5. Required a 90% reduction in emissions of VOC and carbon monoxide by 1975.
6. Published emission standards for aircraft.
7. Funded research and demonstration plants.
8. Furnished grants to states, cities, and towns to help them combat air and water pollution

EPA's law-enforcement efforts are supported by the National Enforcement Investigation Center in Denver, Colorado, which gives assistance to federal,

state and local law enforcement agencies. This unit has helped to clamp down on the “midnight dumping” of toxic waste and the deliberate destruction or falsification of documents.

## 4.2 Other Environmental Agencies

Today, almost every U.S. state has an environmental agency. Arguably, the most famous of these is the California Air Resources Board (CARB), which pioneered regulations to mitigate smog in Los Angeles. In addition to administering state programs for improving air and water quality, the Texas Commission on Environmental Quality (TCEQ) participates in making plans to prevent and react to industrial terrorism.

Most countries have environmental agencies. As shown in *Table 4*, some are combined with public health departments, some are combined with energy agencies, and at least one is coupled with tourism. In addition to handling internal issues, most of these agencies administer their country’s participation in international treaties, such as the Kyoto Protocol.<sup>16</sup>

## 4.3 Occupational Safety and Health Administration

Pollution control and safety are two sides of the same coin. In the United States, the Occupational Safety and Health Administration (OSHA) is part of the U.S. Department of Labor. Its legislative mandate is to assure safe and healthful working conditions by:

- Enforcing the Occupational Safety and Health Act of 1970
- Helping states to assure safe and healthful working conditions
- Supporting research, information, education, and training in occupational safety and health

OSHA levies fines against unsafe people and companies. Not surprisingly, a large percentage of the safety infringements cited by OSHA have caused environmental damage or put the environment at risk.

Here is an example. In 1993 OSHA levied fines against the Manganas Painting Company for exposing its workers and the environment to lead during sand-blasting operations. The proposed fines totalled US\$4 million. The contractor appealed, but in February 2002, it pled guilty to knowingly and illegally dumping 55 tons of lead-containing sandblasting material, in violation of the Resource Conservation and Recovery Act (RCRA).<sup>17</sup>

Under the Occupational Safety and Health Act, employers are responsible for ensuring a safe and healthy workplace. One key requirement is that all hazardous chemicals must be properly labeled. Workers must be taught how to handle the chemicals safely, and material safety data sheets must be available to any employee who wishes to see them.

Table 4. Environmental Agencies Around the World

| Country        | Agency   |
|----------------|--|
| Australia      | Department of the Environment and Heritage                                 |
| Austria        | Ministry of Agriculture, Forestry, Environment and Water Management        |
| Brazil         | Ministry of Environment  |
| Canada         | Environment Canada   |
| China          | China Council for International Cooperation on Environment and Development |
| Europe         | European Environment Agency  |
| Finland        | Finnish Environmental Administration                                       |
| Indonesia      | Kementerian Lingkungan Hidup   |
| India          | Ministry of Environment and Forests  |
| Japan          | Department of the Environment of Japan                                     |
| Kuwait         | Environment Public Authority   |
| Malaysia       | Department of Environment Malaysia   |
| Mexico         | Secretariat of Environment and Natural Resources                           |
| Norway         | Ministry of Environment  |
| Saudi Arabia   | Presidency of Meteorology and Environment                                  |
| Singapore      | National Environment Agency  |
| South Africa   | Department of Environmental Affairs and Tourism                            |
| Thailand       | Ministry of Natural Resources and Environment                              |
| United Kingdom | Environment Agency   |
| United States  | Environmental Protection Agency  |

#### 4.3.1 Material Safety Data Sheets (MSDS)

Material Safety Data Sheets (MSDS) include the following information:

**Material identification.** The name of the product and the manufacturer's name, address, and emergency phone number must be provided

**Hazardous ingredients.** The sheet must give the chemical name for all hazardous ingredients comprising more than 1% of the material. It must list cancer-causing materials if they comprise more than 0.1%. Listing only the trade name, only the Chemical Abstract Service (CAS) number, or only the generic name is not acceptable.

If applicable, exposure limits are listed in this section of the MSDS. The OSHA permissible exposure limit (PEL) is a legal, regulated standard. Other limits may also be listed. These include recommended exposure limits (REL) from the National Institute for Occupational Safety and Health (NIOSH) and threshold limit values (TLV) from the American Conference of Governmental Industrial Hygienists (ACGIH). Sometimes, short-term exposure and/or ceiling limits are shown. The ceiling limit should never be exceeded.

**Physical properties.** These include the appearance, color, odor, melting point, boiling point, viscosity, vapor pressure, vapor density, and evaporation rate. The vapour pressure indicates whether or not the chemical will vaporize when spilled. The vapor density indicates whether the vapor will rise or fall. Odor is important because a peculiar smell is the first indication that something has leaked.

**Fire and explosion hazard data.** This section provides the flash point of the material, the type of extinguisher that should be used if it catches fire, and any special precautions.

The flash point is the lowest temperature at which a liquid gives off enough vapor to form an explosive mixture with air. Liquids with flash points below 100°F (37.8°C) are called *flammable*, and liquids with flash points between 100 and 200°F (37.8 and 93.3°C) are called *combustible*. Flammable and combustible liquids require special handling and storage.

The four major types of fire extinguishers are Class A for paper and wood, Class B for flammable liquids or greases, Class C for electrical fires, and Class D for fires involving metals or metal alloys.

**Health hazard data.** This section defines the symptoms that result from normal exposure or overexposure to the material or one of its components. Toxicity information, such as the result of studies on animals, may also be provided. The information may also distinguish between the effects of acute (short term) and chronic (long-term) exposure. Emergency and first-aid procedures are included in this section.

**Reactivity data.** This section includes information on the stability of the material and special storage requirements.

Unstable chemicals can decompose spontaneously at certain temperatures and pressures. Some unstable chemicals decompose when they are shocked. Rapid decomposition produces heat, which may cause a fire and/or explosion. It also may generate toxic gas. Hazardous polymerization, which is the opposite of hazardous decomposition, also can produce enough heat to cause a fire or explosion.

Concentrated acids and reactive metals are hazards when mixed with water. They should be stored separately in special containers.

**Spill, leak, and disposal procedures.** This part of the MSDS gives general procedures, precautions and methods for cleaning up spills and disposing of the chemical.

**Personal protection information.** This section lists the protective clothing and equipment needed for the safe handling of the material. Requirements can differ depending on how the chemical is used and how much of it is used.

Protective equipment and clothing can include eye protection (safety glasses or face shields), skin protection (clothing, gloves, shoe covers), self-contained breathing equipment, and/or forced-air ventilation (fume hoods).

## 5. KEY REGULATIONS

In this section, we describe important environmental legislation. Most of our examples come from the United States. We apologize for this, but only a little. Historically, the United States has pioneered environmental regulations, and many countries have followed suit. Recently, the European Commission

took the lead in promoting climate-control treaties, including the Rio and Kyoto Protocols. These are discussed in Sections 5.13.2 and 5.13.3.

## 5.1 Clean Air Acts

The first clear-air acts in the English-speaking world were implemented by Parliament in 1956, in response to the “deadly fog” incidents around London. Since then, the United States government has passed several clean-air acts, including:

- Clean Air Act of 1963
- Motor Vehicle Air Pollution Control Act of October 20, 1965
- Clean Air Act Amendments of October 15, 1967
- Air Quality Act of November 21, 1967
- Clean Air Act of 1970
- Clean Air Act Amendments of 1975, 1977, and 1990<sup>18</sup>

For convenience, the entire package often is called just the Clean Air Act (CAA) or the Clean Air Act Amendments (CAAA). Its continued strength demonstrates that Americans are serious about stopping air pollution.

The CAA of 1970 and its amendments contributed extensively to cleaner air in the United States. Significantly, it inspired similar legislation by many nations around the world. According to the EPA, between 1978 and 1988, lead pollution in the United States decreased by 89%, nitrogen oxides by 14%, carbon monoxide by 32%, sulfur dioxide by 37%, and ozone by 21%.

Since passage of the 1990 CAAA, individual and corporate polluters can be jailed for breaking environmental laws. Goals of the 1990 CAAA are:

1. To reduce SO<sub>2</sub> and NO<sub>x</sub> emissions from coal-burning power plants by 50% and 10%, respectively, by the year 2000.
2. To reduce smog, ozone, and carbon monoxide by requiring automakers to sell autos that burn clean alternative fuels in cities with bad air pollution.
3. To reduce airborne toxic chemicals by 75% in the 1990s by compelling plants to use the best available control technology (BACT), especially for chemicals suspected of causing cancer in humans.

The 1990 CAAA required EPA to set National Ambient Air Quality Standards (NAAQS) for pollutants considered harmful to public health and the environment. As shown in *Table 5*, EPA set two types of standards. Primary standards are designed to protect public health, including the health of sensitive people such as asthmatics, children, and the elderly. Secondary standards are designed to protect public welfare by improving visibility and decreasing damage to animals, crops, vegetation, and buildings. In the table, units of measure are parts per million (ppm) by volume, milligrams per cubic meter of air (mg/m<sup>3</sup>), and micrograms per cubic meter of air (μg/m<sup>3</sup>).

Table 5. U.S. National Ambient Air Quality Standards

| Pollutant        | Primary Standard                   | Averaging Times      | Secondary Standard                |
|------------------|------------------------------------|----------------------|-----------------------------------|
| Carbon monoxide  | 9 ppm (10 mg/m <sup>3</sup> )      | 8-hour <sup>1</sup>  | None                              |
|                  | 35 ppm (40 mg/m <sup>3</sup> )     | 1-hour <sup>1</sup>  | None                              |
| Lead             | 1.5 µg/m <sup>3</sup>              | Quarterly            | Same as Primary                   |
| Nitrogen dioxide | 0.053 ppm (100 µg/m <sup>3</sup> ) | Annual               | Same as Primary                   |
| PM10             | 50 µg/m <sup>3</sup>               | Annual <sup>2</sup>  | Same as Primary                   |
|                  | 150 µg/m <sup>3</sup>              | 24-hour <sup>1</sup> |                                   |
| PM2.5            | 15 µg/m <sup>3</sup>               | Annual <sup>3</sup>  | Same as Primary                   |
|                  | 65 µg/m <sup>3</sup>               | 24-hour <sup>4</sup> |                                   |
| Ozone            | 0.08 ppm                           | 8-hour <sup>5</sup>  | Same as Primary                   |
|                  | 0.12 ppm                           | 1-hour <sup>6</sup>  | Same as Primary                   |
| Sulfur Oxides    | 0.03 ppm                           | Annual               | –                                 |
|                  | 0.14 ppm                           | 24-hour <sup>1</sup> | –                                 |
|                  | –                                  | 3-hour <sup>1</sup>  | 0.5 ppm (1300 µg/m <sup>3</sup> ) |

<sup>1</sup> Must not be exceeded more than once per year.

<sup>2</sup> Annual mean PM10 at each monitor in an area must not exceed 50 µg/m<sup>3</sup>.

<sup>3</sup> The 3-year average of mean PM2.5 from all monitors must not exceed 15 µg/m<sup>3</sup>.

<sup>4</sup> The 3-year average of the 98th percentile of 24-hour concentrations at each monitor in an area must not exceed 65 µg/m<sup>3</sup>.

<sup>5</sup> The 3-year average of the fourth-highest daily-maximum 8-hour average concentrations of ozone in an area must not exceed 0.08 ppm.

<sup>6</sup> The standard is met when the expected number of days per calendar year with maximum hourly average concentrations above 0.12 ppm is less than or equal to 1.

The 1990 CAAA are designed to bring the United States into compliance with the NAAQS. The main sections of the Amendments are:

Title I – Non-Attainment

Title II – Mobile Sources

Title III – Air Toxics

Title IV – Acid Rain

Title V – Operating Permits

Title VI – Stratospheric Ozone and Global Climate Protection

Title VII – Enforcement

Title VIII – Miscellaneous (Outer Continental Shelf, Border Areas)

Title IX – Clean Air Research

Title X – Disadvantaged Business Concerns

Title XI – Clear Air Employment transition Assistance

Titles with a major impact on the petroleum processing industry are summarized below. State and local regulations can be more stringent than federal Clean Air Acts. For example, in the San Francisco Bay Area,<sup>19</sup> average daily CO emissions from oil refineries may not exceed 400 ppm, regardless of the CO concentration in ambient air.

### 5.1.1 Title I – Non-Attainment

**Non-attainment categories.** Title I divided cities and metropolitan areas into several categories for ozone (*marginal, moderate, serious, severe,*

*extreme*) and two categories for carbon monoxide. Areas with *moderate* ozone had to achieve a 15% reduction in volatile organic compounds (VOC) by 1996. For areas with ozone problems that are *serious*, *severe* or *extreme*, VOC must be reduced by 3% per year until attainment is achieved. Major NO<sub>x</sub> sources had to reduce emissions by the same schedule, unless EPA agreed that NO<sub>x</sub> reduction would not be beneficial.

**State Implementation Plans.** Each American state was required to develop a state implementation plan (SIP) within 2 years. If EPA decided that an SIP was inadequate, it had the right to impose a federal implementation plan (FIP). In practice, EPA's first response was to ask for a revised SIP.

**Ozone.** Ground-level ozone is generated by photolytic reactions between NO<sub>x</sub>, VOC, and oxygen. Non-attainment ozone areas had to correct (update) their RACT, I/M, and CTG guidelines. RACT = reasonably available control technology, I/M = inspection and maintenance, CTG = control technology guidelines, and Non-CTG = plants that do not meet CTG.

Areas with moderate or worse air quality were required to use Stage II vapor recovery, in which special nozzles and coaxial hoses collect VOC from the fuel tanks of automobiles as they are being fuelled. The VOC are routed to a storage tank at the filling station. Moderate areas also were required to use basic I/M and RACT on new sources and on non-CTG existing sources from which potential NO<sub>x</sub> emissions exceeded 100 tons per year. For serious, severe and extreme ozone areas, RACT is required on plants from which NO<sub>x</sub> could exceed 50, 25, and 10 tons per year, respectively. These areas also had to implement transportation control measures (TCM) to limit the number of vehicles on the road. Extreme areas were required to add peak-hour traffic controls. Eleven new CTGs were issued for coatings in aerospace and shipbuilding factories, for marine vessels, and for consumer products.

**CO and Particulates.** For CO and PM<sub>10</sub>, Title I required oxygenated gasoline in the winter for areas where the ambient CO level exceeded 9.4 ppm. For areas where CO exceeded 12.7 ppm, enhanced I/M and predictions of "vehicle miles travelled" (VMT) were required. As in severe ozone areas, serious CO areas had to impose TCMs. Areas where PM<sub>10</sub> levels exceeded EPA limits had to reach compliance by December 1994, with possible extensions to 2001. Moderate PM<sub>10</sub> areas had to adopt RACT, and serious areas had to adopt BACT (best available control technology).

### 5.1.2 Title II – Mobile Sources

The mobile sources section of the 1990 CAA amendments promulgated regulations for automobiles, trucks, and other moving vehicles. It included the following sections:

**Emission Standards.** Full-useful-life emission standards for gasoline-powered vehicles are shown in *Table 6*. Tier I limits for automobiles were phased in between 1994 and 1996. Tier II standards are based on California's



LEV II program (LEV = low-emission vehicles). The Tier II phase-in began in January 2004. By 2009, sport utility vehicles (SUVs), minivans, and pickup trucks have to meet the same emission standards as automobiles. For the first time, vehicles and fuels are treated as a single system. Tier II allows vehicle manufacturers to certify a mix of vehicles (“fleet”) if average NO<sub>x</sub> emissions for the fleet are less than 0.07 grams/mile (Bin 5). Tier II “bins” differ mainly in allowed NO<sub>x</sub> emissions. To obtain alternative motor vehicle credits, such as those described in the Energy Policy Act of 2004,<sup>20</sup> hybrid and alternative-fuel vehicles must meet or exceed Tier II, Bin 5 emission standards.

Table 6. Tier I & Tier II Emission Standards for Gasoline-Powered Vehicles (Full Useful Life)

|                           | NMHC/<br>NMOG, gpm | CO<br>gpm  | NO <sub>x</sub><br>gpm | PM<br>gpm   | HCHO<br>gpm  |
|---------------------------|--------------------|------------|------------------------|-------------|--------------|
| <b>Tier I</b>             |                    |            |                        |             |              |
| LDV and LDT (<3,751 lbs.) | 0.31               | 4.2        | 0.60                   | 0.10        | –            |
| LDT (3,751-5,700 lbs.)    | 0.40               | 5.5        | 0.97                   | 0.10        | –            |
| LDT (>5,750 lbs.)         | 0.56               | 7.3        | 1.53                   | 0.12        | –            |
| <b>Tier II</b>            |                    |            |                        |             |              |
| Bin 6                     | 0.09               | 4.2        | 0.09                   | 0.01        | 0.018        |
| <b>Bin 5</b>              | <b>0.09</b>        | <b>4.2</b> | <b>0.07</b>            | <b>0.01</b> | <b>0.018</b> |
| Bin 4                     | 0.07               | 2.1        | 0.04                   | 0.01        | 0.011        |
| Bin 3                     | 0.055              | 2.1        | 0.03                   | 0.01        | 0.011        |

gpm = grams/mile, LDV = light-duty vehicles, LDT = light-duty trucks

**Reformulated Gasoline.** Reformulated gasoline (RFG) is designed to reduce CO, air toxics, and VOC. Adding oxygen compounds lowers CO emissions, limiting benzene reduces air toxics, and controlling volatility limits VOC emissions. Table 7 lists the RFG specification that took effect in 1995.

Table 7. Tier I RFG Specifications

| Property                | Specification |
|-------------------------|---------------|
| Oxygen, wt%             | 2.0 max       |
| Benzene, vol%           | 1.0 max       |
| RVP, Summer             |               |
| Class B (psi)           | 7.2 max       |
| Class B (kPa)           | 50 max        |
| Class C (psi)           | 8.1 max       |
| Class C (kPa)           | 56 max        |
| VOC (summer)            | 15% reduction |
| Air toxics              | 15% reduction |
| Sulfur                  | Same as 1990  |
| T90, olefins, aromatics | Same as 1990  |

T90 = the temperature at which 90% of a gasoline blend evaporates.

RVP = Reid vapour pressure

Air toxics = benzene, formaldehyde, and butadiene

Oxygen can be added as ethanol, MTBE (methyl t-butyl ether), ETBE (ethyl t-butyl ether), or TAME (t-amyl methyl ether).

RFG was implemented in two phases. The Phase I program started in 1995 and mandated RFG for 10 large metropolitan areas. Several other cities and four entire states joined the program voluntarily. In the year 2000, about 35% of the gasoline in the United States was reformulated.

The regulations for Phase II, which took force in January 2000, are based on the EPA Complex Model, which estimates exhaust emissions for a region based on geography, time of year, mix of vehicle types, and – most important to refiners – fuel properties.

**Low-sulfur gasoline.** When fossil fuels are burned, the sulfur they contain is converted into SO<sub>2</sub> and sulfates. SO<sub>2</sub> contributes to acid rain, and sulfates become particulate matter. In the United States, the phase-in of low-sulfur gasoline began in January 2004. By 2006, the average sulfur level must be less than 30 wppm with a cap of 80 wppm. In parts of the Western U.S., the 30/80 rule will not take effect until 2007.

**Low-sulfur diesel.** From 1991 in Sweden, 1995 in California, and 1998 in the rest of the United States, the sulfur content of on-road diesel has been limited to <500 wppm sulfur. Recently, EPA imposed tighter limits on sulfur in both on-road and non-road diesel (*Table 8*). Non-road diesel is used in farm equipment, railroad engines, fork lifts, boats, and ships. Non-road rules also apply to diesel-powered generators, mining equipment, and baggage-handling equipment in airports.

*Table 8.* Clean Fuels: U.S. Limits on Sulfur in Gasoline and Diesel

|                  | Fuel Sulfur Content, wppm |              |              |
|------------------|---------------------------|--------------|--------------|
|                  | 2004 Level                | Target Level | Target Date  |
| Gasoline         | >300                      | 30           | 2004 – 2008  |
| Diesel, on-road  | 500                       | 15           | July 1, 2006 |
|                  | -                         | -            | July 1, 2010 |
| Diesel, off-road | 2000 – 3500               | 500          | 2007         |
|                  | -                         | 15           | 2010         |

### 5.1.3 Title III – Air Toxics

The 1990 CAA Amendments listed 189 hazardous air pollutants. It also told EPA to establish regulations for each pollutant and to publish a schedule for regulating the sources thereof. For the petroleum refining industry,<sup>21</sup> EPA issued regulations for the following:

|                        |                            |
|------------------------|----------------------------|
| 2,2,4-Trimethylpentane | Methyl-t-butylether (MTBE) |
| Benzene                | Naphthalene                |
| Cresols/cresylic acid  | Phenol                     |
| Ethylbenzene           | Toluene                    |
| Hexane                 | Xylenes                    |
| Methyl ethyl ketone    |                            |

Due to the shortage of environmental acronyms in 1990, the 1990 CAAA defined a few new ones – MACT and LAER – for maximum achievable control technology and lowest achievable emission rate. It stated that MACT must be used for new sources of air toxics, and it set a schedule for applying MACT to existing sources. Title III also required hazard assessments and risk management plans to protect against accidental releases of air toxics and other toxic chemicals. It also required the establishment of an independent chemical safety board to investigate major accidents, conduct research, and promulgate regulations for the reporting of accidental releases.

#### **5.1.4 Title IV – Acid Rain**

This Title required a 10 million ton per year reduction in SO<sub>2</sub> emissions from power plants, including those in refineries, with a goal of capping SO<sub>2</sub> emissions at about 8.9 million tons per year by 2000. Sources were given allowances based on previous emission reductions and past energy use. Each allowance is worth 1 ton per year of SO<sub>2</sub> and can be bought, sold, traded or banked to offset future emissions violations. Title IV also required a 2 million ton per year reduction in NO<sub>x</sub> emissions from power plants.

To measure SO<sub>x</sub> and NO<sub>x</sub>, continuous monitors are required. Opacity meters are required to measure PM, such as that emitted by FCC regenerators.

#### **5.1.5 Title VIII – Enforcement**

The 1990 CAAA made Clean Air Act easier to enforce, and also made them more consistent with other environmental statutes, including the Clean Water Act and the Resource Conservation and Recovery Act (RCRA). An array of new penalties were added, ranging from wrist slaps to jail time. These were enacted so officials could do a better job of matching a penalty to the severity of a crime.

Before 1990, criminal acts against the environment were misdemeanors, but the 1990 CAAA converted them into felonies. The CAAA also added sanctions for endangerment with air toxics. As an alternative to prosecuting every violation in court, EPA gained the authority to levy administrative fines up to US\$200,000 and to issue field citations up to US\$5,000. The fines can be challenged in court, but if the offender is found guilty, fines levied by the courts are likely to be higher than the fines levied by EPA.

In environmental lawsuits filed by citizens, courts gained the right to levy fines in addition to issuing injunctions. District courts were given jurisdiction over lawsuits filed against EPA for unreasonable delay, etc.

After the government proves that a violation has occurred, the burden of proof is on the accused. This makes it easier for EPA to convict and punish ongoing and recurring violations.

## 5.2 River and Harbor Act, Refuse Act

In 1899, the River and Harbor Act was passed to control obstructions to navigation. The Act required congressional approval for the building of bridges, dams, dikes, causeways, wharfs, piers, or jetties, either in or over a navigable waterway. The Act also made it illegal to discharge debris into navigable water without a permit. In 1966, a court held that the River and Harbor Act made it illegal to discharge industrial waste without a permit, not just directly into navigable waters, but also into associated tributaries and lakes, i.e., just about every puddle of open water in the United States. This led to the Refuse Act Permit Program of 1970, under which specific kinds of pollution are allowed under permits issued by the Army Corps of Engineers. Every application for a permit is reviewed by EPA. If EPA concludes that the discharge described in the application will harm the environment, the Army Corp of Engineers denies the permit.

The penalties for violating permits are severe. For a first offense, a person who violates a permit through negligence can be fined up to US\$25,000 per day or imprisoned for up to a year. For a second offense, the maximum penalties double. For willful violations, fines can be as high as US\$50,000 per day and prison terms can last 3 years. If a willful act causes serious bodily injury, the violator can be fined \$250,000 or sent to jail for 15 years. In addition, the corporation that employs the guilty person can be fined up to \$1,000,000. False reports also can be punished by fines or imprisonment.

In this context, “guilty person” refers to the corporate officer responsible for the facility from which the illegal discharge originates. In other words, a negligent act by a sloppy operator can send the Big Boss to jail.

Some examples of the fines levied under these Acts are:

**Example 1.** In June 1999, a pipeline ruptured in Bellingham, Washington, dumping 236,000 gallons of gasoline into nearby Hannah Creek and Whatcom Creek. The gasoline ignited, killing two boys and a young man. It also did extensive damage to waters, shorelines and other natural resources. In December 2002, two companies and three employees agree to pay damages and fines totaling US\$36 million.

**Example 2.** After the 1989 oil spill in Prince William Sound, Exxon Shipping Company pled guilty to violating the Clean Water Act, the Refuse Act, and the Migratory Bird Treaty Act. In addition, Exxon Corporation pled guilty to violating the Migratory Bird Treaty Act. The corresponding fines – US\$150 million – were the largest ever assessed for environmental pollution.

## 5.3 Federal Water Pollution Control Act

The original Federal Water Pollution Control Act (FWPCA) was approved on July 9, 1956. The present Act includes the following:

- Pollution Control Act Amendments of July 20, 1961

- Water Quality Act of October 2, 1965
- Clean Water Restoration Act of November 3, 1966
- Water Quality Improvement Act of April 3, 1970
- Federal Water Pollution Control Act of 1972
- Clean Water Acts of 1977, 1981, and 1987

The FWPCA of 1972 gave EPA greater authority to fight water pollution. While implementing the Act, EPA cooperates with the U.S. Coast Guard and the Secretary of the Interior. Individual states have primary responsibility for enforcing water quality standards, but if the states fail to meet expectations, EPA can take civil or criminal action under the Refuse Act.

The FWPCA prohibits the discharge of harmful amounts of oil into navigable waters. If oil is spilled, the owner or operator is liable for cleanup costs. Initially, the bill authorized \$24.6 billion for water pollution control over three years. The goal of the law was to eliminate the pollution of U.S. waterways by municipal and industrial sources by 1985.

#### **5.4 Clean Water Acts, Water Quality Act**

The main objective of the Clean Water Acts (CWA) of 1977, 1981 and 1987 is to maintain the “chemical, physical, and biological integrity of the nation’s waters.” It seeks to have “water quality which provides for the protection and propagation of fish, shellfish and wildlife and provides for recreation in and on the water.” Under these Acts, each state is required to set its own water quality standards. All publicly owned municipal sewage treatment facilities are required to use secondary treatment for wastewater. To help states and cities build new or improved water treatment plants, Congress provides construction grants, which are administered by EPA. EPA allocates funds to states, which in turn distribute money to local communities. Between 1972 and 1982, EPA approved construction grants worth nearly \$33 billion. Between 1982 and 1992, another \$24 billion was approved.

Community programs are monitored by EPA. They must meet treatment requirements to obtain permits under the National Pollutant Discharge Elimination System (NPDES).

The Water Quality Act of 1987 requires discharge permits for all point sources of pollution. More than 95% of all major facilities now comply with 5-year NPDES permits, which specify the types and amounts of pollutants that legally can be discharged. When permits are renewed, they can be modified to reflect more stringent regulations. Violators are subject to enforcement actions by EPA, including criminal prosecution.

The authority of the EPA was strengthened under the 1987 Clean Water Act. The allowable sizes of fines were increased, and violators found guilty of negligence could be sent to prison. Violators found guilty of endangerment can be fined up to US\$250,000 and imprisoned for up to 15 years.

## **5.5 Marine Protection, Research, and Sanctuaries Act**

The Marine Protection, Research, and Sanctuaries Act of 1972 gave authority to the EPA to protect oceans from indiscriminate dumping. The Agency designates sites at which dumping is allowed and issues dumping permits. Fines can be imposed for illegal dumping.

## **5.6 Safe Drinking Water Act**

Since the 1970s, the assurance of safe drinking water has been a top priority for EPA, along with individual states and over 53,000 community water systems (CWSs). The CWSs supply drinking water to more than 260 million Americans – about 90% of the population.<sup>22</sup>

The Safe Drinking Water Act of 1974 was amended in 1977 and again in 1986. It empowered EPA to set national standards for drinking water from surface and underground sources. It also authorized EPA to give financial assistance to states, which are in charge of enforcing the standards. Aquifers are protected from wastes disposed in deep injection wells, from runoff from hazardous waste dumps, and from leaking underground storage tanks. In 1987, EPA also established maximum contaminant levels for volatile organics (VOC) and 51 manmade chemicals. Standards for other chemicals were added as their toxicity was determined. At present, health and safety standards have been established for 91 microbial, chemical, and radiological contaminants.

During 2005 – 2008, the EPA, the states, and the CWSs will continue to focus on supplying safe drinking water. In addition, they plan to work toward the following ambitious goal: By 2008, 95% of the population will have access to drinking water that meets all applicable health-based standards. To meet this goal, EPA identified five key objectives:

- To continue to develop and revise drinking water standards
- To implement drinking water standards and other program requirements
- To promote sustainable management of the nation's water infrastructure
- To protect sources of drinking water from contamination
- To assure that the water infrastructure is safe from terrorist and other intentional acts.

## **5.7 Resource Conservation and Recovery Act (RCRA)**

In the United States, solid wastes are regulated by the following:

- Solid Waste Disposal Act of 1965
- Resources Recovery Act of 1970
- Resource Conservation and Recovery Act of 1976 (RCRA)

In 1965, the Solid Waste Disposal Act provided financial grants to develop and demonstrate new technologies in solid waste disposal. The Resources Recovery Act of 1970 emphasized recycling and by-product recovery.

By 1976, problems caused by the accumulation of large quantities of hazardous waste prompted Congress to pass the Resource Conservation and Recovery Act (RCRA). This legislation gave EPA the responsibility of developing a “cradle to grave” approach to hazardous waste.

Under RCRA, hazardous waste is tracked from its source to every destination, including final disposal. Tracking is based on transportation manifests, other required records, and the issuance of permits.

EPA classifies wastes according to four measurable characteristics, for which there are standardized tests. The characteristics are:

- Ignitibility
- Corrosivity
- Reactivity
- Extraction procedure toxicity (EP)

In 1980, the Waste Oil Recycling Act (WORA) empowered EPA to encourage the development of state and local programs for recycling waste motor oil. That same year, WORA was amended to strengthen its enforcement provisions.

A **generator** of hazardous waste is responsible for the following:

1. Determining if a waste is hazardous
2. Obtaining a facility permit if the waste is stored on the generator’s property for more than 90 days
3. Obtaining an EP identification number
4. Using appropriate containers and labeling them properly for shipment
5. Preparing manifests for tracking hazardous waste
6. Assuring through the manifest system that the waste arrives at the designated facility
7. Submitting to EPA an annual summary of activities

Prior to shipping hazardous waste, the generator must prepare a manifest which includes the following:

1. Name and address of the generator
2. Name of all transporters
3. Name and address of the facility designated to receive the waste
4. EPA identification number of all who will handle the waste
5. Department of Transportation (DOT) description of the waste
6. Amount of waste and number of containers
7. Signature certifying that the waste has been properly labeled and packaged in accordance with EPA and DOT regulations

To send waste away from its site, the generator must use EPA-approved transporters. It must also keep records of all hazardous waste shipments and immediately report those that fail to reach the facility shown on the manifest.

A **transporter** of hazardous waste must:

1. Obtain an EPA identification number
2. Comply with the manifest system for tracking hazardous waste
3. Deliver the entire quantity of hazardous waste to the facility specified by the manifest
4. Retain copies of manifests for three years
5. Comply with Department of Transportation rules for reporting discharges and spills.
6. Cleanup any spills that occur during transportation. All spills must be reported to both EPA and the DOT.

Any person who owns or operates a hazardous waste facility must receive a permit from the EPA. Standards for facilities that *treat, store, or dispose* of hazardous waste are designed to:

1. Promote proper treatment, storage, and methods of disposal
2. Provide states with minimum standards acceptable to EPA
3. Provide technical support to states that lack hazardous waste management programs

The RCRA amendments of 1984 and 1986 extended the act to cover underground storage tanks, especially those used for gasoline and other petroleum liquids. At the time, about 15% of the nation's 1.4 million gasoline storage tanks were leaking. Most of these leaks have since been repaired.

## 5.8 Superfund, CERCLA

Years ago, people were less aware of the dangers of dumping chemical wastes. On many properties, dumping was intensive and/or continuous. This created thousands of hazardous sites, many of which were uncontrolled and/or abandoned. On December 11, 1980, in response to public concern, Congress passed the Comprehensive Environmental Response Compensation and Liability Act (CERCLA), which authorized EPA to locate, investigate, and remediate the worst of these hazardous sites.

CERCLA established the Superfund, which provides emergency cleanup funds for chemical spills and hazardous waste dumps. The Superfund allows the government to take immediate action to cleanup spills or dumps where the responsible party cannot be identified easily. The Superfund draws about 90% of its money from taxes on oil and selected chemicals. The remainder comes from general tax revenues.

Except in an emergency, state agencies are consulted before the federal government takes action. When it does so, it uses one of three approaches:

1. If the owner of the hazardous site cannot readily be identified, the federal government may proceed with the cleanup
2. If the owner can be identified but refuses to clean the site, or if the owner's efforts are not up to par, the federal government can take charge of the cleanup. The owner must pay the cost, whatever it happens to be.



3. When the owner can be identified and decides to do the work, the federal government monitors the project and gives official approval when the work is completed according to standards.

CERCLA covers a wide range of sites. In addition to land-based dumps, it applies to spills into waterways, groundwater, and even the atmosphere. Initial funding for the Act was US\$1.6 billion over 5 years. In 1986, the Superfund Amendment and Reauthorization Act (SARA) extended the program by five years and increased the fund to US\$8.5 billion. It also tightened cleanup standards and enhanced EPA's enforcement powers. The Emergency Planning and Community Right-to-Know Act (EPCRA), also known as SARA Title III, encourages and supports emergency planning efforts at state and local levels. It also gives information to the public and local governments on potential chemical hazards in their communities. This piece of legislation has helped to reduce pollution and improve safety all across the land.

In 1984, Hazardous and Solid Waste Amendments (HSWA) were passed because citizens were concerned about the potential contamination of ground water by hazardous waste disposal sites.

In 1978, the Federal Insecticide, Fungicide, and Rodenticide Act (FIFRA) of 1947 was amended to give EPA authority to control pollution from DDT, mercury, aldrin, toxaphene, parathion and related chemicals. About 1 billion pounds of pesticides, fungicides, and rodenticides are used every year in the United States. While they contribute enormously to the success of agriculture, they can be harmful to animals, birds and humans if not used properly.

## **5.9 Toxic Substances Control Act (TSCA)**

The Toxic Substances Control Act (TSCA) of 1976 gave EPA the authority to regulate the development, distribution, and marketing of chemical products. Manufacturers, importers, and processors must notify EPA within 90 days before introducing a new chemical to the market. Certain tests (e.g., fish-kill tests) must be conducted to determine toxicity. Approved chemicals must bear warning labels.

Many chemicals are restricted or banned under TSCA.

- The manufacture, processing and distribution of completely halogenated chlorofluorocarbons (CFCs) is banned, except for a small number of essential applications.
- Chromium (VI) may not be used as a corrosion inhibitor in comfort cooling towers (CCTs) associated with air conditioning and refrigeration systems.
- Nitrosating agents may not be mixed with metalworking fluids that contain specific substances.
- The import, manufacture, processing, or distribution of PCBs is banned unless EPA agrees that the PCBs will be “totally enclosed.”

## 5.10 Asbestos School Hazard Abatement Act

The Asbestos School Hazard Abatement Act (SHAA) of 1984 was passed to encourage the removal of asbestos from schools. In 1986, the Asbestos Hazard Emergency Response Act was passed to correct in deficiencies in the previous Act. The final rule, issued in 1987, required local education agencies to:

1. Inspect school buildings for asbestos-containing materials
2. Submit asbestos management plans to state governors
3. Reduce or completely eliminate all asbestos hazards

## 5.11 Stockholm Conference

The United Nations plays an important role in international pollution abatement. In June 1972, the U.N. Conference on the Human Environment was held in Stockholm, Sweden. The main purpose of the conference was to provide guidelines for action by governments and international environmental organizations. The conference took several important steps, including:

1. Approving a Declaration on Human Environment.
2. Approving an action plan based on five subject areas:
  - Human settlements
  - Environmental resource management
  - Pollutants of international significance
  - Training, education, and information
  - Development and the environment
3. Recommending the establishment of a new United Nations institution to coordinate international activities.

## 5.12 Control of Dumping at Sea

On November 13, 1972, the Convention on the Dumping of Wastes at Sea was agreed in London by representatives of 91 countries, including all of the world's principle maritime nations. The list of substances that may not be dumped includes biological and chemical warfare agents, certain kinds of oil, certain pesticides, durable plastics, poisonous metals and their compounds, and high-level radioactive waste. Enforcement is left to individual countries.

## 5.13 Climate Control: Rio and Kyoto<sup>23,24</sup>

### 5.13.1 Rio Earth Summit

In 1992, during the "Earth Summit" in Rio de Janeiro, 154 nations plus the European community signed the United Nations Framework Convention on

Climate Change (UNFCCC). At the time, the Earth Summit was the largest-ever gathering of Heads of State. Effective on March 21, 1994, the UNFCCC called on industrial nations to voluntarily reduce greenhouse gas emissions to 1990 levels by the year 2000.

In many respects, the Rio Declaration resembled the Declaration on Human Environment issued by the Stockholm Conference in 1972. The 27 non-binding principles of the Rio Declaration included the “polluter pays” concept and the “precautionary principle.” The latter recommends that, before a construction project begins, an impact study should be conducted to identify and forestall potential harm to the environment.

The declaration asserted that present-day economic development should not undermine the resource base of future generations. It also affirmed that industrial nations pollute more than developing countries. (For example, on a per capita basis, the United States emits 25 times more CO<sub>2</sub> than India.) On the other hand, industrial nations have advanced technology and greater financial resources, which enable them to contribute more to environmental protection.

### 5.13.2 Kyoto Protocol

In 1997, representatives of 171 countries convened in Kyoto, Japan to strengthen the UNFCCC with specific, binding commitments. The Kyoto Protocol focused on controlling emissions of 6 greenhouse gases – CO<sub>2</sub>, CH<sub>4</sub>, N<sub>2</sub>O, hydrofluorocarbons (HFCs), perfluorocarbons (PFCs) and sulfur hexafluoride (SF<sub>6</sub>).

The last three chemicals do not act directly as greenhouse gases, but they deplete ozone in the upper atmosphere. Without an ozone layer, certain CO<sub>2</sub>-consuming algae may no longer be protected from harmful UV radiation, and a major sink for CO<sub>2</sub> may be destroyed.

The Protocol divided countries into categories – industrialized (Annex I), economy-in-transition (EIT), developing, and least developed. *Table 9* lists several “Annex I” parties and their 1990 emissions of CO<sub>2</sub>.

*Table 9.* 1990 Emissions of CO<sub>2</sub> by Selected Countries<sup>23</sup>

| Country             | 1990 CO <sub>2</sub> Emissions<br>(10 <sup>6</sup> kg/year) | Emissions Relative<br>to Japan |
|---------------------|---|--------------------------------|
| Australia           | 288,965   | 0.25                           |
| Canada              | 457,441   | 0.39                           |
| Iceland             | 2,172   | 0.0                            |
| Japan               | 1,173,360   | 1.00                           |
| Norway              | 35,533  | 0.03                           |
| Poland              | 414,930   | 0.35                           |
| Romania             | 171,103   | 0.15                           |
| Russia              | 2,388,720   | 2.04                           |
| USA                 | 4,957,022   | 4.22                           |
| 15 EC member states | 3,322,990   | 2.83                           |

The Protocol focused on establishing legally binding emissions targets, mechanisms for implementation, minimizing the burden placed on developing countries, accounting, reporting, review, and compliance. Parties to the Protocol agreed to develop internal climate-control programs entailing:

- National climate-change mitigation measures
- Provisions for developing and transferring environmental technology
- Provisions to maintain carbon sinks, such as forests, which remove more greenhouse gases from the air than they emit.
- Preparations for adapting to climate change
- Plans to engage in climate research and information exchange
- Plans to promote education, training and public awareness

The parties agreed to a 5% global reduction of greenhouse gases, versus 1990 levels, by 2008 – 2012. *Table 10* shows emissions targets for selected countries.

*Table 10. Kyoto Protocol: Reduction Targets for Emissions of Greenhouse Gases*

| Country   | Target <sup>a</sup> |
|---|---------------------|
| European Community, Bulgaria, Czech Republic, Estonia, Latvia, Lithuania, Liechtenstein, Monaco, Romania, Slovakia, Slovenia, Switzerland | -8%                 |
| United States <sup>b</sup>  | -7%                 |
| Canada, Hungary, Japan, Poland  | -6%                 |
| Croatia   | -5%                 |
| New Zealand, Russia, Ukraine  | No change           |
| Norway  | +1%                 |
| Australia <sup>b</sup>  | +8%                 |
| Iceland   | +10%                |

<sup>a</sup> The base year is 1990 for most countries. For some EIT countries, the base year is flexible.

<sup>b</sup> Declared that it will not ratify the Protocol.

By June 2001, more than 150 multi-country projects had been registered with the UNFCCC. Most of these related to renewable energy and energy efficiency, but the largest involved forest preservation or restoration.

### 5.13.3 Plan B for Climate Control: Contraction and Convergence

In 2002, the United States refused to ratify the Kyoto Protocol. Australia soon followed suit. Near the end of 2003, the European Union, the Protocol's biggest supporter, reported that only two member states – Sweden and the UK – were on course to meet their targets. An article in *New Scientist* by Fred Pearce<sup>24</sup> summarized his view of the Kyoto Protocol at the end of 2003.

“The Kyoto Protocol is dying a death of a thousand cuts,” he wrote. “...These blows follow a history of bureaucratic squabbling and political posturing by the Protocol's signatories, and many observers now fear that it has been damaged beyond repair. So does the world have a Plan B for bringing the emissions of greenhouse gases under control?”

“The answer is yes, and it goes by the name ‘contraction and convergence,’ or C&C. The idea has been around for a decade, but lately it has been gaining ever more influential converts, such as the UK’s Royal Commission on Environmental Pollution, the UN Environment Programme, the European Parliament and the German Advisory Council on Global Change, which last week released a report supporting the idea...”

Pearce goes on to say that while Kyoto has become a convoluted, short-term measure to mitigate climate change, C&C could provide a simple, fair, long-term solution. Under C&C, per capita emissions will converge, year by year, towards a common target. In effect, after the target date, every person in the world would have an equal right to pollute.

“On the face of it,” Pearce says, “C&C seems anathema to countries like the US, which would have to buy large numbers of pollution credits in the early years. But it does meet most of the criticisms made by the Bush administration of the Kyoto protocol.

“In particular, Bush called it unfair that Asian trading competitors, as developing nations, had no targets. Under C&C every nation would ultimately have the same target. Some, such as China, already have per-capita emissions in excess of targets they might have to meet by mid-century.

“But perhaps the greatest attraction of C&C is the complete break it would make from the horse-trading, short-term fixing and endless complications that have plagued efforts to bring the Kyoto Protocol into effect.”

If the past can predict the future, politics will continue to dominate the debate about global warming until it becomes a clear and present danger. If so, we hope there will still be time to do something about it.

## **6. POLLUTION CONTROL TECHNOLOGY**

In response to environmental regulation, the refining industry reduced pollution by:

- Reducing fugitive hydrocarbon emissions from valves and fittings
- Removing sulfur from refinery streams and finished products
- Adding tail-gas units to sulfur recovery plants
- Reducing the production of NO<sub>x</sub> in fired heaters
- Scrubbing SO<sub>x</sub> and NO<sub>x</sub> from flue-gases
- Reducing the production of CO<sub>2</sub> by increasing energy efficiency

The technology behind these actions is explained below.

### **6.1 Particulate Matter**

In refineries, coking operations and FCC regenerators are the main sources of PM emissions. Coke-derived PM<sub>10</sub> can be reduced by building enclosures

around coke-handling equipment – conveyor belts, storage piles, rail cars, barges, and calciners.

For flue gas from FCC regenerators, many licensors offer scrubbing technology. ExxonMobil offers wet-gas scrubbing (WGS), which removes particulates, SO<sub>x</sub> and NO<sub>x</sub>.<sup>25</sup> UOP and Shell Global Solutions offer third-stage separator (TSS) technology, which removes PM in conjunction with flue-gas power recovery.<sup>26</sup>

## 6.2 Carbon Monoxide and VOC

CO from by partial combustion in FCC regenerators is converted to CO<sub>2</sub> in CO boilers. Flue gas from other boilers, process heaters, and power plants can also contain some CO, which can be diminished by the installation of high-efficiency burners and/or the implementation of advanced process control.

Fugitive emissions (leaks) from storage tanks, sewers, process units, seals, valves, flanges, and other fittings<sup>27</sup> can contain both CO and volatile organic compounds (VOC). Floating roofs can be added to open tanks, and tanks that already have a roof can be fitted with vapor recovery systems. Open grates above sewers can be replaced with solid covers. Emissions from seals, valves, etc., can be pin-pointed with portable combustible-gas detectors. Repairs can then be made at convenient times, e.g., during a maintenance shutdown.

## 6.3 Sulfur Oxides

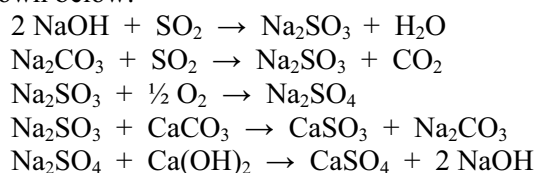
**Sources of SO<sub>x</sub> in refineries.** Fuel-oil fired heaters and the regenerators of FCC units are major sources of refinery SO<sub>x</sub> and NO<sub>x</sub> emissions. The most obvious way to reduce SO<sub>x</sub> from a heater is to burn low-sulfur fuels. Switching fuels requires no capital investment, but it is probably the most expensive solution due to the relatively high cost of low-sulfur fuels.

A large fraction of the sulfur in the feed to an FCC unit ends up in coke on the catalyst. SO<sub>x</sub> are formed in the regenerator when the coke is burned away. Removing sulfur from FCC feed with a pretreater decreases SO<sub>x</sub> emissions.

**Flue gas desulfurization.** Processes for removing sulfur oxides from stack gases include dry absorption, wet absorption, carbon adsorption, and catalytic oxidation. As mentioned above, ExxonMobil offers wet-gas scrubbing (WGS) technology, which simultaneously removes particulates, SO<sub>x</sub> and NO<sub>x</sub>.<sup>25</sup>

Historically, wet flue-gas desulfurization processes used aqueous slurries of lime, dolomite, and/or sodium hydroxide. Sulfur oxides react with lime or limestone (CaCO<sub>3</sub>) to produce calcium sulfate (CaSO<sub>4</sub>) and calcium sulfite (CaSO<sub>3</sub>), which precipitate from the scrubbing solution. The products move to a settling tank, in which the solid calcium salts separate from the solution as the scrubbed gas goes up the stack. After some time, the solids are removed and sent to a sanitary landfill. The solution is recycled, and fresh lime is added as needed.

The “dual alkali” approach starts with solutions or slurries of sodium hydroxide (NaOH), sodium carbonate (Na<sub>2</sub>CO<sub>3</sub>), or sodium bicarbonate (NaHCO<sub>3</sub>). These compounds react with SO<sub>2</sub> to give sodium sulfite (Na<sub>2</sub>SO<sub>3</sub>) and sodium bisulfite (NaHSO<sub>3</sub>), which stay dissolved in the solution. Some of the sodium sulfite reacts with excess oxygen in the flue gas to give sodium sulfate. Sulfate and sulfite are removed by reaction with lime or limestone (CaCO<sub>3</sub>). The sodium hydroxide solution is recycled. Make-up hydroxide is added as needed to compensate for losses. Selected dual-alkali reactions are shown below:



In a carbon adsorption process developed by Lurgi, hot flue gas first goes through a cyclone or dust collector for particulate removal. The gas is cooled with water and sent to an adsorption tower packed with activated carbon. The carbon adsorbs SO<sub>x</sub>. Water is sprayed into the tower intermittently to remove the adsorbed gas as a weak aqueous acid. The scrubbed gas goes out the stack. The acid goes to the gas cooler, where it picks up additional SO<sub>x</sub> by reacting with incoming flue gas. Cooler discharge is sold as dilute sulfuric acid.

In the Reinluft carbon adsorption process, the adsorbent is a slowly moving bed of carbon. The carbon is made from petroleum coke and activated by heating under vacuum at 1100°F (593°C).

Flue-gas scrubbing with catalytic oxidation (Cat-Ox) is an adaptation of the contact sulfuric acid process, modified to give high heat recovery and low pressure drop. In the Monsanto process, particulates are removed from hot flue gas with a cyclone separator and an electrostatic precipitator. A fixed-bed converter uses solid vanadium pentoxide (V<sub>2</sub>O<sub>5</sub>) to catalyze the oxidization of SO<sub>2</sub> to SO<sub>3</sub>. Effluent from the converter goes through a series of heat exchangers into a packed-bed adsorption tower, where it contacts recycled sulfuric acid. The tower overhead goes through an electrostatic precipitator, which removes traces of acid mist from the scrubbed gas. Liquid from the tower (sulfuric acid) is cooled and sent to storage. Some of the acid product is recycled to the absorption tower.

In a flue-gas desulfurization process from Mitsubishi Heavy Industries (MHI), manganese dioxide (MnO<sub>2</sub>) is the absorption agent. The final product is ammonium sulfate (NH<sub>4</sub>)<sub>2</sub>SO<sub>4</sub>, which is an excellent fertilizer. MHI claims better than 90% removal of SO<sub>x</sub> with this process.

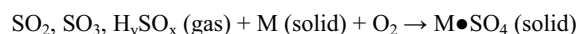
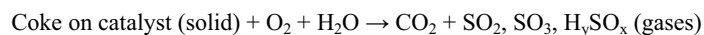
The Wellman-Lord process uses a solution of potassium sulfite (K<sub>2</sub>SO<sub>3</sub>) as a scrubbing agent. K<sub>2</sub>SO<sub>3</sub> adsorbs SO<sub>2</sub> to give potassium bisulfite (KHSO<sub>3</sub>). The bisulfite solution is cooled to give potassium pyrosulfite (K<sub>2</sub>S<sub>2</sub>O<sub>5</sub>). This can be stripped with steam to release SO<sub>2</sub>, which is fed to a sulfuric acid plant.

**FCC SO<sub>x</sub> transfer additives.** Arguably, SO<sub>x</sub> transfer additives are the most cost-effective way to lower SO<sub>x</sub> emissions from a full-combustion FCC unit. These materials, first developed by Davison Chemical, react with SO<sub>x</sub> in the FCC regenerator to form sulfates (*Figure 1*). When the sulfated additive circulates to the riser/reactor section, the sulfate is chemically reduced to H<sub>2</sub>S, which is recovered by amine absorption and sent to a sulfur plant.

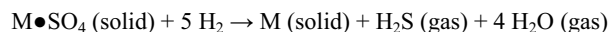
In summary, sulfur that would have gone up the stack as SO<sub>x</sub> goes instead to the sulfur plant as H<sub>2</sub>S.

In some units, SO<sub>x</sub> additives can reduce FCC SO<sub>x</sub> emissions by more than 70%. This can have a dramatic effect on the design and/or operation of upstream and downstream equipment – FCC feed pretreaters, FCC gasoline post-treaters, and flue-gas scrubbers for FCC regenerators.

#### FCC Regenerator (Oxidizing Environment)



#### FCC Riser-Reactor (Reducing Environment)

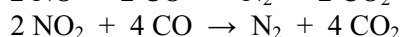
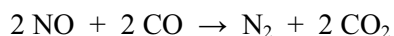


*Figure 1.* Mechanism of SO<sub>x</sub> transfer in FCC units.

**Hydrogen Sulfide Removal.** When sulfur-containing feeds pass through hydrotreaters or conversion units, some or most of the sulfur is converted into H<sub>2</sub>S, which eventually ends up in off-gas streams. Amine absorbers remove the H<sub>2</sub>S, leaving only 10-20 wppm in the treated gas streams. H<sub>2</sub>S is steam-stripped from the amines, which are returned to the absorbers. The H<sub>2</sub>S is piped to the refinery sulfur plant, where it is converted into sulfur.

## 6.4 Nitrogen Oxides

NO<sub>x</sub> are formed in several ways. In high-temperature heaters and FCC regenerators, NO<sub>x</sub> are produced by the reaction of nitrogen with oxygen. In FCC regenerators, NO<sub>x</sub> are produced from the nitrogen deposited with coke on spent catalysts. FCC NO<sub>x</sub> emissions go up when (a) the catalyst contains more combustion promoter, (b) when oxygen in the flue gas goes up, (c) at higher regenerator temperatures, and (d) at higher feed nitrogen contents. Combustion promoter is a noble-metal material that accelerates the reaction between CO and O<sub>2</sub> to form CO<sub>2</sub>. By removing CO, the promoter inhibits the following reactions:





Dual-alkali flue-gas scrubbing as described in Section 6.3 only removes about 20% of the NO<sub>x</sub> from a typical flue gas. Therefore, instead of simple scrubbing, chemical reducing agents are used. In selective catalytic reduction (SCR) processes, anhydrous ammonia is injected into the flue gas as it passes through a bed of catalyst at 500 to 950°F (260 to 510°C). The reaction between NO<sub>x</sub> and ammonia produces N<sub>2</sub> and H<sub>2</sub>O.

The MONO-NO<sub>x</sub> process offered by Huntington Environmental Systems employs a non-noble metal catalyst. For SO<sub>x</sub>, NO<sub>x</sub> and VOC removal, Ducon uses ceramic honeycomb or plate-type catalysts in which titanium dioxide is the ceramic and the active coatings are vanadium pentoxide and tungsten trioxide (WO<sub>3</sub>). The working catalyst temperature ranges from 600 to 800°F (315 to 427°C). For NO<sub>x</sub> abatement, Ducon provides complete ammonia injection systems with storage tanks, vaporizers and injection grids. Either anhydrous or aqueous ammonia can be used.

NO<sub>x</sub>-removal catalysts are offered by Haldor-Topsøe, KTI, and others. The Thermal DeNO<sub>x</sub> process offered by ExxonMobil is non-catalytic.

## 6.5 Greenhouse Gases, Stratospheric Ozone

Refineries have reduced emissions of greenhouse gases – primarily CO<sub>2</sub> – by improving energy efficiency, which cuts back on fuel requirements. Like other factories in countries that have signed the Montreal Protocol, refineries are switching to ozone-friendly heat-transfer fluids in air conditioners.

## 6.6 Waste Water

In refineries, the treatment of wastewater (*Table 11*) purifies process water, runoff from storms, and sewage. These may contain oil, suspended solids, dissolved salts, phenols, ammonia, sulfides, and other materials. They come from just about every process unit, especially those that use wash water, condensate, stripping water, caustic, or neutralization acids.

### 6.6.1 Primary Treatment

Primary treatment uses a settling pond to allow most hydrocarbons and suspended solids to separate from the wastewater. The solids drift to the bottom of the pond, hydrocarbons are skimmed off the top, and oily sludge is removed. Difficult oil-in-water emulsions are heated to expedite separation.

Acidic wastewater is neutralized with ammonia, lime, or sodium carbonate. Alkaline wastewater is treated with sulfuric acid, hydrochloric acid, carbon dioxide-rich flue gas, or sulfur.

*Figure 2* is a simplified sketch of an API oil-water separator. The large capacity of these separators slows the flow of wastewater, allowing oil to float

Table 11. Refinery waste water treatment in a nutshell.

| Designation        | Source   |
|--------------------|--|
| Oil-Free Water     | Oil-free storm runoff                                      |
|                    | Steam turbine condensate                                   |
|                    | Air-conditioner cooling water                              |
|                    | Cooling water from light-oil units (C <sub>5</sub> -minus) |
|                    | Cooling-tower blowdown                                     |
| Oily Cooling Water | Clean water from treatment plants                          |
|                    | Oily storm runoff  |
| Process Water      | Cooling water from heavy-oil units (C <sub>5</sub> -plus)  |
|                    | Uncontrolled blowdown                                      |
| Sanitary Water     | Desalter water   |
|                    | Excess sour water  |
|                    | Water drawn from oil-storage tanks                         |
|                    | Accumulator draws  |
|                    | Treating plant waste                                       |
|                    | Barometric condensers                                      |
|                    | Slop-oil breaks  |
| Sanitary Water     | Ballast water  |
|                    | Employee locker rooms                                      |
|                    | Cafeteria  |
|                    | Office buildings   |
| Sanitary Water     | Control rooms  |
|                    | Destination  |
| Oil-Free Water     | Oil/water separator  |
| Oily Cooling Water | Oil/water separator  |
| Process Water      | API Separator, activated sludge treatment                  |
| Sanitary Water     | Municipal water treatment plant                            |

to the surface and sludge to settle out. They are equipped with a series of baffles and a rotating endless-belt skimmer, which recovers floating oil. Accumulated sludge is removed through sludge hoppers at the bottom.

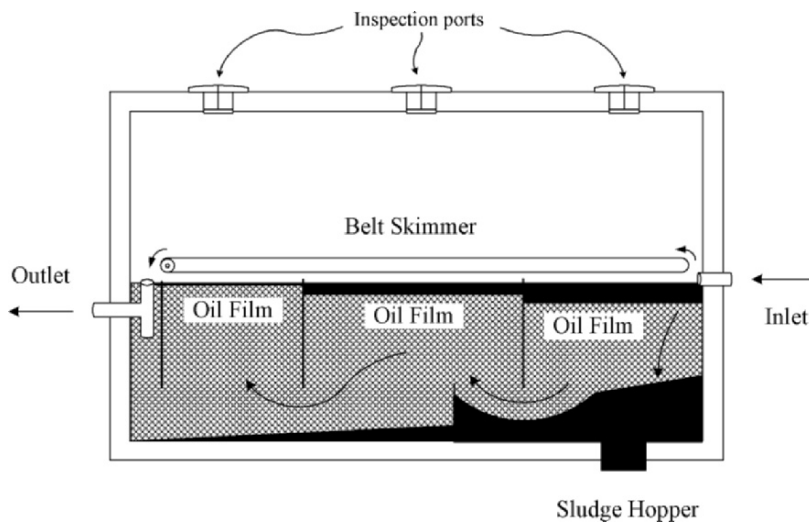


Figure 2. API oil/water separator: simplified sketch

### 6.6.2 Secondary Treatment

A small amount of suspended solids remains in the water after primary treatment. These are removed by filtration, sedimentation or air flotation. Flocculation agents may be added to consolidate the solids, making them easier to remove by sedimentation or filtration. Activated sludge, which contains waste-acclimated bacteria, digests water-soluble organic compounds, in either aerated or anaerobic lagoons. Steam-stripping is used to remove sulfides and ammonia, and solvent extraction is used to remove phenols.

### 6.6.3 Tertiary Treatment

Tertiary treatment removes specific pollutants, including traces of benzene and other partially soluble hydrocarbons. Tertiary processes include reverse osmosis, ion exchange, chlorination, ozonation, or adsorption onto activated carbon. Compressed air or oxygen can be used to enhance oxidation. Spraying water into the air or bubbling air through the water removes remaining traces of volatile chemicals such as phenol and ammonia.

## 6.7 Cleaning Up Oil Spills

Oil spills can be caused by natural seepage, leaky storage tanks, petroleum exploration and production activities, the on-purpose flushing of fuel tanks at sea, and accidents such as those described in Section 3.

The cleanup of oil spills includes containment, physical and mechanical removal, chemical and biological treatment, and natural forces. Land-based spills are easier to clean than spills onto open water, which are spread quickly by currents and winds.

### 6.7.1 Natural Forces

Several natural forces tend to remove oil spills. These include evaporation, spreading, emulsification, oxidation, and bacterial decomposition.

**Evaporation.** A large portion of an oil spill may simply evaporate before other methods can be used to recover or disperse the oil. Rates of evaporation depend on the ambient temperature and the nature of the oil.

**Spreading.** The fact that spilled oil spreads quickly across the surface of water is a “good news, bad news” story. The good news is that spreading increases rates of evaporation and air oxidation. The bad news is that the more dispersed the oil becomes, the harder it is to collect.

As with evaporation, rates of oil-spill dispersion depend upon ambient conditions and the nature of the oil. Not surprisingly, oil disperses best in fast-moving turbulent water.

**Oxidation.** Freshly spilled crude oil has a natural tendency to oxidize in air. Sunlight and turbulence stimulate the process. Oxidation products include organic acids, ketones and aldehydes, all of which tend to dissolve in water. As a spill ages, oxidation slows as “easy” molecules disappear from the mix. Compared to other natural forces, oxidation plays a minor role in removing oil spills.

**Emulsification.** When crude oil spills at sea, it emulsifies rapidly. Two kinds of emulsions are formed – oil-in-water and water-in-oil. Oil-in-water emulsions, in which water is the continuous phase, readily disperse, removing oil from the spill. However, this kind of emulsion requires the presence of surface-active agents (detergents).

The composition of water-in-oil emulsions varies from 30% to 80% water. These are extremely stable. After several days, they form “chocolate mousse” emulsions, which are annoyingly unresponsive to oxidation, adsorption, dispersion, combustion, and even sinking. The most effective method for mousse emulsions is physical removal. Mousse contains roughly 80% water, so after a 40 to 50% loss of light-ends through evaporation, a spill of 200,000 barrels oil can form 400,000 to 500,000 barrels of mousse.

### 6.7.2 Containment and Physical Removal

**Booms.** When oil is spilled on water, floating booms may be used for containment. A typical boom extends 4 inches (10 cm.) above the surface and 1 foot (30 cm.) below. Foam-filled booms are lightweight, flexible, and relatively inexpensive. Typically used for inland and sheltered waters, they are made from polyvinyl chloride (PVC) or polyurethane. Rectangular floats allow them to be wound onto a reel for storage.

Inflatable booms use less storage space and can be deployed from ships or boats in open water. Towed booms (*Figure 3*) are good for preventing dispersion of oil by winds and currents.

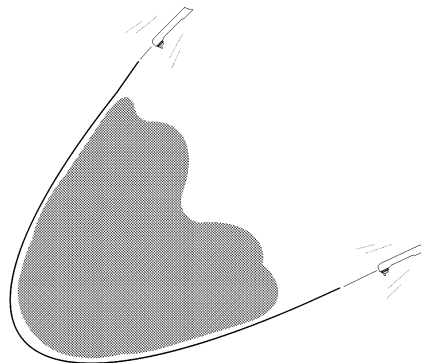


Figure 3. Boom barrier towed by ships

Beach booms are modified for use in shallow water or tidal areas. Water-filled tubes on the bottom of the boom elevate it above the beach when the water level is low and allow the boom to float when the water level rises.

**Skimmers and pumps.** After a spill is contained, skimmers and pumps can pick up the oil and move it into storage tanks. Weir skimmers are widely used because they are so simple. Modern designs are self-adjusting and circular so that oil can flow into the skimmer from any direction. They can be fitted with screw pumps, which enable them to process many different types of oil, including highly viscous grades. Cutting knives keep seaweed and trash from fouling the pumps. Screw pumps can develop high pressure differentials, which gives them higher capacities than other kinds of pumps.

Another kind of skimmer is an oleophilic (“oil loving”) endless belt. The belt picks up oil as it passes across the top of the water. As the belt returns to its starting point, it is squeezed through a wringer. Oil recovered by the wringer flows into containers, where it is stored until it can be moved to a land-based processing facility.

Another method uses a subsurface impeller to create a vortex, similar to the vortex that forms as water flows out of a bathtub. (Figure 4.) This funnels water down through the impeller and creates a bowl of oil in the middle of the vortex. A pump is used to remove oil from the bowl.

### 6.7.3 Adsorbents

Oil spills can be treated with absorbing substances or chemicals such as gelling agents, emulsifiers, and dispersants.

When applying adsorbents, it is important to spread them evenly across the oil and to give them enough time to work. When possible, innocuous substances should be used. Straw is cheap, and it can absorb between 8 and 30 times its own weight in oil. When it is saturated, the straw is loaded into boats with rakes or a conveyor system and transported to land. Oil can be recovered from the straw by passing it through a wringer.

Synthetic substances may also be used adsorbing oil spills. Polymers such as polypropylene, polystyrene, and polyurethane have been used successfully. Polyurethane foam is especially good. It can be synthesized onsite easily, even aboard a ship. It adsorbs oil readily and doesn’t release its load unless it is squeezed. Best of all, a batch of polyurethane can be used again and again.

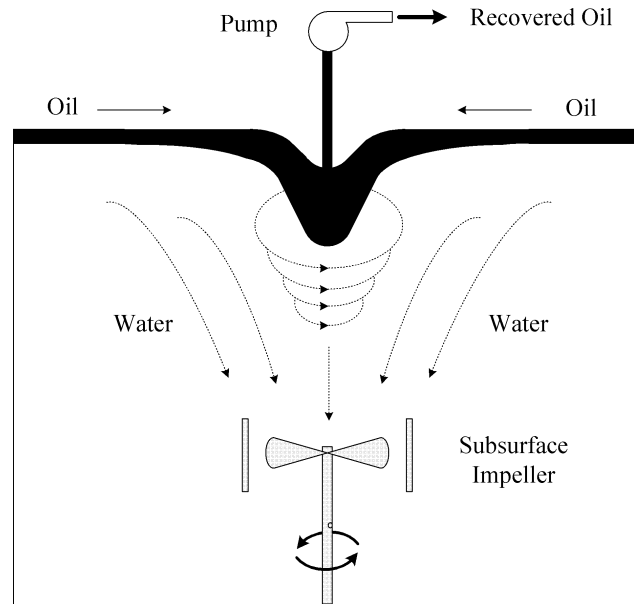


Figure 4. Free vortex skimmer for oil recovery

#### 6.7.4 Dispersion Agents

Dispersion chemicals act like detergents. One part of the molecule is oil-soluble while the other is water-soluble. In effect, the oil dissolves in water and diffuses quickly away from the spill. Dispersants reduce the tendency of oil to cling to partly immersed solids, such as walls, docks, buoys and boats.

#### 6.7.5 Non-dispersive Methods

Non-dispersive methods for removing oil spills include gelling, sinking, and burning.

**Gelling.** Fatty acids and 50% sodium hydroxide can be added to a spill to trigger a soap-forming reaction. The resulting gel does not disperse. Instead, it remains in place to block the spread of non-gelled oil.

**Oil sinking.** Sinking an oil spill keeps it from reaching shorelines, where it can devastate marine life. Sinking is best used in the open sea. In shallow water near the coast, it can cause more problems than it solves. Amine-treated sand is the most common sinking agent. To initiate sinking, a sand/water slurry is sprayed onto the oil slick through nozzles. The required sand/oil ratio is about 1-to-1. The oil sticks to the treated sand, which sinks toward the bottom of the sea. According to many experts, the oil-coated sand remains in place for many years. According to others, it can damage fragile ecosystems on the ocean floor.

During a full-scale test 15 miles from the coast of Holland, Shell Oil used amine-treated sand to sink a 100-ton slick of Kuwaiti crude in less than 45 minutes. Oil removal exceeded 95%.

Other materials have been used for oil sinking. These include talc, coal dust, cyclone-treated fly ash, sulfur-treated cement, and chalk. In general, a 1-to-1 ratio of sinker weight to oil weight is needed to sink a fresh spill. If weathering takes place, the density of the oil increases and less sinking agent is needed. It has been estimated that the cost for sinking is similar to the cost for dispersion. However, in open seas under high winds and waves, it may be difficult to spread the sinking agent.

**Burning.** Freshly spilled crude oil in a confined area may be combustible. However, after several hours, the spill may have thinned due to spreading and the most volatile components may have evaporated. If so, it may not be possible to ignite the remaining material. The addition of gasoline or kerosene can restore combustibility.

Burning is not used much anymore. It seldom removes much oil, and it can generate concentrated, unpredictable pockets of atmospheric CO and SO<sub>2</sub>, both of which are poisonous.

#### 6.7.6 Cleanup of Oil Contaminated Beaches

For cleaning oil from beaches, farm machinery and earthmoving equipment have been used to good effect. In many cases, a layer of straw is spread across the oil. After a few days, the oil-laden straw is raked onto a conveyor, screened to drop out sand, and sent to wringer. Recovered oil is trucked away to a refinery. The spent straw, which still contains some oil, can be blended with coal and burned in a power plant, or simply incinerated. The separated sand is washed and returned to the beach.

When beach pollution is severe, oily sand is removed with earthmoving equipment. When beach pollution is mild, sand removal may not be needed. Instead, detergents can be used. They must be used cautiously to minimize harm to marine life. Wave action does a great job of mixing detergent into the sand. Usually, the detergent is applied about one hour before high tide. When the tide comes in, the washing begins. If high-tide washing is inappropriate, high-pressure hoses can be used. Hoses are also effective for cleaning oil off of walls and rocks.

**Froth flotation.** In the froth-flotation process, oil-soaked sand from a polluted beach is poured into a vessel, where it is mixed with water and cleaned with a froth of air bubbles. Aided by chemical or physical pre-treatment, the froth strips oil away from the sand. Due to its low density and the action of the bubbles, the oil floats to the top of the vessel, where it is drawn off and sent to a separating chamber, where entrained water is removed. Tests show that sand containing 5,000 ppm of oil can be cleaned

down to 130 ppm, generating effluent water with 165 ppm of oil. Usually, the cleaned sand is returned directly to the beach.

**Hot water cleanup.** When milder methods fail to give the desired degree of cleanup, hot water can mobilize some of the oil still trapped within the polluted sand. This method is used as a last resort because of the damage it does to inter-tidal ecosystems.

### 6.7.7 Amoco Cadiz Oil Spill Cleanup: A Case Study

As mentioned, for two weeks after the *Amoco Cadiz* ran aground off the coast of Brittany, severe weather restricted cleanup efforts. Eventually, the entire cargo – more than 1.6 million barrels of crude oil – spilled into the sea. The resulting slick was 18 miles wide and 80 miles long. The oil polluted 200 miles of coastline, including beaches, harbors and habitats for marine life.

A 2.5 mile permanent boom protected the Bay of Morlaix. Although it required constant monitoring, the boom functioned well because the bay was protected from severe weather and the brunt of the oil slick. In other areas, booms were largely ineffective due to strong currents, and also because they were not designed to handle such enormous amounts of oil. Skimmers were used in harbors and other protected areas. Vacuum trucks removed oil from piers and boat slips where seaweed was especially thick. “Honey wagons” – vacuum tanks designed to handle liquefied manure – were used to collect emulsified oil along the coast.

Oil-laden seaweed was removed from the beaches with rakes and front-end loaders. Farm equipment was used to plow and harrow the sand, making it more susceptible to wave and bacterial action. Prior to harrowing, chemical fertilizers and oleophilic bacteria were applied to the sand.

At first, authorities decided against using dispersants in sensitive areas and along the coastal fringe. Meanwhile, the spill formed a highly stable water-in-oil emulsion (“chocolate mousse”). On the open sea, the French Navy applied both dilute and concentrated dispersants, but good dispersion was hard to achieve because in some places the mousse emulsion was several centimeters thick. If dispersants been dropped from the air at the source of the spill – in days instead of weeks – the formation of mousse emulsion might have been prevented.

About 650 metric tons of chalk was applied in an effort to sink the oil. But after one month at sea, the oil was so viscous that the chalk just sat on top of it. Rubber powder made from ground-up tires was applied to absorb the oil. The French Navy used water hoses to spread most of the powder. Some was applied manually from small fishing boats. Because it stayed on top of the oil, the rubber powder had little effect; wave action wasn’t strong enough to mix it into the oil, most of which was trapped inside the chocolate mousse emulsion.



During the third and fourth months of the cleanup, high-pressure hot water (fresh water at 2,000 psi, 80° - 140°C) was very effective in cleaning oil from rocky shores. A small amount of dispersant was applied to prevent oiling of clean rocks during the next high tide. The mouths of several rivers contained oyster beds and marshes that required manual cleaning. Soft mud river banks were cleaned with low-pressure water. To improve oil-collection efficiency, a sorbent was mixed with water and poured in front of the wash nozzles. The oil was collected downstream by a local invention called an "Egmolap." This device was good at collecting floating material in sheltered areas.

## 6.8 Solid Waste Recovery and Disposal

Contaminated solids are produced during the drilling of oil wells, the transportation of crude oil, and in oil refineries. All oil-contaminated solids are considered hazardous and must be sent to hazardous-waste landfills. The transportation and disposal of hazardous waste costs an order of magnitude more than the transportation and disposal of sanitary waste. Thus, there is a huge economic incentive to remove oil from contaminated solids before they leave a site.

Table 12 shows the sources of solid wastes in a modern oil refinery. These data, provided by the American Petroleum Institute, are based on a "typical" 200,000 barrels-per-day high-conversion refinery. A plant this size produces about 50,000 tons per year of solid waste and about 250,000 tons per year of waste water. As discussed above, all waste water must be purified before it leaves the plant.

Table 12. Breakdown of Refinery Solid Wastes

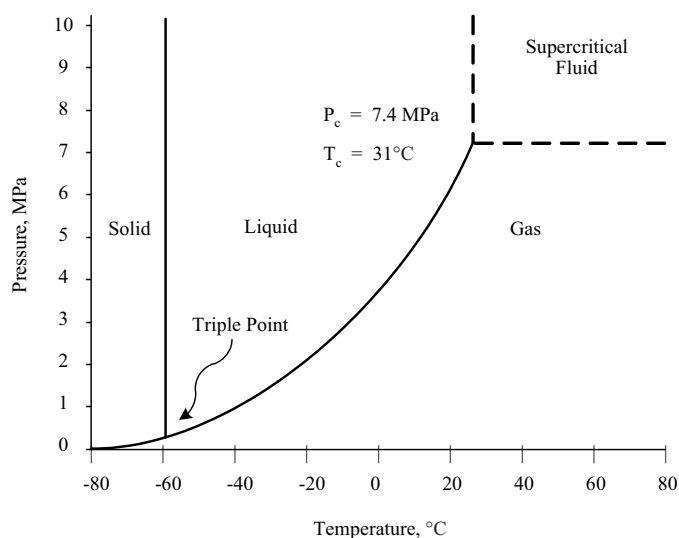
| Solid Waste                         | Percent of Total (wt%) |
|-------------------------------------|------------------------|
| Pond sediments                      | 8.4                    |
| Sludge from biological treatment    | 18.9                   |
| Solid from DAF/IAF treaters         | 15.4                   |
| API separator sludge                | 13.2                   |
| Miscellaneous sludge                | 17.5                   |
| Off-grade coke                      | 1.9                    |
| Spent catalysts                     | 6.4                    |
| Slop oil emulsion solids            | 4.4                    |
| Spent solvents, chemicals           | 3.8                    |
| Contaminated soils and other solids | 6.7                    |
| Heat exchanger cleaning sludge      | 0.1                    |
| Tank sludge                         | 3.4                    |

DAF = dissolved air flotation

IAF = induced air flotation

### 6.8.1 Super-critical Fluid Extraction

A supercritical substance exists as a single fluid phase. Simultaneously, it can have liquid-like solvating powers and gas-like diffusivity and viscosity; its surface tension is zero. Ammonia, argon, propane, xenon, water, CO and CO<sub>2</sub> are used for supercritical extraction. The phase diagram in *Figure 5* shows that the super-critical region for CO<sub>2</sub> lies above 88°F (31°C) and 1058 psig (7.4 MPa). The CO<sub>2</sub> triple point, where solid, liquid and gas phases exist simultaneously, occurs at -69.9°F (-56.6°C) and 57.8 psig (0.5 MPa).



*Figure 5.* Phase diagram for carbon dioxide.

With non-toxic gases such as CO<sub>2</sub>, the SFE process is simple. Untreated solids are placed in an extraction chamber and CO<sub>2</sub> is added. Pressurizing the CO<sub>2</sub> converts it into an effective solvent. By manipulating temperature and pressure, operators can extract the material of interest with high selectivity. After the extracted material dissolves in the CO<sub>2</sub>, it goes to a collection vessel, where the pressure is reduced. At low pressure, CO<sub>2</sub> loses its solvating power and separates from the extract. The CO<sub>2</sub> is recovered, condensed and recycled. In SFE with CO<sub>2</sub>, no liquid solvents are used. The CO<sub>2</sub> is recycled, so the process is not considered to be a contributor to global warming.

SFE is common in the food, pharmaceutical and cosmetic industries, where it extracts caffeine from coffee beans, bitter from hops, tar and nicotine from tobacco, and other natural compounds from spices, flowers, aromatic woods, and medicinal plants.

Since about 1990, SFE with CO<sub>2</sub> has been used in oil fields to remove oil from drill cuttings. CO<sub>2</sub> is especially good for this purpose because it can be used onsite. It is non-toxic (except when it suffocates), relatively unreactive, and it doesn't burn. On drill cuttings and other oil-contaminated soils and sands, it penetrates the mineral structure, removing both the free-oil phase and the oil trapped in the solid matrix. The process removes more than 99.9% of the oil, leaving no toxic residue. The required time is short – about 10 to 60 minutes per batch.

### 6.8.2 Sludge

According to RCRA, oil-containing sludge from storage tanks and refinery water treatment facilities is by definition hazardous, and should be sent to a hazardous land fill. In most cases, a lot of the sludge can be dissolved with detergents and/or solvents (such as hot diesel oil) and blended into crude oil. Alternatively, dissolved sludge can go to delayed cokers, asphalt plants, carbon black plants, or cement kilns.

In one method, hot water and a chemical are circulated through the tank. On top of the water, a hydrocarbon such as diesel is added. The density difference between warm water and the hydrocarbons in the sludge causes the sludge to rise, allowing the chemical to strip out water and solids. The method recovers good-quality oil, which can be processed in the refinery, and leaves behind a relatively clean layer of solids on the tank bottom.

Tanks associated with slurry oil from FCC units present an interesting challenge. It can be very expensive to take these tanks out of service, the sludge is loaded with finely divided FCC catalyst particles, and slurry-oil sludge is difficult to dissolve. Recently, a process called Petromax has been used to liquefy slurry-oil sludge, allowing it to be pumped out of tanks with ordinary equipment, even while the tanks are still in use.<sup>28</sup>

Some service companies use robots, cutting wands, and other sophisticated devices to clean tanks completely without sending people inside. These methods are especially valuable when the tank contents are toxic. One such company is Petrochemical Services, Inc., which pioneered the use of robots in tank-cleaning operations.

Blending mobilized sludge into crude oil is limited by specifications on basic sediment and water (BS&W). This seems equivalent to moving waste from one place to another, but it really isn't. The dissolution of tank sludge separates useful oil from inorganic solids (sand, clay, salts, and metal oxides) and refractory organics (asphaltenes, long-chain waxy paraffins, kerogen, and coke).

### 6.8.3 Spent Catalysts

Many refinery catalysts are regenerated several times. The regeneration of FCC catalysts occurs in the (aptly named) regenerator. Catalysts from fixed-bed units can be regenerated in place, but usually they are sent off-site to a facility that specializes in catalyst regeneration.

Eventually, even the hardiest catalysts reach the end of their useful life. When this happens, they are sent to a metals reclaimer, which recovers saleable products such as alumina, silica,  $\text{MoO}_3$ ,  $\text{V}_2\text{O}_5$ , nickel metal, and various forms of cobalt.

The reclamation company makes money on both ends of the plant – from the refiner who must dispose of the catalyst, and from the customer who buys reclaimed products.

## 7. FICTION VS. FACT

In today's popular culture, Big Oil is a convenient villain. Catastrophic oil spills, tragic explosions, and price fluctuations capture front-page headlines, stimulate editorials, and spark conspiracy-theory discussions on talk radio and television news. *On Deadly Ground* (1994) is one of the latest in a succession of action films that portray oil executives as ruthless sociopaths.

This is understandable. The petroleum industry is far from blameless. Its early history was dominated by nature-despoiling oil booms and greedy oil barons. Its recent history is punctuated by ecological disasters.

But our personal experience differs from popular culture. Between us, we have been employed by three different oil companies, and we have provided services to scores of others. Without exception, the people we deal with – from managers and engineers to operators, and office workers – rank safety and environmental compliance as their top two work-place priorities.

Things used to be different. Before the 1970s, “miners’ asthma,” dead forests downwind from coal-fired power plants, and pools of poison around abandoned strip mines were just part of the price we paid for cheap power and minerals. In some locales, smoky flares in refineries were the rule, not the exception. More often than not, news of a river catching fire caused laughter instead of outrage.

In contrast, today we believe that our fundamental rights include clean air, clean water, and a healthy workplace. We are products of the same social movement that created the United States Environmental Protection Agency (EPA), the Occupational Safety and Health Administration (OSHA), and similar agencies around the world. We were part of that movement, as were many of the people who now work for Big Oil. Governments are providing the “stick” – steep fines and possible jail time for corporate executives – but the “carrot” comes from a basic change in our fundamental values.

We may never see a movie in which an oil executive saves the day. But someday, perhaps, public perception will catch up with the following reality: Accidents may happen and mistakes might be made, but their impact and frequency are minimized by the bright, devoted people who work in today's refineries. While providing us with clean fuels and basic chemicals, they do their level best to protect the world from pollution, making it a better place for all of us and our children.

## 8. REFERENCES

1. Shaheen, E.I. *Technology of Environmental Pollution Control*, 2<sup>nd</sup> ed., PennWell Books: Tulsa, 1992.
2. Margulis, L.; Sagan, D. *What Is Life? The Eternal Enigma*, University of California Press: Berkeley, 2000
3. "AQMD Adopts Regulation to Reduce Particulate Emissions from Oil Refineries," *AQMD Advisor*, Nov. 7, 2003
4. U.S. Environmental Protection Agency, *Air Trends: Stratospheric Ozone*, National Service Center for Environmental Publications: Cincinnati, OH, 2004
5. *Policy Implications of Greenhouse Warming: Mitigation, Adaptation, and the Science Base*, National Academy Press: Washington, D.C., 1992
6. McIntyre, S.; McKittrick, R. "Corrections to the Mann et. al. (1998) Proxy Data Base and Northern Hemispheric Average Temperature Series," *Energy and Environment* **2003**, 14 (6), 751
7. Lower, S.K. *Carbonate Equilibria in Natural Waters*, [www.chem1.com/acad/pdf/3carb.pdf](http://www.chem1.com/acad/pdf/3carb.pdf)
8. "Air Quality in the UK," *Postnote*, November 2002 (188)
9. Proceedings of the symposium: "Twenty Years after the Amoco Cadiz," Brest, France October 15-17, 1998.
10. "Chernobyl Powers Down Permanently," *CNN.com*, Dec. 15, 2000, <http://www.cnn.com/2000/WORLD/europe/12/15/chernobyl.shutdown/>
11. Grushevoi, G. World Uranium Hearing, Salzburg, 1992, 259-260.
12. Weber, U. "The Miracle of the Rhine," *UNESCO Courier*, June 2000.
13. "Tankers Have Spill-Free Year in Alaska," *USA Today*, July 11, 2004.
14. Maslow, A.H., *Toward a Psychology of Being*, 3<sup>rd</sup> ed., Wiley: New York, 1998.
15. Seebauer, E.G., "Whistleblowing: Is It Always Obligatory?" *Chemical Engineering Progress*, 2004, (6), 23
16. Depledge, J.; Lamb, R. *Caring for Climate: A Guide to the Climate Change Convention and the Kyoto Protocol*, Courir-Druck: Bonn, 2003
17. "Bridge Painting Company and Its President Plead Guilty to Federal Crimes Relating to the Dumping of Lead Waste," *Business and Legal Reports*, Feb. 15, 2002.
18. 40 CFR Parts 50-99.
19. BAAQMD 9-10, "NOx and CO from Boilers, Steam Generators, and Process Heaters in Petroleum Refineries," Jan. 5, 1994
20. H.R. 4503, 862
21. "National Emission Standards for Hazardous Air Pollutants: Petroleum Refineries; Final Rule," 40 CFR Part 9, 60 and 63, *Federal Register* **1995**, 60 (160), 43244
22. "2003 - 2008 EPA Strategic Plan. Goal 2: Clean and Safe Water," U.S. Environmental Protection Agency: Washington, D.C., 2003

23. *Kyoto Protocol to the United Nations Framework Convention on Climate Change*, UNFCC: Bonn, Germany, 1998
24. Pearce, F. *New Scientist*, December 10, 2003
25. <http://www.prod.exxonmobil.com/refiningtechnologies/>
26. Couch, K.A.; Seibert, K.D.; Van Opdorp, P. "Controlling FCC Yields and Emissions: UOP Technology for a Changing Environment, AM-04-45, NPRA Annual Meeting, San Antonio, TX, March 23-25, 2003
27. "Cleaner Production Initiatives – BP Kwinana Refinery," Department of the Environment and Heritage: Canberra, Australia, 2004.
28. "World Energy Interviews Barry Rosengrant, Chief Executive Officer of Petromax," *World Energy* **2004**, 7 (2).

## INDEX

- Aniline Point, 107
- API Gravity, 104, 107
- ASTM, 49
  - D1159, 124, 125, 126
  - D1218, 109
  - D1319, 124-126, 129
  - D1322, 109
  - D1552, 104, 110
  - D1655, 181
  - D189, 108
  - D2007, 118-123
  - D2386, 108
  - D2500, 108
  - D2549, 118, 119-121, 123
  - D2699, 50
  - D2700, 50
  - D2786, 119, 131, 135, 141
  - D287/1298, 104, 107
  - D2892, 105, 106
  - D3228, 108
  - D323, 109
  - D3230, 109
  - D3239, 119, 131, 136, 140, 141
  - D36, 111
  - D4057, 103
  - D4294, 104, 110, 136
  - D445, 110
  - D4502, 143, 146
  - D4629, 108
  - D5, 111
  - D5186, 129
  - D5236, 106
  - D5291, 104, 110
  - D5307, 104
  - D5453, 104, 110
  - D5773, 108
  - D5853, 104, 109
  - D5949, 108
  - D5972, 108
  - D611, 107
  - D613, 56, 143, 146
  - D664, 110
  - D97, 104, 109
  - D975, 181
  - D976, 57
  - D5854, 103
- Alkylation, 44
  - Sulfuric Acid, 44
  - Hydrofluoric Acid (HF), 45
- Amoco Cadiz (1978), 402-403, 441
- Aromatic Sulfur Types, 135-136
- Asphalt, 47
  - Production, 47
  - Properties, 111
  - Road-Tar, 47
  - Roofing, 47
- Atmospheric distillation, 18
- Auto Oil I & II, 57, 58
- Benfield process, 65
- Biodegradation, 95
- Biodesulfurization, 348-352
- Bitumen, 91
- Blending,
  - Diesel, 56
  - Gasoline, 50
- Bhopal, India (1984), 403-404
- Bromine Number, 124, 125
- BTX, 149, 150, 157, 164
- Carbenium Ion Beta Scission, 151
- Carbenium Ions, 151, 155
- Carbon Monoxide, 396, 431
- Catagenesis, 92, 95
- Catalysts, 25, 31, 34, 37, 40, 43
  - Acid Function, 232-233
  - Acidic, 44
  - Activation, 199, 240-241
  - Alkylation, 44
  - Deactivation, 38, 241-242, 275-276
  - FCC, 171-174
  - Hydrocracking, 200
  - Hydroprocessing, 195-200
  - Hydrotreating, 199-200
  - Impregnation, 198, 238-239
  - Isomerization, 41
  - Light Olefin Production, 153-155
  - Manufacturing, 234-239
  - Metal Function, 234
  - Noble Metal, 199, 356-360
  - Poisons, 19, 250
  - Preparation, 196-199
  - Reforming, 37
  - Regeneration, 243, 275-276
  - Shape Selective, 12
  - SPA, 44
  - Suppliers, 255
  - Ultra Deep HDS, 299

- Catalytic Converters, 13, 58
- Catalytic Cracking, 25, 156, 164
  - Fluid (FCC) 25, 32
  - Houdry (HCC), 27
  - Residue FCC, 28
- Catalytic Processes, 150
- Catalytic Pyrolysis Process (CPP), 154, 157-160
- Catalytic Reforming,
  - Continuous Catalytic Regeneration (CCR), 37, 39
  - Cyclic, 37
  - Semi-regenerative, 38
- Caustic Scrubber, 41
- Cetane Index, 56, 57
- Cetane Number, 56
- Chernobyl (1986), 404-406
- Class-Type Separation, 118-131
- Claus Reactions, 61
- Claus Process, 61
- Clean Air Act, U.S., 12, 13, 52, 317, 415-420
- Clean Fuels, 181
- Clean Water Acts, 422
- Cloud Point, 58, 108
- Coefficient of Thermal Expansion (CTE), 24
- Coke,
  - Formation, 190-191
  - Needle, 23
  - Shot, 23
  - Sponge, 23
- Coking, 22
  - Delayed, 22
  - Fluid, 24
- Composition,
  - Crude Oil, 96
  - Petroleum, 95
- Contaminated Beaches Cleanup, 440-441
- Cracking Mechanism, 151
- Cracking Reactions, 187-190, 227-231
- Crude Assay, 103-111
  - Property Measurement/Assay Grid, 107
- Cyclic Reformer, 37
- Deasphalting, 19
- Deep Catalytic Cracking (DCC), 156-157
- Deep Dearomatization (Hydrogenation), 355-362
- Deep Desulfurization, 317-362
- Deep Upgrading of Heavy Crude, 150
- Dehydrocyclization, 36
- Dehydrogenation, 36
- Deoiling, 21
- Deposition of Organic-Rich Sediments, 82-86
- Depositional Environment, 85, 88, 94
- Dewaxing, 21
- Diagenesis, 88
- Diesel,
  - Additives, 59
  - Blending, 56
  - Clean, 57
- Distillation, 15, 105, 106
  - Atmospheric, 15
  - HiVac, 106
  - Vacuum, 19
- Edeleanu Process, 21
- Environmental Protection Agency (EPA), 411-412
- Extraction, 20
- Extractive Desulfurization (EDS), 373-378
  - Synergism with HDS, 376-378
- Federal Water Pollution Control Act, 421-422
- Fixed Bed Hydrotreater, 34
- Fluid Cat Cracking (FCC), 153,160,167, 169-175, 179
  - Catalysts, 171-174, 445
  - Chemistry and Kinetics, 171
  - Effect in Air Quality, 396-397, 431-434
  - Gasoline Post-Treating, 55
- Fluorescent Indicator Adsorption (FIA), 124, 126
- Freezing Point, 56, 108
- Gasoline,
  - Additives, 53
  - Blending, 50
  - FCC, 55
  - Low sulfur, 54
  - Reformulated (RFG), 51,52
- GC-AED, 124, 258-259, 306-308
- GC-FID, 124
- GC-EIMS, 131, 135, 137, 144
- GC-FIMS, 131-136, 141-142
- GC-MS, 114, 124
- Generation of Oil and Gas, 89
- Greases, 47
- Greenhouse Gases, 399-400, 428-430, 434
- HDM (hydrodemetallation), 262, 273-274
- HDN (Hydrodenitrogenation), 186-187, 226-227, 273-274
- HDO (Hydrodeoxygenation), 273-274
- HDS (Hydrodesulfurization), 184-185, 226, 258
  - Catalysts, 283-290
  - Chemistry, 264-269



- Deep, of Diesel, 271-273
- Deep, of FCC Gasoline, 280-283
- Deep, of Gasoline, 269-271
- Deep, Reactor Design, 279
- Inhibition, 275
- Mechanistic Pathways, 328-330
- Reactivities of Sulfur Compounds, 324-328
- Synergism with Extractive Desulfurization, 376-378
- Ultra Deep, of Diesel, 297-316
- High-Conversion Oil Refinery, 178
- History,
  - Hydrocracking, 219-221
  - Petroleum Production, 1
  - Petroleum Processing, 11
- Hydrocarbon Type Analysis,
  - by Mass Spectrometry, 131-135
  - by Boiling Point, 137-141
- Hydrocracker, 177
  - Design and Construction, 243-245
  - Ebullated Bed Units, 34, 210-211
  - Licensors, 255
  - Mild (MHC), 181
  - Operation, 245-246
  - Single Stage Once-Through, 221-222
  - Single Stage with Recycle, 222-223
  - Trickle Bed Units, 204-210
  - Two Stage Recycle, 209, 224
- Hydrocracking, 28, 29, 33, 36, 177-217, 219-225, 257
  - Catalysts, 200, 231-243
  - Chemistry, 225-231
  - Comparison with FCC, 215
  - Flow Schemes, 221
  - History, 219-221
  - "In-Between" Process, 181
  - Process Variables, 246-255
  - Reaction Kinetics, 192-195
  - Separate Hydrotreat Two Stage, 224-225
  - Similarities and Differences with Hydrotreating, 178-180
- Hydrofinishing, 257
- Hydrogen addition, 14
- Hydroprocessing, 182, 257
  - Catalysts, 195-196
  - Chemistry, 182-195
  - Economics, 212-214
  - Licensors, 216
  - Objectives, 180-181
  - Process Conditions, 211-212
  - Reactor Design, 382-388
  - Reactor Internals, 381-393
  - Yields and Product Properties, 212
- Hydrotreating, 28, 29, 31, 177-217, 257-294
  - Catalysts, 199-200, 262-263
  - Diesel, 32
  - FCC Feed, 32, 352-353
  - Gasoline/Naphtha, 31
  - Kerosene, 31
  - Lube, 32
  - Process Flow, 276-279
  - Processes, 261-262
  - Pyrolysis Gasoline, 33
  - Similarities and Differences with Hydrocracking, 178-180
- Increasing Propylene Production, 150, 157
- IP 391, 118
- Isodewaxing, 12, 46
- Isomerization, 36, 40
  - Catalysts, 40, 41
  - C<sub>4</sub>, 41
  - C<sub>5</sub>C<sub>6</sub>, 41
- Jet Fuel, 55
- Kerogens, 80, 81, 86, 87, 88, 91, 97
  - Formation, 88
  - Quality, 89
  - Type (Classification), 89
  - van Krevelen Diagram, 78, 89
- Kerosene, 55
- Kuwait (1991), 408
- Kyoto Protocol, 428-429
- Light Cycle Oils (LCO), 321
  - Undercutting, 353-355
- Light Olefin Production, 149, 151-153
- Linear Hourly Space Velocity (LHSV), 28
- London Fog (1952), 402
- Low Sulfur Gasoline, 54-55
- Mass Spectrometry, 131-137
- Material Safety Data Sheet (MSDS), 413-414
- Mercaptan, 108
  - Formation, 191-192
- Merichem LO-CAT Process, 62
- Metagenesis, 92
- Metals, 108
- Metathesis of ethylene and butene-2, 165
- Methanol to Olefin (MTO) Process, 164
- MFI type zeolite, 154, 155
- Mobil Olefin Interconversion (MOI), 163
- Micro Carbon Residue, 109
- Nelson Index, 70
- Neural Network Correlation, 142-147

- Nitrogen Content, 109
- Nitrogen Oxides, 397, 433-434
- Occupational Safety and Health Administration (OSHA), 412
- Octane number,
  - Research (RON, RONC), 50
  - Motor (MON, MONC), 50
- OCTGAIN, 12, 75, 282
- Oil Expulsion, 93-95
- Oil Spill Cleanup, 436-442
- Olefin Production Technology, 167
- Olefins Conversion Technology (OCT), 164-165
- Oxidative Desulfurization, 346-347
- Ozone, 397-398
- Particulate Matter (PM), 395-396, 430-431
- PetroFCC, 160-161
- Petroleum,
  - Abiogenic, 80,81
  - Accumulation, 81
  - Biogenic, 79, 80
  - Composition, 95-96, 259-260
  - History of Production, 1
  - History of Processing, 11
  - Modern Processing, 14
  - Origin, 79, 80
  - Processes, 258
  - Reservoir Rocks, 81
  - Seal Rocks, 81
  - Synthetic, 5
  - System, 81
  - Traps, 81
- PIONA Analysis, 122-123, 134, 141-142, 144
- Pollution Control, 395-446
  - Technology, 430-446
- Pour Point, 104, 109
- Prediction of Crude Assay Properties, 112-116
  - from NMR Measurements, 113
  - from Chromatographic Measurements, 113
  - from GC-MS Measurements, 114
  - from NIR Measurements, 115
- Primary Cracking, 151, 153
- Primary Migration, 93
- Primary Water Treatment, 63, 435
- Prime-G, 12, 75, 280-281
- Prince William Sound, Alaska (1989), 407-408
- Propane Catalytic Cracking (PCC), 164
- Propylur Process, 161-162
- Protolytic Cracking, 151
- Pump Octane, 50
- Quench Mixing Chamber Design, 388-389
- Quench Zone, 30
- Redox Cycle of Organic Carbon, 84
- Reforming, 37, 39
- Refractive Index, 109
- Refractory Sulfur Compounds, 271, 299
- Resid FCC, 157
- Reservoir Alteration, 95
- Resource Conservation and Recovery Act (RCRA), 423-425
- Rio Earth Summit, 427-428
- ROSE Process, 20, 75
- RVP, 52, 109
- Safety Drinking Water Act, 423
- Salt Content, 110
- SAP, 121-123
- Saturation Reactions, 182-184
- SCANfining, 12, 75, 280-281
- Secondary Cracking, 151, 153, 156
- Secondary Migration, 93
- Secondary Water Treatment, 63, 436
- Selective Adsorption, 341-346
- Selective Catalyst Reduction (SCR) Process, 60
- Selectivity to Ethylene, 149, 165, 166
- Selectivity to Propylene, 149, 165, 166
- Simulated Distillation,
  - Whole Crude, 104
- Smoke Point, 56, 110
- Solid Waste, 401
  - Recovery and Removal, 442-445
- Solvent Refining, 14
- SOAP, 123-131
- SOx, 396-397, 431-433
  - Abatement, 59
  - Transfer Additives, 60, 433
- Source Rock, 81, 82, 85, 88, 89, 91-94
- Specifications,
  - Diesel Fuels, 297-298, 373
- SPE (Solid Phase Separation), 121-131
- Steam Cracking, 149
- Stockholm Conference, 427
- Sulfur,
  - Compounds in Transportation Fuels, 321-324
  - Compound Reactivities in HDS, 324-328
  - Content, 104, 110
  - Regulations,
    - of Diesel and Jet Fuels, 319
    - of Gasoline, 318

- Removal by Selective Adsorption, 55
- Supercritical Fluid Extraction, 443-444
- SUPERFLEX Process, 162
- Superfund, 425-426
- S Zorb, 12, 75, 340-341
- TBP Curve, 106
- Tertiary Water Treatment, 63, 436
- The Rhine (1986), 406
- Thermal Cracking, 23
- Thermal Sulfate Reduction, 95
- Thermostat Catalytic Cracking (TCC), 169
- Total Acid Number, 110
- Toxic Substance Control Act (TSCA), 426
- Ultra Deep HDS, 297-316
  - Case Studies, 309-315
- Catalysts, 301-303, 309
  - Design Approaches, 330-352
  - Inhibitors for the Hydrogenation Route, 303-309
- Ultra-clean Distillate Fuels, 317-362
- Ultra-low Sulfur Diesel (ULSD), 54-55, 181, 297, 373
- Vacuum Residue, 28
- Visbreaking, 22
- Viscosity, 111
- Waste Water, 63, 434-436
- Water and Sediment, 111
- Waxes, 46
- Y zeolite, 153, 154, 156
- ZSM-5 zeolite, 25, 46, 151, 152, 154, 166

Practical Advances in  
Petroleum Processing  
Volume 2

# Practical Advances in Petroleum Processing Volume 2

Edited by

**Chang S. Hsu**

*ExxonMobil Research and Engineering Company  
Baton Rouge, Louisiana, USA*

and

**Paul R. Robinson**

*PQ Optimization Services  
Katy, Texas, USA*

 Springer

Chang S. Hsu  
ExxonMobil Research and Engineering Co.  
10822 N. Shoreline Avenue  
Baton Rouge, Louisiana 70809  
USA  
chang.samuel.hsu@exxonmobil.com

Paul R. Robinson  
PQ Optimization Services  
3418 Clear Water Park Drive  
Katy, Texas 77450  
USA  
paul-robinson@houston.rr.com

Cover design by Suzanne Van Duyne (Trade Design Group)

Front cover photo and back cover photo insert: Two views of the OMV plant in Schwechat, Austria, one of the most environmentally friendly refineries in the world, courtesy of OMV. Front cover insert photo: The Neste Oil plant in Porvoo, Finland includes process units for fluid catalytic cracking, hydrocracking, and oxygenate production. The plant focuses on producing high-quality, low-emission transportation fuels. Courtesy of Neste Oil.

Library of Congress Control Number: 2005925505

ISBN-10: 0-387-25811-6

ISBN-13: 978-0387-25811-9

©2006 Springer Science+Business Media, Inc.

All rights reserved. This work may not be translated or copied in whole or in part without the written permission of the publisher (Springer Science+Business Media, Inc., 233 Spring Street, New York, NY 10013, USA), except for brief excerpts in connection with reviews or scholarly analysis. Use in connection with any form of information storage and retrieval, electronic adaptation, computer software, or by similar or dissimilar methodology now known or hereafter developed is forbidden.

The use in this publication of trade names, trademarks, service marks and similar terms, even if they are not identified as such, is not to be taken as an expression of opinion as to whether or not they are subject to proprietary rights.

Printed in the United States of America

9 8 7 6 5 4 3 2 1

springeronline.com

## CONTENTS

### 15. Conventional Lube Basestock Manufacturing

*B. E. Beasley*

|   |    |
|---|----|
| 1. Lube Basestock Manufacturing .....   | 1  |
| 2. Key Base Stock Properties .....  | 3  |
| 2.1 Lube Oil Feedstocks .....   | 4  |
| 3. Base Stock Composition .....   | 5  |
| 4. Typical Conventional Solvent Lube Processes .....  | 5  |
| 4.1 Lube Vacuum Distillation Unit (VDU) or Vacuum<br>Pipestill (VPS) - Viscosity and Volatility Control ..... | 6  |
| 4.2 Solvent Extraction - Viscosity Index Control .....  | 6  |
| 4.3 Solvent Dewaxing - Pour Point Control .....   | 6  |
| 4.4 Hydrofinishing - Stabilization .....  | 6  |
| 4.5 Solvent Deasphalting.....   | 7  |
| 4.6 Refined Wax Production .....  | 7  |
| 5. Key Points in Typical Conventional Solvent Lube Plants .....   | 8  |
| 6. Base Stock End Uses .....  | 8  |
| 7. Lube Business Outlook .....  | 9  |
| 8. Feedstock Selection .....  | 9  |
| 8.1 Lube Crude Selection .....  | 9  |
| 9. Lube Crude Assays .....  | 11 |
| 10. Vacuum Distillation .....   | 12 |
| 10.1 Feed Preheat Exchangers .....  | 15 |
| 10.2 Pipestill Furnace .....  | 15 |
| 10.3 Tower Flash Zone .....   | 15 |
| 10.4 Tower Wash Section .....   | 15 |
| 10.5 Wash Oil .....   | 16 |
| 10.6 Purpose of Pumparounds .....   | 16 |
| 10.7 Tower Fractionation .....  | 16 |
| 10.8 Fractionation Packing .....  | 16 |
| 10.9 Bottoms Stripping Section .....  | 18 |
| 10.10 Side Stream Strippers .....   | 18 |
| 10.11 Overhead Pressure .....   | 18 |

|        |   |    |
|--------|---|----|
| 10.12  | Tower Overhead Pressure with Precondensers .....                                | 19 |
| 10.12a | Tower Overhead Pressure without Precondensers.....                              | 19 |
| 10.13  | Tower Pressure - Ejectors .....   | 19 |
| 10.14  | Factors Affecting Lube Distillate Feed .....                                    | 20 |
| 11.    | Pipestill Troubleshooting .....   | 20 |
| 11.1   | Material Balance and Viscosity Measurements .....                               | 20 |
| 11.2   | Tower Pressure Survey .....   | 21 |
| 12.    | Solvent Extraction .....  | 22 |
| 12.1   | The Characteristics of a Good Extraction Solvent .....                          | 24 |
| 12.2   | Extraction Process .....  | 25 |
| 12.3   | Extraction Process Variables .....  | 28 |
| 12.4   | Solvent Contaminants .....  | 28 |
| 12.5   | Solvent Recovery .....  | 28 |
| 12.5.1 | Raffinate Recovery .....  | 29 |
| 12.5.2 | Extract Recovery .....  | 29 |
| 12.6   | Minimizing Solvent Losses .....   | 29 |
| 12.6.1 | Recovery Section .....  | 29 |
| 12.6.2 | Other Contributors to Solvent Losses .....                                      | 29 |
| 13.    | Corrosion in NMP Plants .....   | 30 |
| 14.    | Extraction Analytical Tests .....   | 30 |
| 15.    | Dewaxing .....  | 31 |
| 16.    | The Role of Solvent in Dewaxing .....   | 32 |
| 17.    | Ketone Dewaxing Processes .....   | 34 |
| 17.1   | Incremental Ketone Dewaxing Plant .....   | 34 |
| 17.2   | DILCHILL Dewaxing .....   | 35 |
| 17.3   | Dewaxing Process Variables .....  | 37 |
| 18.    | Process Variable Effects .....  | 37 |
| 18.1   | Crude Source Affects Dewaxed Oil Yield .....                                    | 37 |
| 19.    | Solvent Composition .....   | 38 |
| 19.1   | Miscible and Immiscible Operations .....  | 38 |
| 19.2   | Effect of Viscosity on Filtration Rate .....                                    | 40 |
| 19.3   | Effect of Chilling Rate on Filtration Rate and Dewaxed<br>Oil Yield .....       | 40 |
| 19.4   | Effect of Temperature Profile .....   | 41 |
| 19.5   | Effect of Solvent Dilution Ratio .....  | 41 |
| 19.5.1 | Filtration Rate .....   | 41 |
| 19.5.2 | DWO Yield .....   | 42 |
| 19.6   | Effect of Water .....   | 42 |
| 19.7   | Effect of Increased Raffinate VI .....  | 43 |
| 19.8   | Effect of Pour Point Giveaway on Product Quality and<br>Dewaxed Oil Yield ..... | 43 |
| 20.    | Scraped Surface Equipment .....   | 43 |
| 21.    | Filters .....   | 45 |



|   |    |
|---|----|
| 21.1 Filter Operation/Description .....             | 45 |
| 21.2 Filter Media .....                             | 47 |
| 22. Cold Wash Distribution .....                    | 50 |
| 23. Wash Acceptance .....                           | 52 |
| 24. Wash Efficiency .....                           | 54 |
| 25. Filter Hot Washing .....                        | 55 |
| 26. Dewaxed Oil/Wax-Solvent Recovery .....          | 57 |
| 27. Solvent Dehydration .....                       | 58 |
| 28. Solvent Splitter .....                          | 58 |
| 29. 2-Stage Dewaxing .....                          | 59 |
| 30. Deoiling .....                                  | 59 |
| 31. Propane Dewaxing .....                          | 63 |
| 31.1 Effect of Water .....                          | 66 |
| 32. 2-Stage Propane Dewaxing .....                  | 66 |
| 32.1 Propane Deoiling .....                         | 66 |
| 32.3 Propane Filter Washing with Hot Kerosene ..... | 66 |
| 33. Dewaxing Aids .....                             | 67 |
| 34. DWA Mechanism .....                             | 68 |
| 35. Asphaltene Contamination .....                  | 69 |
| 36. Regulatory Requirements .....                   | 69 |
| 37. Glossary .....                                  | 70 |
| 38. Acknowledgements .....                          | 77 |
| 39. References and Additional Readings .....        | 77 |

## 16. Selective Hydroprocessing for New Lubricant Standards

*I. A. Cody*

|   |     |
|---|-----|
| 1. Introduction .....                                       | 79  |
| 2. Hydroprocessing Approaches .....                         | 83  |
| 3. Chemical Transformations .....                           | 85  |
| 3.1 Ring Conversion .....                                   | 85  |
| 3.2 Paraffin Conversion .....                               | 88  |
| 3.3 Saturation .....  | 91  |
| 4. Process Combinations .....                               | 96  |
| 4.1 Ring Conversion-Hydroisomerization-Hydrofinishing ..... | 96  |
| 4.2 Extraction-Hydroconversion .....                        | 99  |
| 5. Next Generation Technology .....                         | 101 |
| 6. References .....   | 103 |

## 17. Synthetic Lubricant Base Stock Processes and Products

*Margaret M. Wu, Suzzy C. Ho, and T. Rig Forbus*

|   |     |
|---|-----|
| 1. Introduction .....                     | 105 |
| 1.1 Why Use Synthetic Lubricants? .....   | 106 |
| 1.2 What is a Synthetic Base Stock? ..... | 106 |

|   |     |
|---|-----|
| 1.3 A Brief Overview of Synthetic Lubricant History .....                                   | 107 |
| 2. Overview of Synthetic Base Stocks .....  | 108 |
| 3. Synthetic Base Stock - Chemistry, Production Process,<br>Properties and Use .....        | 109 |
| 3.1 PAO .....   | 109 |
| 3.1.1 Chemistry for PAO Synthesis .....   | 110 |
| 3.1.2 Manufacturing Process for PAO .....   | 112 |
| 3.1.3 Product Properties .....  | 112 |
| 3.1.4 Comparison of PAO with Petroleum-based Mineral<br>Base Stocks .....                   | 113 |
| 3.1.5 Recent Developments - SpectraSyn Ultra as Next<br>Generation PAO .....                | 116 |
| 3.1.6 Applications .....  | 116 |
| 3.2 Dibasic, Phthalate and Polyol Esters - Preparation,<br>Properties and Applications..... | 118 |
| 3.2.1 General Chemistry and Process .....   | 118 |
| 3.2.2 Dibasic Esters .....  | 119 |
| 3.2.3 Polyol Esters .....   | 120 |
| 3.2.4 Aromatic Esters .....   | 121 |
| 3.2.5 General Properties and Applications of Ester Fluids                                   | 121 |
| 3.3 Polyaklylene Glycols (PAG) .....  | 123 |
| 3.3.1 Chemistry and Process .....   | 123 |
| 3.3.2 Product Properties .....  | 124 |
| 3.3.3 Application .....   | 125 |
| 3.4 Other Synthetic Base Stocks .....   | 125 |
| 4. Conclusion .....   | 126 |
| 5. Acknowledgement .....  | 127 |
| 6. References .....   | 127 |

## **18. Challenges in Detergents and Dispersants for Engine Oils**

*James D. Burrington, John K. Pudelski, and James P. Roski*

|   |     |
|---|-----|
| 1. Introduction .....                                       | 131 |
| 2. Engine Oil Additive and Formulation .....                | 131 |
| 2.1 Detergents .....  | 132 |
| 2.2 Dispersants .....                                       | 134 |
| 3. Performance Chemistry .....                              | 137 |
| 4. Current Dispersant and Detergent Polymer Backbones ..... | 138 |
| 5. Future Polymer Backbones .....                           | 140 |
| 6. Future Trends .....                                      | 142 |
| 6.1 Advanced Fluids Technology .....                        | 143 |
| 6.2 Technologies for New Product Introduction .....         | 144 |
| 6.3 Performance Systems .....                               | 146 |
| 7. Summary and Conclusions .....                            | 146 |

|                           |     |
|---------------------------|-----|
| 8. Acknowledgements ..... | 147 |
| 9. References .....       | 147 |

## **19. The Chemistry of Bitumen and Heavy Oil Processing**

*Parviz M. Rahimi and Thomas Gentzis*

|   |     |
|---|-----|
| 1. Introduction .....   | 149 |
| 2. Fractional Composition of Bitumen/Heavy Oil .....  | 150 |
| 3. Heteroatom-Containing Compounds .....  | 154 |
| 4. Properties of Asphaltenes (Solubility, Molecular Weight, Aggregation) .....                                      | 157 |
| 4.1 Chemical Structure of Asphaltenes .....   | 159 |
| 4.2 Thermal Chemistry of Asphaltenes .....  | 160 |
| 5. Chemistry of Upgrading .....   | 163 |
| 5.1 Reaction of Feedstock Components - Simplification of Upgrading Chemistry .....                                  | 168 |
| 6. Application of Hot Stage Microscopy in the Investigation of the Thermal Chemistry of Heavy Oil and Bitumen ..... | 171 |
| 6.1 Effect of Feedstock Composition .....   | 171 |
| 6.2 Effect of Boiling Point .....   | 172 |
| 6.3 Effect of Additives .....   | 174 |
| 6.4 Effect of Deasphalting .....  | 174 |
| 7. Stability and Compatibility .....  | 175 |
| 7.1 Physical Treatment .....  | 175 |
| 7.1.1 Effect of Distillation .....  | 175 |
| 7.1.2 Effect of Addition of Diluent .....   | 177 |
| 7.1.3 Thermal/Chemical Treatment .....  | 177 |
| 8. References .....   | 179 |

## **20. Mechanistic Kinetic Modeling of Heavy Paraffin Hydrocracking**

*Michael T. Klein and Gang Hou*

|   |     |
|---|-----|
| 1. Introduction .....   | 187 |
| 2. Approach and Overview .....                                    | 188 |
| 3. Model Development .....  | 191 |
| 3.1 Reaction Mechanism .....                                      | 191 |
| 3.2 Reaction Families .....                                       | 192 |
| 3.2.1 Dehydrogenation/Hydrogenation .....                         | 192 |
| 3.2.2 Protonation/Deprotonation .....                             | 192 |
| 3.2.3 Hydride and Methyl Shift .....                              | 194 |
| 3.2.4 PCP Isomerization .....                                     | 194 |
| 3.2.5 $\beta$ -Scission .....                                     | 194 |
| 3.2.6 Inhibition Reaction .....                                   | 195 |
| 3.3 Automated Model Building .....                                | 196 |
| 3.4 Kinetics: Quantitative Structure Reactivity Correlations .... | 198 |

|   |     |
|---|-----|
| 3.5 The C <sub>16</sub> Paraffin Hydrocracking Model Dignostics ..... | 198 |
| 4. Model Results and Validation .....                                 | 199 |
| 5. Extension to C <sub>80</sub> Model .....                           | 201 |
| 6. Summary and Conclusion .....                                       | 202 |
| 7. References .....   | 203 |

## 21. Modeling of Reaction Kinetics for Petroleum Fractions

*Teh C. Ho*

|  |     |
|--|-----|
| 1. Introduction .....  | 205 |
| 2. Overview .....  | 206 |
| 2.1 Partition-Based Lumping .....                                    | 206 |
| 2.2 Total Lumping .....  | 207 |
| 2.3 Reaction Network/Mechanism Reduction .....                       | 207 |
| 2.4 Mathematical Approaches to Dimension Reduction .....             | 208 |
| 3. Partition Based Lumping .....                                     | 209 |
| 3.1 Top-down Approach .....  | 209 |
| 3.2 Bottom-up Approach .....   | 211 |
| 3.2.1 Mechanistic Modeling .....                                     | 212 |
| 3.2.2 Pathways Modeling .....  | 215 |
| 3.2.3 Quantitative Correlations .....                                | 217 |
| 3.2.4 Carbon Center Approach .....                                   | 218 |
| 3.2.5 Lumping via Stochastic Assembly .....                          | 218 |
| 4. Mathematical Reduction of System Dimension .....                  | 220 |
| 4.1 Sensitivity Analysis .....                                       | 220 |
| 4.2 Time Scale Separation .....                                      | 221 |
| 4.3 Projective Transformation .....                                  | 221 |
| 4.3.1 First Order Reactions .....                                    | 221 |
| 4.3.2 Non-Linear Systems .....                                       | 223 |
| 4.3.3 Chemometrics .....   | 224 |
| 4.4 Other Methods .....  | 224 |
| 5. Total Lumping: Overall Kinetics .....                             | 224 |
| 5.1 Continuum Approximation .....                                    | 225 |
| 5.1.1 Fully Characterized First Order Reaction Mixtures .....        | 226 |
| 5.1.2 Practical Implications .....                                   | 227 |
| 5.1.3 Partially Characterized First Order Reaction<br>Mixtures ..... | 228 |
| 5.1.3.1 Plug Flow Reactor .....                                      | 229 |
| 5.1.3.2 CSTR .....   | 230 |
| 5.1.3.3 Diffusional Falsification of Overall<br>Kinetics .....       | 231 |
| 5.1.3.4 Validity and Limitations of Continuum<br>Approach .....      | 232 |
| 5.1.3.5 First Order Reversible Reactions .....                       | 232 |
| 5.1.3.6 Independent <i>n</i> th Order Kinetics .....                 | 233 |

|  |     |
|--|-----|
| 5.1.3.7 Uniformly Coupled Kinetics .....                   | 233 |
| 5.1.4 Upper and Lower Bounds .....                         | 234 |
| 5.1.5 One Parameter Model .....                            | 235 |
| 5.1.6 Intraparticle Diffusion .....                        | 236 |
| 5.1.7 Temperature Effects .....                            | 237 |
| 5.1.8 Selectivity of Cracking Reactions .....              | 237 |
| 5.1.9 Reaction Networks .....                              | 238 |
| 5.2 Discrete Approach: Nonuniformly Coupled Kinetics ..... | 238 |
| 5.2.1 Homologous Systems .....                             | 239 |
| 5.2.2 Long-Time Behavior .....                             | 239 |
| 6. Concluding Remarks .....                                | 241 |
| 7. References .....  | 242 |

## 22. Advanced Process Control

*Paul R. Robinson and Dennis Cima*

|                                |     |
|--------------------------------|-----|
| 1. Introduction .....          | 247 |
| 2. Useful Definitions .....    | 247 |
| 3. Overview of Economics ..... | 249 |
| 4. Source of Benefits .....    | 250 |
| 5. Implementation .....        | 253 |
| 6. Costs .....                 | 254 |
| 7. References .....            | 255 |

## 23. Refinery-Wide Optimization with Rigorous Models

*Dale R. Muft, Clifford C. Pedersen, Maurice D. Jett, Sriganesh Karur, Blaine McIntyre, and Paul R. Robinson*

|  |     |
|--|-----|
| 1. Introduction .....                                    | 257 |
| 2. Overview of Suncor .....                              | 257 |
| 3. Refinery-Wide Optimization (RWO) .....                | 259 |
| 4. Rigorous Models for Clean Fuels .....                 | 261 |
| 4.1 Feedstock and Product Characterization .....         | 262 |
| 4.2 Aspen FCC Overview .....                             | 262 |
| 4.3 Aspen Hydrocracker .....                             | 266 |
| 4.3.1 Reaction Pathways .....                            | 269 |
| 4.3.2 Catalyst Deactivation Model .....                  | 271 |
| 4.3.3 AHYC Model Fidelity .....                          | 272 |
| 4.4 Clean Fuels Planning .....                           | 272 |
| 4.4.1 Hydrogen Requirements for Deep Desulfurization ... | 272 |
| 4.4.2 Effects of Hydrotreating on FCC Performance .....  | 274 |
| 5. Conclusions .....                                     | 278 |
| 6. Acknowledgements .....                                | 278 |
| 7. References .....                                      | 278 |

## 24. Modeling Hydrogen Synthesis with Rigorous Kinetics as Part of Plant-Wide Optimization

*Milo D. Meixell, Jr.*

|  |     |
|--|-----|
| 1. Introduction .....  | 281 |
| 2. Steam Reforming Kinetics .....  | 283 |
| 2.1 Methane Steam Reforming Kinetic Relationships .....                                      | 283 |
| 2.2 Naphtha Steam Reforming Kinetic Relationships .....                                      | 286 |
| 2.3 Coking .....   | 292 |
| 2.4 Catalyst Poisoning .....   | 294 |
| 3. Heat Transfer Rates and Heat Balances .....   | 295 |
| 3.1 Firebox to Catalyst Tube .....   | 297 |
| 3.2 Conduction Across Tube Wall .....  | 299 |
| 3.3 Fouling Resistance .....   | 299 |
| 3.4 Inside Tube to Bulk Fluid .....  | 300 |
| 3.5 Bulk Fluid to Catalyst Pellet .....  | 300 |
| 3.6 Within the Catalyst Pellet .....   | 301 |
| 3.7 Convection Section .....   | 301 |
| 3.8 Fuel and Combustion Air System .....   | 302 |
| 3.9 Heat Losses .....  | 302 |
| 4. Pressure Drop .....   | 302 |
| 4.1 Secondary Reformer Reactions and Heat Effects .....                                      | 303 |
| 4.2 Model Validation .....   | 304 |
| 4.2.1 Validation Case 1 (Naphtha Feed Parameter Case)...                                     | 305 |
| 4.2.2 Validation Case 1a (Naphtha Feed Simulate Case)...                                     | 307 |
| 4.2.3 Validation Case 2 (Butane Feed Parameter Case)....                                     | 307 |
| 4.2.4 Validation Case 3 (Primary and Secondary Reformer<br>Butane Feed Reconcile Case) ..... | 309 |
| 5. References .....  | 311 |
| <b>Appendix A</b> Simulation Results .....   | 313 |
| Primary Reformer .....   | 313 |
| Adiabatic Pre-Reformer .....   | 317 |
| Oxo-Alcohol Synthesis Gas Steam Reformer .....   | 317 |
| <b>Appendix B</b> Case Study of Effects of Catalyst Activity in a<br>Primary Reformer .....  | 318 |

## 25. Hydrogen Production and Supply: Meeting Refiners' Growing Needs

*M. Andrew Crews and B. Gregory Shumake*

|  |     |
|--|-----|
| 1. Introduction .....                                | 323 |
| 2. Thermodynamics of Hydrogen .....                  | 324 |
| 3. Technologies for Producing Hydrogen .....         | 326 |
| 3.1 Steam Methane Reforming (SMR) Technologies ..... | 326 |
| 3.1.1 Maximum Steam Export .....                     | 326 |

|                                      |     |
|--------------------------------------|-----|
| 3.1.2 Limited Steam Export .....     | 327 |
| 3.1.3 Steam vs. Fuel .....           | 328 |
| 3.1.4 Minimum Export Steam .....     | 329 |
| 3.2 Oxygen Based Technologies .....  | 330 |
| 3.2.1 SMR/O <sub>2</sub> R .....     | 330 |
| 3.2.2 ATR .....                      | 331 |
| 3.2.3 POX .....                      | 332 |
| 3.2.4 Products .....                 | 332 |
| 3.2.5 H <sub>2</sub> /CO Ratio ..... | 332 |
| 3.2.6 Natural Ratio Range .....      | 333 |
| 3.2.7 CO <sub>2</sub> Recycle .....  | 333 |
| 3.2.8 Import CO <sub>2</sub> .....   | 335 |
| 3.2.9 Membrane .....                 | 335 |
| 3.2.10 Cold Box .....                | 335 |
| 3.2.11 Steam .....                   | 335 |
| 3.2.12 Shift Converter .....         | 335 |
| 3.2.13 Other Considerations .....    | 335 |
| 3.3 Technology Comparison .....      | 336 |
| 3.3.1 Process Parameters .....       | 337 |
| 3.3.2 Export Steam .....             | 339 |
| 3.3.3 Economic Considerations .....  | 340 |
| 3.3.4 Oxygen Availability .....      | 340 |
| 3.3.5 Hydrocarbon Feedstock .....    | 340 |
| 3.3.6 H <sub>2</sub> /CO Ratio ..... | 340 |
| 3.3.7 Natural Gas Price .....        | 340 |
| 3.3.8 Capital Cost .....             | 340 |
| 3.3.9 Conclusions .....              | 341 |
| 3.4 Hydrogen Purification .....      | 341 |
| 3.4.1 Old Style .....                | 341 |
| 3.4.2 Modern .....                   | 342 |
| 4. Design Parameters for SMR's ..... | 343 |
| 4.1 Function .....                   | 343 |
| 4.2 Feedstocks .....                 | 344 |
| 4.3 Fuels .....                      | 344 |
| 4.4 Design .....                     | 344 |
| 4.5 Pressure .....                   | 345 |
| 4.6 Exit Temperature .....           | 346 |
| 4.7 Inlet Temperature .....          | 346 |
| 4.8 Steam/Carbon Ratio .....         | 347 |
| 4.9 Heat Flux .....                  | 347 |
| 4.10 Pressure Drop .....             | 348 |
| 4.11 Catalyst .....                  | 348 |
| 4.12 Tubes .....                     | 349 |

|   |     |
|---|-----|
| 4.13 Burners .....                                  | 349 |
| 4.14 Flow Distribution .....                        | 350 |
| 4.15 Heat Recovery .....                            | 350 |
| 5. Environmental Issues .....                       | 351 |
| 5.1 Flue Gas Emissions .....                        | 351 |
| 5.2 Process Condensate (Methanol and Ammonia) ..... | 352 |
| 5.3 Wastewater .....                                | 354 |
| 6. Monitoring Plant Performance .....               | 355 |
| 7. Plant Performance Improvements .....             | 357 |
| 8. Economics of Hydrogen Production .....           | 359 |
| 8.1 Overall Hydrogen Production Cost .....          | 361 |
| 8.2 Overall Production Cost Comparison .....        | 361 |
| 8.3 Evaluation Basis .....                          | 362 |
| 8.4 Utilities .....                                 | 362 |
| 8.5 Capital Cost .....                              | 363 |
| 8.6 “Life of the Plant” Economics .....             | 363 |
| 8.7 Sensitivity to Economic Variables .....         | 364 |
| 8.8 Feed and Fuel Prices .....                      | 365 |
| 8.9 Export Steam Credit .....                       | 366 |
| 9. Conclusion .....                                 | 366 |
| 10. Additional Reading .....                        | 367 |

## 26. Hydrogen: Under New Management

*Nick Hallale, Ian Moore, and Dennis Vauk*

|   |     |
|---|-----|
| 1. Introduction .....                   | 371 |
| 2. Assets and Liabilities .....         | 372 |
| 3. It's All About Balance .....         | 373 |
| 4. Put Needs Ahead of Wants .....       | 375 |
| 5. Beyond Pinch .....                   | 382 |
| 5.1 Multi-Component Methodology .....   | 383 |
| 5.2 Hydrogen Network Optimization ..... | 384 |
| 6. You Don't Get Rich by Saving .....   | 388 |
| 7. Conclusions .....                    | 391 |
| 8. References .....                     | 392 |

## 27. Improving Refinery Planning Through Better Crude Quality Control

*J. L. Peña-Díez*

|   |     |
|---|-----|
| 1. Introduction .....                                   | 393 |
| 2. Crude Oil Quality Control .....                      | 394 |
| 3. New Technologies in Crude Oil Assay Evaluation ..... | 396 |
| 3.1 Analytical Methods .....                            | 397 |
| 3.2 Chemometric Methods .....                           | 397 |



|   |            |
|---|------------|
| 3.3 Other Alternatives .....                | 398        |
| 4. Crude Assay Prediction Tool (CAPT) ..... | 398        |
| 4.1 Model Description .....                 | 398        |
| 4.2 Potential Applications .....            | 402        |
| 4.3 Model Results .....                     | 403        |
| 5. Concluding Remarks .....                 | 405        |
| 6. References .....                         | 406        |
| <b>Index</b> .....                          | <b>409</b> |

## Chapter 15

# CONVENTIONAL LUBE BASESTOCK MANUFACTURING

B. E. Beasley, P. E.  
*ExxonMobil Research & Engineering Co.*  
*Process Research Lab*  
*Baton Rouge, LA 70821*

This chapter reviews the basic unit processes in modern conventional lube manufacturing. As this is a large subject area, this chapter will focus on giving the reader an overview of the major processes most frequently found in the lube manufacturing plant. It will not cover all technologies or processes, nor will it discuss detailed plant design and operation as this would easily require another book. The reader should come away with a general understanding of the conventional lube manufacturing process and key factors affecting the unit processes.

### 1. LUBE BASE STOCK MANUFACTURING

Lubes and specialties include a number of products that have a variety of end uses. Some end uses include:

- Automotive: engine oils, automatic transmission fluids (ATF's), gear oils.
- Industrial: machine oils, greases, electrical oils, gas turbine oils.
- Medicinal: food grade oils for ingestion, lining of food containers, baby oils.
- Specialty: food grade waxes, waxes for candles, fire logs, cardboard.

Lube manufacturing is complex and involves several processing steps. Crude is distilled and the bottoms, atmospheric resid, is sent to a vacuum distillation unit (VDU) sometimes called a vacuum pipestill (VPS) for further fractionation. Vacuum fractionation is used to separate the atmospheric resid into several feed streams or distillates. Conventional solvent processing uses selected solvents in physical processes to remove undesirable molecules

(asphaltenes, aromatics, *n*-paraffins). Hydroprocessing is used to convert or remove the trace undesirables such as nitrogen, sulfur and multi-ring aromatics or to enhance base stock properties to make specialty, high quality products.

The manufacture of lubes and specialty products makes a significant contribution to refining profitability even though volumes are relatively small.

The business drivers of the lube business are for increased production to reduce per barrel costs, to reduce operating expense (OPEX) and for higher quality products to meet ever-increasing product quality standards.

Refiners produce **base stocks** or **base oils** and lube oil blenders produce **finished oils or formulated products**. See the American Petroleum Institute's API-1509.

- **base stocks** are products produced from the lube refinery without any additives in the oil
- **base oils** are blends of one or more base stock
- **finished oils** or **formulated** products are blends of baseoil with special additives

Lube Base stocks are given various names. Some of the common names include:

1. Neutrals - from virgin distillates ex. 100N, 150N, 600N, etc
2. Bright stock - from Deasphalted Oil (DAO), ex BS150
3. Grades - ex. SAE 5, 10, 30, etc.; ISO 22, 32, etc.

The most common name is **neutral** (N) which was derived in the days when the lube distillates were acid treated (sulfuric acid) followed by clay filtration. After clay treating the oil was acid free or **neutral**. The viscosity number in this example, 150 N, is the approximate viscosity of the base stock (Note: the ASTM viscosity classification refers to an industrial oil grade system, not the base stock viscosity system) expressed in Saybolt Seconds Universal (SSU) at 100°F.

Bright stock is a heavy lube grade that is made from deasphalted resid. The name refers to the “bright” appearance of the product as compared to the resid feed. Bright stocks are very viscous; a typical bright stock, BS150, has a viscosity of 150 SSU at 210°F.

Grades may refer to the actual viscosity. For example, ISO (International Standards Organizations) industrial oil grades = cSt at 40°C or the reference may be arbitrary such as SAE (Society of Automotive Engineers) engine oil grades.

There are many other grade names that are used to differentiate special products. These products may have special qualities that may make them very profitable even though they tend to be lower volume products.

Base stocks are assigned to five categories (see API-1509 Appendix E).

- Group I base stocks contain less than 90 percent saturates and/or greater than 0.03 percent sulfur and have a viscosity index greater than or equal to 80 and less than 120.

- Group II base stocks contain greater than or equal to 90 percent saturates and less than or equal to 0.03 percent sulfur and have a viscosity index greater than or equal to 80 and less than 120.
- Group III base stocks contain greater than or equal to 90 percent saturates and less than or equal to 0.03 percent sulfur and have a viscosity index greater than or equal to 120.
- Group IV base stocks are poly-alpha-olefins (PAO).
- Group V base stocks include all other base stocks not included in Groups I-IV.

## 2. KEY BASE STOCK PROPERTIES

**Viscosity** is a key lube oil property and is a measure of the fluidity of the oil. There are two measures of viscosity commonly used; **kinematic** and **dynamic**. The **kinematic** viscosity is flow due to gravity and ranges from approximately 3 to 20 cSt (centistokes) for solvent neutrals and about 30-34 cSt at 100°C for Bright stock. The **dynamic** viscosity is flow due to applied mechanical stress and is used to measure low temperature fluidity. Brookfield viscosity for automobile transmission fluids (ATF's) at -40°C and cold cranking simulator (CCS) viscosity for engine oils at -25°C are examples of dynamic viscosity measurements.

Lube oil **volatility** is a measure of oil loss due to evaporation. Noack volatility measures the actual evaporative loss which is grade dependent, and a function of molecular composition and the efficiency of the distillation step. The volatility is generally lower for higher viscosity and higher VI base stocks. The gas chromatographic distillation (GCD) can be used to measure the front end of the boiling point curve and may be used as an indication of volatility, e.g. 10% off at 375°C.

**Viscosity index** or **VI** is based on an arbitrary scale that is used to measure the change in viscosity as a function of temperature. The scale was first developed in 1928 and was based on the "best" and "worst" known lubes at the time. The best paraffinic lube was assigned a value of VI = 100 and the worst naphthenic was assigned a VI = 0. The quality of Base stock has been improved dramatically since 1928 with the VI of high quality Base stock in the 140+ range.

**Pour point** is the temperature at which the fluid ceases to pour and is nearly a solid. Typically the pour point ranges from -6 to -24°C for heavy to light neutrals.

The **cloud point** is the temperature at which wax crystals first appear.

**Saturates, aromatics, naphthenes** are measures of these molecular types present in the Base stock.

**Color** (appearance) and **Stability** are the measure of color and change in presence of light or heat.

**Conradson carbon (CCR)** or **Micro-Carbon Residue (MCR)** is a measure of the ash left after flame burning.

## 2.1 Lube Oil Feedstocks

Lube plant feedstocks are taken from the bottom of the crude barrel (see Figure 1).

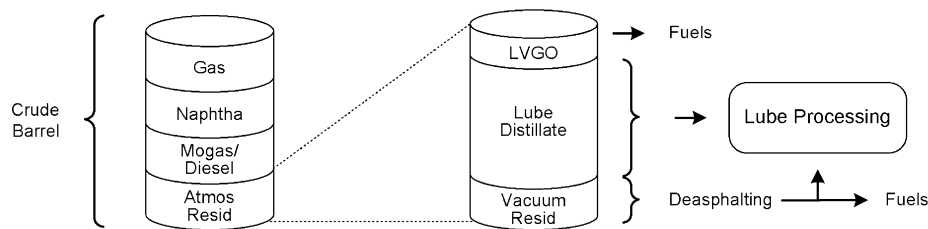


Figure 1. Lube Plant Feedstocks Are Taken from the Bottom of the Crude Barrel.

Lube crudes are generally paraffinic or naphthenic in composition. A paraffinic crude is characterized by a higher wax content. West Texas and Arab Light are good quality paraffinic crudes. Naphthenic crudes are characterized by their low wax content and they make base stocks with low viscosity index, e.g. Venezuelan and Californian.

In conventional solvent lubes the atmospheric resid (bottoms from the crude distillation tower) is upgraded to lube products through the following processes:

- vacuum distillation
- solvent extraction (N-methyl-2-pyrrolidone (NMP), furfural, phenol)
- solvent dewaxing (methyl ethyl ketone (MEK)/methyl isobutyl ketone (MIBK), MEK/toluene, propane)
- hydrofinishing (may be integrated with extraction)
- propane deasphalting
- hydroprocessing for higher quality

| Molecule                      | Structure             | Base Stock Quality Affected     | Process Involved           |
|-------------------------------|-----------------------|---------------------------------|----------------------------|
| N-Paraffin                    |                       | High Pour, VI<br>No S and CCR   | Dewaxing                   |
| I-Paraffin                    |                       | High VI and Sats<br>Medium Pour |                            |
| 2-Ring Naphthene              |                       | Medium VI, Low Pour, High Acids | Extraction, Hydrofinishing |
| 1-Ring Aromatic               |                       | Medium to High VI               | Extraction                 |
| Multi-Ring Naphthene          |                       | Low VI, Low Pour, High Acids    | Extraction, Hydrofinishing |
| Multi-Ring Aromatic           |                       | Low VI, Low Pour                | Extraction                 |
| Organic Sulfur                |                       | Good Stability<br>Antioxidant   | Hydrofinishing             |
| Organic Nitrogen              |                       | Poor Stability                  | Hydrofinishing             |
| Aliphatic Sulfur and Nitrogen | R-S R-N               | Removed by Hydrofinishing       | Hydrofinishing             |
| Asphaltenes                   | Condensed Multi-Rings | High CCR<br>Poor Color          | Distillation, Deasphalting |

Figure 2. Lube Oil Molecules Contribute to Lube Oil Properties

### 3. BASE STOCK COMPOSITION

Lube oil is produced from a wide variety of crude oil molecules. The molecular types and effect on lube oil quality is summarized below along with the lube process that acts on them.

### 4. TYPICAL CONVENTIONAL SOLVENT LUBE PROCESSES

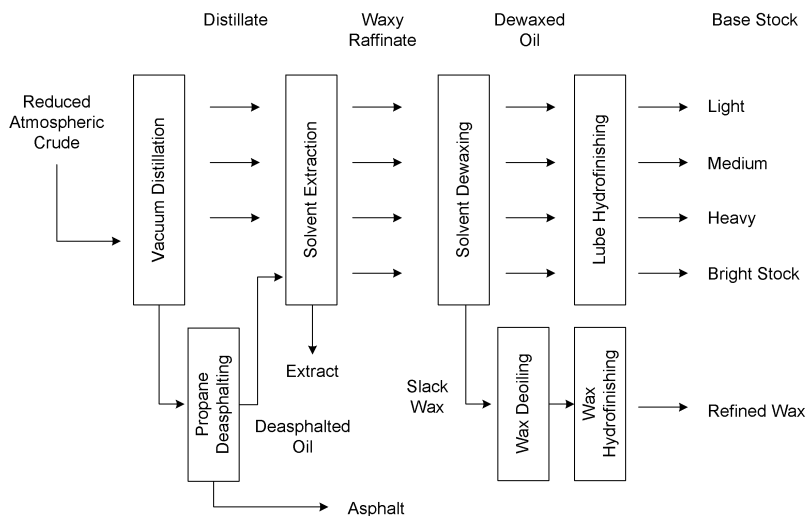


Figure 3. Typical Lube Process Flowchart

#### **4.1 Lube Vacuum Distillation Unit (VDU) or Vacuum Pipestill (VPS) - Viscosity and Volatility Control**

The VPS is generally the first process unit. The VPS's goal is to fractionate the atmospheric resid or reduced crude so that the base stock will have the desired viscosity. The fractionation also controls the volatility and the flash point. The boiling point separation is accomplished by using high efficiency distillation/fractionation hardware. Secondary effects include asphalt segregation in the Vacuum Resid from the VPS (potential by-product), reduction in Conradson carbon and color improvement.

#### **4.2 Solvent Extraction - Viscosity Index Control**

Extraction is typically the second process although this is not always the case. The primary goal of extraction is to remove aromatics and polar molecules. This is accomplished through solvent extraction of the distillate using NMP, furfural, or phenol. By removing aromatics, the VI is raised. Secondary effects of extraction include reduction in the refractive index, reduction in density, reduction in Conradson carbon and improvement in color, color stability and oxidative stability.

#### **4.3 Solvent Dewaxing - Pour Point Control**

Conventional solvent dewaxing is an energy- and cost-intensive process, and you therefore want to operate on the fewest number of molecules consistent with a high product yield. Therefore you do extraction first to remove the non-lubes molecules and you do dewaxing last on the raffinate. But you optimize the total OPEX per volume through the entire process. If somehow it made better economics to do the DWX first, even though it is expensive, you would do it that way.

The primary goal of solvent dewaxing is to make the pour and cloud point requirements. This is accomplished by paraffin separation by solubility of non-paraffins in cold solvent, fractional crystallization, and filtering the solid paraffins from the slurry. This may be done in "ketone" units which use MEK, MEK/MIBK, MEK/Toluene solvents or in propane units which use liquefied propane as the solvent. Secondary effects include viscosity increase, density increase, sulfur increase, and reduction in VI.

#### **4.4 Hydrofinishing - Stabilization**

Hydrofinishing follows extraction or dewaxing. The primary goal is to improve appearance (color, color stability, and oxidative stability) and to remove impurities such as the solvent, nitrogen, acids and sulfur to meet the

required specification. This is accomplished by hydrogen saturation and chain breakage that uses hydrogen at mild pressures and temperatures in the presence of a catalyst. Secondary effects include slight improvement in VI, slight improvement in saturates, reduction in viscosity, lower acidity, and reduction in Conradson Carbon.

#### 4.5 Solvent Deasphalting

When used, it is always ahead of extraction. The primary goal is to remove asphaltenes, which could be a possible byproduct and to make the viscosity specification that is required. This is accomplished by asphaltenes separation by solubility of non-asphaltenes in a solvent and precipitation of asphaltenes using e.g. propane as a solvent. Secondary effects include Conradson Carbon reduced, metals reduced, saturates increased, viscosity index increased, and color improved.

#### 4.6 Refined Wax Production

Wax deoiling and hydrofinishing follows the dewaxing unit. The primary goal is to reduce the oil content of the wax and to meet melting point and needle penetration requirements. This is accomplished by soft wax solubility and physical separation in the deoiling equipment. Hydrofinishing's primary goal is to saturate residual oxygenates and aromatics. Secondary effects include removal of impurities and color improvement.

A summary of the main and secondary lube qualities, by processing step, is shown in Figure 4.

|                            | Distillation      | Deasphalting    | Extraction                    | Dewaxing     | Hydrofinishing           |
|----------------------------|-------------------|-----------------|-------------------------------|--------------|--------------------------|
| Feed Stock                 | Atmospheric Resid | Vacuum Resid    | Distillate or Deasphalted Oil | Raffinate    | Raffinate or Dewaxed Oil |
| Lube Product               | Distillate        | Deasphalted Oil | Raffinate                     | Dewaxed Oil  | H/F Oil                  |
| By-Products                | Vacuum Resid      | Asphalt         | Extract                       | Wax          | Naphtha                  |
| Main Lube Quality Improved | –                 | Con Carbon ↓    | VI ↑                          | Pour Point ↓ | Color                    |
| Other Quality Changes      |                   |                 |                               |              |                          |
| Density (SG)               | Varies            | ↓               | ↓                             | ↑            | ↓                        |
| Gravity (API)              | Varies            | ↑               | ↑                             | ↓            | ↑                        |
| Viscosity                  | Varies            | ↓               | ↓                             | ↑            | ↓                        |
| Viscosity Index (VI)       | –                 | ↑               | “↑”                           | ↓            | ↑ (slightly)             |
| Color (ASTM)               | ↓                 | ↓               | ↓                             | –            | “↓”                      |
| Pour Point                 | –                 | –               | –                             | “↓”          | –                        |
| Cloud Point                | –                 | –               | –                             | ↓            | –                        |
| Conradson Carbon           | ↓                 | “↓”             | ↓                             | ↑            | ↓                        |
| Sulfur                     | –                 | ↓               | ↓                             | ↑            | ↓                        |
| Nitrogen                   | –                 | ↓               | ↓                             | ↑            | ↓                        |
| Saturates                  | –                 | ↑               | ↑                             | ↓            | ↑ (slightly)             |
| Flash Point                | ↓                 | –               | –                             | –            | –                        |
| Refractive Index           | –                 | ↓               | ↓                             | ↑            | ↓                        |

Figure 4. Summary of Lube Process Impact on Product Quality



## 5. KEY POINTS IN TYPICAL CONVENTIONAL SOLVENT LUBE PLANTS

- Majority of operations are “blocked operation” instead of “in-step”. Blocked operation requires intermediate tankage between units and allows the optimum operation of each unit on each viscosity grade.
- The dewaxer is the most expensive unit to build, has the highest operating costs and is the most complex to operate. Therefore, you want to operate on the fewest number of molecules consistent with a high product yield.
- Bright stock is the most expensive conventional lube to manufacture and requires the addition of a deasphalting unit.
- Integration of extraction and hydrofinishing units saves energy, and the elimination of a hydrofiner furnace saves capital. However, this arrangement is less flexible than a standalone hydrotreater.

There are exceptions to the general flow. Some plants that process extremely high wax content crudes position dewaxing after vacuum distillation. Some plants position high-pressure hydrotreating upstream of dewaxing.

Hydroprocessed lubes will be covered in other chapters and includes:

- Lubes hydrocracking
- Wax isomerization
- White Oils hydrogenation
- Catalytic dewaxing

Other processes include:

- Clay Contacting or Acid Treating, both are older stabilization processes
- Duo-Sol, a process that combines propane deasphalting and solvent extraction

## 6. BASE STOCK END USES

Conventional lube Base stocks are formulated into a multitude of finished products:

- Engine Oils
- Transmission Fluids
- Gear Oils
- Turbine Oils
- Hydraulic Oils

Metal Working (Cutting) Oils

- Greases
- Paper Machine Oils

Specialty products may include:

- White Oils: Foods, Pharmaceuticals, Cosmetics.
- Agricultural Oils: Orchard Spray Base Oils.
- Electrical Oils: Electrical Transformers (Heat Transfer).

## 7. LUBE BUSINESS OUTLOOK

Lubricant base stocks are produced in approximately 170 refineries worldwide that have a total capacity of over 900 kBD. The average capacity utilization is somewhere around 80%, to meet an industry demand of just over 700 kBD. About 75% of the total production is solvent-based refining, most making Group I quality base stocks. However, almost all new capacity is hydroprocessing-based, making Group II or Group III base stocks.

The lubricant market is roughly equally split between transportation lubricants (engine crankcase oils, transmission fluids, greases, etc.) and industrial process oils. Demand is growing at an average rate of only 1% / year, as robust growth in the developing economies (e.g. China, India) is being partially offset by declining demand in the mature markets (N. America, Europe) due to extended drain intervals for the higher quality engine oils. Engine builders tend to drive the transportation lubricant quality, as economic and environmental drivers push engine oils towards better oxidation stability, better low temperature properties, lower volatility, and lower viscosity. These desired characteristics drive formulators to favor hydroprocessed base stocks which have higher VI. However many other applications, such as most industrial and process oils, as well as older engine oils, still favor the characteristics of solvent-refined Group I base oils, which are expected to continue to play an important role in meeting the world's lubricant needs for year's to come.

## 8. FEEDSTOCK SELECTION

Crude selection is extremely important for the profitable production of lubes. Only a limited number of crudes contain a sufficient quantity of lubes quality molecules. Downstream unit operability is affected by crude selection, as are rates and yields. Typically, manufacturers would prefer operating at maximum throughput, thereby spreading costs over a larger volume. Poor crude selection can result in downstream bottlenecks reducing overall throughput.

### 8.1 Lube Crude Selection

Lube oil manufacturers may have a lube crude approval (LCA) process to assess the opportunity to manufacture Base stocks from crudes available in

the marketplace. The LCA process defines the detailed steps to qualify a new crude for purchase by the refinery to make base stocks and / or wax products.

The first step entails identifying economically attractive crudes. These crudes are characterized, or assayed, to quantify their lube yield and qualities. The assay process includes subjecting a small sample of the crude to an atmospheric distillation, vacuum distillation, extraction and dewaxing to produce the desired base stock products. This information enables the manufacturer, through the use of modeling techniques, to predict the process response of the crude of interest to make the required Base stock products. These modeling techniques may also allow the manufacturer to investigate process variables and operating optimization for distillation, extraction, and dewaxing to assess manufacturing flexibility. Not all crudes are acceptable for Base stock manufacturing as yields may be too low or Base stock products may not meet requirements.

With an acceptable assessment of the new crude, the refiner may elect to validate the crude for Base stock manufacture. This may entail running a plant test to make Base stock products from the new crude. The products made from the plant test are typically blended into formulated oils and subjected to testing to demonstrate acceptable product performance.

Results of the plant test are reviewed with a focus on lube plant manufacturing performance and Base stock product quality to determine if the new crude can be approved for Base stock manufacture.

1) Lube plant manufacturing performance - actual rate, yield and operability. The actual operating conditions are compared to the predicted processing conditions to assess if the new crude processed as expected.

2) Base stock product quality - Plant testing protocol should be defined to ensure base stock products meet acceptable quality specifications. Care should be taken to avoid making base stocks that may not be representative of how the crude will typically be processed to make base stocks. The range of acceptable base stock qualities should be defined by the test protocol. Plant test product disposition may need to be defined as part of the plant test. Options may include blending the plant test products to dilute the new crude component or quarantining the product tank until product testing has been completed. Product testing failure will prevent the crude from being approved.

Results from the manufacturing test will determine if the crude will be accepted. The certification test must have been acceptable and the crude processed as expected. There must not be any evidence that Base stock quality is unacceptable. If the above is completed successfully, the crude may be approved and added to the manufacturer's list of approved crudes.

The approval protocol may require periodic re-evaluation of the crude in recognition that the crude may change.

## 9. LUBE CRUDE ASSAYS

A lube crude assay is a laboratory process to measure the lube processing response from crude to base oil. It is an important step in a manufacturer's lube crude selection. A crude assay will include process yields for desired base oils at their quality specifications. The manufacturer can use the assay data to predict the process response for their refinery and to assess the desirability of purchasing particular crude. The assay results may be used to calculate the impact on profitability.

Key steps to complete a typical lube assay include:

- Secure a representative sample of the crude. This may best be achieved by collecting a sample at a load port.
- Fractionate the crude into discreet components first to separate the light, non-lubes boiling material. The bottoms are then sent to a high vacuum distillation. The distillation produces several distillate blends
- for extraction. The distillates produced are sufficient to cover the Base stock viscosity range.
- The distillates are then extracted using a lab pilot unit and the preferred extraction solvent (ex. furfural, NMP or phenol). Waxy raffinates are produced from the extraction.
- The waxy raffinates are then dewaxed using solvents of interest (MEK, MEK/MIBK, MEK/toluene, etc.) to produce a dewaxed oil and a slack wax.
- The dewaxed oils will be characterized to quantify their properties and yields. This will enable an economic assessment to be made with respect to the crude's lube potential.

There are several lube assay objectives in distillation. One is to relate key lube properties such as viscosity, sulfur, density, refractive index, etc. to boiling point. A second is to determine the yield of material boiling in the lube range and a third is to determine the yield of material boiling in the asphalt range.

The objectives of the lube assay extraction are to generate data, which will determine the ability of the crude to produce base oil capable of meeting the base oil specifications. Obviously this is of great importance in the selection of lube crudes for the plant. Key lube oil qualities related to process response are determined over the full lube oil viscosity range. Yields are used in manufacturing economic calculations. All crudes were not created equal, although there may be similarities in a given region. For example, Middle Eastern crudes may contain high sulfur, high aromatics and high iso-paraffins while North Sea crude may be low in sulfur, contain high saturates, and have a medium wax content. There are always outliers in every region. Crude production from a given "field" may change over time. If so, this may require that the assay is repeated to update the crude's relevant information to remain current.

In summary, the lube assay will characterize the potential of a crude to produce a specific Base stock (viscosity, viscosity index, saturates, wax, sulfur, basic nitrogen, etc) and to determine the expected yields from distillation, extraction and dewaxing.

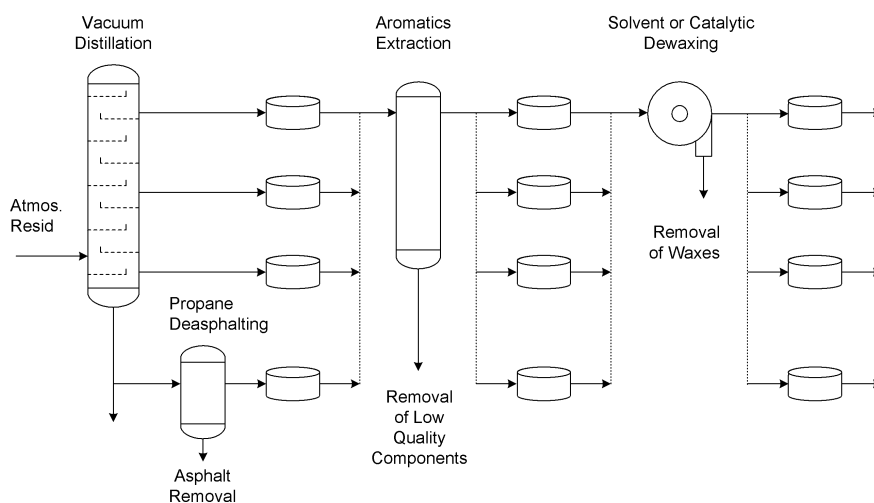


Figure 5. Lube Manufacturing Scheme

## 10. VACUUM DISTILLATION

Vacuum distillation is used to fractionate the heavier molecules in the crude. In the majority of plants it is the beginning point for lube manufacturing. Vacuum distillation is applied to avoid the high temperature fractionation, which would lead to undesirable coking and loss of lube oil yield.

Crude oil was first distilled in batch distillation, like a lab technique, beginning in the 1850s. Advancements were made by increasing the size of the batch vessel. A continuous process was developed by using a series of batch stills - called a battery. The first continuous pipestill appeared in the 1920s and the “modern” pipestill came on the scene in the 1930s. A typical lube vacuum distillation unit is shown below (Fig 6).

Vacuum distillation equipment is often referred to as the vacuum distillation unit (VDU) or vacuum pipestill (VPS).

The objective of the VPS is to achieve on test product quality for viscosity, volatility and flash point. Maximizing the yield of the most valuable products requires using the right cutting schemes. Steady control will minimize distillate variability. Good fractionation makes for sharp separation which is beneficial to good performance in downstream equipment. VPS per barrel costs can be minimized by operating the VPS at high capacity with long

run lengths and making the best use possible of utilities and chemicals per barrel.

Fractionation is the separation by boiling point of light and heavy components in the distillation tower achieved by intimate contact between hot rising vapor with the cooler falling liquid. The hot vapor strips the lighter components from the liquid and the cold liquid condenses heavier components from the vapor. Stripping requires heat in order to vaporize the lighter components and the condensation of heavy components releases heat. Good contact between the phases is essential to achieve maximum fractionation efficiency. In the presence of vapor the liquid may be carried upward in the form of a mist, foam or spray and may contaminate the desired distillates with heavy components. The contamination is known as entrainment and should be avoided.

The concept of a “theoretical stage” is a useful one and refers to the length of the VPS section required for the vapor and the liquid to reach equilibrium. The sharpness of the separation between adjacent streams may be measured in theoretical stages or minimum number of theoretical stages (Nm) which represents the number of theoretical stages at infinite reflux to effect the separations.

Sidestreams from the distillation tower are typically named from the top (lighter products) down to the bottom (heavier streams). Typical atmospheric and vacuum sidestream nomenclature for a typical atmospheric and vacuum tower is shown below (typical boiling point range of fractionated stream).

Table 1. Typical Distillation Tower Sidestream Names

| Name | Description   |
|------|---|
| AOH  | atmospheric overhead (-30 to 200 °C)                        |
| A1SS | atmospheric 1, or first, sidestream (150 to 210 °C)         |
| A2SS | atmospheric 2, or second, sidestream (175 to 300 °C)        |
| A3SS | atmospheric 3, or third, sidestream (190 to 400 °C)         |
| LVGO | light vacuum gas oil, vacuum tower overhead (200 to 400 °C) |
| V1SS | vacuum 1, or first, sidestream (350 to 425 °C)              |
| V2SS | vacuum 2, or second, sidestream (390 to 600 °C)             |
| V3SS | vacuum 3, or third, sidestream (450 to 620 °C)              |
| VRES | vacuum resid stream (500 to >900 °C)                        |

Cut points are used to describe the pipestill product. Volume cut points are the cumulative yield on the crude and are expressed as a liquid volume percent of product. Temperature cut points are the boiling points that correspond to the volume cut point.

A key objective of the VPS is to set the viscosity of the final product. This basic product property is set in the distillation by setting the cut points of the product streams. Volatility, another key product specification is the amount of material removed at a certain temperature and is controlled in the distillation by cut point targets and front-end fractionation. It affects engine oil

thickening and evaporative losses. The flash point is the ignition temperature above the liquid surface and affects engine oil thickening. It is a safety concern for storage of liquid product. Cut point targets and fractionation in the main tower and stripper are used to control the product flash point.

Distillate yields are affected by crude type, product viscosity and volatility specifications, the distillation tower cutting scheme, fractionation efficiency and the theoretical stages between the sidestreams. Poor fractionation efficiency can be caused by operating at feed rates above equipment design. If the feed is significantly lighter than the tower is designed to handle, fractionation efficiency may suffer. Mechanical damage such as dislodged or damaged internals, leaks or plugs in spray headers used to distribute liquids in the tower, leaking trays, etc. will degrade fractionation efficiency. Insufficient wash oil or reflux in the tower contributes to poor separation. Poor distribution of liquid or vapor reduces contact and leads to poor fractionation efficiency. Pumparounds are used to remove heat from the tower and to adjust the vapor-liquid flow in the tower. When pumparound duties get out of balance, fractionation efficiency is reduced. This can be because of reflux rates being above or below design specifications and also if flooding or entrainment is occurring in overloaded sections of the tower.

Poor tower fractionation efficiency may adversely affect downstream lube operations. Insufficient separation of light grade front ends may result in light oil carryover in extraction, increasing solvent ratio requirements, possibly reducing throughput and increasing energy usage. Dewaxing throughput and yields are adversely affected across all grades by the presence of “tail ends”.

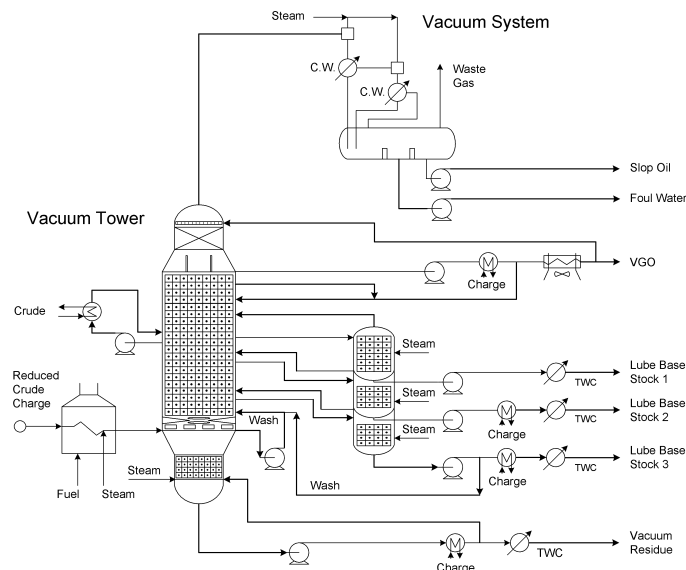


Figure 6. Typical Lube Vacuum Tower Design

## **10.1 Feed Preheat Exchangers**

Feed preheat exchangers are used to recover heat from sidestreams and pumparounds and to make the overall distillation more energy efficient. Preheating minimizes the loss of heat to the atmosphere or cooling water. Heat integration reduces fuel consumption in the furnace and steam may be generated for stripping in the vacuum unit. Atmospheric and vacuum units may be heat integrated.

## **10.2 Pipestill Furnace**

The furnace partially vaporizes the feed to the tower. A typical furnace has multiple parallel passes and the outlets are combined as feed to the distillation tower. Steam may be injected into the vacuum furnace coil to increase vaporization of feed at a lower temperature and to reduce the residence time. The vacuum cut points are set by the extent of the vaporization in the flash zone where temperatures may range from 390-420°C. Furnace firing is controlled to achieve the desired vacuum cut point.

## **10.3 Tower Flash Zone**

The flash zone is a large area in the tower that allows for the disengagement of liquid and vapor. The height of the zone affects the separation. The flash zone is designed to facilitate disengagement. Internals in this section consist of annular rings or vapor horns and collector rings for the bottoms stripping inlet.

## **10.4 Tower Wash Section**

The wash section cleans entrained liquids from the flash zone vapor phase. Vapor in excess of the amount needed to meet distillate requirements is referred to as overflash. The wash section condenses the overflash. It also provides some fractionation between the heavy lube sidestream and the vacuum resid stream.

The wash zone may include a Glitsch grid or random packing. An open structure gives a low-pressure drop while providing a high surface area to capture and retain resid. The resid is washed away by the wash oil that is applied through a spray header. The overflash, or spent wash, may be 40-50% resid and is removed and either sent to tankage as another sidestream or returned to the bottoms section for stripping. Maintaining wash oil flow is extremely important to efficient long-term operation. Loss of wash oil will result in rapid fouling.



## 10.5 Wash Oil

The wash oil that is used for de-entrainment is also important for improving the separation between the bottom side stream and the resid stream. Separation is enhanced by condensation of the overflash by vaporizing the bottom sidestream. The amount of overflash that is required is affected by packing type, depth and source of the wash oil. Overflash flow rates should be carefully monitored to make sure that there is no degradation in the bottom side stream fractionation, that there is no increase in pitch entrainment to the heavy solvent neutral stream and there are no major increases in coking in the wash bed zone.

## 10.6 Purpose of Pumparounds

Pumparounds are used to remove heat from the tower and to adjust the vapor-liquid flow in the tower. They condense vapors rising in the tower and create an internal reflux for the fractionation stages below the pumparound. They also reduce vapor loads in sections of the tower above the pumparound. A pumparound takes liquid from the tower, cools it, and returns it higher up in the tower. The liquid condenses the vapors in the pumparound section creating liquid reflux for fractionation lower in the tower. Vacuum pipestills do not use overhead reflux seen in other distillation towers, a top pumparound is used instead.

## 10.7 Tower Fractionation

As mentioned earlier, fractionation is used to generate the various product sidestreams off the tower by condensing rising hot vapor with falling colder liquid. At each stage in the fractionation section the highest boiling components are condensed, releasing heat that boils the lowest boiling point components, putting them into the vapor phase. Contacting between the phases is needed for the heat and mass transfer. Contacting equipment may include bubble cap trays, sieve trays, Glitsch grid, structured packing and many others. The number of theoretical stages between adjacent sidestreams typically varies from 1 to 3. The current trend is toward using packing.

## 10.8 Fractionation Packing

Packing used for fractionation can also reduce the pressure drop ( $\Delta P$ ) in a tower compared to trays. Tray designs are more limited in  $\Delta P$  reduction. The packing surface allows intimate contact between vapor and liquid without having to have the vapor pass through the liquid. The liquid phase coats the packing surface as a film so the liquid phase movement is

restricted only by the resistance of the packing surface. Packing has been used in high liquid loading service such as pumparounds and also in main fractionation sections. Packing is sensitive to liquid maldistribution so spray rates, pan level control and pumparound rate control are critical. A high quality liquid distributor is preferred.

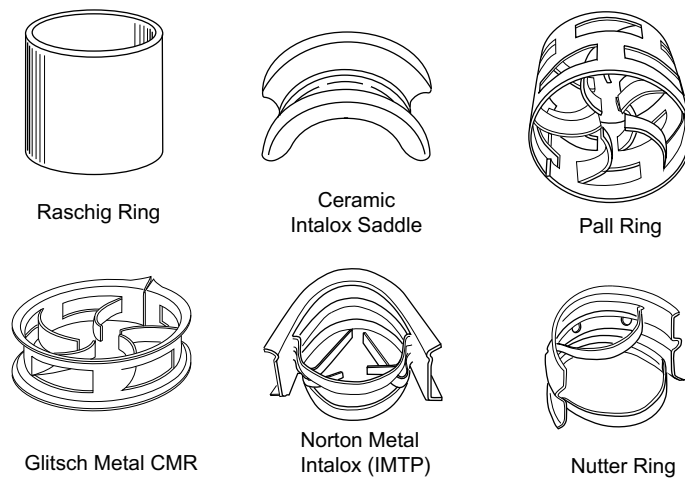


Figure 7. Various Types of Random Fractionation Packing (Drawing courtesy ExxonMobil Research and Engineering)

### Structured Packing

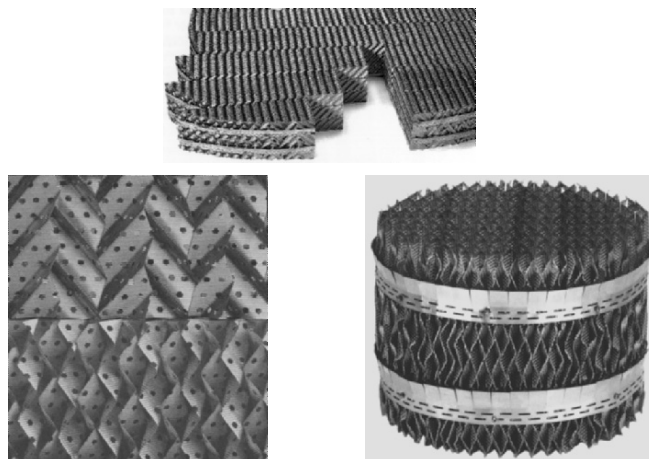


Figure 8. Various Types of Structured Fractionation Packing (photos by Ted Sideropoulos courtesy ExxonMobil Research and Engineering)

If the liquid flow to the packing is low and a spray distributor is used, the sprays can collapse so that the liquid contact with the vapor degrades causing low viscosity and poor volatility of the stream below. If the pumparound rate is too high, liquid may be atomized at the spray distributor and the small liquid droplets may be entrained upwards. If the liquid stream is from the pumparound, the product above the pumparound will be contaminated with heavy components. If there is leakage or overflow from the sidestream draw off pan, the falling liquid does not contact the vapor and it will reduce the viscosity of the stream below and also result in poor volatility.

## 10.9 Bottoms Stripping Section

The objective of the bottoms stripper is to strip distillate from the flash zone liquid, revaporize residual distillate that may be in the spent wash, and correction of bottoms flash. The bottom stripper typically has a design of 4 to 6 bubble cap trays or sieve trays. Some of the newer designs are using packing. Steam is used to reduce the hydrocarbon partial pressure to vaporize lighter molecules. A quench recycle is used to cool the stripped bottoms below 360°C (680°F) to reduce coking and cracking of the hydrocarbons.

## 10.10 Side Stream Strippers

Lube distillates are sent at their bubble points to side stream strippers. Steam is injected, reducing the partial pressure of hydrocarbons which effectively removes lighter hydrocarbons; improving volatility beyond that obtainable without side stripping. Ten to thirty percent of the stream may be removed in the stripper. If the heavier streams are not stripped this will reduce the yield of lighter lubes. Stripping is an important part of the overall operation to achieve the best separation and produce the desired products. A stripper typically consists of 4 to 6 sieve trays but packing may also be used.

## 10.11 Overhead Pressure

Pressure has a very large effect. Low pressure (15 to 100 mmHg overhead) is employed to reduce boiling points, allowing operation at temperatures low enough to minimize thermal degradation and cracking. The overhead vapors include steam, light hydrocarbons, and inerts. In the lower pressure design (15 to 50 mmHg) there is no precondenser before the first ejector. In higher pressure designs (40 to 100 mm Hg) a precondenser is employed and overhead pressure is dictated by condensing temperature (vapor pressure of water at the condensing temperature). Steam ejectors or vacuum pumps compress to atmospheric pressure and pump away the non-condensable hydrocarbons and inerts. Precondensers will reduce the overall load on the

compression system. Ejectors use steam for compression in 2 or 3 stages. Each ejector typically has an intercondenser. Secondary and tertiary ejectors may sometimes be replaced by a liquid ring vacuum pump.

## 10.12 Tower Overhead Pressure With Precondensers

In a precondenser design, the lower the cooling water temperature the higher the achievable vacuum. The precondensers must operate below the water dew point to condense steam in the overheads. To achieve lowest tower pressure the tower should be operated at a low top temperature to minimize condensable hydrocarbons. Inerts should be minimized by reducing air egress and by keeping the bottoms temperature at or below 360°C to avoid excess thermal cracking and the formation of light gases. Cooling water flow should be sufficient to minimize the cooling water outlet temperature which sets the equilibrium conditions in the precondenser and therefore the achievable tower vacuum.

### 10.12a Tower Overhead Without Precondensers

In no precondenser designs, pressures can be lower than the vapor pressure of water at the condensing temperature. Lower pressure has both advantages and costs:

Advantages:

1. Higher distillate/resid cut-point
2. Less furnace coil and stripping steam required
3. Pressure is controlled at a constant value (vs. varying with cooling media temperature)

Costs:

1. Higher ejector steam rate
2. Larger diameter tower

## 10.13 Tower Pressure - Ejectors

The steam ejectors pump away the remaining vapor pressure of water, hydrocarbons and inerts. Ejector systems typically have two stages or three by 50% ejectors. Because of the criticality for tower operation most systems are oversized and it may be possible for the tower to operate with one 50% ejector in each stage. Intercondensers (1st stage) and after condensers (2nd stage) condense the steam from the ejectors, tower steam and condensable hydrocarbons. Motive steam flow must be maintained for best operation.

## 10.14 Factors Affecting Lube Distillate Production

- Crude Type
- Equipment Operation
  1. Cutting scheme selected
  2. Fractionation efficiency
  3. Pumparound heat removal capability
  4. Sidestream product stripper operation
  5. Equipment constraints
  6. Operational Stability
- Product Inspection Measurement precision

Table 2. Nominal Lube Product Boiling Range

|                | Two Product<br>Sidestreams, °C | Three Product<br>Sidestreams, °C | Two Product<br>Sidestreams, °F | Three Product<br>Sidestreams, °F |
|----------------|--------------------------------|----------------------------------|--------------------------------|----------------------------------|
| Vacuum Gas Oil | 345 - 385                      | 345 - 370                        | 650 - 725                      | 650 - 700                        |
| Light Neutral  | 385 - 455                      | 370 - 425                        | 725 - 850                      | 700 - 800                        |
| Medium Neutral | -----                          | 425 - 490                        | -----                          | 800 - 915                        |
| Heavy Neutral  | 455 - 540                      | 490 - 550                        | 850 - 1005                     | 915 - 1025                       |
| Overflash      | 540 - 580                      | 550 - 580                        | 1005 - 1075                    | 1025 - 1075                      |
| Vacuum Resid   | 580+                           | 580+                             | 1075+                          | 1075+                            |

Table 3. 2-Sidestream vs. 3-Sidestream Product Comparison

| Two Sidestream Products          |                          | Three Sidestream Products        |                          |
|----------------------------------|--------------------------|----------------------------------|--------------------------|
| Viscosity<br>(SSU at 100°F/38°C) | Yield on Crude<br>(Vol%) | Viscosity<br>(SSU at 100°F/38°C) | Yield on Crude<br>(Vol%) |
| 150                              | 9.8                      | 100                              | 9.2                      |
| 450                              | 8.5                      | 300                              | 7.7                      |
|                                  |                          | 700                              | 5.3                      |
| Total                            | <u>18.3</u>              | Total                            | <u>22.2</u>              |
| Resid (1000 + °F)<br>(538 + °C)  | 18.3                     | Resid (1075 + °F)<br>(579 + °C)  | 16.8                     |

## 11. PIPESTILL TROUBLESHOOTING

### 11.1 Material Balance and Viscosity Measurements

1. Tabulate rates of crude feed, reduced crude, overhead condensate rate, and all VPS sidestream and bottoms rates for material balance calculations.
2. Take a sample of VGO and each sidestream and measure viscosities (100°C) of all the VPS products.
3. Calculate yields, cumulative yield ranges and mid yield points for all the VPS products and combine with measured viscosities.
4. Compare viscosity to yield for each product. Compare to assay or lab generated distillation cuts and viscosities.

## 11.2 Tower Pressure Survey

- Use the same vacuum gauge to measure tower absolute pressures. (Pressures are low and different gauges can have calibration offset. Best results are obtained by moving the same gauge to the desired locations.)
  1. Make pressure measurement at flash zone, tower top and points in between.
  2. Determine Delta P across the strippers, both with steam on and with steam off.
  3. Measure ejector inter-stage pressures and condenser Delta P, noting temperature differences between condenser liquid and vapor outlet as well as Delta T across the condensers.
  4. Determine pressure drop across spray nozzles.
  5. Measure the transfer line pressure drop.
  6. Measure the ejector motive steam pressure.
  7. Measure the steam source pressure.
- Inferences based on findings
  1. If overall **tower pressure** drop is too low from the flash zone to the top then there may be damage to the tower internals or hydraulic problems. If the pressure drop is too high then flooding, plugging or internal damage may be indicated.
  2. **Pumparounds** typically have higher pressure drop than the fractionating sections.
  3. No or low Delta P in a **tower section** may indicate missing trays or absence of liquid. High Delta P in a tower section may indicate that the drawoff is partially restricted or blocked, that may be due to high liquid rates in that section of the tower, flooding, or too much stripping steam.
  4. Check **spray nozzle** Delta P, actual vs. expected. If higher than expected, the spray nozzle may be plugged. If lower than expected, the header may be leaking or missing a nozzle(s).
  5. If **Stripper** Delta P is too high then this may be an indication that too much steam is being used. If the Delta P is too low there may be too little steam being used if the trays or packing are damaged.
  6. If the **precondenser** Delta P is too high this may be an indication of poor design, flooding or fouling. If too low, equipment damage may be indicated.
  7. Review **ejector interstage** pressures vs. design. Low interstage pressure may be an indication of 2nd stage overload.
  8. **Tower pressure cycling** may be due to steam ejector underload and high ejector discharge pressure.
  9. **Condenser** liquid and vapor temperatures should be about 3°C apart. If the temperature difference is greater than this it may be an indication of bypassing.

10. Increase in cooling water temperature (in vs. out) should be about 5-8°C. If too low this may indicate fouling or bypassing. If too high cooling water rate may be too low.
- Comparison to Design
    1. Cooling Water - Higher / lower rate than design
    2. Vacuum system - Higher / lower rate than design
    3. Steam Injection - Higher / lower rate than design

## 12. SOLVENT EXTRACTION

The properties of the lube oil that are set by the extraction process are the viscosity index (VI), oxidation stability and thermal stability. These properties are related to aromatics, aliphatic sulfur, total sulfur and nitrogen levels present in the base stock.

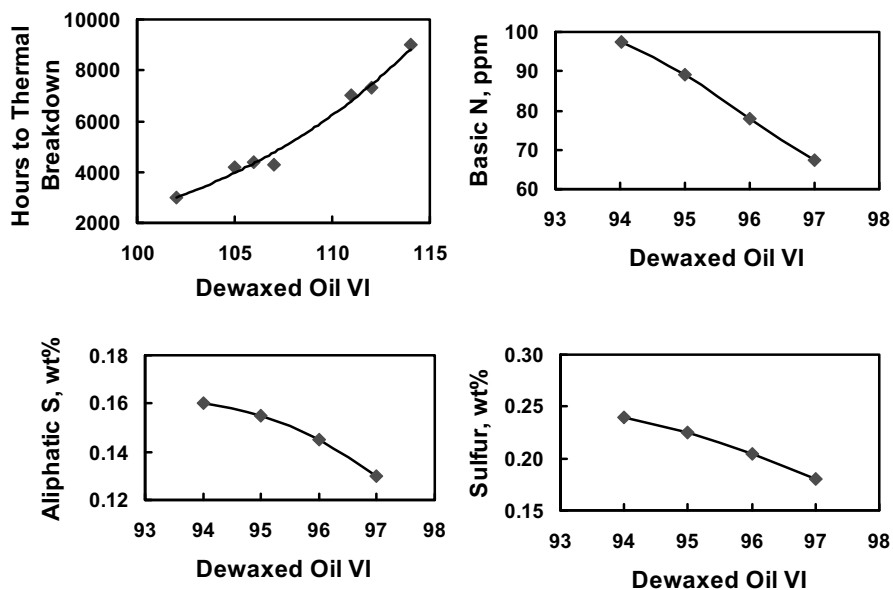


Figure 9. Typical impact Of Extraction On VI And Lube Oil Properties

Base stock VI has historically been used as a performance indicator for the base stock. The VI specification sets the extraction severity required to achieve the target. VI is also an indicator of relative stability from the same feed. VI is crude sensitive under constant extraction conditions.

Table 4. Impact of Molecular Type on Lube Oil VI and Stability

|                 | VI        | Stability |
|-----------------|-----------|-----------|
| Paraffins       | Excellent | Good      |
| Mono-Naphthenes | Good      | Fair      |
| Poly-Naphthenes | Fair      | Fair      |
| Mono-Aromatics  | Good      | Fair      |
| Poly-Aromatics  | Poor      | Poor      |

Molecular structure affects Lube quality. Solvent extraction and dewaxing processes preferentially separate the molecules as shown in Figure 10. Extraction separates *n*-paraffins, *i*-paraffins, naphthenes and some aromatics from the distillate into the raffinate phase. Dewaxing rejects the *n*-paraffins and some *i*-paraffins from the raffinate to produce a dewaxed oil or base stock. The dewaxed oil will contain the “slice” of molecular types as shown in Figure 10.

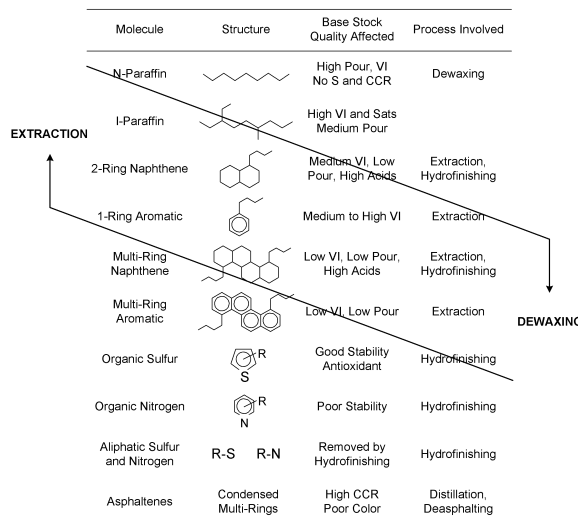
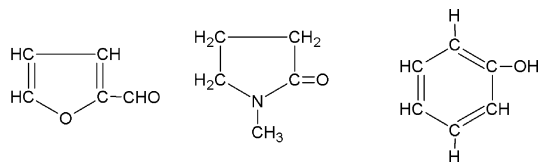


Figure 10. Principal Molecular Types And Their Effect On Lube Quality

The extraction process is a physical separation that is used in all conventional lube plants. The solvent is added to the distillate and then separated to produce a raffinate (the desired product) and an extract that contains a higher percentage of aromatics and impurities. Typical solvents used are N-methyl-2-pyrrolidone, furfural, and phenol. Properties of the solvents are shown in Figure 11.





| Solvent                    | Furfural | N-Methyl-2-pyrrolidone | Phenol |
|----------------------------|----------|------------------------|--------|
| Molecular Weight           | 96       | 99.1                   | 94.1   |
| Specific Heat @ 130°F      | 0.42     | 0.47                   | 0.56   |
| Boiling Point @ 1 atm., °F | 323      | 399                    | 359    |
| Flash Point, °F            | 137      | 187                    | 175    |
| Viscosity @ 140°F, Cp      | 0.95     | 1.02                   | 2.58   |
| Melting Point, °F          | -37      | -11.6                  | 105.6  |
| Latent Heat @ b.p., Btu/lb | 194      | 187                    | 206    |
| Toxicity                   | moderate | low                    | high   |
| Specific Gravity @ 20°C    | 1.16     | 1.03                   | 1.07   |

Figure 11. Physical Properties Of Typical Extraction Solvents

## 12.1 The Characteristics of a Good Extraction Solvent

A good extraction solvent will have a high selectivity for the undesirable components of the distillate stream. The solvent must also have good solvent power so that a low solvent to feed ratio may be used in the extraction plant. The solvent promotes rapid mass transfer. The solvent partitions between the raffinate and extract phases and must be recovered. Easy recovery via distillation is desired. A high density is also a characteristic of a good extraction solvent as this allows rapid separation of the oil and solvent phases. High demulsibility is needed for a rapid separation of the oil and solvent. The solvent must be chemically and thermally stable or inert in the lube extraction and recovery equipment. The ideal solvent would work for a wide range of feed stocks that the refiner might process. Solvent must be available at a reasonable cost and be non-corrosive to conventional materials of construction and it must be environmentally safe.

Table 5. NMP Relative To Furfural

| NMP Solvent Property |  |
|----------------------|--|
| Thermally Stable     | Heat integration with no measurable solvent decomposition    |
| More Selective       | Higher yields at lower solvent treats                        |
| Lower Latent Heat    | Requires less energy for solvent recovery                    |
| Chemically Stable    | Eliminates the need for feed deaerator for removal of oxygen |
| Higher Boiling Point | More efficient heat integration                              |

Table 6. NMP Relative to Phenol

| NMP Solvent Property                    |  |
|---|--|
| Lower toxicity                          | Much safer   |
| More selective                          | Higher yields and/or lower solvent treats  |
| Lower Latent heat                       | Less energy required for solvent recovery  |
| Higher Boiling point                    | More efficient heat integration  |
| Lower Melting point                     | Less steam tracing required, less chance of solidifying in piping                |
| No hydrogen bonding effect with the oil | More efficient stripping, easier to achieve low solvent concentration in product |
| No azeotrope                            | Simplifies water recovery  |

## 12.2 Extraction Process

Distillate is brought in contact with the solvent, and aromatics and polars are preferentially dissolved in the solvent phase. Saturates do not dissolve and remain in the hydrocarbon or dispersed phase. The hydrocarbon phase is lower in density than the solvent phase and rises as bubbles through the continuous phase. After separation the raffinate and extract solution are sent to their respective solvent recovery sections. Integration of a hydrofiner on the raffinate product is in some lube plants for heat integration because this eliminates the need for an additional hydrofiner furnace.

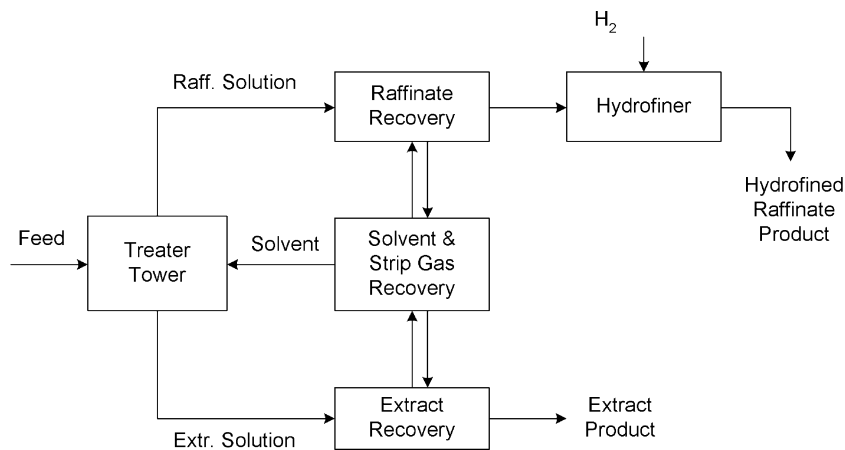


Figure 12. Simplified Extraction Flow Diagram

There are several types of continuous treater tower designs used in conventional lube plants. These include trayed towers, packed towers and rotating disc contactors (see Figure 13). The treater tower internals are designed to promote contact and separation of the oil and the solvent phases.

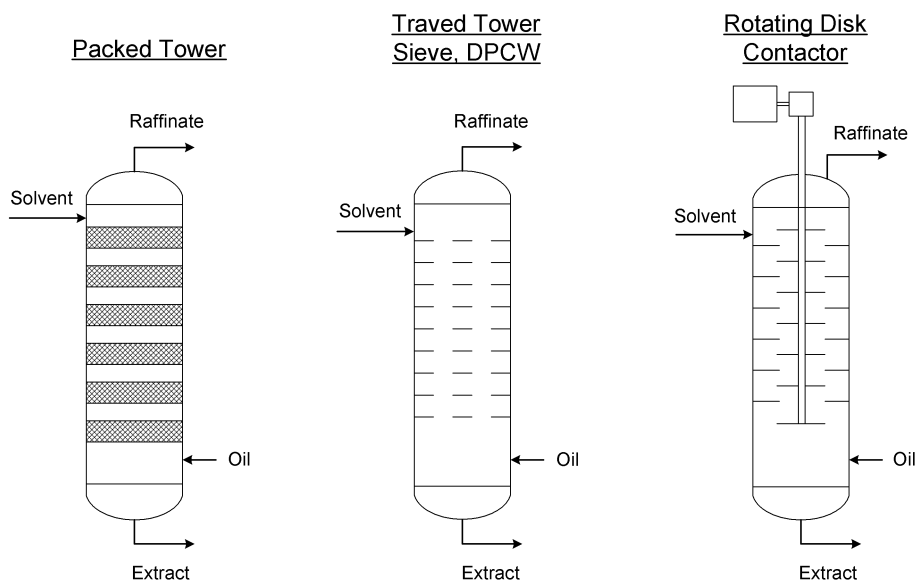


Figure 13. Types of Continuous Extractors

An example of a tray design is shown below.

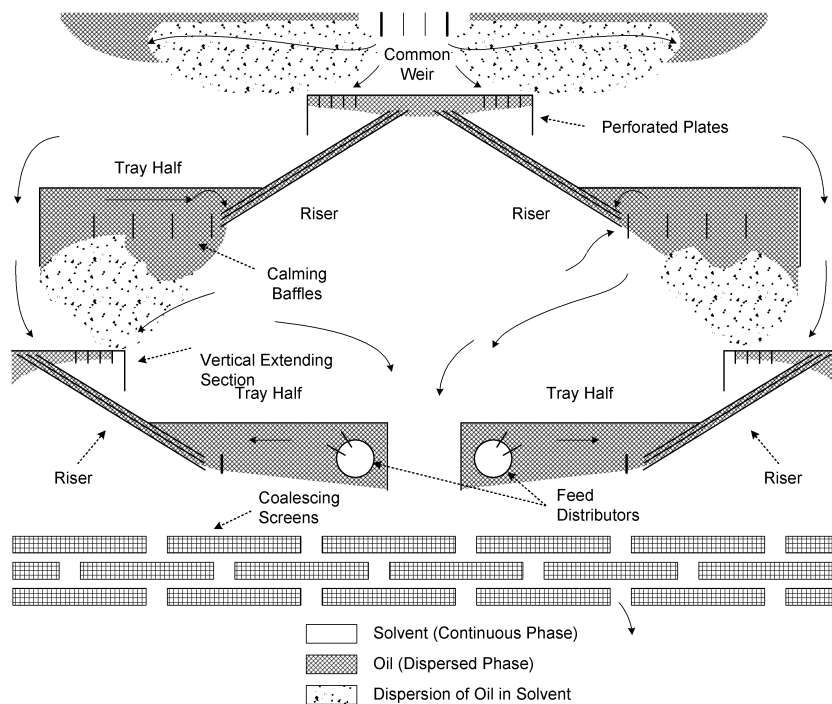


Figure 14. ExxonMobil® Patented Dual Pass Cascade Weir Tray

An example of a typical rotating disc contactor is shown below.

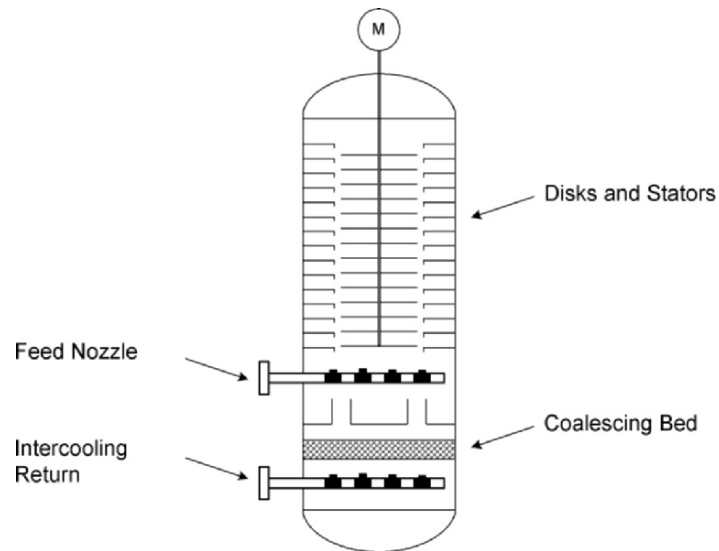
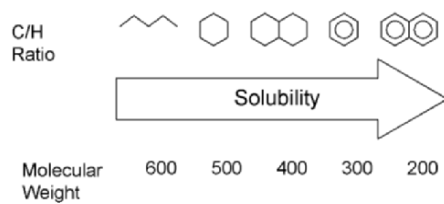


Figure 15. Typical Rotating Disc Contactor

There are several factors that affect extraction efficiency and in general the efficiency depends on the mixing/settling and coalescence characteristics of the system. Important factors include:

1. Hardware and staging
2. Throughput
3. Viscosity/Gravity of Oil/Solvent
4. Solvent dosage and composition
5. Temperature and temperature gradient
6. Solvent quality
7. Dispersion energy

Effect of Oil Composition on Solubility



Effect of Dosage on Solubility

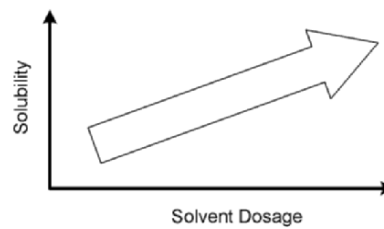


Figure 16. Effect On Oil Composition And Dosage On Solubility

### 12.3 Extraction Process Variables

INDEPENDENT variables are controlled by the operator and include:

- Treat Ratio - the volume ratio of solvent to feed
- Solvent Composition (water for NMP, Phenol)
- Bottom and Top treater temperature

DEPENDENT variables rely on the independent variables.

- Raffinate Quality
  - Viscosity Index
  - Saturates content as an indicator of the degree of aromatic removal
  - Sulfur
- Raffinate Yield - primarily dependent on the treat ratio at constant VI

### 12.4 Solvent Contaminants

Water from steam stripping in the solvent recovery section must be removed. In the furfural solvent system water is removed for process effectiveness and product quality. Water contamination in furfural reduces DWO VI and leads to furfural degradation. In NMP and phenol systems excess water is removed for process control.

Oil in the solvent results from incomplete solvent-oil separation and may be due to entrainment from flash vessels, volatilization or stripper flooding. Characterization of the solvent contamination by GCD can be used to determine if contamination is occurring by light or heavy oil fractions. A light oil contamination suggests that the accumulation of distillate in the front end. Presence of heavy oil suggests entrainment oil in the solvent, which can reduce raffinate yield and increase the treat rate required.

### 12.5 Solvent Recovery

The objectives of solvent recovery sections are to:

- Recover furfural/NMP/phenol from product streams
  - Purify furfural/NMP/phenol for recycle
  - Maximize energy efficiency while recovering solvent
- Simplified recovery sections are shown below

### 12.5.1 Raffinate Recovery

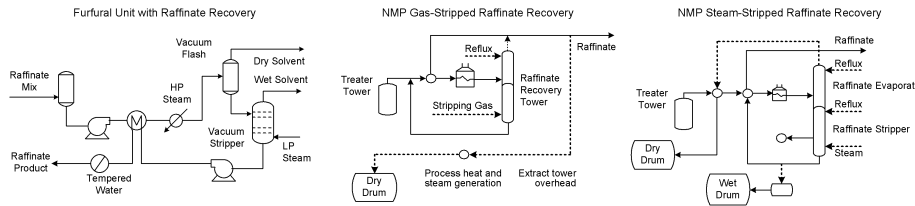


Figure 17. Typical Raffinate Recovery Diagrams

### 12.5.2 Extract Recovery

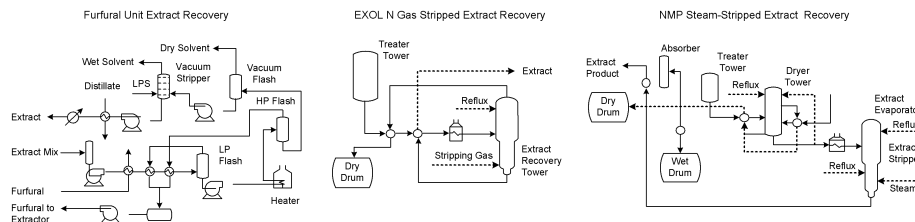


Figure 18. Typical Extract Recovery Diagrams

## 12.6 Minimizing Solvent Losses

### 12.6.1 Recovery Sections

NMP concentration in the product can be readily reduced to <20 ppm and furfural to <50 ppm, but keeping solvent loss low requires energy and the final concentration is an optimization problem. The furnace coil outlet temperature is a function of the pressure. Typical furnace COT's are higher for NMP than furfural due to solvent boiling points and the concern for furfural degradation. If fuel gas failure occurs at the furnace the plant immediately goes on oil recycle. The solvent concentration in the product can rise to several percent if the COT is too low. Too high of a furnace temperature leads to an increase in solvent decomposition and to premature furnace coking.

### 12.6.2 Other Contributors to Solvent Losses

- Some solvent is lost through line flushing during product sampling. To reduce losses, send sample line flushings back to the unit.
- Address miscellaneous leaks at flanges.

- The start-up and shutdown operation typically will increase solvent losses in the year the shutdown is taken. Consider ways to minimize solvent left in vessels.
  - Check valves on bypass lines that may not hold and may allow bypassing of solvent.
  - Water sent to the wastewater treatment unit might contain solvent.
  - Phenol will oxidize and form deposits in the unit.
- Effective solvent loss performance is considered to be:
- NMP = <0.03 Lbs/Bbl feed,
  - Phenol = <0.1 Lbs/Bbl feed,
  - Furfural = <0.2 Lbs/Bbl feed
- Furfural will decompose when exposed to oxygen or excessive temperatures.
- Sources of oxygen ingress include:
- Pump suctions
  - Vacuum systems
  - Oil feed poorly deaerated
  - Poor/non-existent inert gas blanketing

### 13. CORROSION IN NMP PLANTS

NMP, by itself, is not corrosive to carbon steel. However, because of NMP's high dielectric constant, other corrosive compounds will readily ionize in NMP and become very aggressive. The NMP condensing circuit may be at risk to accelerated corrosion from accumulated corrosive elements or corrosion/erosion from high velocities.

The refiner can take the following corrective actions. Avoid corrosive species ingress into the circuit. Remove H<sub>2</sub>S from recycle stripping gas with a ZnO bed. Neutralize acids with neutralizing additives or caustic injection. Consider alloy upgrade in areas of known corrosion or areas of known impingement or very high velocity, such as 316 SS impingement baffles in exchangers. Insulate the overhead line to the first condenser to avoid premature condensation leading to impingement issues.

### 14. EXTRACTION ANALYTICAL TESTS

There are numerous analytical tests that are used to assess the extraction operation and to help optimize the treater tower. A few of the most important tests are listed below in Table 7.

Table 7. Typical Analytical Tests for Extraction

| TEST                             | ASTM Test No.     | APPLICATION  |
|----------------------------------|-------------------|--|
| Refractive Index @ T°C           | D 1218            | Correlation with dewaxed oil quality: VI, saturates etc<br>Better for yield calculations than relying on process flow meters |
| Density at 15°C                  | D 4052            | Better for yield calculations than relying on process flow meters  |
| Water in Solvent by Karl Fischer | D 6304-3, E 203-1 | Process optimization (NMP, Phenol)   |
| Treater Carryunder               |                   | Measures the amount of distillate bypassing the treater and being downgraded from lubes to fuel                              |
| Oil in solvent                   |                   | Oil in solvent adversely affects raffinate yield   |
| 1. Percent                       |                   |  |
| 2. Characterization              |                   |  |
| <b>DEWAXED OIL</b>               |                   |  |
| Viscosity                        | D 445             | Primary base stock specification   |
| VI                               | D 2270            |  |
| Molecular Analysis               | D 2007, D2887     | Troubleshooting  |
|                                  | D 2140, D2501     | Base stock quality   |

## 15. DEWAXING

Waxy raffinates from extraction are not useful as lubes because they contain too much wax. Referring to our molecular drawing (Figure 10) we can see that the objective of dewaxing is to remove the paraffins from the raffinate to produce a final Dewaxed Oil base stock that when additized becomes the finished lubricant.

Dewaxing is a physical process that adds solvent to a raffinate (or distillate) and once the mixture is cooled, the n-paraffins drop out of solution as solid wax crystals. The slurry is filtered to remove the wax crystals and produce a dewaxed oil or base stock and a valuable wax by-product. Waxes may be further refined to make hard waxes by melting and separating the soft wax. Hard waxes may meet FDA standards for use in direct or indirect contact with food.

The majority of dewaxing processes today use Methyl Ethyl Ketone (MEK), Methyl IsoButyl Ketone (MIBK), mixtures of MEK and MIBK, or mixtures of MEK and Toluene or propane. There are advantages and disadvantages to each solvent system.



Dewaxing sets the primary properties shown in Table 8.

Table 8. Properties Set by Dewaxing

| Dewaxed Oil Properties   | Wax Properties     |
|--------------------------|--------------------|
| Pour Point               | Oil Content        |
| Cloud Point              | Melting Point      |
| Low Temperature Fluidity | Needle Penetration |

A general flow plan for a dewaxing plant is shown below.

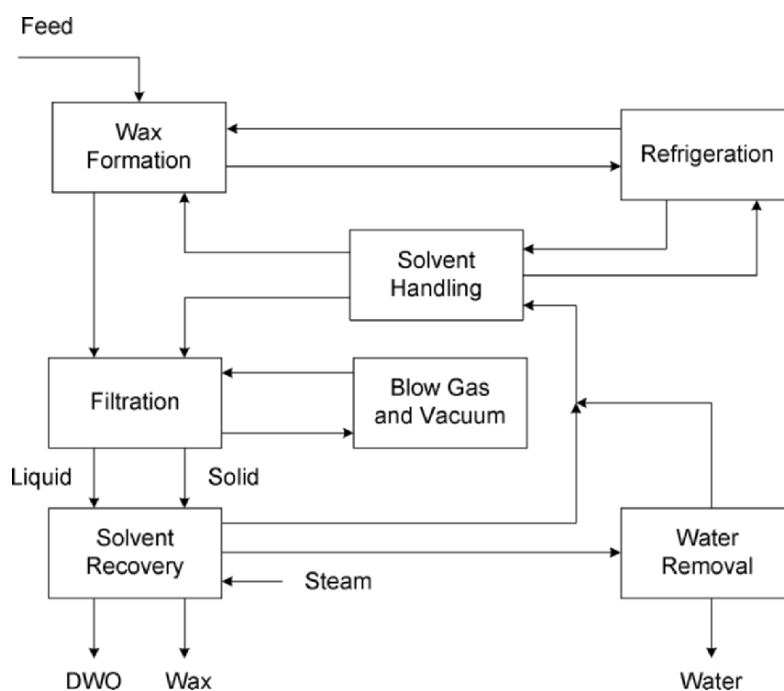


Figure 19. Simplified Dewaxing Flow Diagram

## 16. THE ROLE OF SOLVENT IN DEWAXING

As solvent is added to the waxy raffinate the oil is diluted and the viscosity of the oil solvent mixture decreases allowing filtration to take place more easily. The polarity of the oil-solvent mixture increases, decreasing the solubility of the wax and promoting the formation of more compact wax crystals. But as solvent is added the resulting filtrate becomes more dilute, loading up filtrate pumps and solvent recovery facilities.

Properties to Consider in Selecting a Dewaxing Solvent:

1. Solubility
2. Selectivity
3. Solvent boiling point lower than the boiling point of the oil
4. Low heat capacity
5. Heat of vaporization
6. Low viscosity
7. Non-Toxic
8. Non-corrosive
9. Low freezing point
10. Inexpensive
11. Readily Available

Ketone units typically use a dual solvent system consisting of MEK and either MIBK or Toluene. The MEK acts as an antisolvent to reject wax molecules from solution. This reduces refrigeration requirements but excessive MEK may cause oil phase separation. The second solvent keeps the oil in solution but also dissolves some wax. MIBK and toluene act as prosolvents.

Solvent properties are compared in the table below.

*Table 9. Typical Dewaxing Solvent Properties*

| Solvent | Wax Solubility<br>g/100 ml | Viscosity<br>@ 0°C, cSt | BP, °C | Latent Heat of<br>Vaporization, cal/g | Specific Heat,<br>cal/g-°C |
|---------|----------------------------|-------------------------|--------|---------------------------------------|----------------------------|
| MEK     | 0.25                       | 0.40                    | 80     | 106                                   | 0.55                       |
| MIBK    | 0.90                       | 0.61                    | 116    | 87                                    | 0.46                       |
| Toluene | 13.0                       | 0.61                    | 111    | 99                                    | 0.41                       |

MEK/MIBK refrigeration requirements are lower than MEK/Toluene because the Pour-Filter spread is smaller due to the lower wax solubility. The Pour-Filter spread is the difference between the Dewaxed Oil pour point and the filtration temperature required to meet the Dewaxed Oil pour point specification. Wax has a higher solubility in Toluene than MIBK and MEK/Toluene systems will require a lower filtration temperature to achieve the same pour point. MEK/MIBK solvent mixture viscosity is lower than MEK/Toluene. Filtration rates are higher for MEK/MIBK. Toluene costs less than MIBK.

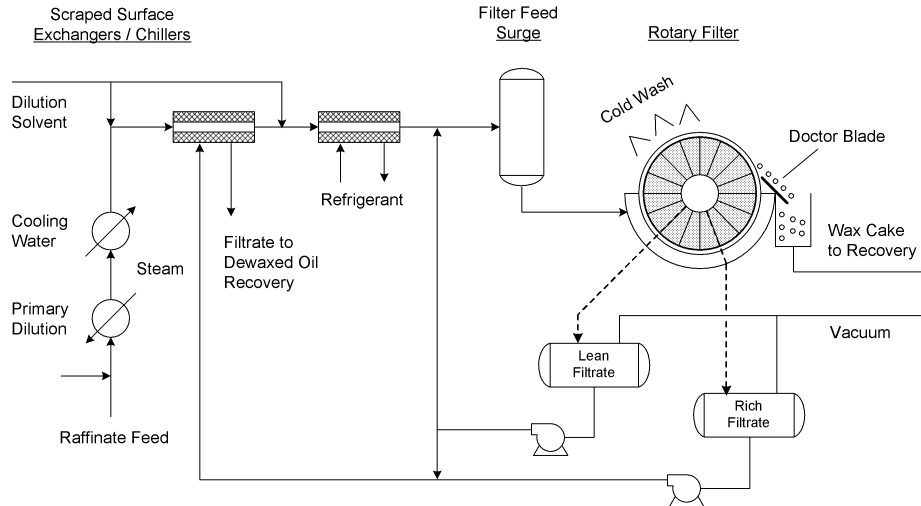


Figure 20. Simplified Incremental Dilution Dewaxing

## 17. KETONE DEWAXING PROCESSES

### 17.1 Incremental Ketone Dewaxing Plant

Incremental ketone dewaxing plants (see Figure 20) use a combination of Scraped Surface Exchangers that use cold filtrate for cooling the slurry followed by Scraped Surface Chillers, which use a refrigerant (propane, propylene, ammonia) to cool the slurry to the filtration temperature. Solvent may be added at the beginning or along the train in “increments”.

Solvent may be mixed with raffinate before the scraped service exchanger as primary dilution. The slurry passes through a feed heat exchanger to melt any crystals that may have formed in tankage. The slurry temperature is then reduced in a feed pre-cooler. The slurry flows to the Scraped Surface Exchangers and through the tube side of the exchanger. Cold filtrate from the filters is used to cool the feed below the cloud point and initiate crystallization. Solvent may be added in increments to reduce the slurry viscosity and enhance heat transfer. Slurry flows to Scraped Surface Chillers and through the tubeside. Propane, propylene or ammonia are typical refrigerants used on the shell side. The slurry exits the last scraped surface temperature at filtration temperature and enters the filter feed drum. The slurry flows by gravity to the filters where the wax crystals are filtered across a rotary vacuum filter. Wax is removed from the filter and sent to the wax recovery section. Oil and solvent—filtrate—is collected and sent through the shell side of the Scraped Surface Exchangers on its way to the Dewaxed Oil recovery section. Filtrate may also be recycled back to the slurry to adjust the final dilution before filtering.

## 17.2 DILCHILL™ Dewaxing

In DILution CHILLing the Scraper Surface Exchangers (SSE) are replaced with a multistage crystallizer. Cold Solvent is added at each stage and the slurry is mixed with an impeller. The crystallizer replaces all the SSEs with a single mixer.

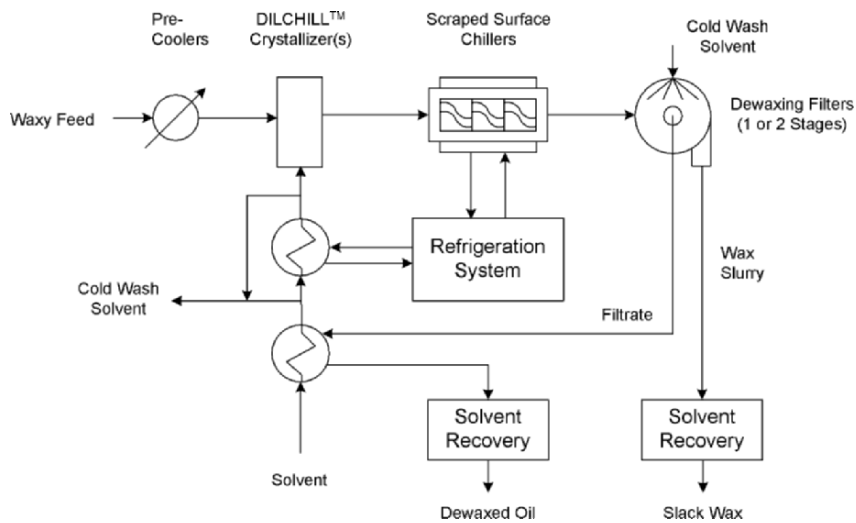


Figure 21. Simplified DILCHILL™ Dewaxing

The key features of DILCHILL™ are summarized below:

- Less oil is occluded in the wax crystal due to the vigorous “micromixing” in the crystallizer
- Higher filtration rates and lower oil-in-wax are achieved as a result of compact, spherical crystals
- Lower dilution solvent
- Lower operating costs
- Easier Operation
- Higher Service Factor.

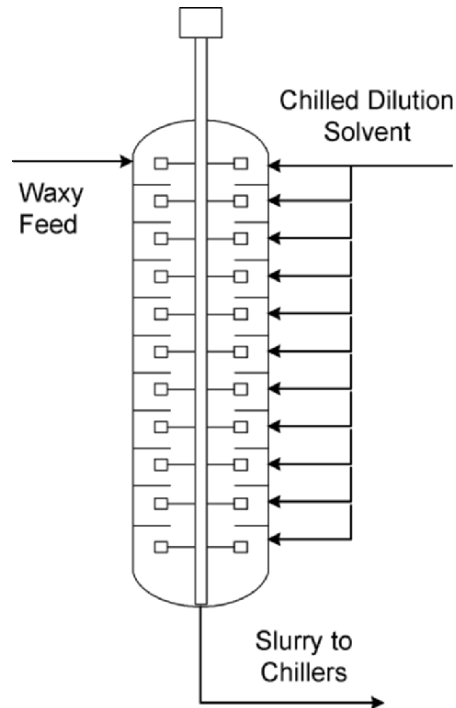
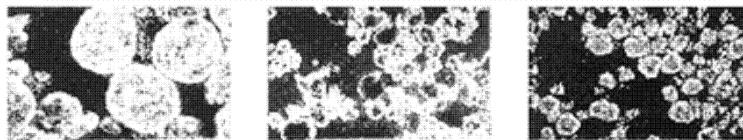
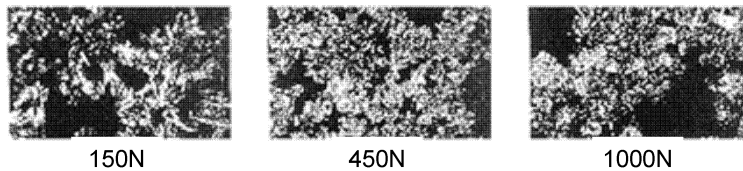


Figure 22. Simplified DILCHILL™ Tower

### Wax Crystals from DILCHILL™ Dewaxing



### Wax Crystals from Conventional Dewaxing



Optimum Crystal Formation Leads to Faster Filter Rates,  
Lower Solvent/Oil Ratios and Lower Oil-in-Wax Content

Figure 23. Comparison of Wax Crystals Formed in DILCHILL™ and Incremental Dewaxing

### 17.3 Dewaxing Process Variables

INDEPENDENT variables are controlled by the operator and include:

- Charge Rate
- Solvent Composition
- Precooler Outlet Temperature
- Dilution Ratio (Increments)
- Chilling Rate
- Filter Wash Solvent Ratio
- Wash Temperature
- Mixing Energy (DILCHILL™ Only)
- Filtration Temperature
- Filter Speed
- Dewaxing Aids

DEPENDENT variables rely on the independent variables:

- Filter Feed Rate
- Dewaxed Oil Quality
  - Cloud Point
  - Pour Point
  - Low Temperature Properties
- Dewaxed oil yield
- Wax Yield
  - Oil in Wax
  - Melting Point
  - Needle Penetration

## 18. PROCESS VARIABLE EFFECTS

### 18.1 Crude Source Affects Dewaxed Oil Yield

As was mentioned earlier, crude selection can have an influence on downstream units. The table below shows the impact of crude source on dewaxed oil yield.

*Table 10. Typical Basestock Yields for Two Different Crudes*

| <b>Basestock</b>        | <b>Arab Light</b> | <b>Statford</b> |
|-------------------------|-------------------|-----------------|
| Minimum Fluid Point, °C | Yield, Vol%       | Yield, Vol%     |
| 100 SUS                 | -18               | 81              |
| 300 SUS                 | -9                | 81              |
| 700 SUS                 | -7                | 85              |
| Bright stock            | -7                | 85              |

## 19. SOLVENT COMPOSITION

### 19.1 Miscible and Immiscible Operation

MEK is an antisolvent for the wax and helps to reduce its solubility. If the MEK content is too high the Basestock may become insoluble and a phase separation will occur. MIBK or Toluene is added to help solubilize the oil. Both of these prosolvents have a higher affinity for wax molecules than MEK. The higher the concentration of prosolvent the more wax stays in solution, and ends up in the filtrate. This raises the pour point of the dewaxed oil and since the manufacturer must meet dewaxed oil pour point specification the manufacturer is forced to reduce the filtration temperature to remove more wax. The reduction in filtration temperature increases the viscosity of the slurry and filtration rates are slower and oil removal from the wax cake becomes more difficult. Thus the objective is to use the maximum amount of MEK without having a phase separation. A plot of the phase separation temperature or miscibility temperatures vs. solvent composition may be used to help set the optimum solvent composition.

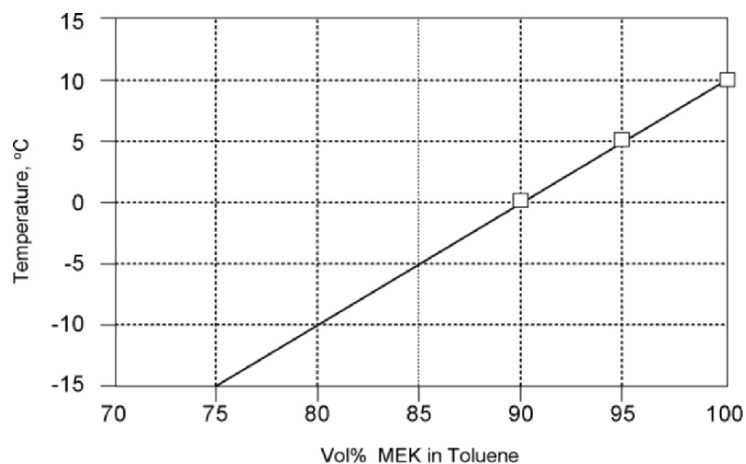


Figure 24. Typical Heavy Neutral Miscibility Curve

The ideal would be to operate as close to the miscibility curve as possible. However, this curve shifts depending on the Basestock. Wax molecules in heavier grades come out of solution earlier and this has the effect of shifting the miscibility curve to the left. Plants equipped with solvent splitters to separate the MEK from the MIBK or Toluene after it has been recovered in the DWO and Wax recovery sections may blend to the optimum solvent composition for each Basestock. Manufacturers without the capability to change solvent composition will set the plant solvent composition based on

the heaviest grade to avoid immiscible operation. This increases the pour filter spread, because the prosolvent composition is too high for the lighter grades. This will also affect plant processing capacity.

The shift from miscible to immiscible operation occurs over a narrow range of solvent composition. When the plant moves deep into immiscible operation and phase separation occurs, the oily phase, containing the desirable high VI molecules, will hang up in the filter cake and be very difficult to remove, increasing the oil in wax content of the wax and reducing dewaxed oil yield. Dewaxed oil properties may be adversely affected, and VI may decrease. Interestingly, in severely immiscible operation the dewaxed oil pour point may actually decrease as the waxy molecules remain in the wax cake.

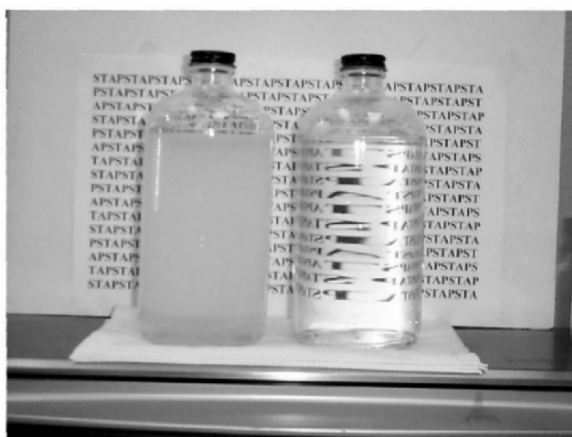


Figure 25. Comparison of Immiscible and Miscible Filtrates (photo by B.E. Beasley courtesy ExxonMobil Process Research)

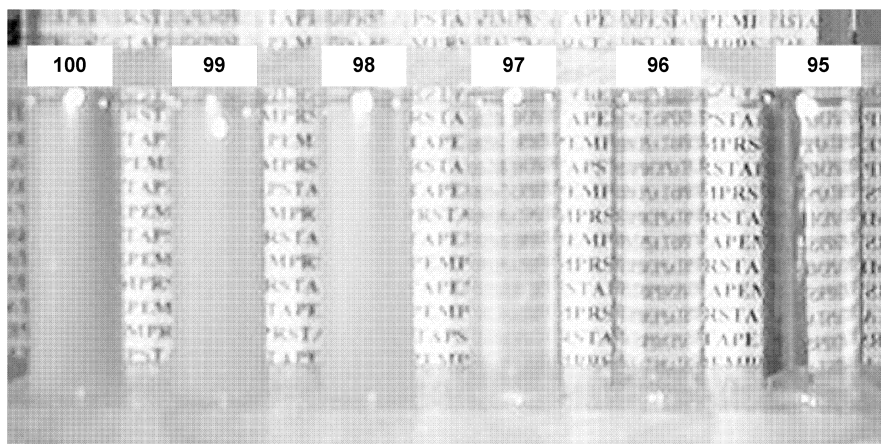


Figure 26. Impact Of Change In Solvent Composition On Miscibility (photo by B.E. Beasley courtesy ExxonMobil Process Research)



## 19.2 Effect of Viscosity on Filtration Rate

Higher viscosity Base stocks will filter more slowly. Increasing the MEK concentration in the solvent reduces the slurry viscosity but the maximum amount of MEK is limited by miscibility considerations.

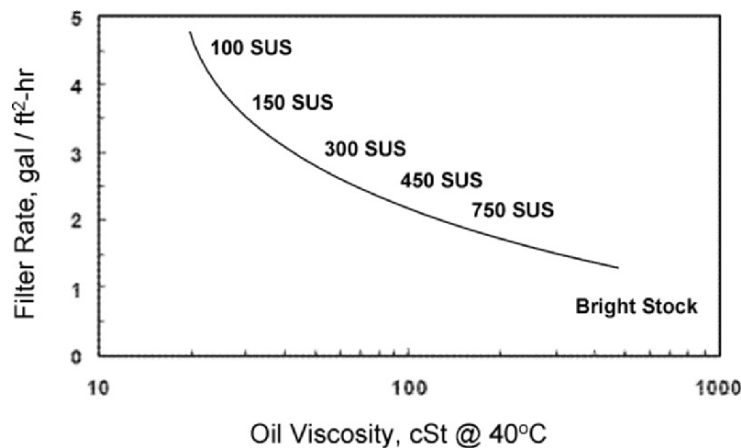


Figure 27. Effect Of Oil Viscosity On Filtration Rate

## 19.3 Effect of Chilling Rate On Filtration Rate and Dewaxed Oil Yield

Increasing the chilling rate forces wax molecules to come out of solution quicker. When the wax molecules come out of solution they may either form a separate nucleus (nucleation) or attach onto an existing nucleus (growth). When the chilling rate is high, nucleation is favored over growth with the result that the average crystal size is smaller, the wax is more difficult to filter, and the wax retains a higher oil content.

Table 11. Example of Effect of Chilling Rate on Yield and Filtration Rate

| Chilling Rate, °C/min | DWO Yield, Vol% | Filter Rate, Gal/ft <sup>2</sup> -hr |
|-----------------------|-----------------|--------------------------------------|
| 2.2                   | 85.3            | 2.00                                 |
| 4.4                   | 82.0            | 1.94                                 |
| 6.7                   | 81.3            | 1.92                                 |
| 8.9                   | 79.8            | 1.90                                 |

## 19.4 Effect of Temperature Profile

The preferred temperature profile for incremental and DILCHILL™ dewaxing is a linear profile. Both methods of dewaxing add solvent, either in increments along the SSE/SSC train or in stages in the crystallizer. Thus the flow rate increase from the feed to the filters. Other temperature profiles are possible. Filtration rates in plants with a convex temperature profile are typically not as good as those with a linear profile. This may be due to the very high chilling rates in the SSC or last few DILCHILL™ stages, required to reach the filtration temperature, and which favors nucleation at the expense of growth and leads to smaller average crystals. Typically concave profiles offer no advantage over linear. In the rare case where a concave profile has produced improved filtration rates, it has been surmised that a high chilling rate at the beginning of the train, which will favor nucleation, was needed to establish “seed” crystals for growth.

## 19.5 Effect of Solvent Dilution Ratio

### 19.5.1 Filtration Rate

Solvent may be added in increments along the SSE/SSC train or in the DILCHILL™ Crystallizer. The solvent reduces the slurry viscosity and facilitates filtration. When the dilution is too low, the slurry viscosity will be too high, and the slurry filtration will be reduced. This is often referred to as VISCOSITY limited. When the dilution is too high, the volume of liquid to be filtered exceeds the capacity of the filter (filter cake resistance is limiting) and the filtration is said to be hydraulically limited. This balance results in an optimum dilution ratio dependent on the Basestock being processed, the solvent composition being used and the crystallization, which sets the filter cake resistance (see Figure 28). Light Basestock operations are more likely to be Chilling or Refrigeration limited rather than Filtration limited because the Light Basestock pour points are typically lower than the heavy grades while the average wax crystal size is larger, reducing wax cake resistance.

### 19.5.2 DWO Yield

Increasing the dilution ratio will reduce the Oil in Wax and increase the dewaxed oil yield.

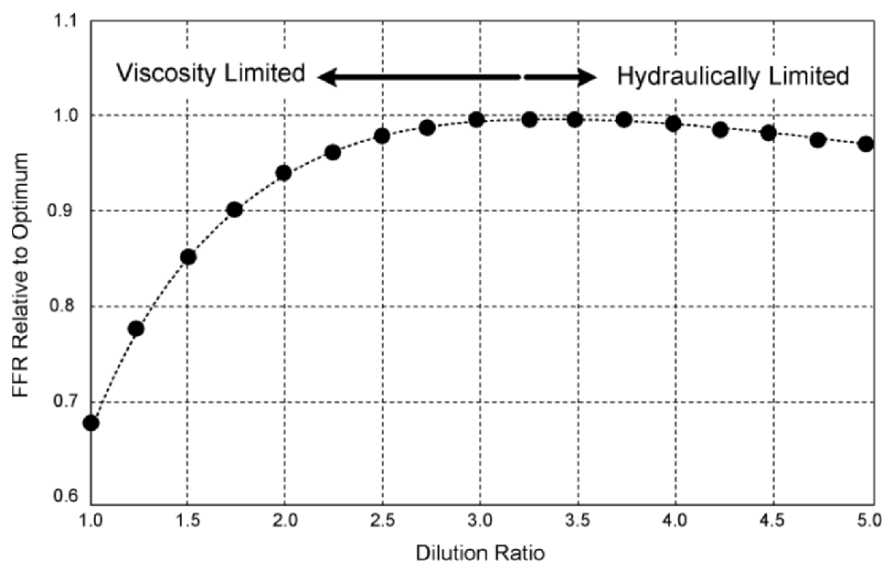


Figure 28. Effect Of Dilution Ratio On Filtration Rate, Heavy Neutral

## 19.6 Effect of Water

Water may enter with the feed from the extraction process or from tankage. It may also enter the system from leaks in water coolers or condensers that are used in the dewaxing plant, or it may reenter the solvent system through inadequate performance of the dehydrator section in the plant. Water is a strong anti-solvent, and reduces the solubility of wax and oil molecules so that they come out of solution at a higher temperature. This has the effect of shifting the miscibility curve to the left. Typically the increase in water concentration from the normal levels is an indication of a process/equipment problem and the root cause must be found and dealt with quickly.

Excessive water may drop out of solution and form ice in the slurry or on the inside of the scraped surface equipment. It may also flow downstream to the filters where it may be captured in the wax cake or on the filter cloth.

## 19.7 Effect of Increased Raffinate VI

Raffinate VI may be increased in extraction through more severe extraction. This increases wax concentration in the raffinate stream. These waxy molecules will come out of solution in the dewaxer at a higher temperature, resulting in the miscibility curve shifting to the left. This will require the manufacturer to add more prosolvent to avoid immiscible operation.

## 19.8 Effect of Pour Point Giveaway on Product Quality and Dewaxed Oil Yield

When a Basestock produces a dewaxed oil with a lower pour point than the specification, the plant is “giving away” this product quality. The economic penalty for pour point give away is lower filtration rate and lower throughput and decreased dewaxed oil yield. Lower pour point also means that more wax has been removed and this will lower the dewaxed oil VI.

Table 12. Examples Of Quality Giveaway

| Base Stock       | Pour Point Reduction, °C | Typical VI Loss | Typical Yield Loss, vol% |
|------------------|--------------------------|-----------------|--------------------------|
| Solvent Neutrals | 3                        | 1               | 1.0                      |
| Bright Stock     | 3                        | 0.5             | 1.0                      |

## 20. SCRAPED SURFACE EQUIPMENT

SSEs and SSCs are used in incremental dewaxing and SSCs in DILCHILL™ dewaxing. SSEs and SSCs are double pipe exchangers with slurry inside the central tube and the cooling media (filtrate or refrigerant) in the annular area around the inside tube (pipe). Tubes are typically stacked in groups of 8, 10 or 12 and internal flow may be in parallel or series. Internal pipe diameters are typically 6, 8, 10, 12 inches.

A shaft extends the length of the inner pipe. Spider bearings are used for shaft support. Each shaft is fitted with a scraping blade; there are two leading designs. The shaft extends through a seal or packing at the drive end. A sprocket is attached to the shaft outside the tube and the shaft is turned by a lubricated chain that is connected to all the sprockets in a tube back and to a fixed speed drive motor mounted above the tube bank. Shaft speeds range from 2-30 rpm.

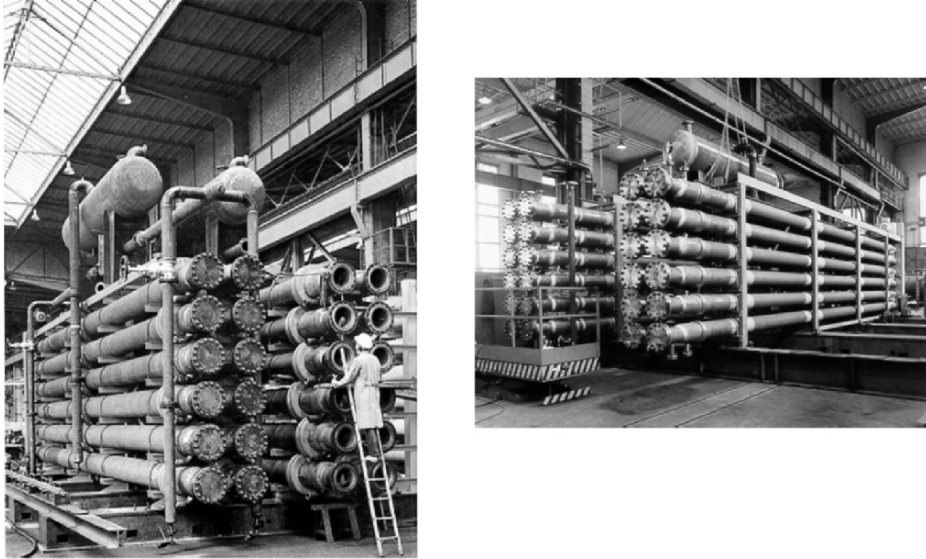


Figure 29. Scraped Surface Equipment (photos reprinted courtesy Borsig®)

Borsig GmbH and Armstrong International, Inc. are the leading designers of scraper internals. Both use blades that are softer than the pipe, so that the blades will wear down first. Each uses a spring to apply pressure on the scraper blade to push it against the tube wall so that it scrapes the wax off the wall as the internal shaft is turned.

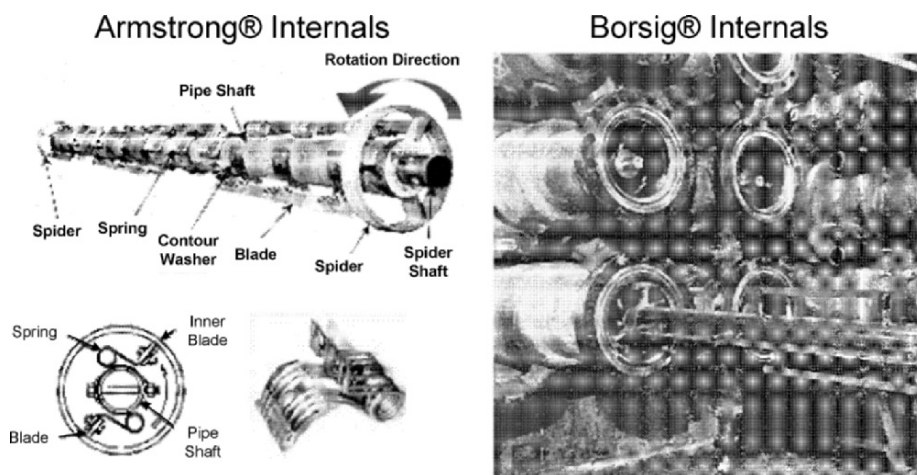


Figure 30. Scraped Surface Equipment (Photos reprinted courtesy Armstrong® and Borsig®)

Both designs attempt to accomplish wax removal from the wall by scraping while maximizing open cross sectional area in the tube. Wax will tend to accumulate on cold internals like the Spider bearing and other surfaces affixed to the shaft. The build up of wax will increase the pressure drop. When pressure drop becomes limiting, the equipment will either be taken off-line and cleaned with hot solvent or cleaned on-line. Various methods have evolved to optimize the cleaning with minimum impact on the process.

SSEs and SSCs require very high maintenance support in comparison to other equipment in the plant. Shear pins protecting the internal shaft from damage will fail and the shaft will stop turning. This reduces the effective heat transfer, which can limit the plant throughput if the plant is near a chilling or refrigeration limit. Seals and packing will leak, contributing to solvent loss in the plant. Poorly lubricated chains will break or jump off the sprockets. SSEs and SSCs overall heat transfer coefficients are low. Performance should be monitored, which is typically not an easy task. Internals must be overhauled when performance has permanently degraded.

## **21. FILTERS**

### **21.1 Filter Operation/Description**

Filters are used to separate the wax crystals from the slurry. The slack wax and filtrate are collected and sent to their respective recovery sections in the plant to recover and recycle solvent.

Rotary vacuum filters are used in ketone dewaxers and rotary pressure filters are used in propane plants. The principles of operation are the same. A typical filter is shown in Figure 30.

The filter drum rotates at speeds from 0.2 - 1.6 rpm. The surface of the drum is divided into segments that run the length of the filter. Newer designs have 30 segments. Each segment has a lead and trail pipe connected to the segment in several locations running the length of the drum. The segment lead and trail pipes combine so that there are 30 lead and trail pipes, one for each segment, that carry filtrate to the master valve, which is also called the trunnion valve. The master valve is stationary while the filter drum rotates. The master valve has internal bridge blocks that effectively segregate the filtrate collected from the filter into as many as four distinct compartments or "pick-ups".

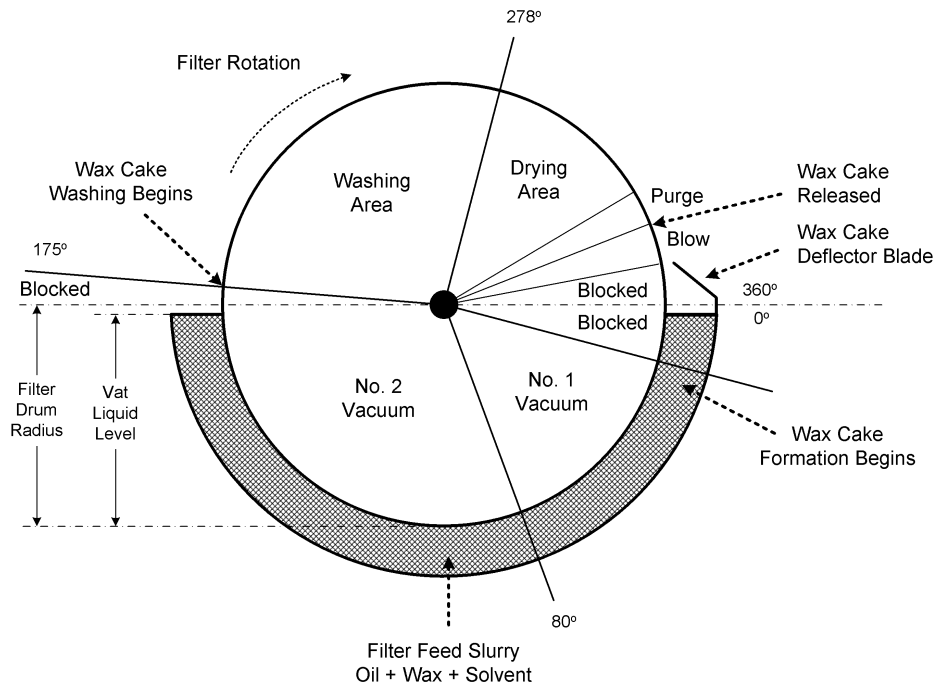


Figure 31. Typical Filter Wash - Dry Segments

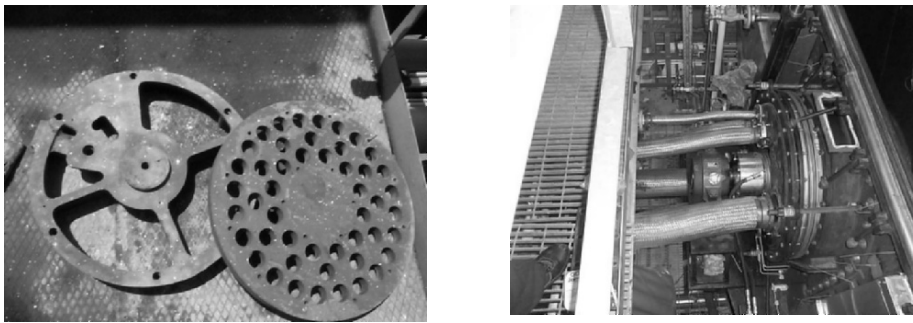


Figure 32. Filter Master Valve (photos by B.E. Beasley courtesy ExxonMobil Process Research)

Starting from the deflector blade (see Figure 31), the drum rotates into the slurry in the vat and filtration begins at the first “wet pick up” port or “No. 1 vacuum”. The filter segment continues its rotation into the “2nd wet pick up” or “No. 2 vacuum”. The rotation continues and the filter moves into the wash area or “first dry pick-up” and finally into the “drying area” or “second wet pickup”. The drying area may also be washed with cold solvent. The filter

rotates into the Purge zone where N<sub>2</sub> blow gas is applied to the trail pipe while the lead pipe stays under vacuum. The purge zone clears out the filtrate in the pipes and increases the dewaxed oil yield by preventing the filtrate in the pipes from being blown back through the pipes and into the wax scroll with the wax. Finally the segment moves into the blow gas zone and blow gas is applied to the lead and trail pipes and the cake “pops” off of the filter and slides across the deflector blade and into the wax scroll.

The scroll is an Archimedes screw that moves slack wax from the outer ends of the filter to a center pipe. The slack wax falls down the pipe and may either proceed down a slide where it may be combined with slack wax from other filters into a slack wax drum or into a wax “boot” or vessel. This is a small drum dedicated to the filter. From the large wax drum or the wax boot the slack wax is pumped to either wax recovery, the second stage of dewaxing or deoiling depending on the plant configuration.



Filter Drum



Solvent wash sprays and drip pipe



Wax scroll

Figure 33. Typical Rotary Vacuum Filter (photos by B.E. Beasley courtesy ExxonMobil Process Research)

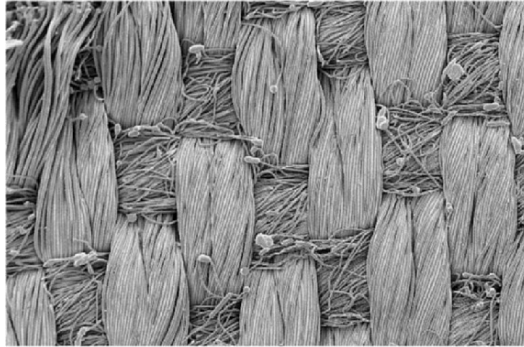
## 21.2 Filter Media

The filter drums used in ketone dewaxing (rotary vacuum) and in propane dewaxing (Rotary pressure) have filter cloths secured to the drum surface. The filter cloth retains the wax crystals while allowing the filtrate to pass through the filter cake, through the filter cloth and into the internals of the filter drum and eventually to the filtrate receiver drum.

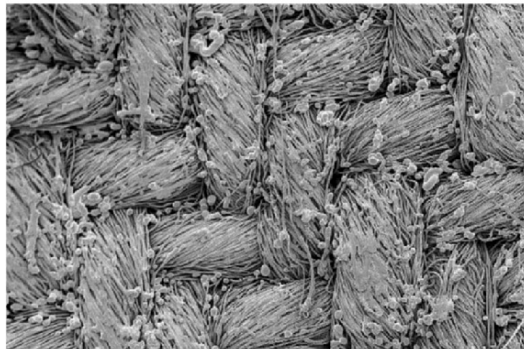
Many different types of material have been used over the years. These include woven and non-woven materials, single and dual layer cloths. A few examples are shown below.



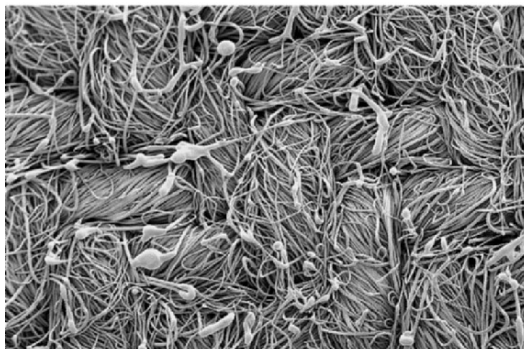
SATIN WEAVE



Twill Weave



PLAIN WEAVE



NON-WOVEN

Figure 34. SEM of Typical Filter Medium (photos reprinted courtesy Madison U.S. Filter)

The requirements of a good filter cloth are:

1. Low Interfacial Resistance for high filtration rates

2. High filtration rates lead to high wash acceptance or lower filter speeds for increased dewaxed oil yields
3. Elimination of wax bleed through and haze formation
4. Thermally stable at hot wash temperature
5. Chemically stable in ketone and propane service

A comparison of typical filter cloth materials is included below.

Additional considerations include the mechanical stresses generated in vacuum and pressure filters that lead to fabric stretch and wear associated with filter blow gas. The filter cloth may suffer mechanical damage during installation, or from exposed deflector blades or other sharp or raised edges. The cost of the filter cloth is minor compared to the lost production time incurred when a filter has to be re-clothed or when the dewaxed oil quality does not meet product specification.

Fiber selection, fabrication technique (woven, non-woven) and cloth finishing all play an important role in determining filter cloth performance.

The ExxonMobil® Patented proprietary filter cloth has been used in ketone and propane dewaxing service for many years. It has higher resistance to fouling due to several unique design features and can achieve >15% improvement in filtration relative to woven cloths.

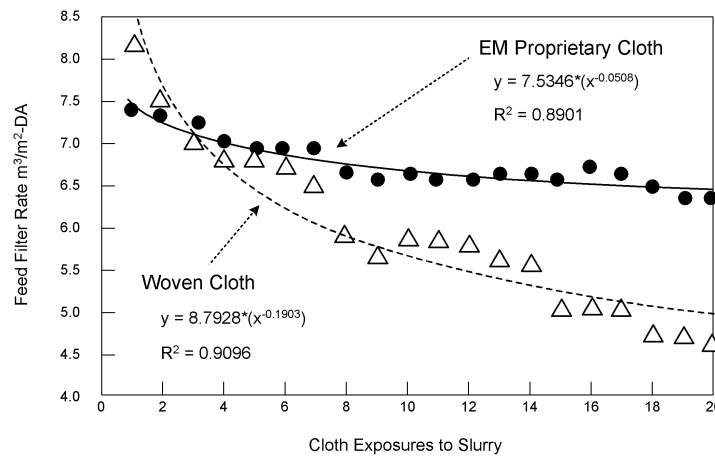


Figure 35. Typical Filter Cloth Fouling

Filter cloth is cut the length of the filter and depending on the width, several sections are required. The cloth sections are held in place on the surface of the drum by a caulking bar which is hammered into the caulking bar groove during the cloth installation. A steel wire is wrapped, under tension, around the drum to further secure the cloth. The wire will tend to migrate away from the drive end and many filters have installed a take-up tensioner device to extend the length of time before wire breakage occurs.



Upper left: Caulking bars hammered into caulking bar groove

Upper right: Removal of excess cloth. A small cloth strip is used in all grooves that do not have cloth overlap to provide tight fit.

Lower left: Technicians tamp down the caulking bar as the wire is wound onto the drum.

Lower right: Wire tension take up device.

*Figure 36. Filter Cloth Installation (photos by B.E. Beasley courtesy ExxonMobil Process Research)*

## 22. COLD WASH DISTRIBUTION

Cold ketone wash is applied to the filters through either sprays or drip pipes or both. There are advantages and disadvantages to both designs and both are in practice today. Cold wash is essential to reduce the Oil in wax, increase dewaxed oil yield and increase the wax product value.

Good distribution is necessary to spread the wash fully over the wax cake and avoid dry sections. The wash must not impinge with excessive velocity onto the wax cake in order to avoid knocking it off or digging channels or grooves. The wash system should be resistant to fouling. Spray nozzles and drip pipes are the major wash distribution systems in use today. Both are acceptable provided the system is properly designed and operated within the design parameters.

ExxonMobil patented Drip Pipes provide excellent coverage and are capable of good turndown. Wash falls by gravity onto the wax cake

minimizing potential dislodging of the cake by wash impingement. Stainless steel construction and upstream filtration prevent fouling.

- Poor wash distribution can result from collapsed sprays creating a wide area without coverage.
- If cold wash flow from the spray nozzles is too high wax may actually be blown off the filter cake. Evidence of this may be seen as an accumulation of wax on the filter windows.
- Conventional (not ExxonMobil) drip pipes may not be balanced, resulting in some areas with no flow and some areas with too much flow.
- Excessive wash flow rates through the spray nozzles may cut grooves in the cake and wash wax and solvent back into the vat, resulting in recycling.
- Combinations of too high a flow through conventional drip pipes will collapse spray cones. Excess accumulation in a local area may cut grooves in the wax cake.

### Poor Distribution from Conventional Drip Pipe

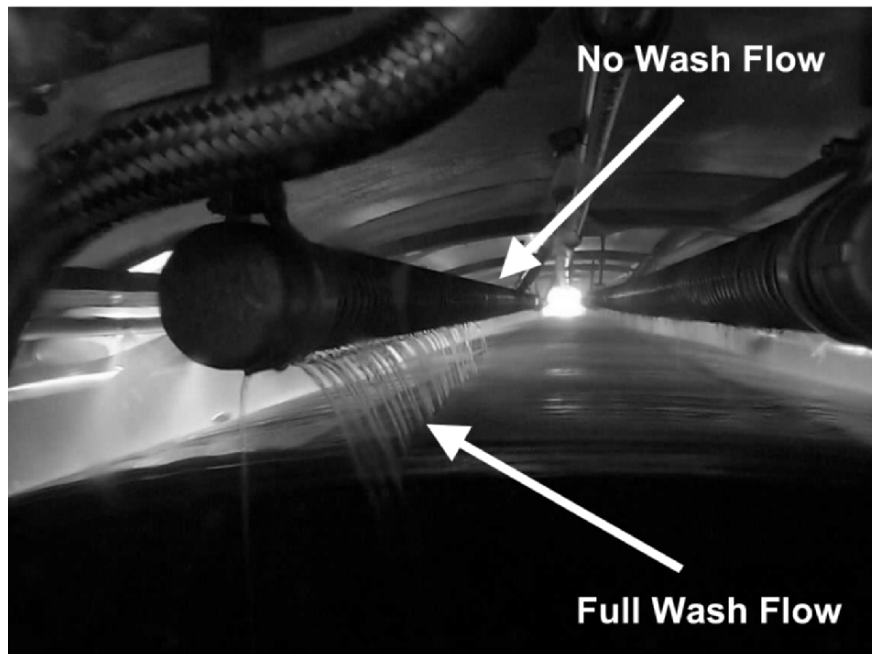


Figure 37. Example Of Poor Filter Cold Wash Distribution (photo by D. S. Sinclair courtesy ExxonMobil Process Research)

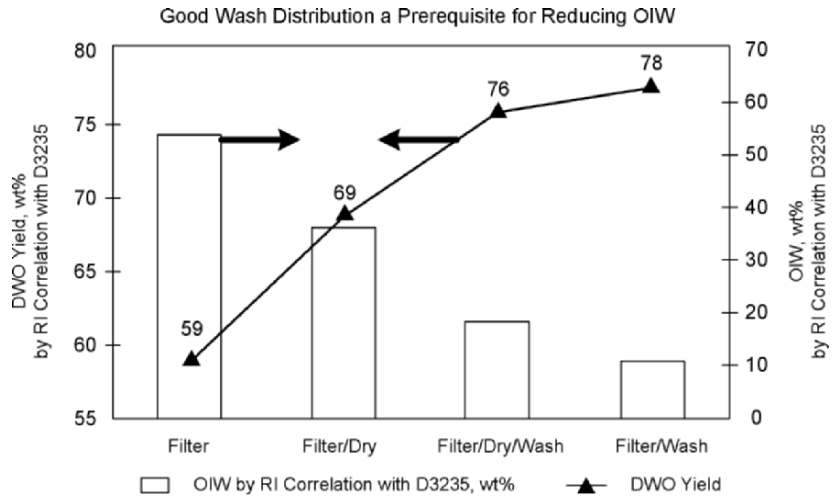


Figure 38. Effect Of Filter-Wash-Dry Sequence On Oil Yield (Lab) (photo by B.E. Beasley courtesy ExxonMobil Process Research)

Impact of Wash Application on Filter Feed Rate (FFR)

Drying out / compressing wax cake due to lack of wash over part of top pickup zone affects both DWO yield and FFR

- Recent plant tests redistributed wash solvent to prevent large “dry” area on descending side of filter, gave 15% increase in FFR
- Graph shows effect of continuing to apply vacuum without wash and then reapplying wash. FFR improved but did not come back up to previous level

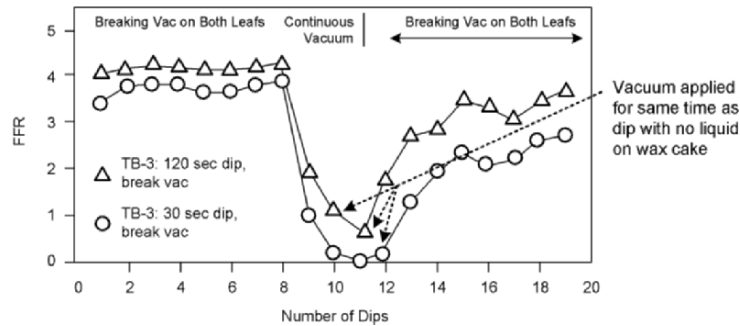


Figure 39. Impact of Wash Application on Feed Filtration Rate (FFR)

**23. WASH ACCEPTANCE**

Wash acceptance is the amount of wash that can be accepted through the wax cake before it begins to spill or run off the wax cake. The volume of filtrate collected as a function of time decreases in a square root relationship, for non-compressible wax cakes, until the end of the filtration step. At that point filtration is complete, the wax cake formation has stopped and the wash

is applied to the cake. The flow of wash through the cake is at the same rate as the last increment of filtrate just at the final moment of filtration (ignoring for the moment slight differences in liquid viscosity and wax cake compressibility). If too little wash is applied the Oil in Wax will be higher than optimum and yield will be lower. If excess wash is applied the excess wash will roll off into the filter vat or into the scroll.

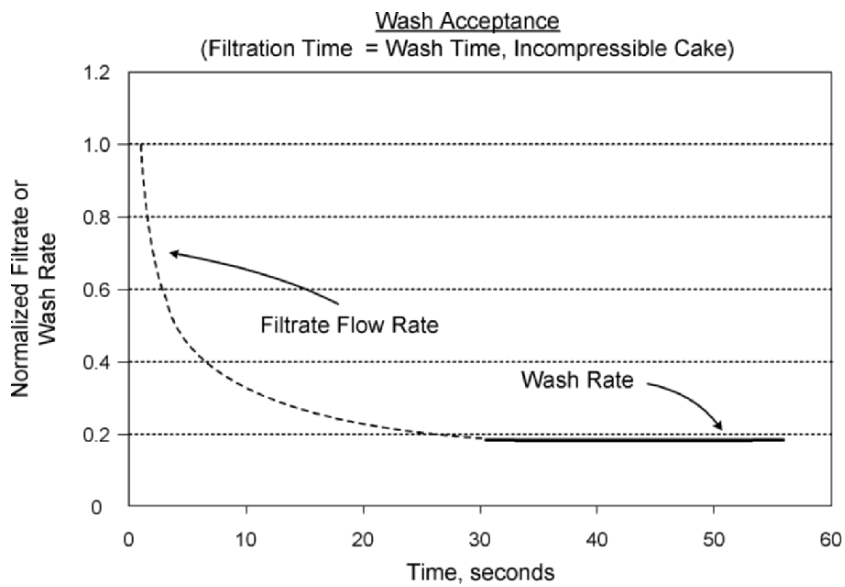


Figure 40. Filtrate Volume Versus Time

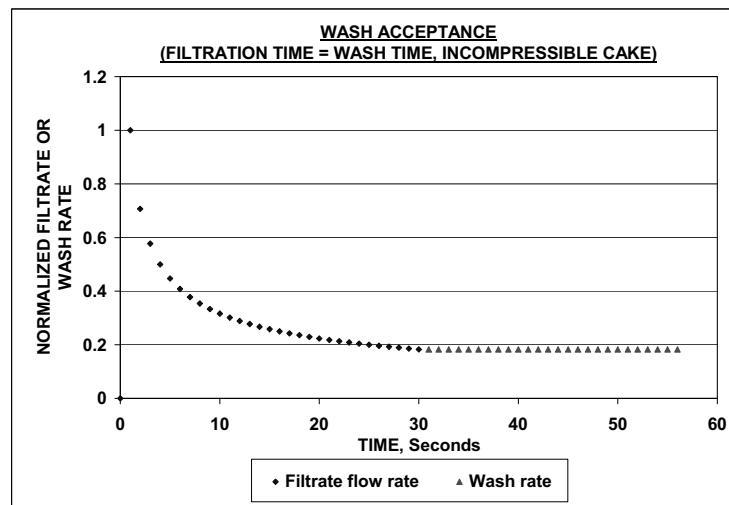


Figure 41. Normalized Filtrate Or Wash Rate Versus Time

## 24. WASH EFFICIENCY

Cold wash, distributed over the wax cake by drip pipes or sprays, will displace the cake liquids, reducing the Oil in Wax and increasing the yield. This occurs in two steps. The first step is a piston displacement where the wash liquid pushes out the cake liquids. In the second step, oil from within the wax crystal diffuses into the low oil concentration wash liquid. The theoretical reduction in oil content may be predicted by the Butler equation <sup>1</sup>.

The wash efficiency is defined as the actual oil in wax obtained for a given amount of wash applied relative to that predicted by the Butler curve. Efficiencies may be less than 100%. This may result from:

1. Poor spray distribution
2. Fouled, leaking or missing spray nozzles
3. Poor distribution along the drip pipe, "out of level" on older designs
4. Fouled drip pipes
5. Area of excessively fouled filter cloth may occur when "drying" is practiced
6. Cracked filter cake, solvent flows through crack instead of cake
7. Wash rate exceeding wash acceptance
8. Wash temperatures significantly lower than filtration temperature, seals off wax crystals

Wash efficiencies may be found to exceed 100%. This may be due to:

1. Hydraulic compression of the wax cake, "squeezing" oil out of the cake without using any wash solvent such as may occur in the drying section of the filter
2. Higher crystal or wax cake compressibility in the presence of wash.

Some plants will dedicate a significant portion of the filter area to "drying" and will block off sprays or drips in this area. The intent is to reduce the Oil in Wax to increase yield and possibly debottleneck wax recovery. An unintended consequence is that the vacuum that remains on in this section will pull the wax cake into the filter cloth, accelerating the filter fouling which will reduce wash acceptance and increase oil in wax. It will also require more frequent filter washing which will reduce plant throughput. These competing factors must be balanced by the manufacturer to achieve the optimum filter performance.

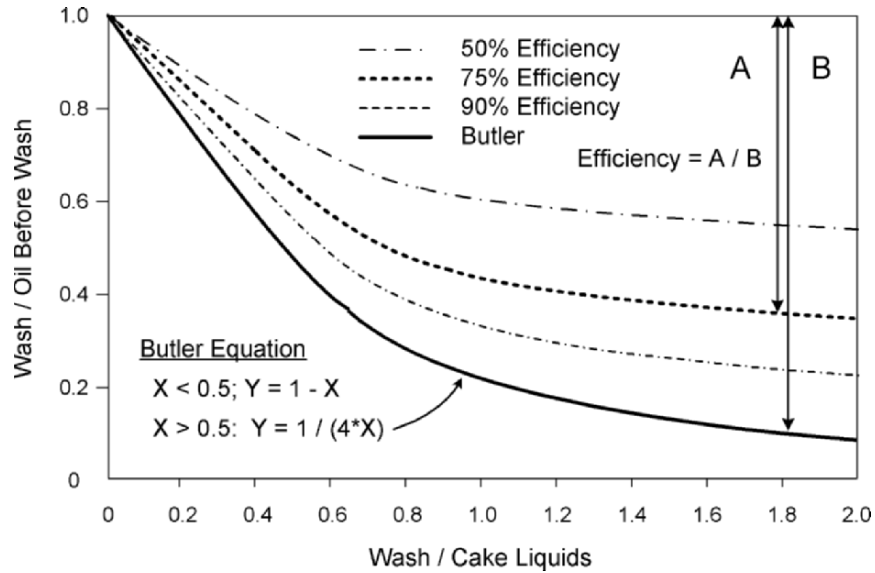


Figure 42. Wash Efficiency

## 25. FILTER HOT WASHING

The filtration rate of a filter decays over time due to plugging of the filter cloth by small wax crystals. A typical decay curve is shown below. The feed rate measured by flow meter is plotted against the number of “DIPS” or exposures of the filter cloth to the wax slurry. The shape of the decay curve depends on the filter media, in this case an ExxonMobil proprietary cloth.

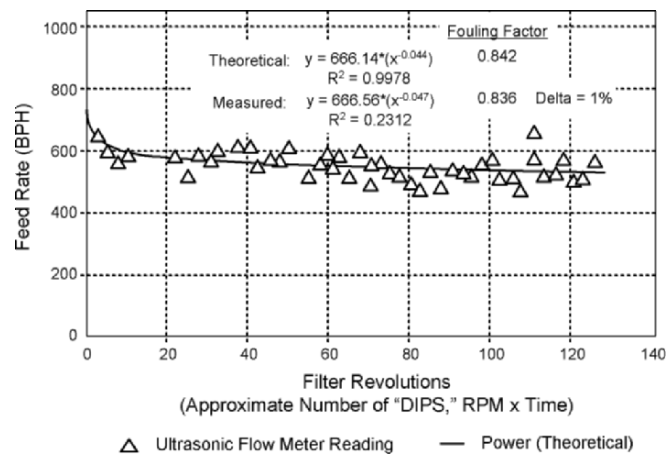


Figure 43. Feed Rate Decay Curve (Light Neutral)



As the filtration rate decays, throughput is lost and at some point the filter must be taken offline and washed to restore the filtration rate. The time that the filter is off-line also represents lost production. The optimum time between washes is the economic balance between production lost due to the decay curve compared to the time to wash the filter and bring it back on line. An example of a series of decays and washes are shown below. If the shape of the decay curve is known and the wash time is known the optimum wash time may be found analytically.

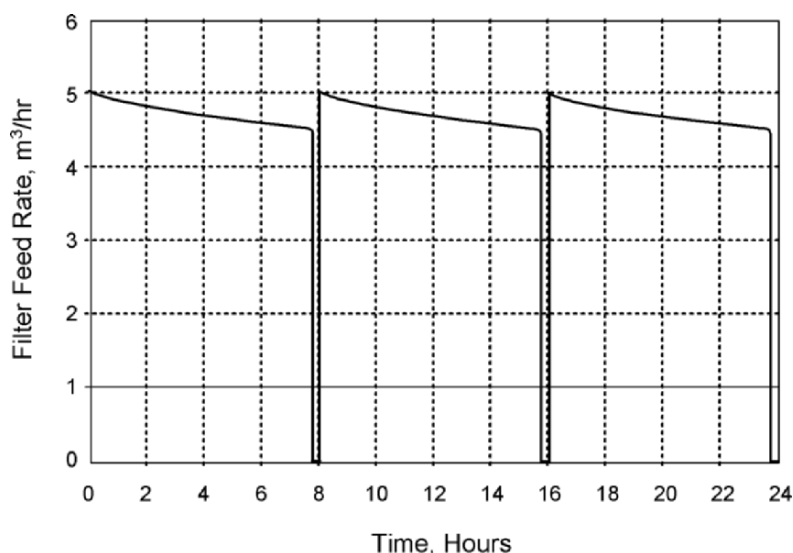


Figure 44. Filter Feed Rate Decay Curves And Filter Washes

Hot ketone solvent is used to wash the filters. Cold wash solvent is blocked off and hot solvent flows through the same sprays or drip pipes, over the filter cloth, melting the wax crystals, cleaning the cloth. Filter washings are collected in a filter washing drum. The washings may be:

1. Injected with the feed as “predilution”
2. Injected between 1st and 2nd filter stages
3. Injected into the appropriate stage of the DILCHILL™ crystallizer
4. Sent to wax recovery.

Hot wash temperature is controlled. If the temperature is too low it may not adequately melt the wax crystals. If the wash temperature is too high wire migration may occur resulting in reduced wire life and/or an increase in the frequency of wire retensioning.

## 26. DEWAXED OIL/WAX-SOLVENT RECOVERY

The objective of the Dewaxed oil and wax recovery section is to remove solvent from the product stream for recycle back to the chilling train and the filters. This is done using low and high pressure flashes and a high temperature flash followed by steam stripping and vacuum drying (dewaxed oil). Solvent concentrations are reduced to meet the product specification. High concentrations in the product represent avoidable solvent losses and increase operating expenses. In some cases excessive high temperature operation in the recovery section can lead to light oil vaporization and accumulation in the solvent. This represents avoidable excess energy costs. The operation of the solvent recovery system becomes an economic optimization problem.

Dry “Waxy Solvent” from wax recovery should be segregated from the Dry “Clean” solvent recovered from the Dewaxed Oil recovery section. “Waxy solvent” tends to have wax in it and cannot be chilled to the same temperature as that of the “Clean” solvent from the dewaxed oil recovery. It may be cooled and temperature blended with the “Clean” and used as filter wash. Flow restrictions may be set on flow to wax recovery to prevent wax carryover and downstream fouling.

Wet solvent from the stripper and solvent from the low pressure flash is sent to the dehydrator for solvent recovery.

A typical recovery section is shown below.

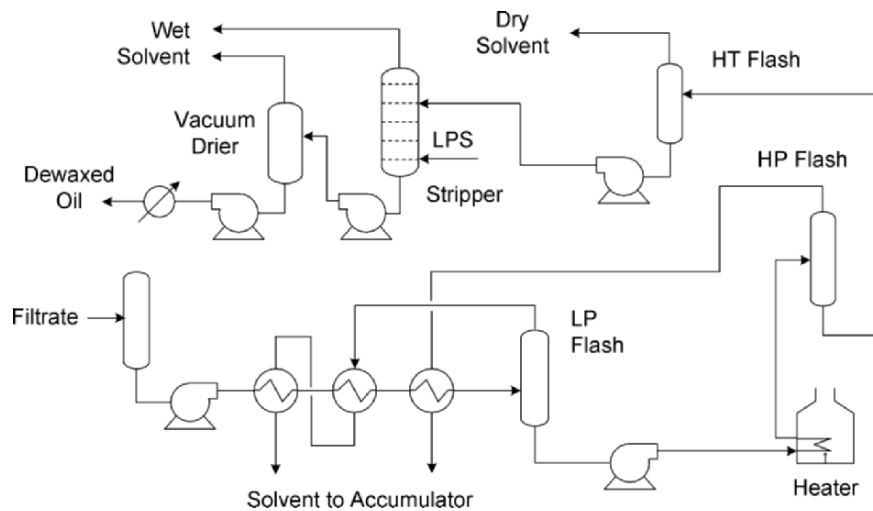


Figure 45. Typical Dewaxed Oil Recovery Section Flow Diagram

## 27. SOLVENT DEHYDRATION

Solvent from the low pressure flashes are sent to the dehydrator tower. Overheads from the dehydrator tower are combined with stripper overheads and the overhead from the water tower and sent to the decanter. The solvent rich phase from the decanter is sent back to the dehydrator. The water rich phase to the water tower. Dry solvent from the dehydrator bottoms is returned to the unit. The water from the water tower is sent to waste water treatment.

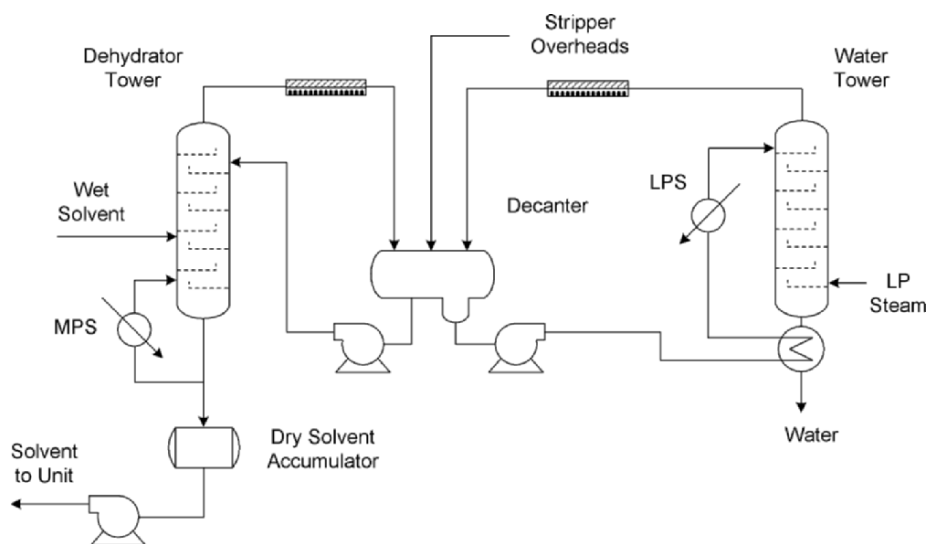


Figure 46. Typical Solvent Dehydration Flow Diagram

## 28. SOLVENT SPLITTER

The solvent splitter allows the manufacturer to separate the solvent mixture back into MEK and MIBK or Toluene which can then be added back to the solvent mixture in the plant to optimize the solvent composition and minimize the “pour - filter” temperature spread to achieve maximum throughput.

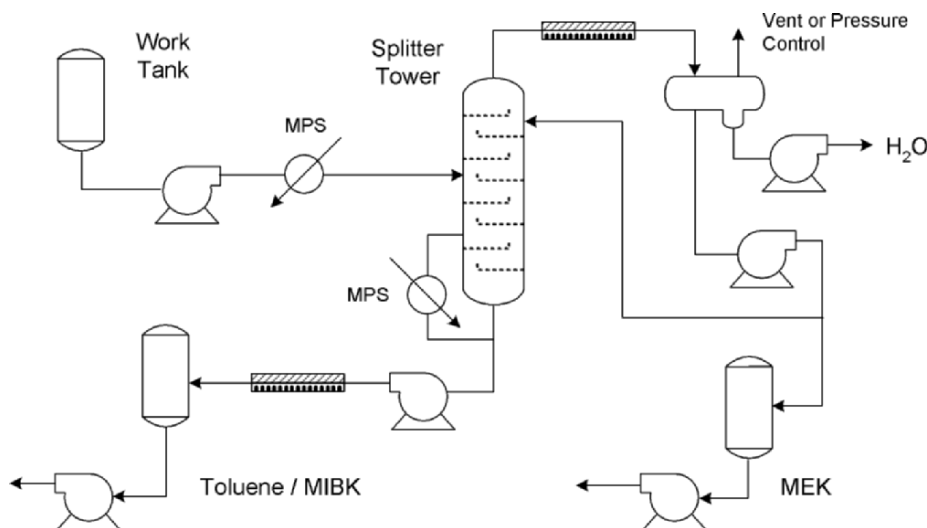


Figure 47. Typical Solvent Splitter Flow Diagram

## 29. 2-STAGE DEWAXING

A second stage of filtration can be used to reduce the oil in wax and to increase the dewaxed oil yield. Solvent (called repulp or repuddle) is added to the wax from the first stage, typically in the wax scroll or wax boot depending upon the plant design, and pumped to a filter feed drum that feeds the second stage of filters.

Filtrate from the second stage is “lean” in oil and can be used in first stage operation. It may be blended with “fresh” solvent and used as first stage wash, or it may be added as the final increment of dilution in an incremental plant. Recycling the 2nd stage filtrate reduces the overall solvent usage.

## 30. DEOILING

The deoiling process is used to produce a hard wax containing a very low oil content. Waxes produced in deoiling have melting point and needle penetration specifications. Waxes intended for food grade use must also meet UV absorption specifications and require wax hydrotreating.

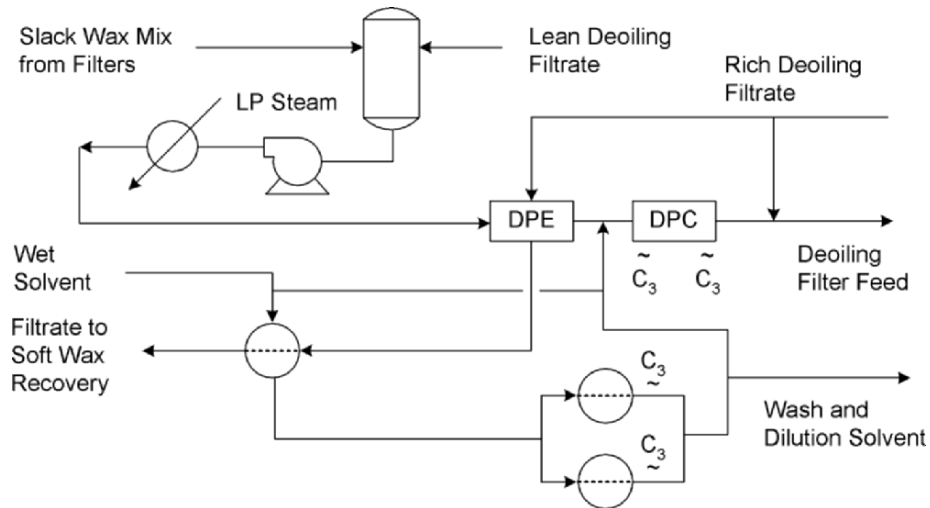


Figure 48. Typical Chilling Section In Recrystallization Deoiling

In recrystallization deoiling, lean solvent is added to the wax from the dewaxing plant and the resulting slurry is pumped through a heat exchanger where the wax crystals are melted. The wax is then recrystallized in SSEs and SSCs. Typically two stages of deoiling are used to meet the low Oil in Wax specification.

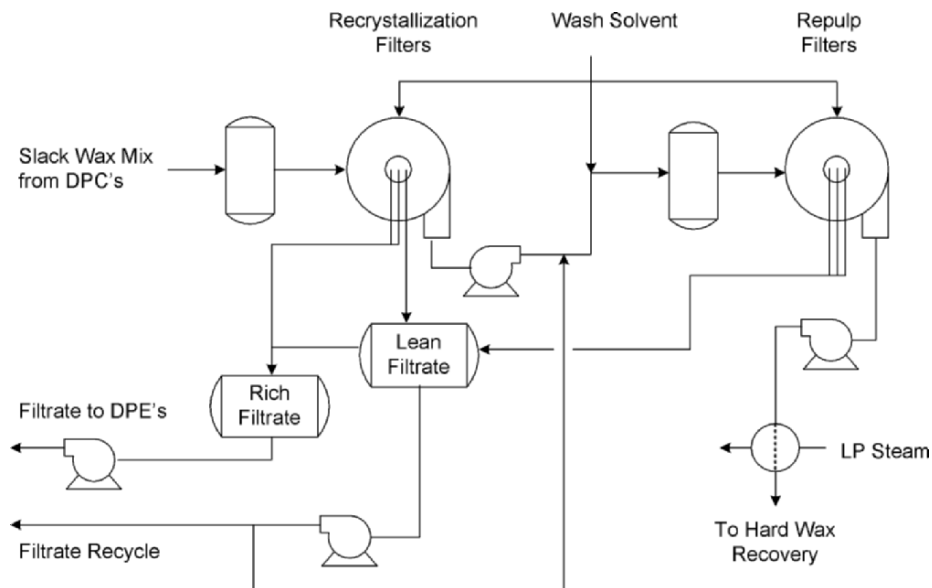


Figure 49. Typical Filtration Section In Recrystallization Deoiling

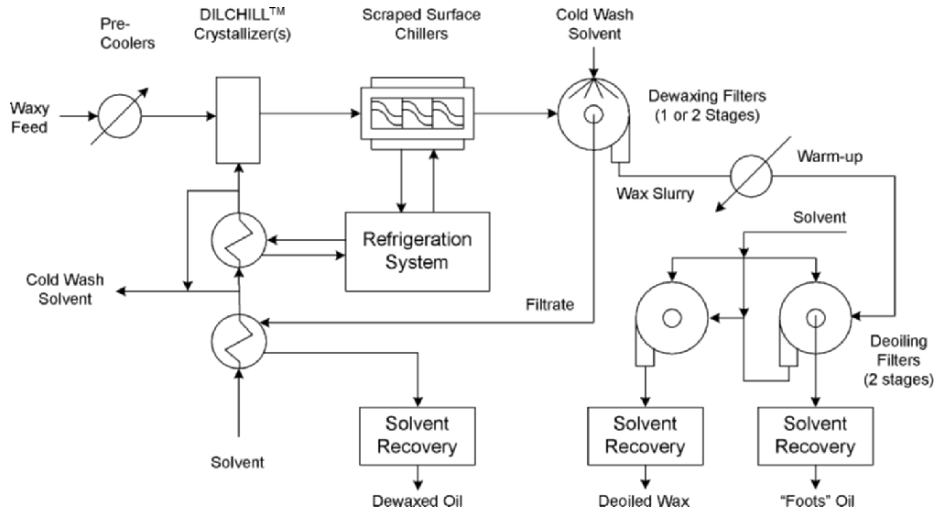


Figure 50. Simplified DILCHILL™ Dewaxing/Warm-up Deoiling Flow Diagram

DILCHILL™ dewaxing is ideally suited for Warm-up deoiling. The spherical nature of the crystals facilitates the melting of the softwax and re-crystallization is not required.

The Deoiling (Filtration) temperature in the deoiling plant is key to meeting final wax properties. As the temperature is increased the soft wax melts and is removed, leaving behind the higher melting, harder wax. Needle penetration decreases while melting point increases. The melting point and needle penetrations define the specification “box” for the manufacturer. Usually the “box” is wide enough that a range of Deoiling temperatures may be used that will produce a hard wax that meets all product specifications. In this case, the manufacturer will select the lowest deoiling temperature that will achieve the desired product properties, because this will give the manufacturer the maximum yield.

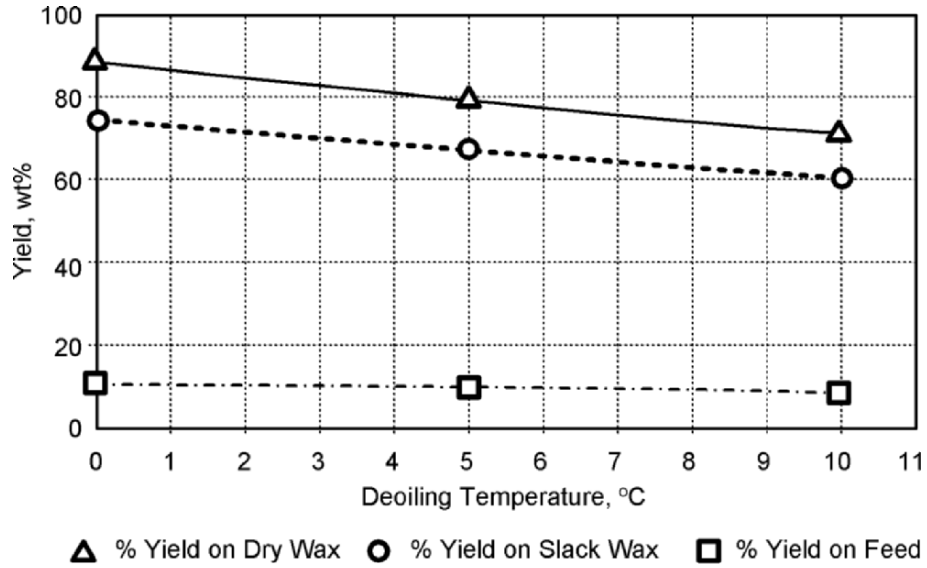


Figure 51. Typical Light Neutral Refined Wax Yields Versus Deoiling Temperature

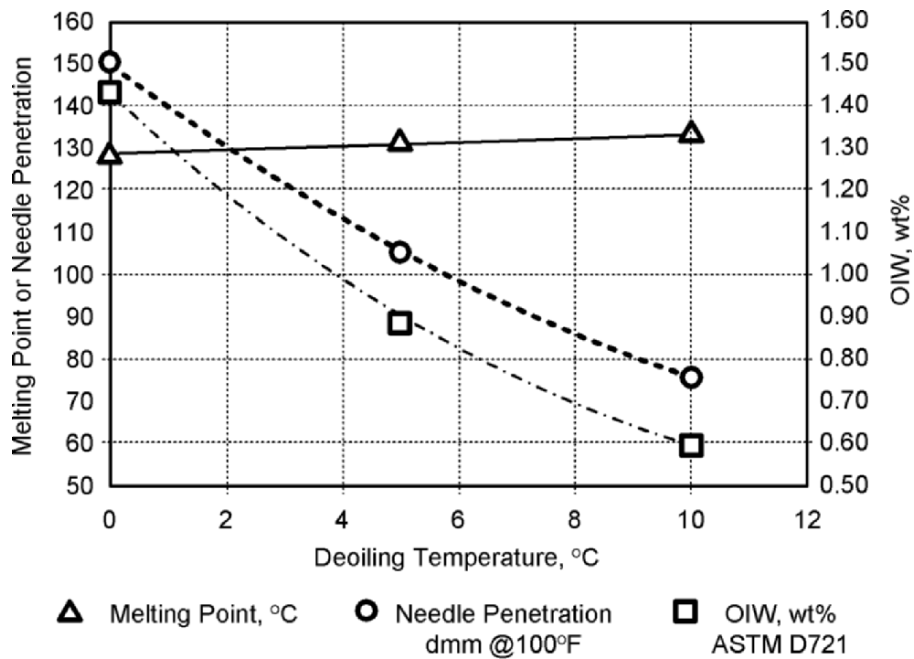


Figure 52. Typical Light Neutral Melting Point and Needle Penetration Versus Deoiling Temperature

Table 13. Comparison of Dewaxing, 2-Stage Dewaxing and Deoiling Heavy Neutral

| Yields, vol%         | 1-Stage Dewaxing | 2-Stage Dewaxing | 1-Stage Dewaxing<br>2-Stage Deoiling |
|----------------------|------------------|------------------|--------------------------------------|
| Dewaxed oil          | 68               | 73               | 68                                   |
| Slack Wax            | 32               | 27               | 0                                    |
| Soft Wax (Foots Oil) | 0                | 0                | 19                                   |
| Finished Wax         | 0                | 0                | 13                                   |

### 31. PROPANE DEWAXING

Propane dewaxing uses liquid propane as the solvent. Propane is normally a gas at ambient temperature and the vessels in the unit must be pressure vessels. This also includes the filter. Filtration in propane dewaxing is pressure filtration vs. ketone dewaxing which uses vacuum filtration. The propane temperature depends on the pressure, so that it is of paramount importance that the pressure be controlled. It is often said that in propane dewaxing propane is always either flashing or condensing. This adds an additional level of complexity that is not present in ketone dewaxing.

There are advantages and disadvantages to ketone vs. propane dewaxing. A brief comparison is shown below.

Table 14. Propane Vs. Ketone Dewaxing

|                       | Propane          | Ketone |
|-----------------------|------------------|--------|
| Higher filter rates   |                  |        |
| 150N                  | 30-50            | 7-9    |
| 600N                  | 18-30            | 4-5    |
| Bright stock          | 10-15            | 2-3    |
| Lower dilution ratios |                  |        |
| 150N                  | 1.2-1.6          | 2      |
| 600N                  | 1.4-2.0          | 3      |
| Bright stock          | 2-2.2            | 4      |
| Economics             |                  |        |
| Investment            | -40%             | base   |
| Utilities             | Less             | base   |
| Operating costs       | More             | base   |
| Pour point            | Limited to -15°C |        |
| 2-stage               | yes              | yes    |
| Deoiling              | yes              | yes    |



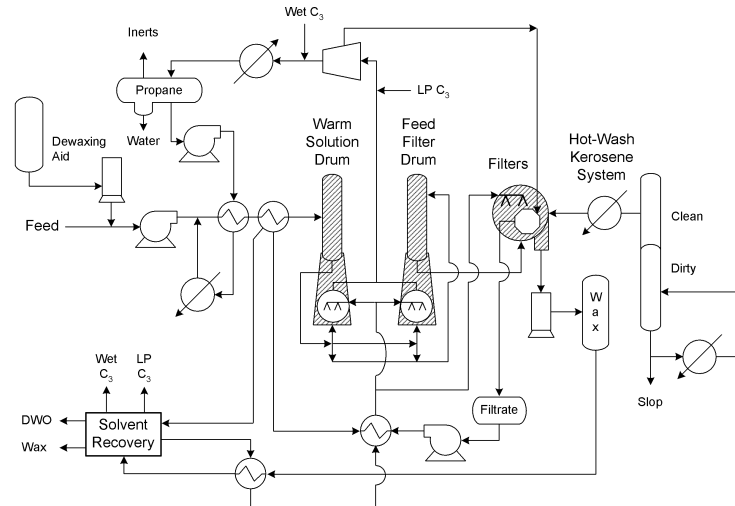


Figure 53. Simplified Propane Dewaxing Plan

Warm liquid propane is added to waxy raffinate and the slurry is prechilled in a shell and tube prechiller, with the slurry in the tube side. The Warm Dilution Ratio is controlled by the operator. Like the feed precooler in ketone dewaxing the outlet temperature of the prechillers is maintained just above the cloud point of the slurry to avoid fouling in the prechiller. Some newer designs use a prechiller tower.

The feed solution passes through the prechillers and into the warm solution drum. Up to this point the propane dewaxing process is a continuous process. The warm solution drum alternates feeding one of two chillers and the process now becomes a batch process.

Large batch chillers cylindrical (older) or spherical in design accept prechilled slurry from the warm solution drum and batch chilling begins. Pressure on the chiller is slowly released and the liquid propane evaporates, cooling the batch of slurry in the chiller.

In older plants control of the “vent gas” sets the chilling rate. This may be done with two pressure control valves (chiller vent valves). Advanced control and valve design has been successfully applied to allow adequate pressure control using a single valve.

Make-up propane is added to replace the vented propane so that at the end of the cycle the dilution in the slurry, the cold dilution ratio (CDR) is at the desired target. Similar to ketone dewaxing where the filtration rate depends on the solvent dilution to the filters, the filtration rate in propane dewaxing is dependent on the CDR that is also the dilution that will be seen at the filters. The CDR also has a big influence on the Pour point. Wax molecules are highly soluble in propane, more than Toluene. Increasing the CDR will carry more wax molecules into the filtrate and increase the pour point of the dewaxed oil. This requires the manufacturer to reduce the filtration

temperature (by reducing the filtration pressure) to compensate. Because of the large pour-filter spread that exists in propane dewaxing the base stock pour point is typically limited to -15. This is a drawback for the propane dewaxing process.

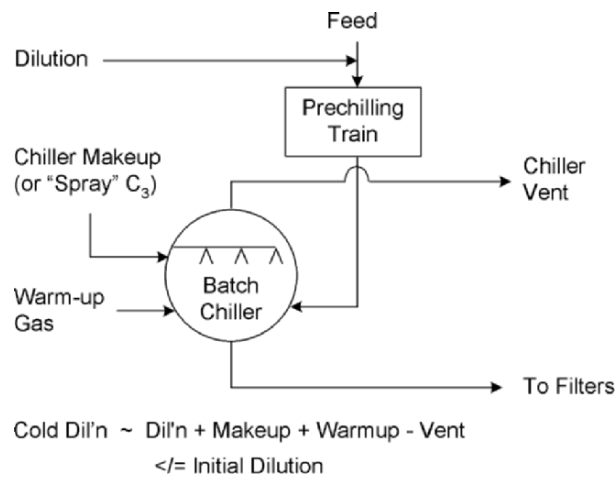


Figure 54. Simplified Propane Dewaxer Chilling Section

Slurry in the chiller is cooled to the target conditions and then the bath is transferred to the filter feed drum that provides holding capacity for the filters.

Under ideal conditions the transfer of the cold slurry would occur the moment after the chiller target temperature has been reached. In practice two conditions may exist. If the chiller final chill temperature has been reached and the filters are not ready to accept the new batch, then the slurry is held in the chiller and the slurry “waits” for the filters. This is referred to as “wait time”. If the filters are ready to accept the next batch of feed but the chiller has not reached its final chill temperature so that it is ready for transfer the filter levels will drop and the filters will be starved for feed. This is referred to as “starve time”. Chilled slurry is transferred to the filters. After transfer has been completed the chiller is warmed by pressuring with propane, which condenses on the walls of the chiller. The wall temperature is “warmed-up” to a high enough temperature so that when the prechilled slurry from the warm solution drum is fed to the chiller shock chilling at the wall will not occur. Warm-up takes time which limits production. The steps in the chiller cycle are:

1. Fill with prechilled slurry
2. Chill slurry to target temperature by venting propane, add make-up to make target CDR
3. Wait time for filters
4. Transfer slurry to filter feed drum
5. Warm-up

Total cycle times may range from 20 to 30 minutes.

Rotary Pressure filters are used to filter the slurry. Filtration rate is a function of the pressure drop across the filter. The temperature of the slurry also depends on the pressure. This requires carefully controlled pressure balance from the filter feed drum to the filters and to the filtrate drum. If the pressure in the filtrate drum is too high the temperature will be high and the resulting dewaxed oil pour point will be too high. If the filter pressure is not increased to maintain the Delta P then filtration rate will also be reduced.

Wax and propane and oil and propane are sent from the filters to their respective recovery sections. High pressure flash, low pressure flash, stripper and drier vessels are used to recover propane from the product.

### **31.1 Effect of Water**

Solvent “Drip Pipes” which are used to distribute the liquid propane wash over the wax cake in the filters, will foul if the water content in the propane is too high. The water freezes and will reduce the wash flow and/or may change the wash distribution. The Oil in Wax will increase and the overall dewaxed oil yield will drop. Methanol or acetone may be added to the propane to “de-ice” the drip pipes.

## **32. 2 -STAGE PROPANE DEWAXING**

Two stage dewaxing may be used to reduce the Oil in Wax and increase Dewaxed oil yield and to reduce solvent requirements. Repulp/repuddle propane is added to the slack wax from the first dewaxing stage. The slurry is pumped to the second stage filters. Control of the pressure balance is critical to avoid shock chilling and second stage bog-downs that will limit plant throughput. Second stage filtrate may be used as first stage wash or as dilution.

### **32.1 Propane Deoiling**

Propane deoiling is accomplished using high pressure filters that are required to handle the higher temperatures that must be used to melt the softwax. The finished wax produced from deoiling is a valuable by-product and margins may at times exceed dewaxed oil margins.

### **32.2 Propane Filter Washing with Hot Kerosene**

Temperatures required to successfully melt the wax from the filter cloth do not allow the use of liquefied propane due to the very high pressure required.

Instead kerosene is used to wash the filters. Kero wash temperature is typically controlled. If the wash temperature is too low the wax crystals will not be melted, and if the wash temperature is too high wire migration will increase leading to reduced wire life and/or more frequent wire retensioning.

### 33. DEWAXING AIDS

DeWaxing Aids (DWA) may be used in ketone dewaxing but are always used in propane dewaxing. Typically the DWA doses used in propane plants are 2-3 times higher than in ketone plants. While DWAs are economically justified for use on all grades in the propane plant, performance on light neutrals in ketone plants has typically not been economically justified.

DWAs are expensive and may represent the single largest controllable operating expense in the propane plant. Filtration rates in the propane plant may be improved from a level that is almost inoperable to several times the highest rate experienced in the ketone dewaxing plant. Oil in wax may be greatly reduced, increasing overall yield and enhancing the wax product value.

DeWaxing Aids (DWA) are required to achieve high filtration rates in propane dewaxing. Typically a dewaxing aid consists of a polymer backbone with alkyl side chains. Factors affecting the DWA performance include:

1. Raffinate Feed
2. Polymer “backbone” chemistry
3. Molecular weight, number distribution
4. Side chain distribution
5. Active Ingredient
6. DWA ratio (when combined with other additives) in blend
7. DWA dose, the concentration used
8. Asphaltene contamination
9. Regulatory Requirements (FDA approval)

Major DWA Polymer Backbone Chemistries include:

1. Poly Alkyl Methyl Acrylate (PAMA)
2. Poly Alkyl Acrylate (PAA)
3. Co-Polymerization of PAMA, PAA
4. Di Alkyl Fumerate Vinyl Acetate (DAFVA)
5. Ethylene Vinyl Acetate (EVA)
6. Wax Naphthalene Condensate

Molecular weights of the DWA may vary from 10,000 to 1,000,000. Molecular number, the “branchiness” may range from 7,000 to 300,000. Side chain lengths may vary from C<sub>14</sub>-C<sub>26</sub> and with various distributions.

Active ingredient may range from 10-100% with 15-30 most typical. Dewaxed oil (Light or Heavy Neutral) or toluene may be used as diluent. DWA viscosity will depend on the active ingredient, and the diluent and the viscosities can be quite high and may affect pumpability.

Typically DWA is stored at elevated temperatures. Positive displacement or centrifugal pumps are used for injection and various meters may be used to monitor the flow rate. Mass flow meters have been used with great success in the application.

### 34. DWA MECHANISM

The exact mechanism of how the Dewaxing aid works is still being studied. Leading theories include:

1. Co-crystallization of the DWA into the wax crystal matrix that changes growth direction of crystal planes
2. Agglomeration Mechanism
3. Wax Crystal Modifier that associates with the surface to change crystal growth plane

Studies have shown that DWAs may be combined to give synergistic performance. Currently, because of the large number of variables (feed, DWA chemistry, etc.) it is not possible to predict DWA performance a-priori and DWAs must be tested in a pilot plant that can simulate the propane dewaxing process. Lab and analytical tests typically over predict DWA performance due to favorable conditions of the lab and inability to simulate the plant.

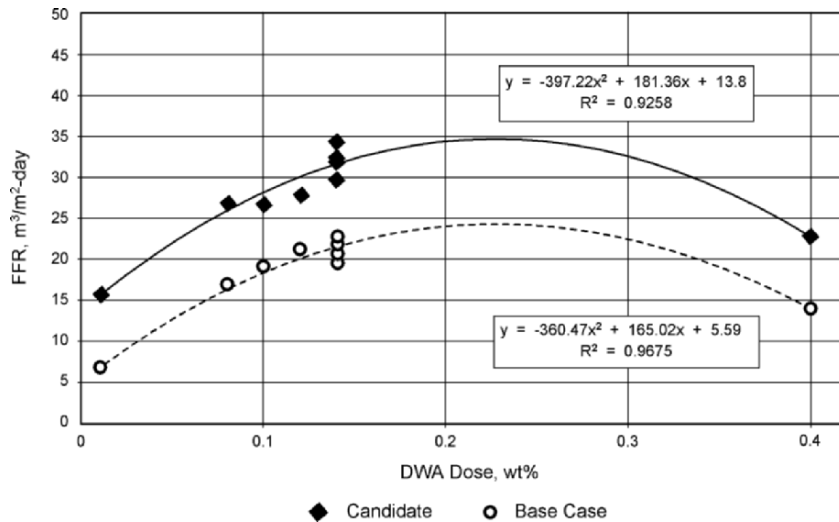


Figure 55. Light Neutral DWA Dose Response Curve, DWA Ratio 1:1

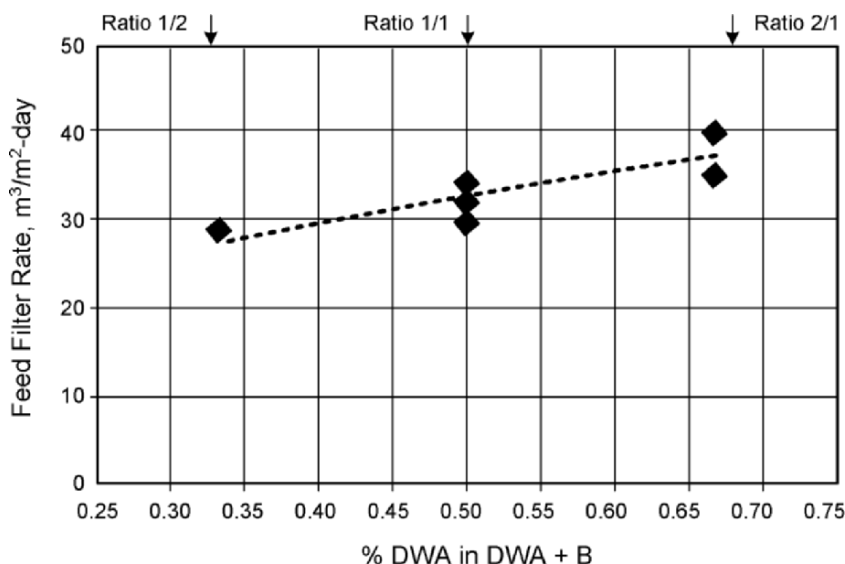


Figure 56. Effect of DWA Ratio on Light Neutral

### 35. ASPHALTENE CONTAMINATION

The presence of asphaltenes in the feed to the propane dewaxer or in the propane will significantly reduce the filtration rate and must be avoided. Asphaltenes may be present in the heavy neutral due to entrainment from the VPS section below the heavy sidestream drawoff. Contamination may occur if the lube deasphalting unit (LDU) and propane dewaxer share propane.

### 36. REGULATORY REQUIREMENTS

The manufacturer using DWAs must determine if a FDA approved DWA is required in their product market. The number of DWAs meeting FDA technical requirements is small and these DWAs command a premium in the marketplace. The qualification of new DWAs is expensive and takes a long time. DWA chemistry type, Molecular weight (Mw), Molecular number (Mn), PolyDispersity (PDI = Mw/Mn), unreacted monomer concentration and concentration in the final product are some of the major factors the FDA considers and the candidate must pass technical specifications in these areas in order to obtain approval.

Table 15. Analytical Tests in Dewaxing

| TEST                             | ASTM Test No                               | APPLICATION  |
|----------------------------------|--|--|
| Pour Point                       | D 97, D 5949,<br>D 5950, D 5985,<br>D 6749 | Key specification for dewaxed oil  |
| Oil-in-wax %                     | D 721, D 3235                              | Wax specification, measure of yield performance                              |
| RI @ T °C                        | D 1218                                     | Yield calculation, solvent composition                                       |
| Miscibility Curve                |  | Used to set solvent composition for each stock to avoid immiscible operation |
| Gas Chromatographic Distillation | D 2887                                     | GCDs may be for troubleshooting and predicting dewaxing performance          |
| Feed Cloud Point                 | D 2500, D5551<br>D 5771, D 5772,<br>D 7773 | Helps set feed precooler outlet temperature                                  |
| Water-in-Solvent                 | D 6304-03,<br>E 203-1                      | Excess water may lead to immiscible operation and icing of solvent chillers  |

### 37. GLOSSARY

|                  |  |
|------------------|--|
| Aromatic         | An unsaturated ring compound having a basic 6-carbon-atom ring with either a hydrogen atom or a chain joined to each carbon atom.  |
| API              | American Petroleum Institute   |
| ATF              | Automatic transmission fluid   |
| Base oil         | “A base oil is the base stock or blend of base stocks used in API licensed oil “ (See API 1509)  |
| Base stock       | “A base stock is a lubricant component that is produced by a single manufacturer to the same specifications (independent of feed source or manufacturer’s location); that meets the same manufacturer’s specification; and that is identified by a unique formula, product identification number, or both.” (See API 1509) |
| Base stock slate | “A base stock slate is a product line of base stocks that have different viscosities but are in the same base stock grouping and from the same manufacturer.” (See API 1509)   |
| Batch            | Any quantity of material handled or considered as a unit in processing.  |
| Batch treat      | A treatment of a limited quantity of material with chemicals or solvent to improve quality.  |
| Blowback         | The term applied to blowgas usage. Blowback Gas used to “blow” the wax cake from the filter cloth by being applied under pressure beneath the cloth  |

|                     |  |
|---------------------|--|
| Bright Stock        | A Vacuum Distillation Tower Bottoms that has been deasphalted and extracted or hydrotreated and probably dewaxed as a heavy Base stock   |
| Caulking Grooves    | “U-shape” piece of metal welded to the drum deck. The resultant “grooves” are used with “caulking bars” that hold the filter cloth in place on the surface of the filter drum. The grooves are slightly slanted inward at the top to provide tension on the bar and help hold the caulking bar in the groove. The upper edges of the U shape are lipped to provide an edge to retain the grid on which the filter cloth rests. |
| CCR                 | Conradson Carbon Residue   |
| Controlled Chillers | SSE using cold filtrate to cool the slurry   |
| Carryover           | Term in solvent extratic which refers to entrainment of heavy phase into the light phase and out with the raffinate solution (essentially solvent at the tower top).   |
| Carryunder          | Term in solvent extratic which refers to entrainment of light phase which has not settled from the heavy phase and exits with the extract solution (essentially feed at the tower bottom).   |
| Centistoke          | The worldwide unit of kinematic viscosity.   |
| Coalescence Rate    | Relative rate at which fine, small droplets form larger droplets, which settle faster, forming a clarified oil layer.  |
| Continuous Phase    | Heavy, NMP-rich phase which forms an unbroken stream through the treater in solvent extraction.  |
| Corrosion           | The gradual eating away of metallic surfaces as the result of oxidation or other chemical action. It is caused by acids or other corrosive agents.   |
| Crystallization     | May be defined as a phase change in which a crystalline product is obtained from a solution  |
| Cut                 | The portion or fraction of a crude oil boiling within certain temperature limits.  |
| Cut point           | The temperature limit of a cut or fraction, usually but not limited to a true boiling point basis.   |
| DAO                 | Deasphalted Oil: The extract or residual oil from which asphalt and resins have been removed by an extractive precipitation process called deasphalting.   |
| DAU                 | DeAsphalting Unit: A process for removing asphalt from reduced crude or vacuum residua (residual oil) which utilizes the different solubilities of asphaltic and nonasphaltic constituents in light hydrocarbon liquids, e.g., liquid propane.   |
| Density             | The mass of a unit volume of a substance.  |



|                       |  |
|-----------------------|--|
| Deck Pipes            | Each segment of a dewaxing filter is drained by a series of pipes located along side each caulking groove  |
| DILCHILL™             | DILution CHILLing. ExxonMobil process where chilled solvent is added stagewise to an agitated tower. Mixing, cooling and crystallization occur in the tower  |
| Dilution Ratio        | Term used in solvent dewaxing to refer to the ratio of solvent to waxy raffinate feed (vol/vol)  |
| Dispersed Phase       | Light, oil-rich phase which “bubbles” through continuous phase, then settles, and repeats the process on each tray in solvent extraction.  |
| Distillate            | Product of distillation collected by passing vapors through a condenser.   |
| DPC                   | Double Pipe Chiller  |
| DPE                   | Double Pipe Exchanger  |
| Drum                  | The horizontal drum on which the filter cloth is applied to its circumference surface in solvent dewaxing.   |
| Dry Wax               | The solid component present in a waxy feed at a certain oil pour point if all oil were removed from it   |
| DWO                   | DeWaxed Oil  |
| Entrainment           | Entrainment is the carryover of liquid by the vapor phase. Liquid may be in the form of a spray, foam or mist.   |
| EXOLFINING™           | An ExxonMobil® extraction process used to extract aromatics from lube feedstocks to improve the viscosity index and quality of lubricating oil base stocks, integrated with HYDROFINING                                  |
| Extract               | In solvent refining processes, that portion of the oil which is dissolved in and removed by the selective solvent; the solvent rich phase. Contains a low percentage of oil which is typically high in aromatic content. |
| Extraction            | The process of separating a material, by means of a solvent, into a fraction soluble in the solvent and an insoluble residue.  |
| Feed Retention Drum   | Feed solution hold up drum   |
| Feed Solution         | Waxy feed plus warm propane in propane dewaxing.   |
| FFR                   | Feed Filter Rate ( $M^3/day/M^2$ of filter cloth). Refers to feed only in solvent dewaxing.  |
| Filter Cloth Blinding | Term applied to the reduction in filter rate due to wax or ice particles plugging up the flow paths in the filter cloth  |
| Filter Hood           | The top part of the filter outer enclosure   |

|                        |  |
|------------------------|--|
| Filtrate (or Wet) Port | The section or nozzle on the master valve that collects filtrate from the vat slurry   |
| Filtrate               | Liquid product (oil plus solvent) in solvent dewaxing.   |
| Final Dilution         | The last increment of solvent added after the shock chillers in incremental dilution solvent dewaxing.   |
| Foots Oil              | The soft wax melted or dissolved/washed away during wax deoiling. In the old days, it was the oil drawn from the bottom (foot) of a pan separator for the wax formed in a wax “sweater”.       |
| Fractionation          | Fractionation is the separation of light and heavy fractions in the distillation tower.  |
| Furfural               | An aldehyde obtained from corn shucks, wheat, or oat hulls, used in an extraction process for removing aromatic, naphthenic, olefinic and unstable hydrocarbons from a lubricating oil charge. |
| Haze                   | Visible, uncombined or flocculated, wax or water in Dewaxed Oil  |
| Hot Wash               | The technique or the hot solvent used to periodically melt and dissolve wax out of the filter cloth  |
| Immiscible             | Two separate phases, one oil rich and one solvent rich, which will not mutually dissolve. Normally not desirable in solvent dewaxing   |
| Incremental Dilution   | Refers to the addition of solvent, in increments to the waxy raffinate feed as it flows through the heat exchanger equipment leading to the solvent dewaxing filters.                          |
| Internal Reflux        | Portion of the light phase which springs from the heavy phase due to lower temperature at treater bottoms, and recycles back up the tower in the dispersed phase of solvent extraction.        |
| Kinematic viscosity    | The ratio of the absolute viscosity of a liquid to its specific gravity at the temperature at which the viscosity is measured.   |
| L/S                    | Liquids to solids ratio in the wax cake. The liquids consist of oil and solvent OR liquids to solids in the filter vat   |
| LHU                    | Lube Hydrofining unit to improve color stability of lube oils using hydrogen   |
| Lead Pipes             | The pipes on the leading side of each segment as the drum rotates  |
| Lubricant              | Any substance interposed between two surfaces in relation to motion for the purpose of reducing the friction and/or the wear between them.   |
| LPS                    | Low Pressure Steam   |

|                         |  |
|-------------------------|--|
| LVPS                    | Lubes Vacuum PipeStill   |
| Master Valve            | Trunnion Valve, The stationary sectioned casting in contact with the rotating end of the drum (i.e., the wear plate) at which the lead and trail pipe manifolds are dead-ended in solvent dewaxing filtration. |
| MEK                     | Methyl Ethyl Ketone or loose term for ketone dewaxing unit   |
| MEK OIW Test            | Oil content of wax using ASTM D921 (MEK solvent at -25°F)  |
| MIBK                    | Methyl IsoButyl Ketone   |
| Miscible                | Two or more liquids which mix to form one homogeneous phase. Usually preferred in solvent dewaxing. Refers to oil and solvent mixture  |
| Miscibility temperature | Temperature at which solvent and feed are completely miscible - all feed dissolved in solvent - and there is no phase separation in treater tower or in dewaxer slurry.  |
| MPS                     | Medium Pressure Steam  |
| NMP                     | N-methyl-2-pyrrolidone, a solvent used as an alternate to furfural and phenol for the extraction of lubricating oil fractions.   |
| Naphthene               | A group of cyclic hydrocarbons also termed cycloparaffins. Polycyclic members are also found in the higher boiling fractions.  |
| Naphthenic crudes       | Class designation of crude oils containing predominantly naphthenes or asphaltic compounds.  |
| Neutral                 | A VPS distillate, extracted and dewaxed, made into a Base stock  |
| Normal paraffin         | A straight chain hydrocarbon in which no carbon atom is united with more than two other carbon atoms.  |
| Pale oil                | A petroleum lubricating or process oil refined until its color is straw to pale yellow.  |
| Paraffin-base crudes    | Crude containing paraffin wax and practically no asphalt or naphthenes.  |
| Paraffinic              | Describing the paraffin nature or composition of crude petroleum or products therefrom.  |
| Paraffins               | A homologous series of open-chain saturated hydrocarbons of the general formula $C_nH_{2n+2}$ of which methane ( $CH_4$ ) is the first member.   |
| Paraffin wax            | A colorless wax extracted from paraffin-base lubricating oils. Typically solid at room temperature.  |
| PDU                     | Propane Dewaxing Unit to remove wax from oil using propane as a solvent  |

|                                 |   |
|---------------------------------|---|
| PNA                             | PolyNuclear Aromatic. A compound composed of two or more aromatic rings (see aromatic). These compounds may impart unwanted color, cause stability problems and are classified as carcinogens.                                      |
| Polarity                        | A measure of the asymmetric distribution of a molecule's electrical charge. MEK>MIBK>H <sub>2</sub> O   |
| Pour Point                      | The temperature at which oil will not pour  |
| Pre-dilution                    | Solvent addition occurring before the precoolers. Sometimes called primary dilution.  |
| Prechillers                     | In propane dewaxing, Shell and Tube exchangers that chill the feed solution before batch chillers   |
| Raffinate                       | In solvent-refining practice, that portion of the oil which remains undissolved and is not removed by the selective solvent; the solvent lean phase. Contains a low percentage of solvent and typically a low aromatic content oil. |
| Rectification                   | Rectification is the removal of heavy material from the vapor phase in fractionation.   |
| Saybolt Universal Seconds (SUS) | A measure of kinematic viscosity, expressed as the time in seconds for 60 ml of fluid to flow through a standard Saybolt Universal viscometer at a specified temperature. ASTM Method D-88 describes the method and apparatus.      |
| Scale Wax                       | Wax with an oil content of 1-5%, e.g. Wax from a 2-stage dewaxer  |
| Segment                         | Each solvent dewaxing filter drum segment is made up of a pair of the caulking grooves running longitudinally on the drum deck with the grid in between   |
| Selectivity                     | A measure of the ability of a solvent to separate compounds of different structure, e.g. aromatics from paraffins from naphthenes.  |
| Service factor                  | A quantity which relates the actual on-stream time of a process unit to the total time available for use of the unit. Frequently a ratio of the number of actual operating days divided by 365.                                     |
| Settling Rate                   | Rate at which droplets of the dispersed phase rise through and separate from the continuous phase.  |
| Shock Chillers                  | Double pipe exchangers (see SSE) that use propane or propylene as a refrigerant in solvent dewaxing. Rapid cooling rates (>2%/min) "shock" the slurry resulting in smaller crystals and lower FFR.                                  |

|                           |  |
|---------------------------|--|
| Shock Chilling            | Rapid uncontrolled crystallization, characterized by high nucleation rates producing very small average crystal size.  |
| Slack Wax                 | Wax with an oil content >5%, e.g. Wax from a 1-Stage Dewaxer   |
| Solubility                | Degree to which the oil (especially the aromatic fraction) dissolves in the solvent. This is a function of aromatic type and concentration, changes from one grade to another as well as for the same grade from one crude to another, for a given solvent.  |
| Solvent neutral oil (SNO) | A paraffinic base oil which has been solvent refined, dewaxed, and finished and is ready to be used in blending or compounding.  |
| SSC                       | Scraped Surface Chiller. Usually a double pipe design of 6, 8, 12 inch diameter with internal scrapers to remove wax from the cold walls. Typically a refrigerant such as propane, propylene or ammonia is used on shell side. Used in conventional dewaxing |
| SSE                       | Scraped Surface Exchanger. Usually a double pipe design of 6, 8, 12 inch diameter with internal scrapers to remove wax from the cold walls. Typically cold filtrate is used on shell side. Used in conventional dewaxing                                     |
| SSU                       | See Saybolt Universal Seconds.   |
| Stability                 | Resistance to chemical change.   |
| Stripping                 | Stripping is the removal of light material from the liquid phase.  |
| TAN                       | Total Acid Number  |
| Third Phasing             | Immiscible condition in a dewaxer where you have two liquid phases and a solid (wax phase)   |
| Trail (or Lag) Pipes      | The pipes on the trailing side of each segment as the drum rotates   |
| Trunnion Valve            | Master Valve, the stationary sectioned casting in contact with the rotating end of the drum (i.e., the wear plate) at which the lead and trail pipe manifolds are dead-ended   |
| Vat                       | The bottom part of the filter outer enclosure into which the filter feed slurry flows  |
| Viscosity Index           | A measure of the change in viscosity with temperature; ASTM D-2270.  |
| VPS (VDU)                 | Fractionation equipment, a vacuum pipestill (VPS) or vacuum distillation unit (VDU) is used to distill atmospheric bottoms into gas oil or lube distillate cuts.   |

|                         |   |
|-------------------------|---|
| VTB                     | Vacuum tower (VPS/VDU) bottoms, or vacuum residue or vacuum resid   |
| Warm-up                 | A step in the batch chiller sequence during which the chiller internal metal wall is warmed in preparation of accepting feed, and avoiding shock chilling at the wall                           |
| Warm Solution Drum Wash | Drum containing prechilled feed solution<br>Generally the term used for the cold solvent applied to the wax cake in solvent dewaxing.   |
| Wax Cake                | A cake formed on the surface of the filter in solvent dewaxing. Typically consists of a Liquids (solvent plus oil) to Solids (oil free wax) ratio of 2-10. Wax Doctor Knife dislodges the cake. |
| Wax, Refined            | Wax of, usually, 0.5-2% oil-in-wax produced from deoiling   |
| Wax, Scale              | Wax of, usually, 2-10% oil-in-wax produced from two stage dewaxing.   |
| Wax Scroll              | The screw conveyor rotating in the wax trough. All scrolls in dewaxing service are the center- discharge type   |
| Wax, Slack              | Wax of, usually, <10% oil-in-wax produced from one stage dewaxing.  |
| Wax Trough              | The semi-circular channel that the wax cake falls into after blow gas dislodges it and into which the wax doctor knife deflects it  |

### 38. ACKNOWLEDGEMENTS

A Special Editorial thanks to Mike Davis and XB Cox at ExxonMobil Research and Engineering Co., for their comprehensive detailed review and recommendations.

Special thanks to ExxonMobil employees and annuitants: Bob Aupperlee, Doug Boate, Joe Boyle, Barry Deane, Sasha Glivicky, Dave Mentzer, Dominick Mazzone, Chuck Quinlan, Ken Del Rossi, Evelino Ruibal, Dave Sinclair, Bernie Slade, and Howard Spencer.

### 39. REFERENCES AND ADDITIONAL READINGS

1. Butler, R. M.; Tiedje, J. L. "The Washing of Wax Filter Cakes," *Can. J. Technol.* **1957**, *3(1)*, 455-467.
2. Citarella, V. A.; Ruibal, E. A.; Zaczepinski, S.; Beasley, B. E. "Crystallization Technique to Simplify Dewaxing", *Pet. Technol. Quarterly*, Winter **1999/2000**; pp. 37-43.
3. Klamann, D. *Lubricants and Related Products*, Verlag Chemie GmbH, D-6940: Weinheim, 1984.

4. Sequeira, A. "Lubricant Baseoil and Wax Production", Marcel Dekker: New York, 1994.
5. Fiocco R.J. "Development of the Cascade Weir Tray for Extraction", *AIChE Symposium Series, New Developments in Liquid-Liquid Extraction*, ISEC 83, **1984**, 80, 89-93.
6. Sankey, B. M. et al. "EXOL N:New Lubricants Extraction Process", *Proc. Tenth World Petroleum Congress*, **1979**, 4, 407-14.
7. Bushnell, J.D.; Fiocco, R.J. "Engineering Aspects of the Exol N Lube Extraction Process", *Proc. - Refining Department American Petroleum Institute*, **1980**, 59, 159-67.
8. Sankey, B.M. "A New Lubricants Extraction Process", *Can. J. Chem. Eng.*, **1985**, 63, 3-7.
9. Davis, M. B. et al. "The EXOL N Extraction Process - Flexibility and High Efficiency to Meet Modern Lubes Product Requirements", *Advances in Production and Application of Lube Base Stocks*, Indian Institute of Petroleum, Nov. 23-5, 1994, Tata McGraw Hill, New Delhi, India, pp. 24-32.
10. Gudelis et al. "Improvements in Dewaxing Technology", *American Petroleum Institute Proceedings - Division of Refining*, **1973**, 53, 725-37.
11. Bushnell, J. D.; Eagan, J. F., "Commercial Experience with DILCHILL™ Dewaxing", paper F&L-75-50, 1975, NPRA Fuels and Lubricants Meeting, Sept., 11-12, 1975, Houston, Texas,
12. Gudelis, D. A. et al, "New Route to Better Wax", *Hydrocarbon Process.*, **1973**, 52(9), 141-6.
13. Wax HYDROFINING™, *Pet./Chem. Eng*, **1970**, 42(9), p. 36.
14. *The Exxon Wax HYDROFINING™ Process*, Exxon Research and Engineering Co, Technology Licensing Division, February, 1986.
15. Eagen, J.F., et al., "Successful Development of Two New Lubricating Oil Dewaxing Processes", *Proc. Ninth World Petroleum Congress*, Vol. 5, Applied Science: London, 1975; pp. 345-357.
16. *Engine Oil Licensing and Certification System*, American Petroleum Institute, API 1509, Fifteenth Edition, April 2002.
17. R.R. Savory, "Chaper 11: Base Oil Processes", *Modern Petroleum Technology, Volume 2 Downstream*, The Institute of Petroleum, John Wiley and Sons, 2000.
18. B.C. Deane, "Chapter 25: Base Oil Quality", *Modern Petroleum Technology, Volume 2 Downstream*, The Institute of Petroleum, John Wiley and Sons, 2000.

## Chapter 16

# SELECTIVE HYDROPROCESSING FOR NEW LUBRICANT STANDARDS

I. A. Cody

*ExxonMobil Research and Engineering Co*

*Process Research Laboratories*

*Baton Rouge, LA 70805*

## 1. INTRODUCTION

World basestock demand is expected to remain steady or rise only slightly in the next decade, but the nature of basestocks is anticipated to change dramatically, primarily driven by tougher specifications for automotive lubricants.<sup>1,2</sup> Automobile manufacturers continue to seek lubricants that provide better fuel economy, lower emissions and longer life; for the refiner this means producing basestocks with lower viscosity, lower volatility and higher saturates content. Lower viscosity of the formulated oil can improve both cold start performance and fuel economy by reducing friction in the engine. Lower volatility directly lowers emissions and minimizes oil thickening, extending oil change intervals.<sup>3,4</sup> Also, with less volatiles there is less stress on catalytic converters. Higher saturates can help make oils more stable by lessening oxidation, thereby extending service. These trends in formulated oil performance present difficulties to the refiner in making suitable basestocks for these formulations using conventional processing strategies. For example, lower viscosity cannot be achieved merely by cutting a lighter stock because that would increase volatility. Conversely, cutting deeper to resolve volatility adversely affects fluidity and fuel economy. Separations-based processing alone can be inadequate because the hydrocarbon molecules with the required properties are not abundant in many of the mineral crudes refined today. Accordingly, many lube refiners have elected to incorporate new conversion technologies<sup>5</sup> to boost populations of the desired molecules by selectively transforming the indigenous hydrocarbons. At the same time, some of the largest oil companies are poised



to invest in “Gas-to Liquids” (GTL) technologies that can produce basestocks with excellent properties. This chapter describes some of the current and future hydroprocessing technology that can generate basestocks capable of meeting the new standards in lubricant quality.

Until recently, improvements in standards for passenger vehicle lubricants (PVL’s) and commercial vehicle lubricants (CVL’s) were achieved largely with the use of better additives, such as anti-oxidants, antiwear agents, detergents, and viscosity improvers. In the 1990’s that began to change as the equipment manufacturers accelerated efforts to improve automotive performance (see Table 1). Additives alone have not been able to address the new requirements, resulting in dramatic changes to basestock properties and consequent refining strategies.

*Table 1. Evolution of Multi-Grade PVL’s*

|                  |                      |   |
|------------------|----------------------|---|
| 1930             | API/SA               | Mineral Oil + castor oil<br>No/few additives<br>No performance requirements   |
| 1950s            | API/SB               | Antioxidants, antiwear introduced<br>Take head off to “de-coke” engine after 20,000 miles   |
| 1960s            | API/SC               | Detergency to control high temperature deposits<br>Multi-grade introduced   |
| 1964-1980s       | API/SC to SG         | Tripartite of ASTM.SAE/API control quality<br>Requirements (new additive technology)  |
| 1990-<br>present | GF, CF<br>Categories | Rapid change, Equipment manufacturers control quality<br>targets (better basestocks for e.g. fuel efficiency, reduced<br>emissions) |

A simple measure of the impact on basestocks resulting from changing engine oil specifications is the empirical property of viscosity index (VI). For example, in North America in the past decade, SAE 5W-30 oils have required the light basestock VI target to increase from about 100 to 115 due to the progressively tougher ILSAC, GF-1, GF-2 and GF-3 standards. This target is achievable only in low yield from most crudes by the conventional, separations based, processing steps of vacuum distillation, solvent extraction, and solvent dewaxing. Similar trends have occurred with ACEA requirements in Europe.

VI is a convenient guide to low temperature viscosity and volatility, properties that really underpin automotive oil performance. This is illustrated in Figure 1. Basestocks meeting the 5W specification have a kinematic viscosity of about 4 to 4.5 cSt at 100c, and, until the 1990’s, the acceptable limit of formulated oil volatility for this grade was as high as 30 wt%, as measured by the Noack volatility test.<sup>6</sup> Basestocks with about 95 VI could be blended to this target and at the same time stay below the maximum allowable low temperature dynamic viscosity limit for a 5W- oil. However, in subsequent years, the industry impetus to reduce volatility while maintaining low kinematic and dynamic viscosity has resulted in ever higher VI

basestocks to achieve GF-1, then GF-2, and now GF-3. Today, with a 5W formulated oil volatility of 15 wt % Noack, basestocks suitable for GF-3 require about 115 VI. Further changes in basestock quality are expected in 2003 with the introduction of GF-4.

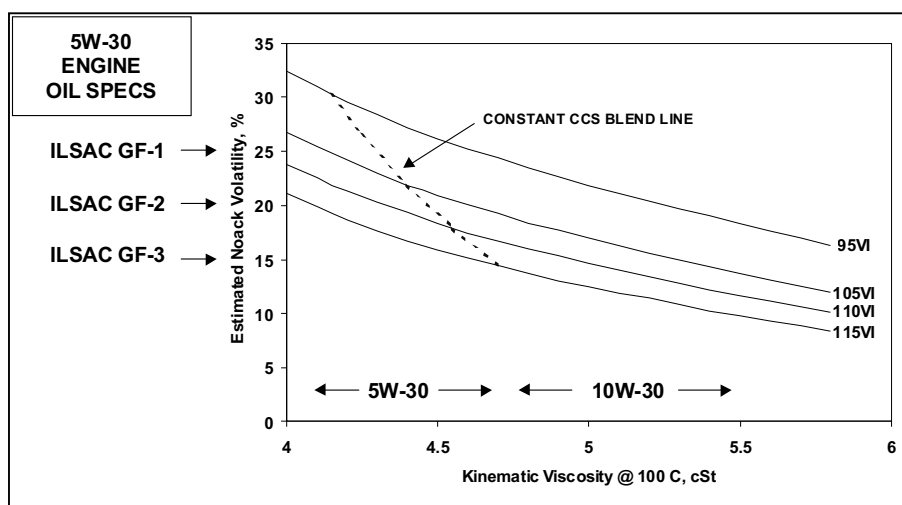


Figure 1. Higher VI basestocks required to blend lower volatility engine oils (from reference 3)

Basestocks with higher VI provide value to the formulator in two ways: the “volatility@viscosity” relationship is better and at the same time the low temperature viscometric properties are improved. The sloping blendline in Figure 1 shows that the same low temperature Cold Cranking Simulator (CCS) viscosity value is achieved at higher kinematic viscosity when the basestock VI is higher. This allows the refiner the additional flexibility to cut a basestock with higher kinematic viscosity, still meeting the CCS target and lowering volatility even further.

Refiners have only two ways to tailor basestock volatility while holding viscosity constant. One is tighter fractionation: by narrowing the boiling range distribution of a basestock, populations of low boiling hydrocarbons are minimized and volatility is accordingly improved. Since the mid-boiling point remains constant, the volatility@viscosity relationship is also improved. However, this strategy has limited value because volatility improvements are ultimately dictated by the nature of the molecules within the boiling range envelope. Step improvements in volatility@viscosity can only be achieved by raising VI.

This is evident in Figure 2, which shows the relationship between boiling point (and the associated Noack volatility) for a basestock with a typical boiling range distribution versus kinematic viscosity. Each curve represents a class of lube hydrocarbons that have been assayed into fractions with viscosities spanning the typical lube range of 10 to 1000 cSt at 40°C

(corresponding to light basestocks to Brightstocks derived from vacuum tower bottoms). Boiling point rises (and volatility falls) as viscosity increases for a given hydrocarbon class. But to raise boiling point while maintaining viscosity requires a shift to a new class, linked to a higher VI. For example, at 30 cSt @ 40°C a basestock with 100 VI has a mid boiling point around 425°C, i.e. about 15 wt% Noack volatility, whereas a basestock of the same 40°C viscosity with 140 VI has a mid-boiling point of about 465°C, fully 40°C higher boiling point. This corresponds to a Noack volatility of less than 12 wt%.

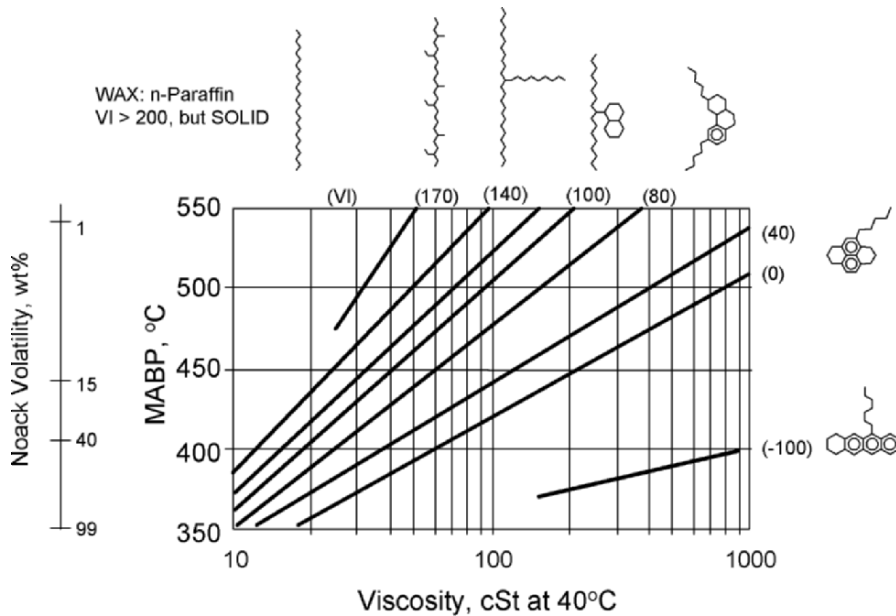


Figure 2. Isoparaffin molecules needed for better volatility (from reference 10)

Viewed in the context of the specification changes discussed above, while 100 VI was sufficient to achieve 15 wt% Noack volatility in a 10W type PVL, i.e. with basestock viscosity around 30 cSt, 115 VI or greater is needed to achieve that same volatility standard in a 5W formulation at 25 cSt. The molecular implications of VI improvement associated with increasing boiling point while fixing viscosity are shown in the perimeter of the chart: the basestocks must comprise hydrocarbons that have regions of more paraffinic character with fewer ring clusters, either naphthenic or aromatic. Ultimately, straight chain normal paraffins have the best volatility@viscosity characteristic, but, since they also have high melting points (i.e. are waxes), they are unsuitable for use in automotive lubricants across the full temperature range of application. From a purely viscometric and boiling point perspective, the most attractive hydrocarbons for lubrication are the lightly branched isoparaffins.

In large part, hydroprocessing technology has been introduced to make basestocks with higher boiling point for a given viscosity by selectively boosting the population of isoparaffins with catalytic methods that eliminate or convert ring species and/or that isomerize normal paraffins. An associated benefit of hydroprocessing is that aromatic ring species become saturated, contributing to an overall improvement in oxidation performance of the finished oil.

Hydroprocessing is the means by which refiners are now producing basestocks with higher saturates and VI, typified by the API basestock categories, Group II and III, see Table 2.

Group IV basestock, typified by polyalphaolefins, derived from the oligomerization of selected olefins, represent the pinnacle of basestock performance, but, because of their high cost to manufacture, have so far occupied only a small niche in top tier.

Lower cost Group III basestocks, particularly those derived from GTL, are expected to partially displace PAO's.

Table 2. American Petroleum Institute (API) Basestock Categories

| API Group | Sats |        | Sulfur | VI     | Typical Manufacturing Process          |
|-----------|------|--------|--------|--------|--|
| I         | <90% | and/or | >0.03% | 80-119 | Solvent Processing                     |
| II        | 90+% | and    | <0.03% | 80-119 | Hydroprocessing                        |
| III       | 90+% | and    | <0.03% | 120+   | GTL; Wax Isom.; Severe hydroprocessing |
| IV        |      |        |        |        | Polyalphaolefins (PAO)                 |
| V         |      |        |        |        | All other basestocks                   |

## 2. HYDROPROCESSING APPROACHES

Today, hydroprocessing plays many roles in the manufacture of basestocks and specialties. In some cases all-catalytic technologies have replaced separations based processing, while in others, refiners have inserted hydroprocessing into the pre-existing solvent-based technology train. The first strategy involves higher capital cost but can provide lower overall operating expense; the second offers a lower capital cost route that can leverage the existing facilities.

A composite of several possible schemes for basestock and specialties manufacture (that no single lube plant employs in total) is illustrated in Figure 3.

Group I basestocks are generally made by the traditional separations-based sequence of distillation, solvent extraction, and solvent dewaxing. These steps tailor the volatility, viscosity and low temperature properties by shaping the boiling range, and then removing the most aromatic species (by extraction with e.g. furfural, phenol or N-methyl pyrrolidone) followed by fractional crystallization (to separate the highest melting species, generally paraffins) using ketones. An alternative to solvent dewaxing of raffinates is

catalytic dewaxing in which the wax is converted to lower melting products by either boiling range conversion or isomerization. This step is lower cost than solvent dewaxing and is used in areas where wax is valued as fuel only. An example of this technology is ExxonMobil's MLDW™ process.<sup>7</sup>

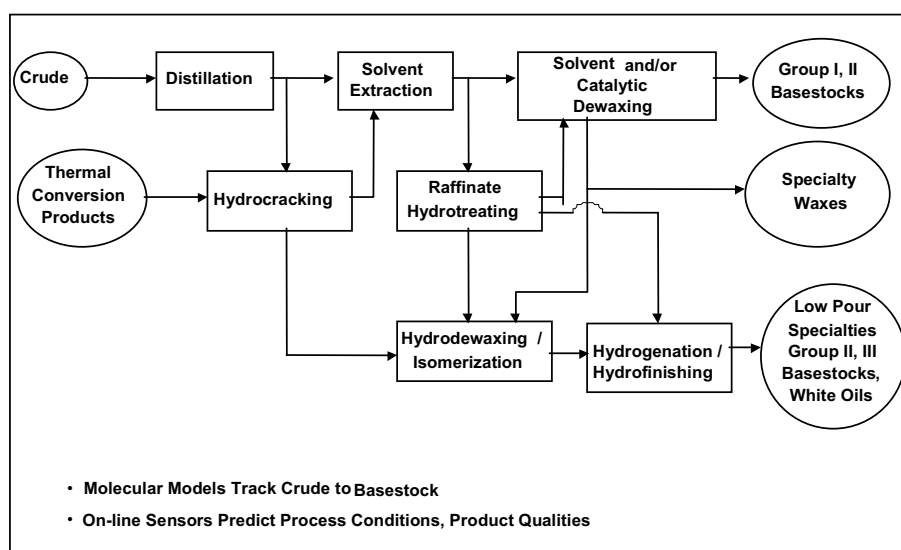


Figure 3. Hydroprocessing technology developed for entire process train

Finally, a hydrofinishing step is often used to improve color and stability by saturation of trace multiring species and by removing some residual polar hydrocarbons, e.g. those containing nitrogen. Basestocks from typical crudes have VI ranging from 95 to 105, with saturates contents 65 to 85% and sulfur levels usually above 0.1 wt%.

An “all catalytic” approach to basestock manufacture is to feed virgin gas oils (from vacuum distillation of crude) and/or thermally converted feeds, such as coker gas oils, through a sequence of hydrocracking, hydrodewaxing, and hydrofinishing (hydrogenation).<sup>8</sup> In the first step, a high pressure, high temperature, hydrocracker operation generates species that have increasing paraffinic character. Next, the lube boiling fractions are block processed through a moderate pressure hydrodewaxing step, in which the most highly paraffinic hydrocarbons are hydroisomerized into isoparaffins. Finally, the hydrodewaxed streams cascade over a saturation catalyst operating at moderate to high pressures to hydrogenate most of the remaining aromatics into naphthenes. Depending on the gas oil properties (such as wax content) and the processing severity, basestocks meeting Group II and III requirements, i.e. with saturates in the high 90’s and VI’s ranging all the way to 150, can be produced. Such processes are more flexible than separations based refining approaches in that they can utilize a wider range of crudes and

achieve unique properties. For example, basestocks may have excellent low temperature viscosity, features attractive for use as refrigerator oils and transformer oils; others may be deeply saturated to meet the most stringent specifications for use as “white” oils for application in the food and cosmetics industries.

Some refiners use combinations of separation and catalytic processes to retain specialties like waxes, a by-product of the solvent dewaxing step, and/or to leverage the hydroprocessing step. A raffinate hydroprocessing step inserted between extraction and solvent dewaxing can be designed to achieve the same kind of basestock upgrading achieved by a VGO hydrocracker but at milder conditions using less hydrogen. At the same time the extraction step preceding the hydroprocessor can operate at higher yields and rates because it is not needed to achieve final basestock property targets like VI. ExxonMobil’s Raffinate Hydroconversion (RHC™) process is a recent example of this approach.<sup>9,10</sup>

An alternative process may involve a sequence of raffinate hydrotreating, hydrodewaxing and a hydrofinishing step. In either case, a range of Group II and III basestocks and specialties with excellent properties are feasible.

To optimize overall processing, comprehensive models are increasingly used to relate crude and vacuum distillate properties to the required process conditions needed for the catalysts to mediate the desired reactions. In particular, a compositional modeling technology, “Structure-Oriented Lumping” (SOL) developed by ExxonMobil, provides a way to describe crudes, intermediates, and finished oils mathematically by combining high-detail hydrocarbon analysis and reaction rules.<sup>11</sup> SOL, in combination with refinery process models, makes it possible to evaluate the economics of any lube crude and predict refining yields and product performance. Supplementing the models are on-line sensors that provide immediate feedback on the approach to target.

### **3. CHEMICAL TRANSFORMATIONS**

Three classes of catalyzed chemical transformation characterize how modern hydroprocessing is used to improve basestock properties—two concerning ring structures and the other paraffins.

#### **3.1 Ring Conversion**

The most facile reactions in a hydrotreating or hydrocracking environment involve the removal of sulfur and nitrogen. These species are present in both aliphatic and ring structures, and at moderate severity conditions essentially complete ejection can be achieved of even the most refractory of these heteroatoms, such as those embedded in structurally

hindered rings. For example on a medium viscosity raffinate feed (5 cSt at 100C), conditions around 350°C and about 40 bar H<sub>2</sub> partial pressure and at 1.0 space velocity on a contemporary hydrotreating catalyst comprising Co, Ni, Mo or W on an alumina support may be sufficient to convert most liquid phase sulfur and nitrogen into H<sub>2</sub>S and NH<sub>3</sub>. Their removal opens out the heterocycle into a more aliphatic arrangement, resulting in a modest increase in basestock VI. Generally, these transformations alone are insufficient to improve basestock properties to the level needed to meet current and future automotive standards. Instead, higher severity processing is required.

At the next level, the reaction that contributes most to VI improvement with contemporary catalysts at hydrotreating conditions is ring de-alkylation of multiring hydrocarbons. As side chains are cleaved by a beta scission step, both the side chain and ring fragments may fall below the front of the lube boiling range, leaving behind more paraffinic hydrocarbons in the lube range. Conditions to achieve this transformation must also be conducive for ring saturation, requiring moderate to high pressures. Accordingly, the remaining rings in the lube range become progressively more naphthenic. The “saturation-de-alkylation” zone typically occurs at reactor temperatures from 350°C to 380°C (assuming 1.0 space velocity) which requires pressures to be higher than about 60 bar H<sub>2</sub> in order for the aromatic-naphthene equilibrium to favor saturation. (See below for further discussion of saturation strategies).

At the end of the hydroconversion scale, both ring and paraffin type hydrocarbons undergo hydrogenolysis as hydrotreating gives way to hydrocracking, resulting in a significant shift of lube range hydrocarbons to lower boiling species. Hydrocracking is generally mediated by catalysts with an acid function to promote the formation of carbenium ions, leading to carbon-carbon cleavage.<sup>12</sup> These reactions are prominent above about 380°C (at 1.0 space velocity), and require pressures of 100 bar H<sub>2</sub> or higher to sustain saturation rather than aromatics formation mitigating both coke on the catalyst (associated with catalyst deactivation) and poorer basestock oxidation stability.

The overall change in composition of the remaining lube range (343°C+) hydrocarbons resulting from the progressive hydroconversion of a heavy lube distillate is illustrated in Figure 4. Looking at the composition on a dewaxed oil basis, it is evident that paraffins and mononaphthenes grow in population at the expense of aromatics and polynaphthenes. Viscosity declines, as does the average boiling point of the 343°C+ envelope. However, the net gain in paraffinic character of the basestock means that viscosity must decline faster than the mid-boiling point, corresponding to a VI rise. That is, for the highly hydroconverted product, the mid-boiling point rises substantially over the mid-boiling point of the feed at a given viscosity.

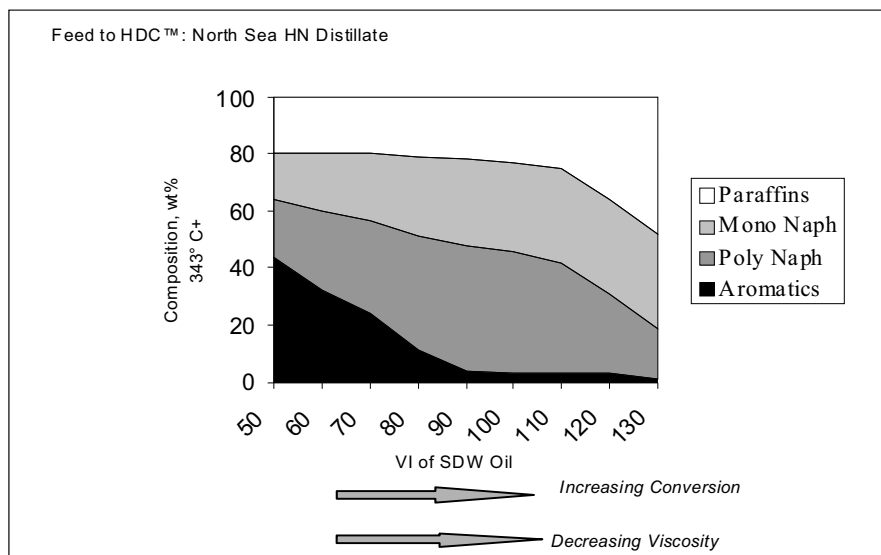


Figure 4. Hydrocracking impact on base stock composition

Selective ring conversion of a raffinate can also be a very effective route to improved basestock properties. This is dramatically illustrated by comparing the profiles of a Group I basestock made from conventional separations-based processing with a Group II basestock derived from a similar raffinate, but converted by a moderate severity hydrotreating type process, RHC™.

Both the conventional basestock (100VI) and the RHC™ derived basestock (116 VI) were separated in a thermal diffusion column, see Figure 5. Thermal diffusion is an analytical technique that applies a thermal gradient across a narrow annular wall, driving the basestock sample in this space to move in a convection cycle.<sup>13</sup> After about one week, the sample separates by density with the least dense, paraffinic species, at the top and most dense, clustered ring species, at the bottom, as shown in the right-hand illustration. Samples from each of ten ports can be characterized both for basestock properties and composition.

The plot of VI against port number reveals that the Group I basestock has a very wide range of properties, with VI's spanning from +170 to -160; port 10 comprises a high concentration of multiring species. However, these species are mostly absent in the Group II basestock; the combination of extraction and RHC™ has selectively eliminated the “port 10” components found in the feed, with little else altered. As a consequence, the basestock “volatility@viscosity” is greatly improved.



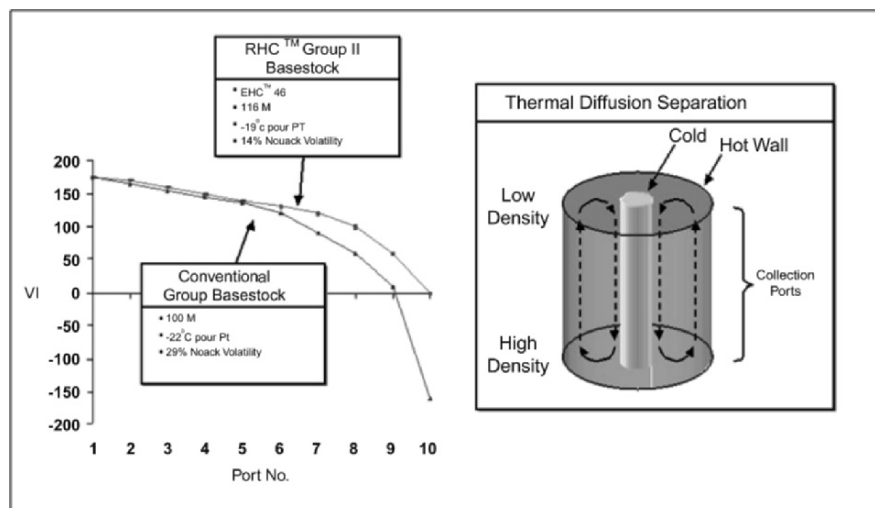


Figure 5. Basestock property improvement in RHC™ is by ring conversion (from ref. 10)

### 3.2 Paraffin Conversion

Contemporary catalysts used for lubes hydrotreating or hydrocracking do not typically exploit the high VI potential associated with the waxy paraffinic component of distillates or raffinates. Paraffins either go through these processes little changed, or, at more severe hydrocracking conditions, are converted along with other non-paraffins into lower valued fuels.

In general, catalysts that function well for boiling range conversion and ring conversion processing are not suitable for selective paraffin conversion. Paraffin conversion can be mediated by amorphous surface catalysts such as platinum on fluorided-alumina, but the most effective catalysts are those that possess shape selectivity. These catalysts are able to selectively process paraffins in an environment that excludes most other non paraffins. On such catalysts, access of hydrocarbons to the catalytic conversion sites is governed by the molecular cross section of the molecule rather than adsorption energy. Ring containing species that may preferentially adsorb onto the amorphous surface of an alumina supported hydrotreating catalyst on account of their greater bulk and polarity, are mostly denied entry to the regular microporous surfaces that characterizes modern “dewaxing” catalysts.

Two distinct kinds of “Catalytic Dewaxing” are in use today. One involves the boiling point conversion of the paraffin components of waxy feeds by selective hydrocracking and the other by selective hydroisomerization.

An example of the first kind of process that has been in use since the late 1970’s is MLDW™, a very durable technology that handles feedstocks across the entire lube boiling range, utilizing the zeolite ZSM-5.<sup>14</sup> This unique

material has also been used in chemicals and fuels applications: non-equilibrium product distributions can be forced by limiting access and diffusion of reactants into the micropores and by preventing certain products from forming because of internal pore geometry constraints. The microporous network of ZSM-5 consists of two intersecting channels with pores of size and shape to admit normal and monobranched paraffins, but little else. One channel runs sinusoidally along the crystals with a nearly circular pore (5.5 Å diameter), whereas the crossing channel is straight and has an elliptical section (5.1, 5.5 Å). Several generations of this catalyst have been employed since its inception, resulting in catalysts today that have a higher resistance to coking with consequent better activity and longevity.

MLDW™ technology offers interesting options to the refiner. It has a lower operating cost process than solvent dewaxing and can lead to basestocks with excellent low temperature properties. Also, for higher viscosity grades, particularly Brightstock, yield and VI at the target pour can match or exceed that of the comparable solvent dewaxed basestock. Countering this, the potentially valuable wax component of the waxy feed is downgraded to light fuel, and on medium and low viscosity lube grades, yield and VI are generally lower than that of solvent dewaxed basestocks with the same pour point.

Alternate approaches to MLDW™ emerged in the 1990's in the form of Chevron's IsoDewaxing™<sup>15, 16</sup> and ExxonMobil's MSDW™ process<sup>17</sup> as the industry trend toward greater hydroprocessing continued to grow. The new technologies are based on the hydroisomerization of paraffins rather than selective hydrocracking, and are applied downstream of a hydroprocessing step such as a lube hydrocracker or hydrotreater. In this environment, the feeds to the hydrodewaxer are "cleaner", with fewer coke precursors and polars, allowing highly shape selective microporous materials to be used. Yields and properties of the basestocks from these processes are boosted because the wax component of the feed is transformed selectively into high VI isomerate.

These new processes differ from earlier commercial forms of hydroisomerization technologies that utilized amorphous bifunctional acidic, noble metal catalysts supported on fluorided aluminas and silica-aluminas. The amorphous catalyst processes were the first to illustrate that hydroprocessed waxy feeds could be manipulated into valuable isoparaffins with exceptional properties.<sup>18</sup>

For example, thermal diffusion of a wax isomerate derived from the hydroisomerization of a heavy slack wax using a fluorided alumina catalyst reveals the profile shown in Table 4. Notably, there are samples from most ports with both high VI and low pour point, testifying to molecules present that are not common in mineral basestocks derived from separations processes or even in basestocks made from hydroprocessing by only ring conversion methods.

Table 3. Thermal Diffusion Illustrates Unique Properties of Wax Isomerates (from Ref. 18)

| Sample Port    | VI  | Pour Point, °C |
|----------------|-----|----------------|
| (whole sample) | 143 | -21            |
| 1              | 173 | -6             |
| 3              | 161 | -21            |
| 5              | 146 | -34            |
| 7              | 134 | -46            |
| 10             | 95  | -31            |

Feed: heavy grade slack wax; Catalyst: Pt-fluorided alumina

Ultimately the shortcoming of amorphous catalysts is that, unlike microporous catalysts, they allow access to all the molecules in the feed, making it difficult to achieve an adequate reduction in paraffin melting point without also over-converting (by hydrocracking) the isomerates in the lube range to lower boiling fuels. Figure 6 illustrates in a simplified way how the relative kinetics for hydroisomerization and hydrocracking dictate the selectivity of the process.

Paramount to an effective hydroisomerization process is that the relative rate ( $k_1$ ) of paraffin (wax) conversion to isoparaffin well exceeds the rate of isoparaffin conversion into fuels ( $k_2$ ) or of paraffin conversion directly to fuels ( $k_3$ ). As conversion of wax progresses, e.g. with increasing reactor temperature or by extending residence time, the yield of isomerate at first rises sharply, reaches a maximum, and then declines as more of the isomerate produced is hydrocracked to fuels. For example, with  $k_2$  at about one-fifth of  $k_1$  ( $k_3$  is generally very low and can be ignored in this discussion), yields of isomerate may reach 60%, meaning that 60% of the wax component of the feed has converted to isomerate. However, at this maximum there is still a component of feed with melting point above the target, i.e. counted as wax, that remains and must be removed by an additional step, such as solvent dewaxing, for the isomerate basestock to meet all the specified properties. In this process a balance has to be struck to achieve sufficient hydroisomerization to lube isomerate, minimizing fuel production, yet ensuring that there is not too much residual wax in the isomerate that might impose a limit in the downstream solvent dewaxer. Overall, this is a relatively inefficient process because the additional solvent dewaxing step can add significantly to the manufacturing cost.

With the advent of microporous hydroisomerization catalysts, it became possible for the first time to achieve the desired pour point in one step. As shown in Figure 6, MSDW technology achieves complete wax disappearance (to the target pour point). A high percentage of the high melting paraffins are converted into desirable isoparaffins with minimal conversion to fuels products, corresponding to a very high  $k_1/k_2$ . This is believed to be a consequence of the isoparaffins being shape constrained against further reaction, diffusing intact from the pores of the catalyst.<sup>17</sup>

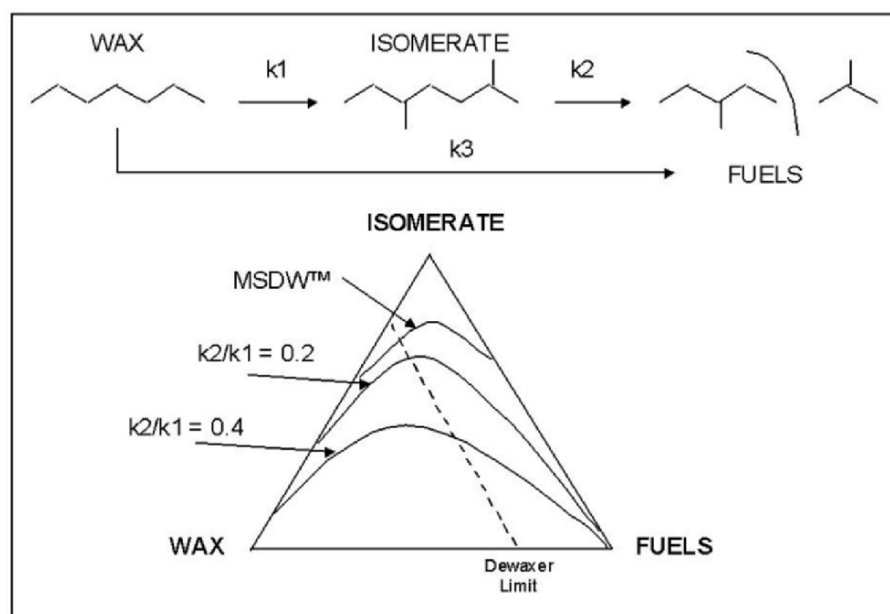


Figure 6. Hydroisomerization Kinetics

A specific example of the upgrading power of selective hydroisomerization technology is shown in Figure 7; a hydrotreated heavy grade slack wax with 30% entrained oil in wax is converted to an isomerate with 150 VI at 0°F pour point at a yield of greater than 70%.

These technologies are effective on a wide range of hydroprocessed stocks of varying wax content from light grades to Brightstock. Basestocks from these processes typically have superb low temperature viscometric properties.

With this level of hydrodewaxing capability, some refiners have moved to “all catalytic” processes with a ring conversion hydroprocessing step complemented by a single step paraffin conversion process that achieves the desired low temperature specifications by completely converting residual wax components, primarily into lube range isomerate.<sup>19</sup> (See further discussion under “Process Combinations”, below.)

### 3.3 Saturation

While ring and paraffin conversion technologies are effective in creating more paraffinic streams with excellent volatility@viscosity, as well as low temperature property characteristics, they may not necessarily provide basestocks or finished oils that are also oxidatively stable.

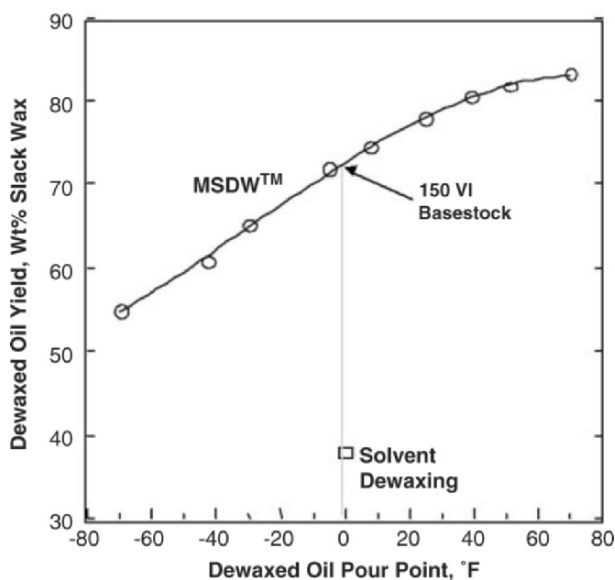


Figure 7. MSDW™ selectively converts wax to high VI isomerate

A factor that directly relates to the oxidative stability of basestocks, particularly Group II and III basestocks, is the extent of ring hydrogenation (saturation). At first sight, saturation appears straightforward. If there is enough driving force to reach equilibrium (i.e. sufficient reactor temperature, catalyst activity, and residence time), then the bulk measure of saturates associated with ring structures will simply be a function of pressure. This is shown in Figure 8, representing the saturates equilibrium of a medium grade raffinate; at higher  $H_2$  pressure and lower reactor temperature, conditions are favorable for producing highly saturated basestocks.

In reality, particularly with conventional hydrotreating type processes, the driving force may be insufficient to approach equilibrium. For example, the catalyst mediating the saturation reaction may have low activity for hydrogenation and/or the residence time for the reaction may be too brief, resulting in a basestock that falls well short of the equilibrium lines defined by the process  $H_2$  pressure. Furthermore, polar compounds present in the feed may hamper the inherent saturation activity by poisoning sites that mediate hydrogenation.

The properties of basestocks cannot be fully described by focusing on bulk saturates alone. Within the envelope of saturates are one, two, three, and higher ring classes, each of which behaves differently, both in terms of the kinetics and equilibrium for saturation. A crucial point is that the conditions favoring an increased rate of saturation of a particular ring class may promote

unfavorable equilibrium (i.e. the formation of aromatics) in another class.<sup>20</sup> This is illustrated in Figure 9.

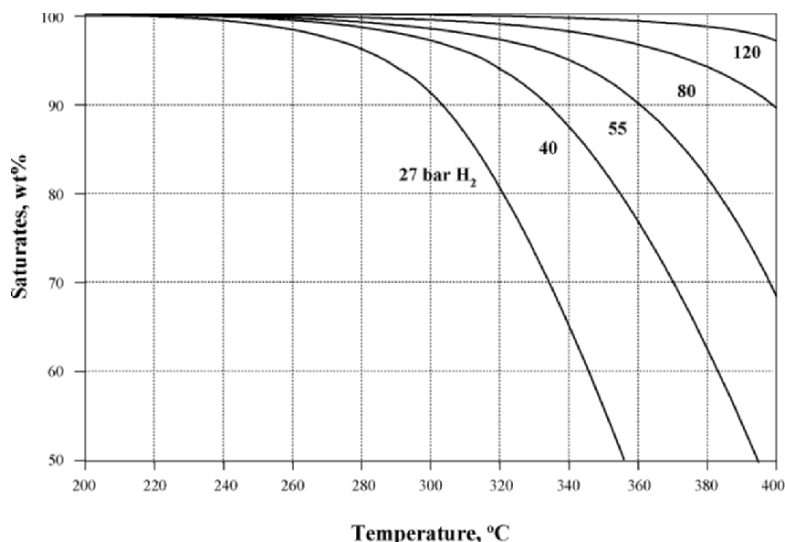


Figure 8. Estimate of Equilibrium Saturates

Single aromatic rings, whether linked to an aliphatic chain or a naphthene ring, have the characteristic of being kinetically slow to saturate, yet favored thermodynamically. By contrast, clustered aromatic rings may saturate rapidly, yet be unfavored thermodynamically. These conflicting trends can make it difficult to achieve complete saturation at one set of conditions.

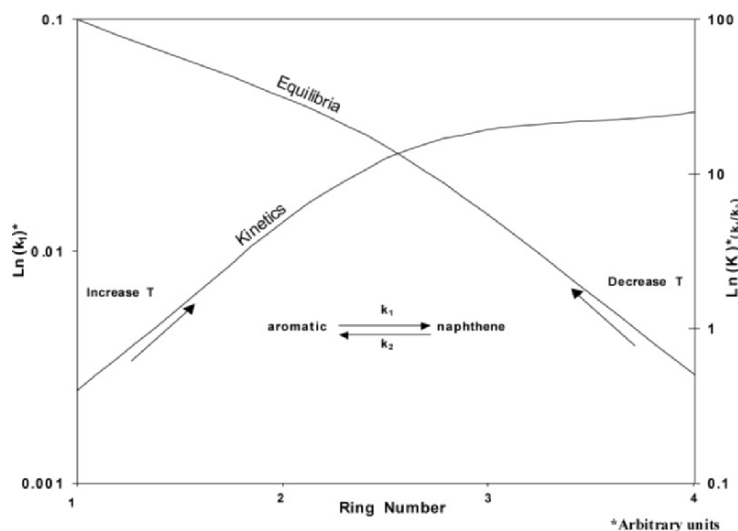


Figure 9. Kinetics and equilibria differ with ring class

For example, by increasing the reactor temperature, the rate of saturation of an isolated one or two-ring aromatic will increase because the forward reaction is well favoured over the reverse reaction (ring dehydrogenation), resulting in an overall increase in the population of naphthenes. Since most ring species in a typical lube raffinate or distillate feed are one or two ring aromatics, the net result of increasing temperatures in a hydrotreater or hydrocracker is to increase the overall saturates content. However, this action will have the reverse effect on aromatics centered in a cluster. At higher temperatures, complete saturation of a four ring aromatic cluster is not favored thermodynamically, and any increase in temperature only makes saturation of this ring class more difficult by tipping the equilibrium further in favor of dehydrogenation. So, while the majority of aromatic species may become saturated at moderate temperatures and pressures in a hydrotreater, the aromaticity of, e.g., three-plus ring species may increase, resulting in basestocks that are colored and/or exhibit higher UV absorbances and oxidative instability.

Two primary strategies are used to achieve nearly complete saturation across all ring classes. An effective but relatively costly approach is to use higher pressure. This works well because it forces the aromatic/naphthenic equilibrium toward naphthenic molecules, allowing the higher ring class species to remain mostly saturated at temperatures needed to kinetically drive the lower ring classes into naphthenes.

An alternate strategy, broadly applied, is temperature-staged processing. In this approach, a lower temperature stage is used following first stage processing such as hydrotreating, hydrocracking, or hydrodewaxing. Provided that process  $H_2$  pressures are not too low, e.g. 40 bar or greater, the higher temperature step can do an effective job of converting mono-aromatics into naphthenes, even though there may be considerable reversal of higher ring classes back toward aromaticity. Then, as product from this reactor cascades to the lower temperature step, nearly complete saturation of all ring classes may be achieved; the higher ring class aromatics convert rapidly to naphthenes because the reaction is still kinetically viable and the conditions more thermodynamically favorable.

Temperature staging is used in the RHC<sup>TM</sup> process<sup>10</sup> to achieve a highly saturated, oxidatively stable, colorless basestock. This process incorporates three reactors, the first two (referred to as stage 1) operating at higher temperatures to achieve ring conversion for desired volatility@viscosity improvements and to drive saturation of mono-aromatics. Product from these reactors cascades to a lower temperature third reactor (stage 2), comprising a sulfur tolerant catalyst. At such conditions, equilibrium favors near complete saturation of clustered rings, resulting in excellent color and UV stability. In Figure 10, the equilibrium curve for higher ring classes (i.e. 3 ring and greater) aromatics is shown. With the catalyst and conditions chosen for the first stage, liquid effluent from the first stage can have residual aromaticity

above the targeted level needed to ensure subsequent basestock stability. But, this is overcome in the second stage by operating at mild conditions. Even at short residence times, a temperature can be chosen that balances kinetics and equilibrium such that the residual clustered ring aromatics are readily saturated to a low level, ensuring excellent stability.

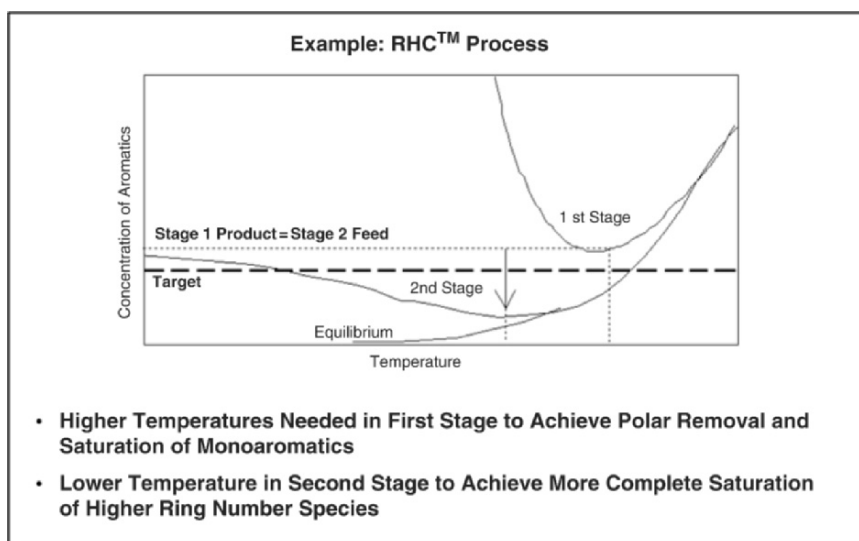


Figure 10. Temperature Staging for More Complete Saturation

The conflicting tug of the kinetics of saturation versus equilibrium has a direct bearing on process conditions and choice of catalyst to mediate the reaction. In some scenarios, a base metal, sulfided catalyst (such as Ni and Mo sulfides on alumina) is preferred, even though this type of catalyst has only moderately active hydrogenation sites compared to noble metal catalysts. This is because the gas stream cascading from the first stage is sour, containing  $H_2S$  and  $NH_3$  that may significantly poison noble metal sites and erode catalyst performance. Base metal sulfided catalysts are much less susceptible to poisoning in this environment, making them a cost effective candidate in a process of this type *providing* there is sufficient pressure to offset the higher temperatures needed to drive saturation with a less active hydrogenation catalyst (per the guidelines shown in Figure 8). Conversely, in an environment where gas and liquid feeding to a saturation unit have only low levels of polars, noble metal catalysts may be preferred because they offer the greatest inherent activity for hydrogenation, allowing lower reactor temperatures and pressures to be employed while achieving near-complete saturation of all ring classes.



## 4. PROCESS COMBINATIONS

### 4.1 Ring Conversion-Hydroisomerization-Hydrofinishing

Since 1965, a prevailing reason for using hydroconversion technologies has been feed flexibility; the envelope of crudes viable for lubes applications is considerably broadened when there is a hydroprocessing step in the manufacturing sequence. For example, crudes with high aromaticity such as Maya and Alaska North Slope can be upgraded by ring conversion to make moderate quality basestocks that would not be possible by solvent processing. However, as basestock specifications have continued to tighten, and VI requirements increase, processes such as lube hydrocracking that utilize only a ring conversion step incur high yield losses even on good crudes.

Figure 11 illustrates that, relative to VGO from a good lube crude such as Arab Light, the additional conversion required to upgrade VGO's from poorer crudes grows considerably as the basestock target VI increases. On the same 370°C+ basis, yields from poorer quality VGO's may be lower by a factor of three when the basestock VI target is above 110. The lower slope for VI improvement of the poorer feed is indicative of a lack of molecules amenable to upgrading by de-alkylation, a sign that much of the ring population consists of clusters with only short aliphatic side chains.

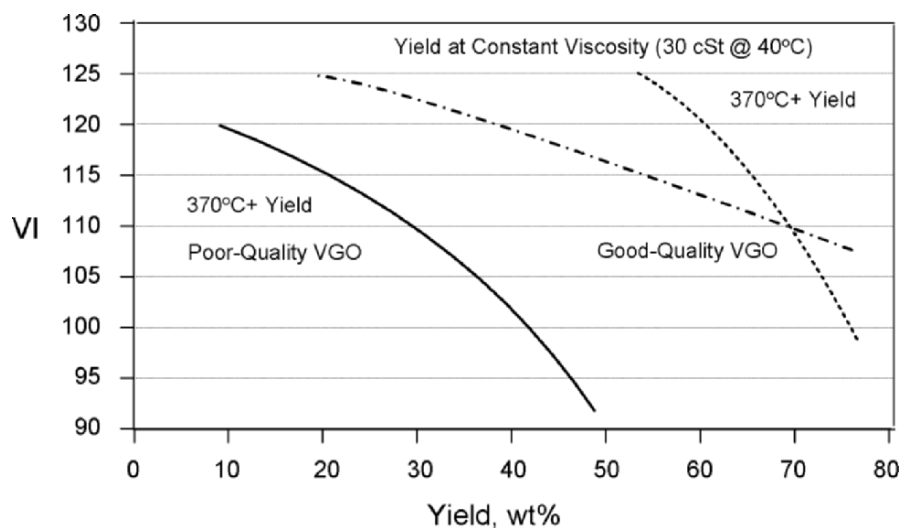


Figure 11. Yield loss is high with ring conversion alone (from reference 21)

Note though that even “good” VGO feeds can be reduced to low yields of basestock when a high VI target is fixed on a particular viscosity grade, e.g. 30 cSt @ 40C. Clearly the kind of ring conversion technology that typifies many hydroprocessing operations today is not very efficient at achieving

basestock properties needed for modern automotive use. Above 110, additional improvements in VI are very costly, causing at least a 3% loss for each unit of VI improvement at a fixed viscosity.

The situation improves considerably when the hydroconversion step is combined with a selective hydrodewaxing step, employing a catalyst such as MSDW-2™. Since the paraffinic components of the VGO can be selectively converted to very high VI isomerate, this permits hydrocracking severity and conversion to be reduced while achieving the same nominal basestock properties. For example, a VGO with 20% wax may have an additional uplift of 5 to 6 VI points associated with the selective paraffin conversion step. This can result in an overall yield of basestock at an improved 115 VI that is 15 to 20 wt% greater than that achieved by the hydrocracking step alone. In this way, selective hydrodewaxing can be a very effective lever to increase quality and/or basestock volumes, as well as to further extend feed flexibility.<sup>21</sup>

The layout of an integrated Lube Hydrocracking-Hydrodewaxing Complex, used by ExxonMobil in Singapore, is shown in Figure 12.

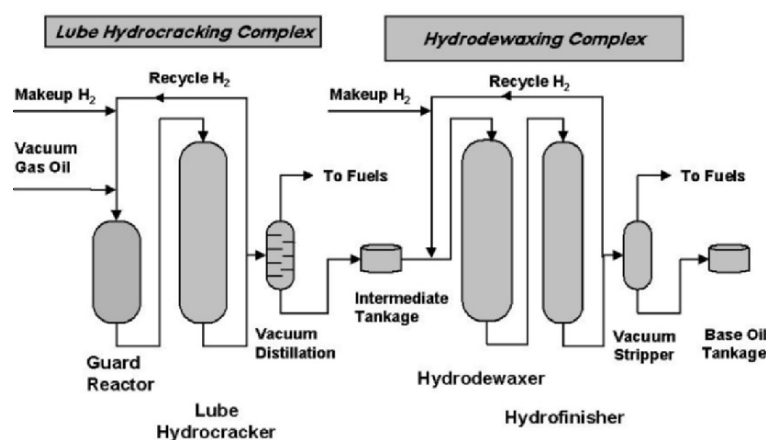


Figure 12. Hydrocracking-Hydrodewaxing Complex

This combination of technologies opens up new opportunities to the refiner. For example, waxier crudes become viable since there is no longer a (potentially rate limiting) solvent dewaxing step involved. With increasing wax content in the VGO feed there has to be a rebalancing of the upgrading load from the hydrocracker, placing a greater burden on the hydrodewaxer. For the same target basestock properties, feed to the hydrodewaxer will now have lower VI, potentially more aromatics and residual polars, as well as more wax to convert to isomerate. This can be a problem for some hydrodewaxing catalysts, because, despite their inherently excellent selectivity for converting polar free paraffinic feeds into isomerate, they can be intolerant of even quite low levels of residual nitrogen leading to much less

selective performance. Some degree of polar tolerance in the hydrodewaxing step has significant ramifications, because if the refiner can operate the hydrocracker to a VI target rather than to a residual polars target, the overall yield from the process can be greatly improved.

This is because the hydrocracker lubes fraction VI target and an essentially polar free lubes fraction target may be separated by considerable additional conversion, see Figure 13. For example, the extra conversion required to progress from 10 ppm residual nitrogen in a hydrocracked VGO down to 1 ppm nitrogen may exceed 30 wt%! Fortunately, the latest generation of hydrodewaxing catalysts are more tolerant, permitting much greater process flexibility.

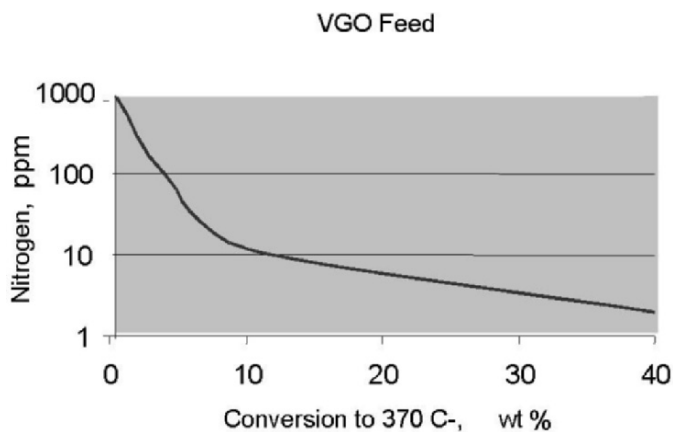


Figure 13. Hydrocracker yields strongly influenced by nitrogen target (from reference 21)

A caveat here is that for the overall process scheme of Figure 12 to be robust, the hydrofinisher must also be more tolerant of polars since the effluent gas and liquid flow directly to it from the hydrodewaxer. These hydrodewaxing and hydrofinishing catalysts need to operate in tandem to achieve a wax free, highly saturated, stable basestock. Here too, the most recent versions of hydrofinishing catalyst, exemplified by Exxonmobil's MAXSAT™, have a corresponding resilience to polars while retaining a high activity for saturation of all ring classes, Figure 14.<sup>21</sup>

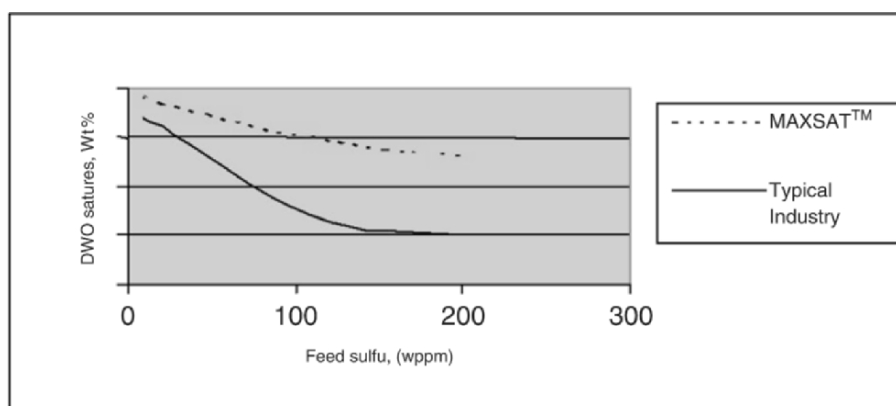


Figure 14. MAXSAT™ polar tolerance is outstanding (from reference 21).

## 4.2 Extraction-Hydroconversion

Another process combination that is very effective in meeting modern basestock standards is linking extraction with a hydroconversion step. Both processes help reduce populations of low VI ring structures to improve volatility at a given viscosity, but there are optimal ways to operate the combined process by playing on the strength of each. A good example is the RHC™ process, illustrated in Figure 15.

An important aspect of this process is the use of raffinate feeds that are “under-extracted” relative to the raffinates required to meet typical Group I basestock properties using extraction only. In the combined process this lower severity mode takes best advantage of the extraction step because a higher percentage of the species removed into the extract phase are clustered aromatic ring structures with few aliphatic characteristics. In other words, the species that have the *least* potential to be converted into more highly paraffinic structures in the subsequent hydroconversion step are removed more selectively when the extraction treat is mild.

Furthermore, the increased raffinate yield associated with under-extraction more than offsets yield loss in the subsequent hydroprocessing step. There are some trade-offs, like higher hydrogen consumption in the hydroconversion step and possibly shortened catalyst life, but the overall advantage weighs heavily toward using under-extracted raffinate feeds. The RHC™ process has been found to be most effective with raffinate feeds having a VI (on a dewaxed oil basis) in the range of 80 to 95.

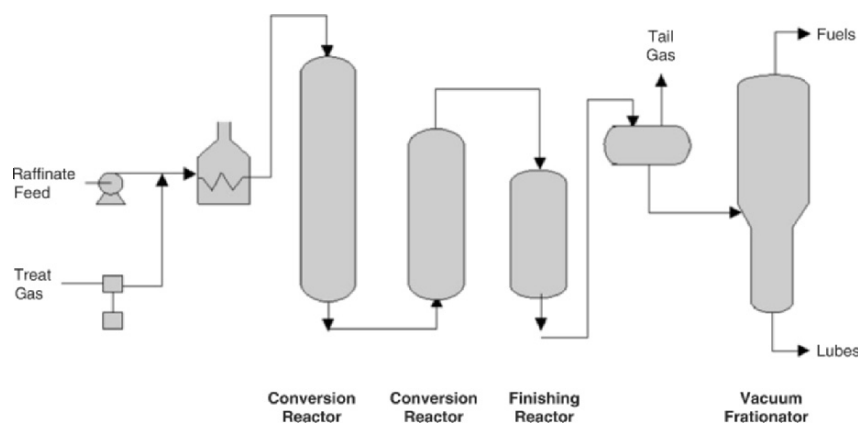


Figure 15. Raffinate Hydroconversion Process™

The combination of extraction and hydroprocessing is a very efficient route to basestocks needed for GF-3 quality. Extraction alone is inappropriate because of an inability to selectively remove multiring naphthenes (these tend to be split evenly between the raffinate and extract phases). Yields by extraction to the same basestock property levels may be less than half of that achieved by RHC™. Also, VGO hydrocracking, i.e. with no pre-extraction step, requires more severe conditions and has potentially lower yields than RHC™ because of the higher conversion needed to offset the highly negative VI characteristics of refractory multi-ring species present in the distillate feed.

The RHC™ process exploits the two factors that influence volatility@viscosity, basestock VI and boiling range distribution. This occurs because the hydroprocessing step not only raises VI by ring conversion, but is also effective in shifting the highest boiling species to the middle of the boiling range. After vacuum stripping, a narrower boiling fraction is formed, effectively lowering volatility at the viscosity target. In fact, this works better when more of the upgrading workload is placed on the hydroprocessing step and less on extraction, that is, using under-extracted feeds. Figure 16 illustrates how this benefit is achieved on a raffinate feed derived from a 250N lube distillate.

In this example, the nominal target properties for the basestock from the RHC™ process were set at 112 VI, 7% Noack volatility, and, following vacuum stripping and solvent dewaxing, a pour point of -18°C. The base operation is shown with a raffinate extracted to achieve typical Group I basestock properties (103VI, on a dewaxed basis) then hydroprocessed to 112 VI. From this platform, as feed VI declines, the basestock yield at target properties rises, a testament to the greater ability of hydroconversion to raise VI, versus extraction capability in this range. The extra advantage of using lower VI raffinates in the hydroprocessing step is that the resultant basestock

has *lower* viscosity for the same VI and volatility (by as much as 0.1 cSt, associated with using a raffinate feed with 85 VI rather than 95 VI). This credit can be taken as improved low temperature viscometric properties and/or as a yield increase resulting from being able to operate to a lower VI target, achieved by lowering conversion in the hydroprocessing step.

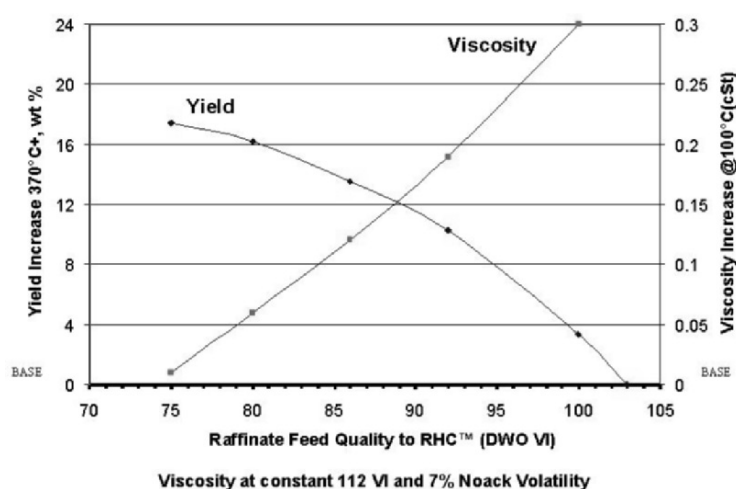


Figure 16. Yield and property improvements with under-extracted feeds (from Ref. 10)

A further embellishment to this process results from combining extraction and hydroconversion with a selective hydrodewaxing step, as discussed above.

## 5. NEXT GENERATION TECHNOLOGY

The next steps in technologies for better basestocks are likely to include conversion of natural gas into high quality fuels, and, potentially, basestocks and specialties. Although Fischer-Tropsch (FT) chemistry has been around since the catalysis discovery in 1923, it has had only minor impact on the traditional petroleum market, and none at all on the world of lubricants. But now, advances in catalysts and process design have significantly reduced costs and improved flexibility to the point where major oil companies such as Shell Gas and Power, ExxonMobil Corp., and Sasol Ltd. are technically ready for larger scale plants. While a major part of product from GTL will be diesel, it is expected that some basestocks can be also produced with properties ranging from those of the best Group III's made today from petroleum waxes, to the current benchmark for excellence, synthetic Group IV basestocks. The difference is that GTL basestocks volumes could well exceed the relatively small market for today's Group III and PAO applications and be produced at

much lower operating cost than any currently made basestock. They have the potential to revolutionize the basestock business.<sup>22</sup>

The nominal sequence for making GTL basestocks as shown in Figure 17 can provide a reference for this if needed. First, natural gas (predominantly methane) is mixed with oxygen and converted into synthesis gas, a 2:1 mixture of H<sub>2</sub> and CO. Synthesis gas is then knitted into extended -CH<sub>2</sub>- links using highly selective FT catalysts, forming paraffins with carbon numbers ranging from one to hundreds.

In the last step, the fraction above about C<sub>20</sub> is selectively hydroisomerized into iso-paraffins, yielding basestocks with viscosities ranging from about 3 to 10 cSt @ 100°C (or higher, depending on the technology). Catalysts used in preliminary demonstrations are in the same family as those used today for hydrodewaxing of hydroprocessed petroleum streams. They create very stable isoparaffinic basestocks with exceptional high and low temperature viscometric properties and low volatility.

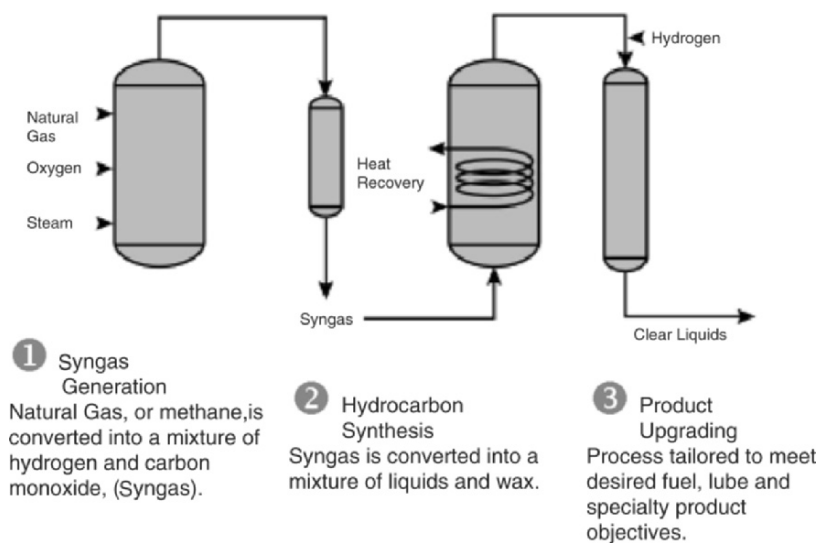


Figure 17. AGC-21 Process

Looking into the next decade, there should be even greater opportunities in lube processing to manipulate basestock properties to meet ever tightening specifications. More streams will be available for upgrading that are relatively free of polar and aromatic species, permitting highly selective lube catalysis. It may be possible, for example, to open rings more efficiently and to be more precise with placement and type of branch created in hydroisomerization processes.

As more is learned about how properties and performance relate to hydrocarbon structure, hydroprocessing will continue to evolve, providing ever more subtle routes to superior lubricants.

## 6. REFERENCES

1. Carnes, K., *Lubr. World*, **2001**, *11(10)*, 16-20.
2. Carnes, K., *Lubr. World*, **2002**, *12(2)*, 16-20.
3. Deane, B.C.; Choi, E.; Crosthwait, K., The Relationship of Base Oil Volatility to Oil Loss in Automotive Applications, 1997 NPRA Annual Meeting, March 16-18, 1997, San Antonio, (AM-97-40)
4. Choi, E.; Deane, B.C., Base Oil Volatility and Oil Consumption, 1998 NPRA Annual Meeting, March 16-17, 1998, San Antonio, (AM-98-47)
5. Rousmaniere, J., Group I Base Oils Decline in North America, *Lubr. World*, **2000**, *10(11)*, 14-16.
6. Noack, K., *Angewandte. Chemie*, **1936**, *49*, 385.
7. Smith, K.W.; Chen, N.Y., New Processes for Dewaxing Lube Basestocks, *Oil Gas J.*, **1970**, *78(21)*, 75, May 1970.
8. Wuest, R.G.; Anthes, R.J.; Hanlon, R.T.; Jacob, S.M.; Loke, L.; Tan, C.T., An Early Change, *Lubr. World*, **2000**, *10(2)*, 12-15..
9. Gallagher, J.E.; Cody, I.A.; Claxton, A.A., Raffinate Hydroconversion, *Lubr. World*, **2000**, *10(2)*, 16-19.
10. Cody, I.A.; Deane, B.C.; Claxton, A.A.; Gallagher, J.E.; May, C.J., Efficient Raffinate Hydroconversion Process for High Quality Lube Basestocks, 16th World Petroleum Congress, Calgary, Canada, June 11-15, 2000.
11. Jacob, S.M.; Banta, F.X.; Hoo, T.M.; McGuinness, M.P.; Quann, R.J.; Sanchez, E.; Staffeld, P.O.; Wells, M.E.; Wuest, R.G., Compositional Modelling of Lube Processes and Lube Base Oil Processing for the 21st Century, AIChE Spring National Meeting, March 10, 1998 (Paper 25c).
12. Scherzer, J.; Gruia, A.J., *Hydrocracking Science and Technology*, Marcel Dekker Inc., 1996
13. White, J.R.; Fellows, A.T., Thermal Diffusion Efficiency and Separation of Liquid Petroleum Fractions, *Ind. Eng. Chem.*, **1957**, *49(9)*, 1409-1418.
14. Kokotailo, G.T., *Nature*, **1978**, *272*, 437.
15. Lok, B.K.; King, R.R.; Lee, S.K.; Wilson, M.M.; Lopez, J., Cost Effective Mineral Oils with Synthetic Performance, AIChE Spring Meeting, February 25-29, 1998, New Orleans; Paper No. 67(d).
16. Miller, S., Wax Isomerization for Improved Lube Quality, AIChE, Spring National Meeting, March 8-12, 1998, New Orleans; Paper No. 25(b)
17. Helton, T.E.; Degnan, T.F.; Mazzone, D.N.; McGuinness, M.P.; Jacob, S.M.; Dougherty, R.C., Mobil's Lube Hydroprocessing Technologies --A Legacy of Catalytic Innovation and Commercial Success, AIChE Spring National Meeting, March 10, 1998 New Orleans; Paper No. 25(d).
18. Cody, I.A.; Ball, K.J.; Murphy, W.J.; Ryan, D.G.; Silbernagel, B.G., Exxsyn 6 --Exxon's New Synthetic Basestock, ACS National Meeting, Base Oil Symposium, San Diego, March 16,17, 1994.
19. Wuest, R.G.; Anthes, R.J.; Hanlon, R.T.; Jacob, S.M.; Loke, L.; Tan, C.T., Commercialization of Mobil's All Catalytic Lube Technology and Next Generation Improvements, AIChE Spring National Meeting, March 14-18, 1999, Houston, TX, Session 31(e).
20. Frye, C.G., Equilibrium Hydrogenation of Multiring Aromatics, *J. Chem. Eng. Data*, **1969**, *14*, 372.



21. Hilbert, T.; Cody, I.A.; Hantzer, S., Process Options for Producing Higher Quality Basestocks, NPRA, Lubricants and Waxes Meeting, November 8-9, 2001, Houston (LW-01-128).
22. Cox, X.B.; Burbach, E.R.; Lahn, G.C., The Outlook for GTL and Other High Quality Lube Basestocks, 2001 NPRA National Meeting, May 25, 2001, New Orleans, LA. (AM-01-64).

## Chapter 17

# SYNTHETIC LUBRICANT BASE STOCK PROCESSES AND PRODUCTS

Margaret M. Wu<sup>(a)</sup>, Suzzy C. Ho<sup>(b)</sup>, and T. Rig Forbus<sup>(c)</sup>

*(a) ExxonMobil Research & Engineering Co. Annandale, NJ 08801*

*(b) ExxonMobil Chemical Co. Synthetic Division, Edison, NJ 08818*

*(c) The Valvoline Co. of Ashland, Inc., Lexington, KY 40512*

### 1. INTRODUCTION

This chapter reviews the product and process for synthetic base stocks produced from chemicals of well-defined chemical structures and in processes tailored to optimize important properties and performance features. These synthetic base stocks are critical components used in the formulation of many synthetic lubricants. (In this chapter, we use “synthetic base stock“ to represent the base fluid and “synthetic lubricant“ to represent formulated, finished lubricant product.)

At the start of this chapter, we briefly discuss the background and the driving force for using synthetic lubricants. The major part of the chapter discusses the key synthetic base stocks - chemistry, synthesis processes, properties, their applications in synthetic lubricant formulation and advantages compared to petroleum-derived base stocks.

Many U.S. base oil manufacturers and formulators include some Group II+ and Group III base stocks as synthetic, as their manufacturing process includes varying degrees of chemical transformation. These base stocks are usually produced by hydroprocessing or hydroisomerization, which is typically part of a refining process<sup>1</sup>. Discussion of these hydroprocessed base stocks can be found in the previous chapter. In this chapter, we limit discussion to those synthetic base stocks produced from chemicals of well-defined composition and structure.

## 1.1 Why Use Synthetic Lubricants?

Synthetic lubricants are used for two major reasons:

- When equipment demands specific performance features that can not be met with conventional mineral oil-based lubricants. Examples are extreme high or low operating temperature, stability under extreme conditions and long service life.
- When synthetic lubricants can offer economic benefits for overall operation, such as reduced energy consumption, reduced maintenance and increased power output, etc.

Conventional lubricants are formulated based on mineral oils derived from petroleum. Mineral oil contains many classes of chemical components, including paraffins, naphthenes, aromatics, hetero-atom species, etc. Its compositions are pre-determined by the crude source. Modern oil refining processes remove and/or modify the molecular structures to improve the lubricant properties, but are limited in their ability to substantially alter the initial oil composition to fully optimize the hydrocarbon structures and composition. Mineral oils of such complex compositions are good for general-purpose lubrication, but are not optimized for any specific performance feature. The major advantages for mineral oils are their low cost, long history and user's familiarity. But this paradigm is now changing.

The trend with modern machines and equipment is to operate under increasingly more severe conditions, to last longer, to require less maintenance and to improve energy efficiency. In order to maximize machine performance, there is a need for optimized and higher performance lubricants. Synthetic lubricants are designed to maximize lubricant performance to match the high demands of modern machines and equipment, and to offer tangible performance and economic benefits.

## 1.2 What Is a Synthetic Base Stock?

Synthetic lubricants differ from conventional lubricants in the type of components used in the formulation. The major component in a synthetic lubricant is the synthetic base stock. Synthetic base stocks are produced from carefully-chosen and well-defined chemical compounds and by specific chemical reactions. The final base stocks are designed to have optimized properties and significantly improved performance features meeting specific equipment demands. The most commonly optimized properties are:

- **Viscosity Index (VI).** VI is a number used to gauge an oil's viscosity change as a function of temperature. Higher VI indicates less viscosity change as oil temperature changes - a more desirable property. Conventional 5 cSt mineral oils generally have VIs in the range of 85 to 110. Most synthetic base stocks have VI greater than 120.

- **Pour point and low temperature viscosities.** Many synthetic base stocks have low pour points, -30 to -70°C, and superior low-temperature viscosities. Combination of low pour and superior low-temperature viscosity ensures oil flow to critical engine parts during cold starting, thus, offering better lubrication and protection. Conventional mineral oils typically have pour points in the range of 0 to -20°C. Below these temperatures, wax crystallization and oil gelation can occur, which prevent the flow of lubricant to critical machine parts.
- **Thermal/oxidative stability.** When oil oxidation occurs during service, oil viscosity and acid content increase dramatically, possibly corroding metal parts, generating sludge and reducing efficiency. These changes can also exacerbate wear by preventing adequate oil flow to critical parts. Although oil oxidation can be controlled by adding antioxidants, in long term service and after the depletion of antioxidant, the intrinsic oxidative stability of a base stock is an important factor in preventing oil degradation and ensuring proper lubrication. Many synthetic base stocks are designed to have improved thermal oxidative stability, to respond well to antioxidants and to resist aging processes better than mineral oil.
- **Volatility.** Synthetic base stocks can be made to minimize oil volatility. For example, polyol esters have very low volatility because of their narrow molecular weight distribution, high polarity and thermal stability. Similarly, careful selection and processing of raw materials can influence the finished properties of polyalphaolefins (PAO) base stocks.
- **Other properties,** including friction coefficient, traction coefficient, biodegradability, resistance to radiation, etc. can be optimized for synthetic base stocks as required for their intended applications.

### 1.3 A Brief Overview of Synthetic Lubricant History

Significant commercial development of synthetic lubricants started in the early 1950's with the increased use of jet engine technology<sup>2</sup>. Jet engines must be lubricated properly in extremely high and low temperature regimes where mineral lubricants could not adequately function. Esters of various chemical structures were synthesized and evaluated. Initially, dibasic esters were used as base stock. Later, polyol esters with superior thermal/oxidative stability, lubricity and volatility were developed to meet even more stringent demands. These polyol esters are still in use today.

Another early application that demanded the use of synthetic lubricants came in the mid-1960s during oil drilling in Alaska where conventional mineral oil lubricants solidified and could not function in the severe Alaskan cold weather<sup>3</sup>. Initially, a synthetic lubricant based on an alkylbenzene base stock of excellent low temperature flow properties was used in the field. This base stock was soon replaced by another base stock with better overall properties, namely polyalphaolefins (PAO).

Research on PAO began at Socony-Mobil in early 1950s<sup>4</sup>. The early researchers recognized the unique viscometric properties that could be attained by the proper selection of starting olefins and reaction conditions in the PAO synthesis. After many years of continuous improvements in optimizing the compositions, processes and formulations, Mobil Corporation introduced a synthetic automotive engine oil, Mobil SHC™ in Europe in 1973, followed by a fuel-saving SAE 5W-20 Mobil 1™ in the US. The product was a commercial success and successive generations of Mobil 1™ continue to be the leading synthetic automotive crankcase lubricant today<sup>5</sup>.

Since the early introduction of synthetic lubricants in automotive and industrial applications, many products from numerous companies have followed. The total synthetic lubricant market in 1998 amounted to about 200 million gallons/yr, approximately 2% of the total lubricant volume<sup>5</sup>. However, it is estimated to grow at 5-10% per year, much higher than conventional lubricant (less than 2% per year). Although the volume of synthetic lubricants is relatively small compared to conventional lubricants, the overall economic impact from synthetic lubricants is much larger than just the volume number alone, since synthetic lubricants improve energy efficiency, productivity, reliability and reduce waste, etc.

## 2. OVERVIEW OF SYNTHETIC BASE STOCKS

Of the total world wide synthetic base stock volume, over 80% are represented by three classes of materials<sup>6</sup>

- PAO (45%)
- Esters, including dibasic ester and polyol esters (25%)
- Polyalkyleneglycol (PAG) (10%)

Other smaller volume synthetic base stocks include alkylaromatics, such as alkylbenzenes and alkyl naphthalenes, polyisobutylenes, phosphate esters and silicone fluids. Among these synthetic base stocks, with the exception of phosphate esters and silicones, the starting materials are all derived from basic petrochemicals - ethylene, propylene, butenes, higher olefins, benzene, toluene, xylenes, and naphthalenes, as illustrated in Figure 1.

As expected, the major producers of PAO, esters, PIB and alkylaromatics are integrated petroleum companies that supply conventional mineral oil base stocks and petrochemicals as well as various synthetic base stocks. PAG, phosphate esters and silicone fluids are manufactured by chemical companies that produce these fluids on a much larger scale mainly for other applications. Their use as lubricant base stocks is only a fraction of the total market. Table 1 summarizes the major synthetic base stock producers.

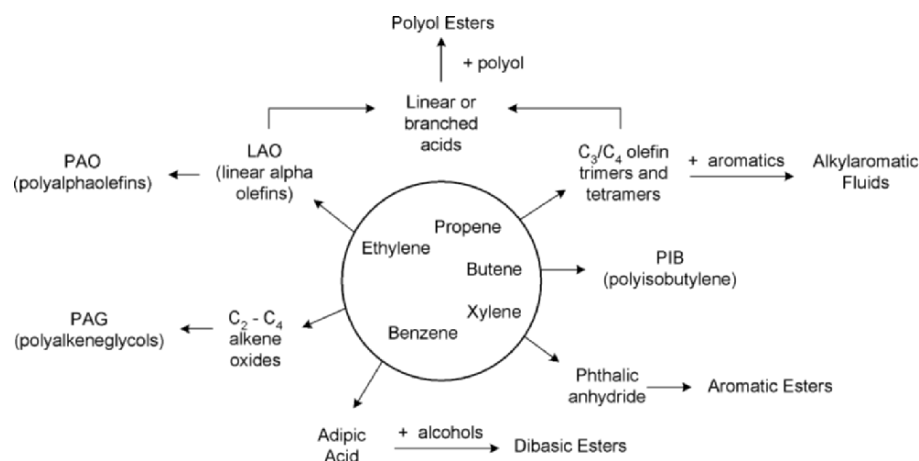


Figure 1. Most synthetic base stocks are derived from petrochemicals

Table 1. Summary of major synthetic base stocks and producers

| Synthetic Base Stock | Major Manufacturer  | Relative price* |
|----------------------|---|-----------------|
| PAO                  | ExxonMobil Chemical Co.,<br>BP, Chevron Phillips Chemical Co., Fortum               | 4               |
| Dibasic ester        | ExxonMobil Chemical Co., Henkel Corp., Hatco Corp., Inolex Chemical Co.             | 5               |
| Polyol ester         | ExxonMobil Chemical Co., Henkel Corp., Hatco Corp., Inolex Chemical Co., Kao Corp., | 7-10            |
| PAG                  | Dow Chemical Co., BASF  | 4-10            |
| Alkylaromatic        | ExxonMobil Chemical Co., Pilot Chemical Co., Inolex Chem. Co.                       | 4-8             |
| Mineral oil          | ExxonMobil, Motiva Enterprise, ChevronTexaco, Valero, BP, Shell, etc.               | 1               |

\* Estimated relative price vs. Group I mineral oil

### 3. SYNTHETIC BASE STOCK - CHEMISTRY, PRODUCTION PROCESS, PROPERTIES AND USE

#### 3.1 PAO

PAO with viscosities of 2 to 100 cSt at 100°C are currently produced and marketed commercially<sup>7</sup>. The low viscosity PAO of 4 to 6 cSt account for more than 80% of the total volume. The remaining are mainly medium to high viscosity products of 10 to 100 cSt.

### 3.1.1 Chemistry for PAO Synthesis

1-Decene is the most commonly used starting olefin for PAO (Figure 2). It is produced as one member of the many linear alpha-olefins (LAO) in an ethylene growth process, which yields  $C_4$  to  $C_{20}$  and higher LAO according to the Schulz-Flory distribution<sup>8</sup>. Typically, 1-decene constitutes about 10-25% of the total LAO fraction, depending on the process technology.

To make PAO, the linear 1-decene is further polymerized using Friedel-Crafts catalysts to give  $C_{20}$ ,  $C_{30}$ ,  $C_{40}$ ,  $C_{50}$ , and higher olefin oligomers.

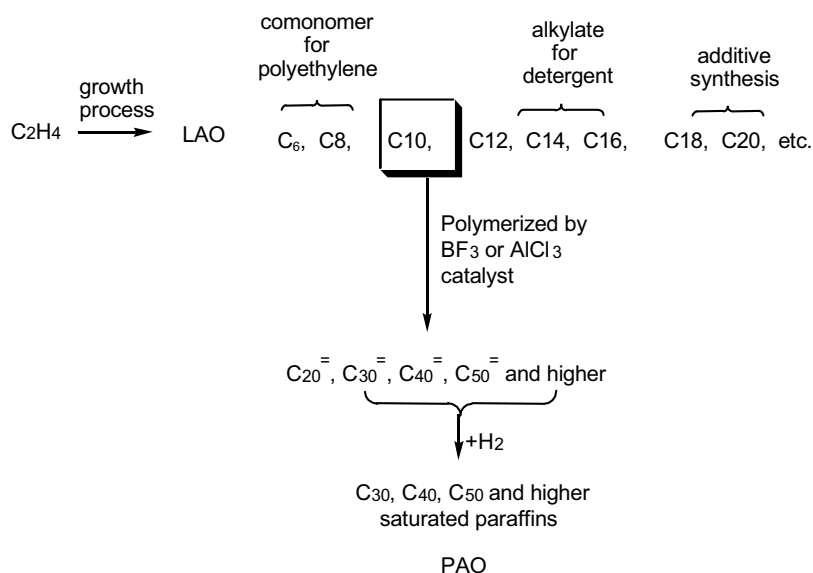


Figure 2. Reaction scheme for converting ethylene into PAO

The degree of polymerization depends on the type of catalyst used and reaction conditions<sup>9</sup>. Generally,  $BF_3$  type catalysts give a lower degree of polymerization. By careful choice of co-catalyst types and reaction conditions, the  $BF_3$  process produces mostly  $C_{30}$  to  $C_{50}$  oligomers that yield low viscosity base stocks of 4-8 cSt.  $AlCl_3$ -based catalysts are more suitable for higher viscosity PAO synthesis because they produce oligomers with  $C_{60}$ ,  $C_{70}$  and higher olefin enchainment species. If a  $C_{20}$  fraction is produced, it is usually separated and recycled. Fractions containing  $C_{30}$  and higher olefin oligomers are then hydrogenated to yield fully saturated paraffinic PAO.

PAO is a class of molecularly engineered base stock with optimized viscosity index, pour point, volatility, oxidative stability and other important lubricant base oil properties. Researchers at ExxonMobil have systematically synthesized polyalphaolefin oligomers of  $C_{30}$  to  $C_{40}$  by  $BF_3$  catalysis and compared their lubricant properties, as summarized in Table 2.<sup>10</sup>

Table 2. Lubricant base stock property comparison: C<sub>30</sub>-C<sub>42</sub> hydrocarbons made from different olefins

| Name                | Carbon Number | Kinematic Viscosity, cSt, at |      |         | Viscosity Index | Pour Point, °C |
|---------------------|---------------|------------------------------|------|---------|-----------------|----------------|
|                     |               | 100°C                        | 40°C | -40°C   |                 |                |
| Propylene decamers  | C30           | 7.3                          | 62.3 | >99,000 | 70              | --             |
| Hexene pentamers    | C30           | 3.8                          | 18.1 | 7,850   | 96              | --             |
| Octene tetramers    | C32           | 4.1                          | 20.0 | 4,750   | 106             | --             |
| Decene trimers      | C30           | 3.7                          | 15.6 | 2,070   | 122             | <-55           |
| Undecene trimers    | C33           | 4.4                          | 20.2 | 3,350   | 131             | <-55           |
| Dodecene trimers    | C36           | 5.1                          | 24.3 | 13,300  | 144             | -45            |
| Decene tetramers    | C40           | 5.7                          | 29.0 | 7,475   | 141             | <-55           |
| Octene pentamers    | C40           | 5.6                          | 30.9 | 10,225  | 124             | --             |
| Tetradecene trimers | C42           | 6.7                          | 33.8 | Solid   | 157             | -20            |

These data show that the oligomers made from propylene, 1-hexene and 1-octene have relatively low VI and very high viscosity at -40°C. Oligomers from 1-tetradecene have high VI but also have undesirable high pour point and are solid at -40°C. Oligomers from 1-decene have the best combination of high VI, low pour point and -40°C viscosity.

Historically, the market dynamics of LAO supply and demand further drove the trend toward the use of 1-decene as a raw material. Among all the major LAO from the ethylene growth process (Figure 2), C<sub>6</sub> and C<sub>8</sub> LAO are used as co-monomer in the linear low-density polyethylene production; C<sub>12-16</sub> LAO are used in the manufacture of linear alkylbenzene detergent; C<sub>18</sub> and C<sub>20</sub> LAO are used in additives. 1-Decene is not in high demand for other chemical manufacturing and its use as raw material for synthetic base stocks makes a perfect match. When 1-decene supply became tight, other LAO, such as C<sub>8</sub> and C<sub>12</sub>, have been successfully incorporated with 1-decene as the starting olefins for PAO production. Since 2001, 1-decene supply has increased significantly due to several LAO expansion projects and new production coming on-line around the world<sup>11</sup>.

The chemical composition of PAO is very simple. Using 4 cSt PAO as an example, it is made of ~ 85% C<sub>30</sub> and ~15% C<sub>40</sub> hydrocarbons. It has a narrow molecular weight distribution compared to typical 4 cSt mineral oils. The gas chromatograms in Figure 3 show that 4 cSt PAO has few low



molecular weight components of less than  $C_{30}$  that can degrade oil volatility, flash and fire point. Figure 3 also shows that the  $C_{30}$  fraction of PAO is not a single compound but a mixture of many isomers. This is because the PAO from  $BF_3$  process contains many isomers, each with different types of branching<sup>12</sup>. This irregular branching may be beneficial to some of PAO's low temperature properties, e.g. pour point.

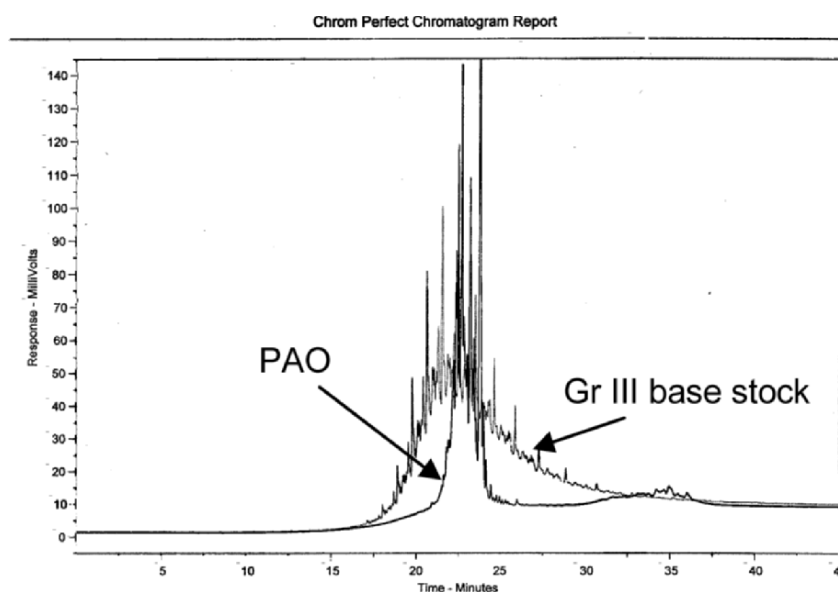


Figure 3. Gas chromatograph comparison of a 4 cSt PAO with a 4 cSt Group III base stock

### 3.1.2 Manufacturing Process for PAO

Commercial production of PAO using a  $BF_3$  catalyst generally involves a multi-stage, continuous stirred tank reactor (CSTR) process<sup>9</sup>. In early production technology, the catalyst was destroyed with diluted aqueous alkali after polymerization. More recent patents disclosed improved processes using  $BF_3$  catalyst recycle to reduce catalyst usage, minimize process waste and improve process economics<sup>13</sup>.

### 3.1.3 Product Properties

The physical properties of some commercial PAO are summarized in Table 3.<sup>7</sup>

Table 3. General product properties of commercial PAO from ExxonMobil Chemical Company

| Fluid type                      | SHF-20 | SHF-41 | SHF-61/63 | SHF-82/83 | SHF-101 | SHF-403 | SHF-1003 |
|---------------------------------|--------|--------|-----------|-----------|---------|---------|----------|
| Kinematic Viscosity @100°C, cSt | 1.7    | 4.1    | 5.8       | 8.0       | 10.0    | 39      | 100      |
| Kinematic Viscosity @40°C, cSt  | 5      | 19     | 31        | 48        | 66      | 396     | 1,240    |
| Kinematic Viscosity @-40°C, cSt | 262    | 2,900  | 7,800     | 19,000    | 39,000  | --      | --       |
| Viscosity Index                 | --     | 126    | 138       | 139       | 137     | 147     | 170      |
| Pour Point, °C                  | -66    | -66    | -57       | -48       | -48     | -36     | -30      |
| Flash Point., °C                | 157    | 220    | 246       | 260       | 266     | 281     | 283      |
| Specific Gravity @15.6°C/15.6°C | 0.798  | 0.820  | 0.827     | 0.833     | 0.835   | 0.850   | 0.853    |

### 3.1.4 Comparison of PAO with Petroleum-based Mineral Base Stocks

PAO have different chemical compositions compared to mineral oil base stocks. The American Petroleum Institute (API) categorizes lubricant base stocks into five categories, designated Group I to V. The definition of each base stock group is summarized in Table 4.

Table 4. Definition of API category I to V lubricant base stock

| Description   | % Saturates | % Sulfur | VI     |
|---|-------------|----------|--------|
| Group I (Conventional, solvent refined)*  | <90         | >0.03    | 80-120 |
| Group II (Hydroprocessed)*  | >= 90       | </= 0.03 | 80-120 |
| Group III (Severely hydroprocessed or isomerized wax)*  | >= 90       | </= 0.03 | >=120+ |
| Group IV Polyalphaolefins   |             |          |        |
| Group V All other base stocks not included in Group I, II, III or IV (e.g. esters, PAG, alkylaromatics, etc.) | --          | --       | --     |

\* - comments in parentheses are not included in the original API definition

PAO is classified by itself as a Group IV base stock. In addition to the differences listed in Table 3, PAO also contains no cyclic paraffins, naphthenes or aromatics, whereas Group I, II and III base stocks contain different amounts of aromatics ranging from <1% to >40%<sup>14</sup>. With the increasing presence of aromatics and/or naphthenes, oxidative stability and low temperature properties of these fluids are typically degraded. Also, as shown earlier in Figure 3, PAO have discrete carbon numbers with relatively long linear hydrocarbon branches, whereas mineral base stocks contain a continuum of carbon number. As a result, PAO usually have lower volatility.

Table 5 compares the basic properties of low and high viscosity PAO versus Group I to Group III mineral oil base stocks.

Table 5. Typical property comparison of PAO with Group I to III mineral oil

|                                  | Low Viscosity |        |         |     | High Viscosity |           |
|----------------------------------|---------------|--------|---------|-----|----------------|-----------|
|                                  | Grp I         | Grp II | Grp III | PAO | Bright stock   | PAO stock |
| Kinematic Viscosity @100°C, cSt  | 3.8           | 5.4    | 4.1     | 4.1 | 30.5           | 100       |
| Kinematic Viscosity @40°C, cSt   | 18            | 30     | 19      | 19  | 470            | 1,240     |
| Viscosity Index                  | 92            | 115    | 127     | 126 | 94             | 170       |
| Pour Point, °C                   | -18           | -18    | -15     | -66 | -18            | -30       |
| Cold Crack Simulator @ -20°C, cP | --            | --     | 750     | 620 | --             | --        |
| Noack Volatility, wt%            | 32            | 15     | 14      | 12  | --             | --        |
| Aniline point, °C                | 100           | 110    | 118     | 119 | 97             | >170      |

- PAO have superior viscometrics properties compared to mineral oil base stocks.

Data in Table 5 show that PAO has higher VI and lower pour point than Group I and II base stocks. Compared to Group III base stocks, PAO has comparable VI, but much lower pour point and improved low-temperature viscosity as measured by Cold Cranking Simulator (CCS) viscosity at -20°C. In an actual engine oil formulation, this lower CCS viscosity observed with PAO results in a wider SAE cross-grade (5W-40) than with Group III base stock (10W-40)<sup>15</sup>. The lower low-temperature viscosity translates into better fuel economy during the engine warm up period.

- PAO has lower volatility.

Data in Table 5 show that PAO has lower volatility than Group I to III base stocks. This lower volatility is the result of the unique chemical compositions of PAO - 100% relatively linear paraffin, little low molecular weight hydrocarbons of less than C<sub>30</sub> (Figure 3). Low volatility is advantageous for decreased oil consumption and reduced emissions.

- PAO show intrinsic oxidative stability and excellent response to antioxidant additive treatment.

It has been demonstrated that the un-formulated PAO base stock treated with 0.5 wt% antioxidant resists oxidation for more than 2500 minutes in a standard rotary bomb oxidation test (RBOT, D2272 method). In comparison, similarly treated Group II and III base stock started to oxidize much earlier, at less than 800 or 1700 minutes, respectively<sup>16</sup>.

This oxidative stability translates into performance advantages in actual engine oil tests (Figure 4).<sup>15</sup>

Figure 4 shows that a fully formulated engine oil with PAO has much lower viscosity increase than with Group III or with Group I/II base stocks in standard length, 64-hour ASTM Sequence IIIIE engine test. In an extended-length, 256-hour test, the viscosity increase for PAO-based lubricant is still much less than the maximum increase allowable for this test. In contrast, Group III or Group I/II based engine lubricants become too viscous to measure. Performance advantages in fuel efficiency and oil consumption are also reported.<sup>17</sup>

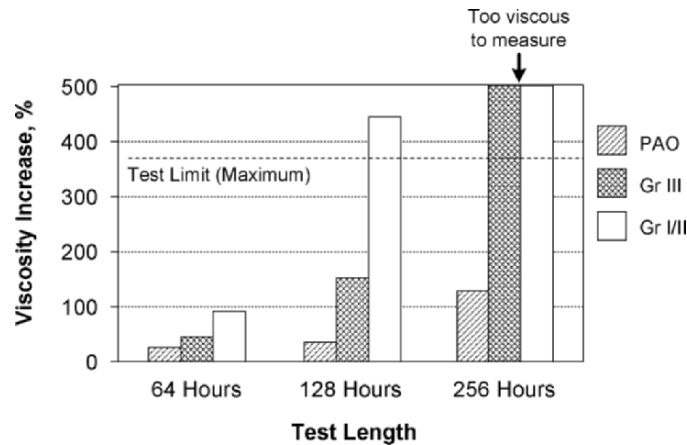


Figure 4. Comparison of viscosity increase in ASTM Sequence IIIE engine test for fully formulated lubricants based on PAO vs. Group III or I/II base stocks<sup>17</sup>

- PAO are available in wide viscosity range.

PAO are available from 2 to 100 cSt at 100°C. The high viscosity PAO maintain excellent VI and low pour point (Table 3 and 5), in a manner that is superior to the highest viscosity mineral oil base stock - bright stock. High viscosity PAO are important when blending with low viscosity fluid to formulate high viscosity grade industrial oils. When used to blend with low viscosity mineral oil, the high viscosity PAO also significantly improves the oxidative stability of the blended base stocks compared to using mineral bright stock<sup>15</sup>.

- PAOs have high aniline point, indicating low polarity.

Table 5 shows that low viscosity PAO has a higher aniline point than Group I mineral oils, 119°C vs. 100°C (Table 5). A more pronounced difference is observed for high viscosity fluids (>170°C vs. 97°C). The higher aniline points of PAO mean that they are much less polar than Group I oils. Generally, lubricant additives and oil oxidation by-products are highly polar chemical species. As aniline point has relevance to solvency, additives and oil oxidation by-products are not very soluble in PAO alone. As a result, a polar co-base stock, such as ester or alkylaromatic, is usually added to the formulation to improve the solvency of PAO in a finished lubricant. These co-base stocks can also assist other performance features, such as seal compatibility and improved lubricity.

- PAO possess other important properties, depending on application:
  - Compatibility or miscibility with mineral oil at all concentration levels without phase separation or detrimental effects when cross-contamination occurs
  - Hydrolytic stability

- 10% higher thermal conductivity and heat capacity than comparable mineral oil, allowing equipment to run at lower temperature and improve wear performance<sup>18</sup>
- Lower traction coefficients than conventional fluids, resulting in better energy efficiency for many industrial oil applications<sup>6</sup>
- PAO are non-greasy and non-comedogenic

In summary, PAO have superior VI, pour point, low-temperature viscosity, volatility, and oxidative stability and are available in a wide viscosity range compared to conventional Group I, II or III mineral oils.

### 3.1.5 Recent Developments – SpectraSyn Ultra as Next Generation PAO

Following the success with PAO, ExxonMobil Chemical Co. recently introduced a new generation of PAO, trade-named SpectraSyn Ultra<sup>TM</sup>. SpectraSyn Ultra<sup>TM</sup> is produced from the same raw material as PAO, 1-decene, using proprietary catalyst technology<sup>19, 20</sup>. Table 6 summarizes the properties of commercial SpectraSyn Ultra<sup>TM</sup> products.

Compared to traditional PAOs, SpectraSyn Ultra<sup>TM</sup> PAO have even higher VI, lower pour point and are available in higher viscosity ranges. This unique class of fluid can be used in automotive engine oil and industrial oil formulations to provide advantages in terms of shear stability, viscometrics properties, thickening power and increased lubricant film thickness.

Table 6. Product properties of next generation PAO - SpectraSyn Ultra<sup>TM</sup>

| Product                         | SpectraSyn Ultra <sup>TM</sup> 150 | SpectraSyn Ultra <sup>TM</sup> 300 | SpectraSyn Ultra <sup>TM</sup> 1000 |
|---------------------------------|------------------------------------|------------------------------------|-------------------------------------|
| Kinematic Viscosity @100°C, cSt | 150                                | 300                                | 1,000                               |
| Kinematic Viscosity @40°C, cSt  | 1,500                              | 3,100                              | 10,000                              |
| Viscosity Index                 | 218                                | 241                                | 307                                 |
| Pour Point, °C                  | -33                                | -27                                | -18                                 |
| Flash Point., °C                | >265                               | >265                               | >265                                |
| Specific Gravity @15.6°C/15.6°C | 0.850                              | 0.852                              | 0.855                               |

### 3.1.6 Applications

PAO is the workhorse base stock for most synthetic lubricants. Low viscosity PAO are used in synthetic automotive crankcase and gear lubricants, industrial oils and greases. High viscosity PAO have found great utility in industrial oils and greases.

**Synthetic automotive engine oils** command the largest volume among synthetic lubricant products. Taking advantage of the many superior properties of PAO base stocks, performance advantages of synthetic engine oils based on PAO over mineral oil-based engine oils are well-documented in scientific and trade literature<sup>21</sup>. They include:

- Improved engine wear protection
- Extended oil drain interval
- Excellent cold starting performance
- Improved fuel economy
- Reduced oil consumption
- Excellent low-temperature fluidity and pumpability
- High temperature oxidation resistance

Many of these performance advantages are directly attributable to the intrinsically superior properties of PAO, such as high VI, low pour point, low low-temperature viscosity, high oxidative stability, low volatility, etc.

The advantage of using synthetic engine oil is further supported by the fact that many automakers use synthetic lubricant as the “factory fill” lubricant for their high performance cars. For example, in 2003, Mobil 1™ is used as factory-fill lubricant for the Corvette, all Porsches, Mercedes-Benz AMG models, Dodge Viper, Ford Mustang Cobra R and Cadillac XLR<sup>22</sup>.

PAO blended with mineral oil are also used in many partial synthetic lubricant formulations. In this case, PAO is used as a blending stock to improve the volatility, high or low-temperature viscosity, oxidative stability, etc. of the mineral oil blend.

**Synthetic industrial oils and greases**, formulated with PAO, have many specific performance and economic advantages over conventional lubricants<sup>6,21a</sup>. For example, in industrial gear/circulation oils, PAO-based lubricants offer the following documented advantages:

- Energy savings, longer fatigue life and lowered temperatures of operation due to lower traction coefficients
- Wider operating temperature range due to higher VI and better thermal-oxidative stability
- Reduced equipment down-time, reduced maintenance requirements and longer oil life due to the excellent stability of PAO base stock

Because PAO is available in high viscosity grades (up to 100 cSt at 100°C), high ISO grade synthetic industrial oils with improved performance features are more easily formulated. This option is not available for mineral oil-based lubricants.

In compressor oil applications, PAO-based lubricants have advantages due to their better chemical inertness and resistance to chemical attack. Synthetic compressor oils are used in corrosive chemical environments, for example, in sulfuric acid or nitric acid plants. PAO-based lubricants are also used in refrigeration compressor applications due to their excellent low temperature fluidity, lubricity and generally wider operating temperature range.

Other synthetic industrial oil applications with PAO-based lubricants, include gas turbine, wind turbine and food-grade gear lubricants. Synthetic greases based upon PAO are used in industrial equipment, aviation and automotive applications that take advantage of the wide operating

temperature range, high degree of stability and other desirable properties and features offered by PAO base stocks.

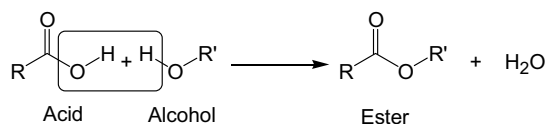
Recently, PAO is finding its way into personal care products such as shampoos, conditioners and skin lotions because it provides emolliency in addition to good skin feel and is non-greasy and non-comedogenic. It is also used in off-shore drilling fluids because of its good lubricity. New applications for PAO are continuously emerging.

### 3.2 Dibasic, Phthalate and Polyol Esters - Preparation, Properties and Applications

Lard and vegetable oil, both ester-type compounds derived from natural sources, have been used as lubricants throughout human history. After World War II, thousands of synthetic esters were prepared and evaluated as lubricant base stocks for jet engine lubricants.<sup>2</sup>

#### 3.2.1 General Chemistry and Process

Esters are made by reacting carboxylic acids with alcohols. The elimination of water is shown by the following equation:



The reaction proceeds by heating the mixture to 150°C or higher with or without a catalyst<sup>9</sup>. Catalysts such as p-toluenesulfonic acid or titanium(IV) isopropoxide, are typically used to facilitate reaction rates. The reaction is driven to completion by continuous removal of water from the reaction medium. Sometimes, one component is used in a slight excess to ensure complete conversion. The final product is purified over an adsorbent to remove trace water and acids, both of which are detrimental to base stock quality. Commercially, esters are generally produced by batch processes.

The choice of acid and alcohol determines the ester molecular weights, viscometrics and low temperature properties, volatility, lubricity, as well as the thermal, oxidative and hydrolytic stabilities<sup>23</sup>. The structure-property relationships of ester base stocks are well documented in the literature. Compared to PAO and mineral oil, ester fluids have a higher degree of polarity, contributing to the following unique properties:

- Superior additive solvency and sludge dispersancy
- Excellent lubricity
- Excellent biodegradability
- Good thermal stability

Three classes of esters are most often used as synthetic base stocks - dibasic ester, polyol ester and aromatic ester. Some basic properties of these esters are summarized in the Table 7.

Table 7. Basic properties of ester base stocks

| Acid   | Alcohol                             | Viscosity, cSt |      | VI  | Pour Point, °C | Wt% Volatility <sup>(a)</sup> | Wt% Biodegradability <sup>(b)</sup> |
|--|-------------------------------------|----------------|------|-----|----------------|-------------------------------|-------------------------------------|
|  |                                     | 100°C          | 40°C |     |                |                               |                                     |
| <b>Dibasic ester</b>                                 |                                     |                |      |     |                |                               |                                     |
| Adipate  | Iso-C <sub>13</sub> H <sub>27</sub> | 5.4            | 27   | 139 | -51            | 4.8                           | 92                                  |
| Sebacate   | Iso-C <sub>13</sub> H <sub>27</sub> | 6.7            | 36.7 | 141 | -52            | 3.7                           | 80                                  |
| <b>Polyol ester</b>                                  |                                     |                |      |     |                |                               |                                     |
| n-C <sub>8</sub> /C <sub>10</sub>                    | PE <sup>(c)</sup>                   | 5.9            | 30   | 145 | -4             | 0.9                           | 100                                 |
| n-C <sub>5</sub> /C <sub>7</sub> /iso-C <sub>9</sub> | PE                                  | 5.9            | 33.7 | 110 | -46            | 2.2                           | 69                                  |
| n-C <sub>8</sub> /C <sub>10</sub>                    | TMP <sup>(c)</sup>                  | 4.5            | 20.4 | 137 | -43            | 2.9                           | 96                                  |
| Iso-C <sub>9</sub>                                   | TMP                                 | 7.2            | 51.7 | 98  | -32            | 6.7                           | 7                                   |
| n-C <sub>9</sub>                                     | NPG <sup>(c)</sup>                  | 2.6            | 8.6  | 145 | -55            | 31.2                          | 97                                  |
| Di- and mono-acids                                   | NPG                                 | 7.7            | 40.9 | 160 | -42            | --                            | 98                                  |
| <b>Aromatic Esters</b>                               |                                     |                |      |     |                |                               |                                     |
| Phthalate  | Iso-C <sub>13</sub> H <sub>27</sub> | 8.2            | 80.5 | 56  | -43            | 2.6                           | 46                                  |
| Phthalate  | Iso-C <sub>9</sub>                  | 5.3            | 38.5 | 50  | -44            | 11.7                          | 53                                  |
| Trimellitate   | Iso-C <sub>13</sub> H <sub>27</sub> | 20.4           | 305  | 76  | -9             | 1.6                           | 9                                   |
| Trimellitate   | C <sub>7</sub> /C <sub>9</sub>      | 7.3            | 48.8 | 108 | -45            | 0.9                           | 69                                  |

(a) Noack Volatility : 250°C, 20 mm-H<sub>2</sub>O, and one hour with air purge

(b) by CEC-L-33-A-96 test, % degradable in 21 days

(c) PE: pentaerythritol, TMP: trimethylolpropane, NPG: neopentylglycol

### 3.2.2 Dibasic Esters

Dibasic esters are made from carboxylic diacids and alcohols. Adipic acid (hexanedioic acid) is the most commonly used diacid (Figure 5). Because it is linear, adipic acid is usually combined with branched alcohols, such as 2-ethylhexanol or isotridecanols (C<sub>13</sub>H<sub>27</sub>OH) to give esters with balanced VI and low temperature properties (Figure 5). Dibasic ester is most often used as a co-base stock with PAO to improve solvency and seal swell properties of the final lubricants.

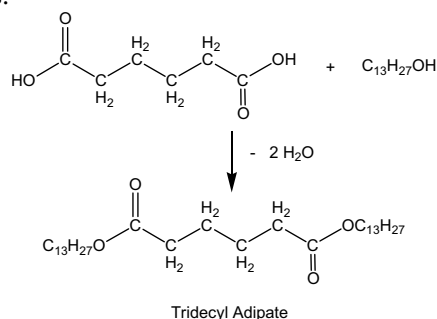


Figure 5. Synthesis of adipate ester



### 3.2.3 Polyol Esters

The most common polyols used to produce synthetic polyol ester base stocks are pentaerythritol (PE), trimethylolpropane (TMP) and neopentylglycol (NPG), (Figure 6). By carefully choosing the degree of branching and size of the acid functions, polyol esters with excellent viscometric properties - high VI and very low pour points - can be produced (Table 6).

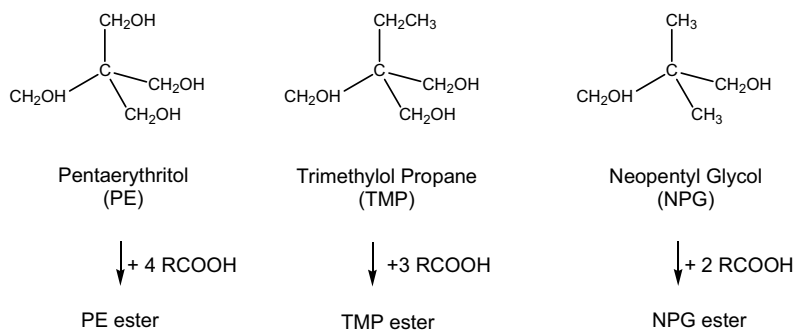


Figure 6. Synthesis of polyol esters

In addition to excellent viscometric properties, polyol esters have the best thermal resistance to cracking. This is because polyols lack  $\beta$ -hydrogen(s) adjacent to the carbonyl oxygen and thus can not undergo the same facile  $\beta$ -H transfer reaction as the dibasic esters (Figure 7). This cracking by  $\beta$ -H transfer leads to two neutral molecules and is a relatively low energy process. Polyol esters can only be cracked by C-O or C-C bond cleavage, leaving two free radicals - a very high-energy process requiring extremely high temperature. Therefore, polyol esters are thermally stable up to 250°.

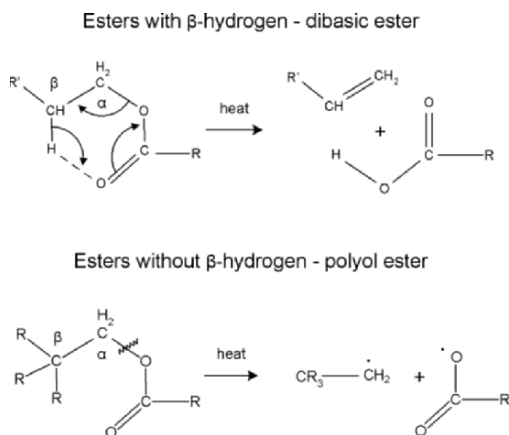


Figure 7. Cracking reaction mechanism for esters -  $\beta$ -H effect

Among the three polyol ester types, the thermal stability ranking is: PE esters > TMP esters > NPG esters.

### 3.2.4 Aromatic Esters

Phthalic anhydride or trimellitic anhydride are converted into esters by reactions with alcohols as shown in Figure 8. Phthalic anhydride is produced cheaply and in large volume from oxidation of ortho-xylene. The largest use of phthalate esters is in the plasticizer market. Only a small fraction of its production is consumed by the synthetic lubricants market. Phthalate esters generally have superior hydrolytic stability than adipic esters because the ortho di-ester groups are electronically less available and sterically more hindered<sup>24</sup>. However, they have lower VIs, 50-70, because of their high polarity and the presence of branched alcohol chains. They are used in special industrial oil applications where VI is not a critical parameter. Trimellitate esters are specialty products and relatively expensive. They are of high viscosity and usually are more resistant to oxidation than adipic esters.

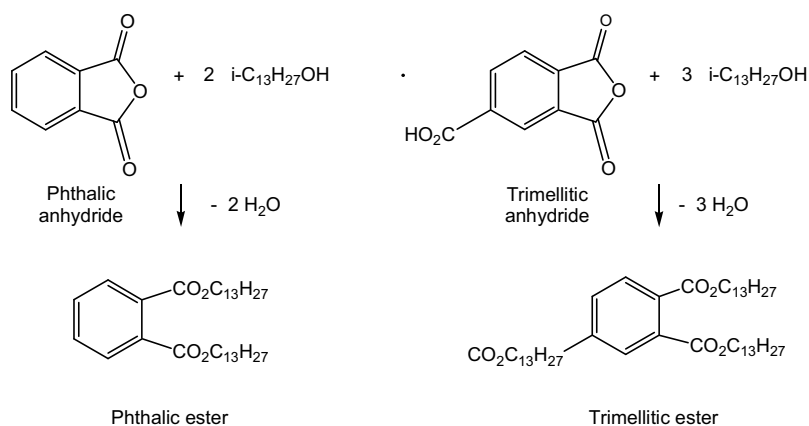


Figure 8. Synthesis of phthalate and trimellitate esters

### 3.2.5 General Properties and Applications of Ester Fluids

**Solvency and dispersancy** - Ester fluids are quite polar due to their high oxygen contents. They have high solubility for many commonly used additives. They also have high solubility for the polar acids and sludges generated by oxidation processes during service. This property makes ester based lubricant “clean“ compared to hydrocarbon-based lubricants. Typically, low viscosity ester fluids are soluble with non-polar PAO base stocks. These properties make them excellent for use as co-base stocks with PAO in many synthetic automotive and industrial lubricants. Generally, 5 to 25% esters are used with PAO in finished lubricant formulations.

**Hydrolytic stability**<sup>24</sup> - Hydrolysis of esters to give acids and alcohols is a facile reaction and can proceed at elevated temperatures in the presence of water. Hydrolysis of ester generates acid that can be very corrosive to metal components and can catalyze the base stock decomposition process. Therefore, hydrolytic stability of esters is an important issue. Much work has been carried out to improve the hydrolytic stability by varying the composition of acids and alcohols. Generally, esters made from aromatic acids or from more sterically hindered acids, such as 2-alkyl substituted acids or neo-acids, have improved hydrolytic stabilities. Proper branching of the acids protect the carbonyl ester function from the detrimental attack of water. The presence of impurity, such as trace acid or metal, can catalyze the decomposition and hydrolysis of ester. Compared to PAO or alkylaromatic base stocks, ester hydrolysis is always an issue of concern in many lubrication applications.

**Volatility** - Ester fluids generally have lower volatility compared to PAO and mineral oil of comparable viscosities. A General volatility ranking for base stocks are as follows:

PE ester > TMP ester > dibasic ester > PAO >> Group I or II mineral oil.

**Lubricity** - Polar ester fluids show mild boundary film protection at lower temperature. At lower temperature, esters interact with the metal surface via polar interaction, forming a chemisorbed surface film, which can provide better lubrication than the less polar mineral oil or non-polar PAO. When esters decompose, they produce acids and alcohols. Higher molecular weight acids can bind with the metal surfaces to form a film that can offer some degree of wear protection and friction reduction. However, none of these interactions are strong enough to persist when surface or oil temperature rises much above 100°C. At higher temperature, significant wear protection can only be achieved by the use of anti-wear or extreme-pressure (EP) additives. A drawback for the ester high polarity is that esters can compete with metal surface for polar additives, resulting in less efficient usage of anti-wear and EP additives. Therefore, in formulations using esters, it is important to choose the proper additives and concentration levels to obtain the full benefit of the lubricity from both the additives and esters.

**Biodegradability** - By carefully choosing the molecular compositions, esters of excellent biodegradability can be produced. Generally, esters from more linear acids and alcohols have better biodegradability.

**Applications**<sup>25</sup> - Esters, both dibasic and polyol esters, are used as co-base stocks with PAO or other hydrocarbon base stocks in synthetic automotive engine lubricants and industrial lubricants. Polyol esters are used in aircraft turbine oils due to their excellent thermal and oxidative stabilities, good lubricity, high VI and excellent low temperature properties (<-40°C)<sup>21a</sup>. Esters are also used in synthetic compressor oils for ozone-friendly refrigeration units. Because of their high biodegradability and low toxicity, esters are often the base oils of choice for many environmentally-aware

lubricants or single-pass lubrication applications where ecological impact is critical.

Although ester chemistry has been studied extensively, new esters with unique performance improvements have continuously been reported in the literature<sup>26</sup>. For example, esters with high stability were made from highly branched acids and polyols. Polyol esters formulated with ashless additives can be used as high performance biodegradable hydraulic fluids.

### 3.3 Polyalkylene Glycols (PAG)

PAG is an important class of industrial chemicals. Its major use is in polyurethane applications. Outside of polyurethane applications, only 20% of the PAG is used in lubricant applications. Compared to PAO or esters, PAG have very high oxygen content and hydroxyl end group(s). These unique chemical features give them high water solubility and excellent lubricity. PAG was first developed as water-based, fire-resistant hydraulic oils during World War II for military use. Other applications have been developed subsequently to take advantage of their unique properties.

#### 3.3.1 Chemistry and Process

PAG are synthesized by oligomerization of alkylene oxides over a base catalyst with an initiator R'OH (Figure 9)<sup>27</sup>. When the initiator is water (R'=H), the final PAG has two hydroxyl end groups. When the initiator is an alcohol (R=alkyl group), one of the end groups is an alkoxy group (RO-). The most commonly used alcohol is n-butanol, although large alcohols have also been used for special applications. Phenol, thiols or thiophenol are also used as initiators.

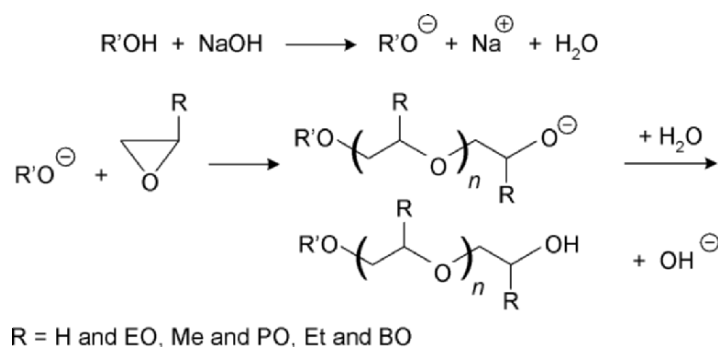


Figure 9. Reaction scheme for PAG synthesis

Ethylene oxide (EO), propylene oxide (PO), butylene oxides (BO) or combinations of these epoxides are used as starting materials for PAG syntheses. Longer chain alkylene oxides are sometimes added to improve their compatibility with hydrocarbons. PAG with a wide range of viscosities,

VIs, pour points, water solubilities and oil-compatibilities are produced by choosing the proper initiators, monomers, reaction conditions and post treatments. The reaction is highly exothermic (22.6 kcal/mole) and heat removal is important to avoid side-reactions or broadening of the product molecular weight distribution.

### 3.3.2 Product Properties

Table 8 summarizes the typical lubricant properties of selected PAG produced from EO, PO and BO with several different initiators.<sup>28</sup>

Table 8. Lube properties of PAG fluids from EO, PO and BO with different initiator

|                         | AO Type | End Group | Avg. MW | KV <sub>100°C</sub> cSt | KV <sub>40°C</sub> cSt | VI  | Pour Point, °C | Density, g/cm <sup>3</sup> | Solubility in oil | Solubility in water |
|-------------------------|---------|-----------|---------|-------------------------|------------------------|-----|----------------|----------------------------|-------------------|---------------------|
| E300                    | EO      | OH/OH     | 300     | 5.9                     | 36                     | 118 | -10            | 1.125                      | i                 | s                   |
| E600                    | EO      | OH/OH     | 600     | 11.0                    | 72                     | 154 | 22             | 1.126                      | I                 | s                   |
| P425                    | PO      | OH/OH     | 425     | 4.6                     | 33                     | 26  | -45            | 1.007                      | --                | --                  |
| P1200                   | PO      | OH/OH     | 1200    | 13.5                    | 91                     | 161 | -40            | 1.007                      | --                | i                   |
| PB200                   | PO      | Bu/OH     | 910     | 8.3                     | 44                     | 180 | -48            | 0.9831                     | --                | i                   |
| EP530                   | EO/PO   | OH/OH     | 2000    | 25                      | 168                    | 192 | -32            | 1.017                      | --                | --                  |
| EPB100                  | EO/PO   | Bu/OH     | --      | 4.8                     | 101                    | 174 | -57            | 1.0127                     | --                | s                   |
| EPB260                  | EO/PO   | Bu/OH     | --      | 11.0                    | 56.1                   | 210 | -37            | 1.0359                     | --                | s                   |
| B100-500                | BO      | OH/OH     | 500     | 5.1                     | 44.3                   | 3   | -30            | 0.975                      | s                 | s                   |
| B100-2000               | BO      | OH/OH     | 2000    | 24.7                    | 234.7                  | 142 | -26            | 0.970                      | s                 | i                   |
| 1500 MW poly BO Mono-ol | BO      | Bu/OH     | 1500    | 15.8                    | 117.1                  | 153 | -30            | 0.961                      | s                 | i                   |

EO-based fluids are typically waxy and have poor low temperature properties. They have high water miscibility and are typically used to formulate water-based lubricants, especially fire-resistant hydraulic oil. PO-based fluids are excellent lubricant base stocks with high VI and low pour point. They have lower solubility in water than EO-based fluids but are not oil miscible.

EO/PO-based fluids have a better combination of VI and low pour points than PO-based products. They are used as base stocks in industrial circulation/gear oils.

BO-based PAG have improved oil solubility and are not water-soluble.

PAG generally have excellent lubricity and low friction coefficients compared to mineral oil as shown in Table 9. These properties result from the facile surface chemisorption of the oxygenate functions or through hydrogen bonding of the terminal OH groups with the metal surface.

Other unique properties for PAG include:

- superior solvency - they dissolve additives, decomposition products and sludges
- non-varnishing and low ash - they leave little or no residue or carbon black upon decomposition

Table 9. Lubricating properties of selected PAG fluids<sup>28</sup>

| Fluid Type | Mol. weight | V100°C<br>,cSt | V40°C<br>cSt | VI  | Pour point, °C | Four ball wear scar, mm (a) | Four ball seizure load, kg (a) | Friction coefficient (b) | Soluble in (c) |
|------------|-------------|----------------|--------------|-----|----------------|-----------------------------|--------------------------------|--------------------------|----------------|
| EO/PO      | 500         | 4.6            | 19           | 161 | -46            | 0.53                        | 120-140                        | 0.15                     | water          |
| EO/PO      | 1300        | 15             | 76           | 218 | -42            | 0.44                        | 180-200                        | 0.11                     | water          |
| PO         | 700         | 6              | 27           | 179 | -44            | 0.53                        | 160-180                        | 0.19                     | oil (d)        |
| PO         | 1300        | 14             | 73           | 193 | -35            | 0.57                        | 120-140                        | 0.12                     | none           |

(a) by DIN 51350 method

(b) determined by oscillation of a steel ball on a steel disc at 30°C under a load of 200 N

(c) determined by mixing equal proportions of water and PAG or oil and PAG.

(d) partially soluble in oi

### 3.3.3 Application

The major use of PAG is in the industrial oil area<sup>29</sup>:

- Fire resistant hydraulic fluids. Water-soluble PAG are fire resistant, low toxicity and have excellent lubricity and anti-wear properties.
- Textile oils. PAG are non-varnishing, non-staining and can be washed away with water.
- Compressor and refrigeration oils. Low solubility of many industrial gases, such as natural gas and ethylene, makes PAG suitable for gas compressor applications. PAG are compatible with new refrigerants (HFC-143a) and have excellent anti-wear properties.
- Metal working fluids. PAG are non-varnishing, have excellent lubricity and anti-wear properties.
- Circulation/bearing/gear oil. Low friction coefficients and traction properties of PAG lead to lower operating temperature and energy consumption. They have good anti-wear properties and are non-varnishing.

## 3.4 Other Synthetic Base Stocks

**Polyisobutylene (PIB)** fluids are produced by the oligomerization of isobutylene in a mixed C<sub>4</sub> stream over a BF<sub>3</sub> or AlCl<sub>3</sub> catalyst. PIB are seldom used by themselves. They are typically used as blend stocks or as additives to increase lubricant viscosity. Table 10 summarizes the typical properties of selected PIB fluids<sup>30</sup>. The VI and pour points of PIB are comparable to those of conventional mineral oil. PIB usually have a lower flash point and decompose easily into monomer at 200°C and higher. The advantages of PIB are their high compatibility with most synthetic or mineral base stocks and their relatively low cost compared to other synthetic base stocks.

Table 10. Typical physical properties of PIB available from BP Chemical Co.

|                                 | H-25 | H-50 | H-100 | H-300 | H-1500 |
|---------------------------------|------|------|-------|-------|--------|
| Kinematic Viscosity @100°C, cSt | 50   | 100  | 200   | 605   | 3000   |
| Viscosity Index                 | 87   | 98   | 121   | 173   | 250    |
| Pour Point, °C                  | -23  | -13  | -7    | 3     | 18     |
| Bromine Number (?)              | 27   | 20   | 16.5  | 12    | 8      |
| Flash Point, °C (a)             | 171  | 193  | 232   | 274   | 307    |
| Molecular Weight (b)            | 635  | 800  | 910   | 1300  | 2200   |

(a) by Cleveland open cup ASTM D92 method.

(b) by gel permeation chromatography.

**Alkylbenzenes and alkylnaphthalenes** are produced by the alkylation of benzene or naphthalene with olefins using Friedel-Crafts alkylation catalysts<sup>31</sup>. Their typical properties are summarized in Table 11. One unique feature of these alkylaromatic fluids is their very low pour points. Alkylbenzenes are often mentioned in the patent literature as components for CFC or HCFC refrigeration compressor oil. Alkylnaphthalenes are used in synthetic automotive engine oil, rotary compressor oils, and other industrial oils.

Table 11. Properties of alkylbenzene and alkylnaphthalenes base stocks

| Fluid type                      | Di-alkylbenzenes            | Di-alkylbenzenes      | Alkylnaphthalenes                  |
|---------------------------------|-----------------------------|-----------------------|------------------------------------|
| Commercial source               | V-9050 from Vista Chem. Co. | Zero 150 from Chevron | Synesstic™ 5 from ExxonMobil Chem. |
| Kinematic Viscosity @100°C, cSt | 4.3                         | 4.4                   | 4.7                                |
| Kinematic Viscosity @40°C, cSt  | 22.0                        | 33.5                  | 28.6                               |
| VI                              | 100                         | 25                    | 74                                 |
| Pour Point, °C                  | -60                         | -40                   | -39                                |
| Flash Point, °C                 | 215                         | 170                   | 222                                |
| Aniline Point, °C               | 78                          | --                    | 33                                 |

**Phosphate esters** are produced from phosphorus oxychloride with various alcohols or phenols, or combinations of these hydroxyl compounds<sup>32</sup>. These fluids generally have good thermal and oxidative stabilities and fire-resistancy. However, because of their high polarity, poor VI-pour point balance, facile hydrolysis<sup>33</sup> and inferior elastomer and paint compatibility, their use in general lubrication is limited. The major use for phosphate esters is in fire-resistant hydraulic oils.

#### 4. CONCLUSION

Synthetic lubricants have significantly raised the performance level of automotive and industrial lubricants with the help of high-quality PAO base stocks and tailored high-performance additive technologies. Equipment builders, industrial users and general consumers have taken advantages of the enhanced performance benefits afforded by synthetic lubricants - reduced

maintenance and waste, lower emissions and pollution, higher reliability and efficiency, etc. As a result, in the last ten years, synthetic lubricants have enjoyed yearly growth rates of 5-10%, a range considerably higher than for conventional lubricants<sup>34</sup>. This growth rate has occurred despite the higher initial costs of synthetic products. The higher initial costs have been economically offset by the extended life and performance benefits afforded by synthetic lubricants.

This trend is expected to continue in the finished lubricants market. In the short-term, the growth for some PAO-based synthetic lubricants may slow temporarily due to new competition from hydroprocessed base stocks<sup>35</sup>. However, high-performance synthetic base stocks and finished lubricants should continue to prove their enhanced and well-documented values as further demands on lubricant performance grow. The knowledgeable user, who treats the lubricant as an active machine component and understands the enhanced performance and associated economic benefits, will continue to demand greater efficiency, reduced maintenance, lower emissions and longer service life, etc, offered by high-quality synthetic lubricants. These factors should increase market value and continue market growth for advanced synthetic lubricants. To meet this demand, the leaders of the lubricant industry will need to respond by developing and marketing next-generation, high performance base stocks and products. ExxonMobil's SpectraSyn Ultra<sup>TM</sup> and Mobil 1<sup>TM</sup> with SuperSyn<sup>TM</sup>-Antiwear technology are current examples of this leadership.

## 5. ACKNOWLEDGEMENT

The authors thank Hal Murray for his assistance in literature search and Andrew Jackson, Mike Thompson, Charles Foster and Joan Kaminski for their valuable comments about this chapter.

## 6. REFERENCES

1. *J. Synth. Lubr.*, **2002**, 18-4, Publisher's Note.
2. G. J. Bishop, Aviation Turbine Lubricant Development, *J. Synth. Lubr.*, **1987**, 4-1, 25.
3. Harlacher, E. A.; Krenowics, R.A.; Putnick, C.R. Alkylbenzene Based Lubricants. *Prep. 52D26P*, 86th AICHE national meeting, Houston, April 1-5 1979.
4. (a) Garwood, W. E., Synthetic Lubricant, US Patent 2,937,129, 1960.  
(b) Hamilton, L. A. and Seger, F. M. Polymerized Olefins Synthetic Lubricants, US Patent 3,149,178, 1964.
5. (a) *Lubricants World*, "On Track for Growth", June 1999, 19.  
(b) After-Market Business Vol. 100, n3, p. 32, March 2000 "It's Brand vs. Commodity in Choosing Motor Oil"  
(c) Business Wire (23 July 2002), p. 328 "Mobil 1 Chosen as Factory-Fill Motor Oil for Cadillac XLR"



6. Murphy, W. R.; Blain, D. A.; Galiano-Roth, A. S.; Galvin P. A. Synthetic Basics - Benefits of Synthetic Lubricants in Industrial Applications, *J. Synth. Lubr.*, **2002**, 18-4, 301.
7. www.exxonmobilsynthetics.com or ExxonMobil Chemical Synthetics, P. O. Box 3272, Houston, TX 77253-3272 (281-570-6000)
8. Lappin, G. R. *Alpha-Olefins Application Handbook*, Lappin, G. R.; Sauer, J. D. (Eds.), Marcel Dekker: New York, 1989; 35.
9. (a) Sacks, M. A private report of Process Economic Program, SRI International, Report no. 125, *Synthetic Lubricant Base Stocks*, May 1979  
(b) Bolan, R. E. A private report of Process Economic Program, SRI International, Report no. 125A, *Synthetic Lubricant Base Stocks*, Sept. 1989
10. Brennan, J. A. Wide-Temperature Range Synthetic Hydrocarbons Fluids, *Ind. Eng. Chem. Prod. Res. Dev.*, **1980**, 19, 2-6
11. (a) "Strong Demand for Synthetic Lubricants Lead to Increased Investment in LAO Production", *Ind. Lubr. Tribology*, **2002**, 54(1), 32. (b)  
[http://www.the-innovation-group.com/ChemProfiles/Alpha Olefins \(Linear\).htm](http://www.the-innovation-group.com/ChemProfiles/Alpha Olefins (Linear).htm)
12. Shubkin R.L.; Baylerian, M. S.; Maler, A. R. Olefin Oligomer Synthetic Lubricants : Structure and Mechanism of Formation, *Ind. Eng. Chem. Prod. Res. Dev.*, **1980**, 19, 15-19
13. Hope, K. D.; Ho, T. C.; Archer, D. L.; Bak, R. J.; Collins, J. B.; Burns, D. W. Process for Recovering Boron Trifluoride From a Catalyst Complex, US Patent 6,410,812, 2002.
14. Cerny, J.; Pospisil, M.; Sebor, G. Composition and Oxidative Stability of Hydrocracked Base Oils and Comparison with a PAO, *J. Synth. Lubr.*, **2001**, 18-3, 199.
15. *ExxonMobil Chemical Co. Sales Brochure*. ExxonMobil Chemical Synthetics, P. O. Box 3272, Houston, TX 77253-3272 (281-570-6000)
16. Lubes-n-Greases, March 2002, p. 39, PAO Problem Solver by Chevron Phillips Chemical Co.
17. Mattei, L.; Pacor, P.; Piccone, A. Oils With Low Environmental Impact for Modern Combustion Engines, *J. Synth. Lubr.*, **1995**, 12-3, 171.
18. (a) *Synthetic Lubricants and High Performance Functional Fluids*, 2nd ed., Rudnick, L. R.; Shubkin, R. L. (Eds.), Marcel Dekker: New York, 1999; 21.  
(b) Lubes-n-Greases, January 2003, p. 39, PAO Problem Solver by Chevron Phillips Chemical Co.
19. (a) Wu, M. M. High Viscosity-Index Synthetic Lubricant Compositions, US Patent 4,827,064, 1989.  
(b) Wu, M. M. High Viscosity-Index Synthetic Lubricant Process, US Patent 4,827,073, 1989.
20. (c) ExxonMobil SuperSyn™ - A New Generation of Synthetic Fluid, Society of Tribologists and Lubrication Engineers Annual Meeting, Las Vegas, Nevada, May 26, 1999
21. (a) Law, D. A.; Lohuis, J. R.; Breaux, J. Y.; Harlow, A. J.; Rochette, M. Development and Performance Advantages of Industrial, Automotive and Aviation Synthetic Lubricants, *J. Synth. Lubr.*, **1984**, 1-1, 6-33.  
(b) Bergstra, R. J.; Baillargeon, D. J.; Deckman, D. E.; Goes, J. A. Advanced Low Viscosity Synthetic Passenger Vehicle Engine Oils, *J. Synth. Lubr.*, **1999**, 16-1, 51.  
(c) Bleimschein, G.; Fotheringham, J.; Plomer A. On the Road to New Diesel Regs - Synthetic Lubes Push on With Fuel to Burn, *Lubes-n-Greases*, November 2002, p. 22
22. www.mobill.com What auto experts say.
23. (a) Szydywar, J. Ester Base Stocks, *J. Synth. Lubr.*, **1984**, 1-2, 153.  
(b) Debuan, F.; Hanssle, P. Aliphatic Dicarboxylic Acid Esters for Synthetic Lubricants, *J. Synth. Lubr.*, **1985**, 1-4, 254.  
(c) Zeman, A.; Koch, K.; Bartle, P., Thermal Oxidative Aging of Neopentylpolyol Ester Oils: Evaluation of Thermal-Oxidative Stability by Quantitative Determination of Volatile Aging Products, *J. Synth. Lubr.*, **1985**, 2-1, 2-21.

- (d) Denis, J. The Relationships between Structure and Rheological Properties of Hydrocarbons and Oxygenated Compounds Used as Base Stocks, *J. Synth. Lubr.*, **1984**, 1-3, 201.
24. Boyde, S. Hydrolytic Stability of Synthetic Ester Lubricants, *J. Synth. Lubr.*, **2000**, 16-4, 297.
25. Carnes, K, Ester? Ester Who? *Lubricants World*, October 2002, p. 10
26. (a) Schlosberg, R. H.; Chu, J. W.; Knudsen, G. A.; Suciu, E. N.; Aldrich, H. S. High Stability Esters for Synthetic Lubricant Applications, *Lubr. Eng.*, **2001**, 21.  
(b) Duncan, C.; Reyes-Gavilan J.; Costantini, D.; Oshode, S. Ashless Additives and New Polyol Ester Base Oils Formulated for Use in Biodegradable Hydraulic Fluid Applications, *Lubr. Eng.*, September 2002, p. 18
27. Kussi, S. Chemical, Physical and Technological Properties of Polyethers as Synthetic Lubricants, *J. Synth. Lubr.*, **1985**, 2-1, 63.
28. The Dow Chemical Co., Midland, Michigan 48674, Dow Polyglycol product brochure. [www.dow.com](http://www.dow.com)
29. Matlock, P. L.; Brown, W. L.; Clinton, N. A. Polyalkylene Glycols, Chapter 6, In *Synthetic Lubricants and High Performance Functional Fluids*, 2nd Ed. Rudnick, L. R.; Shubkin, R. L. (Eds.), Marcel Dekker: New York, 1999; p. 159.
30. [www.bpchemicals.com/polybutene/](http://www.bpchemicals.com/polybutene/)
31. Wu, M. M. Alkylated Aromatics, Chapter 7, In *Synthetic Lubricants and High Performance Functional Fluids*, 2nd Ed. Rudnick, L. R.; Shubkin, R. L. (Eds.), Marcel Dekker: New York, 1999; p. 195.
32. Marino, M. P.; Placek, D. G., Phosphate Esters, Chapter 4, *Synthetic Lubricants and High Performance Functional Fluids*, 2nd Ed. Rudnick, L. R.; Shubkin, R. L. (Eds.), Marcel Dekker: New York, 1999; p. 103
33. Okazaki, M. E.; Abernathy, S. M. Hydrolysis of Phosphate-Based Aviation Hydraulic Fluids, *J. Synth. Lubr.*, **1993**, 10-2, 107.
34. Petroleum Technology Quarterly, Vol. 4, #4, Winter/2000, p. 22
35. Slower growth forecast for PAO lubes, Lube Report, Industry News from *Lubes-n-Greases*, Vol. 2 Issue 16, April 17, 2002.

## Chapter 18

# CHALLENGES IN DETERGENTS AND DISPERSANTS FOR ENGINE OILS

James D. Burrington\*, John K. Pudelski, and James P. Roski  
*The Lubrizol Corporation, 29400 Lakeland Blvd, Wickliffe, OH 44092*

### 1. INTRODUCTION

This chapter will focus on the function and chemistries of today's detergents and dispersants, and how they are being transformed to meet increasing performance and cost demands. A significant trend to address market needs by the combination of additive chemistry with additional technologies will also be presented and some examples discussed.

### 2. ENGINE OIL ADDITIVE AND FORMULATION

Detergents and dispersants are the dominant performance additives components in engine oil formulations. For example, a "typical" gasoline engine oil contains 5-20% of a performance package, which is the largest component, on average, after base oil. The additive supplier supplies the oil marketer with the additive performance package, the pour point depressant, and the viscosity modifier (sometimes known as the viscosity index improver). In a typical crankcase oil the performance package is between 5 and 20% of the formulation. A typical level is about 10%. The viscosity modifier cannot be blended with the performance package and is supplied separately. The performance package is dominated by dispersant and detergent.

The dispersant and detergent together make up about 55-70% of the performance package. Thus, the chemistry of the total package and finished oil is greatly influenced by these two components. As in this example (Figure 1) of a "typical" finished engine oil, the detergent and dispersant must not

only perform their intended chemical functions, but must also provide the proper bulk and rheological properties consistent with the application.

### Formulating a Performance Package for Passenger Car Motor Oils: Additive Company Perspective

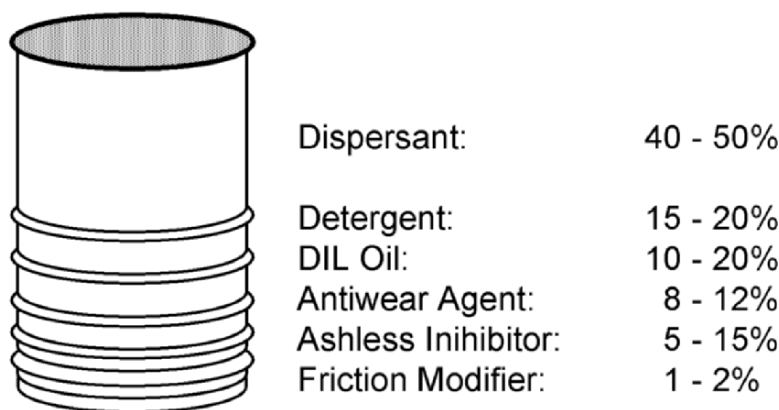


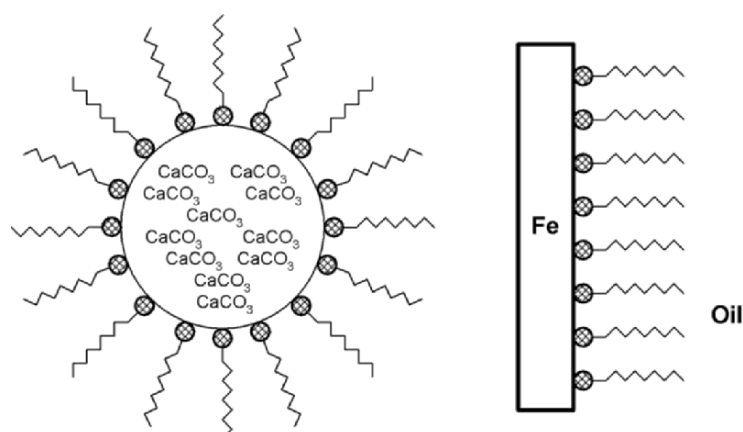
Figure 1. A typical finished engine oil

## 2.1 Detergents

The detergent functions to solubilize polar components, inhibit rust & corrosion, and prevent high temperature deposits, in part, through neutralization of acids. They are composed of two components, a substrate or surfactant and a colloidal inorganic phase, generally resulting from the overbasing process. The major variables effecting performance are the substrate, which is generally sulfonate, phenate, or salicylate, the metal, which is generally Ca, Mg or Na, the degree of overbasing or conversion, which is the level of basic phase present relative to the amount of surfactant. The structural features of a detergent responsible for these unique properties is shown in Fig. 2.

The combination of a surfactant molecule with a colloidal inorganic core results in a micellar-type structure as shown in the figure. This gives both the ability to solubilize polar materials in a continuous matrix of oil, and provides acid neutralization capacity, which is also intimately contacted with the oil in a dispersed amorphous colloidal phase, shown in the figure as  $\text{CaCO}_3$  for a Ca-detergent. This basic colloidal carbonate neutralizes acids formed during the combustion process, such as nitric acid, sulfuric acid, and

hydrochloric acid, which lead to metal corrosion and wear, as well as organic acids, which lead to polymerization, viscosity increase and resin formation. Nitro-hydroxy-carbonyl-compounds also form and, if not neutralized, are the precursors of varnish and sludge.



Overbased & surfactant components work in synergy to:

- Inhibit rust and corrosion
- Reduce high temperature deposits
- Inhibit oil degradation
- Solubilize polar contaminants

Figure 2. Detergents: Surfactant/base oil synergies

The surfactant component of the detergent can also form a protective layer on metal parts as shown here, resulting in the inhibition of rust and corrosion. Together, the surfactant and the basic components work in synergy to inhibit rust and corrosion and oil degradation, reduce high temperature deposits and solubilize polar components.

This is an idealized representation of a detergent. Calcium carbonate is suspended in oil with a sulfonate or phenate. The excess calcium carbonate provides a base reserve to oils and neutralizes acids that are formed during combustion. Detergents are also effective at keeping surfaces in the engine clean. The metals used to make detergents are typically calcium, magnesium, and sodium. Calcium is the most common.

The need for this acid neutralization capacity is evident from Fig. 3, which shows the continual decrease in total base number (TBN) and increase in total acid number (TAN) for a high- and low-TAN gasoline engine oil. The TBN/TAN equivalence point occurs at around 3000 to 6000 miles. (The metal content in the drain increases after the equivalence point is reached in field testing.) Typically, at this point, acids build up to unacceptable levels, and it is, therefore, desirable to change the oil before the TBN and TAN cross.

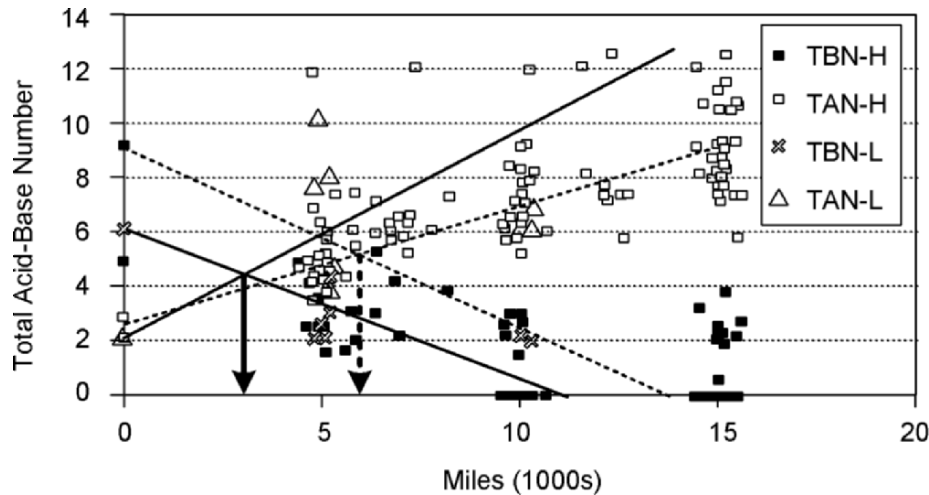


Figure 3. Field testing data demonstrate the need for base capacity (solid lines: TBN, dotted lines: TAN)

These are data from a recent field test showing the decrease in TBN and the increase in TAN with usage. Drain recommendations are often determined by this type of testing. In this example the oil represented by the blue (darker) lines has a lower TBN initially than the oil represented by the pink (lighter) lines. It is not surprising that the cross over point occurs sooner with the lower TBN oil. It is evidence such as this that results in oils with higher TBN being recommended for longer drain intervals.

Another important detergent function is the prevention of high temperature deposit. These deposits, such as the varnish shown in Fig. 4 result, in part, from the acidic precursors formed from high temperature reaction of nitrogen oxides and oxygen with the mixture of fuel and lubricant. The pictures show the effect when these high temperature deposit-forming processes *are* (acceptable) and when they *are not* (unacceptable) sufficiently controlled.

## 2.2 Dispersants

Dispersants function to suspend soot, thereby mitigating the deleterious effects of large particle agglomerates inside the crankcase. Dispersants include a polymer backbone component, which is predominantly polyisobutylene, or PIB, connected to a polar group, normally an amino group. There are two major classes of dispersants, both of which use PIB and a polar amine group: succinimide dispersants, which use maleic anhydride hook, and Mannich dispersants which use formaldehyde. The major variables affecting performance are the nature of the backbone (composition and structure) and the nature, and relative levels of, the hook and polar group.

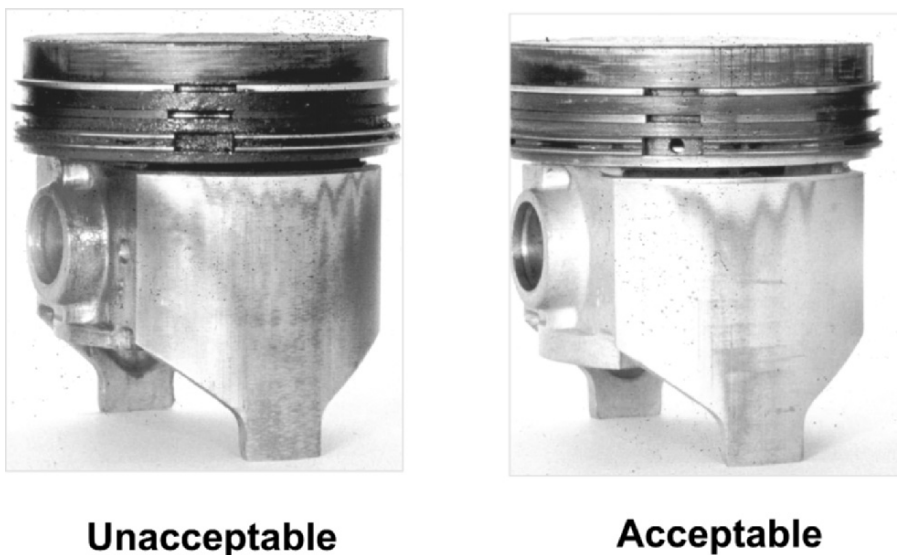


Figure 4. Detergents prevent high temperature deposits

In practice, the dispersant, like the detergent, also solubilizes polar contaminants, but in this case is designed with a longer tail ( $M_n$  = thousands vs. hundreds for detergents) to provide greater steric stabilization to the dispersed carbon (or other contaminant) particle in the micellar structure (Fig. 5). A polyamine head group is used, which is tailored specifically for strong adsorption of soot particles. The nature of the dispersant interactions is tailored to meet the performance characteristics of the particular engine and application. Like detergents, dispersants have been finely tuned over decades to arrive at an optimal structure and composition of the various parameters.

Thus, the combination of the longer hydrocarbon chain and the polar amine head group provides for: (1) the suspension of soot particles (Fig. 6) and the reduction in the corresponding wear and viscosity increases; (2) the solubilization of other polar contaminants; and (3) the prevention of low temperature deposits.

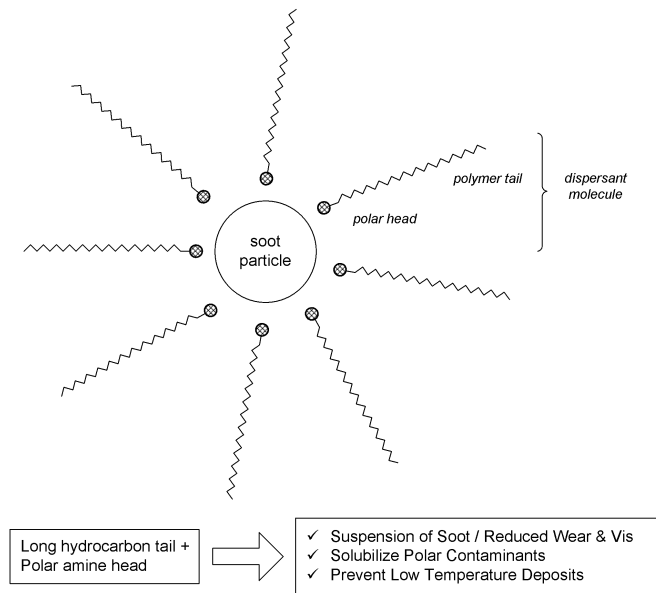


Figure 5. Dispersant chemistry

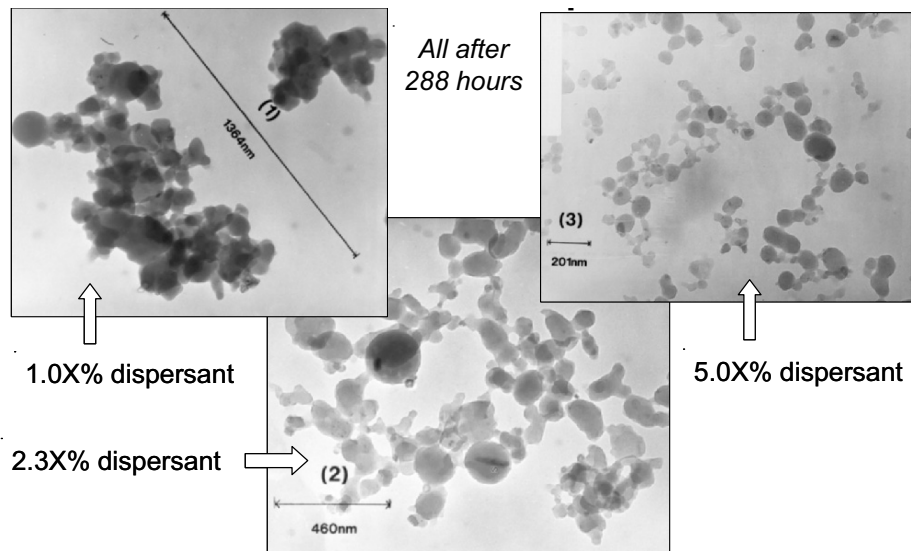


Figure 6. Soot particle growth in a sequence VE test



### 3. PERFORMANCE CHEMISTRY

The rest of this chapter will discuss the chemistries of these additive systems, the opportunities for performance improvements based on chemistry and incorporation of other technologies with additives. Dispersants and detergents are an important class of performance products made by Lubrizol and other additives suppliers based on alkyl succinimides, succans and phenols. These molecules represent a class of surfactant-type materials which are composed of alkyl chains of varying lengths and polar heads.

The dispersant or detergent molecule can be pictured as a “typical” functionalized molecule with a non-polar tail connected to a polar head via a hook connecting group (Fig.7). Detergents generally employ an alkylated aromatic sulfonate, phenol or salicylate where the hydrocarbon chain is a C<sub>12</sub>-C<sub>32</sub>, typically C<sub>16</sub>, linear or branched alpha olefin or olefin oligomer mixture. These are converted to the corresponding sulfonate, phenate or salicylate salt (usually Ca, Mg or Na) and converted to an “overbased” product with a metal base and CO<sub>2</sub> to incorporate an amorphous carbonate phase which provides base capacity. Again, the short chain and polar head surfactant combination provides the mechanism for solubilization of polars and adsorption/protection of metals. The base capacity neutralizes acid, which can contribute to high temperature deposits.

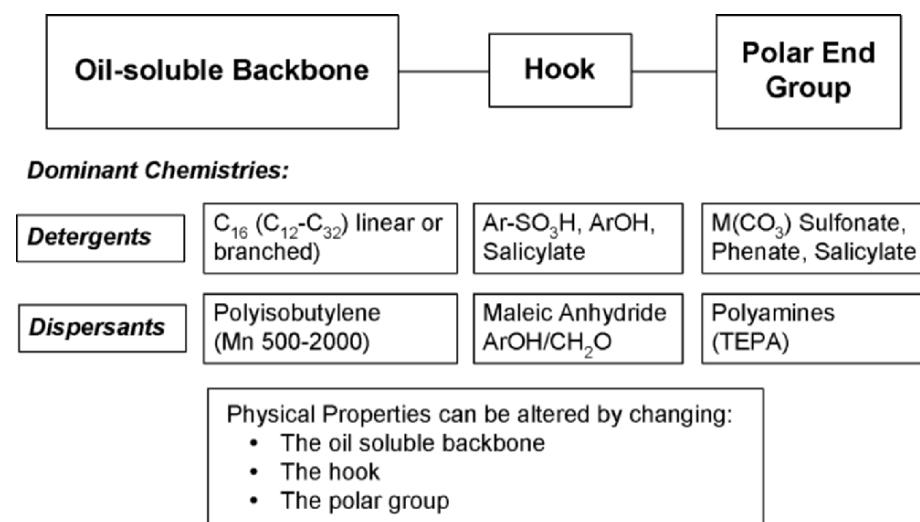


Figure 7. Typical functional molecules

Dispersants, on the other hand, utilize longer alkyl chains, mainly polyisobutylene of 500-2000 Mn. For succinimide-types, these are converted to the succinic anhydride intermediates (or succans) by reaction with maleic

anhydride, and subsequently to the final succinimide dispersant by condensation with a polyamine such as TEPA. For Mannich-types, the long-chain alkylphenol is converted with formaldehyde and the amine to the corresponding dispersant. The polyamine end group strongly adsorbs to soot particles as they are formed in the combustion process and the longer tail provides the steric stabilization of the dispersant/soot micelle structure to inhibit agglomeration into larger, more harmful wear particles.

The physical properties of these end products can be tailored by controlling the nature of each component and the relative amounts of hooks and end groups per molecular chain. These have been optimized over several decades, resulting in today's cost effective and high performance products. But despite the large body of knowledge regarding these structure-function relationships, there are only a handful of chemistries commonly in actual commercial use today for production of detergents and dispersants. This is especially true of the "hooks", and "polar end groups", which generally make up only 10% by weight or less of the product, and where the cost effective polyamine succinimides (from maleic anhydride and polyamines) and overbased alkyl sulfonates and phenates dominate dispersants and detergents, respectively. While polyisobutylene and aromatic alkylate backbones are most commonly used, there has been a significant emphasis on backbone modifications as a means to greater leverage of chemical and physical properties, for optimal cost and performance, particularly for dispersants.

*Table 1.* Currently available backbones

| Backbones               | Sources (Examples)                 |
|-------------------------|------------------------------------|
| Conventional PIB        | Lubrizol, BP                       |
| High vinylidene PIB     | BASF, BP, Nippon Petrochemical Co. |
| Olefin copolymer (OCP)  | Mitsui, ExxonMobil                 |
| Poly alpha olefin (PAO) | Mitsui, ExxonMobil                 |

#### 4. CURRENT DISPERSANT AND DETERGENT POLYMER BACKBONES

While dispersant hydrocarbon backbones are currently dominated by conventional polyisobutylene, many more backbones are on the horizon with the potential to provide improved properties, processing, overall performance per cost, and the ability to optimize properties to respond to specific engine performance characteristics. Some of these (Fig. 8) include high vinylidene PIB, olefin copolymers (OCP) and poly-alpha olefins (PAO). Each of these will be discussed in terms of their structure and reactivity, physical properties and how these translate into strengths and weaknesses in the final application.

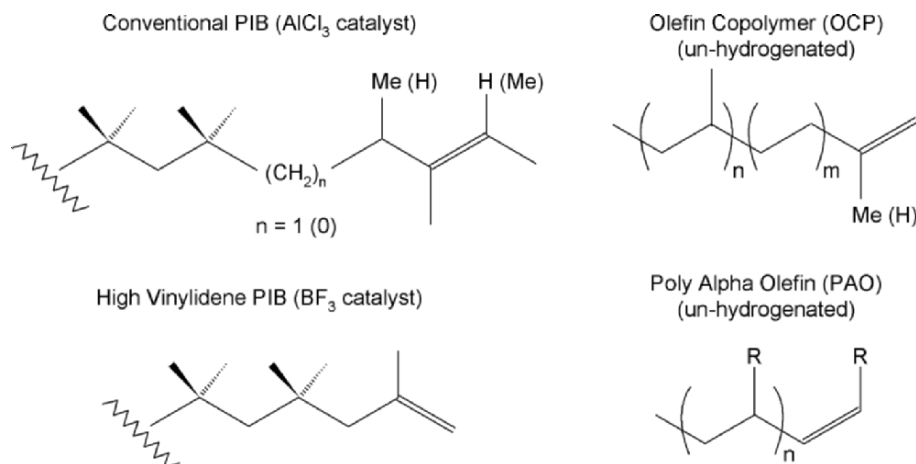


Figure 8. Polyolefin backbone structures

Conventional PIB, made using  $\text{AlCl}_3$  as the isobutylene polymerization catalyst, has a distinctive 5-carbon end grouping with either a tetra- or trisubstituted terminal olefin. High vinylidene PIB, on the other hand, which can be made from a  $\text{BF}_3$ -based catalyst, contains a predominance (usually >70%) of the more straightforward gem-disubstituted vinylidene group. These PIB's have similar physical and rheological properties dictated by the common gem-di-methyl groups on every other carbon of the backbone, while the reactivities with the olefinic end groups are very different. Olefin copolymers and poly alpha olefins, on the other hand, have very different rheological properties than either of the PIB's, but are more similar to high vinylidene PIB in chemical reactivity. These properties are discussed in more detail below, first dealing with their relative reactivities.

Shown here are some representative structures of common backbones and their corresponding succinic anhydrides. Conventional PIB, with multiple allylic carbon atoms, is ideally suited to maleination reaction conditions which promote the formation of diene intermediate, as has been proposed for chlorine-assisted maleination. The diene, once formed, undergoes rapid Diels-Alder reaction with maleic anhydride to form the corresponding polyisobutenyl succinic anhydride, or PIBSA. The vinylidene-type polymers, on the other hand, are more suited to the thermal succination process, thought to proceed by an ene reaction as shown. PAO can also be made with a high degree of vinylidene end groups.

The vinylidene-type containing backbones - that is, high vinylidene PIB, OCP's and PAO's, are also the good reactants for the acid catalyzed alkylation of phenol. The resulting long-chain alkyphenols are intermediates for the Mannich-type dispersants.

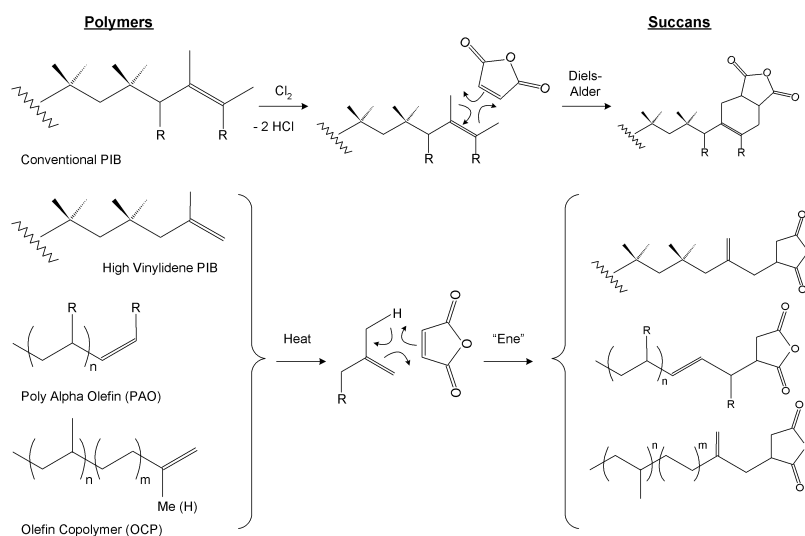


Figure 9. Succination chemistry

## 5. FUTURE POLYMER BACKBONES

Besides reactivity, there are also a number of other properties that are desirable in an “ideal” polymer backbone for detergents and dispersants. As we have discussed, high reactivity with maleic anhydride and phenol is of course important. For example, conversion to dispersants is also key to achieve high conversions at low temperatures, short reaction times, and with minimal excess and decomposition of maleic anhydride. Good overall viscometrics and low temperature properties are becoming increasingly important, especially in light of high energy efficiency and low emissions formulations. These requirements will also drive changes to other formulation components, making it important to use dispersants and detergents with broad flexibility in formulating. Of course, backbones must be produced at low overall cost with minimal capital outlay by well-developed, commercialized (or at least commercializable) processes.

A summary of the strengths and weaknesses of current backbones against these criteria is presented in Table 2.

Conventional PIB has the advantage of providing very low cost products that utilize tried and true technology and already having large volume capacity in place. However, the process is not amenable to thermal processing technology and the resulting products can limit flexibility in formulating to an optimal elemental composition.

As has been discussed, high vinylidene PIB is more thermally reactive,<sup>3</sup> giving more process and formulation flexibility, but requires more expense and is thinner than conventional PIB. The OCP and PAO's have excellent

reactivity and improved low temperature viscometrics, but are even more expensive.

Table 2. Polyolefin backbone alternatives

|  | Low Overall Cost | Reactive w/MAA (thermal) | Reactive w/Phenol | Low Capital Requirements (mainly succination) | Viscosity Credit / Thickening Power | Low Temperature Performance | Low Treat Rate | Process / Formulation Flexibility | Developed Technology | Commercially Available |
|--|------------------|--------------------------|-------------------|---|-------------------------------------|-----------------------------|----------------|-----------------------------------|----------------------|------------------------|
| Conventional PIB (AIC13)               | +                | -                        | -                 | +   | +                                   | -                           | 0              | -                                 | +                    | +                      |
| High Vinylidene PIB (BF <sub>3</sub> ) | -                | +                        | +                 | -   | -                                   | -                           | 0              | +                                 | +                    | +                      |
| LZ High Vinylidene PIB (developmental) | +                | +                        | +                 | -   | +                                   | -                           | 0              | +                                 | -                    | -                      |
| OCP, PAO                               | --               | ++                       | ++                | -   | -                                   | +                           | +              | +                                 | +                    | +                      |
| Branched Polyethylene (potential)      | +                | ++                       | ++                | -   | -                                   | +                           | +              | +                                 | -                    | -                      |

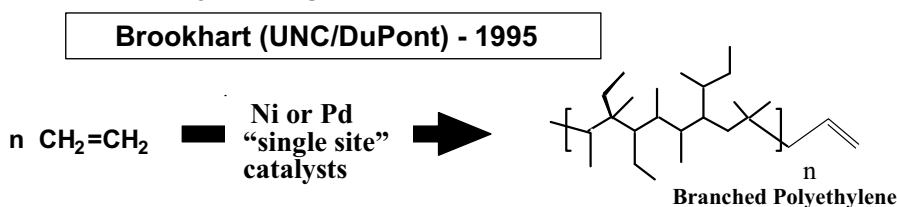
This situation leads to several opportunities for improvement, two of which are: (in the shorter term) to reduce the cost of high vinylidene PIB, and, (in the longer term) for maximal performance, to provide a backbone that has OCP/PAO-type performance at PIB cost. The first opportunity is discussed below.

A catalytic process for producing high vinylidene PIB using a non-BF<sub>3</sub> catalyst was discovered and patented at Lubrizol,<sup>1</sup> uses a solid heteropolyacid-based heterogeneous catalyst,<sup>2</sup> and produces PIB from IOB with high >70% terminal olefin content, and thus, has high reactivity with maleic anhydride and phenol. In addition, it has a unique molecular weight distribution, which gives it and the resulting dispersant products unique properties, especially viscometrics. The process is very efficient, with almost no by-products, is amenable to continuous or batch processing and has a simple product recovery stage. At the heart of this process is a heteropolyacid-based catalyst.

Besides reduced overall cost because of the simplified process and materials requirements, it also provides some improvement in thickening power lost from the BF<sub>3</sub>-produced material, while maintaining the good reactivity properties. However, this process is not yet fully developed, so the total costs are not yet fully certain.

Another alternative backbone, this time moving to a more OCP/PAO-type architecture, is shown in Fig. 10.

- **Branched Ethylene Oligomers**



- **Many variations of catalysts, MW, and branching level/length**

- ✓ Grubbs / Caltech
- ✓ Turner / Symyx
- ✓ Others

- **Terminal olefin: thermal succination reactivity**

- **Potential: PE-like price; PAO-like properties:**

- ✓ Low deposit detergents
- ✓ High performance dispersants
- ✓ Alternative to PAO in other additives

*Figure 10.* New backbone: branched polyethylene

Branched backbones resulting from polymerization of homopolymerization of ethylene was first reported by Brookhart at UNC/Chapel Hill and co-workers at DuPont in 1995.<sup>4</sup> The discovery generated a flurry of literature reports and patents with many claims around the materials and the catalysts, the majority of which are Ni and Pd systems with diimide ligands. The excitement was based on the possibility of generating branched backbones with broad range of molecular weights solely from ethylene. Since then, many other groups have investigated these so-called “single-site”, late transition metal systems for production of branched polyethylenes, including Bob Grubbs at Caltech and workers at Symyx. The latter investigation involved the use of combinatorial-type methods for rapid screening of di and multi-dentate ligands for catalysts for ethylene polymerization activity.

Included in the reported literature of these single-site Ni and Pd catalysts are branched polyethylenes in the dispersant MW ranges and with terminal olefins, which provide thermal succination reactivity to provide PAO-like properties such as low deposits and low temperature performance, at polyethylene-type prices.

These alternate backbones are summarized in the Table 2.

## 6. FUTURE TRENDS

Besides these new backbones, there are also many other approaches being pursued to improve detergents and dispersants to better address market needs.

Cost reduction activities by reducing treat rate and process improvements are continually occurring, as are formulating approaches to improved compatibility with low friction/fuel economy systems, improved viscometrics and incorporation of EP/antiwear and low S/P/CI and ashless components.

In the longer term, customers are continually expecting extended life and durability while demanding lower cost, compatibility with catalyst systems and accountability for everything with which the lube comes into contact during its lifetime. These broader and more demanding challenges will be difficult to address with chemistry and formulation technology alone. Presented below is the growing trend to incorporate other technologies and systems to complement the work that detergents and dispersants do as chemical additives.

These trends include:

- Advanced fluids technology
- Technologies for new product introduction, and
- Performance systems

## **6.1 Advanced Fluids Technology**

The evolution of Advanced Fluids Technology through improvements in understanding of compatibility of key components with each other and with base oils is having a significant impact on our ability to predict performance based on high speed computations. Simple empirical models which may have worked in the past are inadequate for today's and future complex formulations. The resulting solutions provide advanced fluids technology not possible even 2-3 years ago. This is described in more detail below.

As an example, some of the major interactions of base oil with additives to be considered in the design of a lubricant package are shown in Fig. 11. This list isn't complete by any means, but it gives a feel for some of the major issues in base oil quality.

The properties are particularly important to dispersant and detergent surface activity, chemical activity, thermal/oxidative stability and solvent power. Furthermore, maximum performance for one test requires very different and frequently conflicting properties.

Before talking about specific issues, it's worth reminding ourselves about the reasons we use additives at all. With respect to our today's oil industry customers, it is suggested if all oils were perfect, then additives would not be so widely needed. Yet today we see great improvements in base oil quality in combination with additive developments which – together – give us outstanding finished lubricant performance. The conflicting requirements for a dispersant formulation are discussed below.

## Major Interactions of Base Oil with Additives

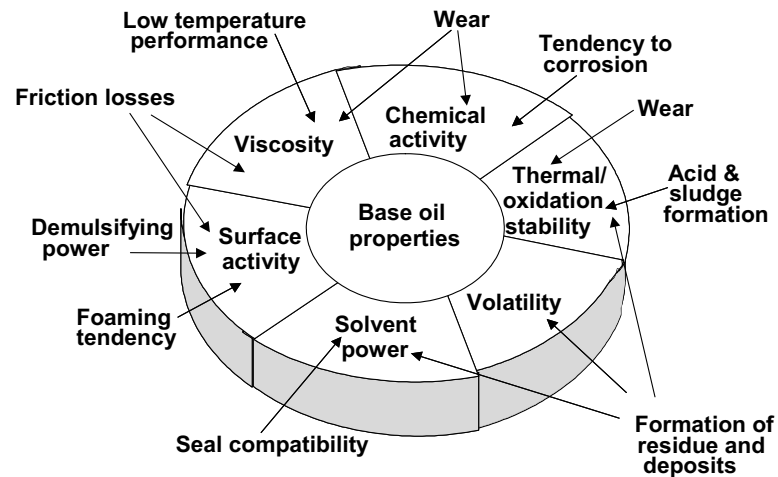


Figure 11. Major interactions of base oil with additives

Four of the performance criteria for dispersants are shown on each axis of Fig. 12; the higher the performance, the larger the area of the figure. The typical dilemma is represented by the dotted lines. Thermal stability and soot control require high conversion normally and high TBN dispersants, which are also the ones which attack seals and give poor VE (sludge) performance. Adjusting the formulation with this conventional wisdom to improve seal compatibility and VE performance results in unacceptable thermal stability. The solid line is a computer-generated formulation, which takes into account many more variables and interactions than would be possible without a very large statistical design and computational power. This design is shown in more detail in Fig. 13.

## 6.2 Technologies for New Product Introduction

The way in which a thorough understanding of structure-performance relationships is obtained is through statistically designed experiments. This design results in a better balance between the competing requirements by consideration of a large statistically designed matrix of variables, including PIB mol. wt. and mol. wt. cut-off, succination level, amine type, and amine charge. Two new formulations were identified which significantly improved performance (the lower the number the better) over the current baseline. Continued use of these powerful, but computationally demanding statistical



models will continue to improve our abilities for formulation to competing requirements.

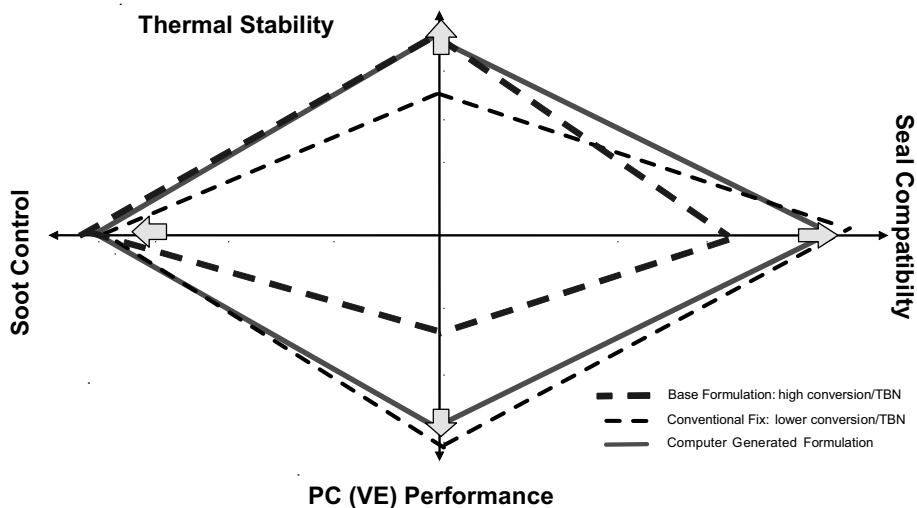


Figure 12. Multiple dispersant requirements

- **Large statistically designed matrix run**
- **Variables included:**
  - PBU mol wt
  - PBU mol wt “cut”
  - Succination level
  - Amine type
  - Amine charge
- **2 formulations were better in all areas of performance**

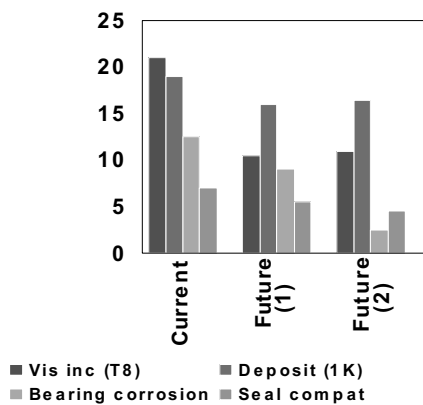


Figure 13. Balance between competing requirements

### 6.3 Performance Systems

*Performance Systems* integrate mechanical, chemical and electronic technologies. An example is Lubrizol's water-blended emulsion fuel system called PuriNOx.<sup>5</sup> PuriNOx is a fill-and-go solution for the simultaneous reduction of both particulate and NOx without the need for engine modifications. Typical results are 50% particulate reduction and 30% NOx reduction by simply switching to PuriNOx fuel, with no other modifications.

The system is composed on the additive package, which includes dispersant-type chemistry, water, diesel fuels and season components, and a blending unit, which includes the mechanical and electronic components necessary to provide a stable water-fuel emulsion, the final PuriNOx fuel product. The system is currently being used in several key cities in North America and Europe with emissions problems for both off and on-road applications.

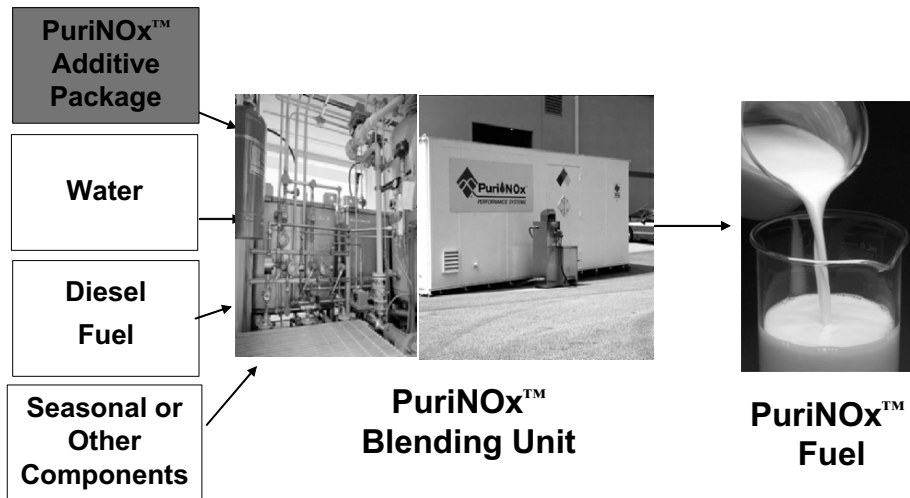


Figure 14. PuriNOx water blended fuel

## 7. SUMMARY AND CONCLUSIONS

In summary, dispersants and detergents perform critical functions in lubricants, and the chemistry has been well-optimized over the years for existing PIB backbones. However, new backbones provide the potential for beyond-incremental improvements in performance and cost. Integration of additives chemistry with artificial intelligence, and mechanical and electronic

systems will provide the technological basis for future step changes in performance.

## 8. ACKNOWLEDGEMENTS

The authors thank the following people for their help in preparing this talk: John Pudelski (Co-author, Dispersants), Jim Roski (Co-author, Detergents), John Johnson (Lubrizol High Vinylidene PIB), Saleem Al-Ahmad (Branched Polyethylene), William Chamberlin (Performance Testing Examples), Steve Di Biase (Trends & New Technologies), Richard Biggin, Phillip Shore and Tom Curtis (Advanced Fluids Technology Example), and Casimir Trotman-Dickenson (Detergents).

## 9. REFERENCES

1. US Pat 5,710,225, **1998**.
2. Burrington, J.D.; Johnson, J.R.; Pudelski, J.K., *Top. Catal*, 2003, 23(1-4).
3. US Pat. 5,286,823; EP Pat 145 235; US Pat 5,068,490; RP Pat 322 241; EP Pat 481 297; US Pat 4,152,499.
4. US Pat. 5,880,323, **1999**.
5. Daly, D. T.; Langer, D. A., *Prep. Am. Chem. Soc. Div. Pet. Chem.*, **2000**, 45(1), 28-31.

## Chapter 19

# THE CHEMISTRY OF BITUMEN AND HEAVY OIL PROCESSING

Parviz M. Rahimi and Thomas Gentzis\*

*National Centre for Upgrading Technology*

*1 Oil Patch Drive, Suite A202, Devon, Alberta, Canada T9G 1A8*

*\*Current address: CDX Canada Co., 1210, 606-4th Street SW,*

*Calgary, Alberta, Canada T2P 1T1*

## 1. INTRODUCTION

Petroleum consists of a complex hydrocarbon mixture. The physical and chemical compositions of petroleum can change with location, age and depth. Beside carbon and hydrogen, the organic portion of petroleum contains compounds combined with sulphur, oxygen and nitrogen, as well as metals such as nickel, vanadium, iron, and copper.

In recent years, technological advancements in bitumen and heavy oil processing and the stabilization of crude oil prices have made production of synthetic crude oil from these resources attractive and economical. With the goal of processing heavy oil, bitumen, and residua to obtain gasoline and other liquid fuels, an in-depth knowledge of the constituents of these heavy feedstocks is an essential first step for any technological advancement.

It is well established that upgrading and refining of different feedstocks is related to their chemical properties. Since petroleum is composed of complex hydrocarbon mixtures, it is impossible to identify each individual component and its upgrading chemistry. Most investigations, to date, relate the thermal or catalytic behavior of petroleum feedstocks to their fractional composition. The hydrocarbon components of petroleum fall into three classes:<sup>1</sup>

1. *Paraffins* - saturated hydrocarbons, straight or branched chains but no ring structures;
2. *Naphthenes* - saturated hydrocarbons with one or more rings; these hydrocarbons may have one or more paraffinic side chains;

3. *Aromatics* - hydrocarbons with one or more aromatic nuclei; these hydrocarbons may be connected to naphthenic rings and/or paraffinic side chains.

In general, as the MW (molecular weight, or boiling point) of the petroleum fraction increases, there is a decrease in the amount of paraffins and an increase in the amount of naphthenes and aromatics.

This chapter briefly reviews the topics related to bitumen and heavy oil properties and their thermal chemistry; it includes:

- the chemical composition of heavy oil and bitumen in terms of fractional composition — an overview of the methods that have been applied to the separation of petroleum into hydrocarbon types;
- asphaltenes – physical and chemical properties, stability and thermal chemistry;
- chemistry of bitumen and heavy oil upgrading;
- reaction chemistry of bitumen components;
- application of hot stage microscopy;
- stability and compatibility of petroleum.

## 2. FRACTIONAL COMPOSITION OF BITUMEN/ HEAVY OIL

Conversion (upgrading) of bitumen and heavy oils to distillate products requires reduction of the MW and boiling point of the components of the feedstocks. The chemistry of this transformation to lighter products is extremely complex, partly because the petroleum feedstocks are complicated mixtures of hydrocarbons, consisting of  $10^5$  to  $10^6$  different molecules.<sup>2</sup> Any structural information regarding the chemical nature of these materials would help to understand the chemistry of the process and, hence, it would be possible to improve process yields and product quality. However, because of the complexity of the mixture, the characterization of entire petroleum feedstocks and products is difficult, if not impossible. One way to simplify this molecular variety is to separate the feedstocks and products into different fractions (classes of components) by distillation, solubility/insolubility, and adsorption/desorption techniques.<sup>2</sup> For bitumen and heavy oils, there are a number of methods that have been developed based on solubility and adsorption.<sup>1</sup> The most common standard method used in the petroleum industry for separation of heavy oils into compound classes is SARA (saturates, aromatics, resins, and asphaltenes) analysis.<sup>3</sup> Typical SARA analyses and properties for Athabasca and Cold Lake bitumens, achieved using a modified SARA method, are shown in Table 1. For comparison, SARA analysis of Athabasca bitumen by the standard ASTM method is also shown in this table. The discrepancy in the results between the standard and modified ASTM methods is a result of the aromatics being eluted with a

mixture of 50/50vol% toluene/pentane in the modified method instead of 100 vol% pentane in the standard method. A different SARA composition was reported by Clark and Pruden when heptane was used to precipitate asphaltenes.<sup>4</sup> Compositional analyses, including SARA, for a number of Chinese and Middle Eastern vacuum residu were reported by Liu et al.<sup>5</sup> These authors also used modified SARA, which was developed in their laboratory (Table 2). In general, regardless of the method used, the properties of the feedstocks as determined by the SARA method give some indication of the “processability” or problems that may occur during upgrading of these relatively heavy materials. The knowledge of the chemical composition of the feedstocks, as will be shown later, plays a major role in predicting their behaviour in terms of phase separation, coke formation, molecular interactions, and the cause of catalyst deactivation.

Table 1. Properties and SARA fractionation results for Athabasca and Cold Lake bitumens

|                  | Athabasca          |       | Athabasca |      | Cold Lake          |       |
|------------------|--------------------|-------|-----------|------|--------------------|-------|
|                  | Modified ASTM 2007 |       | ASTM2007  |      | Modified ASTM 2007 |       |
| API Gravity      |                    |       | 8.05      |      | 10.71              |       |
|                  | <b>MW</b>          |       | <b>MW</b> |      | <b>MW</b>          |       |
| Saturates (wt%)  | 381                | 17.27 | 16.9      | 378  | 20.74              | 21.52 |
| Aromatics (wt%)  | 408                | 39.7  | 18.3      | 424  | 39.2               | 23.17 |
| Resin (wt%)      | 947                | 25.75 | 44.8      | 825  | 24.81              | 39.36 |
| Asphaltene (wt%) | 2005               | 17.28 | 17.18     | 1599 | 15.25              | 15.95 |
| Carbon (wt%)     |                    | 83.34 |           |      | 83.62              |       |
| Hydrogen (wt%)   |                    | 10.26 |           |      | 10.5               |       |
| Sulfur (wt%)     |                    | 4.64  |           |      | 4.56               |       |
| Oxygen (wt%)     |                    | 1.08  |           |      | 0.86               |       |
| Nitrogen (wt%)   |                    | 0.53  |           |      | 0.45               |       |
| Residue (wt%)    |                    | 0.15  |           |      | 0.01               |       |

Table 2. SARA composition of various crudes<sup>5</sup>

| Sample     | Saturates | Aromatics | Resin | C7 Asphaltene |
|------------|-----------|-----------|-------|---------------|
|            | wt%       | wt%       | wt%   | wt%           |
| Daqing     | 34.8      | 35.5      | 29.5  | 0.0           |
| Dagang VR  | 27.8      | 28.7      | 43.4  | 0.0           |
| Guado VR   | 14.6      | 33.0      | 47.7  | 4.7           |
| Shengli VR | 16.1      | 30.6      | 51.1  | 2.2           |
| Huabei VR  | 37.6      | 31.4      | 29.9  | 1.1           |
| Liaohe VR  | 20.8      | 31.8      | 41.6  | 5.7           |
| Oman VR    | 26.3      | 40.6      | 31.2  | 2.0           |
| S-A-L VR   | 16.5      | 49.5      | 26.8  | 7.3           |

Since the trend with petroleum, including bitumens, is towards heavier feedstocks, greater emphasis will be placed here on the composition of material with high boiling point and molecular weight (MW). In a series of papers, Boduszynski<sup>6,7</sup> and Altgelt and Boduszynski<sup>8,9</sup> published data on the composition of heavy petroleum fractions up to the AEBP (atmospheric equivalent boiling point) of 760°C. The fractions were obtained by a combination of DISTACT distillation and sequential elution fractionation (SEF). Data from this work showed that heavy crude oils and petroleum residues had a wide range of MW distributions that extended to relatively small molecules. Quantitative analysis demonstrated that the MWs of most

heavy petroleum components did not exceed 2000 g/mol. The hydrogen deficiency (aromaticity) of the petroleum fractions increased with increasing boiling point. The carbon content of petroleum feedstocks and their products varied over a narrow range (80-85wt%) whereas the difference between the hydrogen content of the feed and products varied over a much wider range (5-14wt%). Wiehe<sup>10</sup> suggested that the use of hydrogen concentration rather than H/C atomic ratio was more instructive for assessing fuel materials and processes. The work by Boduszynski<sup>6,7</sup> also showed that the distribution of sulphur, nitrogen and oxygen constituents of petroleum increased with increasing AEBP. It was further demonstrated that S and N associated with metals also occur in the same molecular structure.<sup>6</sup>

Recently, Chung et al.<sup>11</sup> applied SFE (Supercritical Fluid Extraction) to reveal properties of Athabasca bitumen resid. Using this technique, it was possible to fractionate Athabasca bitumen vacuum bottoms (VB) into narrow cut fractions (based on boiling point), the properties of which are shown in Table 3. Approximately 60 wt% of the residue was composed of relatively small molecules (500-1,500 g/mol). The remaining 40 wt% contained larger molecules, including asphaltenes, with an average MW of 1,500-4,200 g/mol. As the MW of the fractions increased, the fractions became more refractory (higher contents of S, N, metals and MCR (Micro Carbon Residue)). The fractions also became more deficient in hydrogen (lower H/C ratio). The use of this fractionation technique resulted in the removal of all asphaltenes and the concentration of the refractory material in the highest boiling point fraction. In comparison to oil sands bitumen, conventional crude oils are of better quality in terms of asphaltenes content. The crudes consist of small amounts of asphaltenes, a moderate amount of resins and a significant amount of oils.<sup>12</sup>

Table 3. Characteristics of Athabasca bitumen vacuum bottom fractions obtained by SFE technique<sup>11</sup>

|                                   | Fraction No. |       |       |       |       |       |       |       |       |                  |                    |
|-----------------------------------|--------------|-------|-------|-------|-------|-------|-------|-------|-------|------------------|--------------------|
|                                   | 1            | 2A    | 2B    | 3     | 4     | 5     | 6     | 7     | 8     | 9                | Pitch <sup>b</sup> |
| Pressure MPa                      | 4-5          | 5-5.5 | 5.5-6 | 6-7   | 7-8   | 8-9   | 9-10  | 10-11 | 11-12 | >12              |                    |
| Wt% of pitch                      | 12.7         | 9.8   | 7.6   | 10.6  | 6.5   | 4.4   | 3.3   | 2.6   | 2.1   | 40.4             | 100                |
| Density, g/mL at 20°C             | 0.975        | 0.993 | 1.006 | 1.023 | 1.043 | 1.054 | 1.065 | 1.068 | 1.074 | N/A <sup>c</sup> | 1.087              |
| Molecular weight, Da              | 506          | 755   | 711   | 799   | 825   | 948   | 1134  | 1209  | 1517  | 4185             | 1191               |
| Sulfur, wt%                       | 4.0          | 4.5   | 5.0   | 5.4   | 6.0   | 6.2   | 6.5   | 6.8   | 6.8   | 7.6              | 6.5                |
| Nitrogen, ppm                     | 3080         | 4100  | 4330  | 5070  | 6160  | 6810  | 7370  | 7530  | 7900  | 10500            | 4600               |
| Carbon, wt%                       | 84.5         | 83.5  | 83.5  | 84    | 83    | 84    | 83    | 83    | 82.5  | 78.5             | 82.7               |
| Hydrogen, wt%                     | 11.5         | 11.15 | 10.95 | 10.55 | 10.25 | 10.05 | 9.8   | 9.7   | 9.5   | 8                | 9                  |
| C/H (atomci)                      | 0.612        | 0.624 | 0.635 | 0.664 | 0.675 | 0.697 | 0.706 | 0.713 | 0.724 | 0.818            | 0.766              |
| Aromatic carbon <sup>a</sup> , fa | 0.26         | 0.29  | 0.25  | 0.33  | 0.36  | 0.40  | 0.37  | 0.43  | 0.43  | 0.49             | 0.41               |
| Nickel, ppm                       | 12.8         | 21.3  | 30.1  | 44.8  | 71.1  | 89.7  | 123   | 138   | 162   | 339              | 148                |
| MCR, wt%                          | 5.6          | 7.9   | 10.8  | 14.3  | 18.2  | 21.5  | 24.7  | 26.5  | 28.7  | 78.9             | 26.7               |
| Saturates, wt%                    | 26.8         | 164   | 9.7   | 4.1   | 1.4   | 0.7   | 0.6   | 0.1   | 0     | 0                | 6.3                |
| Aromatics, wt%                    | 57.2         | 62.4  | 65.7  | 66.7  | 63.9  | 53.3  | 45.4  | 45.9  | 40.8  | 2                | 33                 |
| Resin, wt%                        | 15.9         | 21.2  | 24.6  | 29.2  | 34.8  | 46    | 54    | 53.8  | 59.2  | 9.4              | 29.4               |
| Asphaltenes, wt%                  | 0            | 0     | 0     | 0     | 0     | 0     | 0     | 0     | 0     | 88.03            | 31.4               |

<sup>a</sup> C13-NMR. <sup>b</sup> Pitch = 524°C + fraction <sup>c</sup> N/A - not applicable

In recent years, the increased interest in refining of heavy crudes and processing VB from oil sands has clearly shown the need for a deeper knowledge of the composition and the chemical structure of these materials. At the National Centre for Upgrading Technology (NCUT) in Devon, Alberta, Canada, a series of fundamental studies was undertaken in order to understand the chemistry of bitumen and heavy oil VB and relate their chemical compositions to processing chemistry. The chemical properties of a number of heavy oils and bitumen VB are shown in Table 4. The data show that although the Forties VB contained a higher percent of pitch compared with the other resids, it also contained less asphaltenes, MCR, metal content, and heteroatoms. In order to gain more insight into the chemical properties of these vacuum residues, the maltenes (pentane solubles) of Athabasca, CL, and Forties VB were subjected to separation using a method similar to SARA analysis. VB maltenes were separated into saturates ( $M_1$ ), mono/di-aromatics ( $M_2$ ), polyaromatics ( $M_3$ ) and polars ( $M_4$ ). The data for Athabasca bitumen were first reported by Dawson et al.<sup>13</sup> and are compared with other feedstocks in Table 5.

Different laboratories may use different methods for the evaluation of feedstock quality. Method variation makes it difficult to compare the data among laboratories. For example, when comparing the properties of different feedstocks – for instance their SARA analysis – the feedstocks should have been distilled to the same nominal cut point. The data in Table 5 show that

Table 4. Properties of Feedstocks

| Analyses                         | Forties VB | CLVB  | Lloyd VB/CLVB  |
|----------------------------------|------------|-------|----------------|
| Density (15°C, g/mL)             | 1.039      | 1.039 | 1.03           |
| Oils (wt%)                       | 91.76      | 75.6  | -              |
| Asphaltenes (wt%)                | 8.15       | 24.4  | 20.9           |
| Aromaticity, <sup>13</sup> C NMR | 30         | 35    | 33 (31)        |
| Pitch Content (+525°C, wt%)      | 93.7       | 75.4  | 74.1           |
| MCR (wt%)                        | 16.3       | 20.2  | 18 (18)        |
| Molecular weight (g/mol)         | 948        | 1071  | 687 (800)      |
| Viscosity (cST)                  |            |       |                |
| 100°C                            | 509.1      | 2748  | 80.8 (at 60°C) |
| 120°C                            | 185.9      | 1010  | -              |
| 135°C                            | 100.8      | 377.8 | -              |
| Elemental (wt%)                  |            |       |                |
| Carbon                           | 87.1       | 82.66 | 84.44          |
| Hydrogen                         | 10.6       | 9.82  | 9.69           |
| Nitrogen                         | 0.43       | 0.51  | 0.58           |
| Sulphur                          | 1.24       | 5.42  | 5.43           |
| Oxygen                           | <0.5       | 0.8   |                |
| Ash                              | -          | 0.04  | 0.1            |
| H/C                              | 1.46       | 1.42  | 1.37           |
| Metals (ppmw)                    |            |       |                |
| Vanadium                         | 29         | 269   | 207            |
| Nickel                           | 13         | 104   | 96             |
| Iron                             | 3          | 175   | -              |



Table 5. Components of vacuum resids (wt% on heavy oil/bitumen)

|              | Pitch (+525°C) | Maltenes (wt%) | Asphaltenes (wt%) | Saturates (M1) | Mono-diaromatics (M2) | Polyaromatics (M3) | Polars (M4) |
|--------------|----------------|----------------|-------------------|----------------|-----------------------|--------------------|-------------|
| Athabasca VB | 96.4           | 59.9           | 40.1              | 3.36           | 3.18                  | 38.1               | 15.36       |
| Cold Lake VB | 75.4           | 75.6           | 24.4              | 11.12          | 4.76                  | 41.52              | 18.22       |
| Forties VB   | 93.7           | 90.9           | 9.1               | 14.5           | 8.83                  | 51.11              | 16.35       |

Athabasca bitumen VB and Forties VB have similar pitch contents (fractions boiling above 525°C) and that the concentrations of subcomponents of maltenes are also comparable. However, CLVB (Cold Lake vacuum bottoms) has much lower pitch content and the product composition cannot directly be compared with the other two feedstocks.

Another widely used technique for the separation of heavy oils into subcomponents is IEC (Ion Exchange Chromatography). In this method, the petroleum samples are separated into acid, base and neutral fractions. Walton<sup>14</sup> reported this technique in 1992, and it has also been used extensively by Green et al.<sup>15</sup> in studying the relationships between the composition of different feedstocks with product slate and composition in catalytic cracking. The properties of the Hamaca resid from Venezuela and its fractions, using the technique developed by Green, were reported by Rahimi et al.<sup>16</sup> and are shown in Table 6.

Table 6. Properties of Hamaca resid (+510°C) and its fractions

|              | Amphoterics | Bases | Acids | Aromatics | Saturates | Hamaca resid    | Losses |
|--------------|-------------|-------|-------|-----------|-----------|-----------------|--------|
| Yield (wt%)  | 30          | 9.8   | 8.9   | 41.1      | 5.7       |                 | 4.5    |
| MW, VPO      | 1832        | 1048  | 996   | 600*      | 620*      | NA <sup>a</sup> |        |
| TGA 600°C    | 43.4        | 19.2  | 24.9  | 5.5       | 0         | NA <sup>a</sup> |        |
| Residue, wt% |             |       |       |           |           |                 |        |
| C            | 83          | 84.5  | 83.6  | 84.6      | 85.2      | 85.9            | NA     |
| H            | 8.2         | 9.6   | 10.4  | 11.5      | 15        | 9.7             | NA     |
| N            | 2.1         | 1.7   | 1.8   | ND        | ND        | 0.9             | NA     |
| O            | 2.9         | 1.6   | 2.5   | 1.6       | <0.1      | 2.2             | NA     |
| S            | 2.8         | 2.8   | 2.3   | 2.5       | <0.05     | 4.0             | NA     |

<sup>a</sup> NA, not applicable. ND, not detectable. \* values by desorption chemical ionization MS.

### 3. HETEROATOM-CONTAINING COMPOUNDS

Bitumens and heavy oils present a challenge for upgrading, partly because of their high levels of metals, N, S and O. There have been numerous publications related to organometallic compounds in heavy oils and bitumen, and the effects that they have during thermal and catalytic processing.<sup>11,17-22</sup> The concentrations of heteroatom-containing molecules such as sulphur, nitrogen and oxygen may be relatively small, but their influence during upgrading can be significant. Although heteroatoms are mostly concentrated in the heavier fractions, they are present throughout the range of boiling points. The presence of these molecules creates considerable process constraints during catalytic upgrading, causing catalyst poisoning and

deactivation. In the finished products, these heteroatom-containing compounds also may cause problems, including lack of stability on storage and discolouration. Moreover, because of environmental issues future transportation fuels will contain no or significantly less heteroatoms compared with fuels today. Sulphur compounds in heavy oils, bitumen and transportation fuels have been studied by a number of investigators.<sup>1,23-28</sup> It has been shown in the asphaltene fraction of petroleum that some of the sulphur in the sulphidic form connects two-ring structures (bridge) that can be easily cleaved under HDS conditions (300-345°C) and hydrogen pressures of 500-1,000psi.<sup>1,29</sup> Most S compounds are relatively easy to remove during hydrotreating. However, there are some that are very resistant and create problems during HDS reactions. There are excellent reviews by Whitehurst et al.<sup>30</sup>, Toshiaki et al.<sup>31</sup> and Te et al.<sup>32</sup> regarding the HDS of polyaromatic S compounds. In general, it has been shown that the sulphur in ring compounds such as thiophene and benzothiophene can be removed rather easily during hydrotreating. Alkylation of the parent dibenzothiophene, especially at the 4 and 6 positions, reduces the catalyst activity for S removal because of steric hindrance.

Other molecules containing nitrogen and oxygen have a strong inhibition effect on desulphurization reactions.<sup>33-35</sup> H<sub>2</sub>S, which is produced during HDS reactions, is also known to act as an inhibitor.

Because of the current limitations in HDS technology, Whitehurst et al, suggested alternative approaches listed below:<sup>30</sup>

1. Development of higher activity catalysts.
2. Altering the desulphurization reaction pathways for hindered sulphur compounds by using zeolite-containing catalysts.
3. HDS reactions that take place in more than one stage: modifying the feed in the first stage, such as isomerization of alkyl groups in hindered alkyldibenzothiophenes, to produce less sterically hindering positions for sulphur removal.
4. Developing a novel reactor design: knowledge of the composition and reactivity of sulphur compounds in different ranges has led to the design of a novel reactor. In this design, the desulphurization of lighter sulphur-containing compounds occurs in the top part of the reactor (co-current with the hydrogen stream). The higher boiling-point sulphur compounds react more efficiently, in the presence of catalyst, in a countercurrent mode.<sup>36</sup>
5. Developing a process other than hydrotreating: this involves the selective adsorption of sulphur compounds on materials such as activated carbon<sup>37</sup> and/or selective oxidation of the sulphur compounds followed by extraction<sup>38-41</sup>.

There has been a significant increase in the number of studies to understand hydrotreating reactions for the development of HDN catalysts. Nitrogen compounds are known to be catalyst poisoning in hydrotreating

processes<sup>42</sup> and are involved in the formation of gum, causing severe stability problems in the finished petroleum products<sup>43</sup>.

Nitrogen content in petroleum and bitumen is much lower than sulphur content (0.1-0.9wt%), although some crude oils may contain up to 2wt%.<sup>1</sup> The amount of N increases as a function of boiling point, in a similar fashion to S. It has been shown that N concentration increases significantly around 350°C and continues to rise.<sup>23</sup> Nitrogen compounds can be classified into a) basic, including pyridine and its derivatives; b) neutral, including alkylindoles and alkylacridines; and c) acidic, including indoles, carbazoles, amides, and nonmetallic porphyrins.<sup>1</sup> Holmes,<sup>44</sup> demonstrated that most of the nitrogen in oil sands bitumen is tied up in pyridinic structures, including quinolines and acridines. Some molecules contain more than one N compound and others contain other elements such as oxygen and S in addition to nitrogen.<sup>45</sup> It should be pointed out that porphyrins are also considered nitrogen-containing molecules and their concentration is relatively high in the heavy distillates and asphaltene fractions.

Although the chemical structures of some common N compounds are similar to their S counterparts, they behave differently under hydrotreating conditions. Based on the resonance energy of two-ring (Benzo[*b*]thiophene 56 kcal/mole vs. Indole 43 kcal/mole) structures there is no reason to believe that N removal would be more difficult than S removal.<sup>42</sup> However, from the available published data on N compounds, it can be concluded that the removal of nitrogen is indeed more difficult when compared with the removal of sulphur. Basic N compounds with a relatively low MW can be extracted with dilute mineral acids. Nitrogen compounds such as pyridine, quinoline, and isoquinoline also can be extracted from petroleum distillates using dilute mineral acids. However, the carbazole, indole, and pyrrole types of N compounds cannot be extracted with these acids.<sup>1</sup> In addition, N compounds can easily adsorb on the catalyst surface and inhibit other hydrotreating reactions. Removal of N requires prehydrogenation followed by hydrogenolysis of strong C-N bonds. In the transportation of fuels, traces of N compounds can have a significant effect on the stability of those fuels.

The oxygen content of petroleum is relatively small (<1wt%) and is concentrated in the heavier fractions (>350°C boiling point). The chemical functionalities of the oxygen-containing molecules include the following: hydroxyl groups (phenols), carboxyl groups (carboxylic acids and esters), carbonyl groups (ketones), and cyclic and acyclic ethers.<sup>9</sup> Phenols, carboxylic acids and naphthenic acids have been identified in a number of crude oils.<sup>47</sup> Ketones, esters, ethers, and anhydrides are difficult to identify because most of them occur in the higher molecular weight, nonvolatile residues.<sup>1</sup> Various analytical techniques, including LC and HPLC, have been developed to identify and quantify acidic compounds. Recently, using Ion Cyclotron Resonance Mass Spectrometry, Marshall et al.<sup>48</sup> identified over 3000 acids in heavy petroleum. However, in day-to-day refinery operation, a standard

method (titration) is used for the measurement of the *total acid number*. In some crude oils, the concentration of acids reaches approximately 1 wt%. The presence of these acids is known to cause problems with corrosion in pipelines during transportation. It has been suggested that naphthenic acids react with iron salts to form iron naphthenates.<sup>49</sup> Upon decomposition of iron naphthenate, FeO is formed that reacts with S compounds such as H<sub>2</sub>S, thiols, and disulphides to produce iron sulphide (Figure 1). Iron sulphide is involved in the fouling of refinery equipment. Formation of gum and sludge during storage of fuels can be attributed, in part, to the presence of phenolic compounds.<sup>50</sup>

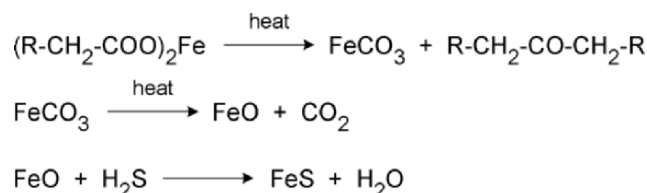


Figure 1. Mechanism of formation of FeS<sup>49</sup>

#### 4. PROPERTIES OF ASPHALTENES (SOLUBILITY, MOLECULAR WEIGHT, AGGREGATION)

Petroleum consists of four hydrocarbon-types (saturates, aromatics, resins, and asphaltenes) that may be defined in terms of solubility, polarity, and MW.<sup>1</sup> Of these structural types, asphaltenes have markedly adverse effects on the processability of petroleum and play a significant role in the physical properties of heavy oils and bitumen. Because of these effects, in this chapter, asphaltenes will be discussed in detail in terms of their properties, composition, and thermal chemistry during upgrading, as well as their influence on instability/incompatibility during the production, transportation and upgrading of petroleum.

Asphaltenes are probably the most studied fraction of petroleum and bitumen. By definition, they are a solubility class: a fraction of petroleum that is not soluble in paraffinic solvents but soluble in aromatic solvents. In general, they are believed to contain large polynuclear aromatic ring systems ranging between 6 and 20 rings. The condensed aromatic structures bear alkyl side chains varying in size between 4 and 20 carbons.<sup>51-53</sup> Asphaltenes are also known to self-associate (aggregate) in solutions. The difficulty in measuring the MW of asphaltenes has been related to this phenomenon. Asphaltenes MWs as high as 300,000 g/mol (using the ultracentrifuge technique) have been reported.<sup>53</sup> Using the VPO technique, a MW of 80,000 g/mol for the same asphaltenes was reported.<sup>53</sup> Even lower MWs (1,000-5,000 g/mol) were

reported in the same study for the same material using VPO under different conditions.

In terms of processability, aggregation of asphaltenes can hinder the conversion of heavy residues to lighter products and can enhance coke formation. Using surface tension measurements and rheological data, Sheu et al.<sup>54-55</sup> and Storm et al.<sup>56</sup> have shown that asphaltenes exhibit properties similar to colloids. These colloids exist in the heavy oil matrix in a micelle form.<sup>57</sup> Since the mole fraction of resins is higher than asphaltenes in petroleum, micelles are richer in resins. Asphaltenes also exhibit properties of colloidal systems such as the 'critical micelle concentration' (CMC) at which aggregates begin to form.

According to the asphaltenes-resin model, resins provide steric stabilization against precipitation of asphaltenes in petroleum fractions. The precipitation and phase separation of asphaltenes upon the addition of a nonpolar solvent can be rationalized in terms of a reduction in the solubility parameter or the polarity of the hydrocarbon medium.<sup>58-60</sup> The most direct evidence for the presence of asphaltenes aggregates in oil has been demonstrated by means of SANS (Small Angle Neutron Scattering). Ravey et al.<sup>61</sup> and Overfield et al.<sup>62</sup> further demonstrated that the physical dimensions and shape of the aggregates are a function of the solvent used. Ravey et al.<sup>61</sup> demonstrated that asphaltenes from Middle Eastern crude oils form sheet-like aggregates in tetrahydrofuran. Sheu et al.<sup>54</sup> showed that Ratawi asphaltenes in toluene and pyridine solutions form spherical aggregates having diameters between 60 and 66 Å. Watson and Barteau<sup>62</sup> observed STM (Scanning Tunneling Microscope) images of Ratawi asphaltenes aggregates separated from pyridine solutions, which showed that the asphaltenes aggregates formed orderly flat arrays covering hundreds of angstroms of the surface. The self-aggregation of asphaltenes plays an important role in the chemistry of asphaltenes conversion during thermal treatment of petroleum residues<sup>63</sup> and will be discussed in detail later in this chapter. Neves et al.<sup>64</sup> using light scattering and electrophoresis techniques, determined the aggregate size and charges present in asphaltenes from a Brazilian crude oil. When n-heptane was added to a mixture of asphaltenes in toluene, depending on concentration, the size of aggregate changed significantly varying between 125-186 nm in high concentration solutions to 238-398 nm in the low concentration solutions. It was also shown that asphaltenes possess a positive charge.

Asphaltenes from Athabasca bitumen were first separated using n-pentane by Pasternak and Clark in 1951.<sup>65</sup> In most refinery practices, the solvent of choice is n-heptane and asphaltenes are defined as materials soluble in toluene or a solvent having a solubility parameter in the 17.5-21.6 Mpa<sup>1/2</sup> range. As the carbon number of the extracting solvent increases, the amount of asphaltenes that precipitate decreases. Fundamentally, it is important to note that during asphaltene precipitation by any solvent, smaller asphaltene molecules, as well as some maltene materials, co-precipitate because of

chemisorption. In order to obtain “pure asphaltenes,” Strausz et al.<sup>66</sup> suggested that after standard asphaltenes extraction, the material should be further extracted by acetone for one week. Following this procedure would result in asphaltenes that do not contain any foreign material. The formation of aggregates in Athabasca bitumen has been studied in detail by Murgich and Strausz.<sup>67</sup> It has been shown that the molecular shapes of asphaltenes and resins play a significant role in the sizes and lifetimes of the aggregates.

#### 4.1 Chemical Structure of Asphaltenes

Recent studies by Strausz et al.<sup>68-70</sup>, Strausz et al. and Peng et al.<sup>71-72</sup>, and Murgich et al.<sup>73</sup> revealed the close structural similarities of asphaltenes from different sources. Asphaltenes are thought to be molecular units consisting of small- to mid-size alkyl and naphthoaromatic hydrocarbons. Some units contain S and to a lesser extent N. The molecular units are linked together by C-C, C-S, and C-O linkages. A molecular representation of a petroleum asphaltenes model has been given by Artok et al.<sup>74</sup> This model was based on extensive analytical data using <sup>1</sup>H and <sup>13</sup>C NMR, GPC, pyrolysis gas chromatography/mass spectrometry, and MALDI TOF (Matrix-assisted laser desorption/ ionization time-of-flight) mass spectrometry.

Chemical and degradation methods were employed by Peng et al.<sup>72</sup> to study the structure of Athabasca asphaltenes. In the oxidation reaction of asphaltenes, the RICO (Ruthenium Ions Catalyzed Oxidation) reaction permits the selective oxidation of aromatics while leaving saturated hydrocarbons intact. A two-dimensional structure for Athabasca asphaltenes having the general formula of C<sub>412</sub>H<sub>509</sub>S<sub>17</sub>O<sub>9</sub>N<sub>7</sub>, a H/C ratio of 1.23 and MW of 6,239 g/mol was proposed by Strausz et al. Recently, Leon et al.<sup>75</sup> investigated the structural characterization and self-association of asphaltenes having different origins. These authors argued that problems during crude oil production could be related to the asphaltene properties. They showed that n-heptane asphaltenes from two problematic crude oils had higher aromaticity, lower H/C atomic ratio, and significantly lower CMC (in different solvents) compared with the properties of asphaltenes derived from non-problematic crude oils. Although the data from this work could explain operational problems during crude oil production, the average structural model proposed for asphaltenes contains highly fused aromatics. This model is significantly different from the asphaltenes model proposed by Strausz et al.<sup>66</sup>, which contains a smaller number of fused aromatic rings. In another study, Shirokoff et al.<sup>76</sup> investigated the structure of Saudi crude asphaltenes using compositional analysis as well as XRD (X-Ray Diffraction). Based on these analyses, it was concluded that the n-pentane asphaltenes derived in these crudes contained condensed aromatic sheets with a tendency to stack. The condensed aromatics had naphthenic and alkyl chains on their periphery. Yen

et al.<sup>77</sup> postulated a similar structure with less dense alkyl regions on the periphery of asphaltene particles.

The effect of asphaltenes on the physical properties of heavy oils and bitumen has been studied extensively.<sup>78-82</sup> It has been demonstrated that the viscosity of petroleum is significantly influenced by the presence and concentration of asphaltenes. Storm et al.<sup>81</sup> demonstrated that when the relative viscosity of heavy oils was plotted versus asphaltenes concentration in both toluene (at room temperature) and vacuum residue (at 93°C), a straight line resulted. Thus, it was concluded that toluene is as good a solvent for asphaltenes as for vacuum resid. However, the amount of solvation is temperature dependent. By analyzing the temperature dependency of solvation, Storm et al. showed that the forces holding asphaltenes in the resid are very weak. Moreover, the fact that the solvation constant is the same for toluene at 25°C as in a vacuum resid at 93°C implies that the forces between asphaltene colloidal particles and toluene are weaker.

In a similar study aimed at shedding light on the aggregation of asphaltenes, Rao and Serrano<sup>78</sup> studied the physical interactions of asphaltenes in heavy oil. The viscosities of Arab resids containing different amounts of asphaltenes were measured in toluene at 27°C. It was concluded that aggregation of asphaltenes in heavy oils is stepwise and causes high viscosity and an apparent increase in MW. At low asphaltene concentrations, smaller aggregates were formed that could be dissociated to monomers at the processing temperature. However, at high asphaltene concentrations, the aggregates could not be dissociated and formed asphaltene clusters. Aggregate formation can cause process upset and limit process yields. Since formation of aggregates is stepwise and reversible, dissociation of asphaltene clusters to monomers may be accomplished by diluting the resid with an appropriate solvent, thus improving the process efficiency.

The dependency of feedstock viscosity on asphaltenes concentration has significant implications, because reducing viscosity could make pipeline transportation of heavy oil less dependent on diluent. Removal of even 100wt% asphaltenes from Athabasca bitumen does not reduce viscosity enough to meet pipeline specifications in Alberta (viscosity of 350 cSt at operating temperature, °API of 19, and BSW of <0.5 vol%). However, removal of approximately 30 wt% of asphaltenes has been shown to reduce diluent requirement by almost 30%. The benefit of partial removal of asphaltenes on thermal processing will be discussed later.

## 4.2 Thermal Chemistry of Asphaltenes

Asphaltenes are considered “bad actors” in refinery upgrading processes, because they cause coke and sludge formation, and in catalytic processes because they cause severe catalyst deactivation. It is widely accepted that petroleum is colloidal in nature and that asphaltenes exist in the petroleum in

a micelle form. The formation of micelles is believed to be primarily due to the interaction between asphaltene species or asphaltene-resin fractions. The nature of the intermolecular or intramolecular forces that cause the formation of asphaltene micelles is not clear at present. It has been suggested that a number of forces may be involved including Van der Waals attraction, dipole-dipole interaction, hydrogen bonding, electron-transfer or charge transfer between aromatics ( $\pi$ - $\pi$  bonding), and porphyrin interaction.<sup>83-84</sup> Wiehe<sup>84</sup> stated that the primary interaction between asphaltene molecules is the Van der Waals attraction between large areas of flat polynuclear aromatics. He used the solubility parameter to measure the attractive interaction between petroleum molecules, which is inversely related to the hydrogen content of the fractions. Using the generated phase diagram, it was shown that asphaltene molecules are relatively insoluble because of their high molecular weight and low H/C atomic ratio (high aromaticity). Wiehe also proposed a hybrid model for petroleum materials. According to this model, the asphaltenes are held in a delicate balance that can be easily upset by the addition of saturates or by the removal of resins and small aromatics.<sup>85</sup> During thermal treatment of petroleum feedstocks, the asphaltene micelles break down to form smaller aggregates. Further heating can result in the breakup of the protective resin layer and, finally, at about 300°C, the cores become “bare” resulting in precipitation of asphaltenes.

From a processing point of view, the microphase behaviour of asphaltenes plays an important role during catalytic and thermal upgrading of heavy oils and bitumens.<sup>86-87</sup> Storm et al. demonstrated that during hydroconversion of vacuum residues, the amount of sediment formation (cyclohexane insolubles) is strongly related to the amount of heptane insolubles in the residues.<sup>86</sup> When the heptane asphaltenes were removed from the residue, no sediment was formed. The authors further showed that a specific fraction of the residue, namely the pentane insoluble-heptane soluble fraction (which is relatively rich in hydrogen), plays an important role in reducing coke formation. They reasoned that the hydrogen in this fraction is used to cap the radicals generated in the asphaltenic-rich phase during conversion, hence retarding the formation of less soluble molecules.

Other properties of the feedstocks that could be correlated to the sediment formation are the degree of condensation of polynuclear aromatics and the degree of alkyl-substitution of polynuclear aromatics. In a later publication, Storm et al.<sup>87</sup> suggested the involvement of “macrochemistry” in the formation of sediment during hydroprocessing at lower temperatures. These particles (sediments) are then converted to macroscopic particles at higher temperatures. According to this model, grouping of certain molecules in the resid results in the formation of micelles with a dimension of 0.004:μm. Rheological and SAXS (Small Angle X-ray Scattering) results showed that these small particles could be transformed into larger two-dimensional particles with dimensions of 0.02-0.03:μm. As discussed earlier, these



microstructure particles form well below temperatures that are characteristic of chemical reactions. Also, during low severity catalytic hydrocracking, polymerization between the larger two-dimensional particles does not occur and only a semisolid, which is soluble in the reaction media, is formed. However, at higher reaction temperatures, polymerization of the particles takes place and results in the formation of insoluble coke. It was thought that if the flocculation of larger particles could be interrupted below reaction temperatures, coke formation could be reduced. To reduce flocculation, Storm et al.<sup>87</sup> used 1 wt% of a polymeric additive (functionalized polypropyleneoxide diol with  $\text{PCl}_3$ ) in a series of hydrocracking experiments with VB from Arabian medium and heavy crude oils. It was shown that the use of the additive, which was soluble in the heavy asphaltenic phase, interrupted the coalescence of asphaltic micelles required for coke formation. Thus, in these experiments, pitch conversion, desulphurization, and demetallation were improved and the formation of sediment was reduced.

In the pendant-core model proposed by Wiehe<sup>88</sup>, every molecule in petroleum consists of two building blocks: an aromatic core, which is coke-producing, and a pendant block, which is attached to the core and can be cracked to produce volatile liquids. Using this model, the building blocks of each hydrocarbon type, including asphaltenes, were constructed. As the polarity or the boiling point of petroleum fractions increases, the core part of the fraction or its aromaticity also increases. As the resins and asphaltene fractions contain more cores, these fractions contribute significantly more coke than the other petroleum fractions during thermal processes. It has also been suggested that coke formation is the result of separation of a second liquid phase formed from partially converted asphaltene cores. The liquid-liquid phase separation is evidenced by the presence of spherical liquid crystalline coke called mesophase. The stacking of the polynuclear aromatic structure, present in asphaltenic material, forms the mesophase. During residue hydrocracking, mesophase lacks a significant degree of ordering (fast solidification) as a result of the high reactivity of the asphaltene cores. Wiehe<sup>2</sup> has shown in the thermal conversion of Cold Lake (CL) vacuum resid that there is a delay in coke formation (an induction period) and that the onset of coke formation is triggered by phase separation.

As indicated earlier, there is a delicate balance between the concentration of resins and asphaltenes in petroleum fractions. Any interruption in the ratio of asphaltenes:resins can cause operational problems because of asphaltene precipitation (coke formation) and plant shutdown. It is therefore crucial, if coke formation is to be minimized, to monitor the ratio of asphaltenes:resins during the thermal processing of bitumens and heavy oils. Clarke and Pruden<sup>89</sup> developed a heat transfer analysis technique that can detect the onset of asphaltene precipitation. They showed that precipitated asphaltenes could be re-peptized using polynuclear aromatic compounds such as phenanthrene. It has been demonstrated in the 5000 bbl/d CANMET hydrocracking unit

operated by Petro-Canada at its Montreal refinery, that the recycling of heavy resids during the hydrocracking of heavy oils improves the plant's operability, resulting in higher conversions.<sup>90</sup> In Texas City, the H-Oil process for the catalytic conversion of resid blends has shown that the presence of highly aromatic byproduct streams is most effective in minimizing asphaltene precipitation and solids formation.<sup>91</sup> The review by Mansoori<sup>92</sup> on asphaltene deposition and control during production suggested that the addition of resins (peptizing agents) in proper amounts might prevent or control the heavy organic deposition problem.

Considering the "average chemical structure" of asphaltene as proposed by Strausz et al.<sup>66</sup>, understanding the chemistry of asphaltene conversion could be extremely complicated. The literature suggests that asphaltene, apart from producing coke, are also converted to lower molecular weight components that are later converted to liquid and gaseous products. Calemma et al.<sup>93</sup> studied the pyrolysis kinetics of four different asphaltene using TGA/FTIR (Thermo Gravimetric Analyzer/Fourier Transform Infrared Spectroscopy). They concluded that for asphaltene containing more sulphur, the activation energy was lower by about 2 Kcal/mole. The data were interpreted on the basis of weaker bond strength in C-S and S-S bonds, which are approximately 10 Kcal/mole lower than in C-C bonds. The data also showed that the activation energy increased at higher conversion. The results were explained as follows: as the reaction proceeds, the structures in the asphaltene become more aromatic (dehydrogenation) and the alkyl groups attached to the rings become shorter. These reactions make the subsequent decomposition more difficult, which translates to higher activation energy for decomposition reactions.<sup>94</sup> Rahimi et al.<sup>95</sup> have shown that approximately 50 wt% of asphaltene from Athabasca bitumen can be converted to maltene at a relatively moderate severity.

During the thermal cracking of vacuum residues, maltene play an important role in the conversion of asphaltene. Wiehe<sup>60</sup> has shown that in the hydrocracking of CL VB (Cold Lake Vacuum Bottoms), the presence of maltene in the resid increases (prolongs) the coke induction period significantly. The results were interpreted based on the effectiveness of maltene as hydrogen donors to cap free radicals produced by the thermal cracking of asphaltene.

At this stage, a general overview of the chemistry of upgrading is necessary prior to discussing the conversion of bitumen and heavy oil constituents at elevated temperatures.

## 5. CHEMISTRY OF UPGRADING

It is well documented that the conversion of resid to lighter products, whether or not in the presence of hydrogen and/or a catalyst, is largely thermally driven.<sup>91,96</sup> The hypothetical molecular structure of bitumen and

asphaltenes consists mostly of C-C, C-H, C=C (in the aromatic rings) and to a lesser degree C-S, C-O, C-N, S-H, and O-H. The metal impurities are mostly attached to nitrogen in porphyrin and non-porphyrin structures. Since most of the chemical reactions during bitumen upgrading are thermally driven, there is no selectivity in bond cleavage. Under non-selective thermal reaction conditions, the weakest bonds break first. The bond dissociation energies of the most common bonds are shown in Table 7. According to this table, C-S (sulphide) has the lowest bond dissociation energy and will break first at a relatively moderate severity. At low to moderate severities in typical visbreaking conditions (380°C-410°C), 10-20wt% pitch conversion can be achieved without major coke formation. Under these conditions, the changes to the molecular structure of bitumen are relatively small since most of the C-C bonds remain intact. A significant MW reduction must take place before bitumen molecules are converted to distillates. The following chemical reactions are known to occur during this transformation to distillates:

1. homolytic cleavage of C-C bonds;
2. side chain fragmentation (cleavage);
3. ring growth;
4. hydrogen shuttling;
5. hydrogenation of aromatics/dehydrogenation of cycloparaffins;
6. ring opening;
7. heteroatom and metals removal.

*Table 7. Bond dissociation energies*

| <b>Bonds</b>                            | <b>Kcal/mole</b> |
|---|------------------|
| H-H                                     | 103              |
| C-C                                     | 83-85            |
| C-H                                     | 96-99            |
| N-H                                     | 93               |
| S-H                                     | 82               |
| O-H                                     | 110-111          |
| C=C                                     | 146-151          |
| C-N                                     | 69-75            |
| C-S                                     | 66               |
| Ar-CH <sub>2</sub> -CH <sub>2</sub> -Ar | 71               |
| Ar-H                                    | 111              |

The most important reaction in upgrading that leads to a significant molecular weight reduction and produces distillate fractions is probably cleavage of the C-C bonds. The bond dissociation energies for C-C bond cleavage can vary depending on the type of molecules. It has been suggested that the reaction mechanism for the cleavage of C-C bonds during upgrading is free radical in nature, and proceeds through a free radical chain mechanism.<sup>97</sup>

The reaction kinetic (homolysis) of a hypothetical molecule (M) proceeding through a free radical chain mechanism is shown in Figure 2. The overall reaction rate is related to the rate of the initiation step. If one assumes

that the initiation step involves the homolytic cleavage of the C-C bond, then one can calculate the half-life ( $t_{1/2}$ ) for the reaction. For example, the  $t_{1/2}$  for the cleavage of the C-C bond in  $\text{PhCH}_2\text{-CH}(\text{CH}_3)_2$  is 2.4 hours at  $540^\circ\text{C}$  and 46.3 days at  $440^\circ\text{C}$ . The fact that thermal hydrocracking of bitumens and heavy oils can be accomplished at a much lower temperature and a relatively high conversion indicates that the cleavage of C-C bonds is not a rate-determining step. The initiation step may involve cleavage of the C-S bond, or the breakage of the C-C bonds must be accomplished by a mechanism other than homolytic cleavage.

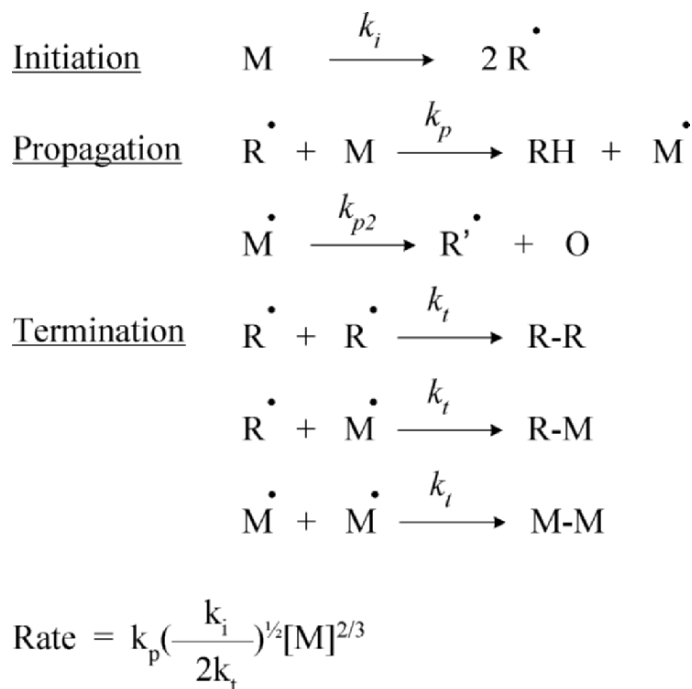


Figure 2. Radical chain mechanism for homolysis of a hypothetical molecule M

There are a number of mechanisms proposed for the initiation step of the cleavage of strong C-C bonds. These reactions are shown in Figures 3 to 5. In the radical hydrogen transfer mechanism proposed by McMillen et al.<sup>98</sup>, there is a direct transfer of hydrogen from a radical to another molecule. Another mode of transferring H atoms includes RRD (Reverse Radical Disproportionation), proposed by Stein et al.<sup>99</sup> Besides transferring an H atom from solvents, a free H atom can also be produced by  $\beta$ -elimination from various radicals or by the reaction of a stabilized radical with molecular hydrogen<sup>100</sup> (Figure 5).

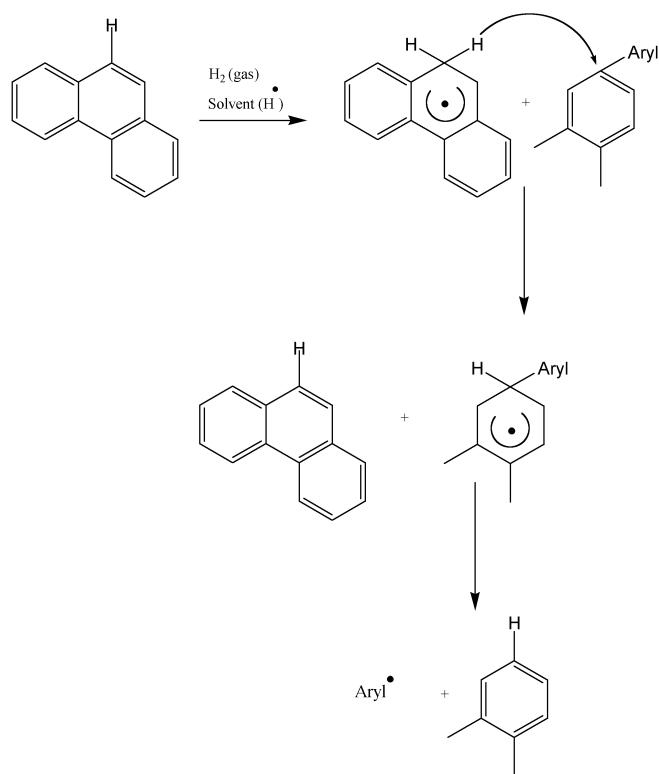


Figure 3. Radical hydrogen transfer for the cleavage of C-C bond<sup>98</sup>

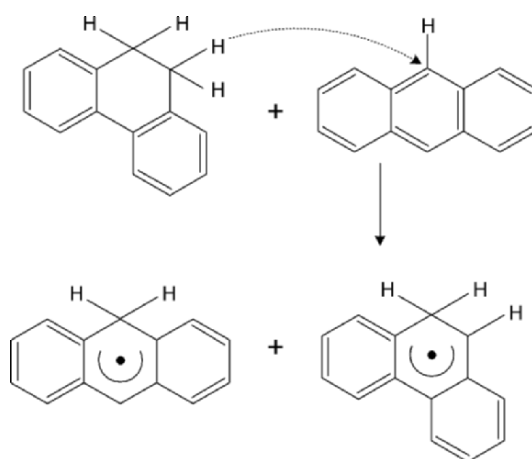
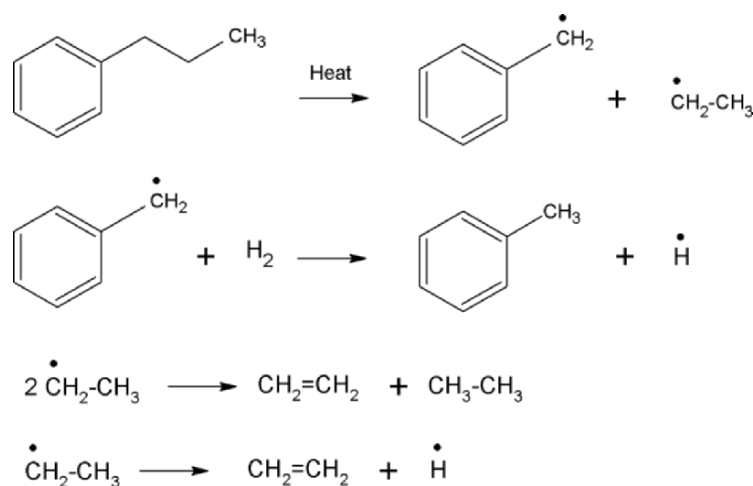


Figure 4. Reverse radical disproportionation mechanism for H-transfer<sup>99</sup>

Figure 5. Formation of H by  $\beta$  elimination<sup>100</sup>

An alternative reaction mechanism to unfavorable homolytic C-C bond cleavage is the electron transfer mechanism shown in Figure 6. In this reaction, an electron is transferred from an aromatic core of a molecule to a metal (Ni, V, or Fe) to produce a radical cation. An electron transfer mechanism has been proposed for the reaction of the model in the presence of carbon black, and with tetralin as the solvent.<sup>101</sup> In this model, selective C-C bond cleavage (at the position of poly condensed aromatic moiety) is achieved at 320°C in the presence of carbon black where no thermal reaction is known to occur. The authors rationalized their observations based on the aforementioned electron transfer mechanism. The selective C-C bond cleavage occurs by an electron transfer from the condensed aromatic ring to the carbon black surface, which has become positively charged at a reaction temperature of 320°C. This reaction mechanism has been recently disputed by Penn et al.<sup>102</sup> They argue the C-C bond cleavage is caused by a radical hydrogen transfer mechanism in which the H atom adds to the ipso position of the polyaromatic moiety. It is also possible that this electron transfer may occur during bitumen and heavy oil upgrading since there is a significant concentration of transition metals capable of accepting electrons from highly condensed poly aromatics.

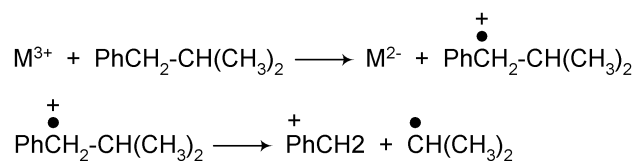


Figure 6. Cleavage of C-C bond via electron transfer mechanism

Whatever the reaction mechanism, it has been demonstrated in heavy oil upgrading that the conversion to lighter products is mainly thermally driven, whether or not the reaction is carried out in the presence of hydrogen and/or a metal catalyst.<sup>103-106</sup>

## 5.1 Reaction of Feedstock Components - Simplification of Upgrading Chemistry

The chemistry of resid upgrading is extremely complicated.<sup>107-110</sup> This is in part due to the complexity of the chemical nature of the feedstocks. In order to understand the chemistry of upgrading, it would be helpful to reduce this complexity prior to reaction, by separating the feedstocks (bitumen and heavy oils) into well-known components such as SARA – saturates, aromatics, resins and asphaltenes – which are useful tools in understanding bitumen chemistry.

Speight<sup>111</sup> investigated the chemistry of the thermal cracking of asphaltenes from Athabasca bitumen and deasphalted oil using a destructive distillation technique. A comparison of the analytical data from the feedstocks and products indicated that considerable changes occurred during cracking. The H/C atomic ratio data showed that simultaneous hydrogenation and dehydrogenation reactions took place. The results also indicated that DAO was more thermally labile than asphaltenes. Approximately 83 wt% of the DAO was converted into resins (maltenes), light oil and gases. In contrast, only 52 wt% of asphaltenes was converted into cracked products. The presence of n-paraffins in the light oil fractions indicated dealkylation (side chain fragmentation) of alkylaromatic compounds. A separate investigation of the thermal reaction of Athabasca bitumen at 440°C for 30 minutes using a micro-autoclave showed that approximately 46 wt% of pentane solubles (maltenes) was formed.<sup>112</sup> Further analysis revealed that the maltenes consisted of 17 wt% saturates, 5 wt% mono-/diaromatics, 20.5 wt% polyaromatics and 3.5 wt% polar compounds.

In a recent study by Rahimi et al.<sup>113</sup>, partial deasphalting of Athabasca bitumen resulted in bitumen with an improved quality in terms of lower viscosity, MCR, and metals content. The better quality of the deasphalted oil was reflected in its coking behaviour. At laboratory conditions comparable to a delayed coking operation, deasphalted bitumen produced similar liquid yield but lower coke yield compared with the coking of the whole bitumen. Also, the liquid product resulting from the coking experiments of the partially deasphalted bitumen feed had less olefins. This product would be more stable and would need less hydrogen during upgrading and refining.

Klein et al.<sup>114</sup> investigated the pyrolysis kinetics of resids, isolated asphaltenes and maltenes from Hondo, Arabian heavy, Arabian light, and Maya oils. At 400°C and 425°C, isolated asphaltenes reacted selectively to form maltenes. At higher temperatures (450°C), asphaltenes reacted

predominantly to form coke. Furthermore, pyrolysis of the maltenes indicated that asphaltenes and coke were formed in the following order:



Karacan and Kok recently studied the pyrolysis of two crude oils and their SARA fractions.<sup>115</sup> Differential scanning calorimetry and thermogravimetry techniques were used to evaluate the pyrolysis behaviour of the feedstocks. The results indicated that the pyrolysis mechanisms depend on the nature of the constituents. Thermogravimetric data showed that asphaltenes are the main contributors to coke formation and that resins are a second contributor. The weight loss for the SARA components was additive. The authors argued that each fraction in a whole crude oil follows its own reaction pathway and there is no interaction or synergy between the components.

The chemistry of upgrading is expected to become significantly more complex when vacuum bottoms are processed. Dawson et al.<sup>116</sup> investigated the thermal behaviour of Athabasca bitumen VB and SARA fractions at temperatures between 420°C and 460°C. Detailed product analyses revealed that saturates and mono- and diaromatics are relatively unreactive, whereas polyaromatics and resins are converted to smaller molecules including saturates. The aromatic fraction constituted the major components of the vacuum residues. Approximately 54 wt% of CLVB consisted of polyaromatic hydrocarbons.<sup>117</sup> The upgrading chemistry of this fraction was investigated in a batch autoclave at different severity conditions (420°C-440°C, 30 min, 13.9 MPa H<sub>2</sub>). The product analyses showed that at all severities the aromatic fraction (M<sub>3</sub>) not only decomposed to form smaller molecules but also polymerized to form larger molecules and a small amount of coke (Table 8). The reaction sequence can be summarized as :

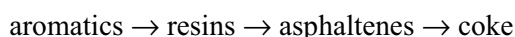


Table 8. Thermal hydrocracking of polyaromatics derived from Cold Lake vacuum bottoms

| Products (wt%)   | 420°C | 440°C | 450°C |
|------------------|-------|-------|-------|
| Gases            | 5.6   | 14.3  | 11    |
| Asphaltene       | 6.0   | 9.5   | 12    |
| Coke             | 0.7   | 0.5   | 0.3   |
| Maltenes         |       |       |       |
| Saturates        | 10.3  | 15    | 21.7  |
| Mono-diaromatics | 8.4   | 9.8   | 9.1   |
| Polyaromatics    | 57.8  | 33.1  | 41.6  |
| Polars           | 11.2  | 17.7  | 4.6   |

Furthermore, the analysis of polyaromatic fractions following the reaction (M<sub>3</sub> products) showed that these molecules had relatively lower MW, shorter chains and were more aromatic. The results of this work confirm that side chain fragmentation and hydrogenation/dehydrogenation reactions are major routes in the thermal cracking of heavy oils and bitumen (see Tables 9-10).



Table 9. NMR analysis of M3 fractions from different sources

| Source      | Aliphatic carbon types (wt %) |                   |                        |               |        |
|-------------|-------------------------------|-------------------|------------------------|---------------|--------|
|             | Alpha CH <sub>3</sub>         | Naphthenic (Beta) | >C <sub>6</sub> Chains | Paraffinic CH | Others |
| Feed        | 8.5                           | 4.9               | 6.1                    | 9.4           | 24.2   |
| 420°C       | 6.8                           | 2.8               | 4.4                    | 9.3           | 18.1   |
| 440°C       | 6.6                           | 1.7               | 1.1                    | 5.1           | 13.9   |
| 440°C (cat) | 7.6                           | 3.1               | 4.3                    | 8.5           | 19.6   |
| 450°C       | 7.1                           | 1.5               | 0.9                    | 5.2           | 14.3   |

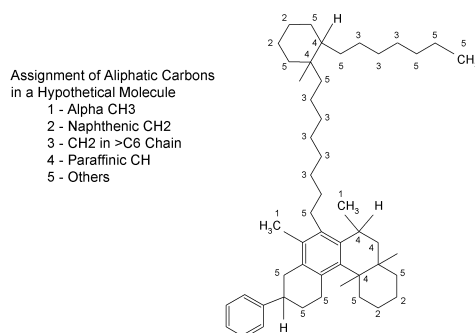
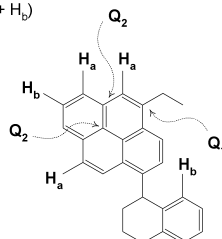


Table 10. NMR analysis of M3 fractions from different sources

| Source      | Aromatic carbon types (wt%) |      |       |      |     |       | Aromaticity | Cluster size* |
|-------------|-----------------------------|------|-------|------|-----|-------|-------------|---------------|
|             | Q1                          | Q2   | Q1+Q2 | Ha   | Hb  | Ha+Hb |             |               |
| Feed        | 9.0                         | 8.5  | 17.5  | 5.8  | 6.3 | 12.1  | 0.36        | 14            |
| 420°C       | 11.1                        | 10.1 | 21.2  | 11.1 | 8.7 | 19.8  | 0.50        | 12            |
| 440°C       | 11.4                        | 20.2 | 31.6  | 15.7 | 8.1 | 23.8  | 0.66        | 18            |
| 440°C (cat) | 10.4                        | 10.7 | 21.1  | 10.8 | 9.4 | 20.3  | 0.49        | 12            |
| 450°C       | 14.3                        | 13.1 | 27.4  | 17.2 | 9.3 | 26.5  | 0.65        | 11            |

\* $\chi_b = /$  (cluster size) given in reference (7)

$$X_b = Q_2 / (Q_1 + Q_2 + H_a + H_b)$$



In an attempt to correlate the thermal cracking behavior of heavy oils to their properties, Liu et al.<sup>118</sup> studied the thermal cracking of 40 heavy oil fractions obtained by supercritical extraction from six Chinese light crude oils and oils from Oman and Saudi Arabia. The thermal cracking experiments were performed at 410°C, 0.1 MPa N<sub>2</sub> for 1 hour. A non-linear regression fit indicated that the thermal cracking of the fractions could be correlated with the H/C, S (wt%), N (wt%) and molecular weight. A similar correlation was obtained with SARA analysis, S, and MW. In this study, the coke yields

(toluene insolubles) correlated with the concentration of asphaltenes/resins plus aromatics of the cracked residues. These results were rationalized in terms of coke formation, not only from asphaltenes but also as a result of the phase separation of the colloidal system in the residues.

## **6. APPLICATION OF HOT STAGE MICROSCOPY IN THE INVESTIGATION OF THE THERMAL CHEMISTRY OF HEAVY OIL AND BITUMEN**

Investigating the effects of process variables on coke formation is usually achieved by autoclave and pilot plant experiments, which are time consuming and expensive. Another tool that offers the advantage of real-time observation of the thermal reaction is hot-stage microscopy. This section reviews the usefulness of hot-stage microscopy for a better understanding of bitumen chemistry.<sup>119</sup>

The coke induction period (the time that is required for coke precursors or mesophase to start forming at a specific temperature) during thermal processing of heavy oils and bitumen is an important measurement for understanding operational problems. These problems may include coke formation and fouling in heat exchangers and fractionators leading to an unscheduled plant shutdown. The induction period coincides with the moment at which the asphaltenes in the reaction system reach their maximum concentration.<sup>120</sup> At the National Centre for Upgrading Technology's laboratory, hot-stage microscopy techniques were used to investigate those parameters that influence the thermal chemistry pathways during upgrading of petroleum feedstocks. Such studies could lead to possible solutions aimed at reducing coke and maximizing product yields. The parameters studied included the following: feed composition (i.e., SARA, acid, base); boiling point range (343°C-675°C); degree of asphaltenes removal (0-18 wt%, C<sub>5</sub> asphaltenes); coke suppressing agent (H-donors); and solid additives (clays) that inhibit coalescence of coke precursors.

### **6.1 Effect of Feedstock Composition**

The thermal chemistry of heavy oils and bitumen is extremely complicated because of wide variations in chemical compositions. The most refractory components in petroleum feedstocks are asphaltenes, which contribute the most to coke formation during thermal cracking. Next to asphaltenes, resins and large aromatics also contribute to coke. To investigate the effect of these three heavy oil components on the mesophase induction period, Athabasca bitumen fractions containing varying amounts of asphaltenes (obtained by supercritical fluid extraction) and Venezuelan heavy

oil fractions varying in polarity (obtained by Ion Exchange Chromatography) were selected.

One of the Athabasca bitumen fractions investigated under a hydrogen atmosphere consisted of 88 wt% asphaltenes. This fraction exhibited a very short induction period (48 minutes at room temperature), as expected for a highly-asphaltenic feed. These results are consistent with the findings of Wiehe<sup>120</sup>, who demonstrated, using an autoclave, that Cold Lake asphaltenes (neat) formed coke immediately with no induction period. Using hot-stage microscopy it is also possible to follow the coalescence of mesophase particles in real-time and observe the changes in the apparent viscosity and, finally, the solidification process (Figure 7a). The second feedstock examined was a fraction of Athabasca bitumen containing 45.4 wt% resins, 54.0 wt% aromatics and no asphaltenes. The coke induction period was significantly longer (~72 minutes) compared with the fraction containing asphaltenes. This fraction developed mesophase of various sizes during thermal treatment, which later coalesced to form bulk mesophase and even-flow domains (Figure 7b).

In another study, in order to examine the relationship between reactivity and composition of a Venezuelan heavy oil, the Hamaca resid (510°C+) was separated into fractions including amphoteric, acidic, basic, neutral and aromatic.<sup>121</sup> Results showed that the amphoteric fraction exhibited the shortest induction period for coke formation (50 minutes), followed by the basic and the acidic fractions. Amphoterics contain polynuclear aromatic systems having 5-6 rings per system<sup>122</sup>; as such, they are the most viscous and showed the fastest solidification. The basic fraction, which consists of 4 aromatic rings per system, showed a longer induction period (58 minutes). The acidic fraction, with only 1-3 aromatic rings per system, had an induction period of 68 minutes. The neutral fraction, which contains non-basic nitrogen and oxygen species, formed small mesophase spheres (Figure 7c) and the induction period was 82 minutes. The aromatic fraction had the longest induction period of 93 minutes and developed large mesophase (Figure 7d). The total resid containing all of the above components had an induction period of 61 minutes, indicating the synergy or interaction among the components during thermal reaction.

## 6.2 Effect of Boiling Point

Recently, major synthetic oil producers in Western Canada have switched from atmospheric bottoms to vacuum resids for processing bitumen. This raises the question of what impact this change might have on the coke induction period during thermal processing of these materials. To address this question, Athabasca bitumen (+343°C) was fractionated using Distact distillation into four distillates and resids.<sup>123</sup> The selected boiling point cuts were 525°C, 575°C, 625°C, and 675°C. The coke induction periods of bitumen

and its resid fractions were measured under hydrogen and nitrogen atmospheres. The results indicated no major differences in the coke induction periods between bitumen (68 minutes) and the four fractions (68, 66, 77 and 61 minutes, respectively). This may have important process implications in that processing higher boiling fractions does not necessarily shorten the coke induction period.

Fig 7a: Semicoke formation from asphaltenes

Fig 7b: Semicoke formation from resins

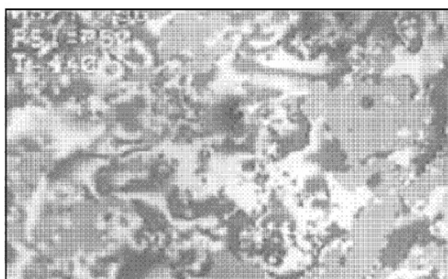


Fig 7c: Mesophase from neutral fraction

Fig 7d: Mesophase from aromatic fraction

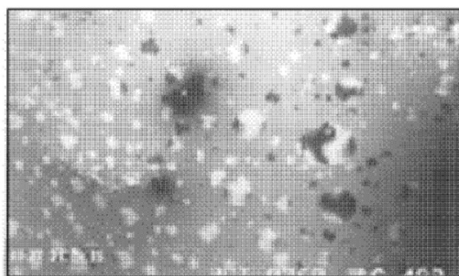
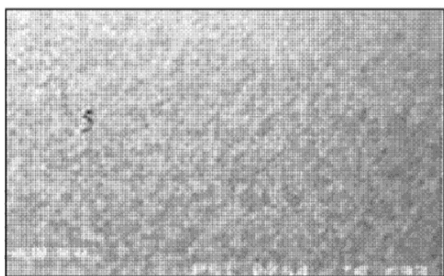
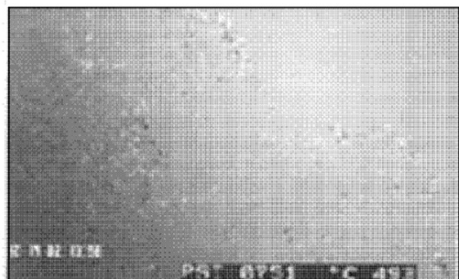
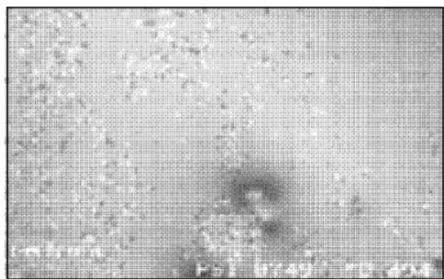


Fig 7e: Mesophase in presence of clay

Fig 7f: Mesophase in presence of H-donor



40 microns

Figure 7. Effect of different variables on mesophase formation

### 6.3 Effect of Additives

Coke formation during thermal treatment of bitumen proceeds via the formation of mesophase spheres that coalesce to form larger mesophase, which eventually deposits as coke on the surfaces of equipment. If the coalescence process can be slowed down or prevented, the size of mesophase would be smaller and, consequently, be carried out of the process lines and vessels without fouling the equipment. To investigate the effectiveness of clay minerals as additives that interfere with the growth of mesophase, three clays (kaolinite, illite and montmorillonite) were added to Athabasca bitumen at concentrations of 2 wt% and 5 wt%.<sup>124</sup> Although the presence of clays did not result in a delay of the coke induction period, the presence of kaolinite reduced the size of mesophase and decreased the mesophase coalescence under nitrogen (Figure 7e). Thus, it was deduced that clays may reduce or prevent fouling on the walls of furnaces, exchangers and reaction vessels during bitumen upgrading.

Liquid additives, such as hydrogen donors, have also been shown to reduce coke formation during heavy oil hydroprocessing.<sup>125</sup> It has been shown that H-donors have the ability to scavenge free radicals, to act as antioxidants, and to inhibit coke formation while improving asphaltene conversion. In order to examine the effectiveness of hydrogen donors on the induction period during upgrading, Athabasca bitumen vacuum bottoms was mixed with 5 wt% of an H-donor derived from a petroleum stream.<sup>126</sup> The results showed that the H-donor prolonged the coke induction period by as much as 20 min. It was also clear from the visual observation under microscope that the presence of additives reduced the rate of mesophase formation under nitrogen gas (Figure 7f).

### 6.4 Effect of Deasphalting

Asphaltenes are known to be the most refractory components in heavy oils and bitumen and can be converted to coke during thermal cracking. Therefore, it would be beneficial to selectively remove, if possible, the "worst" asphaltenes using solvents with different solubility parameters (polarity). To achieve the above objective, Athabasca bitumen was treated with mixtures of pentane and toluene ranging from P/T = 100, 90/10, 85/15, 75/25 and 65/35. As the pentane to toluene (P/T) ratio decreased the amount of asphaltenes remaining in the partially deasphalted oil (PDAO) increased and their quality deteriorated, as indicated by progressively higher MCR content. To investigate the effect of asphaltene removal on the coke induction period, the PDAOs were subjected to hot-stage microscopy studies.<sup>127</sup> It was shown that, as the P/T ratio decreased (solubility parameters increased), the coke induction period became shorter, ranging from 72 minutes

at P/T=100 to 60 minutes at P/T=65/35. This study shows that deasphalting enhances the bitumen quality and results in a lower coking propensity.

## 7. STABILITY AND COMPATIBILITY

In nature, the components of petroleum, including bitumen and heavy oils, are in a fine balance. Any changes to this balance, as a result of physical or chemical treatments, can result in instability followed by asphaltene precipitation, phase separation and sediment formation. In fact, the changes to the properties of petroleum occur from the time of its production and throughout transportation and processing. Asphaltene precipitation can also occur when two petroleum streams are incompatible. Using the colloidal hybrid model for petroleum discussed earlier by Wiehe,<sup>84</sup> it is relatively easy to follow the changes in the structure of petroleum as a result of physical and chemical treatment. Either removing or converting the resins layer that protects (peptizes) asphaltene, results in instability of asphaltene and, finally, insolubility in the media and precipitation. To prevent further system deterioration, one must bring asphaltene back into the solution (re-peptize), for example by the addition of small amounts of dispersants.

There are no standard tests for measuring the onset of asphaltene precipitation. Among the techniques and analytical methods frequently used to measure sediment and asphaltene onset for the adjustment of different process parameters in the refineries are:

1. spot test (ASTM-D-4740-95);
2. total sediment (ASTM-4870-96);
3. solubility parameters, optical microscope;<sup>128</sup>
4. light scattering (PORLA);<sup>129</sup>
5. peptization value (P-value);<sup>130</sup>
6. colloidal instability index (CII);<sup>131-132</sup>
7. coking index<sup>133</sup>.

In recent years there has been a significant effort by different groups<sup>129, 134-135</sup> to automate the measurement of asphaltene precipitation. This will, supposedly, create more reliable and consistent data.

In this section the stability and compatibility of petroleum will be discussed in terms of physical treatment such as distillation, deasphalting and diluent addition for pipeline transportation, and in terms of chemical treatment such as upgrading.

### 7.1 Physical Treatment

#### 7.1.1 Effect of Distillation

Any physical treatment that may disturb the balance existing between components of oil may cause instability in the system and, finally, asphaltene

precipitation. One such physical treatment is distillation. Conversion of Athabasca bitumen to synthetic crude oil at both Syncrude Canada and Suncor Energy Inc., has changed from processing full-range bitumen (atmospheric bottoms, 343°C) to processing vacuum tower bottoms (524°C). Due to improvements in distillation technology, it is feasible to go to even deeper cut points without any cracking by using a short path distillation unit.

At the National Centre for Upgrading Technology in Canada, full-range Athabasca bitumen was distilled into four fractions using a DISTACT unit. The results on SARA analysis of the original feed and the fractions are shown in Table 11, and reveal that as the boiling point increased, the saturates, aromatics and resins decreased, whereas the asphaltenes content ( $C_5$ ) increased significantly. As a result, the ratio of resins/asphaltenes decreased from 1.49 in the full-range bitumen to 0.30 in the fraction with a nominal boiling point of 675°C. As shown in Table 12, the stability as defined by the ratio of solubility number and peptization value (p-value) point to a less stable feedstock as the boiling point increases (although all fractions are stable and have values well above 1, which is considered to be the borderline between stable and unstable material). The fouling tendency as measured by the colloidal instability index (CII) showed that the feedstocks with a CII greater than about 0.6 would have a greater chance of forming deposits or coke when subjected to thermal treatment.<sup>132</sup> From the data in Table 12, it could be concluded that, although all the distillate fractions from Athabasca bitumen are stable, distillation into deeper cuts removed the asphaltenes' protective layers, making them more prone to separation/deposition and, subsequently, to coke formation.

*Table 11.* Effect of distillation cut point on SARA analysis of Athabasca bitumen

| Cut point, °C | Saturates, wt% | Aromatics, wt% | Resins, wt% | Asphaltenes, wt% | Resins/asph |
|---------------|----------------|----------------|-------------|------------------|-------------|
| 343           | 17.3           | 39.7           | 25.8        | 17.3             | 1.49        |
| 525*          | 5.9            | 31.8           | 20.8        | 41.5             | 0.50        |
| 575           | 5.3            | 30.9           | 19.7        | 44.1             | 0.45        |
| 625           | 4.8            | 23.3           | 17.1        | 54.7             | 0.31        |
| 675           | 3.5            | 20.4           | 17.5        | 58.5             | 0.30        |

\* From DISTACT distillation

*Table 12.* Effect of cut point on satiability and solubility parameters of Athabasca bitumen

| Cut point, °C | Resins/asph | $S_{BN}/I_N$ | P-value | CII** |
|---------------|-------------|--------------|---------|-------|
| 343           | 1.49        | 3.5          | 3.6     | 0.53  |
| 525*          | 0.50        | 3.0          | 3.1     | 0.90  |
| 575           | 0.45        | 2.4          | 2.7     | 0.98  |
| 625           | 0.31        | 2.5          | 2.4     | 1.5   |
| 675           | 0.30        | 2.4          | 2.5     | 1.6   |

\* From DISTACT distillation

\*\* Colloidal Instability Index =  $(S+Asph)/(A+P)$

### 7.1.2 Effect of Addition of Diluent

Heavy oils and bitumen are very viscous (>100,000 cP) and as such cannot be transported by pipeline. The Canadian pipeline specification for viscosity is 350 cSt at operating temperature. At the present time, the viscosity specification is met by the addition of approximately 25 vol% diluent, usually natural gas condensate. Depending on the characteristics of the diluent, i.e., if it is paraffinic, it may cause asphaltene precipitation during pipelining.

It is well known that the presence of asphaltene in heavy oils and bitumen plays an important role in its rheological properties and is responsible for the observed high viscosity of these materials.<sup>81</sup> A recent study by Rahimi et al. showed that the viscosity of Athabasca bitumen varies significantly with the asphaltene concentration.<sup>127</sup> Although the removal of all the asphaltene from Athabasca bitumen (17wt% of C<sub>5</sub> asphaltene) did not result in a product that met the pipeline specification for viscosity, the amount of diluent required to meet that specification was significantly reduced. It was further shown that a large excess of a paraffinic diluent (80 vol%) was required before asphaltene precipitation occurred.<sup>130</sup> In the case of partial deasphalting for the purpose of producing cleaner feedstock, the largest and the most refractory asphaltene could be removed by the addition of a small amount of paraffinic diluent. However, if the diluent in the bitumen is not removed immediately, the remaining asphaltene might precipitate.

### 7.1.3 Thermal/Chemical Treatment

As discussed earlier, the asphaltene molecules are peptized by resins. In the deasphalting process, which is usually performed at low temperatures, the disruption between maltene and asphaltene is done deliberately and results in the precipitation of the latter. However, during thermal processes, the nature and the chemical characteristics of both maltene and asphaltene can change significantly. Because of the nature of the chemical reactions – such as side chain fragmentation – the paraffinic content of the reaction medium will increase. The reaction medium will not keep large molecules in solution and phase separation will occur. The reverse may also occur — wax (long paraffin chain molecules) separates because of a drop in temperature or an increase in the aromaticity of the liquid medium.<sup>136</sup>

There is another type of solid-like (coke-like) material formed during visbreaking and hydrocracking of vacuum residues. This type of solid is usually referred to as sediment or sludge. Sediment may form from both the inorganic or from the organic constituents of petroleum. Formation of sediment and sludge limits process conversion because of its accumulation in downstream equipment.<sup>86</sup> High severity (high conversion) processes promote condensation and polymerization reactions. When the solvent power of the



liquid phase is not sufficient to keep the coke precursors in solution, coke is formed. Even during catalytic hydrocracking, such as in the H-Oil process, the formation of deposits cannot be avoided. The degree and the amount of deposit depend on the severity of the process. It has been shown that during H-Oil operation for moderate resid conversion (60%), there are no problems associated with sediment formation.<sup>137</sup> However, conversions above 60% are accompanied by increased fouling and sedimentation problems in the operating units. The fouling can be 1) the result of asphaltenes precipitation (phase separation) because of the incompatibility of the effluent stream; 2) the result of the formation of polyaromatics (PAH) from naphthenic hydrocarbons by dehydrogenation reactions; and 3) phase separation because of the existence of supercritical conditions in the hydroprocessing equipment.<sup>138</sup> However, the authors of this study believe that reactor fouling is mostly related to the rejection of Ni and V sulphides to the catalyst surface. Moreover, the extract from the deposit formed in the reactor was more aromatic than the feed to the H-Oil unit, indicating dehydrogenation under relatively severe conditions (440°C). From the analyses of the deposits obtained from the vacuum distillation tower, it was concluded that asphaltenes deposition is the major contributor to vacuum tower fouling in the H-Oil process.<sup>137</sup>

Incompatibility is believed to be the major cause of fouling during crude oil refining and hydrotreating when using a fixed-bed reactor.<sup>138,139</sup> Mixing crude oils may cause asphaltenes precipitation (incompatibility), which results in rapid fouling of the preheat exchanger and coking furnace tubes. Wiehe<sup>138</sup> has developed a compatibility model based on solubility parameters of crude oils. This model demonstrates that not only is the ratio of the blend important for obtaining a compatible mixture, but also the correct order of mixing crude oils will determine if the mixture is compatible. The incompatibility of oils has also been shown to result in the plugging of hydrotreaters. In Wiehe's study<sup>139</sup>, the foulant accumulated in the top few inches of the bed and consisted of carbonaceous material with little inorganic matter (ash). In order to apply the oil compatibility model to oils that contain no asphaltenes, Wiehe developed new tests and was able to diagnose and resolve the plugging problem.

Polymerization and retrograde reactions lead to coke formation during thermal treatment of heavy oils and bitumen. Tests have been developed to diagnose the initial stage of the problem and prevent fouling. Depending on the thermal process used, there are different tests available to determine and control the sediment formed. The Shell hot filtration test is a common test used in hydrocracking to determine the stability of the operating process without possible shutdown. The amount of solids (n-heptane insoluble) formed is measured at intervals, and should not exceed a certain percentage (0.15-0.5 wt%) so that the stability of the operation can be maintained.

In visbreaking, which is a relatively mild thermal cracking process, the amount of asphaltenes in the visbroken residue (+350°C) increases and the ability of the medium to disperse asphaltenes decreases. The flocculation ratio of different concentrations of the resid is first determined using various concentrations of a binary solvent (n-heptane and xylene). A plot of the flocculation ratio versus the dilution ratio is then constructed. Extrapolation of the flocculation ratio to zero on the X-axis produces a value that is called the P-value (peptization value). This value must be higher than 1.1 (P-value of the tar 350°C+ > 1.1). The stability of visbroken products from Athabasca bitumen obtained at different severities was reported recently by Rahimi et al.<sup>130</sup> During thermal reaction, the asphaltene aromatic cores, which were stabilized by aliphatic side chains and the presence of resins, were exposed by the cracking off of the side chains and by the conversion of resins. Thus, as the severity of the thermal process increased, the asphaltenes became increasingly less soluble (increased insolubility number). Thermal reactions also produce light hydrocarbons by breaking off the side chains from aromatic rings. This can result in a decrease in the solvency of the media (decreased solubility blending number). However, for the very aromatic Athabasca bitumen the solubility blending number remained nearly constant with increasing severity, showing that the light aromatic and light saturated products compensated for each other. Therefore, partially thermally cracked feedstocks are not only unstable because of the presence of olefins and diolefins, but also because the solubility of asphaltenes has significantly been reduced. The addition of hydroaromatic compounds (H-donors) significantly improves the quality and the stability of the visbroken tars.<sup>140</sup>

The stability of the reaction products in reactors can significantly be improved by controlling the resin:asphaltene ratio. Benham and Pruden<sup>90</sup> demonstrated in the CANMET Hydrocracking Process® that controlling the ratio of polar aromatics to asphaltene is the key to achieving a better unit operability and to obtaining higher pitch conversion and lower coke yield. By recycling the heavy gas oil fraction that is rich in polar aromatics, asphaltene could be kept in peptized form leading to high pitch conversion with low coke yield.

## 8. REFERENCES

1. Speight, J.G. *The Chemistry and Technology of Petroleum*, 3rd ed., Dekker: New York, 1998; 215 pp.
2. Wiehe, I.A. Tutorial on Resid Conversion and Coking, Proc. 2<sup>nd</sup> Intl. Conf. on refinery processing, AIChE 1999 Spring National Meeting, Houston, TX, March 14-18, 499-505.
3. ASTM. 1995. *Annual Book of Standards*. American Society for Testing and Materials: Philadelphia, PA; Method D-2007.
4. Clarke, P.; Pruden, B. Asphaltene precipitation from Cold Lake and Athabasca bitumen, *Pet. Sci. Technol.*, **1998**, 16(3&4), 287-305.

5. Liu, C.; Zhu, C.; Jin, L.; Shen, R.; Liang, W. Step by step modeling for thermal reactivities and chemical compositions of vacuum residues and their SFEF asphalt, *Fuel Process. Technol.*, **1999**, *59*, 51-67.
6. Boduszynski, M.M. Composition of heavy petroleum. 1. Molecular weight, hydrogen deficiency, and heteroatom concentration as a function of atmospheric equivalent boiling point up to 100°F (760°C), *Energy Fuels* **1987**, *1*, 2-11.
7. Boduszynski, M.M. Composition of heavy petroleum. 2. Molecular characterization, *Energy Fuels* **1988**, *2*, 597-613.
8. Altgelt, K.H.; Boduszynski, M.M. Composition of heavy petroleum. 3. An improved boiling point-molecular weight relation, *Energy Fuels* **1992**, *6*, 68-77.
9. Boduszynski, M. M.; Altgelt, K.H. Composition of heavy petroleum. 4. Significance of the extended atmospheric equivalent boiling point (AEBP) scale, *Energy Fuels* **1992**, *6*, 72-76.
10. Wiehe, I.A. The pendant-core building block of petroleum residua, *Energy Fuels* **1994**, *8*, 536-544.
11. Chung, K. H.; Xu, C.; Hu, Y.; Wang, R. Supercritical fluid extraction reveals resid properties, *Oil Gas J.*, **1997**, *95*, 66-69.
12. Koots, J.A.; Speight, J.G. Relation of petroleum resins to asphaltenes, *Fuel*, **1975**, *54*, 179-184.
13. Dawson, D.W.; Chornet, E.; Tiwari, P.; Heitz, M. Hydrocracking of individual components isolated from Athabasca bitumen vacuum resid, *Prep. Div. Petrol. Chem.*, American Chemical Society, Dallas national meeting, 1989, *34* (2), 384-394.
14. Walton, H.F. Ion exchange chromatography, In *Chromatography*, 5<sup>th</sup> ed., *Fundamentals and applications of chromatography and related migration methods*, E. Heftmann (Ed.), Elsevier: Amsterdam, 1996; Chapter 5, pp. A227-A265.
15. Green, J.B.; Zagula, E.J.; Reynolds, J.W.; Wandke, H.H.; Young, L.L.; Chew, H. Relating feedstocks composition to product slate and composition in catalytic cracking. 1. Bench scale experiments with liquid chromatographic fractions from Wilmington, CA, >650°F resid, *Energy Fuels* **1994**, *8*, 856-867.
16. Rahimi, P.M.; Gentzis, T.; Cottó, E. Investigation of the thermal behavior and interaction of Venezuelan heavy oil fractions obtained by ion exchange chromatography, *Energy Fuels* **1999**, *13*, 694-701.
17. Pearson, C.D.; Green, J.B. Comparison of processing characteristics of Mayan and Wilmington heavy residues. 2. Characterization of vanadium and nickel complexes in acid-base-neutral fractions, *Fuel* **1989**, *68*, 456.
18. Speight, J.G., *Fuel science and technology handbook*, Marcel Dekker: New York, 1990; Chapter 3, p.80.
19. Quann, R.J.; Ware, R.A. Catalytic hydrodemetallation of petroleum, *Adv. Chem. Eng.*, **1988**, *14*, 96-259.
20. Franceskin, P.J.; Gonzalez-Jiminez, M.G.; Darosa, F.; Adams, O.; Katan, L. "First observation of an iron porphyrin in heavy crude oil," *Hyperfine Interact.* **1986**, *28*, 825.
21. Biggs, J.C.; Brown, R.J.; Fetzer, W.R. Elemental profiles of hydrocarbon materials by size exclusion chromatography/inductive coupled plasma atomic emission spectroscopy, *Energy Fuels* **1987**, *1*, 257-262.
22. Ware, R.A.; Wei, J. "Catalytic hydrodemetallation of nickel porphyrins," *J. Catal.* **1985**, *93*, 100-121.
23. Altgelt, K.H.; Boduszynski, M.M. *Composition and Analysis of Heavy Petroleum Fractions*, Marcel Dekker: New York, NY, 1994; 495p.
24. Strausz, O.P.; Lown, E.M.; Payzant, J.D. Nature and geochemistry of sulphur-containing compounds in Alberta petroleum, In *Geochemistry of Sulphur in Fossil Fuels*, ACS Symposium series 429. W.L. Orr; C.M. White (Eds.) American Chemical Society: Washington, D.C., 1990; Chapter 22, 366-395.
25. Payzant, J.D.; Montgomery, D.S.; Strausz, O.P. Novel terpenoid sulphoxides and sulphides in petroleum, *Tetrahedron Lett.*, **1983**, *24*, 651.

26. Cyr, T.D.; Payzant, J.D.; Montgomery, D.S.; Strausz, O.P. A homologous series of novel hopane sulphides in petroleum, *Org. Geochem.*, **1986**, *9*, 139-143.
27. Sarowha, S.L.S.; Dogra, P.V.; Ramasvami, V.; Singh, I.D. Compositional and structural parameters of saturate fraction of Gujarat crude mix residue, *Erdol Kohle*, **1988**, *41*, 124-125.
28. Waldo, G.S.; Carlson, R.M.K.; Maldowan, J.M.; Peters, K.E.; Penner-Hahn, J.E. Sulphur speciation in heavy petroleum: Information from x-ray absorption near-edge structure, *Geochim. Cosmochim. Acta*, **1991**, *55*, 801-814.
29. Shaw, J.E. Molecular weight reduction of petroleum asphaltenes by reaction with methyl iodide-sodium iodide, *Fuel* **1989**, *68*, 1218-1220.
30. Whitehurst, D.D.; Isoda, T.; Mochida, I. Present state of the art and future challenges in hydrodesulphurization of polyaromatic sulphur compounds, *Adv. Catal.*, **1998**, *42*, 345-471.
31. Kabe, T.; Ishihara, A.; Qian, W. *Hydrodesulfurization and hydrodenitrogenation*. Kodansha Ltd.: Tokyo, 1999.
32. Te, M.; Fairbridge, C.; Ring, Z. Various approaches in kinetic modeling of real feedstock hydrodesulfurization, *Pet. Sci. Technol.*, **2002**, in Press
33. Kabe, T.; Ishihara, A.; Nomura, M.; Itoh, T.; Qi, P. Effects of solvents in deep desulfurization of benzothiophene and dibenzothiophene, *Chem. Lett.*, **1991**, *12*, 2233-2236.
34. Nagai, M.; Kabe, T. Selectivity of molybdenum catalyst in hydrodesulfurization, hydrodenitrogenation, and hydrodeoxygenation: Effect of additives on dibenzothiophene hydrodesulfurization, *J. Catal.*, **1983**, *81*, 440-449.
35. Whitehurst, D.D.; Mitchell, T.O.; Farcasiu, M.; Dickert, J.J. Exploratory studies in catalytic coal liquefaction, *Report on EPRI Project*, **1979**, 779-18.
36. Sucharek, A.J. How to make low sulfur, low aromatics, high cetane diesel fuel – Synsat technology, *Prep. Div. Pet. Chem.*, American Chemical Society, **1996**, *41*, 583.
37. Savage, D. W.; Kaul, B.K. Deep desulfurization of distillate fuels, U.S. Patent: 5454933, 1995.
38. Bonde, S.E.; Gore, W.; Dolbear, G.E.; Skov, E.R. Selective oxidation and extraction of sulfur-containing compounds to economically achieve ultra-low proposed diesel fuel sulfur requirements, *Prep. Div. Pet. Chem.*, American Chemical Society, 219<sup>th</sup> National Meeting, San Francisco, CA, March 26-31, 2000; 364-366.
39. Collins, F.M.; Lucy, A.R.; Sharp, C. Oxidative desulphurization of oils via hydrogen peroxide and heteropolyanion catalysts, *J. Mol. Catal. A: Chemical*, **1997**, *117*, 397-403.
40. Dolbear, G.E.; Skov, E.R. Selective oxidation as a route to petroleum desulfurization, *Prep. Div. Pet. Chem.*, American Chemical Society, 219<sup>th</sup> National Meeting, San Francisco, CA, March 26-31, 2000; 375-378.
41. Zannikos, F.; Lois, E.; Stournas, S. Desulfurization of petroleum fractions by oxidation and solvent extraction, *Fuel Process. Technol.*, **1995**, *42*, 35045.
42. Ho, T.C. "Hydrodenitrogenation catalysis," *Catal. Rev.-Sci. Eng.*, **1988**, *30 (1)*, 117-160.
43. Mushrush, G.W.; Speight, J.G. Petroleum products: Instability and Incompatibility, *Applied Energy Technology Series*, Taylor & Francis, 1995, 183,pp.
44. Holmes, S.A., Nitrogen functional groups in Utah tar sand bitumen and product oils, *AOSTRA J. Res.*, **1986**, *2*, 167-175.
45. McKay, J.F.; Weber, J.H.; Latham, D.R. Characterization of nitrogen bases in high-boiling petroleum distillates, *Anal. Chem.*, **1976**, *48*, 891-898.
46. Satterfield, C.N.; Cocchetto, J.F. Pyridine hydrodenitrogenation: An equilibrium limitation on the formation of pyridine intermediate, *AIChE J.*, **1975**, *21(6)*, 1107-1111.
47. Seifert, W.K.; Teeter, R.M. Identification of polycyclic aromatic and heterocyclic crude oil carboxylic acids, *Anal. Chem.*, **1970**, *42*, 750-758.
48. Qian, K.; Robbins, W.K.; Hughey, C.A.; Cooper, H.J.; Rodgers, R.P.; Marshall, A.G. Resolution and identification of elemental compositions for more than 3000 crude acids in

- heavy petroleum by negative-ion microelectrospray high-field fourier transformed ion cyclotron resonance mass spectrometry, *Energy Fuels* **2001**, *15*, 1505-1511.
49. Panchal, C.B. Fouling induced by dissolved metals, *Proc. Intl Conf. on Petroleum Phase Behavior and Fouling*, AIChE Spring National Meeting, Houston, TX, March 14-18, 1999, 367-372.
  50. Motahashi, K.; Nakazono, K.; Oki, M. Storage stability of light cycle oil: studies for the root substance on insoluble sediment formation, *Proc. 5<sup>th</sup> Intl. Conf. on Stability and Handling of Liquid Fuels*, Rotterdam, The Netherlands, October 3-7, 1994, 829-844.
  51. Hasan, M.-U.; Ali, M. F. Structural characterization of Saudi Arabian extra light and light crudes by <sup>1</sup>H and <sup>13</sup>C NMR spectroscopy, *Fuel* **1989**, *68*, 801.
  52. Mojelsky, T.W.; Ignasiak, T.M.; Frakman, Z.; McIntyre, D.D.; Lown, E.M.; Montgomery, D.S.; Strausz, O.P. Structural features of Alberta oil sands bitumen and heavy oil asphaltenes, *Energy Fuels* **1992**, *6*, 83.
  53. Payzant, J.D.; Lown, E.M.; Strausz, O.P. Structural units of Athabasca asphaltenes: the aromatics with linear carbon framework, *Energy Fuels* **1991**, *5*, 445.
  54. Sheu, E.Y.; Storm, D.A.; DeTar, M.M. Asphaltenes in polar solvents, *J. Non-Cryst. Solids*, **1991**, *341*, 131-133.
  55. Sheu, E.Y.; DeTar, M.M.; Storm, D.A.; DeCanio, S.J. Aggregation and kinetics of asphaltenes in organic solvents, *Fuel* **1992**, *71*, 299-302.
  56. Storm, D.A.; Barresi, R. J.; DeCanio, S.J. Colloidal nature of vacuum residue, *Fuel* **1991**, *70*, 779-782.
  57. Speight, J.G. *Petroleum Chemistry and Refining*, Applied Technology Series, Taylor & Francis, 1998; 116.
  58. Speight, J.G. *The Chemistry and Technology of Petroleum*, 2<sup>nd</sup> ed., Marcel Dekker: New York, NY, 1991.
  59. Wiehe, I.A. Solvent-resid phase diagram for tracking resid conversion, *Ind. Eng. Chem. Res.*, **1992**, *31*, 530-536.
  60. Wiehe, I.A. A phase-separation kinetic model for coke formation, *Ind. Eng. Chem. Res.*, **1993**, *32*, 2447-2454.
  61. Ravey, J.C.; Decouret, G.; Espinat, D. Asphaltene macrostructure by small angle neutron scattering, *Fuel* **1988**, *67*, 1560-1567.
  62. Watson, B.A.; Barteau, M.A. Imaging of petroleum asphaltenes using scanning tunneling microscopy, *Ind. Eng. Chem. Res.*, **1994**, *33*, 2358-2363.
  63. Overfield, R.E.; Sheu, E.Y.; Shina, S.K.; Liang, K.S. SANS study of asphaltene aggregation, *Fuel Sci. Technol. Int.*, **1989**, *7*, 611-624.
  64. Neves, G.B.M.; dos Anjos de Sousa, M.; Travalloni-Louvisse, A.M.; Luca, E.F.; González, G. Characterization of asphaltene particles by light scattering and electrophoresis, *Pet. Sci. Technol.*, **2001**, *19 (1&2)*, 35-43
  65. Pasternack, D.S.; Clark, K.A. The components of the bitumen in Athabasca bituminous sand and their signification in the hot water separation process, *Alberta Research Council Report*, **1951**, No. 58, 1-14.
  66. Strausz, O.P.; Mojelsky, T.W.; Faraji, F.; Lown, E.M. Additional structural details on Athabasca asphaltene and their ramification, *Energy Fuels* **1999**, *13*, 207-227.
  67. Murgich, J.; Strausz, O.P. Molecular mechanics of aggregates of asphaltenes and resins of Athabasca oil, *Pet. Sci. Technol.*, **2001**, *19 (1&2)*, 231-243
  68. Strausz, O.P.; Mojelsky, T.W.; Lown, E.M. The molecular structure of asphaltenes; an unfolding story, *Fuel* **1992**, *71*, 1355-1363.
  69. Peng, P.; Morales-Izquierdo, A.; Hogg, A.; Strausz, O.P. Molecular structure of Athabasca asphaltenes; Sulfide, ether, and ester linkages, *Energy Fuels*, **1997**, *11*, 1171-1187.
  70. Strausz, O.P.; Mojelsky, T.W.; Lown, E.M.; Kowalewski, I.; Behar, F. Structural features of Boscan and Duri asphaltenes, *Energy Fuels* **1999**, *13*, 228-247.
  71. Peng, P.; Morales-Izquierdo, A.; Lown, E.M.; Strausz, O.P. Chemical structure and biomarker content of Jingshan asphaltenes and kerogens, *Energy Fuels* **1999**, *13*, 248-265.

72. Peng, P.; Fu, J.; Sheng, G.; Morales-Izquierdo, A.; Lown, E.M.; Strausz, O.P. Ruthenium-ions-catalyzed oxidation of an immature asphaltene: Structural features and biomarker distribution, *Energy Fuels* **1999**, *13*, 266-286.
73. Murgich, J.; Abanero, J.A.; Strausz, O.P. Molecular recognition in aggregates formed by asphaltene and resin molecules from the Athabasca oil sand, *Energy Fuels*, **1999**, *13*, 278-286.
74. Artok, A.; Su, Y.; Hirose, Y.; Hosokawa, M.; Murata, S.; Nomura, M. Structure and reactivity of petroleum-derived asphaltene, *Energy Fuels* **1999**, *13*, 287-296.
75. Leon, O.; Rogel, E.; Espidel, J. Structural characterization and self-association of asphaltenes of different origins, *Proc. Intl. Conf. on Petroleum Phase Behavior and Fouling*, 3<sup>rd</sup> International Symposium on Thermodynamics of Heavy Oils and Asphaltenes, AIChE Spring National Meeting, Houston, TX, March 14-18, 1999; 37-43.
76. Shirokoff, J.W.; Siddiqui, M.N.; Ali, M.F. Characterization of the structure of Saudi crude asphaltenes by X-ray diffraction, *Energy Fuels* **1997**, *11*, 561-565.
77. Yen, T.F.; Saraceno. Investigation of the nature of free radicals in petroleum asphaltenes and related substances by electron spin resonance, *J. Anal. Chem*, **1962**, *34*, 694.
78. Rao, B.M.L.; Serrano, J.E. Viscosity study of aggregation interactions in heavy oil, *Fuel Sci. Technol. Int.*, **1986**, *4*, 483-500.
79. Mehrotra, A.K. A model for the viscosity of bitumen/bitumen fractions-diluent blends, *J. Can. Pet. Technol.*, **1992**, *31(9)*, 28-32.
80. Schramm, L.L.; Kwak, J.C.T. The rheological properties of an Athabasca bitumen and some bituminous mixtures and dispersions, *J. Can. Pet. Technol.*, **1988**, *27*, 26-35.
81. Storm, D.A.; Sheu, E.Y.; DeTar, M.M.; Barresi, R.J. A comparison of the macrostructure of Ratawi asphaltenes in toluene and vacuum residue, *Energy Fuels* **1994**, *8*, 567-569.
82. Storm, D.A.; Barresi, R.J.; Sheu, E.Y. Rheological study of Ratawi vacuum residue in the 298-673 K temperature range, *Energy Fuels* **1995**, *9*, 168-176.
83. Li, S.; Liu, C.; Que, G.; Liang, W.; Zhu, Y. A study of the interactions responsible for colloidal structures in petroleum residua, *Fuel* **1997**, *14*, 1459-1463.
84. Wiehe, I. Tutorial on the phase behavior of asphaltenes and heavy oils, Third international symposium on the thermodynamics of heavy oils and asphaltenes, AIChE Spring National Meeting, Houston, TX, March 14-18, 1999, 3-8.
85. Panchal, C.B. Petroleum fouling mechanism, predictions and mitigation, AIChE short course, AIChE Spring National Meeting, Houston, TX, March 14-18, 1999.
86. Storm, D.A.; Decanio, S.J.; Edwards, J.C.; R.J. Sheu, Sediment formation during heavy oil upgrading, *Pet. Sci. Technol.*, **1997**, *15*, 77-102.
87. Storm, D.A.; Barresi, R.J.; Sheu, E.Y.; Bhattacharya, A.K.; DeRosa, T.F. Microphase behavior of asphaltic micelles during catalytic and thermal upgrading, *Energy Fuels* **1998**, *12*, 120-128.
88. Wiehe, I.A., The pendant-core building block model of petroleum residua, *Energy Fuels* **1994**, *8*, 536-544.
89. Clarke, P.F.; Pruden, B.B. Asphaltene precipitation: Detection using heat transfer analysis, and inhibition using chemical additives, *Fuel* **1997**, *76*, 607-614.
90. Benham, N.K.; Pruden, B.B., CANMET residuum hydrocracking: Advances through control of polar aromatics, *NPRA Annual Meeting*, San Antonio, TX, March 17-19, 1996, offprint.
91. Beaton, W.I.; Bertolacini, R.J., Resid hydroprocessing at Amoco, *Catal. Rev.-Sci. Eng.*, **1991**, *33*, 281-417.
92. Mansoori, G.A. A review of advances in heavy organics deposition control, Internet: <http://www.uic.edu-mansoori/hod.html>
93. Calemma, V.; Montanari, L.; Nali, M.; Anelli, M. Structural characteristics of asphaltenes and related pyrolysis kinetics, *Prep. Div. Pet. Chem.*, American Chemical Society National Meeting, Washington D.C., August 21-26, 1994; 452-455.
94. Poutsma, M.L. Free-radical thermolysis and hydrogenmolysis of model hydrocarbons relevant to processing of coal, *Energy Fuels* **1990**, *4*, 113-131.

95. Rahimi, P.M.; Dettman, H.D.; Dawson, W.H.; Nowlan, V.; Del Bianco, A.; Chornet, E. Coke formation from asphaltenes – solvent and concentration effects, CONRAD workshop on bitumen upgrading chemistry, June 7-8, 1995, Calgary, Alberta.
96. Heck, R.H.; Diguseppi, F.T. Kinetic effects in resid hydrocracking, *Energy Fuels* **1994**, *8*, 557-560.
97. Gray, M. R., *Upgrading Petroleum Residues and Heavy Oils*, Marcel Dekker: New York, NY, 1994.
98. McMillen, D.F.; Malhotra, R.; Nigenda, S.E. The case for induced bond scission during coal pyrolysis, *Fuel* **1989**, *68*, 380-386.
99. Stein, S.E.; Griffith, L.L.; Billmers, R.; Chen, R.H. Hydrogen transfer between anthracene structures, *J. Phys. Chem.*, **1986**, *90*, 517.
100. Vernon, L.W. Free radical chemistry of coal liquefaction: Role of molecular hydrogen, *Fuel* **1980**, *59*, 102.
101. Farcasiu, M.; Petrosius, S.C. Heterogeneous catalysis: Mechanism of selective cleavage of strong carbon-carbon bonds, *Prep. Div. Fuel Chem.*, American Chemical Society National Meeting, Washington D.C., August 20-25, 1994; 723-725.
102. Penn, J.H.; Wang, J. Radical cation bond cleavage pathways for naphthyl-containing model compounds, *Energy Fuels* **1994**, *8*, 421-425.
103. Miki, Y.; Yamada, S.; Oba, M.; Sugimoto, Y. Role of catalyst in hydrocracking of heavy oil, *J. Catal.* **1983**, *83*, 371-383.
104. Le Page, J.F.; Davidson, M. *IFP publication*, **1986**, *41*, 131
105. Heck, R.H.; Rankel, L.A.; DiGuseppi, F. T. Conversion of petroleum resid from Maya crude: Effects of H-donors, hydrogen pressure and catalyst, *Fuel Process. Technol.*, **1992**, *30*, 69-81.
106. Gray, M.R.; Khorasheh, F.; Wanke, S.E.; Achia, U.; Krzywicki, A.; Sanford, E.C.; Sy, O.K.Y.; Ternan, M. Rate of catalyst in hydrocracking of residue from Athabasca bitumen, *Energy Fuels* **1992**, *6*, 478-485.
107. Sanford, E.C. Mechanism of coke prevention by hydrogen during residuum hydrocracking, *Prep. Div. Pet. Chem.*, American Chemical Society, National Meeting, Denver, CO, March 28, April 2, 1993; 413-416.
108. Sanford, E.C. Influence of hydrogen and catalyst on distillate yields and the removal of heteroatoms, aromatics, and CCR during cracking of Athabasca bitumen residuum over a wide range of conversions, *Energy Fuels* **1994**, *8*, 1276-1288.
109. Srinivasan, N.S.; McKnight, C.A. Mechanism of coke formation from hydrocracked Athabasca residuum, *Fuel* **1994**, *73*, 1511-1517.
110. Nagaishi, H.; Chan, E.W.; Sanford, E.C.; Gray, M.R. Kinetics of high-conversion hydrocracking of bitumen, *Energy Fuels* **1997**, *11*, 402-410.
111. Speight, J.G. Thermal cracking of Athabasca bitumen, Athabasca asphaltenes, and Athabasca deasphalted heavy oil, *Fuel* **1970**, *49*, 134-145.
112. Rahimi, P.; Dettman, H.; Gentzis, T.; Chung, K.; Nowlan, V. Upgrading chemistry of Athabasca bitumen fractions derived by super critical fluid extraction, Presented at the 47<sup>th</sup> CSCHE conference, Edmonton, Alberta, Canada, October 5-8, 1997.
113. Rahimi, P.M.; Parker, R.J.; Hawkins, R.; Gentzis, T.; Tsapraillis, H. Processability of partially deasphalted Athabasca bitumen, *Prep. Div. Pet. Chem.*, American Chemical Society, National Meeting, San Diego, CA., April 1-5, 2001, 74-77.
114. Yasar, M.; Trauth, D.M.; Klein, M.T. Asphaltene and resid pyrolysis 2: The effect of reaction environment on pathways and selectivities, *Prep. Div. Fuel Chem.*, American Chemical Society, National Meeting, Washington, D.C., August 23-28, 1992; 1878-1885.
115. Karacan, O.; Kok, M.V. Pyrolysis analysis of crude oils and their fractions, *Energy Fuels* **1997**, *11*, 385-391.
116. Dawson, W.H.; Chornet, E.; Tiwari, P.; Heitz, M. Hydrocracking of individual components isolated from Athabasca bitumen vacuum resid, *Prep. Div. of Pet. Chem.*, American Chemical Society, National Meeting, Dallas, TX, April 9-14, 1989; *34*, 384-394.

117. Rahimi, P.; Dettman, H.; Nowlan, V.; DelBianco, A. Molecular transformation during heavy oil upgrading, *Prep. Div. Pet. Chem.*, American Chemical Society, National Meeting, San Francisco, CA, April 13-17, 1997; 23-26.
118. Liu, C.; Zhu, C.; Jin, L.; Shen, R.; Liang, W. Step by step modeling for thermal reactivities and chemical compositions of vacuum residues and their SFEF asphalts, *Fuel Process. Technol.*, **1999**, *59*, 51-67.
119. Rahimi, P.; Gentzis T.; A Delbianco, Application of Hot-Stage Microscopy in the Investigation of the Thermal Chemistry of Heavy Oils and Bitumen – an Overview, Symp. on Kinetics Mechanism of Petroleum Processing, 222<sup>nd</sup> ACS National Meeting, Chicago, Illinois, USA, August 26-30, 2001.
120. Wiehe, I.A. A phase separation kinetic model for coke formations, *Ind. Eng. Chem. Res.*, **1993**, *32*, 2447.
121. Rahimi, P.; Gentzis, T.; Cotté E. Investigation of the thermal behavior and interaction of Venezuelan heavy oil fractions obtained by ion-exchange chromatography, *Energy Fuels*, **1999**, *13*, 694.
122. Speight, J.G. *The Chemistry and Technology of Petroleum*, 3<sup>rd</sup> Ed., Marcel Dekker: New York, 1999.
123. Rahimi, P.; Gentzis, T.; Taylor, E.; Carson, D.; Nowlan, V.; Cotté, E. The impact of cut point on the processability of Athabasca bitumen, *Fuel*, 2001, forthcoming.
124. Rahimi, P.; Gentzis, T.; Fairbridge, C. Interaction of clay additives with mesophase formed during thermal treatment of solid-free Athabasca bitumen fraction, *Energy Fuels*, **1999**, *13*, 817.
125. Kubo, J.; Higashi, H.; Ohmoto, Y.; Aroa, H. Heavy oil hydroprocessing with the addition of hydrogen-donating hydrocarbons derived from petroleum, *Energy Fuels*, **1996**, *10*, 474.
126. Rahimi, P.; Gentzis, T.; Kubo, J.; Fairbridge, C.; Khulbe, C. Coking propensity of Athabasca bitumen vacuum bottoms in the presence of H-donors – formation and dissolution of mesophase from a hydrotreated petroleum stream (H-donor), *Fuel Proc. Technol.*, **1999**, *60*, 157.
127. Rahimi, P.; Gentzis, T.; Ciofani, T. Coking characteristics of partially deasphalted oils, Proc. AIChE Spring Nat. Mtg., Session 71 – Advances in Coking, Atlanta, GA, 428, 2000.
128. Wiehe, I.A.; Kennedy, R.I. The oil compatibility model and crude oil incompatibility, *Energy Fuels*, **2000**, *14*, 56.
129. Vilhunen, J.; Quignard, A.; Pilvi, O.; Waldvogel, J. Experience in use of automatic heavy fuel oil stability analyzer”, *Proc. 7<sup>th</sup> Intl. Conf. of Stability and Handling of Liquid Fuels*, October 13-17, 1997, Vancouver, B.C.; 985-987.
130. Rahimi, P.M.; Parker, R.J.; Wiehe, I.A. Stability of visbroken products obtained from Athabasca bitumen for pipeline transportation, Symp. on Heavy Oil Resid Compatibility and Stability, 221<sup>st</sup> ACS National Meeting, San Diego, CA, USA, April 1-5, 2001.
131. Gaestel, C.; Smadja, R.; Lamminan, K.A. Contribution a la Connaissance des proprietes des bitumen routiers. *Rev. Gen. Routes Aerodromes*, **1971**, *85*, 466.
132. Asomaning, S.A.; Watkinson, A.P. Petroleum stability and heteroatoms species effects on fouling heat exchangers by asphaltenes. *Heat Transfer Eng.*, **2000**, *12*, 10-16.
133. Schabron, J.F.; Pauli, A.T.; Rovani Jr., J.F.; Miknis, F.P. Predicting coke formation tendencies,” *Fuel*, **2001**, *80*, 1435-1446.
134. Van den Berg, F. Developments in fuel oil blending, Proc. 7<sup>th</sup> Intl. Conf. on Stability and Handling Fuels, September 22-26, 2000, Graz, Austria; 165-172.
135. Pauli, A.T. Asphalt compatibility testing using the automated Heithaus titration test, *Prep. Div. Fuel Chem.*, American Chemical Society, **1996**, *41*, 1276-1281.
136. Speight, J.G. *Petroleum Chemistry and Refining*, Taylor & Francis, 1998.
137. Bannayan, M. A.; Lemke, H.K.; Stephenson, W. K. Fouling mechanism and effect of process conditions on deposit formation in H-Oil equipment, Catalysis in petroleum refining and petrochemical industries, 1995. *Proc. 2<sup>nd</sup> Intl. Conf. on Catalysts in Petroleum Refining and Petrochemicals Industries*, Kuwait, April 22-26, 1995, Absi-Halabi et al. Editors, Elsevier Science publisher. 1996; 273-281.



138. Wiehe, I. A. "Prevention of fouling by incompatible crudes with the oil compatibility model," *Proc. Intl. Conf. Petroleum Phase Behavior and Fouling*, AIChE Spring National Meeting, Houston, TX, March 14-18, 1999; 354-358.
139. Wiehe, I. A. "Mitigation of the plugging of hydrotreater with the oil compatibility model," *Proc. Intl. Conf. Petroleum Phase Behavior and Fouling*, AIChE Spring National Meeting, Houston, TX, March 14-18, 1999; 405-411.
140. DelBianco, A.; Garuti, G.; Pirovano, C.; Russo, R. "Thermal cracking of petroleum residues. 3. Technical and economical aspects of hydrogen donor visbreaking," *Fuel*, **1995**, *74*, 756-760.

## Chapter 20

# MECHANISTIC KINETIC MODELING OF HEAVY PARAFFIN HYDROCRACKING

Michael T. Klein\* and Gang Hou

*Department of Chemical Engineering, University of Delaware, Newark, DE 19716*

*\*Present Address: Department of Chemical and Biochemical Engineering*

*School of Engineering, Rutgers University, Piscataway, NJ 08854*

### 1. INTRODUCTION

Catalytic hydrocracking is a flexible process for the conversion of heavy, hydrogen-deficient oils into lighter and more-valuable products. Part of its flexibility is its ability to handle a wide range of feeds, from heavy aromatics to paraffinic crudes and cycle stocks. The ability to extend this flexibility to “customized” product slates depends on the ability to control and manipulate the process chemistry, which is, in turn, enhanced by a rigorous representation of the process chemistry. This motivates the present interest in a heavy paraffin hydrocracking kinetics model.

Traditional hydrocarbon conversion process models have implemented lumped kinetics schemes, where the molecules are aggregated into lumps defined by global properties, such as boiling point or solubility. Molecular information is obscured due to the multi-component nature of each lump. However, increasing environmental concerns and the desire for better control and manipulation of the process chemistry have focused attention on the molecular composition of both the feedstocks and their refined products. Modeling approaches that account for the molecular fundamentals underlying reaction of complex feeds and the subsequent prediction of molecular properties require an unprecedented level of molecular detail.

This is because modern analytical measurements indicate the existence of the order of  $10^5$  ( $O(10^5)$ ) unique molecules in petroleum feedstocks. In modeling terms, each species corresponds to one differential equation in a deterministic modeling approach. Therefore not only the solution but also the formulation of the implied model is formidable. This motivated the

development of computer algorithms not only to solve but also to formulate the model.

These algorithms have now been organized into a system of kinetic modeling tools – the *Kinetic Modeler's Toolbox (KMT)* - that build and solve the kinetic models on the computer automatically.<sup>1</sup> Monte Carlo techniques are used to model the structure and composition of complex feeds. Graph theory techniques are then utilized to generate the reaction network.<sup>2-4</sup> Reaction family concepts and Quantitative Structure-Reactivity Correlations (QSRC) are used to organize and estimate rate constants. The computer-generated reaction network, with associated rate expressions, is then converted to a set of differential equations, which can be solved within an optimization framework to determine the rate parameters in the model. This automated modeling process enables the modeler to focus on the fundamental chemistry and speed up the model development significantly.

This chapter describes the application of these tools to the development of a mechanistic kinetic model for the catalytic hydrocracking of heavy paraffins. The basic approach and overview synopsis are presented first. This is followed by a detailed description of the steps involved in model formulation, optimization, and use.

## 2. APPROACH AND OVERVIEW

Molecular-level modeling can be at either the pathways or the mechanistic level. Pathways-level models include only observable molecules, whereas mechanistic models include reactive intermediates (e.g., carbenium ions) as well. Compared with pathways-level modeling, mechanistic modeling involves a large number of species, reactions, and associated rate constants in the governing network because of the explicit accounting of all reaction intermediates. This can render mechanistic modeling very tedious. However, mechanistic models comprise more fundamental rate constant information and thus can be better extrapolated to various operating conditions and feeds.

This paper thus describes the construction of various mechanistic models for paraffins ranging from C<sub>16</sub> to C<sub>80</sub>. All the models incorporate mechanistic acidic chemistry and pathways-level metal chemistry for the prototypical bifunctional hydrocracking catalyst, which has both a metal function for hydrogenation/dehydrogenation and an acid function for isomerization and cracking.

Much of the complexity of these models is better considered bookkeeping than fundamental. That is, there are only roughly 10 different types of reactions or “reaction operators” underlying the process chemistry, which can comprise thousands of literal reactions because of the statistical or combinatorial explosion of matching these reaction operators with all of the feed and product molecules susceptible to each. A related simplification is

that the large demand for rate parameters can be handled by organizing the reactions involving similar transition states into one reaction family, the kinetics of which are constrained to follow a Quantitative Structure-Reactivity Correlation (QSRC) or Linear Free Energy Relationship (LFER).

The present modeling approach exploited these notions. The molecules in the paraffin hydrocracking reaction mixture were thus grouped into a few species types (paraffins, olefins, ions, and inhibitors such as  $\text{NH}_3$ ), which, in turn, reacted through a limited number of reaction families on the metal (dehydrogenation and hydrogenation) and the acid sites (protonation, hydride-shift, methyl-shift, protonated cyclopropane (PCP) isomerization,  $\beta$ -scission, and deprotonation). As a result, a small number of formal reaction operations could be used to generate hundreds of reactions.

Figure 1 shows the mechanistic reactions for paraffin hydrocracking via the dual site (both metal site and acid site) mechanism. Each reaction family had a single associated reaction matrix, which was used to generate all possible mechanistic reactions.<sup>2</sup> The reaction matrices are summarized in Table 1.

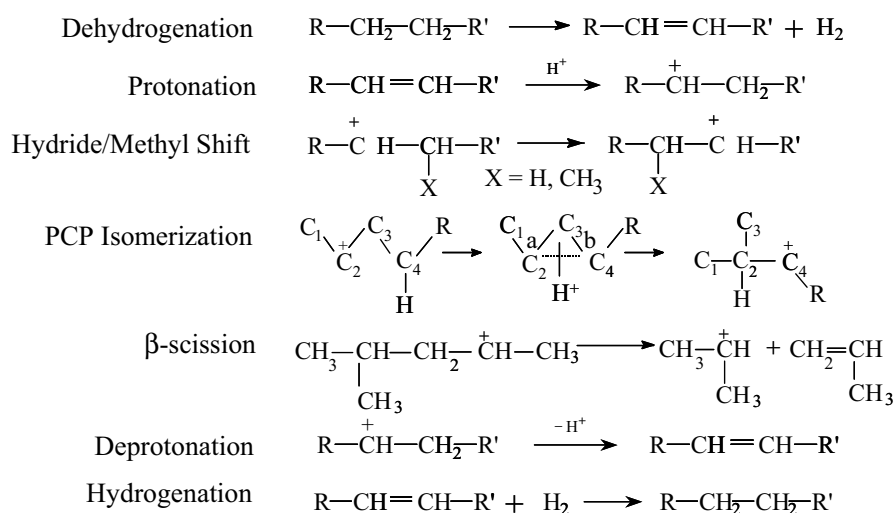


Figure 1. Paraffin Hydrocracking Reaction Families at the Mechanistic Level

The rate constant information was organized with a QSRC/LFER for each reaction family, as shown in Eq. 1.

$$E^* = E_0^* + \alpha \Delta H_{rxn} \quad (1)$$

Eq. 1 is called the Polanyi relationship, which relates the activation energy of each reaction to its heat of reaction. A single frequency factor was used for

each reaction family. The use of QSRC/LFER for heterogeneous mechanistic models has been demonstrated by Korre<sup>5</sup> and Russell<sup>6</sup> for hydrocracking, Watson et al.<sup>7,8</sup> and Dumesic et al.<sup>9</sup> for catalytic cracking, and Mochida and Yoneda<sup>10-12</sup> for dealkylation and isomerization.

Table 1. Reaction Matrices for Paraffin Hydrocracking Reactions at the Mechanistic Level.

| Reaction Family   | Reactant Matrix   |
|---|---|
| Dehydrogenation<br>Test: The string C - C is required   | $\begin{array}{c} \text{C} \\ \text{C} \\ \text{H} \\ \text{H} \end{array} \left  \begin{array}{cccc} 0 & 1 & -1 & 0 \\ 1 & 0 & 0 & -1 \\ -1 & 0 & 0 & 1 \\ 0 & -1 & 1 & 0 \end{array} \right $   |
| Hydrogenation<br>Test: The string C = C is required   | $\begin{array}{c} \text{C} \\ \text{C} \\ \text{H} \\ \text{H} \end{array} \left  \begin{array}{cccc} 0 & 1 & -1 & 0 \\ 1 & 0 & 0 & -1 \\ -1 & 0 & 0 & 1 \\ 0 & -1 & 1 & 0 \end{array} \right $   |
| Protonation<br>Test: The string C = C is required.  | $\begin{array}{c} \text{C} \\ \text{C} \\ \text{H}^+ \end{array} \left  \begin{array}{ccc} 0 & -1 & 1 \\ -1 & 0 & 0 \\ 1 & 0 & 0 \end{array} \right $   |
| Deprotonation<br>Test: The string C+ - C is required.   | $\begin{array}{c} \text{C}^+ \\ \text{C} \\ \text{H} \end{array} \left  \begin{array}{ccc} 0 & 0 & 1 \\ 0 & 0 & -1 \\ 1 & -1 & 0 \end{array} \right $   |
| Hydride Shift and Methyl Shift<br>Test: The string C+ - C - X is required in the carbenium ion (X = H or C) | $\begin{array}{c} \text{C}^+ \\ \text{C} \\ \text{X} \end{array} \left  \begin{array}{ccc} 0 & 0 & 1 \\ 0 & 0 & -1 \\ 1 & -1 & 0 \end{array} \right $   |
| PCP Isomerization<br>Test: The string C+ - C - C is required in the carbenium ion                           | $\begin{array}{c} \text{C}^+ \\ \text{C} \\ \text{C} \\ \text{H} \end{array} \left  \begin{array}{cccc} 0 & 0 & 1 & 0 \\ 0 & 0 & -1 & 1 \\ 1 & -1 & 0 & -1 \\ 0 & 1 & -1 & 0 \end{array} \right $ |
| $\beta$ -Scission<br>Test: The string C+ - C - C is required in the carbenium ion                           | $\begin{array}{c} \text{C}^+ \\ \text{C} \\ \text{C} \end{array} \left  \begin{array}{ccc} 0 & 1 & 0 \\ 1 & 0 & -1 \\ 0 & -1 & 0 \end{array} \right $   |

The remainder of this paper describes the division of the paraffin hydrocracking reactions into mechanistic families with a unique reaction matrix operator for each reaction family. The reaction rules and QSRCs used are then discussed for each reaction family. The technical specifications and the iteration process to find the optimum subset of the mechanistic model will also be discussed.

### 3. MODEL DEVELOPMENT

This section first discusses the reaction mechanism for paraffin hydrocracking and the thus-derived modeling specifications for each reaction family. This is followed by a discussion of the automated model building algorithm and the QSRC/LFERs used to organize the rate parameters. Finally, the thus-developed C<sub>16</sub> paraffin mechanistic hydrocracking model diagnostics are presented.

#### 3.1 Reaction Mechanism

The mechanism of paraffin hydrocracking over bifunctional catalysts is, essentially, the carbenium ion chemistry of acid cracking coupled with metal-centered dehydrogenation/hydrogenation reactions. The presence of excess hydrogen and the hydrogenation component of the catalyst result in hydrogenated products and inhibition of some of the secondary reactions and coke formation.

These mechanistic features were elucidated in detail in the 1960s. Based on the pioneering work of Mills et al.<sup>13</sup> and Weisz<sup>14</sup>, a carbenium ion mechanism was proposed, similar to catalytic cracking plus additional hydrogenation and skeletal isomerization. More recent studies of paraffin hydrocracking over noble metal-loaded, zeolite based catalysts have concluded that the reaction mechanism is similar to that proposed earlier for amorphous, bifunctional hydrocracking catalysts.<sup>15-17</sup>

As shown in Figure 1, the elementary steps used to model the mechanism of paraffin hydrocracking over a bifunctional catalyst are as follows:

1. Dehydrogenation of paraffins to olefins on metal sites,
2. Protonation of olefins to carbenium ions on acid sites,
3. Carbenium ion hydride shift on acid sites,
4. Carbenium ion methyl shift on acid sites,
5. Protonated cyclopropane (PCP) intermediate mediated branching of carbenium ion on acid sites,
6. Carbenium ion cracking through  $\beta$ -scission on acid sites,
7. Deprotonation of carbenium ions to olefins on acid sites, and
8. Hydrogenation of olefins to paraffins on metal sites.

The KMT model building algorithm contained a reaction matrix for each of the foregoing reaction steps. The model species were also classified into paraffins, olefins, carbenium ions and H<sup>+</sup> ion categories. Algorithms were deployed to identify the degree of branching of each species (1, 2, 3, and more) and the type of carbenium ions (primary, secondary, and tertiary).

The model building process was guided by a set of user-supplied reaction rules that pruned the model from the essentially infinite set of feasible reactions to the kinetically significant subset. These rules enjoy two ultimate

foundations: kinetics and analytical chemistry. Kinetics was used to “rule out” feasible but kinetically insignificant reactions, such as reactions leading to the formation of primary carbenium ions. A set of organizational rules was deployed to maintain a reasonable correspondence between the level of detail in the model and in available analytical measurements. The specifics for each reaction family are described in turn.

## 3.2 Reaction Families

### 3.2.1 Dehydrogenation/Hydrogenation

In a typical hydrocracking process, the dominant reactions on the metal sites of the catalyst are mainly dehydrogenation and hydrogenation. Very little hydrogenolysis occurs. The metal component of the catalyst dehydrogenates the paraffin reactants to produce reactive olefin intermediates, hydrogenates the olefins, and also prevents catalyst deactivation by hydrogenating coke precursors.

The mechanism of the dehydrogenation reaction involves stripping of two hydrogen atoms by the metal component of the catalyst. The molecular topology test for the dehydrogenation reaction is a search for a C - C string in the molecule.

Figure 2 shows the number of olefins as a function of the carbon number. It can be seen that the number of possible olefins increase almost exponentially with the carbon number, and even one paraffin can form thousands of olefins. Thus the inclusion of all possible olefins and their reactions would generate an enormously large model. Thus, in order to develop a reasonably sized mechanistic model, certain rules were used for this reaction, as summarized in Table 2. All n-paraffins were allowed to undergo dehydrogenation reactions at all sites, whereas all iso-paraffins were allowed to undergo dehydrogenations only at the C - C bonds  $\beta$  to the branch. This rule was based on the relative rate of reactions of these olefins on the acid site.

### 3.2.2 Protonation/Deprotonation

Protonation transforms an olefin into a carbenium ion. This reaction is much faster than other acid site reactions, and is close to equilibrium under commercial operating conditions. The protonation reaction involves attack of  $H^+$  at a C=C bond. Only three atoms change connectivities during this reaction, as shown in the reaction matrix of Table 1.

Mechanistic insights from the literature were used to synthesize the tests and rules. The deprotonation reaction, which converts carbenium ions to olefins, involves breakage of a C-H bond to give  $H^+$  and an olefin. The deprotonation test required a connected C<sup>+</sup> and C atom. The rules are

summarized in Table 2. Primary carbenium ions were not allowed to form from protonation due to their thermochemistry.

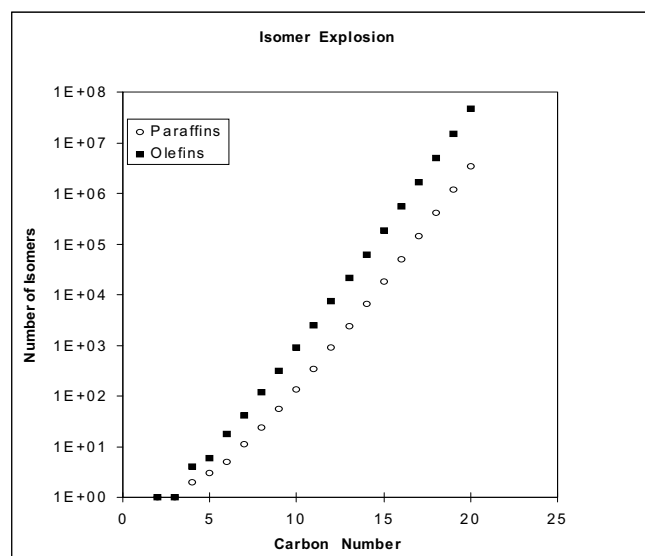


Figure 2. Number of Paraffins and Olefins as a Function of Carbon Number

Table 2. Reaction Rules for Mechanistic Paraffin hydrocracking Reaction Families

| Reaction Family                 | Reactant Rules   |
|---------------------------------|--|
| Dehydrogenation / Hydrogenation | Dehydrogenation is allowed everywhere on n-paraffins but only $\beta$ to branch on iso-paraffins. Formation of di-olefins is not allowed.  |
| Protonation / Deprotonation     | Primary carbenium ions are not allowed to form.  |
| Hydride Shift and Methyl Shift  | Primary carbenium ions are not allowed to form. Only migration to stable or branched ions is allowed. Number of reactions allowed is a function of branch number.  |
| PCP Isomerization               | Primary and methyl carbenium ions are not allowed to form. PCP-isomerization increases either the number of branches or the length of the side chains. PCP-isomerization to form vicinal branches is not allowed. Only methyl and ethyl branches are allowed; A maximum of three branches is allowed. Number of reactions allowed is a function of branch and carbon number. |
| $\beta$ -Scission               | Methyl and primary carbenium ions are not allowed to form.   |



### 3.2.3 Hydride and Methyl Shift

Hydride and methyl shifts are responsible for changes in the position of carbenium ions. The net effect is generally to create a stable ion, e.g., tertiary ion, from a less stable ion, e.g. secondary ion. The methyl shift can also change the location of a branch position, which creates isomers.

The rate of hydride shift is considered to be much faster than alkyl shift due to the ease of moving  $H^+$  as compared to the alkyl group. The hydride shift reaction test required a  $C^+ - C - H$  string in the molecule; that for the methyl shift reaction required a  $C^+ - C - (CH_3)$  string.

The rules are summarized in Table 2. The reactions were allowed for all ions. The number of reactions allowed was constrained as a function of number of branches on the ions. This provided the proper spectrum of isomers and also kept the number of species and reactions manageable and in alignment with available analytical chemistry.

### 3.2.4 PCP Isomerization

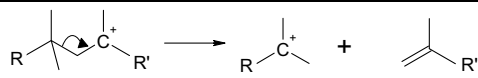
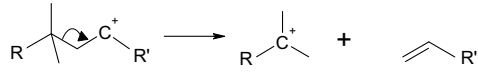
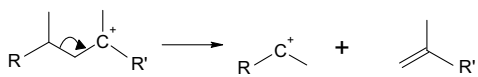
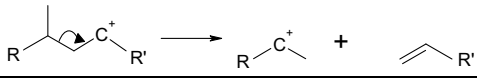
The branching isomerization reaction shown in Figure 1 is postulated to proceed via a protonated cyclopropane (PCP) intermediate with the charge delocalized over the ring.<sup>18</sup> The test for this reaction required a  $C^+ - C - C$  string in the molecule. The rate of this reaction is slower than that of hydride/methyl shift. This reaction was further categorized into two types, isomA and isomB, depending on the identity of the bond to be broken in the three-membered ring intermediate.

The rules for this reaction had a dramatic effect on the size of the generated model. The final set of rules used for the model building is summarized in Table 2. As was the case for the hydride shift/methyl shift, the isomerization reaction was allowed for all paraffins and iso-paraffins and the number of reactions was constrained as a function of the number of carbons and branches on the ions to provide the proper spectrum of isomers and an alignment with analytical chemistry.

### 3.2.5 $\beta$ -Scission

The  $\beta$ -scission reaction is one of the key carbon number reducing reactions for iso-paraffins. The rate of this reaction is dependent on the acidity of the catalyst.  $\beta$ -scission can lead to the formation of tertiary and secondary carbenium ions, but no primary ions were allowed to form. Several  $\beta$ -scission mechanisms have been suggested for the cracking of branched secondary and tertiary carbenium ions, as summarized in Table 3.<sup>19</sup>

Table 3.  $\beta$ -scission mechanisms for carbenium ion conversion over bifunctional hydrocracking catalyst

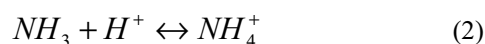
| Type | Min C# | Ions Involved           | Rearrangement  |
|------|--------|-------------------------|--|
| A    | 8      | Tert $\rightarrow$ Tert |  |
| B1   | 7      | Sec $\rightarrow$ Tert  |  |
| B2   | 7      | Tert $\rightarrow$ Sec  |  |
| C    | 6      | Sec $\rightarrow$ Sec   |  |

Type A  $\beta$ -scissions convert a tertiary carbenium ion to another tertiary carbenium ion. This is the fastest and the most likely to occur. The reaction rates decrease in the order of A, B1, B2 and C. Each type of reaction requires a minimum number of carbon atoms in the molecule and a certain of branching in order to occur. The proposed  $\beta$ -scission mechanisms suggest that paraffins may undergo several isomerizations until a configuration is attained that is favorable to  $\beta$ -scission.

The test for this reaction requires a C<sup>+</sup> - C - C string. The rules are summarized in Table 2. Unstable species, such as methyl and primary carbenium ions, were not allowed to form from this reaction.

### 3.2.6 Inhibition Reaction

Nitrogen inhibition effects were accounted for via the dynamic reduction of acid sites by the protonation and deprotonation of the Lewis base on the acid sites. For example, the following ammonia inhibition reaction was included in the reaction network.



This inhibitor protonation/deprotonation will compete with hydrocarbon protonation/deprotonation and thus reduce the available number of acid sites for hydrocarbons. This is expressed in the site balance of Eq. 3, which depicts the conservation of the total ion concentration.

$$H_0^+ = H^+ + \sum_{i=1}^N R^+ + NH_4^+ \quad (3)$$

### 3.3 Automated Model Building

The reaction matrices of Table 1, the reaction rules of Table 2, the QSRC/LFER correlations of Eq. 1, and the automated model-building algorithm of Figure 3 were used to construct various kinetic model versions for mixtures containing molecules from  $C_8$  to  $C_{24}$ .

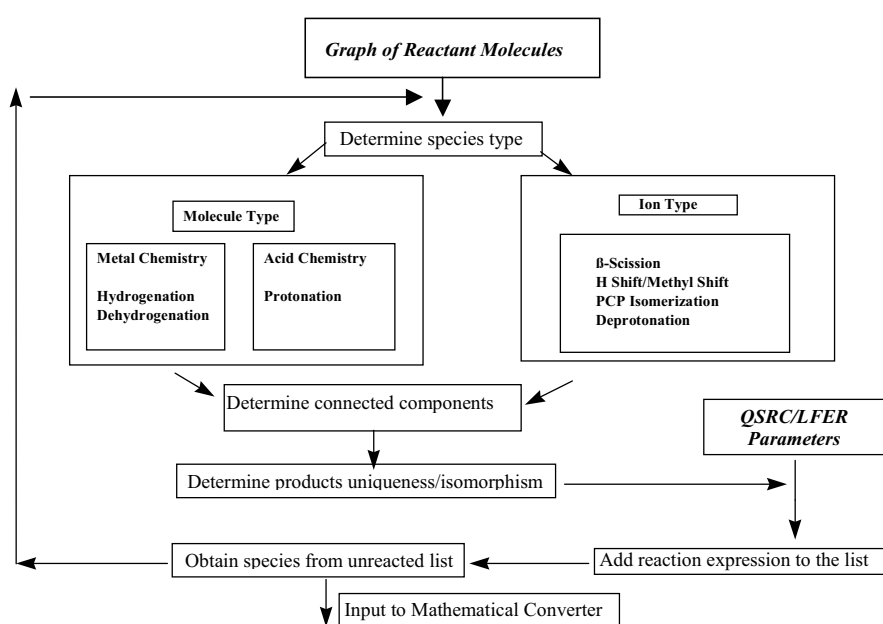


Figure 3. Algorithm for Automated Paraffin Hydrocracking Mechanistic Modeling

Figure 4 depicts a representative result that is presented here to show the types of output that can be obtained. This illustrates the mechanistic level sequences for a large paraffin molecule undergoing various reactions, including dehydrogenation, protonation, H/Me-shift, various isomerizations, the formation of the configuration to carry out the  $\beta$ -scission into a smaller ion and olefin, and then finally deprotonation and hydrogenation to smaller paraffin molecules. It shows that the reactions leading to the formation and subsequent cracking of a tertiary carbenium ion are preferred in the complete reaction network. These insights accrued from building relatively small models guided the extension of model building process to the heavier paraffin hydrocracking model up to as high as  $C_{80}$ , as discussed in detail below.

The model building algorithm shown in Figure 3 classified the molecular graphs of the reactants into the families of molecules and ions. The molecules were further filtered to undergo specific metal and acid chemistries. For example, paraffins were only allowed to undergo dehydrogenation reactions on the metal sites, whereas olefins were allowed to hydrogenate on the metal

site and protonate on the acid sites. The rate parameters derived from the QSRC/LFER for each fundamental reaction family are considered fundamental because of the elementary step nature of the model.

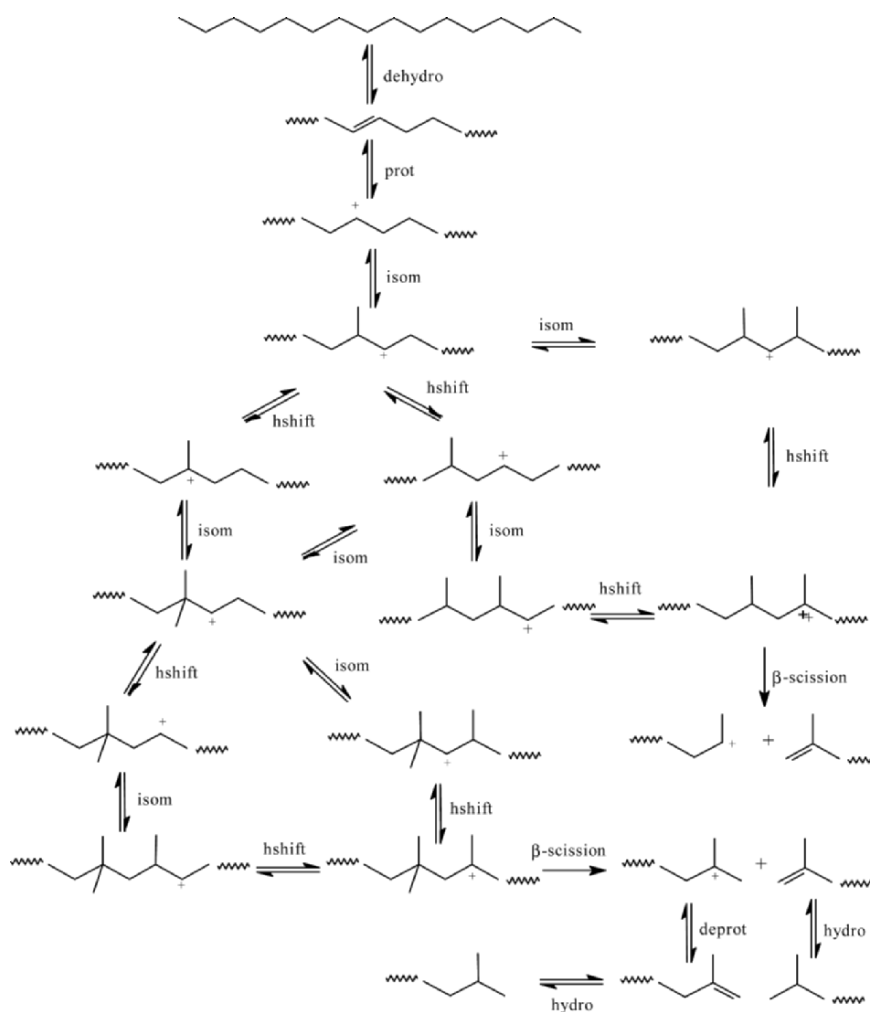


Figure 4. Representative Reaction Network of Paraffin Hydrocracking at the Mechanistic Level

The mechanistic paraffin hydrocracking model builder has a database of all reaction matrices and rules for all mechanistic paraffin hydrocracking reactions, involving both metal and acid chemistries, with the flexibility of changing them. A detailed library of paraffins, olefins, and ion intermediates consisting of their connectivity and thermodynamic information was built

using the MOPAC computational chemistry package. The reactor balances equations were generated for a plug flow reactor (PFR) with molar expansion.

### 3.4 Kinetics: Quantitative Structure Reactivity Correlations

The rate constants within each reaction family were described in terms of a reaction family-specific Arrhenius  $A$  factor and the Polanyi relationship parameters that related the activation energy to the enthalpy change of reaction, as shown in Eq. 1.

The Polanyi relationship and the Arrhenius expression can be combined to represent the rate constant,  $k_{ij}$ , where  $i$  denotes the reaction family and  $j$  denotes the specific reaction in the family, and is shown in Eq. 4:

$$k_{ij} = A_i \exp(-(E_{o,i} + \alpha_i * \Delta H_{rxn,j}) / RT) \quad (4)$$

The acidity of the catalyst was captured by a single parameter  $\Delta H_{stabilization}$ , signifying the relative stabilization of the  $H^+$  ion as compared to other carbenium ions. Since the reactions on the acid site are rate controlling, this was a useful way to capture the catalyst property (acidity) in the rate constant formalism, as shown in Eq. 5.

$$k_{ij} = A_i \exp(-(E_{o,i} + \alpha_i * (\Delta H_{rxn,j} - \Delta H_{stabilization})) / RT) \quad (5)$$

In short, each reaction family could be described with a maximum of three parameters ( $A$ ,  $E_o$ ,  $\alpha$ ). Procurement of a rate constant from these parameters required only an estimate of the enthalpy change of reaction for each elementary step. In principle, this enthalpy change of reaction amounted to the simple calculation of the difference between the heats of formation of the products and reactants. However, since many model species, particularly the ionic intermediates and olefins, were without experimental values, a computational chemistry package, MOPAC,<sup>20</sup> was used to estimate the heat of formations “on the fly”. The organization of the rate constants into quantitative structure-reactivity correlations (QSRC) reduced the number of model parameters greatly from  $O(10^3)$  to  $O(10)$ .

### 3.5 The $C_{16}$ Paraffin Hydrocracking Model Diagnostics

A  $C_{16}$  hydrocracking model with 465 species and 1503 reactions was built automatically in only 14 CPU seconds on a Pentium Pro 200 PC. The corresponding plug flow reactor (PFR) model with molar expansion was then

generated automatically and solved in 76 CPU seconds in once-through mode. Table 4 summarizes the characteristics of the C<sub>16</sub> model.

The species distribution in Table 4 shows there were more intermediate olefins and ions than paraffins. The reaction distribution in Table 4 shows that each reactant molecule went through various rearrangements to form the right configuration before the  $\beta$ -scission. In this model, all type A, B1, and B2  $\beta$ -scission reactions were allowed; type C reaction was ignored in the final model after the optimization with experimental results showed the C-type cracking to be insignificant. Hydride shift, methyl shift, and isomerization reactions were restricted for hydrocarbons having more than eight carbon atoms. All *n*-paraffins, and selected iso-paraffins were used to represent the portion of the feedstock larger than C<sub>9</sub>. This not only helped to keep the model size reasonable, but also resulted in the inclusion of components with different reactivities in the feedstock where detailed characterization was not available.

Table 4. Characteristics of the C<sub>16</sub> Paraffin Hydrocracking Model

| Species                 | #   | Reactions                 | #    |
|-------------------------|-----|---------------------------|------|
| Molecule                |     | Dehydrogenation           | 233  |
| Hydrogen                | 1   | Hydrogenation             | 233  |
| Paraffins               | 64  | Deprotonation             | 328  |
| Olefins                 | 233 | Protonation               | 328  |
| Ion                     |     | Hydride and Methyl Shift  | 168  |
| H-ion                   | 1   | PCP Isomerization         | 174  |
| Carbenium Ions          | 165 | $\beta$ -Scission         | 37   |
| Inhibitor               | 1   | Inhibition                | 2    |
| Total Number of Species | 465 | Total Number of Reactions | 1503 |

#### 4. MODEL RESULTS AND VALIDATION

The C<sub>16</sub> models were tuned with pilot plant data on a commercial Pt-Zeolite catalyst using the optimization program GREG<sup>21</sup> coupled with an equation solver. The objective function was the square of the difference between predicted and experimental yields weighted by the experimental standard deviation, as shown in Eq. 6,

$$F = \sum_{i=1}^M \sum_{j=1}^N \left( \frac{y_{ij}^{\text{model}} - y_{ij}^{\text{exp}}}{\sigma_j} \right)^2 \quad (6)$$

where *i* is the experiment number and *j* is the species or lump number, and  $\sigma_j$  is the experimental measurement deviation.

The A factors for the acid chemistry were obtained from the literature<sup>7,8</sup> and held constant during optimization. The A factors for reactions on the metal sites were constrained to fall between  $1 \leq A_j \leq 20$ . The Polanyi  $\alpha$ 's in the QSRC formalism were held at 0.5, based on guidelines from literature.<sup>7-9</sup>

Further, the  $E_0$ 's were constrained by the relation between activation energies and heat of reaction shown in Eq. 7.

$$E_{backward} - E_{forward} = \Delta H_{rxn} \quad (7a)$$

$$E_{oj,forward} = E_{oj,backward} \quad (7b)$$

$$\alpha_{j,forward} = 1 - \alpha_{j,backward} \quad (7c)$$

In summary, only the  $E_0$ 's, and one catalyst stabilization parameter were optimized by matching with the experimental data.

The model was optimized with the lumped data from experiments (the unconverted  $C_{16}$ , the mono-branched and multi-branched  $C_{16}$ , and all the cracked products). Then the model was used to predict the carbon number distribution and iso-to-normal ratio for the various carbon numbers. Figures 5a and 5b show the parity plots for the  $C_{16}$  paraffin hydrocracking for both (a) the lumped observations and (b) the carbon number distribution at various conditions (T, P, LHSV and  $NH_3$ ). The agreement between the predicted and experimental data sets for all the high and low yield compounds is good, as all predictions are within the experimental error. The good prediction validates the fundamental nature of the model.

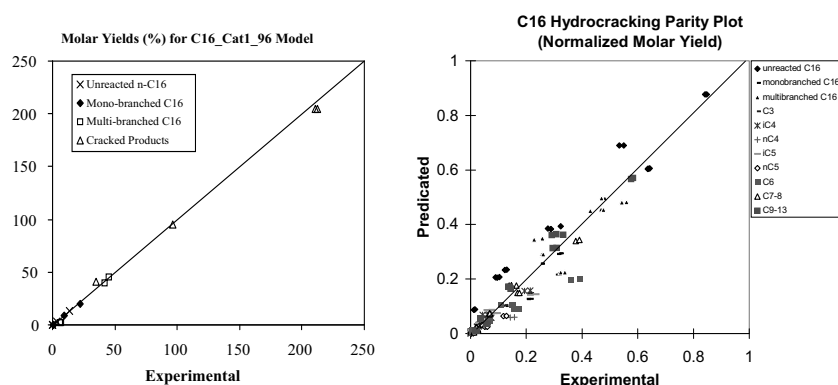


Figure 5. Parity Plots for  $C_{16}$  Paraffin Hydrocracking Model at Various Operation Conditions (T, P, LHSV, and Inhibition)

Various insights were obtained from the optimization results. For this set of paraffin hydrocracking experiments on a commercial bifunctional Pt-Zeolite catalyst, the results showed that the reaction rates ranked as: A-type Cracking > H/Methyl Shift > PCP Isomerization > B1-type Cracking > B2-type Cracking >> C-type Cracking. Thus the cracking products actually evolve from A-type cracking of tri-branched ions or B-type cracking of di-branched ions. Wherever several reaction pathways are possible, the one leading to the formation and subsequent cracking of a tertiary carbenium ion

is preferred. Furthermore, the cracking of smaller paraffins via  $\beta$ -scission is less likely to occur, which explains their high yields even at high conversions. Also, from the product molecular structure point of view, PCP isomerization always leads to branching, A-type cracking always leads to branched isomers, and B-type cracking always leads to normal or branched isomers.

Practically no methane and ethane formation were observed from the experiments. This confirmed our modeling rule that no primary ions were allowed because of their instability compared to more-stable secondary and tertiary ions. This modeling rule basically eliminated the formation of methane and ethane via the carbenium ion mechanism in the reaction network. This also partially explains why the long chain paraffins tend to crack in or near the center.

The mechanistic notion that secondary carbenium ions are isomerized to more stable tertiary ions prior to cracking, as well as the high rate of H-shift to the tertiary carbenium ion, explains the high iso-to-normal ratio for paraffins in the product. The iso-to-normal ratio in the product paraffins increases with decreasing reaction temperature because at higher temperatures the cracking rate of isoparaffins increases faster than that of the n-paraffins.

The ammonia inhibition reduces not only the cracking activity but also the iso-to-normal ratio in the product paraffins because of its partial neutralization of the acid sites on the hydrocracking catalyst.

The tuning results indicated that the rate-determining reactions (isomerization and  $\beta$ -scission) occurred at the acid sites, whereas the metal sites served only the rapid hydrogenation and dehydrogenation function. This confirmed that the hydrocracking process studied was "ideal".

## 5. EXTENSION TO C<sub>80</sub> MODEL

Various model building and control strategies were exploited to construct a high carbon number model based on the leanings from the C<sub>16</sub> model. These strategies are described elsewhere.<sup>1</sup> In short, by restricting the isomorphic criteria to the carbon and branch number level in the generalized isomorphism algorithm, molecules with the same carbon number and branch number were lumped into a representative molecular structure. This allowed construction of a molecule-based paraffin hydrocracking model at the pathways level for a feedstock up to C<sub>80</sub>.

Figure 6 summarizes the essence of this model at the carbon and branch number level. The complexity is reduced to several PCP isomerizations (normal, 1, 2, 3 branch) and cracking (type A and type B) reactions. This captures all the key observations from the paraffin hydrocracking reaction mechanism: paraffins go through isomerizations before cracking; PCP isomerization always leads to branching, A-type cracking always leads to branched isomers, and B-type cracking always leads to normal or branched



isomers; all the cracking products actually come from A-type cracking of tri-branched isomers or B-type cracking of di-branched isomers, and the C-type cracking can be neglected.

The thus-deduced  $C_{80}$  paraffin hydrocracking model containing 306 species and 4671 reactions was automatically generated on the computer. This model can thus be further tuned to capture the carbon number distribution and iso-to-normal ratio in the paraffin hydrocracking process.

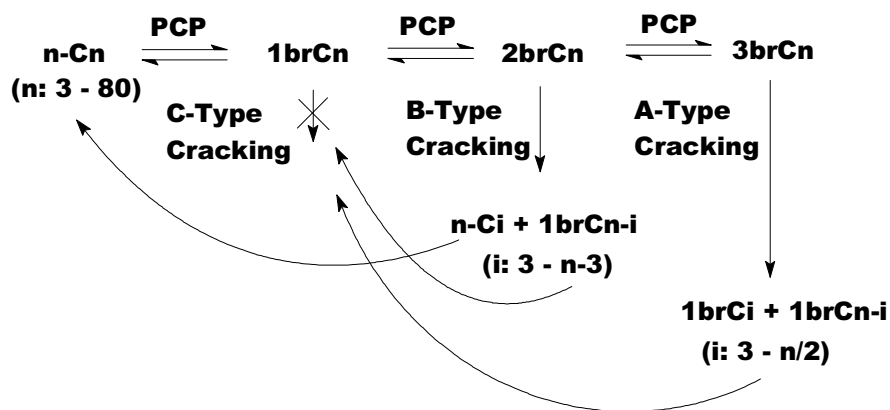


Figure 6. Mechanism Deduced Reaction Pathways at the Carbon Number and Branch Paraffin Hydrocracking Reaction Number Level

## 6. SUMMARY AND CONCLUSIONS

Graph theoretic concepts were used to construct a paraffin hydrocracking mechanistic model builder incorporating bi-functional catalysis with metal and acid functions. The complete automated approach was successfully demonstrated for a  $C_{16}$  paraffin hydrocracking model with 465 species and 1503 reactions at the mechanistic level.

The reaction family concept was exploited by representing the reactions by various reaction families incorporating the metal function (dehydrogenation/hydrogenation) and the acid function (protonation/deprotonation, H/Me-shift, PCP isomerizations, and  $\beta$ -scission). The optimized  $C_{16}$  model provided excellent parity between the predicted and experimental yields for a wide range of operating conditions. This shows that the fundamental nature (feedstock and catalyst acidity independent) of the rate parameters in the model.

Various insights were obtained from the optimization results of the detailed  $C_{16}$  model: the skeletal isomerizations precede the cracking reactions; PCP isomerization led to branching, A-type cracking led to branched isomers, and B-type cracking led to normal or branched isomers; all the cracking

products normally come from A-type cracking of tri-branched isomers or B-type cracking of di-branched isomers.

The generalized isomorphism algorithm was applied at the carbon and branch number level to reduce the complexity and explosion of modeling heavy paraffin hydrocracking. A thus-deduced C<sub>80</sub> paraffin hydrocracking model with 306 species and 4671 reactions at the pathways level was developed from the teachings of the C<sub>16</sub> model.

## 7. REFERENCES

1. Hou, G., Integrated Chemical Engineering Tools for the Building, Solution, and Delivery of Detailed Kinetic Models and Their Industrial Applications, Ph.D. Dissertation, University of Delaware, 2001.
2. Broadbelt, L. J.; Stark, S.M.; Klein, M. T., Computer Generated Pyrolysis Modeling: On-the-Fly Generation of Species, Reactions and Rates, *Ind. Eng. Chem. Res.*, **1994**, *33*, 790-799.
3. Broadbelt, L. J.; Stark, S. M.; Klein, M. T., Computer Generated Reaction Networks: On-the-fly Calculation of Species Properties using Computational Quantum Chemistry, *Chem. Eng. Sci.*, **1994**, *49*, 4991-5101.
4. Broadbelt, L. J.; Stark, S. M.; Klein, M. T., Computer Generated Reaction Modeling: Decomposition and Encoding Algorithms for Determining Species Uniqueness, *Comput. Chem. Eng.*, **1996**, *20*, 2, 113-129.
5. Korre, S. C., Quantitative Structure/Reactivity Correlations as a Reaction Engineering Tool: Applications to Hydrocracking of Polynuclear Aromatics, Ph.D. Dissertation, University of Delaware, 1994.
6. Russell, C.L., Molecular Modeling of the Catalytic Hydrocracking of Complex Mixtures: Reactions of Alkyl Aromatic and Alkyl Polynuclear Aromatic Hydrocarbons, Ph.D. Dissertation, University of Delaware, 1996.
7. Watson, B. A.; Klein, M. T.; Harding, R. H., Mechanistic Modeling of n-Heptane Cracking on HZSM-5", *Ind. Eng. Chem. Res.*, **1996**, *35*(5), 1506-1516.
8. Watson, B. A.; Klein, M. T.; Harding, R. H., Catalytic Cracking of Alkylcyclohexanes: Modeling the Reaction Pathways and Mechanisms, *Int. J. Chem. Kinet.*, **1997**, *29*(7), 545.
9. Dumescic, J. A.; Rudd, D. F.; Aparicio, L. M.; Rekoske, J. E.; Trevino, A. A. *The Microkinetics of Heterogeneous Catalysis*, American Chemical Society, Washington D.C. (1993).
10. Mochida, I.; Yoneda, Y., Linear Free Energy Relationships in Heterogeneous Catalysis I. Dealkylation of Alkylbenzenes on Cracking Catalysts, *J. Catal.*, **1967**, *7*, 386-392.
11. Mochida, I.; Yoneda, Y., Linear Free Energy Relationships in Heterogeneous Catalysis II. Dealkylation and Isomerization Reactions on various Solid Acid Catalysts, *J. Catal.*, **1967**, *7*, 393-396.
12. Mochida, I.; Yoneda, Y., Linear Free Energy Relationships in Heterogeneous Catalysis III. Temperature Effects in Dealkylation of Alkylbenzenes on the Cracking Catalysts, *J. Catal.*, **1967**, *7*, 223-230.
13. Mills, G. A.; Heinemann, H.; Milliken, T. H.; Oblad, A. G., *Ind. Eng. Chem.*, **1953**, *45*, 134.
14. Weisz, D.B., *Adv. Catal.*, **1962**, *13*, 137.
15. Langlois, G.E.; Sullivan R.F., *Adv. Chem. Ser. 97*, ACS, Washington, D.C., 1970; p.38.
16. Weitkamp, J., *Hydrocracking and Hydrotreating*, ACS Symp. Series 20, Ward, J.W.; Qader, S.A. (Eds), Washington, D.C., 1975; p. 1.
17. Steinberg, K.H.; Becker, K.; Nestler, K.H., *Acta Phys. Chem.*, **1985**, *31*, 441.
18. Brouwer, D. M.; Hogeveen, H., *Prog. Phys. Org. Chem.*, **1972**, *9*, 179.

19. Martens, J.A.; Jacobs, P.A.; Weitecamp, J., *Appl. Catal.*, **1986**, *20*, 239.
20. Stewart, J. J. P., Semiempirical Molecular Orbital Methods in *Rev. Comput. Chem.*, Lipkowitz, K. B.; Boyd, D D. B. (Eds.), VCH Publishers: New York, 1989.
21. Stewart, W. E.; Caracotsios, M.; Sorensen, J. P., Parameter Estimation From Multiresponse Data, *AIChE J.*, **1992**, *38(5)*, 641-650.

## Chapter 21

# MODELING OF REACTION KINETICS FOR PETROLEUM FRACTIONS

Teh C. Ho  
*Corporate Strategic Research Labs.*  
*ExxonMobil Research and Engineering Co.*  
*Annandale, NJ 08801*

### 1. INTRODUCTION

The petroleum industry will face a confluence of new challenges in the decades to come, owing to such factors as (1) rapid changes in market demand for high-performance products, (2) mounting public concerns over emissions and toxicity, and (3) dwindling supply of high-quality crudes. As a result, refiners will have to constantly stretch the limits of existing processes with minimum capital outlays. To this end, a low-cost approach is to develop predictive and robust process models that can take full advantage of modern advances in analytical chemistry, computing, control, and optimization.

Two distinguishing features of petroleum refining are that the number of reacting species is astronomically large and that the feedstock properties are continually changing. Refiners have long wanted to have at their disposal process models that can predict the effects of feedstock/catalyst properties and reactor configuration/conditions. But the daunting complexities of the composition and reactivity of petroleum fractions are such that until recently process models have largely been empirical, requiring constant and costly updating.

It is hardly surprising that model developers have been compelled to drastically simplify model development along two lines. One is what may be called *partition-based lumping*, while the other *total lumping*. In the former case, the reaction mixture is represented by a finite number of lumps and the reactions among them are tracked. The lumped system aims to capture essential features of the real system so that it has sufficient predictive power and robustness over ever-changing feeds and catalysts. In the latter case, the

approach was motivated by the fact that in many situations what really matters is the aggregate, not the individual behavior of the reacting species. For instance, in hydrodesulfurization (HDS) one cares only about the reduction of total sulfur, not of the individual organosulfur species. Basically, all that is needed is to add up all sulfur species into a single total lump whose behavior is the focus of attention.

The purpose of this chapter was to provide a broad-brush survey of available theoretical tools for the two types of kinetic lumping problems. The emphasis will be on the general concept. As such, literature citations are merely illustrative rather than comprehensive. And there are very few examples of applying these tools; the reader should consult the original references for details. Throughout the chapter, scalars are denoted by italic letters, vectors by lower case boldface letters and matrices by capital boldface letters.

## 2. OVERVIEW

### 2.1 Partition-Based Lumping

It is easier to think of petroleum fractions in such top-down terms as specific gravity, average molecular weight, boiling range, solubility, polarity, adsorptivity, and basicity, rather than, say, distinct individual gasoline molecules. The traditional PONA analysis lumps tens of thousands of molecules into just four lumps: paraffins, olefins, naphthenes, and aromatics. As a result, up until the '80s, modeling of petroleum reaction kinetics has largely focused on selecting a small number of easily measurable lumps based on gross properties and developing reaction networks in terms of the preselected lumps. There are many examples of such partition-based lumping approaches for various refining processes.<sup>1-3</sup> For a given process, there can be many lumped models, depending on the objectives and the desired level of detail. For instance, the number of lumps for fluid catalytic cracking (FCC) has been as small as three<sup>1</sup> and as large as 34.<sup>4</sup>

There is a limit to what can be gained by using the foregoing top-down approach in light of the growing need to develop high-resolution models for managing refinery streams at the molecular level. In response to this, many have pioneered multiscale approaches from the bottom up through modeling of the interactions of enormous numbers of, say, elementary reactions. The view is that it is the collective microscopic interactions at the bottom that give rise to the macroscopic kinetic behavior observed at the reactor level. One thus splits the reaction mixture at the molecular level, examines individual reactions, and works all the way up to the global level. Along the way one performs lumping at the local level to keep the number of rate constants and

adjustable parameters at bay, because it is prohibitively costly or near impossible to track individual molecules with today's analytical techniques and computing power. Local lumping is achieved by using many time-honored reaction network reduction techniques and quantitative structure-reactivity relationships (QSRR). Final global lumping is done to predict product quality and properties from molecular composition. In contrast to the top-down route, here lumping is done after significant splitting.

## 2.2 Total Lumping

Total lumping may be viewed as a limiting case of the partitioned-based lumping. Here one is primarily interested in the overall behavior of a petroleum fraction. For instance, refiners would very much like to be able to predict how the overall behavior (e.g., HDS level) changes as feeds vary. Process developers want to know how different reactor types affect the overall behavior. And it is important for catalyst developers to rank exploratory catalysts based on their activities for the overall conversion of the feed. Consider first-order reactions. The concentration of the total lump at time  $t$  is  $C(t) = \sum_i c_{if} \exp(-k_i t)$  where  $c_{if}$  is the feed concentration of the  $i$ th reactant and  $k_i$  the corresponding rate constant. The task is to find an overall kinetics  $dC/dt = R(C)$ , a one-lump model, that can be used for reactor modeling. It is highly desirable to be able to determine  $R(C)$  and  $C$  *a priori* from information on how  $c_{if}$  and  $k_i$  are distributed in the feed. The inverse problem is to infer feed microscopic properties from experimentally determined  $R(C)$  through fitting the  $C$  vs.  $t$  data. Given the vast number of species involved, a mathematically expedient approach has been to treat the mixture as a continuum. In practice, the chemical-analytical characterization data for petroleum fractions are often measured as a continuous function of, say, boiling point, molecular weight, or carbon number.

## 2.3 Reaction Network/Mechanism Reduction

The term kinetic lumping implies some kind of simplification and consolidation of reaction networks. This is essential to both the top-down and bottom-up approaches. To do so, kineticists have long used intuitive approaches based on such concepts as (1) rate-limiting step, (2) quasi-steady state approximation (QSA), (3) quasi-equilibrium approximation (QEA), (4) relative abundance of catalyst-containing species, (5) long-chain approximation, (6) on-plus constitutive equation, and (7) reaction shortsightedness. Helfferich<sup>5</sup> gives comprehensive recipes for these approaches. In the following we dwell on only two of these concepts.

Consider the first-order, two-dimensional reaction system  $A \leftrightarrow B \rightarrow C$ . Let  $k_1$ ,  $k_2$ , and  $k_3$  be the rate constants for the  $A$ -to- $B$ ,  $B$ -to- $A$ , and  $B$ -to- $C$  reactions, respectively. In the QSA,  $k_2 \sim k_3 \gg k_1$ , the ultra reactive  $B$  is maintained at a quasi steady state after the initial transient, so the system becomes one dimensional in that it is essentially governed by the disappearance of  $A$ . In the QEA,  $k_1 \sim k_2 \gg k_3$ , hence  $A$  and  $B$  quickly reach equilibrium after startup. The resulting one-dimensional reduced model simply states that the system is dictated by the slow depletion of the equilibrium pool of  $(A + B)$  due to a “small leak” resulting from  $k_3$ .

Essentially, each of the above systems has two widely different time scales. If the initial transient is not of interest, the systems can be projected onto a one-dimensional subspace. The subspace is invariant in that no matter where one starts, after a fast transient, all trajectories get attracted to the subspace in which  $A$  and  $B$  are algebraically related to each other. In essence, what one achieves is *dimension reduction* of the reactant space through time scale separation. For large, complex systems such as oil refining, it is difficult to use the foregoing ad hoc approaches to reduce system dimensionality manually. Computer codes are available for mechanism reduction by means of the QSA/QEA<sup>6-8</sup> and sensitivity analysis.<sup>9</sup>

## 2.4 Mathematical Approaches to Dimension Reduction

The development of mathematical techniques for kinetic lumping is important in its own right. The reason is that even after significant simplification and reduction, the size of the problem may still be impractically large. Constructing lower dimensional models while retaining salient features of the original system can provide both fundamental insights and computationally feasible means for reactor design (especially hydrodynamically complex ones), control, and optimization. For instance, a widely used FCC 10-lump model<sup>10</sup> can be further reduced to a five-lump model through mathematical means such as projective transformation<sup>11</sup>, sensitivity analysis<sup>12</sup>, and cluster analysis.<sup>13,14</sup>

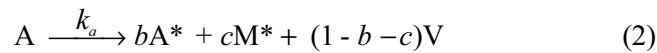
Research on mathematical lumping has focused on constructing kinetic lumps and determining the conditions under which the lumped system can at least approximate the underlying unlumped system. In so doing, one often needs to impose some constraints. Take catalytic reforming as an example. Kinetically and analytically, it makes sense to lump iso and normal paraffins together, but these hydrocarbons have so different octane numbers that they should be separated.

### 3. PARTITION BASED LUMPING

#### 3.1 Top-down Approach

This traditional approach starts with a number of preselected, measurable kinetic lumps and determines the best reaction network and kinetics through experimental design and parameter estimation. The number of lumps depends on the level of detail desired. The lumps, satisfying the conservation law and stoichiometric constraints, are usually selected based on known chemistry, measurability and physicochemical properties (boiling range, solubility, etc.).

To give a flavor of the approach, we consider a simple lumped kinetic model for resid thermal cracking. The model needs to account for an induction time for coke formation, which is due to the phase separation of a second liquid phase formed from partially converted asphaltene cores. That is, coke forms when the solubility limit is exceeded. Wiehe<sup>15</sup> developed a simple first-order kinetic model based on solubility classes, as follows



$$A^*_{\max} = S_1(M + M^*) \quad (3)$$

$$A^*_{\text{ex}} = A^* - A^*_{\max} \quad (4)$$

and at long reaction times,



where  $a$ ,  $b$ ,  $c$ , and  $y$  are stoichiometric coefficients for maintaining carbon and hydrogen balance.  $M$  and  $A$  are maltenes (n-heptene soluble) and asphaltenes (toluene soluble/n-heptane insoluble) in the feed,  $M^*$  and  $A^*$  are the corresponding products, and  $V$  is volatiles. The solubility limit  $S_1$ , given as a fraction of total maltenes, determines the maximum cracked asphaltene concentration in the solution,  $A^*_{\max}$ . The excess asphaltene  $A^*_{\text{ex}}$  separates out as a second phase and produces coke  $C$  (toluene insoluble). With a single set of stoichiometric coefficients, the model correctly predicts the observed induction period and product slates for pyrolysis of both maltenes and whole resid.

Mosby et al.<sup>16</sup> reported a seven-lump residue hydroconversion model. Lumped models for steam cracking of naphtha and gas oils can be found in Dente and Ranzi's review.<sup>17</sup> The literature abounds with FCC kinetic models, with the number of lumps being three<sup>1</sup>, four<sup>18-20</sup>, five<sup>21-25</sup>, six<sup>26</sup>, eight<sup>21</sup>, ten<sup>10</sup>,



11<sup>27</sup>, 17<sup>28</sup>, and 34<sup>4</sup>. The 17- and 34-lump models incorporate a fair amount of cracking chemistry. Figure 1 shows the 10-lump model developed by Weekman et al.<sup>10</sup>, which has been incorporated in an FCC process simulator called CATCRACKER<sup>29</sup>. Dewachtere, et al.<sup>30</sup> combined the 10-lump model with a fluid dynamics model to simulate the feed injection zone in an FCC riser. They found that the feed nozzle with an included angle of 45° produces the most uniform temperature profile at the riser bottom.

Catalytic reforming models developed by Kmak<sup>31</sup> and Ramage et al.<sup>32,33</sup> give a fairly detailed description of the process. In Powell's hydrocracking model<sup>34</sup>, the chemical composition parameters are continuous functions of carbon numbers. Quann and Krambeck<sup>35</sup> developed a kinetic model for olefin oligomerization over the ZSM-5 catalyst.

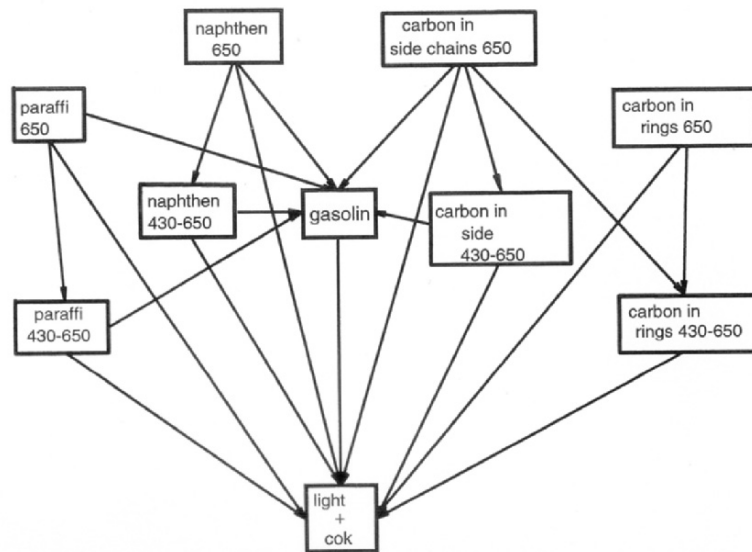


Figure 1. FCC 10-lump Model

The lumped kinetic models developed via the top-down route have limited extrapolative power. The rate “constants” generally depend on feedstock, catalyst, and reactor hardware configuration. As such, the models must be continually retuned for new situations. Moreover, the lack of sufficient molecular information makes it difficult to predict subtle changes in product qualities and properties. The bottom-up approach attempts to rectify this state of affairs, as discussed next.

### 3.2 Bottom-up Approach

Here one deals with individual molecules. The resultant reaction network describes the process chemistry in molecular detail. Broadly speaking, the approach has the following key elements.

(1). *Bookkeeping of Molecules*. Hydrocarbon molecules in petroleum fractions, while huge in number, have only a small number of compound classes (e.g., aromatics, paraffins, etc.) or structural moieties. Their transformation, involving breaking and forming bonds, can be conveniently tracked by matrix operations with a computer.<sup>36-39</sup>

(2). *Splitting and Preprocessing*. The splitting of the mixture can be so fine that individual reactions are formulated in terms of elementary steps or of the single events of which an elementary step consist. These may include surface species such as carbocations in acid-catalyzed reactions. The rate constants are obtained from a variety of sources, such as analogies with liquid- and gas-phase reactions, transition state theory, semiempirical rules, quantum chemical calculations, empirical correlations, existing data bank, etc. Senken<sup>40</sup> reviewed conventional and quantum chemical methods for estimating thermochemical and reaction rate coefficients. Following the splitting is preprocessing of the huge number of individual reactions. This involves simplifying the networks of elementary reactions or single events with such tools as rate-controlling step, QEA, QSA, sensitivity analysis, thermodynamic constraints, etc. The dimension of the thus-reduced networks can still be hopelessly large, necessitating further reduction and parameterizations as discussed next.

(3). *Lumping based on Reaction Families*. That hydrocarbons in petroleum mixtures belong to a limited set of compound classes suggests that they give rise to a finite number of reaction families. For instance, reaction families in hydrocracking include hydrogenation, ring opening, dealkylation, HDS, hydrodenitrogenation (HDN), isomerization, and cracking. The reactions in any given family may be lumped in such a way that a small number of kinetic parameters can define the behavior of the entire family. To achieve this, one usually invokes QSRR, of which linear free energy relationships (LFER) are a prime example. QSRR can be developed from group contribution methods, reaction shortsightedness principle, empirical correlations, etc. The resulting reduced model, compatible with current analytical techniques, retains only the essential chemistry of the process and has a manageable number of parameters to be determined experimentally with judiciously chosen model compounds.

Below we briefly describe two specific bottom-up approaches.

### 3.2.1 Mechanistic Modeling

The models developed here account for unmeasurable intermediates such as adsorbed ions or free radicals. Microkinetic analysis, pioneered by Dumesic and coworkers<sup>41</sup>, is an example of this approach. It quantifies catalytic reactions in terms of the kinetics of elementary surface reactions. This is done by estimating the gas-phase rate constants from transition state theory and adjusting these constants for surface reactions. For instance, isobutane cracking over zeolite Y-based FCC catalysts has 21 reversible steps defined by 60 kinetic parameters.<sup>42,43</sup> The rate constants are estimated from transition state theory

$$k = \frac{k_B T}{h} \exp(\Delta S^\ddagger / R) \exp(-\Delta H^\ddagger / RT) \quad (6)$$

where  $k_B$  is the Boltzmann constant,  $h$  the Planck constant,  $\Delta S^\ddagger$  the standard entropy change, and  $\Delta H^\ddagger$  the enthalpy change from reactants to the transition state. The superscript double dagger denotes a property associated with the transition state. If  $k$  follows the Arrhenius law  $k = A \exp(-E_\alpha/RT)$ , then one can identify the preexponential factor  $A$  with  $\Delta S^\ddagger$  and the activation energy  $E_\alpha$  with  $\Delta H^\ddagger$ .

The entropies of all gas species are obtained from tables of thermodynamic properties. Data on gas phase basicity and proton affinities are used to estimate entropies of carbocations in the gas phase. The entropies of surface species and transition states are expressed in terms of standard entropy changes of adsorption. Some key assumptions are as follows. (1) The coverage of the Brønsted acid sites by carbocations is so low that all of the vibrational and rotational entropy is maintained during adsorption. (2) For  $C_n$  species with  $n \leq 6$ , translational entropy corresponding to 1/2 of one degree of freedom is maintained after adsorption, vs. 1/3 with  $n \geq 7$ . (3) For transition states of reactions involving gas phase and surface species, an additional degree of freedom of translational entropy is maintained upon adsorption compared to a similar surface species. (4) Hydride ion transfer reactions proceed through bulky transition states, and one degree of translational freedom of the corresponding gas phase species is maintained. These assumptions are consistent with adsorption entropy measurements made for  $\text{NH}_3$  on H-mordenite and H-ZSM-5.

An Evans-Polanyi type of correlation is used to parameterize activation energies  $E_\alpha$  based on known thermodynamic properties of gas phase hydrocarbons and carbocations. That is,  $E_\alpha = E_o + \alpha \Delta H$  where  $\Delta H$  is the reaction enthalpy and  $E_o$  and  $\alpha$  are constants for a given reaction family. The reaction families considered are: (a) olefin adsorption/desorption, (b)

carbocation isomerization involving tertiary and secondary ions, (c) oligomerization involving rearrangements between tertiary and primary carbocations, (d)  $\beta$ -scission with the occurrence of the isomerization of a secondary to tertiary carbocation and (e)  $\beta$ -scission. The protolysis reactions are not grouped into one family because each reaction involves the breaking of a different bond (C-H and C-C bonds) and has a different transition state. For hydride ion transfer, the Evans-Polanyi constants are allowed to change slightly. Ethylene production has a separate Evans-Polanyi parameter.

A significant aspect of the microkinetic analysis is the introduction of a catalyst factor  $\Delta H_+$ , the heat of stabilization of a carbocation relative to that of a proton in the zeolite framework. The value of  $\Delta H_+$ , assumed to be constant for all carbocations, is related to the Brønsted acid strength: the lower the value, the stronger the acid site. It may also be defined as the enthalpy of a carbocation transition state relative to the enthalpy of stabilization of a surface proton. The resulting kinetic model reproduces data obtained from a wide range of cracking conditions. The key parameter that changes when modeling calcined USY and steamed USY is  $\Delta H_+$ . It explains why catalysts with lower Brønsted acid strength have a lower coverage of surface carbocations.

The mechanistic modeling approach for large reaction systems (e.g. oil refining) is advanced by the single-event theory developed by Froment and coworkers.<sup>37,44-47</sup> The theory allows the rate constants to be calculated from only a limited set of elementary step rates, which in turn are combinations of more basic molecular rearrangements. The central idea is to link rate constant to molecular structure. The preexponential factor  $A$  (hence the entropy change term; only the internal rotational entropy changes are relevant here) for a given reaction family can be systematically estimated from symmetry change<sup>48,49</sup> in going from the reactant to the transition state. This is done by factoring out a structural parameter  $n_e$  from  $A$  to account for possible chirality. So the rate constant of the elementary step (Eq.1) becomes  $k = n_e \hat{k}$  where  $n_e$  is the number of single events for the elementary step and  $\hat{k}$  the single-event rate constant. A global symmetry number  $\sigma_{gl}$  is defined as  $\sigma_{gl} = \sigma / 2^{n^*}$  where  $\sigma$  is the internal rotational symmetry number and  $n^*$  the number of chiral centers. From this,  $n_e = \sigma_{gl,r} / \sigma_{gl,\neq}$  where the subscript  $r$  refers to the reactant.

As an example, Fig. 2 shows the methyl shift from 2-methyl-3-heptyl carbocation (2m3h) to 3-methyl-2-heptyl (3m2h) carbocation over a solid acid. Both the forward and reverse shift reactions involve secondary carbocations. However, two methyl groups can shift in the forward direction, while only one in the reverse direction. Therefore, different methyl shift rate constants are required to reflect this structural effect. Referring to Fig. 2, each of the 3 methyl groups in 2m3h can be superimposed on itself by a 120 degree rotation and there are no chiral carbon atoms, so  $\sigma = 3 \cdot 3 \cdot 3 = 27$  and  $\sigma_{gl,r} =$

$27/2^0 = 27$ . The transition state is assumed to have a bridging structure, with two chiral carbon atoms. Presumably, the bridging methyl group loses the degree of freedom of internal rotation, so  $\sigma_{gl,\neq} = 3 \cdot 3/2^2 = 9/4$ . Thus  $n_e = 27/(9/4) = 12$  for the forward shift. For the reverse shift,  $n_e = [(3 \cdot 3 \cdot 3)/2]/(9/4) = 6$ . The difference between the forward and reverse rate constants is due solely to the number of single events (or reaction path degeneracy<sup>48</sup>). Importantly, some major assumptions here are: (1) the structure of the transition state is known, (2)  $n_e$  for free carbocations can be used for adsorbed carbocations<sup>50</sup>, and (3) there are no energy differences between the diastereomers. Baltanes et al.<sup>44</sup> gave examples of calculating  $n_e$  for hydroisomerization.

The foregoing discussion deals with the structure effect on  $A$  (or entropy change). The structure effect on the activation energy (or reaction enthalpy change) is described by the Evans-Polanyi relation, with just two parameters ( $E_0$  and  $\alpha$ ) for each single event type, which generally are obtained from model-compound experiments.

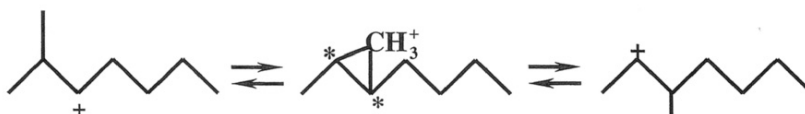


Figure 2. Methyl shift of 2-methyl-3-heptyl carbocation to 3-methyl-2-heptyl carbocation

The number of  $\hat{k}$ 's can be drastically reduced through a number of reaction "rules" for various reaction families. For instance, major reaction families in n-octane hydrocracking are protonation, deprotonation, hydride shift, methyl shift, protonated cyclopropane (PCP) branching, and  $\beta$ -scission. Examples of reaction rules are: (1) methyl and primary carbenium ions, being much less stable than secondary and tertiary ions, are neglected, (2) the protonation rate constant is independent of the olefin and depends on the carbocation type, not on its chain length, and (3) for homologous reference olefins, the deprotonation constants are equal. These rules reduce 383 single event rate constants to 22.

Armed with the reaction network, one can derive the rate equations for the feed components, intermediates and final products. The coupling between the adsorbed and gas-phase species are described by the Langmuir isotherm. Assuming that the rate-determining step is on the acid sites, one then develops the net formation rates for paraffins, olefins and diolefins, as well as those for hydride shift, methyl shift, PCP branching, ring contractions/expansions, and  $\beta$ -scission. These rate equations are combined to develop relations for the net formation of carbocations, which is set equal to zero via the QSA. An overall balance on the acid sites completes the problem statement. Here the lumps

contain all molecules and carbocations, not just “key components.” Froment’s group has used the single event approach to develop kinetic models for FCC of vacuum gas oil.<sup>51</sup>

Klein’s group<sup>52</sup> developed a mechanism-based lumping scheme for hydrocarbon pyrolysis involving free radicals. The model has two submodels. One is a five-component “training set” mixture (5CM) that calculates radical concentrations in terms of 42 representative free radical intermediates. The other is a module in which a feed mixture of many components reacts with the 5CM kernel to provide detailed rates and selectivities. The model retains the essence of pyrolysis chemistry with reasonable CPU demand.

Applying the mechanistic modeling approach to the petroleum refining scale is a big challenge because of the size and stiffness (wide range of time and length scales) of the problem. It is not obvious how this approach can be used to describe coke formation which is an important yet incompletely understood process. A computationally less intensive approach is to sidestep transient intermediates (carbocations or free radicals) and focus on dominant reaction pathways.

### 3.2.2 Pathways Modeling

Quann and Jaffe<sup>39,53</sup> developed what they called the structure-oriented-lumping (SOL) approach. A hydrocarbon molecule is described by a vector whose components, referred to as structural increments, represent the number of specific structural features. These increments are building blocks for constructing molecules. For example, A6 represents a six-carbon aromatic ring present in all aromatics, while A4, a four-carbon aromatic ring, is an incremental structure that must be attached to an A6 or another A4. Figure 3 shows the structure vector and its 22 structural increments that comprise three aromatic (A6, A4, A2) and six naphthenic (N6-N1) ring structures, a -CH<sub>2</sub>- group (R) to specify the carbon number of alkyl chains or paraffins, number of branches in a chain (br), number of methyl substituents (me) on rings, bridging between rings (AA), hydrogen deficiency (H), and heteroatom groups. Each group in the vector has carbon, hydrogen, sulfur, nitrogen, and oxygen stoichiometry and hence molecular weight.

|                         | A6 | A4 | A2 | N6 | N5 | N4 | N3 | N2 | N1 | R | br | me | H | A-A | S  | RS | AN | NN | RN | O  | RO | O= |
|-------------------------|----|----|----|----|----|----|----|----|----|---|----|----|---|-----|----|----|----|----|----|----|----|----|
|                         |    |    |    |    |    |    |    |    |    |   |    |    |   |     |    |    |    |    |    |    |    |    |
| Increment Stoichiometry |    |    |    |    |    |    |    |    |    |   |    |    |   |     |    |    |    |    |    |    |    |    |
| C                       | 6  | 4  | 2  | 6  | 5  | 4  | 3  | 2  | 1  | 1 | 0  | 0  | 0 | 0   | -1 | 0  | -1 | -1 | 0  | -1 | 0  | 0  |
| H                       | 6  | 2  | 0  | 12 | 10 | 6  | 4  | 2  | 0  | 2 | 0  | 0  | 2 | -2  | -2 | 0  | -1 | -1 | 1  | -2 | 0  | -2 |
| S                       | 0  | 0  | 0  | 0  | 0  | 0  | 0  | 0  | 0  | 0 | 0  | 0  | 0 | 0   | 1  | 1  | 0  | 0  | 0  | 0  | 0  | 0  |
| N                       | 0  | 0  | 0  | 0  | 0  | 0  | 0  | 0  | 0  | 0 | 0  | 0  | 0 | 0   | 0  | 0  | 1  | 1  | 1  | 0  | 0  | 0  |
| O                       | 0  | 0  | 0  | 0  | 0  | 0  | 0  | 0  | 0  | 0 | 0  | 0  | 0 | 0   | 0  | 0  | 0  | 0  | 0  | 1  | 1  | 1  |

Figure 3. Structure vectors and 22 structural increments defined in the structure-oriented-lumping (SOL) approach.

Figure 4 gives examples of the use of this vector. The vector components indicate the number of increments in each group. So benzene is represented by A6, with the first component of the vector having a value of one and all others zero. A homologous series is a set of vectors having identical structure increments except for the alkyl chain length and possibly the branching and methyl substituent indicators. This accounting system does not distinguish isomers. A key assumption then is that the isomers of a molecular class for a given carbon number have similar physicochemical and thermodynamic properties. In short, a petroleum mixture is represented by a large set of structure vectors of different weight percents; each vector is a molecule or a collection of isomers.

|                     | A6 | A4 | A2 | N6 | N5 | N4 | N3 | N2 | N1 | R | br | me | H | A_AS | RS | AN | NN | RNO | RO | O= |   |
|---------------------|----|----|----|----|----|----|----|----|----|---|----|----|---|------|----|----|----|-----|----|----|---|
| 2,3,5 Trimethyl<br> | 0  | 0  | 0  | 0  | 0  | 0  | 0  | 0  | 0  | 9 | 3  | 0  | 1 | 0    | 0  | 0  | 0  | 0   | 0  | 0  | 0 |
| Benzene<br>         | 1  | 0  | 0  | 0  | 0  | 0  | 0  | 0  | 0  | 0 | 0  | 0  | 0 | 0    | 0  | 0  | 0  | 0   | 0  | 0  | 0 |
| Naphthalene<br>     | 1  | 1  | 0  | 0  | 0  | 0  | 0  | 0  | 0  | 0 | 0  | 0  | 0 | 0    | 0  | 0  | 0  | 0   | 0  | 0  | 0 |

Figure 4. Examples of SOL molecules

The next step is to define a finite number of reaction rules for the thousands of hydrocarbon components represented by the above 22 structural groups. For a given reaction family, a reaction rule determines if the reactant vector has the required increment(s) for that reaction to occur and then transforms the reactant vector to the product vector according to known chemistry and kinetics. Typically, petroleum process chemistry can be defined by 20-30 reaction families resulting in over 50,000 reactions.<sup>53</sup> Each refining process (e.g., FCC) has its own reaction rules, although all petroleum mixtures have the same vector representation. The lumping part of the approach is done through consolidation of reaction families. The reactions in

the same family are assumed to have the same kinetic constants. In situations where this assumption becomes untenable, a perturbation analysis about equal reactivity may be done to obtain correction terms.<sup>54,55</sup> A more direct approach is to use available QSRR, as discussed in Section 3.2.3.

Many refining process models have been developed using the SOL approach. For FCC, Christensen et al.'s apply 60 reaction rules to more than 30,000 reactions involving over 3000 molecular species.<sup>56</sup> With a single set of kinetic parameters and reactivity relationships, the model can predict both bulk yields/properties and product composition for a range of feeds and catalysts. A smaller size (450 species and 5500 reactions) FCC model was developed by Klein's group.<sup>57</sup> In this model, a stochastic approach was used to describe the molecular structure of the gas oil feed (more on this later). The model reveals that significant protolytic cracking rate defines much of the product distribution for the light catalytic cycle oil, while significant hydride-abstraction defines the gasoline product distribution. Klein's group also developed a pathways-level model for catalytic reforming.<sup>58</sup>

### 3.2.3 Quantitative Correlations

A prominent example of the QSRR is the linear free energy relationship of the form  $\ln k_i = a + bRI_i$  where  $k_i$  and  $RI_i$  are the rate constant and reactivity index for molecule  $i$ , respectively. The constants  $a$  and  $b$  are generally determined from experiments so that the rate constants for all members of the reaction family can be calculated from  $RI_i$ . The choice of  $RI_i$  reflects the controlling mechanism of the reaction, such as carbocation stability in catalytic cracking, or aromatics' electronic properties in hydrogenation<sup>59,60</sup>, or reaction enthalpy in pyrolysis. Mochida and Yoneda<sup>61-63</sup> first demonstrated the use of LFERs for catalytic reactions. Klein and coworkers<sup>64,65</sup> have used LFERs extensively for modeling of reaction kinetics in oil refining. For instance, the number of independent rate constants for modeling individual gas oil reaction is of the order  $10^4$ , whereas that of LFER parameters is of the order ten.<sup>65</sup>

Ho et al. developed a correlation for the poisoning effects of nitrogen compounds on FCC catalysts<sup>66</sup> and a scaling law for estimating the HDS reactivities of middle-distillates in terms of three key properties.<sup>67</sup> For solid acid catalyzed reactions, Sowerby and coworkers<sup>68,69</sup> developed a method for estimating adsorption equilibrium constants from an integrated form of van Hoff's equation.



### 3.2.4 Carbon Center Approach

Allen and coworkers<sup>70-72</sup> introduced a structural lumping approach based on group contribution concepts and pure-compound data. An oil fraction is assembled with a finite number of selected compound classes to capture key structural features of the oil. They calculated the number of CH, CH<sub>2</sub>, CH<sub>3</sub> as well as terminal and nonterminal olefinic and aromatic carbons. They then followed the evolutions of carbon number distributions and carbon types in each compound class.

To illustrate, the FCC feed components are divided into *n*-paraffins, isoparaffins, naphthenes, olefins, and aromatics. Each of the five compound classes can have hundreds of surrogate compounds, each being constructed from the carbon centers (or functional groups) in that class. For instance, *n*-paraffins are built from CH<sub>2</sub> and CH<sub>3</sub>. The cracking rates of these carbon centers are deduced from a small number of model-compound studies. Using the group contribution method reduces the problem of determining cracking kinetics for hundreds of compounds to that of estimating just two dozen parameters. For each compound class, group contribution parameters are determined for each of the following reaction families: cracking, isomerization, cyclization, dehydrogenation, ring opening, dealkylation, and coking. Reaction families neglected are hydrogen transfer and condensation.

The resulting model for cracking over amorphous SiO<sub>2</sub>/Al<sub>2</sub>O<sub>3</sub> has about 25 adjustable parameters that are estimated from pure-compound data. The collective behavior of these hundreds of surrogate compounds predicts the cracking behavior of the FCC feed. The product composition is used to estimate such bulk properties as vapor pressures and octane numbers. A sensitivity analysis shows that it is unnecessary to split each compound class into subsets of different carbon numbers and calculate a carbon center distribution for each carbon number. Using average carbon center distributions gives equally good product composition. In selecting surrogate compounds of a given carbon number within a compound class, one can ignore all molecules of concentrations lower than 10% of the maximum concentration regardless of chemical structure.

### 3.2.5 Lumping via Stochastic Assembly

This lumping approach, introduced by Klein and coworkers<sup>73-75</sup>, deals with reaction systems involving large molecules whose structures are very difficult, if not impossible, to characterize. A case in point is asphaltenes, the portion of a resid that is aromatic-soluble and paraffinic-insoluble. Lumping is achieved by assuming that the reactivity of such large molecules is dominated by the reactivities of a small number of functional groups on the molecules. A

similar lumping approach was also pursued by Gray<sup>76</sup> in his study of hydrotreating kinetics for heavy distillates. This line of approach, similar to that used in the carbon center approach, may be justified by reaction shortsightedness. This principle, as Helfferich<sup>5</sup> put it, says: "The reactivity of a group depends strongly on the local configuration, but little or not at all on the size and shape of the reactant molecules more than two atoms away." Where applicable, this principle can considerably simplify kinetic modeling by using the rate constants for a group of reactions.

For the pyrolysis of asphaltenes, Klein's approach basically consists of the following steps: (1) construction of an ensemble of reactant molecules based on characterization data, (2) development of lumped kinetics for a set of reactive functionalities, and (3) coupling of ensemble with lumped kinetics. This first step is stochastic while the rest are deterministic. Each of the steps is briefly described below.

The construction of a large ensembles of molecules, in which a finite number of functional groups are randomly incorporated in different molecules, is done stochastically with a computer. Since a real asphaltene feed comprises tens of thousands of molecules, its physicochemical properties are best described in terms of distributions rather than average values. The criterion for constructing such ensemble is that distributions of some key properties of the computer-generated ensembles must match those of the asphaltene feed in question. Examples of such distributions are the number of core systems/molecules, number of aromatic carbons/core, number of naphthenic carbons, number of pendants on a core, length of pendants, type of link attaching pendant to core or core to core, length of core-core link, to name a few.

A simple way of constructing each molecule in the ensemble is to connect ring systems (aromatic or naphthenoaromatic) with alkyl chains in a linear fashion subject to stoichiometric constraints. It is easier to construct an ensemble of liquid molecules than solid molecules. The latter requires modeling of three-dimensional structures.

The second step assumes that the reactivity of the ensemble is dominated by a few selected functionalities. The task then is to determine the reaction kinetics for each of the functional groups. Here the art of lumping applies in order to keep the number of kinetic lumps small. Information on reaction pathways and kinetics can be independently obtained from experiments using representative model compounds. For example, butyl benzene pyrolysis<sup>77</sup> may serve as a model system for the pyrolysis of alkyl aromatics moieties in resids.

The final step is to couple the lumped kinetics with the stochastically constructed ensemble. One then follows the reactions by updating the composition of the ensemble as the reactions proceed. The initial reaction

network and pathways are allowed to run to a few conversions. The ensemble is then updated to reflect chemistry by examining concentration of key products. It is important to test the sensitivity of model prediction to various distribution functions.

#### 4. MATHEMATICAL REDUCTION OF SYSTEM DIMENSION

Suppose that one has already used intuitive ad hoc approaches to prune a large reaction model. A natural question then is, can the model be further reduced via some mathematical techniques? What follows is an overview of progress made in this area. Let us first consider the simplest conservation equation governing the fate of  $n$  reacting species

$$\frac{d\mathbf{c}}{dt} = \mathbf{f}(\mathbf{K}; \mathbf{c}), \quad \mathbf{c}(0) = \mathbf{c}_f \quad (7)$$

where  $t$  is a spatial or time variable,  $\mathbf{c}$  the  $n \times 1$  composition vector,  $\mathbf{c}_f$  the feed composition vector and  $\mathbf{K}$  the matrix of rate constants  $k_{ij}$ . The task is to find a lumped system with dimension  $\hat{n} < n$ , which can at least approximately portray the behavior of the underlying unlumped system. We first consider first-order kinetics with  $\mathbf{f} = -\mathbf{K}\mathbf{c}$  where  $\mathbf{K}$  is the  $n \times n$  rate constant matrix.

##### 4.1 Sensitivity Analysis

A kinetic model for oil refining invariably has a multitude of parameters and dependent variables, all of which can be strongly coupled among themselves. Sensitivity analysis can simplify the model by identifying which model parameters or dependent variables are unimportant so they can be lumped or removed from the model on the fly. As a simple example, consider a single first-order reaction with  $c = c_0 \exp(-kt)$ . The sensitivity coefficient is  $s = \partial c / \partial k = -c_0 t \exp(-kt)$ . So  $c$  is not sensitive to  $k$  at very short or very long times but is very sensitive to  $k$  in the neighborhood of  $t = 1/k$ . For large systems, one calculates the sensitivity matrix  $s_{ij} = \partial c_i / \partial k_j$  at the nominal value (or point of interest) of  $\mathbf{K} = \mathbf{K}_0$  where the sensitivity analysis is carried out.<sup>78-</sup><sup>80</sup> Dumesic and coworkers<sup>81</sup> applied sensitivity analysis to catalytic cracking of isobutane. They identified 31 kinetically significant steps out of the 367 steps considered. Another example is that the 20 rate constants in the 10-lump FCC model<sup>10</sup> can be further lumped into 5 coarser lumps for an FCC unit operated in the gasoline mode.<sup>12</sup> Kramer et al.<sup>82</sup> developed a computer code "CHEMSEN" for sensitivity analysis of elementary reaction models.

## 4.2 Time Scale Separation

Suppose that the process time scale (or the time window of interest) is bounded between  $t_{\min}$  and  $t_{\max}$  ( $t_{\min} < t < t_{\max}$ ) and is a small subset of the entire reaction time scale spectrum. Then the species reacting on time scales longer than  $t_{\max}$  remain dormant; their concentrations are hardly different from their initial values. The state of these species may be treated as system parameters. On the other hand, species reacting with time scales shorter than  $t_{\min}$  may be considered relaxed. The relaxed state of these fast-reacting species may be treated as system initial conditions. These considerations naturally help reduce the system dimensionality.

Briefly, a formal treatment is as follows. Let  $\mathbf{X}$  be the matrix of the eigenvectors  $\mathbf{x}_i$  of  $\mathbf{K}$  and  $\mathbf{\Lambda}$  be the diagonal matrix of the corresponding eigenvalues  $\lambda_i$  (i.e.,  $\mathbf{K}\mathbf{x}_i = \lambda_i\mathbf{x}_i$ ). The linear transformation<sup>83</sup>  $\bar{\mathbf{c}} = \mathbf{X}^{-1}\mathbf{c}$  provides a set of pseudospecies called modes, which takes the form  $\bar{\mathbf{c}}(t) = \bar{\mathbf{c}}_f \exp(\mathbf{\Lambda}t)$ ; that is, each of the pseudospecies  $\bar{c}_i$  reacts independently with its own characteristic time scale  $\tau_i = 1/|\text{Re}\lambda_i|$ . If we are interested only in events occurring after  $t \gg 1/|\text{Re}\lambda_k|$ , we can cross off those fast, relaxed modes and project the system to an  $(n - k)$  dimensional subspace spanned by linearly independent eigenvectors  $\mathbf{x}_{k+1}, \mathbf{x}_{k+2}, \dots, \mathbf{x}_n$ . The relaxed modes provide algebraic relations among species. This treatment is commonly called modal analysis. For nonlinear systems such as Eq.(7), one can still gain considerable insights through linearization at a reference state to obtain  $d\mathbf{c}/dt = \mathbf{J}\mathbf{c}$  where  $\mathbf{J}$  is the Jacobin  $\partial\mathbf{f}/\partial\mathbf{c}$ .

## 4.3 Projective Transformation

### 4.3.1 First Order Reactions

The treatment here, due to Wei and Kuo<sup>84</sup>, lumps first-order reactions with  $\mathbf{f} = -\mathbf{K}\mathbf{c}$ . It projects the system onto a lower dimensional space via a linear transformation  $\hat{\mathbf{c}} = \mathbf{M}\mathbf{c}$  where  $\mathbf{M}$  is an  $\hat{n} \times n$  lumping matrix. Thus  $\mathbf{M}$  transforms the  $n$ -tuple vector  $\mathbf{c}$  into an  $\hat{n}$ -tuple vector  $\hat{\mathbf{c}}$  of a lower rank  $\hat{n}$  ( $\hat{n} < n$ ). If the system is exactly lumpable by  $\mathbf{M}$ , then one finds an  $\hat{n} \times \hat{n}$  matrix  $\hat{\mathbf{K}}$  such that

$$\frac{d\hat{\mathbf{c}}}{dt} = -\hat{\mathbf{K}}\hat{\mathbf{c}} \quad (8)$$

This is achievable if and only if<sup>84</sup>

$$\mathbf{MK} = \hat{\mathbf{K}}\mathbf{M} \quad (9)$$

The consequence of the lumpability on the eigenvalues and eigenvectors of the system is that the vector  $\mathbf{M}\mathbf{x}_i$  either vanishes or is an eigenvector of  $\hat{\mathbf{K}}$  with the same eigenvalue  $\lambda_i$ , that is,

$$\mathbf{M}\mathbf{x}_i = \mathbf{0} \text{ or } \hat{\mathbf{K}}(\mathbf{M}\mathbf{x}_i) = \lambda_i(\mathbf{M}\mathbf{x}_i) \quad (10)$$

Hence the matrix  $\hat{\mathbf{K}} = \hat{\mathbf{X}}\Lambda\hat{\mathbf{X}}^{-1}$  has only  $\hat{n}$  eigenvectors  $\hat{\mathbf{x}}_i = \mathbf{M}\mathbf{x}_i$ . Of the original  $n$  eigenvectors,  $n - \hat{n}$  eigenvectors vanish after the projective transformation.

If  $\mathbf{M}$  is known in advance,  $\hat{\mathbf{K}}$  can be found from Eq.(9). To construct  $\mathbf{M}$ , one rewrites Eq.(9) (the superscript T denotes transpose)

$$\mathbf{K}^T\mathbf{M}^T = \mathbf{M}^T\hat{\mathbf{K}} \quad (11)$$

Viewing  $\mathbf{K}^T$  as a mapping, Eq.(11) says that the action of  $\mathbf{K}^T$  on  $\mathbf{M}^T$  is just to create another matrix  $\mathbf{M}^T\hat{\mathbf{K}}$  that still belongs to the same vector space ( $\mathbf{M}^T$  and  $\mathbf{M}^T\hat{\mathbf{K}}$  are both  $n \times n$  matrices). With this property, the mapping  $\mathbf{K}^T$  is said to have invariant subspaces. The spaces spanned by the eigenvectors of  $\mathbf{K}^T$  are invariant subspaces because  $\mathbf{K}^T\mathbf{x}_i = \lambda_i\mathbf{x}_i$ ; i.e.,  $\lambda_i\mathbf{x}_i$  coincides with  $\mathbf{x}_i$ . A straight line containing  $\mathbf{x}_i$  is a one-dimensional invariant subspace of  $\mathbf{K}^T$ . The  $j$ -dimensional subspace spanned by  $\mathbf{x}_1, \mathbf{x}_1, \dots, \mathbf{x}_j$  ( $j < n$ ) are also invariant subspaces. One thus can see that any eigensubspace of  $\mathbf{K}^T$  can be used to construct  $\mathbf{M}^T$ , that is, by letting  $\mathbf{M} = [\mathbf{x}_1, \mathbf{x}_1, \dots, \mathbf{x}_{\hat{n}}]$ , as demonstrated by Li and Rabitz.<sup>85</sup> First-order reactions are therefore always exactly lumpable based on the invariant subspaces of  $\mathbf{K}^T$ . As will be seen later, the existence of invariant subspaces is essential to lumping nonlinear kinetics.

Li and Rabitz<sup>11</sup> used the above approach to further contract the well-known 10-lump FCC model to a five-lump model with essentially the same predictive power for product slate changes. Moreover, if gasoline is the only unlumped species, then three lumps suffice. For nonane reforming, this approach reduces the number of lumps from 14 to 5 without significant errors if the total aromatics is kept unlumped.<sup>86</sup>

In practice, most reaction systems are not exactly lumpable. Hence, approximate lumping is of greatest practical importance. To do so, Kuo and Wei<sup>87</sup> defined an error matrix  $\mathbf{E}$  as  $\mathbf{E} = \mathbf{MK} - \hat{\mathbf{K}}\mathbf{M}$ . The problem then becomes that of minimizing  $\mathbf{E}$ . They gave a detailed account for estimating  $\mathbf{E}$ . Liao and Lightfoot<sup>88</sup> gave a simpler framework for approximate lumping.

### 4.3.2 Non-Linear Systems

Li and Rabitz extended the Wei-Kuo approach to nonlinear kinetics.<sup>11,85,89-92</sup> With  $\hat{\mathbf{c}} = \mathbf{M}\mathbf{c}$ , Eq (7) becomes  $d\mathbf{M}\mathbf{c}/dt = \mathbf{M}\mathbf{f}(\mathbf{c})$  and  $\mathbf{c}(0) = \mathbf{M}\mathbf{c}_f$ . A system is exactly lumpable if  $\mathbf{M}\mathbf{f}(\mathbf{c})$  is a function of  $\mathbf{M}\mathbf{c}$ ; that is,  $\mathbf{M}\mathbf{f}(\mathbf{c}) = \hat{\mathbf{f}}(\mathbf{M}\mathbf{c})$  for every  $\mathbf{c}$ . The resulting lumped system of dimension of  $\hat{n}$  is

$$\frac{d\hat{\mathbf{c}}}{dt} = \hat{\mathbf{f}}(\hat{\mathbf{c}}) \quad (12)$$

Intuitively, one may expect that lumpability suggests that the system should have some degree of “partial linearity,” which is related to the Jacobian matrix  $\mathbf{J}[\mathbf{c}(t)] = \partial\mathbf{f}(\mathbf{c})/\partial\mathbf{c}$ . Indeed, the system is exactly lumpable if and only if for any  $\mathbf{c}$  in the composition space, the transpose of  $\mathbf{J}[\mathbf{c}(t)]$  has nontrivial fixed (i.e.,  $\mathbf{c}$  independent) invariant subspaces. It can be shown that the exactly lumped system is of the form

$$\frac{d\hat{\mathbf{c}}}{dt} = \mathbf{M}\hat{\mathbf{f}}(\bar{\mathbf{M}}\hat{\mathbf{c}}) \quad (13)$$

where  $\bar{\mathbf{M}}$  is one of the generalized inverses of  $\mathbf{M}$  satisfying  $\mathbf{M}\bar{\mathbf{M}} = \mathbf{I}$ . Whether or not the system is exactly lumpable depends on  $\mathbf{f}$  and  $\mathbf{M}$ . When  $\mathbf{f}$  is linear,  $\mathbf{J}^T = \mathbf{K}^T$ , a constant matrix. And the fixed invariant subspaces are nothing but the eigenspaces. While the number of the lumping matrices is infinite, the number of the invariant subspaces is finite. The nonuniqueness of the lumping matrix does not affect the form of the lumped equations. When  $\mathbf{f}$  is nonlinear, not all of the  $\mathbf{J}^T(\mathbf{c})$ -invariant subspaces can be used to construct the lumping matrices. Some of the resulting lumped kinetic equations may have different forms from those for the underlying unlumped system.

In practice, some constraints are usually imposed on the lumped model. For example, certain chemical species (e.g., coke precursors) need to be kept unlumped. In this and similar situations, the lumping matrix needs to reflect the constraint *a priori*. Li and Rabitz also extended their analysis to include nonisothermal effect<sup>91</sup> and intraparticle diffusion.<sup>92</sup>

Li and Rabitz<sup>93,94</sup> developed nonlinear mappings between the original and reduced dimension spaces. That is,  $\hat{\mathbf{c}} = \mathbf{H}(\mathbf{c})$ , which results in a self-contained lumped system of the form  $d\hat{\mathbf{c}}/dt = \hat{\mathbf{f}}(\hat{\mathbf{c}})$ . A necessary and sufficient condition for this to work is that  $\hat{\mathbf{f}}[\mathbf{H}(\mathbf{c})] = \mathbf{f}(\mathbf{c})\partial\mathbf{H}/\partial\mathbf{c}$ . The advantage of this approach is yet to be demonstrated.

### 4.3.3 Chemometrics

Chemometrics<sup>95</sup> is a convenient mathematical tool for developing QSRR or scaling laws that can be embedded in process models.<sup>66,67</sup> It is somewhat analogous to Wei and Kuo's treatment in that it contracts system dimensions through a projective transformation. Each lump is a linear combination of all original variables. The widely used principal component analysis (PCA)<sup>95,96</sup> and partial least squares (PLS)<sup>97</sup> are two examples of chemometric modeling.

The PLS analysis in many cases gives mechanistic insights into the underlying process chemistry, making it possible to construct QSRR from dominant descriptors. In the study of the poisoning effect of organonitrogen compounds on FCC catalysts, Ho et al.<sup>66</sup> compressed 24 structural descriptors into two, each being patient of straightforward physical interpretation. The resulting correlation expresses the poisoning potency as a function of proton affinity and molecular weight. A similar approach gives a property-reactivity correlation for the HDS reactivity of middle distillates.<sup>67</sup> Finally, we remark that chemometrics is just one of many correlation-building tools. The latest developments in this area have been reviewed by Davis et al.<sup>98</sup>

## 4.4 Other Methods

There are other lumping techniques for linear kinetics, such as cluster analysis<sup>13,14</sup>, observer theory<sup>99-100</sup>, singular perturbation<sup>101</sup>, and intrinsic low-dimensional manifolds.<sup>102</sup> Recently, Androulakis<sup>103,104</sup> treated kinetic mechanism reduction as an integer optimization problem with binary variables denoting the existence and nonexistence of reactions and species. The technique is amenable to uncertainty analysis.

## 5. TOTAL LUMPING: OVERALL KINETICS

The problem addressed here can be stated as follows. Let  $c_i(t)$  be the concentration of the individual reactant and  $C(t) = \sum_{i=1}^N c_i(t)$  be the total concentration of all reactants. The aim is to predict the dependence of  $C(t)$  on feed properties and reactor type. It is also of interest to know if an overall kinetics  $R(C)$  can be found for the reaction mixture as a whole. If so, the thus-found  $R(C)$  can be included in the conservation equations for modeling the coupling between kinetics and transport processes in a reactor. The selectivity toward a specific class of reaction intermediates (e.g., gasoline) is also of interest in many situations.

There have been four main lines of attacks to the problem posed here. The first addresses the question of whether one can find an overall kinetics

for, say, a batch or plug flow reactor in the form  $dC/dt = -R(C)$ . There is no fundamental reason why  $R(C)$  should always exist. In fact,  $R(C)$  exists only for certain special reaction mixtures. The second approach is to obtain exact or approximate expressions for  $C(t)$  when  $R(C)$  cannot be found. Both approaches require complete information on the feed composition and reactivity spectra *a priori*; that is, to be working with a fully characterized feed. However, fully characterized petroleum fractions are hard to come by in practice. One has to settle for less, hoping to be able to say something about  $C(t)$  and/or  $R(C)$  with minimum information, that is, for a mixture that has only partially been characterized. This leads to a third approach aimed at finding  $R(C)$  asymptotically for some specific regime of interest. The advantage is that the asymptotic kinetics are not sensitive to the details of the feed properties, thus yielding some rather general results. A fourth approach is to find upper and lower bounds on  $C(t)$ , the tightness of which depending on the quality of available information. These bounds can help choose empirical models and design reactor at least on a conservative basis.

Given the vast number of species in petroleum fractions, for mathematical tractability it pays to approximate the mixture as a continuum. The idea of continuous mixtures, first conceived by deDonder<sup>105</sup>, was propounded in the context of reaction kinetics by Aris and Gavalas.<sup>106</sup> As will be seen later, the continuum approach gives considerable insights into the mixture's behavior. For instance, it provides a theoretical framework for explaining many peculiar behaviors observed in catalytic hydroprocessing (HDS, HDN, and hydrodearomatization). Some examples: (1) the overall HDS or HDN reaction order for the mixture as a whole is higher than that for individual sulfur or nitrogen species; (2) high-activity catalysts show lower overall order than low-activity catalysts; (3) refractory feeds show higher overall order than reactive feeds; (4) the overall HDS order decreases with increasing temperature; and (5) the overall order depends on reactor type (e.g., plug flow vs. stirred tank reactor).

## 5.1 Continuum Approximation

Aris<sup>107</sup> was the first to address the theoretical aspects of total lumping of first-order reactions. Luss and Hutchinson<sup>108</sup> later noticed that serious problems arise if one extends the continuum approach to nonlinear kinetics. Ho and Aris<sup>109</sup> discussed the origin of the difficulties in lumping nonlinear kinetics in continuous mixtures. They proposed a single-component-identity that must be satisfied by any continuum treatment in order to overcome the difficulties. Other aspects of the mathematical and conceptual difficulties have also been examined.<sup>110-112</sup> Krambeck<sup>113</sup> addressed thermodynamic issues. Ocone and Astarita<sup>114</sup> reviewed many aspects of continuous mixtures.



At least three approaches have emerged for total lumping of nonlinear kinetics. Astarita and Ocone's approach<sup>110</sup> is based on the notion that in lumping very many reactions, one should not ignore the interactions between the reactants. They proposed a specific class of interactive kinetics that includes Langmuir-Hinshelwood and bimolecular reactions. Aris<sup>112</sup> used a two-index approach consisting of two steps. First-order reactions (or, more generally, the Astarita-Ocone kinetics) are lumped in the first step to generate nonlinear kinetics which in turn are lumped in the second step. Chou and Ho<sup>111</sup> introduced a reactant-type distribution function that serves as a link between the continuous mixture and its underlying discrete mixture.

Without loss of generality, we use the rate constant  $k$  as the reactant label. The concentration of the total lump  $C(t)$  can be expressed as<sup>111</sup>

$$C(t) = \int_0^{\infty} c(k,t)D(k)dk \quad (14)$$

where  $c(k,t)$  is the concentration of species  $k$  and  $D(k)$  is the reactant-type distribution function. The slice  $D(k)dk$  is the total number of reactant types with  $k$  between  $k$  and  $k + dk$ . For any given finite volume of the mixture, it is the number of reactant types, not the concentration of each reactant type that justifies the continuum hypothesis. Petroleum fractions of similar nature (e.g., gas oils) usually have the same, say, sulfur or nitrogen compound types (i.e.,  $D$  is usually feed invariant), but the concentration of each compound type,  $c(k,t)$ , is feed dependent. For first-order reactions,  $c(k,t) = c_f(k)\exp(-kt)$ . It follows from Eq.(14) that  $C(t)$  is uniquely defined by the product  $D(k)c_f(k) \equiv h(k)$ . This is not the case for nonlinear kinetics in general.

In the following we highlight some significant results obtained from the four approaches mentioned earlier. The majority of them were obtained from the continuum treatment.

### 5.1.1 Fully Characterized First Order Reaction Mixtures

For first-order reactions in a plug flow reactor (PFR),  $C(t) = \int_0^{\infty} h(k)\exp(-kt)dk$ . To portray a wide variety of feed properties with just two parameters, Aris<sup>107</sup> considered a class of feeds that can be characterized by the gamma distribution

$$h(k) = \gamma^{\gamma} (k/\bar{k})^{\gamma-1} \exp(-\gamma k/\bar{k}) / [\bar{k}\Gamma(\gamma)] \quad \gamma > 0 \quad (15)$$

where  $\Gamma$  is the gamma function and  $\gamma$  a feed quality index; the smaller the  $\gamma$  value, the more refractory is the feed. When  $\gamma = 1$  the distribution is exponential, indicating the feed contains a finite amount of unconvertible species. If  $\gamma > 1$ , the distribution is monomodal. Substituting Eq.(15) into

Eq.(14) gives  $C(t) = (1 + \bar{k}t/\gamma)^{-\gamma}$ , implying an overall  $\bar{n}$  th-order kinetics with an overall rate constant  $\bar{k}$ , namely,

$$dC/dt = -R(C) = -\bar{k}C^{\bar{n}}, \quad \bar{n} = 1 + 1/\gamma > 1 \quad (16)$$

Here the overbar indicates kinetic parameters associated with the overall kinetics  $R(C)$ . Thus, the mixture behaves like a single species with a higher-than-first order kinetics. As  $t$  increases, the reactive species disappear rapidly and the mixture becomes progressively more refractory, thus giving rise to a higher overall order. When the spread is broad (small  $\gamma$ ),  $\bar{n}$  is high. When the spread is narrow,  $R(C)$  approaches first order. Equation (16) says that a tough feed with  $\gamma = 1$  gives an overall order of two, while an easy feed with  $\gamma = 2$  gives  $\bar{n} = 1.5$ .

The continuum treatment yields an explicit expression for the overall kinetics whose parameters relate macroscopic behavior to microscopic details of the feed. In the discrete mixture case,  $C$  is the sum of a bunch of exponential functions with a very large number of parameters. All one can say is that the  $\ln C$  vs.  $t$  curve is concave upward<sup>115</sup>, implying that  $C(t)$  can generally be fitted with an overall order higher than one. Sau et al.<sup>116</sup> extended the continuum approach to include the effects of H<sub>2</sub>S inhibition, H<sub>2</sub> partial pressure, and nonisothermality. In many petroleum refining processes,  $k$  can be related to the boiling point distribution.<sup>116-118</sup>

The foregoing results are obtained from a single gamma distribution. In practice, the distributions of sulfur compound types can be monomodal or bimodal. One may use a pair of gamma functions to describe a bimodal distribution. Distributions other than the gamma function have been considered.<sup>119,120</sup> In such cases, one can often obtain explicit expressions for  $C(t)$  but not for  $R(C)$ .

### 5.1.2 Practical Implications

In catalyst exploratory studies, one normally screens a wide variety of experimental catalysts with a standard feed. A catalyst that does not activate the most refractory portion of the feed might well be evaluated by a high-order kinetics. But if the performance of the catalyst is improved (for instance, by the incorporation of a more effective promoter) so that there is no longer a refractory component, then a low overall order would have to be used in evaluating the improved catalyst.<sup>121</sup> In process research work, one generally runs different feeds on a selected catalyst over a wide range of conditions. The overall reaction order is expected to increase when switching from an “easy” feed to a “hard” feed. The extent of this increase could be viewed as an index of feed refractoriness. The overall order is expected to

increase with decreasing reaction severity. In short, the overall reaction order may be viewed as reflecting whether or not (1) the catalyst is active enough to attack the “unconvertibles” or (2) the conditions are severe enough to convert the “unconvertibles.”

Let us cite some experimental results. The HDS rate with a single sulfur compound can often be described by pseudo first order kinetics.<sup>122</sup> By contrast, the HDS rate with a petroleum fraction typically has an overall order between 1.5 and 2.5.<sup>123-125</sup> Sonnemans<sup>125</sup> reported that the overall HDS order increased from 1.5 to 2 when switching from a blend of light coker gas oil and virgin gas oil to a light catalytic cracked oil (LCO). Beuther and Schmid<sup>126</sup> observed that the HDS of petroleum resids followed second-order kinetics. Sonnemans<sup>125</sup> reported an overall order of two for the HDN of LCO and an order of unity for the HDN of virgin gas oils. Heck and Stein<sup>127</sup> found that HDN and hydrodeoxygenation of coal liquids were best described by second-order kinetics. Some of the nitrogen and oxygen compounds in coal liquids are highly aromatic and therefore very refractory.<sup>128</sup> Ozaki et al.<sup>129</sup> observed that the overall HDS order increased with decreasing temperature. Stephan et al.<sup>117</sup> reported that removing H<sub>2</sub>S in the reactor decreased the overall order of HDS of gas oil. Hensley et al.<sup>130</sup> changed  $\bar{n}$  by modifying the support acidity of the hydroprocessing catalysts. The continuum approach used by Inoue et al.<sup>131</sup> allows the overall HDS order to be a variable. Breysse et al.<sup>132</sup> found that the overall HDS orders for three diesel feeds of increasing refractoriness are 2.2, 2.9, and 3.8 over a sulfided catalyst. Catalytic cracking of gas oils is commonly reported to be second order.<sup>133</sup>

The inverse problem is to obtain  $h(k)$  empirically from measured  $C(t)$ . Gray<sup>2</sup> analyzed Trytten et al.’s HDS data<sup>134</sup> and found that  $h(k)$  followed a gamma distribution with  $\gamma = 2$ . Others have also addressed the inverse problem.<sup>117,135,136</sup>

### 5.1.3 Partially Characterized First Order Reaction Mixtures

A partially characterized mixture (PCM) in the present context means that one has some information on the most refractory part of the feed. A problem of practical interest is the total lump’s behavior at large times, or in the high-conversion regime. In oil refining one often wants to achieve the highest permissible conversion. In exploring or developing new catalysts, it is important that competing catalysts be evaluated at high conversions. As will be shown later, developing such long-time, overall asymptotic kinetics allows one to say something rather general about the mixture’s behavior in the absence of detail information. In what follows the subscript  $a$  signifies long-time asymptotic kinetics.

### 5.1.3.1 Plug Flow Reactor

For irreversible first-order reactions in a PFR, Krambeck<sup>137</sup> showed that the asymptotic kinetics  $R_a(C) \propto C^2$  whenever the feed contains a finite amount of unconvertible species. This is also true for reversible first-order reactions.<sup>111</sup> The case where the feed may or may not contain unconvertibles was treated by Ho and Aris.<sup>109</sup> The general treatment of the PCM starts with the expectation that the long-time behavior of the mixture should be governed by the most refractory part of the feed (as will be seen later, this is not always true). To find what goes on at large  $t$ ,  $D(k)$  and  $c_j(x)$  near  $k = 0$  can be expanded as follows<sup>109,138</sup>

$$D(k) \sim k^\mu(d_0 + d_1k + \dots) \sim d_0k^\mu \quad (17a)$$

$$c_j(k) \sim k^\nu(c_0 + c_1k + \dots) \sim c_0k^\nu \quad (17b)$$

in which  $\nu \geq 0$  and  $1 + \mu > 0$ . When the feed has a finite amount of unconvertible species,  $\mu = \nu = 0$ . When  $\mu \leq 0$ , the mixture has a finite number of nearly unreactive reactants. The asymptotic behavior of  $C(t)$  is completely dictated by the feed parameter  $\gamma$  defined as

$$0 < \gamma \equiv \mu + \nu + 1 \quad (18)$$

This parameter characterizes the number of refractory reactant types and their concentrations. A small  $\gamma$  means a refractory feed. For first-order reactions,  $h(k) \sim c_0d_0k^{\gamma-1} = h_0k^{\gamma-1}$  near  $k = 0$ . Then  $C \sim h_0\Gamma(\gamma)/t^\gamma$  as  $t \rightarrow \infty$ , implying an asymptotic power law of the form

$$R(C) \sim R_a(C) = \gamma[h_0\Gamma(\gamma)]^{-1/\gamma} C^{\bar{n}_a}, \quad \bar{n}_a = 1 + 1/\gamma > 1 \quad (19)$$

Thus,  $\bar{n}_a > 1$ , the tougher the feeds, the higher the order. Ho and White<sup>139</sup> determined the asymptotic power-law kinetics for deep HDS of LCO over three different catalysts, with  $\gamma = 0.65$  and hence  $\bar{n}_a = 2.5$ . Sie<sup>124</sup> found that  $\bar{n}_a = 2$  for both gas oil and prehydrotreated gas oil over a sulfided CoMo/Al<sub>2</sub>O<sub>3</sub> catalyst. Ma et al.<sup>140</sup> fractionated a gas oil into five fractions; all give rise to second-order HDS kinetics, whether over a NiMo or a CoMo catalyst. An advantage of the asymptotic analysis is that only local information ( $k \sim 0$ ) is needed for determining the overall rate in a PFR. This is not the case with a CSTR, as discussed below.

### 5.1.3.2 CSTR

Kinetics and catalyst exploratory studies are sometimes conducted in a CSTR. Slurry-phase reactors or ebullating beds, used for upgrading of heavy oils and resids, can be approximated as a CSTR. In a CSTR,  $c(k,t) = c_j(k)/(1 + kt)$  for first-order reactions and

$$C(t) = \int_0^{\infty} \frac{h(k)dk}{1 + kt} \quad (20)$$

The system is more complex in that for each reactant type, there is an exponential distribution of residence times among all the molecules of that reactant. No  $R(C)$  can be found and  $R_a(C)$  admits three possibilities.<sup>141</sup> The case  $\gamma < 1$  (refractory feeds) is similar to the PFR in that  $C \propto 1/t^\gamma$  at large  $t$ , which is dominated by the most refractory reactants. Specifically,  $R_a(C) \sim C^{1/\gamma}$ . For  $\gamma > 1$ ,  $\bar{n}_a = 1$  and  $C \sim I/t$  at large  $t$  (similar to that of its constituents) with  $I \equiv \int k^{-1}h(k)dk$ . Hence the long-time behavior of the mixture is governed by all species – not just by refractory species. Here the feed has a small amount of refractory species, the majority of which have short residence times. As a result, the refractory species cannot be dominating. To calculate  $C$  requires characterizing the whole feed. The situation is very different for the transition case  $\gamma = 1$ , which gives rise to  $C \propto \ln t/t$ . This means that the decay of  $C$ , while governed by the refractory species, is accelerated by the reactive species. One can only define an instantaneous asymptotic order  $\bar{n}_a = d \ln R_a / d \ln C$ , which decreases slowly with conversion, consistent with experiment.<sup>2</sup> At high conversions,  $1 < \bar{n}_a = 1 + 1/|\ln C| < 2$ . For perspective,  $\bar{n}_a$  for a PFR is always higher than that for a CSTR. The CSTR's size is larger than PFR's at constant conversion.<sup>141</sup> The PFR/CSTR reactor size ratio is less sensitive to conversion than in the single-component case.<sup>141</sup>

Experimentally, Rangwala et al.<sup>142</sup> found that the overall kinetics of HDS, HDN, and hydrocracking of a coker gas oil are all first order in a CSTR free of mass transfer effects. Trytten et al.'s CSTR HDS data showed an overall order greater than one.<sup>134</sup> And the PFR gave rise to a higher overall order than the CSTR. Dongen et al.<sup>143</sup> studied hydrodemetallization of heavy residual oils with  $\gamma = 1$ .  $C(t)$  followed 1.5 order kinetics in a CSTR, while the same feed showed an overall order of two in a PFR. All these observations are consistent with the asymptotic kinetics. Although the asymptotic kinetics are developed for long times, they are very useful for modeling the mixture's behavior by power law kinetics.<sup>138</sup>

The overall kinetics represents an averaging over the reactivity and composition spectra. Such averaging should be different in reactors with

different mixing characteristics. Golikeri and Luss<sup>144</sup> were the first to warn that the overall kinetics obtained from the PFR cannot be directly carried over to the CSTR. To the extent possible, it is important to develop if-then rules that can help translate data for different reactors.

Summarizing, a reaction mixture's overall behavior in a CSTR is the result of the interplay of the spreads of reactor residence times, reactant reactivity, and concentration. While all reactants are slowed down compared to those in the PFR, the fast-reacting ones are hampered more than the slow-reacting ones. As a result, the disparities among the species become smaller, making the mixture more homogeneous. A relatively homogeneous feed (high  $\gamma$ ) can be further homogenized in the CSTR to such an extent that its long-time behavior approaches that of a single reactant.

### 5.1.3.3 Diffusional Falsification of Overall Kinetics

A tacit assumption used in the foregoing development is that the system is kinetically controlled. When a single species undergoes an  $n$ th-order reaction, the effect of a severe diffusion limitation is to shift the order from  $n$  to  $(n + 1)/2$ . The order remains intact when  $n = 1$ . Then there remains the question, "Would the overall order of many first-order reactions remain intact if all the constituent reactions become severely diffusion limited?"

For a PFR,  $c(k,t) = c_f(k)\exp[-k\eta(k)t]$  where  $\eta(k)$  is the catalyst effectiveness factor. Denoting  $\bar{n}_d$  as the overall asymptotic order for the mixture controlled by diffusion, Ho et al.<sup>121</sup> showed that  $\bar{n}_d = (\bar{n}_a + 1)/2$ , a relationship similar to that in the single-reactant case. Hence diffusional falsification occurs for mixtures with  $\bar{n}_a \neq 1$ . Since  $\bar{n}_a > 1$  in general, so  $\bar{n}_d < \bar{n}_a$ . Gosselink and Stork<sup>145</sup> found for the HDS of a gas oil that the overall order changed from two to 1.4 in going from ground-up to 3 mm catalyst particles. Stephan et al.<sup>117</sup> observed that the overall order for powder catalyst is three, vs. two for 5 mm pellets.

For a CSTR,  $\bar{n}_d = \bar{n}_a = 1$  when  $\gamma > 1$ ,  $\bar{n}_d = \gamma\bar{n}_a = 1$  if  $1/2 < \gamma < 1$ , and  $\bar{n}_d = \bar{n}_a/2 = 1/(2\gamma)$  for  $0 < \gamma < 1/2$ .<sup>141</sup> Thus, diffusion intrusion lowers  $\bar{n}_d$  only for tough feeds ( $\gamma < 1$ ). For easy feeds ( $\gamma > 1$ ) the asymptotic order is one, with or without severe diffusion limitation. Here diffusion intrusion reduces species reactivity disparity, resulting in a wider region of "single-reactant" behavior (i.e., no shift in reaction order). Before addressing more complex kinetics, let us address the validity and limitations of the continuum theory.

#### 5.1.3.4 Validity and Limitations of Continuum Approach

The concept of a continuum applied to reaction mixtures, arguably, is on a less firm foundation relative to its use in fluid mechanics. A simple thought experiment can show that the continuum approximation must break down for very long times. Consider first-order reactions in a PFR. At sufficiently large  $t$ , the mixture behaves as if there were only one species decaying exponentially, since the concentrations of all other species are exponentially smaller. This counters the power-law decay predicted by the continuum theory. Thus, in order for the continuum theory to be valid, time cannot be unconditionally large, even though the asymptotic kinetics are developed for large times. The issue then becomes one of determining the condition under which the continuum theory and its long-time limit are *both* valid.

For first-order reaction mixtures, the condition is  $1/k^* \ll t \ll 1/\Delta k$ .<sup>139</sup> Here  $k^*$  is a characteristic rate constant for a moderately refractory species and  $\Delta k$  is the difference between the rate constants for two species whose reactivities are adjacent to each other ( $\Delta k \ll k^*$ ). From Houalla et al.'s HDS data<sup>146</sup>,  $k^*$  can be taken as the rate constant for the HDS of dibenzothiophene (DBT). And  $\Delta k$  can be estimated by the rate constants for the HDS of 4-methyl DBT and of 4,6-dimethyl DBT at 300°C and 10.5 MPa over a sulfided Co-Mo/Al<sub>2</sub>O<sub>3</sub> catalyst. The resulting region of validity is  $3.87 \cdot 10^{-3} \ll t \ll 161 \cdot 10^{-3} \text{ h} \cdot \text{g} \cdot \text{cat.} / \text{cm}^3 \text{ feed}$ . This is not stringent at all for the HDS of refractory middle distillates. However, if the regime of very long times ( $t > 1/\Delta k$ ) is of interest, one should use a discrete approach.

#### 5.1.3.5 First Order Reversible Reactions

Hydrogenation of aromatic petroleum fractions is an example of reversible reactions. Wilson et al.'s experiments<sup>147</sup> show how various aromatic ring-number fractions approach equilibrium. Also, the distribution of equilibrium constants within each ring-number fraction is not wide. The hydrogenation of coal extract in a CSTR shows an overall order of unity.<sup>148</sup>

There are a few theoretical studies of the reaction mixture represented by  $c(k, t) \propto c'(k, t)$ .<sup>111,141,149</sup> To examine the mixture's near-equilibrium behavior<sup>141</sup>, let  $c'(k, 0) \sim k^{\gamma-1}(c_0' + c_1'k + \dots)$  for small  $k$  and define  $h'(k) = c'(k)D(k)$ . The equilibrium constant  $K$  is related to  $k$  by the Polyanyi equation  $K(k) = k^\beta/\alpha$  ( $\alpha, \beta$  are constants). Note that  $k$  and  $K$  change in the opposite directions ( $\beta > 0$ ) for hydrogenation of mononuclear aromatics on metal sulfides. The reverse is true for noble metal catalysts.<sup>150</sup>

Both the PFR and CSTR exhibit a much wider variety of asymptotic behaviors than in the irreversible case.<sup>141</sup> Specifically, the PFR admits 13

possibilities, vs. CSTR's 21 possibilities. Still,  $R_a$  for both the PFR and CSTR follows power law in most cases. A striking difference between the two reactors is that when  $\beta < -1$ , the oil's near-equilibrium behavior in a PFR is governed by species of intermediate reactivities, whereas that in a CSTR is governed by either the most refractory species or all species.

### 5.1.3.6 Independent $n$ th Order Kinetics

In heterogeneous catalysis,  $n$ th-order kinetics may be the result of adsorption on a nonideal catalyst surface. In homogeneous systems,  $n$ th-order kinetics may represent the overall rate of the underlying elementary reactions, e.g., the classical Rice-Herzfeld mechanism for thermal cracking of hydrocarbons.<sup>49</sup> For simplicity,  $n$  is assumed to be constant for all species. This is not a strong assumption for many petroleum processes.<sup>128,133,151</sup>

Aris<sup>112</sup> showed that  $\bar{n} = 2$  for a special fully characterized mixture containing a finite amount of unconvertibles. Ho et al.<sup>138</sup> examined the overall kinetics asymptotically and numerically. There exist two critical values of  $n$ , denoted by  $n^*$  and  $n_*$ , which depend on the properties of the most refractory part of the feed; that is:  $n_* = 1 - 1/\nu$  and  $n^* = 1 + 1/(1 + \mu)$ . At large times,  $R_a \sim \bar{k}_a C^{\bar{n}_a}$  in most cases. Specifically, (1)  $\bar{n}_a = n$  when  $n > n^*$ , (2)  $\bar{n}_a = (n\nu + \mu + 2)/(1 + \mu + \nu)$  for  $n_* < n < n^*$ , and  $\bar{n}_a > n$  and 1, (3)  $R_a \propto C^{\bar{n}_a} / |\ell n C|$  when  $n = n^*$ , implying an instantaneous overall order of higher than two, and (4) the total lump depletes in a finite time when  $n \leq n_*$ .

The long-time behavior of  $C$  in cases (2) and (3) is governed by the most refractory species, whereas in case (1) by all species. Case 1 deals with a mixture whose constituents have relatively uniform reactivities. As a result, the overall, asymptotic rate exhibits the same order as that of the individual reactions. But  $\bar{k}_a$ , an average over the entire reactivity spectrum, weighs more heavily toward the refractory end. The asymptotic kinetics can provide guidance for empirical fitting of  $C(t)$  by an  $\bar{m}$ th-order model for all  $t$ . This is because  $\bar{m}$  and  $\bar{n}_a$  behave similarly in many respects. Numerical experiments<sup>138</sup> have shown that a continuum of zero-order reactions collectively can give rise to an apparent order of higher than unity if the feed contains high levels of refractory species, consistent with HDN data.<sup>128</sup>

### 5.1.3.7 Uniformly Coupled Kinetics

We have thus far considered systems in which the disappearance of a reactant depends only on the concentration of that reactant. To consider the interactions between reactants, Astarita and Ocone<sup>110</sup> proposed a class of



kinetics of the form  $r_i = -k_i c_i F(\sum_j w_j c_j)$ , which is a special form of the pseudo-monomolecular system discussed by Wei and Prater<sup>152</sup> in a different context. Since the dimensionless function  $F$  depends only on  $y \equiv \sum_j w_j c_j$ ; as such, its influence on all reactants is uniform. This assumption, while restrictive, reduces the problem to that of first-order reaction mixtures on a warped time scale. When  $F(y) = 1/(1 + y)^m$  ( $m$  is assumed to be constant),  $w$  is the adsorption constant in a Langmuir-Hinshelwood mechanism. The  $m = 1$  case is sometimes called the Eley-Rideal mechanism. If  $F(y) = y^{n-1}$ , one speaks of bimolecular power law kinetics. A special case is  $n = 2$  and  $w = k$ , corresponding to mass-action bimolecular kinetics for which each of the bimolecular rate constants is separable. Many useful results are available for this type of continuous mixtures<sup>112, 153-156</sup>; the reader is referred to Ocone and Astarita's review.<sup>114</sup> In the following, we focus on asymptotic kinetics.

Again,  $w$  is also expanded as  $w(k) \sim w_0 k^\xi$  as  $k \rightarrow 0$  ( $\xi + \gamma > 0$ ). For Langmuir-Hinshelwood reactions, competitive adsorption should become increasingly unimportant as time increases, thus degenerating  $R_a(C)$  to that for first-order reactions regardless of reactor type. Indeed,  $R_a(C) \propto C^{\bar{n}_a}$  for a PFR at large  $t$  with  $\bar{n}_a = 1 + 1/\gamma$ .<sup>141</sup> For a CSTR,  $R_a(C)$  degenerates to the three cases for first-order kinetics discussed earlier. For bimolecular power-law kinetics in the PFR,  $\bar{n}_a = [n(\gamma + \xi) - \xi + 1]/\gamma$ .<sup>157</sup> In particular, if the feed has some unconvertibles ( $\mu = \nu = 0$ ) with a nonzero  $w$ , then  $\bar{n}_a = n + 1$ . The corresponding CSTR case is more complex: it admits nine possibilities.<sup>141</sup> In all cases, the PFR gives rise to a higher  $\bar{n}_a$  than the CSTR.

### 5.1.4 Upper and Lower Bounds

It is useful to develop bounds on  $C(t)$  without detailed information on the feed. From the initial behavior of  $C(t)$ , Hutchinson and Luss obtained the following bounds for first-order reaction mixture in a PFR<sup>158</sup>

$$\exp(-M_1 t) \leq C(t) \leq \frac{\chi^2}{M_2} + \frac{M_1^2}{M_2} \exp(-t M_2 / M_1) \quad (21)$$

where  $\chi$  is the standard deviation of  $h(k)$  and  $M_n$  are moments of  $h(k, 0)$ ,  $M_n = \int_0^\infty k^n h(k) dk$ . If  $h(k)$  is unknown, one can measure  $M_0 = C(0)$ ,  $M_1 = -(dC/dt)_{t=0}$ , and  $M_2 = (d^2 C/dt^2)_{t=0}$ . Since  $M_n$  are based on early-time ( $t \rightarrow 0$ ) information, the gap between the bounds increases with  $t$  and approaches  $\chi^2/M_2$  asymptotically. The upper bound is rather conservative at large  $t$  since it approaches  $\chi^2/M_2$ . For instance, for the gamma distribution,  $\chi^2/M_2 = 1/(\gamma + 1)$ , the bound is especially conservative for small  $\gamma$  (refractory feeds). Tighter bounds can be obtained if one also knows that  $c_f(k)$  is monomodal with a

known mode.<sup>158</sup> Gray<sup>2</sup> used Eq.(21) to analyze Trytten et al.'s HDS data<sup>134</sup> and concluded that the bounds are indeed very conservative. The lower bound is the effluent concentration of a single pseudospecies undergoing first-order reaction with the rate constant  $M_1$ . Thus, using the average rate constant would overestimate the overall decay rate of the mixture. Similar bounds have been obtained for a series of  $N$  CSTRs<sup>141</sup> and for independent irreversible  $n$ th-order reactions in a PFR.<sup>108</sup>

For a variety of kinetics, Ho<sup>157</sup> developed a much improved upper bound that requires information on the most refractory part of the feed. The general form of the upper bound is

$$C \leq C_u \equiv 1/(1 + t/\lambda^{1/\tilde{\gamma}})^{\tilde{\gamma}} \quad (22)$$

Table 1 lists  $\tilde{\gamma}$ , a generalized feed refractoriness index, and  $\lambda$  for various kinetics.

Table 1. Parameters for upper bound shown in Eq.(22)

| Kinetics, $-r_i$                               | $\tilde{\gamma}$            | $\lambda$  |
|--|-----------------------------|--|
| $k_i c_i$ and $k_i c_i / (1 + \sum_j w_j c_j)$ | $\gamma$                    | $h_o \Gamma(\gamma)$   |
| $k_i c_i (1 + \sum_j w_j c_j)^{n-1}$           | $\gamma / \varpi^*$         | $h_o \Gamma(\gamma) / (\varpi^{n-1} \varpi^*)^{\gamma/\varpi^*}$   |
| $\sum_j k_{ij} c_i c_j^{**}$                   | 1                           | $1 / \bar{k}_a = \mathbf{e}^T \mathbf{K}_s^{-1} \mathbf{e}$  |
| $k_i c_i^n, n_* < n < n^*$                     | $\gamma / (\nu + 1 - n\nu)$ | $B(\tilde{\gamma}, \bar{\beta} - \tilde{\gamma}) d_o c_o^n \bar{\beta}^{\tilde{\gamma}+1} / (\nu + \bar{\beta})$ |

$\varpi^* \equiv 1 + (n - 1)(\gamma + \xi)$ ,  $\varpi \equiv w_o h_o \Gamma(\gamma + \xi)$ ,  $\bar{\beta} = 1/(1 - n)$ ,  $B$  is the beta function

\*\* This case is discussed in Section 5.2.2.

Note that  $C_u$  itself implies a power law; that is,  $dC_u/dt = -\tilde{\gamma} \lambda^{-1/\tilde{\gamma}} C_u^{1+1/\tilde{\gamma}}$ . As such, if  $R(C)$  is of a power-law form. With gamma distributions for first-order and uniform kinetics in a PFR, the upper bound  $C_u$  becomes exact.<sup>157</sup>

### 5.1.5 One Parameter Model

In many practical situations, one is mainly interested in  $C(t)$ , which for most kinetics (power law, Langmuir-Hinshelwood, bimolecular reactions, etc.) can be accurately estimated or exactly calculated from the following simple expression<sup>141,157</sup>

$$C_q(t) = \frac{1}{(1 + t^{zq} / \sigma^q)^{1/q}} \quad q > 0 \quad (23)$$

Here  $C_q = C(t)/C_f$  and the subscript  $q$  signifies that  $C_q$  depends on the adjustable parameter  $q$ . Both  $z$  and  $\sigma$  can be determined from information on

the most refractory portion of the feed. The parameter  $q$  should be determined experimentally at an intermediate conversion (say, between 45 to 60%) at or in the neighborhood of  $t = t^* = \sigma^{1/2}$ . Once  $C(t^*)$  is known, then  $q = -\ln 2 / [\ln C(t^*)/C_f]$ . This expression, valid for both PFR and CSTR, is obtained from combining the large and small  $t$  asymptotes.

The point here is that Eq.(22) is all that is needed for an estimate of  $C(t)$ , which requires characterization of only the most refractory portion of the feed. A much improved estimate needs a data point on  $C(t)$  at an intermediate conversion, Eq.(23).

### 5.1.6 Intraparticle Diffusion

Here the attention is focused on the behavior of the overall effectiveness factor  $\bar{\eta}$  as a function of an overall Thiele modulus. For a given particle size, the extent of diffusion intrusion depends on the interplay of the reactivities and diffusivities of the constituent species. As discussed before, lumping very many species with widely different reactivities results in a steeper concentration profile than that in the single-reactant case. If the Thiele modulus  $\phi$  follows a gamma distribution with  $\langle\phi\rangle$  being its average, Golikeri and Luss<sup>159</sup> showed for parallel first-order isothermal reactions that the  $\bar{\eta}$  vs.  $\langle\phi\rangle$  curve is similar to that for a single reactant. The asymptotic similarity of catalyst geometry also holds in terms of a generalized Thiele modulus. When the diffusion limitation is severe,  $\bar{\eta}$  is insensitive to how  $\phi$  is distributed. Calculations based on the gamma distribution show that  $\bar{\eta}$  is smaller than that calculated for the single-reactant case. Thus one would overestimate  $\bar{\eta}$  if the conventional  $\eta - \phi$  plot for a single reactant is used. This practice apparently is not uncommon.<sup>115,134</sup> Golikeri and Luss also obtained bounds for  $\bar{\eta}$ .

Ocone and Astarita<sup>160</sup> considered uniformly coupled reactions in an isothermal slab catalyst. All species are assumed to have the same diffusivity, which may correspond to a petroleum fraction of narrow boiling range. A significant result is that  $\bar{\eta}$  can be greater than unity at small Thiele moduli, since the overall kinetics at the catalyst external surface may have a negative order. For nonuniformly coupled bimolecular reactions of the form  $r_i = \sum_j k_{ij} c_i c_j$ , Upper and lower bounds on  $\bar{\eta}$  can be obtained by reducing the problem to that of finding the effectiveness factor for a single second-order reaction<sup>161</sup>. The resulting bounds can be used to estimate  $\bar{\eta}$  based on information about the average and the spread of the individual Thiele moduli. For a given average Thiele modulus,  $\bar{\eta}$  is smaller than that calculated for the single-component case.

### 5.1.7 Temperature Effects

Suppose that the overall kinetics can be written as  $R(C) = \bar{k}f(C)$ . A natural question is: if the individual rate constants  $k_i$  are all Arrheniusic, what is the temperature dependence of the overall rate constant  $\bar{k}$ ? If  $\bar{k}$  happens to be a function of the products, ratios, or ratios of products of  $k_i$ , then it obeys Arrhenius' equation. But there is no a priori reason why this should often be the case in practice. Golikeri and Luss<sup>162</sup> considered  $r_i = k_i c_i^n$  with activation energy  $E_i$  in a PFR. If  $\bar{k}$  is forced to obey the Arrhenius equation with an overall activation energy  $\bar{E}$ , then  $\bar{E} = \Sigma_i(r_i E_i) / \Sigma_i r_i$  at a constant overall conversion, implying that  $\bar{E}$  depends on temperature and concentration. So  $\bar{k}$  in general does not follow the Arrhenius form unless by chance all  $E_i$  are equal. Calculations show that  $\bar{E}$  is sensitive to temperature and/or concentration when  $E_i$  are widely spread. This says that in general the activation energy determined at one conversion level should not be applicable to another conversion level.

Experimentally, however, the overall temperature responses of many refining processes (FCC<sup>163,164</sup>, hydrotreating<sup>148</sup>, hydrocracking<sup>165,166</sup>) can often be adequately described by the Arrhenius equation. It seems, then, that the activation energies do not vary widely, or the temperature range is not very broad, or one of the activation energies may dominate, or a combination of the above. In systems where there is a wide spectrum of activation energies (e.g., pyrolysis of coal, resids, asphaltenes, or tar sands), some researchers<sup>167-170</sup> used the activation energy as the continuous variable for labeling the reactants. The assumption is that all  $k_i$  have the same pre-exponential factor. They found that the overall temperature response could be reasonably described by the mean of a continuous activation energy distribution function (e.g., Gaussian distribution). The mean activation energy determined by the continuum approach is consistent with pyrolysis mechanisms.

### 5.1.8 Selectivity of Cracking Reactions

Laxminarasimhan et al.<sup>171</sup> treated the problem of maximizing the liquid yield in hydrocracking by introducing a distribution function  $p(k, \kappa)$  characterizing cracking stoichiometry

$$\frac{dc(k, t)}{dt} = -kc(k, t) + \int_k^{k_{\max}} p(k, \kappa) \kappa c(\kappa, t) D(\kappa) d\kappa \quad (24)$$

The hydrocracking rate constant  $k$  is assumed to be a monotonic function of boiling point. And  $p(k, \kappa)$  describes the amount of species with reactivity  $k$  that is formed from the cracking of the species with reactivity  $\kappa$ . Its properties are: (1)  $p(k, \kappa) = 0$  for  $k \geq \kappa$ , (2)  $p(k, \kappa) > 0$  and has a finite, small value when  $k \rightarrow 0$ , and (3)  $\int_0^\kappa p(k, \kappa)D(k)dk = 1$ . The reactant-type distribution function  $D(\kappa)$  accounts for the cracking of all species with reactivity  $\kappa$ , since the mass balance is written in the  $k$  space.

A skewed Gaussian-type distribution function can depict the yield distributions. The resulting model reproduces published pilot-plant and commercial data on vacuum gas oil hydrocracking.<sup>118,172,173</sup> This has led to the development of a hydrocracking process model.<sup>118</sup> Selective cracking in FCC has also been addressed.<sup>174</sup> Browarzik and Kehlen<sup>175</sup> used a fragmentation-based model for n-alkane hydrocracking. Similar approaches have been used for polymer reaction systems.<sup>176-179</sup>

### 5.1.9 Reaction Networks

The overall selectivity of a bunch of reaction networks can be quite different from that of a single network, as discussed by Golikero and Luss<sup>180,181</sup> for discrete mixtures and later by Astarita<sup>182</sup> for continuous mixtures. A simple example is the first-order parallel reaction system  $A_i \rightarrow B_i$  and  $A_i \rightarrow C_i$  ( $i = 1, 2, \dots, N$ ). Let  $a_i(t)$ ,  $b_i(t)$ , and  $c_i(t)$  be the individual concentrations and  $A$ ,  $B$ , and  $C$  be the lumped concentrations, respectively (i.e.  $A = \sum a_i$ ). In the single-reactant case, the selectivity  $s(t) = b(t)/c(t)$  is independent of conversion. In the mixture case, however, the selectivity  $S(t) = B(t)/C(t)$  in general depends on conversion and feed composition. Moreover, the equations governing the kinetic behavior of the lumped species are very different from those for individual species and are often of unconventional forms. Numerical experiments indicated that  $S(t)$  may have at most  $N - 2$  extremum points. For a two-species system,  $S(t)$  is a monotonic function of conversion. Thus, while optimum residence time is an issue for the mixture, it is not for a single reactant. For the consecutive system  $A_i \rightarrow B_i \rightarrow C_i$ ,  $B(t)$  can exhibit multiple maxima, and the overall selectivity  $S(t) = B(t)/[A(0) - A(t)]$  depends on the feed composition. Attempts have also been made to treat multi-step reactions in continuous mixtures, which have been reviewed by Ocone and Astarita.<sup>114</sup>

## 5.2 Discrete Approach: Nonuniformly Coupled Kinetics

An exemplary system that captures structural features of the interacting kinetics is described by the following irreversible bimolecular reactions:

$$\frac{dc_i}{dt} = -\sum_{j=1}^N k_{ij} c_i c_j, \quad \frac{dC}{dt} = -\sum_{i=1}^N \sum_{j=1}^N k_{ij} c_i c_j, \quad c_i(0) = c_{if} \geq 0 \quad (25)$$

with  $k_{ij} = k_{ji}$ . A major source of coke in catalytic cracking is the bimolecular reactions between olefins and aromatics. Bimolecular reactions can also be found in pyrolysis, condensation, oligomerization, disproportionation, alkylation, etc.

Here the continuum approach does not offer much advantage because an explicit expression for  $c_i$  is not available. Finding  $C$  or  $R(C)$  is necessarily more difficult than the uniformly coupled case where  $k_{ij} = k_i k_j$ . The problem has been attacked asymptotically along two paths, as highlighted below.

### 5.2.1 Homologous Systems

The system in question is weakly nonuniform in that  $k_{ij}$  do not span a wide range; that is,  $k_{ij} = k_m + \varepsilon_{ij}$  with  $\varepsilon \equiv \max |\varepsilon_{ij}| = \max |k_{ij}/k_m| \ll 1$  where  $k_m$  is a mean rate constant. Explicit expressions for  $C(t)$  in a PFR and CSTRs have been obtained via perturbation about the equal-reactivity limit.<sup>54</sup> As expected, an overall second-order kinetics appear at lowest order. With no more than three terms the perturbation series is accurate for  $\varepsilon$  at least as high as 0.5. Upper and lower bounds for  $C(t)$  and  $c_i(t)$  have also been derived.<sup>183</sup> The same approach can be used for systems in which the coupling is weak, that is,  $k_{ij} \ll k_{ii}$ .<sup>54</sup>

### 5.2.2 Long-Time Behavior

A crucial question here is, what are the consequences of strong interactions between reacting species? To answer this question, we first consider a binary system that can remember its history; that is, its long-time behavior depends on where it starts.<sup>183,184</sup> There are two governing parameters:  $\delta_1 \equiv k_{11} - k_{12}$  and  $\delta_2 \equiv k_{22} - k_{12}$ . Thus the relative magnitude of  $k_{12}$  plays the key role in determining the interaction intensity. To reveal what goes on at large  $t$ , it pays to work with reactant mole fraction  $x_i(t) = c_i(t)/C(t) \geq 0$  and  $x_i(0) = x_{if}$  so  $\sum_i x_i(t) = 1$  at all  $t$ . At large  $t$ ,  $R \sim \bar{k}_a C^2$  and  $x_i(t)$  approaches a steady state  $\bar{x}_i$ . In order of increasing interaction intensity, the system's behavior can be classified as follows.<sup>184</sup>

*Case I. Single steady state ( $\delta_1 > 0$  and  $\delta_2 > 0$ ):* There is very little "cross talk" between the two species. Hence, both species coexist at all  $t$  and  $\bar{k}_a = (k_{11}k_{22} - k_{12}^2)/(k_{11} + k_{22} - 2k_{12})$ . The system is robust in that it has only one realizable steady-state composition ( $\bar{x}_1 = \delta^*$  and  $\bar{x}_2 = 1 - \delta^*$  where  $\delta^* = \delta_2/[\delta_1 + \delta_2]$ ), whatever the feed composition.

*Cases II. Single steady state (Case IIa.  $\delta_1 \geq 0$  and  $\delta_2 \leq 0$ , but not both zero; Case IIb.  $\delta_1 \leq 0$  and  $\delta_2 \geq 0$ , but not both zero):* There is some “cross talk” between a very reactive species and a refractory species. The latter dominates the system’s long-time behavior, which is robust in that  $\bar{k}_a = k_{22}$  and  $\bar{x}_2 = 1$  in Case IIa, and  $\bar{k}_a = k_{11}$  and  $\bar{x}_1 = 1$  in Case IIb.

*Case III. Multiple steady states ( $\delta_1 < 0$  and  $\delta_2 < 0$ ):* Here the cross-reaction dominates the system behavior, which is sensitive to its initial conditions. Specifically,  $\bar{x}_1 = 1$  and  $\bar{k}_a = k_{11}$  for any  $x_{1f} > \delta^*$  and  $\bar{x}_2 = 1$  and  $\bar{k}_a = k_{22}$  for any  $x_{1f} < \delta^*$ . The interior steady state ( $\bar{x}_1 = \delta^*$ ) is unstable and hence unrealizable.

Thus, as the interaction intensifies, steady-state multiplicity and stability come into play. In the case of uniformly coupled bimolecular reactions ( $k_{ij} = k_i k_j$ ), the interaction is not strong enough to induce steady-state multiplicity; the system behaves similarly to Case II above.

The above treatment can be generalized to an  $N$ -component mixture.<sup>184</sup> At steady state, either  $x_i = 0$  or  $(\mathbf{K}\mathbf{x})_i = \mathbf{x}^T \mathbf{K} \mathbf{x}$  for each  $i$  where  $\mathbf{K}$  is the matrix formed by  $k_{ij}$ . Hence the system has two submixtures. One contains  $N_s$  refractory species that survive the reaction after a long time. Another contains  $N - N_s$  reactive species that become exhausted at large  $t$ . Some of the steady states may not be stable and hence unobservable. Principal findings are: (1)  $R(C) = k(t)C^2$  where the instantaneous rate constant  $k(t)$  decreases with  $t$  and eventually approaches a constant  $\bar{k}_a > 0$  if  $k_{ii} > 0$  for every  $i$ , regardless of the feed composition. That is,  $R_a = \bar{k}_a C^2$ . That  $d\bar{k}_a/dt \leq 0$  implies that the instantaneous order of the overall kinetics is greater or equal to two. While  $R_a$  is usually second order, exceptions do exist. (2) The uniqueness of  $\bar{k}_a$  depends on the feed composition, although  $\bar{k}_a$  can be chosen from only a finite number of possibilities. Thus, the system can exhibit a long-term memory. (3) In most cases, each possibility for  $\bar{k}_a$  corresponds to a unique asymptotic mixture composition. However, under special circumstances, a continuum of steady-state compositions can possibly exist; even in this case the number of overall rate constants is always finite. (4)  $\bar{k}_a = 1/(\mathbf{e}^T \mathbf{K}_s^{-1} \mathbf{e})$  where  $\mathbf{e}$  is an  $N_s$ -dimensional vector of all ones and  $\mathbf{K}_s$  the  $N_s \times N_s$  rate constant matrix formed from the surviving species. (5) The long-time behavior of the mixture can be affected by the fast reactions of the system. (6) When the refractory species decay at an asymptotic second-order rate, the reactive species get exhausted asymptotically at a power-law rate with an order less than two. (7) The behavior of the mixture is not oscillatory because  $\mathbf{x}$  cannot return to the same point as time proceeds. (8) Stability plays a

central role in determining the system behavior. One of the stability criteria can be defined in terms of the transition probability matrix of a Markov chain.

Numerical calculations demonstrate that a mixture with as few as three reactants can exhibit a rich variety of behaviors. The results also point to the importance of varying the feed composition in kinetics studies and that long-time rate data can be used for estimating kinetic constants.

## 6. CONCLUDING REMARKS

Over the past two decades, much progress has been made on the theory and practice of kinetic lumping, largely in response to increasingly stringent requirements for fuels/lubes quality, crude slate flexibility, and reactor control and optimization. Several new approaches have been developed for constructing robust process models used in petroleum refining. Along the way, many QSSR and if-then rules have been developed. In certain areas, high-resolution models have proved their worth by making molecular management a reality.

Much remains to be done, however. One of the most challenging areas is to incorporate catalyst properties in kinetic models. For crystalline catalysts with well-characterized structures (e.g., zeolites), some limited progress has been made, but this is far from being the case for structurally complex catalysts such as highly amorphous metal sulfides.

Control and mitigation of coke formation is an integral part of improving existing and developing new refining technologies. Coke on catalyst not only decreases activity, but also greatly affects selectivity. To complicate matters, there are many types of coke for a given process chemistry (e.g., FCC, coking). Reactor fouling caused by carbonaceous deposit (higher H-to-C ratio than coke) remains an important operation issue in many cases. We really do not know much about the fundamentals of these processes. These areas are fertile grounds for further research.

The tradeoff between kinetics and hydrodynamics for hydrodynamically complex systems continue to be a big challenge. For instance, to address problems of fluid maldistribution in trickle bed reactors or the feed injection zone at the base of a FCC riser, one is compelled to sacrifice chemistry. The same is true when one needs to solve control and optimization problems.

Heavy feed processing is certain to become more important in years to come. This is so because refining processes in today's economic climate must be capable of responding to ever-changing feedstocks, cost and availability, as well as changes in market demand. Moreover, the supply of high quality cat feeds is surely dwindling. Many heavy feed catalytic processes involve multiphase flows with multiscale structure. Modeling of such systems requires consideration of linking different time/length scales (e.g., catalyst surface,



intraparticle transport, bubbles/droplets, sprays, etc.) and development of a framework for predictions at the global (reactor, interprocess) scale.

## 7. REFERENCES

1. Weekman, V. W., *Chem. Eng. Prog. Symp. Ser.* **1979**, 75, 3.
2. Gray, M. R., *Upgrading Petroleum Resids and Heavy Oils*, Marcel Dekker, 1994.
3. Sapre, A. V., Kinetic Modeling at Mobil: A Historical Perspective, In *Chemical Reactions in Complex Mixtures*, Sapre, A.V.; Krambeck, F. J. (Eds.), Van Nostrand Reinhold, 1991.
4. Meier, P. E.; Ghonasgi, D. B.; Wardinsky, M. D., US 6,212,488, **2001**.
5. Helfferich, F. G., *Kinetics of Homogeneous Multistep Reactions*, Elsevier, 2001.
6. Chen, J.-Y., *Combust. Sci. Technol.*, **1988**; 57, 89-94.
7. Chen, J.-Y., *Workshop on Numerical Aspects of Reduction in Chemical Kinetics*, CERMICS-ENPC Cite Descartes-Champus Sur Marve, France, September 2, 1997.
8. Sung, C. J.; Law, C. K.; Chen, J.-Y., *Combust. Sci. Technol.*, **2000**, 156, 201-220.
9. Lutz, A. E.; Kee, R. J.; Miller, J. A., SENKIN: A Fortran Program for Predicting Homogeneous Gas Phase Kinetics With Sensitivity Analysis, SAND87-8248, Sandia Nat. Labs, Livermore, 1988.
10. Jacob, S. M.; Gross, B.; Voltz, S. E.; Weekman, V. W., *AIChE J*, **1976**, 22, 701-713.
11. Li, G.; Rabitz, H. *Chem. Eng. Sci.*, **1991**, 46, 583.
12. Pareek, V. K.; Adesina, A. A.; Srivastava, A.; Sharma, R., *J. Mole. Catal.*, **2002**, 181, 263-274.
13. Coxson, P. G.; Bischoff, K. B., *Ind. Eng. Chem. Res.*, **1987**, 26, 1239-1248.
14. Coxson, P. G.; Bischoff, K. B., *Ind. Eng. Chem. Res.*, **1987**, 26, 2151-2157.
15. Wiehe, I. A., *Ind. Eng. Chem. Res.*, **1993**, 32, 2447.
16. Mosby, J. F.; Buttke, R. D.; Cox, J. A., *Chem. Eng. Sci.*, **1986**, 41, 989-995.
17. Dente, M. E.; Ranzi, E. M., Mathematical Modeling of Pyrolysis Reactions. In *Pyrolysis: Theory and Industrial Practice*, Albright, L. F.; Crynes, B. L.; Corcoran, W. H. (Eds.), Academic Press: NY, 1983.
18. Lee, L. S.; Chen, Y. W.; Huang, T. N.; Pan W. Y., *Can. J. Chem. Eng.*, **1989**, 67, 615-619.
19. Gianetto, A.; Faraq, H.; Blasetti, A.; deLasa, H. I., *Ind. Eng. Chem. Res.*, **1994**, 33, 3053.
20. Dave, N. C.; Duffy, G. J.; Udaja, P., *Fuel*, **1993**, 72, 1333-1334.
21. Hagelberg, P.; Eilos, I.; Hiltuneu, J.; Lipiäinen, K.; Niemi, V. M.; Attamaa, J.; Krause, A. O. I., *Appl. Catal.*, **2002**, 223, 73-84.
22. Cerqueira, H.S.; Biscaia, E. C.; Sousa-Augias, E. F., *Appl. Catal.*, **1997**, 164, 35-45.
23. Ancheyta-Juárez, J.; Lopez-Isunza, F.; Aguilar-Rodriguez, E.; Moreno-Mayorga, J., *I&EC Res.*, **1997**, 36, 5170-5174.
24. Rosca, P.; Ionescu, C.; Apostol, D.; Ciuparu, D., *Prog. Catal.*, **1994**, 3, 89-96.
25. Zhang, Y. Y., *Comput. Chem. Eng.*, **1994**, 18, 39-44.
26. Takatsuka, T., Sato, S., Morimoto, Y., Hashimoto, H., *Int. Chem. Eng.*, **1987**, 27, 107-115.
27. Sha, Y.; Deng, X.; Chen, X.; Weng, H.; Mao, X.; Wang, S., *Proc. Int. Conf. Pet. Refin. Petrochem. Proc.*, Hou, X. (Ed.), 1991; 3: 1517.
28. Pitault, I.; Nevicato, D.; Forissier, M.; Bernard, J., *Chem. Eng. Sci.*, **1994**, 49, 4249-4262.
29. Kumer, S.; Chadha, A.; Gupta, R.; Sharma, R., *Ind. Eng. Chem. Res.*, **1995**, 34, 3737.
30. Dewachtere, N. V.; Fromert, G. F.; Vasalos, I.; Markatos, N.; Skandalis, N., *Appl. Thermal Eng.* **1997**, 17, 837-844.
31. Kmak, W. S. AIChE National meeting, Houston, TX, 1972.
32. Ramage, M. P.; Graziani, K. R.; Krambeck, F. J., *Chem. Eng. Sci.*, **1980**, 35, 41
33. Ramage, M.P.; Graziani, K.R.; Schipper, P. H.; Choi, B.C., *Adv. Chem. Eng.*, **1987**, 13, 193-266.

34. Powell, R. T., *Oil Gas J.*, **1989**, 64-65.
35. Quann, R. J.; Krambeck, F. J., Olefine Oligomerization Kinetics over ZSM-5, In *Chemical Reactions in Complex Mixtures*, Sapre, A. V.; Krambeck, F. J. (Eds.), Van Nostrand Reinhold, 1991.
36. Clymans, P. J.; Froment, G. F., *Comput. Chem. Eng.*, **1984**, 8, 137.
37. Baltanas, M. A.; Froment, G. F., *Comput. Chem. Eng.*, **1985**, 9, 71-81.
38. Broadbelt, L. J.; Stark, S. M.; Klein, M. T., *Ind. Eng. Chem. Res.*, **1994**, 33, 790-9.
39. Quann, R. J.; Jaffe, S. B., *Ind. Eng. Chem. Res.*, **1992**, 31, 2483-2497.
40. Senkan, S. M., Detailed Chemical Kinetic Modeling: Chemical Reaction Engineering of the Future, *Adv. Chem. Eng.*, **1992**, 18, 95.
41. Dumesic, J. A.; Rudd, D. F.; Aparicio, L. M.; Rekoske, J. E.; Trevino, A. A., *The Microkinetics of Heterogeneous Catalysis*, Am. Chem. Soc., Washington, DC, 1993.
42. Yaluris, G.; Rekoske, J. E.; Aparicio, L. M.; Madon, R. J.; Dumesic, J. A., *J. Catal.*, **1995**, 153, 54.
43. Yaluris, G.; Madon, R. J.; Dumesic, J. A., *J. Catal.*, **1999**, 186, 134.
44. Baltanas, M. A.; Raemdonck, K. K. V.; Froment, G. F.; Mohedas, S. R., *I&EC Res.*, **1989**, 28, 899.
45. Feng W.; Vynckier, E.; Froment G. F., *I&EC Res.*, **1993**, 32, 2997.
46. Svoboda, G. D.; Vynckier, E.; Debrabandere, B.; Froment, G. F., *I&EC Res.*, **1995**, 34, 3793-3800.
47. Vynckier, E.; Froment G. F., Modeling of Kinetics of Complex Processes Based Upon Elementary Steps. In *Kinetic and Thermodynamic Lumping of Multicomponent Mixtures*, Astarita, G. A.; Sandler, S. I. (Eds.), Elsevier, 1991.
48. Benson, S. W., *Thermochemical Kinetics*, 2nd. ed., John Wiley, 1976.
49. Laidler, K. J., *Chemical Kinetics*, Harper & Row: New York, 1987.
50. Kazansky, V. B.; Senchemya, I. N., *J. Catal.*, **1989**, 119, 108-120.
51. Dewachtere, N. V.; Santaella, F.; Froment, G. F., *Chem. Eng. Sci.*, **1999**, 54, 3653-3660.
52. Fake, D. M.; Nigam, A.; Klein, M. T., *Appl. Catal.*, **1997**, 160, 191-221.
53. Quann, R. J.; Jaffe, S. B., *Chem., Eng. Sci.*, **1996**, 51, 1615
54. Li, B. Z.; Ho, T. C., *Chem. Eng. Sci.*, **1991**, 46, 273-280.
55. Ho, T. C., *J. Catal.*, **1991**, 129, 524.
56. Christensen, G.; Apelian, M. R.; Hickey, K. J.; Jaffe, S. B., *Chem. Eng. Sci.*, **1999**, 54, 2753- 2764.
57. Joshi, P. V.; Lyer, S. D.; Klein, M. T., *Rev. Process. Chem. Eng.*, **1998**, 1, 111-140.
58. Joshi, P. V.; Klein, M. T.; Huebner, A. L.; Leyerle, R. W., *Rev. Process. Chem. Eng.*, **1999**, 2, 169-193.
59. Korra, S.; Neurock, M.; Klein, M. T.; Quann, R. J., *Chem. Eng. Sci.*, **1994**, 49, 4191-4210.
60. Neurock, M.; Klein, M. T., *Polycyclic Aromat. Compd.*, **1993**, 3, 231-46.
61. Mochida, I.; Yoneda, Y., *J. Catal.*, **1967**, 7, 223-230.
62. Mochida, I.; Yoneda, Y., *J. Catal.*, **1967**, 7, 386-392.
63. Mochida, I.; Yoneda, Y., *J. Catal.*, **1967**, 7, 393-396.
64. Nigam, A.; Klein, M.T., *Ind. Eng. Chem. Res.*, **1993**, 32, 1297-303.
65. Watson, B. A.; Klein, M. T.; Harding, R. H., *Appl. Catal.*, **1997**, 160, 13-39.
66. Ho, T. C.; Katritzky, A. R.; Cato, S. J., *I&EC Res.*, **1992**, 31, 1589-1597.
67. Ho, T. C., *Appl. Catal. - A: General*, **2003**, 244, 115-128.
68. Sowerby, B.; Becker, S. J.; Belcher, L. J., *J. Catal.*, **1996**, 161, 377.
69. Sowerby, B.; Becker, S. J., Modeling Catalytic Cracking Kinetics Using Estimated Adsorption Equilibrium Constants, In *Dynamics of Surfaces and Reaction Kinetics in Heterogeneous Catalysts*, Froment, G. F.; Waugh, K. C. (Eds.), Elsevier, 1997.
70. Liguras, D. K.; Allen, D. T., *Ind. Eng. Chem. Res.*, **1989**, 28, 665.
71. Liguras, D. K.; Allen, D. T., *Ind. Eng. Chem. Res.*, **1989**, 28, 674.

72. Allen, D. T., Structural Models of Catalytic Cracking Chemistry, In *Kinetic and Thermodynamic Lumping of Multicomponent Mixtures*, Astarita, G.; Sandler, S. I. (Eds.), Elsevier: Amsterdam, 1991.
73. Nigam, A.; Neurock, M.; Klein, M. T., Reconciliation of Molecular Detail and Lumping: An Asphaltene Thermolysis Example, In *Kinetic and Thermodynamic Lumping of Multicomponent Mixtures*, Astarita, G.; Sandler, S. I. (Eds.), Elsevier: Amsterdam, 1991.
74. Klein, M. T.; Neurock, M.; Nigam, A.; Libanati, C., Monte Carlo Modeling of Complex Reaction Systems: An Asphaltene Example, In *Chemical Reactions in Complex Mixtures*, Sapre, A. V.; Krambeck, F. J. (Eds.), Van Nostrand Reinhold: N.Y., 1991.
75. Trauth, D. M.; Stark, S. M.; Petti's, T. F.; Neurock, M.; Klein, M. T., *Energy Fuels*, **1994**, *8*, 576-88.
76. Gray, M. R., *I & EC Res.*, **1990**, *29*, 505-512.
77. Freund, H.; Olmstead, W. N., *Int. J. Chem. Kinet.*, **1989**, *21*, 561-574.
78. Rabitz, H., Systems Analysis at the Molecular Scale, *Science*, **1989**, *246*, 221.
79. Yetter, R.; Dryer, F.; Rabitz, H., *Combust. Flames*, **1985**, *59*, 107.
80. Hwang, J. T., *Int. J. Chem. Kinet.*, **1983**, *15*, 959.
81. Sanchez-Castillo, M. A.; Agarwal, N.; Miller, C.; Cortright, R. D.; Madon, R. J., Dumesic, J. A., *J. Catal.*, **2002**, *205*, 67-85.
82. Kramer, M. A.; Kee, R. J.; Rabitz, H., CHEMSEN: A Computer Code for Sensitivity Analysis Elementary Chemical Reaction Models. SAND82-8230, Sandia National Labs, Livermore, 1982.
83. Stewart, G. W., *Introduction to Matrix Computation*, Academic Press: NY, 1973
84. Wei, J.; Kuo, J. C. A., *Ind. Eng. Chem.*, **1969**, *8*, 114.
85. Li, G.; Rabitz, H., *Chem. Eng. Sci.*, **1989**, *44*, 1413.
86. Li, G.; Rabitz, H., *Chem. Eng. Sci.*, **1991**, *48*, 1903-1909.
87. Kuo, J.C.; Wei, J., *I & EC Fundam.*, **1969**, *8*, 124-133.
88. Liao, J. C.; Lightfoot, E. N., *Biotechnol. Bioeng.*, **1988**, *31*, 869-879
89. Li, G., *Chem. Eng. Sci.*, **1984**, *39*, 1261
90. Li, G.; Rabitz, H., *Chem. Eng. Sci.*, **1990**, *45*, 977.
91. Li, G.; Rabitz, H., *Chem. Eng. Sci.*, **1991**, *46*, 95.
92. Li, G.; Rabitz, H., *Chem. Eng. Sci.*, **1991**, *46*, 2041.
93. Li, G.; Rabitz, H.; Toth, J., *Chem. Eng. Sci.*, **1994**, *49*, 343-361
94. Li, G.; Tomlin, A. S.; Rabitz, H.; Toth, J., *J. Chem. Phys.*, 1994, *101*, 1172-1187.
95. Sharaf, M. A.; Illman, D. L.; Kowalski, B. R., *Chemometrics*, John Wiley, 1986.
96. Vajda, S.; Valko, P.; Turanti, T., *Int. J. Chem. Kinet.*, **1985**, *17*, 55.
97. Wold, S.; Geladi, P.; Esbensen, K.; Ohman J., *J. Chemom.*, **1987**, *1*, 41
98. Davis, J. F.; Plovuso, M. J.; Hoo, K. A.; Bakshi, B. R., Process Data Analysis and Interpretation, In *Adv. Chem. Eng.* 25, Academic Press, 2000; pp 2-102.
99. Liu, Y. A.; Lapidus, L., *AIChE J.*, **1973**, *19*, 467.
100. Coxson, P. G., *J. Math. Anal. Appl.*, **1984**, *99*, 435-446.
101. Lam, S. H.; Goussis, D. A., *Int. J. Chem. Kinet.*, **1994**, *26*, 441-486
102. Maas, U.; Pope, S. B., *Combust. Flame*, **1992**, *88*, 239-264.
103. Androulakis, I. P., *AIChE J.*, **2000**, *46*, 361.
104. Androulakis, I. P., *AIChE J.*, **2000**, *46*, 1769.
105. DeDonder, Th., Gauthiers-Villars: Paris, 1931.
106. Aris, R.; Gavalas, G. R., *Phil. Trans. Roy. Soc.*, **1966**, *A260*, 351.
107. Aris, R., *Arch. Ratl. Mech. Anal.*, **1968**, *27*, 356.
108. Luss, D.; Hutchinson, P., *Chem. Eng. J.*, **1971**, *2*, 172.
109. Ho, T. C.; Aris, R., *AIChE J.*, **1987**, *33*, 1050.
110. Astarita, G.; Ocone, R., *AIChE J.*, **1988**, *34*, 1299.
111. Chou, M. Y.; Ho, T. C., *AIChE J.*, **1988**, *34*, 1519

112. Aris, R., *AIChEJ.*, **1989**, 35, 539.
113. Krambeck, F. J., *Chem. Eng. Sci.*, **1994**, 49, 4179-4189.
114. Ocone, R.; Astarita, G., Kinetics and Thermodynamics in Multicomponent Mixtures, In *Adv. Chem. Eng.* 24, 1-77, Academic Press: N.Y., 1998.
115. Yitzhaki, D.; Aharoni, C., *AIChE J.*, **1977**, 23, 342.
116. Sau, M., C.; Narasimhan, S. L.; Verma, R. P., A Kinetic Model for Hydrodesulfurization, In *Studies in Surface Science and Catalysis*, Froment, G. F.; Delmon, B.; Grange, P. (Eds.), Elsevier, 1997.
117. Stephan, R.; Emic, G.; Hoffman, H., *Chem. Eng. Process.*, **1985**, 19, 303-315.
118. Narasimhan, C. S. L.; Sau, M.; Verma, R. P., An Integrated Approach for Hydrocracker Modeling, In *Studies in Surface Science and Catalysis*, Froment, G. F.; Delmon, B.; Grange, P. (Eds.), Elsevier, 1997.
119. Harris, C. C.; Chakravarti, A., *Trans. of SME*, **1970**, 247, 162.
120. Boudreau, B. P.; B. R. *Am. J. Sci.*, **1991**, 291, 507-538.
121. Ho, T. C.; Chianelli, R. R.; Jacobson, A., *J. Appl. Catal.*, **1994**, 114, 131.
122. Girgis, M. J.; Gates, B. C., *I&EC Res.*, **1991**, 30, 2021.
123. Ammus, J. M., Androusoopoulos, G. P., *I&EC Res.*, **1987**, 25, 494-501.
124. Sie, S. T., *Fuel Process. Technol.*, **1999**, 61, 149-171.
125. Sonnemans, J. W. M., Hydrotreating of Cracked Feedstocks. Ketjen Catalyst Symposium, 1982.
126. Beuther, H.; Schmid, B. K., 6th World Petroleum Congress Section III, paper 20, PD7, 1963.
127. Heck, R. H.; Stein T. R., *ACS Symp., Ser.* **1977**, 22, 948-961.
128. Ho, T. C., *Catal. Rev.-Sci. Eng.*, **1988**, 30, 117.
129. Ozaki, H.; Satomi, Y.; Hisamitsu, T., *Proc. 9th World Pet. Cong.*, **1976**, 6 PD, 18 (4), 97.
130. Hensley, A. L., Jr.; Tait, A. M.; Miller, J. T.; Nevitt, T. D., US Patent 4,406,779, 1983.
131. Inoue, S.; Takatsuka, T.; Wada, Y.; Hirohama, S.; Ushida, T., *Fuel*, **2000**, 79, 843.
132. Breyse, M.; Djega-Mariadassou, G.; Pessayre, S.; Geantet, C.; Vrinat, M.; Pérot, G.; Lemaire, M.; *Catal. Today*, **2003**, 84, 129-138.
133. Venuto, P. B.; Habob, E. T., Fluid Catalytic Cracking with Zeolite Catalysts, Marcel Dekker: N.Y., 1978.
134. Trytten, L. C.; Gray, M. R.; Sanford, E. C., *I&EC Res.*, **1990**, 29, 725-730.
135. Scott, K. F., *J. C. S. Faraday I*, **1980**, 76, 2065-2079.
136. De Pontes, M.; Yokomizo, G. H.; Bell, A. T., *J. Catal.*, **1987**, 104, 147-155.
137. Krambeck, F. J., ISCRE 8; I. *Chem. Eng. Symp. Ser.*, **1984**, A260, 351.
138. Ho, T. C.; White, B. S.; Hu, R., *AIChE J.*, **1990**, 36, 685.
139. Ho, T. C.; White, B. S., *AIChEJ.*, **1995**, 41, 1513.
140. Ma, X.; Sakanishi, K.; Isoda, T.; Mochida, I., *I&EC Res.*, **1995**, 34, 748-754.
141. Ho, T. C., *AIChE J.*, **1996**, 42, 214.
142. Rangwala, H. A.; Wanke, S. E.; Otto, F. D.; Dalla Lana, I. G., *Prepr. 10th Symp. Catal.*, Kinston, Ont., June 15-18, 1986.
143. Van Dongen, R. H.; Bode, D.; van Der Eijk, H.; van Klinken, J., *I&EC Proc. Res. Dev.*, **1980**, 19, 630.
144. Luss, D.; Golikeri, S. V., *AIChE J.*, **1975**, 21, 865.
145. Grosselink, J. W.; Stork, W. H., *J. Chem. Eng. Process.*, **1987**, 22, 157-62.
146. Houalla, M.; Broderick, D. H.; Sapre, A. V.; N. K.; deBeer, V. H. J.; Gates, B. C.; Kwart, H., *J. Catal.*, **1980**, 61, 523.
147. Wilson, M. F.; Fisher, I. P. Kriz, J. F., *J. Cat.*, **1985**, 95, 155.
148. Chen, J. M.; Schindler, H. D., *I&EC Res.*, **1987**, 26, 921.

149. Aris, R., Multiple Indices, Simple Lumps, and Duplicitous Kinetics. In *Chemical Reactions in Complex Mixtures, The Mobil Workshop*, Sapre, A. V.; Krambeck, F. J. (Eds.), Van Nostrand Reinhold, 1991.
150. Stanislaus, A.; Cooper, B. H., *Catal. Rev. - Sci. Eng.*, **1994**, *36*, 75-123.
151. Shabtai, J.; Yeh, G. J. C., *Fuel*, **1988**, *67*, 314-20.
152. Wei, J.; Prater, C. D., *Advances in Catalysis*, Vol. 3, 1962.
153. Astarita, G., *AIChE J.*, **1989**, *35*, 529.
154. Chou, M. Y.; Ho, T. C., *AIChE J.*, **1989**, *35*, 533.
155. Aris, R. The Mathematics of Continuous Mixtures, In *Kinetics and Thermodynamic Lumping of Multicomponent Mixtures*, Astarita, G. A.; Sandler, S. I. (Eds.), Elsevier: Amsterdam, 1991.
156. Astarita, G.; Nigam, A., *AIChE J.*, **1989**, *35*, 1927.
157. Ho, T. C., *Chem. Eng. Sci.*, **1991**, *46*, 281.
158. Hutchinson, P.; Luss, D., *Chem. Eng. J.*, **1970**, *1*, 129.
159. Golikeri, S. V.; Luss, D., *Chem. Eng. Sci.*, **1971**, *26*, 237.
160. Ocone, R.; Astarita, A., *AIChE J.*, **1993**, *39*, 288.
161. Ho, T. C.; Li, B. Z.; Wu, J. H., *Chem. Eng. Sci.*, **1995**, *50*, 2459.
162. Golikeri S. V.; Luss, D., *AIChE J.*, **1972**, *18*, 277.
163. Pachovsky, R. A.; Wojciechowski, B. W., *J. Catal.*, **1975**, *37*, 120.
164. Pachovsky, R. A.; Wojciechowski, B. W., *J. Catal.*, **1975**, *37*, 358.
165. Köseoglu, R. O.; Phillips, C. R., *Fuel*, 1988, *66*, 741.
166. Köseoglu, R. O.; Phillips, C. R., *Fuel*, 1988, *67*, 906, 1411.
167. Anthony, D. B. Howard, J. B., *AIChE J.*, **1976**, *22*, 625.
168. Schucker R. C., *ACS Symp. Div., Fuel. Chem.*, **1982**, *27*, 214.
169. Braun, R. L.; Burnham, A. K., *Energy Fuels*, **1987**, *1*, 153.
170. Lin, L. C.; Deo, M. D.; Hanson, F. V.; Oblad, A. G., *AIChEJ.*, **1990**, *36*, 1585.
171. Laximinarasimhan, C. S.; Verma, R. P.; Ramachandran, P. A., *AIChEJ.*, **1993**, *42*, 2645.
172. Bennett, R. N.; Bourne, K. H., *ACS Symp. Advances Distillate and Residual Oil Technology*, New York, 1972.
173. El-Kardy; F. Y., *Indian J. Technol.*, **1979**, *17*, 176.
174. Cicarelli, P.; Astarita, G.; Gallifuocco, A., *AIChE J.*, **1992**, *38*, 7.
175. Browarzik, D.; Kehlen, H., *Chem. Eng. Sci.*, **1994**, *49*, 923.
176. Teymour, F.; Campbell, J. D., *Macromolecules*, **1994**, *27*, 2460-2469.
177. Wang, M.; Smith J. M.; McCoy, B. J., *AIChEJ.*, **1995**, *41*, 1521-1533.
178. Kodera, Y.; McCoy, B. J., *AIChE. J.*, **1997**, *43*, 3205-3214.
179. Kruse, T. M.; Woo, O. S.; Broadbelt, L. J., *Chem. Eng. Sci.*, **2001**, *56*, 971-979.
180. Golikeri, S. V.; Luss, D., *Chem. Eng. Sci.*, **1974**, *29*, 845.
181. Luss, D.; Golikeri, S. V., *AIChE J.*, **1975**, *21*, 865.
182. Astarita, G., Chemical Reaction Engineering of Multicomponent Mixtures: Open Problems, In *Kinetics and Thermodynamic Lumping of Multicomponent Mixtures*, Astarita, G. A.; Sandler, S. I. (Eds.), Elsevier: Amsterdam, 1991.
183. Li, B. Z.; Ho, T. C., An Analysis of Lumping Bimolecular Reactions, In *Lumping Kinetics and Thermodynamics*, Astarita, G. A.; Sandler, S. I. (Eds.), Elsevier: Amsterdam, 1991.
184. White, B. S.; Ho, T. C.; Li, H. Y., *Chem Eng. Sci.*, **1994**, *49*, 781.

## Chapter 22

# ADVANCED PROCESS CONTROL

Paul R. Robinson<sup>1</sup> and Dennis Cima<sup>2</sup>

1. *PQ Optimization Services, 3418 Clear Water Park Drive, Katy, TX 77450*
2. *Aspen Technology, Inc., 1293 Eldridge Parkway, Houston, TX 77077*

## 1. INTRODUCTION

At relatively low cost, model-predictive control improves the capability of process units by increasing throughput, improving fractionator performance, decreasing product quality giveaway, reducing operating costs, and stabilizing operations. Figure 1 presents an overview of the scope of refinery software applications and indicates the frequency at which they typically run.

## 2. USEFUL DEFINITIONS

A *proportional-integral-derivative* (PID) controller is a feedback device. A *process value* (PV) is measured by a field transmitter. A controller compares the PV to its *setpoint* (SP) and calculates the required change – for example, a new *valve opening position* (OP) – to bring the PV closer to the SP. The required change is calculated with a PID algorithm. In practice, proportional, integral, and derivative constants are parameters used for tuning.

*Advanced process control* (APC) applications involve the use of control algorithms to provide improved process control when compared to regulatory PID controllers in loops or cascades.

*Traditional Advanced Control* (TAC) employs the use of advanced control algorithms combined with regulatory control functions (i.e., lead/lag, ratio, high/low selectors, etc) to implement a control strategy.

A *programmable logic controller* (PLC) is a small computer used to automate real-world processes. A PLC receives input from various sensors

and responds to changes by manipulating actuator valves according to pre-programmed logic stored in the memory of the PLC.

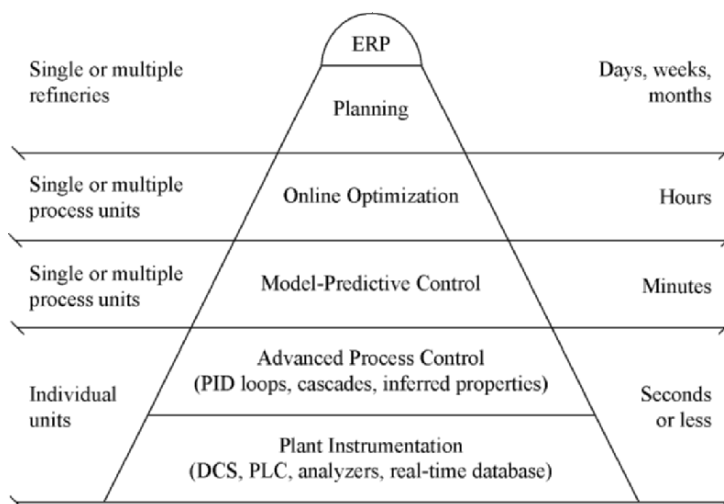


Figure 1. Overview of computer control applications. ERP stands for enterprise resource planning, a software solution that integrates planning, manufacturing, sales, and marketing.

In a **distributed control system** (DCS), process measurements and control functions such as multiple PID loops are connected to application processors, which are networked throughout the plant. A **graphical user interface** (GUI) makes it easier for operators to view data, create plots, change setpoints, and respond to alarms. In addition to process control, modern DCS software includes sophisticated trending and data storage.

**Multivariable process control** (MVPC) applications use one or more independent variables to control two or more dependant variables. If a variable is truly independent, its value is not affected by other process variables. There are two types of independent variables. **Manipulated variables** (MV) can be changed by an operator to control the process. These include setpoints for regulatory PID controllers and valve positions. **Feed-forward** (FF) and **disturbance variables** (DV) affect the process but can't be manipulated. These include ambient temperature, the quality of an external feed, etc.

The value of a dependent variable can be calculated using the values of independent variables and an appropriate dynamic model. **Controlled variables** (CV) are maintained at a desired steady-state target. Constraint variables are maintained between high and low limits. Many variables are dependent, but not all dependent variables are important enough to be controlled by the APC application.

**Model-predictive control** (MPC) uses process models derived from past process behavior to predict future process behaviour.<sup>1</sup> The predictions are used to control process units dynamically at optimum steady-state targets. MPC applications may also include the use of predicted product properties (*inferential analyzers*) and certain process calculations. Model-predictive controllers almost always include multiple independent variables.

In this chapter, when we say “model-predictive control” we mean constrained, multivariable, model-predictive control, which is arguably the predominant type of “advanced control” application in the petroleum refining industry.

### 3. OVERVIEW OF ECONOMICS

Table 1 presents typical benefits for applying model-predictive control to refinery units.<sup>2</sup> After installation of the requisite infrastructure – distributed control system, analyzers, operator terminals, process computer(s) – model-predictive control projects on major refinery units can be completed within 2 to 4 months. The return on investment is quite high; typical payback times usually are 4 to 12 months.

*Table 1.* Typical Benefits of Multivariable Model-Predictive Control

| Process Unit             | Typical Benefits<br>\$U.S./bbl | Source(s)  |
|--------------------------|--------------------------------|--|
| Crude distillation       | 0.015 to 0.03                  | Higher feed rate<br>Reduced product quality giveaway*<br>Increased energy efficiency   |
| Fluid Catalytic Cracking | 0.15 to 0.30                   | Higher feed rate<br>Reduced $\Delta P$ across slide valves<br>Reduced product quality giveaway*<br>Increased energy efficiency                           |
| Catalytic reformer       | 0.10 to 0.20                   | Higher feed rate<br>Maximum coke on catalyst (CCR units)<br>Reduced product quality giveaway*<br>Increased energy efficiency                             |
| Hydrocracker             | 0.10 to 0.20                   | Higher feed rate<br>Improved control of gas/oil ratio<br>Increased T and P stability<br>Reduced product quality giveaway*<br>Increased energy efficiency |
| Gas Oil Hydrotreater     | 0.02 to 0.10                   | Higher feed rate<br>Improved control of gas/oil ratio<br>Increased T and P stability<br>Reduced product quality giveaway*<br>Increased energy efficiency |
| Gas plant                | 0.05 to 0.10                   | Higher feed rate<br>Reduced product quality giveaway*<br>Increased energy efficiency   |
| Product blending         | 0.10 to 0.20                   | Reduced product quality giveaway*  |

\*Equivalent to increased production of desired products



The applications that benefit most from model-predictive control have one or more of the following characteristics:

- High production capacity
- Competing control objectives
- Highly interactive processes
- Unusual dynamic behavior
- Day/night or seasonal variation
- A need to operate close to constraints
- A need to closely track optimization system targets
- A need to transition smoothly from one set of targets to another

In refineries, the largest benefits of model-predictive control come from crude distillation units and gasoline blenders, for which the throughput is high, and from fluid catalytic cracking (FCC) and other conversion units, for which the difference in value between feeds and products usually is high.

#### **4. SOURCES OF BENEFITS**

The benefits of APC and model-predictive control come from one or more of the following:

- Reduced process variability
- Maximizing throughput against multiple process constraints
- Increased yield of high-value products
- Reduced product quality giveaway
- Reduced production losses<sup>3</sup>

These benefits accrue from two sources – increased process capability due to reduced variability, and constraint pushing.

Variability is a characteristic of all continuous processes. As shown in Figure 2, simply reducing variability provides little (if any) benefit. Benefits start to accumulate when operators run the plant closer to true process constraints.

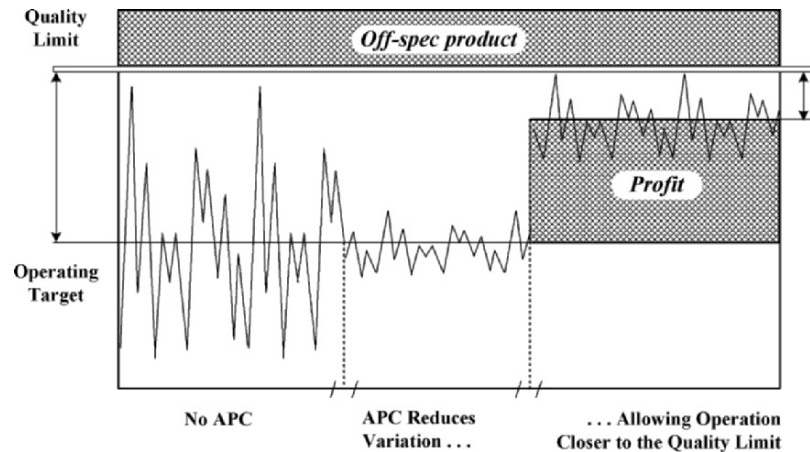


Figure 2. Reduced variation: one source of APC benefits

For example, if a low-pressure hydrotreater must produce off-road diesel fuel with  $\leq 500$  wppm sulfur to meet product specifications, and if there is a severe economic penalty for exceeding the specification, the refiner may set a process target of 350 wppm to ensure that the plant never exceeds the limit. In this case, the difference between the target and the limit – i.e., the cushion – is 150 wppm. A cushion of this size is not atypical for coastal refineries where feed quality and/or hydrogen composition can change significantly from one day to the next, and where there is limited ability to correct a specification violation with blending. But a 30% cushion is expensive, resulting in higher operating cost and accelerated catalyst deactivation. If increased stability allows the process target to be raised from 350 wppm to 450 wppm, hydrogen consumption will decrease, heater firing will decrease and catalyst cycle life will increase significantly.

Figure 3 illustrates how model-predictive control can achieve additional benefits by pushing against process constraints. Plant operators tend to run complex units within a certain comfort range. This comfort range gives an operator extra time or cushion to respond to process changes.

An APC application responds quickly to process changes. A well-tuned model-predictive control application can run outside the comfort range of a human operator while pushing simultaneously against multiple process constraints. More significantly, a model-predictive control application can calculate moves for each MV every minute, which a plant operator cannot. Special techniques, such as move suppression, are used to prevent the plant from moving too far too fast.

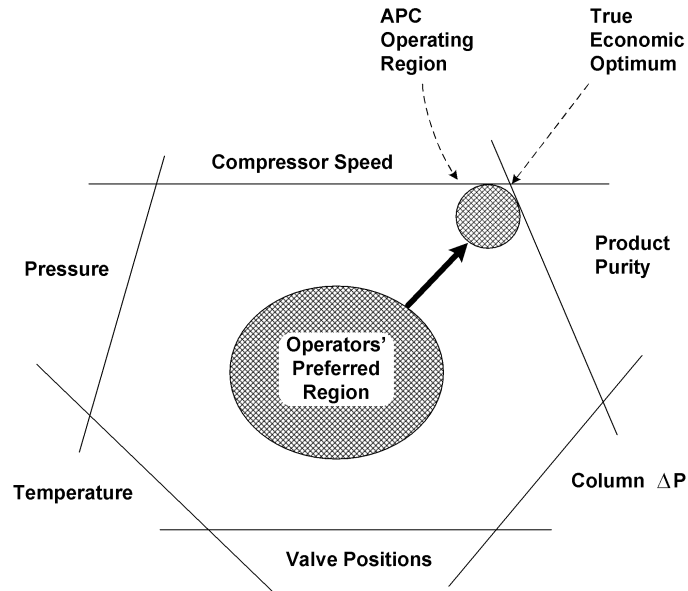


Figure 3. Operating near the right constraints: major source of APC benefits

In certain special circumstances – emergencies, startups, and shutdowns – model-predictive control cannot be used. It is more realistic to say that well-tuned, well-maintained model-predictive control application can emulate the plant’s best operator – every minute of every day. Figure 4 compares the temperature response to a soot-blowing disturbance under three types of control. The solid line shows the open-loop (manual) response. The heavily dotted line shows better response with a PID (feedback) controller. The lightly dotted line shows superb response with model-predictive control.

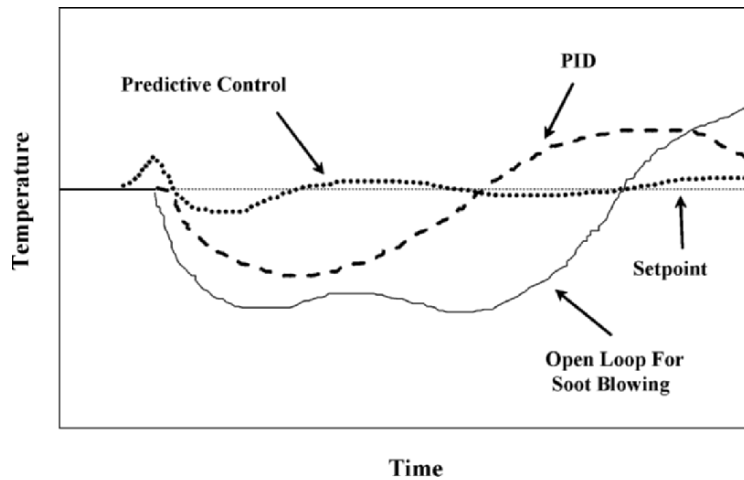


Figure 4. Comparison between open-loop, PID and model-predictive control

## 5. IMPLEMENTATION

The implementation of model-predictive control requires four main steps – plant response testing, model analysis, commissioning, and training.

During the plant response testing phase of a project, independent variables are moved and dependant variable responses are captured electronically. Obtaining good plant test data from which accurate models can be regressed is the key to a successful model-predictive control project. For this reason, special care must be taken to ensure that the underlying instrumentation – meters, analyzers, and PID controllers – are properly tuned and calibrated. Traditionally, independent variables were moved manually during the plant response test, but with recently developed software, an engineer can obtain equivalent plant test data using closed loop testing methods. Proprietary identification software converts response-test data into dynamic models for the plant. Response-test models can be used to predict future plant behavior with the following control equation:

$$\delta CV = [A] \times \Delta I$$

where  $\delta CV$  is the predicted change in a given CV,  $[A]$  is the gain matrix obtained during the model analysis phase, and  $\Delta I$  is a matrix of independent variable changes. Figure 5 shows an example of the control equation in matrix form.

$$\begin{array}{c}
 \delta CV \\
 \downarrow \\
 \begin{bmatrix} \delta CV_1 \\ \delta CV_2 \\ \delta CV_3 \\ \delta CV_4 \\ \delta CV_5 \\ \delta CV_6 \\ \delta CV_7 \end{bmatrix}
 \end{array}
 =
 \begin{array}{c}
 A \\
 \downarrow \\
 \begin{bmatrix} 1 & & \\ 4 & 1 & \\ 6 & 4 & 1 \\ 7 & 6 & 4 \\ 7 & 7 & 6 \\ 7 & 7 & 7 \\ 7 & 7 & 7 \end{bmatrix}
 \end{array}
 *
 \begin{array}{c}
 \Delta I \\
 \downarrow \\
 \begin{bmatrix} \Delta I_1 \\ \Delta I_2 \\ \Delta I_3 \end{bmatrix}
 \end{array}
 =
 \begin{array}{c}
 \begin{bmatrix} 1 \\ 4 \\ 4 \\ -1 \\ -5 \\ -7 \\ -7 \end{bmatrix}
 \end{array}$$

Figure 5. Example of the control equation in matrix form

Model predictions are used to control the plant against constraints, as shown in Figure 3. This is not a trivial matter, because the application must cope successfully with the following:

- Plant/model mismatch
- Instrument failure
- Unmeasured Disturbances
- Input data error
- Diverse process dynamics
- Changing process objectives

Despite these challenges, when implemented by qualified personnel, model-predictive control applications provide considerable value for refiners throughout the world.

## 6. COSTS

Figure 6 illustrates the infrastructure required for computer control. APC and model-predictive control software usually runs on a separate process computer, which uses a “data highway” to communicate with the DCS, the laboratory information management system (LIMS), and a real-time database. Advanced applications receive process values from the DCS, calculate the sizes of MV moves, and send setpoints back to the DCS.

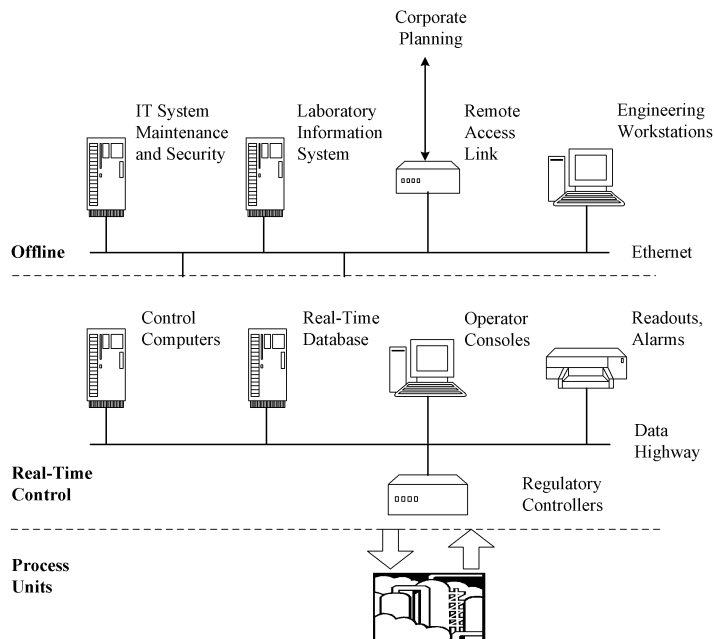


Figure 6. Automation infrastructure

Figure 7 compares the relative costs and benefits of computer applications. As is the case for a personal computer, hardware accounts for most of the cost, but software provides most of the benefit.

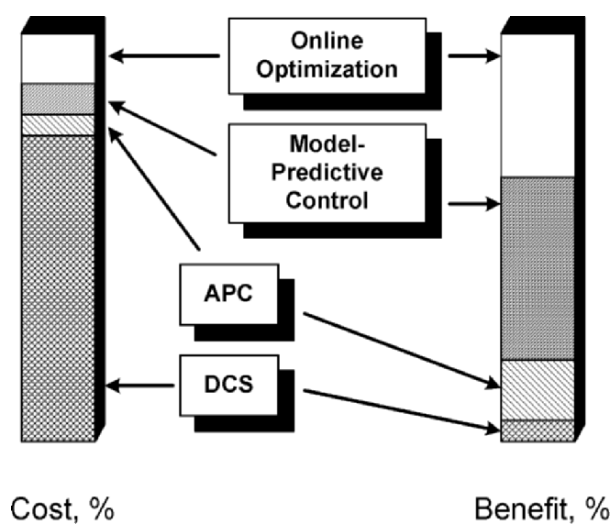


Figure 7. Relative costs and benefits of computer applications in oil refineries

## 7. REFERENCES

1. Cutler, C.R.; Ramaker, B.L. "Dynamic Matrix Control – A Computer Algorithm," AIChE National Meeting, Houston, TX, April 1979.
2. Richard, L.A.; Spencer, M.; Schuster, R.; Tuppinger, D.M.; Wilmsen, W.F., "Austrian Refinery Benefits from Advanced Control," Oil Gas J., March 20, 1995.
3. Vermeer, P.J.; Pedersen, C.C.; Canney, W.M.; Ayala, J.S., Blend Control System All But Eliminates Reblends for Canadian Refiner, Oil Gas J., 95(30), July 28, 1997.

## Chapter 23

# REFINERY-WIDE OPTIMIZATION WITH RIGOROUS MODELS

Dale R. Mudt,<sup>1</sup> Clifford C. Pedersen,<sup>1</sup> Maurice D. Jett,<sup>2</sup> Sriganesh Karur,<sup>2</sup> Blaine McIntyre,<sup>3</sup> and Paul R. Robinson<sup>4</sup>

1. *Suncor, Inc, Sarnia, Ontario, Canada*
2. *Aspen Technology Inc., Houston, Texas*
3. *AspenTech Canada Ltd., Calgary, Alberta, Canada*
4. *PQ Optimization Services, Katy, Texas*

## 1. INTRODUCTION

One reason for writing this chapter is to report the success of real-time, online refinery-wide optimization (RWO) at Suncor-Sarnia using rigorous process models. Another reason is to show how the same rigorous models can be used offline to quantify key non-linear relationships during the evaluation of project ideas, especially those related to the production of clean fuels.

## 2. OVERVIEW OF SUNCOR

Suncor operates a 70,000 barrels-per-day refinery at Sarnia, Ontario, Canada. The refinery processes feeds from the following sources:

- Synthetic crude oil from Suncor's oils sands processing plant at Fort McMurray, Alberta, Canada
- Conventional crude oil
- Condensate
- VGO from a nearby refinery

Figure 1 shows an outline of the plant, which started up in 1953. Synthetic crude and conventional crude oil come to the refinery through the Interprovincial Pipeline, which runs from Edmonton, Alberta to Sarnia,

Ontario. The transit time is about one month. Other crudes are also available from nearby facilities.

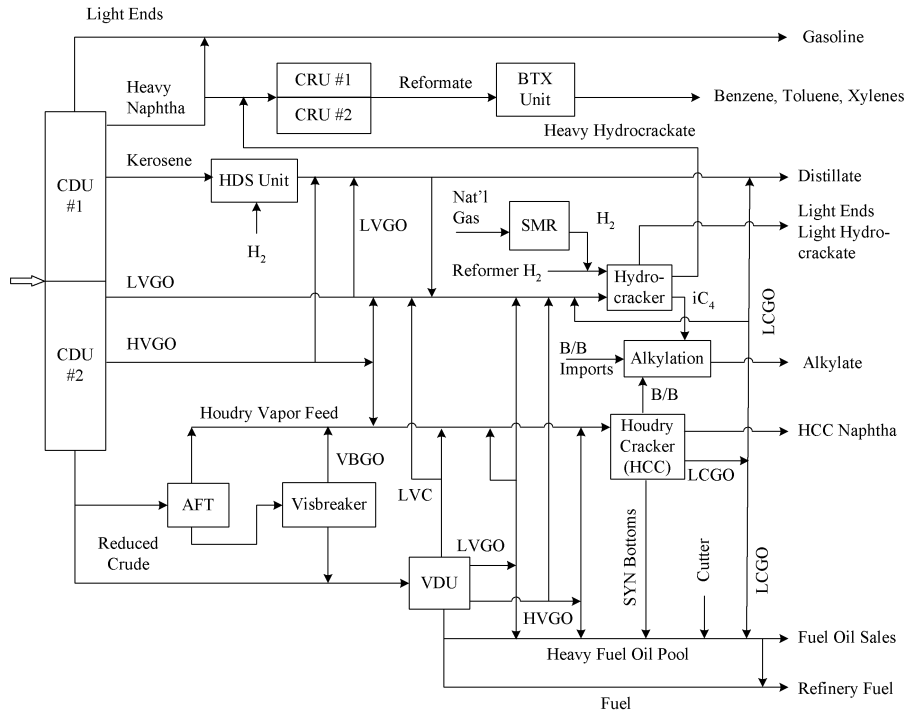


Figure 1. Overview of the Suncor Refinery in Sarnia, Ontario

The refinery includes the following major process units:

- Crude distillation (CDU) — 2 units
- Vacuum distillation (VDU)
- Houdriflow catalytic cracking unit (HCC)
- Catalytic reforming (CRU) — 2 units
- Alkylation unit
- Aromatics recovery unit (BTX)
- Unsaturated gas plant
- Saturated gas plant
- Naphtha hydrotreater
- Diesel / gas oil hydrotreater
- Hydrocracker complex



### 3. REFINERY-WIDE OPTIMIZATION (RWO)

The refinery-wide optimization (RWO) initiative began in July 1998. Three phases were defined for the project:

- Phase 1.** Build a solid and sustainable advanced control and optimization foundation
- Phase 2.** Ensure model consistency between planning, scheduling, and real-time optimization
- Phase 3.** Integrate planning, scheduling, and real-time optimization by linking the optimization models to the refinery LP

Expected benefits from the RWO initiative included:

- Increased refinery throughput
- Improved refinery yields
- Improved gas oil management
- Improved hydrogen management
- Optimum product recoveries
- Reduced energy costs
- Increased ability to respond to market changes

Rigorous models for stand-alone units also can provide significant benefits. Previously,<sup>1</sup> we reported benefits of US\$3,000 per day (US\$0.15 per barrel) for the initial optimizer on the hydrocracking complex; these benefits were in addition to those provided by model-predictive DMC control. For RWO, a revised model based on Aspen Hydrocracker (AHYC) was developed. It includes a catalyst deactivation block, which enhances maintenance turnaround planning by predicting future catalyst activity, product yields and product properties for a variety of assumed feeds and specified operating conditions. This information also is used to impose constraints on present-day operation.

The RWO initiative was driven in part by the need to upgrade or replace software applications that were not Y2K compliant. In addition, the project reduced application maintenance costs because the same software versions are used throughout the plant, and because modern control and optimization software is more user-friendly than it was in the 1980s, when Suncor first began implementing model-predictive control and online optimization.

Table 1 summarizes the scope of the major RWO applications. A large DMCplus application—64 manipulated variables (MV) x 16 feed forward variables (FF) x 168 controlled variables (CV)—controls Plant 1. For Plant 1, the process scope of the controller is equivalent to that of the optimizer, which sends 34 targets to the controller. In Plant 3, separate controllers are used for the hydrogen plant, the HYC, the HYC gas plant, and low-sulfur diesel (LSD) tower, but a single optimizer sends targets to these controllers.

Table 1. Scope of Refinery-Wide Optimization Applications

| <b>Scope</b>                        |   |
|-------------------------------------|---|
| <b>Plant 1</b>                      |   |
| Crude and HCC                       | Preheat Train, Crude Heaters, Crude Tower, Atmospheric Flash Tower, Syn Tower, HCC Heaters, Reactor, Kiln, Steam Coils, Air Blower, Cyclone, Main Fractionator, Unsaturated Gas Plant |
| <b>Plant 2</b>                      |   |
| Crude and Vacuum Reformer 2 and BTX | Preheat Train, Heaters, Atmospheric Tower, Vacuum Tower Heaters, Compressors, Pretreater, Reactors, Flash Drums, Depropanizer, Naphtha Splitter, Absorber/Deethanizer, BTX Complex    |
| <b>Plant 3</b>                      |   |
| SMR, HYC, Gas Plant                 | H <sub>2</sub> Plant, Hydrocracker Reactor Section, Preflash, Main Tower, Absorber/Stripper, Debutanizer, Jet Tower, Diesel Tower, Saturated Gas Plant                                |

The RWO initiative is using the hardware and software in Table 2.

Table 2. Hardware and Software for RWO

| <b>Item</b>           | <b>Vendor</b>                        |
|-----------------------|--------------------------------------|
| DCS Systems           | Honeywell TDC 2000/3000, Foxboro I/A |
| Online Computers      | DEC Alpha (VMS)                      |
| Offline Computers     | Compaq (Windows NT)                  |
| Real-Time Database    | Aspen Infoplus, Honeywell PHD        |
| Control Software      | DMCplus, Aspen IQ                    |
| Optimization Software | Aspen RT-Opt                         |
| Refinery LP           | Haverly GRTMPS                       |

Each optimizer includes an offline version, which is periodically updated with live plant data. Offline models are used for tuning and monitoring the performance of the optimizers. They can also be used for maintenance planning and design studies.

The success of RWO depended heavily upon proper integration of the several separate applications. Integration points fell into three categories (Table 3). Intermediate tanks presented special problems in part because they tend to stratify, but mostly because they complicate time-scale issues. For several critical tanks, open-equation models calculate tank compositions on a regular basis—about every 5 minutes—to provide feed-forward inputs to other optimizers or possibly DMCplus controllers. Special logic is used to compensate for stratification. To date, these tank composition models are performing well.

Table 3. Integration Point categories

| <b>Type of Integration Point</b>  | <b>Time Scale</b> |
|---|-------------------|
| Feed forward information required by the model predictive controllers       | Minutes           |
| Steady state information (inputs to and outputs from) the online optimizers | Hours             |
| Higher level information (inputs to and outputs from) the refinery LP       | Daily             |

Other key integration points are shown in Table 4:

*Table 4. Key Integration Points*

|   |    |                      |
|---|----|----------------------|
| Plants 2 (H <sub>2</sub> from reformer)               | => | Plant 3 (HYC)        |
| Plants 1, 2, and 3 (reformates and HYC light naphtha) | => | Gasoline blender     |
| Plant 3 (HYC heavy naphtha)                           | => | Plant 2 (Reformer 2) |
| Plant 3 (isobutane)                                   | => | Plant 1 (alky feed)  |

Integrating the real-time optimizers into Suncor's planning and scheduling methodology will require consistency between the optimizers and the refinery LP in the following areas:

- Yields and product qualities
- Degrees of freedom
- Constraints

At present, data are transferred manually between the LP and the optimizers. This is beneficial because the models allow us to increase the accuracy of LP shift vectors. A recent publication<sup>2</sup> describes the benefits of running steady-state models in recursion with Aspen PIMS, a widely used LP program. This method may offer the best of both worlds—the practicality of LP technology augmented by the rigor of non-linear, unit-specific models.

During RWO Phase 3, the transfer of data will be automated, section by section, as we gain confidence in the robustness of the individual optimizers, and in the fidelity of the LP solutions.

#### 4. RIGOROUS MODELS FOR CLEAN FUELS

As mentioned above, one purpose of this paper is to show how rigorous models can be used offline to quantify key non-linear process relationships, including those related to manufacturing clean fuels.

At most North American refineries, including Suncor-Sarnia, most of the sulfur in the gasoline pool comes from a catalytic cracking unit. To make low-sulfur gasoline, an Axens Prime-G unit was installed to desulfurize gasoline from the HCC and visbreaker units. Another option would have been to pretreat all of the HCC feed.<sup>3</sup> (Already, hydrocracker bottoms comprise some of the HCC feed, but only a minor fraction.)

To summarize: our RWO experience has demonstrated the following:

- Rigorous optimizers provide significant economic benefits
- Open-equation optimizers can be linked, and linked optimizers can successfully represent non-linear interactions between process units.
- AFCC (modified) and AHYC provide high-fidelity representations of Suncor's HCC and hydrocracker, respectively.

- Therefore, we can conclude that linking AHYC with AFCC will enhance the industry's understanding of FCC feed pretreating, and eventually to operate FCC-plus-pretreater installations as a single, optimized complex.

#### 4.1 Feedstock and Product Characterization

For any rigorous model, success requires detailed, accurate feedstock and product characterizations. For the HCC and hydrocacker, GC/MS,  $^1\text{H}$  NMR,  $^{13}\text{C}$  NMR, HPLC, and standard ASTM methods were used to analyze a battery of feedstock and product samples. The analytical results were used to generate base-case distributions for the components used in the models and to tune reaction kinetics.

In the real world, feedstock properties and product slates are changing continually. In AFCC and AHYC, proprietary feed-adjust models skew the base-case component distribution to match the measured properties of feeds and products.

#### 4.2 Aspen FCC Overview

Aspen FCC (AFCC) is an open-equation, flowsheet-based model designed for both online and offline applications. The model is constructed from individual blocks that represent the separate pieces of equipment—riser, standpipe, slide valve, cyclone, transfer line, etc.—found in commercial FCC units. Each building block is generic and can be configured with dimensions corresponding to a given commercial unit (Table 5).

*Table 5. Aspen FCC Building Blocks*

---

|   |
|---|
| Riser model: hydrodynamics and kinetics         |
| Reactor-vessel cyclones and plenum model        |
| Reactor dilute-phase model                      |
| Reactor dense-bed model                         |
| Reactor stripping zone model                    |
| Catalyst stand-pipe model                       |
| Catalyst slide-valve two-phase flow model       |
| Catalyst transfer-line model                    |
| Regenerator dense-bed model: coke burn kinetics |
| Regenerator freeboard model: coke burn kinetics |
| Regenerator cyclone model                       |
| Feed characterization, component-mapping model  |

---

A typical FCC unit configuration is presented in Figure 2. The diagram shows a simple version of the actual blocks used to model the feed, feed adjust and preheat systems.

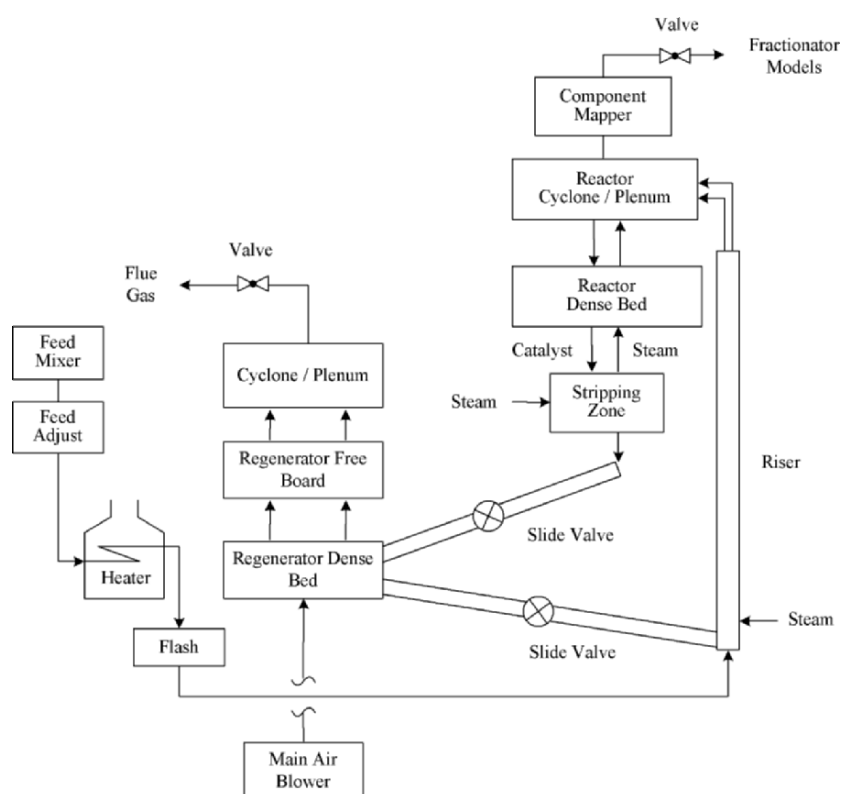


Figure 2. Model Components for Aspen FCC (Riser/Reactor/Regenerator)

In the riser model, detailed hydraulics and heat effects are captured by linking flow equations to kinetics. The riser model can be configured vertically, horizontally, or at any angle of inclination. Multiple risers can be used. The individual risers can process different feeds or the same feed. In essence, any commercial riser/reactor configuration can be simulated with the modular components of AFCC.

Hydrocarbon feed and regenerated catalyst models are connected to the inlet of the Riser model. The catalyst-stream model includes the mass flow, temperature, pressure, enthalpy of the catalyst/coke mixture, particle density of the catalyst/coke mixture, coke-on-catalyst weight fraction and coke composition.

Pressure drop calculations are based on head, acceleration, and frictional effects. Pressure drop through the riser is modeled as a combination of

pressure drop due to vapor and pressure drop due to solids. For the vapor, the frictional contribution is based on friction-factor correlations with the Reynolds number. For catalyst flow, frictional contributions are based on correlations for solid-vapor flow in a conduit. Proper prediction of pressure drop along the riser has a significant impact on predicted yields.

The riser model uses vertical or horizontal slip factor correlations (depending on the riser orientation) to determine the differential velocity between the vapor and the solid phases. The slip calculation is critical for determining bulk density profiles, which govern the path dependence of cracking profiles.

As coke is differentially produced along the length of the riser, additional solids are differentially transferred from the vapor to the catalyst surface. The physical effects of this transfer are described by continuity equations. The molar heat of adsorption for coke laydown is included in the heat balance. The heat of coke desorption is calculated in the regenerator model. Slip-factor correlations are based on fully developed flow. The model applies a correction for the turbulent, high-slip zone at the inlet of the riser.

The riser model effluent is connected to the reactor vessel models. These include the reactor dilute phase, the dense phase, and the cyclone system, which represents the segregation of effluent vapors and catalyst. The cyclone model performs a two-phase, loading-based  $\Delta P$  calculation, for which cyclone inlet and body diameters are used. The cyclone model can be configured with one or two riser inlet ports.

The reactor dilute phase model is identical to the riser model without entry-zone and frictional effects. The reactor dense bed model can be configured to the exact geometry of an operating unit. It is used to represent the inventory of spent catalyst above the stripping zone. For large vessels with significant holdup, this model can be configured as a fluidized bubbling bed system. For low holdup or riser-cracking systems, it is treated as a fluidized bed with a parameterized void fraction.

Spent catalyst and regenerator air are connected to the regenerator model. The regenerator includes three blocks, each of which can be configured for a specific unit. The first block (from the bottom up) is the regenerator dense bed. This model represents the bubbling, fluidized bed where the majority of coke burn occurs. The second block is the regenerator free board (disperse phase), which is the region between the surface of the bubbling bed (dense bed) and the inlet to the cyclones. The third block is the regenerator cyclone model.

The regenerator dense bed is modeled as a bubbling bed with heterogeneous coke burn and CO conversion to CO<sub>2</sub>. Bulk density is modeled as a function of bed height and pressure. Promoters are modeled by updating selected coke-burn parameters. Combustion air composition is determined

independently by the regenerator air model. Therefore, O<sub>2</sub> enrichment can be simulated and optimized.

The regenerator freeboard model represents the vessel region between the surface of the dense bed and the cyclone inlets. Inlets to the model are entrained, regenerated catalyst from the dense-bed model and the combustion-gas stream from the dense bed. Outlets from the model are the freeboard combustion-gas stream and the catalyst stream from the cyclones. The freeboard is modeled as a simple plug-flow reactor with homogeneous CO-to-CO<sub>2</sub> after-burn. Temperatures may rise rapidly in the presence of excess O<sub>2</sub>.

The regenerator cyclone model performs a two-phase, loading-based  $\Delta P$  calculation. Flue-gas compositions are calculated and reported on a standard dry mole percent basis for parameterization purposes. The flue gas stream can be connected to the valve model between the regenerator and CO boiler, or to a downstream power recovery system.

Inputs and outputs for the blocks described below are compatible with the vapor and catalyst streams used in the reactor/regenerator models.

The stripping zone model performs heat, mass and pressure balance calculations around the stripping zone. A tunable stripping efficiency curve is included. The stripping efficiency is related to the ratio of catalyst flow to stripping-steam flow.

The catalyst standpipes create a standing head that drives catalyst circulation. Different FCC designs make more or less use of standpipe technology. Standpipes typically end at a slide valve, which is used to control catalyst circulation. Standpipe diameter and length are variables in the standpipe model.

The catalyst transfer line model represents the pneumatic transport regime in the catalyst transfer line. Transfer-line diameter and length are configurable. Like the riser model, the catalyst transfer line model can be configured as vertical, horizontal or inclined.

The slide valve model calculates  $\Delta P$  for a two-phase, loading-based orifice. The valve coefficient is parameterized from measured slide valve position (percent open) and pressure differential across the slide valve.

Components with similar reaction kinetics are grouped into 21 lumps. These kinetic lumps are listed in Table 6. In practice, the 21 components provide sufficient granularity to model all of the important steady-state cause-and-effect relationships in the FCC reactor-regenerator complex. Kinetic parameters for the riser and reactor models are segregated from the hydraulics and heat balance relationships. This permits different FCC kinetic schemes to be implemented within the same rigorous riser/reactor models. The off-line version of the model includes a simplified fractionator model and a product-property model.

Table 6. Aspen FCC 21 Reactive Lumps

---

|                                      |
|--------------------------------------|
| Gas lump                             |
| Gasoline lump                        |
| 221-343°C (P, N, As, Ar1, Ar2)       |
| 343-510°C (P, N, As, Ar1, Ar2, Ar3)  |
| 510°C-plus (P, N, As, Ar1, Ar2, Ar3) |
| Coke (2 lumps)                       |

---

The simplified fractionator includes a delumper model to convert the 21 kinetic lumps into >80 pure- and pseudo-components, which are then divided into user-specified boiling fractions. A non-linear distribution function generates ideal distillation curves with realistic fraction-to-fraction overlap. The fractionator can inter-convert distillation methods, so a user can calculate D-86, D-1160, D-2887, and/or TBP curves for gasoline and LCO.

The product property model generates the product properties listed in Table 7. During projects, other product property calculations are added as needed. The online application at Suncor-Sarnia does not use the simplified fractionator model. Instead, it uses fully rigorous tray-by-tray models for the HCC fractionation section.

Table 7. Aspen FCC Standard Product Properties

---

| As-Fractionated Product Properties |             |                  |        |             |     |     |      |
|------------------------------------|-------------|------------------|--------|-------------|-----|-----|------|
|                                    | API Gravity | Specific Gravity | Sulfur | Cloud Point | RON | MON | PONA |
| Gasoline                           | x           | x                | x      |             | x   | x   | x    |
| LCO                                | x           | x                | x      | x           |     |     |      |
| HCO                                | x           | x                | x      |             |     |     |      |
| Bottoms                            |             | x                | x      |             |     |     |      |
| Standard-Cut Product Properties    |             |                  |        |             |     |     |      |
| Light Naphtha                      | x           | x                | x      |             | x   | x   | x    |
| Heavy Naphtha                      | x           | x                | x      |             | x   | x   | x    |
| LCO                                | x           | x                | x      | x           |     |     |      |
| Bottoms                            | x           | x                | x      |             |     |     |      |

---

### 4.3 Aspen Hydrocracker

In many respects, AHYC is simpler than AFCC, mainly because it doesn't have to model the flow of a solid phase. Complexity arises for the following reasons:

- A separate reactor is used for each catalyst bed.
- The same set of reactions is used for both fixed-bed hydrotreating and fixed-bed hydrocracking units.
- All recycle loops are closed.
- More components and reactions are required. The model employs 116 components and 195 reactions.



- Catalyst deactivation has a major impact on the economics of a fixed-bed hydrocracker.

AHYC is an update of SARCRACK, a hydrocracker model developed by Sun Oil Company,<sup>4</sup> and modified by Suncor Sarnia with assistance from DMC corporation for online optimization. The component slate and reaction network for AHYC are consistent with publications by Klein, et al., Stangeland,<sup>5</sup> Quann, et al.,<sup>6,7</sup> Filiminov, et al.,<sup>8</sup> and Jacobs.<sup>9</sup>

Figure 3 presents a diagram of the high-pressure reaction section of the hydrocracker at Suncor-Sarnia. The unit is a classical single-stage Unicracker with two reactors. In the first (R1), all three beds are loaded with high-activity hydrodenitrogenation (HDN) catalyst. In the second (R2), all four beds are loaded with a zeolite-based, distillate-selective hydrocracking catalyst. For both reactors, the incoming gas is heated separately. The unit has two separator drums. The hydrogen-rich gas from the overhead of the high-pressure separator (HPS) is recycled. The HPS bottoms flow through a power-recovery turbine (PRT) to the low-pressure separator (LPS). LPS bottoms go through a pre-flash tower to the main fractionator.

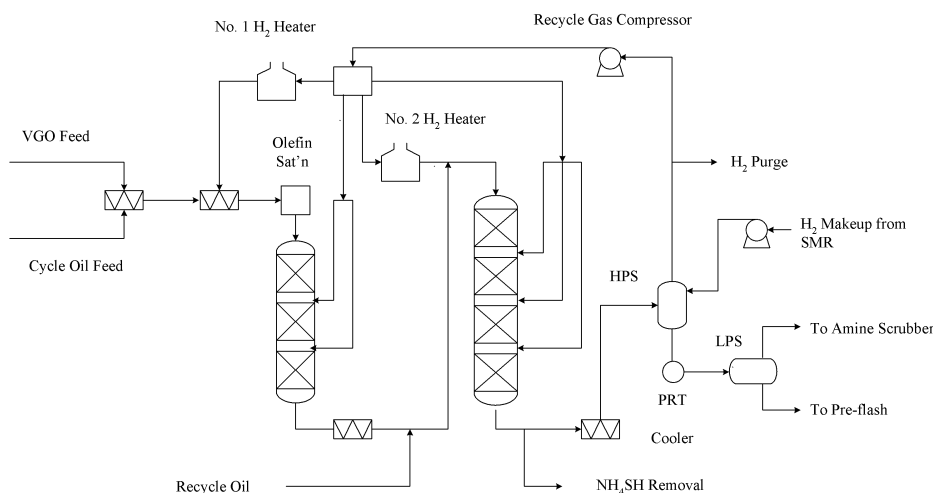


Figure 3. AHYC Model for the Suncor Sarnia Hydrocracker: Reaction Section

Heavy naphtha from the main fractionator goes to the large catalytic reformer, which is used to produce both gasoline and feedstock for the aromatics plant. A portion of the bottoms from the main fractionator is recycled to R2. The remainder goes to the first of two distillation towers for recovery of middle distillate products.

AHYC is an open-equation, flowsheet-based model, which is used both online and offline at Suncor Sarnia, where it was configured and tuned to

rigorously represent the catalyst beds, quench valves, compressors, flash drums, heaters, exchangers, etc., in the commercial unit. A rigorous model for the hydrogen plant, a steam/methane reformer, was linked to the hydrocracker model. The entire fractionation section—comprising a pre-flash tower, main fractionator, all five gas plant towers, and two middle distillate recovery towers—was modeled rigorously.

After R1, a component-splitter model was used to simulate the removal of  $\text{NH}_4\text{HS}$  upstream from the HPS. This is a simplification, but it eliminates the need for a three-phase electrolytic flash model in the HPS, and it has no effect on reaction kinetics, the composition of recycle hydrogen, or the composition of the LPS bottoms.

A relatively simple extent-of-reaction model was used to simulate the saturation of olefins, including the associated consumption of hydrogen and generation of heat. It was assumed that 100% of the olefins in the feed are removed in the first bed of R1.

As mentioned above, each catalyst bed is modeled separately. Kinetic constituents are segregated from hydraulic and heat balance relationships, which permits different kinetic schemes to be implemented within the same mechanical framework.

Trickle-bed hydrodynamics are modeled with equations described by Satterfield.<sup>10</sup> Reaction rates and flash calculations are performed at multiple collocation points in each reactor bed. This enhances the ability of the model to perform an accurate heat-release calculation (see Table 9 below).

A customized version of the Langmuir-Hinshelwood-Hougen-Watson (LHHW) mechanism is used both for reversible (Figure 4) and irreversible reactions (Figure 5). The main steps in this mechanism are:

- Adsorption of reactants to the catalyst surface
- Inhibition of adsorption
- Reaction of adsorbed molecules
- Desorption of products

Several inhibitors are included in AHYC reaction kinetics. These include  $\text{H}_2\text{S}$ , ammonia, and organic nitrogen compounds. The inhibition of hydrodesulfurization (HDS) reactions by  $\text{H}_2\text{S}$  is modeled, and so is the inhibition of acid-catalyzed cracking reactions—dealkylation of aromatics, the opening of naphthenic rings, and paraffin hydrocracking—by ammonia and to a much greater extent by organic nitrogen.

$$\text{Rate} = A * k * \frac{((K_i C_i * K_{H_2} * (P_{H_2})^x / K_{eq}) - K_j C_j) * PF^y}{I_a * I_b * I_c}$$

where A = catalyst activity  
 k = rate constant  
 K<sub>i</sub> = adsorption constants for hydrocarbons  
 C<sub>i</sub> = concentrations of hydrocarbons  
 K<sub>H<sub>2</sub></sub> = adsorption constants for hydrogen  
 P<sub>H<sub>2</sub></sub> = concentrations of hydrogen  
 K<sub>eq</sub> = equilibrium constant  
 PF = pressure factor  
 I<sub>a</sub>, I<sub>b</sub>, I<sub>c</sub>, etc. = inhibition factors

Figure 4. LHHW rate equation for reversible reactions.

$$\text{Rate} = A * k * \frac{K_i C_i * K_{H_2} * (P_{H_2})^x * PF^y}{I_a * I_b * I_c}$$

where A = catalyst activity  
 k = rate constant  
 K<sub>i</sub> = adsorption constants for hydrocarbons  
 C<sub>i</sub> = concentrations of hydrocarbons  
 K<sub>H<sub>2</sub></sub> = adsorption constants for hydrogen  
 P<sub>H<sub>2</sub></sub> = concentrations of hydrogen  
 PF = pressure factor  
 I<sub>a</sub>, I<sub>b</sub>, I<sub>c</sub>, etc. = inhibition factors

Figure 5. LHHW rate equation for irreversible reactions (C-C scission reactions such as paraffin hydrocracking, opening of naphthene rings, and ring dealkylation).

#### 4.3.1 Reaction Pathways

The following reaction types were modeled in SARCRACK:

- Hydrodesulfurization (HDS)
- Hydrodenitrogenation (HDN)
- Saturation of aromatics
- Ring opening

- Ring dealkylation
- Paraffin hydrocracking

AHYC also models olefin saturation and (in an empirical way) paraffin isomerization.

The AHYC reaction scheme has the following characteristics:

- 45 reversible aromatics saturation reactions involving components in each major distillation range. The components include naphthene-aromatic compounds.
- 19 irreversible olefins saturation reactions. The model assumes that olefin saturation is complete within the first catalyst bed.
- Saturation and dealkylation for sterically hindered sulfur and nitrogen lumps. This allows AHYC to use different HDS and HDN rates for easy-to-treat and hard-to-treat to sulfur and nitrogen compounds.

Recent publications<sup>11,12,13,14</sup> confirm that a hydrotreater removes sulfur from organic sulfides, disulfides, and mercaptans with relative ease. Thiophenes, benzothiophenes, unhindered dibenzothiophenes and hindered dibenzo-thiophenes are successively harder to desulfurize.

Figure 6 illustrates the so-called “direct” mechanism for the HDS of dibenzothiophene, and Figure 7 shows a widely accepted mechanism for the HDS of hindered dibenzothiophenes. Note that the direct HDS of dibenzothiophene requires 2 moles of hydrogen per sulfur atom, while the HDS of hindered dibenzothiophenes requires 5 moles of H<sub>2</sub> per sulfur atom.

Structural differences between sulfur-containing compounds translate into significantly different HDS reaction rates. Table 8 shows pilot plant data for the HDS of small amounts of pure thiophenes in a clean-diesel solvent. The catalyst and temperature were the same for each compound. Note that HDS rates for the first three compounds, which are unhindered, are 30 to 100 times faster than rates for the last three compounds, which are hindered.

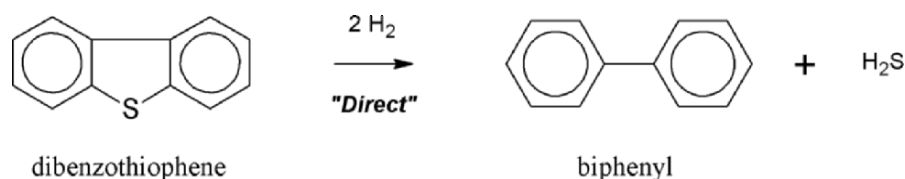


Figure 6. Direct mechanism for the hydrodesulfurization of dibenzothiophene

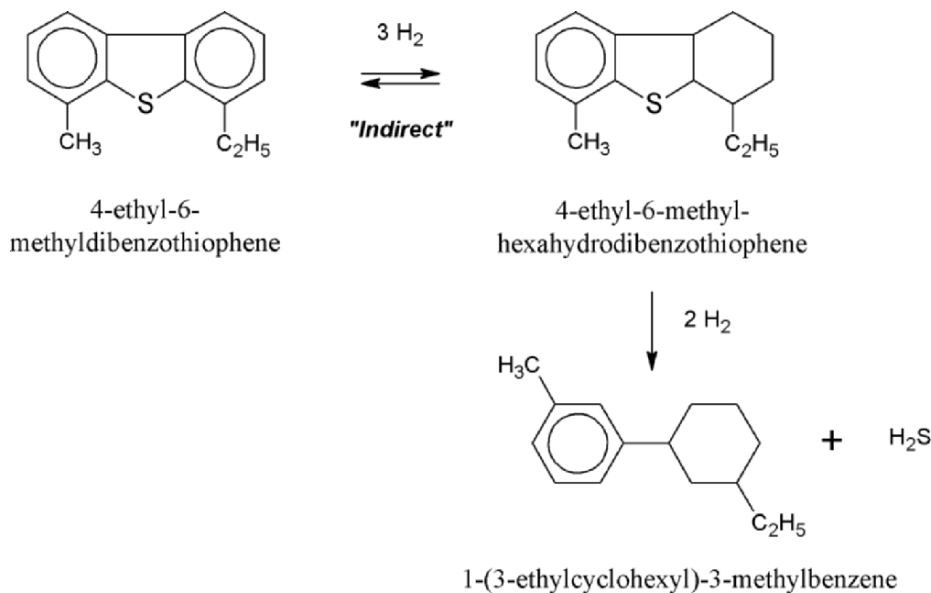


Figure 7. Mechanism for the hydrodesulfurization of hindered dibenzothiophenes

Table 8. Relative Reaction Rates of Hindered and Unhindered Sulfur Compounds

| Sulfur Compound           | Rel. HDS Rate | Boiling Point (°F) | Boiling Point (°C) |
|---------------------------|---------------|--------------------|--------------------|
| Thiophene                 | 100           | 185                | 85                 |
| Benzothiophene            | 30            | 430                | 221                |
| Dibenzothiophene          | 30            | 590                | 310                |
| Methyldibenzothiophene    | 5             | 600 - 620          | 316 - 327          |
| Dimethyldibenzothiophene  | 1             | 630 - 650          | 332 - 343          |
| Trimethyldibenzothiophene | 1             | 660 - 680          | 349 - 360          |

### 4.3.2 Catalyst Deactivation Model

In AHYC, the catalyst deactivation model calculates the deactivation rate as function of the following:

- Coke precursors in the feed
- Time on stream
- Average bed temperature for each catalyst bed
- H<sub>2</sub> partial pressure

The model predicts future catalyst activity, required temperature, yields, hydrogen consumption, and product properties. Alternatively, if the catalyst cycle life is fixed, the model can compute the optimal changes in feed rate, feed properties and/or conversion needed to reach the target end-of-run date.

Figure 10 shows how the deactivation model can be used to predict future temperatures required to hit a user-selected process objective. The process

objective can be sulfur removal, nitrogen removal, or hydrocarbon conversion—for example, the conversion of 650°F-plus to 650°F-minus (343°C-plus to 343°C-minus) material.

At the hydrocracker at Suncor Sarnia, the deactivation model is applied to each catalyst bed. This enables the development of strategies to bring all catalyst beds to end-of-run at (roughly) the same time, and prediction of future yields, selectivity and product properties.

### 4.3.3 AHYC Model Fidelity

Table 9 presents data from an AHYC project at a U.S. East Coast refinery. The data show the excellent fit that can be achieved with the model. During that project, AHYC predictions were compared to step-test gains from a model-predictive controller. The optimizer matched most gains within +/- 20% (relative). This shows that the model does a good job of predicting process behavior under conditions well away from those at which it was tuned.

Table 9. Aspen Hydrocracker Model Fidelity

| Variable         | Measured Value     |         | Predicted Value            |         | Offset    |
|------------------|--------------------|---------|----------------------------|---------|-----------|
| Conversion       | 63.6 wt% feed      |         | 63.54 wt% feed             |         | 0.057     |
| R1 WART*         | 724°F              | 384.4°C | 724°F                      | 384.4°C | 0.55°F    |
| R2 WART          | 723°F              | 383.9°C | 723°F                      | 383.9°C | -0.71°F   |
| N at R1 exit     | 61 wppm            |         | 59 wppm                    |         | 2 wppm    |
| N at R2 exit     | 3 wppm             |         | 3 wppm                     |         | 0 wppm    |
| S at R1 exit     | 300 wppm           |         | 299 wppm                   |         | 1 wppm    |
| S at R2 exit     | 33 wppm            |         | 33 wppm                    |         | 0 wppm    |
| H2 makeup        | 40.5 million scf/d |         | 47,800 Nm <sup>3</sup> /hr |         | -1 Mscf/d |
| R1B1 outlet temp | 707°F              | 375°C   | 707°F                      | 375°C   | 0.001°F   |
| R1B2 outlet temp | 762°F              | 405.6°C | 762°F                      | 405.6°C | 0.009°F   |
| R2B1 outlet temp | 761°F              | 405°C   | 761°F                      | 405°C   | 0.008°F   |
| R2B2 outlet temp | 760°F              | 404.4°C | 760°F                      | 404.4°C | 0.002°F   |
| R3B1 outlet temp | 725°F              | 385°C   | 725°F                      | 385°C   | 0.001°F   |
| R3B2 outlet temp | 726°F              | 385.6°C | 726°F                      | 385.6°C | 0.001°F   |
| R3B3 outlet temp | 743°F              | 395°C   | 743°F                      | 395°C   | 0.003°F   |

\* WART = weighted average reactor temperature

## 4.4 Clean Fuels Planning

### 4.4.1 Hydrogen Requirements for Deep Desulfurization

We ran a series of case studies to calculate the hydrogen requirements for deep desulfurization in a high-pressure gas-oil hydrotreater.

For the saturation of aromatics in a hydrotreating or hydrocracking unit, equilibrium effects, which favor formation of aromatics, start to overcome kinetic effects above a certain temperature. This causes a temperature-dependent “aromatics cross-over” effect, which explains the degradation of important middle distillate product properties—including kerosene smoke point and diesel cetane number—at high process temperatures near the end of catalyst cycles. The cross-over temperature is affected by feed quality and hydrogen partial pressure, so it can differ from unit to unit.

Figure 8 shows results from a case study in which the weighted average reactor temperature (WART) was changed over a wide range in a model based on the treating section of the Suncor Sarnia hydrocracker. Even though the WART was changed, the reactor temperature profile—equal outlet temperatures for the catalyst beds—was the same for every case.

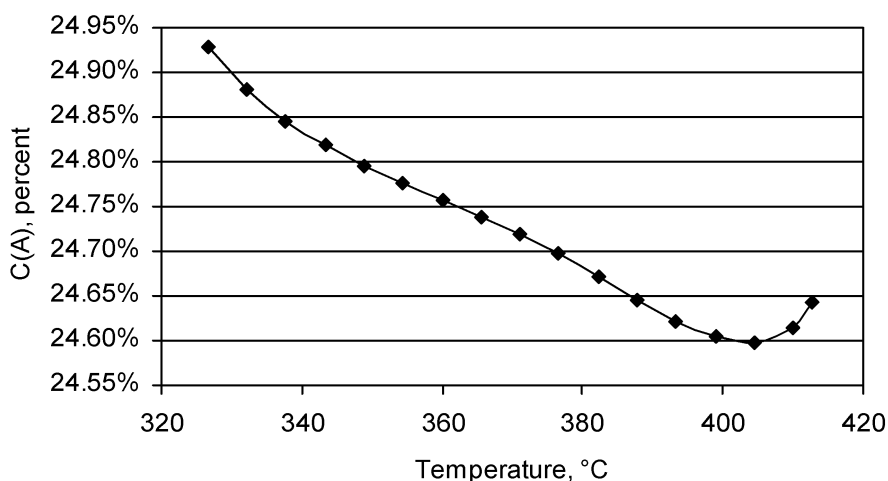


Figure 8. Product Aromatics versus Temperature

The y-axis shows the mole fraction of total aromatics remaining in product. For this case study, the feed rate, feed type, and catalyst activity were kept constant, which means that deactivation effects were not included. With less-active end-of-run catalysts, the rates of forward (saturation) reactions are inhibited, so the aromatics cross-over effect is amplified.

Figure 9 shows results of a case-study in which the product sulfur was kept constant (fixed) at different levels between 500 and 15 wppm. Required WART and hydrogen makeup flow are plotted on the y-axis. Because the product sulfur was fixed, another normally fixed variable can be allowed to vary. For this study, the chosen variable was WART.

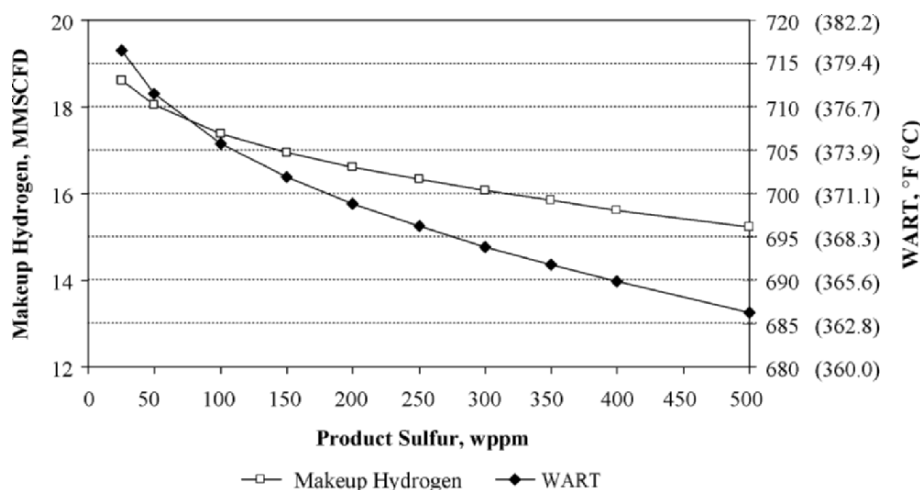


Figure 9. Aspen Hydrocracker case study results: hydrogen consumption and weighted average reactor temperature (WART) versus product sulfur content.

Again, we ran the case study using the hydrotreating portion of the Suncor-Sarnia hydrocracker model with an equal-outlet temperature profile. For 500 wppm sulfur in the product, the makeup  $H_2$  flow is 15.2 MMSCFD. For 15 wppm, the makeup flow is 18.6 MMSCFD, more than 40% higher. Higher WART leads to increased conversion, increased HDN, and (up to point) increased saturation of aromatics. This explains why the hydrogen consumption increased so much—and so non-linearly—when the target product sulfur content went from 500 wppm to 15 wppm.

We can also keep WART constant and achieve the desired level of HDS by allowing changes in LHSV. When this is done, the effect on hydrogen consumption is less severe. But in the real world, decreasing the LHSV is equivalent to lowering feed rate or adding a reactor, both of which are expensive. The WART-based trend shown here is more relevant to an existing unit.

Figure 9 is consistent with the existence of both hindered and unhindered sulfur compounds in the feed. As mentioned above, the last traces of sulfur in diesel oil are locked inside highly hindered hydrocarbon molecules, which have to be cracked open before the sulfur can be removed.

#### 4.4.2 Effects of Hydrotreating on FCC Performance

Many refiners are including the hydrotreating of FCC feed in their plans to make clean fuels. To demonstrate the feasibility of running a rigorous model for an FCC-plus-pretreater complex, we connected AHYC to AFCC. To link



the two, we created a component mapper model to compress the 97 reactive components from AHYC into the 21 lumps used in AFCC. We then connected the unconverted oil stream from the AHYC fractionator model to the feed-adjust block of AFCC.

Initially, the combined model was huge, containing more than 1.2 million non-zero terms in its matrix of variables. To allow the model to run in a reasonable amount of time on a Pentium III computer, we made some simplifications. In the reduced model, the four catalyst bed models are still fully rigorous. However, the hydrogen furnaces are represented with a heat-exchanger model, quench valves are modeled with mixers, a component splitter model is used for the wash-water system, and a group of component splitters is used for the fractionation section. These changes reduce the number of equations and non-zeros to 130,000 and 680,000 respectively. Despite these simplifications, the slimmed-down model remains, in our collective opinion, a useful tool for offline what-if studies and for economic comparisons of different process options.

We first looked at the effect of varying the amount of hydrotreated material in an FCC feed blend from 0.0 to 96.7 vol%. Table 10 presents selected process conditions for the feed hydrotreater, which achieved 90% desulfurization and roughly 23 wt% conversion of vacuum gas oil to middle distillate and naphtha.

Table 10. Feed Pretreater Operating Conditions

| Variable                                | Units            | Value  |
|---|------------------|--------|
| Feed rate                               | b/d              | 39,000 |
| Number of catalyst beds                 |                  | 4      |
| Weighted average reactor temperature    | °F               | 720    |
|   | °C               | 382    |
| LHSV                                    | hr <sup>-1</sup> | 1.2    |
| Hydrogen partial pressure               | psig             | 2000   |
|   | barg             | 136    |
| Hydrotreater feed sulfur                | wt%              | 1.95   |
| Sulfur in hydrotreated FCC feed         | wt%              | 0.195  |
| Conversion of 343°C-plus to 343°C-minus | wt%              | 23.0   |

We modeled the effect of feed hydrotreating in two ways. The first and most logical approach was to model the pretreating of the 100% of the FCC feed. We simply operated the pretreater model at several different severities and watched the response of the FCC model. Complications arose because upstream conversion in the pretreater affects the amount of feed going to the FCC model. When we compensated by increasing or decreasing the overall fresh feed rate to maintain a constant feed rate to the FCC, conversion in the pretreater changed due to the corresponding differences in LHSV. This is a classical—and very realistic—economic optimization problem, for which the

combined AHYC/AFCC model is well suited. However, it doesn't easily lend itself to creating straight-forward graphs for publications.

In another approach to modeling the effects of FCC feed pretreating, the FCC model receives a blend of hydrotreated feed from AHYC with straight-run feed from a tank model. The latter case is discussed here.

Table 11 shows the properties of the four FCC feed blends that were used in the combined hydrotreater/FCC simulations. Table 12 presents FCC conversion and yield data. In each case, we held the FCC riser outlet temperature at 1030°F (544°C).

Table 11. FCC Feed Properties for Blends of Straight-run and Hydrotreated Feeds

| Variable                   | Units | Case 1 | Case 2 | Case 3 | Case 4 |
|----------------------------|-------|--------|--------|--------|--------|
| Straight-run VGO           | b/d   | 30,000 | 20,000 | 10,000 | 1,000  |
| Hydrotreated VGO (90% HDS) | b/d   | 0      | 10,000 | 20,000 | 29,000 |
| Total Feed Rate            | b/d   | 30,000 | 30,000 | 30,000 | 30,000 |
| API gravity                | °API  | 22.60  | 24.57  | 26.58  | 28.44  |
| Specific gravity           |       | 0.9182 | 0.9067 | 0.8951 | 0.8847 |
| Sulfur                     | wt%   | 1.95   | 1.38   | 0.80   | 0.26   |
| Basic Nitrogen             | wppm  | 417    | 380    | 344    | 310    |
| CCR                        | wt%   | 0.730  | 0.525  | 0.315  | 0.122  |
| Vanadium                   | wppm  | 3.1    | 2.1    | 1.1    | 0.2    |
| Nickel                     | wppm  | 5.2    | 3.5    | 1.8    | 0.3    |
| Sodium                     | wppm  | 1.3    | 0.9    | 0.5    | 0.1    |
| Iron                       | wppm  | 2.6    | 2.1    | 1.5    | 1.1    |
| Copper                     | wppm  | 0.2    | 0.2    | 0.1    | 0.1    |
| UOP K Factor               |       | 11.67  | 11.79  | 11.92  | 12.03  |

Table 12. FCC Conversion and Yields

| Variable                                   | Units | Case 1 | Case 2 | Case 3 | Case 4 |
|--|-------|--------|--------|--------|--------|
| Net conversion                             | Vol%  | 74.39  | 78.45  | 82.01  | 84.88  |
|  | Wt%   | 73.11  | 77.05  | 80.61  | 83.56  |
| <b>Yields</b>                              |       |        |        |        |        |
| Fuel gas (H <sub>2</sub> -C <sub>2</sub> ) | FOE*  | 5.68   | 5.83   | 5.95   | 6.03   |
| C <sub>3</sub>                             | Vol%  | 16.48  | 17.07  | 17.55  | 17.90  |
| C <sub>4</sub>                             | Vol%  | 25.38  | 26.71  | 27.90  | 28.88  |
| C <sub>5</sub>                             | Vol%  | 0.85   | 0.93   | 1.00   | 1.06   |
| Naphtha                                    | Vol%  | 44.46  | 47.13  | 49.55  | 51.53  |
| LCO  | Vol%  | 19.13  | 16.56  | 14.15  | 12.20  |
| Bottoms                                    | Vol%  | 4.56   | 2.92   | 1.62   | 0.63   |
| Coke                                       | Wt%   | 5.30   | 5.30   | 5.30   | 5.30   |
| Total liquid                               |       | 116.54 | 117.16 | 117.74 | 118.23 |
| Flue gas SOx                               | wppm  | 390    | 296    | 180    | 60     |

Figure 10 shows that the sulfur content of FCC gasoline is essentially linear with respect to the percent of hydrotreated oil in the FCC feed blend. Figure 11 shows that relatively more sulfur goes into heavy FCC products (LCO, HCO and slurry oil) at higher percentages of hydrotreated oil in the feed.

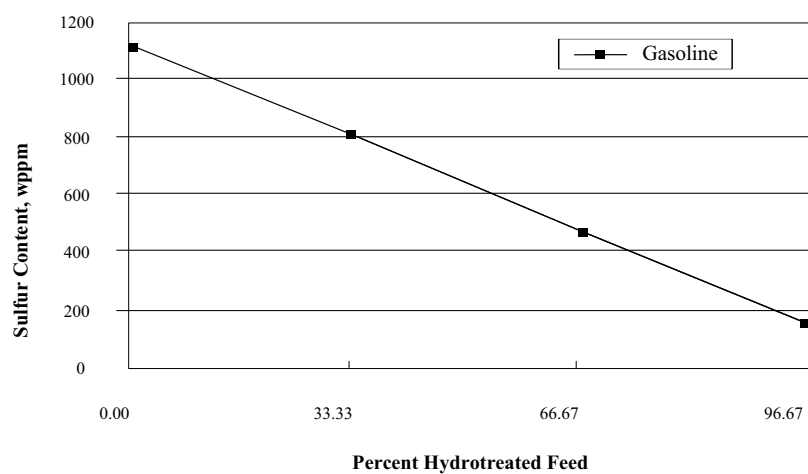


Figure 10. Sulfur in FCC gasoline versus percent hydrotreated oil in the FCC feed.

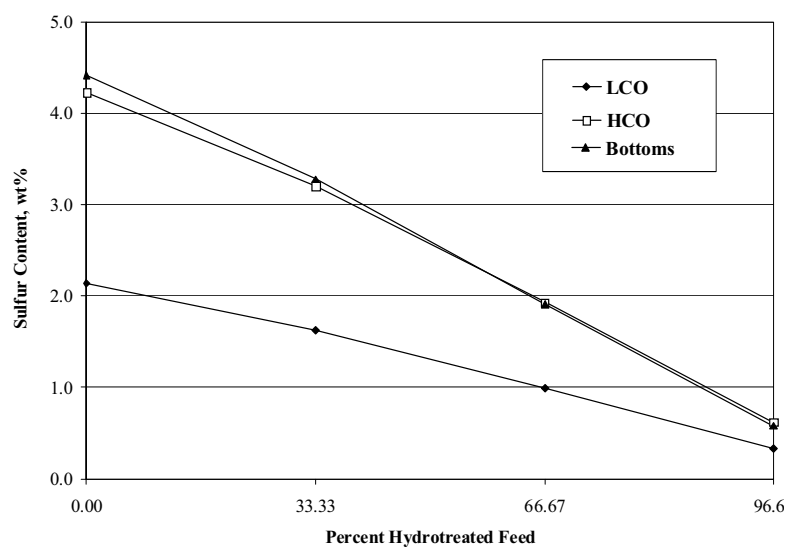


Figure 11. Sulfur in heavy FCC products versus percent hydrotreated oil in the FCC feed.

This is consistent with the easy-sulfur/hindered-sulfur hypothesis, which predicts that nearly all of the sulfur left behind after high-severity hydrotreating is encased in hindered compounds. These compounds contain multiple aromatic rings, so they more likely (relative to other sulfur compounds) to be incorporated into the coke that forms on FCC catalysts. When the coke is burned away, the sulfur is converted into sulfur oxides (SO<sub>x</sub>), which ends up in the regenerator flue gas.

## 5. CONCLUSIONS

Rigorous models are being used for closed-loop real-time optimization at the Suncor refinery in Sarnia, Ontario. Single-unit rigorous models—and combinations of models similar to those being used in Sarnia—can be used offline to quantify non-linear relationships between important refinery units, such as the FCC and its associated feed pretreater. These relationships are important when planning for clean fuels, especially when selecting and designing processes for hydrogen production and deep desulfurization.

## 6. ACKNOWLEDGEMENTS

We are pleased to thank the following people for their contributions to RWO and to the development of Aspen FCC or Aspen Hydrocracker: John Adams, John Ayala, Darin Campbell, Steve Dziuk, Fernando Garcia-Duarte, Steve Hendon, Nigel Johnson, Ajay Lakshmanan, Jiunn-shyan Liou, Skip Paules, Rosalyn Preston, and Charles Sandmann.

## 7. REFERENCES

1. Pedersen, C.C.; Mudt, D.R.; Bailey, J.K.; Ayala, J.S. "Closed Loop Real Time Optimization of a Hydrocracker Complex," NPRA Computer Conference, CC-95-121, November 6-8, 1995.
2. English, K.; Dunbar, M. "Using Steady State Models to Generate LP Model Inputs," NPRA Computing Conference, CC-97-131, November 16-19, 1997.
3. Shorey, S.W.; Lomas, D.A.; Keesom, W.H. "Improve Refinery Margins and Produce Low-Sulfur Fuels," World Refining Special Edition: Sulfur 2000, Summer 1999, p. 41.
4. Lapinas, A.T.; Klein, M.T.; Gates, B.D.; Macris, A.; Lyons, J.E. "Catalytic Hydrogenation and Hydrocracking of Fluorene: Reaction Pathways, Kinetics and Mechanisms," *Industrial and Engineering Chemistry Research*, 30 (1), 1991, 42.
5. Stangeland, B.E. "Kinetic Model for the Prediction of Hydrocracker Yields," *Industrial & Engineering Chem., Process Des. Development*, 13 (1), 1974, 71.

6. Quann, R.J. "Hydrocracking of Polynuclear Aromatic Hydrocarbons. Development of Rate Laws through Inhibition Studies," *Industrial & Engineering Chemistry Research*, 36 (6), 1997, 2041.
7. Jacob, S.M.; Quann, R.J.; Sanchez, E.; Wells, M.E. "Compositional Modeling Reduces Crude-Analysis Time, Predicts Yields," *Oil & Gas Journal*, July 6, 1998, p. 51.
8. Filimonov, V.A.; Popov, A.A.; Khavkin, V.A.; Perezhigina, I.Ya.; Osipov, L.N.; Rogov, S.P.; Agafonov, A.V. "The Rates of Reaction of Individual Groups of Hydrocarbons in Hydrocracking," *International Chemical Engineering*, 12 (1), 1972, 21.
9. Jacobs, P.A. "Hydrocracking of n-Alkane Mixtures on Pt/H-Y Zeolite: Chain Length Dependence of the Adsorption and the Kinetic Constants," *Industrial & Engineering Chemistry Research*, 36 (8), 1997, 3242.
10. Satterfield, C.N. "Trickle-Bed Reactors," *AIChE Journal*, 21 (2), 1975, 209.
11. Callejas, M.A.; Martinez, M.T. "Hydrocracking of a Maya Residue. Kinetics and Product Yield Distributions," *Industrial & Engineering Chemistry Research*, 38 (9), 1999, 3285.
12. Cooper, B.H.; Knudsen, K.G. "Ultra Low Sulfur Diesel: Catalyst and Processing Options," NPRA Annual Meeting, Paper No. AM-99-06.
13. Cooper, B.H.; Knudsen, K.G. "What Does it Take to Produce Ultra-Low-Sulfur Diesel?" World Refining, November 2000, p. 14.
14. Bjorklund, B.L.; Howard, N.; Heckel, T.; Lindsay, D.; Piasecki, D. "The Lower It Goes, The Tougher It Gets," NPRA Annual Meeting, Paper No. AM-00-16, March 26-28, 2000.

## Chapter 24

# **MODELING HYDROGEN SYNTHESIS WITH RIGOROUS KINETICS AS PART OF PLANT-WIDE OPTIMIZATION**

Milo D. Meixell, Jr.  
*Aspen Technology, Incorporated*  
*Advanced Control and Optimization Division*  
*Houston, Texas*

## **1. INTRODUCTION**

Hydrogen for industrial use is manufactured primarily by steam reforming hydrocarbons, or is available as a byproduct of refinery or chemical plant operations. Hydrogen demand usually is significantly greater than that available as a byproduct, and many times the plant's ability to supply hydrogen limits overall plant throughput. An operating plant can exploit existing in-place steam reformer and related equipment designs with rigorous models that employ kinetics. During plant design kinetics models are not necessarily used because experience and more simple models using "approach to equilibrium", space velocity, maximum heat flux, and other parameters allow designers to build hydrogen plants to supply whatever hydrogen amount, purity, and pressure that is desired. The objective of suppliers of hydrogen plants is to establish an economic feasible design, given these predetermined criteria. Additional hydrogen, or less expensive hydrogen can be manufactured from these facilities, after construction, when rigorous models are used in on-line, closed loop optimization systems. These systems manipulate independent operating conditions (degrees of freedom), maximize or minimize an objective function (usually operating profit), while honoring numerous constraints, such as tube metal temperatures, pressure drops, pressures, damper and valve positions. A good kinetic model is the cornerstone of the predictive capabilities of such on-line optimization

systems. An on-line optimization system exploits equipment under operating demands and constraints that were not necessarily anticipated during design.

The steam reformer and associated models represent the most significant models in an overall hydrogen or synthesis gas plant real-time, closed-loop optimization project. The reformer does the great majority of converting the feedstock (i.e. natural gas, butane or naphtha, plus steam) to the primary reactant for downstream synthesis reactors, hydrogen. Consequently, detailed modeling is required to predict the correct product yields from varying feed stock composition at various operating conditions. Additionally, the primary reformer is subject to numerous constraints, such as tube metal temperatures, that also demand detailed modeling to predict. The primary reformer consumes significant energy, and the methane slip or hydrogen purity from it affects operating conditions in downstream equipment. The optimization system must be able to exploit these reactors if optimal plant operation is to be achieved.

The reformer reactions (reforming and water gas shift) are modeled using the best available heterogeneous kinetic relationships from the literature,<sup>1-4</sup> and have been validated with industrial data and literature data<sup>28</sup> over a wide range of conditions. Equilibrium relationships are appropriately incorporated into the rate relationships, but the model does not use the empirical "approach to equilibrium temperature" as the basis for predicting outlet compositions. Nor does the model use "pseudo-homogeneous" rate relationships.

The steam reformer model can handle feeds from methane to naphtha, with all the typical components that are present in natural gas, as well as recycled synthesis purge gas, or hydrogen recovery unit tail gases. Naphtha feed is characterized as about 30 chemical species, some of which are pure components, and some are hydrocarbon fractions (pseudo components). Each hydrocarbon species participates in a reaction that includes adsorption onto the catalyst, reforming, and desorption. The model includes diffusion effects within the catalyst, as well as heat transfer resistance from the bulk gas to the catalyst surface.

Since the model is based on mechanistic rate relationships, the composition profiles (as well as temperature and pressure) are calculated at positions from the inlet of the catalyst tube to the outlet. The differential reaction rate relationships, as well as the mass balances, heat balances, and pressure drop relationships are solved simultaneously. A global spline collocation algorithm is used to pose the problem, and an SQP algorithm (sequential quadratic programming) solves the relationships.

The heat transfer rate from the primary reformer fire box to the catalyst tubes is calculated along the tube using radiant and convective heat transfer relationships. Heat transfer is also calculated from the tube outer surface, across the tube metal, through the inside tube surface film to the bulk fluid, and finally from the bulk fluid to the catalyst particles. Measurements of the catalyst temperatures at several positions along the tube, as well as measured

tube skin temperatures provide feedback that is used to update heat transfer parameters, as well as to validate the model.

Pressure drop calculations are included, which use the Ergun relationship.<sup>5</sup> This relationship predicts the pressure drop through packed beds, such as the primary reformer catalyst tubes and the secondary reformer (auto-thermal) bed. Measurements provide feedback that is used to update appropriate parameters in this relationship.

The kinetics developed for natural gas and naphtha steam reforming in fired and auto-thermal reactors were put to more stringent tests by applying them to two other reactors. One is a “pre-reformer”, an adiabatic fixed bed typically used upstream of a fired tube reformer for debottlenecking. The other reactor is a fired furnace with high carbon dioxide content in the feed, making a 1:1 ratio hydrogen to carbon monoxide synthesis gas, at 3.5 bars (as opposed to the typical 40 bars pressure in many steam reformers), which is processed in downstream Fischer-Tropsch reactors, ultimately making oxo-alcohols. Calculated and measured yields and temperature profiles in these reactors, using the same kinetics, are in excellent agreement.

These rigorous models, developed from credible literature sources, and validated against industrial data over a wide range of conditions, are the foundation of several plant-wide optimization systems, including those for hydrogen, ammonia, methanol, and oxo-alcohol plants.

## 2. STEAM REFORMING KINETICS

The reaction scheme and associated kinetics are based on methane reforming and “heavier hydrocarbon” reforming studies reported in the literature. The methane reforming relationships must be included in any model processing heavier hydrocarbons since methane is generated from these feeds, and subsequently reacts. The primary source of information used for methane reforming is Xu and Froment’s most recent literature articles on intrinsic kinetics and on using these along with diffusional resistance relationships to model industrial reformers.<sup>1, 2, 6</sup> The source of information for higher hydrocarbon steam reforming is based upon the work of Rostrup-Nielsen of Haldor-Topsøe A/S, as well as that of others, whose work Rostrup-Nielsen has referenced extensively.<sup>3, 4, 7</sup>

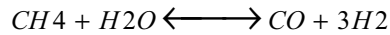
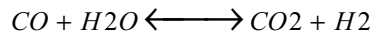
### 2.1 Methane Steam Reforming Kinetic Relationships

Numerous reaction mechanisms were investigated by Froment, and the best reaction scheme is shown in Figure 8 and Table 3 of Reference 1. “Best” was determined by “model discrimination” methods described by Froment. The kinetic expressions used for methane reforming account for adsorption of all the reacting species present ( $\text{CO}$ ,  $\text{H}_2$ ,  $\text{CH}_4$ , and  $\text{H}_2\text{O}$ ), as well as reaction



on the surface. The intermediate, adsorbed species concentrations, which are unmeasurable (at least in industrial equipment), are eliminated from the mechanistic steps (at steady-state), and only stable species concentrations (partial pressures) appear in the net reaction stoichiometry and the reaction rate expressions.

Net Reaction Stoichiometry:



Reaction Rate Relationships:

$$r_1 = \frac{\frac{k_1}{p_{H_2}} \left( p_{CO} * p_{H_2O} - \frac{p_{H_2} * p_{CO_2}}{K_1} \right)}{\left( DEN \right)^2}$$

$$r_2 = \frac{\frac{k_2}{2.5} \left( p_{CH_4} * p_{H_2O} - \frac{p_{H_2}^3 * p_{CO}}{K_2} \right)}{\left( DEN \right)^2}$$

$$r_3 = \frac{\frac{k_3}{3.5} \left( p_{CH_4} * p_{H_2O}^2 - \frac{p_{H_2}^4 * p_{CO_2}}{K_3} \right)}{\left( DEN \right)^2}$$

$$DEN = 1 + K_{CO} * p_{CO} + K_{H_2} * p_{H_2} + K_{CH_4} * p_{CH_4} + K_{H_2O} * p_{H_2O} / p_{H_2}$$

The reaction rate “constants”,  $k_i$ 's, are functions of temperature, activation energies, and frequency factors, in the classic Arrhenius form:

$$k_i = A_i * e^{-E_i / RT}$$

$$i = 1 \text{ to no. of reactions } (\cong 30)$$

Similarly, the adsorption equilibrium constants are functions of temperature, heats of adsorption, and a frequency factor:

$$K_i = A_i * e^{\Delta H_i / RT}$$

$$i = \text{CO, H}_2, \text{CH}_4, \text{H}_2\text{O}$$

The reaction equilibrium “constants” are functions of temperature. The equilibrium constants as a function of temperature are listed in References 3 and 4. Those of Reference 3 were used, and have been tabulated and regressed, with results listed in Appendix E.

$$K_i = f(T)$$

$$i = 1 \text{ to no. of reversible reactions}(= 3)$$

The kinetics discussed so far are intrinsic kinetics that are valid in the absence of diffusional or heat transfer resistances. Bulk phase concentrations (partial pressures) and temperatures are not present at the active sites within the catalyst pellets, since the pore structure offers very significant resistance to diffusion, and mild resistance to heat transfer exists between the bulk phase and the pellet surface. Little resistance to heat transfer exists within the pellets (Reference 4, page 69).

The diffusional effects are accounted for using the classic “effectiveness factor”<sup>2, 8, 9, 10, 11</sup>.

$$\eta = \frac{\text{actual rate throughout pellet with resistances}}{\text{rate evaluated without resistances}}$$

Evaluating the numerator of this expression requires simultaneous integration of the rate and diffusion relationships. Froment presents the results of that integration in Figure 6 of Reference 2. Rostrup-Nielsen lists results of Haldor-Topsøe’s calculations on page 69 of Reference 4. These results are qualitatively similar, but differ in value due to numerous factors. Simplification of the effectiveness factor calculation can be applied for conditions which cause the diffusional resistance to be large (Reference 8, page 431), and that simplification is implied in many of Haldor-Topsøe’s equations (Reference 4, pages 37, 69 and Reference 9). The simplification (Reference 8, page 434) is:

$$\eta = \frac{3}{r_p} \sqrt{\frac{K(D_e)}{k(K+1)\rho_p}}$$

Satterfield (Reference 10, page 78) gives further insight to the simplification, when the diffusivities of the forward and reverse reactions are not equal.

Since the kinetics used in the DMCC model are those of Froment, the effectiveness factor profiles in the primary reformer model are based upon his results. Rather than incur the computational burden of calculating the effectiveness factors for each reaction on-line, they are entered as a function of length as constant profiles. Since the effectiveness factors are primarily functions of the catalyst pellet size, pore size, and pore size distribution, and since they are relatively weak functions of operating conditions over the normal range of these conditions, the effect of imposing them as constant profiles is very small. The results of reactor simulations with the effectiveness factor profiles fixed agree very well with measured results from industrial reformers, and with results presented in the literature. Off-line calculations can be done to update the effectiveness factors if catalyst pellet size or pore size are changed significantly, or ultimately these calculations can be added to the on-line model. It is essential that effectiveness factors are used in conjunction with the intrinsic kinetic rate parameters, since the effectiveness factors account for phenomena that attenuate the intrinsic rates by factors on the order of 100. That is, effectiveness factors are on the order of 0.01.

The relationship among actual reaction rate, intrinsic rate, effectiveness factor, and catalyst activity is:

$$r_{i, \text{observed}} = \eta_i * \alpha * r_{i, \text{intrinsic}}$$

where:

$\eta$  = effectiveness factor

$\alpha$  = relative catalyst activity

(accounting for aging, sintering, pore closure, etc.)

$r_{i, \text{intrinsic}}$  = rate calculated with bulk fluid conditions

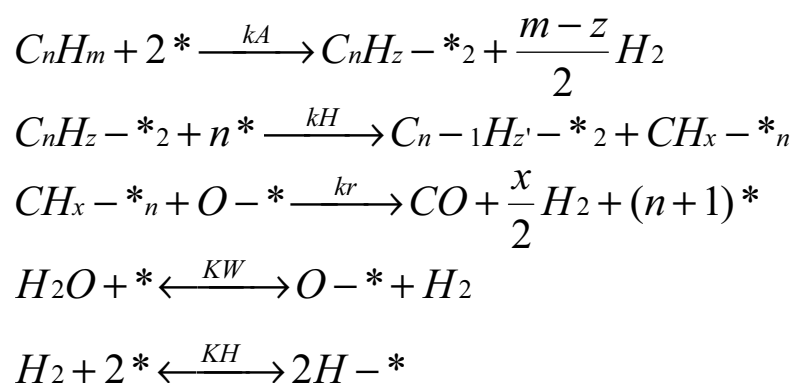
The catalyst activity is calculated as a parameter, updated from operating data.

## 2.2 Naphtha Steam Reforming Kinetic Relationships

Several intrinsic reaction rate relationships have been derived for steam reforming of “higher hydrocarbons” (i.e. higher in carbon number than methane), based on Langmuir-Hinshelwood adsorption and reaction mechanisms (Reference 3, pages 118 and 174, Reference 4, page 54). These reaction rates (as with the reactions associated with the reforming of methane) are greatly attenuated in industrial tubular reactors by mass transfer resistance within the catalyst pellet and, to a lesser degree, by heat transfer resistance from the bulk fluid to the catalyst pellet surface. As with any intrinsic rate relationships, these rate expressions must be used in conjunction with a

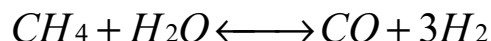
reactor model that accounts for these resistances for the model to be useful in assessing reformer performance, and predicting performance as independent conditions are manipulated. The relationship among intrinsic rates, observed rates, mass and heat transfer resistances, and catalyst activity has been shown in the Methane Steam Reforming Kinetic Relationships section.

One of the mechanisms (Reference 4, page 54) is based on the following sequence of adsorption, reaction, and desorption:



The “\*” symbol represents an active site on the catalyst surface. Concentration of  $C_n H_z - * _2$  is generally assumed to be negligible, so the step 2 rate “constant”,  $k_H$  does not appear in the final rate expression. The rate constants  $k_A$  and  $k_r$  (adsorption and reforming) do appear in the rate expression.  $K_W$  and  $K_H$  are the adsorption equilibrium “constants” for water and hydrogen, respectively.

The mechanisms account for chemisorption of the hydrocarbon and steam, followed by  $\alpha$ -scission of the carbon-carbon bonds. The resulting adsorbed  $C_1$  species react with adsorbed steam to form carbon monoxide and hydrogen. These mechanisms alone would result in no formation of methane, which is of course generated from naphtha feed stocks which are totally free of methane. Methane concentrations of 8 to 10 mole percent (dry basis) are typical at the outlet of industrial naphtha steam reformers. Methane is generated when the hydrogen partial pressure is sufficiently high so that the reverse of the methane reforming reaction:



is favored. This reaction, along with reforming to carbon dioxide, and the water gas shift reaction are solved simultaneously with the reforming reactions for the higher hydrocarbons. The mechanisms for these reactions are documented in the “Methane Steam Reforming” section.

Competition between methane and the higher hydrocarbons for reactive sites on the catalyst surface is limited to a narrow axial position in the reactor tube, since the higher hydrocarbon species reform quickly, and since methane concentration buildup due to the reverse of the aforementioned methane reforming reaction is only significant after the great majority of the higher hydrocarbons are gone. The hydrogen partial pressure is only high enough to favor the reverse of the methane reforming reaction when the higher hydrocarbon species have essentially disappeared. Therefore the denominator of the higher hydrocarbon rate relationships do not contain a methane adsorption term, nor does the denominator in the methane reforming reaction rate expressions have higher hydrocarbon adsorption terms. Rate expressions can be derived for the region in which the higher hydrocarbon and methane compete for active catalyst sites, however results of simulating a reactor with such a model will be essentially unchanged from the results obtained by applying the rate expressions discussed here.

The concentration profiles that result from solving the methane and the higher hydrocarbon reaction rates simultaneously agree well with the profiles reported by others,<sup>12,13</sup> and the reactor effluent species concentrations agree well with those observed from industrial reformers (Appendix A). The effluent concentrations are fairly insensitive to reaction rates, since industrial reformers operate near equilibrium conditions. Effluent conditions will only be noticeably affected by reaction rates as the catalyst activity declines significantly. The temperature profile, especially in the first on third of the reactor which is furthest from equilibrium, is affected significantly by reaction rates, and therefore is the most affected by the catalyst activity. The case study results in Appendix B illustrate the concentration profiles, and the effects of catalyst activity on temperature profiles.

From Reference 4:

$$r_i = \frac{k_A * p_{CnHm}}{\left(1 + \frac{n * k_A}{kr * K_W} * \frac{p_{CnHm}}{p_{H_2}} * p_{H_2} + K_W * \frac{p_{H_2O}}{p_{H_2}} + \sqrt{K_H * p_{H_2}}\right)^{2n}}$$

The  $2n$  exponent in the denominator appears to be in error, since similarly derived rate expressions, listed below, have exponents of 2. Also, the  $2n$  exponent leads to very unreasonable results for rates of reaction of higher carbon number hydrocarbons.

From References 3 and 13:

$$r_i = \frac{k_A * p_{CnHm}}{\left(1 + \frac{n * k_A}{kr * K_W} * \frac{p_{CnHm}}{p_{H_2}} * p_{H_2} + K_W * \frac{p_{H_2O}}{p_{H_2}}\right)^2}$$

From Reference 3, including Boudart's interpretation of hydrogen and hydrocarbon site differences:

$$r_i = \frac{k_A * p_{CnHm} / p_{H_2}^{y/2}}{\left(1 + \frac{n * k_A}{kr * K_W} * \frac{p_{CnHm}}{p_{H_2}} * p_{H_2}^{(1-y/2)} + K_W * \frac{p_{H_2O}}{p_{H_2}}\right)^2}$$

The rate expression from "Catalytic Steam Reforming" (1984) can be modified to include Boudart's hydrogen site interpretation, and can be solved in its original form, or the modified form by manipulating the value of "y". A "y" value of zero restores the relationship to its original form. Additionally, that rate expression can be transformed into essentially the expression from "Steam Reforming Catalysts" (1975) by manipulating the value of KH. A small value of KH transforms the 1984 expression into the 1975 one. Generally, the final term in the denominator of the 1984 rate expression (the term including KH) is much smaller than the other terms.

The rate expression from "Catalytic Steam Reforming" (1984), modified to include the Boudart interpretation of the hydrogen site versus hydrocarbon site difference, is the relationship used in the model. The apparent error in the 2n exponent of the denominator has been corrected, and an exponent of 2 is used.

$$r_i = \frac{k_A * p_{CnHm} / p_{H_2}^{y/2}}{\left(1 + \frac{n * k_A}{kr * K_W} * \frac{p_{CnHm}}{p_{H_2}} * p_{H_2}^{(1-y/2)} + K_W * \frac{p_{H_2O}}{p_{H_2}} + \sqrt{K_H * p_{H_2}}\right)^2}$$

Each naphtha species is individually reformed, with its distinct set of rate "constants", kr and kA. Each of these is a function of temperature and has its own pre-Arrhenius factor, as well as an activation energy (for kr), and heat of adsorption (for kA). The same KH and KW is used for each reaction. These too are functions of temperature, with their Arrhenius factors and heats of adsorption taken from Froment's most recent work<sup>1</sup>. The kr and kA values for each reforming reaction for hydrocarbons higher than methane are derived from rate data reported in the literature,<sup>3,4,19</sup> and validated with overall

reformer outlet compositions measured in industrial furnaces. Each reaction also has an effectiveness factor associated with it.

Naphtha is characterized as about thirty components, pure or pseudo (several species of similar structure lumped together). The distribution of these components is chosen to best match measured specific gravity, volume average boiling fractions (ASTM-D86 method), and normal paraffinic, branched paraffinic (iso-paraffins), naphthenic, and aromatics (PINA) contents.

Numerous other rate expressions for steam reforming of higher hydrocarbons are listed in the literature (Reference 4, pages 55 & 57). Many of these are simplifications of the relationships shown here, with assumptions imposed on the relative contribution of the various terms. These assumptions may be valid for some operating conditions, or for some catalysts. Many of the rate expressions are simple “power law” relationships that are difficult to relate to mechanistic pathways, and to physical attributes of the catalyst or the reacting species. The rate expression chosen for the model is one that has a broad range of applicability, for different catalyst types, and wide operating conditions.

Specific catalysts are characterized in part by their relative values of  $k_r$ ,  $K_W$ , and  $k_A$ . The water adsorption equilibrium constant,  $K_W$ , is affected by the catalyst support. Alumina supports have lower values of  $K_W$  than magnesia supports.<sup>13</sup> Alkali content increases  $K_W$ . Increased alkali concentrations tend to decrease  $k_r$ , though. Catalysts’ shape and size affect pressure drop and effectiveness factors. Their pore structure affects their effectiveness factors as well. Additionally, the support affects the catalyst crush strength, and tendency to hold together under adverse conditions (i.e. wetting) that may be encountered during unplanned plant outages, severe operating conditions, or start-up conditions. Migration of catalyst additives into equipment downstream of the reformers has caused fouling problems in some plants. Catalysts must maintain their activity and strength for several years to be commercially viable.

The following reactions are used in the primary reformer model, for butane and naphtha feeds. The model interprets the “StmReforming” qualifier, and determines the correct stoichiometry. The “User1” and “User2” qualifiers direct the model to use either the Froment reaction rate relationships, or the naphtha reaction rate relationships.

```

Reaction Mechanism = start
!
! USER1 REACTIONS:
!
! Water Gas Shift

CO          +   H2O   =>  CO2  +   H2           :User1

```

```

! Methane Reforming to CO

CH4          +  H2O   =>  CO   +  H2   :StmReforming   :User1

! Methane Reforming to CO2

CH4          + 2*H2O  =>  CO2  + 4*H2   :User1
!
! USER2 REACTIONS:
!
! Reforming of Higher Hydrocarbons to CO & H2 (Irreversible)

Ethane       +  H2O   =>  CO   +  H2   :StmReforming   :User2
Propane      +  H2O   =>  CO   +  H2   :StmReforming   :User2
Isobutane    +  H2O   =>  CO   +  H2   :StmReforming   :User2
N-Butane     +  H2O   =>  CO   +  H2   :StmReforming   :User2
Isopentane   +  H2O   =>  CO   +  H2   :StmReforming   :User2
N-Pentane    +  H2O   =>  CO   +  H2   :StmReforming   :User2
Cyclopentane +  H2O   =>  CO   +  H2   :StmReforming   :User2
Iso-C6       +  H2O   =>  CO   +  H2   :StmReforming   :User2
N-Hexane     +  H2O   =>  CO   +  H2   :StmReforming   :User2
Cyclo-C6     +  H2O   =>  CO   +  H2   :StmReforming   :User2
Benzene      +  H2O   =>  CO   +  H2   :StmReforming   :User2
Iso-C7       +  H2O   =>  CO   +  H2   :StmReforming   :User2
N-Heptane    +  H2O   =>  CO   +  H2   :StmReforming   :User2
Cyclo-C7     +  H2O   =>  CO   +  H2   :StmReforming   :User2
Toluene      +  H2O   =>  CO   +  H2   :StmReforming   :User2
Iso-C8       +  H2O   =>  CO   +  H2   :StmReforming   :User2
N-Octane     +  H2O   =>  CO   +  H2   :StmReforming   :User2
Cyclo-C8     +  H2O   =>  CO   +  H2   :StmReforming   :User2
Aromatic-C8  +  H2O   =>  CO   +  H2   :StmReforming   :User2
Iso-C9       +  H2O   =>  CO   +  H2   :StmReforming   :User2
N-Nonane     +  H2O   =>  CO   +  H2   :StmReforming   :User2
Cyclo-C9     +  H2O   =>  CO   +  H2   :StmReforming   :User2
Aromatic-C9  +  H2O   =>  CO   +  H2   :StmReforming   :User2
Iso-C10      +  H2O   =>  CO   +  H2   :StmReforming   :User2
Cyclo-C10    +  H2O   =>  CO   +  H2   :StmReforming   :User2
N-Decane     +  H2O   =>  CO   +  H2   :StmReforming   :User2
Aromatic-C10 +  H2O   =>  CO   +  H2   :StmReforming   :User2

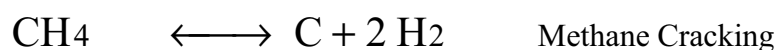
Reaction Mechanism = end

```



### 2.3 Coking

Coke deposition is a potential problem in steam reformers, and is favored by low steam to carbon ratio and high temperatures. High hydrogen composition also lowers the potential for carbon deposition. The following three reactions can deposit solid carbon, and the thermodynamic equilibrium relationships for these reactions, when carbon is graphite, are well known.<sup>3, 4, 13, 20, 21, 22, 23</sup>



Also, higher hydrocarbons can form carbon (3).



Equilibrium relationships with carbon of other forms has also been investigated and results reported in the aforementioned references. Whisker or filamental carbon is the form of carbon favored on nickel catalysts, and equilibrium of the aforementioned reactions with this form of carbon is reasonably well understood.

The first three carbon depositing reactions involve only methane and carbon monoxide, and are of particular interest in plants with methane feeds. These reactions can also occur in reformers with higher molecular weight feedstocks, since the reactants exist a short distance into the reformer tube, even when no methane exists in the feed. As mentioned in Reference 23, "The mechanism of thermal cracking (pyrolysis) of higher hydrocarbons is more complicated." Reference 13 highlights the relative risk of carbon laydown from several paraffinic, aromatic, and olefinic compounds.

Many literature articles imply that carbon deposition can be predicted and avoided by using equilibrium calculations. This implication is not correct, and several references acknowledge this fact. For methane feeds the equilibrium calculations provide reasonable guidelines, or "rules of thumb", but still are not definitive in predicting whether coke formation will be encountered. For these feeds if the conditions (composition, temperature, and pressure) are constrained so that at equilibrium (with the appropriate carbon form) no carbon exists, then it is likely that none will deposit. As clearly

stated in Reference 4, page 82, “The principle (of equilibrated gas) is *no law of nature*...It is merely a rule of thumb, indicating process conditions which are critical for carbon formation”. From page 85 of Reference 4, “The principle of equilibrated gas is no law of nature. Rates of carbon formation may be too slow. On the other hand, carbon formation may occur in spite of the principle, if the *actual* gas in the bulk phase, and thus the exterior of the catalyst pellet, shows affinity for carbon formation...Carbon formation is then a question of kinetics and the local approach to the reforming equilibrium.” Obviously, the defining relationships which would indicate whether carbon will deposit are the reaction rates associated with the actual gas (not the equilibrated gas), and include the carbon forming as well as the carbon gasifying reactions. These rates have been extensively studied<sup>3,4,20</sup> and are not presently well enough understood to justify including their reactions in the model. Reference 23 states “...the process conditions at which deposition (carbon) occurs can only be determined experimentally for each particular catalyst.”

Chapter 5 of Reference 4 presents several mechanisms for coking reactions, for methane as well as higher hydrocarbons. The rate expressions presented cannot be directly and practically used in a reformer reactor model, since many of them are for “without steam present” conditions. Section 2.2 of Chapter 5 presents an empirical approach, which uses a critical steam to carbon ratio for each hydrocarbon species. Critical steam to carbon ratios must be established by experiment. This kind of simple empirical relationship can be added as a model and connected to the reformer model, if the need arises. Presently when applied on-line, operating conditions must be empirically constrained to avoid coke formation. Experience and advice from catalyst vendors can be used to establish the empirical guidelines. Consequently, operating conditions cannot as closely approach coking conditions as would be possible if the coking rates were well defined. Even if these rates were well defined, on-line analysis of reformer conditions (naphtha feed components of high coking potential, and down the tube temperatures) may still dictate that operating conditions be empirically established.

Some confusion may exist pertaining to how catalyst activity affects coke deposition, or the potential for coke deposition. There are three distinct effects of catalyst activity. First, an inactive catalyst can deliver a specified reformer outlet “methane slip” at only slightly higher outlet temperature compared to a catalyst that is significantly more active. Results in Appendix B and Figure 12 of Reference 23 show this significant rise of temperature. For the few furnaces with in-the-tube temperature measurements and the ability to control firing profiles, this rise of temperature can be avoided by automatically adjusting firing profiles. The allowable temperatures along the tube must be empirically determined, as mentioned. Results in Appendix B illustrate this effect as well. Reformers without in-the-tube temperature measurements, or ones with limited capability of controlling firing profiles

(i.e. top or floor fired) are at higher risk of coking due to inactive catalyst, since the rise in outlet temperature is subtle, and the rise in the process temperature near the tube inlet many times goes unnoticed. The third effect of catalyst activity on coking is its influence on the coking reaction rates, which as shown are relatively poorly understood. It is clear that the first two effects of catalyst activity are captured well in this model, and that the effect on coking rate is not required to predict, and empirically avoid the higher temperatures near the tube inlet that arise due to inactive catalysts operated at a firing profile similar to that used for active catalysts.

Typical operating conditions in industrial reformers are sufficiently far from coking conditions so that significant benefits can be obtained by applying the model, and constraining operating conditions empirically, as related to coking limits. Many times product values (hydrogen, ammonia or methanol) are sufficiently different from fuel values so that plant-wide optimum operating conditions are at a high steam to carbon ratio (where hydrogen production is favored, but at higher energy usage), and coking limits are not of concern. Plant operators, designers of steam reformers, and catalyst vendors many times focus only on minimum steam to carbon ratios as being “optimum”, due to thermodynamic (energy per ton of product), and not economic objective functions.

## 2.4 Catalyst Poisoning

Catalyst “poisoning” is generally regarded as any process by which the number of catalyst active sites are reduced, and can occur due to sulfur coverage of active nickel sites, sintering of the nickel into fewer active sites, or coke deposition. The model lumps all those effects into the “activity” parameter.

The catalyst activity in the model can be a function of tube length, but typically is specified as uniform along the length. Measured data from an industrial reformer is essentially never available to allow the calculation of the activity profile. Even in reformers with in-the-tube temperature measurements, this information is usually insufficient to determine activity as a function of length. Process gas composition is required as a function of length to establish the activity profile. Clearly, such information can only be obtained in a laboratory environment.

References 23 and 24 address sulfur poisoning in significant detail. Reference 23 illustrates the relative activity of a catalyst as a function of mean sulfur coverage. Also, that reference lists a Temkin-like adsorption isotherm for equilibrium sulfur coverage, as a function of temperature, hydrogen, and hydrogen sulfide mole fraction. As stated, it takes years to establish sulfur equilibrium in a reformer.

A reasonable approach might be to “enhance” the model by imposing an activity profile by incorporating the sulfur equilibrium, or approach to

equilibrium isotherm, along the tube length. Without on-line, real time, or at least infrequent laboratory analysis of feed sulfur content, the model would have insufficient information to establish the sulfur isotherm, and subsequent activity profile. Sulfur levels in feed stocks may be very low ( $\approx 5$  ppb) and difficult to detect. Also, it would be desirable to have feedback of sulfur content on the catalyst as a function of position in the tube, as well as feed sulfur history over the entire catalyst run length to properly validate the model. In view of these issues, and since the model with a uniform activity profile agrees well with measured conditions and outlet compositions, there appears little incentive to extend the modeling functionality in this area at this time.

### 3. HEAT TRANSFER RATES AND HEAT BALANCES

Heat transfer rates are calculated to the catalyst tube from the firebox flue gas, through the tube wall, tube fouling, and inside tube film to the bulk fluid, as well as from the bulk fluid to the catalyst surface. As reported in the literature, the catalyst pellets are assumed to have a uniform temperature, since very little resistance to intra-pellet heat transfer exists.

Heat balances are determined for all the reactor models discussed. Therefore the heat duties of the radiant tubes, convection section heaters, waste heat boilers, and associated steam drums are all explicitly calculated and reported. Heat losses are part of the models, as described in the "Heat Losses" section. The enthalpies of all the streams entering and leaving each piece of equipment are calculated and reported. These streams include, for example, the process, fuel, air, and flue gas. Combustion, and all reaction related heat effects, are handled in models using enthalpies of all species including heats of formation based on of the elements at their standard states, so heats of reaction are avoided.

Heat balance terms such as furnace stack heat loss as a fraction of fired fuel heating value and furnace efficiency are not calculated, mainly since these "indices of performance" are not required in an optimization system that has the plant-wide operating profit as an objective function. These indices are remnants of local equipment or design "optimization" approaches. Typically a plant's operation should not be constrained nor its performance judged by these indices. Models can of course be easily used to calculate these indices, and "plant built" to the furnace models to perform these calculations on-line.

Heat transfer rates are calculated to the catalyst tube from the firebox flue gas, through the tube wall, tube fouling, and inside tube film to the bulk fluid, as well as from the bulk fluid to the catalyst surface. As reported in the literature, the catalyst pellets are assumed to have a uniform temperature, since very little resistance to intra-pellet heat transfer exists.

Heat balances are determined for all the reactor models discussed. Therefore the heat duties of the radiant tubes, convection section heaters, waste heat boilers, and associated steam drums are all explicitly calculated and reported. Heat losses are part of the models, as described in the "Heat Losses" section. The enthalpies of all the streams entering and leaving each piece of equipment are calculated and reported. These streams include, for example, the process, fuel, air, and flue gas. Combustion, and all reaction related heat effects, are handled in models using enthalpies of all species including heats of formation based on of the elements at their standard states, so heats of reaction are avoided.

Heat balance terms such as furnace stack heat loss as a fraction of fired fuel heating value and furnace efficiency are not calculated, mainly since these "indices of performance" are not required in an optimization system that has the plant-wide operating profit as an objective function. These indices are remnants of local equipment or design "optimization" approaches. Typically a plant's operation should not be constrained nor its performance judged by these indices. Models can of course be easily used to calculate these indices, and "plant built" to the furnace models to perform these calculations on-line.

Heat transfer rates are calculated to the catalyst tube from the firebox flue gas, through the tube wall, tube fouling, and inside tube film to the bulk fluid, as well as from the bulk fluid to the catalyst surface. As reported in the literature, the catalyst pellets are assumed to have a uniform temperature, since very little resistance to intra-pellet heat transfer exists.

Heat balances are determined for all the reactor models discussed. Therefore the heat duties of the radiant tubes, convection section heaters, waste heat boilers, and associated steam drums are all explicitly calculated and reported. Heat losses are part of the models, as described in the "Heat Losses" section. The enthalpies of all the streams entering and leaving each piece of equipment are calculated and reported. These streams include, for example, the process, fuel, air, and flue gas. Combustion, and all reaction related heat effects, are handled in models using enthalpies of all species including heats of formation based on of the elements at their standard states, so heats of reaction are avoided.

Heat balance terms such as furnace stack heat loss as a fraction of fired fuel heating value and furnace efficiency are not calculated, mainly since these "indices of performance" are not required in an optimization system that has the plant-wide operating profit as an objective function. These indices are remnants of local equipment or design "optimization" approaches. Typically a plant's operation should not be constrained nor its performance judged by these indices. Models can of course be easily used to calculate these indices, and "plant built" to the furnace models to perform these calculations on-line.

### 3.1 Firebox to Catalyst Tube

Firebox flue gas to catalyst tube heat transfer is primarily governed by radiation, but convection, although proportionally small, is included. The relationships used are derived from Chapter 19 of *Process Heat Transfer* by D. Q. Kern.<sup>14</sup>

$$Q = \sigma * F * \alpha * A_{cp} * (T_g^4 - T_{ff}^4) + h_c * A_o * (T_g - T_s)$$

Where:

- Q** = total heat transferred
- $\sigma$**  = Stefan-Boltzmann constant
- F** = Overall view (exchange) factor (See Kern, Figure 19.15)
- $\alpha$**  = Cold plane effectiveness factor (See Kern, Figure 19.11)
- $A_{cp}$**  = Cold plane area (of both sides of tube bank, or row)
- $T_g$**  = Effective temperature of radiating gas, absolute
- $T_{ff}$**  = Temperature of tube front face (surface), absolute
- $h_c$**  = Convective heat transfer coefficient
- $A_o$**  = Outside area of tube
- $T_s$**  = Average outside tube surface temperature, absolute
- $T_{ff}$**  =  $T_s * PMDF$
- PMDF** = Peripheral maldistribution factor  
(accounts for circumferential heat flux maldistribution)

This equation is essentially Equation 19.9 from Kern, modified to allow variation of conditions along the tube length. The model integrates this heat transfer relationship along the length of the tube, while simultaneously solving the kinetics, pressure drop relationships, and all other equations related to the reformer (and the rest of the plant).

The effective gas radiating profile as a function of length is related to the burner placement in the firebox, as well as to the relative burner firing rates. The overall effective gas radiating profile is built up from the individual burner row profiles. The individual burner row profiles are similar to normal distributions of temperatures around the centerline location of the burners. The effects of adjacent burner rows overlap. Amplitudes of the temperature distributions are related to the firing rates of the burners. These amplitude to burner firing rate relationships have been derived from the steady-state gains of step response models relating “catalyst” temperatures (i.e. in the tube temperatures) to burner firing rates, and are included in the model. The chain ruling that may seem required to establish the relationship of the effective

temperature profile amplitudes to the firing rates is implicitly done, since the steady-state gain relationships are added as constraints, and the amplitude variables then become dependent variables. Furthermore, the steady-state gain relationship intercept values are updated as parameters, for measured values of burner firing rates and measured “catalyst” temperatures. By this means the solution to the Parameter or Reconcile case (calculated prior to each Optimize case) can precisely match the measured down the tube temperatures, including the tube inlet (convection section heater outlet), in-the-tube “catalyst” temperatures, as well as tube outlet temperature. The Appendix A simulation results and discussion illustrate that care must be taken so that the measured catalyst temperatures are not matched with unreasonable effective gas radiating and flux profiles.

Few plants have measured temperatures inside the catalyst tubes. When those temperatures are not available there may be little justification for building models that relate the individual burner profiles to an overall effective gas radiating profile. An overall effective radiating temperature profile is still justified, but without measured feedback, its shape cannot be effectively updated on-line. A simpler gas temperature model can then be employed. Without in the tube temperature measurements it follows that temperature profile control in the tube is not practical. The absolute level of the radiating gas temperature, both in the case when the profile is built up from burner profiles and when it is not, is determined from actual operating conditions (namely measured or specified outlet temperature). The level of the temperature profile is that at which the resulting integrated heat transfer rate supplies the required heat to achieve the specified tube outlet temperature.

An important constraint on the effective gas radiating temperature profile is its relationship to the “bridgewall” temperature, which is the temperature of the flue gas leaving the radiating temperature after it has given up the total heat absorbed in the radiant section tubes and lost (small) from the radiant section walls. This relationship is in many cases handled by a radiant section efficiency parameter. This model does not use that approach, but uses an offset between the length average effective gas radiating temperature and the bridgewall temperature as the analogous parameter. Others, such as Wimpres of C. F. Braun & Co. have used a similar approach.<sup>27</sup> The offset parameter is updated on-line, and is determined by firebox heat balance determined from heat absorbed on the process side, fuel firing rate, and arch oxygen measurements. Heat balances using measured bridgewall temperatures from conventional thermocouples should not be attempted, due to the reasons explained in the “Convection Section” section of this report. The measured fuel flow, for the observed radiant duty, affects this parameter the most. The effective radiating gas temperature profile is not tied to the flue gas temperature at other than the bridgewall position, since the effective temperature (the radiation “source” temperature) is a result of all refractory as

well as flue gas temperatures in line-of-sight of the tube front face temperature (radiation “sink” temperature) at any position. If the heat balance with the flue gas were calculated all along the tube, and if that temperature were used as the radiating source temperature, the resulting heat flux profile would not reflect the actual phenomena occurring, and would be significantly in error for most, if not all, industrial furnaces.

The following chart shows a typical net effective gas radiating temperature profile, along with the individual burner row by burner row profiles.

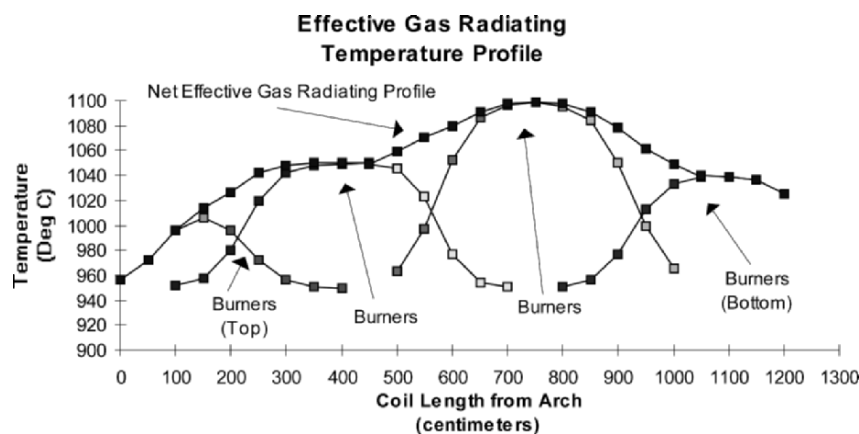


Figure 1. Effective Gas Radiating Temperature Profile

### 3.2 Conduction Across Tube Wall

Heat transfer across the tube wall occurs by conduction. The one-dimensional form of Fourier’s law of heat conduction (page 245 of Reference 25) is used as the governing relationship between heat flux, thermal conductivity, and temperature gradient. The tube wall thickness is an explicit “discretized” variable in the model. It therefore can vary with length, although most tubes are of uniform thickness. The thermal conductivity is also a model variable, but is considered constant as a function of length.

### 3.3 Fouling Resistance

A fouling (or “coke”) layer is included in the tube reactor model. Fouling thickness in the model can vary with length. The fouling thermal conductivity is a variable whose value can be specified, and is assumed invariant with length. Theoretically, measured tube metal temperatures at various lengths can be used to “back out” the apparent fouling profile, although inherent errors in pyrometer measurements make this impractical. With little or no



fouling the outside tube metal temperature profile approaches the shape of the process (inside the tube) temperature profile, and with appreciate fouling the outside metal temperature profile approaches the shape of the effective radiating gas profile. Hence, the fouling, even if assumed uniform, can be used as a parameter to more closely match tube metal temperatures close to the tube inlet, while the “peripheral maldistribution factor” can be used as a parameter to match the hottest measured tube metal temperature, usually near the tube outlet.

### 3.4 Inside Tube to Bulk Fluid

The inside tube surface to bulk fluid heat transfer coefficient is calculated using the Sieder-Tate correlation for turbulent flow (similar to Dittus-Boelter), as listed in Reference 15:

$$\frac{h D}{k} = 0.023 (\text{Re}^{0.8} \text{Pr}^{0.3}) \left( \frac{\mu}{\mu_0} \right)^{0.14}$$

Where:

- h = Inside heat transfer coefficient
- D = Inside tube diameter
- k = Process fluid thermal conductivity
- Re = Reynolds Number
- Pr = Prandtl Number
- $\mu$  = Bulk fluid viscosity
- $\mu_0$  = Fluid viscosity at the tube wall

### 3.5 Bulk Fluid to Catalyst Pellet

Heat transfer to the pellet is calculated by applying Equation 28 of Chapter 14 in Reference 31:

$$\Delta T_{\text{film}} = (T_{\text{gas}} - T_{\text{pellet surface}}) = \frac{L * (-\text{rate}) * (-\Delta H_r)}{h_s}$$

This relationship assumes that all the reactions occur inside the pellets, and that none occurs in the bulk fluid. This is a very good assumption in a steam reformer. The heat of reaction is backed out of the heat effects, since heats of reaction are not explicitly used elsewhere. Heats of formation are based on elements at their standard reference states, so the overall heat effects (sensible plus reaction) are included in enthalpies.

The bulk fluid to catalyst pellet heat transfer coefficient,  $h_s$ , is calculated as a function of fluid properties, catalyst size, and fluid temperature using the heat transfer relationship from Reference 11, page 89, Table 4.2:

$$\frac{h_s D_p}{\lambda_f} = 2 + 1.1 \text{Pr}^{1/3} \text{Re}^{0.6}$$

### 3.6 Within the Catalyst Pellet

Little resistance to heat transfer exists within the catalyst pellet (Reference 4, page 69). Consequently, the catalyst temperature is assumed to be uniform, at the catalyst surface temperature.

### 3.7 Convection Section

The convection section pre-heaters are modeled using standard heat exchanger models. Considerable differences between measured and calculated temperatures exist on the flue gas side, especially at the higher flue gas temperatures leaving the firebox, or just above the auxiliary burners. These discrepancies can be explained by the shortcomings associated with standard thermocouples employed in high temperature service. The main problem with these thermocouples is that they cannot come close to thermal equilibrium with the very hot flue gas, so their measurements are consistently low. This problem is well understood, and documented in several heat transfer texts.<sup>16,17,18</sup> Reference 16 illustrates the large errors that can arise in high temperature environments, and Reference 17 highlights the futility of using temperatures measured with conventional thermocouples as the bases for heat balances. Reed, in Reference 17, states, "...experience shows that an attempt at heat balance where gas temperatures are taken from fixed thermocouples is largely a pointless exercise in calculation because of inaccuracy of gas temperature measurement and thus, gas heat content". Illustrations on pages 33-17 and 33-18 of Reference 18 show thermocouples that are specially designed for high temperature measurements.

The measured fuel flows, arch oxygen composition, and high pressure steam drum heat balance confirm that the heat duties calculated from the process side (as opposed to the flue gas side) are most accurate, as would be expected. The high pressure steam system and boiler feed water measurements impact significantly on the convection section heat balance since boiler feed water preheat and steam superheat duties make up the majority of the convection section duty. The high pressure steam import flow, and the expected versus measured and calculated synthesis gas compressor steam turbine performance further support that the process side, and not the flue gas side measurements are the most accurate.

### 3.8 Fuel and Combustion Air System

The fuel-air mixtures are combusted in “extent of reaction” models. Complete combustion to water vapor and carbon dioxide is assumed, with no residual carbon monoxide remaining. The model can be implicitly kept valid by lower bounding the flue gas oxygen content so complete combustion is maintained.

Combustion air preheat is modeled with standard heat exchanger models.

### 3.9 Heat Losses

The firebox model has a heat loss term that can be calculated as a parameter, however the loss term is essentially a small difference between large numbers (total heat fired minus total heat absorbed in radiant plus convection sections), so it is subject to large relative errors. Additionally, the heat “loss” may be calculated as a heat gain depending on the accuracy of the fired and absorbed heat duties. To keep the heat loss from the firebox reasonable, it is typically set to a small value, on the order of 1% of the heat fired.

There is also a heat loss term associated with the high-pressure steam drum. This term is typically used to understand the whether significant errors exist in boiler feed water flows, steam flows and temperatures, furnace convection section measurements, and fuel flow and composition measurements. During the optimization system commissioning sensitivity of this term to the aforementioned measurements helps those commissioning the system eliminate the worst measurements, and establish the validity of the models.

## 4. PRESSURE DROP

Pressure drop calculations in the primary and secondary reformer models are based on the Ergun<sup>5</sup> relationship, as presented in Reference 25. Both the laminar flow and turbulent flow terms are included. The natural parameter that arises from the Ergun equation, which can be updated with measured pressure drop information, is the “TURBULENT\_DP\_COEF” term in the models of both the primary and secondary reformers. This term affects only the pressure drop, whereas another term, the bed void fraction, which might also have been used as the parameter to update with measure pressure drop, also affects all the reaction rates. The bed void fraction affects the amount of catalyst in a fixed volume reformer tube, and is not an appropriate parameter to use in this case. The void fractions of typical packed beds are shown in Figure 5.70 of Reference (26). Void fractions of 0.4 to 0.6 are typical, and can be determined for specific catalysts sizes and shapes from vendor specification sheets, by measurement, or, with more difficulty, by calculation.

The “TURBULENT\_DP\_COEF” is the appropriate performance indicator for catalyst pressure drop, and is a better indicator than pressure drop itself, since it is independent of all the known effects of flow rate (both hydrocarbon and steam), gas density, viscosity, catalyst particle diameter, and void fraction. Pressure drop itself is important though, due to the stress it imposes on the catalyst (which raises the potential for crushing) and normally the optimization system has an upper bound on pressure drop. That bound may or may not be active at the solution, depending on the catalyst condition, and whether the solution is maximizing throughput.

The pressure drop profile illustrated is for a primary reformer when the pressure drop across the catalyst was fairly high. The differential pressure indicator showed a 2.9 kg/cm<sup>2</sup> drop across the catalyst tubes.

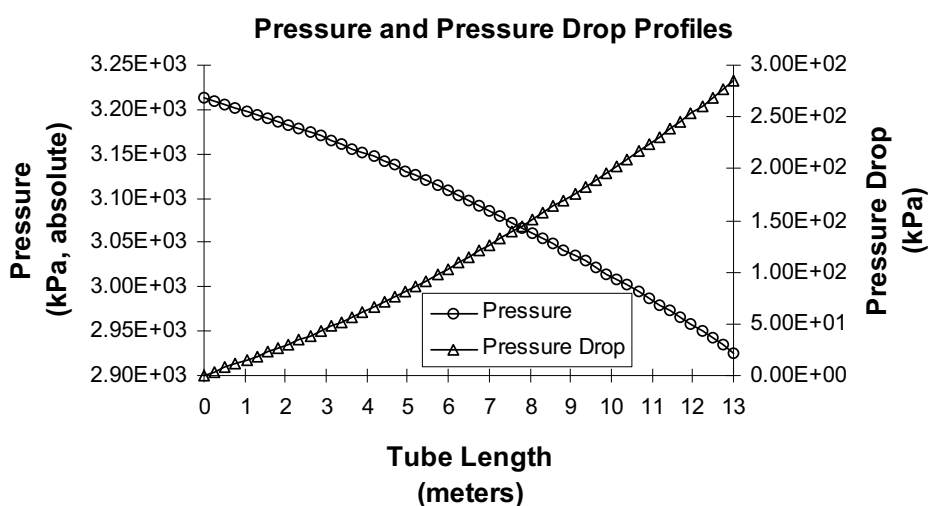


Figure 2. Pressure and Pressure Drop Profile

#### 4.1 Secondary Reformer Reactions and Heat Effects

Most steam reformers are process furnaces, transferring the required endothermic heat from a firebox to the process inside catalyst-packed tubes. Some steam reformers are “auto-thermal”, getting their heat from oxidation reactions occurring within the catalyst bed. Secondary reformers in ammonia plants are an example of auto-thermal steam reformers.

There are several categories of reactions and heat effects calculated in the secondary reformer model. First, the primary reformer effluent is mixed with the process air. Then, the effect of consuming the oxygen that is admitted with the process air is determined. This effect was investigated by simulating several possible reaction pathways. The results were insensitive to the pathway chosen, so the simplest, and also the most thermodynamically

avored route was used. This assumes that all the oxygen preferentially reacts with primary reformer effluent hydrogen. Sufficient hydrogen exists under all reasonable operating conditions so oxygen is the limiting reactant, therefore no methane is oxidized. The model includes oxidation of methane as a possible pathway, however it is presently not activated. That pathway can be activated without modifying the model by just changing input data (extent of reaction). The adiabatic “flame” temperature is calculated for this oxidation set of reactions, and the outlet from this “extent of reaction” model is the inlet to the secondary reformer packed catalyst bed.

This model assumes that the oxidation is complete before the top of the catalyst bed, and that only methane reforming as described by References 1 and 2 occur in the reactor bed. The same kinetic rate expressions are used as in the primary reformer. The catalyst activity is of course different from the primary reformer activity, and is determined from operating data. An initial estimate of its value, relative to the primary reformer activity, was calculated as the primary reformer activity, times the nickel weight percent ratio, times the density ratio of the catalysts. This estimate assumes that the nickel mass in either catalyst supplies similar number of active sites. The activity calculated in this manner is close to the reconciled activity, based on measured compositions in the primary and secondary outlet, and operating conditions. Effluent compositions are very insensitive to assumptions concerning how the oxygen is reacted. For example, if some of the methane from the primary effluent is oxidized, rather than only hydrogen, the results are essentially unchanged. The high temperatures in the reactor cause the reaction rates to be relatively high, bringing the outlet near equilibrium. This near equilibrium condition is a state, and not a path function, so it is not surprising that various reaction pathways affect the results so little.

The reactor bed is not assumed to be adiabatic, but loses heat from its walls. Presently a constant heat flux from the walls is assumed. A flux profile can easily be imposed, based on heat transfer driving force, but its effect will be negligible. In fact, if the reactor were assumed adiabatic the results would be essentially unchanged. The heat loss from the reactor walls was retained, so that the effects of the heat losses can be easily demonstrated.

## 4.2 Model Validation

The primary reformer models has been validated by comparing calculated to measured results, and by comparing predicted to observed results. Three cases of calculated versus measured results are presented, one for naphtha feed, and the other for butane feed. One case of predicted versus observed results is presented, for a naphtha feed. The on-line, closed-loop optimization system continuously supplies validation results, by reporting differences (biases) between calculated and measured results on every optimization cycle.

These results, along with calculated parameters, can be monitored by trending their values as a function of time.

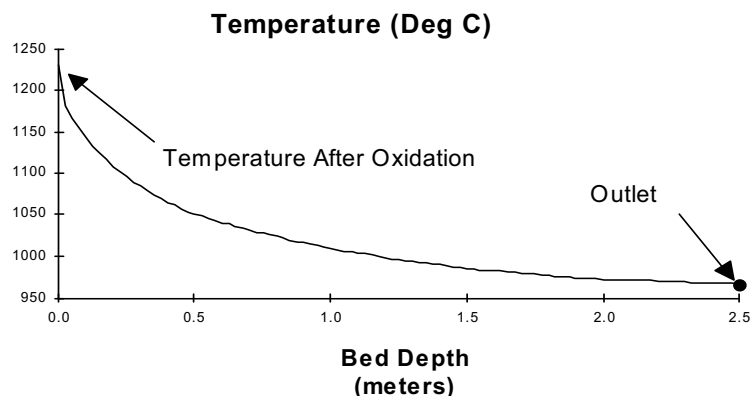


Figure 3. Temperature Profile as a function of Bed Depth

The first two validation cases are Parameter cases, while the third is a Reconcile case. In the first two cases only primary reformer calculations are done, while in the third case both primary and secondary reformer calculations are performed. The Parameter cases manipulate the process steam flow and outlet temperature to match observed outlet  $\text{CO}_2$  and  $\text{CH}_4$ . In the Reconcile case the best values for the primary and secondary reformer catalyst activities are determined as well, using an objective function which minimizes the differences between calculated and observed outlet compositions of both reformers, calculated and observed primary outlet temperature, and calculated and observed process steam flow rate.

#### 4.2.1 Validation Case 1 (Naphtha Feed Parameter Case)

The feed composition used for this validation case was characterized as listed in Table 1.2, based on measured naphtha gravity, ASTM-D86 volume versus boiling point, and PINA (paraffin, isoparaffin, naphthinic, and aromatic content) information, plus recycle desulfurization hydrogen stream measurements. The feed is a mix of the naphtha and desulfurization hydrogen streams. This naphtha feed molecular weight is 65.923.

Table 1.0 Validation Case 1 - Operating Conditions

|                    |  |
|--------------------|--|
| Feed               | Naphtha  |
| Feed rate          | 17.7 Tonnes/h  |
| Process steam rate | 79.0 Tonnes/h<br>(Parameterized to 82.92 to match effluent $\text{CO}_2$ ) |
| Inlet temperature  | 470°C  |
| Outlet temperature | 760°C (Parameterized to 761.99 to match $\text{CH}_4$ )                    |

Table 1.1 Validation Case 1 - Outlet Compositions

| Component       | Calculated<br>Dry mole % | Observed<br>Dry mole % |
|-----------------|--------------------------|------------------------|
| HYDROGEN        | 63.9077                  | 63.6                   |
| NITROGEN        | 0.3675                   | 0.4                    |
| ARGON           | 0.0060                   | ---                    |
| CARBON MONOXIDE | 9.0188                   | 9.2                    |
| CARBON DIOXIDE  | 16.4000                  | 16.4                   |
| METHANE         | 10.3000                  | 10.3                   |

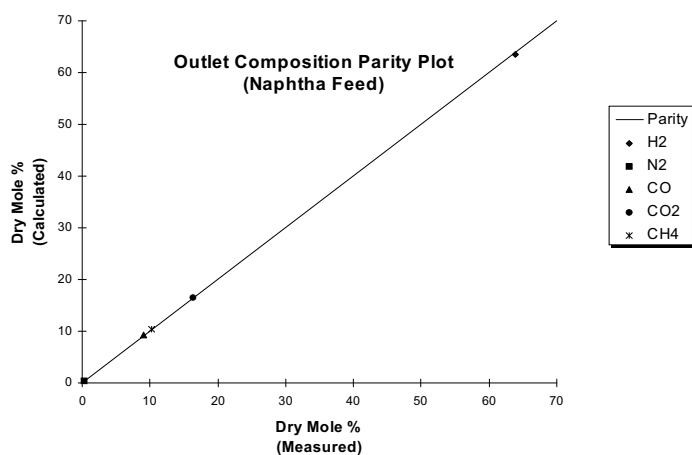


Table 1.2 Validation Case 1 - Feed Composition

| Component       | Mole%  |
|-----------------|--------|
| HYDROGEN        | 13.807 |
| NITROGEN        | 4.610  |
| ARGON           | 0.075  |
| CARBON MONOXIDE | 0.000  |
| CARBON DIOXIDE  | 0.000  |
| METHANE         | 0.258  |
| ETHANE          | 0.000  |
| PROPANE         | 0.000  |
| ISOBUTANE       | 0.932  |
| n-BUTANE        | 1.792  |
| ISOPENTANE      | 17.142 |
| n-PENTANE       | 24.221 |
| CYCLOPENTANE    | 2.553  |
| ISO-C6          | 10.628 |
| n-HEXANE        | 7.386  |
| CYCLO-C6        | 5.952  |
| BENZENE         | 2.064  |
| ISO-C7          | 2.639  |
| n-HEPTANE       | 1.952  |
| CYCLO-C7        | 1.441  |
| TOLUENE         | 0.391  |
| ISO-C8          | 0.621  |
| n-OCTANE        | 0.509  |

|              |       |
|--------------|-------|
| CYCLO-C8     | 0.314 |
| AROMATIC-C8  | 0.150 |
| ISO-C9       | 0.155 |
| n-NONANE     | 0.103 |
| CYCLO-C9     | 0.087 |
| AROMATIC-C9  | 0.066 |
| ISO-C10      | 0.048 |
| CYCLO-C10    | 0.027 |
| n-DECANE     | 0.047 |
| AROMATIC-C10 | 0.030 |
| WATER        | 0.000 |

#### 4.2.2 Validation Case 1a (Naphtha Feed Simulate Case)

This case is simulated at the same conditions as the Case 1 Parameter case, except at an outlet temperature of 778 Deg C, compared to 762 Deg C.

A comprehensive set of plant operating conditions was not available for this case, but the plant indicated a methane slip of about 8.5 % was observed by the plant for this outlet temperature. The calculated outlet methane dry mole percent of 8.8 % is very close to the 8.5 % that was observed, and since all the independent conditions (feed rate, steam to carbon ratio, etc.) are not precisely known for this case, the “discrepancy” may be easily attributed to differences in simulated versus actual conditions.

Table 1.3 Validation Case 1a - Outlet Compositions

| Component       | Calculated<br>Dry mole % | Observed<br>Dry mole % |
|-----------------|--------------------------|------------------------|
| HYDROGEN        | 65.1413                  | Unavailable            |
| NITROGEN        | 0.3550                   | Unavailable            |
| ARGON           | 0.0058                   | Unavailable            |
| CARBON MONOXIDE | 9.8817                   | Unavailable            |
| CARBON DIOXIDE  | 15.8156                  | Unavailable            |
| METHANE         | 8.8006                   | ≅ 8.5                  |

#### 4.2.3 Validation Case 2 (Butane Feed Parameter Case)

The feed composition used for this validation case was characterized as listed in Table 2.2, based on typical butane feed, plus recycle desulfurization hydrogen stream measurements. The feed is a mix of the butane and desulfurization hydrogen streams.

Table 2.0 Validation Case 2 - Operating Conditions

|                    |  |
|--------------------|--|
| Feed               | Butane   |
| Feed rate          | 17.7 Tonnes/h  |
| Process steam rate | 70.3 Tonnes/h (Parameterized to 70.8 to match effluent CO <sub>2</sub> )                 |
| Inlet temperature  | 473°C  |
| Outlet temperature | 773°C Average (Range: 763 < T < 779)<br>(Parameterized to 779 to match CH <sub>4</sub> ) |



Table 2.1 Validation Case 2 - Outlet Compositions

| Component       | Calculated<br>Dry mole % | Observed<br>Dry mole % |
|-----------------|--------------------------|------------------------|
| HYDROGEN        | 63.6562                  | 63.5                   |
| NITROGEN        | 0.2844                   | 0.3                    |
| ARGON           | 0.0046                   | ---                    |
| CARBON MONOXIDE | 10.3548                  | 10.4                   |
| CARBON DIOXIDE  | 14.7                     | 14.7                   |
| METHANE         | 11.0                     | 11.0                   |

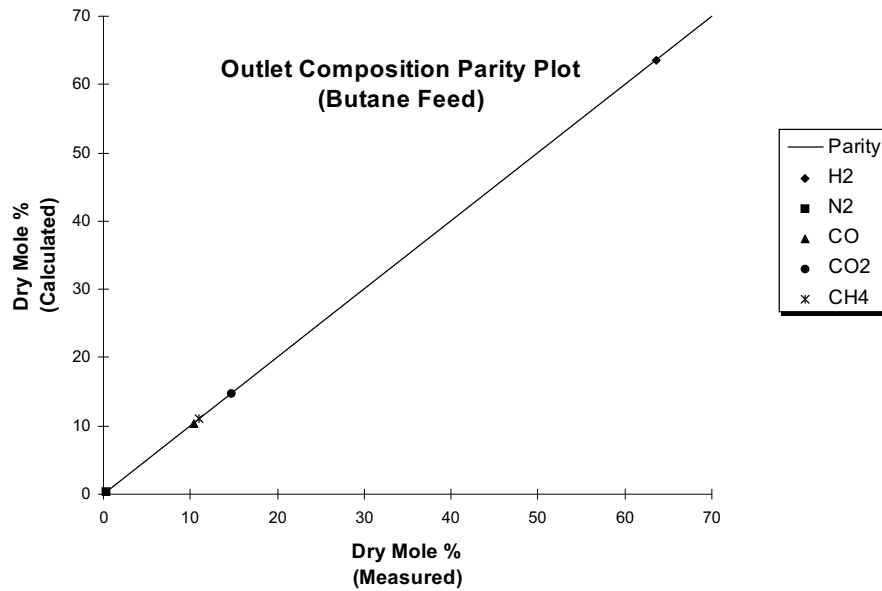


Table 2.2 Validation Case 2 - Feed Composition

| Component       | Mole % |
|-----------------|--------|
| HYDROGEN        | 8.100  |
| NITROGEN        | 2.806  |
| ARGON           | 0.046  |
| CARBON MONOXIDE | 0.000  |
| CARBON DIOXIDE  | 0.000  |
| METHANE         | 0.157  |
| ETHANE          | 0.000  |
| PROPANE         | 0.000  |
| ISOBUTANE       | 0.932  |
| n-BUTANE        | 87.959 |
| ISOPENTANE      | 0.000  |
| n-PENTANE       | 0.000  |

#### 4.2.4 Validation Case 3 (Primary & Secondary Reformer Butane Feed Reconcile Case)

A Reconcile case was executed with the objective function minimizing the sum of the weighted squared differences between the calculated and measured primary outlet compositions, outlet temperature, and secondary reformer outlet compositions. Primary reformer catalyst activity, secondary reformer catalyst activity, primary outlet CO<sub>2</sub> measurement minus calculated value difference, and secondary outlet CH<sub>4</sub> measurement minus calculated value difference were the degrees of freedom (the independent manipulated variables). The degrees of freedom are bounded to assure the results are most reasonable. By posing the problem in this manner the insensitive nature of the catalyst activities (due to near equilibrium conditions) is handled as well as possible. By step bounding the catalyst activities, the errors or “noise” in the composition and process steam flow measurements are not all forced into the catalysts activities, as would be the case if a “square” Parameter case were posed. The best weighting of the terms in the objective function is determined during commissioning when many sets of data are processed in an open-loop mode. Over long time periods (months) the catalyst activities trends downward, since the steps bounds are relative to the activity values from the last solution. Soft bounds (see [DMO]<sup>TM</sup> Users’ Manual) may need to be employed if the data has significant error, causing otherwise (i.e. without soft bounds) infeasible problems to be posed.

This approach allows the relationship between firing duties and catalyst temperatures, if available, (derived from [DMC]<sup>TM</sup> controller steady-state gains) to be used, with all of the intercepts being updated as parameters, determined primarily by the measured catalyst temperatures. The catalyst temperatures are matched precisely at the solution of each Reconcile case.

The overall approach in determining the catalyst activities relies on reformer outlet compositions which are near equilibrium to update rate parameters (catalyst activities). This kind of analysis is inherently problematic, but can be handled as described. Short term trends of the catalyst activities (hourly, daily, or even over a week or so) will be subject to somewhat erratic, noisy behavior, but will not detract significantly from the ability of the models to predict appropriate outlet compositions and reactor temperature profiles. As the catalysts become less active the aforementioned numerical problems diminish, and the activity trends will become smoother, for the same error in measurements, since the outlet conditions become further (but still not very far) from equilibrium.

The feed composition used for this validation case was characterized as listed in Table 3.2, based on typical butane feed, plus recycle desulfurization hydrogen stream measurements. The feed is a mix of the butane and desulfurization hydrogen streams.

As described, the secondary reformer model was solved along with the primary reformer model for Validation Case 3. The results are listed in Table 3.3.

Table 3.0 Validation Case 3 - Operating Conditions

|                    |  |
|--------------------|--|
| Feed               | Butane                                 |
| Feed rate          | 17.451 Tonnes/h                        |
| Process steam rate | 73.556 Tonnes/h (Reconciled to 74.773) |
| Inlet temperature  | 464.2°C                                |
| Outlet temperature | 772.81°C (Reconciled to 772.92)        |

Table 3.1 Validation Case 3 - Outlet Compositions

| Component       | Calculated<br>Dry mole % | Observed<br>Dry mole % |
|-----------------|--------------------------|------------------------|
| HYDROGEN        | 64.3261                  | 66.4770                |
| NITROGEN        | 0.4858                   | 0.2608                 |
| ARGON           | 0.0935                   | ---                    |
| CARBON MONOXIDE | 9.9671                   | 10.4600                |
| CARBON DIOXIDE  | 14.8347                  | 14.896                 |
| METHANE         | 10.2928                  | 10.415                 |

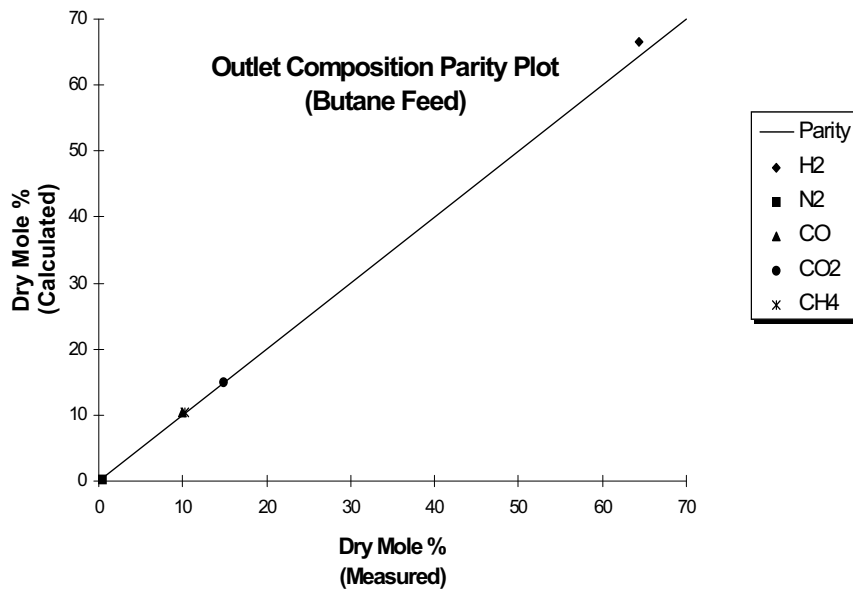


Table 3.2 Validation Case 3 Feed - Composition

| Component       | Mole %  |
|-----------------|---------|
| HYDROGEN        | 10.8684 |
| NITROGEN        | 4.5144  |
| ARGON           | 0.8692  |
| CARBON MONOXIDE | 0.0000  |
| CARBON DIOXIDE  | 0.0000  |
| METHANE         | 2.9427  |
| ETHANE          | 0.0000  |
| PROPANE         | 0.0000  |
| ISOBUTANE       | 0.8121  |
| n-BUTANE        | 79.9885 |
| ISOPENTANE      | 0.0000  |
| n-PENTANE       | 0.0000  |

Table 3.3 Validation Case 3 - Secondary Reformer Outlet Conditions

| Component        | Calculated<br>Dry mole % | Observed<br>Dry mole % |
|------------------|--------------------------|------------------------|
| HYDROGEN         | 52.952                   | 53.553                 |
| NITROGEN         | 22.254                   | 22.254                 |
| ARGON            | 0.327                    | -----                  |
| CARBON MONOXIDE  | 13.818                   | 13.245                 |
| CARBON DIOXIDE   | 10.164                   | 10.583                 |
| METHANE          | 0.4843                   | 0.4843                 |
| Temperature (°C) | 966.82                   | 966.52                 |

The outlet methane concentration bias in the objective function was heavily weighted (to drive it toward zero, since the objective function is the sum of the weighted squares biases) and therefore explains the good agreement between calculated and observed values. The process air flow measurement bias (difference between measured and calculated) was a parameter, so the calculated nitrogen composition is precisely equal to the measured value. The air flow measurement bias was 4.4% of the measured value at the solution. The calculated outlet temperature is surprisingly close to the measured value. The heat balance around the high pressure steam drum required only a 1.2% heat loss to close in this case. That balance is of course affected by numerous other measurements, so the calculated secondary reformer outlet enthalpy can only be said to be part of the overall consistent set of information.

## 5. REFERENCES

1. Xu, J.; Froment, G. F., Methane Steam Reforming, Methanation and Water-Gas Shift: I. Intrinsic Kinetics, *AIChE J.* **1989**, *35* (1), 88.
2. Xu, J.; Froment, G. F., Methane Steam Reforming:II. Diffusional Limitations and Reactor Simulation, *AIChE J.* **1989**, *35* (1), 97.

3. Rostrup-Nielsen, J. R., Steam Reforming Catalysts, An Investigation of Catalysts for Tubular Steam Reforming of Hydrocarbons, Teknisk Forlag A/S, Copenhagen, 1975.
4. Rostrup-Nielsen, J. R., *Catalytic Steam Reforming*, Springer-Verlag: Berlin/Heidelberg/New York, 1984.
5. Ergun, S., Fluid Flow through Packed Columns, *Chem. Eng. Prog.* **1952**, 48 (2), 89.
6. Elnashaie, S. S. E. H. et al., Digital Simulation of Industrial Steam Reformers for Natural Gas Using Heterogeneous Models, *Can. J. Chem. Eng.* **1992**, 70, 786.
7. Boudart, M., Two Step Catalytic Reaction, *AIChE J.* **1972**, 18 (3), 465.
8. Smith, J.M., *Chemical Engineering Kinetics*, 2nd ed., McGraw-Hill: New York, 1970.
9. Rostrup-Nielsen, J. R.; Wristberg, J., Steam Reforming of Natural Gas at Critical Conditions, Natural Gas Processing and Utilisation Conference, Dublin, Ireland, 1976.
10. Satterfield, C. N.; Sherwood, T. K., *The Role of Diffusion in Catalysis*, Addison-Wesley Publishing Company: Reading, Massachusetts, 1963.
11. Rase, H. F., *Fixed-Bed Reactor Design and Diagnostics Gas-Phase Reactions*, Butterworth Publishers: Boston, 1990.
12. Bridger, G. W., Design of Hydrocarbon Reformers, *Chem. Process Eng.*, January, 1972.
13. Rostrup-Nielsen, J. R., Hydrogen via Steam Reforming of Naphtha, *Chem. Eng. Prog.*, September, 1977.
14. Kern, D. Q., *Process Heat Transfer*, McGraw-Hill: New York, 1950, 1990.
15. Greenkorn, R. A.; Kessler, D. P., *Transfer Operations*, McGraw-Hill: New York, 1972.
16. Krieth, *Principles of Heat Transfer*, International Textbooks Co.: Scranton, Pennsylvania, 1965.
17. Reed, R. D., *Furnace Operations*, Gulf Publishing Co.: Houston, Texas, 1976.
18. *Steam - Its Generation and Use*, The Babcock & Wilcox Company, 1972.
19. Rostrup-Nielsen, J. R., Activity of Nickel Catalysts for Steam Reforming of Hydrocarbons, *J. Catal.*, **1973**, 31, 173-199.
20. Froment, G. F.; Wagner, E. S., Steam Reforming Analyzed, *Hydrocarbon Process.*, July, 1992.
21. Colton, J. W., Pinpoint Carbon Deposition, *Hydrocarbon Process.*, January, 1991.
22. Rostrup-Nielsen, J. R., Equilibria of Decomposition Reactions of Carbon Monoxide and Methane Over Nickel Catalysts, *J. Catal.*, **1972**, 27, 343-356.
23. Hansen, J. H. B.; Storgaard, L.; Pedersen, P. S., Aspects of Modern Reforming Technology and Catalysts, AIChE Paper No. 279d, AIChE Ammonia Symposium, *Safety in Ammonia Plants and Related Facilities*, Los Angeles, California, November 17-20, (1991).
24. Christiansen, L. J.; Andersen, S. L., Transient Profiles in Sulphur Poisoning of Steam Reformers, *Chem. Eng. Sci.* **1980**, 35, 314-321.
25. Bird, R. B.; Stewart, W. E.; Lightfoot, E. N., *Transport Phenomena*, John Wiley & Sons, Inc., 1960.
26. Perry, R. H.; Chilton, C. H., *Chemical Engineers' Handbook*, 5th Edition, McGraw-Hill: New York, 1973.
27. Wimpres, N., Generalized Method Predicts Fired-Heater Performance, *Chem. Eng.*, May, 1978.
28. Singh, C. P. P.; Saraf, D. N., Simulation of Side Fired Steam-Hydrocarbon Reformers, *Ind. Eng. Chem. Process Des. Dev.* **1979**, 18(1).
29. Rostrup-Nielsen, J. R.; Christiansen, L. J.; Hansen, J. H., Activity of Steam Reforming Catalysts: Role and Assessment, *Appl. Catal.*, **1988**, 43, 287-303.
30. Phillips, T. R.; Yarwood, T. A.; Mulhall, J.; Turner, G. E., The Kinetics and Mechanism of Reaction Between Steam and Hydrocarbons Over Nickel Catalysts in the Temperature Range 350-500°C, *J. Catal.*, **1970**, 17, 28-43.
31. Levenspiel, O., *Chemical Reaction Engineering*, John Wiley & Sons, Inc., 1962 & 1972.

## APPENDIX A SIMULATION RESULTS

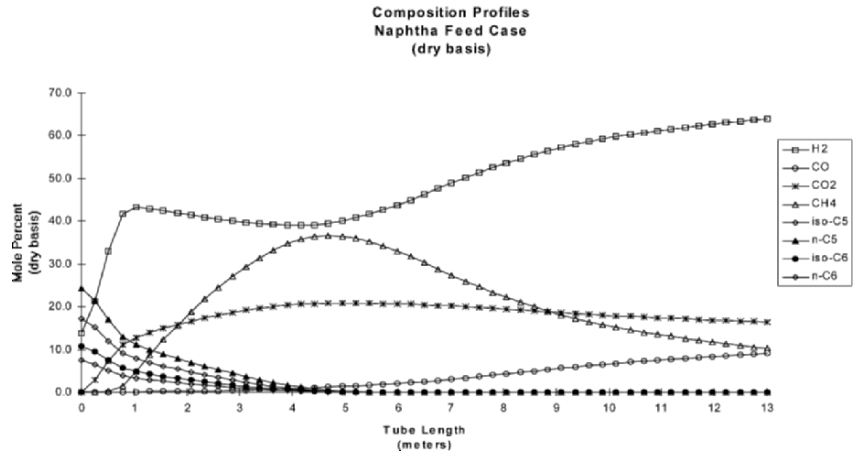
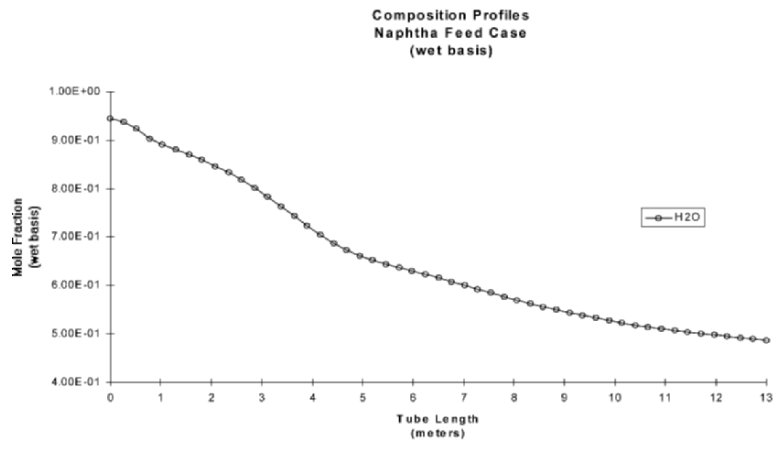
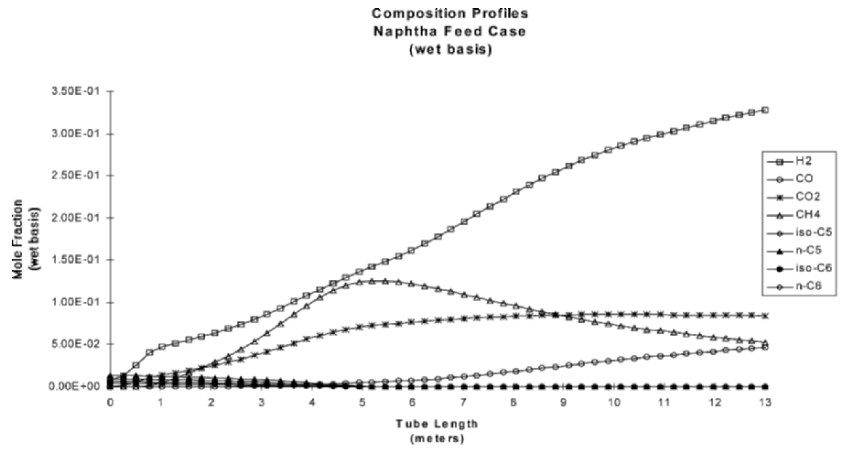
### Primary Reformer

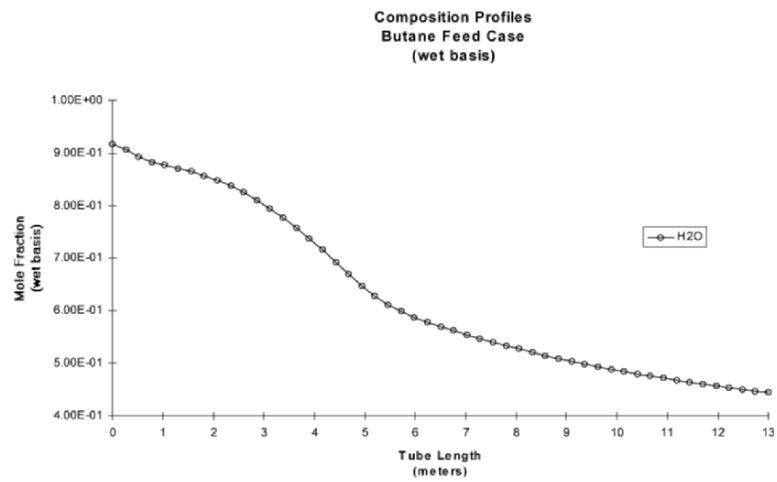
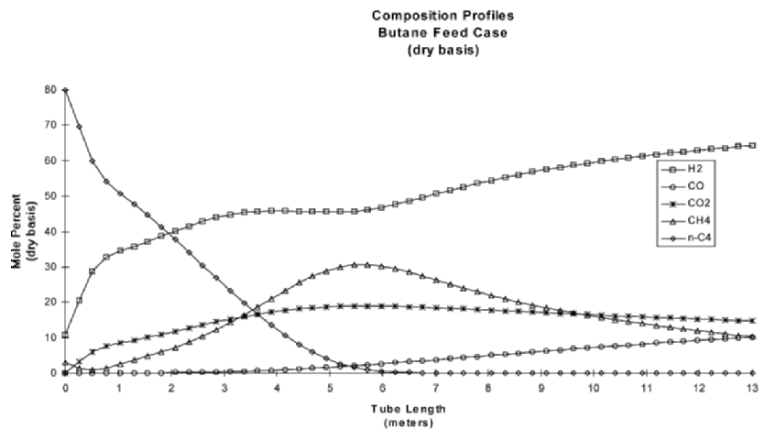
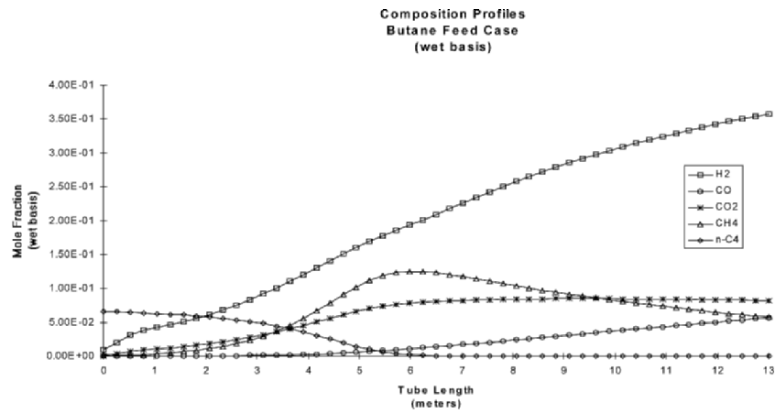
Results are shown for naphtha and butane feeds. The naphtha feed case profiles are results from the “Validation Case 1”, and the butane feed results are from “Validation Case 3” described in the “Model Validation” section.

The calculated versus outlet composition comparisons have been discussed. This section illustrates the profile results, and compares them to literature sources (for compositions), and to measurements (for temperatures). Only the key component concentrations are plotted, such as methane, hydrogen, carbon monoxide, carbon dioxide, and the main hydrocarbon species. The minor hydrocarbon species, nitrogen, and argon concentration profiles are not shown.

Both the naphtha and butane feed cases show the methane profile rising from very low inlet values to a maximum, and falling to the outlet composition. The hydrocarbon species compositions fall quickly, and are essentially zero at about 4 to 6 meters from the tube inlet. These profiles are in close agreement with the profiles shown in References 4 and 13. For more active catalyst, the hydrocarbon species disappear closer to the tube inlet. The simulated temperature profiles are also in good agreement with profiles in those references, but more importantly, they agree precisely with the measured profiles. Reference 23 shows that the temperature profile in a top fired reformer is significantly different than in a wall-fired furnace.

Only one literature reference<sup>12</sup> was found that illustrated the hydrogen composition profile along the catalyst tube. The simulated results agree well with that reference’s profile. At first the dry basis hydrogen composition profile appears strange, since it peaks at a position fairly close to the tube inlet (about 1 to 2 meters), falls, then rises again. On a wet basis the profile is monotonic, and appears reasonable, since no decline occurs. The initial sharp rise in hydrogen concentration is due to the fast rates of reforming of the hydrocarbon species. As carbon dioxide concentration rises, it impedes hydrogen production via the water gas shift reaction, but as shown on the wet basis profile plots, the rate of change is still positive. Since water is a reactant, and not just a diluent of the hydrocarbon to prevent coking, dry basis profiles are misleading. The Reference 12 dry basis hydrogen profile has the same peak and subsequent rise as the results plotted for naphtha feed. The hydrogen profile for butane feed, for the catalyst activity and firing profile representing late June 1994 operation, shows a much more subtle “peak”.

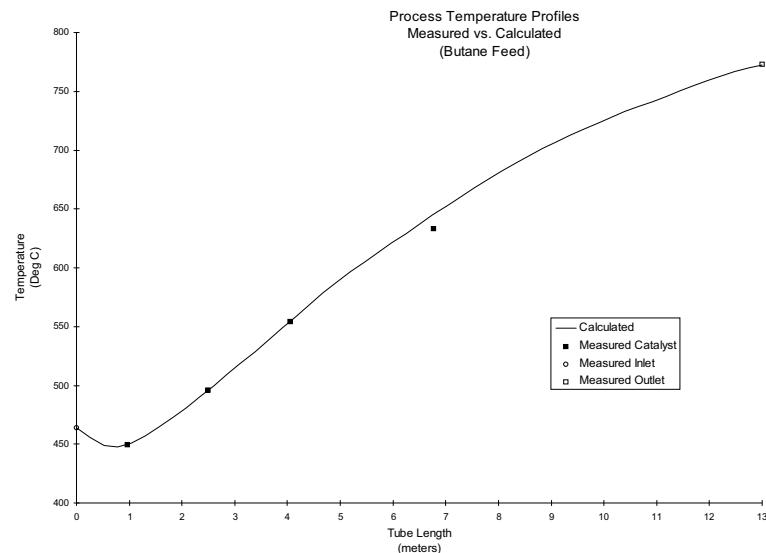






The flux calculated at the top of the tube is quite small, but must be that small to allow the temperature to drop from the measured convection section feed/steam preheat exchanger outlet temperature to the upper most measured catalyst temperature. The small flux is insufficient to supply all the net endothermic heat of reaction, so the temperature drops several degrees. Further down the tube the flux is sufficient to supply the reaction plus sensible heat, and the temperature rises. The flux profile is sensitive to the specified catalyst temperatures. Small discrepancies in the catalyst temperatures (or their position) require that the flux profile change significantly, if all the model and measured temperatures are required to match. Reconciliation of the measured temperatures, with shape constraints (rate of change or inflection point restrictions) on the flux profile can be used to assure a reasonable flux profile.

The measured tube metal temperature (TMT) is precisely matched at the solution of a Parameter or Reconcile case, since the “Peripheral Maldistribution Factor” (See “Firebox to Catalyst Tube” heat transfer section) is used as a parameter to adjust the relationship between the average outside tube metal temperature, calculated assuming uniform heat flux distribution, and the front face tube metal temperature. The front face TMT is higher than the average TMT because heat flux is not uniformly circumferentially distributed. The “Peripheral Maldistribution Factor” is assumed constant in the Simulate or Optimize cases, which is a very good assumption. As mentioned in the “Fouling Resistance” heat transfer section, the fouling can be used to match a measured TMT near the tube inlet.



## **Adiabatic Pre-Reformer**

An adiabatic pre-reformer was modeled with the same kinetics used in the previous models. A reactor bed was configured to represent an industrial reactor that was newly commissioned. Consequently the catalyst activity was assumed to be uniform, that is, no poisoned front had time to be established. The catalyst activity was reconciled so that one temperature in the non-equilibrium zone near the front of the reactor was matched. All other simulated temperatures then also matched the remaining measured temperatures, confirming that the kinetics were yielding appropriate heats of reaction, and composition all along the reactor bed. Effluent compositions were directly measured, and are plotted versus simulated compositions in the parity plot, showing excellent agreement.

Good agreement in this adiabatic reactor further confirms the validity of the kinetics. Issues related to heat transfer do not cloud the kinetics validity in this case.

## **Oxo-Alcohol Synthesis Gas Steam Reformer**

A fired tube reactor was configured to match the dimensions and catalyst loading of an existing oxo-alcohol synthesis gas steam reformer. Simulation results at observed conditions (feed gas composition, outlet temperature, steam to carbon ratio, etc.) agree very well with observed results. Catalyst activity is first determined by matching key effluent composition.

## APPENDIX B CASE STUDY OF EFFECTS OF CATALYST ACTIVITY IN A PRIMARY REFORMER

Several cases were simulated to show the effects of catalyst activity. Plots of key operating conditions illustrate many effects that are unnoticed if only outlet compositions are examined. Table C.1 shows how insensitive the outlet conditions are to catalyst activity, over a wide range. The plot of methane composition as a function of tube length for these cases is much more revealing. The methane compositions for all the cases approach similar values near the tube outlet, but the methane composition profiles are significantly different at positions closer to the inlet.

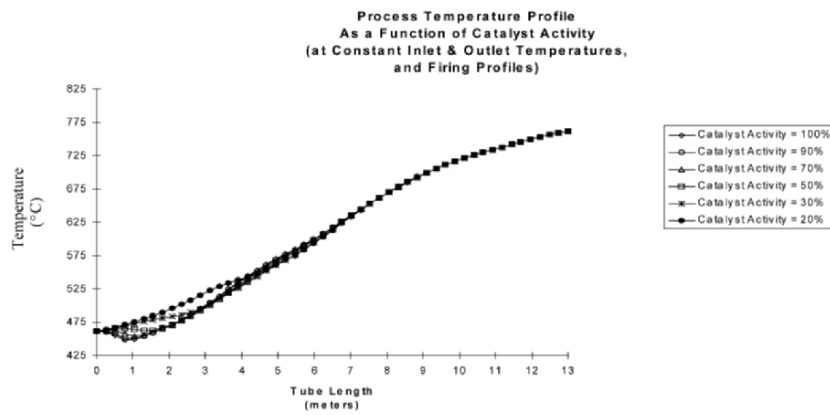
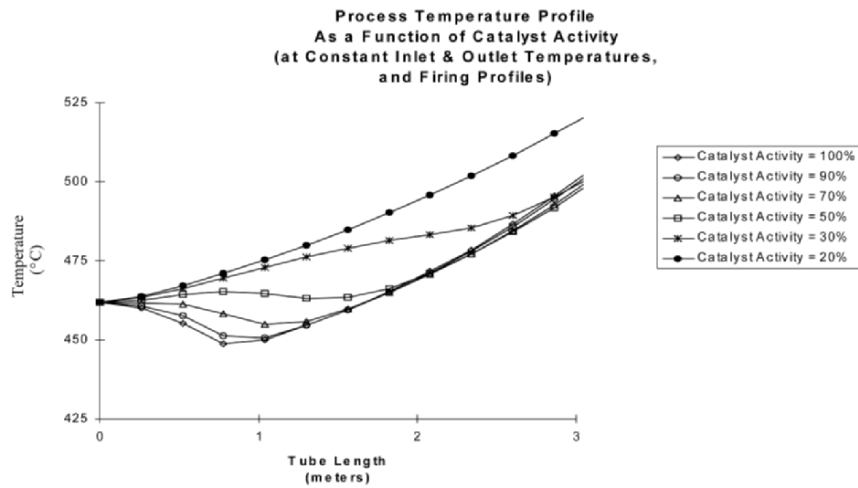
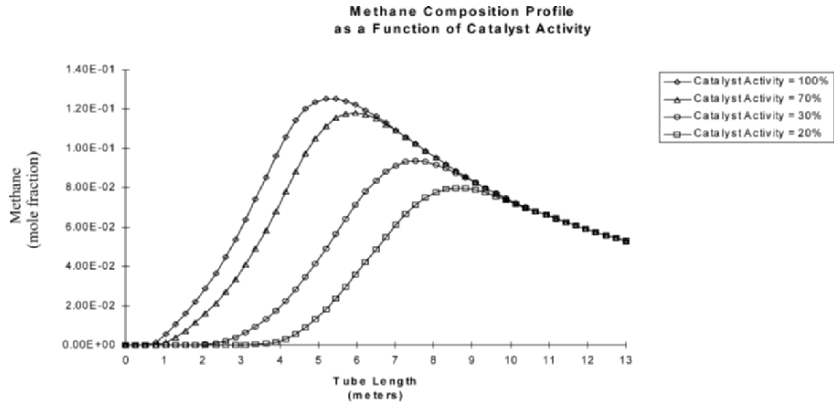
The lower activity cases exhibit operating conditions (temperatures) that are likely to be unacceptable, as shown by the plots of the process temperatures. Both the overall temperature profile, as well as a “close up” of the first 3 meters are shown. As discussed in the “Coking” section, in the paragraph beginning with “Some confusion may exist...”, reformers with less active catalyst operated at similar outlet temperature as with active catalyst, **at similar firing profiles**, exhibit higher, and likely unacceptable temperatures within the tube. The plotted profiles are similar in nature to those shown in Figure 12 of Reference 23. The shapes are different due to top firing<sup>23</sup> and wall firing profile differences. The reason the temperature profiles change is because with less active catalyst, less reaction heat sink exists, and more of the heat input raises the sensible heat of the process fluid, and hence the temperature.

Table B.1 Effluent Composition vs. Catalyst Activity, at Constant Inlet & Outlet Temperatures Naphtha Feed Cases

Inlet Temperature = 462.0°C  
Outlet Temperature = 761.8°C

All cases have the same firing profile (not level).

| Catalyst Activity => | 100%    | 90%     | 70%     | 50%     | 30%     | 20%     |
|----------------------|---------|---------|---------|---------|---------|---------|
| <u>Component</u>     |         |         |         |         |         |         |
| HYDROGEN             | 63.9077 | 63.9072 | 63.9057 | 63.9029 | 63.8962 | 63.8872 |
| NITROGEN             | 0.3675  | 0.3675  | 0.3676  | 0.3676  | 0.3677  | 0.3677  |
| ARGON                | 0.0060  | 0.0060  | 0.0060  | 0.0060  | 0.0060  | 0.0060  |
| CARBON MONOXIDE      | 9.0188  | 9.0186  | 9.0181  | 9.0171  | 9.0146  | 9.0109  |
| CARBON DIOXIDE       | 16.4000 | 16.4001 | 16.4004 | 16.4010 | 16.4026 | 16.4049 |
| METHANE              | 10.3000 | 10.3006 | 10.3022 | 10.3053 | 10.3130 | 10.3233 |



The unacceptable temperatures can be avoided. Two alternatives of avoiding them are simulated, one resulting in different unacceptable operating conditions (high methane slip), and the other with very acceptable conditions.

The first alternative focuses on the unacceptable temperatures encountered in the first few meters of the reactor, which may cause coking. This alternative keeps the temperature at the approximate one meter from the inlet at the same temperature as the base, 100% catalyst activity, case. This temperature was 449°C. Table C.2 and the accompanying plot shows these results. To keep that temperature at 449°C, and maintain the firing profile, the reactor outlet specification has to be relaxed. The independent operating condition is just moved from the reactor outlet, to the catalyst temperature. As illustrated, under these operating conditions, as the catalyst activity falls from 100% to 90%, and 70%, the methane slip rises dramatically. So does the reactor outlet temperature. As mentioned, this alternative is unacceptable, due to very high methane slip.

Table B.2 Effluent Composition vs. Catalyst Activity, at Constant Upper Bed Catalyst Temperature Naphtha Feed Cases

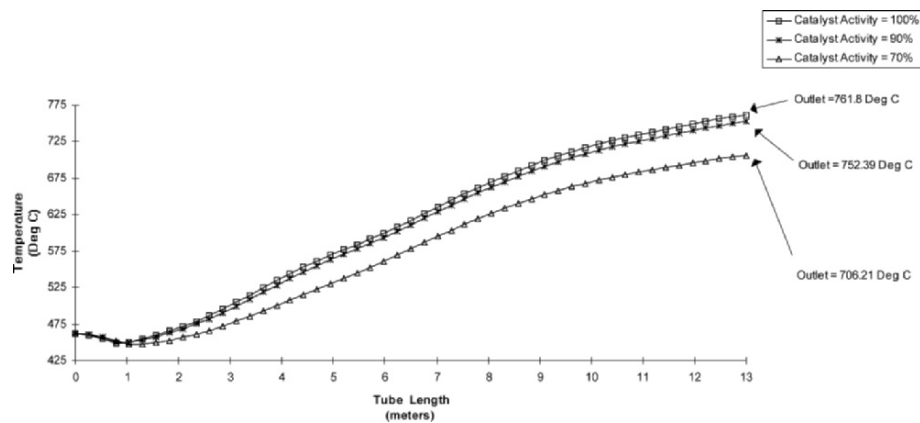
Inlet Temperature = 462.0 °C  
 TI211-1 Temperature = 449 °C

All cases have the same firing profile (not level).

| Catalyst Activity => | 100%    | 90%     | 70%     |
|----------------------|---------|---------|---------|
| <u>Component</u>     |         |         |         |
| HYDROGEN             | 63.9077 | 63.1242 | 58.6711 |
| NITROGEN             | 0.3675  | 0.3755  | 0.4209  |
| ARGON                | 0.0060  | 0.0061  | 0.0069  |
| CARBON MONOXIDE      | 9.0188  | 8.5117  | 6.1219  |
| CARBON DIOXIDE       | 16.4000 | 16.7405 | 18.3063 |
| METHANE              | 10.3000 | 11.2420 | 16.4730 |

The second alternative is to minimize the tube outlet methane slip (dry basis), while modifying the firing profile, keeping the “CAT-1” temperature acceptable (in this case it was upper bounded at 449°C), and while keeping the tube metal temperature (TMT) below acceptable limits. This was posed as an optimization problem. The objective in a plant-wide optimizer is not to minimize the reactor outlet methane content (profit is maximized), but in this sub-plant problem it is the most realistic objective. The ability to modify the firing profile will depend greatly on the control system, burner design, fuel composition, and fire box design. In this case the range over which the optimizer could vary the firing was bounded simply by step bounding the amplitude changes for each burner row. In the overall furnace model the steady-state gain relationship between fuel fired and catalyst temperatures, as well as bounds on the duties that can be fired will constrain the range of

firing. The amplitudes of the firing profiles will all be dependent variables, as described in the “Firebox to Catalyst Tube” heat transfer section.



Results of this alternative for a catalyst activity of 90% show that the tube outlet temperature can be raised to 762.43°C, slightly higher than the base (100% activity) case value of 761.8°C, while not violating the “CAT-1” temperature limit, the TMT limit (of 884.92°C, which is the same maximum as in the base case), nor the step bounds on the firing profile. The reason this case is at a slightly higher outlet temperature (and slightly lower methane slip) than even the base (100% activity) case is because the base case is not an optimized (profile) case. Had the base case been an optimized case, its methane slip would have been slightly lower than the optimized 90% activity case.

The optimized profile was reduced (to its lower step bound) for the top burner row, and increased (to the upper step bounds) for the next two burner rows. The bottom row firing was not at its limit, but the TMT in that section of the tube was at its maximum limit (884.92°C). The resulting reactor outlet compositions show that the methane slip is slightly lower, and hydrogen composition slightly higher than the base case. This is to be expected, even for a less active catalyst, for this system which is close to equilibrium, and at a slightly higher outlet temperature. This solution shows that profile control can essentially overcome the otherwise poor operating conditions that would accompany catalyst activity decline. The optimizer increases the heat flux to the part of the tube in which sufficient reaction heat sink exists, and decreases heat flux to the tube where insufficient reaction exists, and where temperature limits would otherwise be violated. Of course, at lower catalyst activities, and with less range of firing control, the debits associated with catalyst activity decline cannot be avoided. For example, as the catalyst activity falls, the

ability to reduce firing and maintain the “CAT-1” temperature below reasonable limits, while still maintaining a reasonable reactor outlet temperature will cease to exist.

*Table B.3.* Effluent Composition Maximize Outlet Temperature Optimize Case Naphtha Feed Case

*Inlet*      *Temperature* = 462.0°C  
 TI211-1    *Temperature Upper Limit* = 449°C  
 TMT        *Temperature Upper Limit* = 884.9°C

Step Bounds on Firing Profile

| <u>Catalyst Activity =&gt;</u> |  | <u>90%</u> |
|--------------------------------|--|------------|
| <u>Component</u>               |  |            |
| HYDROGEN                       |  | 63.961     |
| NITROGEN                       |  | 0.3670     |
| ARGON                          |  | 0.0060     |
| CARBON MONOXIDE                |  | 9.0552     |
| CARBON DIOXIDE                 |  | 16.3755    |
| METHANE                        |  | 10.2344    |

## Chapter 25

# Hydrogen Production and Supply

## *Meeting Refiners' Growing Needs*

M. Andrew Crews and B. Gregory Shumake

*CB&I Process and Technology*

*Tyler, TX 75701-5013*

### 1. INTRODUCTION

Hydrogen is a key feedstock in many refining operations associated with the production of cleaner gasoline and diesel products. There are several drivers for the increase in hydrogen demand in the refining industry. Crude oil continues to become heavier with additional sulfur and nitrogen species. As the demand for heavy fuel oil diminishes, additional upgrading of the “bottoms” is required to produce a marketable fuel. More stringent environmental regulations have reduced the level of sulfur in both gasoline and diesel products. The combined effect of these trends is that refineries are running short of the necessary hydrogen to meet the increase in hydrotreating and hydrocracking requirements.

There are many routes to the production of hydrogen. In particular, several refinery unit operations produce hydrogen as a by-product. In order to focus the scope of this discussion, this chapter will only cover on purpose hydrogen production. The technologies discussed will be limited to those that can produce hydrogen in sufficient quantities to satisfy typical refinery demands, i.e., from 5 MMSCFD to 200 MMSCFD.

Hydrogen can be produced from a variety of feedstocks and technologies. Feedstock for hydrogen production can range from natural gas to coal and includes all hydrocarbons in-between. The availability of specific feedstock types will limit the number of technology options for the production of hydrogen. The conversion of hydrocarbons to hydrogen requires significant heat input as well as excess (waste) heat resulting from achieving the high

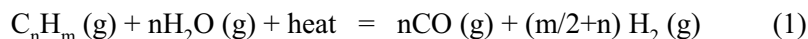


temperatures required to obtain sufficient feedstock conversion. This excess heat is typically recovered to produce steam and can also be recovered to improve the overall efficiency of the technology chosen, but with a significant capital cost impact.

## 2. THERMODYNAMICS OF HYDROGEN

The production of hydrogen from hydrocarbons can be broken down into three key chemical reactions: (1) steam methane reforming, (2) partial oxidation, and (3) water gas shift.

The use of the term 'reforming' in a refinery environment can be confusing as there are several catalytic 'reformer' unit operations that are used to improve the octane numbers of gasoline. In the context of a hydrogen plant a reformer is a furnace or vessel associated with the steam methane reforming reaction. The steam methane reforming reaction produces hydrogen (H<sub>2</sub>), carbon monoxide (CO), carbon dioxide (CO<sub>2</sub>), and un-reacted methane (CH<sub>4</sub>) from hydrocarbons and water based on the following chemical reaction:



The reforming reaction is endothermic and is favored by high temperature and low pressure. In other words, as the net reaction temperature is increased, the higher the conversion of methane and as the pressure at which the reaction takes place is decreased, the methane conversion is increased. Another variable in the reforming reaction is the steam to carbon ratio. As the amount of steam increases above the stoichiometric requirement, the amount of methane conversion also increases. Conversely as the ratio of steam to carbon decreases, the greater the possibility of forming carbon precursors (coking) through alternative reaction pathways. This is an undesirable condition because the formation of carbon can destroy the reforming catalyst, increase the pressure drop through the reformer, increase the reformer tube wall temperature, and consequently require an unscheduled plant shutdown to repair these problems. See Table 1 for equilibrium constant information on the steam methane reforming reaction.

Partial oxidation refers to a chemical reaction where hydrocarbons react with oxygen in a sub-stoichiometric burn reaction to produce carbon monoxide and hydrogen. Partial oxidation technologies require oxygen as a feedstock. Several other reactions take place in the partial combustion zone that contribute to the overall heat provided by the partial oxidation reaction.

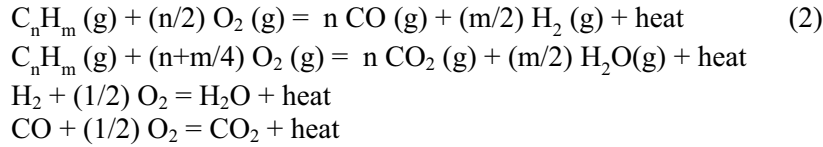
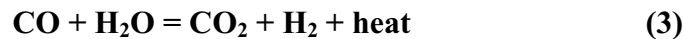


Table 1. Reaction and Equilibrium Constants (Used with Permission of Sud-Chemie)

| Temp., °F | CO + H <sub>2</sub> O = CO <sub>2</sub> + H <sub>2</sub> |                | CH <sub>4</sub> + H <sub>2</sub> O = CO + 3H <sub>2</sub> |                           |
|-----------|--|----------------|---|---------------------------|
|           | ΔH deg., Btu/lb-mole                                     | K <sub>p</sub> | ΔH deg., Btu/lb-mole                                      | K <sub>p</sub>            |
| 200       | -17,570  | 4523           | 90,021  | 7.813 x 10 <sup>-19</sup> |
| 300       | -17,410  | 783.6          | 91,027  | 6.839 x 10 <sup>-15</sup> |
| 400       | -17,220  | 206.8          | 91,957  | 7.793 x 10 <sup>-12</sup> |
| 500       | -17,006  | 72.75          | 92,804  | 2.173 x 10 <sup>-9</sup>  |
| 600       | -16,777  | 31.44          | 93,566  | 2.186 x 10 <sup>-7</sup>  |
| 700       | -16,538  | 15.89          | 94,252  | 1.024 x 10 <sup>-5</sup>  |
| 800       | -16,293  | 9.03           | 94,863  | 2.659 x 10 <sup>-4</sup>  |
| 900       | -16,044  | 5.61           | 95,404  | 4.338 x 10 <sup>-3</sup>  |
| 1000      | -15,787  | 3.749          | 95,880  | 4.900 x 10 <sup>-2</sup>  |
| 1100      | -15,544  | 2.653          | 96,283  | 0.4098                    |
| 1200      | -15,299  | 1.966          | 96,628  | 2.679                     |
| 1300      | -15,056  | 1.512          | 96,922  | 0.1426 x 10 <sup>2</sup>  |
| 1400      | -14,814  | 1.202          | 97,165  | 0.6343 x 10 <sup>2</sup>  |
| 1500      | -14,575  | 0.9813         | 97,378  | 2.426 x 10 <sup>2</sup>   |
| 1600      | -14,344  | 0.8192         | 97,545  | 8.166 x 10 <sup>2</sup>   |
| 1700      | -14,117  | 0.697          | 97,655  | 2.464 x 10 <sup>3</sup>   |
| 1800      | -13,892  | 0.6037         | 97,741  | 6.755 x 10 <sup>3</sup>   |
| 1900      | -13,672  | 0.5305         | 97,786  | 1.701 x 10 <sup>4</sup>   |
| 2000      | -13,459  | 0.4712         | 97,818  | 3.967 x 10 <sup>4</sup>   |
| 2100      | -13,246  | 0.4233         | 97,812  | 8.664 x 10 <sup>4</sup>   |
| 2200      | -13,041  | 0.3843         | 97,791  | 1.784 x 10 <sup>5</sup>   |

The partial oxidation (POX) reaction is highly exothermic and provides the heat required for the steam methane reforming reaction that occurs following the conversion of hydrocarbons to carbon monoxide and hydrogen. The partial oxidation reaction is favored by high temperature and high pressure. However, the higher the pressure the more likely that alternative reaction pathways will lead to the formation of carbon.

The water gas shift (WGS) reaction is where carbon monoxide is 'shifted' on a mole per mole basis to hydrogen by the following reaction:



The water gas shift reaction is favored by low temperature and is mildly exothermic. The WGS reaction is typically the final reaction step that produces hydrogen in a multiple reactor train. Since the WGS reaction is favored by low temperature, it is typically included in the heat recovery train down stream of the high temperature reactors. See Table 2 for thermodynamic and equilibrium data.

Table 2. Equilibrium Constants and Heats of Reaction (Used with Permission of Sud-Chemie)

| CO = 0.5 CO <sub>2</sub> + 0.5 C <sub>(s)</sub> |                      |                           |
|---|----------------------|---------------------------|
| Temp. in °F                                     | ΔH deg., Btu/lb-mole | K <sub>p</sub>            |
| 100   | -37,130.24           | 7.5489 x 10 <sup>9</sup>  |
| 200   | -37,244.17           | 4.7479 x 10 <sup>7</sup>  |
| 300   | -37,313.43           | 1.1237 x 10 <sup>6</sup>  |
| 400   | -37,345.16           | 6.3291 x 10 <sup>4</sup>  |
| 500   | -37,346.08           | 6.4858 x 10 <sup>3</sup>  |
| 600   | -37,321.90           | 1.0223 x 10 <sup>3</sup>  |
| 700   | -37,277.30           | 2.2190 x 10 <sup>2</sup>  |
| 800   | -37,216.05           | 6.1052 x 10 <sup>1</sup>  |
| 900   | -37,141.19           | 2.0628 x 10 <sup>1</sup>  |
| 1000  | -37,055.16           | 8.0522                    |
| 1100  | -36,959.90           | 3.5533                    |
| 1200  | -36,856.96           | 1.7338                    |
| 1300  | -36,747.60           | 9.1957 x 10 <sup>-1</sup> |
| 1400  | -36,632.77           | 5.2304 x 10 <sup>-1</sup> |
| 1500  | -36,513.23           | 3.1565 x 10 <sup>-1</sup> |
| 1600  | -36,389.57           | 2.0036 x 10 <sup>-1</sup> |
| 1700  | -36,262.22           | 1.3284 x 10 <sup>-1</sup> |
| 1800  | -36,131.47           | 9.1460 x 10 <sup>-2</sup> |
| 1900  | -35,997.52           | 6.5074 x 10 <sup>-2</sup> |
| 2000  | -35,860.48           | 4.7655 x 10 <sup>-2</sup> |
| 2100  | -35,720.36           | 3.5799 x 10 <sup>-2</sup> |
| 2200  | -35,577.17           | 2.7506 x 10 <sup>-2</sup> |
| 2300  | -35,430.71           | 2.1563 x 10 <sup>-2</sup> |
| 2400  | -35,280.92           | 1.7210 x 10 <sup>-2</sup> |
| 2500  | -35,127.58           | 1.3960 x 10 <sup>-2</sup> |

### 3. TECHNOLOGIES FOR PRODUCING HYDROGEN

#### 3.1 Steam Methane Reforming (SMR) Technologies

Steam-methane reformers generate the majority of the world's on-purpose hydrogen. A steam-methane reformer (SMR) is a fired heater with catalyst-filled tubes. Hydrocarbon feedstock and steam react over the catalyst to produce hydrogen. The reacted process gas typically exits the reformer at about 1600°F. The flue gas leaving the reformer radiant section is typically about 1900°F.

The flue gas at 1900°F must then be cooled to about 300°F to achieve efficient heat recovery. This heat is recovered in the convection section of the SMR. The process gas at 1600°F must then be cooled to about 100°F before final product purification.

##### 3.1.1 Maximum Steam Export

A maximum export steam plant is defined as a plant that makes the maximum practical quantity of export steam, without auxiliary firing.

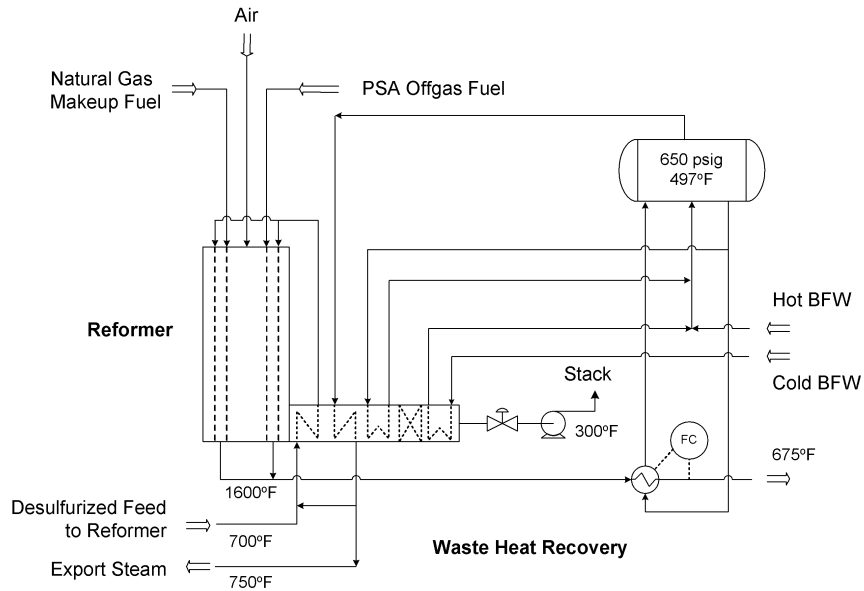


Figure 1. Steam/Methane Reforming with Maximum Steam Export

Table 3 gives a typical feed and utility summary for a maximum export steam plant, as defined above.

Table 3. Maximum Export Steam Feed and Utility Summary

|                    | Units      | Units/M SCF<br>H <sub>2</sub> Product |
|--------------------|------------|---------------------------------------|
| Natural Gas        | MM Btu LHV | 0.450                                 |
| Export Steam       | Lbs        | 86.8                                  |
| Treated Water      | lbs        | 117.0                                 |
| Power              | kWh        | 0.55                                  |
| Cooling Water Circ | gal        | 12.7                                  |

### 3.1.2 Limited Steam Export

A limited export steam plant is defined as a plant that makes some export steam but significantly less than the maximum. This is typically achieved by adding a combustion air preheat unit (CAP). This unit consists of a modular heat exchanger that heats the combustion air to the SMR by heat exchange with the flue gas from the SMR. The hot combustion air reduces the fuel requirement for the SMR, which in turn reduces the steam production.

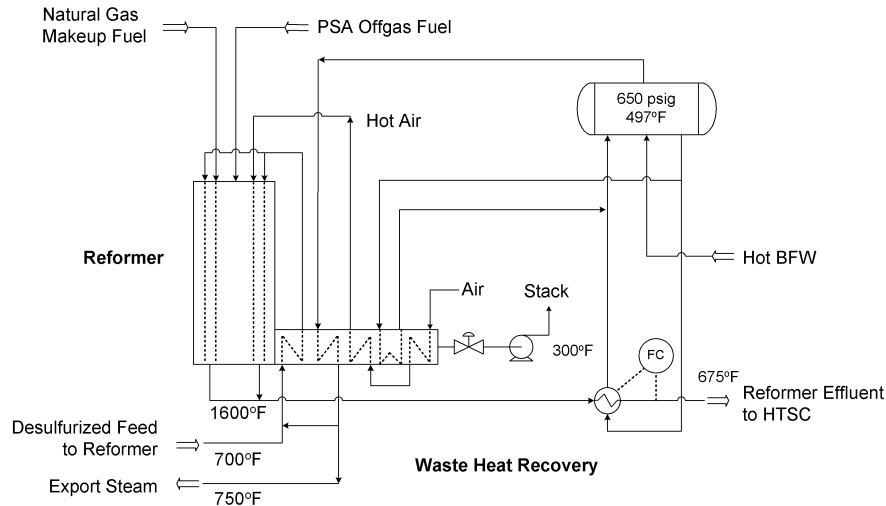


Figure 2. Steam/Methane Reforming with Limited Steam Export

A typical combustion air preheat temperature for this type of plant is approximately 750°F. This permits use of carbon steel ducting in the air preheat distribution system. Table 4 gives a typical feed and utility summary for a limited export steam plant, as defined above.

Table 4. Limited Export Steam Feed and Utility Summary

|                    | Units      | Units/M SCF<br>H <sub>2</sub> Product |
|--------------------|------------|---------------------------------------|
| Natural Gas        | MM Btu LHV | 0.386                                 |
| Export Steam       | lbs        | 38.0                                  |
| Treated Water      | lbs        | 67.7                                  |
| Power              | kWh        | 0.58                                  |
| Cooling Water Circ | gal        | 13.1                                  |

Note that the limited export steam plant makes less than half as much export steam as the maximum steam export case, but also uses less natural gas. At the same time, the limited steam export plant capital cost is higher, because of the addition of the air preheat unit.

### 3.1.3 Steam vs. Fuel

The steam value and fuel price typically determine which of these two cases is the most economic. A high steam value (relative to fuel price) favors the Maximum Steam Export Case. A high fuel price and a low steam value (relative to fuel price) favor the Limited Steam Export Case.

Figure 3 is a plot of natural gas price versus steam value. For a given natural gas price, if the steam value is above the curve, then maximum steam export is favored. But if the steam value is below the curve, then CAP

(limited steam export) is favored. For example, for a natural gas price of 3.00 \$/MM Btu LHV, Figure 3 indicates that if the steam value is above 3.30 \$/M lbs, then steam generation is favored. But if the steam value is below 3.30 \$/M lbs, then CAP (limited steam export) is favored.

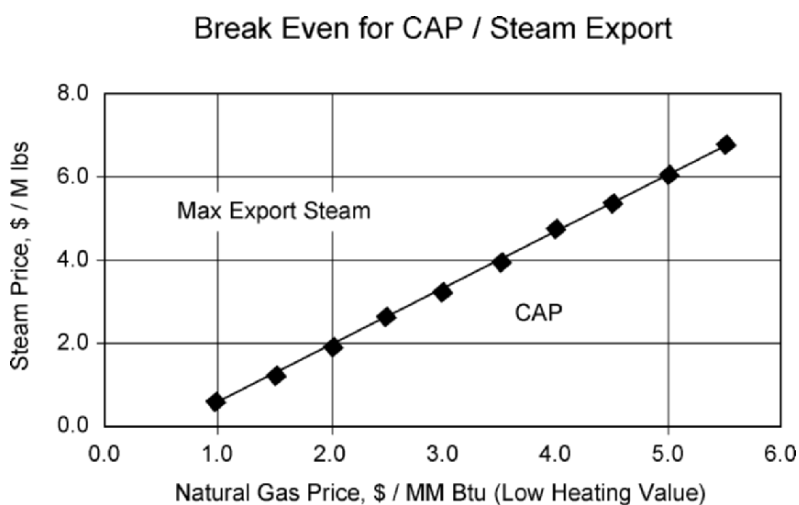


Figure 3. Steam price versus natural gas price

### 3.1.4 Minimum Export Steam

A minimum export steam plant is defined as a plant that optimizes heat recovery in the plant to the maximum extent possible. This is often done when the value of steam is essentially zero or the price of the feedstock and fuel are exceptionally high. Minimum steam export is often achieved by first increasing the SMR process gas inlet temperature and then the combustion air preheat temperature, both of which reduce the fired duty of the SMR. Typical temperatures are 1150°F for the process gas and 900°F for the air preheat. These changes reduce the export steam to a low level, but typically not completely to zero. Additional modifications are required to reduce the export steam to an absolute minimum.

Adding reaction steps to the process can further reduce the amount of feed and fuel required by the hydrogen plant. The first reaction step that can be added is a prereformer. The prereformer is an adiabatic reactor where the feed is heated to approximately 900°F and the gas is partially reformed over a catalyst bed and hydrocarbon components of ethane and heavier are converted to methane. The conversion of ethane plus components to methane is exothermic. If the feedstock is essentially methane (i.e., natural gas), the amount of heat required to drive the steam methane reforming reaction to equilibrium will produce a temperature decrease across the reactor. However,

if the feedstock is butane or heavier, the methane conversion reaction produces more heat than is required by the steam methane reforming reaction and there is a net temperature increase across the reactor.

The prereformer is an excellent way to produce a consistent feed to a steam methane reformer. Heavier feedstocks to the SMR increase the potential for carbon formation. The ultimate in energy recovery can be achieved by utilizing a heat recuperative reforming step in the process. Since the steam methane reforming occurs at high temperature, the reformed gas is typically cooled by generating steam. However, if the heat can be recovered by utilizing it in an additional reforming step, the net heat input required to complete the reaction is reduced and, therefore, the quantity of fuel required to operate the furnace is reduced. The reformer effluent gas is passed through the shell side of a tubular heat exchanger with catalyst filled tubes.

## 3.2 Oxygen Based Technologies

Steam-methane reforming (SMR) has been the conventional route for hydrogen and carbon monoxide production from natural gas feedstocks. However, several alternative technologies are currently finding favor for an increasing number of applications.

These technologies are:

**SMR/O<sub>2</sub>R:** Steam-Methane Reforming combined with Oxygen Secondary Reforming.

**ATR:** Autothermal Reforming.

**POX:** Thermal Partial Oxidation.

Each of these alternative technologies uses oxygen as a feedstock. Accordingly, if low cost oxygen is available, they can be an attractive alternate to an SMR for natural gas feedstocks. Low cost oxygen is now available in many large industrial sites where a large air separation plant already exists or can be economically installed to serve the needs of the area. (Note that unlike ammonia plant technology, air cannot be used in place of oxygen since the contained nitrogen would dilute the hydrogen/carbon monoxide product.)

A brief description of each technology follows.

### 3.2.1 SMR/O<sub>2</sub>R

An SMR/O<sub>2</sub>R essentially consists of an SMR followed by an oxygen secondary reformer (Figure 4). The oxygen reformer is a refractory lined vessel containing catalyst and a burner. The reaction mixture from the SMR is fed to the top of the oxygen reformer where it is mixed with oxygen fed through the burner. Partial oxidation reactions occur in a combustion zone just below the burner. The mixture then passes through the catalyst bed where reforming reactions occur. The gas exits at about 1900°F.

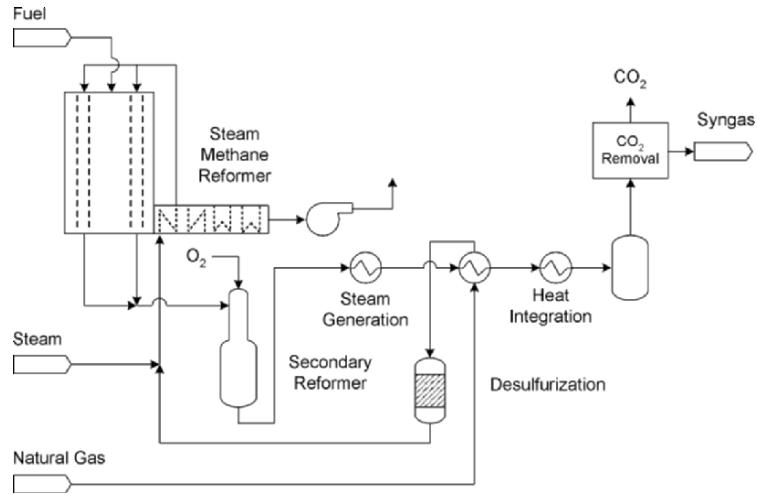


Figure 4. SMR/O2R Plant

### 3.2.2 ATR

An ATR is similar to an oxygen secondary reformer except that it does not receive feed from an SMR. Instead, it is fed directly with a natural gas/steam mixture, which is mixed directly with oxygen from a burner located near the top of the vessel (Figure 5). Again, partial oxidation reactions occur in a combustion zone just below the burner. The mixture then passes through a catalyst bed where reforming reactions occur. The gas exits at about 1900°F.

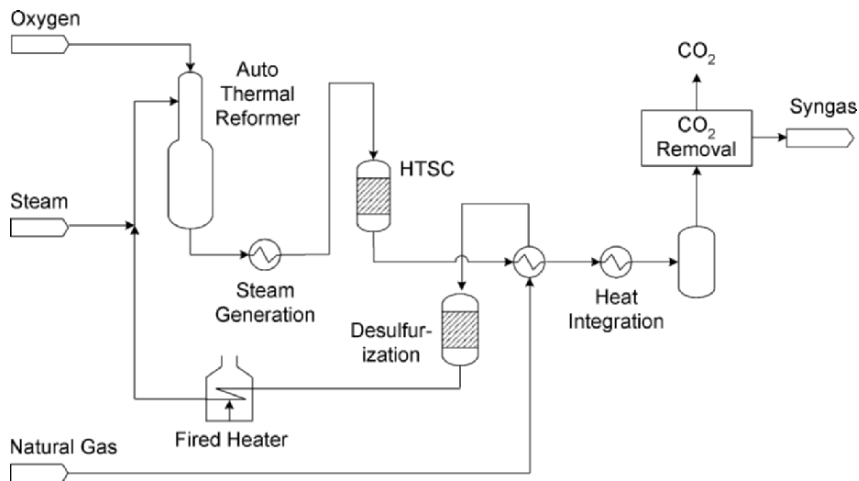


Figure 5. ATR Plant



### 3.2.3 POX

A POX is similar to an ATR except that it does not contain a catalyst and does not require steam in the feed. It is fed directly with a natural gas stream, which is mixed directly with oxygen from a burner located near the top of the vessel. Partial oxidation and reforming reactions occur in a combustion zone below the burner. The gas exits at about 2500°F.

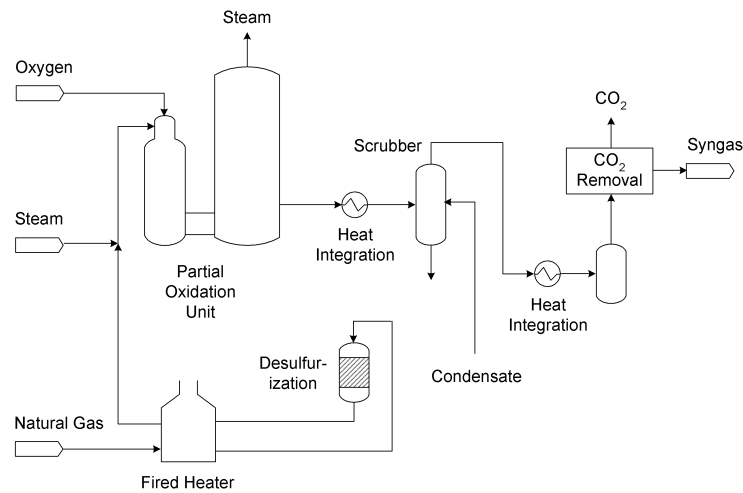


Figure 6. POX Plant

### 3.2.4 Products

The exit gas from each of the above reactors consists of hydrogen, carbon monoxide, carbon dioxide, steam, and residual methane. Small quantities of nitrogen and argon from the original feedstocks may also be present. This gas mixture is then typically processed to yield one or more of the following products:

- (1) High Purity Hydrogen
- (2) High Purity Carbon Monoxide
- (3) A Hydrogen/Carbon Monoxide Gas Mixture

If only hydrogen is required, the plant becomes a hydrogen plant. If only CO is required, the plant becomes a carbon monoxide plant. If both hydrogen and carbon monoxide are required as separate streams, the plant is typically known as a HYCO plant. If only a hydrogen/carbon monoxide mixture is required, the plant is typically known as a synthesis gas (or syngas) plant. If all three products are required, the plant is considered a combination (hydrogen/carbon monoxide/syngas) plant.

### 3.2.5 H<sub>2</sub>/CO Ratio

A key variable in the design of these plants is the product H<sub>2</sub>/CO ratio.

For HYCO and syngas plants, the product H<sub>2</sub>/CO ratio typically varies from 1.0 to about 3.0. But for hydrogen plants, the ratio is almost infinite. And for carbon monoxide plants, the ratio is essentially zero.

### 3.2.6 Natural Ratio Range

Each of the above technologies makes products with inherently different H<sub>2</sub>/CO ratios. The natural ratio range is defined herein as the range of ratios that can be achieved when varying only the CO<sub>2</sub> recycle. The natural ratio ranges for each technology are shown in Table 5, as applicable to natural gas feedstocks. (Other feedstocks will produce a different set of natural ratios).

Table 5. Hydrogen to CO Ratio Summary

|                      | Membrane<br>Or Import CO <sub>2</sub> | Total CO <sub>2</sub><br>Recycle | No CO <sub>2</sub><br>Recycle | Increase<br>Steam | Add Shift<br>Converter |
|----------------------|---------------------------------------|----------------------------------|-------------------------------|-------------------|------------------------|
| SMR                  | <3.0                                  | 3.0                              | 5.0                           | >5.0              | infinity               |
| SMR/O <sub>2</sub> R | <2.5                                  | 2.5                              | 4.0                           | >4.0              | >5.0                   |
| ATR                  | <1.6                                  | 1.6                              | 2.7                           | >2.7              | >3.0                   |
| POX                  | <1.6                                  | 1.6                              | 1.8                           | >1.8              | >2.0                   |

As seen in Table 5, the natural ranges for natural gas are as follows: For the SMR: 3.0 to 5.0. For the SMR/O<sub>2</sub>R: 2.5 to 4.0. For the ATR: 1.6 to 2.65. And for the POX: 1.6 to 1.8. Note that some ranges are broader than others, and that some of the ranges do not overlap.

The technology that offers a natural ratio that spans the required product ratio is considered to have an inherent advantage and merits careful consideration.

### 3.2.7 CO<sub>2</sub> Recycle

CO<sub>2</sub> recycle is the typical means of tailoring the natural ratio span to meet the desired H<sub>2</sub>/CO product requirement.

As noted earlier, carbon dioxide is present in all the reactor effluents. Since CO<sub>2</sub> is considered an impurity, it must typically be eliminated. In most designs, the CO<sub>2</sub> is removed from the process gas by selective adsorption in a suitable solvent such as an amine solution. The CO<sub>2</sub> is then stripped from the solvent as a separate stream.

(Note: synthesis gas for methanol plants typically retains some or all of the carbon dioxide. This is a special case, which is outside the scope of this discussion).

The separate CO<sub>2</sub> stream can be removed from the system or it can be recycled back to the reactor. If it is recycled, the CO<sub>2</sub> can be converted to CO in the reactor by the reverse water gas shift reaction. This reduces the final H<sub>2</sub>/CO ratio because the carbon atoms in the original CO<sub>2</sub> are converted to CO. On the other hand, if the CO<sub>2</sub> is not recycled, the H<sub>2</sub>/CO ratio is

increased, because the carbon atoms in the original CO<sub>2</sub> are not converted to CO. (CO<sub>2</sub> that is not recycled is typically vented to the atmosphere; however, sometimes it is sold as a byproduct).

The natural H<sub>2</sub>/CO range for each technology represents the spread between full CO<sub>2</sub> recycle and no CO<sub>2</sub> recycle. See Figure 7. By operating with partial recycle, any H<sub>2</sub>/CO ratio within the natural range can be achieved.

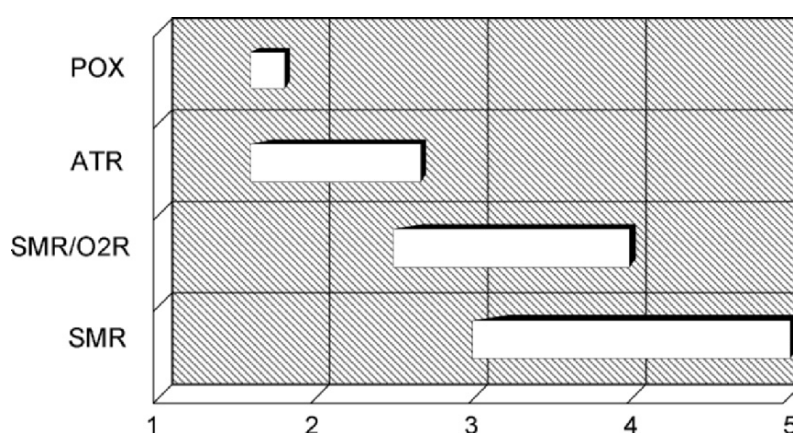


Figure 7. Natural Range of H<sub>2</sub>/CO Ratio

But as noted earlier, some of the natural ratio ranges do not overlap; hence for a given product H<sub>2</sub>/CO ratio, at least some of the technologies will require additional ratio adjustment to meet the product requirements. Fortunately, a number of process techniques are available to do this. The viability of the technology will depend on the economics of using these techniques.

To decrease the ratio below the natural range, common techniques include importing CO<sub>2</sub>; use of a membrane; or use of a cold box. To increase the ratio, common techniques include increasing the quantity of steam in the reactor feed or adding a shift converter. These techniques, along with CO<sub>2</sub> recycle, are summarized in Table 6.

Table 6. Techniques for H<sub>2</sub>/CO Ratio Adjustment

|                         | Decreases Ratio | Increases Ratio |
|-------------------------|-----------------|-----------------|
| Recycle CO <sub>2</sub> | X               |                 |
| Import CO <sub>2</sub>  | X               |                 |
| Use Membrane            | X               |                 |
| Remove CO <sub>2</sub>  |                 | X               |
| Increase Steam          |                 | X               |
| Add Shift Converter     |                 | X               |
| Use Cold Box            |                 | See Note        |

Note: A cold box decreases the ratio with respect to CO and increases the ratio with respect to H<sub>2</sub>.

### 3.2.8 Import CO<sub>2</sub>

The H<sub>2</sub>/CO ratio can be decreased by importing CO<sub>2</sub> as feed to the reactor. The import CO<sub>2</sub> is added to the CO<sub>2</sub> already being recycled. The carbon atoms in the import CO<sub>2</sub> can then be converted to CO by the reverse water gas shift reaction.

### 3.2.9 Membrane

The H<sub>2</sub>/CO ratio can also be decreased by use of a membrane unit. Hydrogen is removed from the membrane as a permeate stream, which reduces the H<sub>2</sub>/CO ratio of the main process stream.

### 3.2.10 Cold Box

A cold box is often used to separate the hydrogen and carbon monoxide into a high purity CO stream and a H<sub>2</sub>-rich stream. This reduces the ratio to near zero with respect to the CO stream. The H<sub>2</sub>-rich stream may undergo further purification (typically in a PSA unit) to yield a high purity H<sub>2</sub> stream. This increases the ratio to near infinity with respect to the H<sub>2</sub> stream.

### 3.2.11 Steam

Adding steam to the reactor converts CO to H<sub>2</sub> by the water gas shift reaction. This increases the H<sub>2</sub>/CO ratio.

### 3.2.12 Shift Converter

A shift converter is a catalytic reactor which catalyzes the conversion of CO to H<sub>2</sub> by the water gas shift reaction. This step can be used to increase the H<sub>2</sub>/CO ratio to a very high value. It is widely used in hydrogen plants.

Table 6 summarizes the ranges achievable by each technology by inclusion of these techniques. Typically, the viability of the technology decreases with the magnitude of the added steps necessary to achieve the required product H<sub>2</sub>/CO ratio.

### 3.2.13 Other Considerations

As stated above, these ratios are based on natural gas feedstocks. If heavier feedstocks are used, the ratios will be lower because the hydrogen to carbon ratio of the feed will be lower.

The above ratios are based on typical reformer outlet temperatures and pressures for each technology. The reformer outlet temperature is typically set by the residual methane requirement. The reformer outlet pressure is typically

set by compression requirements. Some design flexibility often exists between these limits. However, within the normal range of flexibility, the H<sub>2</sub>/CO ratio does not change appreciably with the reformer outlet temperature or pressure. Hence, for a given design, it is normally impractical to achieve a significant change in H<sub>2</sub>/CO ratio by varying the reformer outlet temperature or pressure. Instead, the techniques discussed above should be utilized.

If it is impractical for a given technology to achieve the desired ratio by the techniques discussed above, then excess hydrogen or carbon monoxide containing gas can be burned as fuel in the SMR (for SMR and SMR/O<sub>2</sub>R plants) or in the Process Heater (for ATR or POX plants). If necessary, the Process Heater can be expanded to include a second radiant section to permit burning of excess product by generating steam. Alternatively, a package boiler can be used to burn excess gas and generate steam.

Thus far, considerable discussion has centered on the H<sub>2</sub>/CO ratio, since as noted above, the technology that can most easily achieve the required product H<sub>2</sub>/CO ratio has an inherent initial advantage. But there are other considerations that could over-ride this advantage. These are outlined below.

### 3.3 Technology Comparison

Table 7 is a comparison of some key process advantages and disadvantages for the technologies under consideration for hydrogen/carbon

Table 7. Technology Comparison

|   |  |
|---|--|
| <p><b>SMR</b></p> <p>*Advantages</p> <ul style="list-style-type: none"> <li>- Most commercial experience</li> <li>- Does not require oxygen</li> <li>- Reforming temperature relatively low</li> <li>- Best natural H<sub>2</sub>/CO ratio for hydrogen product</li> </ul> <p>*Disadvantages</p> <ul style="list-style-type: none"> <li>- Natural ratio high for CO product</li> <li>- Highest atmospheric emissions</li> </ul> | <p><b>ATR</b></p> <p>Advantages</p> <ul style="list-style-type: none"> <li>- Natural H<sub>2</sub>/CO ratio often favorable</li> <li>- Lower reforming temperature than POX</li> <li>- Low residual CH<sub>4</sub></li> <li>- Tailor residual CH<sub>4</sub></li> </ul> <p>*Disadvantages</p> <ul style="list-style-type: none"> <li>- Limited commercial experience</li> <li>- CO<sub>2</sub> cycle higher than POX</li> <li>- Require oxygen</li> <li>- Makes carbon (soot)</li> <li>- Complex heat recovery section</li> <li>- Licensed process</li> <li>- Significant third party involvement</li> </ul> |
| <p><b>SMR/O<sub>2</sub>R</b></p> <p>*Advantages</p> <ul style="list-style-type: none"> <li>- Smaller than SMR</li> <li>- Low residual CH<sub>4</sub></li> <li>- Tailor residual CH<sub>4</sub></li> </ul> <p>*Disadvantages</p> <ul style="list-style-type: none"> <li>- Two-step reforming</li> <li>- Higher reforming temperature</li> <li>- Require oxygen</li> </ul>  | <p><b>POX</b></p> <p>*Advantages</p> <ul style="list-style-type: none"> <li>- Does not require feedstock desulfurization</li> <li>- Does not require oxygen</li> <li>- Low residual CH<sub>4</sub></li> <li>- Low natural H<sub>2</sub>/CO ratio</li> </ul> <p>*Disadvantages</p> <ul style="list-style-type: none"> <li>- Narrow H<sub>2</sub>/CO ratio</li> <li>- Cannot tailor residual CH<sub>4</sub></li> <li>- Require oxygen</li> </ul>   |

monoxide plants with natural gas feedstock. Please note that while the oxygen requirement is shown as a disadvantage, it may not be a disadvantage in cases where low cost oxygen is available.

### 3.3.1 Process Parameters

Key process parameters and feedstock requirements for each technology include the following:

**PRESSURE** - Most SMR plants run at reformer outlet pressures between 150 and 400 psig. The maximum pressure is about 550 psig, due to metallurgical considerations in the SMR outlet piping. The same applies to SMR/O<sub>2</sub>R plants.

This limits the final product gas pressure to about 500 psig. Above this, product gas compression is required.

ATR and POX plants can run at much higher pressures. For example, some plants require synthesis gas at about 800 psig; this can be supplied directly from an ATR or POX without synthesis gas compression.

**TEMPERATURE** - SMR plants typically run at reformer outlet temperatures of 1550 to 1700°F.

SMR/O<sub>2</sub>R and ATR plants typically run at outlet temperatures of 1750 to 1900°F.

POX plants typically run at about 2500°F. This high temperature is needed to maintain low residual methane without a catalyst.

**STEAM/CARBON** - Steam is typically required to prevent carbon formation on the reformer catalyst. The steam requirement is generally expressed as the steam/hydrocarbon-carbon ratio (steam/hcc). This is the ratio of the moles of steam to moles of hydrocarbon-carbon in the feed (the carbon in any CO<sub>2</sub> recycle is not included in computation of the ratio).

Both the SMR and SMR/O<sub>2</sub>R plants typically use a 2.5 to 5 steam/hcc ratio for no CO<sub>2</sub> recycle, and a 2/1 steam/hcc ratio when all the CO<sub>2</sub> is recycled. (A lower ratio can be used with CO<sub>2</sub> recycle since the CO<sub>2</sub> makes some H<sub>2</sub>O by the water gas shift reaction). For partial recycle, a ratio between 3/1 and 2/1 is typically used.

ATR plants can operate at a lower ratio, often about 1 to 1.5 with or without CO<sub>2</sub> recycle.

POX plants require no steam. Some soot is formed, but since there is no catalyst, there is obviously no possibility of catalyst bed plugging. With proper design and operation, the soot can be processed and removed in the downstream equipment without affecting the plant on-stream time.

**METHANE SLIP** - The exit gas from each reactor contains some residual methane, which corresponds to unreacted natural gas feed. This is typically referred to as the methane slip. A low methane slip increases the purity of a synthesis gas product. It also reduces the natural gas requirement.

An SMR typically has a relatively high methane slip (3 to 8 mol pct, dry basis). This is primarily because the SMR operates at a lower outlet temperature. The other technologies operate at higher outlet temperatures and typically have low slips (0.3 to 0.5 mol pct, dry basis).

If a methane-wash cold box is used, typically a methane slip of at least 1 to 2 mol percent is required to maintain the methane level in the box. This is not a problem for an SMR design because its methane slip is considerably more than this. It is also easily achieved by the SMR/O<sub>2</sub>R and ATR designs by simply reducing the reactor outlet temperature. However, this methane level is more difficult to achieve with a POX, since in the absence of a catalyst, a high temperature and corresponding low methane slip should be maintained to ensure consistent performance.

**RAW MATERIALS** - Natural gas and oxygen are the two major raw materials. For each technology, the quantities required must be considered on a case-by-case basis, since they depend on the H<sub>2</sub>/CO requirement for each application.

For example, the product H<sub>2</sub>/CO ratio may require that CO<sub>2</sub> be either recycled or vented, depending on the ratio and the technology.

If the required H<sub>2</sub>/CO product ratio is 2.0, all the CO<sub>2</sub> would be recycled in an SMR or SMR/O<sub>2</sub>R design; part of the CO<sub>2</sub> would be recycled in an ATR design; and no CO<sub>2</sub> would be recycled in a POX design.

The extent of CO<sub>2</sub> recycle changes the raw material requirements for a given technology, because if CO<sub>2</sub> is vented, its contained carbon and oxygen is not recovered.

To provide a basis of comparison, a design can be considered wherein all the CO<sub>2</sub> is recycled for each technology. This would normally occur for designs for a H<sub>2</sub>/CO product ratio less than 1.6.

A typical design meeting this requirement would be a carbon monoxide only plant (H<sub>2</sub>/CO ratio of zero). For such a design, we have compared all four technologies for a proposed plant on the US Gulf Coast.

For this plant, the natural gas and oxygen requirements are given in Table 8. The natural gas requirement shown is the net requirement on a heating value basis and includes credit for excess hydrogen at fuel value. (For this plant, all the technologies produce excess hydrogen since CO is the only required product and there is no requirement for product hydrogen).

Table 8. Feedstock Requirements

|                               | Units per 100 SCF CO Product |                      |       |       |
|-------------------------------|------------------------------|----------------------|-------|-------|
|                               | SMR                          | SMR/O <sub>2</sub> R | ATR   | POX   |
| Net Natural Gas* (MM Btu LHV) | 0.729                        | 0.724                | 0.531 | 0.509 |
| Oxygen Import, lb             | 0                            | 14.2                 | 56.5  | 58.7  |

\* includes credit for excess hydrogen at fuel value.

All cases based on full CO<sub>2</sub> recycle.

For the following discussion, the SMR and SMR/O<sub>2</sub>R are called SMR-based technologies because the SMR is the dominant component. And the ATR and POX are called oxygen-based technologies because the partial oxidation reactor is the dominant component.

From Table 8, note that the natural gas requirements for the SMR-based technologies are about the same. Note also that the natural gas requirements for the oxygen-based technologies are about the same. But also note that the oxygen-based technologies require only about 70 percent as much natural gas as the SMR-based technologies.

The natural gas requirement is lower for the oxygen-based technologies because most of the oxygen in the feed reacts with carbon in the natural gas to form carbon monoxide. The oxidation reaction is therefore more efficient for the formation of carbon monoxide, which is the desired product for the referenced plant.

Another reason for the lower natural gas requirement is that for the oxygen-based technologies, the heat required for the reaction is applied directly to the process gas in the reactor vessel. This is more energy efficient than the SMR-based technologies, which require a temperature driving force between the combustion gas and the intube process gas.

With respect to oxygen consumption, the oxygen requirement for the SMR is obviously zero. For the SMR/O<sub>2</sub>R, the oxygen requirement is about 25 percent of that for the ATR or POX.

The ATR and POX oxygen requirements are about the same. This is to be expected, since both technologies use the same direct combustion process, and for the referenced plant, both technologies recycle all the CO<sub>2</sub> and produce essentially the same H<sub>2</sub>/CO product ratio.

### 3.3.2 Export Steam

For the referenced plant, the export steam is relatively low since the excess hydrogen is not burned within the plant to make export steam. Accordingly, the export steam for the SMR, SMR/O<sub>2</sub>R, and POX averaged only about 150 lbs per 1000 SCF of carbon monoxide and any differences were not considered significant. However, the ATR export steam was less than half this value because the energy requirement for the CO<sub>2</sub> removal system is larger.



### 3.3.3 Economic Considerations

The economics of each technology depend on the conditions and requirements of each project and must be studied on a case-by-case basis. Some of the most important considerations are as follows

#### 3.3.4 Oxygen Availability

The availability of oxygen is obviously a key parameter. Since the SMR requires no oxygen, it is the obvious choice if oxygen is unavailable or prohibitively expensive. Studies indicate that the oxygen-based technologies can be attractive if oxygen is available at less than about \$25 per short ton. If oxygen is greater than about \$30 per ton, the SMR is favored.

The oxygen price can be less than \$25 per ton in large industrial sites where a large air separation plant already exists or can be economically installed to serve the needs of the area. Hence, in such cases the oxygen-based technologies merit serious consideration.

#### 3.3.5 Hydrocarbon Feedstock

This section is based on natural gas feedstock. With natural gas, all technologies are technically viable. However, if the feedstock is a heavy hydrocarbon (such as fuel oil or vacuum bottoms), the POX is the only viable technology. This is because the other technologies cannot process feedstocks heavier than naphtha (to avoid carbon deposition on the catalyst).

#### 3.3.6 H<sub>2</sub>/CO Ratio

The importance of the product H<sub>2</sub>/CO ratio has already been discussed extensively. As previously stated, the technology that offers a natural ratio that spans the required product ratio is considered to have an inherent advantage and must be seriously considered.

#### 3.3.7 Natural Gas Price

Since the SMR-based technologies directionally require more natural gas, they are favored by low natural gas prices.

#### 3.3.8 Capital Cost

The SMR-based technologies typically have a somewhat higher capital cost because the SMR furnace with its high alloy tubes and large flue gas heat recovery section is inherently more expensive than the ATR or POX technologies which are refractory lined carbon steel vessels without external flue gas heat recovery.

An SMR has a lower capital cost than an SMR/O<sub>2</sub>R when the operating pressure is relatively low. Since low pressure favors the reforming reaction, under such conditions most of the reforming occurs in the SMR, and the O<sub>2</sub>R does not significantly reduce the size of the SMR. But at higher pressures, an SMR/O<sub>2</sub>R can cost less, because more of the reforming is done in the O<sub>2</sub>R, and the size of the SMR can often be significantly reduced.

The ATR and POX technologies have offsetting capital costs, depending on the extent of CO<sub>2</sub> recycle.

For full CO<sub>2</sub> recycle, the CO<sub>2</sub> removal system is much larger for the ATR than the POX, and the added capital cost associated with this difference tends to make the ATR more expensive overall.

However, for no CO<sub>2</sub> recycle, the ATR tends to cost less than the POX because its reaction and heat recovery section is inherently less expensive and it does not carry any third party royalty.

### 3.3.9 Conclusions

Based on the above, the following conclusions can be drawn.

- 1) The SMR/O<sub>2</sub>R, ATR, and POX technologies can be attractive if low cost oxygen is available.
- 2) For competing technologies, the H<sub>2</sub>/CO product ratio is typically the most important process parameter.
- 3) For low methane slip, the SMR/O<sub>2</sub>R, ATR, and POX technologies are favored.
- 4) For full CO<sub>2</sub> recycle, the POX is typically better than the ATR.
- 5) Relative to the POX, the ATR is a non-licensed technology which avoids third-party involvement.
- 6) The economics of each technology is dependent on the conditions and requirements for each project and must be evaluated on a case-by-case basis.
- 7) The technology with the most favorable H<sub>2</sub>/CO ratio for producing hydrogen is the SMR.

## 3.4 Hydrogen Purification

### 3.4.1 Old Style

Many refiners are still operating hydrogen plants that were designed and built 20 or more years ago. These older plants were generally designed with the best available technology of the time. These typical plants consist of a steam-methane reformer (SMR) to convert the hydrocarbon feed to a syngas

mixture followed by a high temperature shift converter (HTSC) and low temperature shift converter (LTSC) to shift most of the CO to hydrogen. This hydrogen-rich gas is purified by a CO<sub>2</sub> removal unit where a hot potassium carbonate or MEA solution removes the CO<sub>2</sub> and then followed by a methanator to convert the remaining CO and CO<sub>2</sub> to methane and water. The final product gas is typically about 95-97% hydrogen. Figure 8 shows a typical layout for an Old Style hydrogen plant.

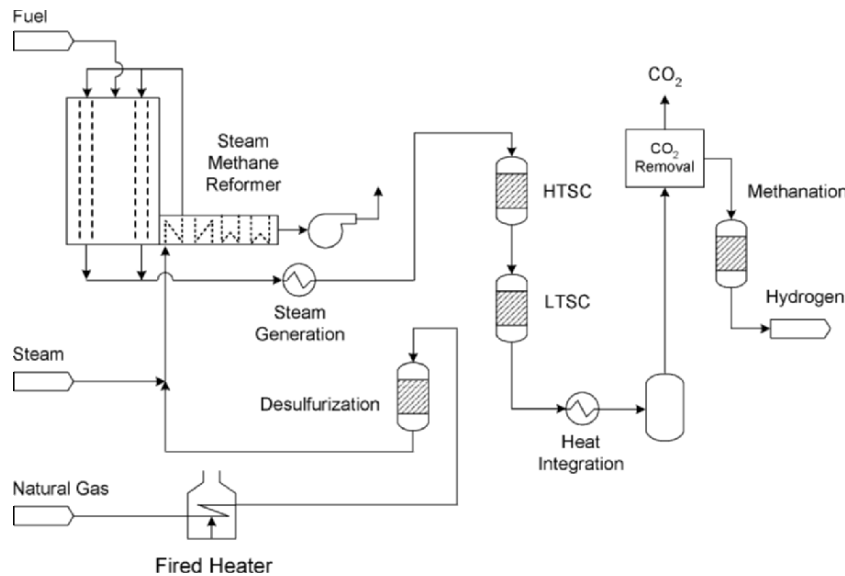


Figure 8. Old Style Hydrogen Plant

### 3.4.2 Modern

The main process difference between a Modern hydrogen plant and an Old Style hydrogen plant is the hydrogen purification technology. A Pressure Swing Adsorption (PSA) unit replaces the CO<sub>2</sub> removal unit and methanator and allows the Modern plant to produce hydrogen product with a much higher purity. In addition, many significant improvements in technology and design allow the Modern plant to operate at much higher efficiency and with substantially lower operating costs.

A Modern hydrogen plant includes an SMR followed by an HTSC. A PSA unit purifies the syngas effluent from the HTSC. The final product gas is typically 99.99% hydrogen. Since the PSA unit removes the impurities from the syngas, an LTSC is not required to further reduce the CO content.

The PSA unit produces an offgas stream that can be used by the SMR as the primary fuel source. In addition, the increase in product purity from the PSA unit has potential benefits in downstream units. For example, the higher

purity hydrogen makeup to a hydrotreater increases reactor hydrogen partial pressure, lowers the recycle flow, and potentially reduces compression costs and/or increases Hydrotreater performance and catalyst run life. Figure 9 shows a typical layout for a Modern hydrogen plant.

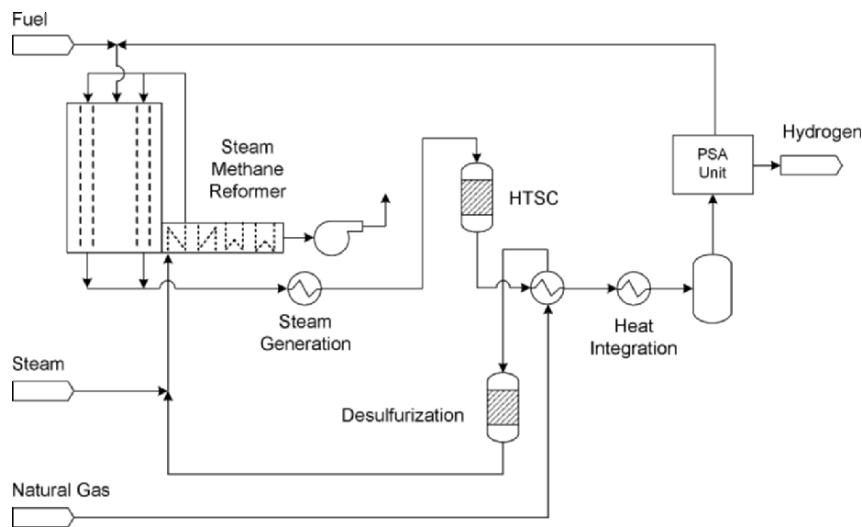


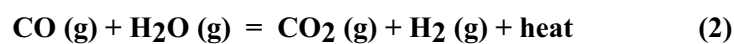
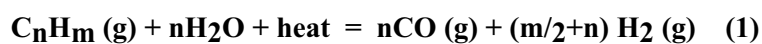
Figure 9. Modern Hydrogen Plant

## 4. DESIGN PARAMETERS FOR SMR'S

Steam reformers are used in hydrogen generation plants throughout the refining and petrochemical industries and are expected to remain the most cost effective approach for on-purpose hydrogen production. The steam reformer for hydrogen plants consists of a fired heater containing catalyst-filled tubes. This article discusses process design considerations for a modern reformer of this type.

### 4.1 Function

The primary function of a steam reformer is to produce hydrogen. Hydrocarbon feed gas is mixed with steam and passed through catalyst-filled tubes. Hydrogen and carbon oxides are produced by the following reactions.



The first reaction is the reforming reaction, and the second is the shift reaction. Both reactions produce hydrogen. Both reactions are limited by thermodynamic equilibrium. The net reaction is endothermic. These reactions take place under carefully controlled external firing, with heat transfer from the combustion gas in the firebox to the process gas within the catalyst-filled tubes.

The carbon monoxide in the above product gas is subsequently shifted almost completely to hydrogen in a downstream catalytic reactor by further utilization of reaction (eqn. 2).

## 4.2 Feedstocks

Typical hydrocarbon feedstocks for the reformer include natural gas, refinery gas, propane, LPG, and butane. Naphtha feedstocks with final boiling points up to about 430°F can also be processed.

## 4.3 Fuels

Typical fuels for the reformer are light hydrocarbons such as natural gas and refinery gas, although distillate fuels are sometimes used. Residual fuels are not utilized since the contained metals can damage the reformer tubes.

In most hydrogen plants, a pressure swing adsorption (PSA) system is used for hydrogen purification. In such plants, a major portion of the reformer fuel is PSA offgas, with the makeup fuel being a hydrocarbon stream as discussed above.

## 4.4 Design

Reformers are fired to maintain a required process gas outlet temperature. Most modern reformers are top-fired. In this design, the burners are located in the top of the furnace, and fire downward. The process gas flows downward through the catalyst-filled tubes in the same direction.

Accordingly, the top-fired design features co-current flow of process gas and flue gas. The co-current flow permits use of (1) the highest flue gas temperature when the intube process gas temperature is lowest, and (2) the lowest flue gas temperature when the intube process gas temperature is highest. This in turn provides tubewall temperatures that are quite uniform over the length of the tube. Because of this uniformity, the average tubewall temperature is lower. And lower tubewall temperatures reduce tube cost and increase tube life.

Another advantage of co-current flow is that as the flue gas cools, it sinks in the same direction as its normal flow. This provides an inherently stable furnace operation. In particular, it avoids flue gas backmixing that inherently occurs in alternative designs. Since there is no backmixing, the flue gas outlet

temperature tends to more closely approach the process gas outlet temperature than in alternative designs. This improves the furnace efficiency.

Note that the highest tubewall temperature occurs at the outlet, which is quite common for this type of furnace. Also note that at the tube outlet, the tubewall temperature is very close to the required process gas outlet temperature. This is because the heat flux at the outlet is quite low, having fallen steadily for the last two-thirds of the tube.

Therefore, the tubewall temperature is minimized for the required process gas outlet temperature, which in turn minimizes the required tubewall thickness.

In addition, note that the flue gas temperature falls off steadily for the last two-thirds of the tube, and is at a minimum at the tube outlet. Since the furnace must be fired to provide the necessary flue gas outlet temperature, the fact that the flue gas outlet temperature is relatively low means that the fuel requirement is minimized.

The burners are housed at the top of the reformer by an enclosure commonly referred to as a penthouse. This housing provides a convenient shelter for the burners and for the inlet piping and valving.

The flue gas is collected at the bottom of the reformer in horizontal fire-brick ducts, often referred to as "tunnels." The flue gas then exits horizontally into a waste heat recovery (WHR) unit. The combustion gas is drawn through the WHR unit by an induced draft fan and the gas is then discharged to the atmosphere through a stack. The WHR unit and fan are essentially at grade, which facilitates operation and maintenance.

When the above features of the top-fired design are considered and weighed against alternative arrangements, the consensus of the industry favors the top-fired design.

The remainder of this section will therefore focus on the top-fired design.

The process considerations discussed below focus on steam reformer parameters specifically related to hydrogen plant design. However, many of these parameters also apply to steam reformers for other types of plants (such as syngas, ammonia, and methanol plants).

## **4.5 Pressure**

The shift reaction equilibrium is independent of pressure. However, the reforming reaction equilibrium is favored by low pressure. Therefore for the overall reaction, the lower the pressure, the higher the conversion of hydrocarbon to hydrogen. Accordingly, from the reaction standpoint, it is best to operate at low pressure.

However, there are other considerations. For example, modern hydrogen plants typically use a pressure swing adsorption (PSA) unit for hydrogen purification. PSA units are more efficient at higher pressure. The minimum pressure for acceptable operation is typically 150 to 200 psig. The optimum

pressure may be 300 to 450 psig. Therefore, to accommodate the PSA unit, the reformer pressure will need to be adjusted accordingly.

Another consideration is product hydrogen pressure requirements. In many applications, the hydrogen product from the hydrogen plant requires subsequent compression to a much higher pressure, for example for refinery hydrotreating applications. In such cases, the compression cost can be reduced considerably if the hydrogen from the hydrogen plant is produced at a higher pressure.

As discussed below, hydrogen plant reformers typically operate at process gas outlet temperatures up to 1700°F. At these temperatures, metallurgical considerations for the outlet piping typically limit the reformer outlet pressure to about 550 psig. This corresponds to a hydrogen product pressure of about 500 psig.

Many hydrogen plant reformers are designed consistent with a hydrogen product pressure of about 300-350 psig. Although this decreases the reforming reaction conversion, the overall plant economics often favors the higher pressure.

On the other hand, if the product pressure requirement is low, then the PSA unit will typically determine the minimum pressure.

Therefore, for hydrogen plants, the reformer outlet pressure typically runs between 150 and 550 psig.

## 4.6 Exit Temperature

The reforming reaction equilibrium is favored by high temperature. At the pressure levels used in hydrogen plants, the reformer process gas exit temperature typically runs between 1500 and 1700°F. Lower temperatures give insufficient conversion. Higher temperatures increase metallurgical requirements, tubewall thickness, and fuel consumption.

## 4.7 Inlet Temperature

The reforming reaction rate becomes significant at about 1000°F, so it is usually advantageous to design for an inlet temperature near this value. This is typically achieved by preheating the reformer feed against the hot flue gas in the WHR section of the reformer.

A higher reformer inlet temperature decreases the absorbed duty requirement and therefore decreases the number of tubes, the size of the furnace, and the fuel requirement. It also decreases the steam generation from the waste heat recovery unit.

If steam has a high value relative to fuel, it may be economical to reduce the reformer inlet temperature somewhat in order to maximize steam generation. In many such cases, the optimum inlet temperature is about 1050°F. This is low enough to maximize steam generation, but high enough to keep the furnace size down.

If steam does not have a high value, the optimum reformer inlet temperature is often about 1100°F. Above this, metallurgical considerations with the inlet piping become a factor.

Up to 1050°F, 2-1/4 Cr -1 Mo material is satisfactory for the inlet piping. At higher temperatures, stainless steel would ordinarily be used, but stainless steel is generally considered unacceptable because of the possibility of chloride stress cracking. Such cracking can occur if the steam in the feed has chloride-containing water droplets carried over from the steam drum. Incoloy is considered the next step up in metallurgy and is not subject to chloride stress cracking, but its cost typically prohibits its use. Accordingly, for metallurgical reasons the maximum inlet temperature should remain at about 1050°F.

#### **4.8 Steam/Carbon Ratio**

The hydrocarbon feed must contain sufficient steam to eliminate carbon formation. The relationship between steam and hydrocarbon is typically expressed as the steam-to-carbon ratio. This corresponds to the moles of steam per mol of carbon in the hydrocarbon. The design steam-to-carbon ratio is typically about 3.0 for all hydrocarbon feedstocks. Lower values (down to about 2.5) can be used for some feedstocks, but there is a higher risk from potential operating upsets that might occur which could drop the ratio down to where carbon formation could occur.

For heavier feedstocks, carbon formation is more likely, and an alkali-based catalyst must be used to suppress carbon formation. Such catalysts are readily available, and it is understood that the 3.0 steam-to-carbon is applicable only if the proper catalyst is chosen. Otherwise, higher steam-to-carbon ratios are required.

#### **4.9 Heat Flux**

The reformer heat flux is typically defined as the heat input per unit of time per square unit of inside tube surface. For a given absorbed duty, the heat flux is therefore determined by the amount of tube surface.

A low heat flux provides extra catalyst volume and lower tubewall temperatures. This provides several advantages: The extra catalyst volume increases the reforming reaction conversion. The lower tubewall temperature reduces the tubewall thickness, which in turn reduces the cost per tube and increases the tube life. The lower tubewall temperature also reduces the fuel requirement.

A high heat flux has the opposite effect, but has the advantage of reducing the number of tubes.

Because of these trade-offs, commercial heat fluxes typically vary from



about 20,000 Btu/hr-ft<sup>2</sup> to 28,000 Btu/hr-ft<sup>2</sup>. A conservative design will typically run from 20,000 to about 25,000 Btu/hr-ft<sup>2</sup>.

The above fluxes are average values for the entire furnace. The point flux is highest in the zone of maximum heat release, and then falls off to a relatively low value at the tube outlet. The maximum point flux is often 35,000 to 40,000 Btu/hr-ft<sup>2</sup>.

#### 4.10 Pressure Drop

The reformer pressure drop depends primarily on the number of tubes, the tube diameter, and the catalyst selection. Typically, the overall design pressure drop will range from 40 to 60 psi.

#### 4.11 Catalyst

Reforming catalysts are typically manufactured in a ring or a modified ring form. The modified ring forms have increased surface area and a higher activity for about the same pressure drop, but they cost more.

Reforming catalysts use nickel as the principal catalytic agent. For heavier feedstocks, an alkali promoter is typically used to suppress carbon formation. For heat fluxes above about 25,000 Btu/hr-ft<sup>2</sup>, modified ring shapes are needed to maintain the reforming reaction conversion.

The reaction conversion is typically measured in terms of "approach to equilibrium." A typical design approach to reforming equilibrium is 20°F. This means that the reforming reaction (equation 1 above) is at equilibrium corresponding to a temperature 20°F lower than the actual temperature. This corresponds to a typical end-of-life catalyst condition. Fresh catalyst typically runs at essentially a 0°F approach to reforming equilibrium (that is, for fresh catalyst the reforming reaction is essentially at equilibrium at the actual temperature). The shift reaction (equation 2 above) is rapid and is considered in equilibrium at all times.

Typical catalyst life is 4 to 5 years. To obtain the performance discussed above over this time frame, the appropriate catalyst must be selected, consistent with the design heat flux and allowable pressure drop.

For higher flux reformers, a dual charge of catalyst is typically used. The top half of the tube is loaded with a high activity catalyst that prevents carbon formation in the zone of maximum flux. The bottom half of the tube can be a more conventional, less expensive catalyst.

Catalyst pressure drop is also an important consideration. Fortunately, the modified ring catalysts can provide higher activity for about the same pressure drop. If significantly higher activity is needed, a higher pressure drop must be accepted.

## 4.12 Tubes

Reformer tubes typically operate at maximum temperatures of 1600 to 1700°F and are designed for a minimum stress-to-rupture life of 100,000 operating hours. Today's preferred metallurgy is a 35/25 Ni/Cr alloy modified with niobium and microalloyed with trace elements including titanium and zirconium.

Smaller tube diameters provide better intube heat transfer and cooler walls. The cooler walls reduce tubewall thickness, which reduces tube cost and increases tube life. The cooler walls also decrease fuel consumption. However, more tubes are required and the pressure drop is higher. Based on these parameters, the optimum inside tube diameter is typically 4 to 5 inches.

Thin walls increase tube life because secondary stresses are minimized during thermal cycling on startups, shutdowns, and upsets. Accordingly, the tubewall thickness should be minimized consistent with meeting the tensile strength requirement. For many applications, the minimum sound wall (MSW) can be as low as 0.25 inches.

Longer tubes provide a longer co-current heat transfer path in the reformer, and thereby reduce the flue gas exit temperature, which conserves fuel. Longer tubes also reduce the number of tubes. However, the pressure drop is higher. The optimum tube length is typically 40 to 45 feet.

Increasing the tube pitch (the center-to-center spacing) reduces the shielding effect between tubes and lowers the peak temperature around the tube circumference. This improvement is significant for short tube pitches, but falls off at longer pitches.

If the pitch is too short, the design must be modified to avoid overlapping the tube inlet flanges. The optimum pitch is typically 2 to 3 tube diameters.

The lane spacing between tube rows must be sufficient to avoid flame impingement from the burners. Typical spacing ranges from 6 to 8 feet.

## 4.13 Burners

The burners are located between the tube rows. Increasing the number of burners reduces the heat release per burner, which permits a smaller flame diameter and reduced lane spacing. The number of burners varies with the design, but a ratio of one burner for every 2 to 2.5 tubes will provide a very uniform heat release pattern and is considered good design practice.

For most hydrogen plants, the burners are a dual-fired design, which will fire both PSA offgas and the supplemental makeup gas. Lo-NO<sub>x</sub> burners are typically used to meet modern environmental requirements. In some burner designs, the makeup gas is used to induce flue gas into the flame, thereby reducing the flame temperature and the NO<sub>x</sub> level. With a properly designed burner, NO<sub>x</sub> levels of as low as 0.025 lbs/MM Btu LHV of heat release can be expected.

#### 4.14 Flow Distribution

It is important to obtain good flow distribution for all reformer streams. The piping should be designed such that the variation in gas flow to the reformer tubes and to the burners does not exceed plus or minus 2.5 percent. Otherwise, the tubewall temperatures may not be sufficiently uniform.

Special consideration must be given to the PSA offgas flow since it is typically available to the burners at only about 3 psig. Even greater consideration must be given for preheated combustion air (if used), since the differential air pressure across each burner is typically no more than 2 inches H<sub>2</sub>O.

To help ensure good distribution, the piping should be as symmetrical as possible, and detailed pressure drop computations should be made and analyzed.

It is especially important that the flue gas tunnels be properly designed. The tunnels are rectangular fire-brick structures located at the bottom of the reformer which serve as horizontal ducts for flue gas removal. Selected bricks are removed along the bottom of the tunnels to provide openings for the flue gas. To ensure plug flow of flue gas down the box, these openings must be designed for uniform flow distribution of the flue gas from the box into the tunnels. To ensure proper design, detailed hydraulic calculations should be made and analyzed.

#### 4.15 Heat Recovery

The flue gas typically exits the radiant box at 1800 to 1900°F. A waste heat recovery (WHR) unit is provided to recover heat from this gas. Typically, this consists of a package unit containing a reformer feed preheat coil, followed by a steam superheat coil (if applicable), followed by a steam generation coil, followed by a boiler feedwater preheat coil. If combustion air preheat is used, the air preheat unit typically replaces the boiler feedwater coil. The flue gas typically exits the WHR unit at about 300°F.

On this basis, and with a typical heat loss of 3 percent of the absorbed duty, the overall efficiency of the reformer (radiant plus WHR) is about 91 percent on an LHV basis.

Steam is also generated in a process steam generator, which extracts heat from the reformer outlet process gas. The WHR unit and the process steam generator typically share a common steam drum.

Steam generation pressure must be sufficient to provide steam to the reformer. Typically, the minimum required pressure is 100-150 psig above the hydrogen product pressure, depending on the plant pressure drop. Significantly higher steam pressures can easily be accommodated, and reformers generating 1500 psig steam are not uncommon in some industries.

## 5. ENVIRONMENTAL ISSUES

The federal government's passage of the Clean Air Act in 1970 set national limits on industrial emissions to reduce air pollution and acid rain. Since 1970, the Clean Air Act has been amended and some states, such as California, have set even stricter limits on several of these emissions. Therefore, a major point of emphasis when designing a hydrogen plant is the reduction of plant emissions. A typical hydrogen plant has three sources of emissions: 1) Flue gas from the combustion chamber of the reformer; 2) Condensate from the process; and 3) Wastewater from the steam generation system.

### 5.1 Flue Gas Emissions

There are five primary pollutants found in the flue gas: nitrogen oxides, carbon monoxide, sulfur oxides, unburned hydrocarbons, and particulates. These components are formed during the combustion process.

The majority of the flue gas emissions consist of the nitrogen oxides (NO<sub>x</sub>). NO<sub>x</sub> is an environmental concern because it can cause photochemical smog and acid rain. The nitrogen oxides from a hydrogen plant primarily consist of nitrogen oxide (NO) and nitrogen dioxide (NO<sub>2</sub>). There are three types of NO<sub>x</sub> formation: prompt NO<sub>x</sub>, fuel NO<sub>x</sub>, and thermal NO<sub>x</sub>. Prompt NO<sub>x</sub> is formed when fragments of hydrocarbons in the fuel combine with nitrogen in the combustion air. This form of NO<sub>x</sub> is considered to be negligible as compared to thermal NO<sub>x</sub> in hydrogen plant applications. Fuel NO<sub>x</sub> is formed when nitrogen-containing hydrocarbons in the fuel are burned. However, this is typically not a concern for hydrogen plants because the makeup fuel is usually natural gas. Thermally produced NO<sub>x</sub> represents the largest contributor to NO<sub>x</sub> formation in a hydrogen plant. Thermal NO<sub>x</sub> is produced by N<sub>2</sub> and O<sub>2</sub> in the combustion air reacting in the hottest part of the burner flame. The rate of thermal NO<sub>x</sub> formation is based on the burner flame temperature, the amount of combustion air, and residence time. As the flame temperature increases, the amount of NO<sub>x</sub> formed increases. Issues such as type of fuel gas, amount of excess air and combustion air temperature affect the amount of thermal NO<sub>x</sub> formation. Therefore, to reduce the flame temperature, many burner manufacturers have developed burner designs that incorporate staged combustion and flue gas recirculation. The recirculation of the flue gas cools the flame thus lowering the amount of thermal NO<sub>x</sub> formation. The recirculation will also lower the amount of CO exiting the burner, as a portion of it will be recycled and combusted.

A NO<sub>x</sub> removal system may be required to meet a site's emission requirements. The typical system used for this case is a Selective Catalytic Reduction unit (SCR). The SCR unit reduces NO<sub>x</sub> by reacting ammonia with the flue gas over a catalyst, which yields nitrogen and water vapor. An SCR

unit can reduce the NO<sub>x</sub> emission from a hydrogen plant by approximately 90%. There is a small slipstream of ammonia, approximately 10 ppmvd that will exit with the flue gas. This unit adds additional capital costs as well as operating costs and ammonia handling issues but is sometimes required as the best available technology (BACT) for NO<sub>x</sub> removal.

The CO, combustion produced particulates, and the unburned hydrocarbons are all related to the amount of excess air, type of fuel, and the amount of mixing of the fuels within the burner. Insufficient air and inadequate mixing can result in incomplete combustion thus raising the amount of CO and unburned hydrocarbons in the flue gas. Particulates formed in the combustion process are very low for gaseous fuels but will increase with the use of liquid fuels.

The sulfur oxides that are formed are directly related to the amount of sulfur found in the fuel. These emissions are typically low when PSA offgas is burned with natural gas. The PSA offgas is sulfur-free due to feedstock pretreatment to protect catalyst beds within the hydrogen plant. Natural gas also typically contains very low levels of sulfur. However, if refinery fuel gases are used as a makeup fuel to the reformer, then the sulfur emissions can increase dramatically as these streams often contain large amounts of sulfur.

Burner manufacturers will have typical values of these emissions for their burners based on actual tests of their burner design. The emission limits of the CO, sulfur oxides, unburned hydrocarbons, and particulates are generally met since light gaseous fuels are typically used as the fuels for the reformer. Table 9 below contains some typical emission values for a standard hydrogen plant utilizing Low-NO<sub>x</sub> burners when burning PSA offgas with natural gas.

*Table 9.* Typical emission values for a standard hydrogen plant

| <b>Emission</b>       | <b>Units</b>                       | <b>Value</b> |
|-----------------------|------------------------------------|--------------|
| NO <sub>x</sub>       | lb/MM Btu LHV                      | 0.03         |
| CO                    | ppmv (3% O <sub>2</sub> dry basis) | 25           |
| Unburned Hydrocarbons | ppmv (3% O <sub>2</sub> dry basis) | 5            |
| Particulates          | lb/MM Btu LHV                      | 0.005        |

## 5.2 Process Condensate (Methanol and Ammonia)

The process condensate from a standard hydrogen plant contains impurities such as dissolved gases, ammonia, methanol, and traces of other organic compounds. The dissolved gases that are found in the process condensate consist of the components in the syngas (CO, CO<sub>2</sub>, H<sub>2</sub>, CH<sub>4</sub>, and N<sub>2</sub>). Henry's Law can be used to calculate the amounts of these gases that are in the condensate.

$$\text{Henry's Law: } P = H \times x$$

where P is Partial Pressure of a Component

H is Henry's Law Constant  
X is Mole Fraction of Component in Solution

The CO<sub>2</sub> represents the largest amount of dissolved gas in the condensate, typically in the range of several 1000 ppmw. The dissolved H<sub>2</sub>, CO, and CH<sub>4</sub> are typically in lower concentrations of less than a hundred ppmw each.

In a hydrogen plant, ammonia is produced in the reformer. The steam methane reformer's operating conditions are similar to that of an ammonia synthesis reactor. The amount of ammonia produced is based on the amount of nitrogen in the feed. Feedstocks with negligible amounts of nitrogen will not produce an appreciable amount of ammonia. Ammonia formation depends on the reaction equilibrium and the residence time inside the reformer. The ammonia equilibrium reaction is given below.

$$[\text{NH}_3] = K_{\text{pNH}_3} * [\text{N}_2]^{0.5} [\text{H}_2]^{1.5} * P_T$$

where [ ] is Mole Fractions  
K<sub>pNH<sub>3</sub></sub> – Equilibrium Constant  
P<sub>T</sub> – Total Pressure, atm

Ammonia formation is lessened due to the fact that the residence time of the steam methane reformer is designed for hydrogen production not ammonia production with recycle. In an NH<sub>3</sub> plant, the ammonia is considered to be at equilibrium in a secondary reformer that is operating approximately 300°F to 500°F higher than a traditional steam methane reformer. Therefore for calculations, the worst case for ammonia production in a hydrogen plant can be assumed to be equilibrium at the reformer outlet temperature plus an additional 300°F.

Methanol is produced as a by-product in the shift converters within the hydrogen plant. In High Temperature Shift Converters (HTSC), the formation of methanol is an equilibrium reaction similar to that of ammonia formation in the reformer. The equilibrium reaction for methanol is given below.

$$[\text{CH}_3\text{OH}] = K_{\text{pCH}_3\text{OH}} [\text{CO}_2][\text{H}_2]^3 P_T^2 / [\text{H}_2\text{O}]$$

where [ ] is Mole Fractions  
K<sub>pCH<sub>3</sub>OH</sub> – Equilibrium Constant  
P<sub>T</sub> – Total Pressure

The typical concentrations of methanol in an HTSC application are approximately 100 to 300 ppmw. In a Low Temperature Shift Converter (LTSC) application, the methanol production is greater than that of an HTSC application. The formation of methanol is not just related to equilibrium for an LTSC but also by the catalyst characteristics and kinetics. Therefore, the catalyst vendor should be contacted in reference to calculating the expected amount of methanol from an LTSC application.

In the majority of hydrogen plants today, the process condensate is used as makeup water to the steam generation system of the plant. Typically, boiler feedwater makeup is mixed with the process condensate and sent to a deaerator. The deaerator uses steam to strip the dissolved gases, namely O<sub>2</sub> and CO<sub>2</sub>, and the other contaminants from the boiler feedwater. These contaminants can be harmful to downstream equipment and boiler operation. These contaminants are then emitted to the atmosphere. Since there are large amounts of CO<sub>2</sub>, the type of deaerator for hydrogen plant use typically has a vertical stripping section consisting of either trays or packing located on top of the deaerator. To calculate the amount of each contaminant leaving the deaerator's stripping section, one can use the equations below.

Mole Fraction Remaining:

$$(Lx_{OUT}) / (Lx_{IN}) = (S-1) / (S^{n+1} - 1)$$

and Mole Fraction Stripped:

$$(Gy_{OUT}) / (Lx_{IN}) = S (S^n - 1) / (S^{n+1} - 1)$$

where G & L are Molar Flow Rates

S – Stripping Factor (KG / L)

n – Number of Equilibrium Stages

K – Vapor-liquid distribution coefficient, (y / x = H / P<sub>T</sub>)

As methanol emissions continue to be monitored more closely, there are some methods of reducing the methanol in the deaerator vent. The vent stream could be condensed and sent to the reformer or the steam system. Catalytic combustion could be used to reduce the methanol. A scrubber system could be added to remove the methanol. In some instances a condensate stripper is added instead of the deaerator to remove the ammonia, methanol, and other contaminants from the condensate. This system recycles the vent stream to the reformer as process steam and the bottoms are mixed with the incoming boiler feedwater makeup. However, this system adds considerable capital cost to a project.

### 5.3 Wastewater

The wastewater from a hydrogen plant typically consists of only the blowdown from the boiler system. The boiler feedwater that feeds the steam generation system has small amounts of impurities such as sodium, chlorides, silica, and organic carbons. These impurities will accumulate within the boiler system and create sludge, scaling of the boiler tubes, and possible carryover of solids into the process steam. Blowdown of the boiler water is performed to prevent these issues from affecting the operation of the steam system. The blowdown is typically sent to the sewer or the on-site waste treatment plant for treatment and disposal.

## 6. MONITORING PLANT PERFORMANCE

There are several areas of focus when monitoring the performance of a hydrogen plant. The first area of focus is the performance of the catalyst beds employed in the hydrogen plant. The Hydrotreater, which converts sulfur compounds to  $H_2S$ , should be checked periodically for pressure drop through the bed. The hydrotreating catalyst life is approximately 3 years. If the catalyst bed's pressure drop is exceeding design then it may be time to change the catalyst out due to catalyst degradation and activity loss.

The next typical catalyst bed in a hydrogen plant is the desulfurizer bed. The desulfurizer removes the  $H_2S$  from the feed gas. The desulfurizer catalyst bed design is based on the loading of the sulfur compounds. Therefore, the exiting gas from the desulfurizer bed should be checked to ensure that the sulfur levels are below 0.1 ppmv. If the original design life of the catalyst bed is known, then periodic feedstock analysis can be used to forecast when the bed may require change out.

Since the reforming reaction constitutes the majority of the hydrogen production in the plant, it is important to monitor the reforming catalyst. The reforming catalyst is typically designed for a 5-year life. Pressure drop measurements should be taken across the catalyst filled tubes in the reformer. If the pressure drop increases as time goes by, this could be an indication that catalyst attrition or possible carbon formation on the catalyst could be taking place. The activity of the catalyst can be checked by comparing the outlet composition of the reformer to the expected composition at the design approach to equilibrium conditions. If the pressure drop increases or the activity has decreased, then it is probably time to change out the reforming catalyst.

The examination of the high temperature shift catalyst is similar to that of the reforming catalyst. The catalyst life for the high temperature shift catalyst is approximately 5 years. Pressure drop readings should be taken to check for possible catalyst attrition. The outlet composition should be validated with the expected composition with the design approach to equilibrium conditions.

The pressure swing adsorption system (PSA) has a catalyst life of approximately 20 years or equal to the expected plant life. However, the hydrogen purity and recovery should be recorded periodically to watch for possible catalyst poisoning. The amount of nitrogen in the feedstock also has an effect on these two operating parameters as well and should be checked. A higher nitrogen content in the feedgas than design could lower the hydrogen recovery in the PSA unit.

The reformer tubes are one of the most important pieces of equipment in a hydrogen plant. These tubes are built from micro-alloyed materials in order to handle the extreme environment in which they are exposed to. The industry standard for reformer tube design is for 100,000 hour life. To ensure that the tubes will last the designed 100,000 hour life, the reformer tubewall



temperature readings should be taken on a regular basis. An optical pyrometer is the instrument of choice for this task. In order to obtain the correct tubewall temperature reading, the tubewall and the furnace background should be shot for each tube reading. The background temperature is required to correct for the background radiation. The equation below can be used to correct the tubewall temperature readings. The emissivity on the pyrometer should be set to 1 before taking the readings.

$$T_t = [(T_{MT}^4 - (1 - e) * T_{MB}^4) / e]^{1/2}$$

where  $T_t$  is True Tube Temperature, °R  
 $T_{MT}$  is Measured Tube Temperature, °R  
 $T_{MB}$  is Measured Background Temperature, °R  
 $e$  is Average furnace emissivity (typical = 0.82)

The maximum allowable tube stress will need to be calculated in order to calculate the actual reformer tube life. This is accomplished by using the Mean Diameter Formula given below.

$$S = (P * D_M) / (2 * t_{MIN})$$

where  $S$  is Tube stress, psi max  
 $P$  is Tube inlet pressure, psig  
 $D_M$  is Tube Mean Diameter =  $(D_O + D_I)/2$   
 $D_O$  is Tube OD, as cast, inches  
 $D_I$  is Tube ID =  $D_O - 2 * t_{MIN} - 2 * CA$   
 $CA$  is Casting allowance, (typically 1/32" on outside wall, 0" on inside wall)  
 $t_{MIN}$  is Minimum sound wall, inches

The Larson-Miller equation correlates the stress-temperature to life of the tubes. The equations below are for Manaurite XM material tubes.

$$S = 0.145 * B * 10^{(-0.0062 * P^2 + 0.2955 * P - 1.5426)}$$

$$P = T * (22.96 + \text{LOG}(t))10^{-3}$$

where  $S$  is Minimum stress to rupture, ksi  
 $B$  is Ratio of minimum to average stress (Typical temperature range,  $B = 0.85$ )  
 $P$  is Larson-Miller parameter, dimensionless  
 $T$  is Tube wall temperature, °K  
 $t$  is tube life, hours

If the measured temperature is less than design, then the reformer tubes should last their expected life. However, if the measured temperature is greater than the design temperature, then the reformer tube life will be shortened. If the actual life of the reformer tubes is below the expected life, then the operating conditions of the reformer should be further investigated.

The steam system is an area that requires constant attention to ensure proper operation of the hydrogen plant. If the steam quality decreases, it can lead to solids carryover from the steam drum. These solids will plate out in the feed preheat coil of the convection section and subsequently lead to an equipment failure and plant shutdown. To reduce the probability of an upset, the steam drum should be manually blowdown on a regular basis to reduce the amount of dissolved solids and other impurities in the steam drum. Next, the boiler feedwater should be analyzed on a regular basis to ensure that the treatment it is receiving is adequate for the desired steam generation conditions.

Cooling water is generally used for the final trim cooling of the process gas before the hydrogen purification step. In most instances, the cooling water is considered to be a dirty medium. Therefore, it is recommended to develop a temperature profile of the cooling water side of the exchanger based on design data. Additional temperature profiles should be developed based on data from the operation of the plant and compared to the original profile. This data can be used as a means to check for fouling of the cooling water side of the exchanger and improper heat transfer through the exchanger.

Another means of monitoring the performance of the hydrogen plant is to check the pressure drop through the entire plant. If the pressure drop is higher than design, then individual pieces of equipment should be checked for excess pressure drop. This may signify several things such as catalyst attrition, excessive exchanger fouling, or equipment failure.

The final method of checking the performance of the unit is to calculate the overall utility consumption of the plant and compare it to the design summary or previous summaries. The feed and fuel flows are typically converted to energy since their utility cost are typically on an energy basis (for example: MM Btu/hr LHV). These numbers as well as the other utility quantities are divided by the hydrogen product flow. This method allows for calculating the total price of hydrogen on a \$/M SCF H<sub>2</sub> basis. Once the summary has been created, comparisons to earlier summaries and analysis of major cost areas can be investigated. The effects of process improvements can be evaluated on this basis.

## **7. PLANT PERFORMANCE IMPROVEMENTS**

The most common method of improving the plant performance is to increase the capacity of the hydrogen plant. The plant design should be evaluated as to its capability to handle an increased load before this is attempted. The process design specifications should be retrieved on all of the relevant plant equipment and compared to the vendor's design specifications. If there are any significant differences between the two sets of specifications, investigation into the cause of the difference is warranted. From this comparison, a final set of equipment design data should be developed for each piece of equipment.

The operating data of the equipment should then be compared to the design capabilities of the equipment in order to set the available capacity increase for each piece of equipment. Compressors should be checked for capacity versus design flow, spillback design, inspection of valves, and motor requirements. The fans should be checked for operating versus design capacity, vane inspection, and motor requirements. The pumps should be checked for operating versus design capacity, inspection of screens and impellers, and motor requirements.

The next area of evaluation consists of the pressure profile of the plant. The operating pressure profile should be compared to the design pressure profile. Any significant differences should be investigated and possibly corrected. An acceptable capacity increase for the equipment should be used to set a proposed capacity increase for the plant. The pressure drop for this raised capacity case should be calculated and compared to design pressure profile. Depending on the results of this calculation, investigation into the available feed pressure may be warranted. Relief settings for the raised capacity case should be evaluated to ensure proper operation. Some pieces of equipment may have to be checked to determine if they can be re-rated for a higher operating pressure than design.

The reformer tubes will need to be evaluated as to their capability of handling an increase in capacity. Temperature readings should be taken at several plant capacity increments (50%, 75%, 100%). This data should be compared with the maximum design tubewall temperature. If the tubewall temperature is approaching the maximum design tubewall temperature, there are several things that can be considered. The catalyst vendor should be contacted about the possibility of a more active reforming catalyst. The burners could be revamped or replaced. The burner pressure drop should be monitored and compared to design data. The excess air used for the combustion should be checked to ensure proper operation. If the burners were to be replaced, it would affect firing capacity, flame pattern, and NO<sub>x</sub> emissions. The reformer tube metallurgy should be checked to see if it could be upgraded. An upgrade in tube metallurgy would affect the tube ID and the design tubewall temperature.

Most hydrogen plants utilize a PSA system for their hydrogen purification. This system should be checked for H<sub>2</sub> purity, and a corresponding H<sub>2</sub> recovery should be calculated. This data should be compared to the original design data of the unit. The cycle times should be compared to the design cycle time. To check the available capacity increase for the PSA unit, the adsorption time should be increased in small increments until the maximum permissible impurity breakthrough occurs. The cycle time should be adjusted and the H<sub>2</sub> recovery calculated. The purge time in this cycle should be compared with the design purge time. The additional purge time is a measure of the additional capacity that is available in the PSA unit.

If the PSA unit is capacity limiting, then the following options should be considered: reduction of offgas drum back pressure, improvement of feed conditions, relaxation of purity specifications, setting unit on automatic purity control, change cycle (equalizations), adsorbent change out, or add additional vessels.

The reduction of the utility consumption of the plant is another method of improving the plant performance. It is important to make certain that the plant is not using an excessive amount of utilities. The reformer is a key target area for this investigation. The burners should be checked to ensure that they are using the correct amount of excess air (typically 10%, 20% for heavier fuels). For example, if the burners were using 20% versus 10% excess air, this would translate to an approximate increase in reformer firing of 10%. Therefore, using the correct amount of excess air does not waste fuel. The bridgewall temperature should also be checked. For every 20°F above the required bridgewall temperature, there is a 1.5% increase in reformer firing. The bridgewall temperature should be set at the temperature required to obtain the process outlet temperature that yields the proper CH<sub>4</sub> slip through the reformer. As discussed above, the PSA recovery should be maximized. For every 1% increase in recovery, there is an approximate savings of 0.5% of feed and fuel. The deaerator vent and steam system blowdowns should be checked. Excessive blowdown adds additional treating chemicals and boiler feedwater flow while reducing the export steam quantity.

Another option is to debottleneck an existing hydrogen plant by revamping or upgrading portions of it. However, these cases should be evaluated on a case-by-case basis as different sites have different utility and/or plot considerations. Some of the upgrades are discussed in Section 8:

## 8. ECONOMICS OF HYDROGEN PRODUCTION

There is a growing focus in the refining industry on hydrogen capacity. Hydrogen is generally required for deep sulfur removal from hydrocarbon products. As sulfur restrictions on gasoline and diesel become increasingly stringent, the refining demand for hydrogen continues to grow.

By evaluating the hydrogen utilization in their facilities, refiners are coming to the realization that they need additional hydrogen supply. There are a number of options available to address this need. Refiners may be able to meet the increased demand by improving operations of their existing hydrogen plants. They may choose to separate hydrogen from waste or off-gas streams or even purchase hydrogen from 3<sup>rd</sup> parties. As an alternative, after careful technical and economic evaluation, they may conclude that the best solution to optimize the economic benefit to them over the longer term is to build a new hydrogen plant.

In recent years, many advances have been made in hydrogen plant technology. Substantial improvements have been incorporated into hydrogen

plant design to significantly improve overall life cycle costs. Based on experience with hydrogen plant benchmarking, it has become clear that the optimum economic solution in some cases may be to replace an existing hydrogen plant with a new modern hydrogen plant.

There are a number of options available to refiners to meet the increase in hydrogen demand. Before deciding to proceed with any option, refiners should conduct a comprehensive technical and economic evaluation of their existing operations and evaluate the technical and economic benefits of the options available to them. The option that provides the optimum economic and operations benefits will be different for each situation and will depend on such things as the existing steam balance, the cost and availability of utilities, plot limitations, and the condition of existing hydrogen plants.

The first option for refiners who are operating Old Style (See Section 3.4) hydrogen plants is to consider ways to increase the capacity of these plants. Following an evaluation of the condition and efficiency of the existing plant, they may be able to effectively increase the capacity by either tightening up on operations or selectively upgrading portions of the old plant.

In many refineries, hydrogen is treated like a utility. There may not be much of a focus on the details of the actual production and the plants are sometimes operated “loose.” In this case, simple operational changes could significantly increase production and efficiency. Refiners could also debottleneck an existing hydrogen plant by revamping or upgrading portions of it. Debottlenecking options can also have a positive efficiency impact. Some of these potential upgrades may include:

Replacing reformer tubes with upgraded metallurgy and thinner walls will allow for more throughput and a higher heat flux, which would increase capacity.

- Adding a Pre-Reformer would unload the primary reformer so capacity can be increased.
- Adding a Secondary Reformer would increase methane conversion, which increases capacity.
- Adding Combustion Air Preheat would lower the fuel requirement and potentially unload the waste heat recovery unit and fluegas fan, resulting in a capacity increase.
- Upgrading the CO<sub>2</sub> removal unit would minimize hydrogen loss in the Methanator, resulting in a potential capacity increase.
- Adding a PSA unit would decrease hydrogen production, but would typically produce more cost effective and higher purity hydrogen.

A second option is to separate hydrogen from a waste stream or an offgas stream that is currently being sent to fuel. This would typically require the addition of separation equipment and possibly some compression. In addition, separating hydrogen out of the fuel system will usually result in additional makeup fuel. This could change the heating value of the refinery fuel system and possibly have an impact on other fuel burning equipment.

A third option is to buy hydrogen from a 3<sup>rd</sup> party. Various industrial gas suppliers are willing to sell hydrogen to refiners either by pipeline or, depending on location, by a stand-alone plant. This option requires a minimal capital investment by the refiner but the delivered hydrogen will probably be more expensive per unit than if self-produced.

The last option is to build a new hydrogen plant. Building a Modern hydrogen plant is typically the most capital intensive of the options available; however, the capital investment could pay off if there is a significant gain in efficiency. Below we will analyze and compare the typical overall production cost of hydrogen between a Modern and an Old Style hydrogen plant.

## 8.1 Overall Hydrogen Production Cost

The most significant economic factor in evaluating options to increase hydrogen capacity is the overall production cost of hydrogen. The overall production cost can be estimated over the life of the hydrogen plant by using the different cost parameters of constructing, operating, and maintaining the hydrogen plant. This overall production cost reflects a complete picture of the hydrogen plant economics over the life of the plant.

The efficiency of producing hydrogen and by-products are very important in minimizing the production cost of hydrogen. Utility costs are the major operating cost in hydrogen production. Utilities typically include usage of feed, fuel, boiler feed water, power, and cooling water, and generation of export steam (steam is typically a by-product of the hydrogen production process). Of these, feed and fuel make up the largest portion of the utility costs. In addition, the credit for export steam can have a significant impact on utility costs, especially when refinery utility costs are favorable for steam production. The remainder of the utilities combined typically make up less than 10% of the total operating cost.

These utility costs, together with other economic parameters applicable to the plant being evaluated, can be incorporated into a cash flow model and the overall production costs of hydrogen can be evaluated. The other economic parameters include such things as capital cost, start-up cost, other operating costs (including catalyst replacement and tube replacement), and maintenance costs. From this model, the internal rate of return (IRR), net present value at various rates of return (NPV), net cash flow, and a generated income statement can also be developed.

## 8.2 Overall Production Cost Comparison

Building a new hydrogen plant is typically not the most appealing alternative to refiners. A new hydrogen plant requires a significant capital investment, and although hydrogen is required to support many of the refinery unit operations, it is generally not viewed as a direct “money maker.”

However, once all factors are taken into account and a total production cost of hydrogen over the life of the plant is determined, the best economic solution may be replacing an Old Style hydrogen plant with a new Modern hydrogen plant. The following evaluation illustrates this potential.

### 8.3 Evaluation Basis

To demonstrate the economics of building a Modern hydrogen plant versus continuing to operate an Old Style plant, two representative plants each producing 90 MM SCFD of contained hydrogen from a natural gas feed will be compared. Natural gas will also be used for fuel, and both plants will export 600 psig superheated steam. The Old Style plant will consist of the major processing units described above and will produce hydrogen with a purity of 95%. Other parameters for the Old Style plant will be based on typical observed values. The Modern plant will consist of the major processing units described above and will produce hydrogen with a purity of 99.99%. The Modern plant design will be based on producing maximum export steam.

This evaluation could be done based on a variety of other plant configurations, but for demonstration purposes, this evaluation is limited to the plant types described. For comparison purposes, the cost of utilities will be based on the following:

|                  |                      |
|------------------|----------------------|
| Natural Gas      | \$4.00 per MM Btu    |
| HP Steam         | \$5.00 per 1000 lbs  |
| Boiler Feedwater | \$0.50 per 1000 lbs  |
| Power            | \$0.05 per kWh       |
| Cooling Water    | \$0.10 per 1000 gals |

### 8.4 Utilities

As previously discussed, the utility costs of a hydrogen plant are among the most important economic factors in determining the overall production cost of hydrogen. Simulation models were built for both the Old Style and Modern plants to calculate utility costs. The Old Style plant utilities are based on a simulation model built to reflect typical plant performance. The Modern plant utilities are based on a simulation model for the design of a typical new plant. Table 10 shows the utilities and utility cost of hydrogen for each plant.

Table 10 clearly illustrates a lower total utility cost for producing hydrogen in the Modern Plant than in the Old Style plant. The Modern plant produces hydrogen at rate of \$1.409 per M SCF of contained hydrogen, while the Old Style plant produces at a rate \$1.908 per M SCF of contained hydrogen. For a plant producing 90 MM SCFD of contained hydrogen, this

Table 10. Utility Cost of Hydrogen Production

| <b>Utilities per 100 SCF Contained Hydrogen</b> |                         |                      |
|---|-------------------------|----------------------|
|   | <b><u>Old Style</u></b> | <b><u>Modern</u></b> |
| Natural Gas Feed, MM Btu LHV                    | 0.275                   | 0.317                |
| Natural Gas Fuel, MM Btu LHV                    | 0.200                   | 0.126                |
| Total Feed,+ Fuel, MM Btu LHV                   | 0.475                   | 0.443                |
| HP Export Steam, lbs                            | 20                      | 90                   |
| Boiler Feedwater, lbs                           | 45                      | 120                  |
| Power, kWh                                      | 0.65                    | 0.52                 |
| Cooling Water, gal                              | 530                     | 8                    |
|   | <b><u>Old Style</u></b> | <b><u>Modern</u></b> |
| Natural Gas Feed, MM Btu LHV                    | 1.100                   | 1.268                |
| Natural Gas Fuel, MM Btu LHV                    | 0.800                   | 0.504                |
| Total Feed,+ Fuel, MM Btu LHV                   | 1.900                   | 1.772                |
| HP Export Steam, lbs                            | -0.100                  | -0.450               |
| Boiler Feedwater, lbs                           | 0.023                   | 0.060                |
| Power, kWh                                      | 0.033                   | 0.026                |
| Cooling Water, gal                              | 0.053                   | 0.001                |
| <b>Total Utility Cost, \$</b>                   | <b>1.908</b>            | <b>1.409</b>         |

difference results in an annual utility savings for a Modern plant of \$16.4 MM. Of course, the utility cost alone does not complete the picture of the overall production cost of hydrogen. We must also evaluate a number of other economic and operating factors.

## 8.5 Capital Cost

Capital must be invested to build the new plant in order to capture the utility savings of the Modern plant. A total capital investment of about \$55 MM would be expected for a new typical 90 MM SCFD hydrogen plant. This approximate installed sales price is based on inside battery limits, natural gas feed, no compression, no buildings, no water treatment units, no SCR's or MCC's, industry engineering standards, and delivery to the US gulf coast. For purposes of comparison, no capital investment is considered for the Old Style plant.

## 8.6 "Life of the Plant" Economics

A cash flow economic model can be generated using the utility costs developed for each plant, the capital cost required for the Modern plant, as well as a number of other economic factors. These other economic factors, along with their associated values are listed below:

- New Plant construction length – 2 years
- Escalation Rate 1.5% for all feed, product and utilities



- Labor – 2 operators per shift
- Overhead – 50% of labor
- Maintenance – 2% of plant cost per year
- Other Misc – 1% of plant cost per year
- Catalyst costs accrued in year of change out
- Reformer tube replacement – every 10 years
- On Stream Time – 98.5%
- Working Capital – 45 days
- Debt Level – Borrow 75% for New Plant
- Cost of Capital – 8%
- Debt Length – 7 years
- Depreciation Life (of Capital Cost) – 10 years
- Tax Rate – 34%
- Project Life – 25 years (includes 2 years of construction)
- Internal Rate of Return – 0% to obtain actual cost of Hydrogen production

This resulting average overall production cost of hydrogen, calculated for the life of the plant, is shown in Table 11.

*Table 11. Overall Production Cost of Hydrogen*

|   | Old Style  | Modern            |
|---|------------|-------------------|
| Plant Capacity, MM SCFD (Contained)               | 90         | 90                |
| Capital Cost, MMS\$                               | -          | 55                |
| Average H2 Production Cost, \$ per 100 SCF        | 1.996      | 1602              |
| Average H2 Production Cost, \$ per year           | 65,568,600 | 52,625,700        |
| <b>Average Annual Production Cost Savings, \$</b> | -          | <b>12,942,900</b> |

The evaluation shows that taking all relevant economic factors into consideration, the overall production cost of hydrogen is lower for the Modern plant. The Modern plant produces hydrogen at a rate of \$1.602 per M SCF of contained hydrogen while the Old Style plant produces hydrogen at \$1.996 per M SCF of contained hydrogen. This lower overall production cost results in an annual savings for the Modern plant of about \$12.9 MM per year. This evaluation proves that for the cases analyzed, it is economically feasible and potentially advantageous to build a new, more efficient hydrogen plant.

## 8.7 Sensitivity to Economic Variables

Economic parameters for each refinery are different. The major parameters that can significantly alter these results are the efficiency of the existing plant, the feed and fuel price, and the export steam credit. The

efficiency of the existing plant can span a wide range and is specific to each plant. For the remaining evaluations, the Old Style plant utilities will be held constant. The overall production cost of hydrogen will be analyzed as a function of the other two major factors, feed and fuel price and export steam credit.

## 8.8 Feed and Fuel Price

The cost of feed and fuel is typically the largest component of the overall production cost of hydrogen. Feed and fuel usually account for more than 80% of the total before the steam credit is taken. The overall operating cost changes significantly as the natural gas price varies. Figure 10 shows the effect of varying the natural gas price. For this evaluation, the export steam credit to natural gas price ratio was held constant.

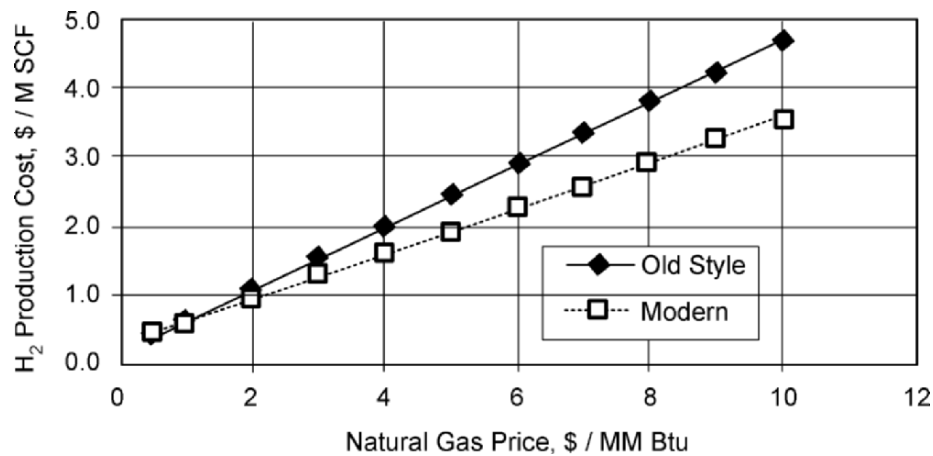


Figure 10. H<sub>2</sub> Production vs Natural Gas Price

As the price of natural gas increases, the Modern plant becomes more favorable. This is due to the overall feed and fuel efficiency advantage of the Modern plant. For example, if the natural gas price were changed from \$4 to \$8 per MM Btu (double the base case credit), the overall production cost would increase by \$1.326 per M SCF of hydrogen for the Modern plant and \$1.804 for the Old Style plant. The higher natural gas price would increase the average annual savings for the Modern plant from \$12.9 MM to \$28.6 MM.

## 8.9 Export Steam Credit

The export steam credit also has a significant effect on the overall production cost. The value a refinery places on steam depends on utility factors and the existing steam balance in the refinery. For example, during the winter, steam tracing is generally used more heavily and the value of steam could be higher than average. Conversely, in the summer, when less steam tracing may be utilized, steam may have a lower than average value. Modern hydrogen plants typically export much more steam due to the fact that they are more efficient and have a CO<sub>2</sub> removal regeneration requirement. Figure 11 shows the effect of varying the export steam credit. For this evaluation, the natural gas price remained the same.

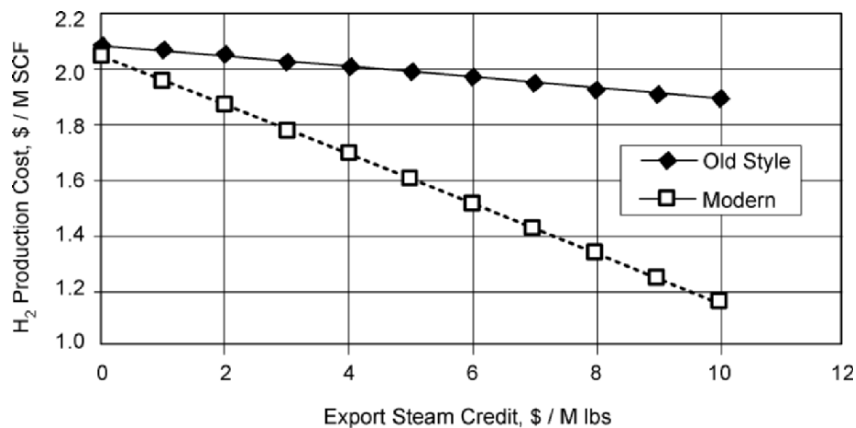


Figure 11. H<sub>2</sub> Production Cost Vs Steam Credit

As the export steam credit increases, the economics for the Modern plant become more favorable. For example, if the export steam credit were changed from \$5 to \$10 per M lbs (double the base case credit), the overall production cost would drop by \$0.450 per M SCF of hydrogen for the Modern plant and \$0.100 for the Old Style plant. The higher steam credit would increase the average annual savings for the Modern plant from \$12.9 MM to \$24.4 MM.

## 9. CONCLUSION

Refiners have a number of different options to consider in addressing the demand for additional hydrogen. A comprehensive technical and economic evaluation of existing operations is required to determine the optimum

solution for each specific application. The optimum solution for each refinery will be different due to site-specific items such as the cost and availability of utilities, plot limitations, refinery steam balance, emission requirements, and the condition of any existing hydrogen plants. The rising cost of utilities, and particularly natural gas, has placed a premium on the overall plant efficiency. Therefore, the overall plant efficiency has not only become a key factor in determining the economics of what option to pursue, but also in the performance enhancement of existing hydrogen plants.

Today's Modern hydrogen plants take advantage of numerous technological improvements and offer a much more efficient plant with lower overall life cycle cost. Once technical and economic evaluations are performed, it should not be surprising that the most economically attractive and most feasible approach may be to build a new hydrogen plant.

## 10. ADDITIONAL READING

1. Tindall, B.M.; King, D.L., Design Steam Reformers For Hydrogen Production, *Hydrocarbon Process.*, July **1994**.
2. Tindall, B.M.; Crews, M.A., Alternative Technologies to Steam-Methane Reforming, *Hydrocarbon Process.*, p. 80, August, **1995**.
3. King, D.L.; Bochow, C.E., What Should and Owner/Operator Know When Choosing and SMR/PSA Plant, *Hydrocarbon Process.*, May **2000**.
4. Hoitsma, K.; Snelgrove, P., Effective Reformer Design and Erection, *World Refining*, p. 24 July/August **2002**.
5. Tindall, B.M.; Crews, M.A., Economics of export steam for hydrogen plants, *Hydrocarbon Engineering*, 39-41, February **2003**.
6. Boyce, C.; Ritter, R.; Crews, M.A., Is It Time For A New Hydrogen Plant, *Hydrocarbon Engineering*, February **2004**.
7. Ernst, W.S.; Venables, S.; Christensen, P.S.; Berthelsen, A.C., Push Syngas Production Limits, *Hydrocarbon Process.*, 100-C through 100-J, March **2000**.
8. de Wet, H.; Shaw, G., Ammonia Plant Safety & Related Facilities, American Institute of Chemical Engineers, Vol. 35, 315-335.
9. Haldor Topsoe A/S, Autothermal Reforming, 10-1 through 10-11, June **1995**.
10. Christensen, T.S.; Primdahl, I.L., Improve Syngas Production Using Autothermal Reforming, *Hydrocarbon Process.*, 39-46, March **1994**.
11. Lawson, A.; Primdahl, I.; Smith, D.; Wang, Shou-I, Carbon Monoxide Production by Oxygen Reforming, Air Products and Chemicals, Inc., 2-21 1475H, March 1990.
12. Jahnke, F.C.; Ishikawa; Rathbone, T., High Efficiency IGCC Using Advanced Turbine, Air Separation Unit, and Gasification Technology, Presentation at the 1998 Gasification Technologies Conference in San Francisco, CA., 1-8, October 1998.
13. Wallace, P.S.; Anderson, M.K.; Rodarte, A.I.; Preston, W.E., Heavy Oil Upgrading by the Separation and Gasification of Asphaltenes, Presented at the 1998 Gasification Technologies Conference in San Francisco, CA., 1-11, October 1998.
14. Liebner, W.; Hauser, N., The Shell Oil Gasification Process (SGP) and its Application for Production of Clean Power, Lurgi and Shell, 1990's.
15. Texaco Development Corporation, Texaco Gasification Process for Gaseous or Liquid Feedstocks, Texaco Image Services Tulsa, January 1993.

16. Heaven, D.L., Gasification Converts A Variety Of Problem Feedstocks And Wastes, *Oil Gas J.*, 49-54, May 27, **1996**.
17. Fong, W.F.; O'Keefe, L.F., Syngas Generation from Natural Gas Utilizing the Texaco Gasification Process, Presented at the 1996 NPRA Annual Meeting in San Antonio, TX., AM-96-68 Pages 1-12, March 17-19, 1996.
18. Stellaccio, R.J., Partial Oxidation Process for Slurries of Solid Fuel, U.S. Patent No. 4,443,230, April 17, 1984.
19. Hauser, N.; Higman, C., Heavy Crude and Tar Sands – Fueling for a Clean and Safe Environment, 6<sup>th</sup> UNITAR Int'l. Conference on Heavy Crude & Tar Sands – Houston, TX., February 12 – 17, 1995.
20. Lurgi Corporation, Integrated Gasification Combined Cycle Process (IGCC), June 1995.
21. Lurgi, Perspectives and Experience with Partial Oxidation of Heavy Residues, Presented at the Tale Ronde – Association Francaise des Techniciens du Petrole – Paris, June 28, 1994.
22. Reed, C.L.; Kuhre, C.J., Make Syn Gas By Partial Oxidation, *Hydrocarbon Process.*, 191-194, September **1979**.
23. Abbott, J., Advanced Steam Reforming Technology in GTL Flowsheets, Syntex (ICI), 1999.
24. Hicks, T., A Decade of Gas Heated Reforming, FINDS, Volume XI, Number 3 Third Quarter 1996.
25. Abbishaw, J.B.; Cromarty, B.J., The Use of Advanced Steam Reforming Technology for Hydrogen Production, Presented at the 1996 NPRA Annual Meeting – San Antonio, TX., AM-96-62 Pages 1-15, March 17-19, 1996.
26. Farnell, P.W., Commissioning and Operation of ICI Katalco's Leading Concept Methanol Process, Prepared for presentation at the AIChE Ammonia Safet Symposium – Tucson, Arizona, September 18-20, 1995.
27. Farnell, P.W., Commissioning/Operation of Leading Concept Methanol Process, Ammonia Technical Manual, 268-277, 1996.
28. Goudappel, E.; Herfkens, A.H.; Beishuizen, T., Gas Turbines for crude oil heating and cogeneration, PTQ Spring 2000, 99-109.
29. Shahani, G.; Garodz, L.; Baade, B.; Murphy, K.; Sharma, P., Hydrogen and Utility Supply Optimization, *Hydrocarbon Process.*, 143-150, September **1998**.
30. Hairston, D., Hail Hydrogen, Chemical Engineering, 59-62, February 1996.
31. Farnell, P.W., Investigation and Resolution of a Secondary Reformer Burner Failure, Prepared for Presentation at the 45<sup>th</sup> Annual Safety In Ammonia Plants and Related Facilities Symposium – Tuscon, Arizona – Paper no. 1D, September 11-14, 2000.
32. Shahani, G.H.; Gunardson, H.H.; Easterbrook, N.C., Consider Oxygen for Hydrocarbon Oxidations, *Chem. Eng. Prog.*, 66-71, November **1996**.
33. Jung, C.S.; Noh, K.K.; Yi, S.; Kim, J.S.; Song, H.K.; Hyun, J.C., MPC Improves Reformer Control, *Hydrocarbon Process.*, 115-122, April **1995**.
34. Baade, W.F.; Patel, N.; Jordan, R.; Sekhri, S., Integrated Hydrogen Supply-Extend Your Refinery's Enterprise, AM-01-19 Presented at the NPRA 2001 Annual Meeting – New Orleans, LA., March 18-20, 2001.
35. Grant, M.D.; Udengaard, N.R.; Vannby, R.; Cavote, C.P., New Advanced Hydrogen Plant in California Refinery by the Topsoe Process, AM-01-27 Presented at the NPRA 2001 Annual Meeting – New Orleans, LA., March 18-20, 2001.
36. Howard, Weil, Labouisse, Friedrichs Inc., GAS-TO-LIQUIDS, SOLIDS-TO-LIQUIDS, LIQUIDS-TO-LIQUIDS, Fischer-Tropsch Technology, 1-54, December 18, 1998.
37. Sanfilippo, D.; Micheli, E.; Miracca, I.; Tagliabue, L., Oxygenated Synfuels from Natural Gas, PTQ Spring 1998, 87-95.

38. Barba, J.J.; Hemmings, J.; Bailey, T.C.; Horne, N., Advances in Hydrogen Production Technology: the Options Available, *Hydrocarbon Eng.*, 48-54, December/January **1997/98**.
39. Dybkjaer, I.; Madsen, S.W., Advanced Reforming Technologies for Hydrogen Production, *Hydrocarbon Eng.*, 56-65, December/January **1997/98**.
40. DaPrato, P.L.; Gunardson, H.H., Selection of Optimum Technology for CO Rich Syngas, *Hydrocarbon Eng.*, 34-40, September/October **1996**.
41. Hutchings, G.J.; Ross, J.R.H.; Kunchal, S.K., *Methane Conversion*, 1-81, 1994-97.
42. ICI Group, ICI Catalysts for Steam Reforming Naphtha, ICI Group 72W/033/1/CAT46, 1-19, 46 Series.
43. Brown, F.C., Alternative Uses for Methanol Plants, PTQ Spring 2000, 83-91.
44. Mii, T.; Hirotsani, K., Economics of a World Class Methanol Plant, PTQ Spring 2000, 127-133.
45. Carstensen, J., Reduce Methanol Formation in Your Hydrogen Plant, *Hydrocarbon Process.*, 100-C – 100-D, March **1998**.
46. LeBlanc, J.R.; Schneider III, R.V.; Strait, R.B., *Production of Methanol*, Marcel Dekker, Inc., 51-132, Copyright 1994 by Marcel Dekker, Inc.
47. Parks, S.B.; Schillmoller, C.M., Improve Alloy Selection for Ammonia Furnaces, *Hydrocarbon Process.*, 93-98, October **1997**.
48. Cromarty, B., Effective Steam Reforming of Mixed and Heavy Hydrocarbon Feedstocks for Production of Hydrogen, Presented at the NPRA 1995 Annual Meeting – San Francisco, CA., March 1995.
49. Martin, R.P., Nitrogen Oxide Formation and Reduction in Steam Reformers, Paper Presented at the International Fertilizer Industry Association, October 2-6, 1994, Amman, Jordan.
50. Clark, L., Controlling NOx, Posted on [www.JohnstonBurner.com](http://www.JohnstonBurner.com), April 1, 2002.
51. Garg, A., Reducing NOx from Fired Heaters and Boilers, Presented at Chemical Engineering Expo 2000 at Houston, TX, 2000.
52. Kunz, R.G.; Smith, D.D.; Patel, N.M.; Thompson, G.P.; Patrick, G.S., Air Products and Chemicals, Inc., Control NOx from Gas-Fired Hydrogen Reformer Furnaces, Paper presented, AM-92-56.
53. Yokogawa, Boiler Blowdown, Analytical-SIC4900-02, Posted on [www.Yokogawa.com](http://www.Yokogawa.com).
54. Harrell, G., Boiler Blowdown Energy Recovery, Energy Matters Newsletter, Winter 2003.

## Chapter 26

# HYDROGEN: UNDER NEW MANAGEMENT

Nick Hallale,<sup>1</sup> Ian Moore,<sup>1</sup> and Dennis Vauk<sup>2</sup>

1. *AspenTech UK Limited, Warrington, UK*

2. *Air Liquide America L.P., Houston, Texas*

## 1. INTRODUCTION

These days, you can't be involved in the oil refining industry without coming across something on hydrogen management. However, most articles and presentations follow the same route, namely discussing the stricter fuel specs on sulfur and aromatics as well as the changing product markets. They then move on to say that more hydrotreating and hydroprocessing will be required as a result. The conclusion? Refineries are going to need more hydrogen. But are they telling the refiners anything that they didn't already know? Of course, some authors go a step further and subtly (or not so subtly) remind the refiner that he or she will need to buy more hydrogen from them or perhaps buy a hydrogen plant from them in the future. As if they really need to have it rubbed in.

This chapter aims to be different. Instead of focusing on the problems, we will look at the opportunities. The intention is to get refiners thinking of their hydrogen as an asset not a liability.

At present, refineries generally fit into one of three situations with respect to hydrogen:

**Type 1:** The refinery has an excess of hydrogen, which is routed to the fuel gas system. Refinery operations are not constrained by hydrogen. The price of hydrogen is based on its fuel gas value. Direct pressure-control letdowns to fuel gas have no economic penalty. In process units, high-pressure purge rates can be increased to increase hydrogen partial pressure in reactors without penalty. In these cases, catalytic reformer hydrogen is normally the only source of hydrogen supply. Typical hydrogen price (depending on marginal fuel price) is €350/tonne (January 2003 prices).

**Type 2:** The refinery is often “short” of hydrogen, with the catalytic reformer acting as the “swing” hydrogen producer. Refinery operations and profitability are constrained by hydrogen. Key process units “compete” for hydrogen, which is priced in the refinery LP model based on plant-wide profitability (e.g. gasoline over-production). Direct pressure-control letdowns have a high economic penalty. In process units, high-pressure purges are minimized, reducing hydrogen partial pressure in the reactors. In these cases, catalytic reformer hydrogen is normally still the only source of hydrogen supply, although Type 2 also applies when on-purpose generation or import capacity is limited and operating at maximum. Under these conditions, hydrogen value can be three times higher – €1000/tonne.

**Type 3:** The refinery can meet hydrogen demand through “on-purpose” hydrogen production (e.g., with an SMR) or through external import. These are the refinery “swing” hydrogen producers. Refinery operations are not constrained by hydrogen. Hydrogen is priced based on its marginal production cost or import value. Direct pressure control letdowns have an economic penalty based on the value of hydrogen as a reactant in process units relative to its value as fuel. In process units, high-pressure purge rates are optimized to balance the value of higher hydrogen partial pressures (better yields, increased capacity, longer catalyst life) against the cost of purge losses. The value of hydrogen depends on whether or not the cost of capital is included in the price. For a refinery that has pre-invested in a hydrogen plant, the marginal production cost could be €500/tonne. If hydrogen is imported from an external supplier, the cost is more likely to approach €900/tonne.

Most refiners are on a painful journey from the fondly remembered days of Type 1 to a current situation of Type 2. Larger and more profitable refineries are developing and implementing plans that take them to Type 3, while a small number may choose to stay within Type 2 because major new investment simply cannot be justified.

## 2. ASSETS AND LIABILITIES

In his book, *Rich Dad, Poor Dad*,<sup>1</sup> best-selling author Robert Kiyosaki explains that the reason most people never become wealthy is because they don't know the difference between assets and liabilities. He keeps away from textbook accountancy and uses a definition of assets and liabilities simple enough for even chemical engineers to understand: *an asset is something that puts money into your pocket while a liability is something that takes money out of your pocket*. Many people view expensive cars, wide-screen TVs and of course their homes as assets, but do these put any money in their pocket? In fact these are all liabilities. True assets are those investments which make



money for their owners, such as real estate, businesses, stocks and shares. Recognising the difference between the two is vital.

What does all this have to do with hydrogen? Well, as we will show, refiners will never get the most value from their hydrogen unless they have the correct view of it. For the most part, refiners tend to view hydrogen as a utility that has to be supplied in order for them to operate. It is a necessary evil whose cost must simply be borne, just like fuel, electricity and water. Supplying hydrogen takes money out of their pockets and so it is a liability. Right?

Wrong! As this article will show, hydrogen - if properly managed - can be an asset, something that *makes* money for the refinery. Just as there are good and bad investments, there are good and bad ways to use hydrogen in a refinery. The secret is in finding the good ways. To do this requires a willingness to question conventional wisdom and to take a wider view of the issues. This chapter will discuss some of the important tools that will help to do this. It will also discuss some of the lessons learned from industrial projects carried out by AspenTech and Air Liquide as part of their alliance called PRO-EN Services.<sup>2</sup>

### 3. IT'S ALL ABOUT BALANCE

Accountants talk about balance sheets. Chemical engineers talk about mass balances. The principle is the same: what goes in must be accounted for. When we are dealing with hydrogen systems, the total amount of hydrogen produced and/or supplied must equal the total hydrogen that is chemically consumed, exported, burned as fuel or flared. Unfortunately, it is very rare to find a refinery where all hydrogen is accounted for. There is usually a poor hydrogen balance to begin with. Stream flow rates and compositions are often not measured and when they are, the data may contain significant inconsistencies. In many cases, large imbalances are often accepted and attributed to "leaks," "distribution losses," "meter error" and "unaccounted flow." If actual currency were involved, the accountants would probably use less euphemistic terms, such as "embezzlement," "fraud," "misappropriation" and "theft." If we take the view that hydrogen is a valuable asset, not having a decent hydrogen balance is tantamount to throwing money away or letting someone steal it. It has been our experience that significant benefits - hundreds of thousands of dollars or more per year - can be achieved by examining the hydrogen balance and finding no-cost "housekeeping" improvements. Simple as this may sound, it can only be realized by understanding the overall hydrogen system and this in turn needs systematic analysis and modelling capabilities.

To give an example, we recently performed a hydrogen system study for a U.S. refinery. The refinery supplemented the hydrogen generated by its two catalytic reformers with purchased hydrogen. Flow rate and composition data were collected from the refinery and used to set up a flow sheet balance with surprising results. We found that hydrogen worth \$2 million per year was being lost to flare and fuel gas through three specific areas, one of which was a leaky valve. We also found other opportunities, including reducing the amount of hydrogen purged for pressure control and avoiding the needless re-compression of rather large gas streams.

So what is needed to set up a hydrogen balance? Firstly, flow rates, compositions and pressures must be determined at certain key points in the hydrogen system. Flow diagrams of the hydrogen-consuming processes are also needed so that reactor and separator configurations as well as recycle locations can be determined.

Secondly, models of the consumers are required. These models need not be totally rigorous ones because this would take far too long in the early stages of a project. However, they should be sufficiently detailed to capture the important operating features of the units as well as to predict their performance. AspenTech has been developing such models using fit-for-purpose simplified models for reactors, flash drums and separation columns, which can be used as building blocks for the entire hydrogen network.

Thirdly, data correction and reconciliation tools are required. During this process, many refiners are surprised to discover that their hydrogen-system flow meter readings, if properly corrected, aren't so bad after all. Think of currency exchange rates. No semi-decent accountant would try to convert South Africa Rands into U.S. Dollars at the exchange rate used in the 1970s. However, it is surprising to see how often people are happy to trust flow meters calibrated with molecular weights that are now quite different from present operation. Because the molecular weight of hydrogen is so low, small changes in stream composition can affect the stream molecular weight significantly. For example, a mixture consisting of 99% hydrogen and only 1% ethane has a molecular weight 14% greater than that of pure hydrogen. Refiners typically correct flow meter readings for temperature and pressure, but not for composition. In other words, if hydrogen were currency, they would be using outdated exchange rates. The software mentioned above can automatically correct measured stream flow rates for deviations from the calibration point. It can also carry out a data reconciliation whereby the user can enter whatever data are available and then specify how much confidence he or she has in each value. For example, a flow rate can be an accurate measurement (within 5%), an accurate estimate (within 20%), a rough

estimate (within 50%) or a guess (within 500%). The software will then reconcile the values to achieve a balance while staying within the confidence bounds. *Figure 1* shows what a completed hydrogen system balance might look like.

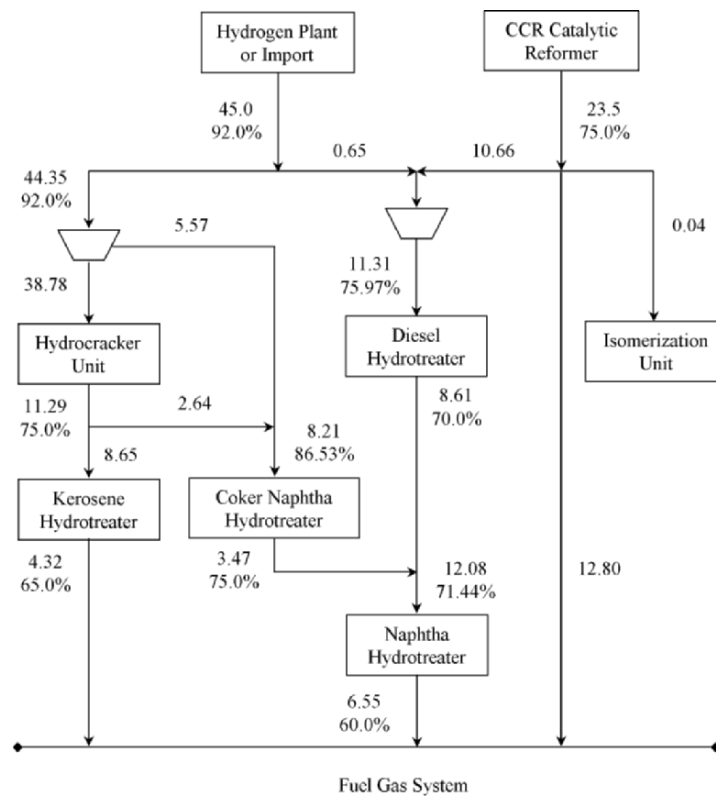


Figure 1. A typical refinery H<sub>2</sub> balance (flows in MMCFD, H<sub>2</sub> purity in mol%)

#### 4. PUT NEEDS AHEAD OF WANTS

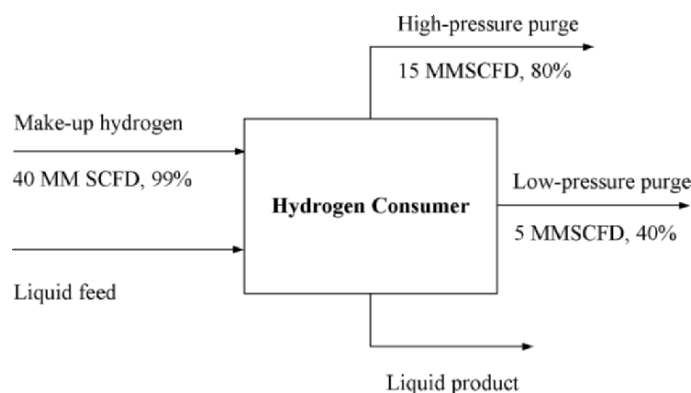
In *Rich Dad, Poor Dad*, Kiyosaki advises that people should not spend money on unnecessary items while trying to build a foundation for wealth. He argues that by delaying gratification now, people will be able to use their money to buy assets which build up enough real wealth so that they can afford anything they want later. The trick is to put needs ahead of wants.

The same principle applies when trying to make more money from hydrogen in refineries. Don't worry, we are not suggesting that refinery operations should have to make do without hydrogen for a few years!

However, we are suggesting that refiners question whether certain units actually need to be fed with hydrogen of very high purity. If there is a supply of hydrogen at 99% purity available, chances are that engineers or operators will claim that their unit “needs” to have 99% pure hydrogen. It is this mindset that needs to be challenged. Once we break away from this, the scope for re-using and recycling hydrogen becomes a lot greater and benefits can be substantial.

One European refinery used a significant flow rate of very pure hydrogen for drying purposes. When questioned about this, the refinery engineers replied that this was the way it had always been done. That made sense because until recently, the refinery had a large surplus of hydrogen. Now, however, that hydrogen is worth several hundred thousand dollars per year. It would be far more sensible to use the offgas from another consumer, accomplishing the same job for free!

Admittedly, most refineries do not have such obvious savings. Most hydrogen consumers require a certain flow rate of gas and hydrogen purity in order to operate properly. The flow rate is needed to maintain a gas to oil ratio high enough to prevent coking, while the purity is required to maintain the required hydrogen partial pressure for effective kinetics. With fixed flow rate and purity demands, it may not look like there is any scope for improvement. However, the opportunities are still there if we know where to look for them. The secret is simple: look at reactor inlets, not make-up streams. *Figure 2* and *Figure 3* illustrate this point. *Figure 2* is a diagram of a hydrogen consumer showing the make-up hydrogen and the high pressure and low pressure purges. Looking at it in this way, it is very easy to be misled into thinking that the unit requires 10,000 sm<sup>3</sup>/hr of hydrogen at 99% purity. However, this is wrong. In order to find the real requirement, one needs to look at the internal workings of the consumer as shown in *Figure 3*.



*Figure 2.* A black-box view can mislead us to think the consumer needs 99% pure hydrogen

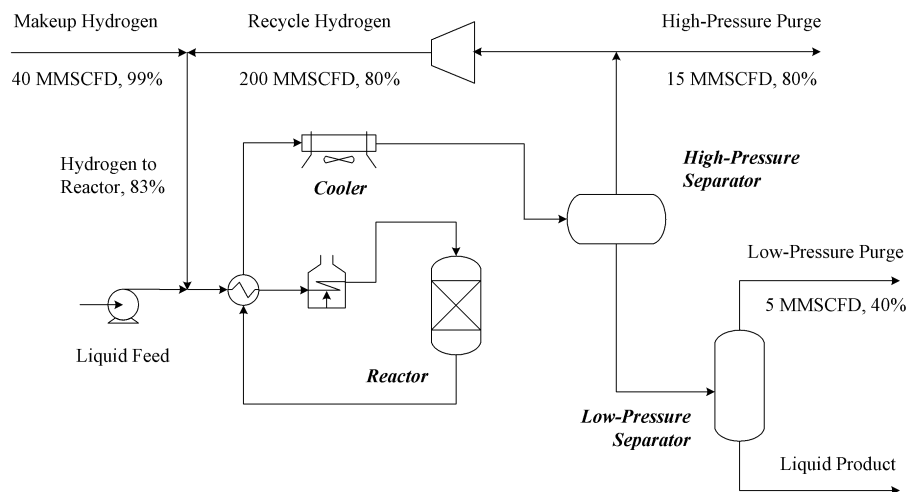


Figure 3. The true reactor inlet purity requirement is only 83%

As can be seen, the hydrogen make-up stream is mixed with hydrogen recycle before being fed to the reactor inlet. Therefore, the purity that the reactor actually sees is only 83%. Recognising this immediately opens up the scope for re-using other gases in the make-up stream and using less of the 99% hydrogen. As long as the flow rate and purity of the hydrogen going into the reactor do not change, the make-up purity is not that important. Put another way, the consumer may “want” 99% purity in the make-up, but it really needs 83% purity at the reactor inlet.

A simple example is shown in *Figure 4* and *Figure 5*. Two consumers are both taking make-up hydrogen from an external supplier at 99% purity, with a total demand of 20,000  $\text{sm}^3/\text{hour}$ . If we make the mistake of saying that the make-up purity must be fixed, there is clearly no scope at all for re-using hydrogen (*Figure 4*).

However, if we do the correct thing and focus on the reactor inlet, *Figure 5* shows that it is possible to re-use the purge from Consumer A as part of the purge from Consumer B. This allows the demand from the external supplier to be reduced by 1710  $\text{sm}^3/\text{hr}$  or 8.7%. With typical hydrogen costs, this could be worth between half a million and a million U.S. dollars per year. The flow rates being compressed by B’s make-up and recycle compressors are lower, giving power-cost savings too. Pretty good value for the cost of a pipe! Notice that Consumer B still has exactly the same flow rate and hydrogen purity at the reactor inlet as before. All that has changed are the make-up and recycle flow rates ... and of course our way of thinking!

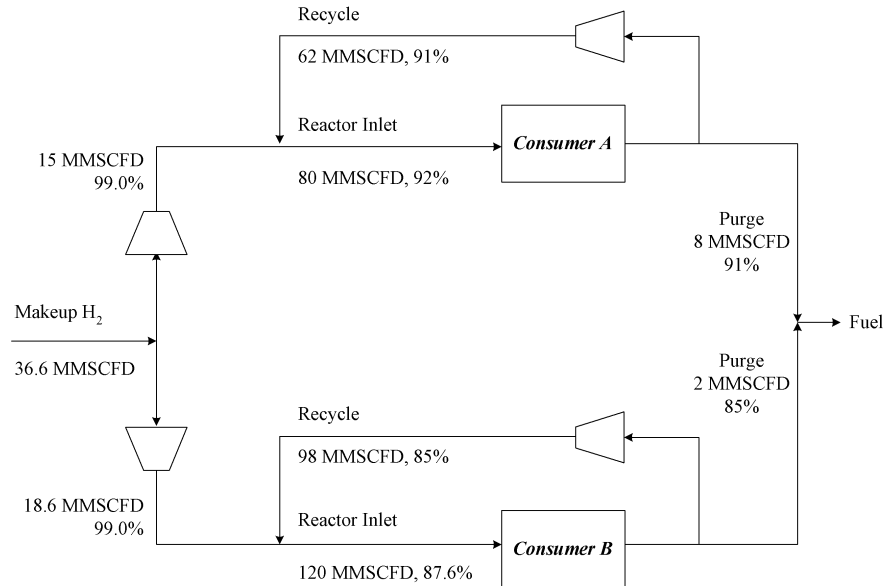


Figure 4. If the makeup purities are fixed, there is no way to reduce the makeup flow rate

Right about now you may be thinking that's all fine and well when there are only two consumers, but real refineries have a lot more than that. Should we use hydrocracker off-gas to feed the diesel hydrotreater, or should we send it to the naphtha hydrotreater? Maybe we should use cat reformer hydrogen instead of imported hydrogen, but should we use it directly or blend it with hydrogen from elsewhere? Maybe that hydrocracker off-gas should be used as fuel instead? Or maybe we could purify it in a PSA. Or why not a membrane? Since we're thinking of PSAs and membranes, maybe we should purify the naphtha hydrotreater off-gas as well? Where should we send the purified product?

At this point, many people might just throw up their hands and forget about the whole thing. What we have right now works, so why mess with it? And if we run out of hydrogen in the future we'll just buy more from a third party and be done with it. But, would you take this attitude with money? Would you be content to let someone steal or gamble away your cash each month while you keep borrowing from the bank in order to replace it? Probably not. So why do it with other assets?

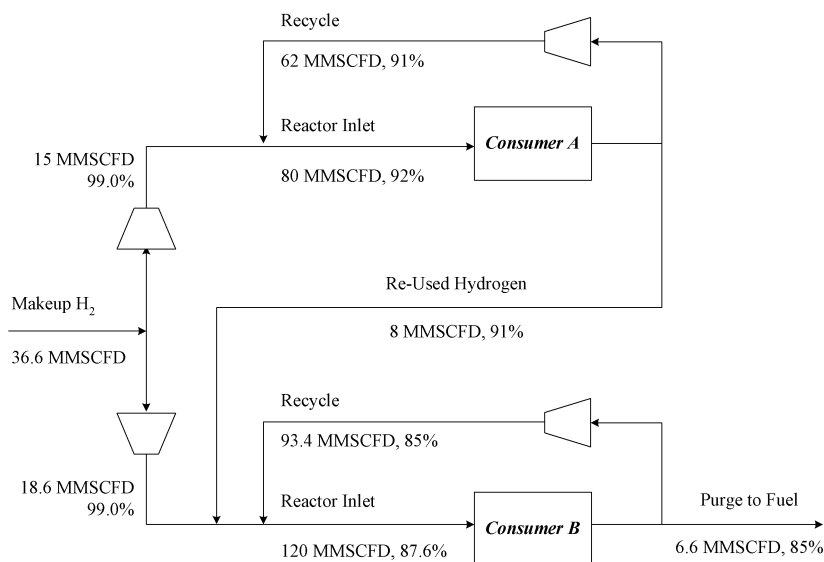


Figure 5. Focusing on reactor purity reduces required H<sub>2</sub> by 8.7%

Wouldn't it be neat if you had a quick and systematic way of cutting out all the fuss and knowing immediately what the maximum hydrogen recovery achievable is? Imagine being able to say to your boss that you know how to recover 15% of the refinery's hydrogen through re-piping, *before* spending any time analyzing all the options? Or perhaps you'll be able to tell him or her that only 1 or 2% can be recovered, so there is no point wasting time looking for a better configuration.

Hydrogen pinch analysis lets you do just that. The method is similar to the well-known energy pinch analysis used for designing heat exchanger networks.<sup>3</sup> Instead of looking at enthalpy and temperature, though, we concern ourselves with gas flow rate and hydrogen purity. The method in its original form aims at maximising the in-plant re-use and recycling of hydrogen to minimise "on-purpose" or "utility" hydrogen production.<sup>4</sup> Later in this article we will discuss whether this is, in fact, the correct thing to do in all cases.

The first step in the Pinch analysis is to plot hydrogen composite curves (Figure 6). These are plots of hydrogen purity versus flow rate for all the sources and all the demands for hydrogen in the refinery. Sources are streams containing hydrogen that potentially could be used. They include catalytic reformer hydrogen, "on-purpose" hydrogen as well as the overhead gases from high and low pressure separators in the various consuming units. When

plotting hydrogen demands, remember the lesson on needs versus wants. Don't base your calculations on make-up purities!

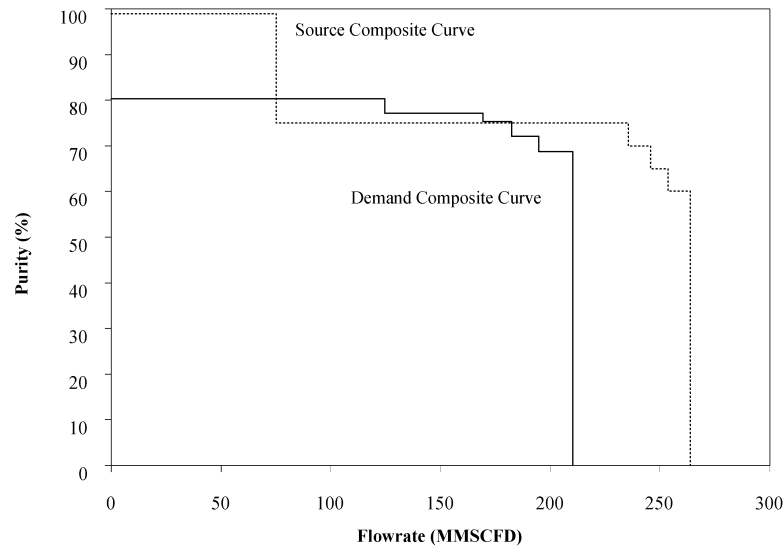


Figure 6. Composite curve showing hydrogen flow and purity

By plotting hydrogen purity versus the area enclosed between the source and sink composites, a hydrogen surplus diagram is constructed (Figure 7). This diagram is analogous to the grand composite curve in heat exchanger network synthesis and shows the excess surplus hydrogen available at each purity level. If the hydrogen surplus is positive throughout the diagram (as is the case in Figure 7), there is some slack in the system.

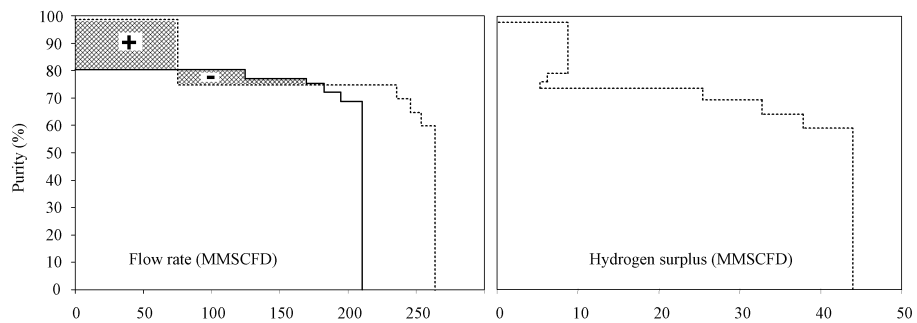


Figure 7. Hydrogen surplus diagram



The hydrogen generation flow rate can be reduced until the surplus is zero (Figure 8). The purity at which this occurs is termed the “hydrogen pinch,” and it is the theoretical limit on how much hydrogen can be recovered from the sources into the sinks. It is analogous to the heat recovery pinch.<sup>3</sup> The “on-purpose” hydrogen flow rate that produces a pinch is the minimum target and is determined *before* any network design analysis. With the appropriate software, a task that would have taken days, weeks or months can be accomplished in hours. If the gap between the target and the current use is large, it is worthwhile spending time reconfiguring the hydrogen network. The key is to avoid cross-pinch hydrogen transfer and to be especially careful about the above-pinch purity, as this is the region that is most tightly constrained. Hydrogen streams with purities greater than the pinch purity should not be used to feed consumers that can use hydrogen below the pinch purity. Also, hydrogen streams above the pinch purity should not be sent to the fuel system or flared. If the gap is not large, your time would be better spent looking at other improvement options, such as purification.

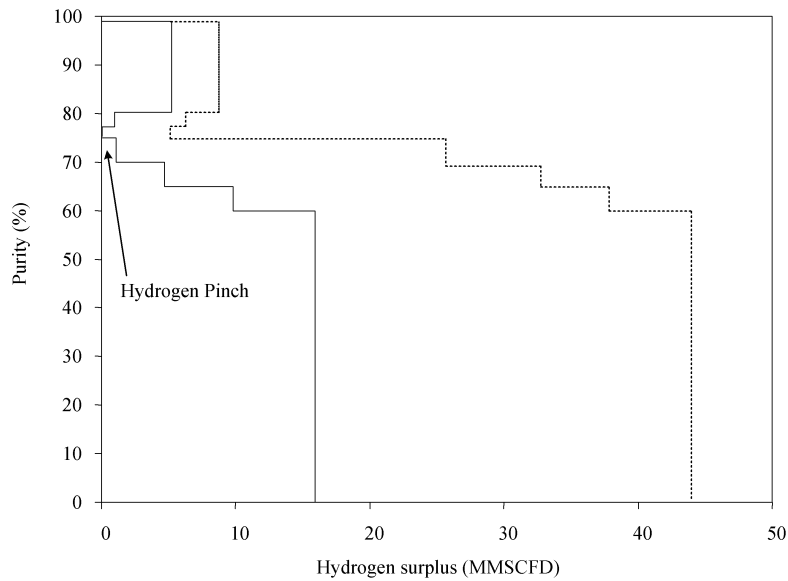


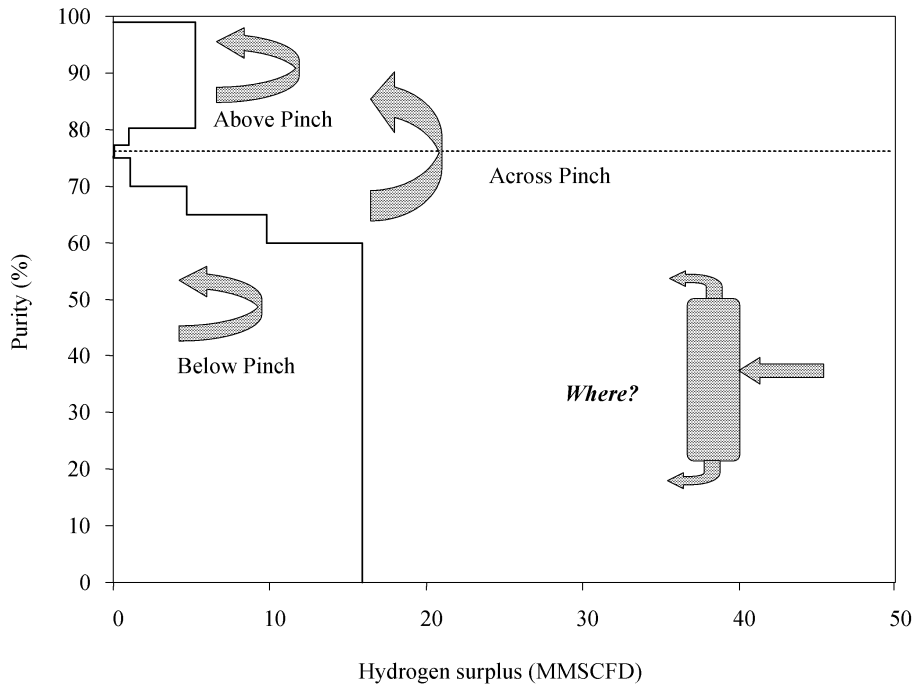
Figure 8. Hydrogen surplus diagram showing pinch point

There are three main options for purification. In case you are wondering, these are *not* PSAs, membranes and cryogenic systems. Those processes all do fundamentally the same thing, which is to split a feed stream into a product stream with a high purity and residue stream with a low hydrogen purity. The options we are talking about relate to the placement of the purifier relative to

the pinch. As *Figure 9* shows, there are three possible placements: above the pinch, below the pinch and across the pinch.

Placing the purifier below the pinch is not a wise idea. This simply takes hydrogen from a region where it is in excess and purifies it before sending it back to the same region. In essence, you would be buying an expensive unit to purify hydrogen for burning!

The best option is to place the purifier across the pinch. This moves hydrogen from a region of excess to a region that is tightly constrained on hydrogen. It frees up hydrogen from “on-purpose” sources, and any hydrogen lost to residue would have ended up in the fuel system anyway.



*Figure 9.* Three ways of placing a purification unit relative to the pinch

## 5. BEYOND PINCH

The pinch analysis approach discussed above is good for getting an immediate overview of the system, setting targets, and even doing some initial screening of ideas. However, in our project work, we have found a number of limitations.

Firstly, it does not fully cope with all the complexities of network design. The two-dimensional representation only considers flow rate and purity, but

does not incorporate other important practical constraints such as pressure, layout, safety, piping, operability and of course capital cost.

One of the more important constraints is stream pressure. The targeting method assumes that any stream containing hydrogen can be sent to any consumer, regardless of the stream pressure. In reality, this is only true if the stream has a sufficiently high pressure. Thus, Pinch analysis targets usually are too optimistic. They can encourage refiners to waste time developing projects that are infeasible or far too expensive due to the need to install compressors. Compressors are among the most expensive capital items in any chemical or refining process. Therefore, a sound retrofit design should make best use of existing compression equipment. Often, the economic feasibility of a hydrogen recovery project is determined by bottlenecks in existing compressors and not by purity and flow rate constraints alone.

Obviously, direct re-use of hydrogen between consumers is only possible if the pressure is sufficient. However, it is certainly possible to re-use a low-pressure hydrogen stream indirectly, i.e. by routing it through an existing compressor, if certain conditions are met. Firstly, there has to be sufficient capacity in a compressor to accommodate the stream; re-using hydrogen will change the make-up and recycle flow rates throughout the system, so capacity might be available in one or more other compressors. Also, the pressure of the re-used stream must satisfy the inlet-pressure requirements of the target compressor. In addition, the discharge pressure of the compressor should be high enough for use in the target consumer.

To account for pressure and other important constraints, a mathematical programming or optimization approach is required. Work on this was started at the University of Manchester Institute of Science and Technology (UMIST), and AspenTech has taken the lead in further development.<sup>5</sup>

## 5.1 Multi-Component Methodology

At this point we should be able to begin process engineering of the proposed re-use project. However, if we were to do so we would find that the simulated benefits are very much lower than those predicted by the optimiser. This is due to another major limitation of the hydrogen pinch approach, its assumption of a binary mixture.

Consider two hydrogen streams, each of 85 mol% purity. The first is ethylene plant export, containing almost 15% methane. The second is catalytic reformer export, containing roughly equal amounts of methane, ethane and propane, plus small amounts of heavier material. Hydrogen pinch techniques cannot differentiate between these streams, and would identify no penalty or benefit from switching between them as a source of make-up gas. Yet in reality the ethylene plant gas would require operation with a much

higher purge rate, due to tendency of methane to build-up in recycle loops. In fact, in certain circumstances it is more efficient to substitute a make-up supply with a lower purity hydrogen source (but lower methane content), while the hydrogen pinch methodology would lead you to do the opposite.

To meet this challenge, we developed a multiple-component optimization methodology that fully accounts for the behaviour of individual components within the process reactors, separators and the recycle gas loop. While in the binary pinch approach the composition and flows of reactor feed and separator gas are fixed, our multiple-component approach allows these compositions to float, so long as constraints such as minimum hydrogen partial pressure and minimum gas-to-oil ratio are met. Simulation models for reactors, high-pressure and low-pressure separators are used to correctly model overall process behaviour. We also developed a network simulation tool based on AspenTech's Aspen Custom Modeler™ (ACM) software.

By extending our analysis to include components other than hydrogen, we can simultaneously optimise downstream amine scrubbers, LPG recovery systems and the entire fuel gas system. Our project experience shows that the benefits from increased LPG recovery can outweigh the value of hydrogen savings.

## 5.2 Hydrogen Network Optimization

While preparing the optimization software, we first set up a superstructure that connects every sink with every source, provided that the source pressure is greater than or equal to the sink pressure. Compressors are included as both sources and sinks. We formulate basic constraints such as balances on total flow rate and hydrogen flow rate, as well as any compressor limitations such as maximum power or maximum throughput. A whole host of other constraints can also be incorporated, such as limited space, no new compressors allowed, and the old favorite: "I don't want to spend any capital!"

Next, we subjected the superstructure to mathematical programming that eliminates undesirable features while satisfying an objective function, which could be minimum hydrogen generation. There is actually no need to limit ourselves to minimising hydrogen generation. For example, we could choose to minimise operating cost or total annual cost. All relevant costs can be considered, including hydrogen cost, compressor power cost, fuel gas credit and capital cost of new equipment. We will not bore you with all the details, as these can be found elsewhere.<sup>5</sup> Suffice it to say that the optimization tool uses a combination of linear and non-linear programming.

The ability to add constraints at will means that all practical considerations can be built in. The cost of adding a constraint can also be determined. For

example, an engineer may say he or she doesn't like the idea of running a long pipe across a road to connect two units. This option can be banned and the optimization carried out again. The difference in cost between the two solutions indicates how much his or her "not liking" the connection will cost. If it costs a million dollars per year, the engineer may decide that he or she doesn't actually mind it *that* much after all!

The other major limitation of pinch analysis is that it gives fundamental guidelines about purification placement, but does not always help with selecting which streams to purify or whether to use a PSA, membrane, cryogenic or other purification process. This is where know-how becomes vital. Purifier experts can rapidly assess different technologies for candidate feed streams, simulate their performance and give quick cost estimates. These experts can weigh the benefits of different options, recognising that each application will be unique. For example, in a recent European study, a refinery was facing a large increase in hydrogen demand to meet upcoming sulfur-in-fuel specifications. In this case, hydrogen recovery was more important than product purity, so Air Liquide experts determined that, for a certain stream, a membrane would be a better choice than a PSA unit.

Another issue with purifiers is that different technologies have very different pressure requirements. A PSA unit gives a product pressure very close to the feed pressure, but the PSA residue pressure is extremely low. On the other hand, a membrane requires a large pressure drop in order to perform properly, the product pressure is much lower than the feed pressure, and the residue pressure is almost the same as the feed pressure. These issues need to be considered in the specific context of the refinery and can be handled easily using the approach described above. Ultimately, economics should determine the optimum trade-off between product purity, product pressure and hydrogen recovery.

Purification expertise also saves time. Hydrogen network analysis experts work in parallel with purification experts to rapidly assess options and develop a project flow sheet. This is much more time-effective than having one company generate a small number of options using Pinch analysis and then sending the options to another company for cost quotes. With the parallel approach, more options are evaluated in less time, and both the network analysis engineers and the purification engineers see the entire picture.

The following case study is representative of a real refinery system, but certain data have been disguised to maintain customer confidentiality. The existing hydrogen system is shown in Figure 10. The objective of the study was to retrofit the network to minimise operating costs. Process and cost data are given elsewhere.<sup>56</sup>

Several constraints were imposed by the refinery:

1. The existing compressors have 5% spare capacity.

2. There is only space on the site for one new compressor and one new purification unit.
3. A payback of more than 2 years will not be acceptable

The network retrofit was designed by setting the objective function to be minimum operating cost while constraining the payback time (capital cost divided by annual operating cost savings) to be two years or less. Figure 10 shows the resulting design. Dotted lines indicate new equipment.

In the recommended project, both a new compressor and a PSA are used and substantial re-piping is required. Notice that the new compressor accommodates the increased recycle requirement for the NHT as well as the need to compress one of the feeds to the PSA so that its product can be used in the hydrocracker.

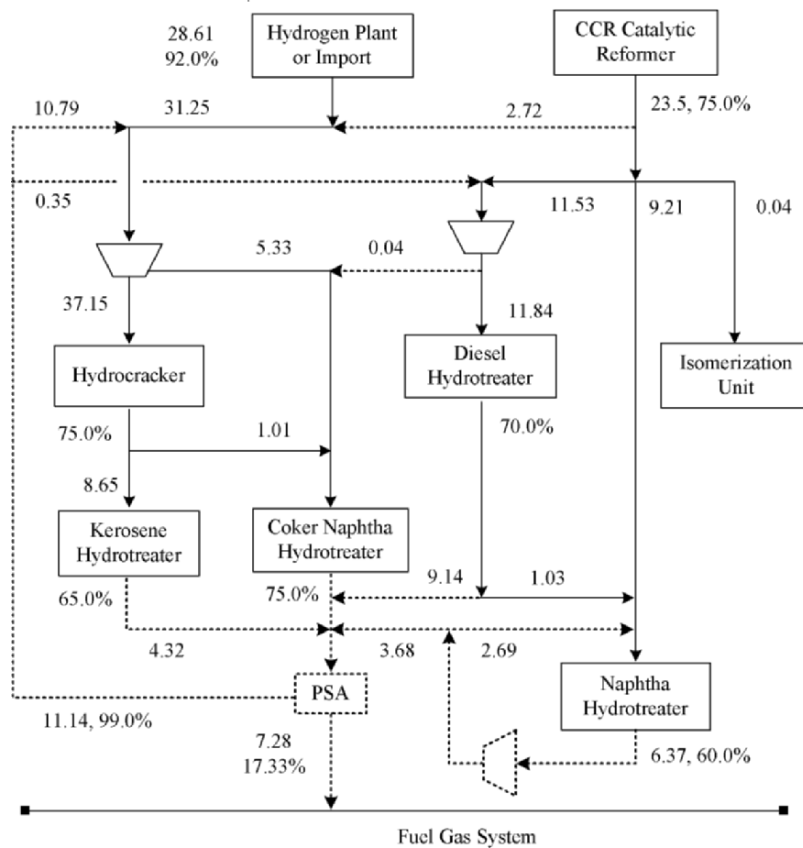


Figure 10. Retrofit for maximum savings with a payback time  $\leq$  two-years

The total capital investment of the retrofit is \$9.8 million and the operating-cost savings are \$6 million per year. The payback period is therefore 1.6 years, which is better than required.

Now, refineries often have limited capital budgets, so even modification with a good payback might be too expensive. It would be valuable to know the maximum savings achievable with a fixed capital budget, say US\$5 million. Adding capital expenditure as an additional constraint and re-optimizing gives the solution shown in Figure 11. The best investment is a PSA unit requiring no new compressor. Notice too that fewer new pipes are installed. The operating cost savings are smaller (only \$3.5 million per year) but this is to be expected.

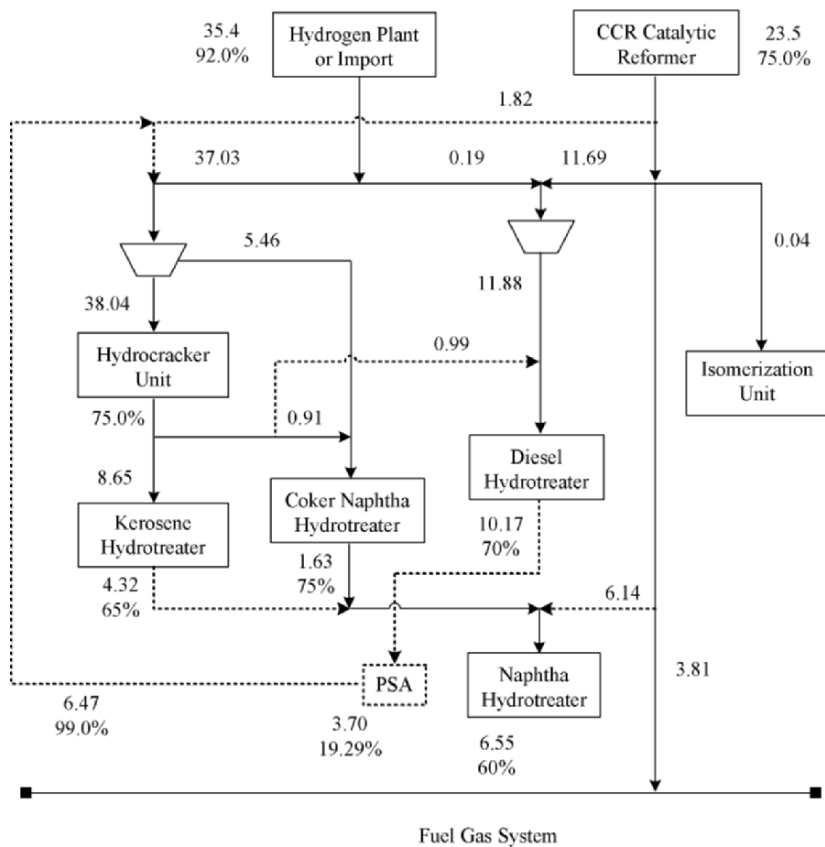


Figure 11. If capital expenditure is limited to US\$5 million, the design changes

## 6. YOU DON'T GET RICH BY SAVING

Up to now, this article has addressed the issue of minimising hydrogen supply, in other words, saving hydrogen. This is certainly a very real problem for refiners, and many of our clients have specified this as their objective. After all, hydrogen is expensive, and a few percent saved can mean millions of dollars per year. However, this is often not the most profitable course of action.

As *Rich Dad, Poor Dad* puts it, nobody has ever become rich by saving money. How many people have become millionaires by opening a savings account? If you put your money in the bank, all you can expect is a modest increase from the interest it earns. When you account for time and inflation, money in the bank actually loses its value gradually. According to Robert Kiyosaki, the rich have their money work for them by investing it in assets that generate passive income. Such investments include real estate, which generates rental income, capital gains, and businesses that generate revenue and dividends.

If you agree that hydrogen is money, let's go a step further and look at hydrogen consumers as investments. Instead of merely *saving* hydrogen, why not consider re-investing it where it will *make* money for you?

How do we re-invest hydrogen? By feeding more and/or purer hydrogen into the appropriate reactors. For example, the hydrogen freed up using the network design methods can be used to process cheaper feed stocks. It could also be used to boost partial pressures to enhance conversion, throughput, yields and catalyst life.

The important question is how do we know which units will be the most profitable ones to invest hydrogen in? When analyzing money investments, there are certain techniques that wise investors use. These include performing a due diligence and analyzing the financial statements and cash flows of the investment. A good return on investment is the goal. Nobody wants an investment that loses money, and likewise a refiner should use hydrogen where it will provide a better return than simply saving it would give. We have our own techniques for analyzing hydrogen investments. They are reactor modelling and refinery LP modelling.

Rigorous kinetic modelling is used to obtain a good understanding of process operation under different feed hydrogen conditions. AspenTech has developed rigorous tools for modelling fixed-bed hydroprocessing units, such as hydrocrackers, reformers, FCC pretreaters, and desulfurization units. They model kinetics for denitrogenation, desulfurization, saturation, and cracking, and are capable of accurately predicting yields, hydrogen consumption and product properties for widely different feeds and operating conditions. These reactor models can easily be connected to rigorous fractionation models,



creating a fully integrated model of the entire hydrotreater, reformer or hydrocracker complex.

The reactor models include a unique catalyst deactivation tool, which allows refiners to minimize catalyst life giveaway and to calculate future conversions, yields, and product properties. Hydrocracking models can be used to optimize tradeoffs between feed rate, conversion, catalyst cycle life, feedstock severity, operating conditions and costs. For recycle hydrocracking units, there are tradeoffs between fresh feed rate and conversion-per-pass in single-stage units, or between 1<sup>st</sup> stage and 2<sup>nd</sup> stage conversion in two-stage units.

It is not necessary to model every reactor and determine the benefits in a trial and error way. A combination of the LP model, understanding of current process operations and constraints, and hydrogen network analysis can be used to develop a short list of key processes and potential changes to those processes. For example, the LP model will show the bottlenecks to increasing refinery profit. If increasing hydrogen partial pressure can eliminate one of these bottlenecks, then this unit will be a candidate for applying rigorous reactor modelling and subsequent process analysis. Hydrogen network analysis can also give insights into process operations. Above a threshold hydrogen purity, hydrotreater operation is insensitive to hydrogen purity. If reducing the hydrogen partial pressure to a hydrotreating reactor gives a large saving in the overall refinery hydrogen target, this unit can be also be selected for rigorous modelling to determine the true impact on reactor operation.

All process changes need to be modelled, the impact on the hydrogen network evaluated, and the final benefit established through the LP model. The reactor models can be linked to Aspen PIMS, a leading PC-based LP software package used by the petroleum and petrochemical industries. By providing automatic updates to Aspen PIMS vectors, the models can enhance detailed operations planning, economic evaluation and scheduling activities. In particular, they can help a refiner decide how best to apportion intermediate heavy distillate streams between different conversion units.

As an illustration, *Figure 12* shows case-study results from a rigorous model for a two-reactor hydrocracker with partial recycle of unconverted oil.<sup>7</sup> The unit runs at about 60% conversion-per-pass. A fixed flow of unconverted bottoms is recycled. The remainder is exported to the FCC unit or heavy diesel blending. At present, the “export” comprises about half of the total unconverted oil.

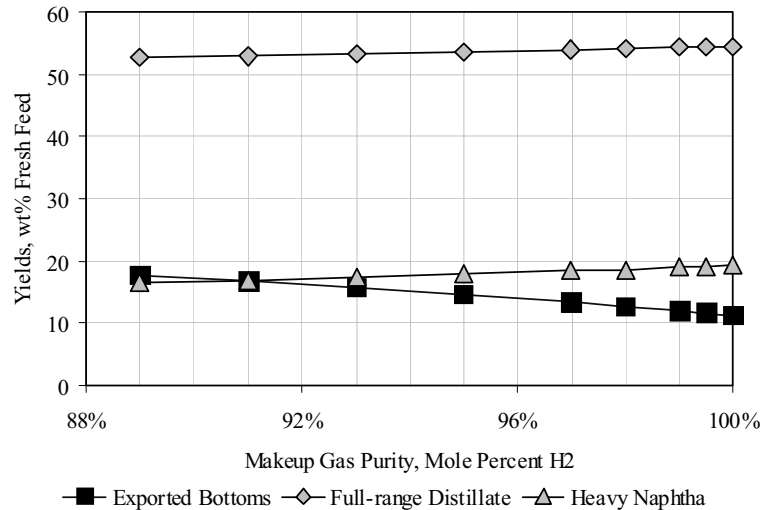


Figure 12. Hydrocracker performance improves with increased hydrogen purity

For the case study, the purity of the make-up hydrogen was varied from the current value (89%) to 100%. The feed rate, recycle oil flow rate, and weighted average reactor temperature (WART) for both reactors was held constant. Under these conditions, the following effects were noted:

1. Full-range distillate yield increases from 52.8% to 54.6%
2. Heavy naphtha yield increases from 16.6% to 19.4%
3. Exported bottoms decreases from 17.8% to 11.3%.

According to the model, the net benefits of increasing the makeup-gas purity from 89% to 100% were on the order of \$2 million per year. But how much would it cost to make available the extra hydrogen needed? Using a simple marginal cost of hydrogen is not the way to answer this.

Figure 13 shows how our network design and analysis tools can fit into an overall profit optimization study. They identify quickly how much additional hydrogen can be made available for certain levels of cost. Typically, a few percent more hydrogen can be squeezed out with simple modifications requiring low or no cost, for example piping modifications. Then there will be a step-change where getting any more hydrogen will require a purification system. Finally, there will be another step-change where purification reaches its limit and any more hydrogen will have to be supplied from external sources, such as imports or a hydrogen plant. Knowing the true cost of providing additional hydrogen makes it easy to weigh it against the benefits that are suggested by process modeling and LP optimization.

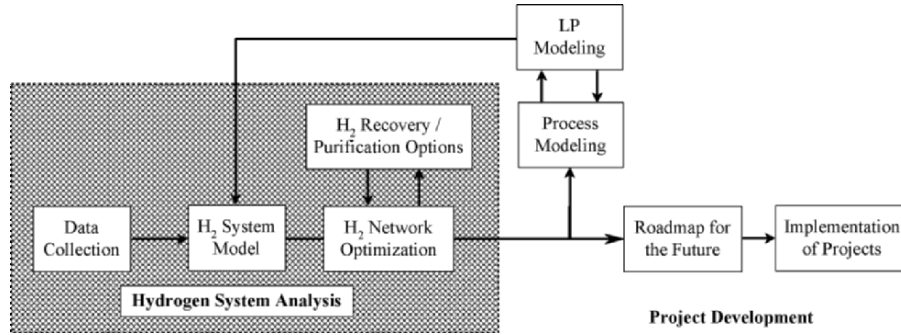


Figure 13. Network design tools compare costs and benefits for project options

Figure 14 shows a typical road-map that can be drawn up, showing where the refinery is now and where it wants to be at different points in the future (e.g. one year, five years, ten years). All of the tools described in this article give the refiner an easier job of planning how to tackle the future. They are used to systematically choose the best set of projects that achieve immediate objectives but also fit in with long-term goals. This avoids the “Regret Capital” syndrome.

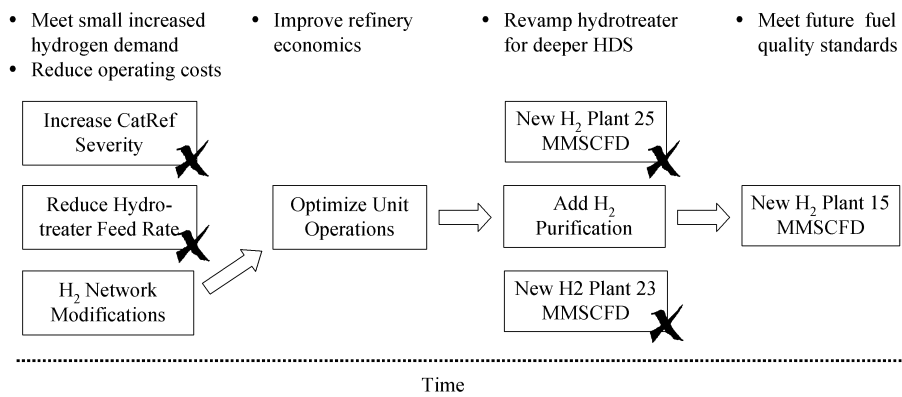


Figure 14. Systematic tools are used to construct a roadmap for the future

## 7. CONCLUSIONS

In conclusion, several hidden opportunities typically are not addressed by refiners when developing plans for Clean Fuels. In our experience:

Time spent in investigating the current balance pays back. This can identify substantial operating savings, and it eliminates “unconscious over-design” in future investments.

Make the best use of hydrogen purity. There is scope to reduce both capital investment and future operating costs by maximizing the benefits from high-purity hydrogen sources. Reactor modelling is an important part of evaluating these benefits and optimizing hydrogen use.

Hydrogen is not the only consideration. A proper methodology for optimization must extend beyond the hydrogen system to include low pressure purges, amine treating, LPG recovery and the fuel gas system. Purification upstream of LPG recovery units can debottleneck those units and increase their overall recovery efficiency, adding significantly to the value of the hydrogen-recovery project. Reducing hydrogen loss to fuel can have both positive implications (improved calorific value) and negative implications (increased fuel oil firing and hence increased SO<sub>x</sub> emissions).

New model-based network optimisation methodologies allow the identification of no- and low-CAPEX projects to improve current operations, particularly for refineries of Types 2 and 3. These savings are often in excess of €1 million/year, with payback times measured in months.

If there is one conclusion you should take away with you, it should be that hydrogen is money. Stop thinking about it as merely an unglamorous utility and start looking at ways to make more money from it. And who knows? By applying these ideas to your personal finances you well may end up becoming a rich dad (or mum) too. We are still working on it!

## 8. REFERENCES

1. Kiyosaki, R.T. and Lechter, S. L. *Rich Dad, Poor Dad*, Warner Books: New York (2000)
2. Cassidy, R.T.; Petela, E. “Life Cycle Utilities Management,” NPRA Annual Meeting, Paper No. AM-01-63 (2001)
3. Linnhoff, B. “Use Pinch Analysis to Knock Down Capital Costs and Emissions,” *Chem. Eng. Progress*, 90 (8), pp. 33-57 (August 1994)
4. Alves, J. “Analysis and Design of Refinery Hydrogen Distribution Systems,” PhD Thesis, University of Manchester Institute of Science and Technology (1999)
5. Hallale, N.; Liu, F. “Refinery Hydrogen Management for Clean Fuels Production,” *Advances in Environmental Research*, 6, 81-98 (2001)
6. Robinson, P.R.; Thiessen, J.M.; Hanratty, P.J.; Mudt, D.R.; Pedersen, C.C. “Plan For Clean Fuel Specifications With Rigorous Models,” NPRA Computer Conference, Paper No. CC-00-143 (2000)

## Chapter 27

# IMPROVING REFINERY PLANNING THROUGH BETTER CRUDE QUALITY CONTROL

J. L. Peña-Díez  
*Technology Centre*  
*Repsol-YPF*  
*P.O. Box 300*  
*28930 Móstoles - Madrid (Spain)*

### 1. INTRODUCTION

Near-term refining trends are demanding continuous improvements to current practices to ensure the profitability to survive in highly competitive global markets. To the common complexity of refinery processes, and the effect of crude oil market volatility and low and cyclic business margins, increasing environmental regulations have made companies face to the need to continuously operate assets at or near the economic optimum.

Refining companies are successfully implementing supply chain integrated solutions to solve these problems and improve refinery operation and profitability. However, these applications depend on the availability of accurate and live data. Some points of the supply chain—in particular planning and operation areas—are greatly influenced by the availability of reliable and updated crude oil libraries reflecting the information of the crude oil and the products that will be obtained in the different processes.

Although the consistency of estimating crude oil relative values with gravity and sulfur-based valuations is still defended<sup>1</sup>, there has been a clear tendency in the oil industry towards product-based valuations, considering the value of the products than can be obtained from a crude oil in a particular refinery. The relative value for the same crude oil may differ from one refinery to another, and LP models are commonly used to maximize crude oil value optimizing the product distribution.<sup>2</sup>

LP crude oil valuation is specific to a refinery and its facilities, markets and constraints.<sup>3</sup> The combination of LP methodologies and refinery simulation models provides the required process and economic data to adequately evaluate crude oil feedstocks. Consistency between the quality of received crude oils and the assay data used with planning LP models is critical to guarantee the success in the optimization process. If crude oil quality suffers significant variations, a continuous assay update is required to take advantage of the benefits offered by supply-chain technologies.

This chapter will briefly review some of the new techniques proposed for crude oil quality control, and an alternative new approach will be presented.

## 2. CRUDE OIL QUALITY CONTROL

Crude oil quality changes with time, although the effect of these variations in planning uncertainties may be significantly different. To illustrate the effect of these quality changes, Figure 1 shows the historical API variation of several representative crude oils.

- The first group of crude oils (A1 and A2) shows a relatively constant quality with time, that makes them desirable from the planning point of view.
- The most common situation is shown in crude oils B1 and B2, with a clear trend in quality with time. This trend will force a periodical update of the assay in the database.
- The third group (crude oils C1 and C2) exhibit significant variations in quality with time without any trend, making planning a very difficult task due to the uncertainty associated to the crude oil quality to be received in the next cargo.

Assays of the crude types B and C will need frequent revisions in the crude oil assay libraries, but the nature will be different. With crude oils from group B there is a continuous need to update the crude assay in the databank, which can be planned following two possible criteria: on a fixed delta time basis or on a delta quality basis, which is the usual procedure.

Crude oils from group C present a more serious problem. A considerable effort in updating crude assays can be made without any improvement, due to the random quality variations. It is very difficult to define the appropriate moment to update the assay, and most of the times different qualities are included in the crude oil library to represent different scenarios

The problem is that these quality variations affect both the planning and operation processes. If planning and operation tools are not updated to reflect the changes in crude oil quality in the form of LP delta vectors for each crude, the model may converge in a solution different from the optimal, and transfer

this uncertainty to the operation in the refinery. Increasing differences are expected to appear between planning and operation.

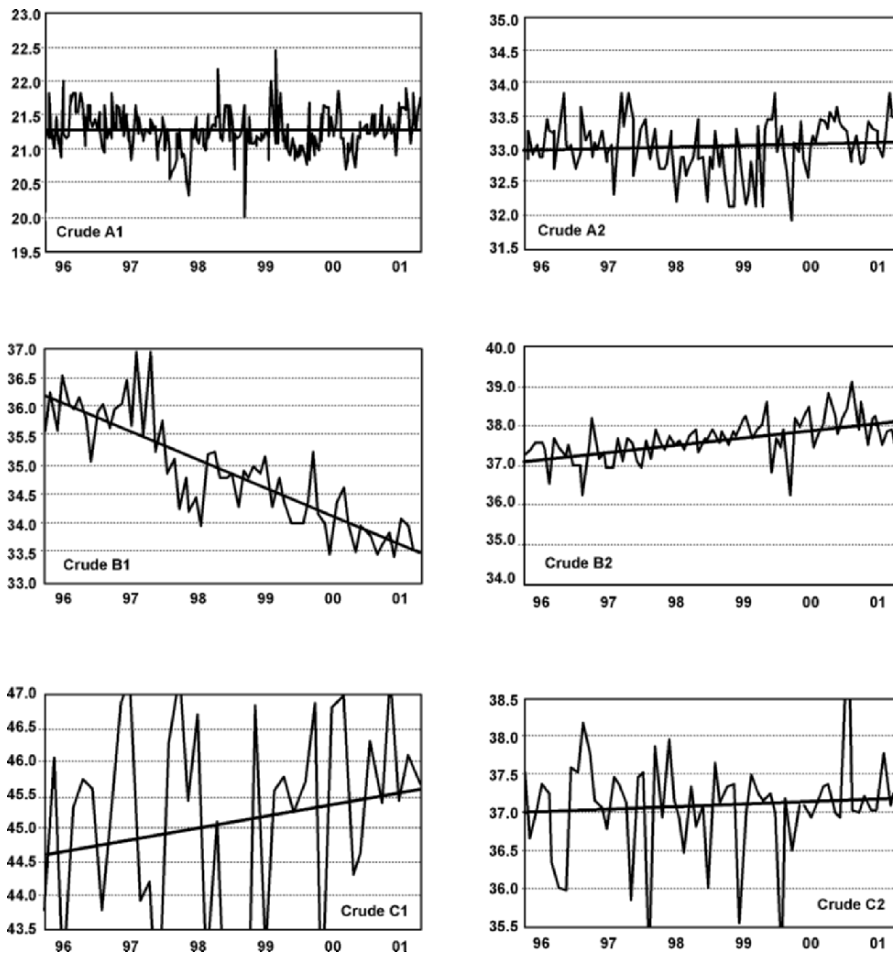


Figure 1. Conventional crude oil assay evaluation procedure

An increase in the quality of the received cargo does not assure a higher profitability, because LP models optimize crude mixtures according to the constraints defined, and perhaps the quality increase will be offset in operation to a specification that can not be reached with the planned yield/profit.

Some authors suggest an existing tradeoff between improving LP predictions with rigorous models and the cost associated to continuously update the crude assay libraries. A conventional crude oil assay evaluation is

long and costly, and alternative methods are needed to take full advantage of the possibilities offered by these supply-chain solutions.

### 3. NEW TECHNOLOGIES IN CRUDE OIL ASSAY EVALUATION

Crude oil evaluation methods have not significantly changed during the last decades. The crude oil is distilled in batch columns to determine the hydrocarbon boiling point distribution (ASTM D2892/5236), and the fractions obtained are analyzed to study the physical properties distribution through the crude oil. Although each company defines the required characterization for the cuts, Figure 2 shows the information commonly included in the assay. Some details of these conventional tests are described in Chapter 3.

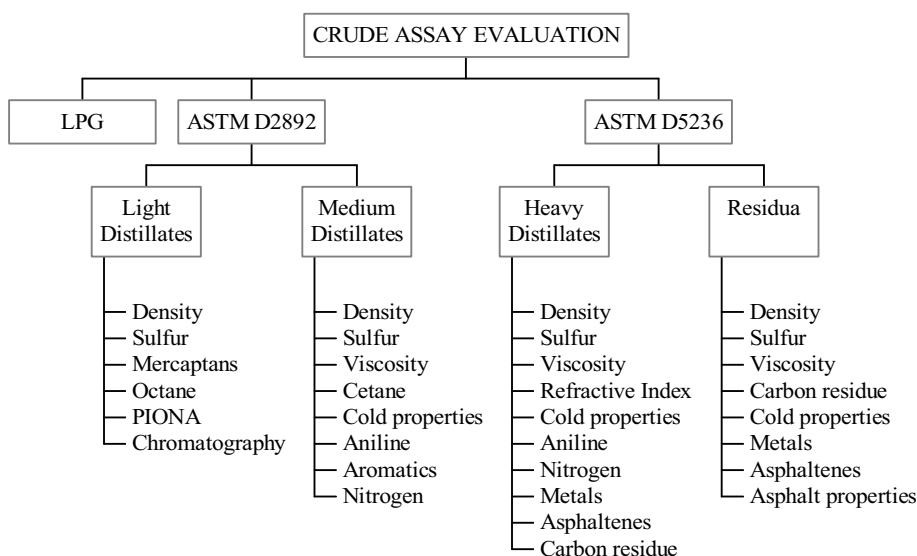


Figure 2. Conventional crude oil assay evaluation procedure

Once the laboratory work is finished, the preliminary assay obtained must be checked with computer assay synthesis models to assure consistency in the distribution of each property between the crude oil and the fractions.

The whole procedure is long and expensive (average 300 man-hours), and must be repeated each time a crude oil quality variation is suspected. Although there are no fixed rules about the recommended assay updating frequency (differences are illustrated in Figure 1), a maximum average assay age of 2-3 years has been proposed.<sup>5</sup> If the refinery has a limited crude basket



this assay updating process is not a problem, but in most cases this maintenance implies a significant investment for the company.

Several references have suggested the need for alternative crude oil evaluation methods. These alternative methods (both analytical and mathematical) should allow keeping the assay information updated under a reasonable cost.

### 3.1 Analytical Methods

The new analytical developments appeared during the last decade are mostly focused on a faster determination of the distillation curve (TBP). HTSD is widely accepted as one of the best alternatives.<sup>6-9</sup> Originally developed as an extension of conventional GC simulated distillation (ASTM D2887/D5307), it provides better information on the crude oil back ends. The technique is currently under study to become an ASTM standard, overcoming the problems related with reproducibility of front and heavy end information.

Infrared spectroscopy<sup>10,11</sup> and NMR<sup>12</sup> are other alternatives proposed, more focused in on-line feed characterization and advanced control projects.

The main disadvantage of the previous methods is that they do not generate fractions to be characterized, and the updated information on product yields may be too limited for LP purposes, although complementary methods have been developed.<sup>7</sup>

GC-MS techniques have also been extensively used as alternative methods for assay evaluation. The method can be applied to the whole crude<sup>13,14</sup> or with a previous SFC fractionation.<sup>15</sup> The possibility to predict product properties relies on the availability of reliable property-composition correlations. Although there are commercial applications<sup>16</sup>, the method is not standardized and problems have been reported on the accuracy of heavy fractions characterization and uncertainty in component identification and quantification due to mass overlapping.

Details of these alternative analytical methods for crude assay can be found in Chapter 3.

### 3.2 Chemometric Methods

Some recent references have demonstrated the power of statistical techniques applied to crude assay prediction.<sup>17,18</sup> The availability of large crude assay databases integrated with advanced statistical methods allows the prediction of updated crude oil assays or isolated physical properties.

Most of these technologies are based on neural networks models, and also provide an error estimate for the predictions, allowing the user to validate the

updated crude oil update and quantify its benefits over the existing one. Usually a previous assay of the crude oil is required to improve accuracy in the predicted assay.

### 3.3 Other Alternatives

The acquisition of a commercial crude oil assay library with periodical updates is a common alternative, which could help refiners solve the planning problem appearing with crude oils type B (Figure 1). However, this approach is not effective with crude oils type C), and the cost is a factor to be considered.

Recently proposed web-based assay sharing systems provide similar benefits, but without the confidence on the availability of the required crude at the required time.

## 4. CRUDE ASSAY PREDICTION TOOL (CAPT)

With the basis of the mentioned requirements and the shortage of commercially available tools, a new technology was developed with the objective to update/complete crude oil assays with limited experimental data using rigorous models. This new technology, registered under the name repCAPT (Repsol-YPF Crude Assay Prediction Tool) was intended to complement conventional evaluation procedures.<sup>19</sup>

The center of this technology is an expert system for crude assay generation. This expert system, which includes a set of mathematical algorithms based in powerful data-mining techniques and first-principle models, may generate a complete crude oil evaluation from variable levels of information available.

The methodology has been designed with flexible inputs, allowing different levels of information to be used in the predictions. It is possible to supply incomplete evaluations from different sources, with the purpose to fill the incomplete information in the crude oil assay according to the standard fractions and properties defined.

With this technique crude oil library quality control can be made at virtually no cost, selecting only specific crude oils to be evaluated in the laboratory and optimizing the information needed for LP planning.

### 4.1 Model Description

The generation of the assay takes places in two stages. The first one is the generation of preliminary TBP and physical properties distribution through

predefined fractions, while the second is the analysis of these properties with first principle models to assure consistency in the assay.

The first stage of the expert system relies on the underlying relationship among thermophysical properties in crude oils. Figure 3 shows the weak correlation between API gravity and sulfur content for crude oils (conventional valuation method, and therefore available for all the cargos), arising from the natural distribution of sulfur compounds in light and heavy crude oil fractions.

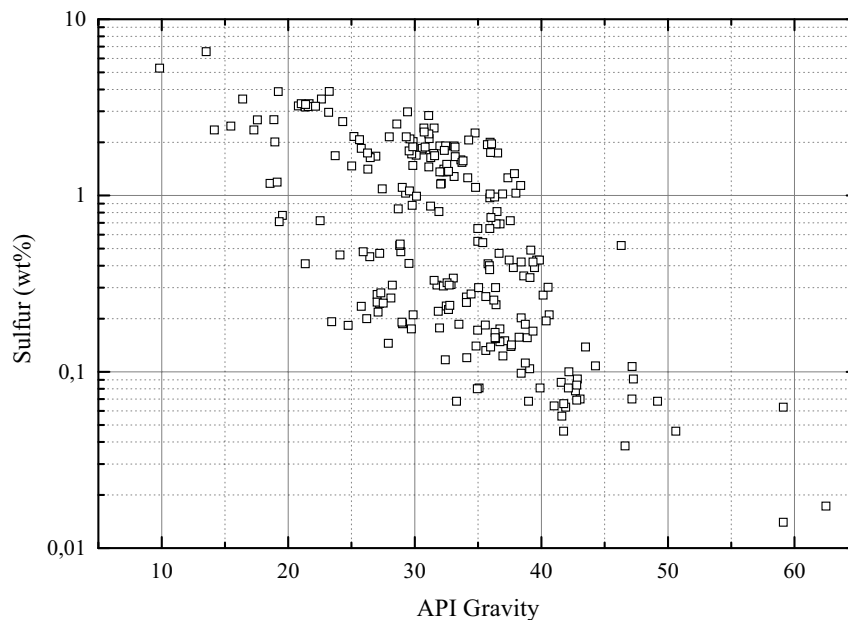


Figure 3. Correlation between crude oil API gravity and sulfur

However, with a third variable (kinematic viscosity at 40°C, Figure 4), the correlation among variables increases, indicating that they are not totally linearly independent. A further increase in this multivariate analysis also shows not only a significant degree of correlation between the bulk properties of a crude oil and the different fractions yields and properties, but even with any other underlying information. One illustrative example is included in Figure 5. A simple principal component analysis of a crude library using basic bulk properties (crude oil density, sulfur, viscosity and pour point) may identify additional information that was not explicit, in this case the geographical origin of the crude oil.

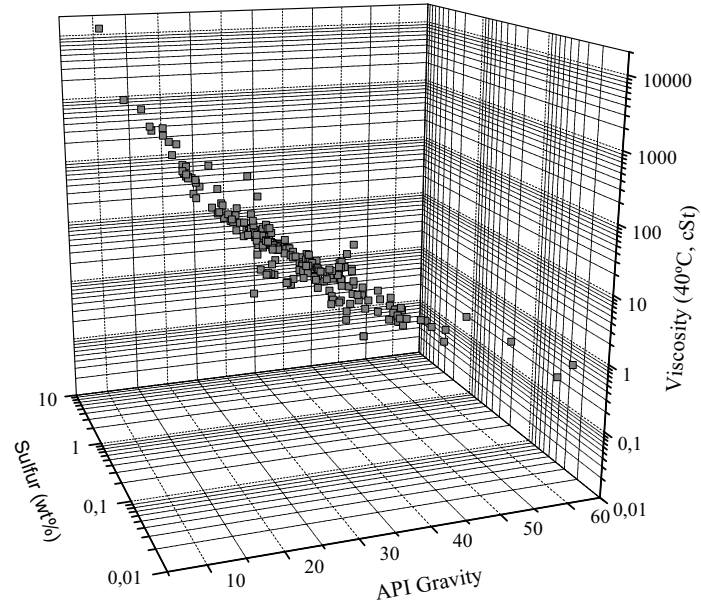


Figure 4. Correlation between crude oil API gravity, sulfur and kinematic viscosity

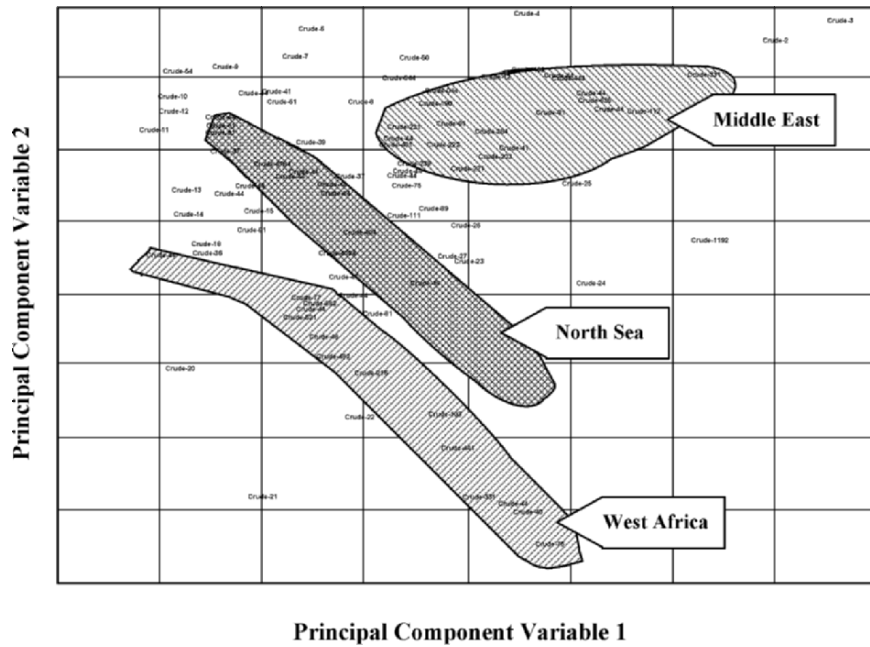


Figure 5. Principal Component Analysis of crude oils bulk properties

From the operational point of view, only a minimum set of crude oil bulk properties will be available to generate the updated assay. This is the less favorable case for the application of the model, and minimum required properties must be carefully selected.

According to the generalized correlations proposed by Riazi and Daubert<sup>20,21</sup>, based on two-parameter equations of state and the theory of intermolecular forces, a minimum of two physical properties are required to characterize non-polar petroleum fluids, one representing the molecular size and another one the molecular energy (or chemical structure). Although most of the published correlations are expressed in terms of boiling point and density, in the application to crude oils it is more appropriate to replace boiling point with kinematic viscosity as an input parameter, unless a reliable simplified distillation procedure is available. Crude oils and heavy petroleum fluids present some degree of polarity and a third bulk property is required to adequately represent the fluid (sulfur content, pour point, etc.).

Although crude oil density, sulfur and viscosity are the minimum typical bulk properties required by the model, sometimes optional laboratory analysis may be required to improve the accuracy of the predictions. The methodology is independent of the available information for the crude oil, and partial crude oil assays can be used. The output information is always a complete updated assay.

One of the expert system requirements is the availability of a homogeneous user-supplied reference crude assay library. The first versions of the technology included predefined correlations to generate preliminary properties. Due to the continuous incorporation of new and updated experimental information to the assay libraries, an on-line correlation development algorithm was implemented in later developments. This algorithm, based in crude assay data-mining through classification neural networks, selects the most appropriate information from the crude oil library to generate the best correlations suitable for the new crude oil. This new approach has greatly simplified the algorithm maintenance, and has allowed us to extend the original technology from crude oils to any intermediate product in the refinery.

The next stage is the validation of the updated assay with first principle models. Most of the petroleum fractions obtained from natural crude oils exhibit a thermodynamic behavior similar to hydrocarbon homologous series, and the consistency can be checked with asymptotic behavior correlations.<sup>22-23</sup> Figure 6 illustrates the ABP behavior for MeABP and liquid molar volume in several crude oils. Similar consistent correlations can be applied for most of the PVT and transport properties of the crude oil.

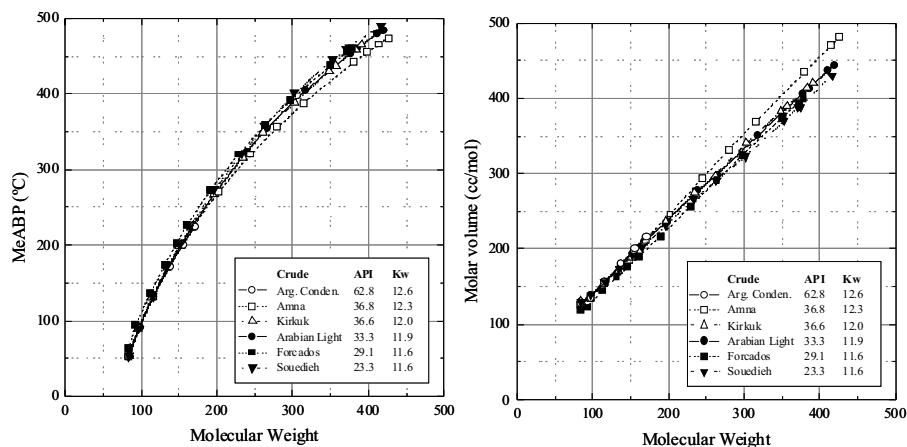


Figure 6. Asymptotic behavior correlations (ABC) for average boiling point and liquid molar volume of crude oil fractions

Property balances with bulk values are checked and consistency analysis of property values in the fractions is performed until the updated assay is validated. When the validation process is finished, the reliability of the updated assay, matching the quality of the received cargo, will be improved for LP optimization.

## 4.2 Potential Applications

The implementation of this technology may provide benefits in planning and operation areas compared with the conventional approach. Some of the benefits expected in the planning area include:

- Extended crude oil quality tracking system.
- Updated assays from existing crude oil libraries.
- Generation of preliminary full assays for new crude oils based on limited laboratory data. The availability of a previous assay is not required.
- Optimization of required laboratory assay updates.
- Conventional crude manager tools: historical crude oil library, crude oil analysis and comparison and mixtures, etc.

The availability of real tank characterization in the operation area allows a more accurate updated planning including final adjustments in crude blending.

Although the technology has been initially implemented in the refining area, additional applications could also be available in the upstream and trading areas.

The system is integrated with unified libraries, updated through the intranet, compiling all the crude oil assay information available. Instant access is provided to crude assay updates, and software interfaces assure integration with other supply chain tools available in planning and operation areas (Figure 7).

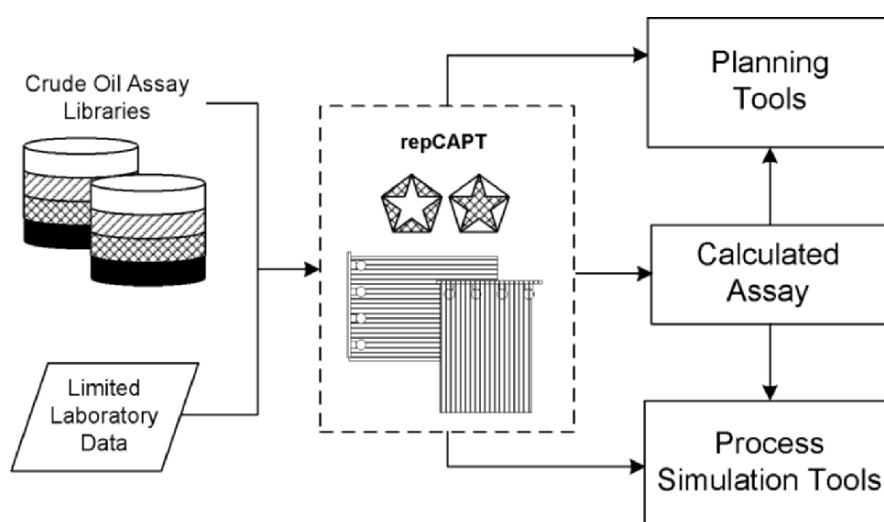


Figure 7. CAPT integration with planning and operation tools

### 4.3 Model Results

The following figures illustrate some representative results of the implementation of repCAPT technology. Figure 8 shows the satisfactory results obtained predicting pure crude oils. Two of the crude oils (i and iii) had not been previously analyzed, and there were no previous assays in the crude oil library. The other two (ii and iv) has a previous analysis in the library, and the updated predicted assays matched the quality of the new cargo better than the existing assays. Although all the predictions were considered satisfactory, the results present a slight higher accuracy when a previous assay was available.

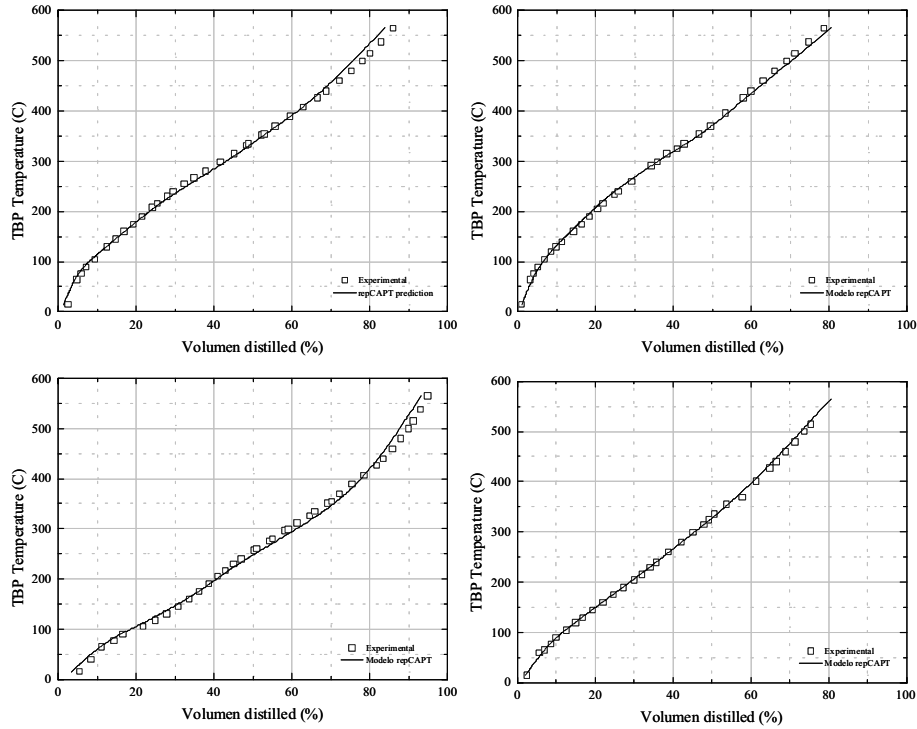


Figure 8. Comparison of predicted TBP for different crude oils

Similar results were also obtained when a real on-tank crude mixture was predicted.<sup>19</sup> The minimum laboratory analyses previously defined were used in all the predictions.

Physical properties are predicted with similar good accuracy, as shown in figure 6 for the crude oil fractions.

Figure 9 illustrates the deviations between experimental and predicted fraction properties. The differences in fraction yields (TBP) are well within the reproducibility of the method ASTM D2892. The rest of the properties of the fractions (specific gravity, sulfur and kinematic viscosity) also present differences close to the accuracy of their analytical techniques, if we consider the propagation of TBP reproducibility error to the physical properties.



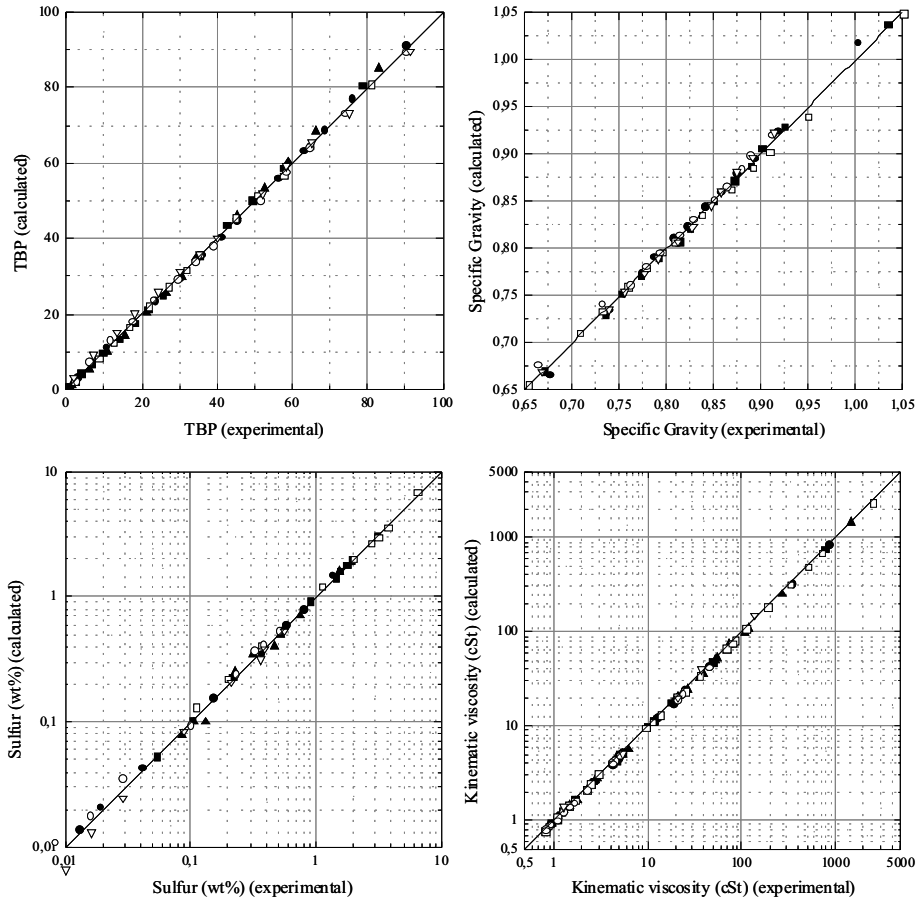


Figure 9. Comparison of experimental vs predicted properties for crude oil fractions (i – TBP, ii – specific gravity, iii – sulfur content, iv – kinematic viscosity)

The rest of the information included in a conventional assay can be predicted with similar quality, although in some cases additional laboratory measurements of crude properties (bulk metals, for example) are required to reach a higher accuracy in the reproduction of the physical properties distribution through the fractions.

## 5. CONCLUDING REMARKS

In this chapter we have reviewed a new methodology to generate complete and reliable crude oil assays from limited laboratory data. This

technology, repCAPT, is an example of the synergies that can be obtained between IT technologies and rigorous chemical engineering models.

The technology continuously updates crude oil libraries with limited cost, allowing supply chain models to optimize refinery planning and operation with reduced uncertainties. Trading areas could also benefit from better crude oil valuations with the updated characterization.

Further research can be expected from the application of repCAPT to Advanced Control Projects. This promising alternative relies on available on-line analyzers for the bulk crude oil physical properties required by the prediction system, or their replacement/supplement in future developments by alternative on-line techniques (NIR, NMR).

Another potential application not covered in this chapter is the extension to the upstream area. Some preliminary results are available in adapting repCAPT to predict the quality of new reservoirs based on the information available for crude oils from the same geographical area. This could turn repCAPT in a valuable tool to generate preliminary quality data for new wells.

## 6. REFERENCES

1. Pavlovic, K.R., "Gravity and Sulfur-based Crude Valuations More Accurate Than Believed", *Oil & Gas J.*, **1999**, 97(47), 51-56.
2. Di Vita, V.B.; Trierwiler, L.D., "The New LP", *ERTC Computing 2003, Milan, Italy, June 23-25, 2003*.
3. Hartmann, J.C.M., "Crude Valuation For Crude Selection", *Petroleum Technology Quarterly* (www.eptq.com), March 2003
4. Ferritto, T., "Crude Oil Properties and their Effect on Linear Programming", *Crude Oil Quality Group Meeting, Denver, CO, February 2, 1999*.
5. COQG. "Panel Discussion On Crude Quality and Refining", *Crude Oil Quality Group Meeting, Houston, TX, September 27, 2001*
6. Villalanti, D; Maynard, J.; Raia, J.; Arias, A., "Yield Correlations Between Crude Assay Distillation and High Temperature Simulated Distillation (HTDS)", *AIChE Spring National Meeting, Houston, TX, March 9-13, 1997*.
7. Alexander, D., "How To Update An Old Assay", *Crude Oil Quality Group Meeting, New Orleans, LA, January 30, 2003*.
8. Thompson, T. "High Temperature Simulated Distillation", *Crude Oil Quality Group Meeting, Houston, TX, October 2, 2003*.
9. Song, C; Lai, W.C.; Reddy, K.M.; Wei, B. "Temperature-Programmed Retention Indices for GC and GC-MS of Hydrocarbon Fuels and Simulated Distillation GC of Heavy Oils" In *Analytical Advances for Hydrocarbon Research*, C.S. Hsu (Ed.), Kluwer Academic/Plenum Publishers: New York, 2003.
10. Hidajat, K; Chong, S.M., "Quality Characterization of Crude Oils by Partial Least Square Calibration of NIR Spectral profiles", *J. Near Infrared Spectrosc.*, **2000**, 8, 53-59.
11. Lambert, D.; Descales, B.; Llinas, R.; Espinosa, A.; Osta, S.; Sanchez, M.; Martens, A., "On-line Near Infrared Optimisation of Refining and Petrochemical Processes", *NIR-95 Conference, Montreal, August 6-11, 1995*.
12. Kane, L., "HPI Control: Consider MRA", *Hydrocarbon Processing*, **2002**, 81(7), 17.

13. Hsu, C. S.; Drinkwater, D. "Gas Chromatography-Mass Spectrometry in the Petroleum Industry" In *Current Practice of Gas Chromatography-Mass Spectrometry*, W. M. A. Niessen (Ed.), Marcel Dekker: New York, 2001.
14. Roussis, S.G.; Fedora, J.W.; Fitzgerald, W.P.; Cameron, A.S.; Proulx, R. "Advanced Molecular Characterization by Mass Spectrometry: Applications for Petroleum and Petrochemicals" In *Analytical Advances for Hydrocarbon Research*, C.S. Hsu (Ed.), Kluwer Academic/Plenum Publishers: New York, 2003.
15. Yoshimoto, N; Kato, H., "Development of Advanced Evaluation Method for Crude Oil", *International Symposium on the Advances in Catalysis and Processes for Heavy Oil Conversion*, San Francisco, CA, April 13-17, 1997
16. Bunger, JW and Associates, Inc., "Z-Basic<sup>TM</sup> Crude Oil Assay", www.jwba.com.
17. Morgan, N., "Crude Oil Intelligence", Review - *The BP Technology Magazine*, **2001**, April, 20-21.
18. Davis, W., "The Assay Simulator – Update Assays Based On Monitoring Data", *Crude Oil Quality Group Meeting, New Orleans, LA, January 30, 2003*.
19. Peña-Díez, J.L.; "Improved Refinery Planning and Operation Through Better Feedstock Characterization", *AspenWorld 2002, Washington, D.C., October 27 – November 1, 2002*.
20. Riazi, M.R.; Daubert, T.E., "Simplify Property Predictions", *Hydrocarbon Processing*, **1980**, 59(3), 115-116.
21. Riazi, M.R.; Daubert, T.E., "Characterization Parameters for Petroleum Fractions", *Ind. Eng. Chem. Res.*, **1987**, 26(4), 755-759.
22. Riazi, M.R.; Al-Sahhaf, T., "Physical Properties of n-Alkanes and n-Alkyl Hydrocarbons: Application to Petroleum Mixtures", *Ind. Eng. Chem. Res.*, **1995**, 34(11), 4145-4148.
23. Marano, J.J.; Holder, G.D.; "General Equation for Correlating the Thermophysical Properties of n-Paraffins, n-Olefins, and Other Homologous Series. 2. Asymptotic Behavior Correlations for PVT Properties ", *Ind. Eng. Chem. Res.*, **1997**, 36(5), 1895-1907.

## INDEX

- Advanced Fluid Technology, 143-144
- Advanced Process Control, 247-255
  - Benefits, 250-253, 255
  - Economics, 249-250
- AGC-21, 102
- Alkyl Benzenes, 126
- Alkyl Naphthalenes, 128
- Ammonia, 352-354
- Aromatic Esters, 121-123
- Aromatics, 150
- Asphaltenes, 157-163, 209
  - Chemical Structure, 159-160, 163
  - Mesophase, 162, 172-173
  - Pendant-Core Model, 162
  - Precipitation, 175-178
  - Properties, 157-159
  - Thermal Chemistry, 160-163
- Automatic Model Building, 196-198
- Automation Infrastructure, 254
- Autothermal Reforming (ATR), 330-331
- $\beta$ -Scission, 194-195
- Bitumen,
  - Composition, 150-154
  - Processing, 149-181
- CANMET Hydrocracking Process, 162-163, 179
- Catalysts,
  - Amorphous Surface, 88
  - Shape Selective, 88
- Catalytic Dewaxing, 88
- Chemometrics, 224
- Clean Fuels,
  - Models, 261-278
  - Planning, 272-278
- Coke Formation, 172-174, 178
- Cold Cranking Simulator (CCS), 81
- Corrosion of NMP Plants, 30
- Crude Assay, 396-405
  - Analytical Methods, 397
  - Chemometric (Mathematical) Methods, 397-398
  - Conventional Evaluation Procedure, 396-397
  - Lube, 11-12
  - Prediction Tool (CAPT), 398
  - Quality Control, 394-396
- CSTR, 230-231
- Deasphalting, 4, 7, 174-175
- Dehydrogenation, 192
- Deprotonation, 192-193
- Dibasic Esters, 107, 118-119
- DISTACT Distillation, 176
- Deoiling, 7, 59-63
- Dewaxing (Solvent), 4, 6, 31-70, 90
  - Cold Wash, 50-55
  - Dewaxing Aids, 67-69
  - DICHILL, 35-36, 43-45
  - Filters, 45-50
  - Hot Washing, 55-56
  - Ketone, 6, 34-63
  - Propane, 6, 63-67
    - Asphaltene Contamination, 69
    - Role of Solvent, 32-33
    - Solvent Recovery, 57-58
- Electronic Transfer Mechanism, 167
- Engine Oils,
  - Additives, 131-136, 138-143
  - Detergents, 131-134
  - Dispersants, 131-132, 134-136
    - Mannich-type, 139
  - Performance Chemistry, 137-138
- Extraction-Hydroconversion, 99-101
- FCC Models, 209-210, 262-266
- Flue Gas Emission, 351-352
- Formulated Lube Oils, 2
- Fouling, 157, 171, 174, 178
  - Resistance in Steam Reformers, 299-300
  - Tendency, 176
- Gas-to-Liquids (GTL), 80, 83, 101-103
- Hard Wax, 59
- H-Oil Process, 163
- Heavy Oil,
  - Composition, 150-154
  - Processing, 149-181
- Heteroatom-Containing Compounds, 154-157
- High Temperature Shift Converter (HTSC), 341, 342
- Hot Stage Microscopy, 171-175
- Hydride Shift, 194
- Hydrocracker Model, 266-272
- Hydrocracking,
  - Combined with Hydrodewaxing, 97
  - Heavy Paraffins, 187-203
  - Kinetic Modeling, 187-203

- Paraffin, 189
  - Reaction Mechanism, 191
- Hydrodesulfurization (HDS),
  - Alternative Approaches, 155
- Hydrofinishing, 4, 6-7
- Hydrogen,
  - Donors, 174, 179
  - Economic of Production, 359-366
  - Management, 371-392
  - Network Optimization, 384-387
  - Production and Supply, 323-367, 388
  - Synthesis, 281-322
  - Thermodynamics, 324-326
- Hydrogenation, 192
- Hydroisomerization, 89-91
- Hydroprocessing, 4, 83-85
- Hydrotreating on FCC Performance, 274-278
- Incompatibility, 178
- Inhibition Reaction, 195
- Ion Exchange Chromatography, 154, 172
- IsoDewaxing, 89
- Kinetic Modeler's Toolbox (KMT), 188, 191
- Kinetics Lumping, 187
  - Bottom-Up Approach, 206-207, 211
  - Mathematical Approaches, 208, 220-224
  - Partition-Based, 205-207, 209-219
  - Structure-Oriented-Lumping (SOL), 215-217
  - Top-Down Approach, 206, 209-210
  - Total, 205-207, 224-241
- Linear Free Energy Relationship, 189-190
- Low Temperature Viscosities, 107
- Lube Business Outlook, 9
- Lube Crude Assay, 11-12
- Lube Feedstock (Crude) Selection, 9
- Lubricant (Lube Oil) Basestocks, 1-5
  - Composition, 4-5
  - End Uses, 8-9
  - Feedstock Selection, 9
  - Group I, 2, 83
  - Group II, 3, 83
  - Group III, 3, 83
  - Group IV, 3, 83
  - Group V, 3, 83
  - High Viscosity Index, 81
- Manufacturing, 1-70
  - Hydroprocessing, 2
  - Solvent Processing, 1-2
- Oxidative Stability, 92, 107
- Properties, 3-4
- Synthetic, 105-107
- Volatility, 81-82, 107
- Lube Crude Assay, 11-12
- Lube Oil Feedstocks, 4
  - Selection, 9-11
- Lube Plants, 8
- Maltenes, 103, 209
- MAXSAT, 98-99
- Methanol, 352-354
- Methyl Shift, 194
- Micelles, 158, 160-161
- MLDW, 188-189
- Mobil 1, 108
- Models,
  - Hydrogen Plant-Wide Optimization, 281-322
  - Refinery-Wide Optimization, 257-278
  - Steam Reformer, 282-283
  - Validation, 304-311
- Model-Predictive Control, 252-254
- Modeling,
  - Graph Theory, 188, 202
  - Linear Free Energy Relationship, 189-191, 217
  - Mechanistic Kinetic for Heavy Paraffins, 187-203
  - Monte Carlo, 188
  - Petroleum Reaction Kinetics, 205-242
  - Quantitative Structure-Reactivity Correlation (QSRC), 188-191, 198, 207, 211, 217
- MSDW, 89, 90
- MSDW-2, 97
- Multi-Grade Passenger Vehicle
  - Lubricants, 80
  - Additives, 80
  - Evolution, 80
- Nitrogen Compounds, 156
- Olefin Copolymers (OCP), 138-141
- Paraffins, 149
  - Conversion, 88-91
- Partial Oxidation (POX), 324-325, 330-341
- Peptization Ratio, 179
- Performance Systems, 146
- Petroleum,
  - Compatibility, 175-180
  - Composition, 149-150, 157
- Phosphate Esters, 126
- Pipestill Troubleshooting, 20-22
- Plants,
  - Carbon Monoxide, 332
  - Hydrogen, 332
  - Environmental Issues, 350-354
  - Models for Optimization, 281-332

- Modern, 342
- Performance Improvements, 357-359
- Performance Monitoring, 354-357
- Old Style, 341-342
- HYCO, 332, 333
- Conventional Solvent Lube, 4, 8
- Synthesis Gas, 332, 333
- Plug Flow Reactor, 229
- Polyalkyleneglycol (PAG), 108-109, 123-125
- Polyalphaolefins (PAO), 107-118, 139-141
  - Applications, 116-118
  - Composition, 111-112
  - Manufacturing Process, 112
  - Next Generation, 116
  - Properties, 111, 112-116
  - Synthesis, 110
- Polyisobutylene (PIB), 125, 139-141
  - High Vinylidene, 139-141
  - PIB Based Dispersants, 134
- Polymerization, 178
- Polyol Esters, 107-109, 120-123
- Pour Point, 107
- Pressure Swing Adsorption (PSA) Unit, 342
- Process Models, 205
- Propane Deasphalting, 4
- Protonated Cyclopropane (PCP)
  - Isomerization, 194
- Protonation, 192-193
- Raffinate Hydroconversion (RHC), 85, 94, 99
- Refinery Planning, 393-394
- Refinery-Wide Optimization, 259-261
- Resid Thermal Cracking, 209
- Ring Conversion, 85-88
  - Combined with Hydroisomerization-Hydrofinishing, 96-99
- Ruthenium Ion Catalyzed Oxidization (RICO), 159
- SARA Analysis, 150-151
- Saturation, 91-95
- Selective Hydrocracking, 88
- Short Path Distillation (DISTACT), 176
- Solvent Deasphalting (see Deasphalting)
- Solvent Dewaxing (see Dewaxing)
- Solvent Extraction, 4, 6, 22-31
  - Analytical Tests, 30-31
  - Characteristics of Good Solvent, 24-25
  - Process, 25-30
- Solvent Lube Processes, 5-7
- Steam Methane Reforming (SMR), 324, 326-331, 333-350
  - Combined with Oxygen Secondary Reforming (SMR/O<sub>2</sub>R), 330-336, 333, 334
  - Design Parameters, 343-350
- Steam Reformers, 282-283, 313-322
  - Catalyst Activity, 318-322
  - Catalyst Poisoning, 294-295
  - Coking, 292-294
  - Heat Balance, 295-296
  - Heat Loss, 302
  - Heat Transfer Rates, 295, 297-302
  - Oxo-Alcohol Synthesis Gas, 317
  - Pressure Drop, 302-303
- Steam Reforming Kinetics, 283-291
  - Butane, 309-311, 315
  - Methane (SMR), 283-286, 324
  - Naphtha, 286-291, 305-308, 314
- Structure-Oriented Lumping (SOL), 85
- Succination Chemistry, 139-140
- Suncor, 257-258
- Supercritical Fluid Extraction (SFE), 152, 171
- Synthetic Lubricant Oils, 105-129
- Thermal Diffusion, 87, 89-90
- Total Acid Number (TAN), 133-134
- Total Base Number (TBN), 133-134
- Upgrading Chemistry, 163-171
- Vacuum Distillation, 4, 6, 12-20
- Visbreaking, 179
- Viscosity Index (VI), 22-23, 80, 106
- Wastewater, 354
- Water Gas Shift (WGS), 325-326
- Wax Deoiling (see Deoiling)